Welcome to Chem 206

Fall Term, 2006, David A. Evans

This course is designed to introduce upper-level undergraduates and beginning graduate students to advanced topics in organic chemistry. The course begins with a discussion of bonding phenomena, an introduction to FMO theory, and stereoelectronic effects. This section will be followed by lectures in conformational analysis in both cyclic and acyclic systems. Following this introduction, a discussion of the important classes of organic reactions will be presented. Topics include rearrangements, cycloadditions, carbonyl additions, and enolate-based transformations.

Problems for this course may be accessed at the following website:
http://daecr1.chem.harvard.edu/problems/

Pavel Nagornyy

Undergraduate: Oregon State

6th-yr Graduate Student

Lab No. Converse 316

Lab Phone: 617-496-8569

Expertise: Organic Synthesis

"The Asymmetric Synthesis of Oasamycin,"
Submitted, Angew. Chem Int Ed. **2006**

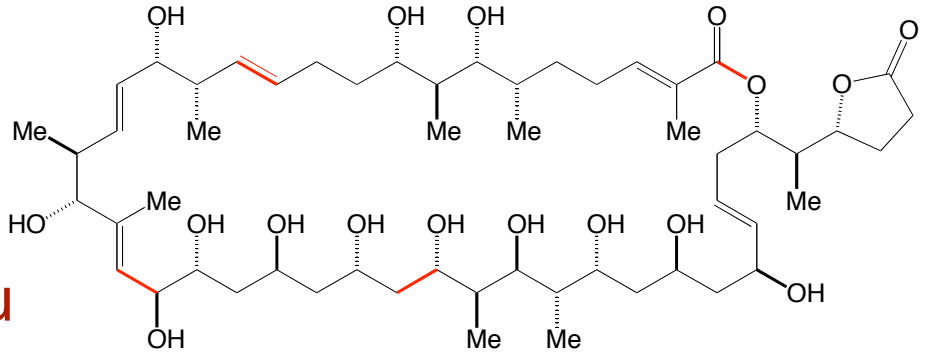

nagornyy@fas.harvard.edu

Head Teaching Fellow

Christian Markert

markert@fas.harvard.edu

Postdoctoral Fellow

University of Basel, Switzerland

Lab No. Converse 306A

Lab Phone: 617-495-5248

Expertise: Catalysis & Synthesis

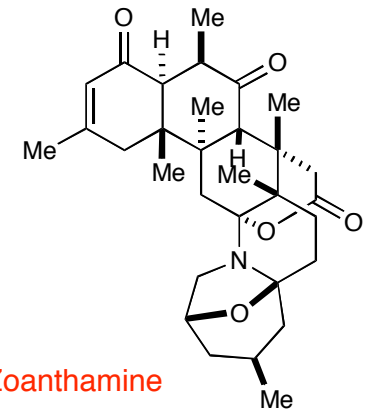

Zoanthamine

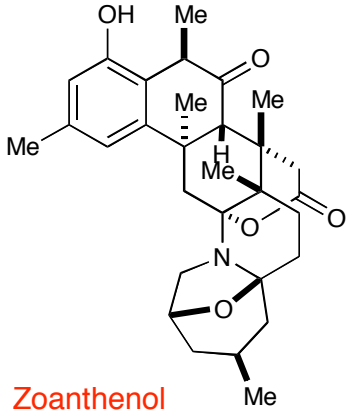

Zoanthenol

C. Markert, A. Pfaltz: 'Screening of Chiral Catalysts and Catalyst Mixtures by Mass Spectrometric Monitoring of Catalytic Intermediates', *Angew. Chem. Int. Ed.* **2004**, *43*, 2498-2500.

Hyun-Ji Song

hsong@fas.harvard.edu

Undergraduate: KAIST, Korea

4th-yr Graduate Student

Lab No. Converse 306B

Lab Phone: 617-495-3245

Expertise: Asymmetric Catalysis

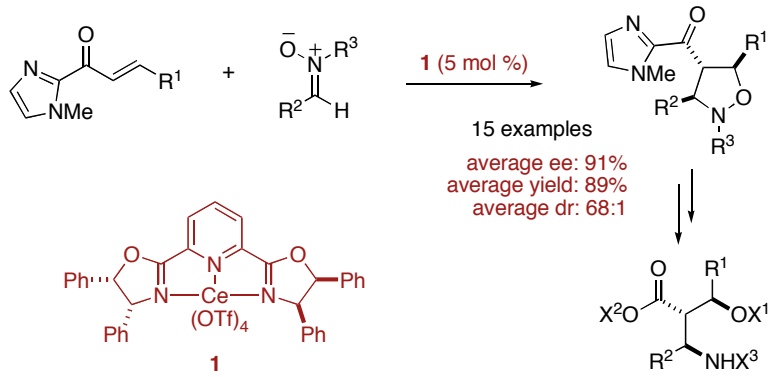

"Enantioselective Nitrone Cycloadditions of Unsaturated 2-Acyl Imidazoles Catalyzed by Bis(oxazolinyl)pyridine-Cerium(IV) Triflate Complexes" Evans, D.A.; Song, H.; *Organic Lett.*, 8, **2006**, 3351-3354

Mathieu Lalonde

Lalonde@fas.harvard.edu

Undergraduate: Univ of Ottawa, Ca

6th-year Graduate Student

Lab No. Mallinckrodt 202F

Lab Phone: 617-496-1836

Expertise: Asymmetric Catalysis

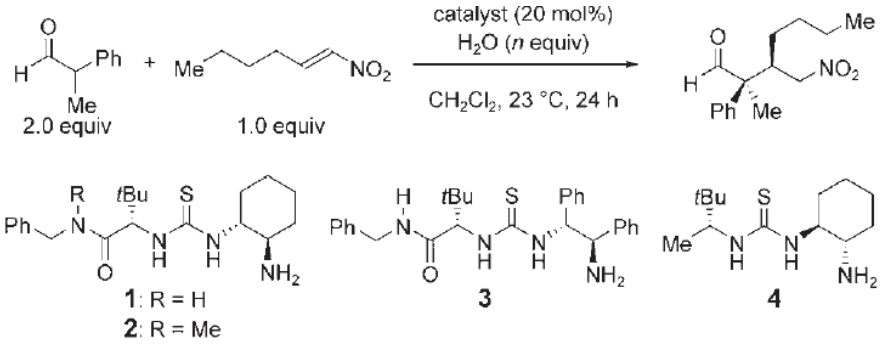

For catalyst **3**, dr >10:1, ee 99%

A Chiral Primary Amine Thiourea Catalyst for the Highly Enantioselective Direct Conjugate Addition of α,α Disubstituted Aldehydes to Nitroalkenes, Mathieu P. Lalonde, Yonggang Chen, and Eric N. Jacobsen*, *Angew.Chemie, Int. Edit*, **2006**, ASAP

Jason Hong

Undergraduate: Yale University

2nd-yr Graduate Student

Lab No. Mallinckrodt 202E

Lab Phone: 617-496-1836

Expertise: Asymmetric Catalysis

Pattern-Based Detection of Different Proteins Using an Array of Fluorescent Protein Surface Receptors, Laura Baldini, Andrew J. Wilson, Jason Hong, and Andrew D. Hamilton, *JACS* **2004,** *126,* 5656

Pattern Recognition of Proteins Based on an Array of Functionalized Porphyrins, Huchen Zhou, Laura Baldini, Jason Hong, Andrew J. Wilson, and Andrew D. Hamilton, *JACS* **2006,** *128,* 2421

jhong@fas.harvard.edu

Significant Dates this Fall

Mon, Sept 25:	Study card day
Mon, Oct 9:	Columbus Day – Class will be held
Fri, Oct 13:	**Exam 1**
Friday, Nov 10:	Veterans Day – Class will be held
Mon, Nov 20:	**Exam 2**
Wed, Nov 22:	No Class in honor of Tom Turkey
Mon, Dec 18:	**Exam 3**
Wed, Dec 20	Winter recess begins
Tuesday, Jan 2	Reading Period begins
Friday, Jan 12	Reading Period ends
Mon, Jan 22	Final Exam (Tentative)

Textbooks

Carey & Sundberg, *Advanced Organic Chemistry, Parts A,B*

Kirby, A. J. *Stereoelectronic Effects*

Web Problems

Challenging Problems in Chemistry and Chemical Biology

http://daecr1.chem.harvard.edu/problems/

Course Grading

3 one-Hour Exams	300 pts
10 Problem Sets	200 pts
Final Examination	300 pts

We will grade your best effort. **We will take your final exam score and manufacture an imaginary hr exam score (IHE).** If this score is better than any of your normalized hourly exam scores, the **IHE** score will replace those lower scores. The **IHE** score will also be used in the event that an hourly exam was missed.

This plan provides you the opportunity to have the final exam count between 37% and 75% of your final grade.

Sections

Sections will begin this week.
Sign up prior to **5 PM this Wednesday**

http://www.courses.fas.harvard.edu/colgsas/1063

http://evans.harvard.edu/problems/

Chemistry 206

Advanced Organic Chemistry

Lecture Number 1

Introduction to FMO Theory

- General Bonding Considerations
- The H_2 Molecule Revisited (Again!)
- Donor & Acceptor Properties of Bonding & Antibonding States
- Hyperconjugation

Reading Assignment for week:

Kirby, Stereoelectronic Effects
Carey & Sundberg: **Part A**; Chapter 1

Fukui, *Acc. Chem. Res.* **1971**, *4*, 57. (pdf)
Alabugin & Zeidan, *JACS* **2002**, *124*, 3175 (pdf)
Robertson, *Org. Letters* **2005**, *7*, 5007 (pdf)

D. A. Evans

Monday,
September 18, 2006

Problems of the Day

The molecule illustrated below can react through either Path A or Path B to form salt **1** or salt **2**. In both instances the carbonyl oxygen functions as the nucleophile in an intramolecular alkylation. What is the preferred reaction path for the transformation in question?

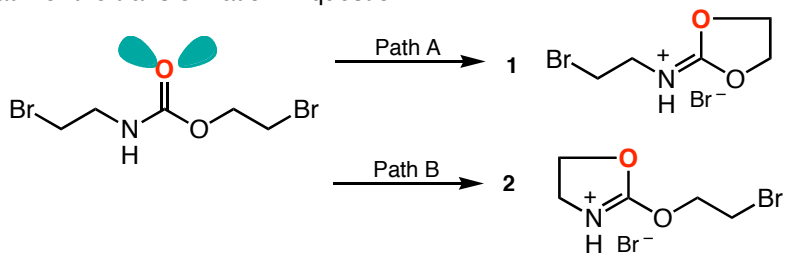

This is a "thought" question posed to me by Prof. Duilo Arigoni at the ETH in Zuerich some years ago

FIRST HOUR EXAM, 2005. The oxidation of acetals by electrophilic ozone is known to be sensitive to structure. Two striking examples of different reactivity are detailed in the questions below. Using clear three-dimensional drawings provide a rationale for the observation that rigid glycoside **A** readily undergoes oxidation but glycoside **B** does not. Be sure to indicate all relevant stereoelectronic interactions.

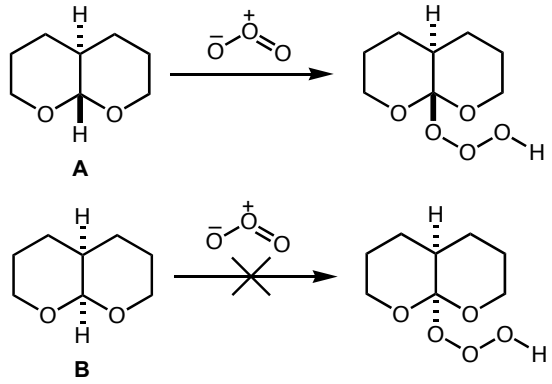

Deslongchamps, *Can. J. Chem.* **1974**, 3651-3664.

Universal Effects Governing Chemical Reactions There are three:

■ Steric Effects

Nonbonding interactions (Van der Waals repulsion) between substituents within a molecule or between reacting molecules

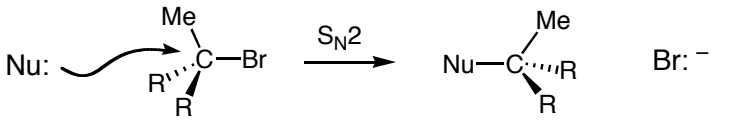

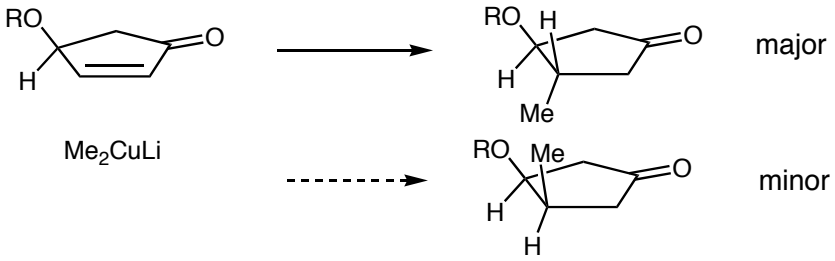

■ Electronic Effects (Inductive Effects):

The effect of bond and through-space polarization by heteroatom substituents on reaction rates and selectivities

Inductive Effects: Through-bond polarization
Field Effects: Through-space polarization

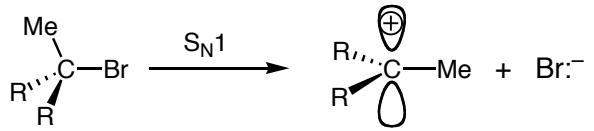

rate decreases as R becomes more electronegative

■ Stereoelectronic Effects

Geometrical constraints placed upon ground and transition states by orbital overlap considerations.

Fukui Postulate for reactions:

"During the course of chemical reactions, the interaction of the highest filled (HOMO) and lowest unfilled (antibonding) molecular orbital (LUMO) in reacting species is very important to the stabilization of the transition structure."

■ General Reaction Types

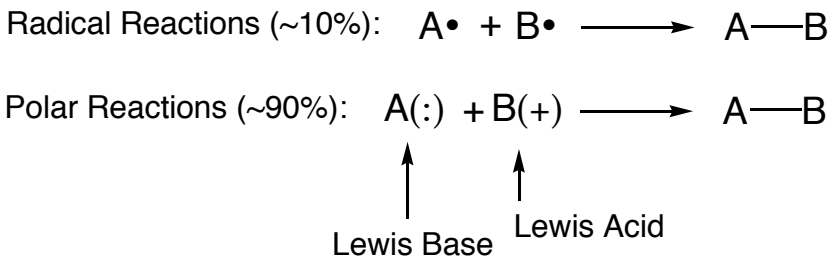

FMO concepts extend the donor-acceptor paradigm to non-obvious families of reactions

■ Examples to consider

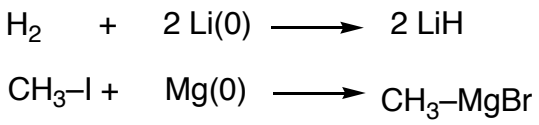

"Organic chemists are generally unaware of the impact of electronic effects on the stereochemical outcome of reactions."

"The distinction between electronic and stereoelectronic effects is not clear-cut."

Steric Versus electronic Effects: Some Case Studies

When steric and electronic (stereoelectronic) effects lead to differing stereochemical consequences

Woerpel etal. *JACS* **1999**, 121, 12208.

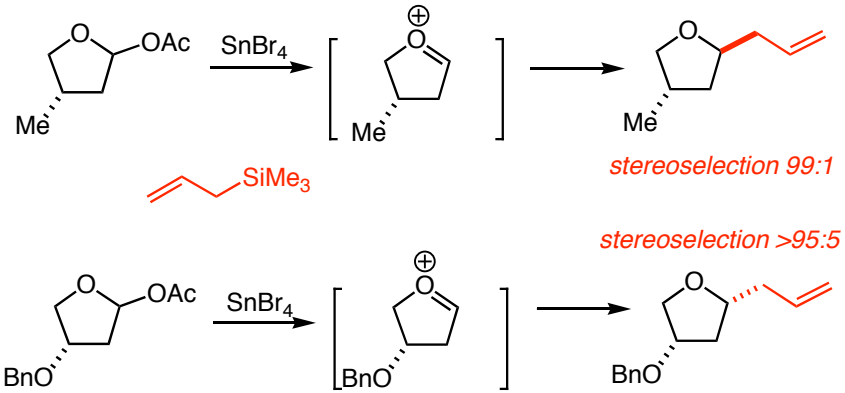

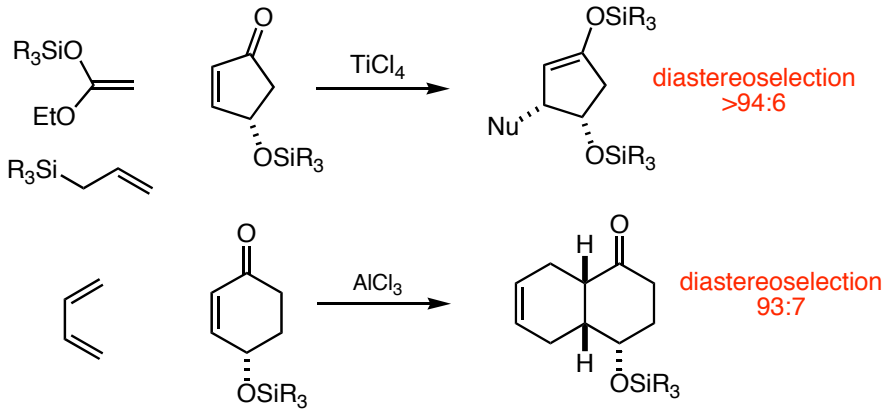

Danishefsky et al *JOC* **1991**, *56*, 387

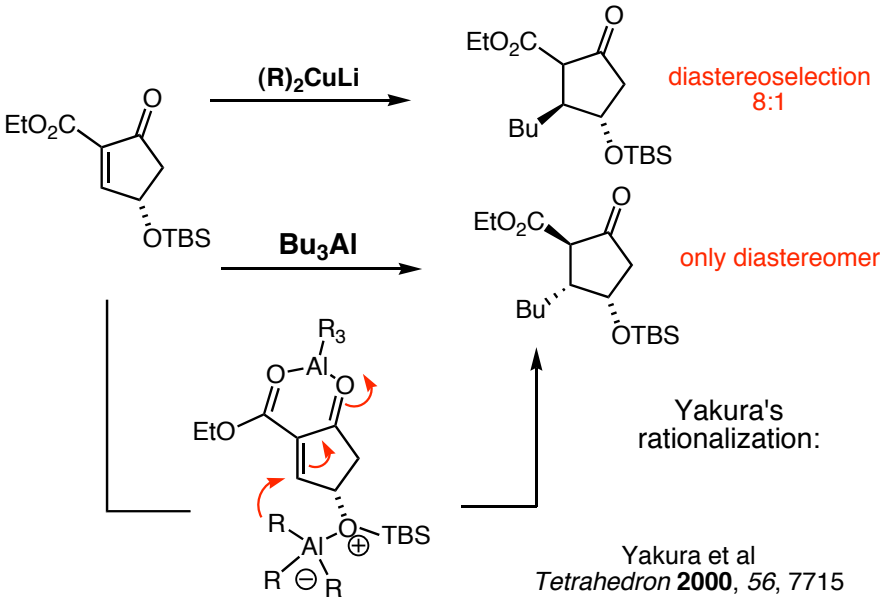

Yakura et al
Tetrahedron **2000**, *56*, 7715

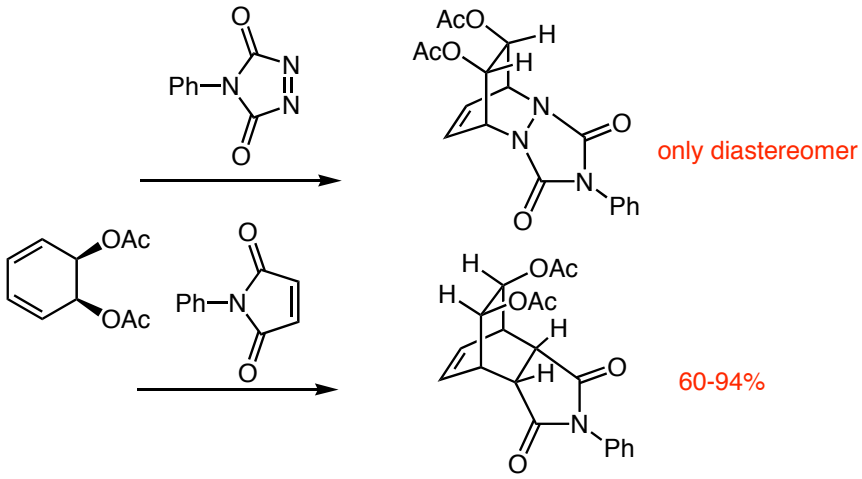

Mehta et al, *Acc Chem. Res.* **2000**, *33*, 278-286

Progress in the Synthesis of the Lituarines: Stereocontrol in Sequential C–C Bond Formation on a Spirobutenolide Template

Jeremy Robertson* and Jonathan W. P. Dallimore

ORGANIC LETTERS

2005
Vol. 7, No. 22
5007−5010

Scheme 2. Conjugate Addition Model Study[1b]

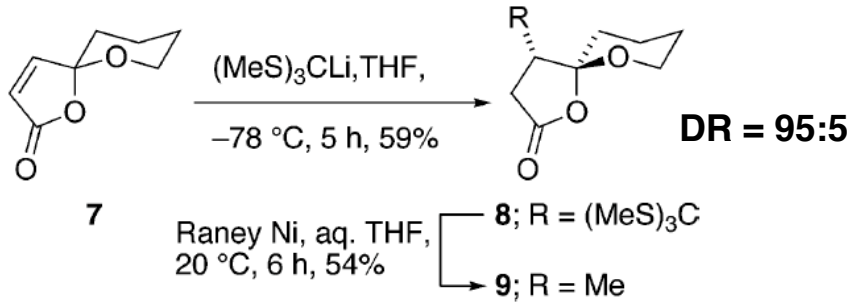

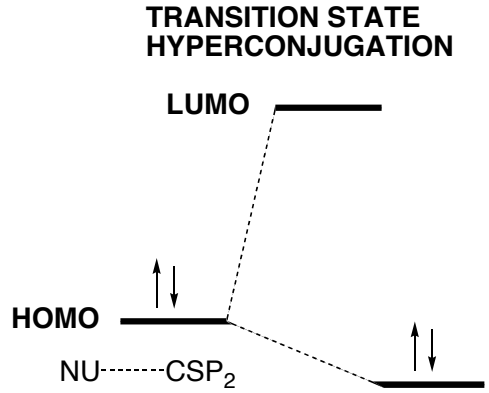

(5) Our working hypothesis is that a stabilizing interaction of the incoming nucleophile, and then the forming C−C bond, with the tetrahydropyran [C(15)−O]σ^* acts cooperatively with electrostatic and solvation effects to favor attack *anti* to the six-membered ring oxygen. Cf. Corey, E. J.; Boaz, N. W. *Tetrahedron Lett.* **1984**, *25*, 3063.

The H_2 Molecule (again!!)

Let's combine two hydrogen atoms to form the hydrogen molecule. Mathematically, linear combinations of the 2 atomic 1s states create two new orbitals, one is bonding, and one antibonding:

■ **Rule one**: A linear combination of n atomic states will create n MOs.

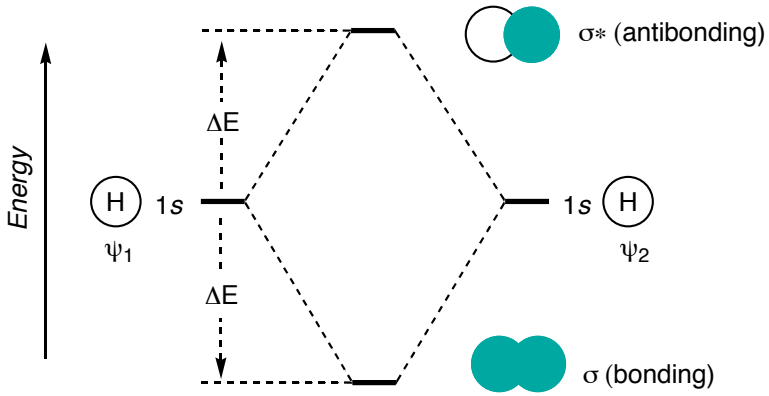

Let's now add the two electrons to the new MO, one from each H atom:

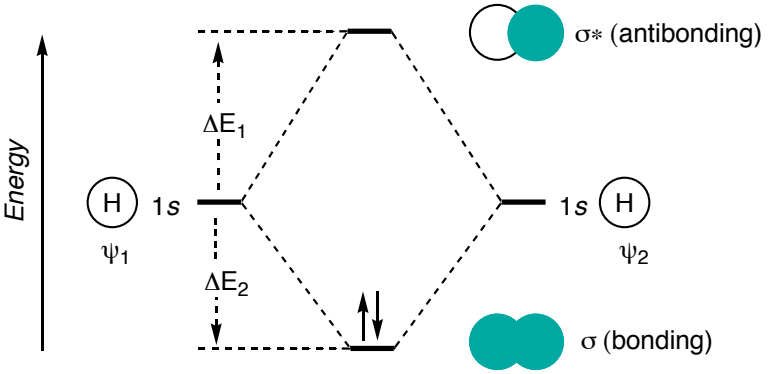

Note that ΔE_1 is greater than ΔE_2. Why?

Linear Combination of Atomic Orbitals (LCAO): Orbital Coefficients

■ **Rule Two**:

Each MO is constructed by taking a linear combination of the individual atomic orbitals (AO):

Bonding MO $\quad \sigma = C_1\psi_1 + C_2\psi_2$

Antibonding MO $\quad \sigma* = C^*_1\psi_1 - C^*_2\psi_2$

The coefficients, C_1 and C_2, represent the contribution of each AO.

■ **Rule Three**: $(C_1)^2 + (C_2)^2 = 1$

The squares of the C-values are a measure of the electron population in neighborhood of atoms in question

■ **Rule Four**: bonding$(C_1)^2$+ antibonding$(C^*_1)^2$= 1

In LCAO method, both wave functions must each contribute one net orbital

Consider the pi–bond of a C=O function: In the ground state pi-C–O is polarized toward Oxygen. Note (Rule 4) that the antibonding MO is polarized in the opposite direction.

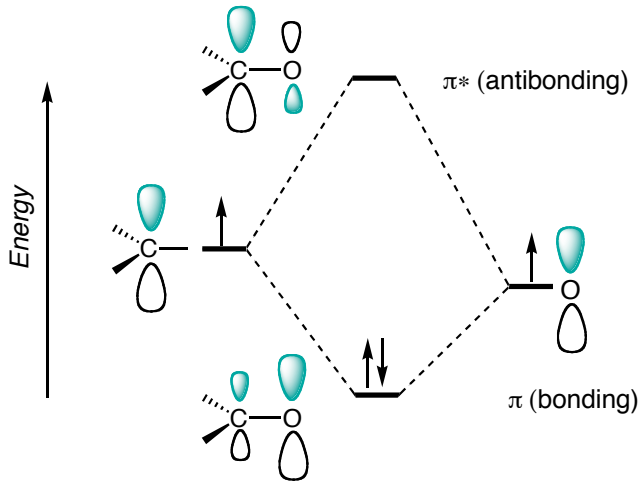

■ *Bond strengths (Bond dissociation energies) are composed of a covalent contribution (δE_{cov}) and an ionic contribution (δE_{ionic}).*

$$\text{Bond Energy (BDE)} = \delta E_{covalent} + \delta E_{ionic}$$

When one compares bond strengths between C–C and C–X, where X is some other element such as O, N, F, Si, or S, keep in mind that covalent and ionic contributions vary independently. Hence, the mapping of trends is not a trivial exercise.

Useful generalizations on covalent bonding

■ *Overlap between orbitals of comparable energy is more effective than overlap between orbitals of differing energy.*

For example, consider elements in Group IV, Carbon and Silicon. We know that C-C bonds are considerably stronger by Ca. 20 kcal mol^{-1} than C-Si bonds.

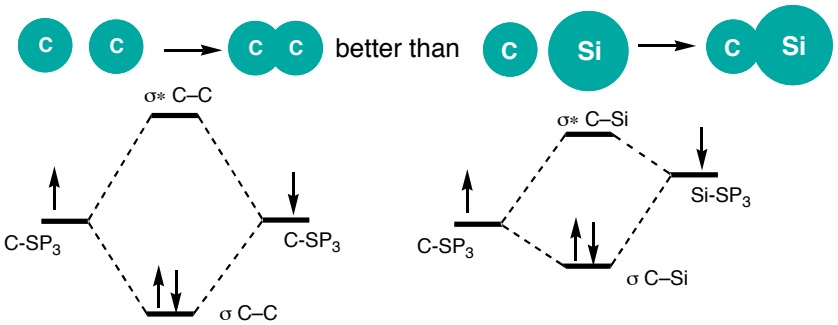

$H_3C–CH_3$ BDE = 88 kcal/mol
Bond length = 1.534 Å

$H_3C–SiH_3$ BDE ~ 70 kcal/mol
Bond length = 1.87 Å

This trend is even more dramatic with pi-bonds:

π C–C = 65 kcal/mol π C–Si = 36 kcal/mol π Si–Si = 23 kcal/mol

■ *Weak bonds will have corresponding low-lying antibonds.*

Formation of a weak bond will lead to a corresponding low-lying antibonding orbital. Such structures are reactive as both nucleophiles & electrophiles

■ *Orbital orientation strongly affects the strength of the resulting bond.*

For σ Bonds:

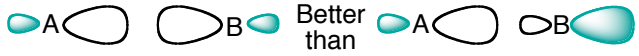

For π Bonds:

This is a simple notion with very important consequences. It surfaces in the delocalized bonding which occurs in the competing anti (favored) syn (disfavored) E2 elimination reactions. Review this situation.

■ *Anti orientation of filled and unfilled orbitals leads to better overlap.*

This is a corrollary to the preceding generalization. There are two common situations.

Case-1: Anti Nonbonding electron pair & C–X bond

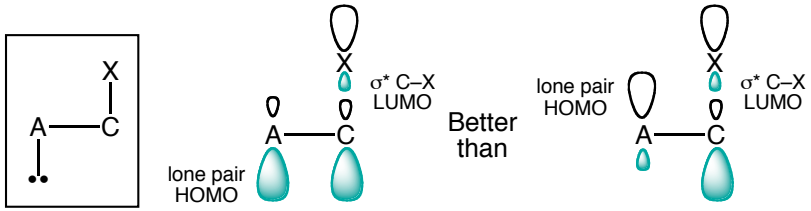

Case-2: Two anti sigma bonds

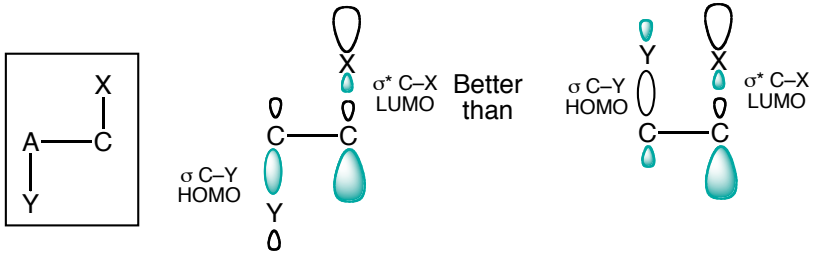

Donor Acceptor Properties of C-C & C-O Bonds

Consider the energy level diagrams for both bonding & antibonding orbitals for C–C and C–O bonds.

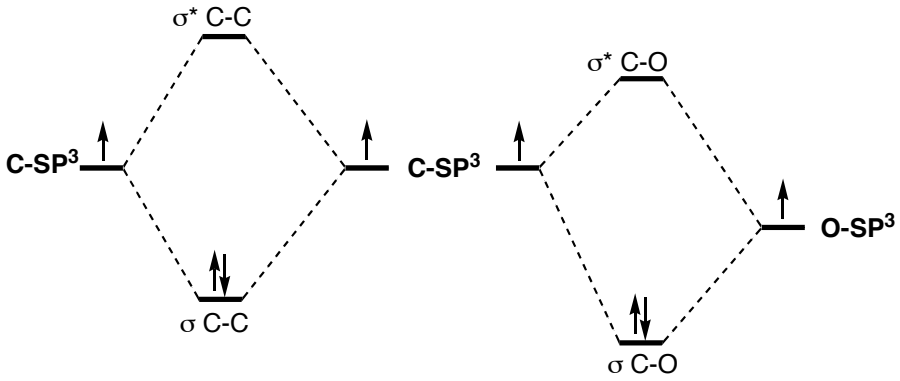

■ The greater electronegativity of oxygen lowers both the bonding & antibonding C-O states. Hence:

- ■ σ C–C is a better donor orbital than σ C–O
- ■ σ*C–O is a better acceptor orbital than σ*C–C

Donor Acceptor Properties of C_{SP3}-C_{SP3} & C_{SP3}-C_{SP2} Bonds

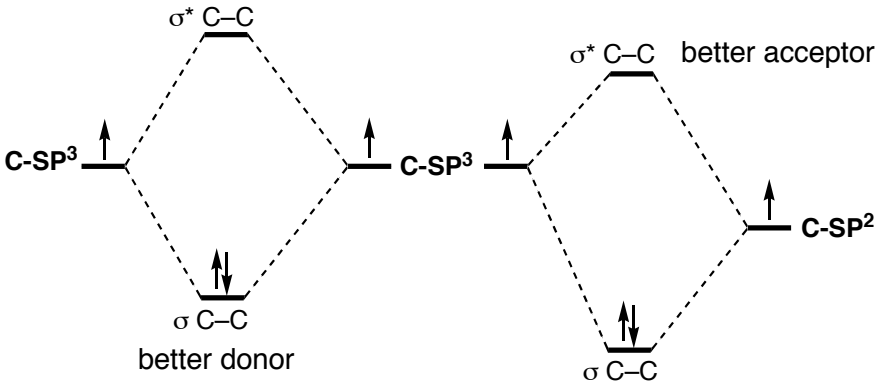

■ The greater electronegativity of C_{SP2} lowers both the bonding & antibonding C–C states. Hence:

- ■ σ C_{SP3}-C_{SP3} is a better donor orbital than σ C_{SP3}-C_{SP2}
- ■ σ*C_{SP3}-C_{SP2} is a better acceptor orbital than σ*C_{SP3}-C_{SP3}

Hierarchy of Donor & Acceptor States

Following trends are made on the basis of comparing the bonding and antibonding states for the molecule CH_3–X where X = C, N, O, F, & H.

σ-bonding States: (C–X)

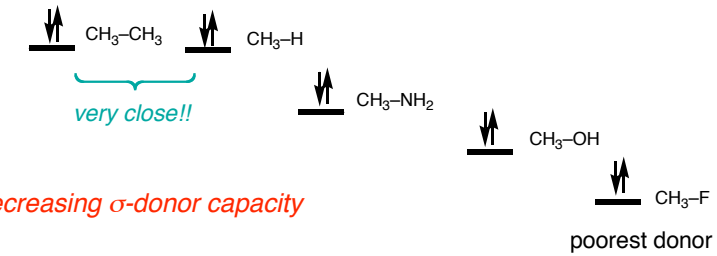

σ-anti-bonding States: (C–X)

For the latest views, please read Alabugin & Zeidan, *JACS* **2002**, *124*, 3175 (pdf)

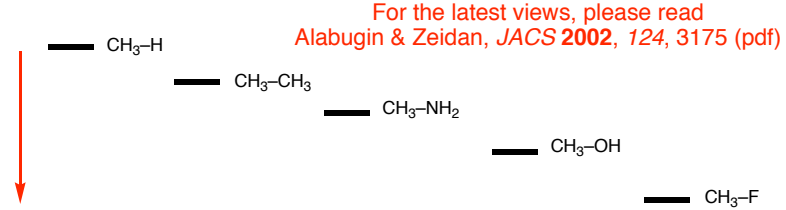

The following are trends for the energy levels of *nonbonding states* of several common molecules. Trend was established by photoelectron spectroscopy.

Nonbonding States

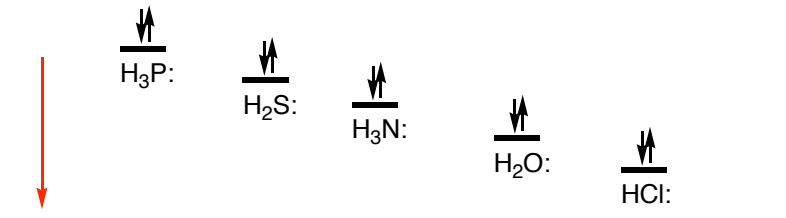

Radial Electron Density of S-States

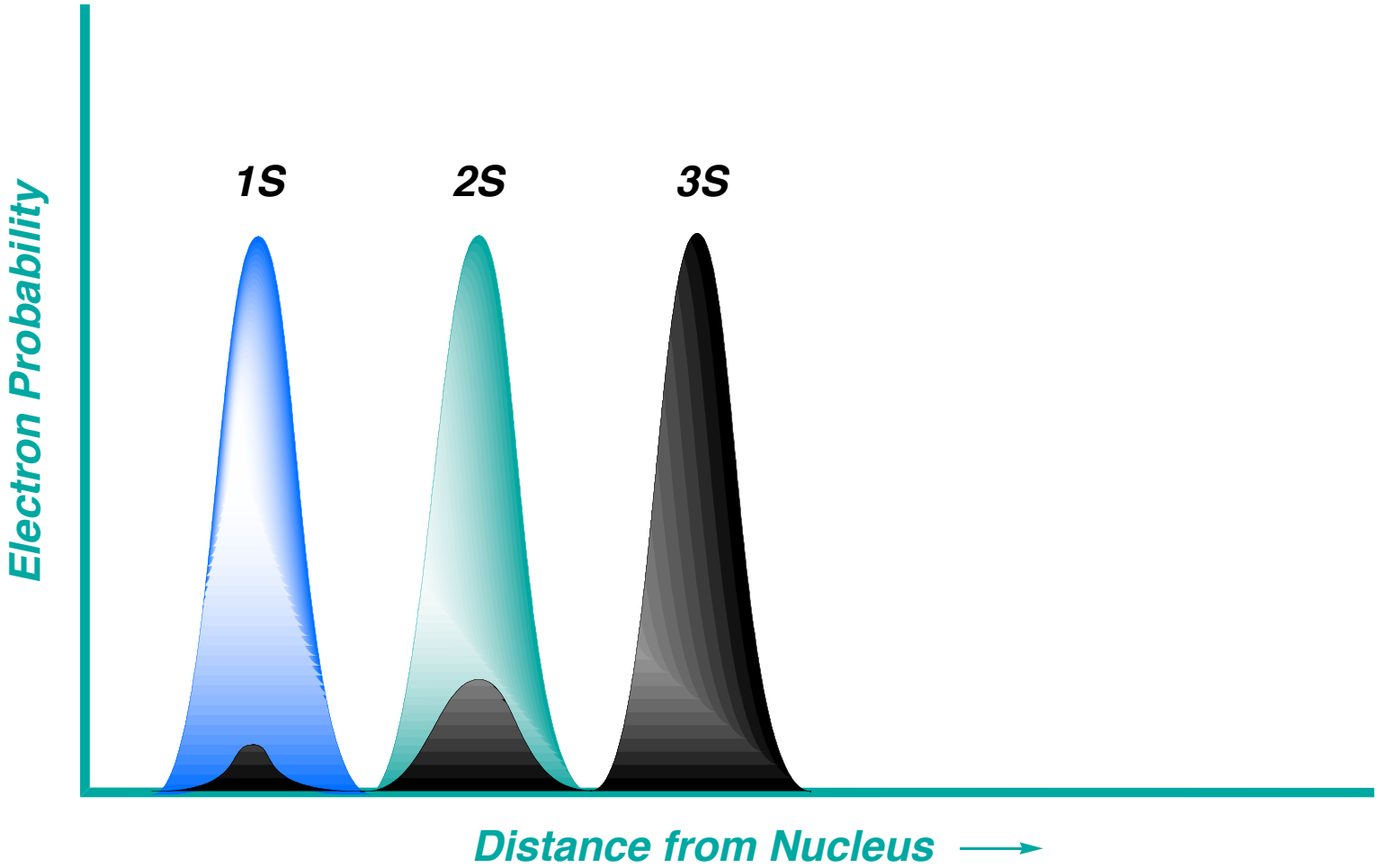

Radial Electron Density of S- & P-States

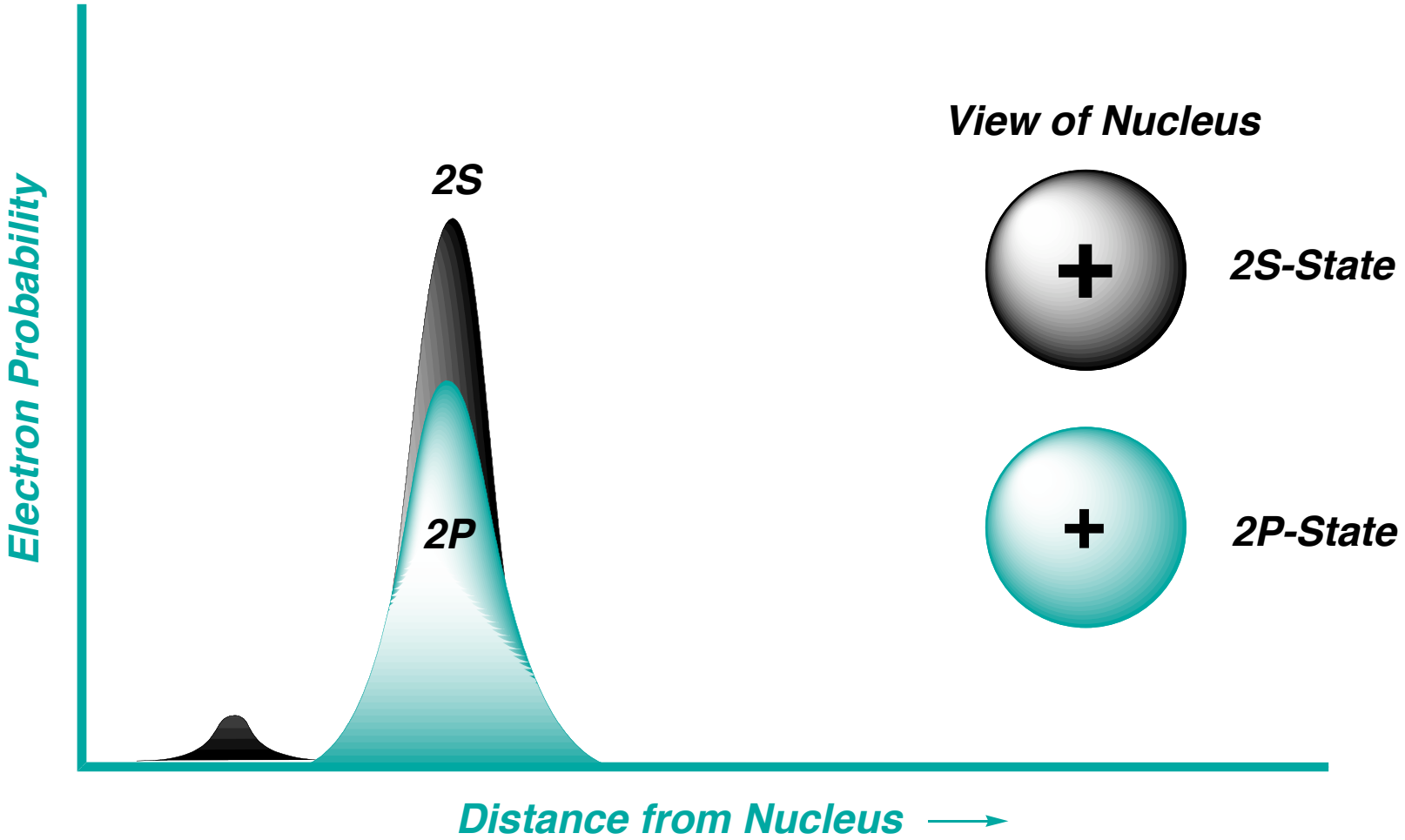

Electrons in 2S states "see" a greater effective nuclear charge than electrons in 2P states.

This becomes apparent when the radial probability functions for S and P-states are examined: The radial probability functions for the hydrogen atom S & P states are shown below.

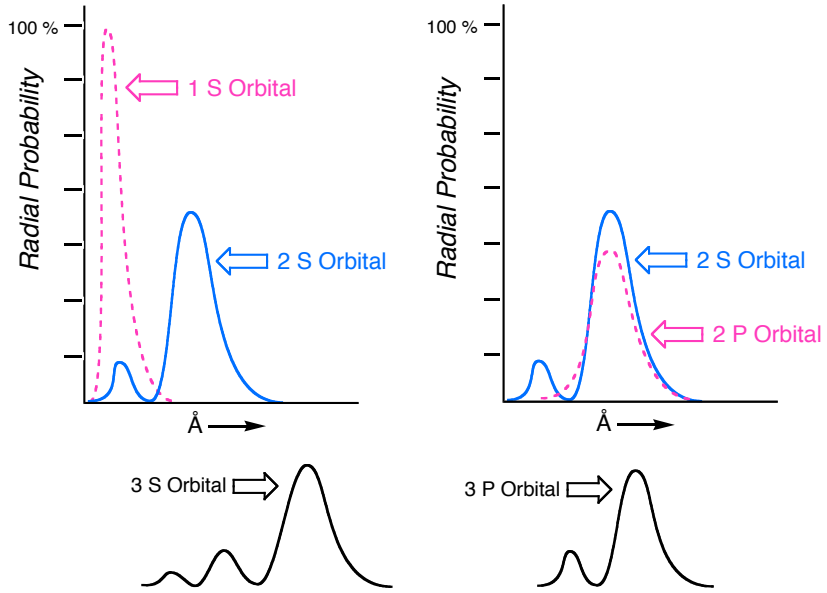

S-states have greater radial penetration due to the nodal properties of the wave function. Electrons in S-states "see" a higher nuclear charge.

Above observation correctly implies that the stability of nonbonding electron pairs is directly proportional to the % of S-character in the doubly occupied orbital

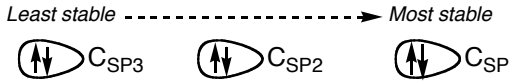

The above trend indicates that the greater the % of S-character at a given atom, the greater the electronegativity of that atom.

There is a linear relationship between %S character & Pauling electronegativity

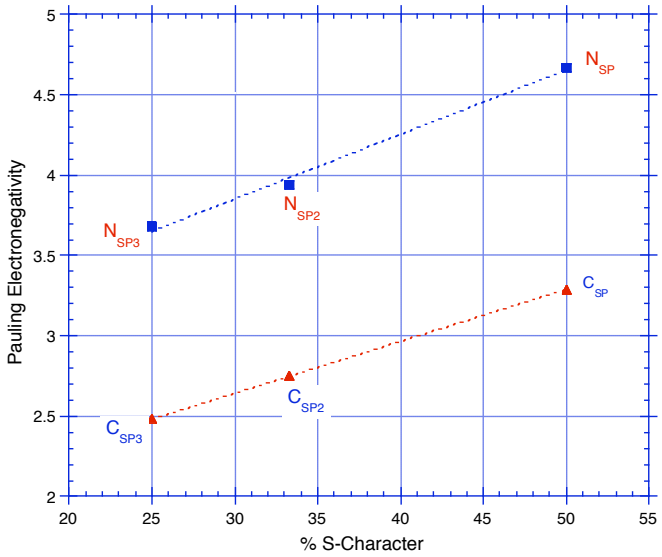

There is a direct relationship between %S character & hydrocarbon acidity

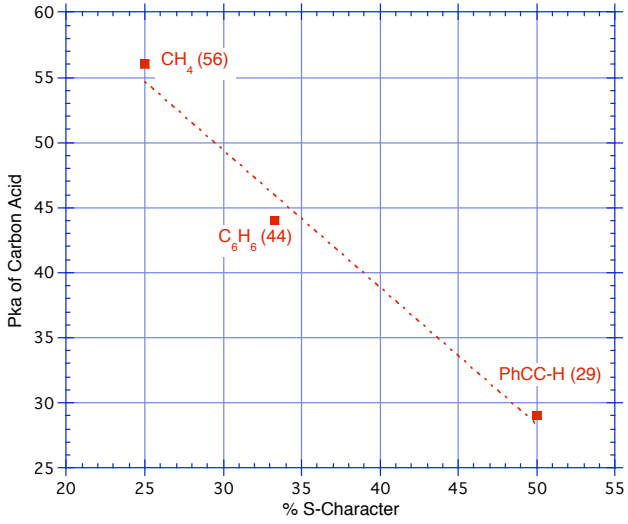

■ The interaction of a vicinal bonding orbital with a p-orbital is referred to as hyperconjugation.

This is a traditional vehicle for using valence bond to denote charge delocalization.

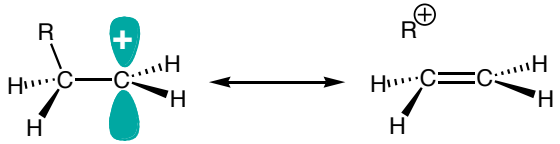

The graphic illustrates the fact that the C-R bonding electrons can "delocalize" to stabilize the electron deficient carbocationic center.

Note that the general rules of drawing resonance structures still hold: the positions of all atoms must not be changed.

Stereoelectronic Requirement for Hyperconjugation:
Syn-planar orientation between interacting orbitals

The Molecular Orbital Description

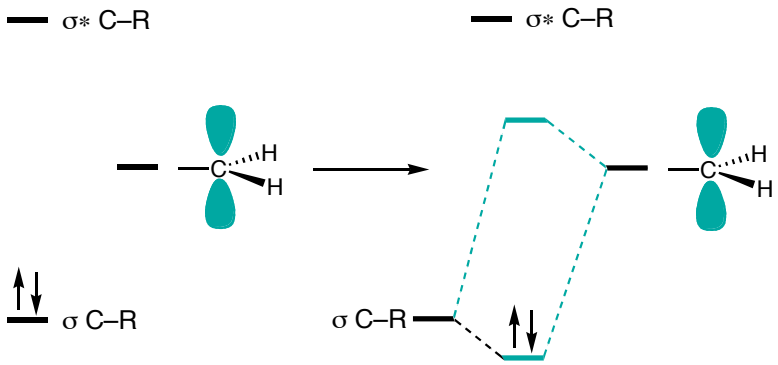

■ Take a linear combination of σ C–R and CSP_2 p-orbital:

"The new occupied bonding orbital is lower in energy. When you stabilize the electrons is a system you stabilize the system itself."

Physical Evidence for Hyperconjugation

■ Bonds participating in the hyperconjugative interaction, e.g. C–R, will be lengthened while the C(+)–C bond will be shortened.

First X-ray Structure of an Aliphatic Carbocation

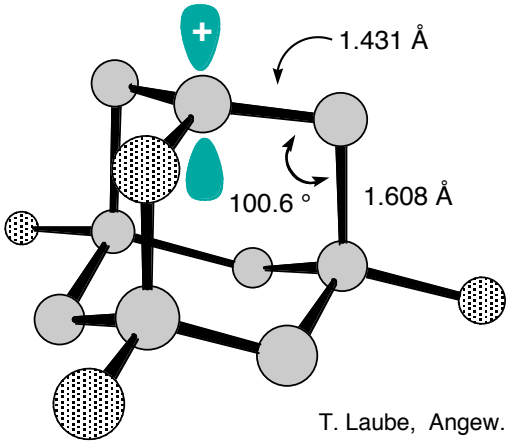

$[F_5Sb–F–SbF_5]^-$

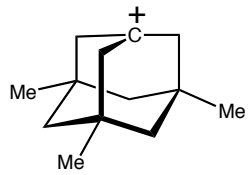

T. Laube, Angew. *Chem. Int. Ed.* **1986**, *25*, 349

The Adamantane Reference (MM-2)

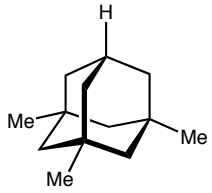

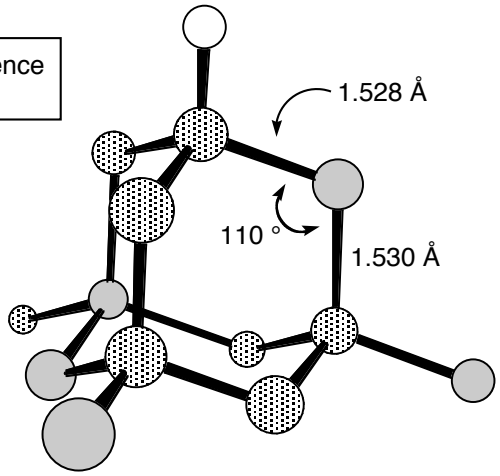

http://www.courses.fas.harvard.edu/colgsas/1063

Chemistry 206

Advanced Organic Chemistry

Lecture Number 2

Stereoelectronic Effects-2

- "Positive" and "Negative" Hyperconjugation
- Anomeric and Related Effects
- Peracid & Dioxirane Epoxidation (Stereoelectronics)

Kirby, Stereoelectronic Effects Chapters 1-5

Carey & Sundberg: **Part A**; Chapter 1, Chapter 3

Fukui, *Acc. Chem. Res.* **1971**, *4*, 57. (pdf)

Alabugin & Zeidan, *JACS* **2002**, *124*, 3175 (pdf)

D. A. Evans

Wednesday, September 20, 2006

Useful LIterature Reviews

Kirby, A. J. (**1982**). The Anomeric Effect and Related Stereoelectronic Effects at Oxygen. New York, Springer Verlag.

Box, V. G. S. (**1990**). "The role of lone pair interactions in the chemistry of the monosaccharides. The anomeric effect." *Heterocycles* **31**: 1157.

Box, V. G. S. (**1998**). "The anomeric effect of monosaccharides and their derivatives. Insights from the new QVBMM molecular mechanics force field." *Heterocycles* **48**(11): 2389-2417.

Graczyk, P. P. and M. Mikolajczyk (**1994**). "Anomeric effect: origin and consequences." *Top. Stereochem.* **21**: 159-349.

Juaristi, E. and G. Cuevas (**1992**). "Recent studies on the anomeric effect." *Tetrahedron* **48**: 5019 **(PDF)**

Carey & Sundberg: **Part A**; Chapter 3 pp 151-156

Database problem 307

Natural bond order (NBO) analysis is a powerful computational tool that allows one to quantitatively estimate the energy of hyperconjugative effects (Alabugin & Zeiden, *JACS* **2002**, *124*, 3175). The stabilizing interactions for the H_1 and H_4 equatorial hydrogens for 1,3-dioxane and 1,3-dithiane are provided below. It is interesting that the two indicated hyperconjugative interactions in dioxane are approximately the same (4.5 vs 4.2) but that the same interactions in dithiane are quite different (6.5 vs 1.8). In fact, the authors refer to C–S bonds as "one directional" acceptor orbitals.

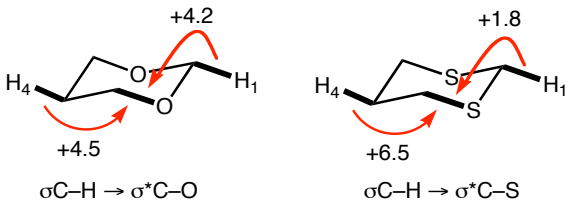

numbers refer to interaction energies in kcal/mol at the B3LYP/6-31+G*** level

There is one quite reasonable qualitative argument that can rationalize the "one directional" character of σ*C–S. Please provide your argument in the space provided below.

■ The interaction of a vicinal bonding orbital with a p-orbital is referred to as hyperconjugation.

This is a traditional vehicle for using valence bond to denote charge delocalization.

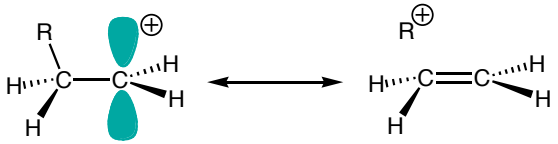

The graphic illustrates the fact that the C-R bonding electrons can "delocalize" to stabilize the electron deficient carbocationic center.

Note that the general rules of drawing resonance structures still hold: the positions of all atoms must not be changed.

Stereoelectronic Requirement for Hyperconjugation:
Syn-planar orientation between interacting orbitals

The Molecular Orbital Description

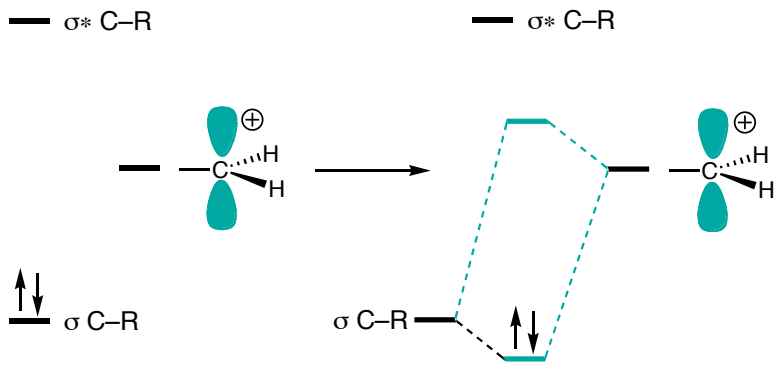

■ Take a linear combination of σ C–R and CSP_2 p-orbital:

"The new occupied bonding orbital is lower in energy. When you stabilize the electrons is a system you stabilize the system itself."

Physical Evidence for Hyperconjugation

■ Bonds participating in the hyperconjugative interaction, e.g. C–R, will be lengthened while the C(+)–C bond will be shortened.

First X-ray Structure of an Aliphatic Carbocation

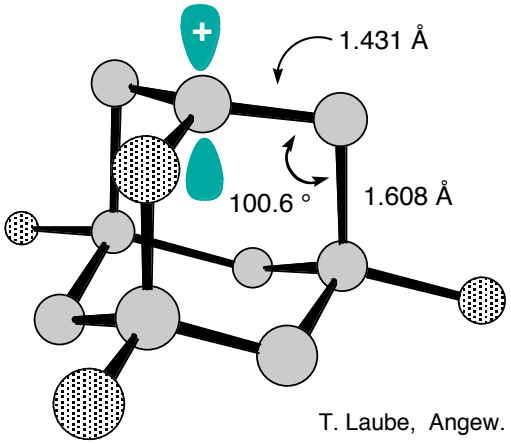

$[F_5Sb–F–SbF_5]^-$

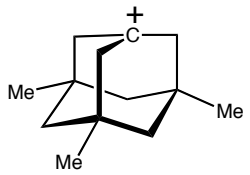

T. Laube, Angew. *Chem. Int. Ed.* **1986**, *25*, 349

The Adamantane Reference (MM-2)

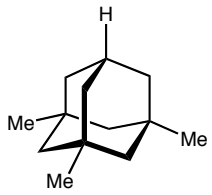

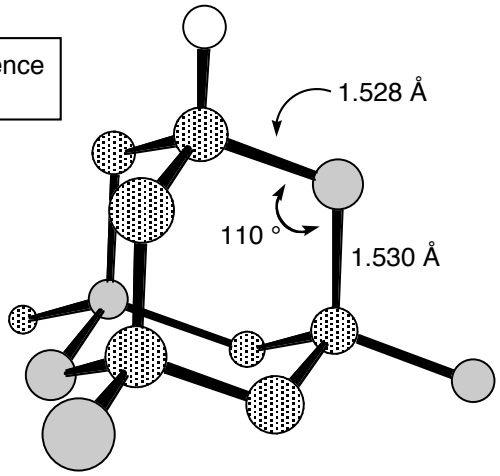

■ Delocalization of nonbonding electron pairs into vicinal antibonding orbitals is also possible

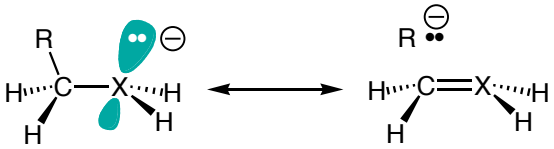

This decloalization is referred to as "Negative" hyperconjugation

Since nonbonding electrons prefer hybrid orbitals rather that P orbitals, this orbital can adopt either a syn or anti relationship to the vicinal C–R bond.

The Molecular Orbital Description

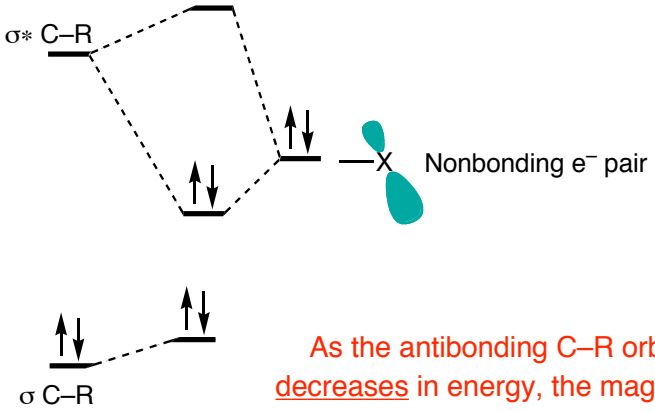

As the antibonding C–R orbital decreases in energy, the magnitude of this interaction will increase

Note that σ C–R is slightly destabilized

Syn Orientation

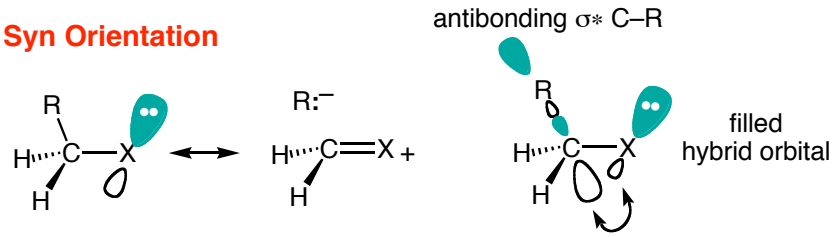

Anti Orientation

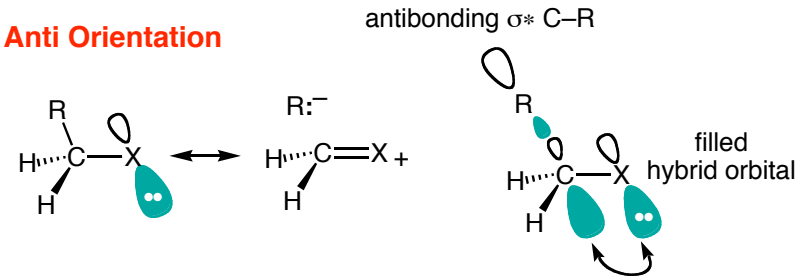

■ Overlap between two orbitals is better in the anti orientation as stated in "Bonding Generalizations" handout.

The Expected Structural Perturbations

Change in Structure	Spectroscopic Probe
■ Shorter C–X bond	X-ray crystallography
■ Longer C–R bond	X-ray crystallography
■ Stronger C–X bond	Infrared Spectroscopy
■ Weaker C–R bond	Infrared Spectroscopy
■ Greater e-density at R	NMR Spectroscopy
■ Less e-density at X	NMR Spectroscopy

The interaction of filled orbitals with adjacent antibonding orbitals can have an ordering effect on the structure which will stabilize a particular geometry. Here are several examples:

Case 1: N_2F_2

This molecule can exist as either cis or trans isomers

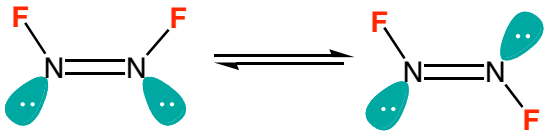

There are two logical reasons why the trans isomer should be more stable than the cis isomer.

■ The nonbonding lone pair orbitals in the cis isomer will be destabilizing due to electron-electron repulsion.

■ The individual C–F dipoles are mutually repulsive (pointing in same direction) in the cis isomer.

In fact the cis isomer is favored by 3 kcal/ mol at 25 °C.

Let's look at the interaction with the lone pairs with the adjacent C–F antibonding orbitals.

The cis Isomer

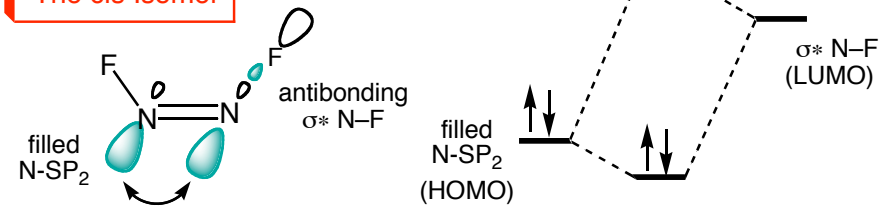

■ Note that by taking a linear combination of the nonbonding and antibonding orbitals you generate a more stable bonding situation.

■ Note that two such interactions occur in the molecule even though only one has been illustrated.

The trans Isomer

Now carry out the same analysis with the same 2 orbitals present in the trans isomer.

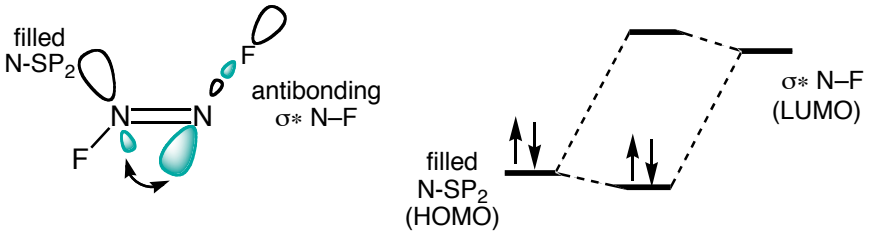

■ In this geometry the "small lobe" of the filled N-SP_2 is required to overlap with the large lobe of the antibonding C–F orbital. Hence, when the new MO's are generated the new bonding orbital is not as stabilizing as for the cis isomer.

Conclusions

■ Lone pair delocalization appears to override electron-electron and dipole-dipole repulsion in the stabilization of the cis isomer.

■ This HOMO-LUMO delocalization is stronger in the cis isomer due to better orbital overlap.

Important Take-home Lesson

Orbital orientation is important for optimal orbital overlap.

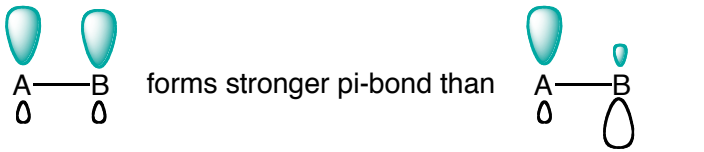

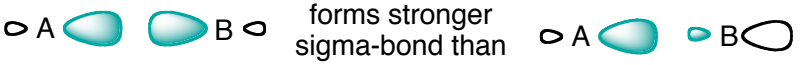

This is a simple notion with very important consequences. It surfaces in the delocalized bonding which occurs in the competing anti (favored) syn (disfavored) E2 elimination reactions. Review this situation.

The Anomeric Effect

It is not unexpected that the methoxyl substituent on a cyclohexane ring prefers to adopt the equatorial conformation.

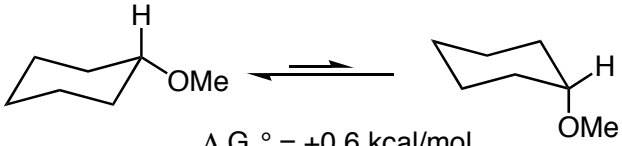

ΔG_c° = +0.6 kcal/mol

What is unexpected is that the closely related 2-methoxytetrahydropyran prefers the axial conformation:

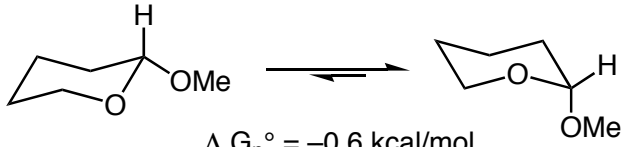

ΔG_p° = –0.6 kcal/mol

That effect which provides the stabilization of the axial OR conformer which overrides the inherent steric bias of the substituent is referred to as the anomeric effect.

Let anomeric effect = A

$$\Delta G_p^\circ = \Delta G_c^\circ + A$$

$$A = \Delta G_p^\circ - \Delta G_c^\circ$$

A = –0.6 kcal/mol – 0.6 kcal/mol = –1.2 kcal/mol

Principal HOMO-LUMO interaction from each conformation is illustrated below:

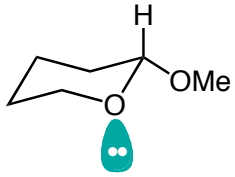

axial O lone pair↔σ* C–H

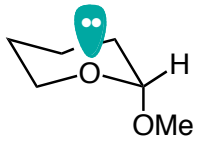

axial O lone pair↔σ* C–O

■ Since the antibonding C–O orbital is a better acceptor orbital than the antibonding C–H bond, the axial OMe conformer is better stabilized by this interaction which is worth ca. 1.2 kcal/mol.

Other electronegative substituents such as Cl, SR etc also participate in anomeric stabilization.

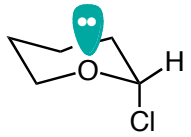

This conformer preferred by 1.8 kcal/mol

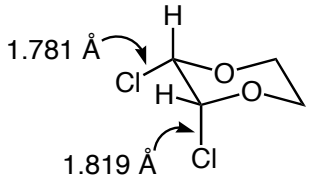

Why is axial C–Cl bond longer ?

axial O lone pair↔σ* C–Cl

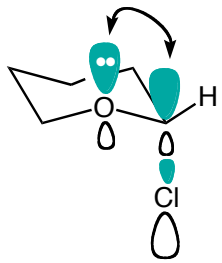

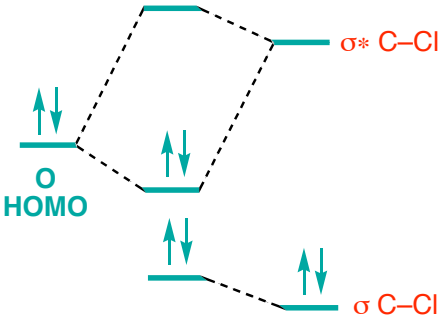

The Exo-Anomeric Effect

■ There is also a rotational bias that is imposed on the exocyclic C–OR bond where one of the oxygen lone pairs prevers to be anti to the ring sigma C–O bond

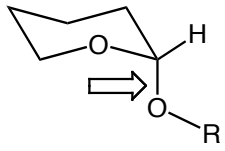

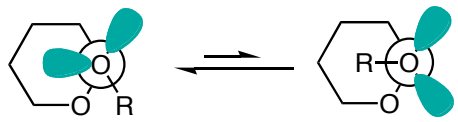

favored

A. J. Kirby, *The Anomeric and Related Stereoelectronic Effects at Oxygen*, Springer-Verlag, 1983
E. Jurasti, G. Cuevas, *The Anomeric Effect, CRC Press*, 1995

Do the following valence bond resonance structures have meaning?

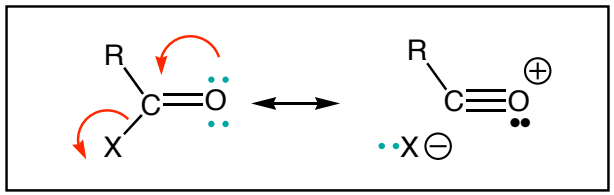

Prediction: As X becomes more electronegative, the IR frequency should increase

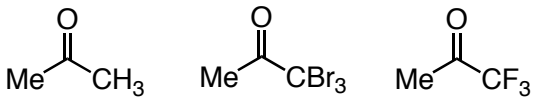

$\upsilon_{C=O}$ (cm^{-1})	1720	1750	1780

Prediction: As the indicated pi-bonding increases, the X–C–O bond angle should decrease. This distortion improves overlap.

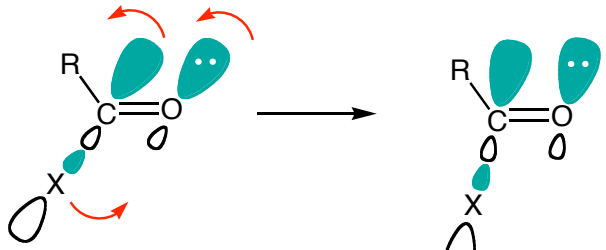

σ* C–X →O lone pair

Evidence for this distortion has been obtained by X-ray crystallography

Corey, *Tetrahedron Lett.* **1992**, *33*, 7103-7106

Aldehyde C–H Infrared Stretching Frequencies

Prediction: The IR C–H stretching frequency for aldehydes is lower than the closely related olefin C–H stretching frequency. For years this observation has gone unexplained.

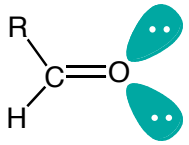

ν C–H = 2730 cm^{-1}

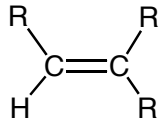

ν C–H = 3050 cm^{-1}

Sigma conjugation of the lone pair anti to the H will weaken the bond. This will result in a low frequency shift.

Infrared evidence for lone pair delocalization into vicinal antibonding orbitals.

The N–H stretching frequency of cis-methyl diazene is 200 cm^{-1} lower than the trans isomer.

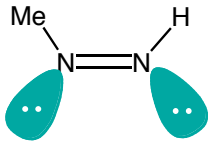

ν N–H = 2188 cm^{-1}

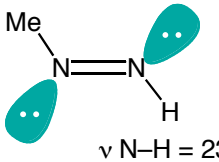

ν N–H = 2317 cm^{-1}

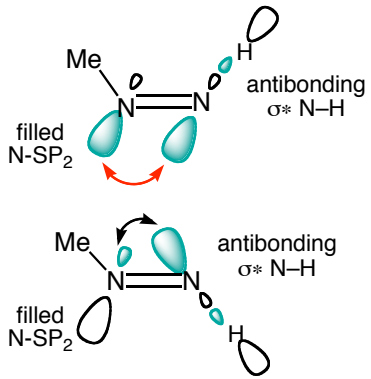

■ The low-frequency shift of the cis isomer is a result of N–H bond weakening due to the anti lone pair on the adjacent (vicinal) nitrogen which is interacting with the N–H antibonding orbital. Note that the orbital overlap is not nearly as good from the trans isomer.

N. C. Craig & co-workers *JACS* **1979**, *101*, 2480.

Observation: C–H bonds anti-periplanar to nitrogen lone pairs are spectroscopically distinct from their equatorial C–H bond counterparts

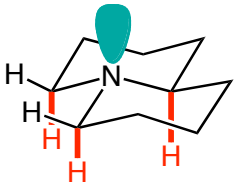

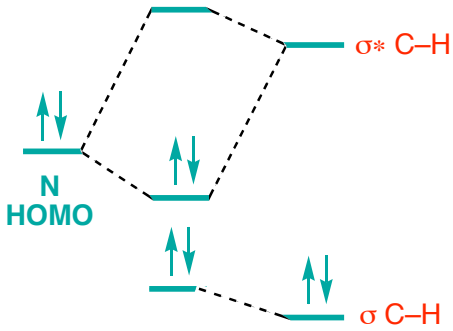

Spectroscopic Evidence for Conjugation

Infrared Bohlmann Bands

Characteristic bands in the IR between 2700 and 2800 cm^{-1} for C-H_4, C-H_6 , & C-H_{10} stretch

Bohlmann, *Ber.* **1958** *91* 2157

Reviews: McKean, *Chem Soc. Rev.* **1978** *7* 399
L. J. Bellamy, D. W. Mayo, *J. Phys. Chem.* **1976** *80* 1271

NMR : Shielding of H antiperiplanar to N lone pair

H_{10} (axial): shifted furthest upfield
H_6, H_4: $\Delta\delta = \delta H_{axial} - \delta H_{equatorial} = -0.93$ ppm
Protonation on nitrogen reduces $\Delta\delta$ to -0.5ppm

H. P. Hamlow et. al., *Tet. Lett.* **1964** 2553
J. B. Lambert et. al., *JACS* **1967** *89* 3761

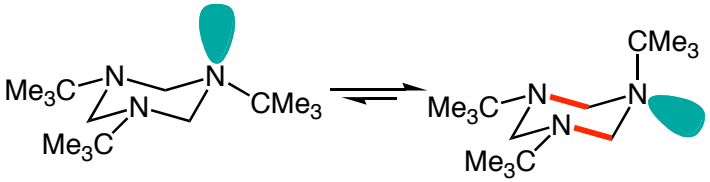

$\Delta G° = -0.35$kcal/mol

A. R. Katritzky et. al., *J. Chemm. Soc. B* **1970** 135

Favored Solution Structure (NMR)

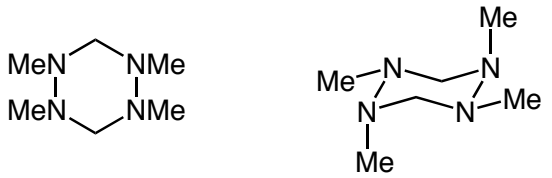

J. E. Anderson, J. D. Roberts, *JACS* **1967** *96* 4186

B Favored Solid State Structure (X-ray crystallography)

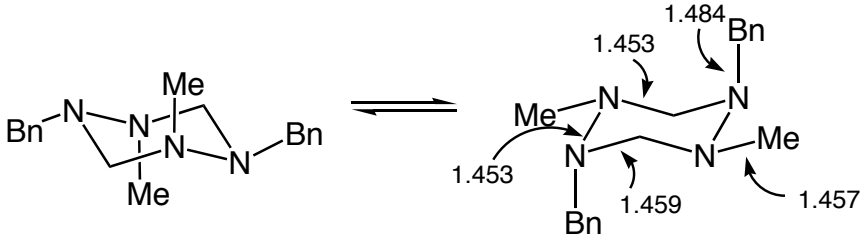

A **B**

Rationalize why **B** might be more stable than **A**.

A. R. Katrizky et. al., *J. C. S. Perkin II* **1980** 1733

■ **Conformations:** There are 2 planar conformations.

(Z) Conformer 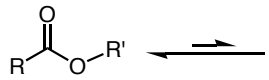 **(E) Conformer**

Specific Case: Methyl Formate 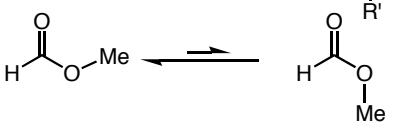 ΔG° = +4.8 kcal/mol

The (E) conformation of both acids and esters is less stable by 3-5 kcal/mol. If this equilibrium were governed only by steric effects one would predict that the (E) conformation of formic acid would be more stable (H smaller than =O). Since this is not the case, there are electronic effects which must also be considered. These effects will be introduced shortly.

■ **Rotational Barriers:** There is hindered rotation about the =C–OR bond.

These resonance structures suggest hindered rotation about =C–OR bond. This is indeed observed:

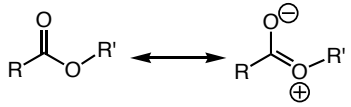

Rotational barriers are ~ 10-12 kcal/mol. This is a measure of the strength of the pi bond.

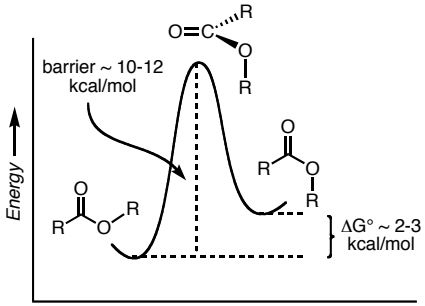

■ **Lone Pair Conjugation:** The oxygen lone pairs conjugate with the C=O.

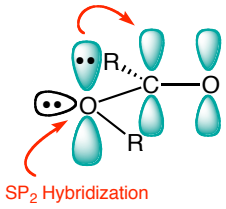

The filled oxygen p-orbital interacts with pi (and pi*) C=O to form a 3-centered 4-electron bonding system.

■ **Oxygen Hybridization:** Note that the alkyl oxygen is Sp2. Rehybridization is driven by system to optimize pi-bonding.

■ **Hyperconjugation:** Let us now focus on the oxygen lone pair in the hybrid orbital lying in the sigma framework of the C=O plane.

(Z) Conformer

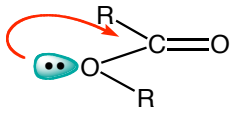

In the (Z) conformation this lone pair is aligned to overlap with σ* C–O.

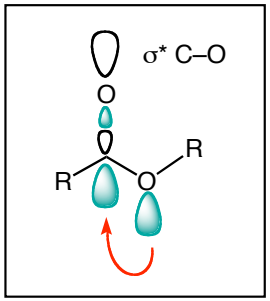

(E) Conformer

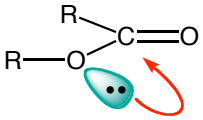

In the (E) conformation this lone pair is aligned to overlap with σ* C–R.

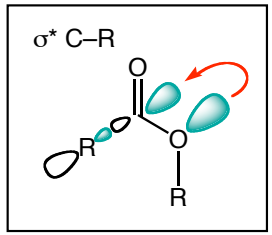

Since σ* C–O is a better acceptor than σ* C–R (where R is a carbon substituent) it follows that the (Z) conformation is stabilized by this interaction.

Esters versus Lactones: Questions to Ponder.

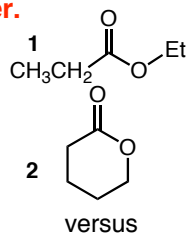

Esters strongly prefer to adopt the (Z) conformation while small-ring lactones such as **2** are constrained to exist in the (Z) conformation. From the preceding discussion explain the following:

1) Lactone **2** is significantly more susceptible to nucleophilic attack at the carbonyl carbon than **1**? Explain.

2) Lactone **2** is significantly more prone to enolization than **1**? In fact the pKa of **2** is ~25 while ester **1** is ~30 (DMSO). Explain.

3) In 1985 Burgi, on carefully studying the X-ray structures of a number of lactones, noted that the O-C-C (α) & O-C-O (β) bond angles were not equal. Explain the indicated trend in bond angle changes.

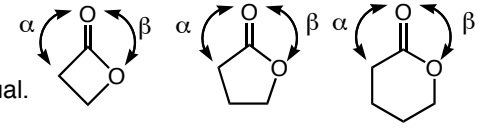

α–β = 12.3 ° α–β = 6.9 ° α–β = 4.5 °

Calculated Structure of ACG–TGC Duplex

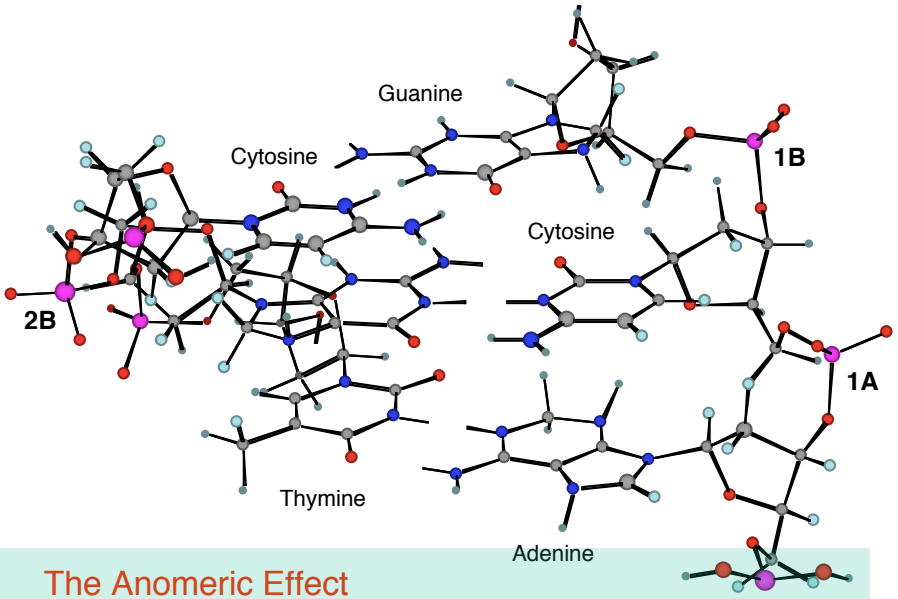

The Anomeric Effect

Acceptor orbital hierarchy: δ^* P–OR * > δ^* P–O$^-$

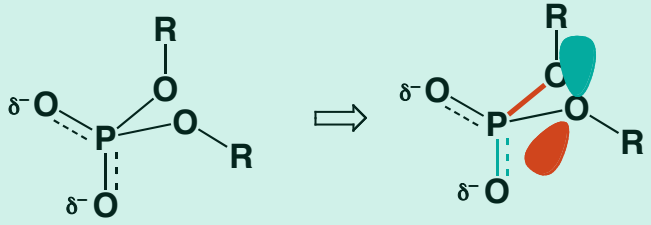

Gauche-Gauche conformation

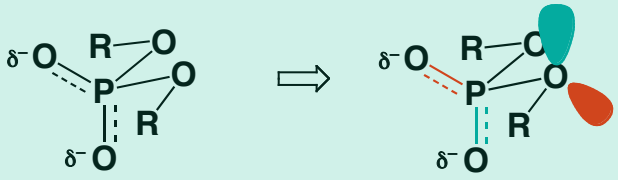

Anti-Anti conformation

Gauche-Gauche conformation affords a better donor-acceptor relationship

The Phospho-Diesters Excised from Crystal Structure

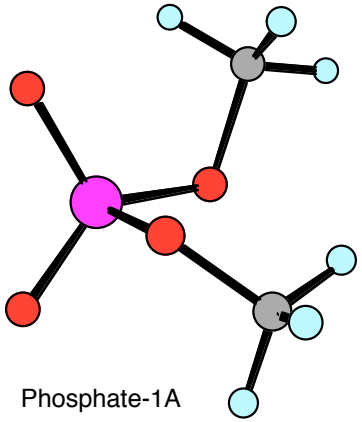

Phosphate-1A

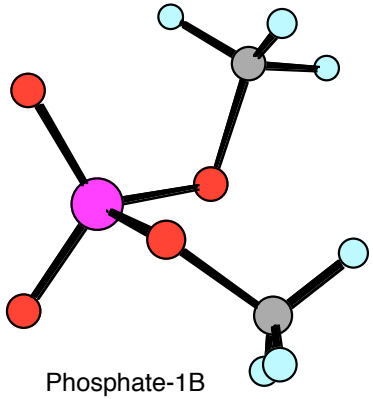

Phosphate-1B

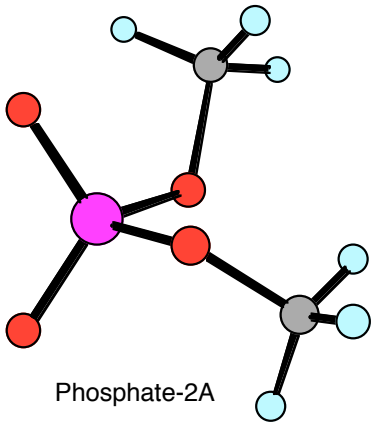

Phosphate-2A

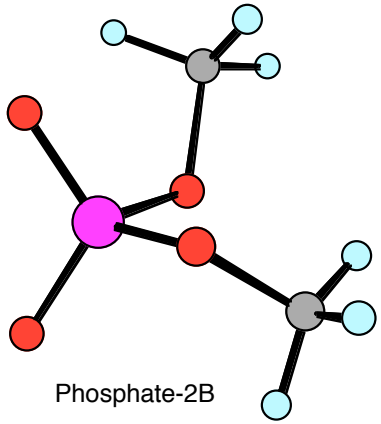

Phosphate-2B

Oxygen lone pairs may establish a simultaneous hyperconjugative relationship with both acceptor orbitals only in the illustrated conformation.

Plavec, et al. (**1996**). "How do the Energetics of the Stereoelectronic Gauche & Anomeric Effects Modulate the Conformation of Nucleos(t)ides? " Pure Appl. Chem. **68**: 2137-44.

The General Reaction:

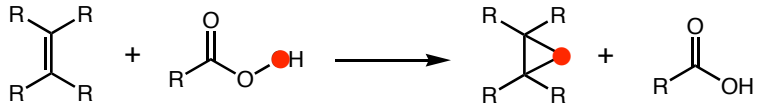

HOMO $\pi C–C$ | LUMO $\sigma^*O–O$

note labeled oxygen is transferfed

O-O bond energy: ~35 kcal/mol

HOMO–LUMO Interactions for Peracid Epoxidation

Since 2 C–O bonds are formed in the epoxidation reaction, there are two HOMO–LUMO pairs that should be considered. They are illustrated below.

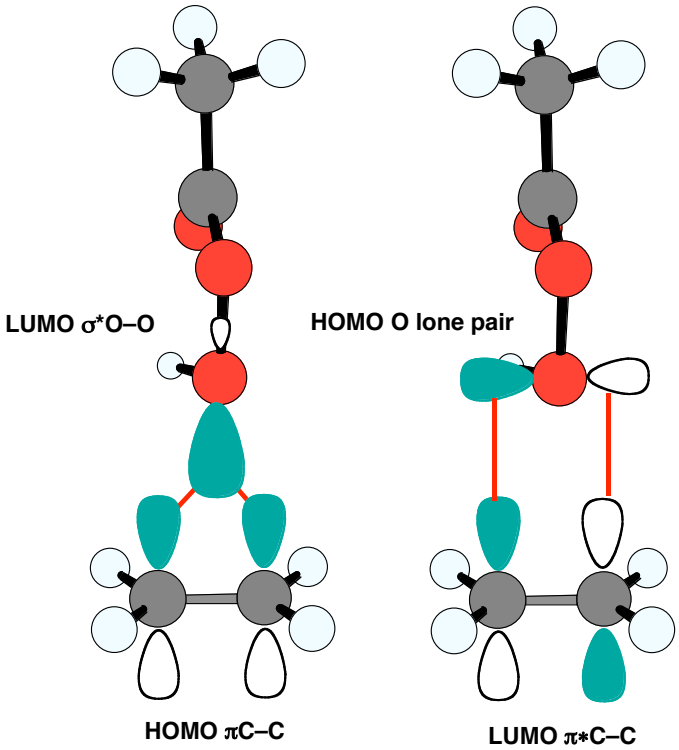

The transition state:

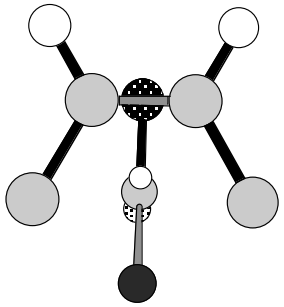

View from below olefin

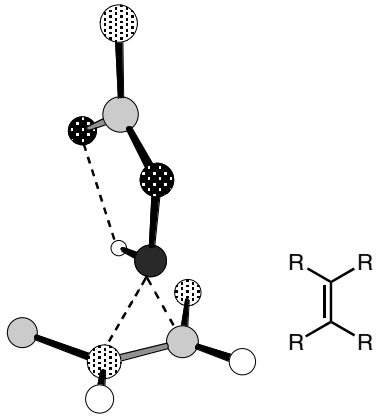

Reaction rates are governed by olefin nucleophilicity. The rates of epoxidation of the indicated olefin relative to cyclohexene are provided below:

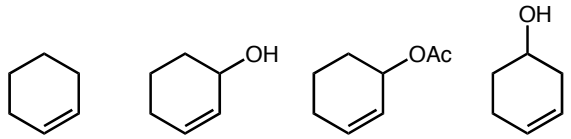

1.0 | 0.6 | 0.05 | 0.4

The indicated olefin in each of the diolefinic substrates may be oxidized selectively.

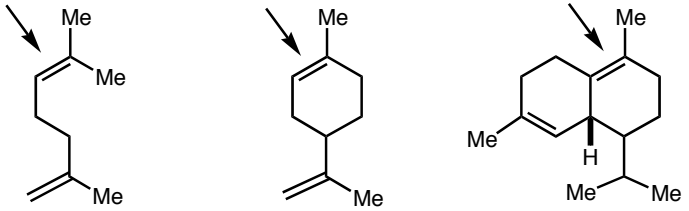

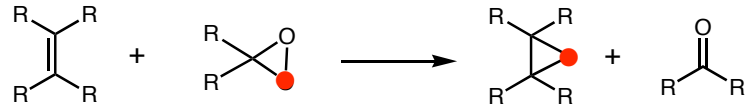

HOMO1
πC–C
LUMO2
π*C–C

LUMO1
σ*O–O
HOMO2
O lone pr

note labeled oxygen is transferfed

O-O bond energy: ~35 kcal/mol

Transition State for the Dioxirane Mediated Olefin Epoxidation

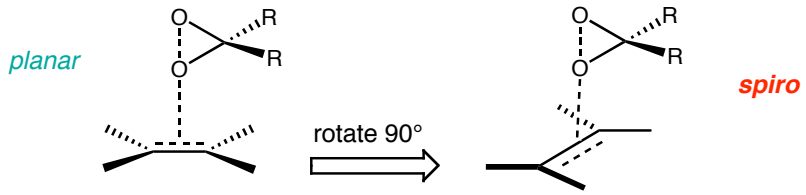

stabilizing $O_{lp} \rightarrow \pi^*$ C=C
cis olefins react ~10 times faster than *trans*

Houk, *JACS*, **1997**, 12982.

■ Synthesis of the Dioxirane Oxidant

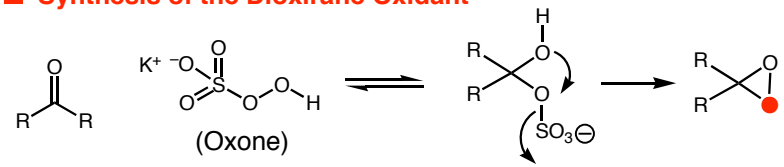

Synthetically Useful Dioxirane Synthesis

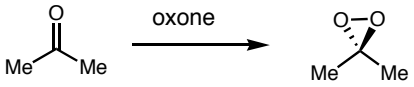

co-distill to give ~0.1 M soln of dioxirane in acetone

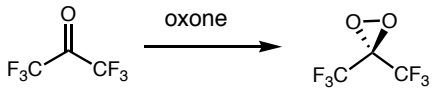

co-distill to give ~0.6 M soln of dioxirane in hexafluoroacetone

Asymmetric Epoxidation with Chiral Ketones

Review: Frohn & Shi, *Syn Lett* **2000**, 1979-2000 **(PDF)**

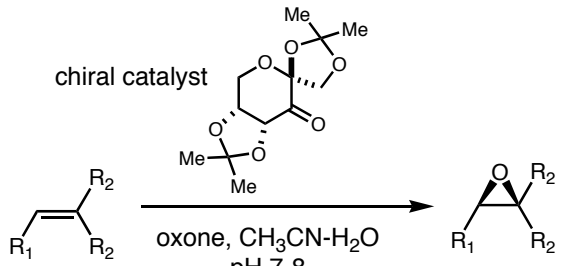

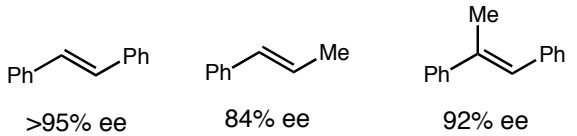

>95% ee | 84% ee | 92% ee

Question: First hour Exam 2000 (Database Problem 34)

Question 4. (15 points). The useful epoxidation reagent dimethyldioxirane (**1**) may be prepared from "oxone" (KO_3SOOH) and acetone (eq 1). In an extension of this epoxidation concept, Shi has described a family of chiral fructose-derived ketones such as **2** that, in the presence of "oxone", mediate the asymmetric epoxidation of di- and tri-substituted olefins with excellent enantioselectivities (>90% ee) (*JACS* **1997**, *119*, 11224).

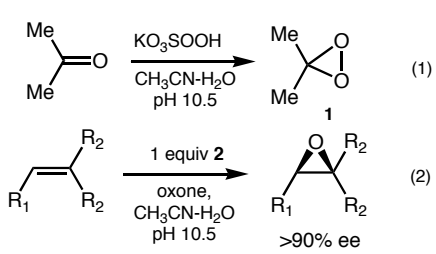

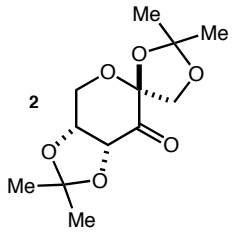

Part A (8 points). Provide a mechanism for the epoxidation of ethylene with dimethyldioxirane (**1**). Use three-dimensional representations, where relevant, to illustrate the ***relative*** stereochemical aspects of the oxygen transfer step. Clearly identify the frontier orbitals involved in the epoxidation.

Part B (7 points). Now superimpose chiral ketone **2** on to your mechanism proposed above and rationalize the sense of asymmetric induction of the epoxidation of trisubstituted olefins (eq 2). Use three-dimensional representations, where relevant, to illustrate the ***absolute*** stereochemical aspects of the oxygen transfer step.

Let R_L and R_S be Sterically large and small substituents.

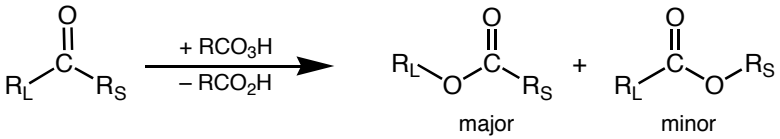

The major product is that wherein oxygen has been inserted into the R_L–C=O bond.

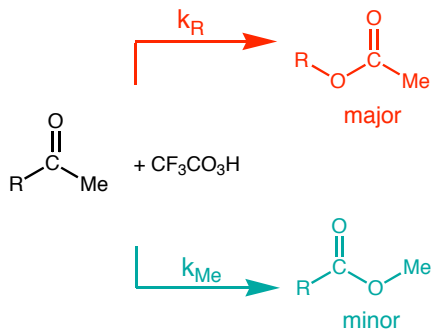

R	k_R / K_{Me}
CH_3CH_2	72
$CH_3(CH_2)_2$	150
$(CH_3)_3C$	830
$PhCH_2$	>2000

The Intermediate

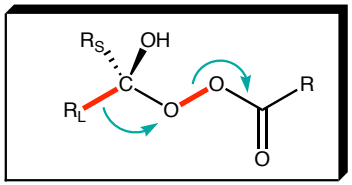

The important stereoelectronic components to this rearrangement:

1. The R_L–C–O–O dihedral angle must be180° due to the HOMO LUMO interaction σ-R_L–C with σ*–O–O.

2. The C–O–O–C' dihedral angle will be ca. 60° due to the gauche effect (O-lone pairsσ*–C–O).

This gauche geometry is probably reinforced by intramolecular hydrogen bonding as illustrated on the opposite page:

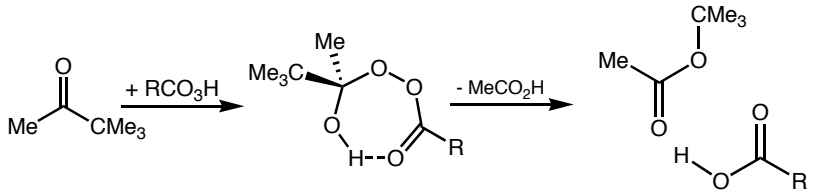

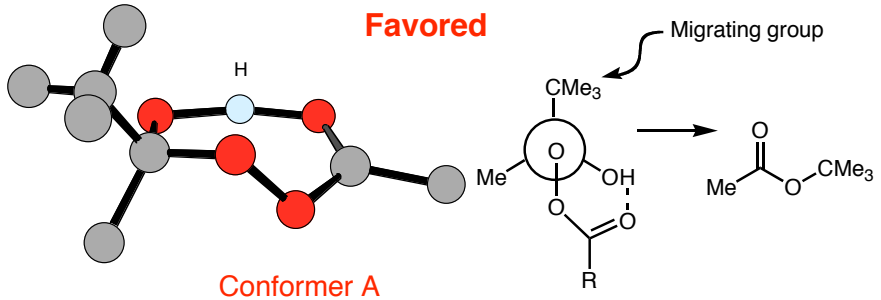

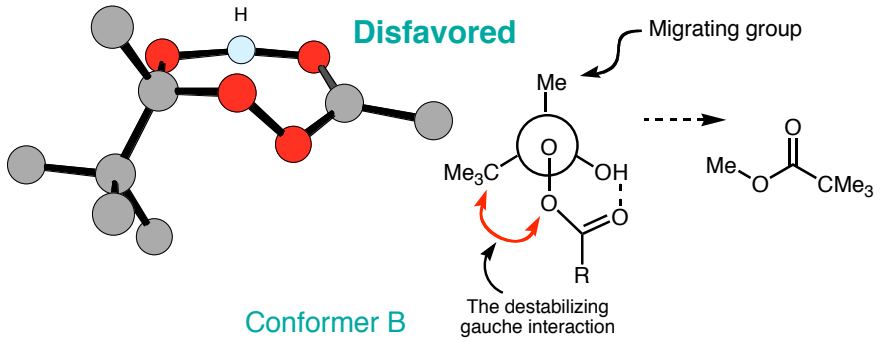

Steric effects destabilize Conformer B relative to Conformer A; hence, the reaction is thought to proceed via a transition state similar to A.

For relevant papers see:
Crudden, *Angew. Chem. Int. Ed* **2000**, *39*, 2852-2855 **(pdf)**
Kishi, *JACS* **1998**, *120*, 9392 **(pdf)**

http://www.courses.fas.harvard.edu/colgsas/1063

Chemistry 206

Advanced Organic Chemistry

Lecture Number 3

Stereoelectronic Effects-3

- The S_N2 Reaction: Stereoelectronic Effects
- Baldwin's Rules for Ring Closure

Read Kirby, Chapter 5, Cary & Sundberg, Chapter 5

Useful LIterature Reviews

Johnson, C. D. (**1993**). "Stereoelectronic effects in the formation of 5- and 6-membered rings: the role of Baldwin's rules." *Acc. Chem. Res.* **26**: 476-82. **(Pdf)**

Beak, P. (**1992**). "Determinations of transition-state geometries by the endocyclic restriction test: mechanisms of substitution at nonstereogenic atoms." *Acc. Chem. Res.* **25**: 215. **(Pdf)**

D. A. Evans

Friday,
September 22, 2006

"Rules for Ring Closure: Baldwin's Rules"

Sir Jack Baldwin

The Primary Literature

Baldwin, *J. Chem. Soc., Chem. Comm.* **1976**, 734, 736.

Baldwin, *J. Chem. Soc., Chem. Comm.* **1977** 233.

Baldwin, *J. Org. Chem.* **1977**, *42*, 3846.

Baldwin, *Tetrahedron* **1982**, *38*, 2939.

Problem 689. Predict the product of the reaction below. Include a rationalization based on a detailed analysis of competing transition state geometries.

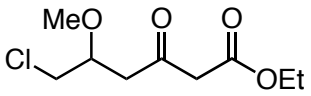

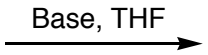

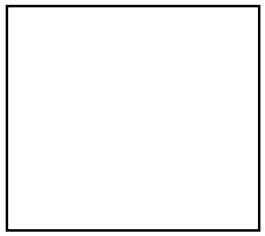

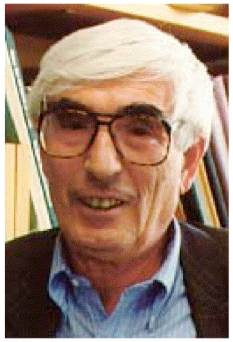

Eidgenössische Technische Hochschule Zürich

Eidgenössische Technische Hochschule Zürich

Prof. Dr. Jack D. Dunitz
Laboratory of Organic Chemistry
ETH Hoenggerberg, HCI
CH-8093 Zürich, Switzerland

Jack Dunitz (1923) studied chemistry at Glasgow University, (Ph.D. 1947) and held research fellowship at Oxford University (1946-1948, 1951-1953), the California Institute of Technology (1948-1951, 1953-1954), the U.S. National Institute of Health, Bethesda MD (1954-1955), and the Royal Institution, London (1956-1957), before taking up a professorship at the ETH-Zürich, a post that he held until his retirement in 1990. He has held Visiting Professorships in the United States, Israel, Japan and the United Kingdom, has been elected to membership of several learned societies, and has received several awards for his work. He has written more than 300 scientific papers.

Prof. Erick Carreira

Erick M. Carreira was born in Havana, Cuba in 1963. He obtained a B.S. degree in 1984 from the Univ. of Illinois at Urbana–Champaign under the supervision of Scott E. Denmark and a Ph.D. degree in 1990 from Harvard University under the supervision of David A. Evans. After carrying out postdoctoral work with Peter Dervan at the California Institute of Technology through late 1992, he joined the faculty at the same institution as an assistant professor of chemistry and subsequently was promoted to the rank of associate professor of chemistry in the Spring of 1996, and full professor in Spring 1997. Since September 1998, he has been full professor of Organic Chemistry at the ETH Zürich.

Eidgenössische Technische Hochschule Zürich

Eidgenössische Technische Hochschule Zürich

Prof. Dr. Albert Eschenmoser
Laboratory of Organic Chemistry
ETH Hoenggerberg, HCI
CH-8093 Zürich, Switzerland

Albert Eschenmoser has been Professor Emeritus at ETH Zurich since 1992.

He was born in Erstfeld (Uri), Switzerland, on August 5, 1925 and received his Dipl.sc.nat. in 1949 and his D.Sci. in 1951 from the Swiss Federal Institute of Technology (ETH), where he became private lecturer in Organic Chemistry in 1956, associate professor in 1960, and full professor for General Organic Chemistry in 1965. In his research in organic and bioorganic chemistry, Eschenmoser has made contributions to theory of terpene biosynthesis, structure elucidation of natural products, stereochemistry and mechanism of organochemical and biochemical reactions, development of new methods for organic synthesis, total synthesis of complex natural products and chemical etiology of nucleic acid structure. Eschenmoser is a member of the German Academy Leopoldina (Halle), Academia Europaea (UK) and the Pontifical Academy (Vatican), a foreign member of the American Academy of Arts and Sciences (Boston), the National Academy of Sciences (Washington), the Royal Society (UK), the Academy of Science in Göttingen, the Croatian Academy of Sciences and Arts (Zagreb), the orden Pour le mérite für Wissenschaften und Künste (Berlin), and the Österreichisches Ehrenzeichen für Wissenschaft und Kunst (Wien), he is a honorary member of the Royal Society of Chemistry (London), Gesellschaft Österreichischer Chemiker (Wien), and the Pharmaceutical Society of Japan. He holds honorary degrees from the Universities of Fribourg, Chicago, Edinburgh, Bologna, Frankfurt, Strasbourg, Harvard, and from The Scripps Research Institute.

Consider the linear combination of three atomic orbitals. The resulting molecular orbitals (MOs) usually consist of one bonding, one nonbonding and one antibonding MO.

Case 1: 3 p-Orbitals

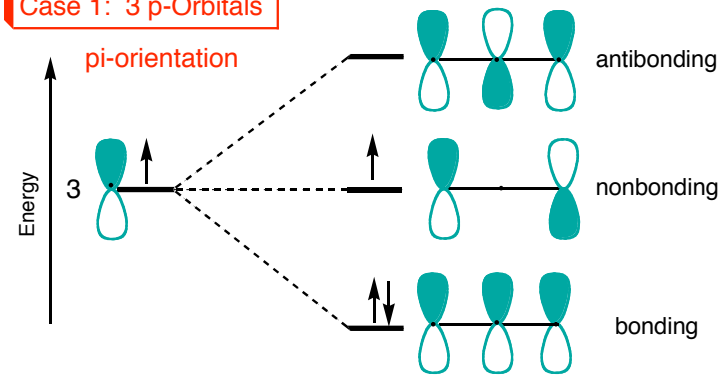

Note that the more nodes there are in the wave function, the higher its energy.

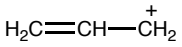

Allyl carbonium ion: both pi-electrons in bonding state

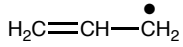

Allyl Radical: 2 electrons in bonding obital plus one in nonbonding MO.

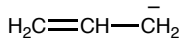

Allyl Carbanion: 2 electrons in bonding obital plus 2 in nonbonding MO.

Case 2: 3 p-Orbitals

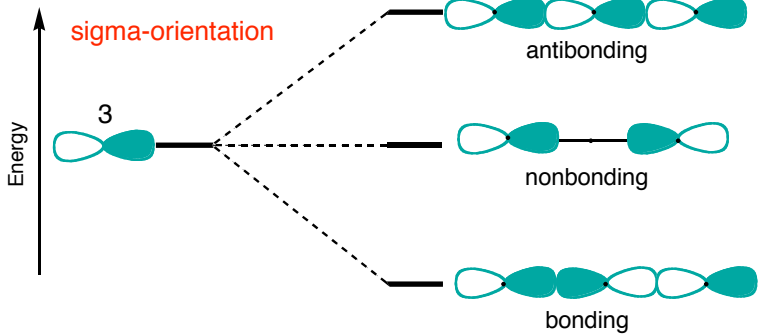

Case 3: 2 p-Orbitals; 1 s-orbital

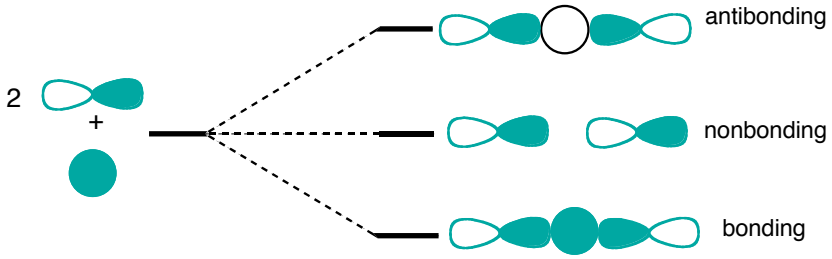

Case 4: 2 s-Orbitals; 1 p-orbital

Do this as an exercise

Examples of three-center bonds in organic chemistry

A. H-bonds: (3–center, 4–electron)

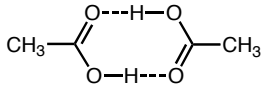

The acetic acid dimer is stabilized by ca 15 kcal/mol

B. H-B-H bonds: (3-center, 2 electron)

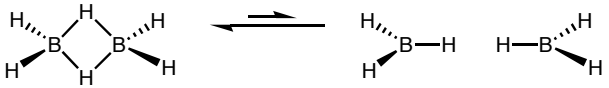

diborane stabilized by 35 kcal/mol

C. The S_N2 Transition state: (3–center, 4–electron)

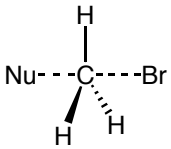

The S_N2 transition state approximates a case 2 situation with a central carbon p-orbital

The three orbitals in reactant molecules used are:
1 nonbonding MO from Nucleophile (2 electrons)
1 bonding MO σ C–Br (2 electrons)
1 antibonding MO σ^* C–Br

Why do S_N2 Rxns proceed with backside displacement?

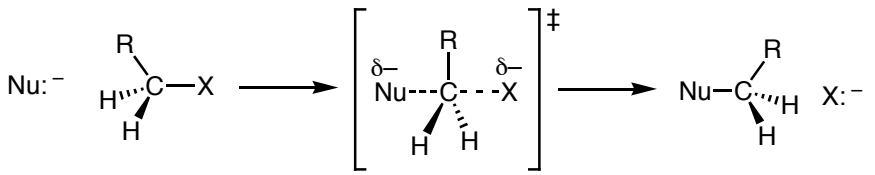

Given the fact that the LUMO on the electrophile is the C–X antibonding orblital, Nucleophilic attack could occur with either inversion or retention.

Inversion

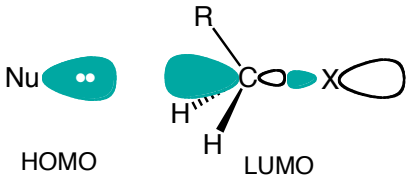

Constructive overlap between Nu & σ*C–X

Retention

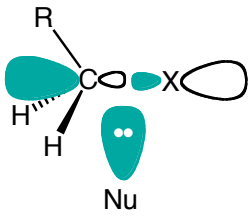

Overlap from this geometry results in no net bonding interaction

Expanded view of σ*C–X

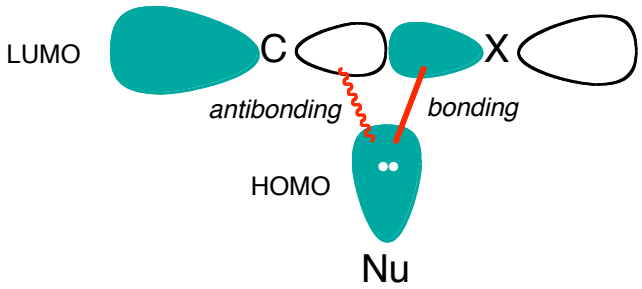

Fleming, page 75-76

Electrophilic substitution at saturated carbon may occur with either inversion of retention

Inversion

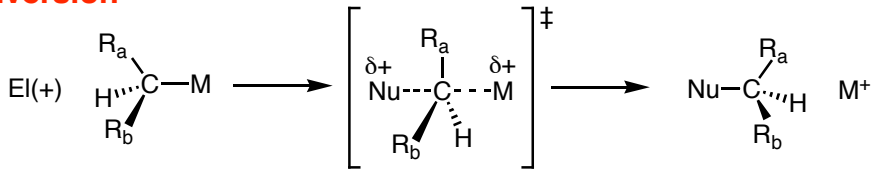

Retention

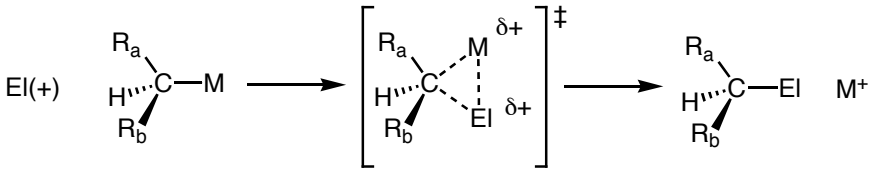

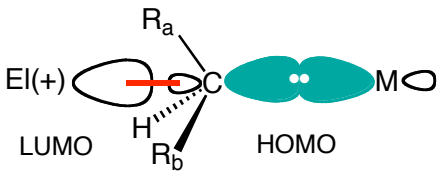

Inversion

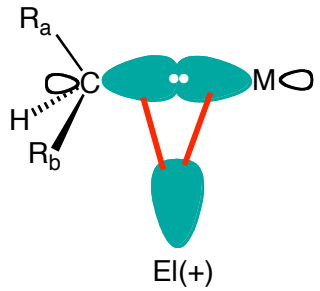

Retention

Examples

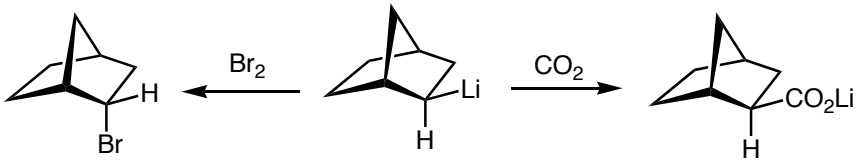

predominant inversion *predominant retention*

Stereochemistry frequently determined by electrophile structure

See A. Basu, *Angew. Chem. Int. Ed.* **2002**, *41*, 717-738 **(PDF)**

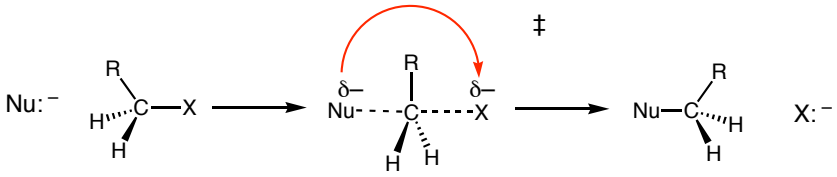

What is the absolute requirement for the Nu–C–X bond angle??
180° +/– ??

Eschenmoser: Tether Nu and X

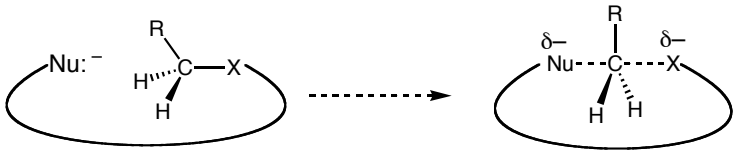

"tethered reactants" "constrained transition state"

Eschenmoser, *Helv. Chim Acta* **1970**, *53*, 2059 **(PDF)**

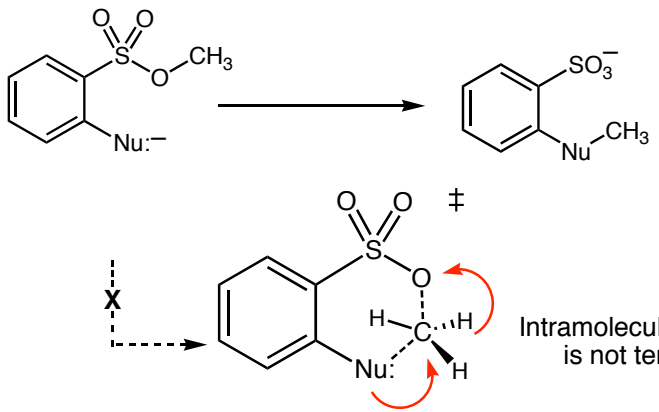

Intramolecular option is not tenable

The reaction illustrated above proceeds exclusively through bimolecular pathway in contrast to the apparent availability of the intramolecular path.

Related Cases: " The Endocyclic Restriction Test"

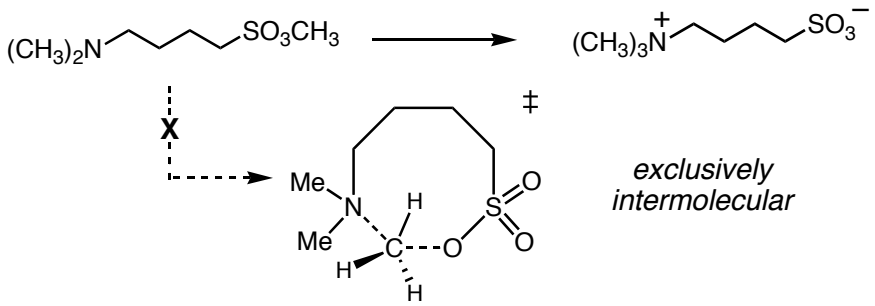

exclusively intermolecular

King, et al. **1982** *Chem Commun.* 175
King, et al. **1982** *Tetrahedron Lett. 23, 4465*

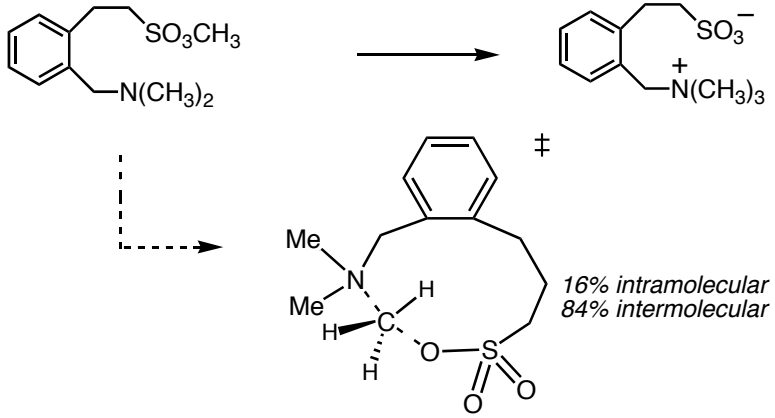

16% intramolecular
84% intermolecular

10-membered transition structure

Hence, the Nu–C–X 180 ° transition state bond angle must be rigidly maintained for the reaction to take place.

"Determinations of transition-state geometries by the endocyclic restriction test: mechanisms of substitution at nonstereogenic atoms",
Peter Beak,
Acc. Chem. Res.; **1992** *25*, 215-222 **(PDF)**

Ring Closure and Stereoelectronic Considerations
An Examination of Baldwin's Rules

"Baldwin's Rules" provides a qualitative set of generalizations on the probability of a given ring closure.

There are circumstances where the "rules" don't apply.

- They do not apply to non-first-row elements participating in the cyclization event. The longer bond lengths and larger atomic radii of 2nd row elements result in relaxed geometrical constraints.

For example, a change in a heteroatom from O to S could result in relaxation of a given geometric constraint.

X = O vs S

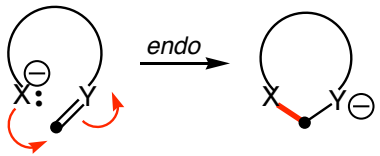

- The "rules" do not apply to electrocyclic processes.

Nomenclature

Classes of Ring Closing Processes

A. Exo-cyclization modes identified by the breaking bond being positioned exocyclic to the forming cycle.

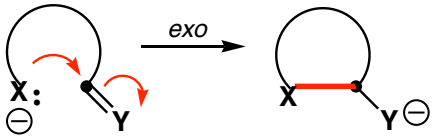

B. Endo-cyclization modes identified by the breaking bond being positioned endocyclic to the forming cycle.

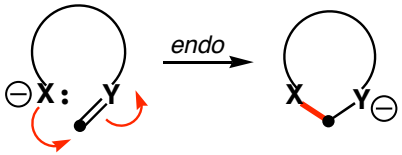

X = first-row element
N, O

C. Nucleophilic ring closures sub-classified according to hybridization state of **electrophilic** component:
(tetrahedral = tet; trigonal = trig; digonal = dig)

D. Nucleophilic ring closures further subclassified according to size of the fomed ring. For example:

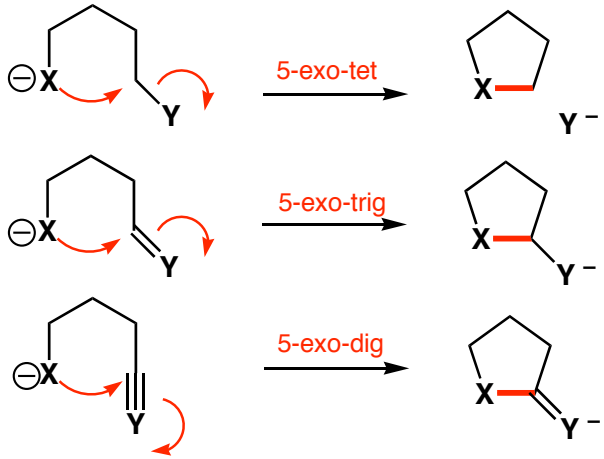

Required trajectories (Baldwin):

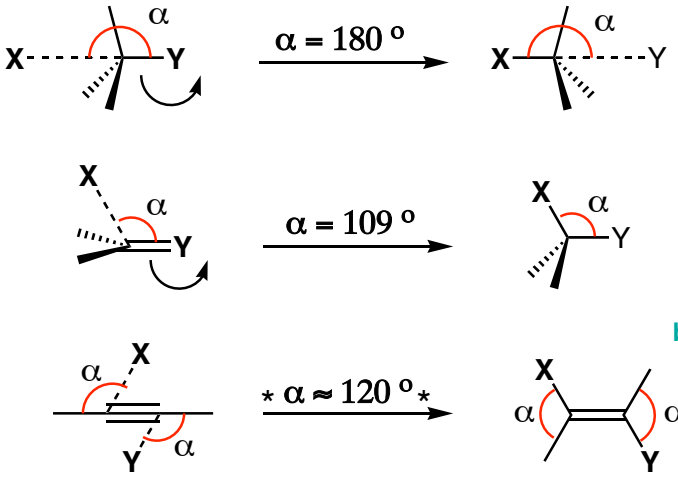

Will come back to this case later

Baldwin, *J. Chem. Soc., Chem. Commun.*, **1976**, 734.

Tetrahedral Carbon

All exo cyclization modes are allowed: (n-exo-tet, n = 3→)

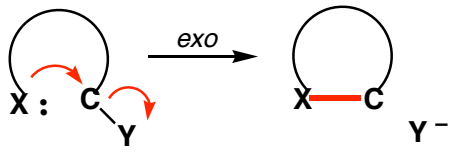

There are stereoelectronic issues to consider for **n-exo-tet** cyclizations

Formation of 3-Membered Rings (3-exo-tet)

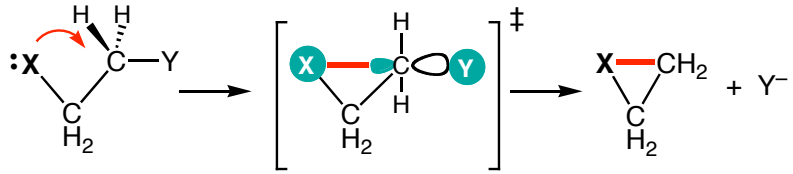

Conformational Effects in Epoxide Ring Formation/cleavage

Those stereoelectronic effects that operate in ring cleavage also influence ring formation. Consider a rigid cyclohexene oxide system:

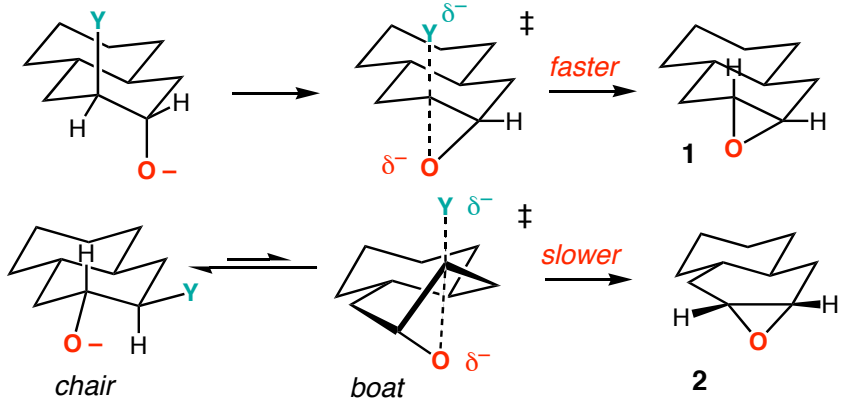

FÜRST-PLATTNER RULE

In this simple model, the transition-state leading to **1** involves the diaxial orientation of nucleophile and leaving group. This orientation affords the best overlap of the anti-bonding C–Y orbital and the nonbonding electron pairs on the nucleophile O$^-$.

In the formation of the diastereomeric epoxide **2**, the proper alignment of orbitals may only be achieved by cyclization through the less-favored boat conformer. Accordingly, while both cyclizations are "allowed", there are large rate differences the the rates of ring closure.

While the FÜRST-PLATTNER RULE deals wilth the microscopic reverse, in the opening of epoxides by nucleophiles, the stereoelectronic arguments are the same.

Stereoelectronic Effects in Epoxide Ring Cleavage

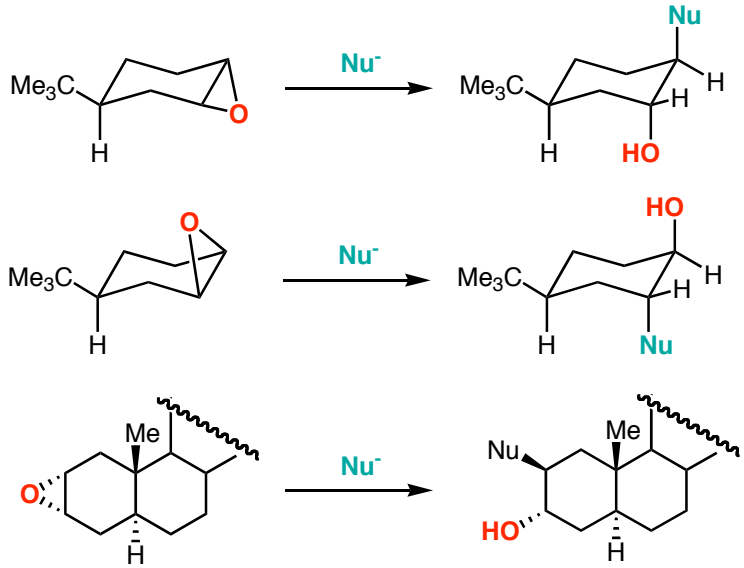

Tetrahedral Carbon

Endo cyclization modes that are disallowed (n-endo-tet, n = 3→~9)

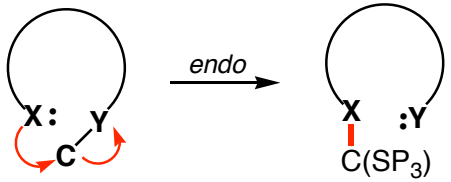

The stereoelectronic requirement for a 180° X–C–Y bond angle is only met when the endo cyclization ring size reaches 9 or 10 members.

Case 1: Eschenmoser, *Helvetica Chim. Acta* **1970**, *53*, 2059.

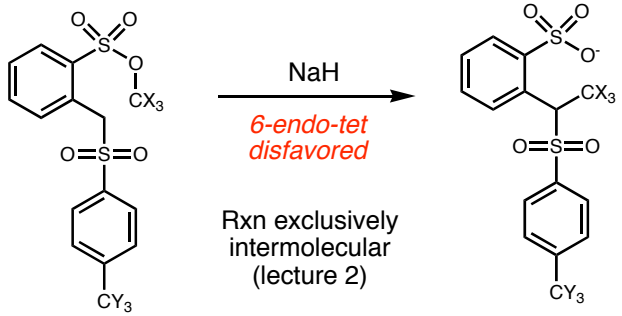

Cyclization exclusively intermolecular. However the exocyclic analog is exclusively intramolecular

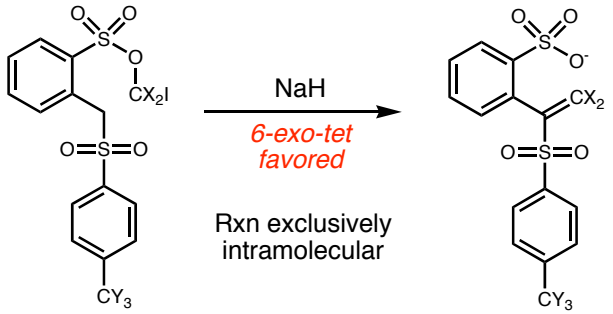

Case 2: King, *J.C.S. Chem. Comm.*, **1979**, 1140.

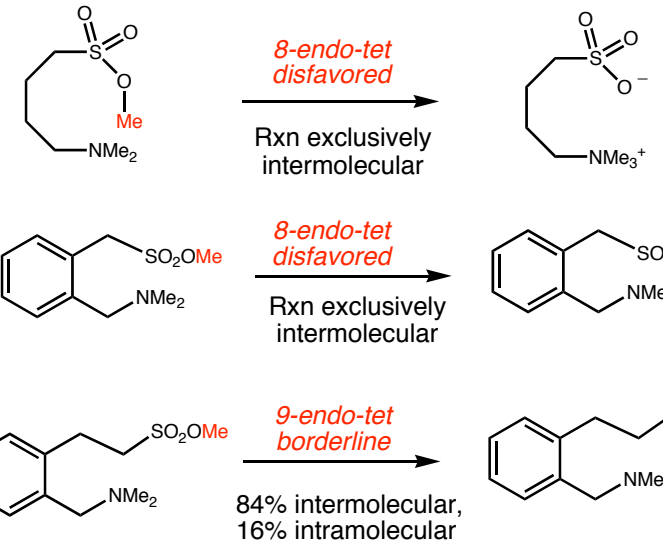

Conclusions

Allowed endo cyclization modes will require transition state ring sizes of at least nine members.

Intramolecular epoxidation has also been evaluated

Beak, *JACS* **1991**, *113*, 6281.

n = 1: rxn exclusively intermolecular
n = 9: rxn is intramolecular

Beak states that the conclusions made with carbon substitution also hold for oxygen atom transfer.

Beak, P. (**1992**). "Determinations of transition-state geometries by the endocyclic restriction test: mechanisms of substitution at nonstereogenic atoms." *Acc. Chem. Res.* **25**: 215.

The General Reaction:

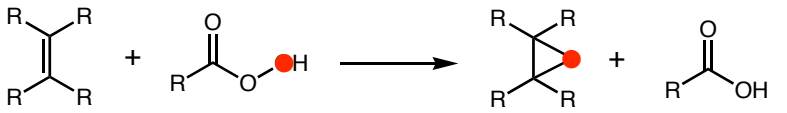

HOMO
πC–C

LUMO
σ*O–O

note labeled oxygen is transferfed

O-O bond energy: ~35 kcal/mol

The transition state:

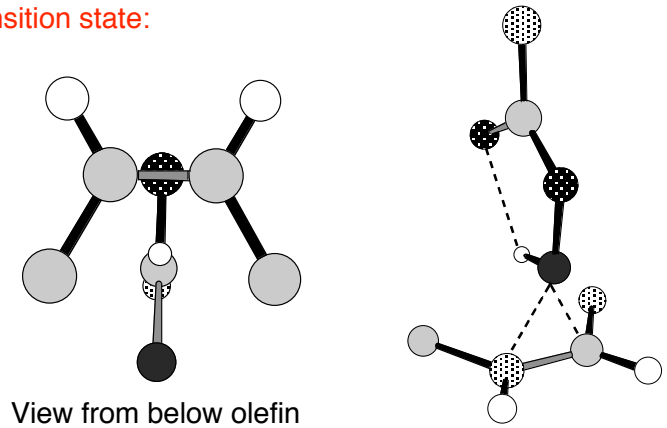

View from below olefin

Per-arachidonic acid Epoxidation

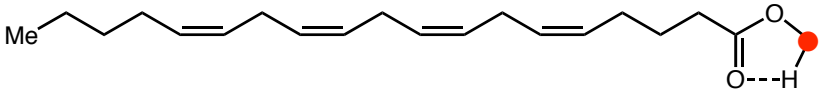

Which olefin is selectively epoxidized??

Per-arachidonic acid Epoxidation

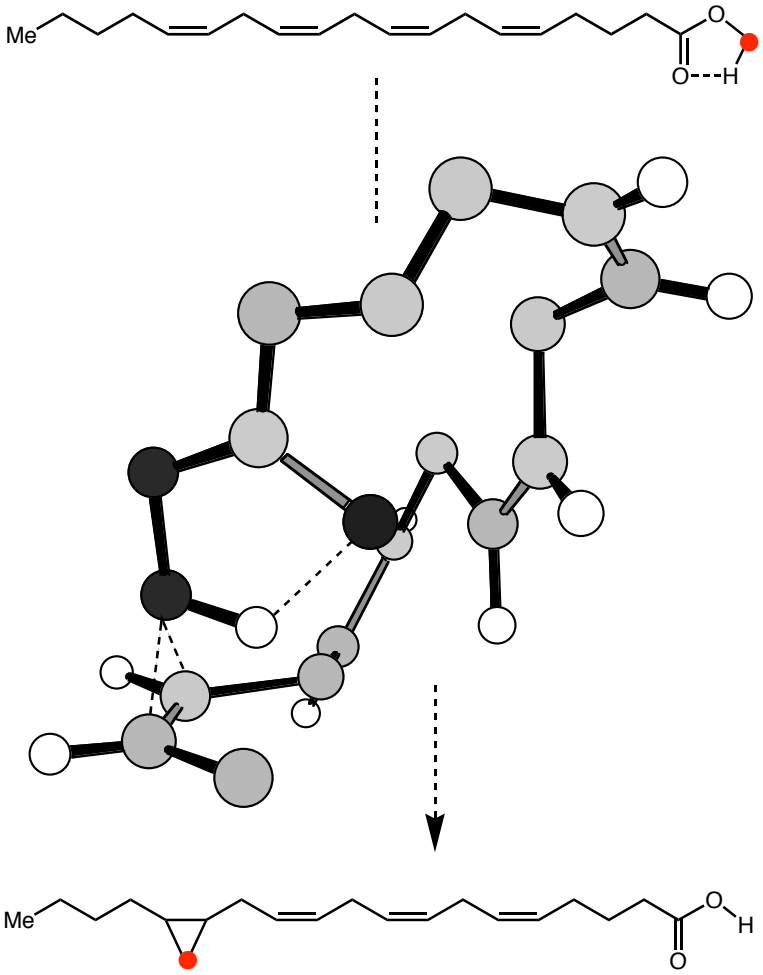

E. J. Corey, *JACS* **101**, 1586 (1979)

For a more detailed study see P. Beak, *JACS* **113**, 6281 (1991)

For theoretical studies of TS see R. D. Bach, *JACS* **1991**, *113*, 2338
R. D. Bach, *J. Org. Chem* **2000**, *65*, 6715

Rules for Ring Closure: SP3 Carbon Versus Silicon

Tetrahedral Silicon

All Endo-Tet cyclization modes are allowed

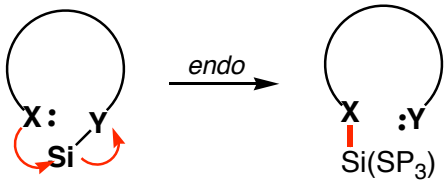

Silicon may readily proceed through a hypervalent intermediate.

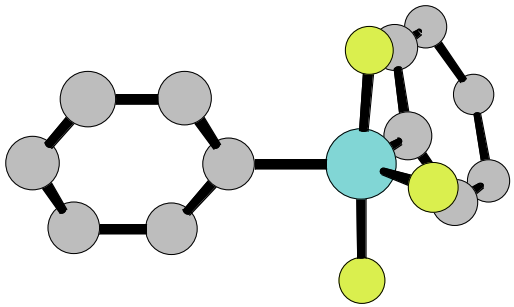

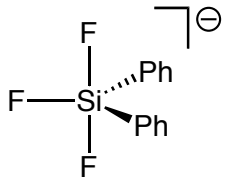

Inorg. Chem. **1984**, *23*, 1378

			5 **B** Boron 10.811	6 **C** Carbon 12.0107
		3S +P	13 **Al** Aluminum 26.981538	14 **Si** Silicon 28.0855
3D				
28 **Ni** Nickel 58.6934	29 **Cu** Copper 63.546	30 **Zn** Zinc 65.39	31 **Ga** Gallium 69.723	32 **Ge** Germanium 72.61

Brook Rearrangements

Explain what drives this rearrangement.

TBS = 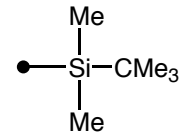

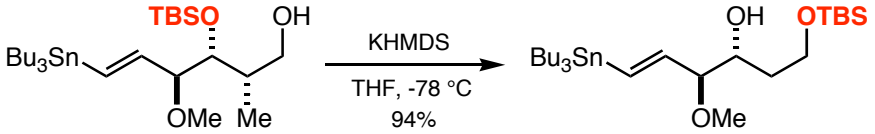

Calter, M. A. Ph. D. Thesis, Harvard University, 1993.

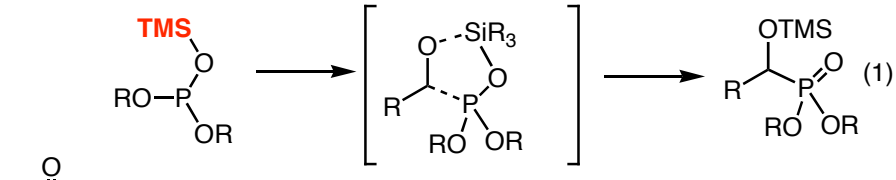

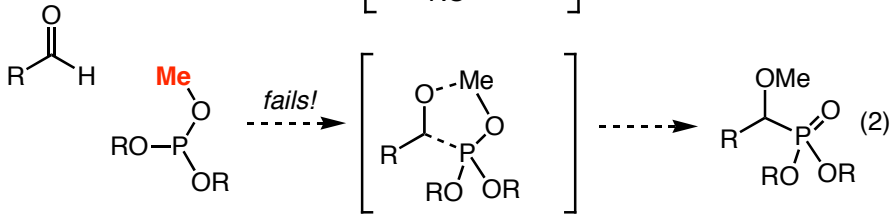

Moser, W. H. "The Brook Rearrangement in Tandem Bond Formation Strategies," *Tetrahedron* **2001**, *57*, 2065-2084

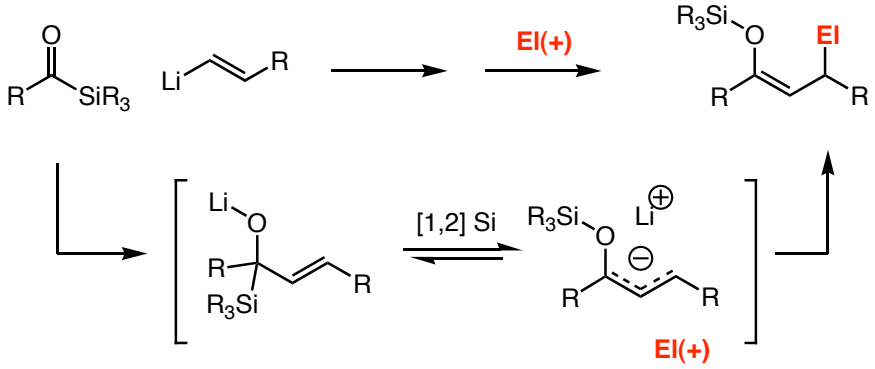

Trigonal Carbon

Endo cyclization modes that are disallowed (3 to 5-endo-trig)

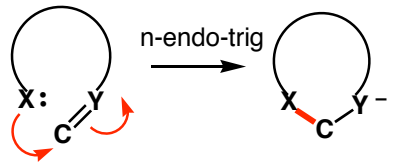

X = first-row element

The 5-endo-trig cyclization is a watershed case

Case 1: Baldwin, *J. Chem. Soc., Chem. Commun.*, **1976**, 734.

however

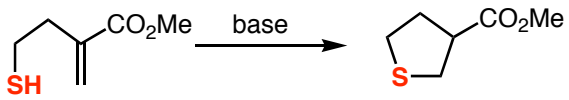

Second row atom relaxes the cyclization geometrical requirement

Case 2: Baldwin, *J. Chem. Soc., Chem. Commun.*, **1976**, 736.

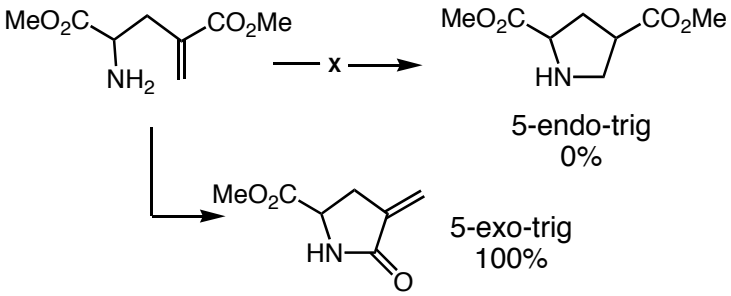

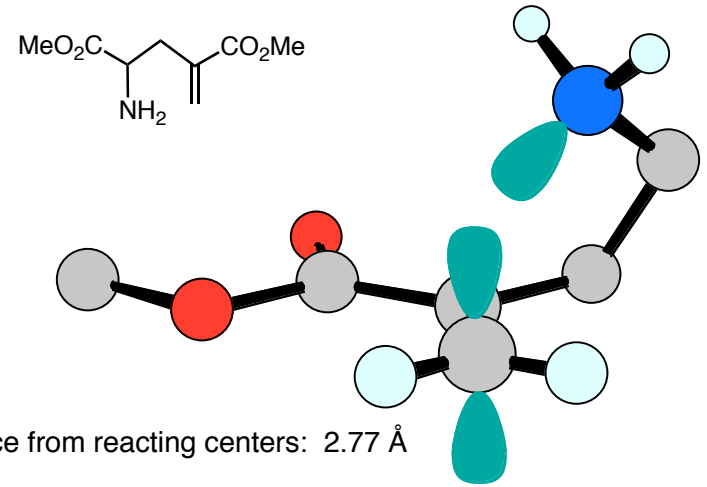

distance from reacting centers: 2.77 Å

It is possible that a "nonvertical" trajectory is operational like that suspected in C=O addition

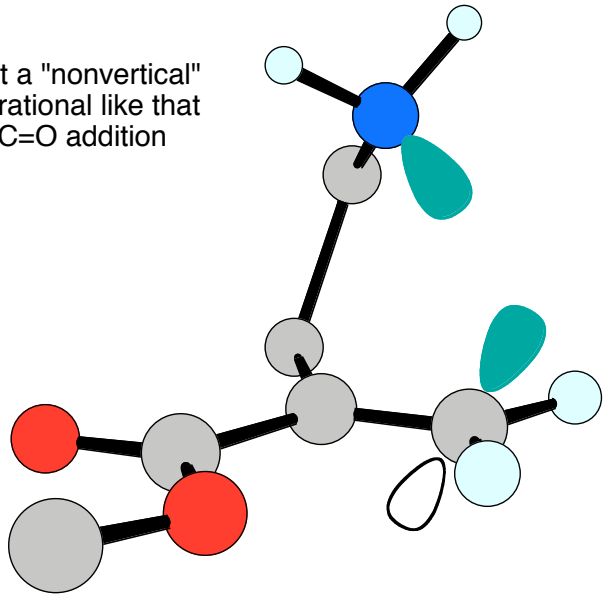

Rules for Ring Closure: SP^2 Carbon & Related Systems

Case 2: continued...

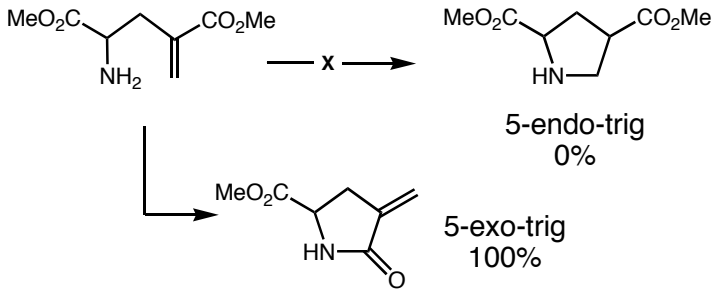

Control experiment: Intermolecular reaction favors conjugate addtion

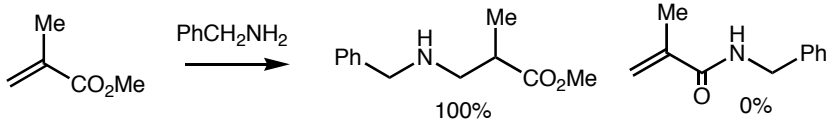

Apparent exceptions to disallowed 5-endo-trig cyclization process

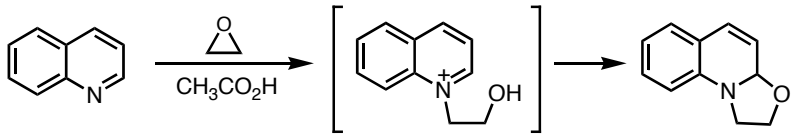

Filer, *J. Am. Chem. Soc.* **1979**, *44*, 285.

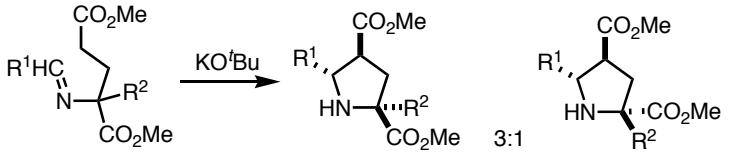

R^1 = aryl, R^2 = aryl, alkyl

Grigg, *J. Chem. Soc., Chem. Commun.* **1980**, 648.

Case 3:

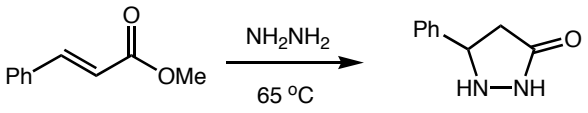

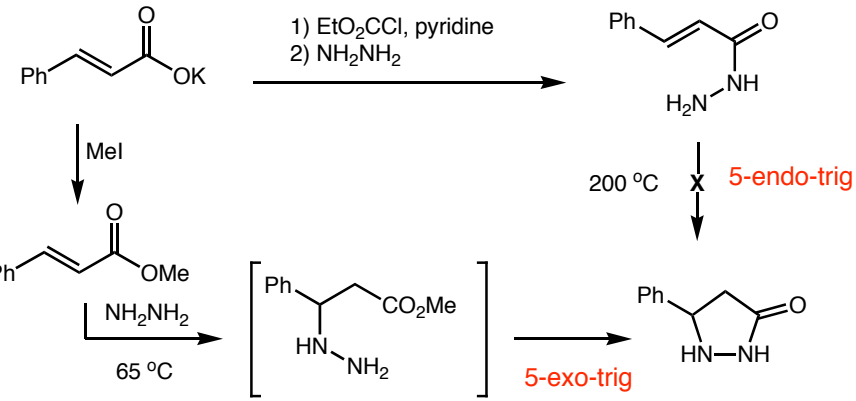

Does the illustrated ketalization process necessarily violate "the rules"?

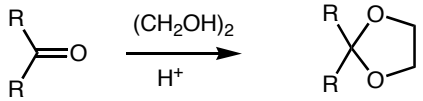

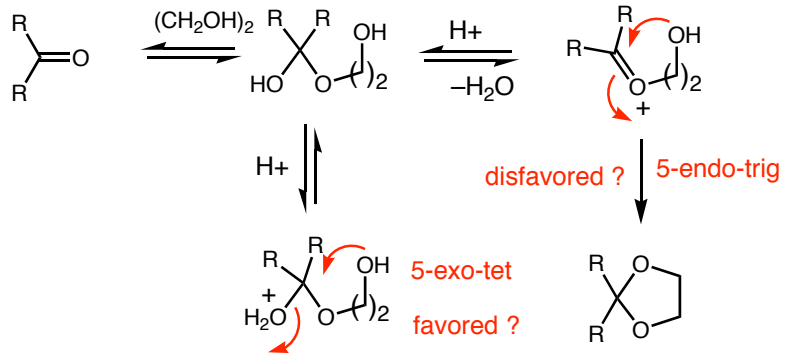

Johnson, C. D. (**1993**). "Stereoelectronic effects in the formation of 5- and 6-membered rings: the role of Baldwin's rules." *Acc. Chem. Res.* **26**: 476-82.

Trigonal Carbon: Exocyclic Enolate Alkylation

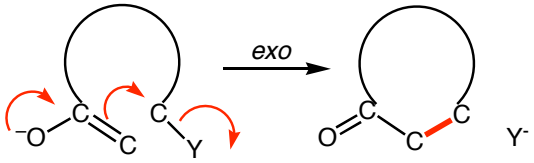

■ By definition, an exo-tet cyclization, but stereoelectronically behaves as an endo trig.

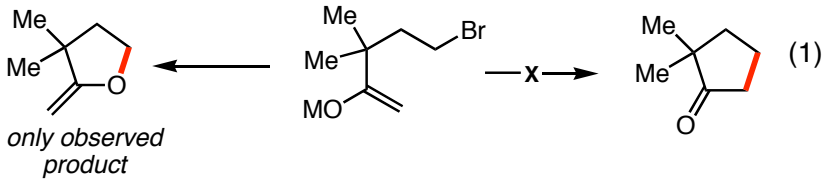

only observed product

However:

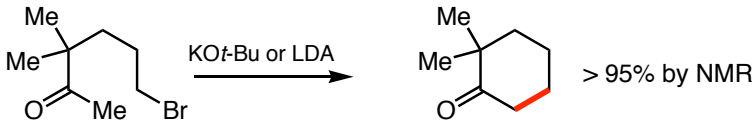

Baldwin, *J. Chem. Soc., Chem. Commun.* **1977**, 233.

■ Given the failure of the enolate alkylation shown above (eq 1), explain why these two cyclizations are successful.

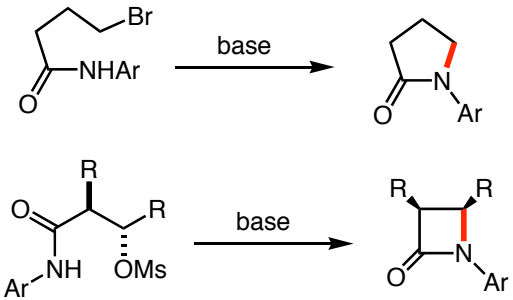

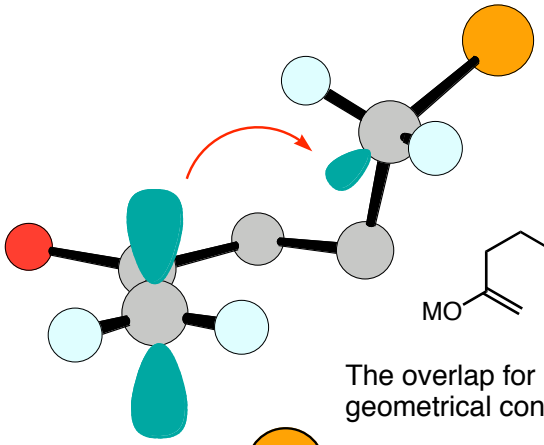

distance between reacting centers: 3.37Å

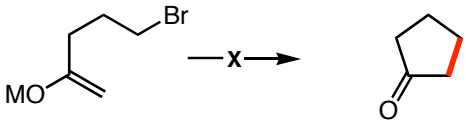

The overlap for C-alkylation is poor due to geometrical constraints of 5-membered ring

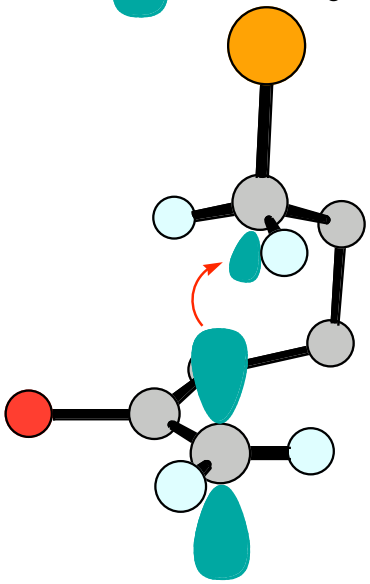

distance between reacting centers: 3.04Å

The relaxed geometrical constraint provided by the added CH_2 group now renders the 6-membered cyclization possible

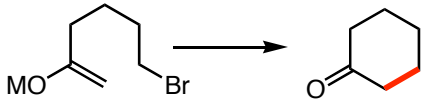

Favorskii Rearrangement (Carey, Pt B, pp 609-610)
Your thoughts on the mechanism

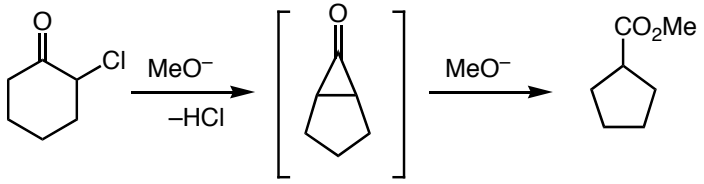

Trigonal Carbon: *Intramolecular Aldol Condensations*

Baldwin, *Tetrahedron* **1982**, *38*, 2939

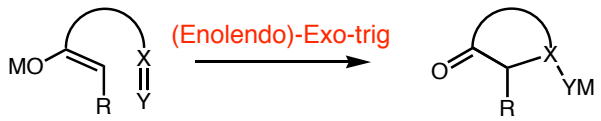

Favored: 6-7-(enolendo)-exo-trig
Disfavored: 3-5-(enolendo)-exo-trig

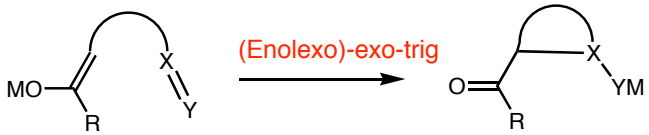

Favored: 3-7-(enolexo)-exo-trig

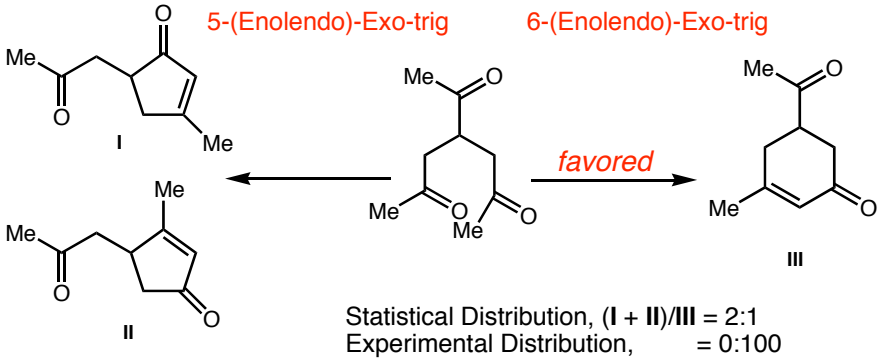

Statistical Distribution, (**I** + **II**)/**III** = 2:1
Experimental Distribution, = 0:100

(KOH, MeOH, r.t., 5 min, 77% y.)

Caution: Baldwin's conclusions assume that the **RDS** is ring closure; however, it is well known (by some!) that the rate determining step is dehydration in a base-catalyzed aldol condensation.

Digonal Carbon: Cyclizations on to Acetylenes

DIGONAL: Angle of approach for attack on triple bonds

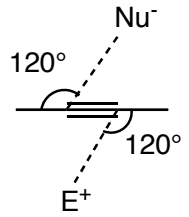

Baldwin:

- 3 and 4-Exo-dig are disfavored
- 5 to 7-Exo-dig are favored
- 3 to 7-Endo-dig are favored

Ab initio SCF 4-31G calculations for the interaction of hydride with acetylene:

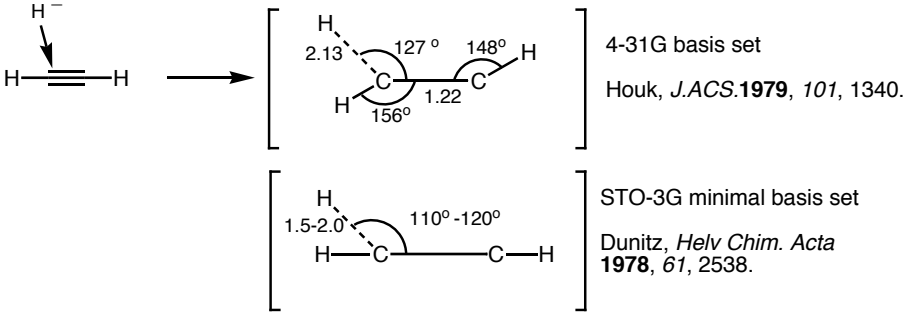

Crystal Structures do not support Baldwin

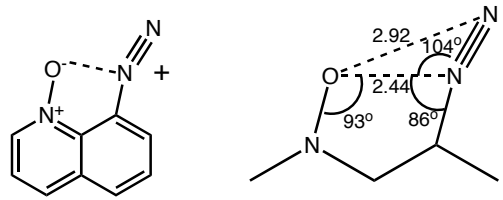

J. Dunitz and J. Wallis *J. C. S. Chem. Comm.* **1984**, 671.

Endo Digonal versus Endo Trigonal Cyclizations

5-endo-trig

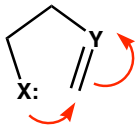

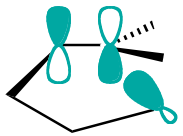

In-plane approach; nucleophile lone pair is orthogonal to π*

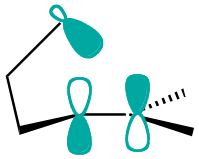

Out-of-plane approach; nucleophile lone pair can't achieve Bürgi-Dunitz angle

5-endo-dig

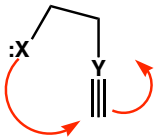

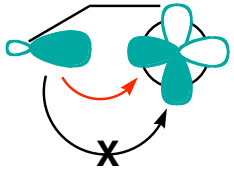

Allowed due to in-plane pi orbitals

For an opposing viewpoint to Baldwin's view of nucleophile trajectories, see Menger's article on directionality in solution organic chemistry: *Tetrahedron* **1983**, *39*, 1013.

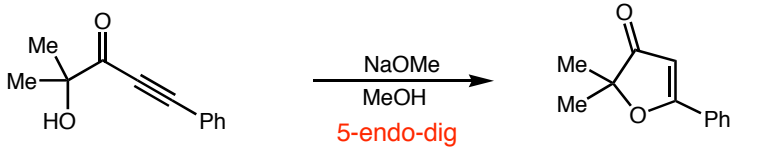

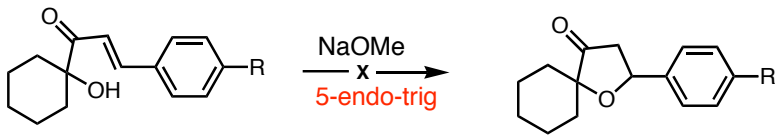

R = H, OMe

however, the acid catalyzed version does cyclize

Baldwin, *J. Chem. Soc., Chem. Commun.*, **1976**, 736.

Johnson, *Can. J. Chem.* **1990**, *68*, 1780

J. Am. Chem. Soc. **1983**, *105*, 5090

J. Chem. Soc., Chem. Commun. **1982**, 36.

■ Indole synthesis:

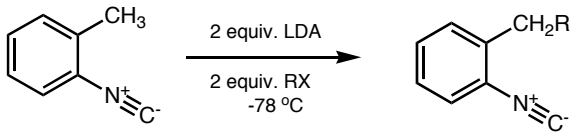

R = Me, Bu, CO_2Me

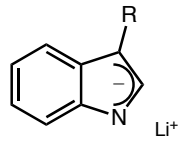

Saegusa, *J. Am. Chem. Soc.* **1977**, *99*, 3532.

■ Spiro dihydrofuranones:

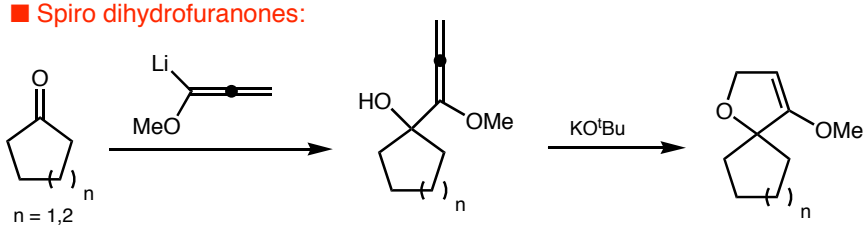

Developing negative charge on the central allenic carbon is in the same plane as the OMe group

Magnus, *J. Am. Chem. Soc.* **1978**, *100*, 7746.

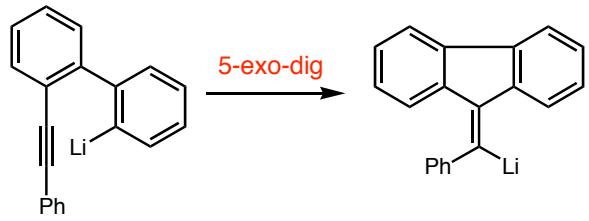

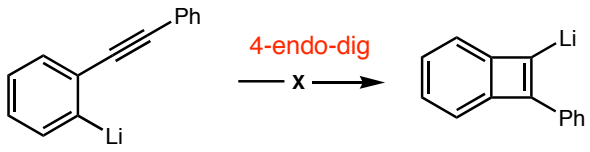

Conclusions and Caveats

■ Baldwin's Rules are an effective first line of analysis in evaluating the stereoelectronics of a given ring closure

■ Baldwin's Rules have provided an important foundation for the study of reaction mechanism

■ Competition studies between different modes of cyclization only give information about relative rates, and are not an absolute indicator of whether a process is "favored" or "disfavored"

■ Structural modifications can dramatically affect the cyclization mode; beware of imines and epoxides

	EXO			ENDO		
	Tet	Trig	Dig	Tet	Trig	Dig
3	√	√	x		x	x
4	√	√	x		x	x
5	√	√	√	x	x	√
6	√	√	√	x	√	√
7	√	√	√	x	√	√

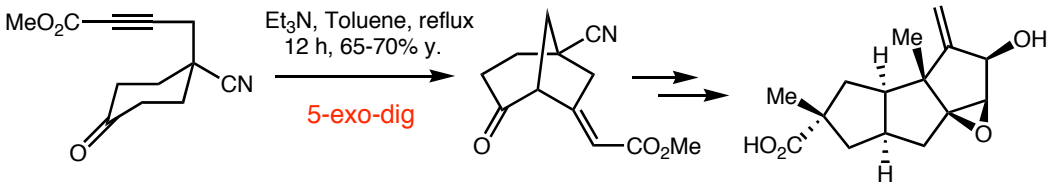

■ Trost, *JACS* **1979**, *101*, 1284

Digonal Cyclizations: Interesting Examples

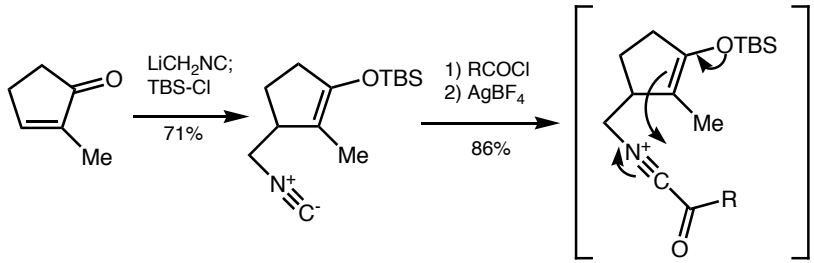

Works for varying ring sizes and R groups; acylnitrilium ion can also work as an electophile in a Friedel-Crafts type of reaction

5-endo-dig

■ Livinghouse, *Tetrahedron* **1992**, *48*, 2209.

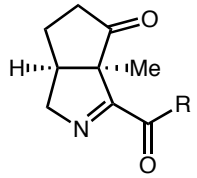

DAE undergraduate, UCLA, 1972

http://www.courses.fas.harvard.edu/colgsas/1063

Chemistry 206

Advanced Organic Chemistry

Lecture Number 4

Conformational Analysis-1

- Ethane, Propane, Butane & Pentane Conformations
- Simple Alkene Conformations

Reading Assignment for week

A. Carey & Sundberg: **Part A**; Chapters 2 & 3

R. W. Hoffmann, *Angew. Chem. Int. Ed. Engl.* ***2000***, *39*, 2054-2070
Conformation Design of Open-Chain Compounds **(handout)**

The Ethane Barrier Problem

F. Weinhold, *Nature* ***2001***, *411*, 539-541
"A New Twist on Molecular Shape" **(handout)**

F. M. Bickemhaupt & E. J. Baerends, *Angew. Chem. Int. Ed.* ***2003***, *42*, 4183-4188,*"The Case for Steric Repulsion Causing the Staggered Conformation in Ethane"* **(handout)**

F. Weinhold,, *Angew. Chem. Int. Ed.* ***2003***, *42*, 4188-4194,*"Rebuttal of the Bikelhaupt–Baerends Case for Steric Repulsion Causing the staggered Connformation of Ethane"* **(handout)**

D. A. Evans

Monday,
September 25, 2006

Problem 61. The following stereoselective hydroboration has been reported by Kishi in his synthesis of monensin (*JACS* **1979**, *101*, 259). Provide the stereostructure of the major product and rationalize the stereochemical outcome as indicated in the directions.

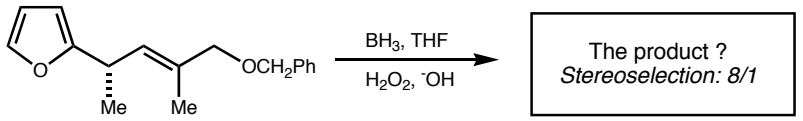

Problem 68. The following stereoselective enolate alkylation has been reported by Kim (*Tetrahedron Lett.* **1986**, *27*, 943). Provide the stereostructure of the major product and rationalize the stereochemical outcome as indicated in the directions.

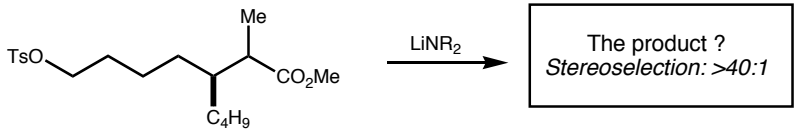

Problem 722. Carbonium ion **A** has been calculated to be 38 kcal/mol more stable than carbonium ion **B** (Jorgensen *JACS* **1985**, *107*, 1496). The profound stabilization of carbonium ions by silicon in this fashion is referred to as the "beta-silicon effect". For example, the S_N1 solvolysis reaction of **1** is 10^{+12} times as fast as the corresponding reaction of **2**. The solvolysis of **2** leads to the olefin. For a good review see: Lambert *Acc. Chem. Res.* **1999**, *32*, 183-190

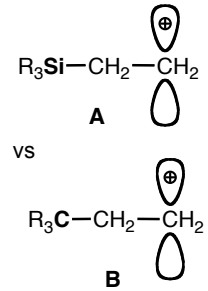

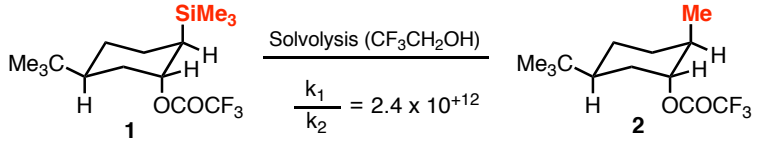

Part A: Identify the HOMO–LUMO interactions in the S_N1 reactions of **1** and **2**.

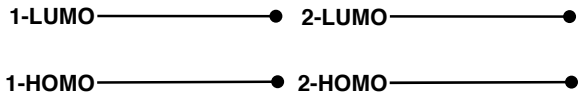

The following discussion is intended to provide a general overview of acyclic conformational analysis

Ethane & Propane

The conformational isomerism in these 2 structures reveals a gratifying level of internal consistency.

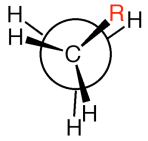

eclipsed conformation

$\Delta E = +3.0$ kcal mol^{-1} (R = H)

$\Delta E = +3.4$ kcal mol^{-1} (R = Me)

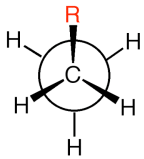

staggered conformation

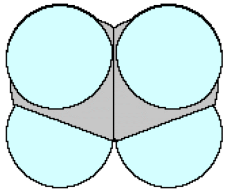

Van derWaals radii of vicinal hydrogens do not overlap in ethane

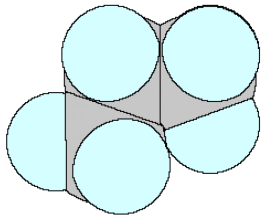

In propane there is a discernable interaction

For purposes of analysis, each eclipsed conformer may be broken up into its component destabilizing interactions.

Incremental Contributions to the Barrier.

Structure	Eclipsed atoms	δ E (kcal mol $^{-1}$)
ethane	3 (H↔H)	+1.0 kcal mol $^{-1}$
propane	2 (H↔H)	+1.0 kcal mol $^{-1}$
	1 (H↔Me)	+1.4 kcal mol $^{-1}$

Ethane Rotational Barrier: The FMO View

F. Weinhold, *Angew. nature* ***2001***, *411*, 539-541 *"A New Twist on Molecular Shape"*

One explanation for the rotational barrier in ethane is that better overlap is possible in the staggered conformation than in the eclipsed conformation as shown below.

In the staggered conformation there are 3 anti-periplanar C–H Bonds

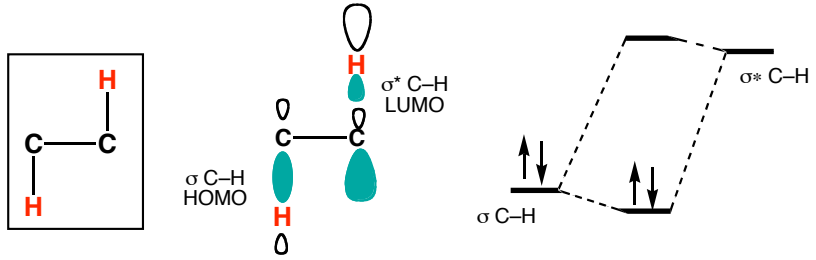

In the eclipsed conformation there are 3 syn-periplanar C–H Bonds

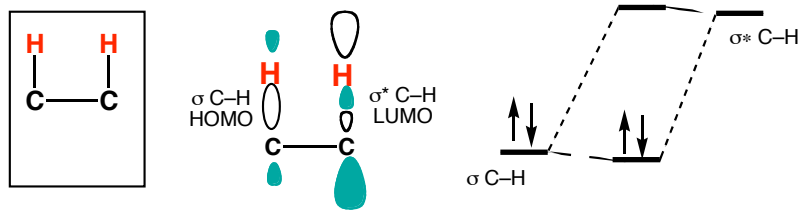

Following this argument one might conclude that:

■ **The staggered conformer has a better orbital match between bonding and antibonding states.**

■ **The staggered conformer can form more delocalized molecular orbitals.**

J. P. Lowe was the first to propose this explanation

"A Simple Molecuar Orbital Explanation for the Barrier to Internal Rotation in Ethane and Other Molecules"
J. P. Lowe, *JACS* **1970**, *92*, 3799

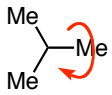

Estimate the rotational barrier about the C1-C2 bond in isobutane

Relationship between ΔG and Keq and pKa

Recall that: $\Delta G^\circ = -RT \ln K$ or $\Delta G^\circ = -2.3RT \log_{10} K$

At 298 K: $2.3RT = 1.4$ (ΔG in kcal Mol^{-1})

$$\Delta G^\circ_{298} = -1.4 \log_{10} Keq$$

Since $pKeq = -\log_{10} Keq$

$$\Delta G^\circ_{298} = 1.4\ pKeq$$

Hence, pK is proportional to the free energy change

Keq	pKeq	ΔG°
1.0	0	0
10	–1	–1.4
100	–2	–2.8 kcal /mol

Butane

Using the eclipsing interactions extracted from propane & ethane we should be able to estimate all but one of the eclipsed butane conformations

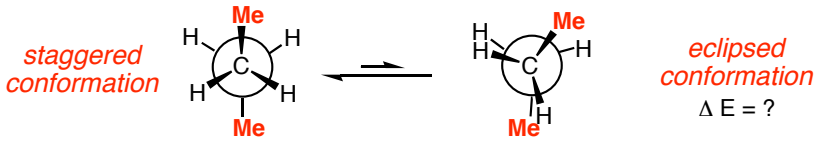

Eclipsed atoms	δ E (kcal mol $^{-1}$)
1 (H↔H)	+1.0 kcal mol $^{-1}$
2 (H↔Me)	+2.8 kcal mol $^{-1}$
Δ E est =	3.8 kcal mol $^{-1}$

The estimated value of +3.8 agrees quite well with the value of +3.6 reported by Allinger (*J. Comp. Chem.* **1980**, *1*, 181-184)

n-Butane Torsional Energy Profile

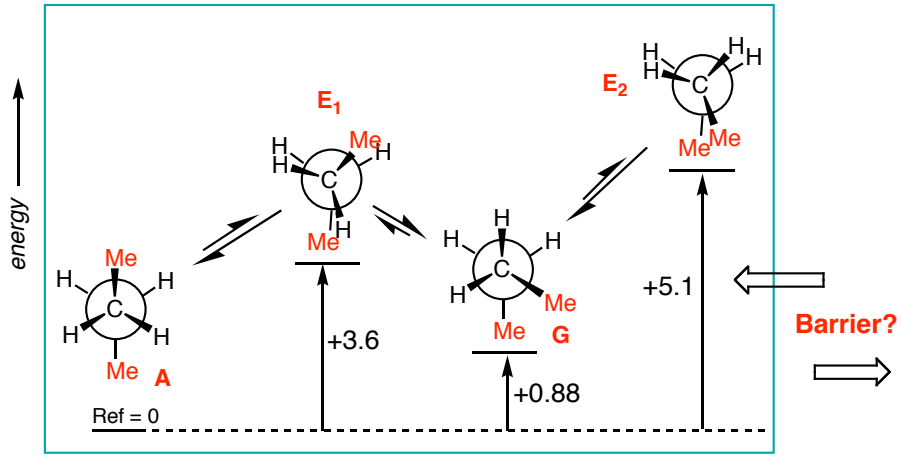

Butane continued

From the torsional energy profile established by Allinger, we should be able to extract the contribution of the Me↔Me eclipsing interaction to the barrier:

staggered conformation ⇌ *eclipsed conformation*

$\Delta E = +5.1$ kcal mol^{-1}

Let's extract out the magnitide of the Me–Me interaction

2 (H↔H) + 1 (Me↔Me) = +5.1

1 (Me↔Me) = +5.1 – 2 (H↔H)

1 (Me↔Me) = +3.1

Incremental Contributions to the Barrier.

Eclipsed atoms	δ E (kcal mol^{-1})
2 (H↔H)	+2.0
1 (Me↔Me)	+3.1

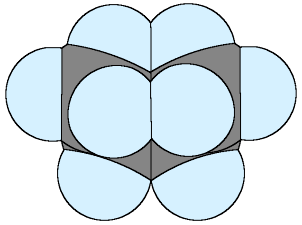

Eclipsed Butane conformation

From the energy profiles of ethane, propane, and n-butane, one may extract the useful eclipsing interactions summarized below:

Hierarchy of Eclipsing Interactions

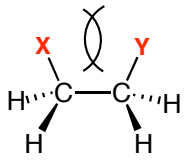

X—Y	δ E kcal mol^{-1}
H—H	+1.0
H—Me	+1.4
Me—Me	**+3.1**

Nomenclature for staggered conformers:

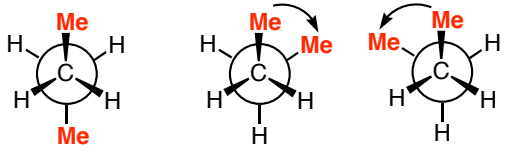

trans or t or (anti)	gauche(+) or g$^+$	gauche(-) or g$^-$
70%	15%	15%

Conformer population at 298 K:

(Klyne, Prelog, *Experientia* **1960**, *16*, 521.)

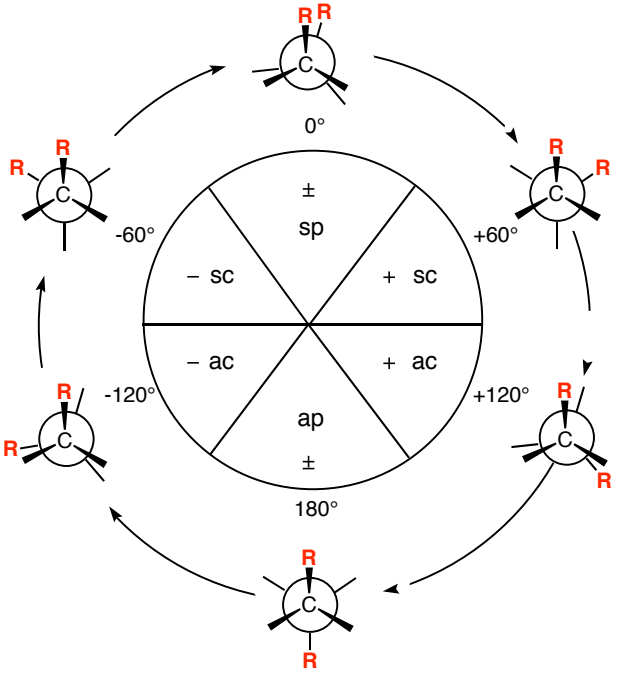

	Torsion angle	Designation	Symbol	*n*-Butane Conformer
Energy Maxima →	0 ± 30°	± syn periplanar	± sp	E_2
Energy Minima ⇢	+60 ± 30°	+ syn-clinal	+ sc (g+)	G
Energy Maxima →	+120 ± 30°	+ anti-clinal	+ ac	E_1
Energy Minima ⇢	180 ± 30°	antiperiplanar	ap (anti or t)	A
Energy Maxima →	-120 ± 30°	- anti-clinal	- ac	E_1
Energy Minima ⇢	-60 ± 30°	- syn-clinal	- sc (g-)	G

n-Pentane

Rotation about both the C_2-C_3 and C_3-C_4 bonds in either direction (+ or -):

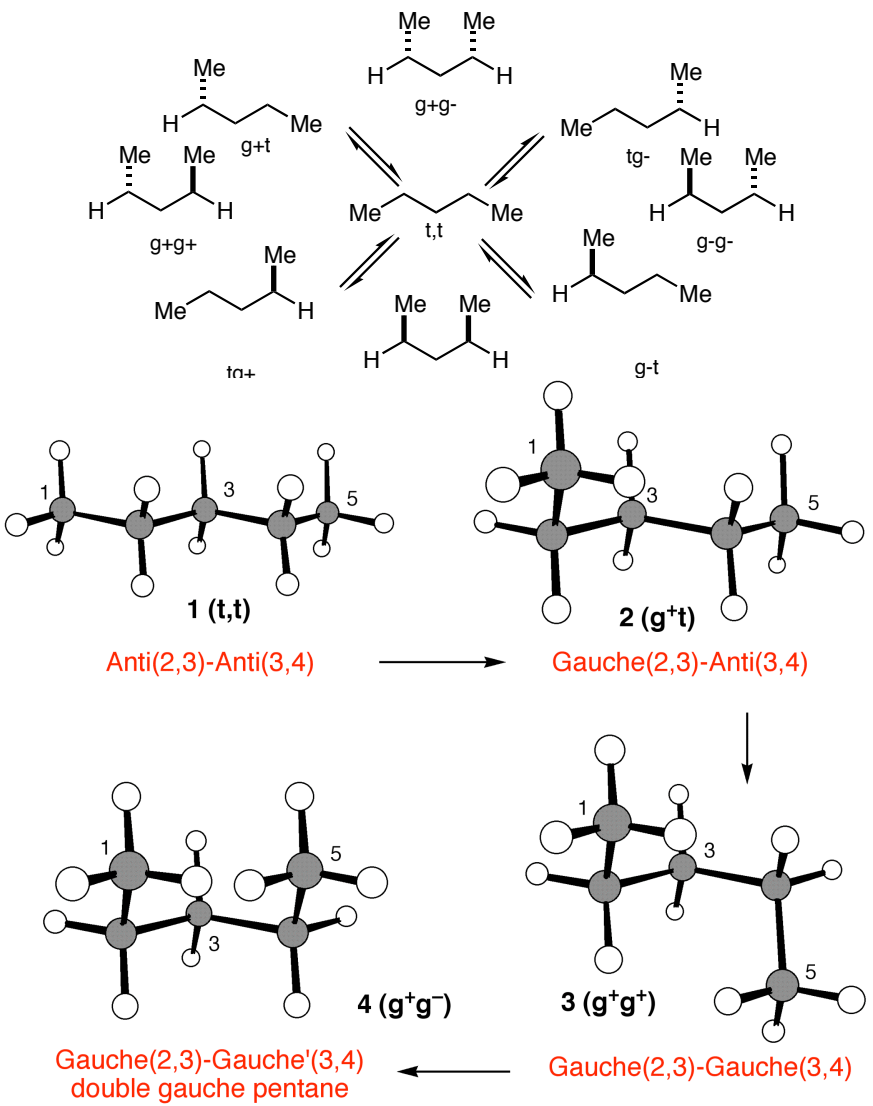

From prior discussion, you should be able to estimate energies of **2** & **3** (relative to **1**). On the other hand, the least stable conformer **4** requires additional data before is relative energy can be evaluated.

The double-gauche pentane conformation

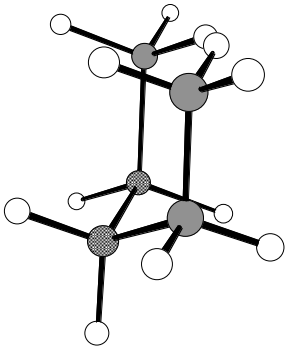

The new high-energy conformation: **(g+g−)**

Estimate of 1,3-Dimethyl Eclipsing Interaction

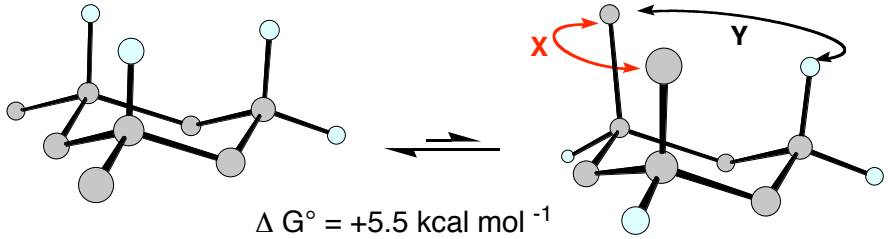

$\Delta G° = +5.5$ kcal mol $^{-1}$

$\Delta G = X + 2Y$ where:

X = 1,3(Me–Me) & Y = 1,3(Me–H)

1,3(Me–H) = Skew-butane = 0.88 kcal mol-1

1,3(Me-Me) = $\Delta G - 2Y = 5.5 - 1.76 = +3.7$ kcal mol-1

1,3(Me↔Me) = + 3.7 kcal mol $^{-1}$

Estimates of In-Plane 1,2 &1,3-Dimethyl Eclipsing Interactions

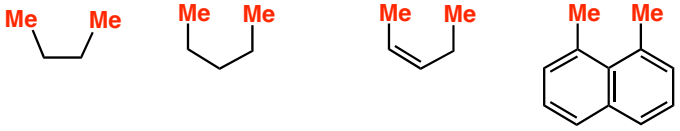

3.1	~ 3.7	~3.9	~ 7.6

It may be concluded that in-plane 1,3(Me↔Me) interactions are Ca +4 kcal/mol while 1,2(Me↔Me) interactions are destabliizing by Ca 3 kcal/mol.

The syn-Pentane Interaction - Consequences

R. W. Hoffmann, *Angew. Chem. Int. Ed. Engl.* ***2000***, *39*, 2054-2070
Conformation Design of Open-Chain Compounds **(handout)**

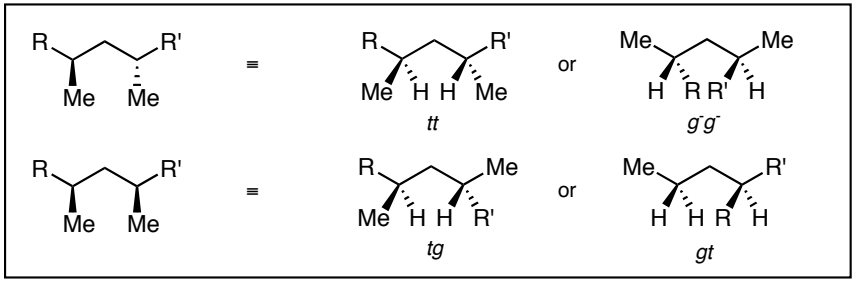

Consequences for the preferred conformation of polyketide natural products

Analyze the conformation found in the crystal state of a bourgeanic acid derivative!

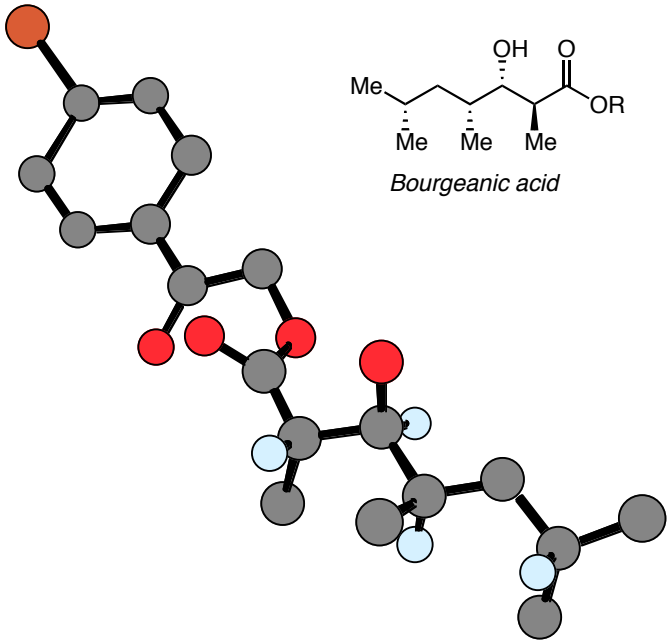

Bourgeanic acid

Lactol & Ketol Polyether Antibioitics

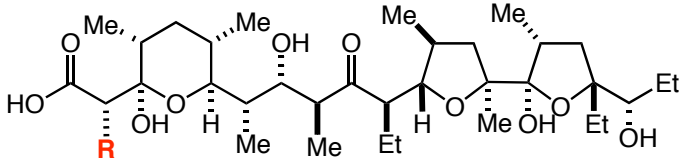

Ferensimycin B, R = Me
Lysocellin, R = H

The conformation of these structures are strongly influenced by the acyclic stereocenters and internal H-bonding

Alborixin R = Me; X-206 R = H

Internal H-Bonding

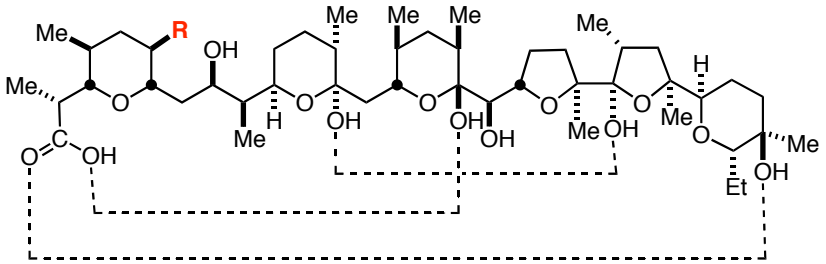

Metal ion ligation sites (M = Ag, K)

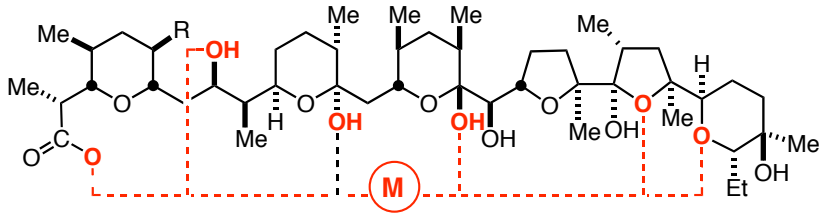

X-ray of Ionophore X-206 · H_2O

Internal H-Bonding

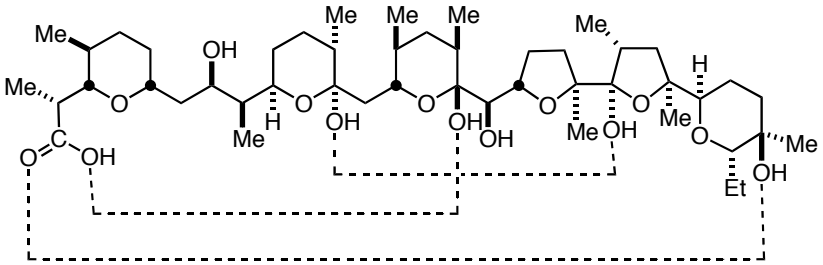

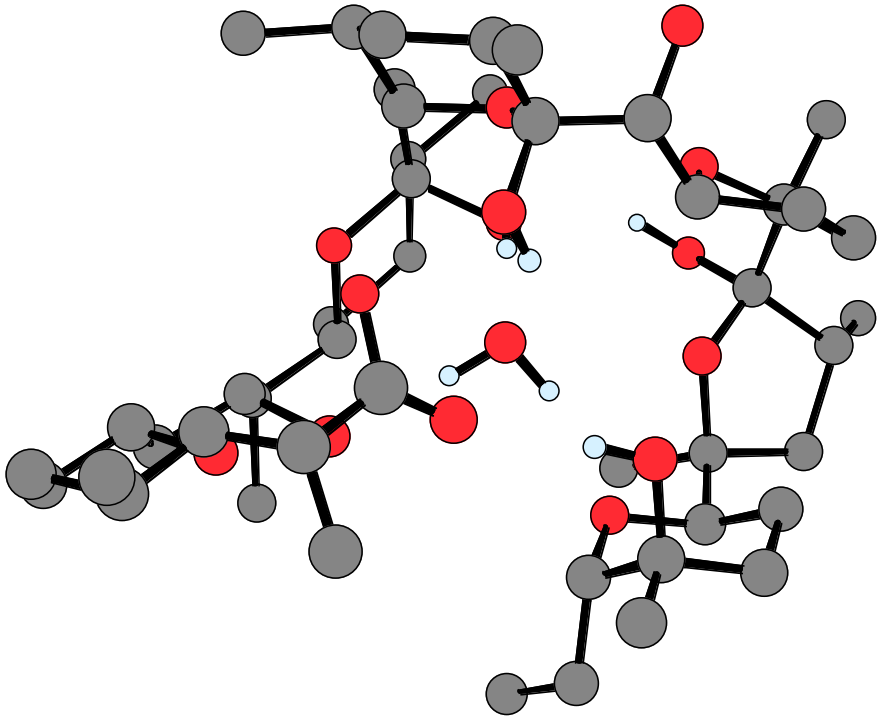

"The Total Synthesis of the Polyether Antibiotic X-206". Evans, D. A.; Bender, S. L.; Morris, J. *J. Am. Chem. Soc.* **1988**, *110*, 2506-2526.

X-ray of Ionophore X-206 - Ag^+ - Complex

Metal ion ligation sites (M = Ag, K)

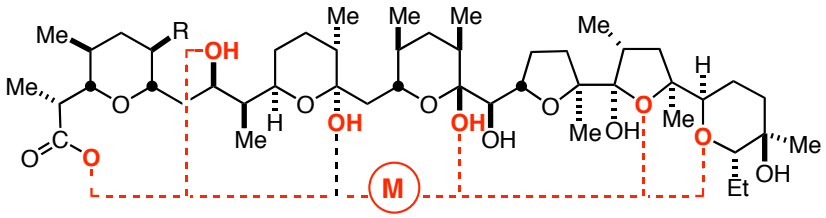

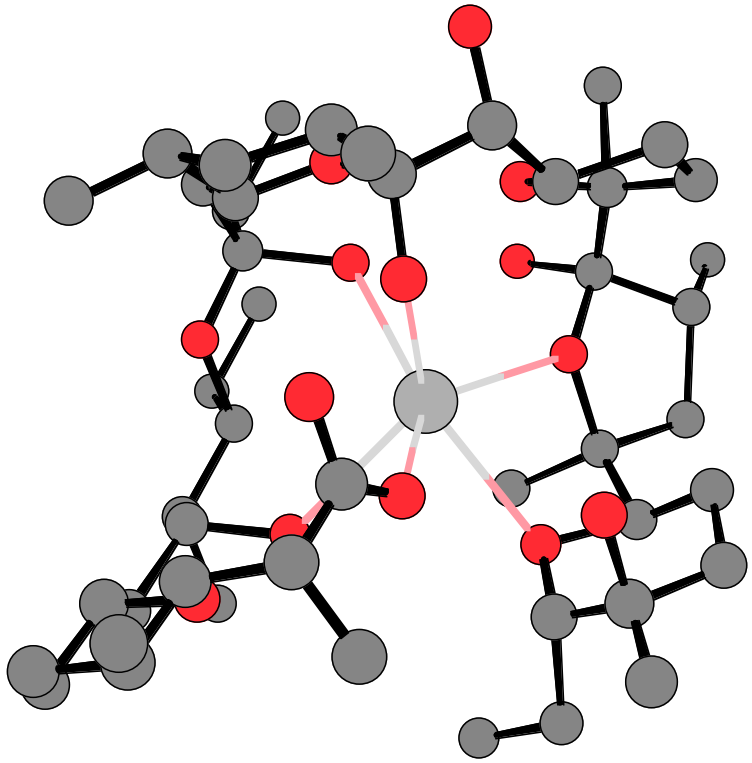

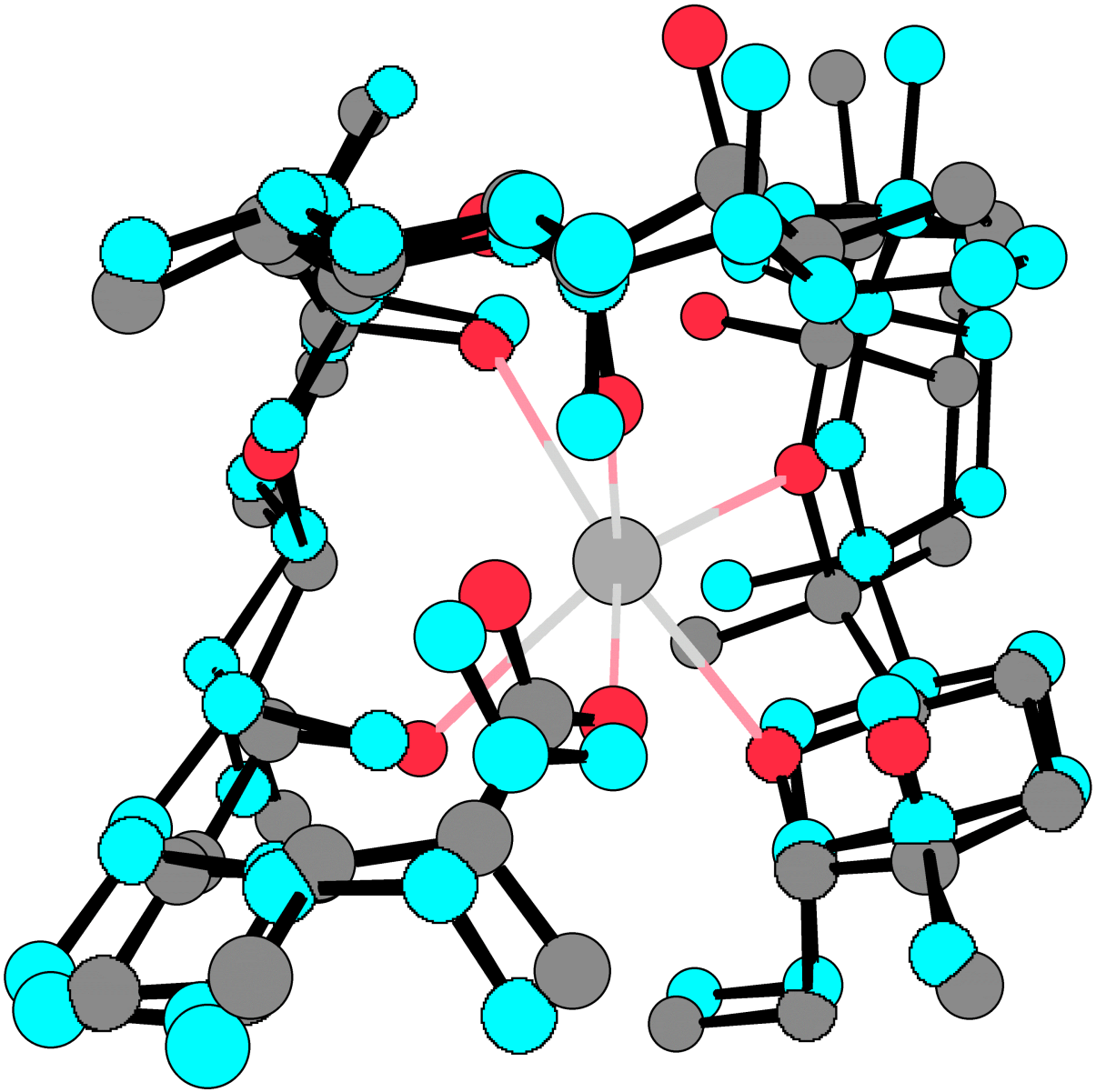

The 1,2-Dihaloethanes

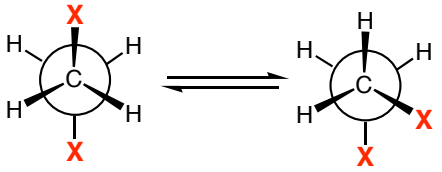

X = Cl; ΔH° = + 0.9–1.3 kcal/mol
X = Br; ΔH° = + 1.4–1.8 kcal/mol
X = F; ΔH° = – 0.6-0.9 kcal/mol

Observation: While the anti conformers are favored for X = Cl, Br, the gauche conformation is prefered for 1,2-difluroethane. Explain.

Relevant Article: *Chem. Commun* **2002**, 1226-1227 **(pdf)**

σ-anti-bonding States: (C–X)

For the latest views, read
Alabugin & Zeidan, *JACS* **2002**, *124*, 3175 (pdf)

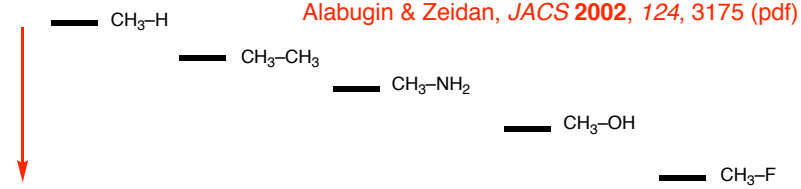

σ-anti-bonding States: (C–X)

For the latest views, read
Alabugin & Zeidan, *JACS* **2002**, *124*, 3175 (pdf)

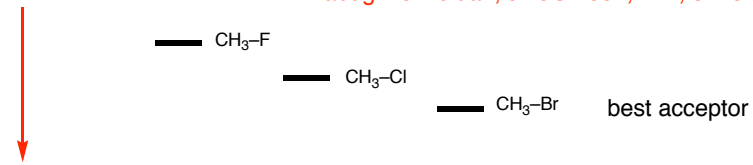

Alabugin & Zeidan, *JACS* **2002**, *124*, 3175 (pdf)

However, the trend of σ acceptor ability being directly proportional to electronegativity is reversed when moving down a group. This reversal is most paradoxical for halogens, where the acceptor ability of C−Hal bonds shows a good linear correlation with the electronegativity of X (Figure 7) but this correlation is *inverse*. In other words, despite the fact that electronegativity *decreases* in the order F > Cl > Br, the acceptor ability of σ^*_{C-X} orbitals *increases* in the order $\sigma^*_{C-F} < \sigma^*_{C-Cl} < \sigma^*_{C-Br}$.[35] These results are especially intriguing since the high acceptor ability of σ^*_{C-F} bonds has a large number of chemical consequences as thoroughly analyzed by Borden in a recent paper.[9f] The consequences of higher acceptor ability of other C−Hal bonds should also be significant.

Several experimental observations support this trend in acceptor ability of C−Hal bonds. The anomeric effect[36] is larger for Br than for Cl,[5a,37,38] and there is a stronger preference for Br than for Cl to be in a pseudoaxial position in α-halocyclo-

Your Thoughts on the trend shown below:

The 1,2-Dihaloethanes

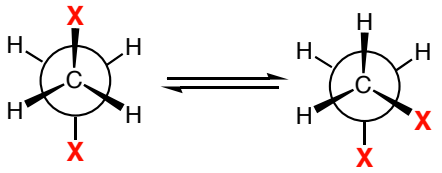

X = Cl; ΔH° = + 0.9–1.3 kcal/mol
X = Br; ΔH° = + 1.4–1.8 kcal/mol
X = F; ΔH° = – 0.6-0.9 kcal/mol

Simple olefins exhibit unusal conformational properties relative to their saturated counterparts

Propane versus Propene

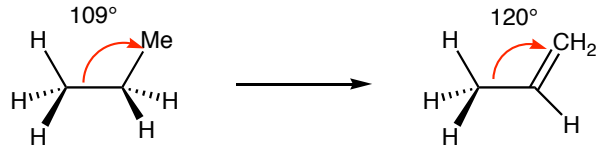

Hybridization change opens up the C–C–C bond angle

■ The Propylene Barrier

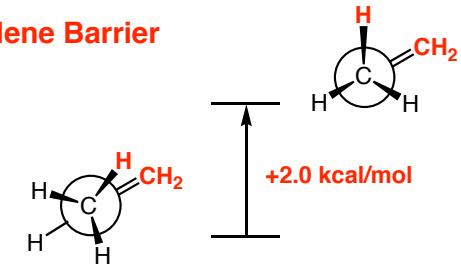

New (de)stabilizing effect

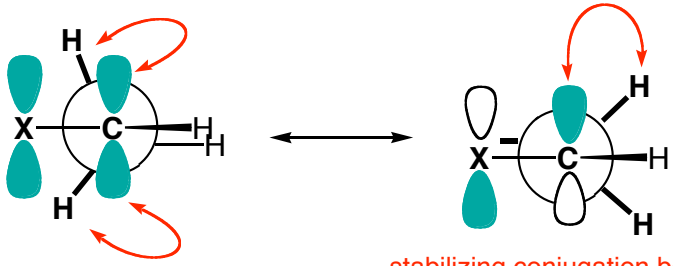

stabilizing conjugation between π*–C–X & σ–C–H

K. Wiberg, *JACS* **1985**, *107*, 5035-5041
K. Houk, *JACS* **1987**, *109*, 6591-6600

Butane versus 1-Butene

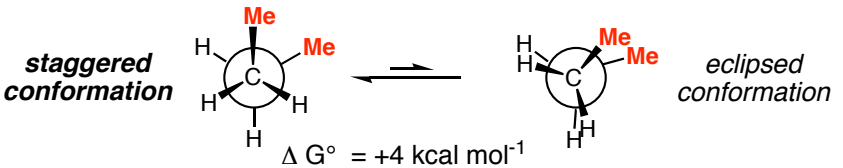

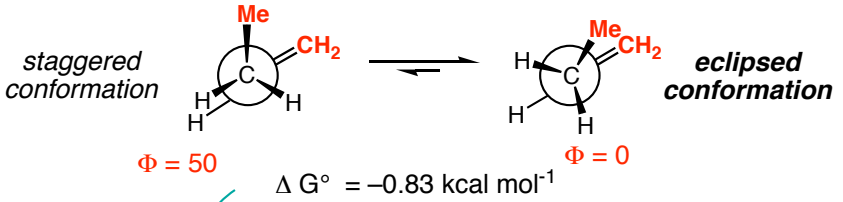

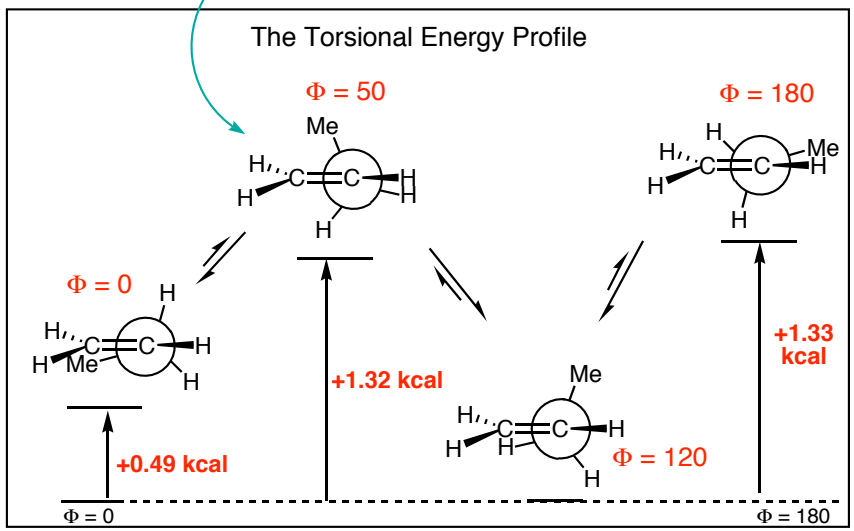

Conforms to *ab initio* (3-21G) values:
Wiberg, K. B.; Martin, E. *J. Am. Chem. Soc.* **1985,** *107,* 5035.

■ Acetaldehyde exhibits a similar conformational bias

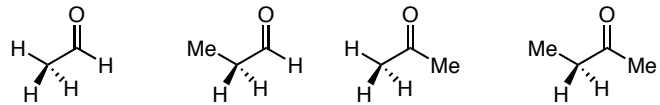

The low-energy conformation in each of above cases is eclipsed

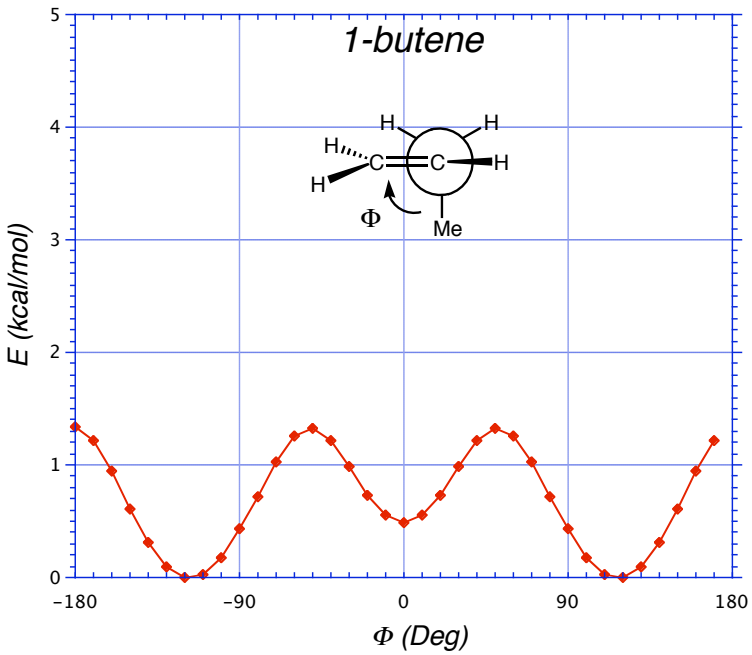

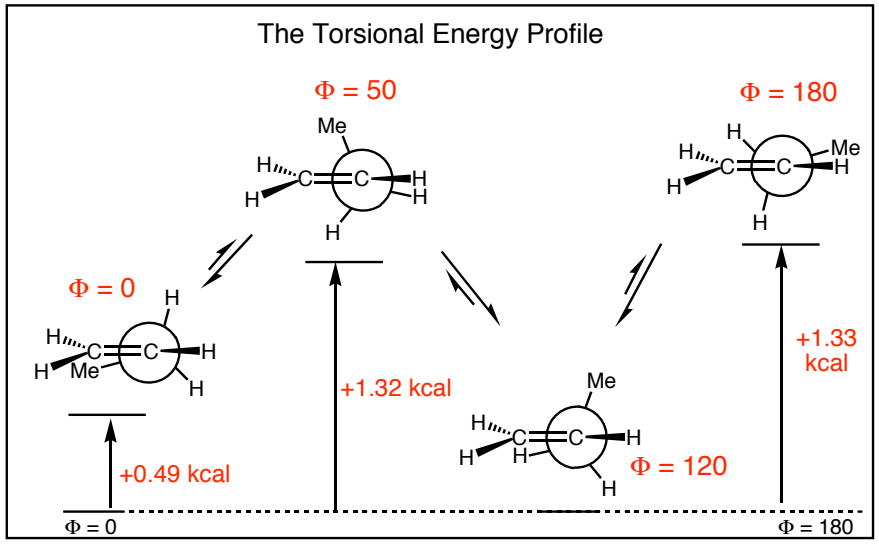

Conforms to *ab initio* (3-21G) values:
Wiberg, K. B.; Martin, E. *J. Am. Chem. Soc.* **1985,** *107,* 5035.

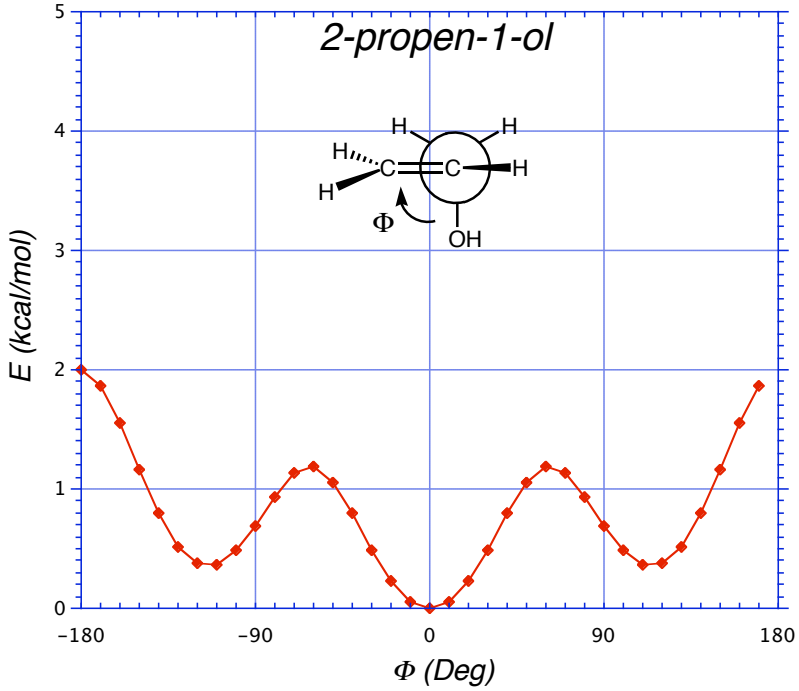

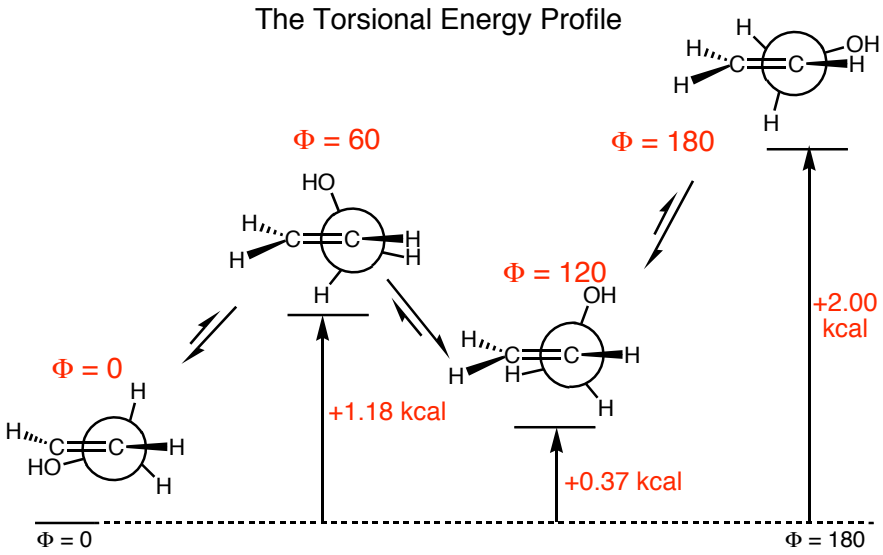

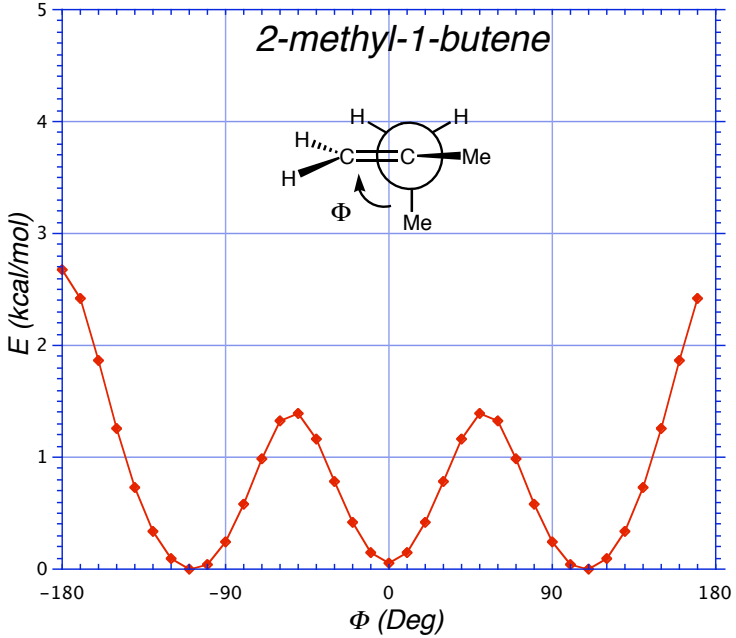
2-methyl-1-butene
E (kcal/mol)
Φ (Deg)
Φ
Me

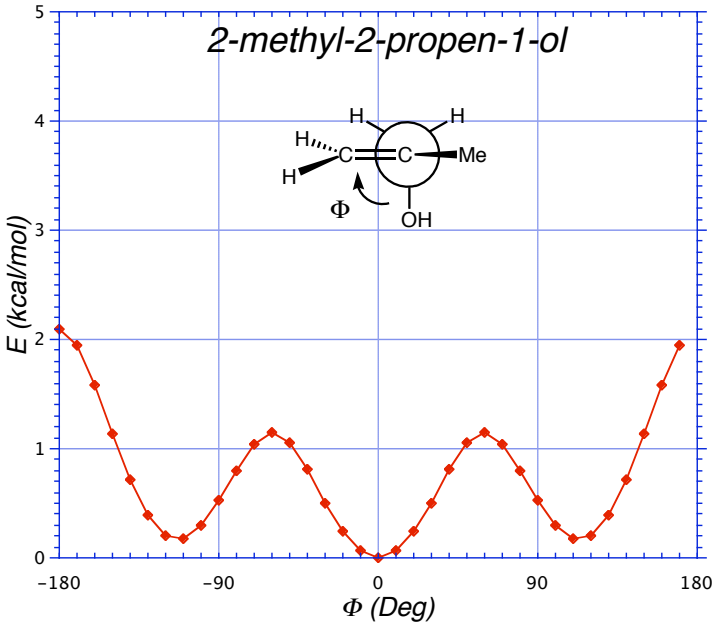
2-methyl-2-propen-1-ol
E (kcal/mol)
Φ (Deg)
Φ
OH
Me

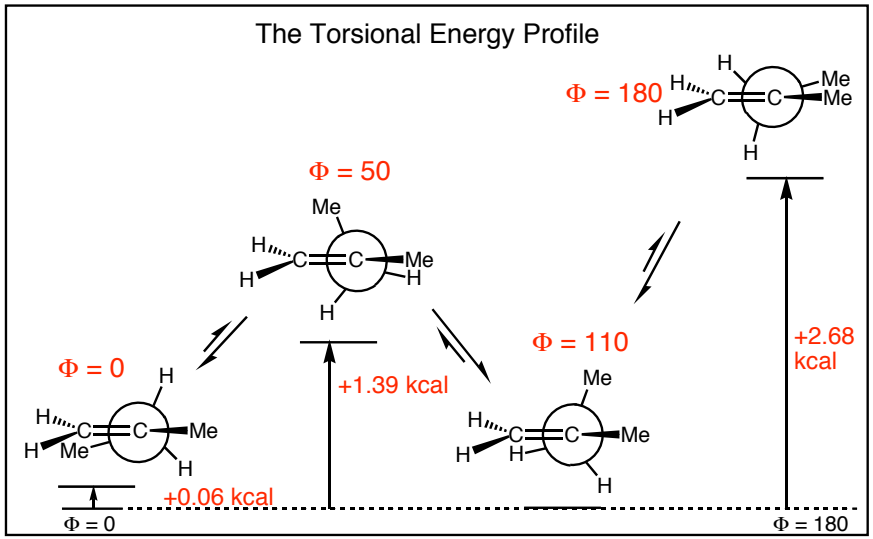
The Torsional Energy Profile
Φ = 180
Φ = 50
Φ = 0
Φ = 110
+1.39 kcal
+2.68 kcal
+0.06 kcal
Φ = 0
Φ = 180

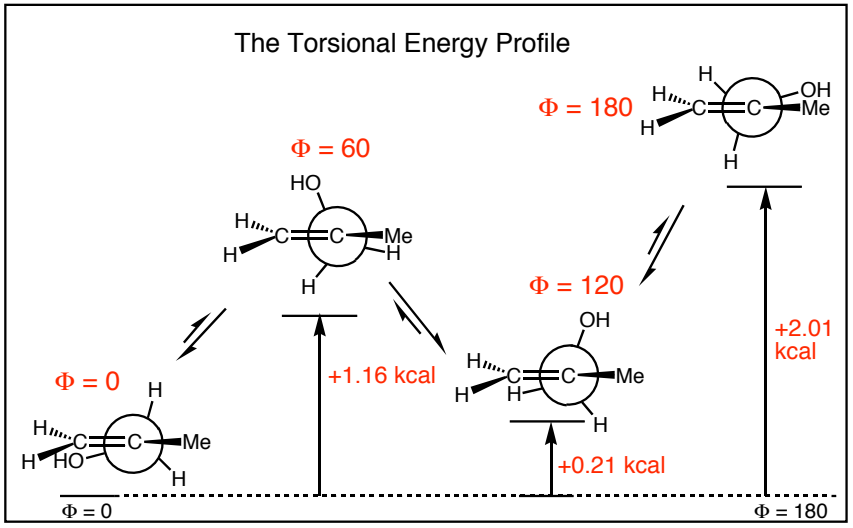
The Torsional Energy Profile
Φ = 180
Φ = 60
Φ = 120
Φ = 0
+1.16 kcal
+2.01 kcal
+0.21 kcal
Φ = 0
Φ = 180

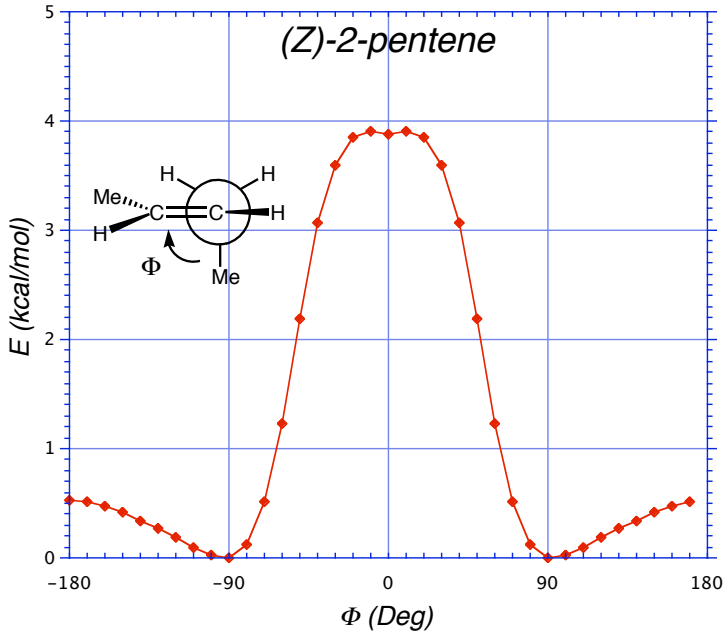

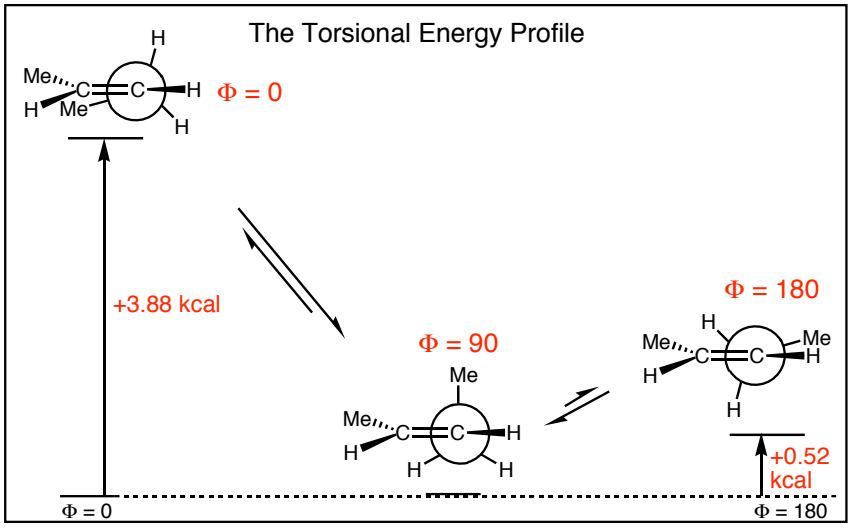

Values calculated using MM2 (molecular mechanics) force fields via the Macromodel multiconformation search.

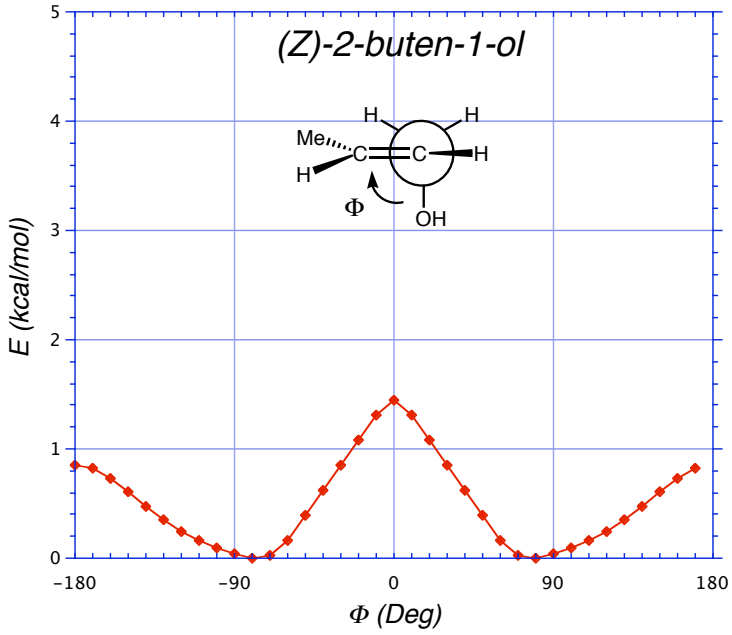

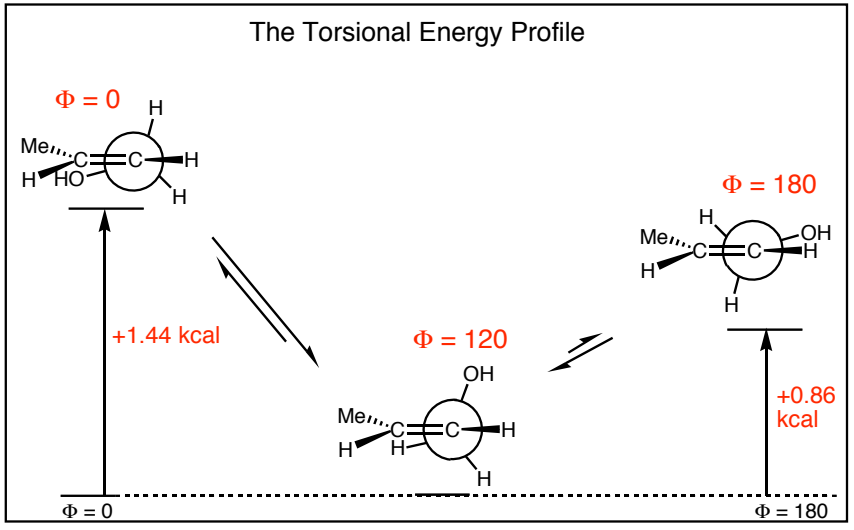

Review: Hoffman, R. W. *Chem. Rev.* **1989,** *89,* 1841.

Useful Destabilizing Interactions to Remember

Hierarchy of Vicinal Eclipsing Interactions

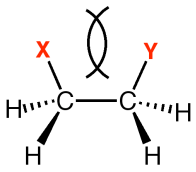

X—Y	δ E kcal mol $^{-1}$
H—H	+1.0
H—Me	+1.4
Me—Me	**+3.1**

Estimates of In-Plane 1,2 &1,3-Dimethyl Eclipsing Interactions

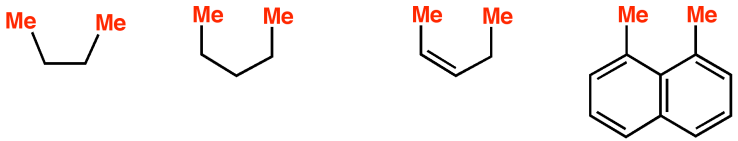

~ 3.1 ~ 3.7 ~3.9 ~ 7.6

It may be concluded that in-plane 1,3(Me↔Me) interactions are Ca +4 kcal/mol while 1,2(Me↔Me) interactions are destabliizing by Ca +3 kcal/mol.

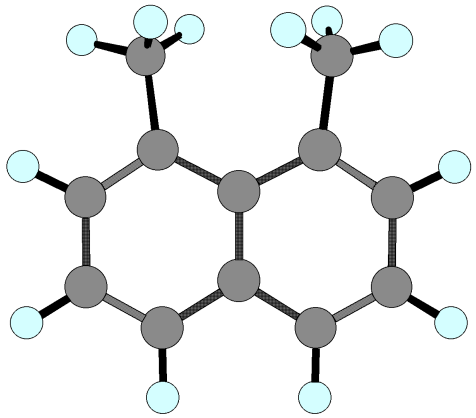

minimized structure

http://www.courses.fas.harvard.edu/colgsas/1063

Chemistry 206

Advanced Organic Chemistry

Lecture Number 5

Acyclic Conformational Analysis-2

■ Introduction to Allylic Strain

■ Reading Assignment for week

A. Carey & Sundberg: **Part A**; Chapters 2 & 3

R. W. Hoffmann, *Angew. Chem. Int. Ed. Engl.* ***2000***, *39*, 2054-2070
Conformation Design of Open-Chain Compounds **(handout)**

R. W. Hoffmann, *Chem. Rev.* **1989**, *89*, 1841-1860
Allylic 1-3-Strain as a Controlling Element in Stereoselective Transformations
(handout)

D. A. Evans

Wednesday,
September 27, 2006

■ Problems of the Day:

Can you predict the stereochemical outcome of this reaction?

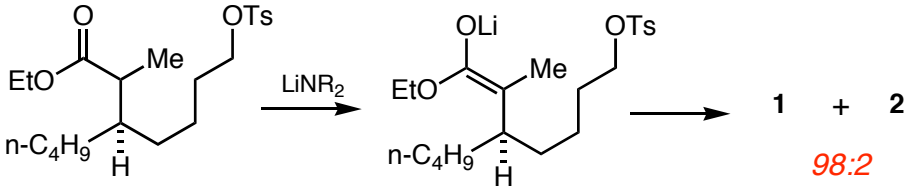

D. Kim & Co-workers, *Tetrahedron Lett.* **1986**, *27*, 943.

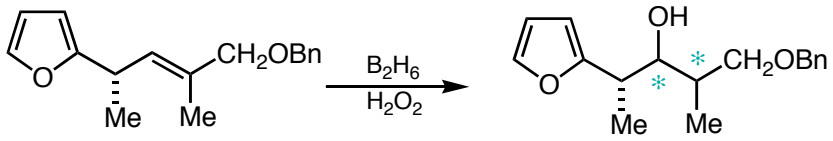

Y. Kishi & Co-workers, *J. Am. Chem. Soc.* **1979**, *101*, 259.

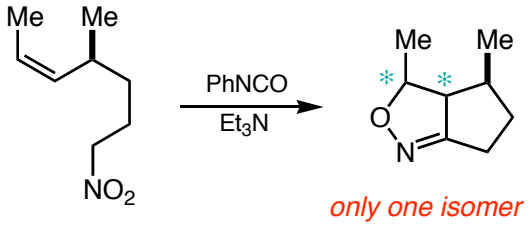

A. Kozikowski & Co-workers, *Tetrahedron Lett.* **1982**, *23*, 2081.

7.46 (d, J = 8 Hz, 2 H). **12:** NMR δ 0.92 (d, J = 7 Hz, 6 H), 1.16–164 (m, 9 H), 1.80 (s, 3 H), 1.87 (s, 3 H), 2.40 (s, 3 H), 3.42 (s, 3 H), 4.04 (dd, J = 11, 4 Hz, 1 H), 5.72 (m, 1 H), 5.88 (t, J = 3 Hz, 1 H), 6.44 (t, J = 2 Hz, 1 H), 7.12 (d, J = 8 Hz, 2 H), 7.30 (d, J = 8 Hz, 2 H). **13:** NMR δ 0.98 (d, J = 8 Hz, 6 H), 1.64 (m, 3 H), 2.89 (br t, J = 8 Hz, 2 H), 3.80 (s, 3 H), 6.43 (d, J = 3 Hz, 1 H), 6.83 (apparent, t, J = 4 Hz, 1 H), 6.93 (d, J = 3 Hz, 1 H), 7.06 (apparent d, J = 4 Hz, 2 H). **15:** NMR δ 1.76 (s, 6 H), 3.52 (d, J = 8 Hz, 2 H), 3.76 (s, 3 H), 5.37 (t, J = 8 Hz, 1 H), 6.36 (d, J = 3 Hz, 1 H), 6.76 (apparent t, J = 4 Hz, 1 H), 6.86 (d, J = 3 Hz, 1 H), 7.00 (apparent d, J = 4 Hz, 2 H). New compounds have been fully characterized by spectral means and have satisfactory elemental composition.

(4) To our knowledge, the directive effect of a benzylic alkylthio group on aromatic ring metalation has not been previously examined. For a leading reference see Slocum, D. W.; Jennings, C. A. *J. Org. Chem.* **1976,** *41,* 3653.
(5) Gjos, N. J.; Gronowitz, S. *Acta Chem. Scand.* **1971,** *25,* 2596.
(6) Plieninger, H.; Hobel, M.; Liede, V. *Chem. Ber.* **1963,** *96,* 1618.
(7) Attempts to use less electron-rich aromatic rings or to cyclize to form five- or seven-membered rings has led to equivocal results.
(8) Brown, R. K. *Chem. Heterocycl. Compd.* **1972,** *25,* 227.
(9) Gassman, P. G.; van Bergen, T. J.; Gilbert, D. P.; Cue, B. W., Jr. *J. Am. Chem. Soc.* **1974,** *96,* 5495.
(10) For a recent approach to 4-substituted oxindoles, see Kozikowski, A. P.; Kuniak, M. P. *J. Org. Chem.* **1978,** *43,* 2083. Renewed interest in ergot alkaloids stems in part from their possible use as prolactin inhibitors or in treatment of Parkinson's disease. See the following. Floss, H. G.; Cassady, J. M.; Robbers, J. E. *J. Pharm. Sci.* **1973,** *62,* 699. Cassady, J. M.; Li, G. S.; Spitzner, E. B.; Floss, H. G.; Clemens, J. A. *J. Med. Chem.* **1974,** *17,* 300.

Barry M. Trost,* Manfred Reiffen, Michael Crimmin
Department of Chemistry, University of Wisconsin—Madison
Madison, Wisconsin 53706

Received August 30, 1978

Total Synthesis of Monensin. 1. Stereocontrolled Synthesis of the Left Half of Monensin[1]

Sir:

Monensin (**1**),[2] produced by a strain of *Streptomyces cinnamonensis*, is perhaps the best known, most historical example from among a group of about 40 naturally occurring

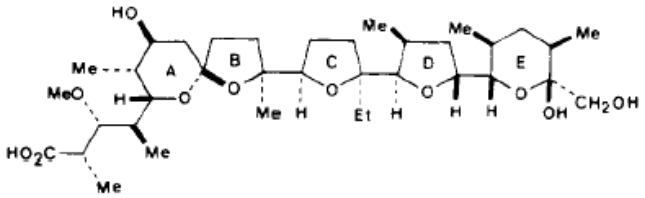

based on an example similar to this case.[8] The origin of the remarkable stereospecificity observed might be related to the conformational preference of **3**; based on the pioneering investigations by Wilson,[9] Herschbach,[10] Bothner-By,[11] and others,[12] the preferred conformation of **3** is assumed to be A. Therefore, hydroboration would take place preferentially from the sterically less hindered α face to yield **4**.

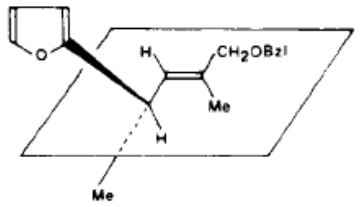

A

We call this Allylic Strain

Methylation of **4** (CH_3I, KH, DMF–THF (1:4), 0 °C, followed by debenzylation (1 atm of H_2, 10% Pd/C, CH_3OH, RT), gave the alcohol **5**[7] (^{1}H NMR ($CDCl_3$) δ 0.96 (3 H, d, J = 7 Hz), 1.27 (3 H, d, J = 7 Hz), 3.21 (3 H, s)) in 88% overall yield. Optical resolution of **5** was achieved in a three-step sequence: (1) (−)-$C_6H_5CH(CH_3)N{=}C{=}O$, Et_3N at 50 °C; (2) separation of the resultant diastereomeric urethanes

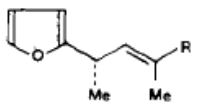

2 R = $CO_2C_2H_5$
3 R = $CH_2OCH_2C_6H_5$

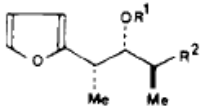

4 R^1 = H, R^2 = $CH_2OCH_2C_6H_5$
5 R^1 = CH_3, R^2 = CH_2OH
6 R^1 = CH_3, R^2 = CHO

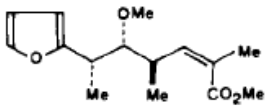

7

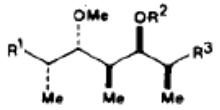

8 R^1 = 2-furyl, R^2 = H, R^3 = CH_2OH
9 R^1 = 2-furyl, R^2 = $CH_2C_6H_5$, R^3 = $CH_2OCH_2OCH_3$
10 R^1 = CO_2CH_3, R^2 = $CH_2C_6H_5$, R^3 = $CH_2OCH_2OCH_3$
11 R^1 = CO_2CH_3, R^2 = $CH_2C_6H_5$, R^3 = CH_2OH

Allylic 1,3-Strain as a Controlling Factor in Stereoselective Transformations

REINHARD W. HOFFMANN

Fachbereich Chemie der Philipps-Universität, Hans-Meerwein-Strasse, D-3550 Marburg, West Germany

Received May 24, 1988 (Revised Manuscript Received August 23, 1989)

Contents

1. Introduction 1841
2. The Concept of Allylic 1,3-Strain 1842
3. Control of Stereoselectivity in Pericyclic Reactions 1843
4. Stereoselective Cyclization Reactions Controlled by Allylic 1,3-Strain 1844
   4.1. Intermolecular Cycloadditions 1844
   4.2. Intramolecular Cycloadditions 1845
   4.3. Iodolactonization Reactions and Related Processes 1846
   4.4. Other Intramolecular Cyclization Reactions 1846
5. Stereoselective Intermolecular Addition Reactions to Double Bonds Controlled by Allylic 1,3-Strain 1847
   5.1. Hydrogenation 1847
   5.2. Hydroboration 1847
   5.3. Epoxidation and Cyclopropanation 1848
6. Diastereoselective Enolate Alkylations Controlled by Allylic 1,3-Strain 1850
7. Chirality Transfer in Reactions of Allylsilanes and Allylboronates 1850
8. Nucleophilic Addition to Double Bonds Controlled by Allylic 1,3-Strain 1851
9. Reactions of Benzylic Systems Controlled by Allylic 1,3-Strain 1853
10. Allylic 1,3-Strain Control of Diastereoselective Reactions Involving Heteroallyl Systems 1853
    10.1. 2-Azaallyl Systems 1853
    10.2. 2-Oxoniaallyl Systems 1854

Prof. Reinhard W. Hoffmann was born in 1933 in Würzburg. He studied chemistry at the Universität Bonn from 1951 to 1958 and received his Dr. rer. nat. with a theses under the direction of Prof. B. Helferich, a former student of Emil Fischer. Prof. Hoffmann spent 2 years as a postdoctoral fellow at The Pennsylvania State University with Prof. G. W. Brindley in the Department of Ceramic Technology followed by another postdoctoral year with Prof. G. Wittig at the Universität Heidelberg working in benzyne chemistry. Subsequent independent studies on heterolytic fragmentation of azo compounds led to the habilitation in 1964. In 1967 Prof. Hoffmann moved as a dozent to the Technische Hochschule Darmstadt and in 1970 to his present position as Professor of Organic Chemistry at the Philipps-Universität Marburg. Over the years Prof. Hoffmann held visiting professorships at the Universität Bern, University of Wisconsin, Madison, and the University of California, Berkeley. His research interests developed from nucleophilic carbenes and electron-rich olefins to the investigation of stereoselective transformations.

The Definition of Allylic Strain

F. Johnson, *Chem. Rev.* **1968**, *68*, 375; *Allylic Strain in Six-Membered Rings*

R. W. Hoffmann, *Chem. Rev.* **1989**, *89*, 1841-1860 **(handout)**

Allylic 1-3-Strain as a Controlling Element in Stereoselective Transformations

Houk, Hoffmann *JACS* **1991**, *113*, 5006

Consider the illustrated general structure where X & Y are permutations of C, N, and O:

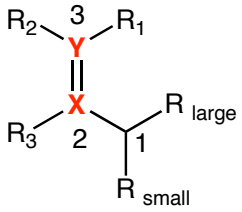

Typical examples:

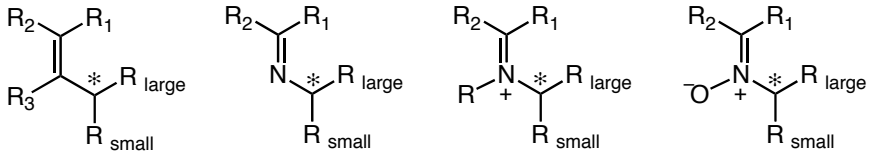

Olefin | Imine | Imonium ion | Nitrone

In the above examples, the resident allylic stereocenter (⁎) and its associated substituents frequently impart a pronounced bias towards reactions occuring at the pi-bond.

Nonbonding interactions between the allylic substituents (R_{large}, R_{small}) & substituents at the 2- & 3-positions play a critical role in defining the stereochemical course of such reactions

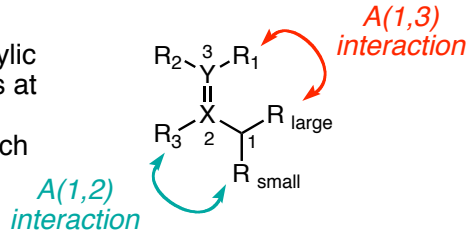

Representative Reactions controlled by Allylic Strain Interactions

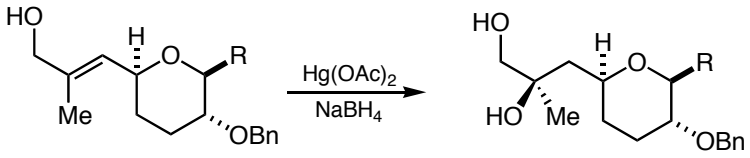

diastereoselection 10:1

M. Isobe & Co-workers, *Tetrahedron Lett.* **1985**, *26*, 5199.

Can you predict the stereochemical outcome of this reaction?

D. Kim & Co-workers, *Tetrahedron Lett.* **1986**, *27*, 943.

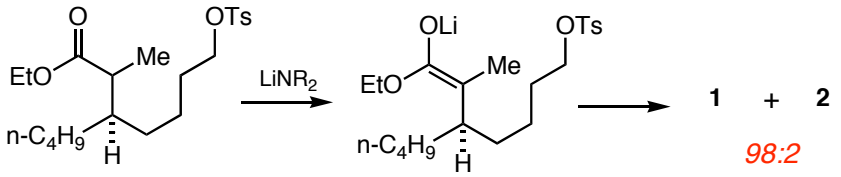

■ Relevant enolate conformations

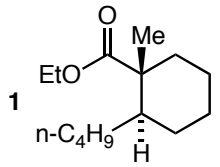

1 ***major***

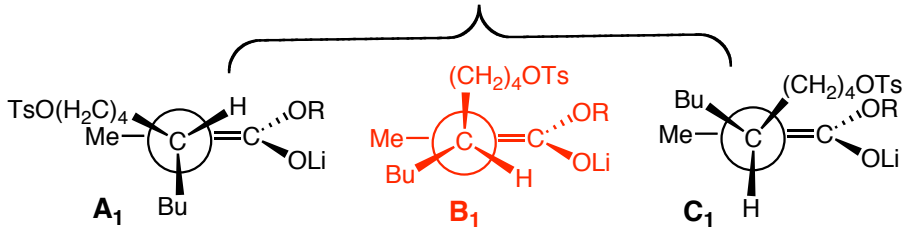

A_1 **B_1** **C_1**

critical conformations

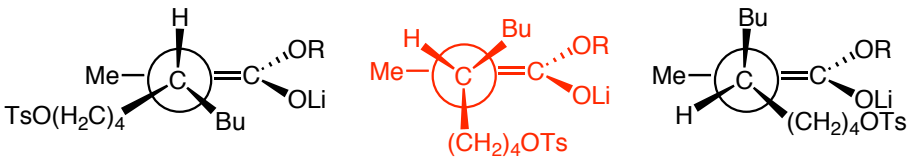

A_2 **B_2** **C_2**

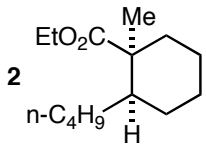

2 ***minor***

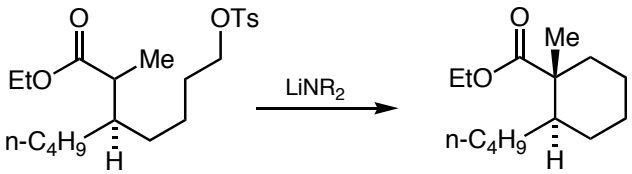

diastereoselection 98:2

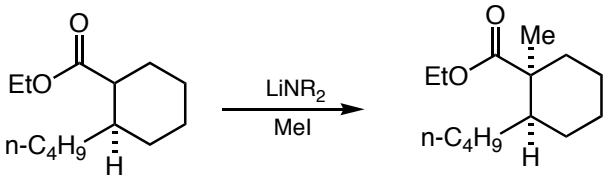

diastereoselection 89:11

D. Kim & Co-workers, *Tetrahedron Lett.* **1986**, *27*, 943.

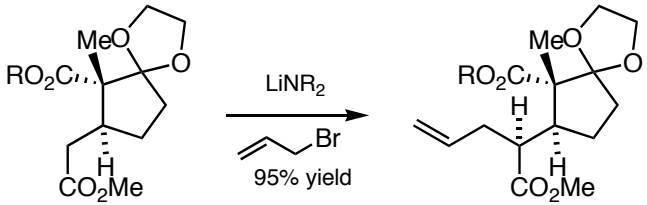

"one isomer"

G. Stork & Co-workers, *Tetrahedron Lett.* **1987**, *28*, 2088.

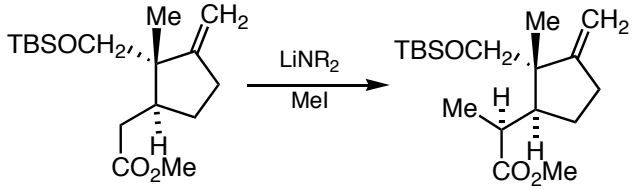

"one isomer"

T. Money & Co-workers, *Chem. Commun.* **1986**, 288.

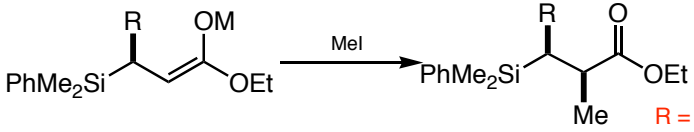

R = Me: *diastereoselection 99:1*

R = Ph: *diastereoselection 97:3*

I. Fleming & Co-workers, *Chem. Commun.* **1984**, 28.

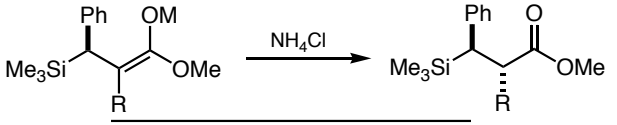

R-substituent	*diastereoselection*
R = Me	87:13
R = Et	80:20
R = $CHMe_2$	40:60 major diastereomer opposite to that shown

I. Fleming & Co-workers, *Chem. Commun.* **1985**, 318.
Y. Yamamoto & Co-workers, *Chem. Commun.* **1984**, 904.

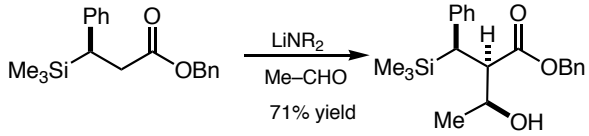

diastereoselection 90:10 at C_3
one isomer at C_2

I. Fleming & Co-workers, *Chem. Commun.* **1986**, 1198.

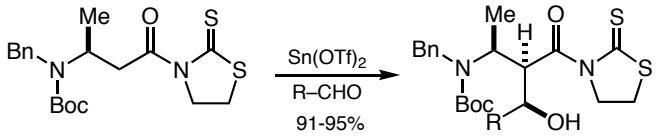

diastereoselection >95%

T. Mukaiyama & Co-workers, *Chem. Letters* **1986**, 637

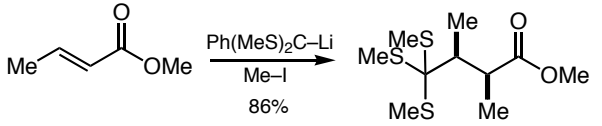

diastereoselection 99:1

K. Koga & Co-workers, *Tetrahedron Letters* **1985**, *26*, 3031.

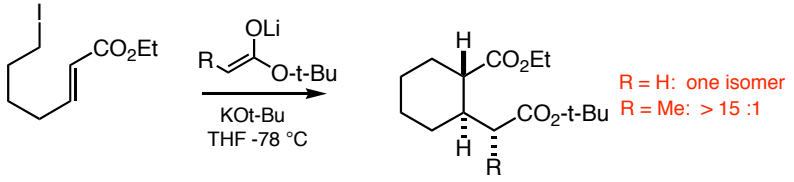

R = H: one isomer
R = Me: > 15 :1

Y. Yamaguchi & Co-workers, *Tetrahedron Letters* **1985**, *26*,1723.

The basic process

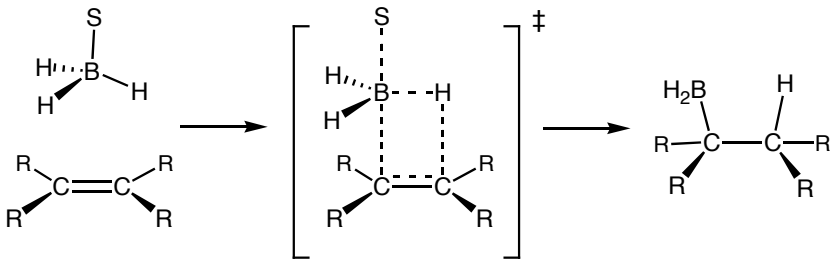

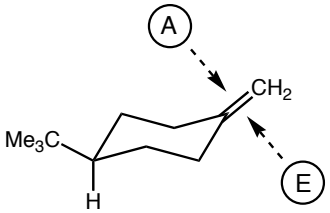

Oxidant	Ratio, A:E	Reference
MCPBA	69:31	*JOC*, **1967**, *32*, 1363
BH_3, H_2O_2	34:66	*JOC*, **1970**, *35*, 2654

Acyclic hydroboration can be controlled by A(1,3) interactions:

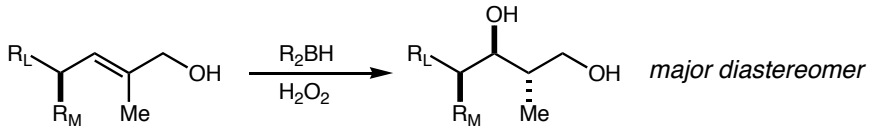

major diastereomer

control elements

A(1,3) allylic strain
Steric effects; R_L vs R_M
Staggered transition states

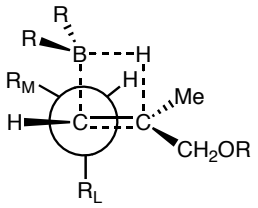

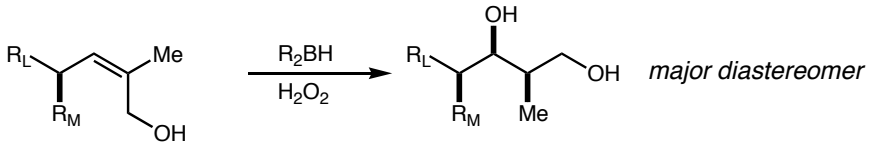

major diastereomer

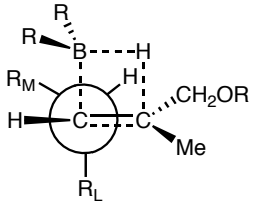

See Houk, *Tetrahedron* **1984**, *40*, 2257

Hydroborations dominated by A(1,3) Strain

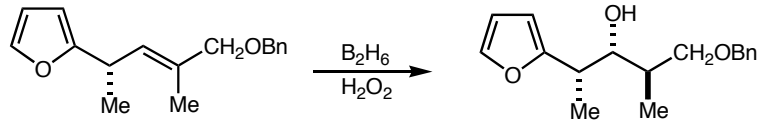

diastereoselection 8:1

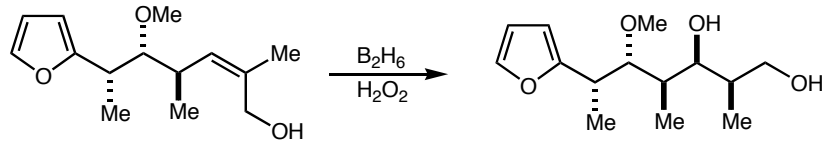

diastereoselection 12:1

Y. Kishi & Co-workers, *J. Am. Chem. Soc.* **1979**, *101*, 259.

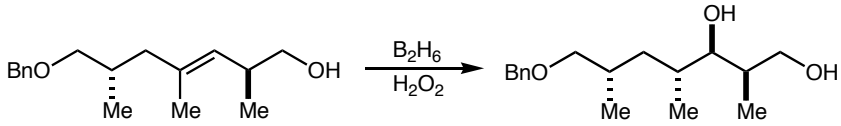

Diastereoselection = 3:1

C. H. Heathcock et. al. *Tetrahedron Lett* **1984** *25* 243.

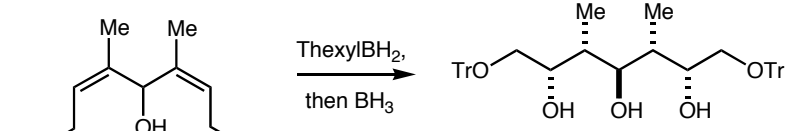

Diastereoselection; 5 : 1

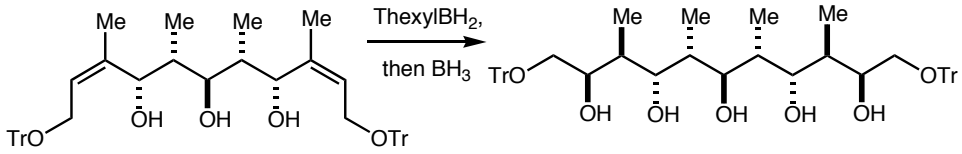

Diastereoselection; 4: 1

Still, W.C.; Barrish, J. C. *J. Am. Chem. Soc.* **1983**, *105*, 2487.

Consider the resonance structures of an amide:

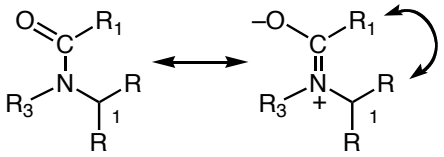

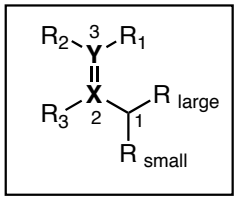

A(1,3) interactions between the "allylic substituent" and the R1 moiety will strongly influence the torsion angle between N & C1.

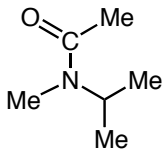

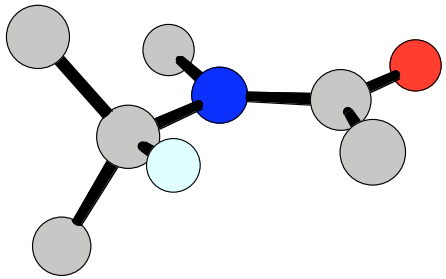

■ conformations of cyclic amides

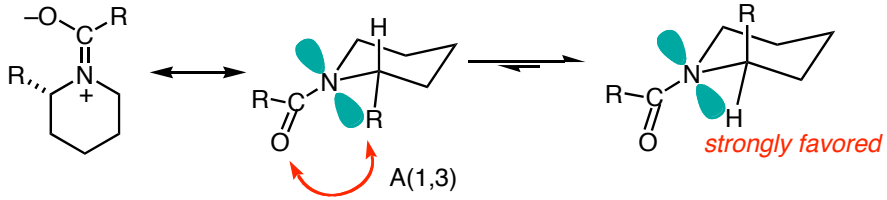

Chow
Can. J. Chem. **1968**, *46*, 2821

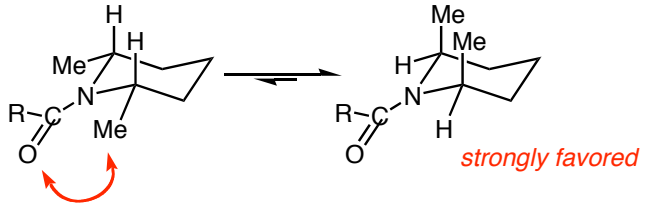

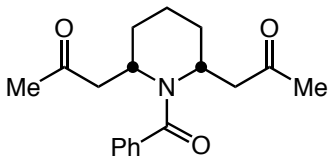

published X-ray structure of this amide shows chair diaxial conformation

Quick, *J. Org. Chem.* **1978**, *43*, 2705

■ Problem: Predict the stereochemical outcome of this cyclization.

D. Hart, *JACS* **1980**, *102*, 397

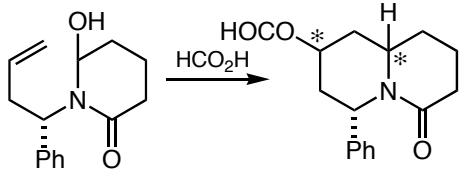

The selection of amide protecting group may be done with the knowledge that altered conformational preferences may result:

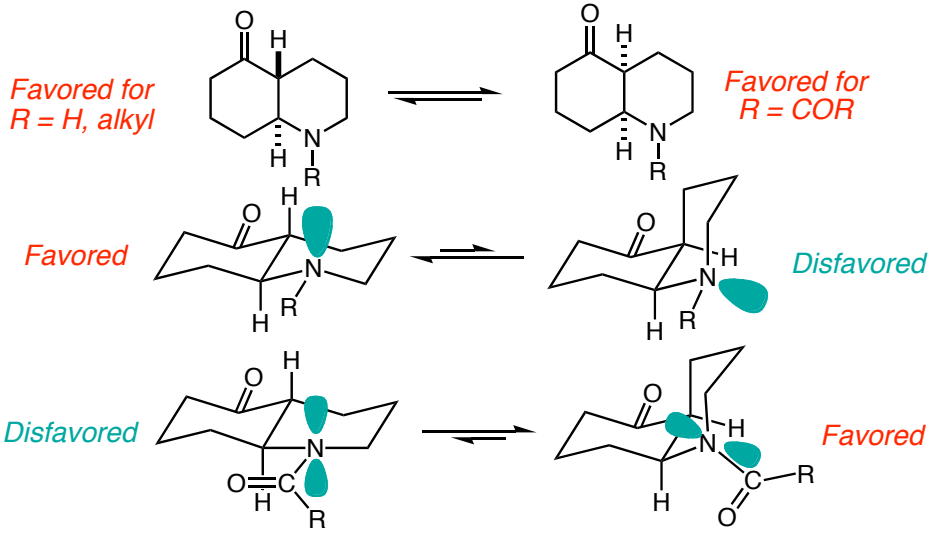

A(1,3) interaction between the C2 & amide substituents will strongly influence the torsion angle between C1 & C2.

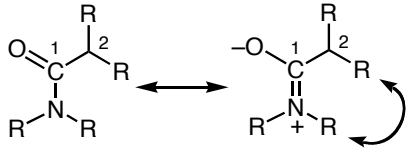

As a result, amides afford (Z) enolates under all conditions

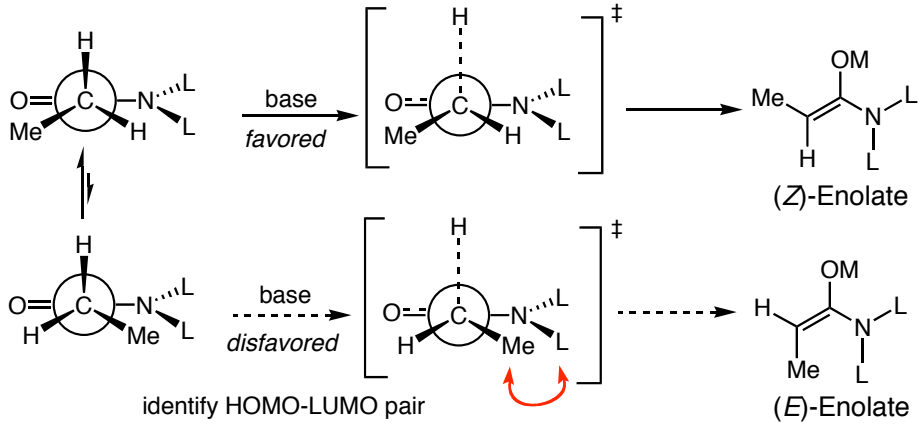

A(1,3) Strain and Chiral Enolate Design

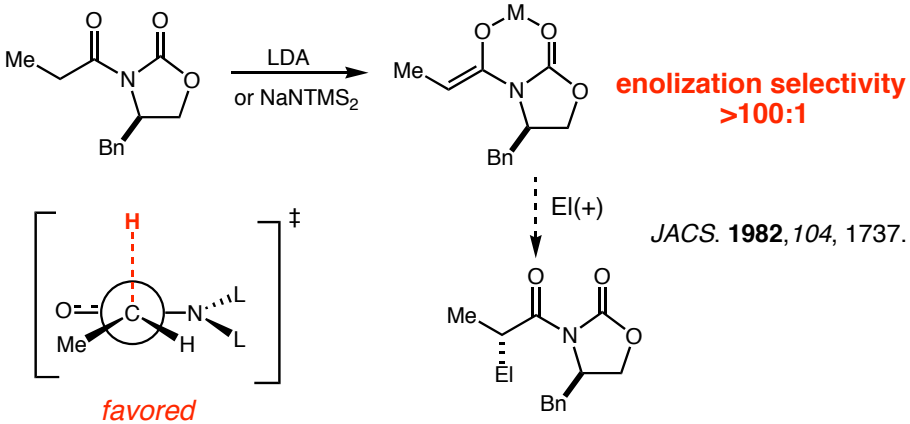

JACS. **1982**,*104*, 1737.

■ In the enolate alkylation process product epimerization is a serious problem. Allylic strain suppresses product enolization through the intervention of allylic strain

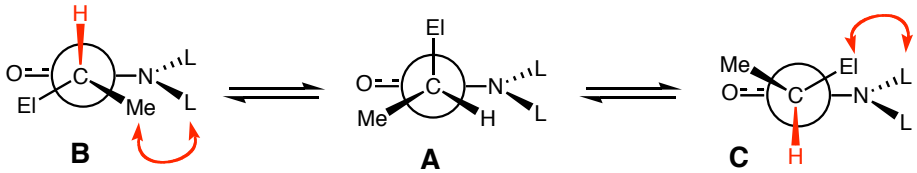

While conformers **B** and **C** meet the stereoelectronic requirement for enolization, they are much higher in energy than conformer **A**. Further, as deprotonation is initiated, A(1,3) destabilization contributes significantly to reducing the kinetic acidity of the system

These allylic strain attributes are an integral part of the design criteria of chiral amide and imide-based enolate systems

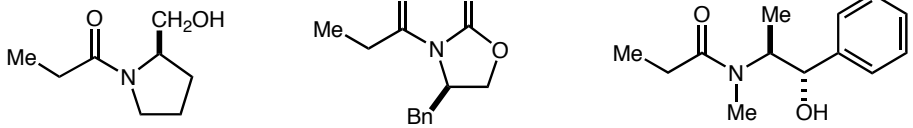

Evans
Tetr Lett. **1977**, *29*, 2495

Evans
JACS **1982**,*104*, 1737.

Myers
JACS **1997**, *119*, 6496

Polypropionate Biosynthesis: The Acylation Event

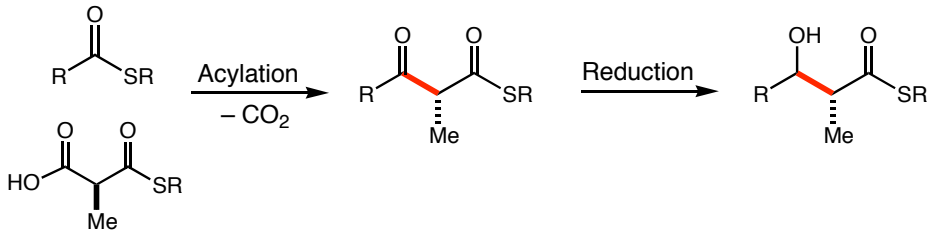

First laboratory analogue of the acylation event

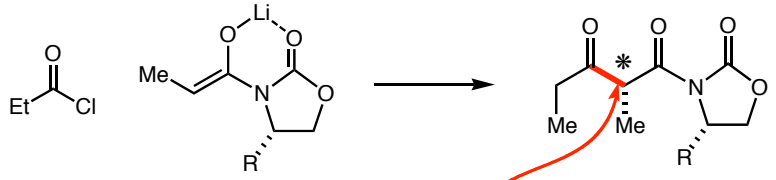

with M. Ennis JACS ***1984****, 106, 1154.*

Diastereoselection ~ 97 : 3

Why does'nt the acylation product rapidy epimerize at the exocyclic stereocenter??

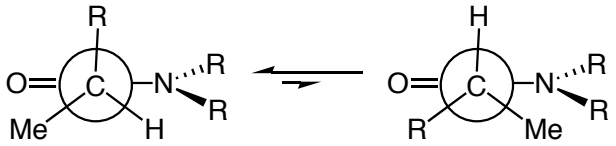

favored

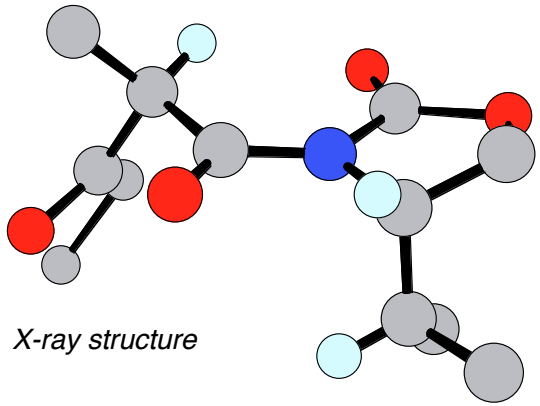

X-ray structure

Discodermolide

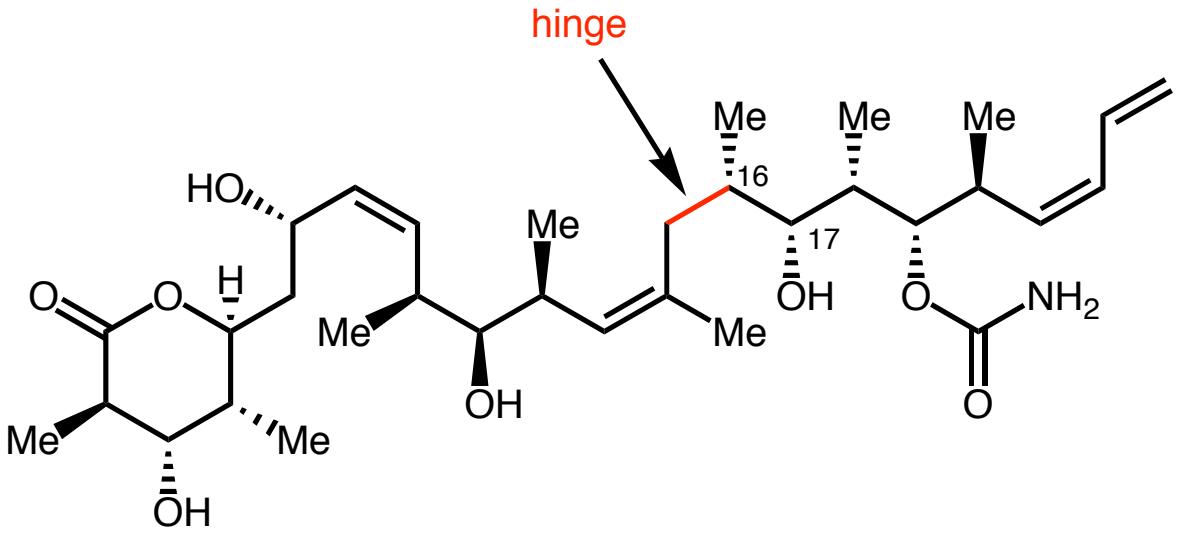

- immunosuppressive activity
- potent microtubule-stabilizing agent
(antitumor activity similar to that of taxol)

The epimers at C16 and C17 have no or almost no biological activity.

The conformation about C16 and C17 is critical to discodermolide's biological activity.

S. L. Schreiber et al. *JACS* **1996**, *118*, 11061.

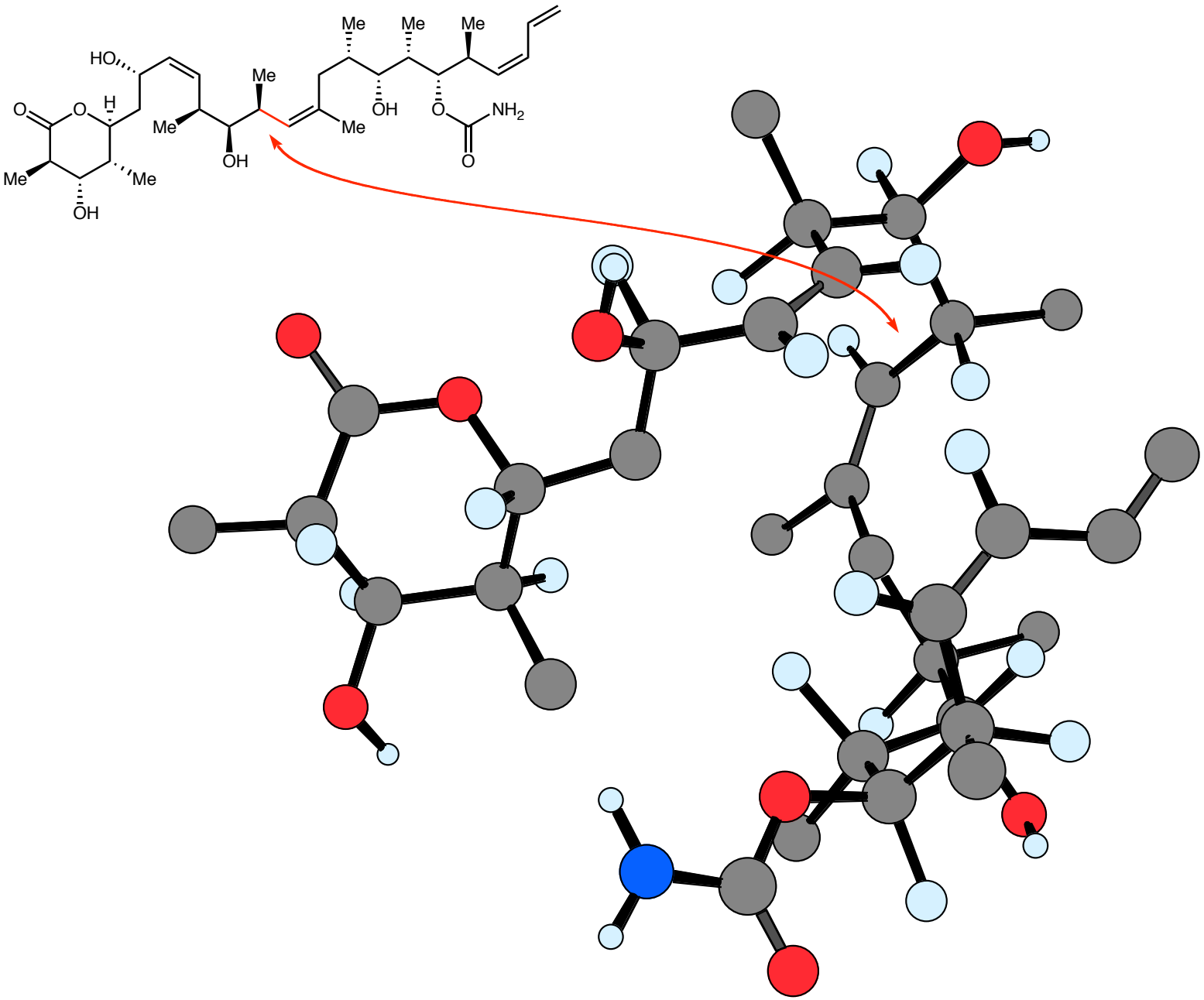
HO
H
O
O
Me
Me
Me
OH
Me
Me
Me
Me
Me
OH
O
NH2
O
Me
OH

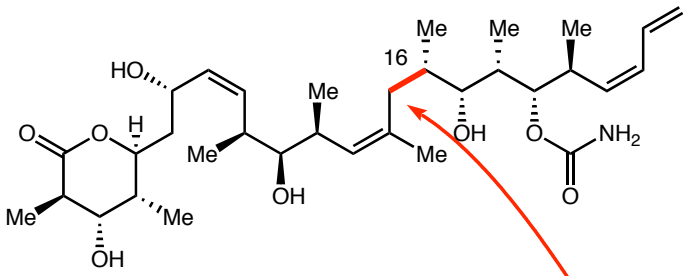
HO
H
O
O
Me
Me
OH
Me
Me
16
Me
Me
Me
OH
O
NH2
O
Me
Me
OH

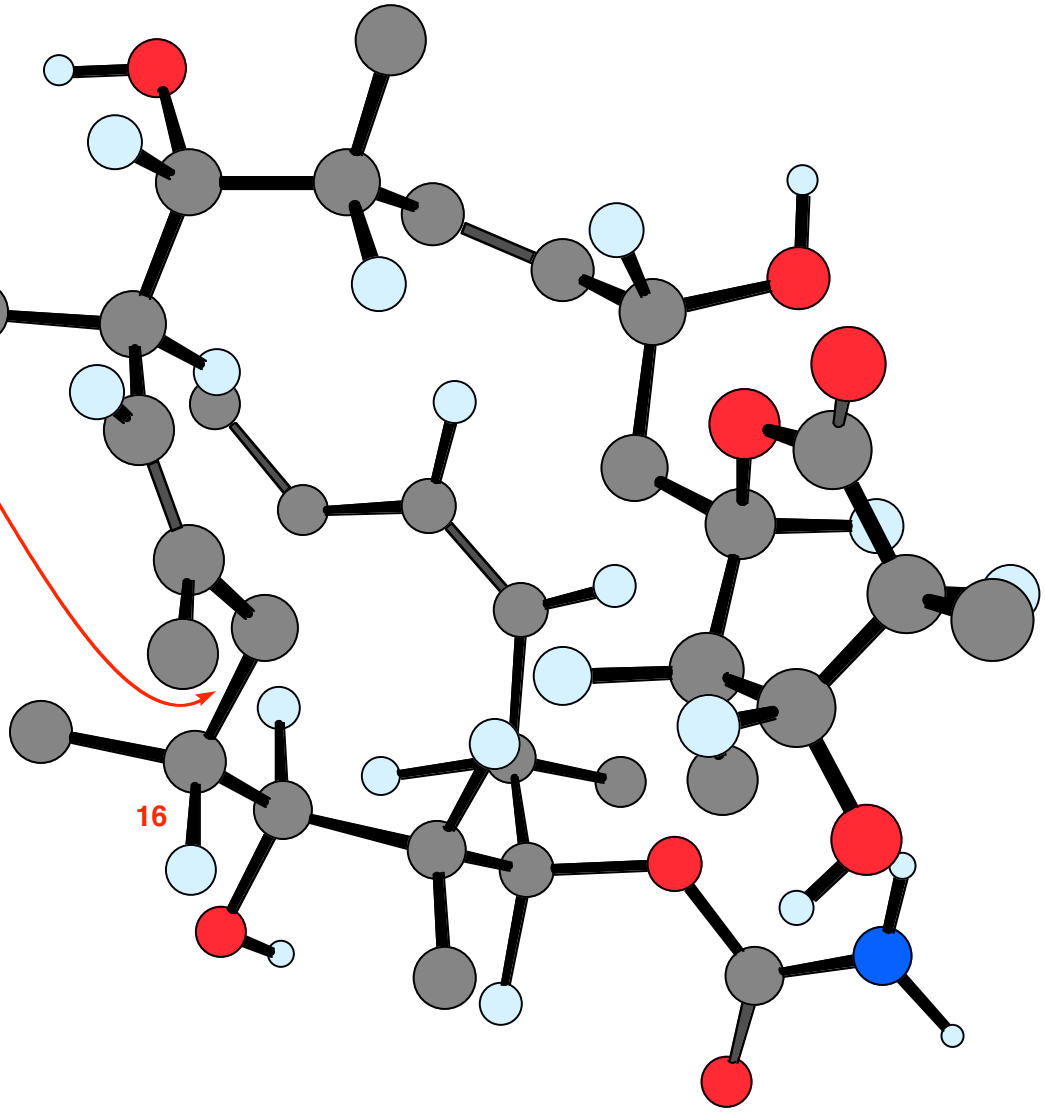
16

http://www.courses.fas.harvard.edu/colgsas/1063

Chemistry 206

Advanced Organic Chemistry

Lecture Number 6

Conformational Analysis-3

- Conformational Analysis of $C_4 \rightarrow C_6$ Rings

- Reading Assignment for week

A. Carey & Sundberg: **Part A**; Chapter 3

Eliel & Wilen, "Stereochemistry of Organic Compounds, "Chapter 11, Configuration and Conformation of Cyclic Molecules, Wiley, 1994

Ribeiro & Rittner, "The Role of Hyperconjugation in the Conformational Analysis of Methylcyclohexane and Methylheterocyclohexanes"
J. Org. Chem., **2003**, *68*, 6780-6787 **(handout)**

Stability Relationships in Bicyclic Ketones,
Synlett **2005,** 2911-2914 **(handout)**

The Application of Cyclobutane Derivatives in Organic Synthesis
Chem Rev. 2003, 103, 1485-1537 **(pdf)**

de Meijere, "Bonding Properties of Cyclopropane & their Chemical Characteristics"
Angew Chem. Int. Ed. **1979**, *18*, 809-826 **(pdf)**

The Application of Cyclobutane Derivatives in Organic Synthesis
Chem. Rev. **2003,** *103,* 1485-1537 **(pdf)**

D. A. Evans

Friday,
September 29, 2006

Conformational Analysis of Cyclic Systems

Three Types of Strain:

Prelog Strain: van der Waals interactions

Baeyer Strain: bond angle distortion away from the ideal

Pitzer Strain: torsional rotation about a sigma bond

Baeyer Strain for selected ring sizes

size of ring	Ht of Combustion (kcal/mol)	Total Strain (kcal/mol)	Strain per CH_2 (kcal.mol)	"angle strain" deviation from 109°28'
3	**499.8**	**27.5**	9.17	24°44'
4	656.1	26.3	6.58	9°44'
5	793.5	6.2	1.24	0°44'
6	**944.8**	**0.1**	0.02	-5°16'
7	1108.3	6.2	0.89	
8	1269.2	9.7	1.21	
9	**1429.6**	**12.6**	1.40	
10	**1586.8**	**12.4**	1.24	
11	**1743.1**	**11.3**	1.02	
12	1893.4	4.1	0.34	
13	2051.9	5.2	0.40	
14	2206.1	1.9	0.14	
15	2363.5	1.9	0.13	

Eliel, E. L., Wilen, S. H. *Stereochemistry of Organic Compounds*
Chapter 11, John Wiley & Sons, 1994.

- Baeyer "angle strain" is calculated from the deviation of the *planar* bond angles from the ideal tetrahedral bond angle.

- Discrepancies between calculated strain/CH_2 and the "angle strain" results from puckering to minimize van der Waals or eclipsing torsional strain between vicinal hydrogens.

Problem: Rationalize the regioselectivity of the following reduction

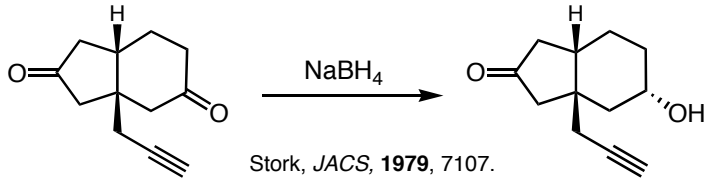

Stork, *JACS,* **1979**, 7107.

Cyclopropane

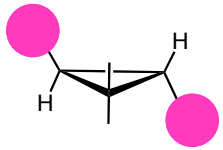

- Necessarily *planar*.
- Subtituents are therefore eclipsed.
- Disubstitution prefers to be *trans*.

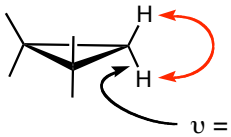

- Almost sp^2, not sp^3

Walsh Model for Strained Rings:

- Rather than σ and σ* c-c bonds, cyclopropane has sp^2 and p-type orbitals instead.

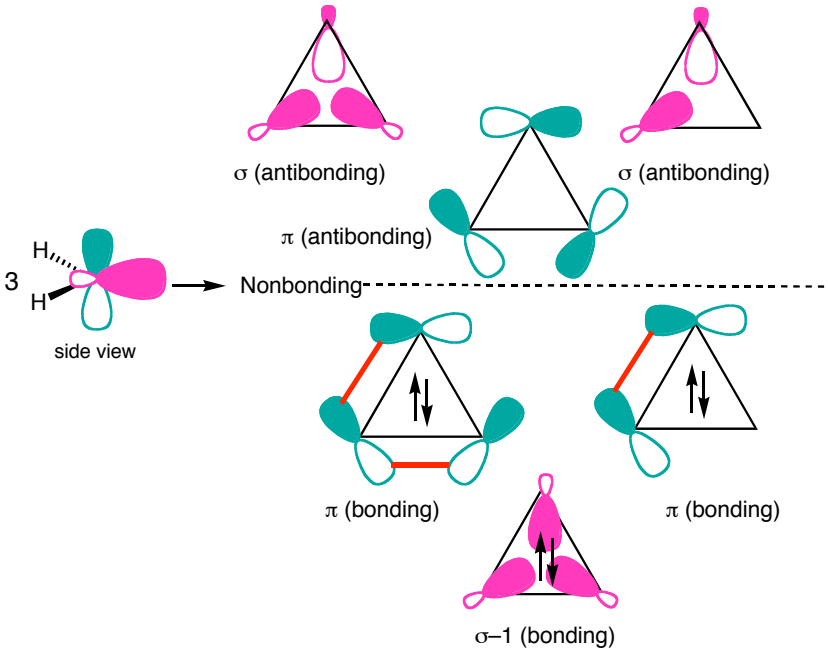

de Meijere, "Bonding Properties of Cyclopropane & their Chemical Characteristics" *Angew Chem. Int. Ed.* **1979**, *18*, 809-826 **(handout)**

de Meijere, A.; Wessjohann, L. "Tailoring the Reactivity of Small Ring Building Blocks for Organic Synthesis." *Synlett* **1990**, 20. **(pdf)**

Carbocation Stabilization via Cyclopropylgroups

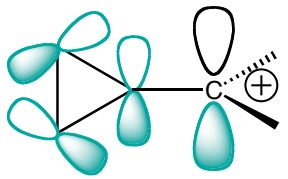

A rotational barrier of about 13.7 kcal/mol is observed in following example:

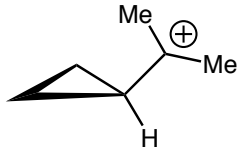

NMR in super acids $\delta(CH_3)$ = 2.6 and 3.2 ppm

X-ray Structures support this orientation

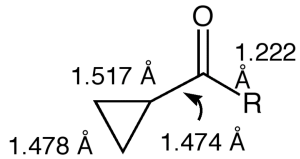

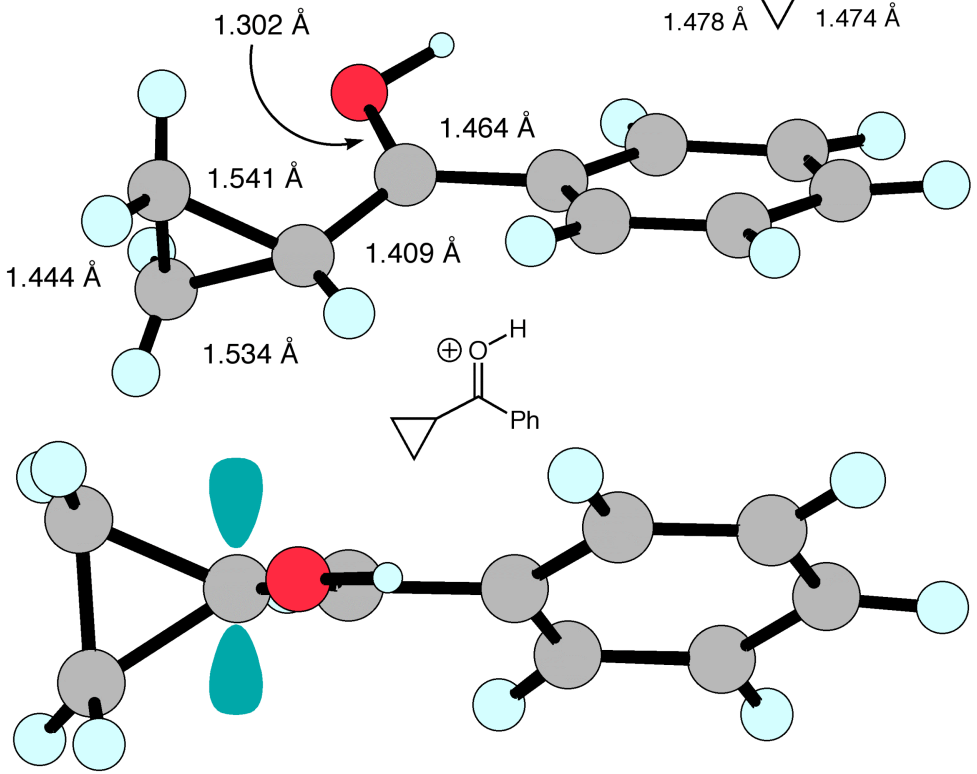

R. F. Childs, *JACS* **1986**, *108*, 1692

Cyclobutane

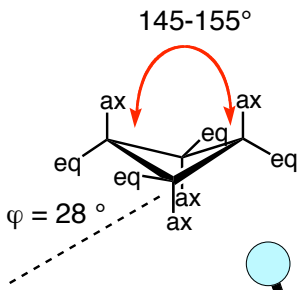

■ Eclipsing torsional strain overrides increased bond angle strain by puckering.

■ Ring barrier to inversion is 1.45 kcal/mol.

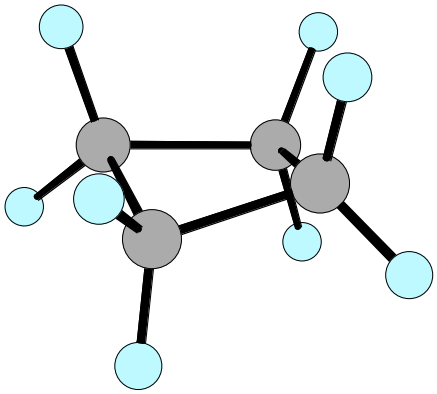

(MM2)

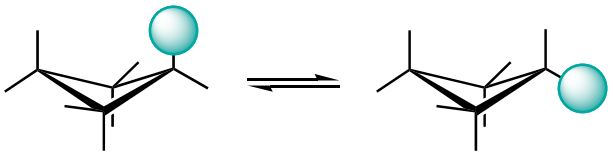

■ **ΔG = 1 kcal/mol favoring R = Me equatorial**

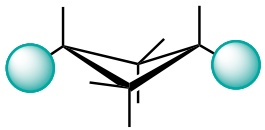

■ 1,3 Disubstitution prefers *cis* diequatorial to *trans* by 0.58 kcal/mol for di-bromo cmpd.

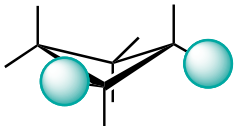

■ 1,2 Disubstitution prefers *trans* diequatorial to *cis* by 1.3 kcal/mol for diacid (roughly equivalent to the cyclohexyl analogue.)

Cyclopentane

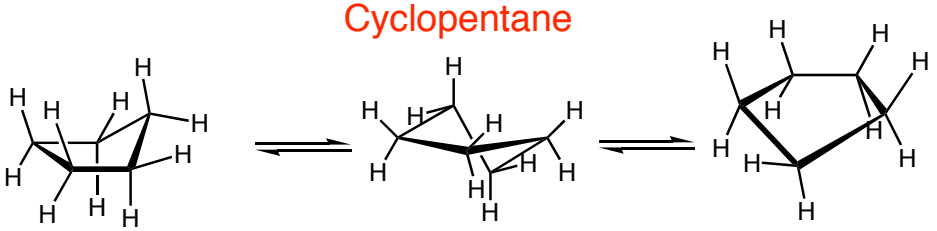

■ Two lowest energy conformations (10 envelope and 10 half chair conformations C_s favored by only 0.5 kcal/mol) in rapid conformational flux (pseudorotation) which causes the molecule to appear to have a single out-of-plane atom "bulge" which rotates about the ring.

■ Since there is no "natural" conformation of cyclopentane, the ring conforms to minimize interactions of any substituents present.

C_sEnvelope

(MM2)

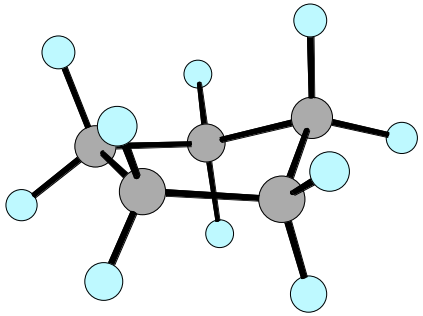

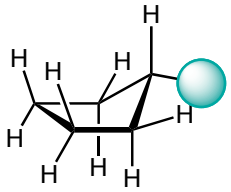

■ A single substituent prefers the equatorial position of the flap of the envelope (barrier ca. 3.4 kcal/mol, R = CH_3).

■ 1,2 Disubstitution prefers *trans* for steric/torsional reasons (alkyl groups) and dipole reasons (polar groups).

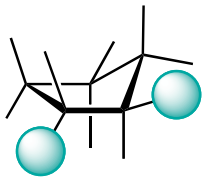

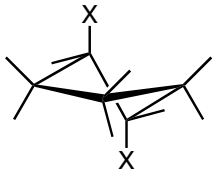

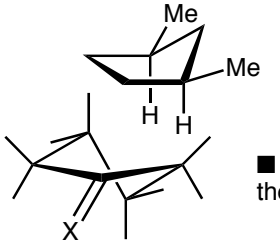

■ 1,3 Alkyl Disubstitution: **Cis**-1,3-dimethyl cyclopentane 0.5 kcal/mol **more stable** than trans.

■ A carbonyl or methylene prefers the planar position of the half-chair (barrier 1.15 kcal/mol for cyclopentanone).

Methylenecyclopentane and Cyclopentene

Strain trends:

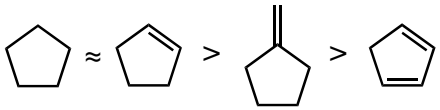

■ Decrease in eclipsing strain more than compensates for the increase in angle strain.

Relative to cyclohexane derivatives, those of cyclopentane prefer an sp^2 center in the ring to minimize eclipsing interactions.

"Reactions will proceed in such a manner as to favor the formation or retention of an exo double bond in the 5-ring and to avoid the formation or retention of the exo double bond in the 6-ring systems." Brown, H. C., Brewster, J. H.; Shechter, H. *J. Am. Chem. Soc.* **1954**, *76*, 467.

Examples:

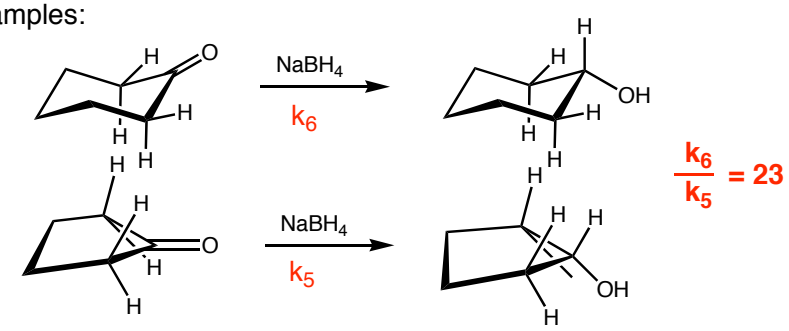

Brown, H. C.; Ichikawa, K. *Tetrahedron* **1957**, *1*, 221.

Problem: Rationalize the regioselectivity of the following reduction

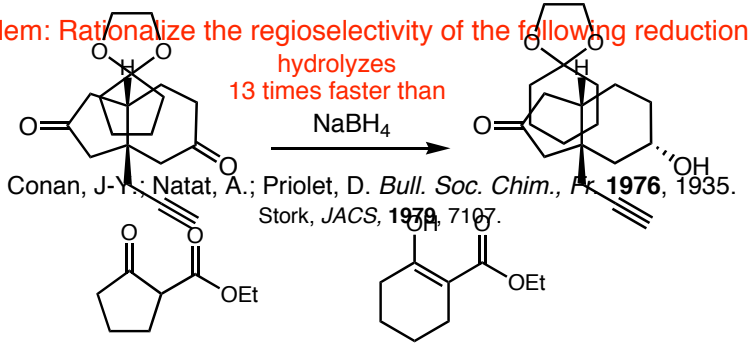

Conan, J-Y.; Natat, A.; Priolet, D. *Bull. Soc. Chim., Fr.* **1976**, 1935.
Stork, *JACS*, **1979**, 7107.

95.5:4.5 keto:enol

76:24 enol:keto

Brown, H. C., Brewster, J. H.; Shechter, H. *JACS* **1954**, *76*, 467.

Cyclohexane Energy Profile (kcal/mol)

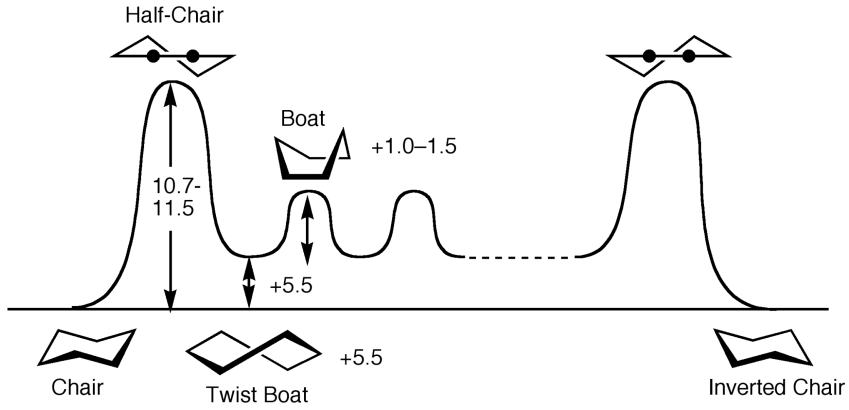

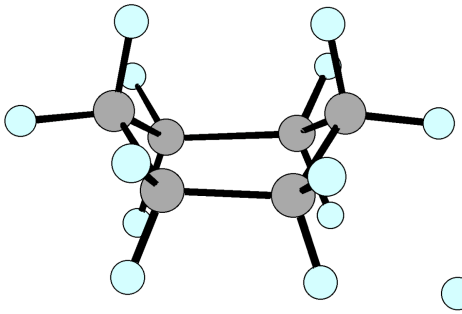

ΔE = +6.5-7.0

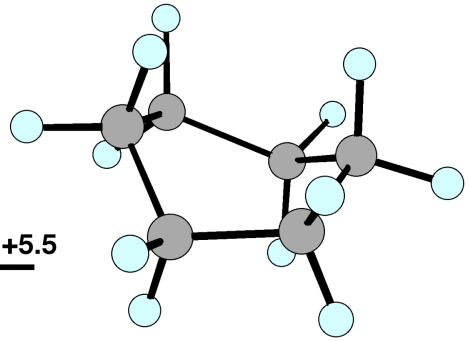

ΔE = +5.5

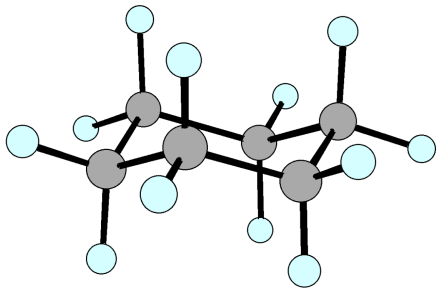

The barrier: +10.7-11.5

E = 0

"Total Synthesis of the Antifungal Macrolide Antibiotic (+)-Roxaticin," Evans, D. A.; Connell, B. T.
J. Am. Chem. Soc., **2003**, *125*, 10899-10905

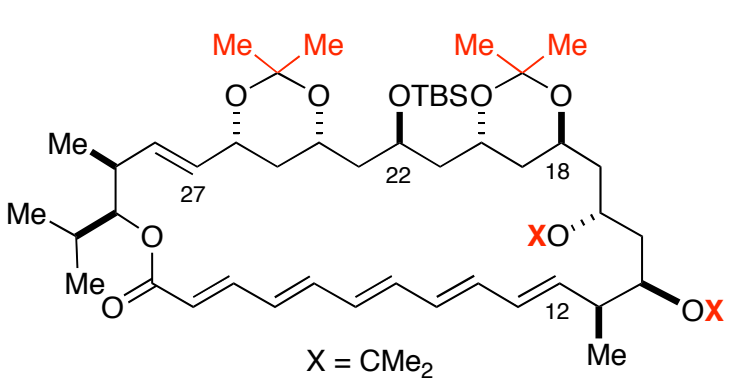

X = CMe_2

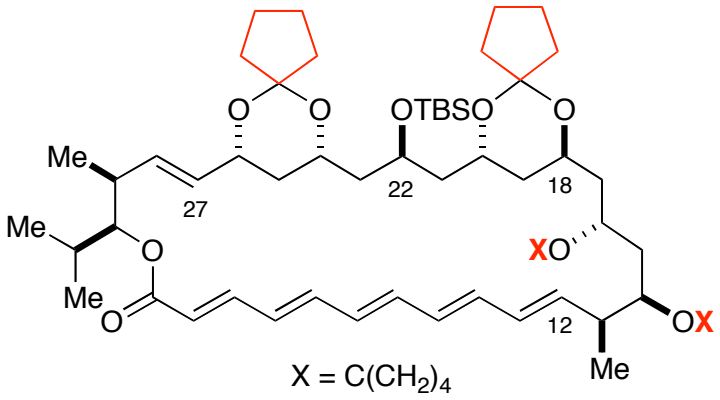

X = $C(CH_2)_4$

<10% | PPTS, rt, MeOH.

63% | PPTS, rt, MeOH.

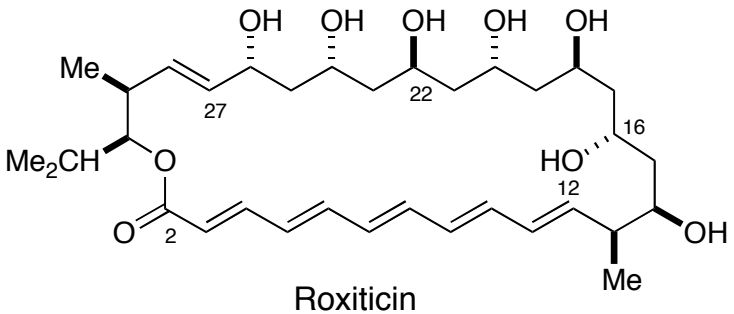

Roxiticin

hydrolyzes
13 times faster than

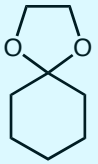

Conan, J-Y.; Natat, A.; Priolet, D. *Bull. Soc. Chim., Fr.* **1976**, 1935.

Zaragozic Acid C Synthesis

J. Leighton, J. Barrow

JACS **1994,** *116,* 12111-12112

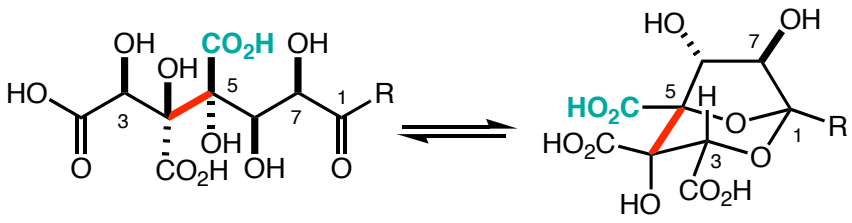

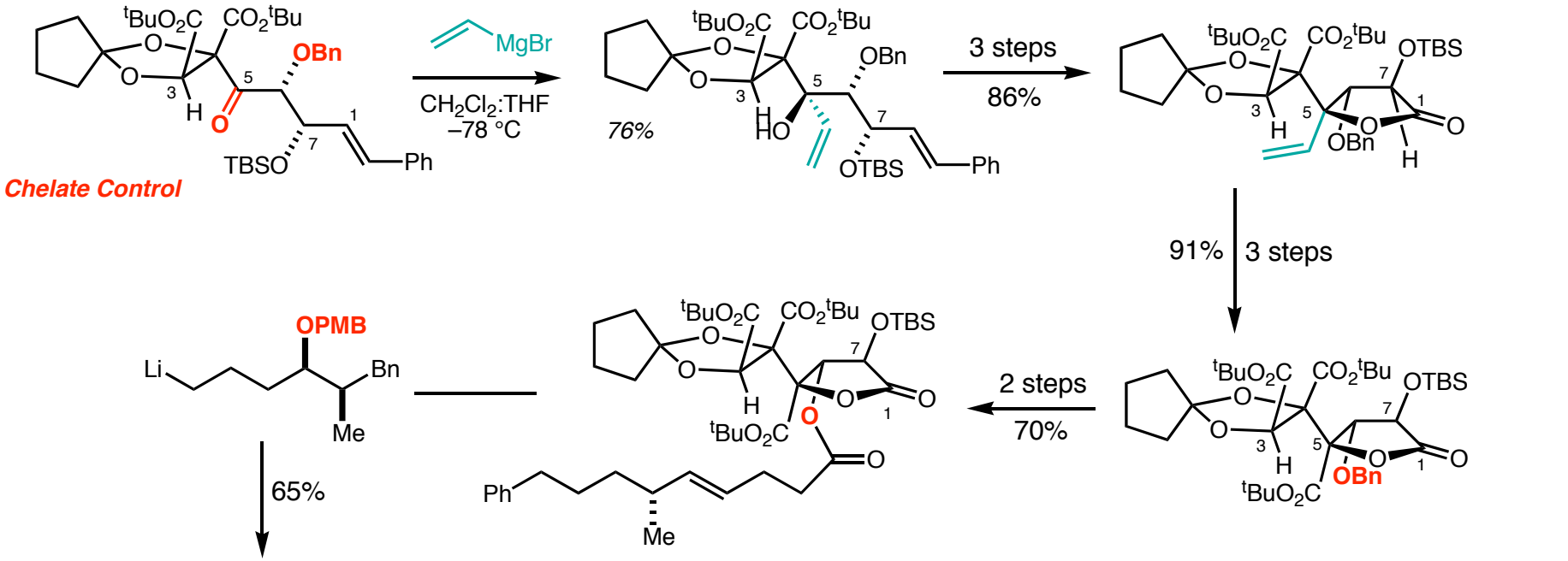

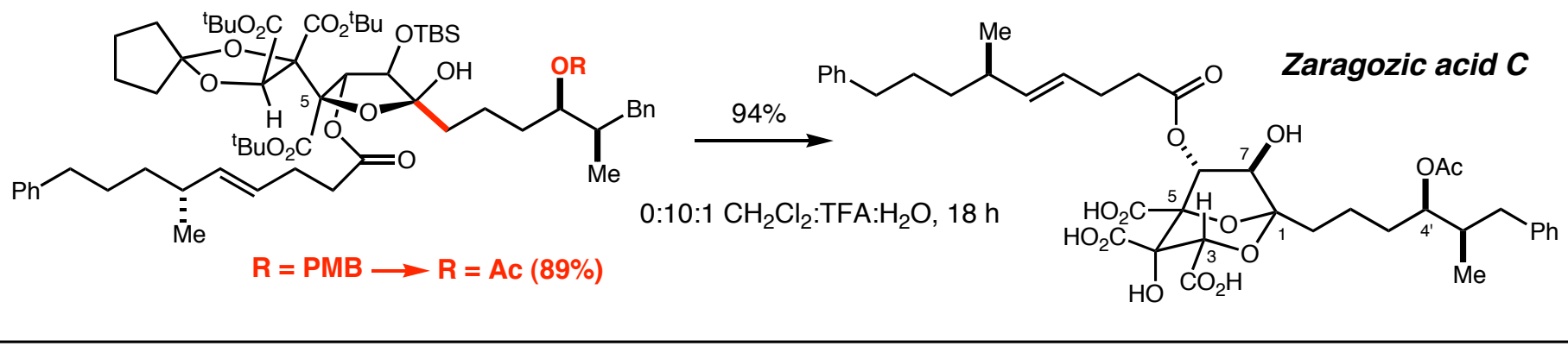

Monosubstituted Cyclohexanes: *A* Values

- Me–axial has **2 gauche butane interactions** more than Me–equatorial.
  Expected destabilization: ≈ 2(0.88) kcal/mol = ~1.8 kcal/mol;
  Observed: 1.74 kcal/mol

- The *A*– Value, or -ΔG°, is the preference of the substituent for the equatorial position.

Table 3.6. Conformational Free Energies ($-\Delta G°$) for Substituent Groups[a]

Substituent	$-\Delta G°$ (kcal/mol)	Reference
–F	0.24–0.28	b
–Cl	0.53	b
–Br	0.48	b
–I	0.47	b
$-CH_3$	1.8	c
$-CH_2CH_3$	1.8	c
$-CH(CH_3)_2$	2.1	c
$-C(CH_3)_3$	> 4.5	d
$-CH=CH_2$	1.7	e
$-C\equiv CH$	0.5	f
$-C_6H_5$	2.9	e
–CN	0.15–0.25	b
$-O_2CCH_3$	0.71	b
$-CO_2H$	1.35	d
$-CO_2C_2H_5$	1.1–1.2	d
–OH (aprotic solvents)	0.52	d
–OH (protic solvents)	0.87	d
$-OCH_3$	0.60	d
$-NO_2$	1.16	b
–HgBr	0	b

C & S, Part A, pg 140

A Values depend on the *relative size* of the particular substituent.

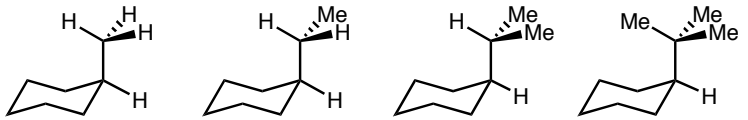

A–Value 1.74 1.80 2.15 5.0

The "relative size" of a substituent and the associated A-value may not correlate. For example, consider the $-CMe_3$ and $-SiMe_3$ substituents. While the $-SiMe_3$ substituent has a larger covalent radius, it has a smaller A-value:

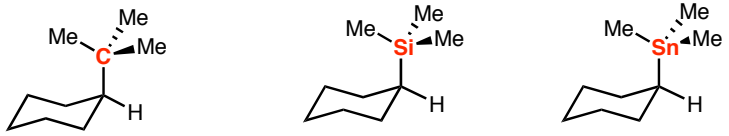

A–Value 4.5-5.0 2.5 1.1

Can you explain these observations?

- The impact of double bonds on A-values:

Lambert, *Accts. Chem. Res.* **1987**, *20*, 454

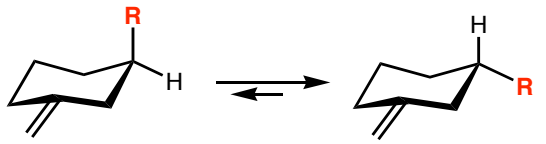

substituent	$-\Delta G°$	A-value (cyclohexane)
R = Me	0.8	1.74
R = OMe	0.8	0.6
R = OAc	0.6	0.71

The Me substituent appears to respond strictly to the decrease in nonbonding interactions in axial conformer. With the more polar substituents, electrostatic effects due to the trigonal ring carbon offset the decreased steric environment.

Bond Lengths and A-Values of Methyl Halides

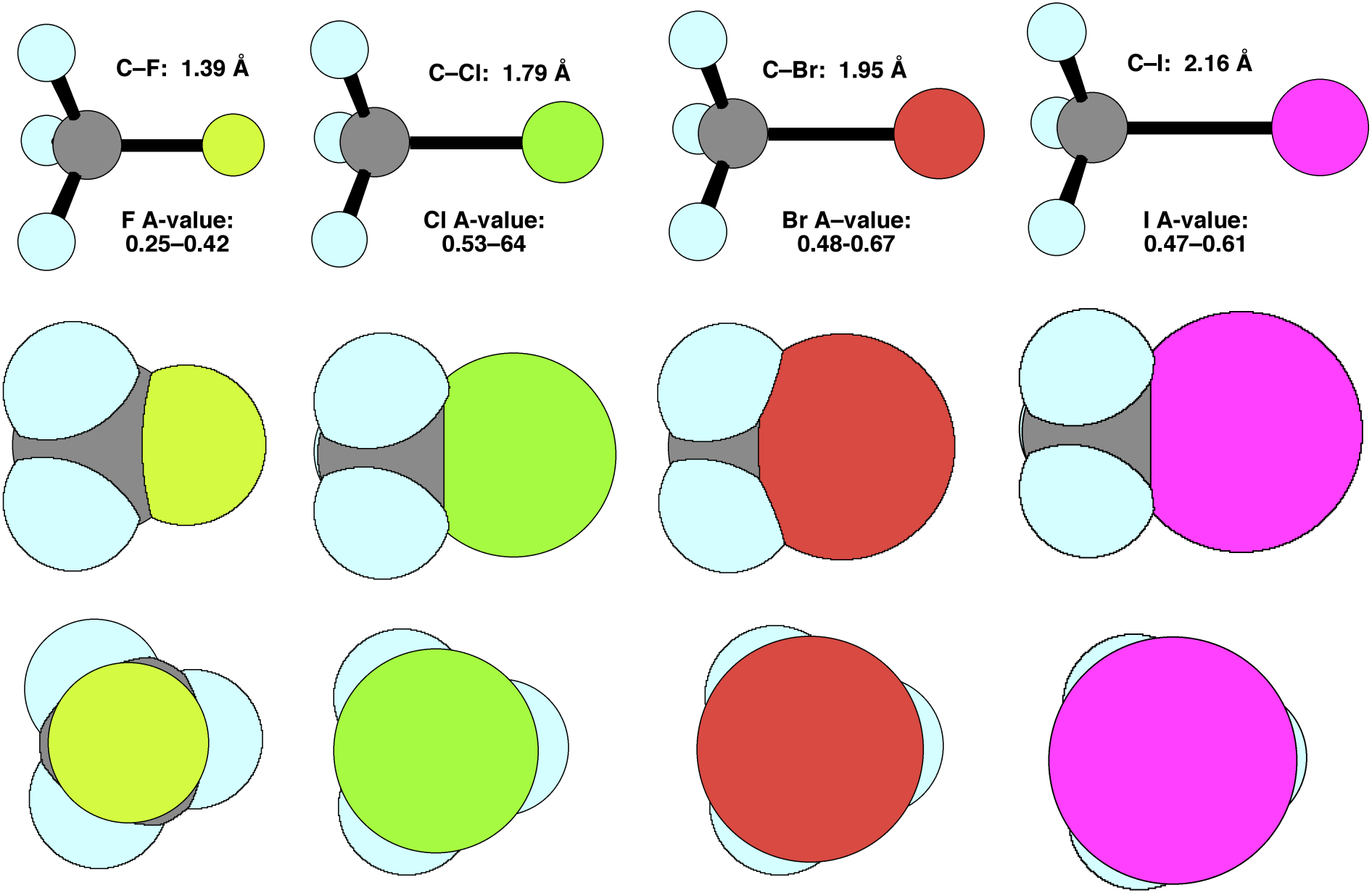

Chem 3D Pro (Verson 5.0)

Impact of Trigonal Carbon

- Let's now compare look at the carbonyl analog in the 3-position

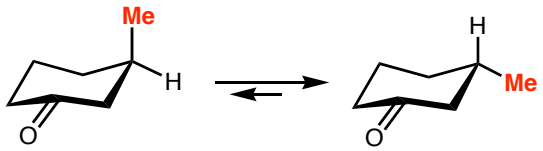

ΔG° = –1.36 kcal/mol
versus –1.74 for cyclohexane

- Let's now compare look at the carbonyl analog in the 2-position

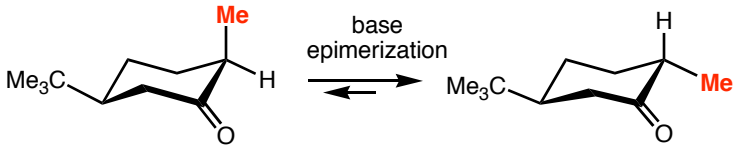

ΔG° = –1.56 kcal/mol
versus –1.74 for cyclohexane

However, the larger alkyl groups do not follow the expected trend. Can you explain? (see Eliel, page 732)

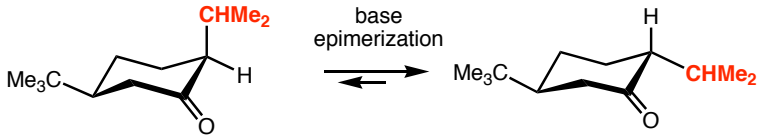

ΔG° = –0.59 kcal/mol
versus –2.15 for cyclohexane

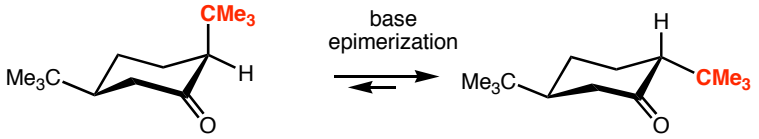

ΔG° = –1.62 kcal/mol
versus –5.0 for cyclohexane

Polysubstituted Cyclohexane *A* Values

- As long as the substituents on the ring do not interact in either conformation, their A-values are roughly additive

1,4 Disubstitution: *A* Values are roughly additive.

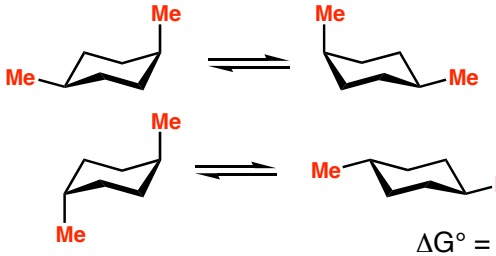

ΔG° = 0 kcal/mol

ΔG° = –2(1.74) = –3.48 kcal/mol

1,3 Disubstitution: *A* Values are only additive in the trans diastereomer

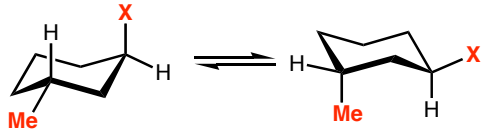

ΔG° = A(Me) – A(X)

The cis Isomer

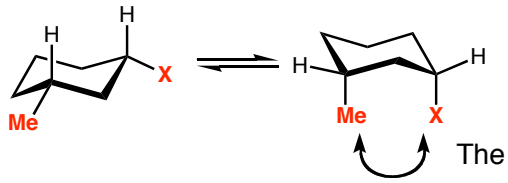

The new interaction!

For X = Me

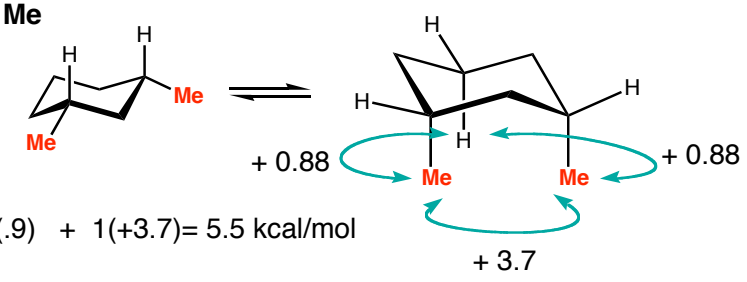

ΔG° = 2(.9) + 1(+3.7)= 5.5 kcal/mol

Let's now consider geminal substitution

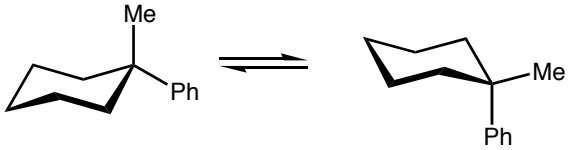

The prediction: $\Delta G° = A(Ph) - A(Me)$

$\Delta G° = +2.8 - 1.7 = +1.1$ kcal/mol

Observed: $\Delta G° = -0.32$ kcal/mol

Hence, when the two substituents are mutually interacting you can predict neither the magnitude or the direction of the equilibrium. Let's analyze this case.

Allinger, *Tet. Lett.* 1971, 3259

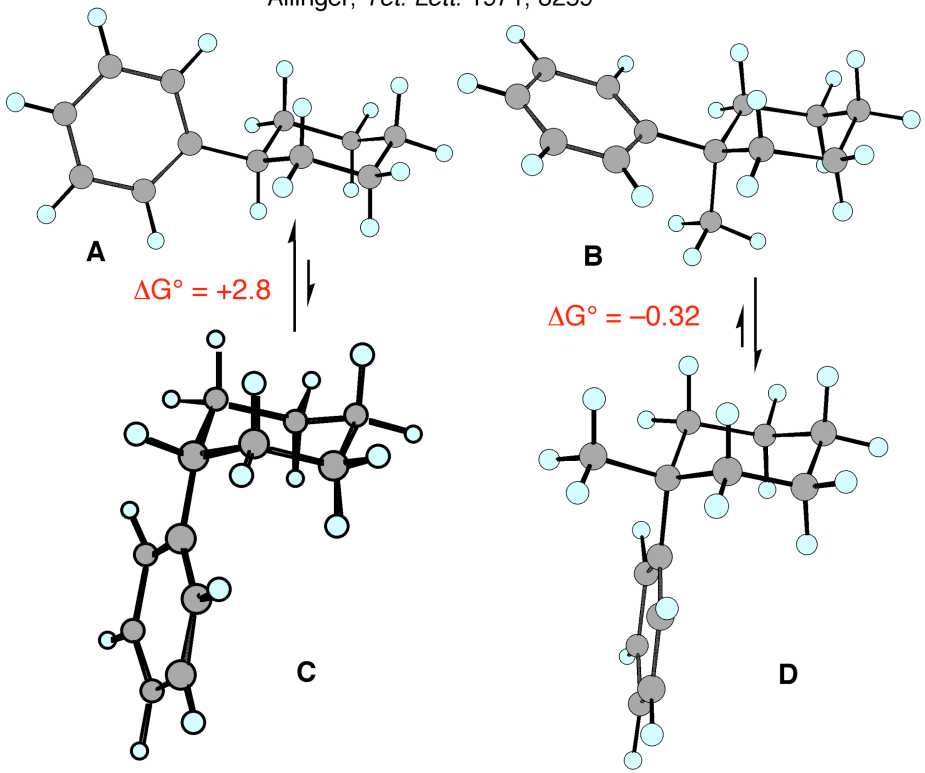

Note the difference in the Ph substituent in **A** & **B**.

Let's now consider vicinal substitution

Case 1:

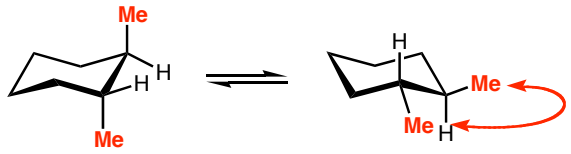

The prediction: $\Delta G°$ = 1 gauche butane – 2A(Me)

$\Delta G° = +0.88 - 2(1.74) = +2.6$ kcal/mol

Observed: $\Delta G° = +2.74$ kcal/mol

If the added gauche butane destabilization in the di-equatorial conformer had not been added, the estimate would have been off.

Case 2:

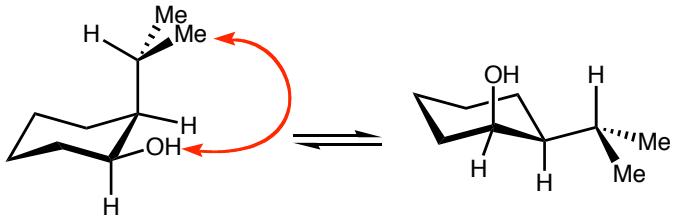

The conformer which places the isopropyl group equatorial is much more strongly preferred than would be suggested by *A*- Values. This is due to a syn pentane OH/Me interaction.

Problem:
Can you rationalize the stereochemical outcome of this reaction?

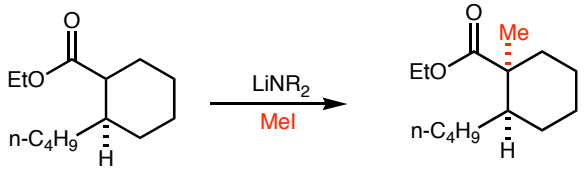

diastereoselection 89:11

D. Kim & Co-workers, *Tetrahedron Lett.* **1986**, *27*, 943.

Heteroatom-Substituted 6-Membered Rings

■ A-values at the 2-position in both the O & N heterocycles are larger than expected. This is due to the shorter C–O (1.43 Å), and C–N (1.47 Å) bond lengths relative to carbon (C–C; 1.53 Å). The combination of bond length and bond angle change increases the indicated 1,3-diaxial interaction (see eq 1, 4).

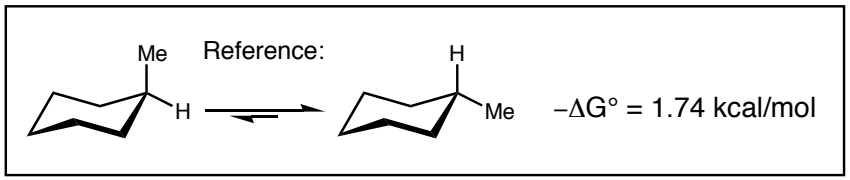

(1) 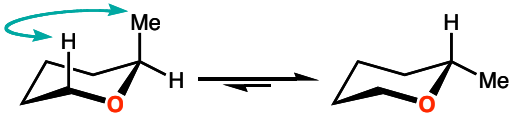 **–ΔG° = 2.86 kcal/mol**

(2) (4) 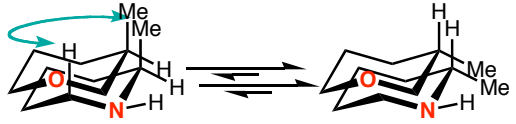 –ΔG° = 1.43 kcal/mol **–ΔG° = 2.5 kcal/mol**

(3) 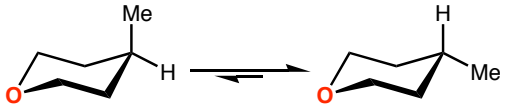 –ΔG° = 1.95 kcal/mol

(4) 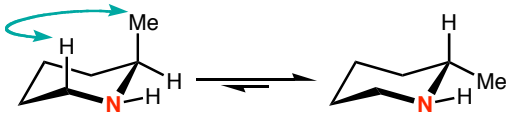 **–ΔG° = 2.5 kcal/mol**

(5) 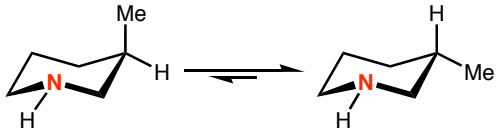 –ΔG° = 1.6 kcal/mol

(6) 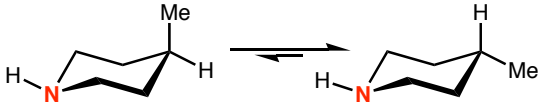 –ΔG° = 1.9 kcal/mol

A-Values for *N*-Substituents in Piperidine

■ Hydrogen is "bigger" than the N–lone Pair.

■ The A-value of N–substituents is slightly larger than the corresponding cyclohexane value. Rationalize

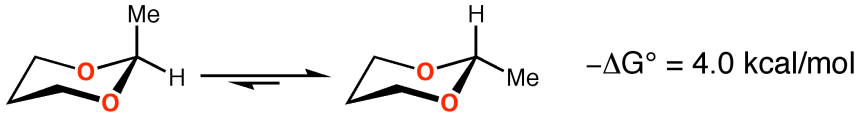

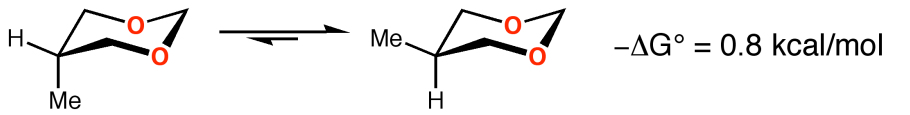

■ The indicated distance is 2.05 Å. The analogous H–H distance in Cyclohexane is 2.45 Å

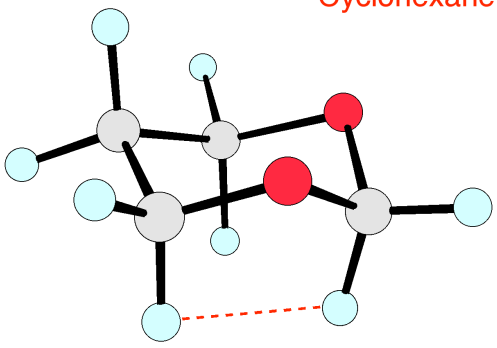

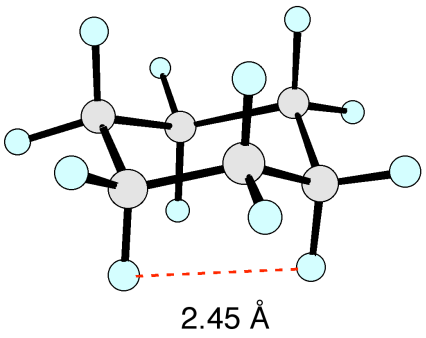

Conformations of Bicyclic Ring Systems

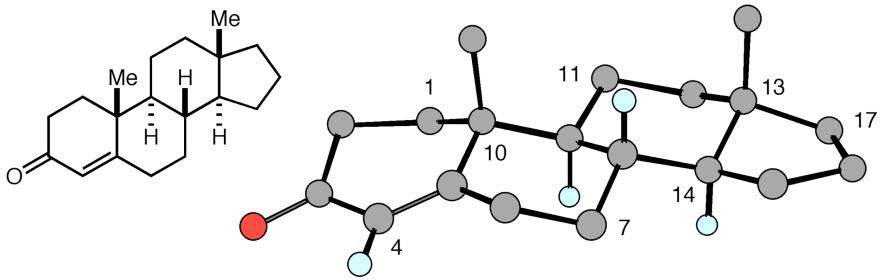

The steroid nucleus provided the stimulation for the development of conformational analysis, particularly of polycyclic ring systems. D. H. R. Barton was awarded a Nobel prize in 1969 for his contributions in this area.

Decalin Ring System (6/6)

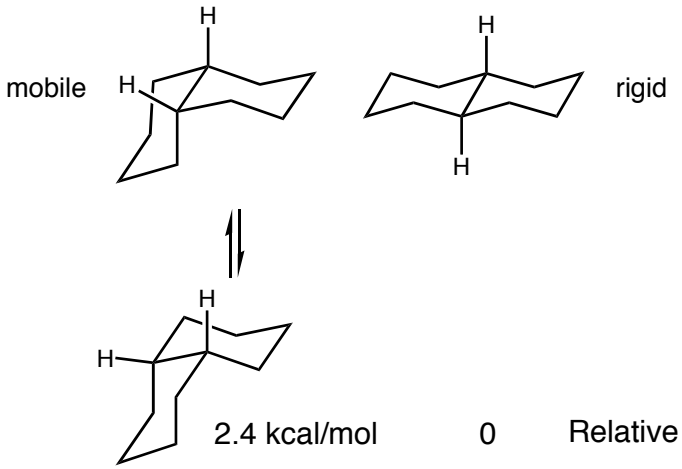

Let's identify the destabilizing gauche butane interactions in the cis isomer

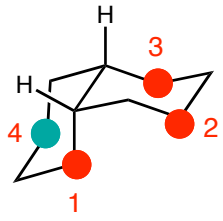

Gauche-butane interactions

C1 → C2
C1 → C3
C4 → C3

ΔG°(est) = 3(0.88) = 2.64 kcal/mol

Estimate the energy difference between the two methyl-decalins shown below.

Hydrindane Ring System (6/5)

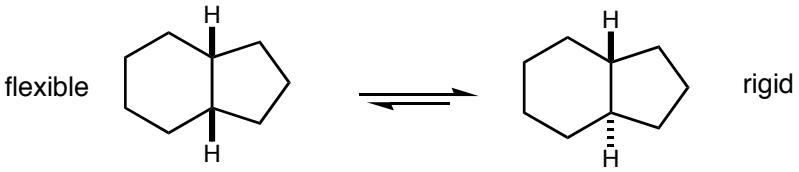

ΔG° = –0.5 kcal/mol (at 23 °C)
ΔG° = 0.0 kcal/mol (at ~200 °C)

■ The turnover to favor the *cis* fusion results from the entropic preference for the less ordered *cis* isomer.

The 5-5 Ring System

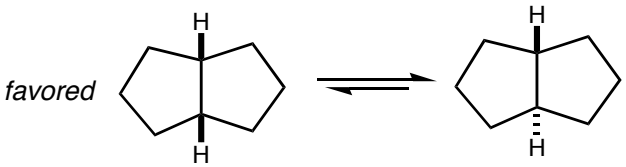

ΔG° = +6.4 kcal/mol

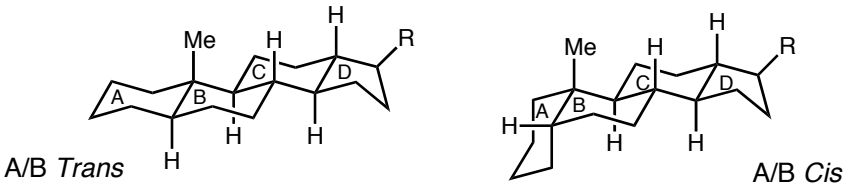

Rationalize the conformational flexibility of a *A/B Trans* vs. *A/B Cis* Steroid!

Different reactivity for axial and equatorial substituents

Axial substituents are more hindered, thus less reactive in many transformations

- Acetylation with Ac_2O/Py

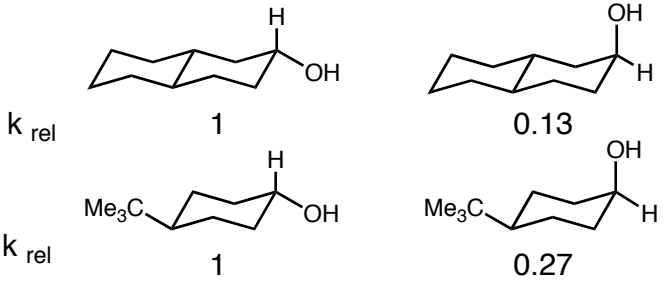

- Acid-catalyzed esterification

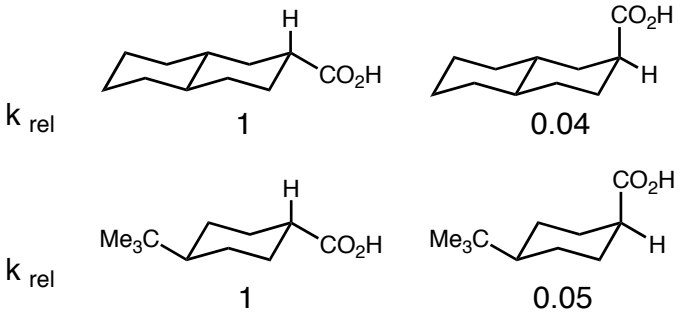

- Ester Saponification

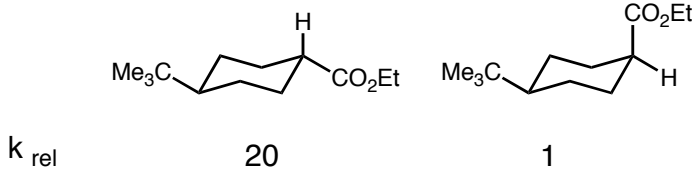

- S_N2 Reactions (Displacement with Ph–S^-)

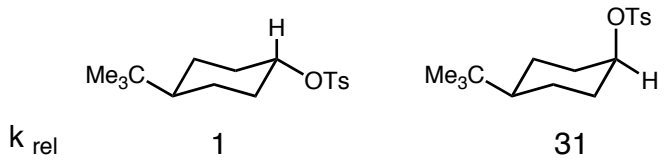

The axial diastereomer is not always slower reacting:

- Alcohol Oxidation with Cr(6+)

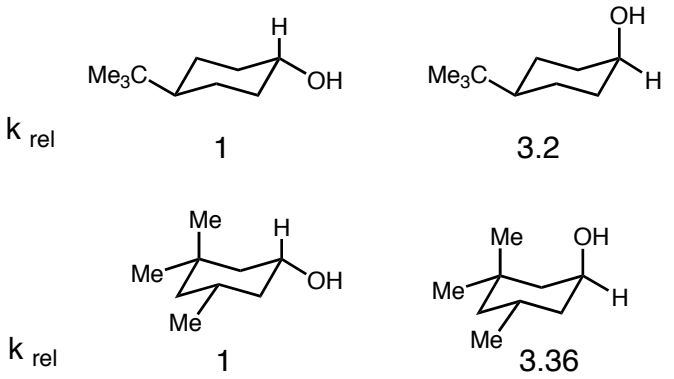

The rate-determining step is breakdown of the chromate ester. This is an apparent case of strain acceleration

For a more detailed discussion of this topic see:
Eliel, E. L., S. H. Wilen, et al. (1994). *Stereochemistry of Organic Compounds pp 720-726*

http://www.courses.fas.harvard.edu/colgsas/1063

Chemistry 206

Advanced Organic Chemistry

Lecture Number 7

Conformational Analysis-4

- Ground State Torsional Effects (Conformational Transmission)
- Conformational Analysis of $C_6 \rightarrow C_8$ Rings continued
- Transition State Torsional Effects

- Reading Assignment for week

A. Carey & Sundberg: **Part A**; Chapter 4
"Study & Descrption of Reaction Mechanisms"

K. Houk, *Science.* **1986**, *231*, 1108-1117
Theory & Modeling of Stereoselective Organic Reactions **(handout)**

Still, W. C.; Galynker, I. *Tetrahedron* **1981**, *37*, 3981**(handout)**

D. A. Evans

Monday,
October 2, 2006

Problems of the Day:

Predict the stereochemical outcome of this reaction. The diastereoselection is 99:1

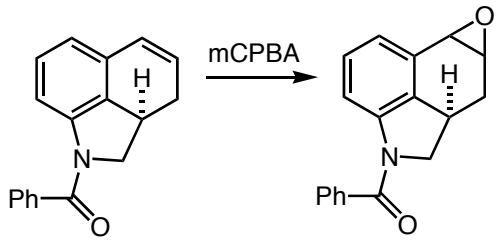

Martinelli, et.al. *Tett. Lett.* **1989**, *30*, 3935

Rationalize the stereochemical outcome of this reaction.

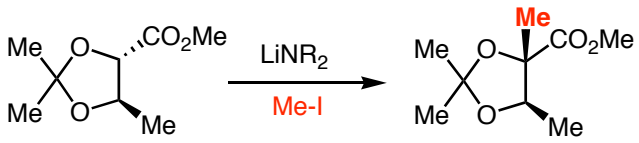

diastereoselection is 8:1.

Ladner, et.al. *Angew. Chemie, Int. Ed* **1982**, *21*, 449-450

Which is the more stable C=C isomer in the two THC structures?

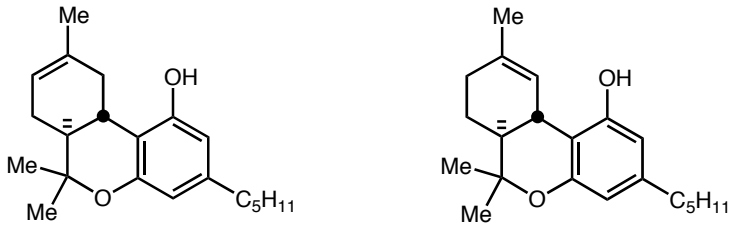

R. W. Kierstead, *JACS* **1967**, *89*, 5934

Cycloheptane

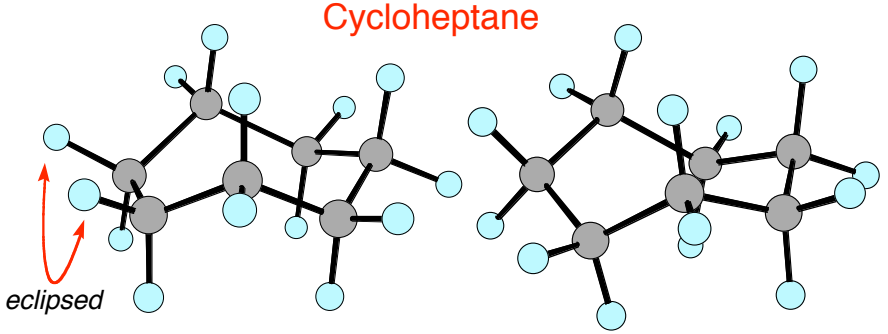

Chair (2.16 kcal/mol)

Twist-Chair (0 kcal/mol)

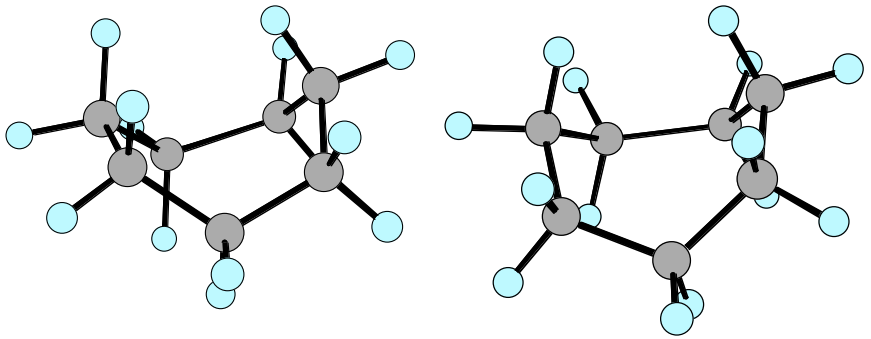

Boat (3.02 kcal/mol)

Twist-Boat (2.49 kcal/mol)

Hendrickson, J. B. *JACS* **1961**, *83*, 4537.
See Eliel, page 762+

Olefins preferentially oriented to eliminate eclipsing interactions.

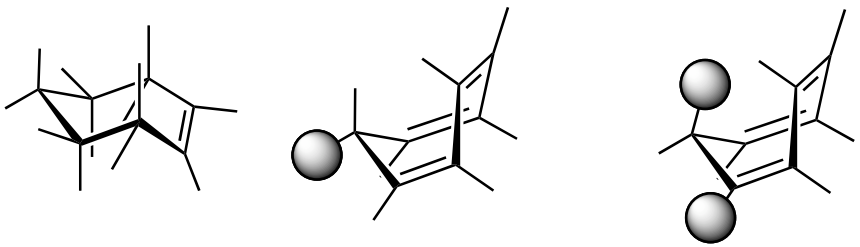

Cyclooctane

Chair-Boat
Lowest-energy conformation

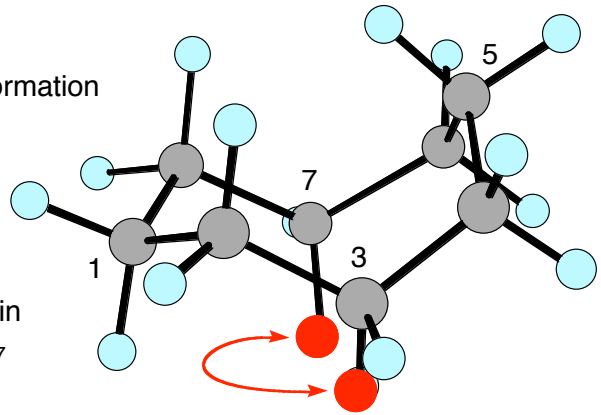

Transannular strain
between C_3 & C_7

Ring strain originates in eclipsing interactions and transannular vanderWaals interactions

Methylene position	1	2	**3**	4	5
ΔG pseudoequatorial **Me** / pseudoaxial **Me** (kcal/mol)	1.8	2.8	**>4.5**	-0.3	6.1

Underside view of boat-chair C3 & C7 eclipsing interactions

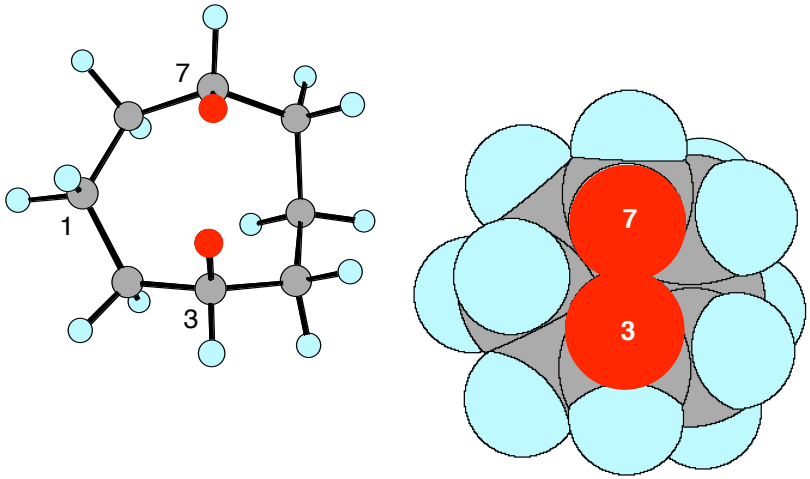

Cyclooctane continued...

Chair-Boat (**BC**)
Lowest-energy conformation

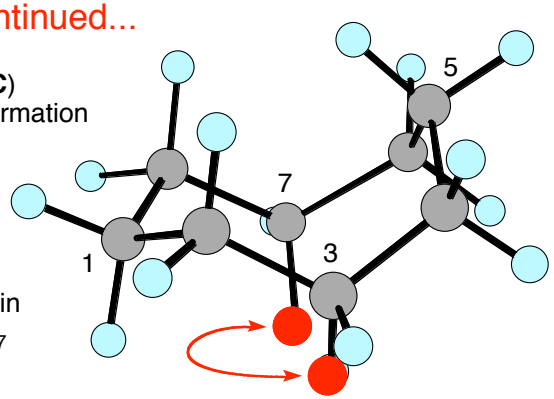

Transannular strain
between C_3 & C_7

Methyl position	1	2	3	4	5
ΔG (pseudoeqatorial) / (pseudoaxial) (kcal/mol)	1.8	2.8	>4.5	-0.3	6.1

Cyclooctane derivatives

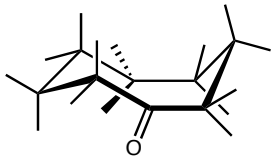

Carbonyl is positioned at C_3 or C_7

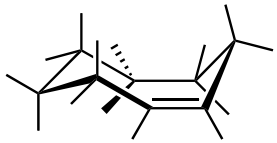

Olefin is positioned at C_3-C_4 or C_6-C_7

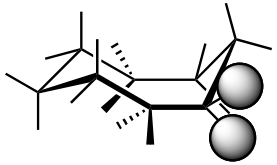

Disubstitution occurs at C_4 or C_6

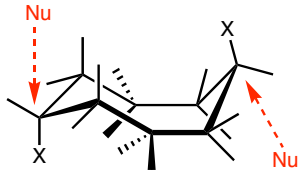

S_N2 occurs at C_1 and C_5

Still, W. C.; Galynker, I. *Tetrahedron* **1981**, *37*, 3981.

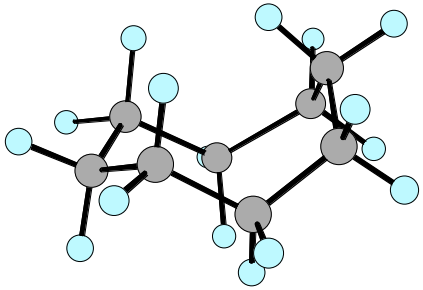

Chair-Boat (**CB**) conformation
reference structure

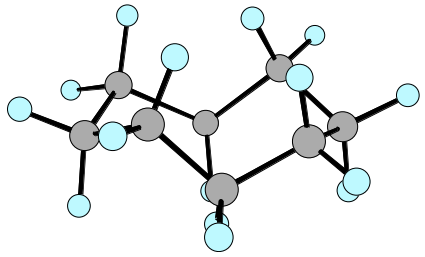

Chair-Chair (**CC**) conformation
(+1–1.6 kcal/mol)

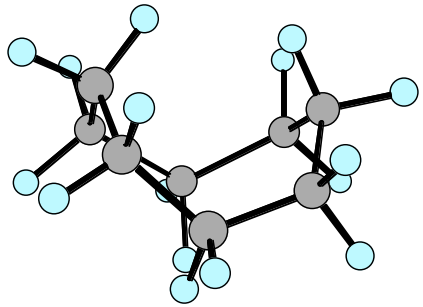

Boat-Boat (**BB**) conformation
(>+ 8 kcal/mol)

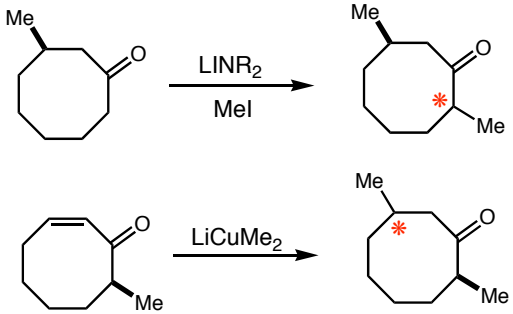

Torsional Effects

Torsional Strain: the resistance to rotation about a bond

Torsional energy: the energy required to obtain rotation about a bond

Torsional Angle: also known as dihedral angle

Torsional steering: Stereoselectivity originating from transition state torsional energy considerations

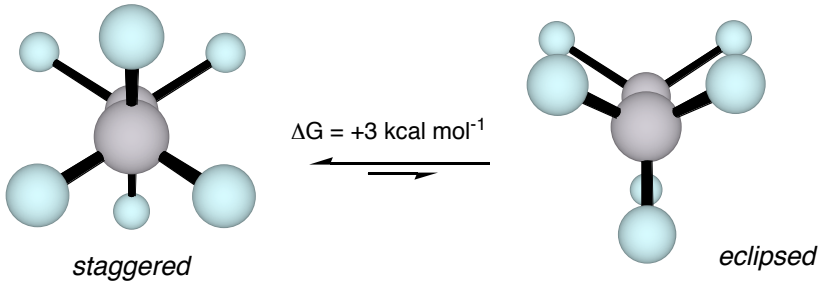

Torsional Strain (Pitzer Strain): Ethane

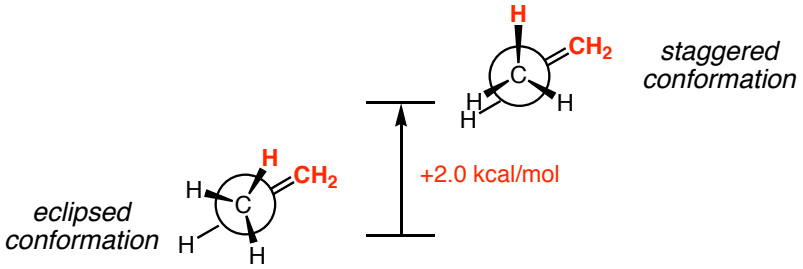

Wiberg K. B.; Martin, E. *J. Amer. Chem. Soc.* **1985**, *107*, 5035-5041.

See Lecture 5 for previous discussion

Relevant Orbital Interactions:

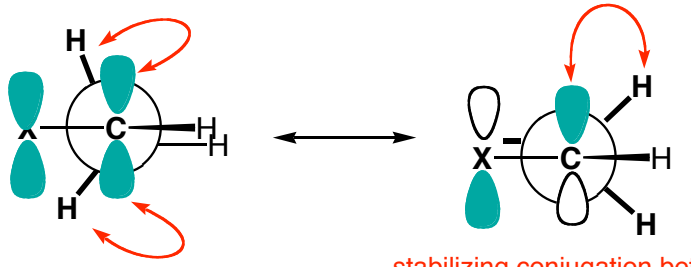

σ C–H & π electrons are destabilizing

stabilizing conjugation between π*–C–X & σ–C–H

Dorigo, A. E.; Pratt, D. W.; Houk, K. N. *JACS* **1987**, *109*, 6591-6600.

Conformational Preferences: Acetaldehyde

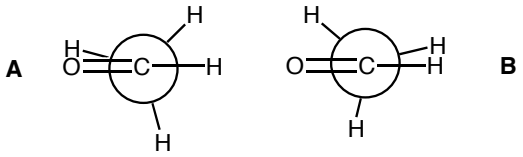

The eclipsed conformation (conformation **A**) is preferred.
Polarization of the carbonyl decreases the 4–electron destabilizing
Rotational barrier: 1.14 kcal/mol

Houk, *JACS* **1983**, *105*, 5980-5988.

Conformational Preferences
1-Butene (X = CH_2); Propanal (X = O)

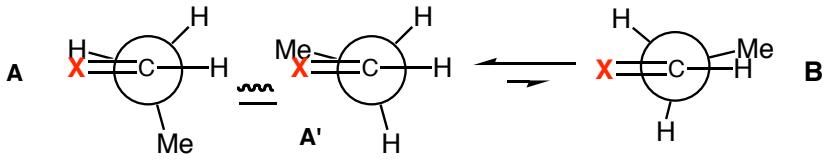

Conformation A is preferred. There is little steric repulsion between the methyl and the X-group in conformation A'.

Observation:
Relative enolate stability correlates to ring junction stereochemistry

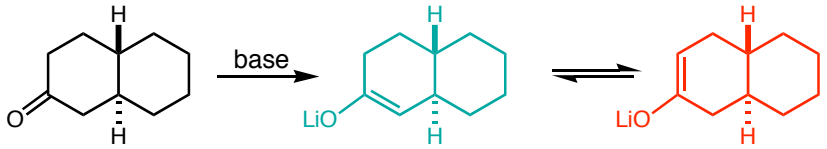

ratio: 13 : 87

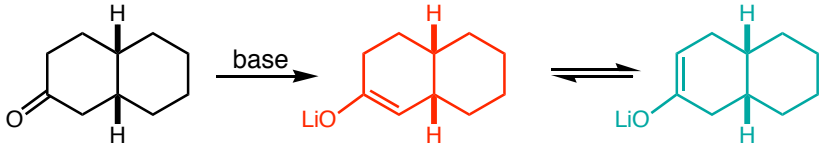

ratio: 70 : 30

House, *JOC* **1965**, *30*, 1341

Observation:
Relative enolate stability seems to be correlated to position of C=C

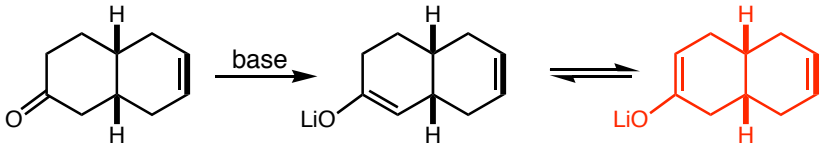

ratio: 10 : 90

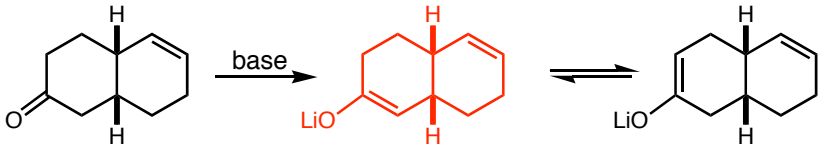

ratio: 92 : 8

How do we explain the experimental observations shown above?

Readings: Velluz etal, *Angew. Chemie, Int Ed.* **1965**, *4*, 181-270 **(pdf)**

Let Φ be defined as the torsion or dihedral angle for butane

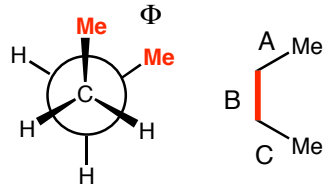

Φ = 60° for butane

Let's now consider cyclohexane

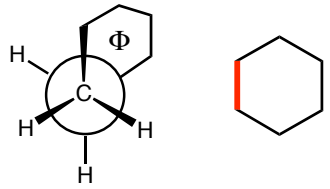

	Perfect chair	**real chair**
	Φ = 60°	**Φ = 56°**
CCC∠	109° 28'	111°

Given cyclohexane with an identified torsion angle ΦR, if ΦR either increases or decreases what effects in angle change are transmitted to ΦO, ΦM, and ΦP?

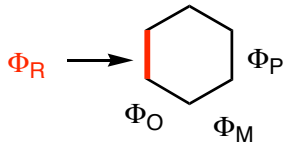

	Φ_R = 56°	Φ_R = 0°	[Δ]
Φ_O	56	15	–41°
Φ_M	56	44	–11°
Φ_P	56	61	+6°

$[\Delta] = \Phi_R(0°) - \Phi_R(56°)$

Operation:

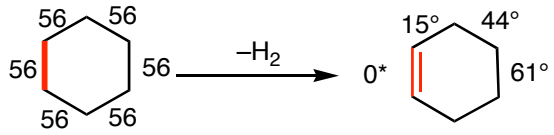

Hence, relative to cyclohexane, the following notation for torsion angle change may be denoted:

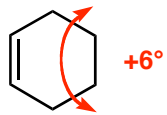

For Φ_P

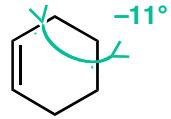

For Φ_M

Dear Class:
During our discussions on "Conformational Transmission", it is assumed (by Velluz) that it is energetically preferable to **decrease** the C–C torsion angle in cyclohexane rather than to **open up** this angle. The plot provided below confirms this assumption.

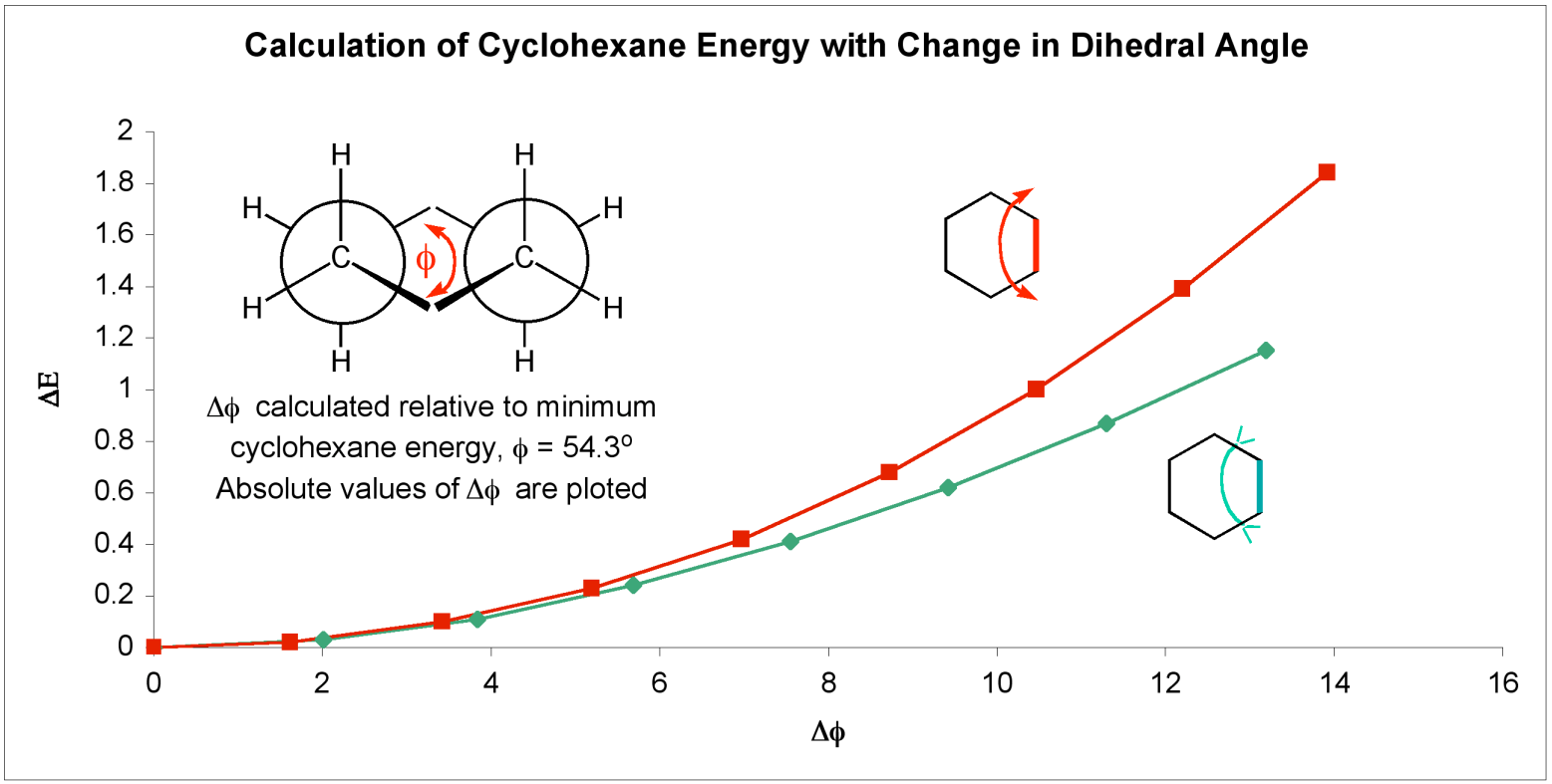

Single-point energy minimizations using molecular mechanics MMFF (Spartan `04)

Operation: *trans*-dimethylcyclohexane

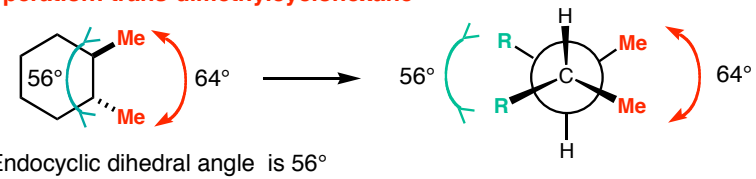

Endocyclic dihedral angle is 56°
Exocyclic dihedral expands correspondingly (+4°): 64°

Operation: *cis*-dimethylcyclohexane

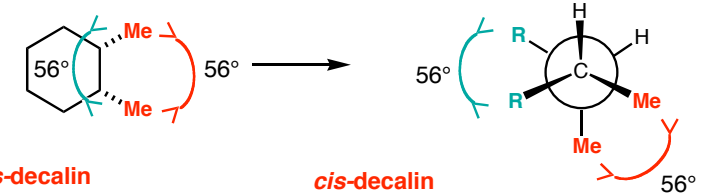

***trans*-decalin**

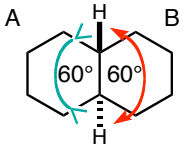

***cis*-decalin**

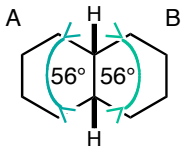

Simple Application: Reinforcing Torsional Effects

Which C=C bond isomer below is more stable?

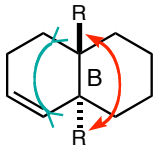

1) C=C will open up ring=B torsion angle
2) Ring B will resist increase in its ring fusion torsion angle
3) Therefore torsion effects are opposed

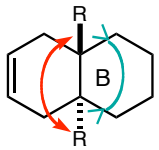

1) C=C will close down ring=B torsion angle
2) Ring B will accomodate decrease in its ring fusion torsion angle
3) Therefore torsion effects are reinforcing

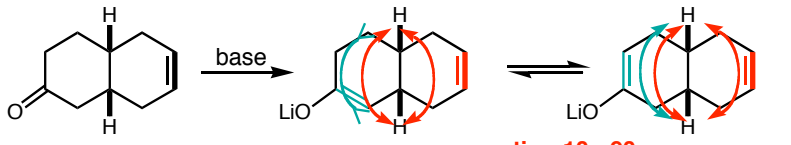

ratio: 10 : 90

effects opposing effects reinforcing

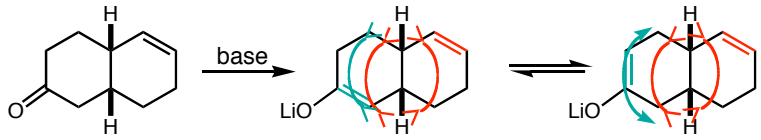

ratio: 92 : 8

effects reinforcing effects opposing

Question: Which is the more stable C=C isomer in the two THC structures?

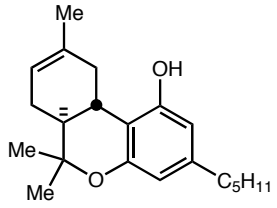

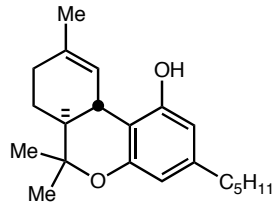

R. W. Kierstead, *JACS* **1967**, *89*, 5934

Question: Which enol acetate is more stable?

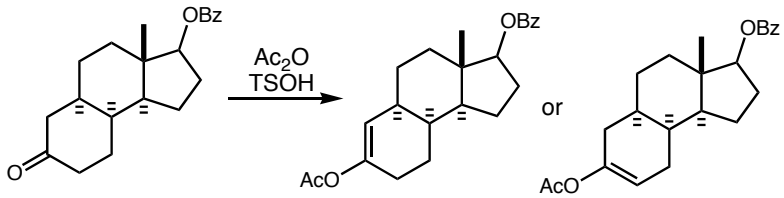

Houk: "Torsional effects in transition states are more important than in ground states"

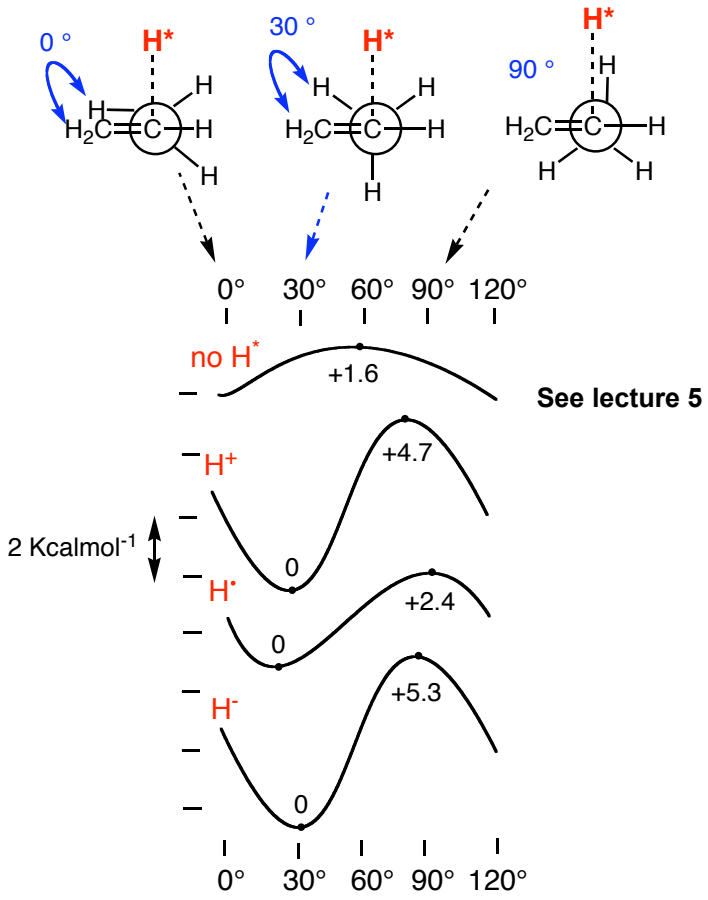

See lecture 5

Houk, *JACS* **1981**, *103*, 2438
Houk, *JACS* **1982**, *104*, 7162

Transition states

H-radical and H-anion: antiperiplanar σ*C–R orbital stabilized the TS illustrated for Nu addition

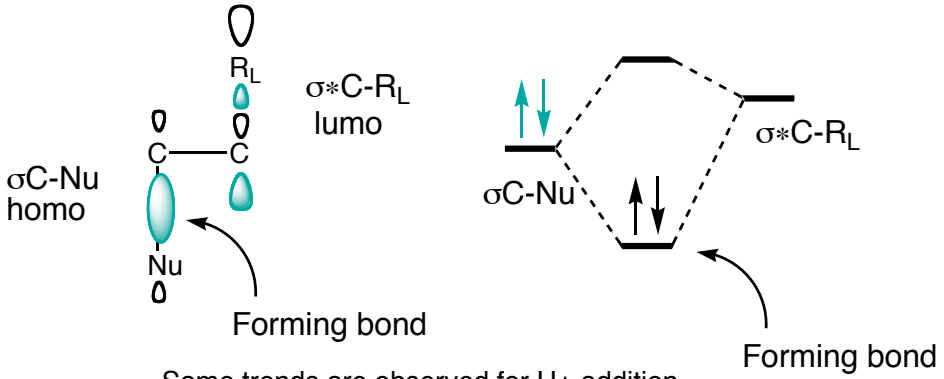

Same trends are observed for H+ addition

Houk, *Science* **1981**, *231*, 1108-1117
"The Theory and Modeling of Stereoselective Organic Reactions"

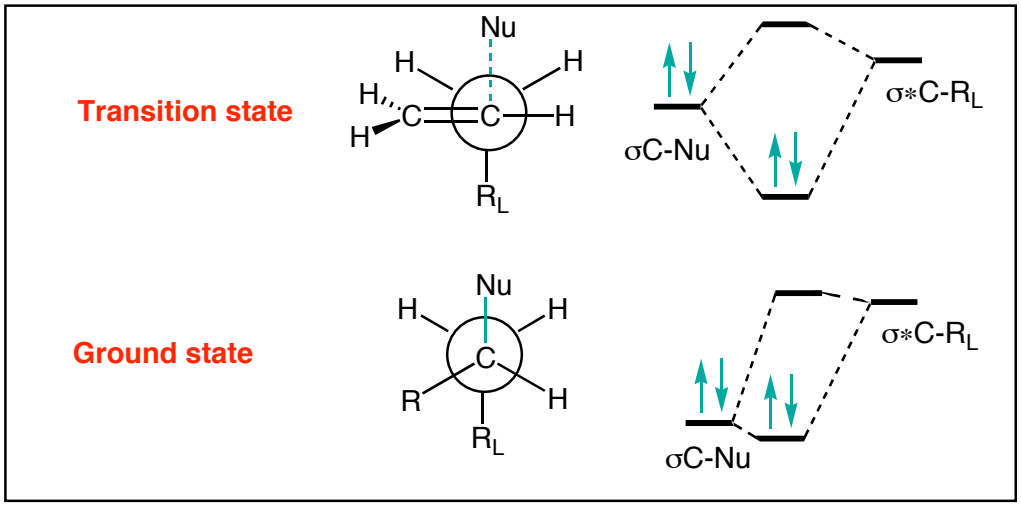

Olefin Addition Reactions: Case one

How do we account for the high exo selectivities in addition reactions to norbornene?

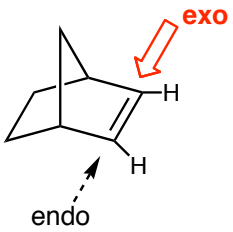

Highly exo selective for electrophilic, nucleophilic and cycloaddition reactions

Rate enhancement due to strain

The Controversy over origin of high exoselectivities

Steric effects

Least nuclear motion

Orbital distortion

Schleyer: torsional steering

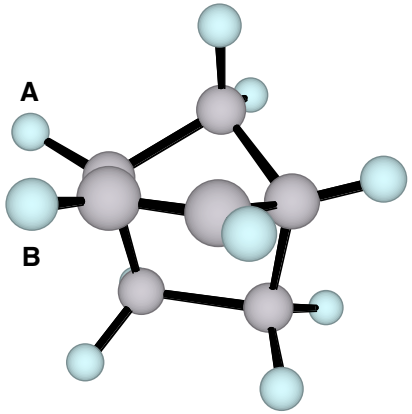

Schleyer, P. R. *J. Amer. Chem. Soc.* **1967**, *89*, 701.

Addition from exo face avoids eclipsing A & B hydrogens

(better hyperconjugative stabilization of transition state)

Olefin Addition Reactions: Case two

How do we account for the high selectilvities in the oxidation of the indicated olefin?

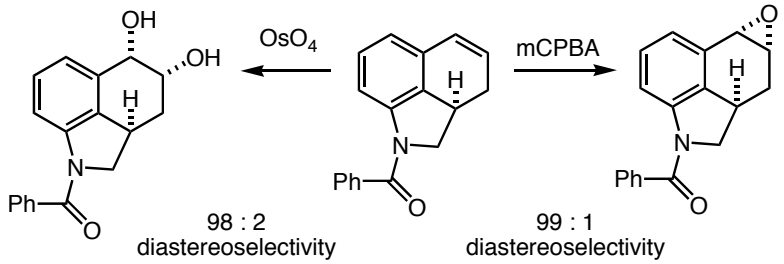

98 : 2 diastereoselectivity

99 : 1 diastereoselectivity

Nitrogen protecting group does not affect selectivities

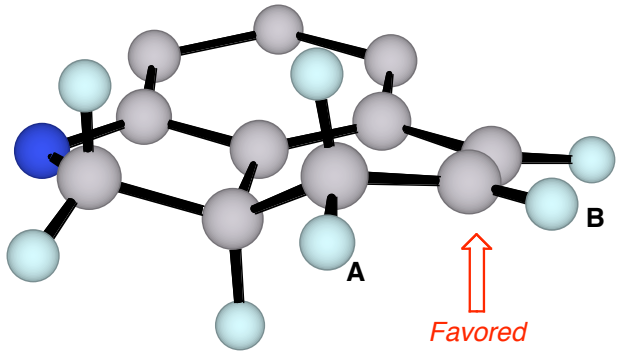

Martinelli, et.al. *Tett. Lett.* **1989**, *30*, 3935

Addition from indicated olefin face avoids eclipsing A & B H's

(better hyperconjugative stabilization of transition state)

Martinelli has carried out further studies on related structures.....

Martinelli: Torsional steering important in selectivity

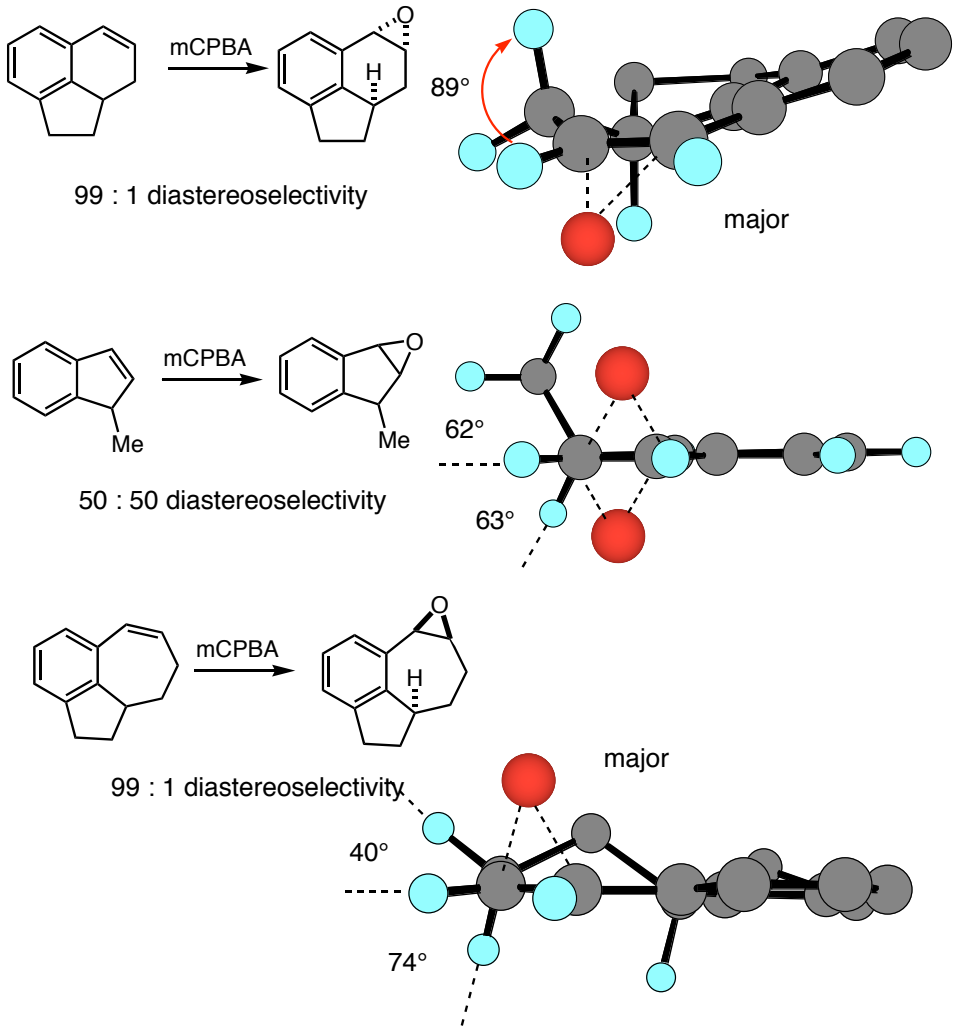

Authors propose that diastereoselection controlled by TS torsional effects

Martinelli & Houk, *J. Org. Chem.* **1994**, *59*, 2204.

Torsional Steering Controls the Stereoselectivity of Epoxidation in the Guanacastepene A Synthesis

Paul Ha-Yeon Cheong,† Heedong Yun,‡ Samuel J. Danishefsky,‡,§ and K. N. Houk*,†

ORGANIC LETTERS
2006
Vol. 8, No. 8
1513−1516

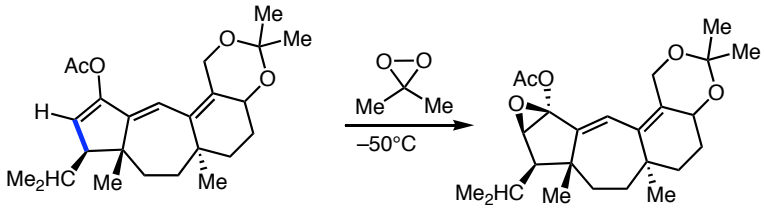

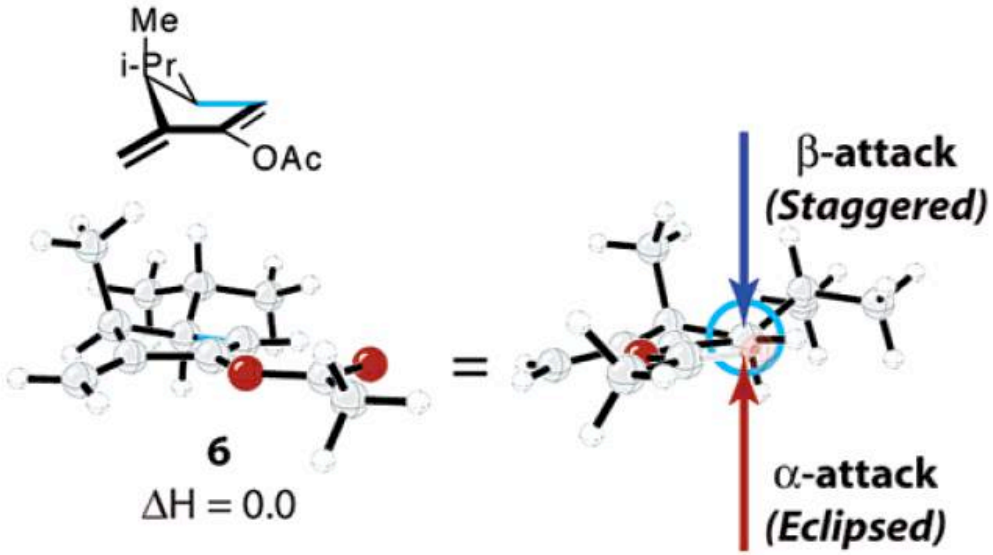

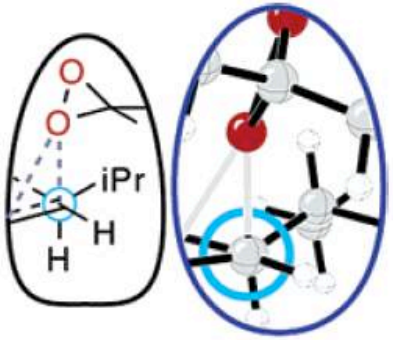

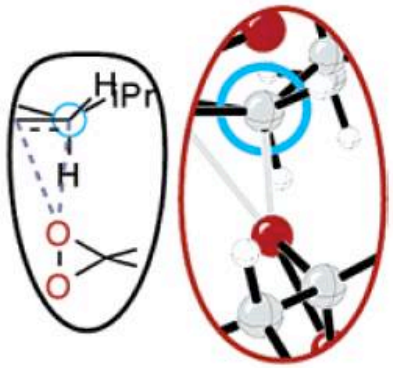

Cyclohexanone Addition Reactions: Hydride Reduction

Stereoselective Reductions: Cyclic Systems

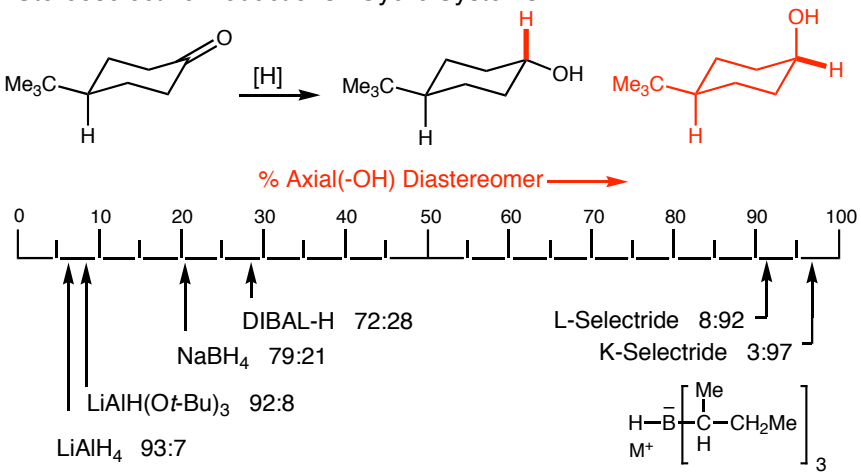

Observation: Increasingly bulky hydride reagents prefer to attack from the equatorial C=O face.

The most stereoselective Reductions

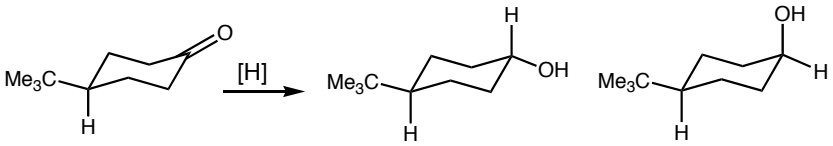

Reagent	Ratio
$KBH(s\text{-}Bu)_3$	03 :97
Li in NH_3	99 :01

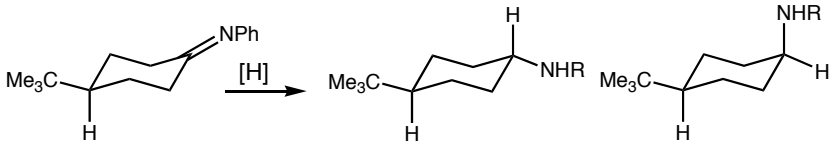

(R)	Reagent	Ratio
R = Bn	$LiBH(s\text{-}Bu)_3$	03 :97
R = Ph	$LiBH(s\text{-}Bu)_3$	01 :99
	Al/Hg/MeOH	~90 :10

Ganem, *Tet. Let* **1981**, *22*, 3447
Hutchins, *JOC* **1983**, *48*, 3412
private communication

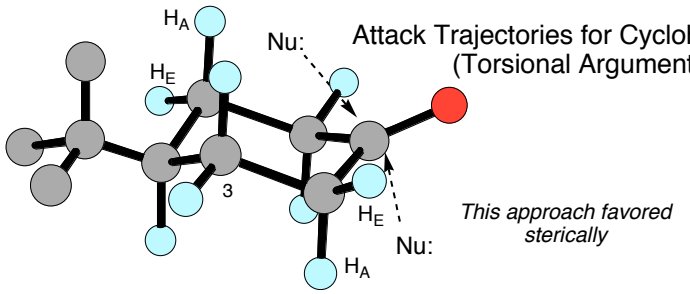

The steric hindrance encountered by Nu-attack from the axial C=O face by the axial ring substituents (hydrogens in this case) at the 3-positions is more severe than the steric hinderance encountered from Nu-attack from the equatorial C=O face.

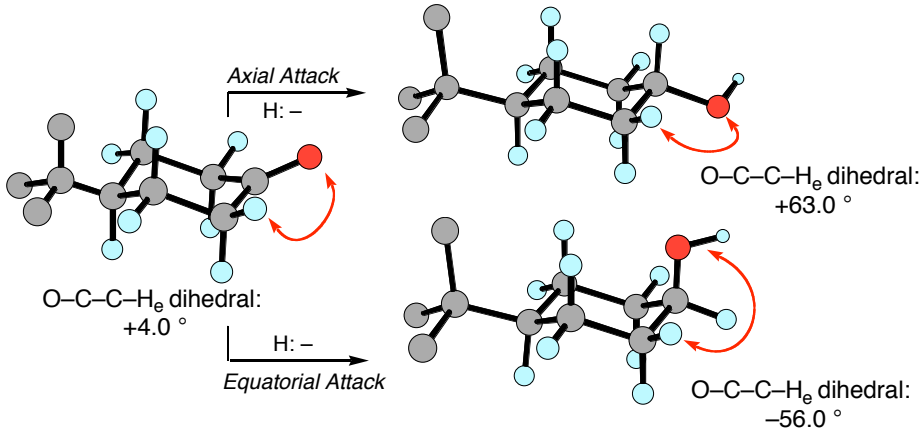

The Issues Associated with the Reduction Process

Steric Effects: Attack across equatorial C=O face sterically more favorable.

Torsional Effects: However, attack across the axial face of the C=O group avoids development of eclipsing interactions in the transition state. (Note the dihedral angle sign changes between reactants & products shown above). These "torsional effects" favor axial attack.

Prediction For "small" hydride reagents such as $LiAlH_4$, torsional effects are felt to be dominant and this explains the predisposition for axial attack.

Prediction For "large" hydride reagents such as $H–BR_4$, steric effects now are dominant and this explains the predisposition for equatorial attack.

http://www.courses.fas.harvard.edu/~chem206/

Chemistry 206

Advanced Organic Chemistry

Lecture Number 8

Olefin Addition Reactions–1

- Hydroboration
- Epoxidation & Directed Epoxidation

Reading Assignment for week

A. Carey & Sundberg: **Part B**; Chapter 4
"Electrophilic Additions to C–C Multilple Bonds"

K. Houk, *Science*. **1986**, *231*, 1108-1117
Theory & Modeling of Stereoselective Organic Reactions ***(Handout)***

K. Houk, *Tetrahedron*. **1984**, *40*, 2257-2274
Theoretical Studies of Stereoselective Hydroboration Reactions ***(Handout)***

Hoveyda, Evans, Fu, *Chem Rev*. **1993**, *93*, 1307-1370
Substrate-Directable Chemical Reactions
(Electronic Handout)

D. A. Evans

Wednesday,
October 4, 2006

Problems of the Day: (To be discussed)

Rationalize the stereochemical outcome of these reactions.

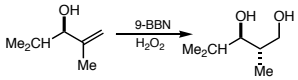

diastereoselection 24:1

W. C. Still & J. C. Barrish, *J. Am. Chem. Soc.* **1983**, *105*, 2487.

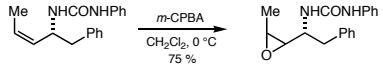

Roush, *J. Org. Chem.* **1987**, *52*, 5127. *Diastereoselection* = 95 : 5

Problem 309. The indicated olefins were subjected to hydroboration/oxidation as shown (*Synlett*, **1993**, 696).

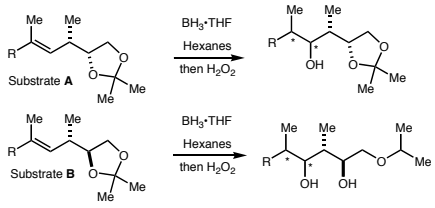

Part A. Please predict the major stereoisomer obtained from these reactions and illustrate your predictions with clear 3D drawings.

Part B. Please also explain the fact that **B** suffers reductive ring opening while **A** does not..

Representative Cis-Addition Processes

- Hydrometallation

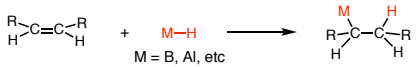

- Hydrogenation

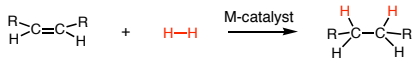

- Group Transfer (epoxidation)

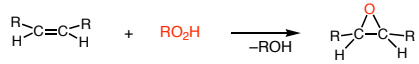

- Group Transfer (dihydroxylation)

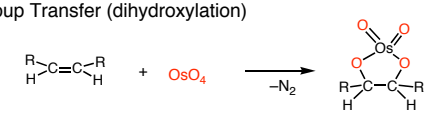

- Group Transfer (cyclopropanation)

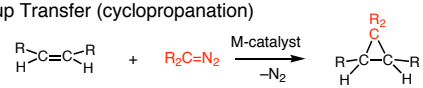

- Cycloadditions (one of many!)

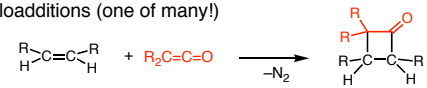

Attributes:

Each process adds to the C=C via a stereospecific process

Intermediates *may* be involved in some of the indicated reactions

Representative Trans-Addition Processes

- Halogenation

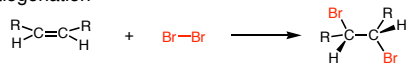

- Oxy–metallation (M = Hg(II), Tl(III))

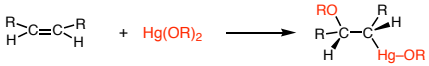

- Oxy–sulfenation (M = S(II), Se(II))

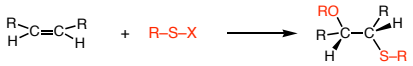

Attributes:

Each process may proceed via an bridged intermediate where X is the initiating electrophile

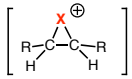

Olefin substitution may disrupt bridging

- Addition of hydrogen halides

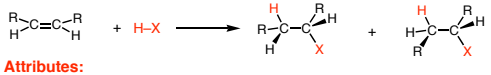

Attributes:

Process may proceed via an bridged intermediate where H+ is the initiating electrophile

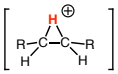

Olefin substitution, reaction conditions as well as halide type may disrupt bridging

The basic process

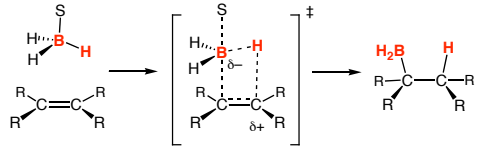

Response to steric effects: Here is a good calibration system:

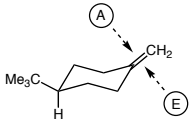

Oxidant	Ratio, A:E	Reference
MCPBA	69:31	*JOC*, **1967**, *32*, 1363
BH_3, H_2O_2	34:66	*JOC*, **1970**, *35*, 2654

Acyclic hydroboration can be controlled by A(1,3) interactions:

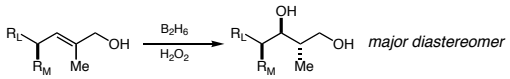

major diastereomer

control elements

A(1,3) allylic strain

Steric effects; R_L vs R_M

Staggered transition states

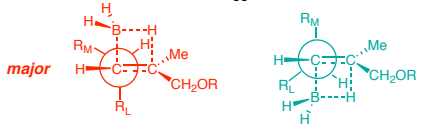

major ***minor***

Houk, "*Theoretical Studies of Stereoselective Hydroboration Reactions*" *Tetrahedron* **1984**, *40*, 2257 **(Handout)**

Hydroborations dominated by A(1,3) Strain

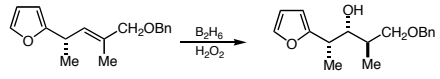

diastereoselection 8:1

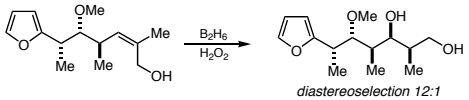

diastereoselection 12:1

Y. Kishi & Co-workers, *J. Am. Chem. Soc.* **1979**, *101*, 259.

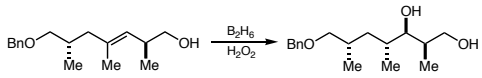

Diastereoselection = 3:1

C. H. Heathcock et. al. *Tetrahedron Lett* **1984** *25* 243.

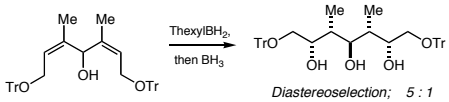

Diastereoselection; 5 : 1

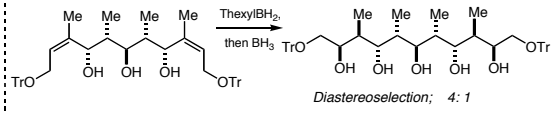

Diastereoselection; 4: 1

Still, W.C.; Barrish, J. C. *J. Am. Chem. Soc.* **1983**, *105*, 2487.

Hydroborations dominated by A(1,2) Strain

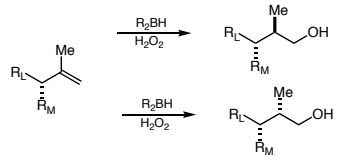

R_2BH structure is a potential variable

Houk's rules: Orient R_L anti-periplanar to incoming reagents to avoid TS eclipsing:

■ Case I: Borane

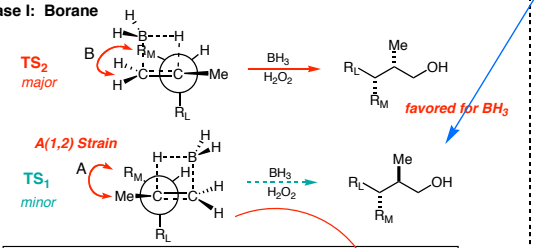

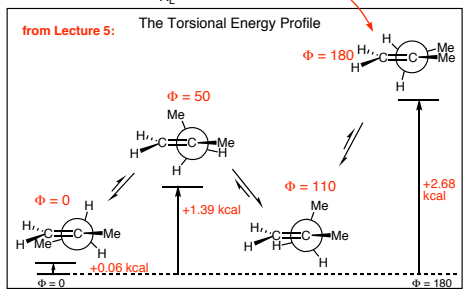

■ Case II: Dialkylboranes

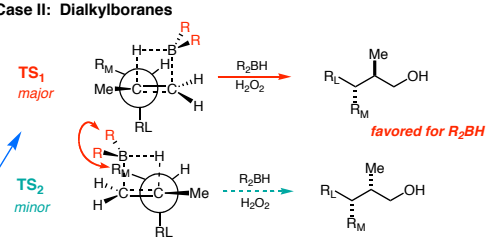

Midland finds that TS_1 favored for R_2BH reagents, but $TS_1 \sim TS_2$ for BH_3

Others have found that TS_1 favored over TS_2 for BH_3

Representative Examples

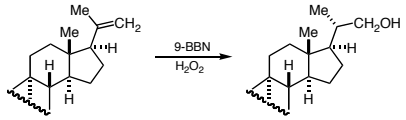

M. M. Midland & Co-workers, *J. Am. Chem. Soc.* **1983**, *105*, 3725..

R_2BH	*diastereoselection*
borane methylsulfide	1 : 1
thexylborane	4 : 1
9-BBN	14 : 1
dicyclohexylborane	26 : 1

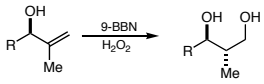

R = n-Bu: *diastereoselection 11:1*
R = $CHMe_2$: *diastereoselection 24:1*

Model is consistent if you presume HO = R_M: R = R_L

W. C. Still & J. C. Barrish, *J. Am. Chem. Soc.* **1983**, *105*, 2487.

Case I: Dialkylboranes

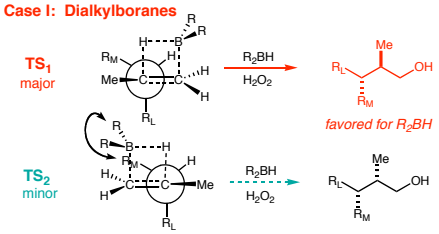

Case II: Borane

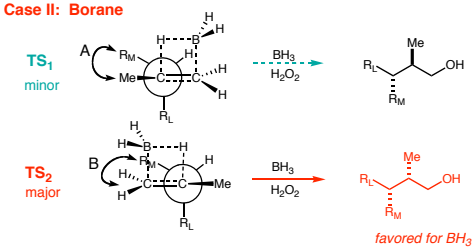

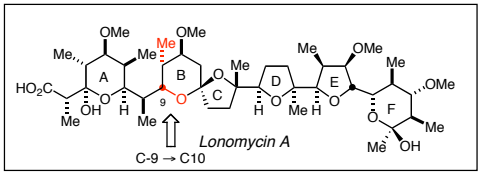

Evans, Ratz, Huff, Sheppard, *JACS* **1995**, *117*, 3448-3467.

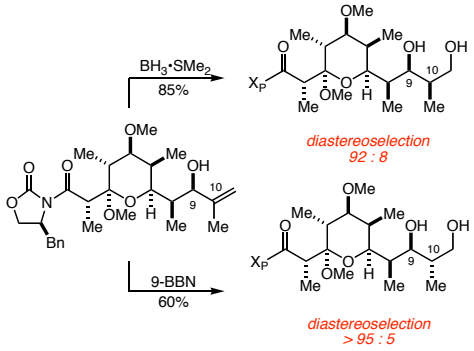

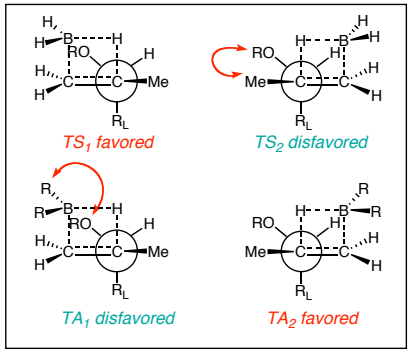

Represetative Hydroboration Examples: Acyclic Control

For each of the examples shown below, attempt to rationalize the stereochemical outcome of the reaction in terms of one of the models presented in the discussion.

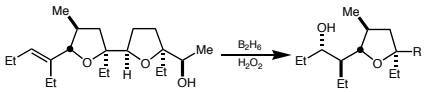

"one isomer"

Y. Kishi & Co-workers, *J. Am. Chem. Soc.* **1978**, *100*, 2933.

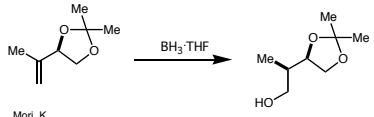

Mori, K.
Tetrahedron **1976**, *32*, 1979

diastereoselection 12:1

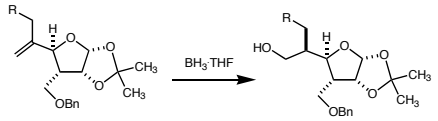

Oikawa et. al.
Tetrahedron Lett. **1983**, *19*, 1987.

R=H; Diastereoselection = 6.8:1
R=OBn Diastereoselection = 6.6:1

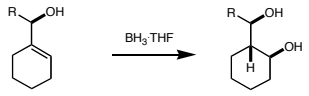

Birtwistle et. al.
Tetrahedron Lett. **1986**, *25*, 243.

R = CH_3; Diastereoselction = 6.7:1
R = isopropyl "One Compound"

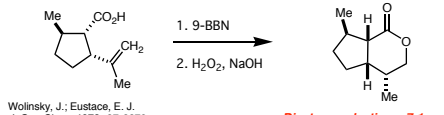

Wolinsky, J.; Eustace, E. J.
J. Org. Chem. **1972**, *37*, 3376.

Diastereoselection = 7:1

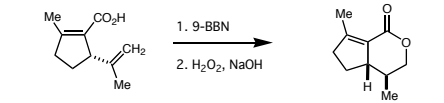

Wolinsky, J.; Nelson, D.
Tetrahedron. **1968**, *25*, 3767.

Diastereoselection = 10:1

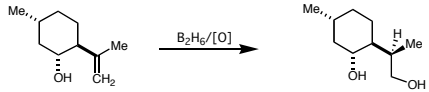

Diastereoselection = 19:1

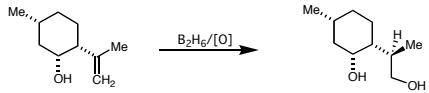

Diastereoselection = 32:1

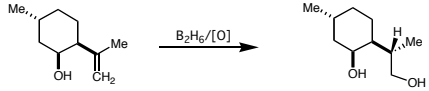

Diastereoselection = 10:1

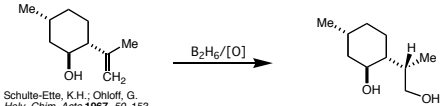

Schulte-Ette, K.H.; Ohloff, G.
Helv. Chim. Acta **1967**, *50*, 153.

Diastereoselection = 4.6:1

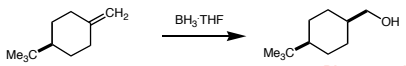

Diastereoselection = 2.1:1

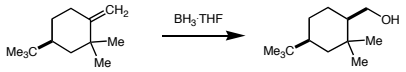

Diastereoselection = 1.2:1

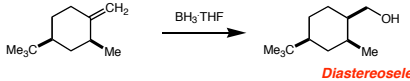

Diastereoselection = 3.3:1

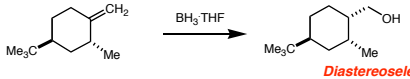

Diastereoselection = 2.4:1

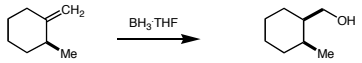

Y. Senda et. al.
Tetrahedron **1977**, *33*, 2933.

Diastereoselection = 4.9:1 (Compare with H.C. Brown's case, with 9-BBN; 1.5:1)

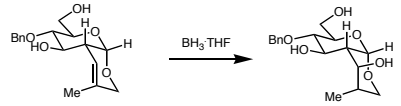

B. Fraser-Reid et. al.
J. Am. Chem. Soc. **1984**, *106*, 731.

Major isomer; no ratio given.

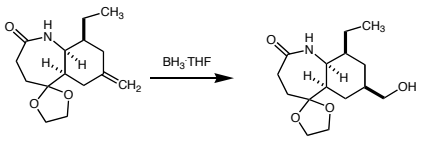

Sallay, S. I.
J. Am. Chem. Soc. **1967**, *89*, 6762.

90% yield, *no diastereoselection given*

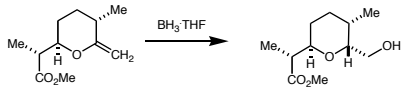

Ley, S. et.al.
J. Chem. Soc. Chem. Commun. **1983** 630.

55% yield with the diastereomeric alcohol produced in an unspecified amount. Recycling of the minor isomer further provided 15% of the desired material

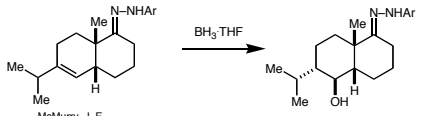

McMurry, J. E.
J. Am. Chem. Soc. **1968**, *90*, 6321.

Minor diastereomer not detected

Stereochemical Control Elements for all reactions

- Steric & Electronic Factors
- Stereoelectronic Considerations
- Associative Substrate-Reagent Interactions

Steric control:

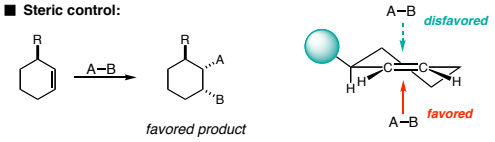

Nonbonding Interactions disfavor the syn diastereoface

Directed Reactions

Review: Hoveyda, Evans, Fu *Chem. Reviews* **1993**, *93*, 1307

Associative Substrate-Reagent Interactions

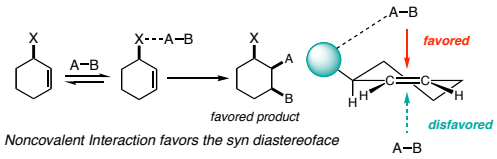

Noncovalent Interaction favors the syn diastereoface

Agenda

- **Directed Oxidations**
  - Epoxidation
  - Hydroboration
- **Directed Reductions**
  - Hydrogenation
  - Hydride reduction
- **Directed C–C Bond Constructions**

Heteroatom-directed Reactions

Mechanism-based: (HO & C=C must be allylic)

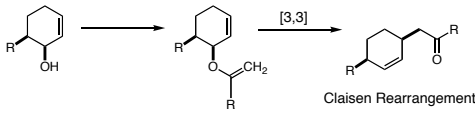

Claisen Rearrangement

via Reagent Ligation

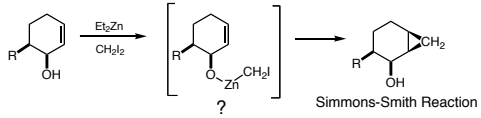

Simmons-Smith Reaction

Hydroxyl-directed Reactions

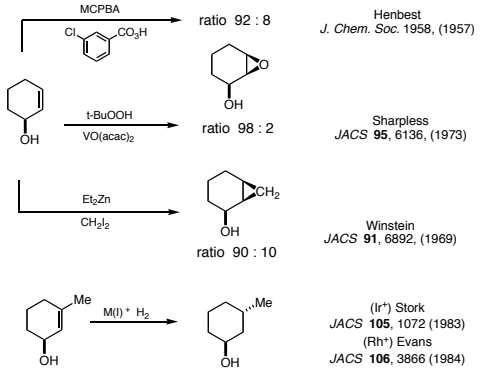

Orientation of the Directing Group

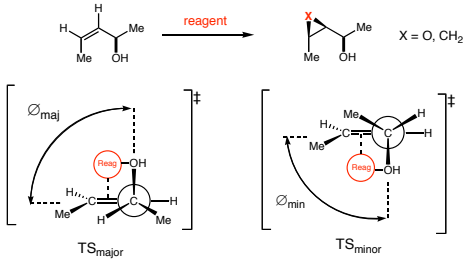

Orientation of directing group is not the same for all reactions

Reagent	Selectivity	Φ Estimate
t-BuO_2H, V $^{+5}$	71 : 29	~ 50 °
RCO_3H	95 : 5	~ 120 °
CH_2I_2, Zn–Cu	> 99 : 1	?

The transition state bite angles for the above reactions are either not known or have been only crudely estimated.

The "best guesses" are provided.

The Directed Peracid Epoxidation

■ **Transition State Hydrogen Bonding: Substrate as H-bond donor (Henbest)**

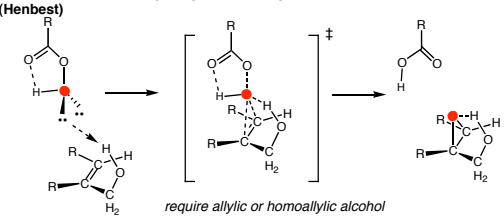

require allylic or homoallylic alcohol

■ **Transition State Hydrogen Bonding: Peracid as H-bond donor (Ganem)**

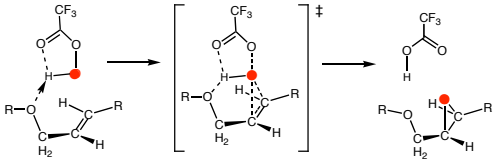

require more acidic peracid both allylic alcohols and ethers OK

	Syn : *Anti* (*m*-CPBA)	*Syn* : *Anti* (CF_3CO_3H)
	24 : 1	50 : 1
	24 : 1	100 : 1
	5 : 1	100 : 1

	Syn : *Anti* (*m*-CPBA)	*Syn* : *Anti* (CF_3CO_3H)
	1 : 7	5 : 1
	1 : 8	12 : 1
	1 : 4	1 : 6

Ganem *Tet. Let.* **1985**, *26*, 4895

Epoxidation of Cyclic Olefins with Amide &Urethane Directing Groups

Substrate	Major Product		Selectivity
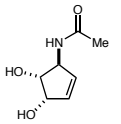	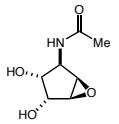		"highly selective"
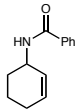	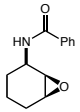		"highly selective"
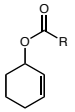	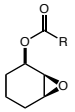	a. R = NH_2	3 : 1
		b. R = NHBn	5 : 1
		c. R = NMe_2	10 : 1
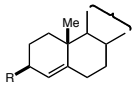	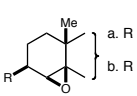	a. R = OCONHBn	>20 : 1
		b. R = $OCONMe_2$	>20 : 1
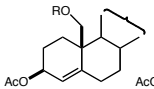	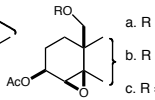	a. R = $CONH_2$	6 : 1
		b. R = CONHBn	>10 : 1
		c. R = $CONMe_2$	2 : 1

Conditions: Perbenzoic acid, or meta-chlorobenzoic acid in benzene.

(Table 11, p1316, from the Evans, Hoveyda, Fu review article)

Epoxidation of Cyclic Homoallylic Alcohols

Substrate	Major Product	Selectivity
	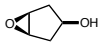	9 : 1
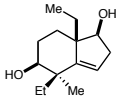	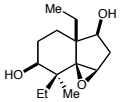	"highly selective"
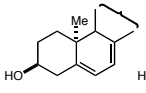	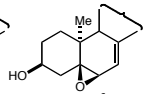	16 : 1
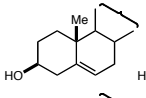	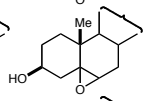	1 : 1
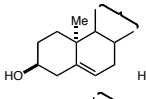	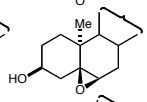	21 : 1
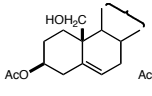	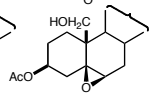	5 : 1

Conditions: Perbenzoic acid, or meta-chloroperbenzoic acid in benzene or cyclopentane.

(Table 14, p1318, from the Evans, Hoveyda, Fu review article)

The Sharpless Epoxidation

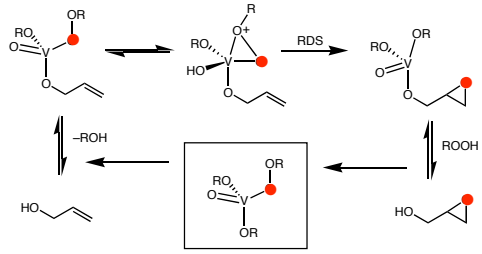

Aldrichimica Acta, **12**, 63 (1979)

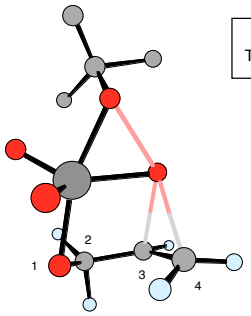

Chem 3D Transition State

O–C_2–C_3–C_4 = 41°
The Sharpless estimate: ~50°

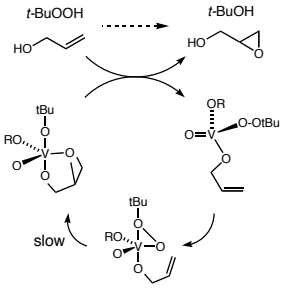

■ The literature precedent: Sheng, Zajecek, *J. Org. Chem.* **1970**, *35*, 1839

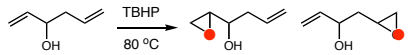

Catalyst { $VO(acac)_2$ 4 : 1 ; $Mo(CO)_6$ 1 : 1

■ Next step: Sharpless, Michaelson *JACS* **1973**, *95*, 6136

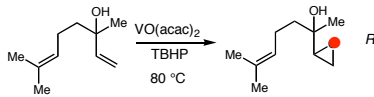

Regioselection 20:1

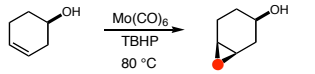

Stereoselection 98:2 (90 % yield)

Relative Rates (Diastereoselectivities) for the Epoxidation of Cyclohexene Derivatives JACS **1973**, *95*, 6136

Substrate	k_{rel}[a,b] (diastereoselectivity[c]) peracid	$Mo(CO)_6$	$VO(acac)_2$
	1.00	1.00	1.00
	0.55 (92 : 8)	4.5 (98 : 2)	>200 (98 : 2)
	0.046 (37 : 63)	0.07 (40 : 60)	--
	0.42 (60 : 40)	11.0 (98 : 2)	10.0 (98 : 2)

[a,b] The relative rate data apply only to a given column.
Values in parenthesis refer to the ratio of syn:anti epoxide.

■ Allylic Alcohols:

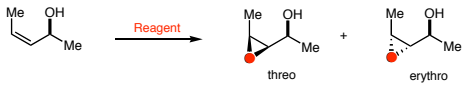

Φ Estimate	Reagent	Ratio
~ 120 °	*m*-CPBA	95 : 5
40-50 °	*t*-BuOOH / $VO(acac)_2$	71 : 29
	t-BuOOH / $Mo(CO)_6$	84 : 16

■ RCO_3H Transition States: Φ ~ 120 °

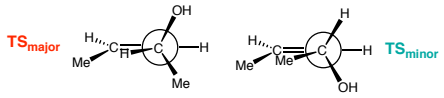

■ V(+) Transition States: Φ ~ 45 °

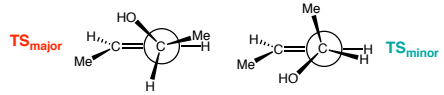

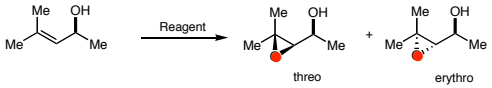

K. Oshima & Coworkers
Tetrahedron Lett. **1980**, *21*, 1657, 4843.

K. B. Sharpless & Coworkers
Tetrahedron Lett. **1979**, *20*, 4733.

Reagent	Ratio
m-CPBA	95 : 5
t-BuOOH / $VO(acac)_2$	86 : 14
t-BuOOH / $Mo(CO)_6$	95 : 5
t-BuOOH / (*t*-BuO)$_3$Al	100 : 0

Reagent	Ratio
m-CPBA	64 : 36
t-BuOOH / $VO(acac)_2$	29 : 71
t-BuOOH / $Mo(CO)_6$	62 : 38
t-BuOOH / (*t*-BuO)$_3$Al	64 : 36

Oshima, *Tetrahedron Lett.* **1982**, *23*, 3387.

R_1	R_2	Yield	Ratio
H	Bu	84 %	99 : 1
C_5H_{11}	Me	70 %	99 : 1

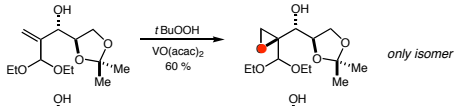

Depezay, *Tetrahedron Lett.* **1978**, *19*, 2869.

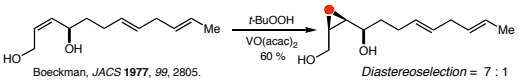

Boeckman, *JACS* **1977**, *99*, 2805. *Diastereoselection* = 7 : 1

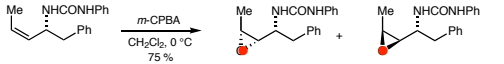

Roush, *J. Org. Chem.* **1987**, *52*, 5127. *Diastereoselection* = 95 : 5

Homoallylic Alcohols (Mihelich, *JACS* **1981**, *103*, 7690)

Diastereoselection > 400 : 1

Control Elements
A(1,3) Strain
Directed Rxn

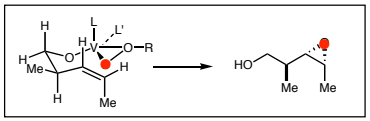

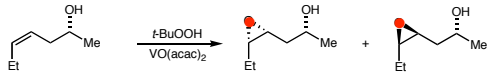

Diastereoselection 12 : 1

Control Elements
Directed Rxn

Prediction

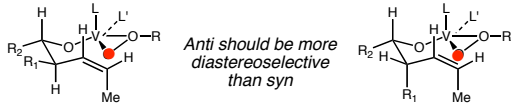

Anti should be more diastereoselective than syn

Anti diastereomer *Syn diastereomer*

Anti diastereomer

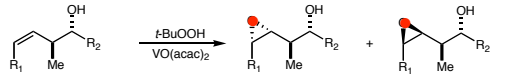

R_1	R_2	Yield	Ratio
C_6H_{13}	Me	92 %	104 : 1
Me	*i*-Pr	97 %	> 400 : 1

Syn diastereomer

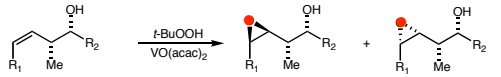

R_1	R_2	Yield	Ratio
C_6H_{13}	Me	73 %	70 : 1
Me	Me	70 %	85 : 1
Me	C_5H_{11}	81 %	16 :1

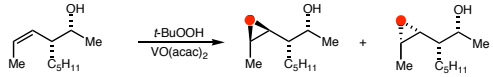

E. D. Mihelich & Coworkers
J. Am. Chem. Soc. **1981**, *103*, 7690.

Diastereoselection = 211 : 1

Epoxidation of Homoallylic Alcohols with TBHP, $VO(acac)_2$

Substrate	Product	Selectivity
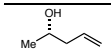	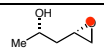	2 : 1
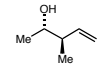		4.6 : 1
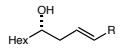 R = $(CH_2)_7CO_2Me$	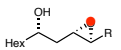	1.4 : 1

Bishomoallylic Alcohols (Kishi, *Tet. Lett.* **1978**, *19*, 2741)

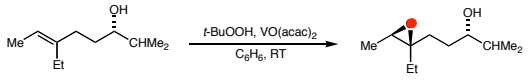

diastereoselection ~ 9 : 1

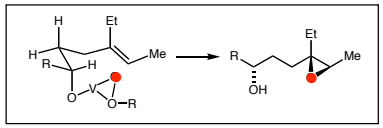

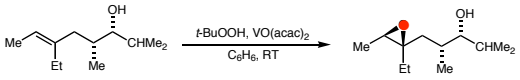

diastereoselection ~ 20 : 1

2nd stereocenter is reinforcing

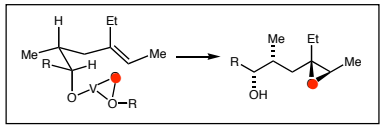

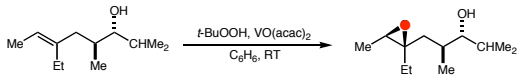

diastereoselection ~ 6 : 1

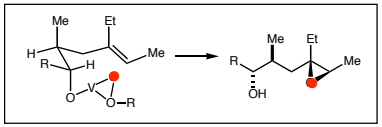

Epoxidation & Cyclization of Bishomoallylic Alcohols

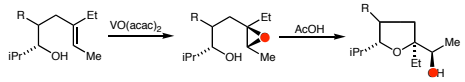

The Kishi Lasalocid Synthesis (*JACS* **1978**, *100*, 2933)

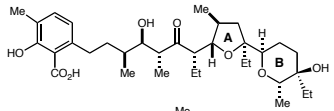

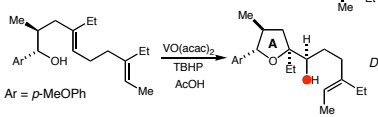

Ar = *p*-MeOPh

Diastereoselection 8:1

Evans X-206 Synthesis JACS **1988**, *110*, 2506.

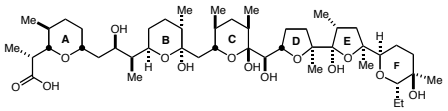

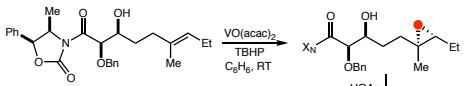

diastereoselection 20 : 1
(89 %)

http://www.courses.fas.harvard.edu/colgsas/1063

Chemistry 206

Advanced Organic Chemistry

Lecture Number 9

Olefin Addition Reactions–2

- Curtin-Hammett Principle
- Hydrogenation

Reading Assignment for week

A. Carey & Sundberg: **Part B**; Chapter 4
"Electrophilic Additions to C–C Multilple Bonds"

Hoveyda, Evans, & Fu (**1993**). *Substrate-directable chemical reactions.* Chem. Rev. 93: 1307-70 ***(pdf)***

J. M. Brown, *Angew. Chem. Int. Edit.* **26**, 190-203 (1987) ***(Handout)***

H. Yamamoto et.al, *Angew. Chem. Int. Ed.* **2005,** *44,* 4389-4391 **(pdf)**

D. A. Evans

Friday,
October 6, 2006

Problems of the Day:

Rationalize the stereochemical outcome of the indicated reaction.

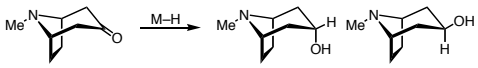

R. Noyori
Bull. Chem. Soc. Japan **47**, 2617, (1974)

R_2AlH	97 : 3
$LiAlH_4$	28 : 72

Problem 579. The following publication (*J. Org. Chem.* **1991**, *56*, 5553) reported the surprisingly selective olefin epoxidation illustrated below. In this reaction, olefin B in **1** was found to be much less reactive than olefin A. Using your knowlege of stereoelectronic effects, provide an explanation for the reduced reactivity of olefin B in diene **1**.

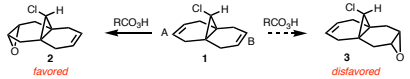

Problem 313. Overman and co-workers recently reported the indicated selective epoxidation in conjunction with a synthesis of briarellins A and E, a new family of diterpenes (*JACS* **2003,** *125,* 6650)**.** It should be noted that the Al(t-BuO)$_3$/(t)-BuOOH reagent system is both highly diastereoselective and site selective. It is also relevant to the mechanism of the reaction that the ring-trisubstituted olefin lacking an allylic oxygen substituent would normally be more prone to epoxidation with a peracid than the acyclic trisubstituted olefin.

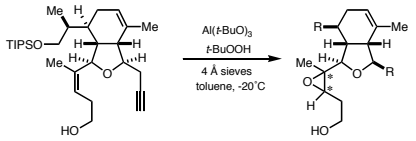

Part. Provide a general mechanism illustrating how the Al(t-BuO)$_3$/(t)-BuOOH reagent epoxidizes olefins. Three-dimensional drawings are recommended.
Part B. Provide a general mechanism illustrating how the above epoxidation proceeds and provide the stereochemistry (*) of the product epoxide along with a stereochemical analysis of the noted face selectivity.

A Brief Introduction to the Curtin-Hammett Principle

J. I. Seeman, *J. Chem,Ed.* **1986,** *63,* 42-48 *The Curtin-Hammett Principle and the Winstein-Holness Equation*

J. I. Seeman, *Chem. Rev.* **1983**, *83*, 84-134. *Effect of Conformational Change on Reactivity in Organic Chemistry. Evaluations, Applications, and Extensions of Curtin-Hammet-Winstein-Holness Kinetics*

Curtin–Hammett Principle

"The product composition, P_A vs P_B is not solely dependent on relative proportions of the conformational isomers in the substrate;

it is controlled by the difference in standard Gibbs energies ($\Delta\Delta G^*$) of the respective transition states."

The C-H principle may be extended to rapidly interconverting diastereomers, or constitutional isomers as well.

Curtin–Hammett Conditions

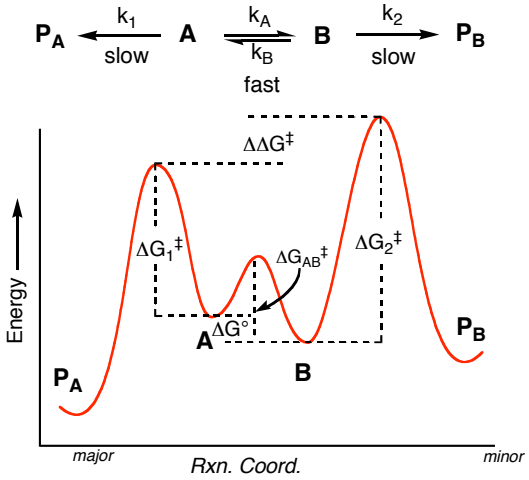

Chem 206, D. A. Evans

"Curtin–Hammett Conditions"

k_1, k_2 << k_A, k_B:

$$P_A \xleftarrow[\text{slow}]{k_1} A \underset{k_B}{\overset{k_A}{\rightleftharpoons}} B \xrightarrow[\text{slow}]{k_2} P_B \quad (1)$$

fast

Case 1: Less stable conformer leads to the **major** product.

If reaction rates are much **slower** than the rate of interconversion, ($\Delta G_{AB}^{\ddagger}$ is small relative to $\Delta G_1^{\ddagger}$ and $\Delta G_2^{\ddagger}$), then the A/B ratio is constant throughout the course of the rxn.

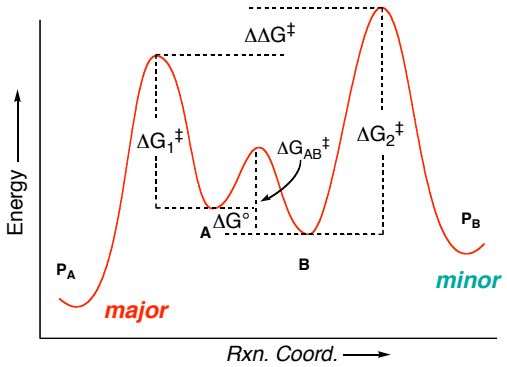

Case 2: Less stable conformer leads to the **minor** product.

If reaction rates are much **slower** than the rate of interconversion, ($\Delta G_{AB}^{\ddagger}$ is small relative to $\Delta G_1^{\ddagger}$ and $\Delta G_2^{\ddagger}$), then the A/B ratio is constant throughout the course of the rxn.

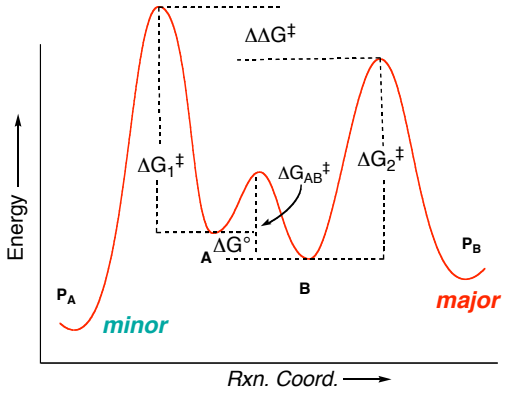

Curtin - Hammett Principle

The product composition is not solely dependent on relative proportions of the conformational isomers in the substrate; it is controlled by the difference in standard Gibbs energies ($\Delta\Delta G^{\ddagger}$) of the respective transition states.

Case 2: Curtin-Hammett Conditons

k_1, k_2 << k_A, k_B: If the rates of reaction are much **slower** than the rate of interconversion, ($\Delta G_{AB}^{\ddagger}$ is small relative to $\Delta G_1^{\ddagger}$ and $\Delta G_2^{\ddagger}$), then the ratio of A to B is constant throughout the course of the reaction.

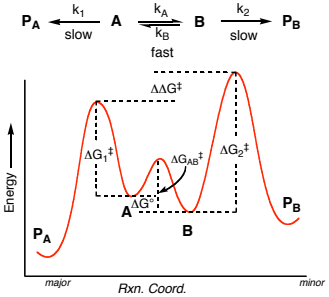

The Derivation:

Using the rate equations $\frac{d[P_A]}{dt} = k_1[A]$ and $\frac{d[P_B]}{dt} = k_2[B]$ we can write:

$$\frac{d[P_B]}{d[P_A]} = \frac{k_2[B]}{k_1[A]} \quad \text{or} \quad d[P_B] = \frac{k_2[B]}{k_1[A]}\, d[P_A] \qquad (2)$$

Since A and B are in equilibrium, we can substitute $K_{eq} = \frac{[B]}{[A]}$

$$\int d[P_B] = \frac{k_2}{k_1} K_{eq} \int d[P_A] \quad \text{Integrating, we get} \quad \frac{[P_B]}{[P_A]} = \frac{k_2}{k_1} K_{eq} \qquad (3)$$

When A and B are in rapid equilibrium, we must consider the rates of reaction of the conformers as well as the equilibrium constant when analyzing the product ratio.

To relate this quantity to ΔG values, recall that $\Delta G^o = -RT \ln K_{eq}$ or $K_{eq} = e^{-\Delta G°/RT}$, $k_1 = e^{-\Delta G_1^{\ddagger}/RT}$, and $k_2 = e^{-\Delta G_2^{\ddagger}/RT}$. Substituting this into the above equation:

$$\frac{[P_B]}{[P_A]} = \frac{k_2}{k_1} K_{eq} = \frac{e^{-\Delta G_2^{\ddagger}/RT}}{e^{-\Delta G_1^{\ddagger}/RT}} (e^{-\Delta G°/RT}) = e^{-\Delta G_2^{\ddagger}/RT} e^{-\Delta G°/RT} e^{\Delta G_1^{\ddagger}/RT} \qquad (4)$$

Combining terms:

$$\frac{[P_B]}{[P_A]} = e^{-(\Delta G_2^{\ddagger} + \Delta G° - \Delta G_1^{\ddagger})/RT} \quad \text{or} \quad \frac{[P_B]}{[P_A]} = e^{-\Delta\Delta G^{\ddagger}/RT}$$

Where $\Delta\Delta G^{\ddagger} = \Delta G_2^{\ddagger} + \Delta G° - \Delta G_1^{\ddagger}$

Curtin - Hammett Principle: The product composition is not solely dependent on relative proportions of the conformational isomers in the substrate; it is controlled by the difference in standard Gibbs energies of the respective transition states.

Within these limits, we can envision three scenarios:

- If both conformers react at the **same rate**, the product distribution will be the same as the ratio of conformers at equilibrium.
- If the **major conformer** is also the faster reacting conformer, the product from the major conformer should prevail, and will not reflect the equilibrium distribution.
- If the **minor conformer** is the faster reacting conformer, the product ratio will depend on all three variables in eq (2), and the observed product distribution will not reflect the equilibrium distribution.

This derivation implies that you could potentially isolate a product which is derived from a conformer that you can't even observe in the ground state!

"Non-Equilibrating Conformers"

k_1, k_2 >> k_A, k_B: If the rates of reaction are **faster** than the rate of interconversion, A and B cannot equilibrate during the course of the reaction, and the product distribution (P_B/P_A) will simply reflect the initial equilibrium composition.

$$\frac{[P_B]}{[P_A]} = \frac{[B]_o}{[A]_o}$$

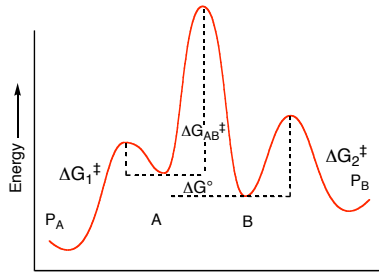

"Non-Equilibrating Conformers"

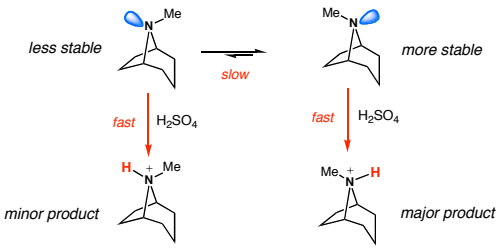

The rates of protonation are much faster than the rates of conformation interconversion

Introduction

Two new classes of potent nonnucleoside reverse transcriptase inhibitors were recently reported by the Merck Research Laboratories: the 3,4-dihydroquinazolin-2(1*H*)-ones[1] and the 1,4-dihydro-2*H*-3,1-benzoxazin-2-ones.[2] Efforts to enhance the clinical utility of these inhibitor classes by deriving compounds that express both high levels of antiviral activity and augmented pharmacokinetic profiles led to one promising compound from each class—L-738,372 and DMP-266. DMP-266 was ultimately

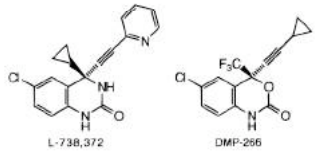

chosen for clinical evaluation[2] and has shown excellent preliminary results for the treatment of HIV when used in combination with indinavir.[3,4] The potential importance of

A Dramatic case from Merck

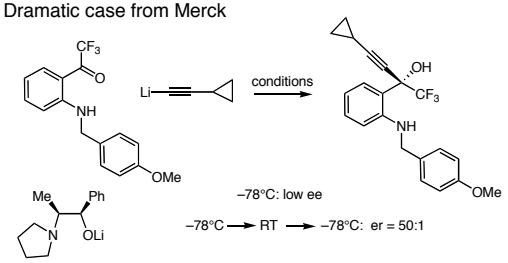

JACS **1998,** *120,* 2028-2038

Tropane alkylation is a well-known example.

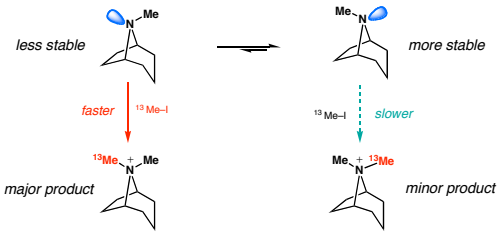

The less stable conformer reacts much faster than the more stable conformer, resulting in an unexpected major product!

JOC **1974** 319

Oxidation of piperidines:

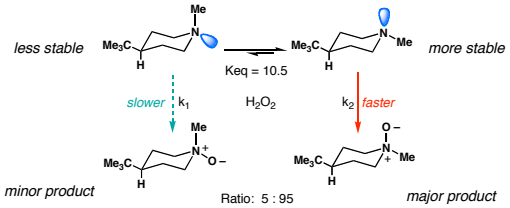

When the equilibrium constant is known, the Curtin-Hammett derivation can be used to calculate the relative rates of reaction of the two conformers. Substituting the above data into $[P_B]/[P_A] = k_2K/k_1$, the ratio $k_2/k_1 \sim 2$.

Note that in this case, the more stable conformer is also the faster reacting conformer!

Tet. **1972** 573
Tet. **1977** 915

Enantioselective Lithiation:

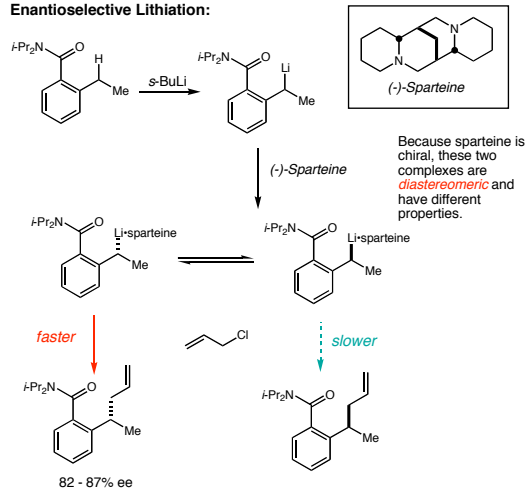

Because sparteine is chiral, these two complexes are *diastereomeric* and have different properties.

Enantioselectivities are the same, regardless of whether or not the starting material is chiral, even at low temperatures. Further, reaction in the absence of (-)-sparteine results in racemic product.

Note that the two alkyllithium complexes MUST be in equilibrium, as the enantioselectivity is the same over the course of the reaction. If they were not equilibrating, the enantioselectivity should be higher at lower conversions.

This is a case of ***Dynamic Kinetic Resolution***: Two enantiomeric alkyl lithium complexes are equilibrating during the course of a reaction with an electrophile.

Beak, *Acc. Chem. Res*, **1996**, 552

The Curtin-Hammett treatment can be extended to ANY case where different products are formed from two rapidly intereconverting starting materials, whether they are conformers, tautomers or isomers.

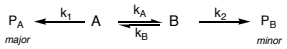

Stannylene ketals provide an efficient way to acylate the more hindered site of 1,2-diols.

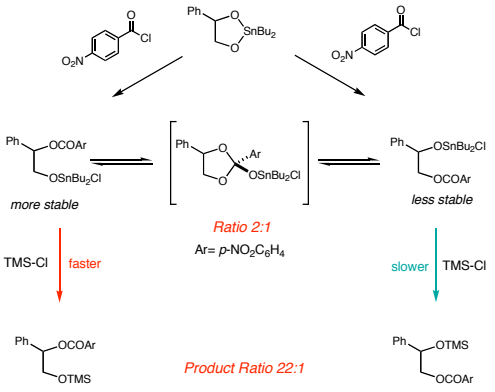

The two stannyl esters are in equilibrium at room temperature, and the more stable isomer is initially formed more slowly. The stannyl esters are allowed to equilibrate before quenching with TMS-Cl, which reacts more rapidly with the less hindered primary alkoxystannane.

JOC **1996**, 5257

"It was pointed out by Professor L. P. Hammett in 1950 (private communication) that ..."

David Y. Curtin, 1954

" Because Curtin is very generous in attributing credit, this is sometimes referrred to as the Curtin-Hammett principle rather than the Curtin principle."

Louis Plack Hammett, 1970

Curtin - Hammett Principle: *The product composition is not solely dependent on relative proportions of the conformational isomers in the substrate; it is controlled by the difference in standard Gibbs energies of the respective transition states.*

THE TAKE-HOME LESSON:

Never assume that the most stable conformation of a compound is the most reactive. It may be, but then again, it may not.

The asymmetric hydrogenation of prochiral olefins catalyzed by Rhodium is an important catalytic process.

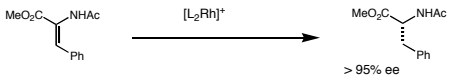

Enantioselectivities are generally very high when the ligand is a chelating diphosphine. (ee's are given for S,S-CHIRAPHOS)

When a chiral ligand is used, there are two diastereomeric complexes which may be formed:

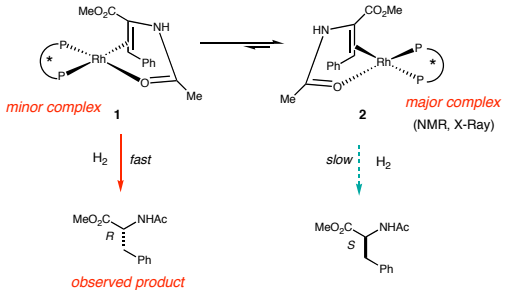

Observations:

- Complex 2 is the only diasteromer observed for the catalyst-substrate complex (1HNMR, X-Ray crystallography) in the absence of hydrogen
- The enantioselectivity is strongly dependant on the pressure of H_2, and degrades rapidly at higher hydrogen pressures
- The observed enantiomer is exclusively derived from the minor complex 2

These observations may be explained using the ***Curtin - Hammett Principle***

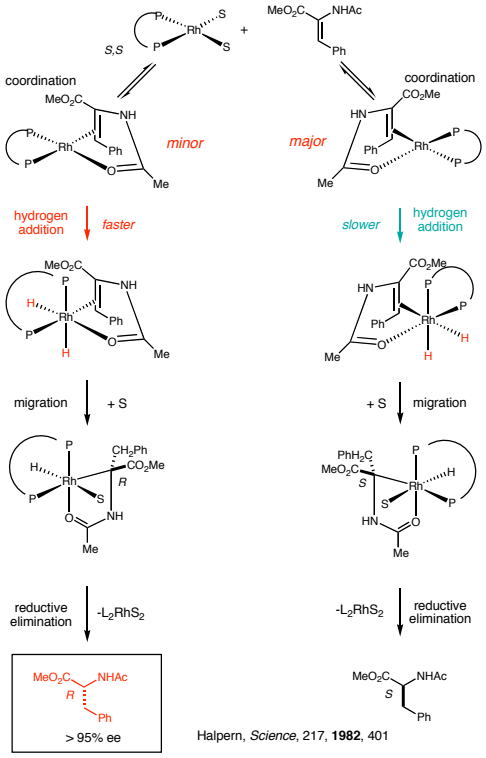

Halpern, *Science*, 217, **1982**, 401

The Hydrogenation Reaction

Review article: J. M. Brown, *Angew. Chem. Int. Edit.* **26**, 190-203 (1987) **(handout)**

■ General Mechanism

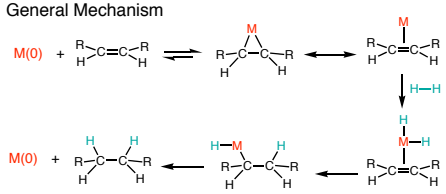

Historically, primary stereochemical control designed around analysis of steric environment in vicinity of C=C.

However, the influence of polar effects was documented

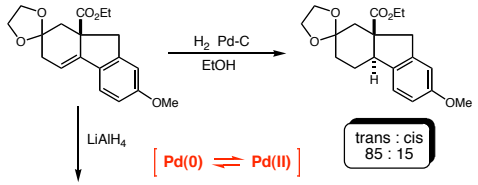

Thompson, *J.Org. Chem.* **36**, 2577 (1971)

Polar functional groups may play a role in controlling the diastereoselectivity of the hydrogenation process;
however, the control elements were not well-defined.

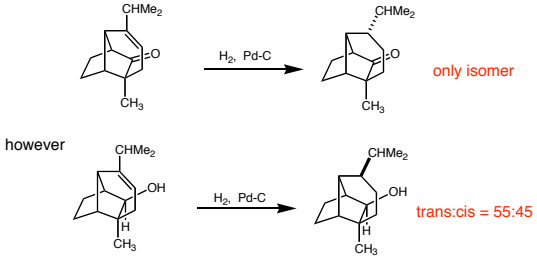

J. E. McMurry & Co-workers, *Tetrahedron Lett.*. 3731 (1970)

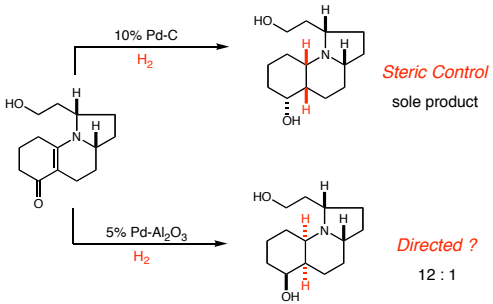

Y. Kishi & Co-workers, *J. Am. Chem. Soc.* **102**, 7156 (1980)

The first rational attempt to identify those FGs which will direct the reaction

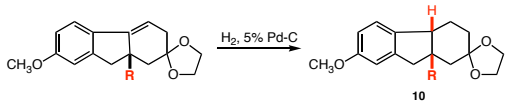

10

R	cis : trans
CH_2OH	95 : 5
CHO	93 : 7
CN	75 : 25
COONa	55 : 45
COOH	18 : 82
COOMe	15 : 85
COMe	14 : 86
$CONH_2$	10 : 90

H. Thompson & Co-workers, *J. Am. Chem. Soc.* **95**, 838 (1973)

The first rational attempt to associate catalyst with substrate:

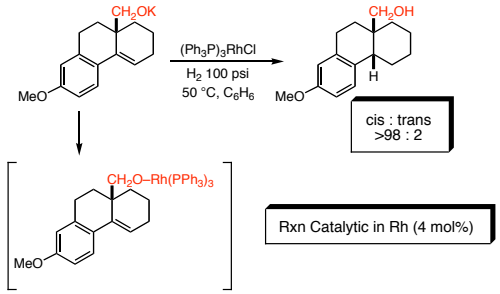

Thompson & Coworkers, *J. Am. Chem. Soc.* **97,** 6232 (1974)

Cationic Hydrogenation Catalysts

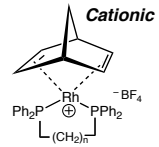

Schrock & Osborne,
J. Am. Chem. Soc. **91**, 2816 (1969)

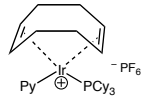

R. Crabtree
J. Organomet. Chem. **168**, 183 (1979)

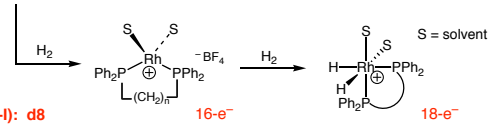

Rh(+I): d8 16-e⁻ 18-e⁻

Mechanism of Hydrogenation Cationic Rhodium-(I) Catalysts.

S = solvent

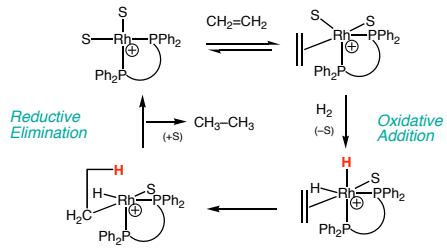

Mechanism of Hydrogenation Cationic Rhodium-(I) Catalysts.

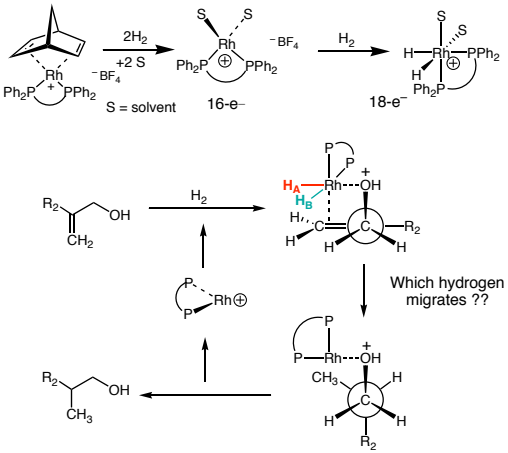

A potential stereoelectronic effect

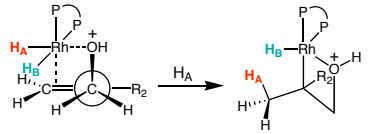

That H atom lying parallel to the pi-system (H_A) should migrate preferentiallyif the dihydride is an intermediate.

D. A. Evans & M. M. Morrissey *JACS* **106**, 3866 (1984)

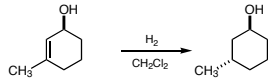

Catalyst	Mol% Catalyst	H_2 Pressure	trans:cis (Yield)
Rh(DIPHOS-4)$^+$	17.5	15 psi H_2	200 : 1 (89%)
	3.5	375 psi H_2	300 : 1 (95%)
Ir(pyr)PCy_3	20.0	15 psi H_2	50 : 1 (82%)
	2.5	15 psi H_2	150 : 1 (85%)

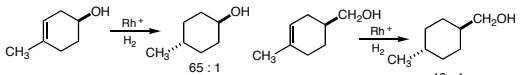

Rh(DIPHOS-4)$^+$ H_2 1000 psi CH_2Cl_2

Excessive Steric Hindrance

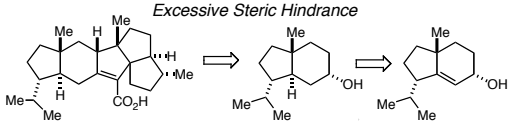

Retigeranic Acid

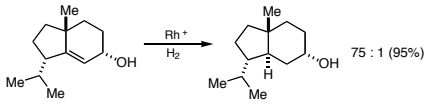

Rh(DIPHOS-4)$^+$ H_2 800 psi THF

THF is important to success of rxn to buffer the Lewis acidity of the catalyst which causes elimination of ROH under normal conditions

Polar functional groups other than OH may also direct the process

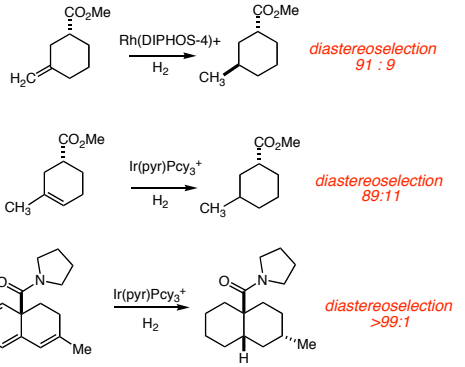

J.M. Brown and S.A. Hall, *J. Organomet. Chem.*, **1985**, *285*, 333.

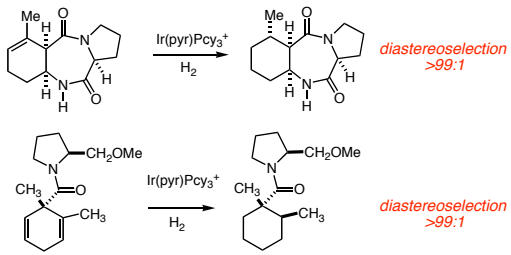

A.G. Schultz and P.J. McCloskey, *J. Org. Chem.*, **1985**, *50*, 5907.

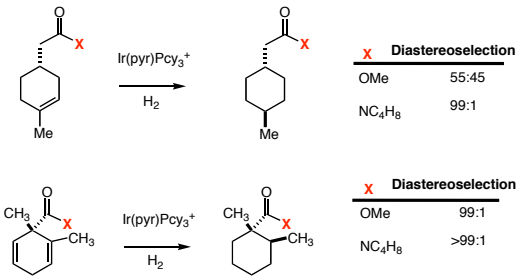

A.G. Schultz and P.J. McCloskey, *J. Org. Chem.*, **1985**, *50*, 5907.

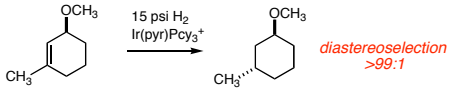

R.H. Crabtree and M.W. Davis, *J. Org. Chem.*, **1986**, *51*, 2655.

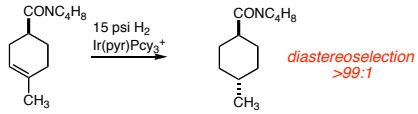

A.G. Schultz and P.J. McCloskey, *J. Org. Chem.*, **1985**, *50*, 5907.

Diastereoselective Hydrogenation: Acyclic Substrates

Acyclic Allylic Alcohols

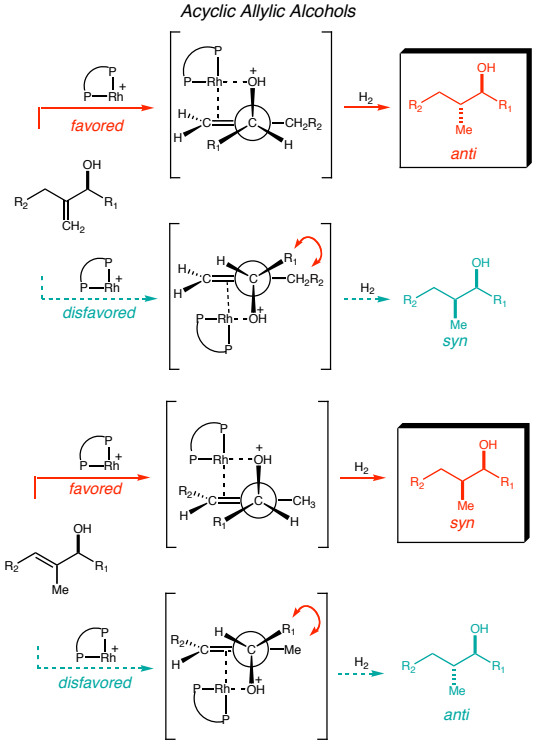

D. A. Evans & M. M. Morrissey *JACS* **106**, 3866 (1984)

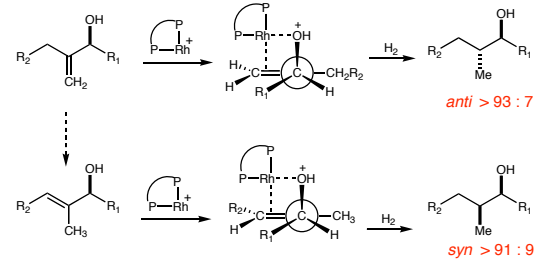

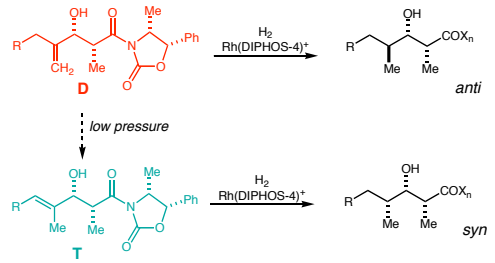

D

T

Anti : Syn Ratio

	Hydroxy-Olefin	15 psi H_2	640 psi H_2
D	R = CH_3	25 : 75 (23%)	93 : 7
	R = $(CH_3)_2CH$	52 : 48 (35%)	94 : 6
	R = Ph	71 : 29 (-)	93 : 7
T	R = CH_3	13 : 87 (6%)	9 : 91
	R = $(CH_3)_2CH$	12 : 88 (8%)	8 : 92
	R = Ph	21 : 79 (-)	6 : 94

Homoallylic Alcohols Evans, Morrissey *Tetrahedron Lett.* **26** 6005 (1985)

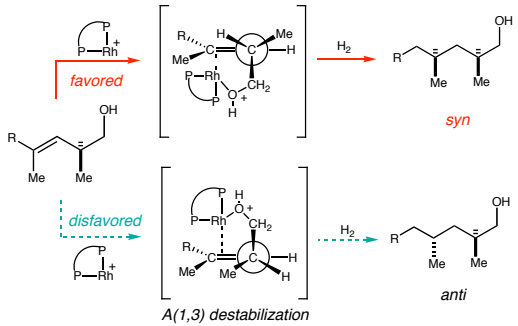

The Premonensin Synthesis

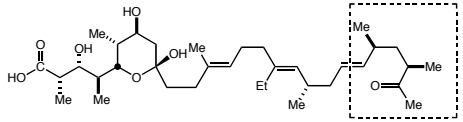

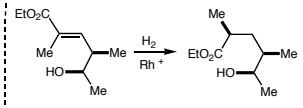

Catalyst	Ratio
Rh(DIPHOS-4)$^+$	85 : 15
Rh(–)(BINAP)$^+$	65 : 35
Rh(+)(BINAP)$^+$	98 : 2 (90%)

Evans, DiMare, *JACS*, **1986**, *108*, 2476)

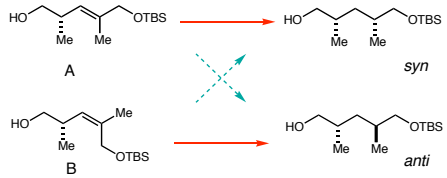

Olefin	Catalyst (H_2 Pressure)	syn : anti
A	Rh(DIPHOS-4)$^+$ (1000 psi)	95 : 5
A	Ir(pyr)PCy_3^+ (15 psi, 2.5 mol%)	73 : 27
B	Rh(DIPHOS-4)$^+$ (1000 psi)	9 : 91

The Ionomycin Synthesis

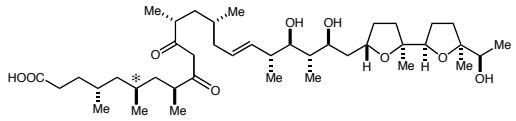

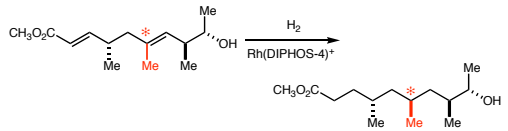

Diastereoselection: 94 : 6 (93%)

with Dow, Shih, Zahler, Takacs, *JACS* **1990**, *112*, 5290

http://www.courses.fas.harvard.edu/colgsas/1063

Chemistry 206

Advanced Organic Chemistry

Lecture Number 10

Olefin Addition Reactions–3

- Olefin Bromination
- Olefin Oxymercuration
- Halolactonization
- Simmons-Smith Reaction

Reading Assignment for week

A. Carey & Sundberg: **Part B**; Chapter 4
"Electrophilic Additions to C–C Multilple Bonds"

Investigation of the early Steps in Electrophilic Bromination through the Study of the Reaction of Sterically Encumbered Olefins
R. S. Brown, *Accts. Chem. Res.* **1997**, *30*, 131 **(handout)**

Bromoniun Ions or β-Bromocarbocations in Olefin Bromination. A Kinetic Approach to Product Selectivities
M-F. Ruasse, *Accts. Chem. Res.* **1990**, *23*, 87 **(handout)**

D. A. Evans

Monday,
October 9, 2006

Predict stereochemical outcome

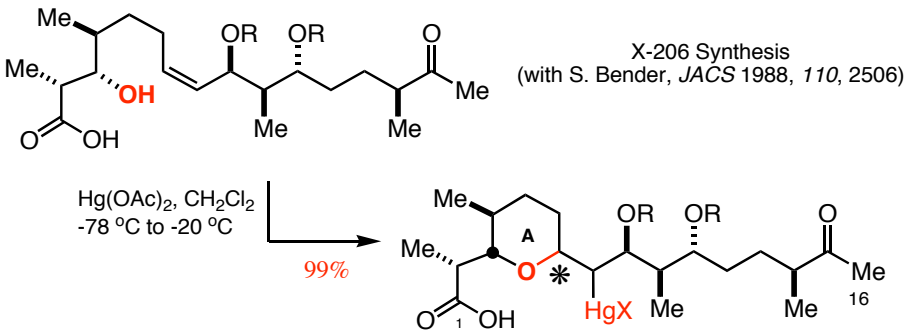

X-206 Synthesis
(with S. Bender, *JACS* 1988, *110*, 2506)

99%, *single diastereomer*

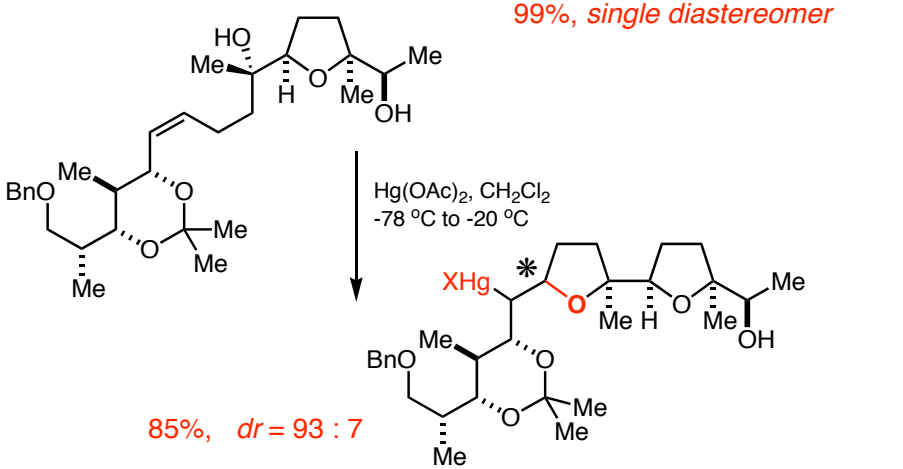

85%, *dr* = 93 : 7

Ionomycin Synthesis
(with Dow & Shih, *JACS* 1990, *112*, 5290)

Introduction

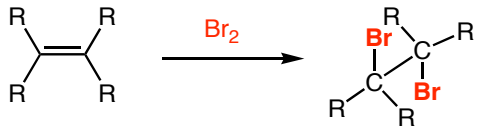

- Reaction is first order in alkene

At low concentrations of Br_2, rxn is also **first order in Br_2**

At higher concentrations of Br_2 in nonpolar solvents rxn is **2nd order in Br_2**.

- Substituent Effects on Bromination Rates

Alkene	k_{rel}
$CH_2=CH_2$	1
$CH_3CH=CH_2$	61
n-$PrCH=CH_2$	70
i-$PrCH=CH_2$	57
t-$BuCH=CH_2$	27
$(CH_3)_2C=CH_2$	5470
cis-$CH_3CH=CHCH_3$	2620
trans-$CH_3CH=CHCH_3$	1700
$(CH_3)_2C=CHCH_3$	130,000
$(CH_3)_2C=C(CH_3)_2$	1,800,000

- Stereochemical outcome versus structure (Br_2 in HOAc @ 25°)

Alkene	% anti addition	Alkene	% anti addition
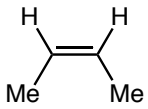	100%	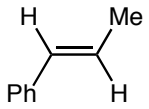	83%
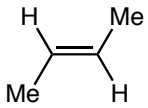	100%	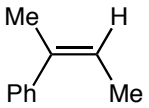	63%
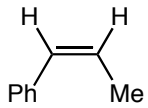	73%	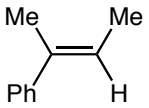	68%

- Bromonium ion origin of the anti (trans) selectivity first suggested by Roberts, *JACS* **1937**, *59*, 947

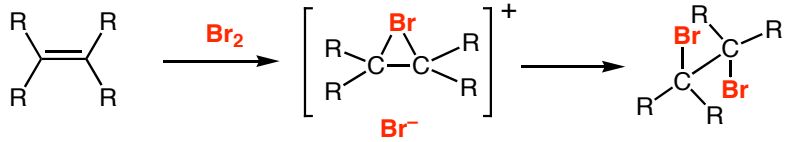

- First X-ray Structure of a bromonuium ion: Brown, *JACS* **1985**, *107*, 4504

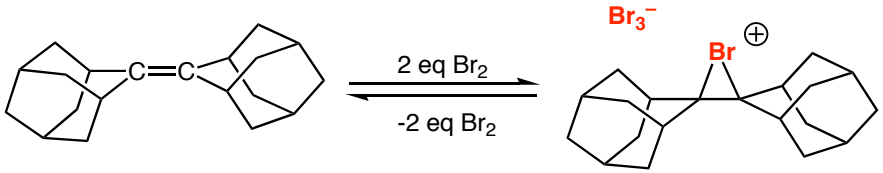

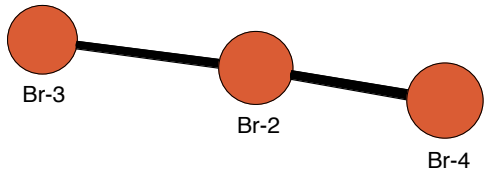

X-ray structure

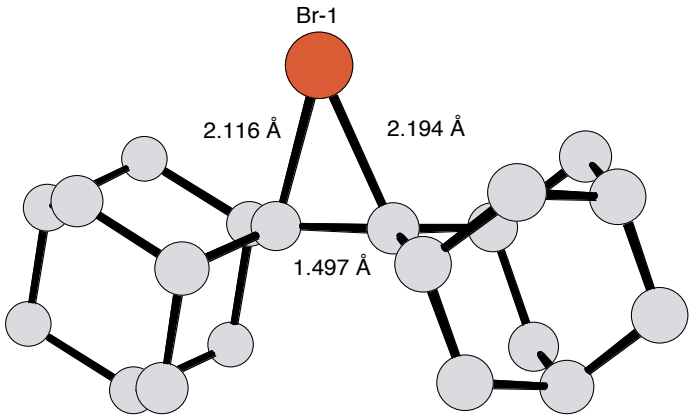

■ Calculated Geometries of Substituted Bromonium Ions
Ruasse, *Chem Commun.* **1990**, 898
More recent calculations: Sigalas, *Tetrahedron* **2003**, *59*, 4749

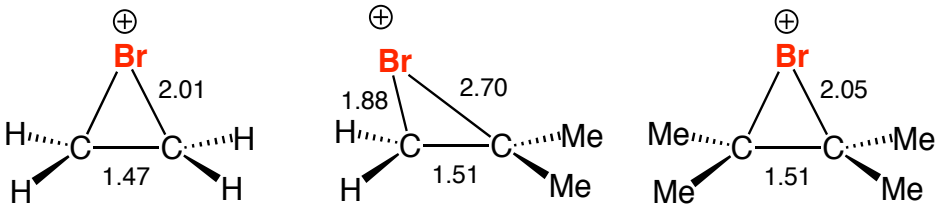

Note; the C–Br bond lengths in previous X-ray structure are 2.116 Å.

■ Bromonium Ions undergo fast exchange with olefins
Brown, *Accts. Chem. Res.* **1997**, *30*, 131

Unprecedented until 1991 (Bennet, JACS **1991**, *113*, 8532)

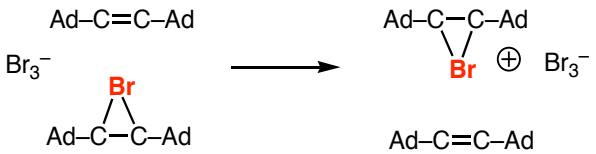

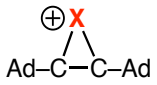

X = Br: exchange rate: 2 x 10^6 M^{-1} s^{-1}
X = I : exchange rate: 8 x 10^6 M^{-1} s^{-1}

There is an intermediate in the halogen transfer (ab initio calcs):

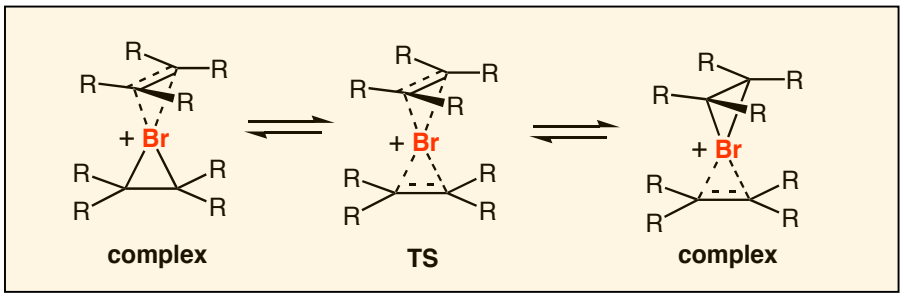

Overall Reaction Mechanism

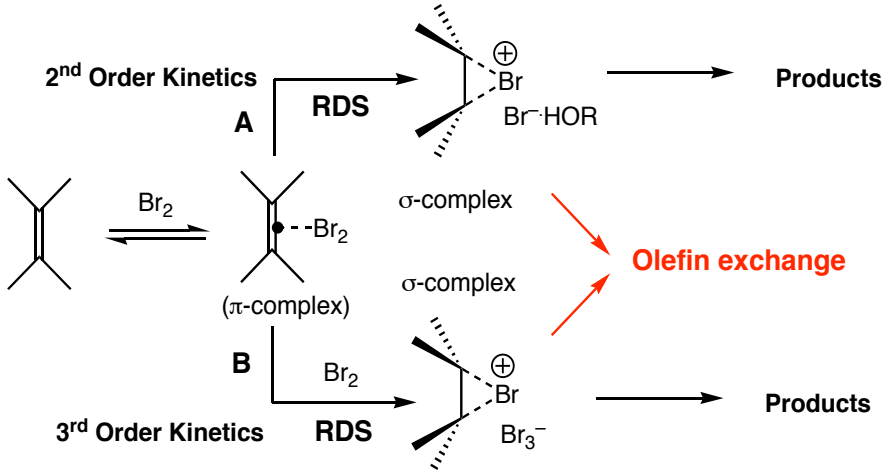

One is not committed to an addition product from the σ-complex

Bromination of Cyclohexene Derivatives **Pasto, *JACS* 1970, *92*, 7480**

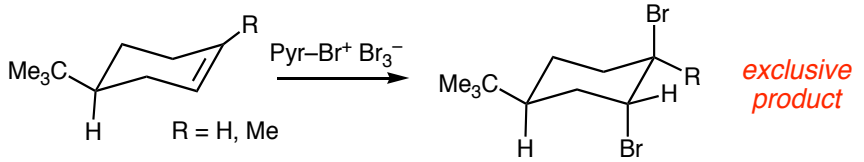

Diaxial opening of bromonium ions may be viewed as an extension of the Furst-Plattner Rule for epoxide ring opening (**Lecture-3**).

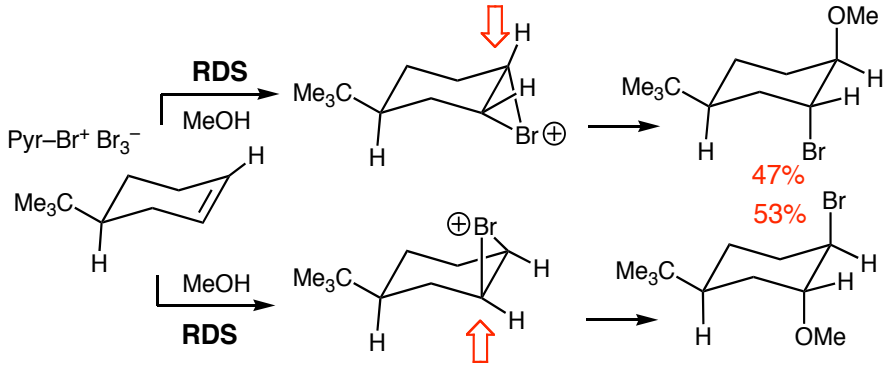

It appears that bromine attack from both olefin faces occurs with near equal probability.

Bromination of Cyclohexene Derivatives Pasto, *JACS* 1970, *92*, 7480

Diaxial opening of bromonium ions may be viewed as an extension of the Furst-Plattner Rule for epoxide ring opening. (Lecture-2)

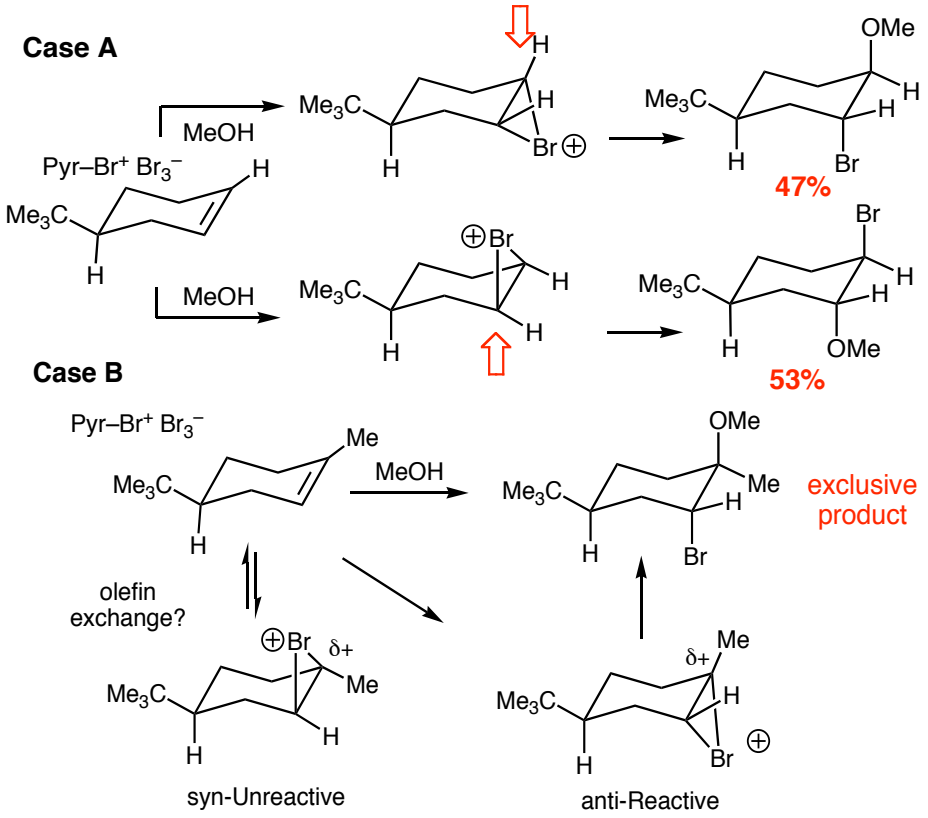

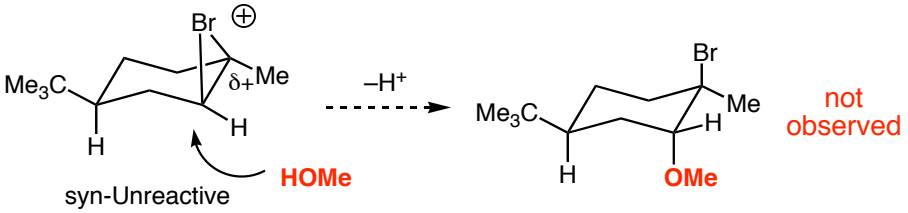

From Case **A**, one assumes that both bromonium ions are formed; however, for the syn isomer to react, ring opening must proceed against the polarization due to Methyl substituent. Therefore it is reasonable that bromoniun ion exchange must be occuring.

Representative Examples of Diastereoselective Bromination

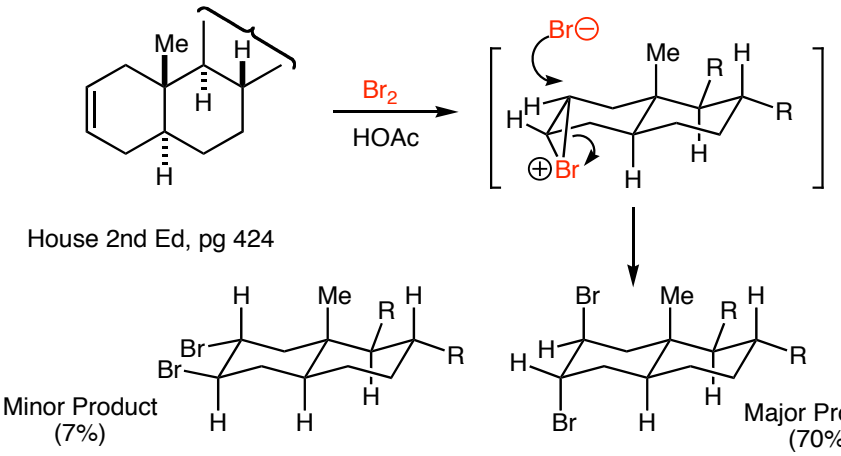

How to generate either epoxide from a conformationaly biased olefin

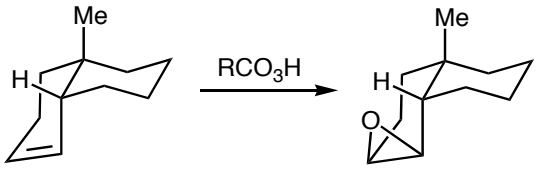

How do we construct the other epoxide diastereomer??

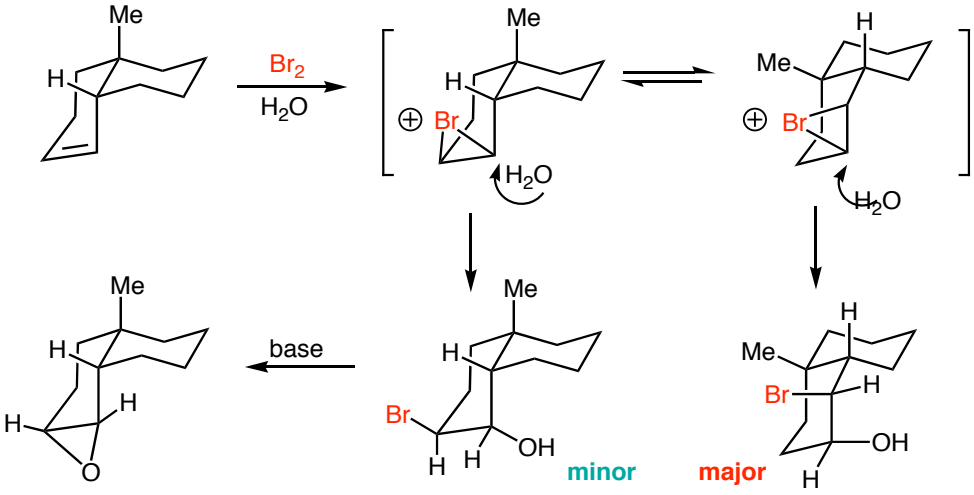

both bromohydrins afford same product

Oxymercuration **Pasto, *JACS* 1970, *92,* 7480**

The basic process:

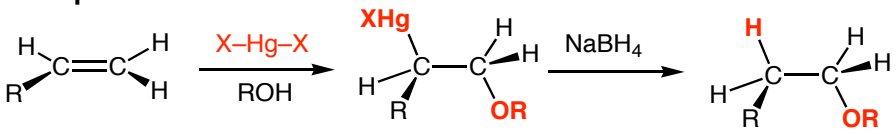

Kinetics: Halpern, *JACS* **1967**, *89*, 6427 Reduction: Pasto, *JACS* **199**, *91*, 719
Overview: B rown, *JOC* **1981**, *46*, 3810.

Oxy-Mercuration & bromination follow identical pathways (Pasto)

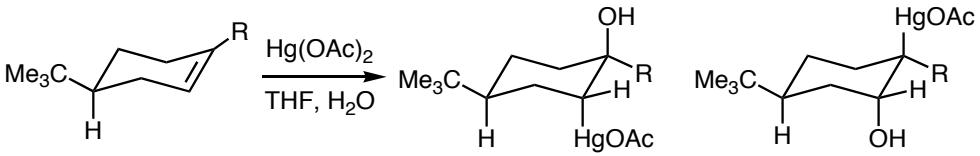

R = H 41% 48%

R = Me 100%

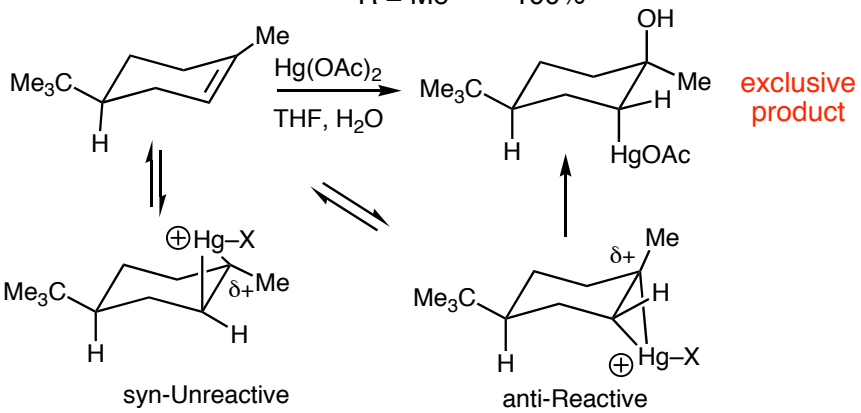

Reduction of the Hg–C bond

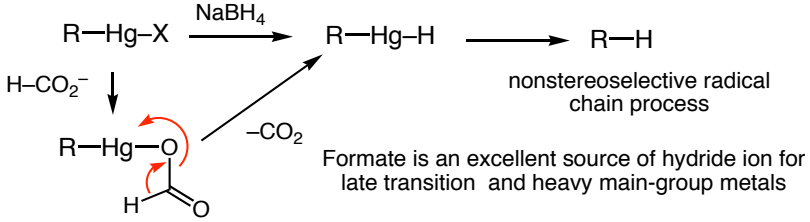

nonstereoselective radical chain process

Formate is an excellent source of hydride ion for late transition and heavy main-group metals

Bromonium and Mercurium Ions; Similarities vs Differences

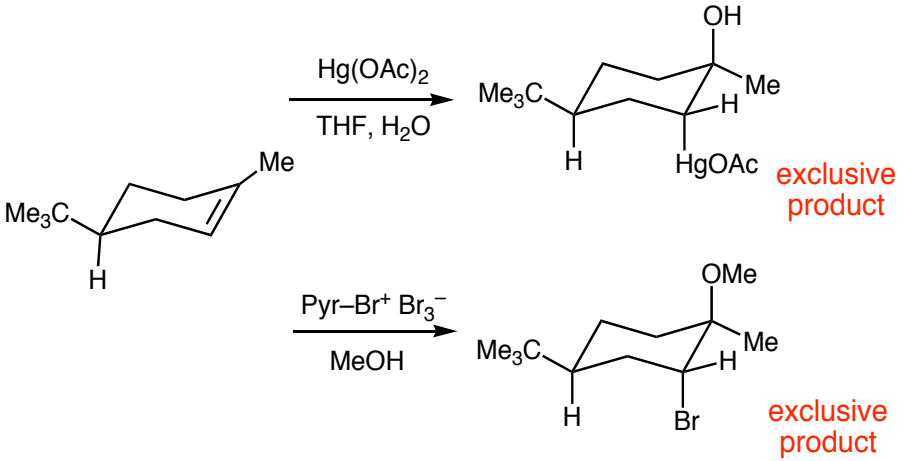

Norbornene Additions: An interesting comparision

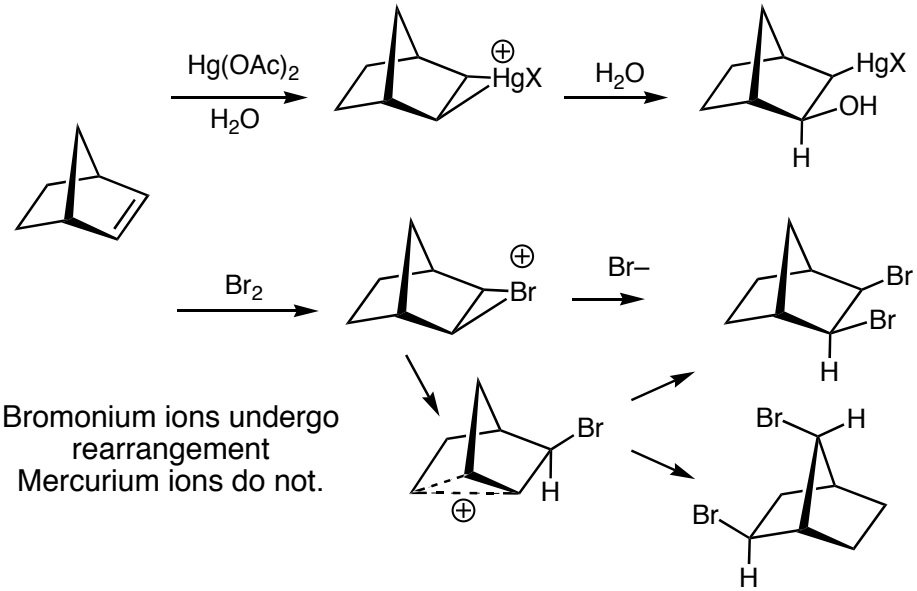

Bromonium ions undergo rearrangement
Mercurium ions do not.

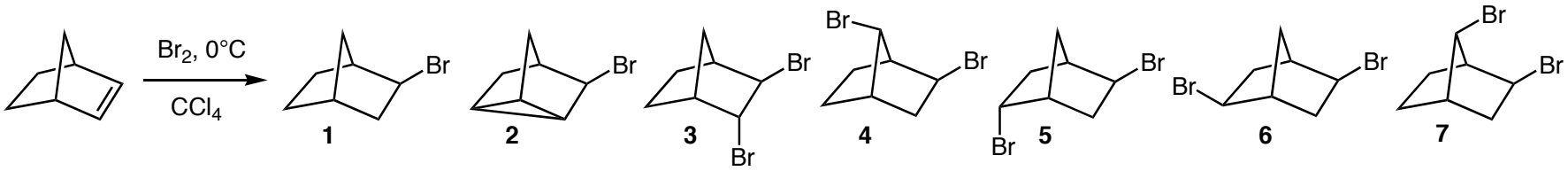

Experiment	1	2	3	4	5	6	7
Normal (0°C)	16.7	34.4	3.0	12.4	3.1	1.9	27.3
Low Temp (-78°C)	10.2	45.5	1.1	9.7	1.7	0.6	30.7
Radical Scavenger	11.4	36.0	3.1	12.1	3.0	1.3	31.8
HBr Scavenger	2.4	42.2	3.6	13.5	3.2	1.5	22.8

All compounds are kinetically controlled addition products as shown by control experiments with HBr. They are not derived from secondary reactions or isomerizations.

Products are not formed via radical chain processes as shown thrrough the use of radical scavengers.

Compound **1** is mainly formed through HBr addition.

Compound **3** is formed in equal amounts from two separate processes as shown by ^{14}C labeling experiments.

Marshall, D. R.; Warnhoff, E. W. *Can. J. Chem.* **1971**, *49*, 885

Diastereoselective ring closures via oxymercuration

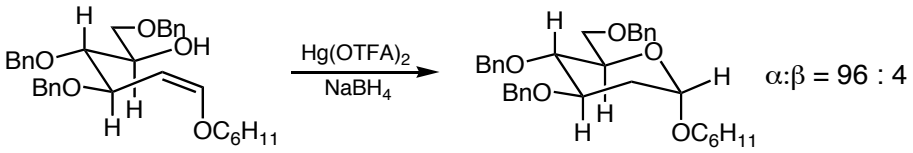

Mukaiyama, *Chem. Lett.* **1981**, 683

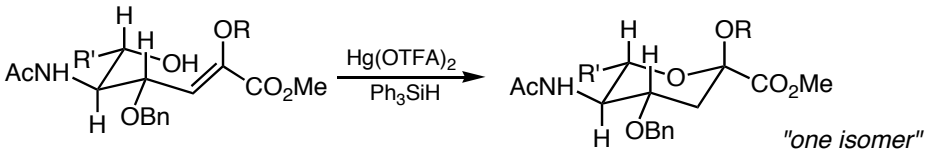

Sinay, *Tet. Lett.* **1984**, *25*, 3071

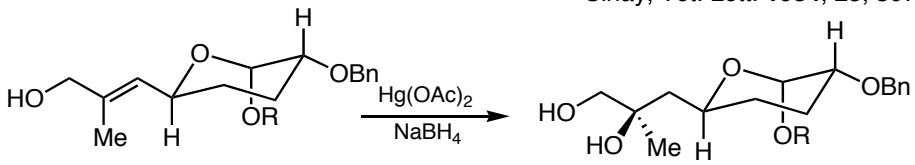

Isobe, *Tet. Lett.* **1985**, *26*, 5199

■ Kinetic vs Thermodynamic control:

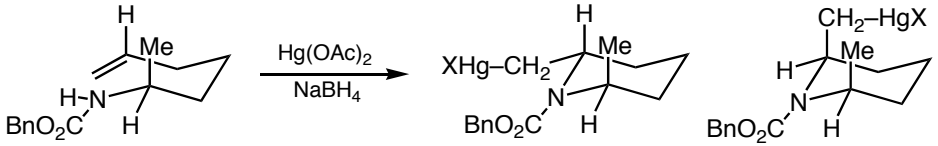

Harding, *JOC* **1984**, 49, 2838

$Hg(OAc)_2$: short rxn times : 40 : 60

$Hg(OTFA)_2$: longer rxn times : 2 : 98

With more electrophilic Hg(II) salt, more polar solvents, and longer rxn times, the rxn may be rendered reversible.

■ Acyclic allylic alcohols:

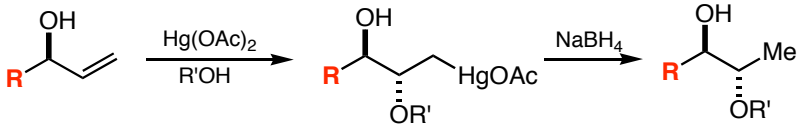

R	R'OH	Ratio	yield
-Et	HOH	76 : 24	65%
-Et	MeOH	93 : 07	72%
-Ph	HOH	88 : 12	66%
-tBu	HOH	98 : 02	70%

Giese, *Tet. Lett.* **1985**, *26*, 1197

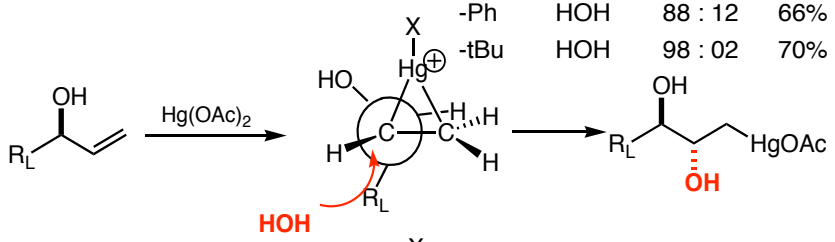

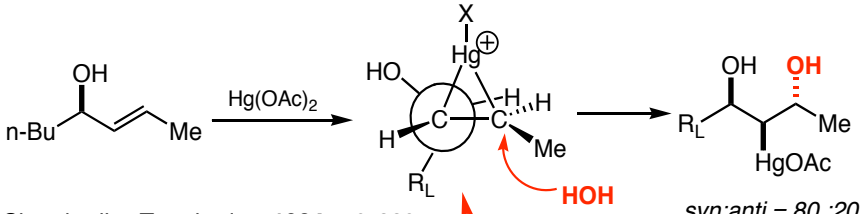

Chamberlin, *Tetrahedron* **1984**, *40*, 2297

syn:anti = 80 :20

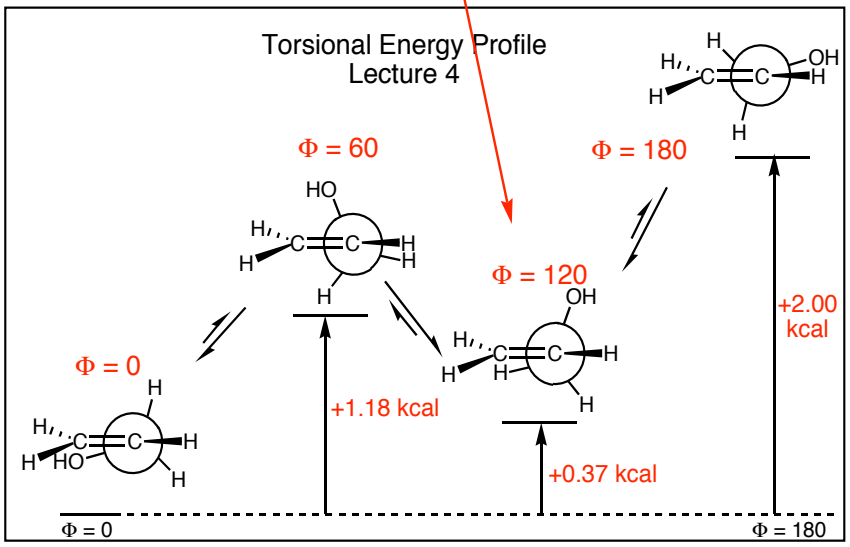

Oxymercuration via Hemiketals & Hemiacetals

J. L. Leighton et. al, *Org. Lett.* **2000**, *2*, 3197-3199

■ General Reaction: diastereoselection >10:1

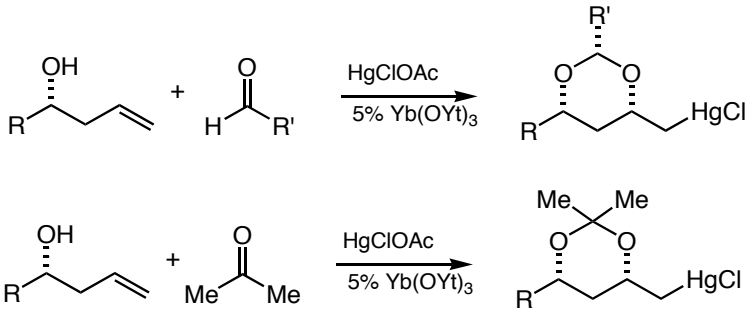

■ Mechanistic Observations:

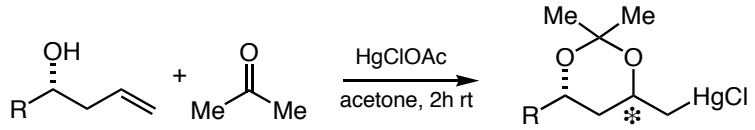

~1:1-mixture of diastereomers
Product formed in low yield.
much recovered starting material

Lewis acid addends were surveyed. the logic for this step was two-fold:

(A) Lewis acid would promote the formation of the putative hemiketal imtermediate.
(B) Lewis acid would promote reversability of the oxymercuration process

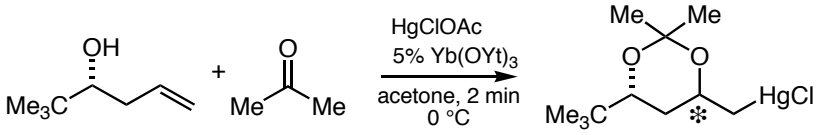

~1:1-mixture of diastereomers

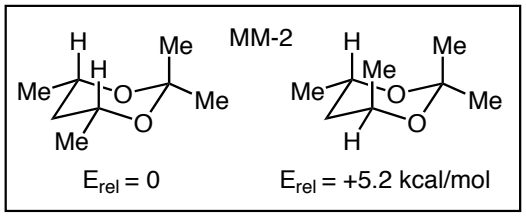

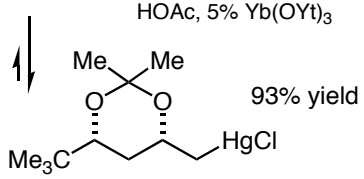

93% yield

Proposed Mechanism

■ Lewis acid catalyzes formation of hemiketal

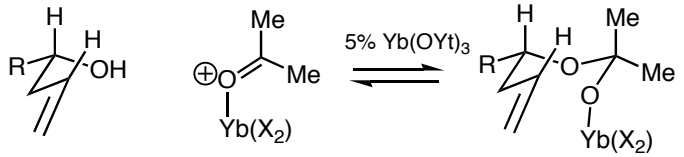

■ The Oxymercuration Step (Kinetic Phase)

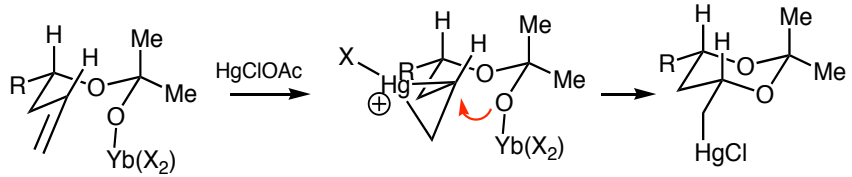

rate-determining step

low diastereoselectivity

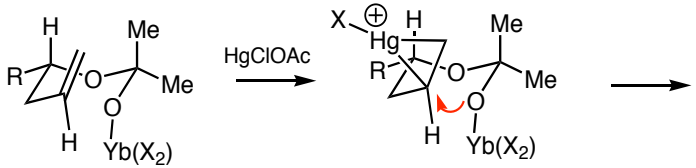

Leighton presumes that mercurium ion formation is rate-determining under kinetic conditions. At higher temperatures and longer reaction times the products are shown to interconvert.

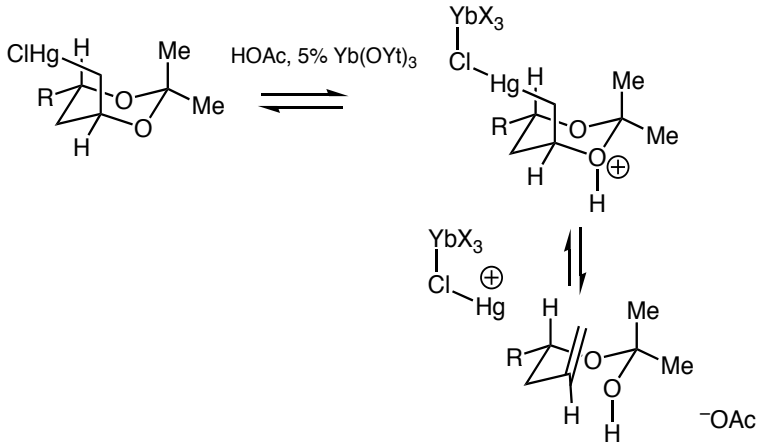

X-206 Synthesis (with S. Bender, *JACS* 1988, *110*, 2506)

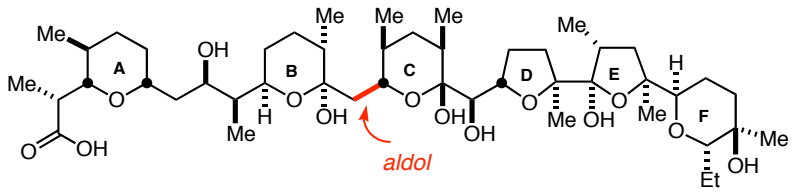

+

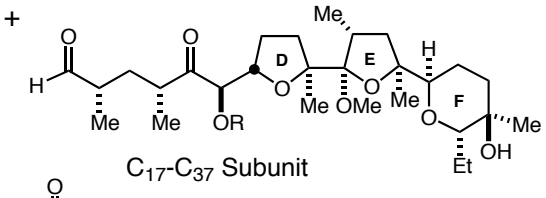

C_1-C_{16} Subunit

C_{17}-C_{37} Subunit

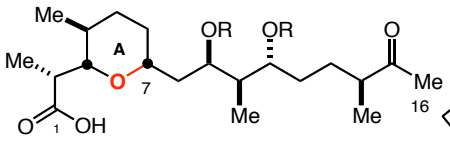

Assemblage strategy for Ring A:

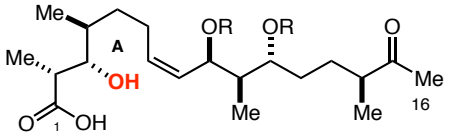

Predicted stereochemical outcome:

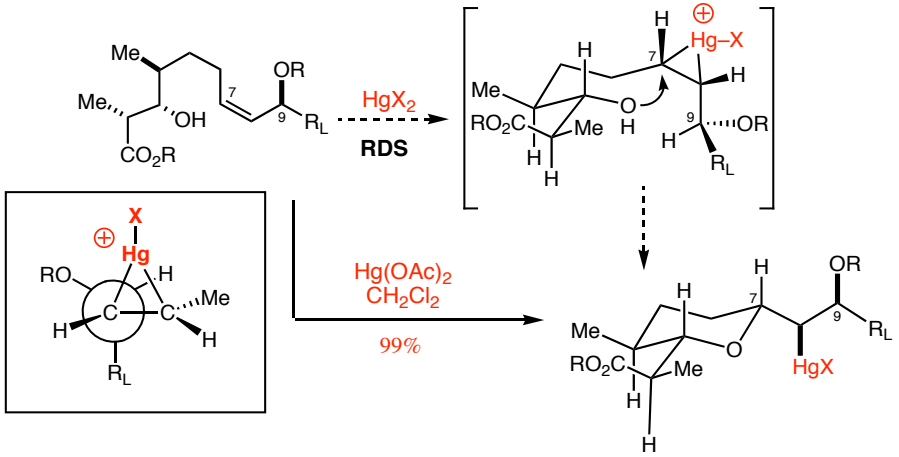

Ionomycin Synthesis (with Dow & Shih, *JACS* 1990, *112*, 5290)

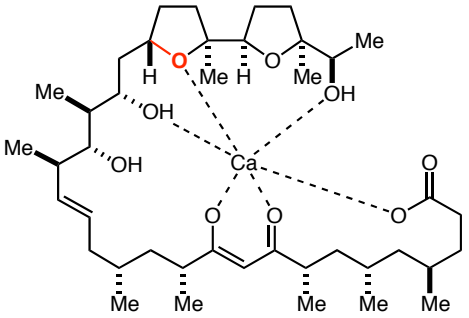

Ionomycin Calcium Complex

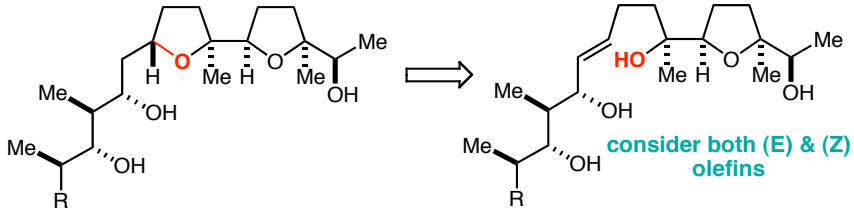

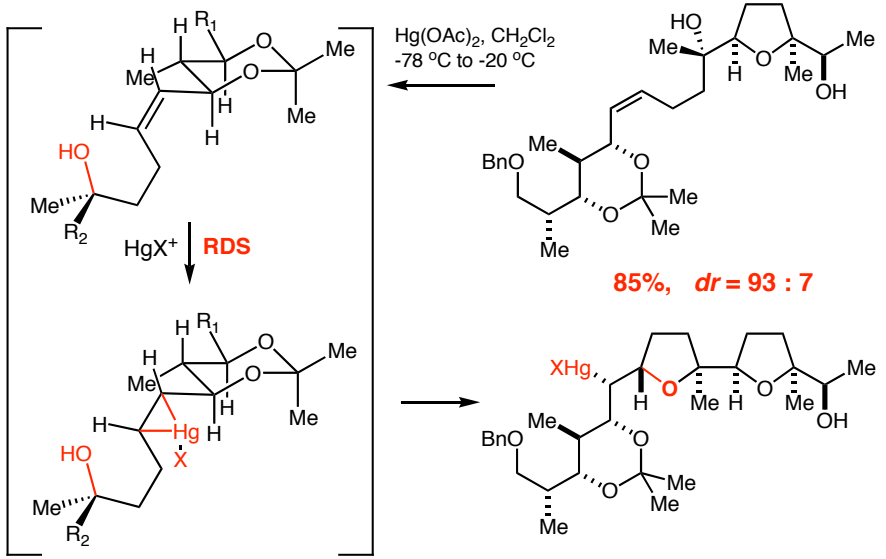

Other electrophilic olefin addition reactions afford the same stereochemical outcome

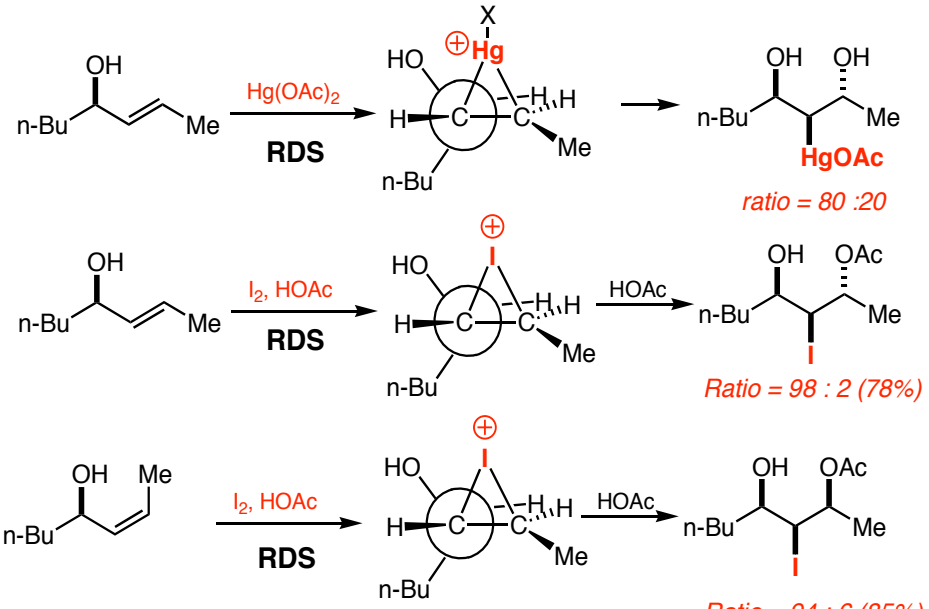

Chamberlin, *Tetrahedron* **1984**, *40*, 2297

Evans, Kaldor, Jones, *J. Am. Chem. Soc.* **1990**, *112*, 7001.

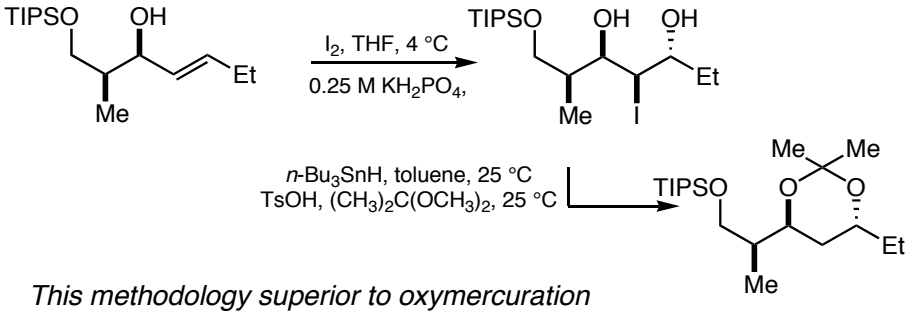

This methodology superior to oxymercuration alternative which was evaluated first

diastereoselection 96 : 4

67% overall

Iodine-induced lactonization is also highly stereoselective

■ Chamberlin (*JACS* **1983**, *105*, 5819)

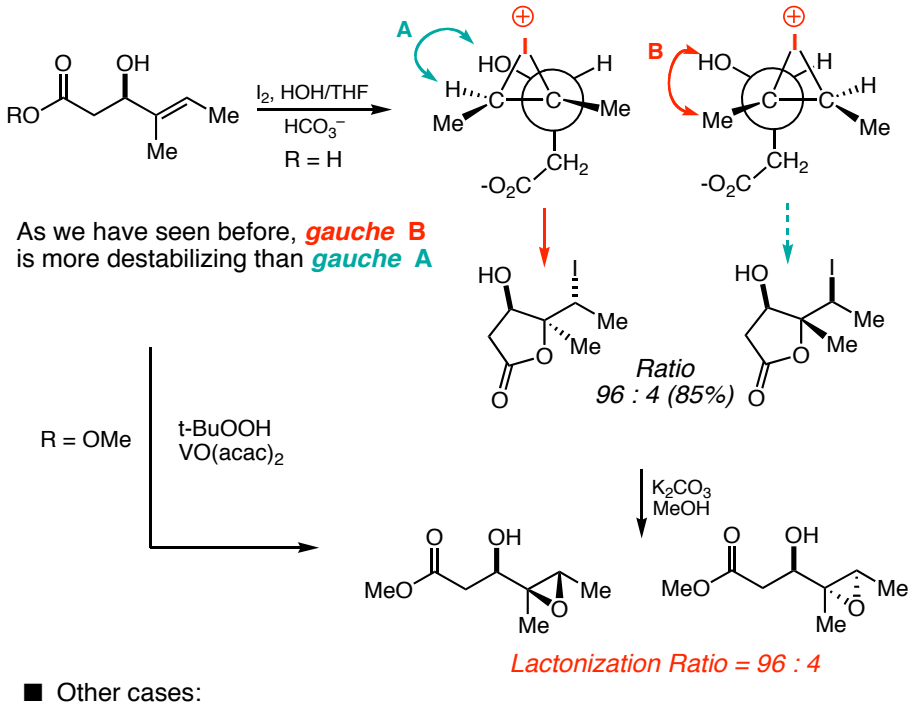

■ Other cases:

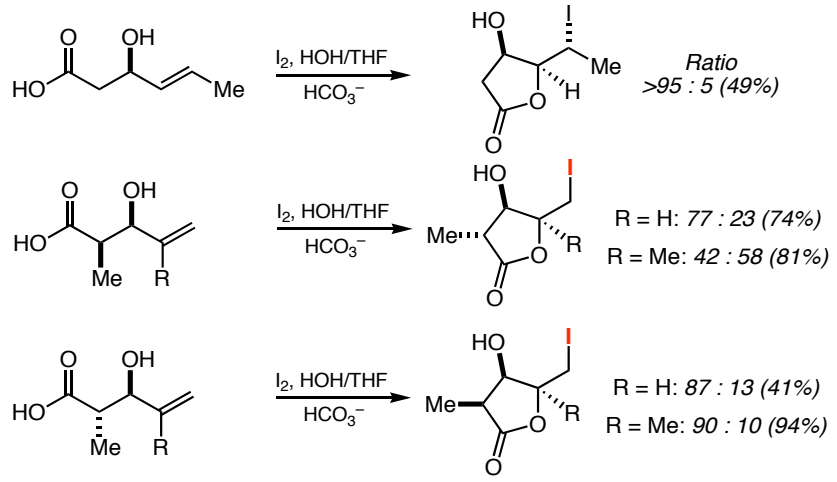

Halogen-induced heterocyclization in the synthesis of monensin

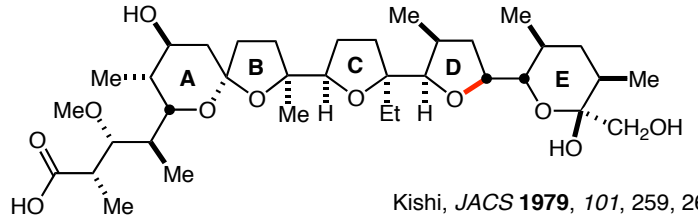

Kishi, *JACS* **1979**, *101*, 259, 260, 262
Still, *JACS* **1980**, *103*, 2117-2121

■ The Kishi Ring D Construction:

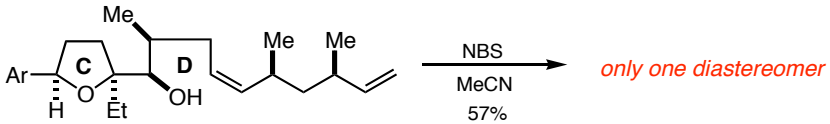

only one diastereomer

■ The Kishi Ring D Construction:

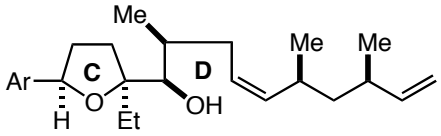

only one diastereomer

Hypothesis-A: Stereocontrol through A(1,3) Strain??

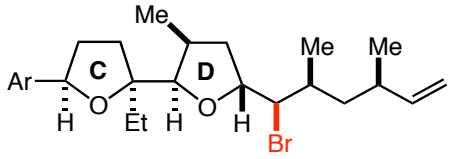

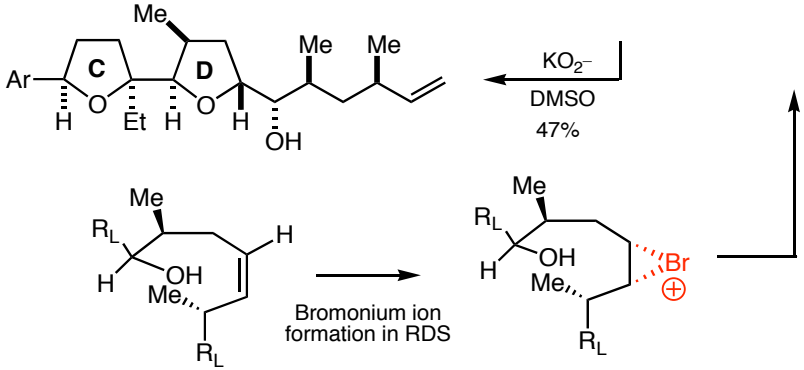

Hypothesis-B:
Stereocontrol through Reversal of Bromonium Ion Intermediate

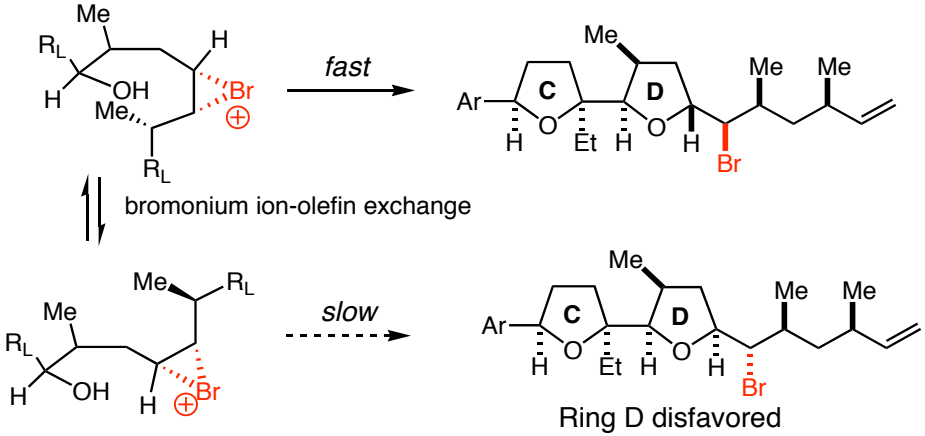

■ The Still Ring E Construction:

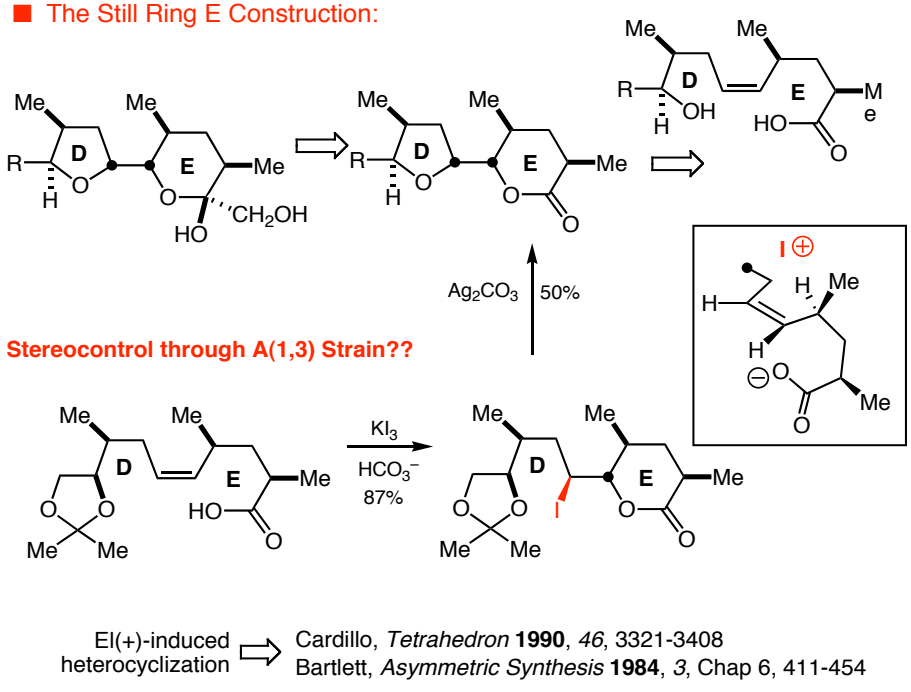

El(+)-induced heterocyclization ⇨ Cardillo, *Tetrahedron* **1990**, *46*, 3321-3408
Bartlett, *Asymmetric Synthesis* **1984**, *3*, Chap 6, 411-454

A complete turnover in olefin diastereofacial selectivity observed when adding *internal* and *external* nucleophiles

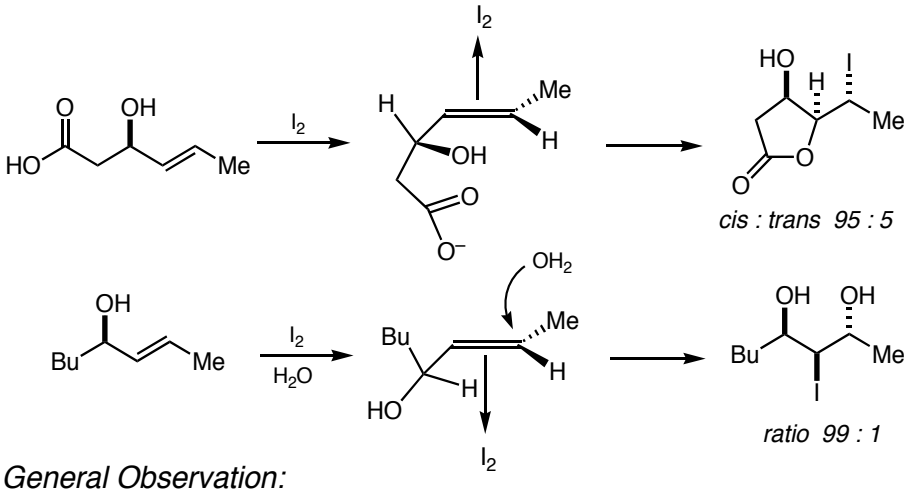

General Observation:

For electrophiles that react via onium intermediates (I_2, Br_2, $Hg(OAc)_2$, PhSeCl), the major diastereomer from electrophile-induced cyclization is **opposite** to that observed in the analogous intermolecular electrophilic addition.

For a review of elctrophilic induced olefin cyclization reactions see:
G. Cardillo & M. Orena, *Tetrahedron* **1990**, *46*, 3321.

Chamberlin & Hehre's Rationalization

- "Facial preferences in electrophilic addition reactions are *not* invariant with respect to the location of the transition state along the reaction coordinate."
- *Change in diastereoselectivity is a consequence of a change in the **rate-limiting step***
  - Addition reactions: Formation of an **onium ion intermediate** (subsequently trapped by a Nu from the medium)
  - Cyclization reactions: Intramolecular attack on a **π–complex** (not an onium ion)
- Analysis of the stereoselectivity of electrophilic addition to chiral olefins:
  1. Relative abundances of conformational minima
  2. *Relative reactivities of the available forms*
  3. Stereoselectivies of the individual conformers

Chamberlin & Hehre, *J. Am. Chem. Soc.* **1987**, *109*, 672-677.

Hehre's Analysis

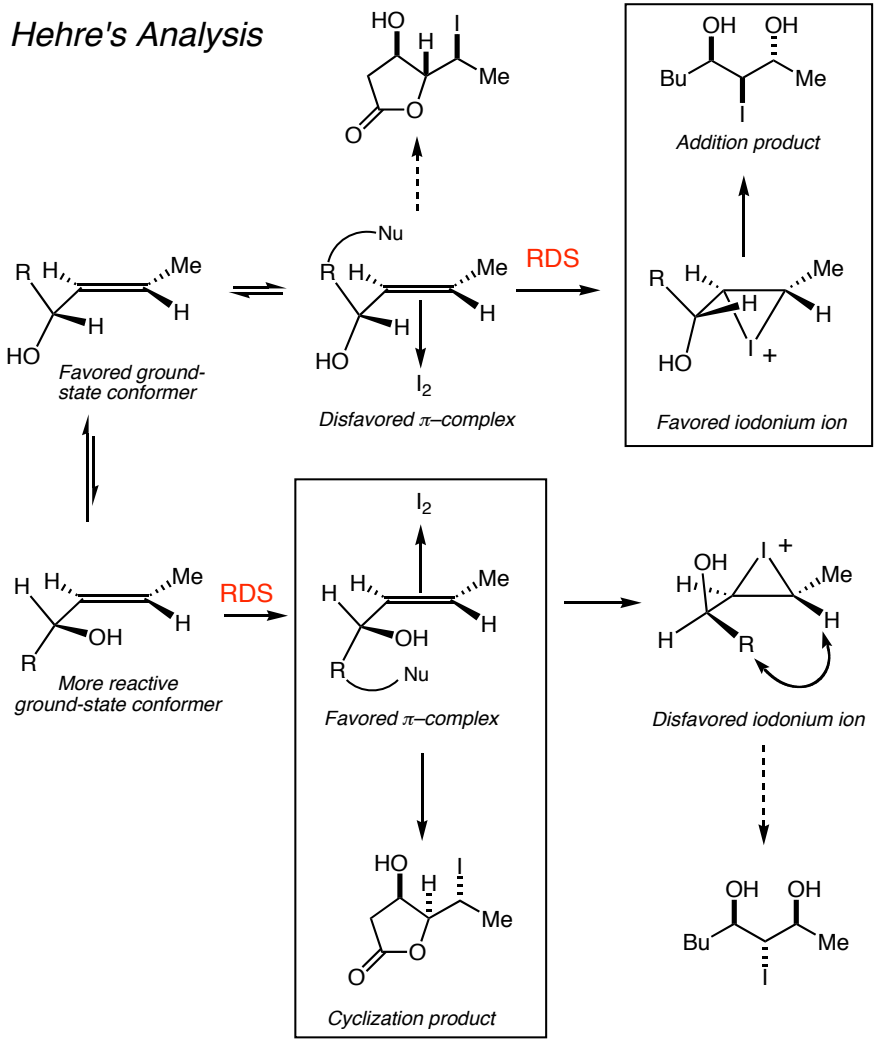

Houk: Argument for the "inside alkoxy effect" in π–complex formation

- π–complex cyclizes if R contains a Nu and its formation is rate determining
- Onium ion formation is rate determing in the addition reactions
- "The presence or absence of an internal nucleophile acts to determine the stereochemical outcome of the reaction by modifying the nature (timing) of transition state.

Tl(+3) and Pb(+4) Good 2-Electron Oxidants

	III	IV
	B	C
	Al	Si
	Ga	Ge
	In	Sn
Hg	Tl	Pb

In Group III and IV the +2 oxidation state becomes increasingly stable. This becomes evident when is is observed that Pb(IV) and Tl(III) are good 2-electron oxidants.

Pb(IV) appears to function as a successive one-electron oxidant as is indicated in the brief summary provided below:

Pb(IV) Oxidation of Alcohols

$$ROH + Pb(OAc)_4 \longrightarrow ROPb(OAc)_3 + HOAc$$
$$ROPb(OAc)_3 \longrightarrow RO\bullet + \bullet Pb(OAc)_3$$
$$RO\bullet + R'H \longrightarrow ROH + R'\bullet$$
$$R'\bullet + Pb(OAc)_4 \longrightarrow R'OAc + \bullet Pb(OAc)_3$$

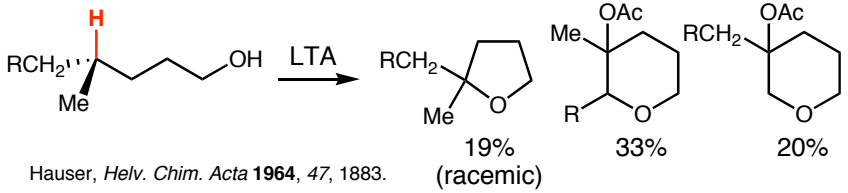

Hauser, *Helv. Chim. Acta* **1964**, *47*, 1883.

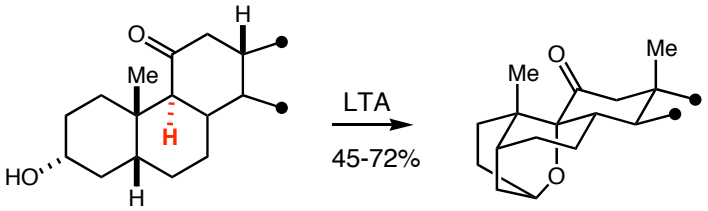

Immer, *Helv. Chim. Acta* **1962**, *45*, 753.

Reactions of Tl(+3) with Olefins

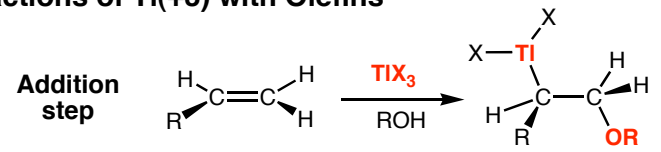

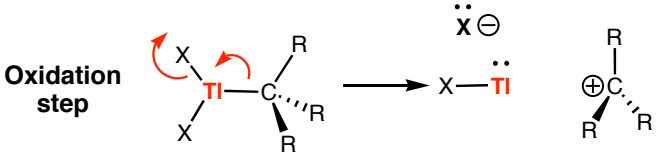

The oxidation step is analogous to a solvolysis of the C–Tl(III) bond. Consequently, the olefin oxythallation step is followed by an oxidation step. Several examples follow using $Tl(NO_3)_3$ (TTN) as the reagent:

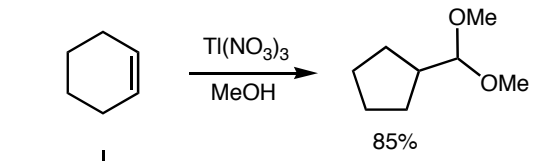

McKillop and Taylor, *JACS*, **1973**, *95*, 3635.

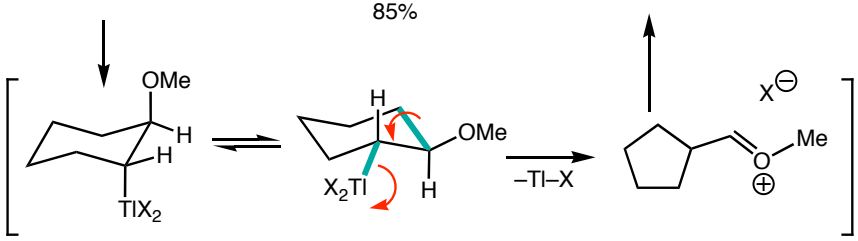

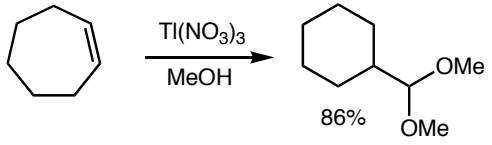

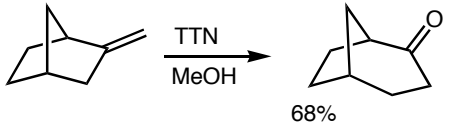

Jones, *JACS*, **1976**, *98*, 8476.

More Reactions of Tl(+3) with Olefins....

TTN = $Tl(NO_3)_3$
TTFA = $Tl(O_2CF_3)_3$

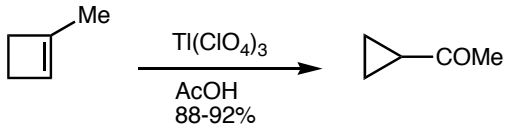

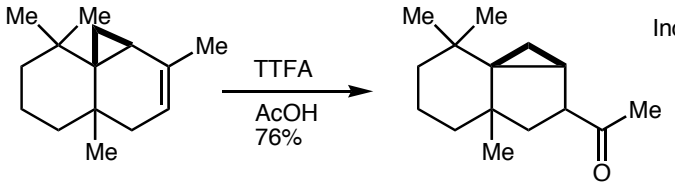

Inoue, *Bull. Chem. Soc. Jpn.* **197**, *51*, 2439.

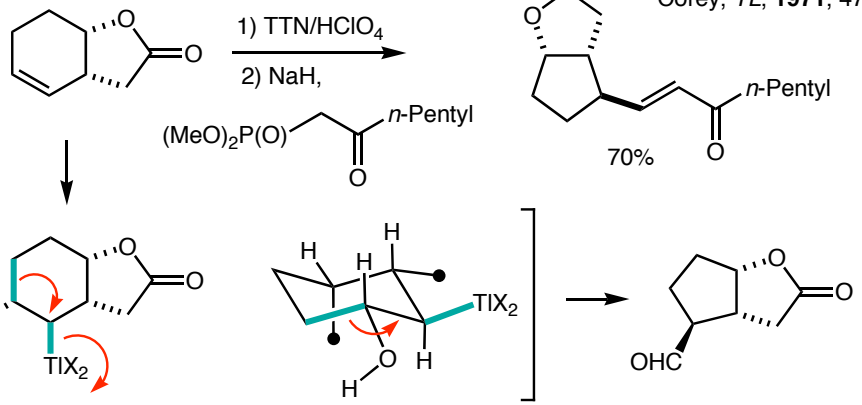

Corey, *TL*, **1971**, 4753.

Oxidative Rearrangements of Styrenes...

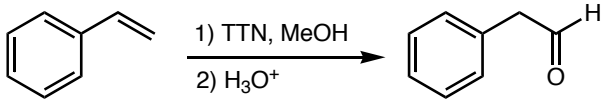

McKillop and Taylor, *JACS*, **1973**, *95*, 3635.

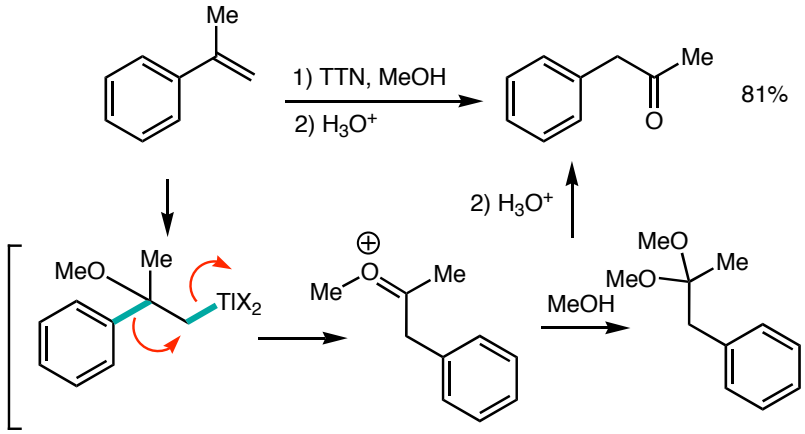

McKillop and Taylor, *JACS*, **1973**, *95*, 3635.

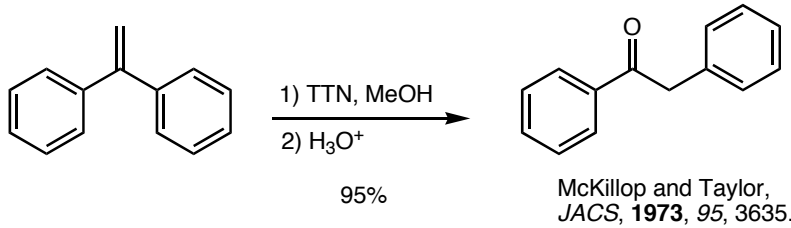

McKillop and Taylor, *JACS*, **1973**, *95*, 3635.

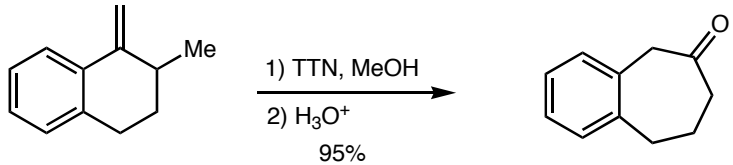

McKillop and Taylor, *TL*, **1977**, 1827.

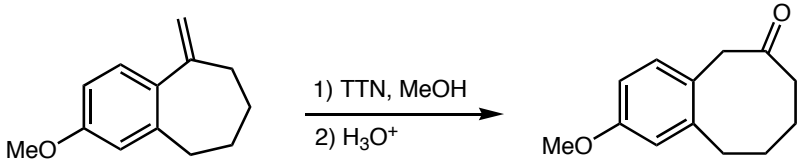

McKillop and Taylor, *TL*, **1977**, 1827.

http://www.courses.fas.harvard.edu/colgsas/1063

Chemistry 206

Advanced Organic Chemistry

Lecture Number 11

Pericyclic Reactions–1

- Introduction to Pericyclic Reactions
- Electrocyclic Reactions
- Sigmatropic Reactions
- Cycloaddition Reactions

Reading Assignment for week:

Carey & Sundberg: **Part A**; Chapter 11
Concerted Pericyclic Reactions

Wednesday,
October 11, 2006

Other Reading Material:

- Woodward-Hoffmann Theory
  R. B. Woodward and R. Hoffmann, *The Conservation of Orbital Symmetry*, Verlag Chemie, Weinheim, 1970.
- Frontier Molecular Orbital Theory
  I. Fleming, *Frontier Orbitals and Organic Chemical Reactions*, John-Wiley and Sons, New York, 1976.
- Dewar-Zimmerman Theory
  T. H. Lowry and K. S. Richardson, *Mechanism and Theory in Organic Chemistry, 3rd Ed.*, Harper & Row, New York, 1987.
- General Reference
  R. E. Lehr and A. P. Marchand, *Orbital Symmetry: A Problem Solving Approach*, Academic Press, New York, 1972.

Problems of the Day:

Predict the stereochemical outcome of this reaction.

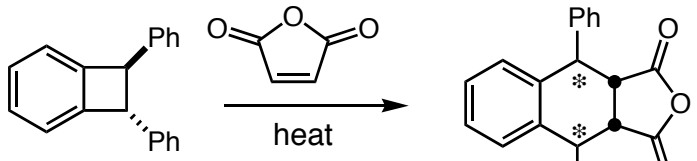

Huisgen, *TL*, **1964**, 3381.

Suggest a mechanism for the following reaction.

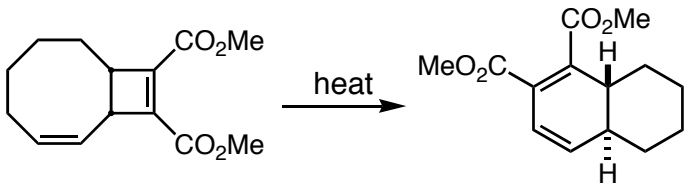

Bloomfield, *TL*, **1969**, 3719.

Pericyclic Reactions - Introduction/Definitions

A pericyclic reaction is characterized as a change in bonding relationships that takes place as a ***continuous, concerted reorganization of electrons***.

The term "***concerted***" specifies that there is ***one single transition state*** and therefore ***no intermediates*** are involved in the process. To maintain ***continuous electron flow***, pericyclic reactions occur through ***cyclic transition states***.

More precisely: The cyclic transition state must correspond to an arrangement of the ***participating orbitals*** which has to ***maintain a bonding interaction*** between the reaction components throughout the course of the reaction.

Some factors to consider in our analysis:

The number of electrons involved has a profound influence on reactivity:

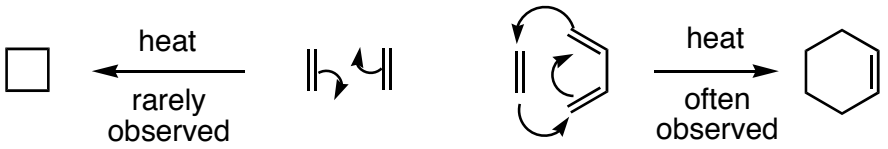

4 electrons 6 electrons

Pericyclic reactions are stereospecific:

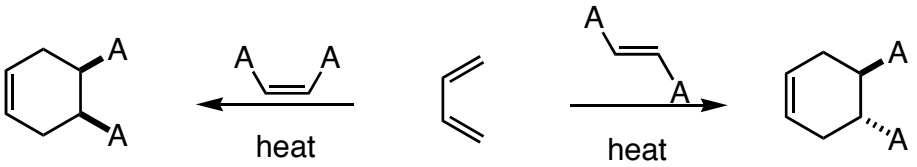

Reactions behave differently depending on the conditions used (i.e. thermal versus photochemical conditions):

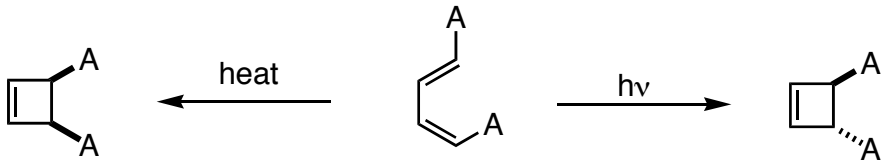

The Theories:

Three theories are commonly used to explain and predict pericyclic reactions. We will only concern ourselves with two of these theories.

1) Fukui: Frontier Molecular Orbital Interactions

Much easier to use than the original orbital symmetry arguments

HOMO/LUMO interactions

2) Dewar-Zimmerman: Aromatic Transition States

The easiest to apply for all reaction types, but it is not as easy to understand why it it valid

Aromatic or antiaromatic transition states

3) Woodward-Hoffmann: Conservation of Orbital Symmetry

First theory to explain and predict the outcome of many reactions

Correlation diagrams

The Five Major Classes of Pericyclic Reactions

(1) ELECTROCYCLIC RING CLOSURE/RING OPENING:

An electrocyclic ring closure is the creation of a new sigma bond at the expense of the terminal p orbitals of a conjugated pi system. There is a corresponding reorganization of the conjugated pi system. We classify the reaction according to the number of electrons involved.

Examples:

A 4 e^- electrocyclic reaction

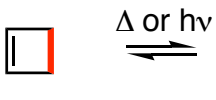

Cyclobutene Butadiene

A 6 e^- electrocyclic reaction

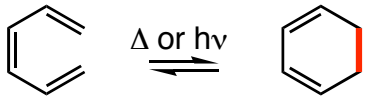

1,3,5-Hexatriene 1,3-Cyclohexadiene

(2) CYCLOADDITION REACTIONS/CYCLOREVERSION REACTIONS:

A cycloaddition reaction is the union of two smaller, independent pi systems. Sigma bonds are created at the expense of pi bonds.

Cycloaddition reactions are referred to as [**m + n**] additions when a system of **m** conjugated *atoms* combines with a system of **n** conjugated *atoms*.

A cycloreversion is simply the reverse of a cycloaddition.

Examples:

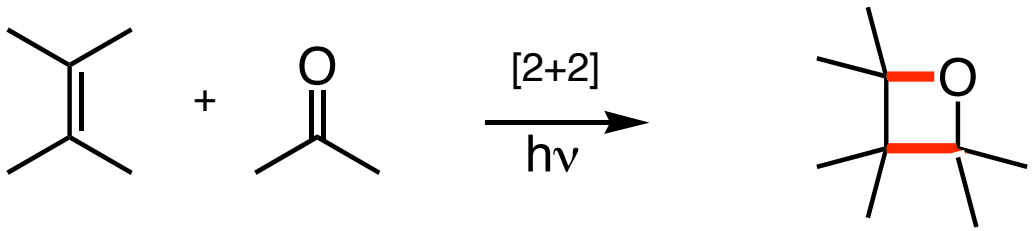

A 2+2 cycloaddition.
The Paterno-Büchi reaction.

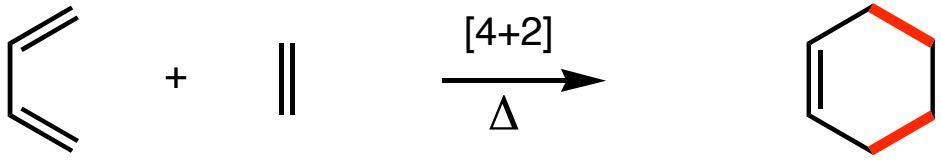

A 4+2 cycloaddition.
The Diels-Alder reaction.

(3) CHELETROPIC REACTIONS:

Cheletropic reactions are a special group of cycloaddition/cycloreversion reactions.

Two bonds are formed or broken at a single atom.

The nomenclature for cheletropic reactions is the same as for cycloadditions.

Examples:

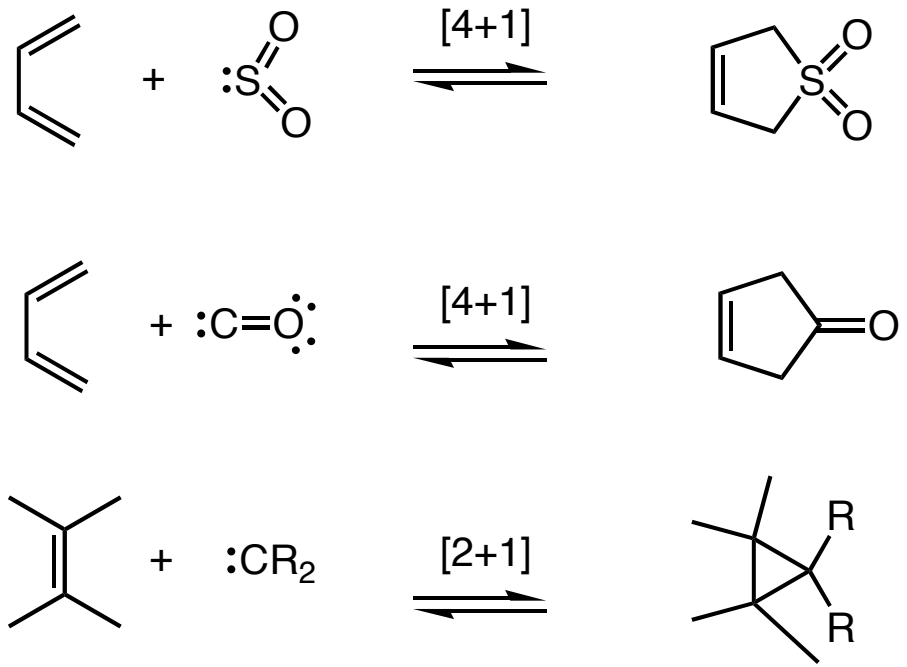

(4) SIGMATROPIC REARRANGEMENTS:

A sigmatropic rearrangement is the migration of a sigma bond from one position in a conjugated system to another position in the system, accompanied by reorganization of the connecting pi bonds.

The number of pi and sigma bonds remains constant.

The rearrangement is an [**m,n**] shift when the sigma bond migrates across **m** atoms of one system and **n** atoms of the second system.

Examples:

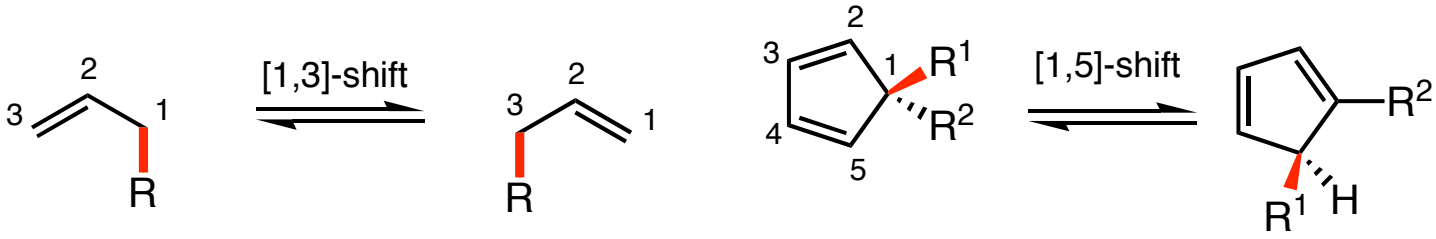

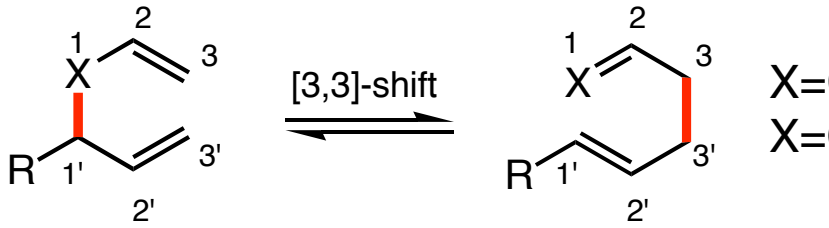

X=CR_2, Cope rearrangement
X=O, Claisen rearrangement

(5) GROUP TRANSFER REACTIONS:

In a group transfer reaction one or more groups get transferred to a second reaction partner.

Examples:

Hydrogen Transfer:

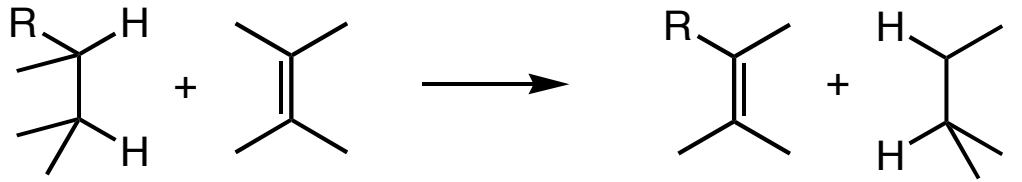

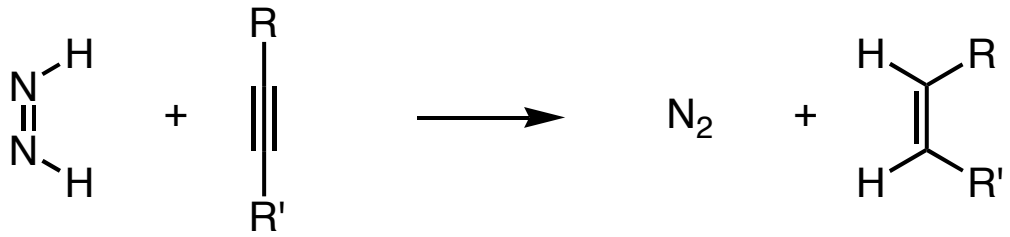

Ene Reaction:

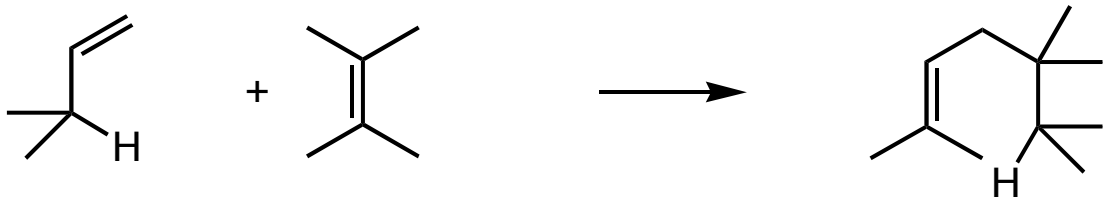

ELECTROCYCLIC RING CLOSURE/RING OPENING:

The Stereochemical issues:

Ring closure can occur in two distinct ways. This has consequences with regard to:

- The orbital lobes that interact
- The disposition of substituents on the termini

Conrotatory Closure: The termini rotate in the **same direction**

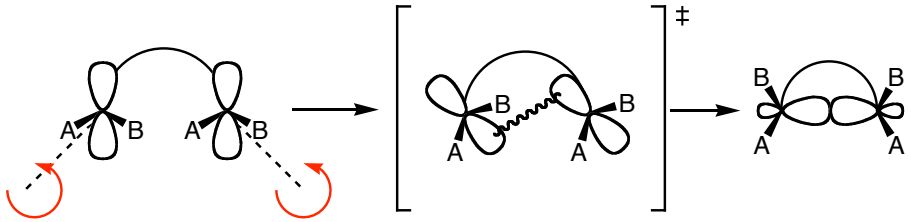

Disrotatory Closure: The termini rotate in **opposite directions**

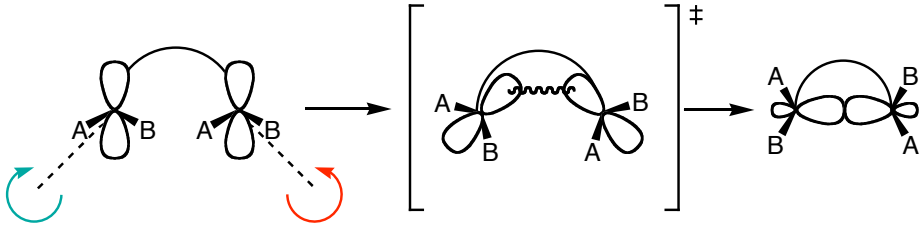

Empirical Observations:

It was noted that butadienes undergo conrotatory closure under thermal conditions, while hexatrienes undergo disrotatory closure under thermal conditions. The microscopic reverse reactions also occur with the same rotational sense (i.e. cyclobutenes open in a conrotatory sense when heated, and cyclohexadienes open in a disrotatory sense when heated.)

Butadiene to cyclobutene: A 4-electron (4q) system

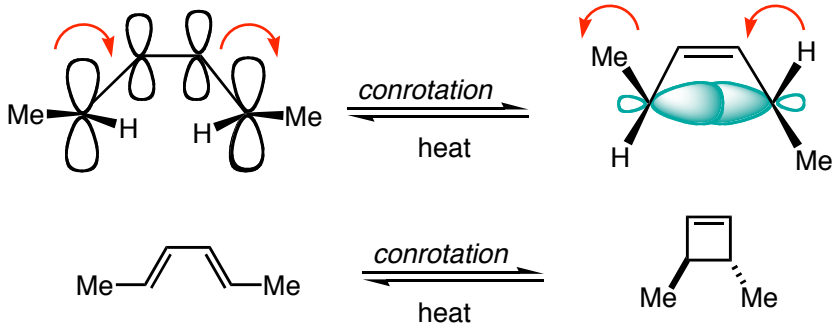

Hextriene to cyclohexadiene: A 6-electron (4q+2) system

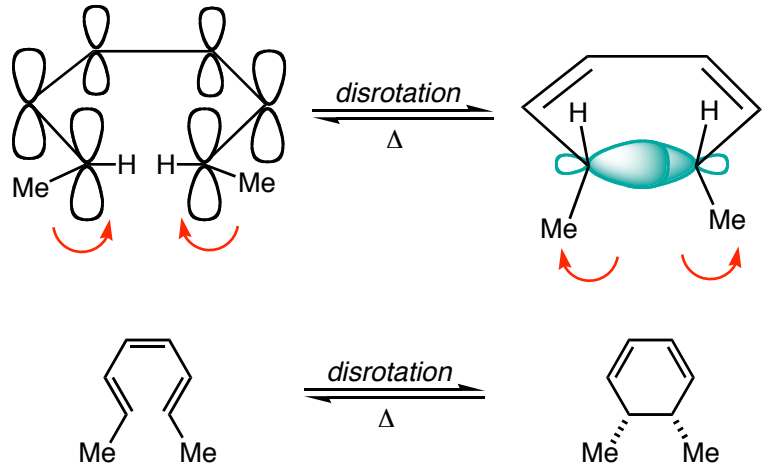

It was also noted that changing the "reagent" from heat to light reversed this reactivity pattern. Under photochemical conditions 4 electron systems undergo disrotatory motion, while 6 electron systems undergo conrotatory motion.

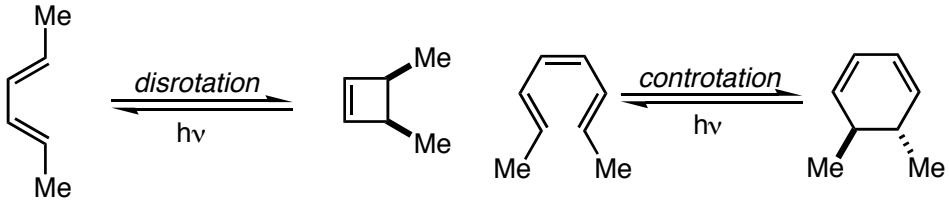

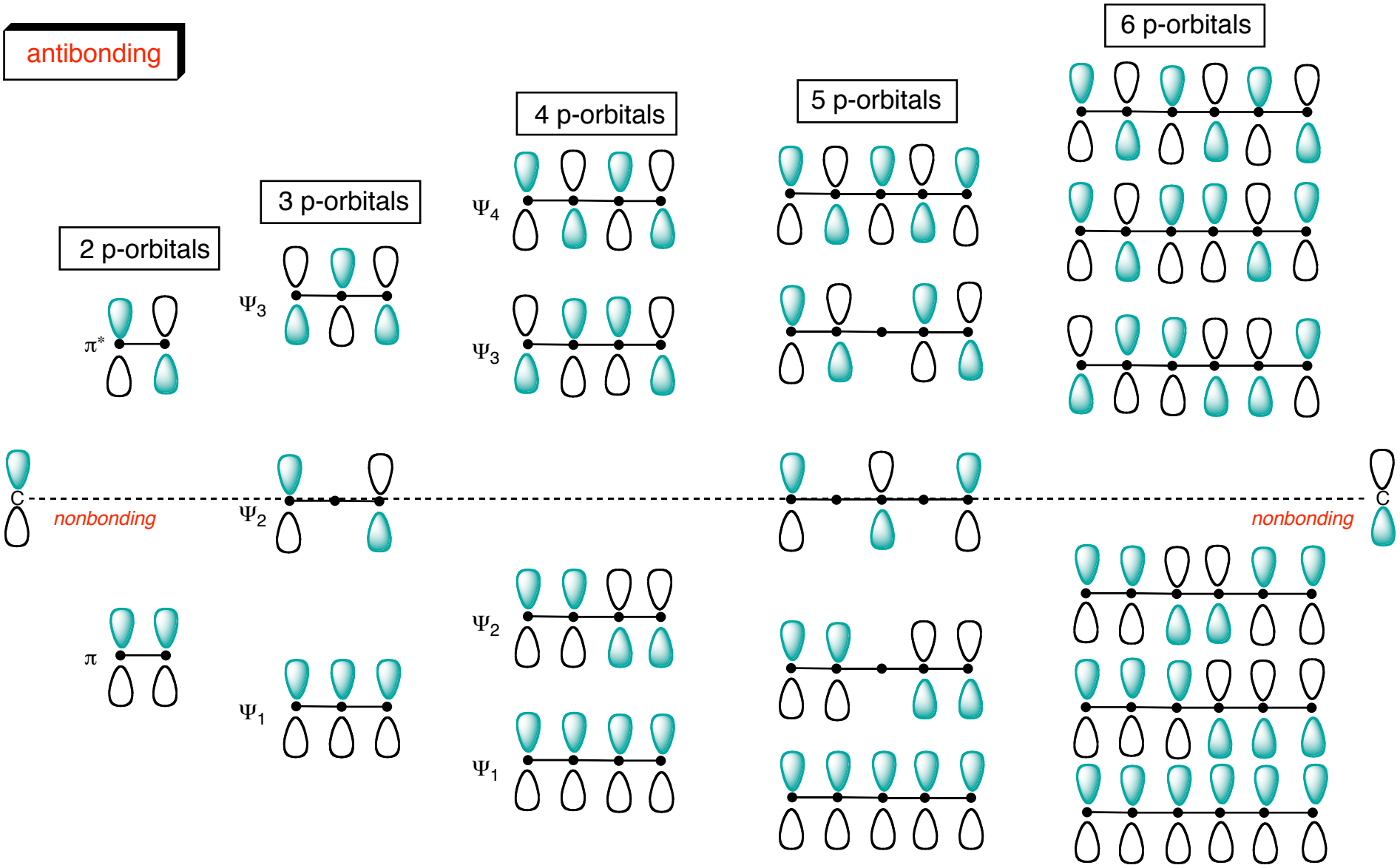

There are no nodal planes in the most stable bonding MO. With each higher MO, one additional nodal plane is added. The more nodes, the higher the orbital energy.

FMO Treatment of Electrocyclic reactions.

Examine the interactions that occur in the HOMO as the reaction proceeds.

If the overlap is constructive (i.e. same phase) then the reaction is "allowed."

If the overlap is destructive (different phases) then the reaction is "forbidden."

Thermal Activation:

Conrotatory Closure: (Allowed and observed)

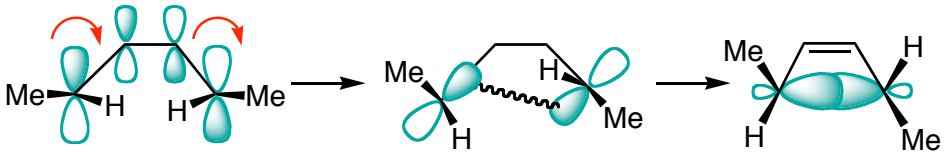

Ψ_2 (diene HOMO) *Constructive overlap*

Disrotatory Closure: (Forbidden and not observed)

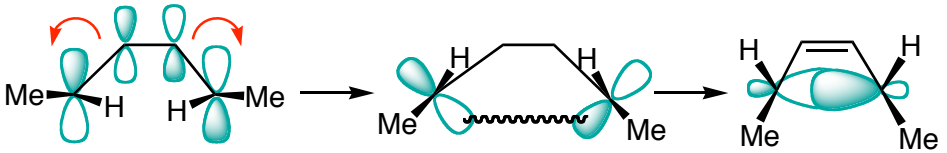

Ψ_2 (diene HOMO) *Destructive overlap*

A similar analysis for the hexatriene system proves that under thermal conditions, disrotation is allowed and conrotation is forbidden.

Photochemical Activation:

When light is used to initiate an electrocyclic rxn, an electron is excited from Ψ_2 to Ψ_3. Treating Ψ_3 as the HOMO now shows that disrotatory closure is allowed and conrotatory closure is forbidden.

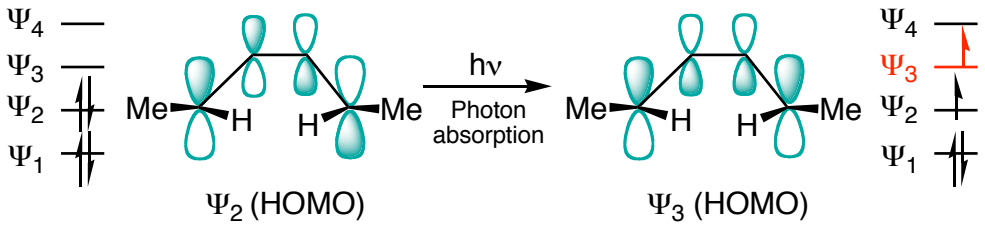

Ψ_2 (HOMO) Ψ_3 (HOMO)

Disrotatory Closure: (Allowed and observed)

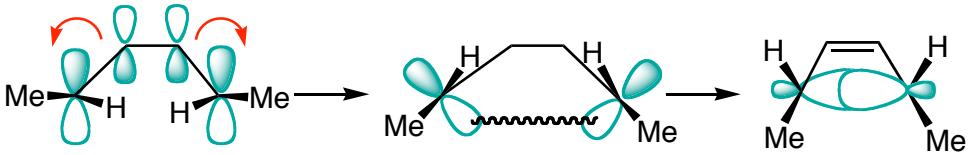

Ψ_3 (new HOMO) *Constructive overlap*

Conrotatory Closure: (Forbidden and not observed)

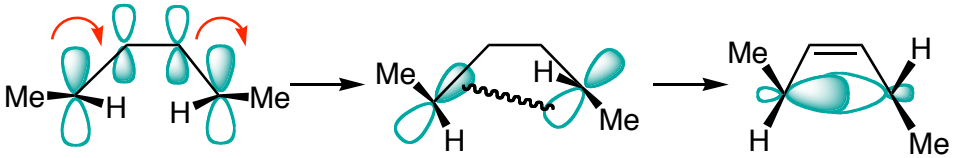

Ψ_3 (new HOMO) *Destructive overlap*

We have so far proven which *ring closures* are allowed and which are forbidden. Do we now have to go back and examine all the *ring openings*?

NO!

The principle of microscopic reversiblity says that if the reaction is allowed in one direction, it must be allowed in the other direction.

The Dewar-Zimmerman analysis is based on identifying transition states as aromatic or anti-aromatic. We will not go into the theory behind why this treatment works, but it will give the same predictions as **FMO** or **Orbital Symmetry** treatments, and is fundamentally equivalent to them.

Using the Dewar-Zimmerman Model:

Choose a basis set of 2p atomic orbitals for all atoms involved (1s for hydrogen atoms).

Assign phases to the orbitals. Any phases will suffice. It is **not** important to identify this basis set with any molecular orbital.

Connect the orbitals that interact in the starting compound, before the reaction begins.

Allow the reaction to proceed according to the geometry postulated. Connect those lobes that begin to interact that were not interacting in the starting materials.

Count the number of phase inversions that occur as the electrons flow around the circuit. Note that a phase inversion **within** an orbital **is not counted**.

Based on the phase inversions, identify topology of system.

Odd number of phase inversions: **Möbius topology**
Even number of phase inversions: **Hückel topology**

Assign the TS as aromatic or antiaromatic, based on number of electrons present.

System	Aromatic	Antiaromatic
Hückel	4q + 2	4q
Möbius	4q	4q + 2

If **TS** is aromatic, then the rxn will be thermally allowed.

If **TS** is antiaromatic, then the rxn will be photochemically allowed.

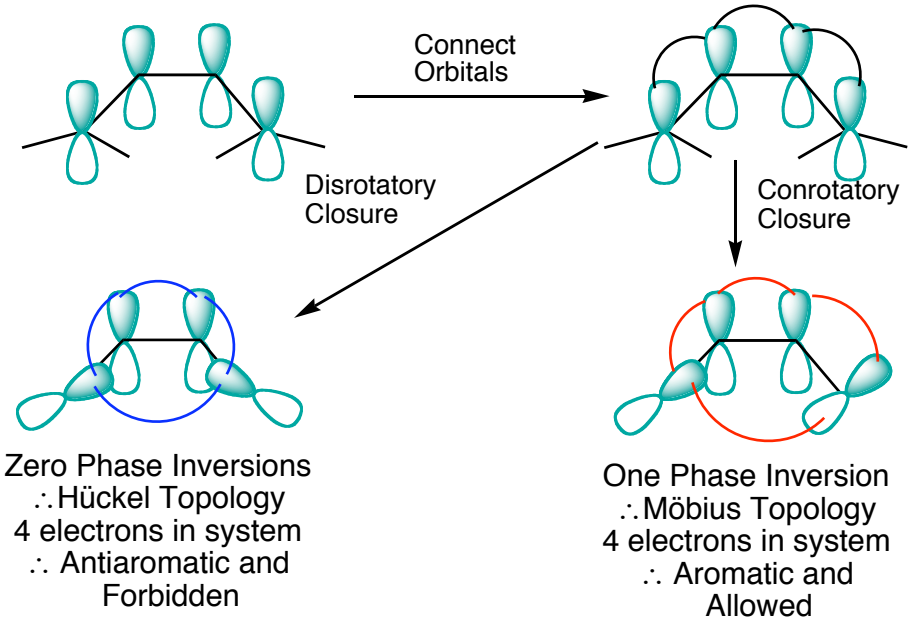

Note that I can change the phase of an abitrary orbital and the analysis is still valid!

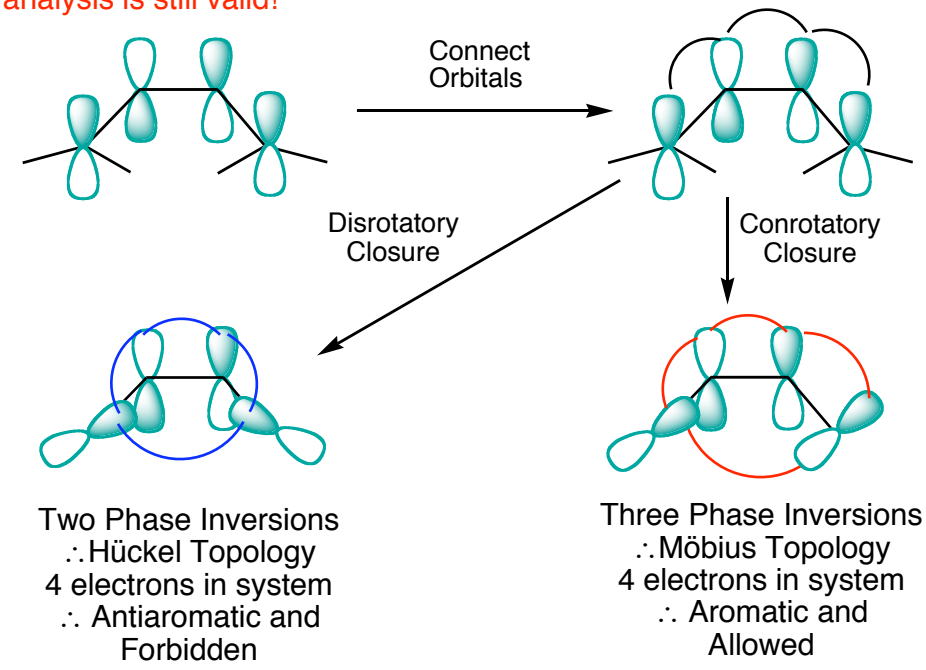

The Stereochemical issues:

The migrating group can move across the conjugated pi system in one of two ways. If the group migrates on the same side of the system, it is said to migrate **suprafacially** with respect to that system. If the group migrates from one side of the pi system to the other, it is said to migrate **antarafacially**.

Suprafacial migration: The group moves across the same face.

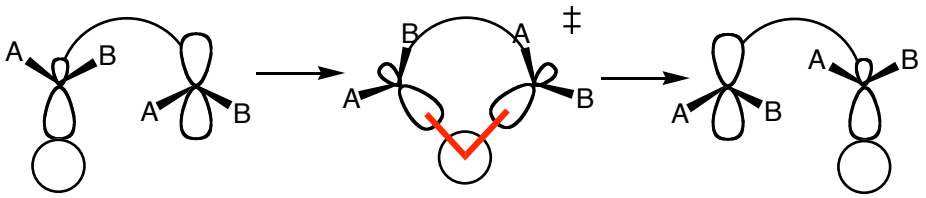

Antarafacial migration: The group moves from one face to the other.

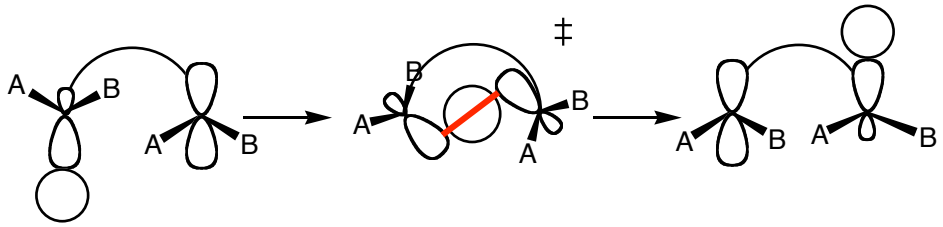

Sigmatropic Rearrangements: FMO Analysis

Imagine the two pieces fragmenting into a cation/anion pair, (or radical pair) next examine the HOMO/LUMO interaction.

If the overlap is constructive at both termini then the reaction is allowed. If the overlap is destructive at either terminus then the reaction is forbidden.

If the migrating atom is carbon, then we can also entertain the possiblity of the alkyl group migrating with inversion of configuration (antarafacial on the single atom).

If the migrating atom is hydrogen, then it cannot migrate with inversion.

[1,3] Sigmatropic Rearrangements (H migration)

Construct TS by considering an allyl anion and the proton (or aradical pair):

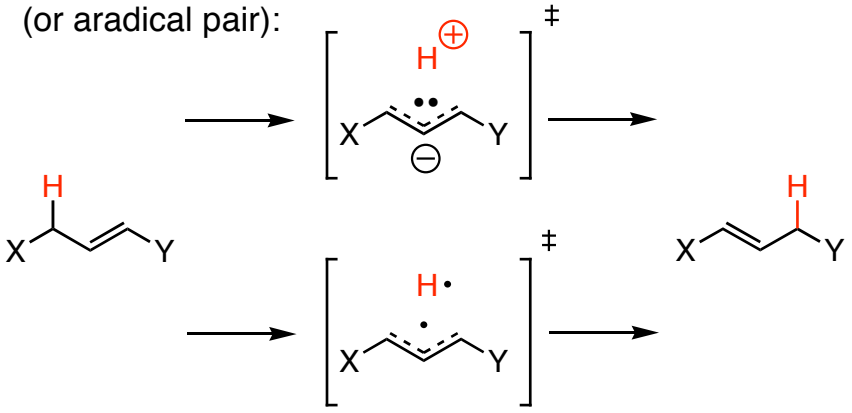

Proton 1S (LUMO)

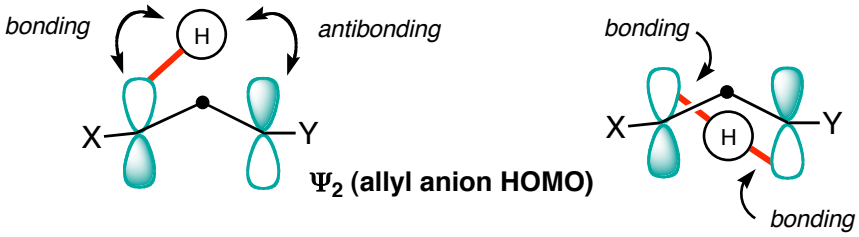

Ψ_2 **(allyl anion HOMO)**

Suprafacial Geometry *Antarafacial Geometry*

The analysis works if you consider the other ionic reaction, or consider a radical reaction. In each case it is the same pair of orbitals interacting.

Suprafacial migration is forbidden and the bridging distance too great for the antarafacial migration. Hence, [1,3] hydrogen migrations are not observed under thermal conditions.

Under photochemical conditions, the [1,3] rearrangement is allowed suprafacially. How would you predict this using FMO?

[1,3] Sigmatropic Rearrangements (C migration)

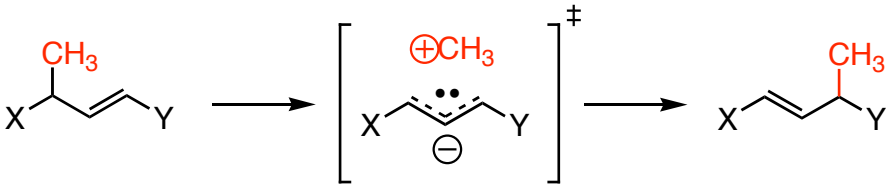

Construct TS by considering an allyl anion and the methyl cation:

Retention at carbon

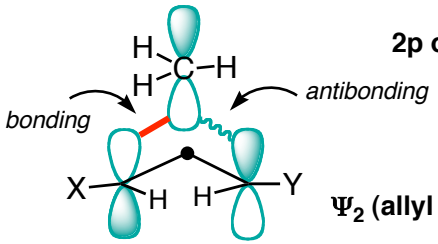

Suprafacial on allyl fragment

2p on Carbon

Ψ_2 (allyl anion HOMO)

Inversion at carbon

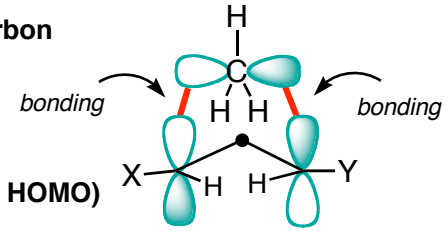

Suprafacial on allyl fragment

The analysis works if you consider the other ionic reaction, or consider a radical reaction. In each case it is the same pair of orbitals interacting.

Under photochemical conditions, the [1,3] rearrangement is allowed suprafacially with retention of stereochemistry.

Stereochemical constraints on the migration of carbon with inversion of configuration is highly disfavored on the basis of strain. Such rearrangements are rare and usually only occur in highly strained systems.

Using a similar analysis, one can prove that [1,5] hydrogen and alkyl shifts should be allowed when suprafacial on the pi component and proceeding with retention. Refer to Fleming for more applications of FMO theory to [1,n] sigmatropic shifts.

Sigmatropic Rearrangements: Dewar-Zimmerman

D–Z also predicts [1,3] suprafacial migration to be forbidden.

The basis set of s and p orbitals with arbitrary phase:

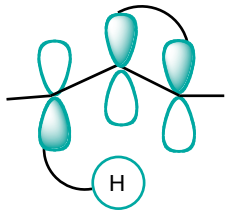

Orbital interactions in the parent system

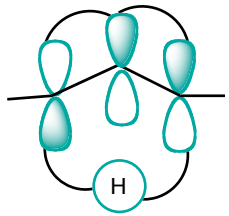

Completing the circuit across the bottom face

Two Phase Inversions
Hückel Topology
Four Electrons
Forbidden thermally

The [1,5] shift of a hydrogen atom across a diene.

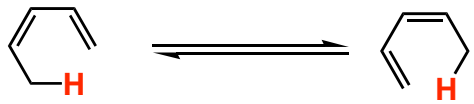

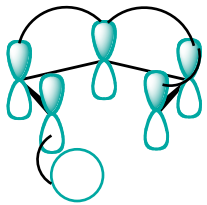

Orbital interactions in the parent system

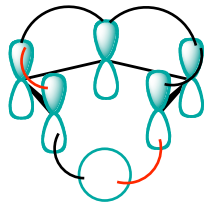

Completing the circuit across the bottom face

Zero Phase Inversions
Hückel Topology
Six Electrons
Allowed thermally

[3,3] Rearrangements:

A thermally allowed reaction is possible in either of two geometries, the "chair" or the "boat" geometry. Depicted below is the "chair" geometry. You should be able to work out the details of the "boat" geometry yourself.

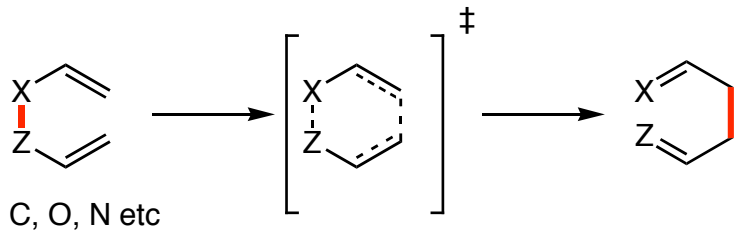

X & Z = C, O, N etc

The FMO Analysis:

Bring two Allyl radicals together to access for a possible bonding interaction between termini.

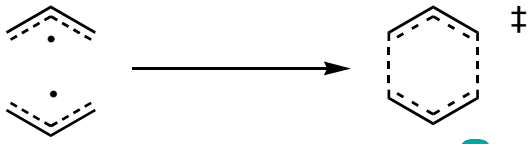

The nonbonding allyl MO Ψ_2

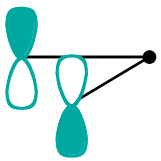

bonding

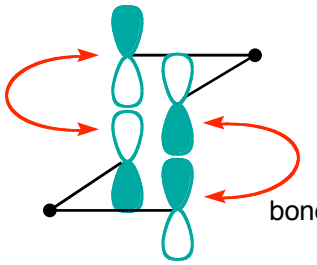

bonding

The Dewar-Zimmerman Analysis:

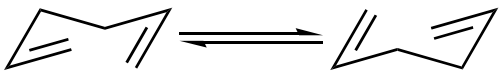

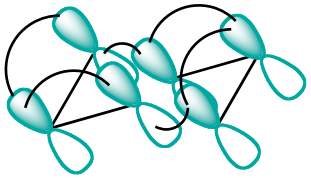

Two Phase Inversions
Hückel Topology
Six Electrons
Allowed Thermally

■ The Toggle Algorithm:

The toggle algorithm is a simple way to take one reaction of each class that you remember is allowed (or forbidden) and derive if the reaction is allowed or forbidden under new conditions.

■ How does it work?

All of the various parameters of the pericyclic reaction are the input variables, the "switches."
The output is either "allowed" or "forbidden."
Write out all the relevant parameters of a reaction together with the known result.
Each time you change a parameter by one incremental value ("toggle a switch"), the output will switch.
This is the prediction of the reaction under the new parameters.

■ So it's nothing really new, is it?

No, its just a convenient way to rederive predictions without memorizing a table of selection rules.

An Example:

Take the [1,3] sigmatropic rearrangement of an alkyl group. We know this is forbidden under thermal conditions in a supra-supra manner, and so we make it the first entry in the table.

Rearrangement	Conditions	Component 1	Component 2	Output
[1,3]	Heat	Suprafacial	Suprafacial	Forbidden
[1,3]	Heat	Antarafacial	Suprafacial	Allowed
[1,3]	Light	Antarafacial	Suprafacial	Forbidden
[1,5]	Heat	Suprafacial	Suprafacial	?

Each incremental change in the "input" registers changes the "output" register by one. Multiple changes simply toggle the output back and forth. What is the prediction in the last line?

The Stereochemical issues:

In a cycloaddition, a pi system may be attacked in one of two distinct ways. If the pi system is attacked from the same face, then the reaction is **suprafacial** on that component. If the system is attacked from opposite faces, then the reaction is **antarafacial** on that component.

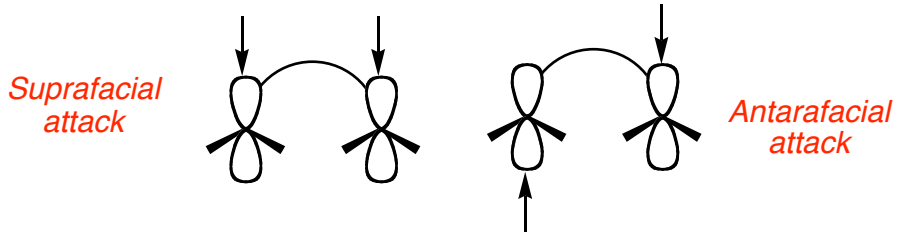

The [2+2] Cycloaddition: FMO Analysis

For the [2+2] cycloaddition two different geometries have to be considered.

Suprafacial/Suprafacial

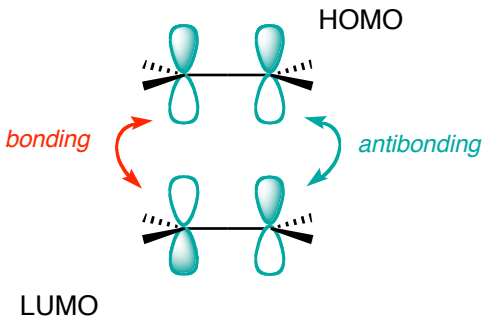

Forbidden

Antarafacial/Suprafacial

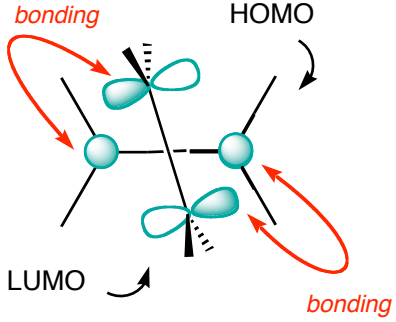

Allowed

The simplest approach (Supra/Supra) is forbidden under thermal activation. The less obvious approach (Antara/Supra) is allowed thermally but geometrically rather congested. It is believed to occur in some very specific cases (e.g. ketenes) where the steric congestion is reduced.

The [4+2] Cycloaddition: Dewar-Zimmerman

The most well known cycloaddition is the Diels-Alder reaction between a four pi component (the diene) and a two pi component (the dienophile). An exhaustive examination of this reaction is forthcoming, so we will limit ourselves to a simple examination.

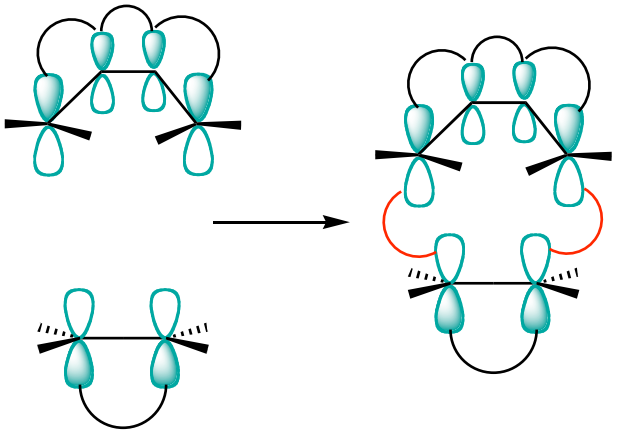

Zero Phase Inversions
Hückel Topology
Six Electrons
Allowed thermally

Summary:

- There are three fundamentally equivalent methods of analyzing pericyclic reactions: Two are much simpler than the third.
  - Fukui Frontier Molecular Orbital Theory
  - Dewar-Zimmerman Hückel-Möbius Aromatic Transition States
  - Woodward-Hoffmann Correlation Diagrams

- Some methods are easier to use than others, but all are equally correct and no one is superior to another. Conclusions drawn from the correct application of one theory will not be contradicted by another theory.

- The principle of microscopic reversibility allows us to look at a reaction from either the forward direction or the reverse direction.

- There is a general trend that reactions will behave fundamentally different under thermal conditions and photochemical conditions.

Question 3. (15 points). Assume that you have a rapidly equilibrating mixture of two conformers **A** and **B** from which two products, $\mathbf{P_A}$ and P_B are produced (eq 1). In the case at hand, $k_2 > k_1$.

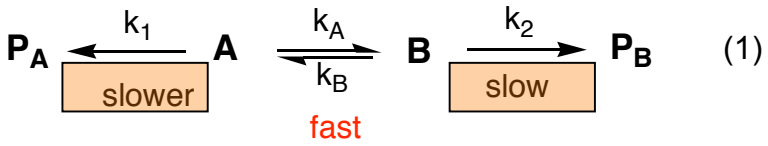

Part A. (10 points). Draw an energy diagram that reflects the situation where the equilibrium population of conformers is the same as the product ratio.

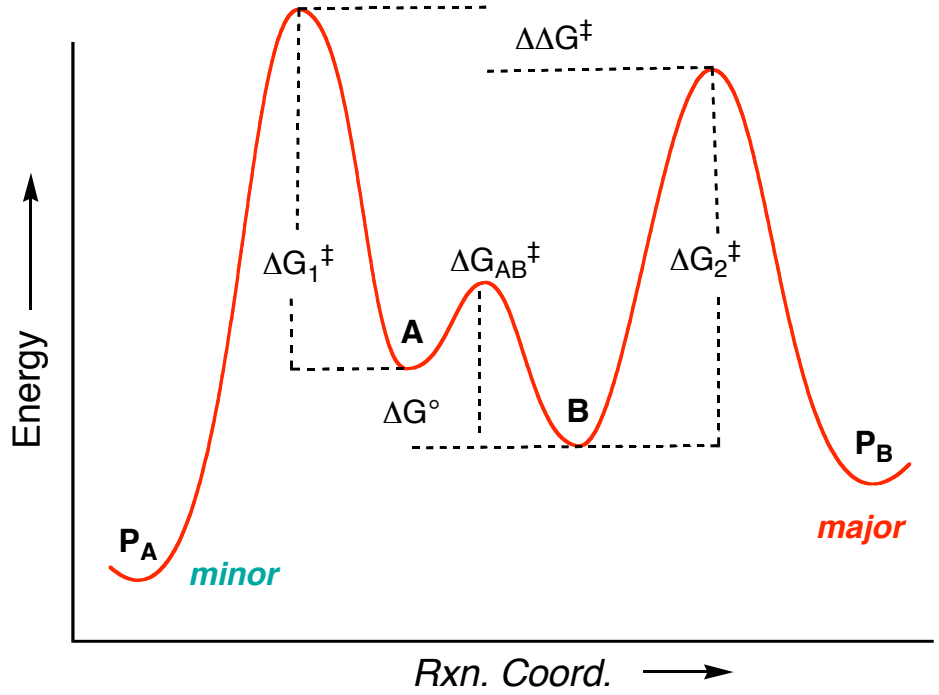

Exam Average

73.5

Part B. (5 points). Provide a concise statement of this circumstance in terms of free energy relationships.

Under this constraint, $\Delta G_1^{\ddagger}$ must equal $\Delta G_2^{\ddagger}$. Accordingly, $\Delta\Delta G^{\ddagger}$ will equal $\Delta G°$.

http://www.courses.fas.harvard.edu/colgsas/1063

Chemistry 206

Advanced Organic Chemistry

Lecture Number 12

Pericyclic Reactions–2

- Electrocyclic Reactions
- Cheletropic Reactions

Reading Assignment for week:

Carey & Sundberg: **Part A**; Chapter 11
Concerted Pericyclic Reactions

"Electronic Control of Stereoselectivities of Electrocyclic Reactions of Cyclobutenes: A Triumph of Theory in the Prediction of Organic Reactions" Houk et al. *Accounts Chem. Res.* **1996**, *29*, 471-477 **(handout)**

"Some New Nazarov Chemstry," Tius, *Eur. J. Chem.* **2005,** 2193-2206 **(pdf)**

C. Palomo, "Asymmetric Synthesis of β-Lactams by Stauginger Ketene-Imine Cycloaddition Reaction, Eur. *J. Org. Chem.* **1999,** 3223-3235 **(pdf)**

D. A. Evans

Monday,
October 16, 2006

Other Reading Material:

C. Palomo, "Asymmetric Synthesis of β-Lactams by Stauginger Ketene-Imine Cycloaddition Reaction, Eur. *J. Org. Chem. 1999*, 3223-3235.

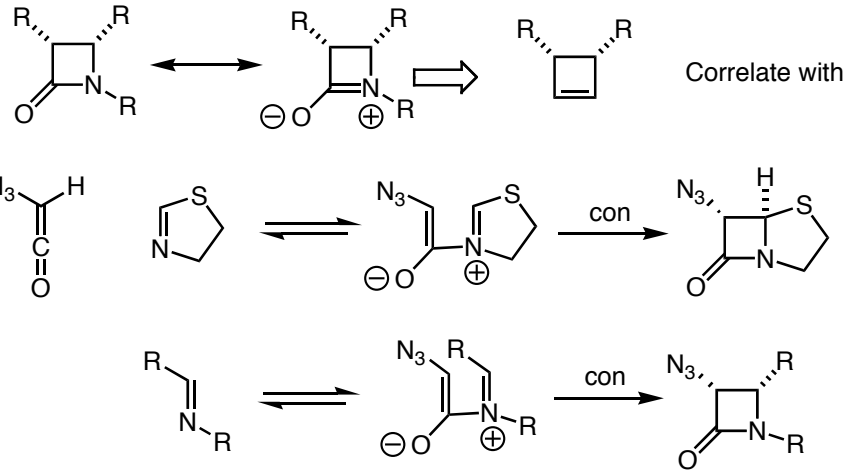

Problems of the Day:

Database Problem 159. The illustrated bicyclic ketone undergoes an isomerization in the presence of a strong base such as potassium hydride upon heating. After quenching the reaction, the new product has been found to have undergone a rather surprising isomerization at the quaternary center.

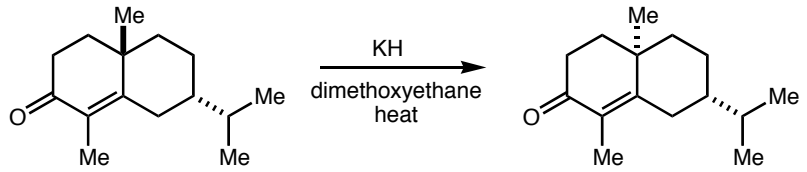

Database Problem 315. Berson and co-workers have studied the thermal isomerization illustrated below (*JACS* **1966,** *88*, 2494-2502). Provide a rationalization of these results. Three-dimensional drawings are recommended.

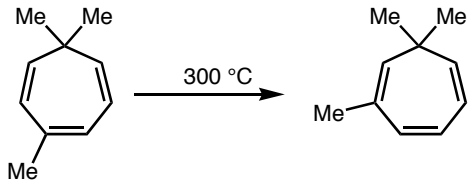

Electrocyclic Reaction - Selection Rules

	Ground State (Thermal process)	Excited State (Photochemical Process)
4n π e⁻ (n = 1,2...)	conrotatory	disrotatory
4n+2 π e⁻ (n = 0,1,2...)	disrotatory	conrotatory

Examples	Ground State	Excited State
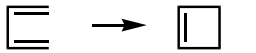	Conrotatory	Disrotatory
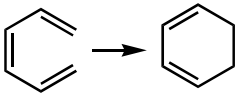	Disrotatory	Conrotatory
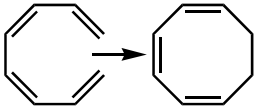	Conrotatory	Disrotatory
	Disrotatory	Conrotatory
	Conrotatory	Disrotatory
	Conrotatory	Disrotatory
	Disrotatory	Conrotatory

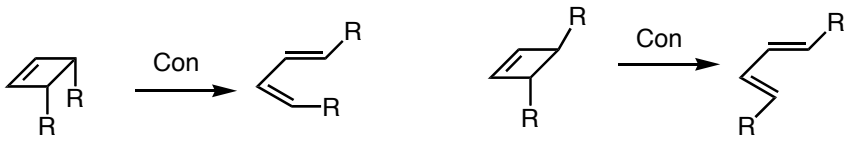

Controtation Ψ_1 and Ψ_2 on to the indicated bonding and anti-bonding orbitals of cyclobutene:

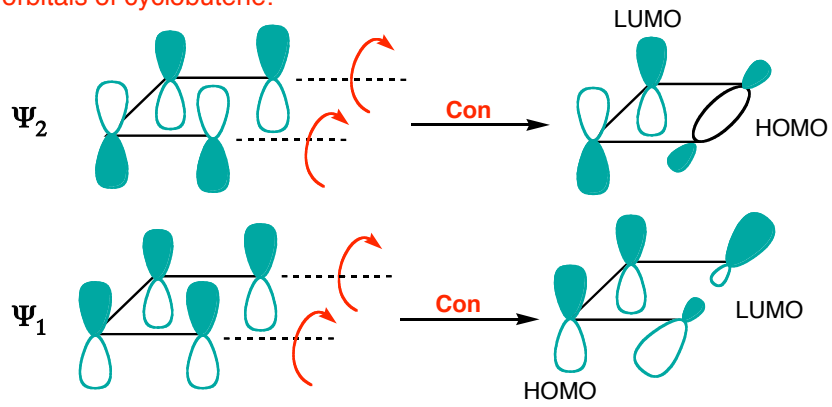

Activation Energy (kcal/mol)
for electrocyclic ring opening

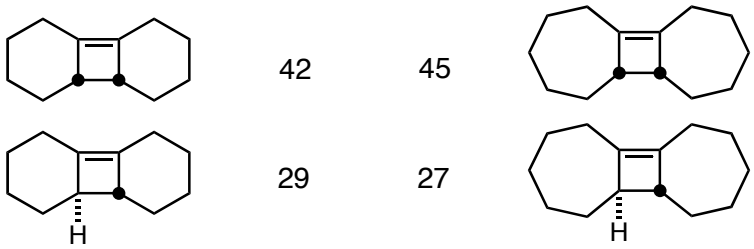

Criegee, *Chem. Ber.* **1968**, *101*, 102.

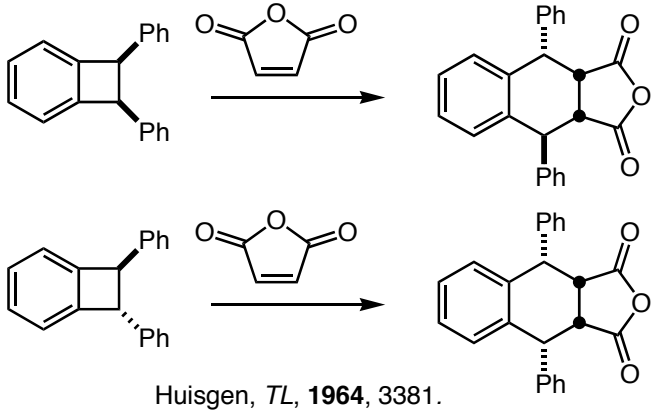

Huisgen, *TL*, **1964**, 3381.

Torquoselectivilty is defined as the predisposition of a given R substituent for a given conrotatory motion

Houk et al. *Acc. Chem. Res* **1996**, 29, 471

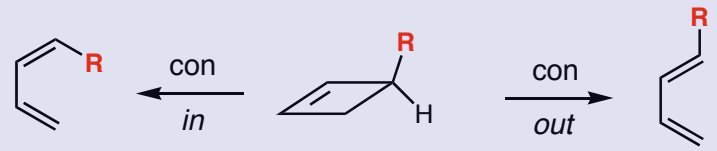

Examples: Donor substituents prefer con–out mode
Pi acceptor substituents prefer con–in mode

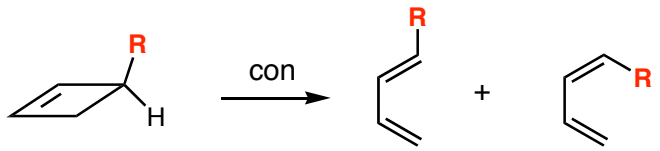

R = Me **only** none
R = CHO none **only**

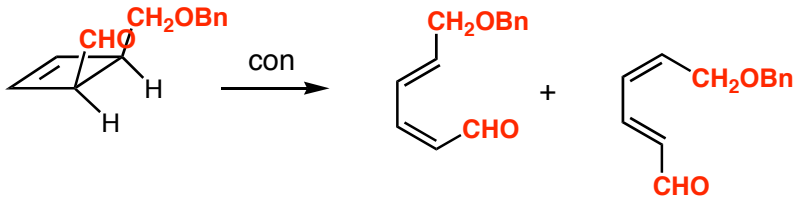

ratio: >20:1

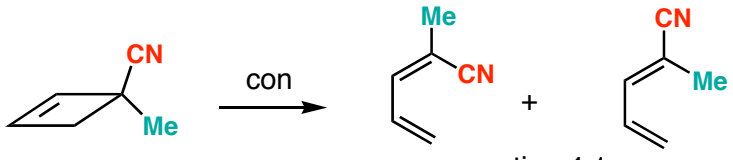

ratio: 4:1

How do we explain? Donor substituents prefer con–out mode
Pi acceptor substituents prefer con–in mode

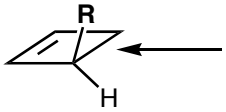

View the 2 conrotatory modes by looking at the breaking sigma bond from this perspective

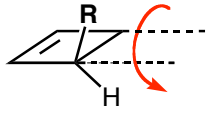

Outward Motion

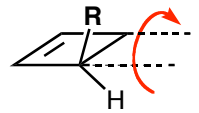

Inward Motion

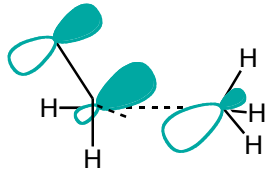

LUMO + p

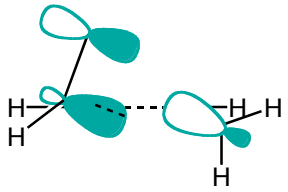

LUMO + p

A **B**

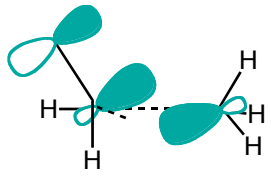

HOMO + p

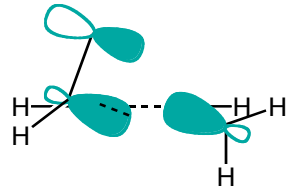

HOMO + p

As conrotation begins the energy of the breaking sigma bond rises steeply. Hyperconjugation with a pi* orbital, while possible in both **A** & **B**, is better in **B**. (Houk)

destabilizing 4 electron interation for donor substituents

stabilizing 2 electron interation for acceptor substituents

Electronic Effects

Synthesis and Thermal Ring Opening of *trans*-3,4-Disilylcyclobutene

Masahiro Murakami and Munehiro Hasegawa*

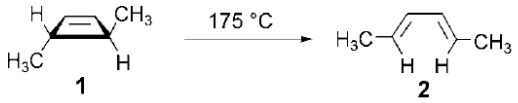

Scheme 1. Ring-opening reaction of *trans*-3,4-dimethylcyclobutene **1**.

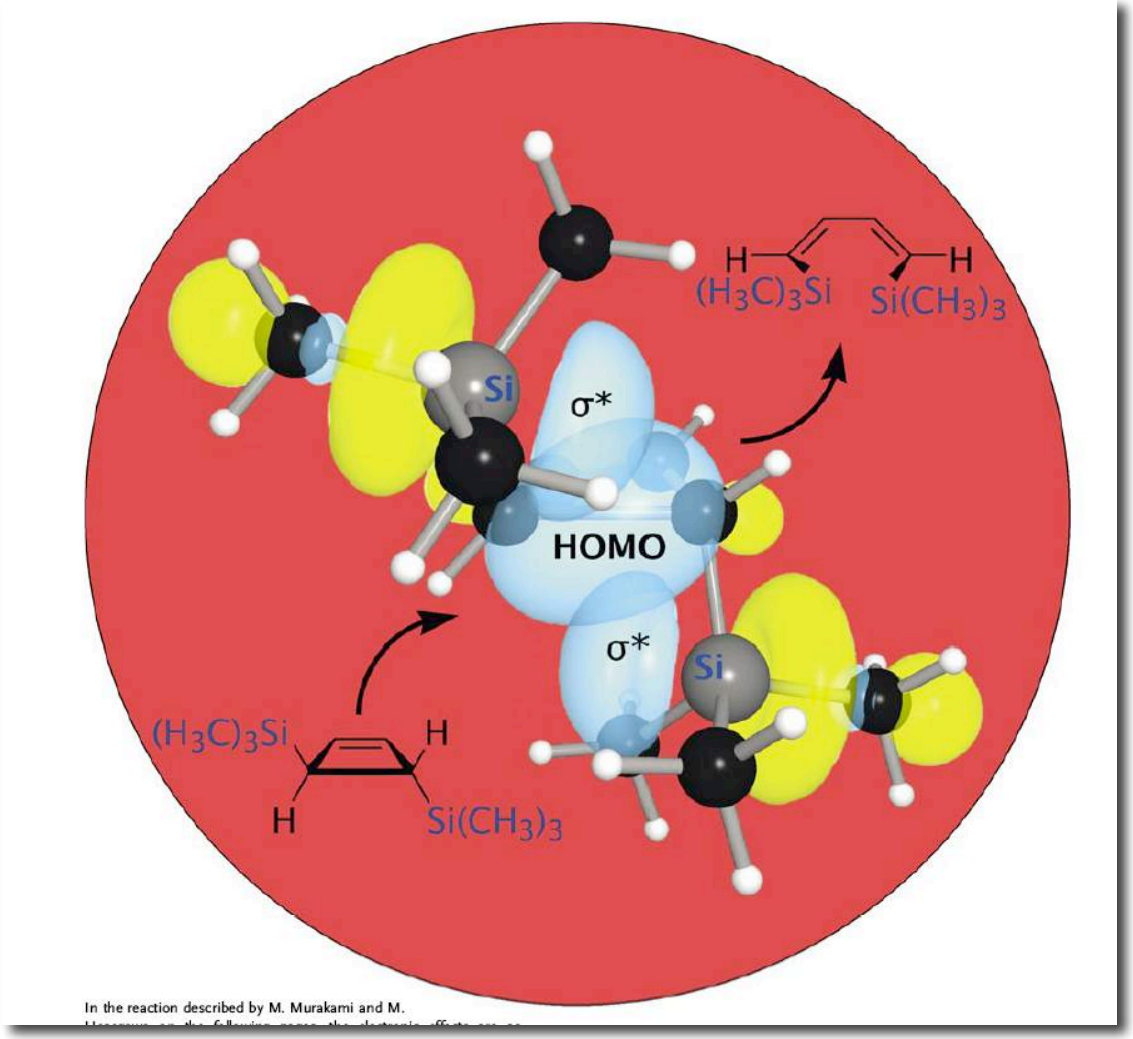

In the reaction described by M. Murakami and M.

How do we explain?

Donor substituents prefer con–out mode

Pi acceptor substituents prefer con–in mode

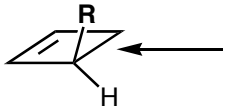

View the 2 conrotatory modes by looking at the breaking sigma bond from this perspective

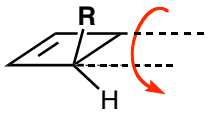

Outward Motion

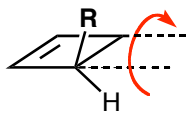

Inward Motion

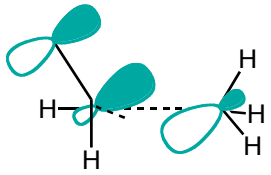

LUMO + p

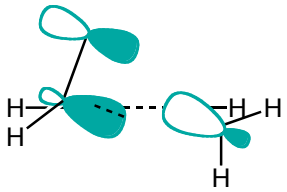

LUMO + p

A **B**

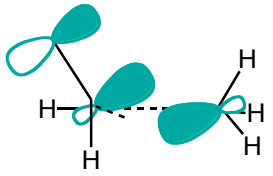

HOMO + p

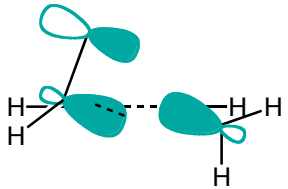

HOMO + p

As conrotation begins the energy of the breaking sigma bond rises steeply. Hyperconjugation with a pi* orbital, while possible in both **A** & **B**, is better in **B**. (Houk)

destabilizing 4 electron interation for donor substituents

stabilizing 2 electron interation for acceptor substituents

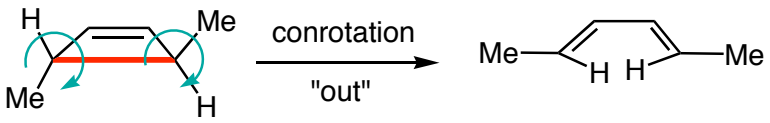

Con-rotation "in" sterically disfavored.

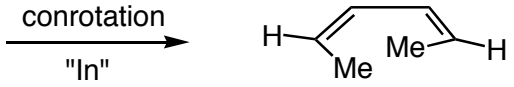

Murakakami *Angew. Chem. Int. Ed.* **2004,** *43*, 4873

What abut Silyl Substitutents?

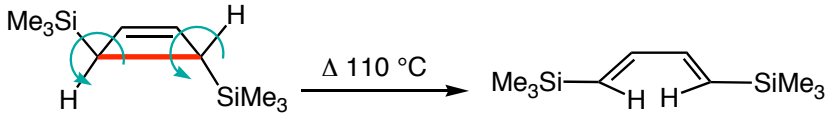

22%

T1/2 = 1.7 hr

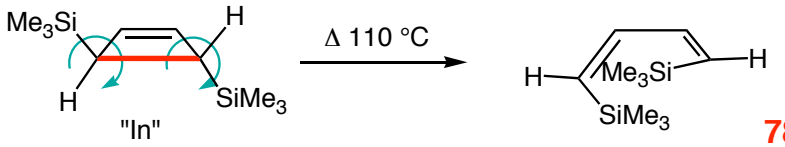

78%

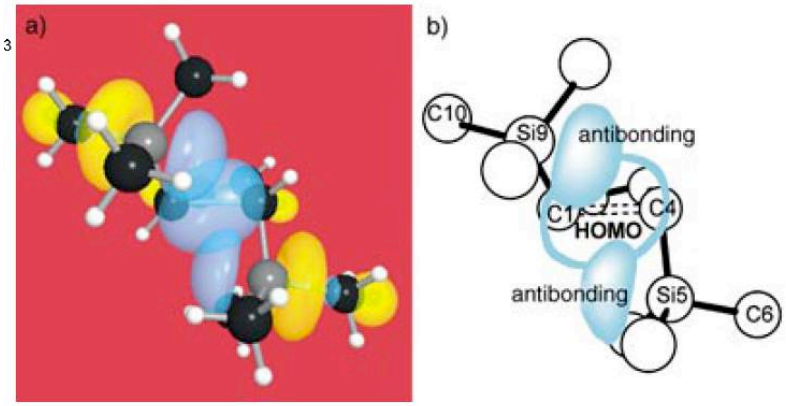

Figure 2. Overlap of the two antibonding orbitals on the silicon atoms with the HOMO in the inward transition state.

Three-Atom Electrocyclizations (2 electrons)

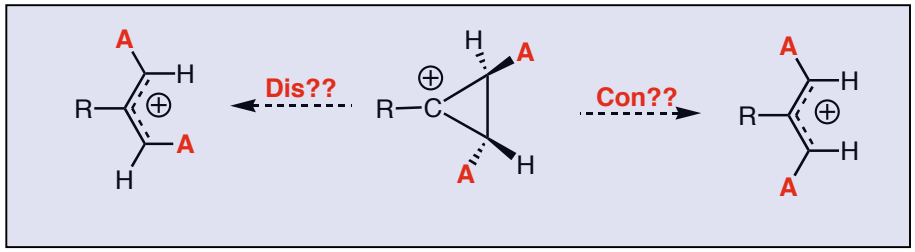

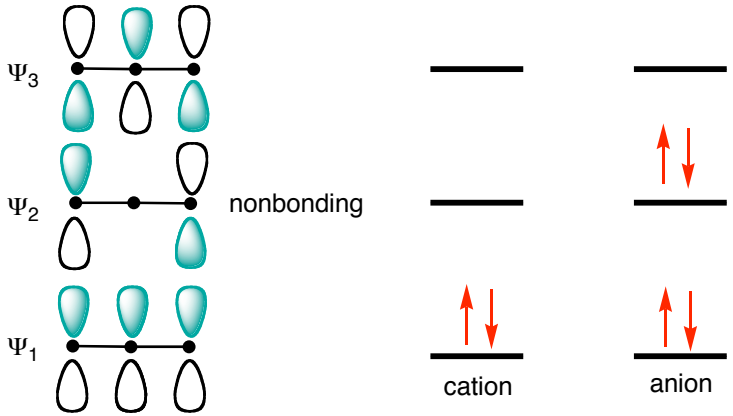

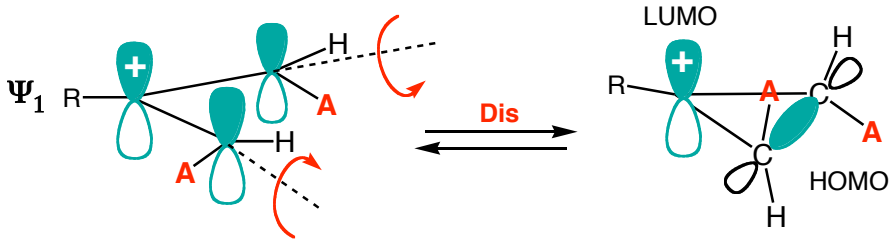

Note that there are two disrotatory modes

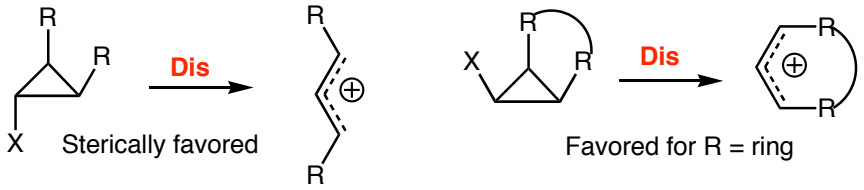

Solvolysis of Cyclopropyl Derivatives

Does solvolysis proceed via cation **1** followed by rearrangement to **2** (Case 1), or does it proceed directly to **2** (Case 2)?

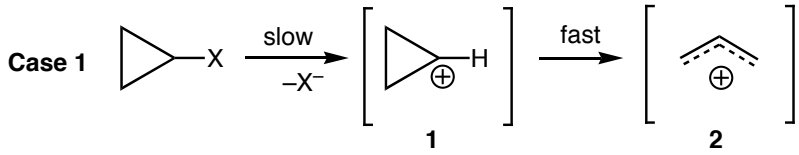

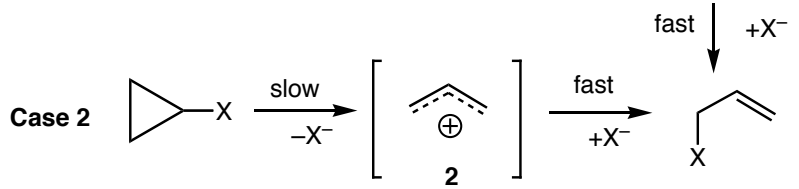

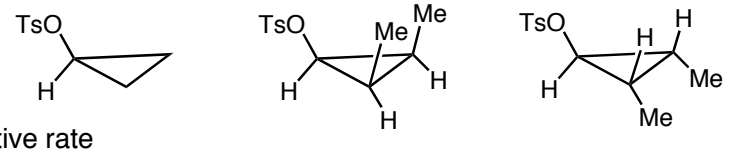

relative rate 1 4 40,000

DePuy, *Accts. Chem. Res.* **1967**, *1*, 33

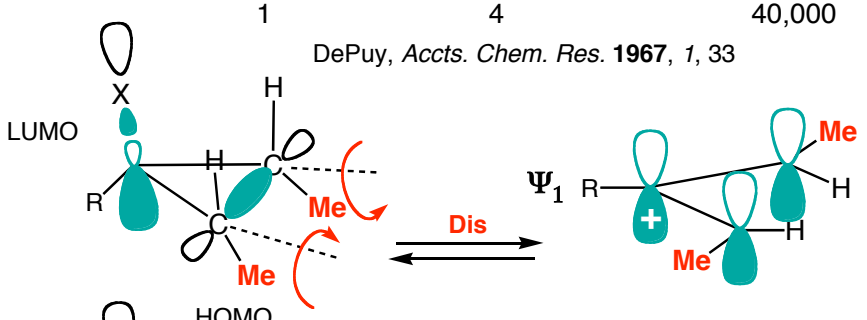

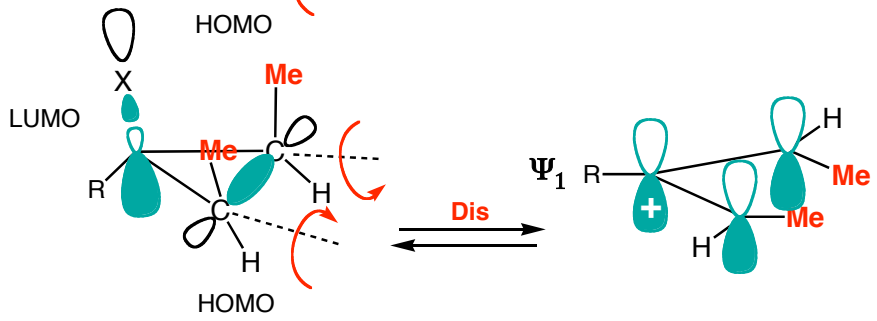

Solvolysis Summary

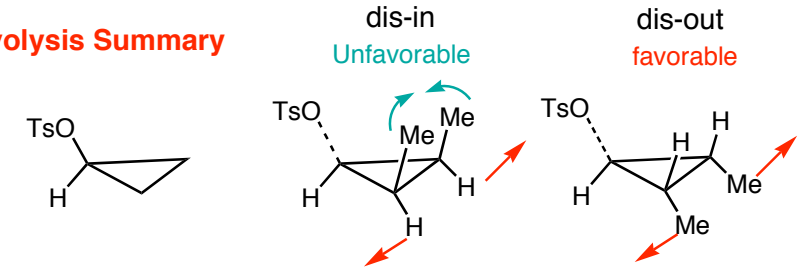

Ring-fused Cyclopropyl Systems

When the cis substiltutents on the cyclopropyl ring are tied together in a ring the following observsations have been made

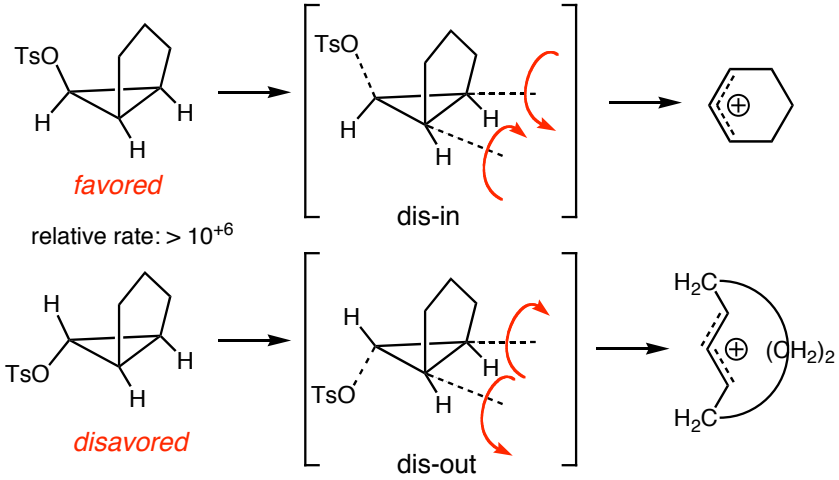

Revisiting the Favorski rearrangement: (Carey, Part A, pp 506-8)

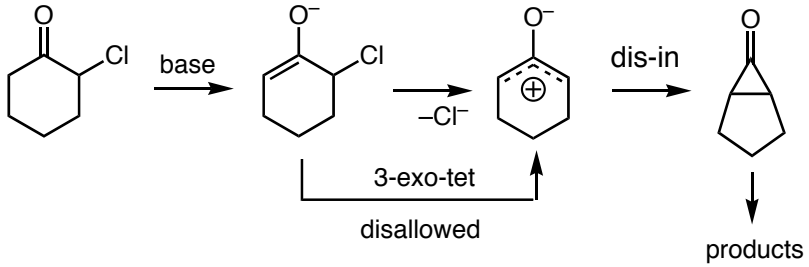

Three-Atom Electrocyclizations (4 electrons)

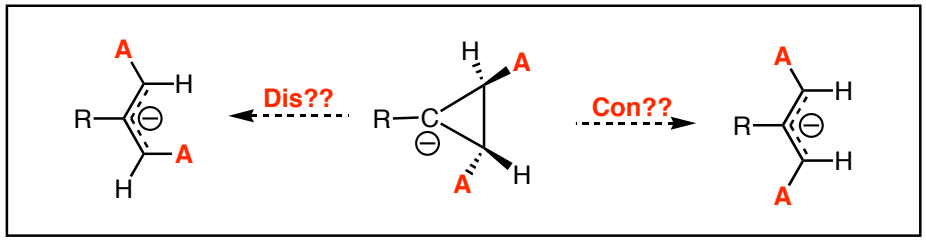

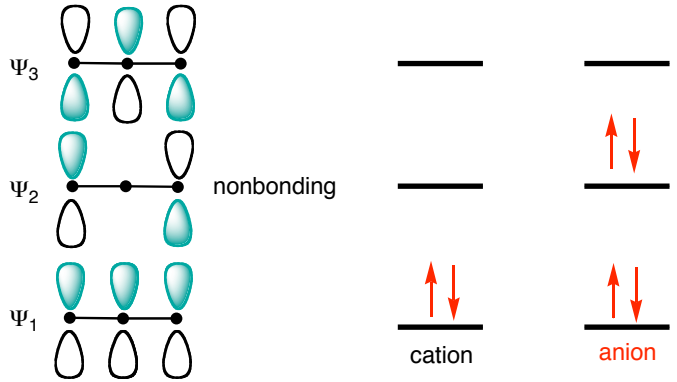

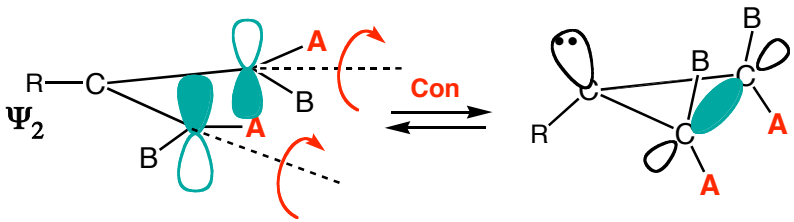

Observation

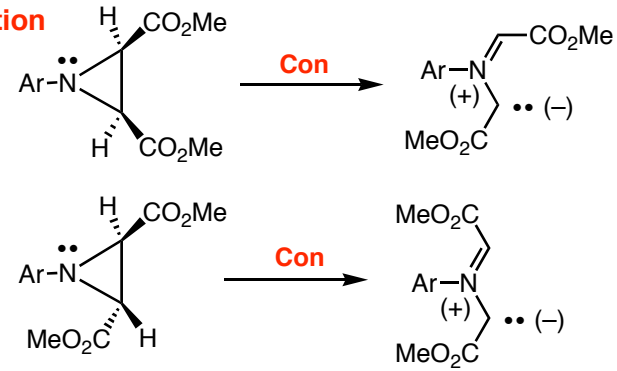

Five-Atom Electrocyclizations (4 electrons)

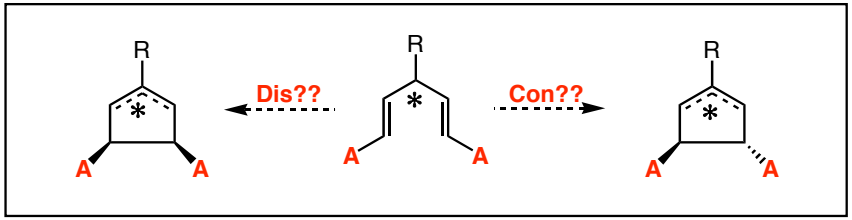

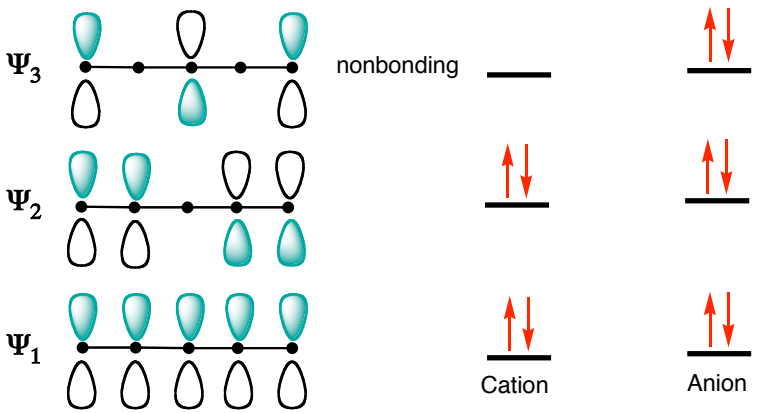

Pentadienyl Cation

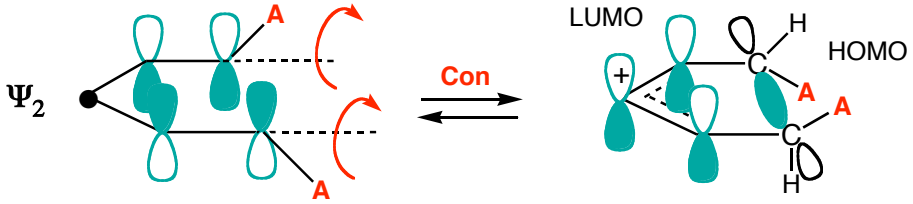

Pentadienyl Anion

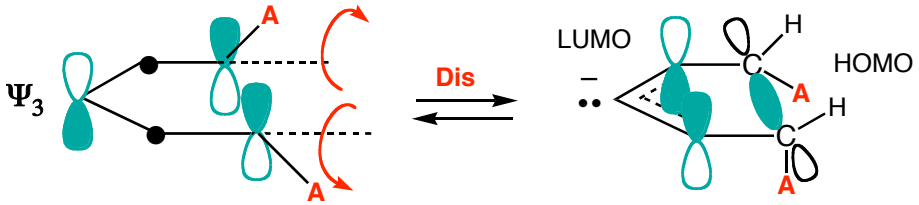

The Nazarov Reaction

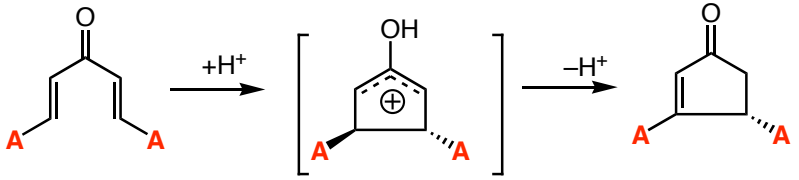

Denmark, S. E. In *Comprehensive Organic Synthesis*; Trost, B. M., Fleming, I., Eds.; Pergamon Press: Oxford, 1991; Vol. 5; pp 751.

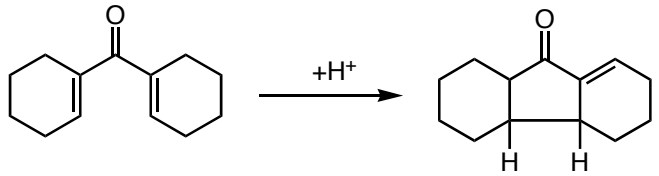

predict stereochemistry

Eight-Atom Electrocyclizations (8 electrons)

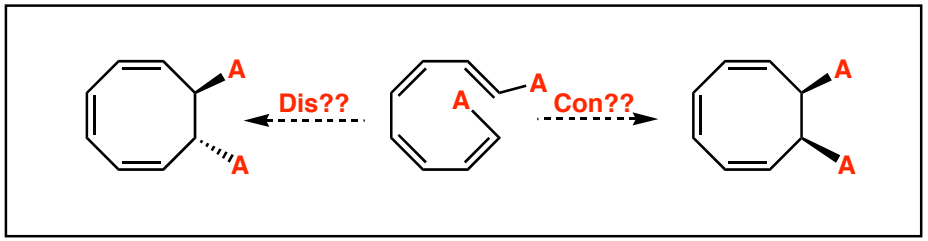

Let's use the "Ready" shortcut to find the homo: Nodes will appear at single bonds

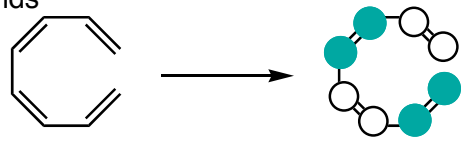

symmetry of homo

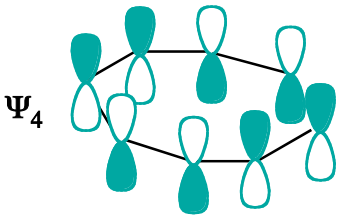

Closure should be conrotatory

Problem 122. The interesting transformation illustrated below was recently reported by F. West and co-workers (*Org. Lett.* **2001**, *3*, 3033-3035). The pivotal reaction upon which this transformation was designed is a pericyclic process that affords a pivotal element of stereocontrol.

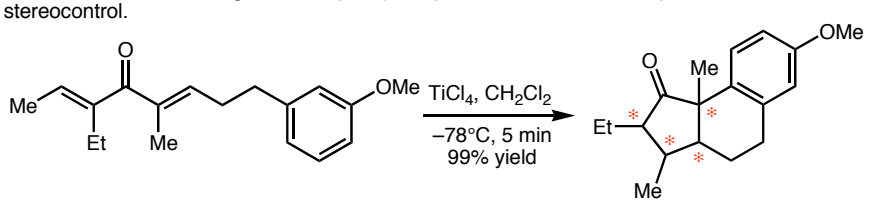

Part A. Identify the pericyclic process that intervenes in the illustrated transformation and illustrate the relative configuration(s) stereocenter(s) that are generated.

Part B. Provide a mechanism for the overall transformation. Since stereochemical issues are at stake, carefully rendered 3-D conformational drawings should be incorporated into your answer.

Problem 158. Danheiser and coworkers (JACS **1986**, *108*, 806) have described an innovative synthesis of the antifungal agent mycophenolic acid. The crucial reaction which resulted in the assemblage of the highly substituted phenolic ring is provided below.

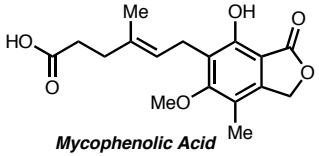

Mycophenolic Acid

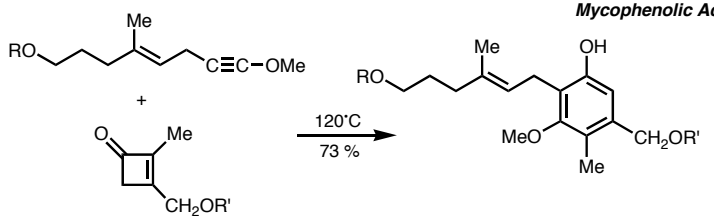

Provide a concise mechanism for this reaction in the space below.

Problem 161. The following transformations entail an "apparent" methyl migration. Address the questions posed below.

Part A. Provide a mechanism for the transformation of **1** to **2**. I represents an ^{18}O label. Classify all pericyclic processes should they intervene.

Part B. Provide a mechanism for the transformation of **3** to **4**. Classify all pericyclic processes should they intervene.

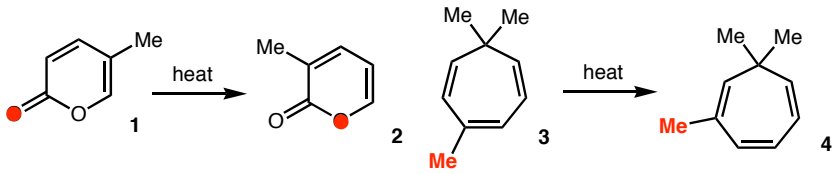

Problem 215. Provide a mechanism for the following set of transformations (*J. Org. Chem.* **1999**, *64*, 2170). It should be noted that compound **A** exhibits a strong carbonyl frequency in the infrared spectrum. Clearly indicate the structure of compound **A** and the relative stereochemistry of any chiral intermediates.

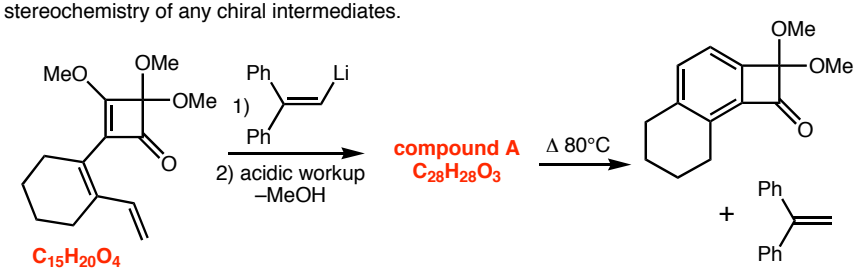

Problem 718. Black proposed that the biosynthesis of endiandric acid B involved a series of pericyclic reactions beginning with the given acyclic starting material. Propose a mechanism for this transformation. You may find it helpful to start with the product and work backwards. Hint: The last step of this mechanism is a Diels-Alder reaction.

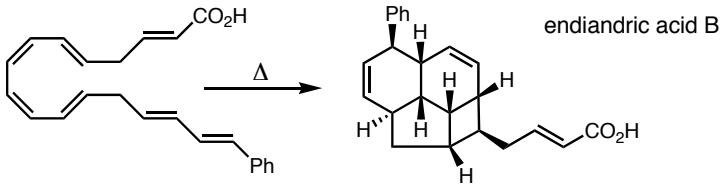

Problem 736. Please provide a mechanism for the following transformation recently reported by Magomedov and co-workers (*JACS* **2004**, 126, 16265) This is one of seven cases reported. *Be sure to classify any pericyclic processes that intervene.*

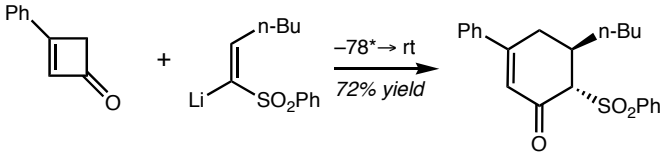

Problem 780. Santilli and co-workers reported this Lewis acid catalyzed reaction (Santilli etal. *JACS* **1991, 113,** 8062-8069). Please provide a reasonable mechanism for this transformation that includes the rationalization of the stereochemical outcome of the transformation.

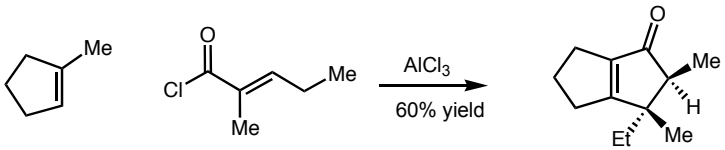

CHELETROPIC REACTIONS: [n+1] Cycloadditions (or Cycloreversions)

Concerted processes in which 2 σ-bonds are made (or broken) which terminate at a single atom.

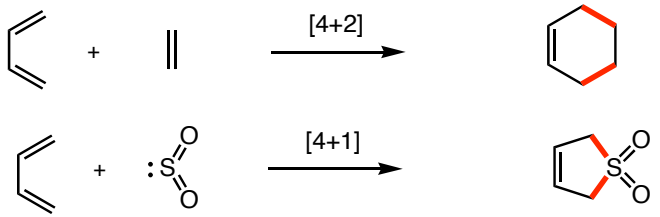

General

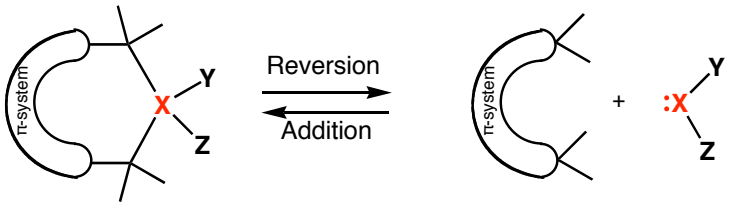

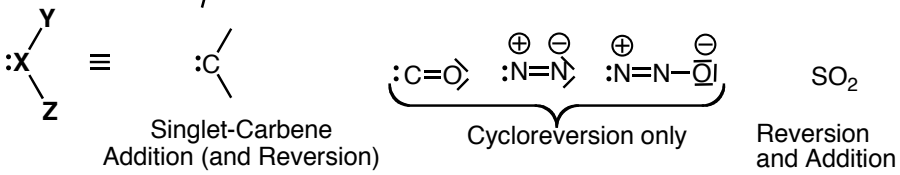

Singlet-Carbene Addition (and Reversion)

Cycloreversion only

SO_2

Reversion and Addition

Frontier Orbitals

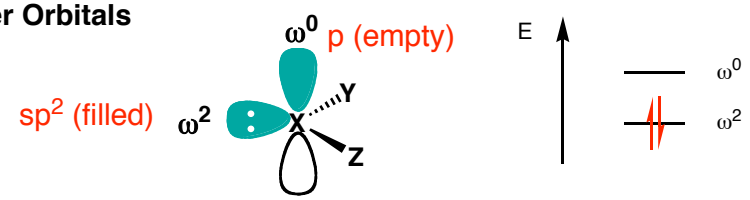

Question: what is orientation of carbene relative to attacking olefin??

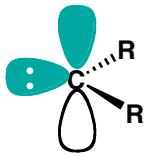

2 + 1 CheletropicReaction: Olefins + Singlet Carbene

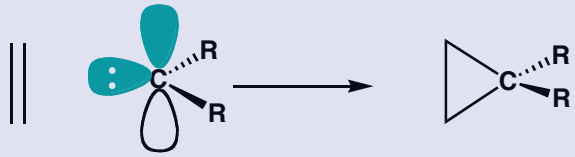

Linear Approach: 2 HOMO-LUMO Interactions

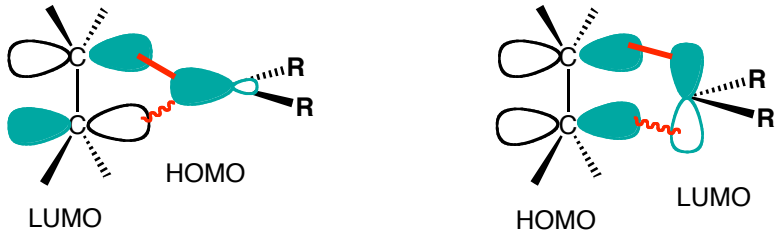

Nonlinear Approach: 2 HOMO-LUMO Interactions

Carry out the analysis of the indicated hypothetical transformation

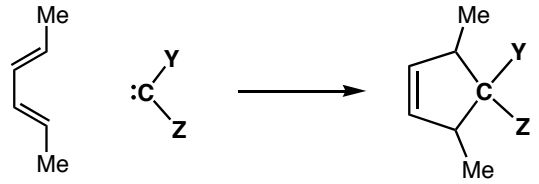

predict approach geometry of carbene

Problem 726. A [4+1] cycloaddition between a diene and a carbene has recently been reported by Spino and co-workers (*JACS*, **2004**, *126*, 9926).

Part A. Using a Dewar-Zimmerman or an FMO analysis, determine if this reaction is thermally allowed. Be sure to consider both the approach and the geometry of the carbene carefully.

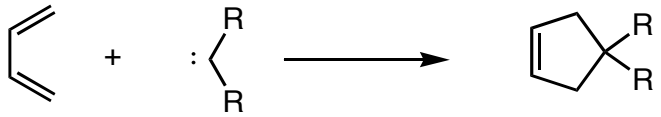

FMO Analysis

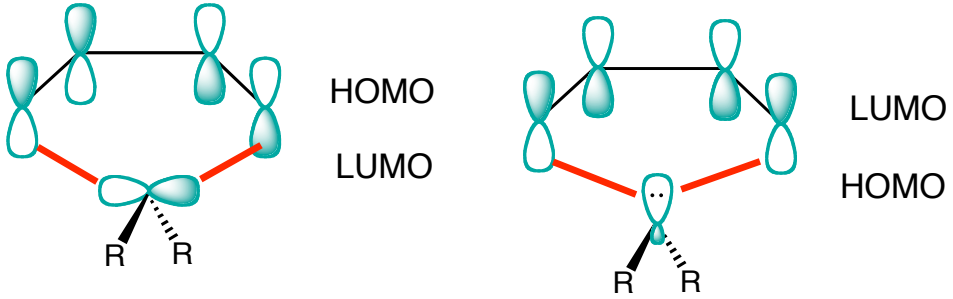

Part B. Provide a mechanism for the following reaction reported by Spino.

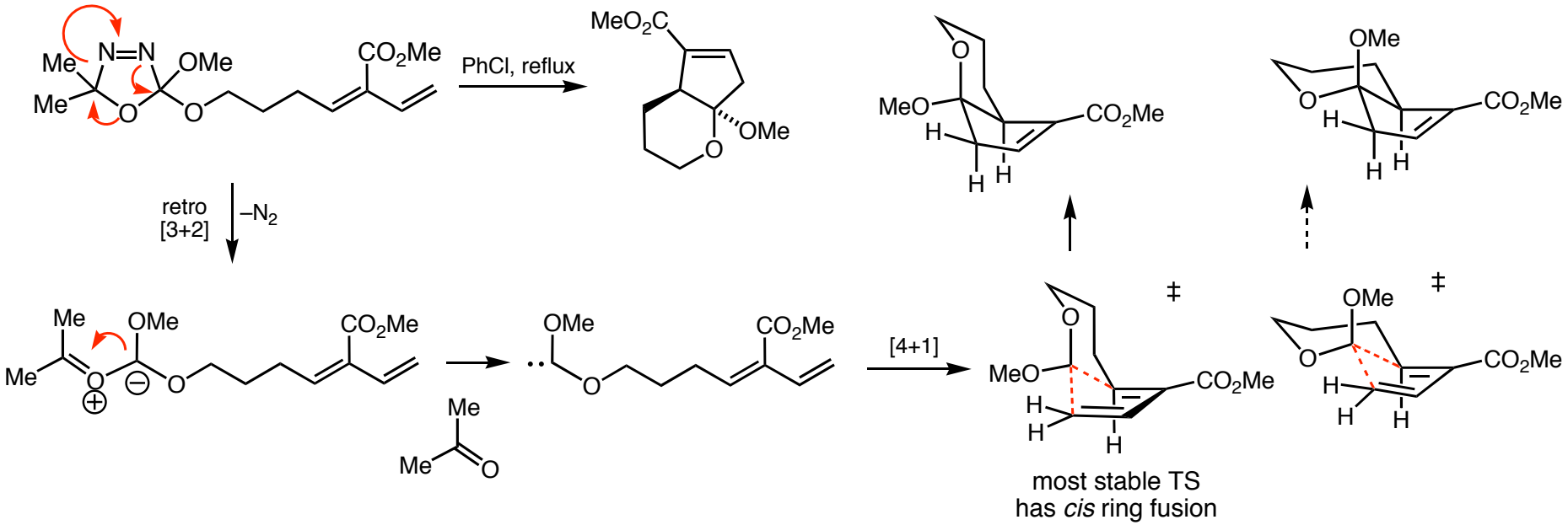

Let's now consider SO_2 as the one-atom component

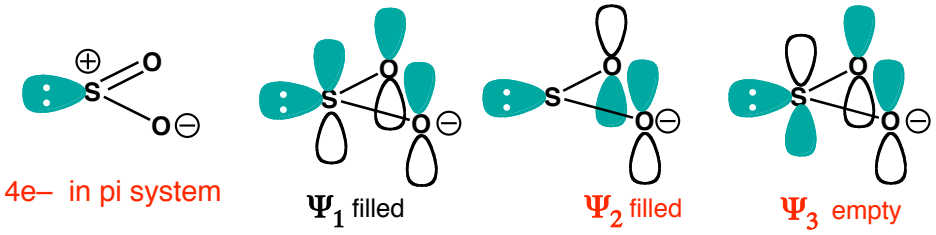

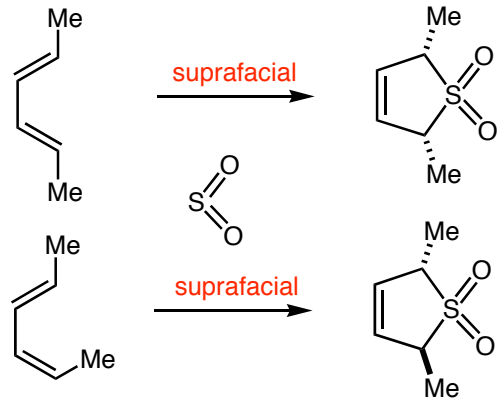

reactions are:
stereospecific & reversible

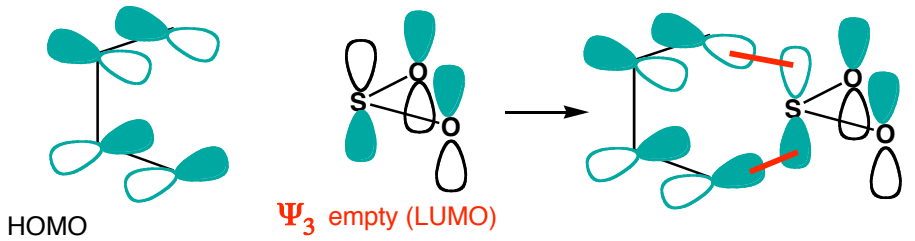

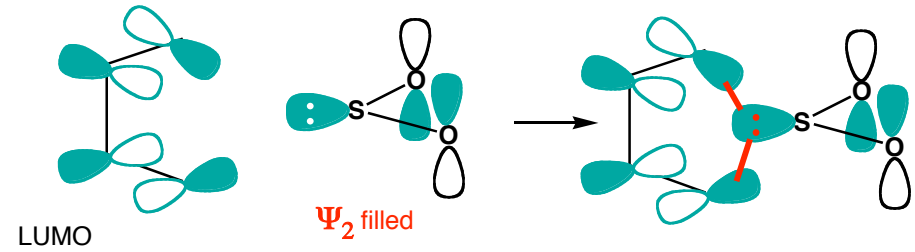

Key step in the *Ramberg Bäcklund* Rearrangement

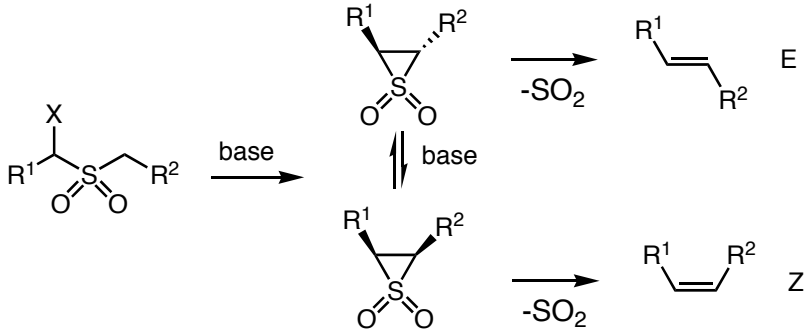

Clough, J. M. *The Ramberg-Backlund Rearrangement.*; Trost, B. M. and Fleming, I., Ed.; Pergamon Press: Oxford, 1991; Vol. 3, pp 861.
"The Ramberg-Backlund Rearrangement.", Paquette, L. A. *Org. React. (N.Y.)* **1977**, *25*, 1.

Analysis of the Suprafacial SO_2 Extrusion (nonlinear)

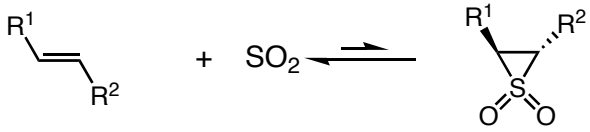

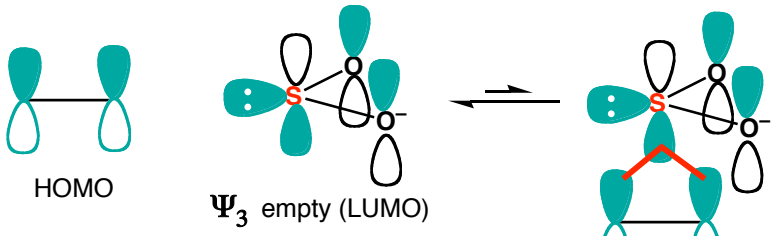

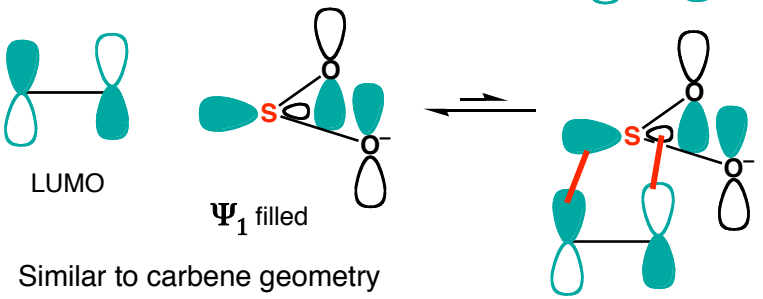

Similar to carbene geometry

http://www.courses.fas.harvard.edu/colgsas/1063

Chemistry 206

Advanced Organic Chemistry

Lecture Number 13

Pericyclic Reactions–3

- Introduction to Sigmatropic Rearrangements
- [2,3] Sigmatropic Rearrangements

Reading Assignment for week:

Carey & Sundberg: **Part A**; Chapter 11
Concerted Pericyclic Reactions

"Pericyclic Reaction Transition States: Passions and Punctilios, 1935-1995 Houk, *Accts. Chem. Res.* **1995**, *28,* 81-90 **(handout)**

"Thermal Reactions of 7-d- and 8-d-Bicyclo[4.2.0]oct-2-enes" Baldwin, Leber, and Powers, *JACS* **2006,** *128,* 10020 **(handout)**

Evans, *Accts. Chem. Res.* **1974**, *7*, 147-55 **(handout)**
(Sulfoxide Rearrangement)

Nakai, *Chem. Rev.* **1986**, *86*, 885-902 (Wittig Rearrangement) **(pdf)**

D. A. Evans

Wednesday
October 18, 2006

Other Reading Material:

[2,3] Sigmatropic Rearrangements

Trost, Ed., *Comprehensive Organic Synthesis* **1992**, Vol 6, Chapter 4.6:

Nakai, T.; Mikami, K. *Org. React. (N.Y.)* **1994**, *46*, 105-209.

Hoffmann, *Angew. Chem. Int. Ed.* **1979**, *18*, 563-572 (Stereochemistry of)

Nakai, *Chem. Rev.* **1986**, *86*, 885-902 (Wittig Rearrangement)

Evans, *Accts. Chem. Res.* **1974**, *7*, 147-55 (Sulfoxide Rearrangement)

Vedejs, *Accts. Chem. Res.* **1984**, *17*, 358-364 (Sulfur Ylilde Rearrangements)

[3,3] Sigmatropic Rearrangements

Trost, Ed., *Comprehensive Organic Synthesis* **1992**, Vol 5,
Chapter 7.1: (Cope, oxy-Cope, Anionic oxy-Cope)
Chapter 7.2, Claisen

S. J. Rhoades, *Organic Reactions* **1974**, *22*, 1 (Cope, Claisen)

S. R. Wilson, *Organic Reactions* **1993**, *43*, 93 (oxy-Cope)

T. S. Ho, *Tandem Organic Reactions* **1992**, *Chapter 12* (Cope, Claisen)

Paquette, L. A. (1990). "Stereocontrolled construction of complex cyclic ketones by oxy-Cope rearrangement." Angew. Chem., Int. Ed. Engl. 29: 609.

Problems of the Day:

Provide a mechanism for this transformation.

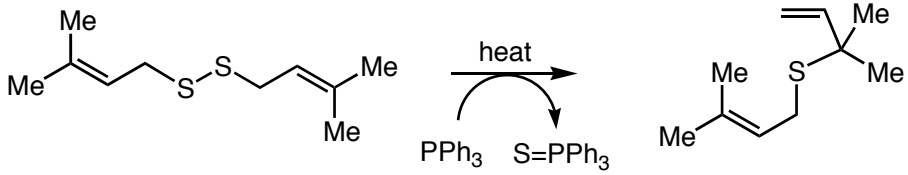

For study on this [2,3] rxn See Baldwin *JACS* **1971**, *93*, 6307

Professor William von Eggers Doering

born: 22 June, 1917, Fort Worth Texas

Professor Doering's parents were both musicians, and met while they were both studying music in Leipzig. When World War I broke out, they moved to the United States, and his father became a vital statistician. His father eventually got a job teaching at Harvard University's School of Public Health, and the family moved to Cambridge. Doering was influenced by his teachers during his early education to pursue science. After graduating from high school, Doering attended Harvard University, where he was inspired to major in chemistry. At Harvard, he took courses with Arthur Lamb, Louis Fieser, Elmer Kohler, and Paul Bartlett. Kohler encouraged Doering to continue on to graduate school, so he earned his Ph.D. in organic chemistry at Harvard in 1943. During his years as a graduate student, he did some research with Louis Fieser on new explosives, including TNT, as well as anti-mustard gas work with Eric Ball. After he completed his PHD, he joined Woodward's team at Harvard, who ultimatelysynthesized quinine. Less than a year later, Doering took an instructorship at Columbia University Doering and spent nine years at Columbia before moving on to Yale University in 1952.

Profesor Doering's major interests have been organic structures and reaction mechanisms. He established the aromatic nature of tropones, tropolones and the tropylium ion. Studies on thermal rearrangements showed that a chair-like transition state is preferred for the Cope rearrangement, and that degenerate Cope rearrangements in bi- and tricyclic systems lead to molecules with "fluxional" structures (i.e. bullvalene). Doering brought carbene chemistry to the attention of organic chemists; he studied carbene insertions, additions to multiple bonds, and intramolecular rearrangements. His interests have been wide-ranging, and he made contributions to the mechanism of solvolysis of tertiary systems, the Diels-Alder reaction, the Baeyer-Villiger rearrangement, the stereochemistry and internal rotations in non-concerted diradical processes, and cis-trans isomerism in higher polyenes.

Professor continues his research to this day and has an active research group in the Naito Laboratory.

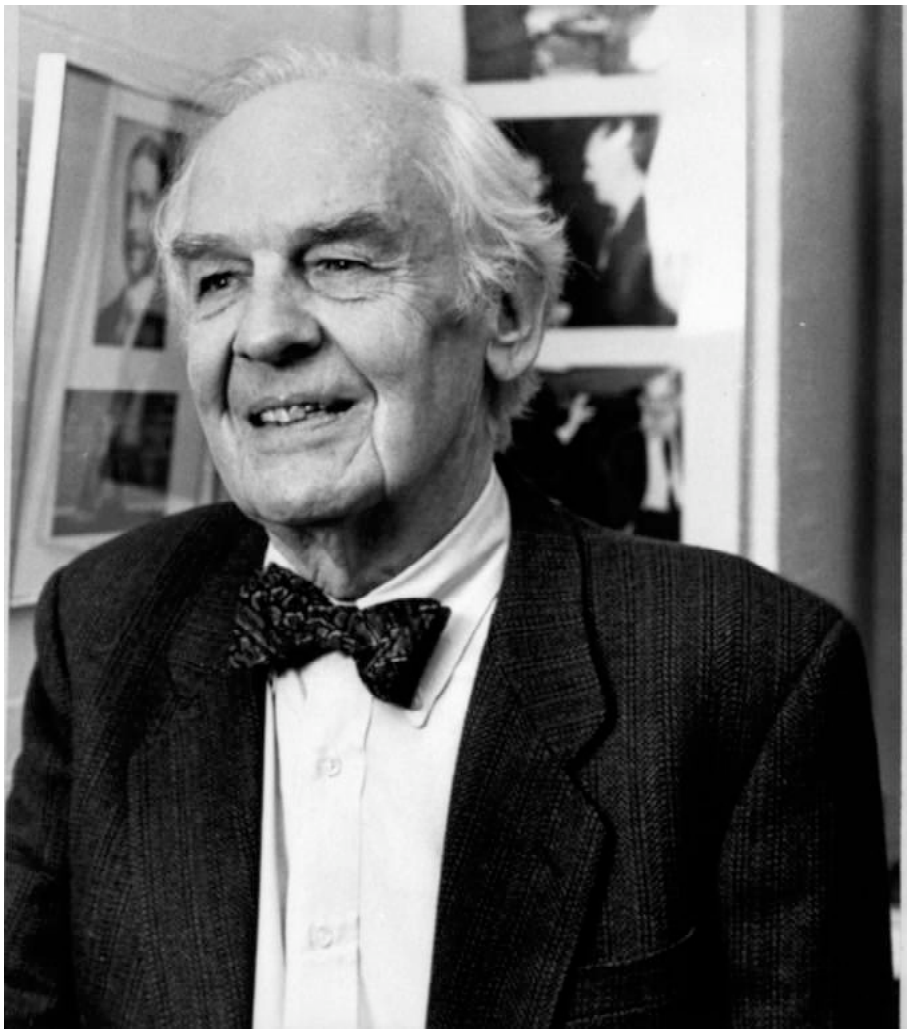

Latest paper

"Effect on Kinetics by Deuterium in the 1,5-Hydrogen Shift of a Cisoid-Locked 1,3(Z)-Pentadiene,2-Methyl-10 methylene-bicyclo[4.4.0]dec-1-ene: Evidence for Tunneling?
William von E. Doering* and Xin Zhao
JACS **2006,** *128*, 9080-9085

Sigmatropic Rearrangements-1

Sigmatropic rearrangements are those reactions in which a sigma bond (& associated substituent) interchanges termini on a conjugated pi system

Examples:

[1,3] Sigmatropic rearrangement

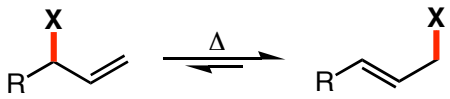

[2,3] Sigmatropic rearrangement

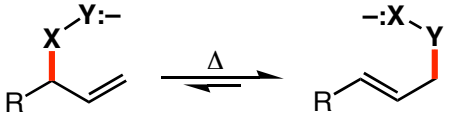

[3,3] Sigmatropic rearrangement

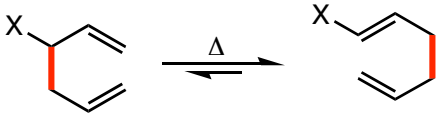

[1,5] Sigmatropic rearrangement

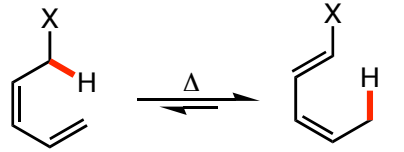

[1,3] Sigmatropic Rearrangements (H migration)

consider the 1,3-migration of H

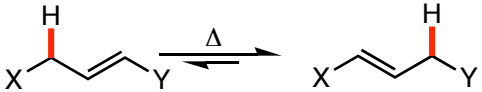

Consider the orbitals needed to contruct the transition state (TS).

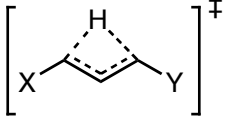

Construct TS by uniting an allyl and H radical:

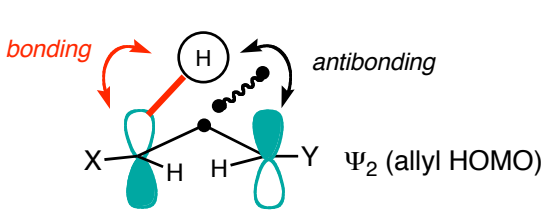

Suprafacial Geometry

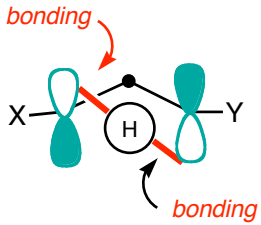

Antarafacial Geometry

Bridging distance too great for antarafacial migration.

[1,3] Sigmatropic Rearrangements (C migration)

consider the 1,3-migration of Carbon

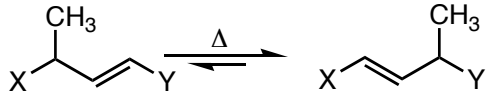

Consider the orbitals needed to contruct the transition state (TS).

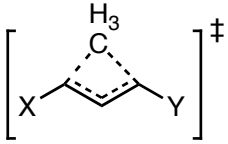

Construct TS by uniting an allyl and Me radicals:

Retention at carbon

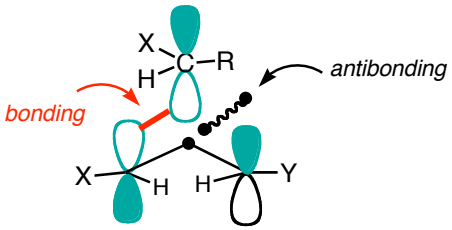

Suprafacial on allyl fragment

Sychronous bonding to both termini cannot be achieved from this geometry

Inversion at carbon

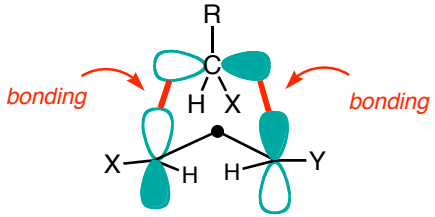

Suprafacial on allyl fragment

Sychronous bonding to both termini is possible from this geometry

❒ The stereochemical constraints on the suprafacial migration of carbon with inversion of configuration is highly disfavored on the basis of strain.

[1,3]-Sigmatropic rearrangements are not common

no observed scrambling of labels

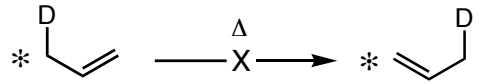

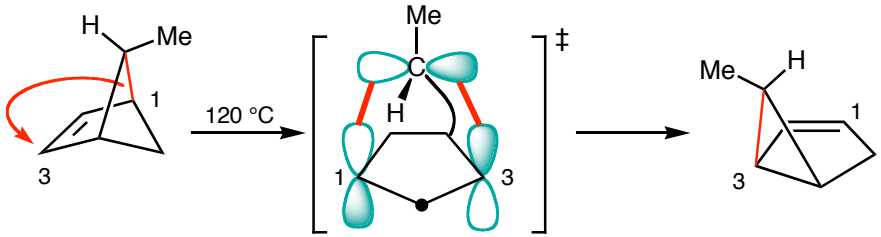

These rearrangements are only seen in systems that are highly strained, an attribute that lowers the activation for rearrangement.

■ [1,3] Sigmatropic Rearrangements (C migration)

"Thermal Reactions of 7-d- and 8-d-Bicyclo[4.2.0]oct-2-enes," Baldwin, Leber, and Powers, *JACS* **2006,** *128,* 10020 **(handout)**

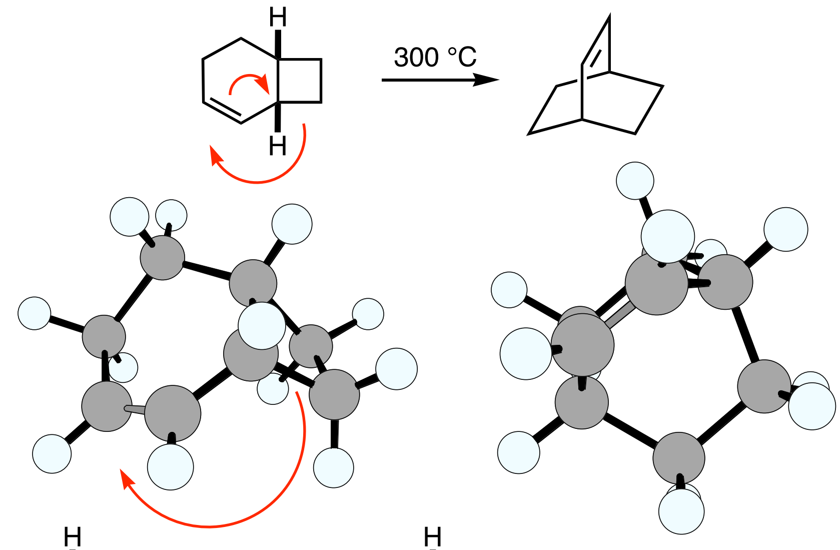

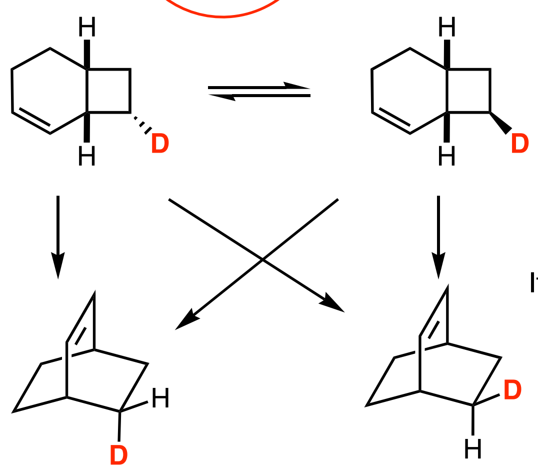

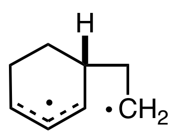

It is concluded that diradical intermediates are involved

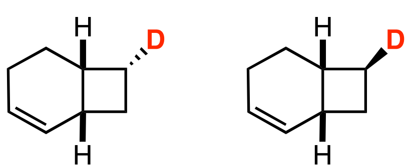

therefore

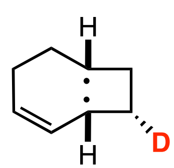

No equilibration

insignificant

■ [1,3] Sigmatropic Rearrangements (C migration)

"New Thermal Reactions of Deuterium-Labeled Bicyclo[3.2.0]hept-2-enes: Bicyclic Skeletal Inversion and Epimerization at C7," *JACS* **2001,** *123,* 8396 **(pdf)**

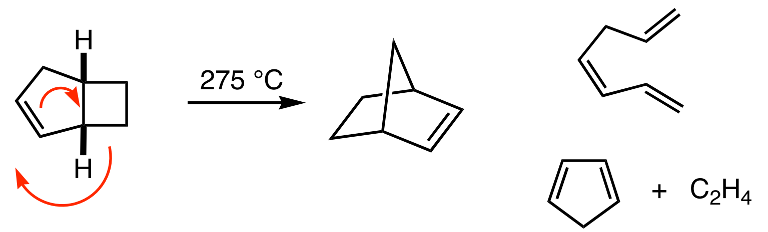

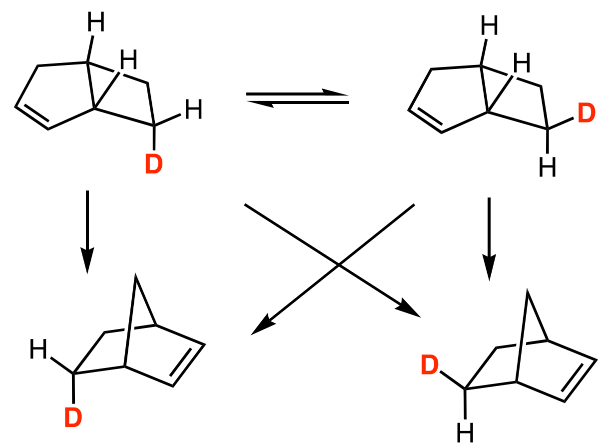

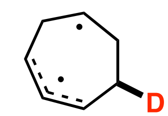

significant

It is concluded that diradical intermediates are involved

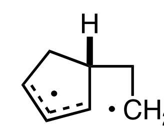

(2) (a) Cocks, A. T.; Frey, H. M. *J. Chem. Soc. A* **1971**, 2564–2566. (b) Baldwin, J. E.; Belfield, K. D. *J. Am. Chem. Soc.* **1988**, *110*, 296–297. (c) Klärner, F.-G.; Drewes, R.; Hasselmann, D. *J. Am. Chem. Soc.* **1988**, *110*, 297–298. (d) Baldwin, J. E.; Belfield, K. D. *J. Phys. Org. Chem.* **1989**, *2*, 455–466. (e) Carpenter, B. K. *Acc. Chem. Res.* **1992**, *25*, 520–528. (f) Carpenter, B. K. *J. Am. Chem. Soc.* **1995**, *117*, 6336–6344. (g) Wilsey, S.; Houk, K. N.; Zewail, A. H. *J. Am. Chem. Soc.* **1999**, *121*, 5772–5786. (h) Baldwin, J. E.; Leber, P. A. *J. Am. Chem. Soc.* **2001**, *123*, 8396–8397.

SIGMATROPIC REACTIONS - FMO-Analysis

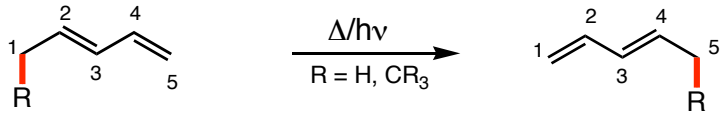

[1,5] Sigmatropic Rearrangements (H migration)

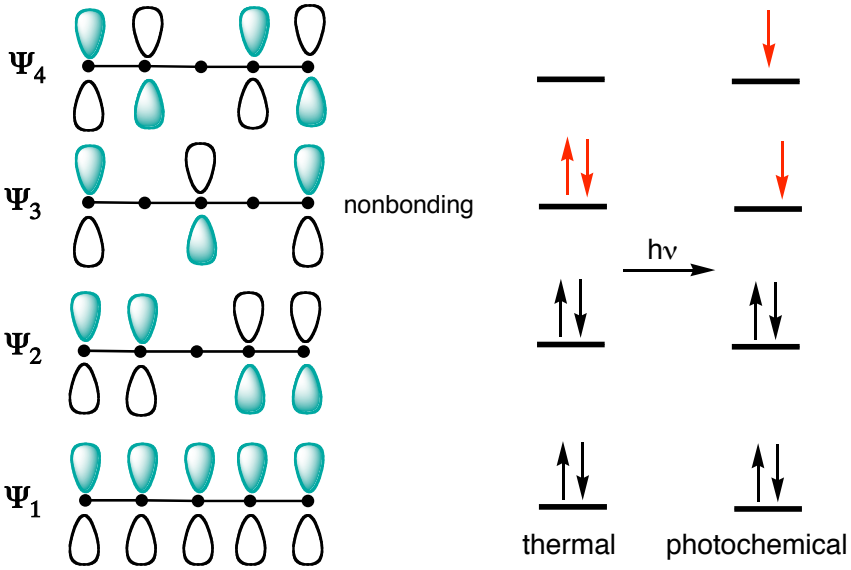

View as cycloadditon between following species:

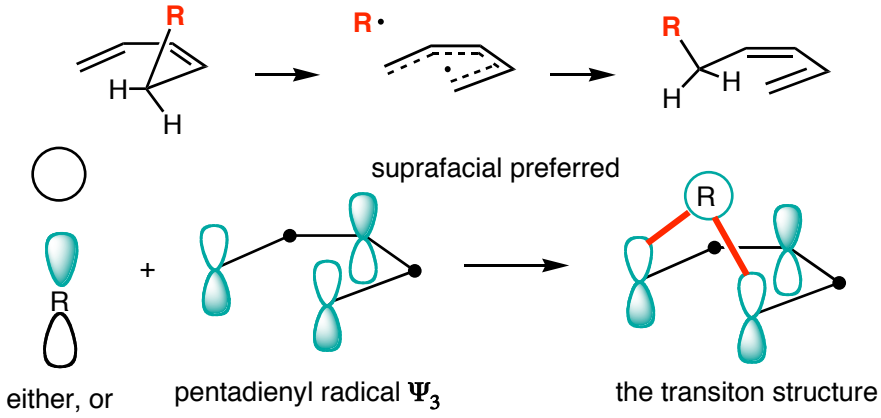

[1,5] Sigmatropic Rearrangements (C migration)

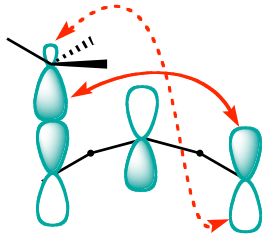

[1s,5s] alkyl shift ⇒ RETENTION

[1a,5a] alkyl shift ⇒ INVERSION disfavored

[1,5] (C migration): Stereochemical Evaluation

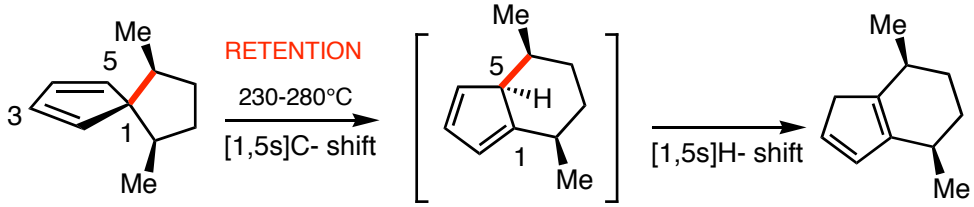

Dewar–Zimmerman Analysis: Retention

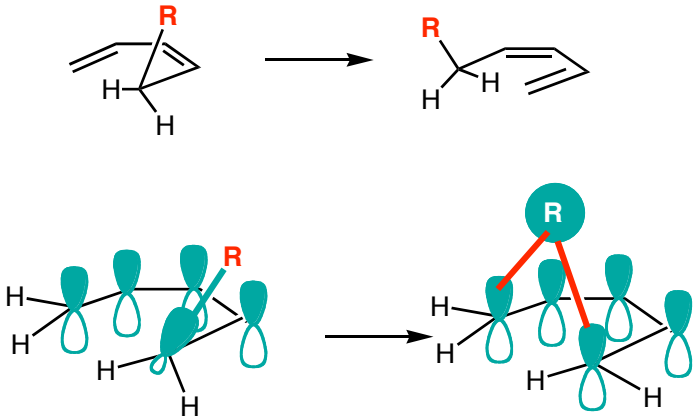

0 phase inversions ⇒ Huckel toplogy
6 electrons
therefore, allowed thermally

Sigmatropic Rearrangements: An Overview

[1,2] Sigmatropic Rearrangements: Carbon

[1,2]-Sigmatropic rearrangements to cationic centers allowed.

Wagner-Meerwein Rearrangement

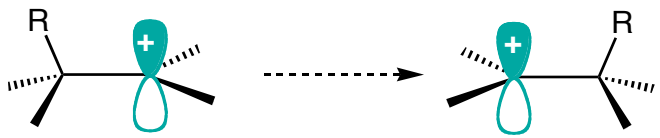

consider as cycloaddition

FMO analysis

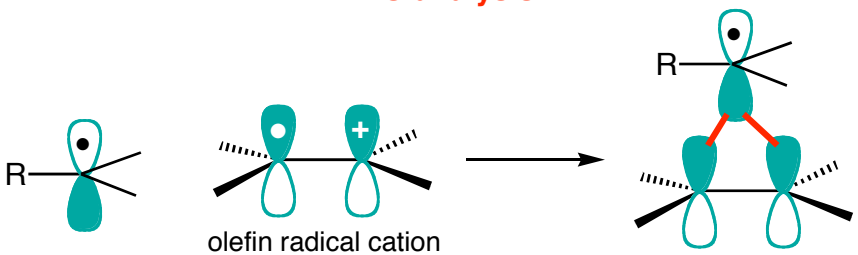

olefin radical cation

transition state

[1,2]-Sigmatropic rearr to carbanionic centers not observed

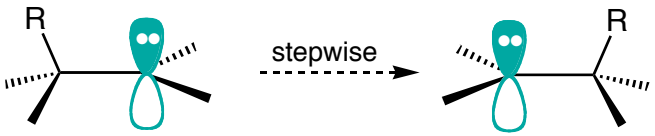

consider as cycloaddition

FMO analysis

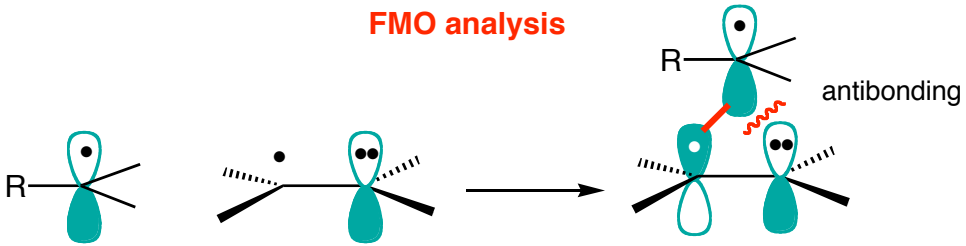

olefin radical anion

transition state

The Wittig Rearrangement [1,2]

"[2,3]-Wittig Sigmatropic Rearrangements in Organic Synthesis.", Nakai, T.; Mikami, K. *Chem. Rev.* **1986**, *86*, 885.
Marshall, J. A. *The Wittig Rearrangement.*; Trost, B. M. and Fleming, I., Ed.; Pergamon Press: Oxford, 1991; Vol. 3, pp 975.

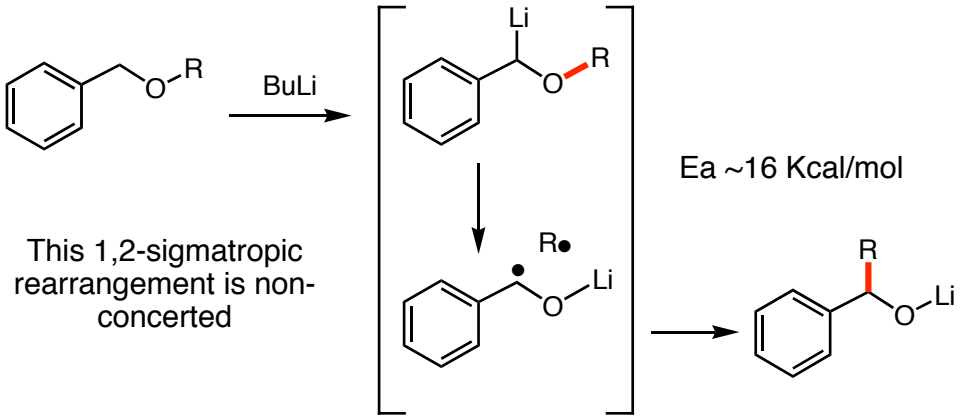

Ea ~16 Kcal/mol

This 1,2-sigmatropic rearrangement is non-concerted

The Wittig Rearrangement [2,3]

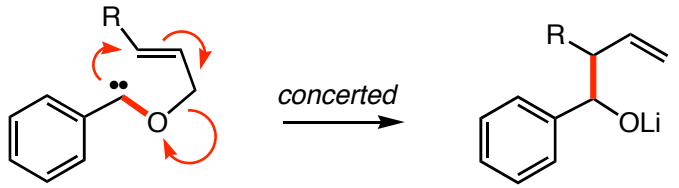

FMO analysis

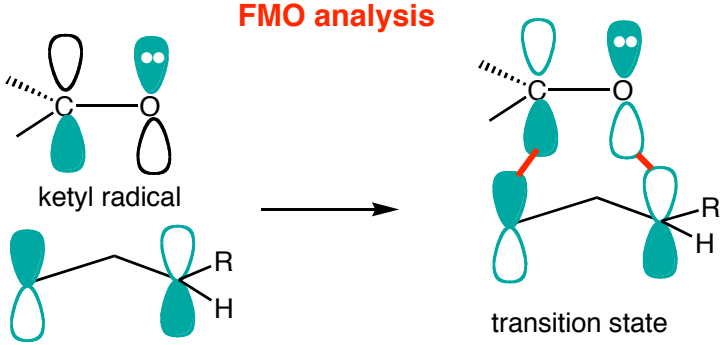

The $\Delta\Delta G^{\ddagger}$ between concerted and non-concerted pathways can be quite small

[2,3] Sigmatropic Rearrangements

■ The basic process:

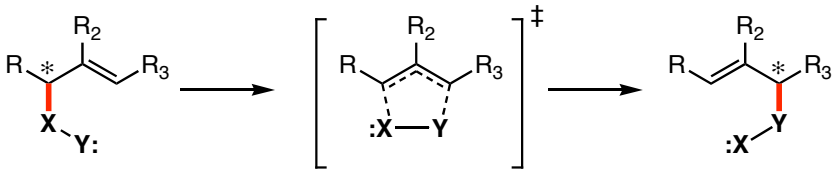

X & Y = permutations of C, N, O, S, Se, P; however X is usually a heteroatom

Attributes: Stereoselective olefin construction & chirality transfer

■ **Representative X-Y Pairs:**

N–O (amine oxides)	S–P, S–N, S–O (sulfoxides)
S–C (sulfur ylids)	O–P (phosphites)
O–C (Wittig rearrangement)	N–N, Cl^+–C (haloium ylids)
N–C (nitrogen ylids)	P–C, C–C (homoallylic anions).
S–S (disulfides)	

An important early paper: Baldwin, *J. Chem. Soc., Chem. Comm.* **1970**, 576

■ X - O, Y = C; Wittig Rearrangement:

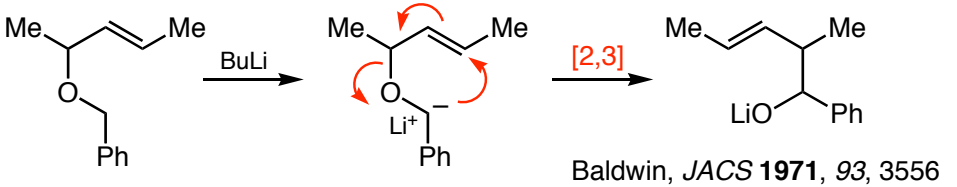

Baldwin, *JACS* **1971**, *93*, 3556

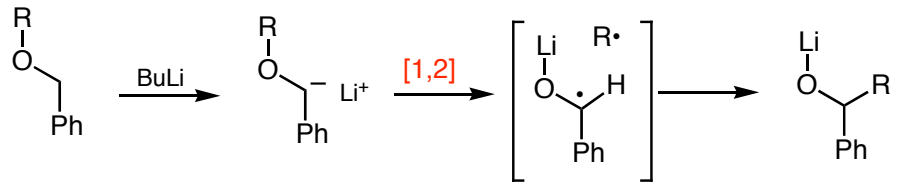

Garst, *JACS* **1976**, *98*, 1526

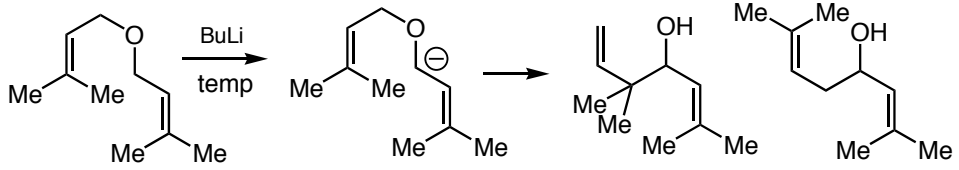

Rautenstrauch, *Chem Commun.* **1979**, 1970 –25 °C ~70% ~30%

■ X - S, Y = C; Sulfonium Ylide Rearrangement:

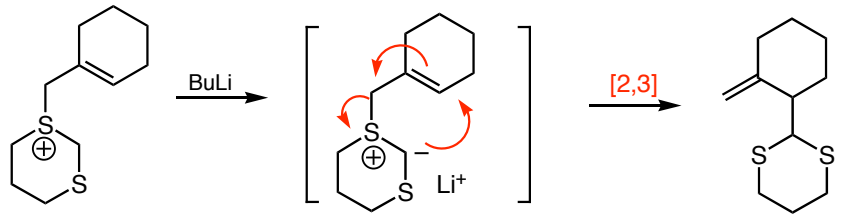

Lythgoe, *Chem Commum* **1972**, 757

■ X - N, Y = C; Ammonium Ylide Rearrangement:

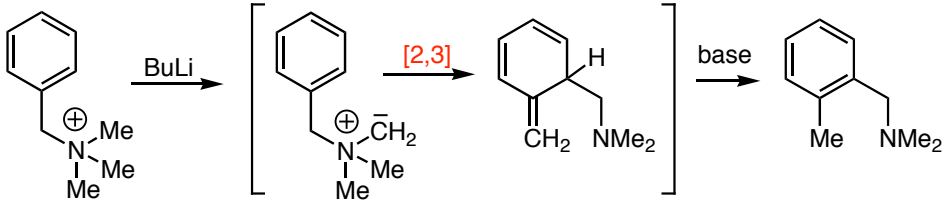

Review, Pines, *Org. Rxns* **1970**, *18*, 416 **Sommelet-Hauser:**

Modern versions of Stevens:

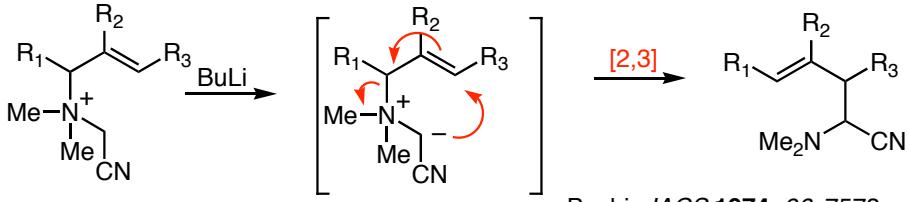

Buchi, *JACS* **1974**, *96*, 7573
Mander, *JOC* **1973**, *38*, 2915
important extension lacking CN FG; Sato, *JACS* **1990**, *112*, 1999

X - O, Y = C; An all-carbon Rearrangement

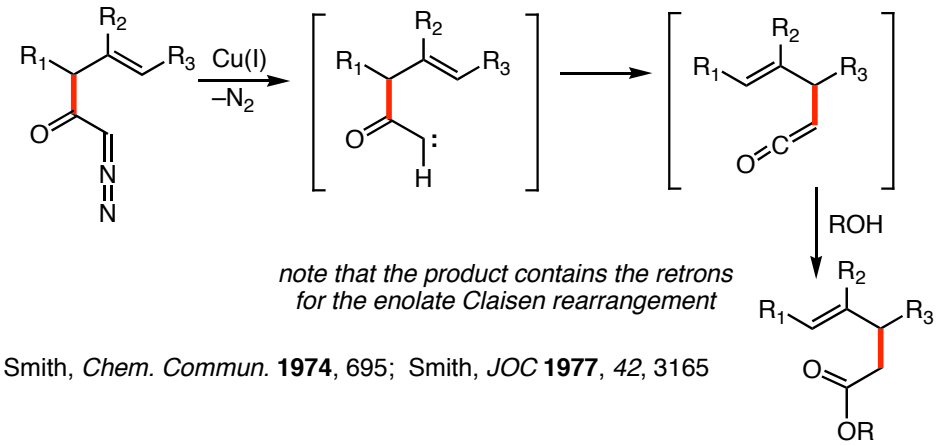

Smith, *Chem. Commun.* **1974**, 695; Smith, *JOC* **1977**, *42*, 3165

X - N, Y = O; Meisenheimer Rearrangement

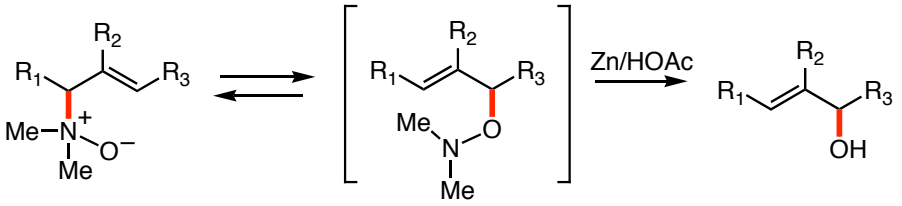

Tanabe, *Tet Let.* **1975**, 3005

X - S, Y = O; Sulfoxide Rearrangement

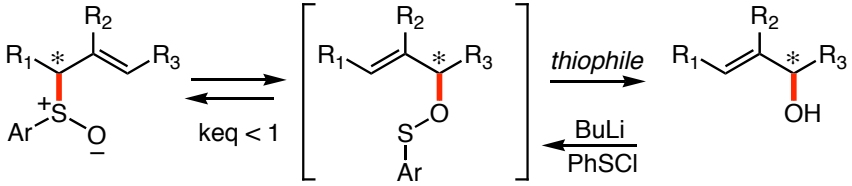

Evans, *Accts. Chem. Res.* **1974**, *7*, 147

X - Se, Y = N; Related Rearrangement

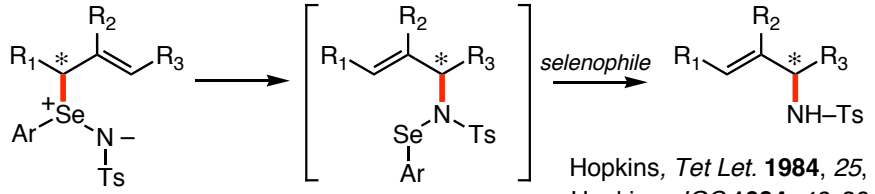

Hopkins, *Tet Let.* **1984**, *25*, 15
Hopkins, *JOC* **1984**, *49*, 3647
Hopkins, *JOC* **1985**, *50*, 417

X - S, Y = N; Related Rearrangement

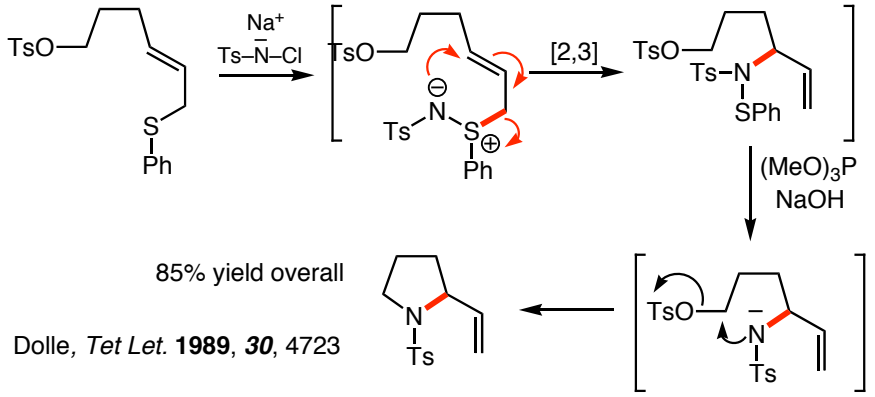

85% yield overall

Dolle, *Tet Let.* **1989**, ***30***, 4723

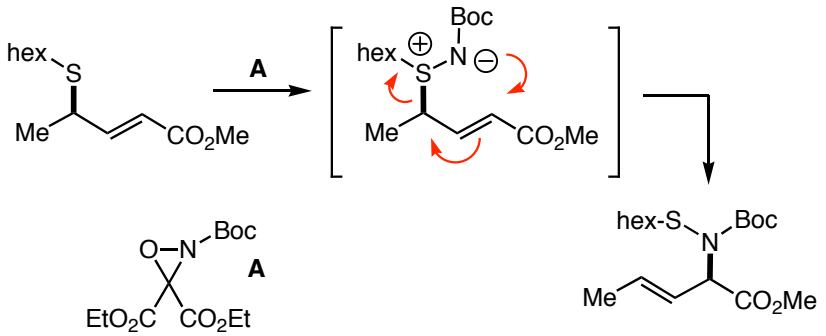

Armstrong et al. *J. Org. Chem.* **2006**, *71*, 4028

■ 1,2-Disubstitution: Good Trans Olefin Selectivity

Starting olefin: Trans

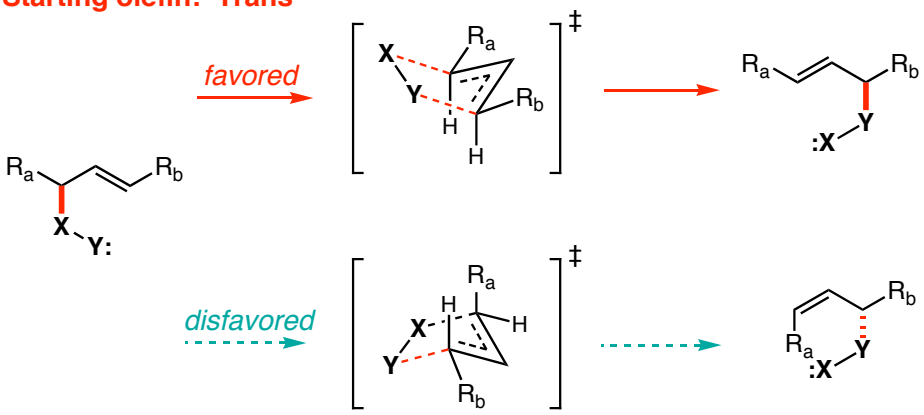

R_a & R_b prefer to orient in pseudo-equatorial positions during rearrangement; nevertheless, this is a delicately balanced situation

Starting olefin: Cis

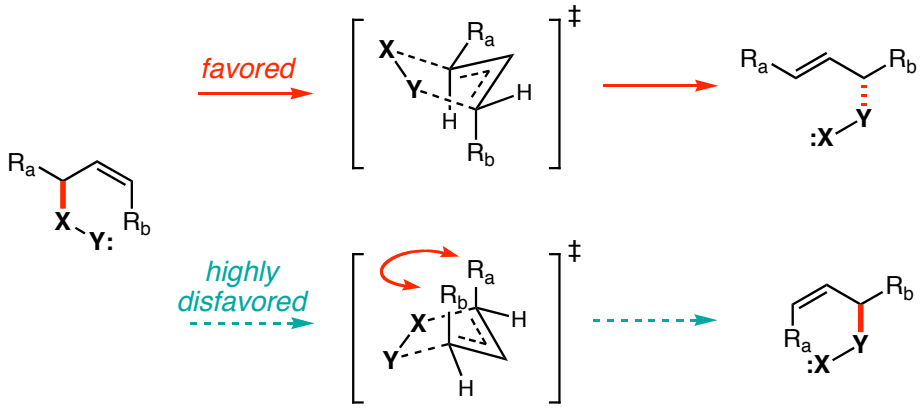

Conclusions

- ❑ Olefin geometry dictates sense of asymmetric induction in rearrangement
- ❑ (Z) Olefin rearrangements might exhibit higher levels of 1,3 induction
- ❑ Product olefin geometry can be either (E) or (Z) from (E) starting material
- ❑ Product olefin geometry will be (E) from (Z) starting material

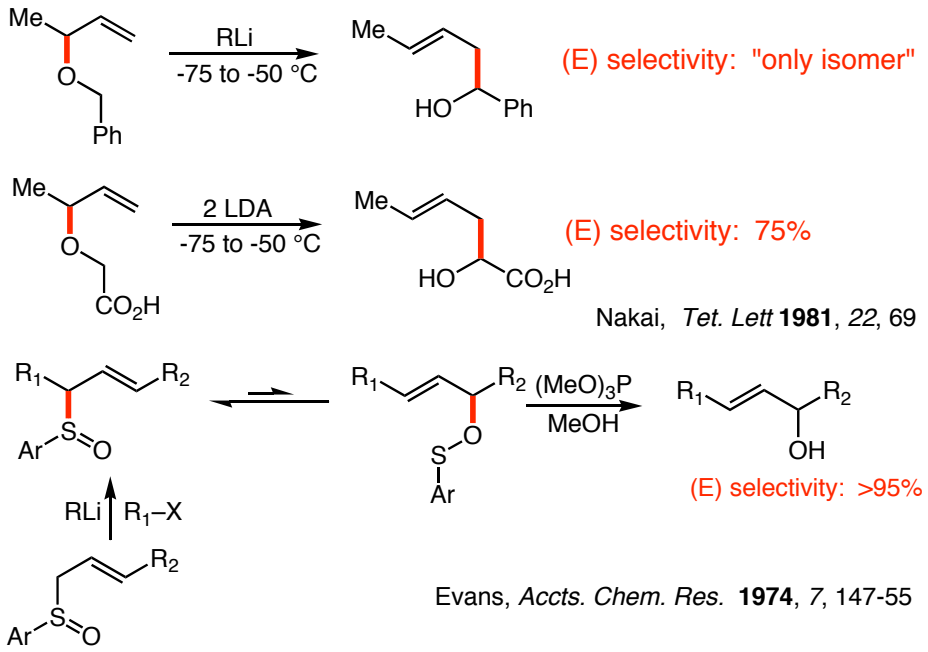

The preceeding transition state models do not explain some of the results:

❑ Cis selectivity has been observed: Still JACS **1978**, *100*, 1927.

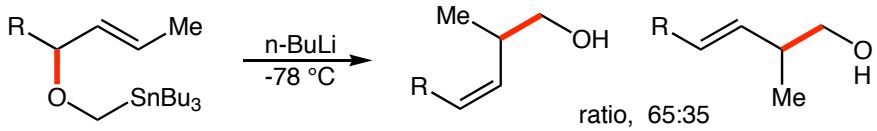

❑ However, Cis selectivity is dependent on starting olefin geometry

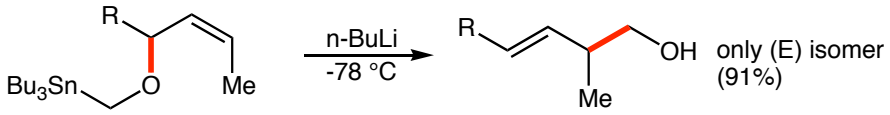

Several theoretical studies have been published: Good reading

Houk JOC **1991**, *56*, 5657 (Sulfur ylide transition states)

Houk JOC **1990**, *55*, 1421 (Wittig transition states)

■ Starting olefin: (E) Trisubstituted

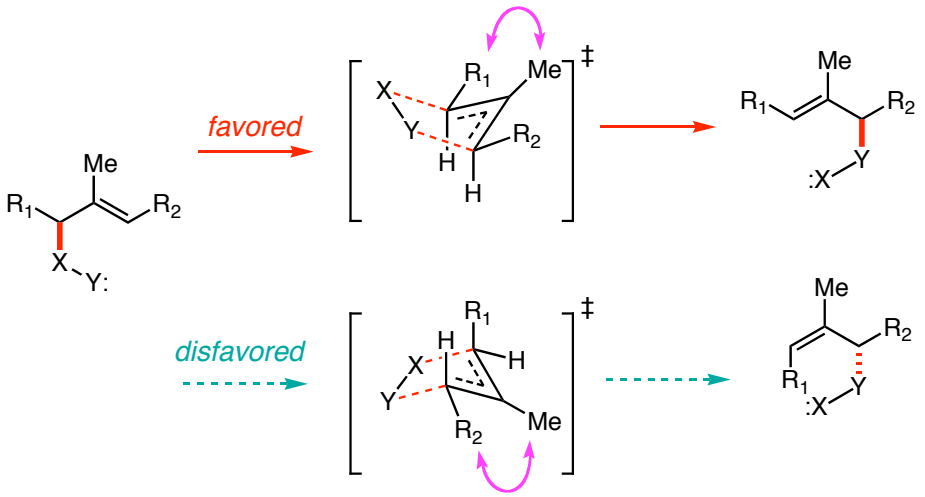

R_1–Me interaction can destabilize the (E) transition state while (Z) TS might be destabilized by R_1 interactions with both X-Y and allyl moiety.

■ Starting olefin: (Z)

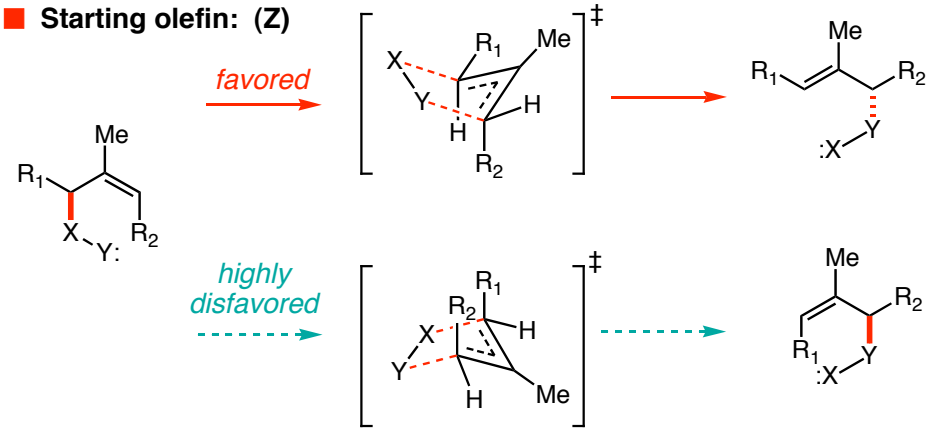

Conclusions

- ❏ Olefin geometry dictates sense of asymmetric induction in rearrangement
- ❏ (Z) Olefin rearrangements might exhibit higher levels of 1,3 induction
- ❏ Product olefin geometry can be either (E) or (Z) from (E) starting material
- ❏ Product olefin geometry will be (E) from (Z) starting material

■ (Z) selectivity has been observed: Still JACS **1978**, *100*, 1927.

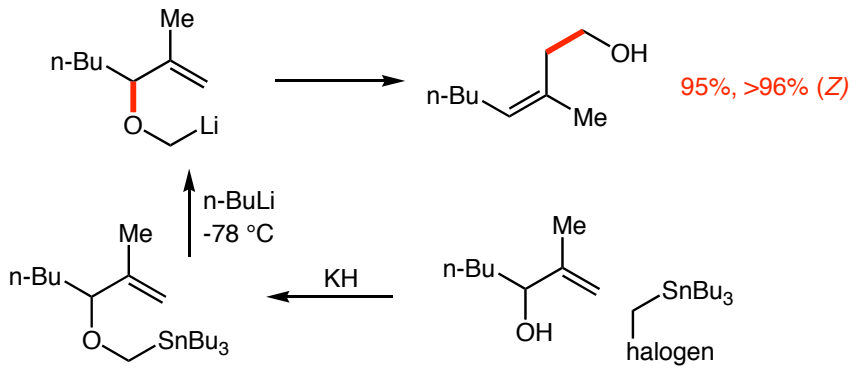

Still says that the TS is early, so that the 1,2 interactions in the TS are most important.

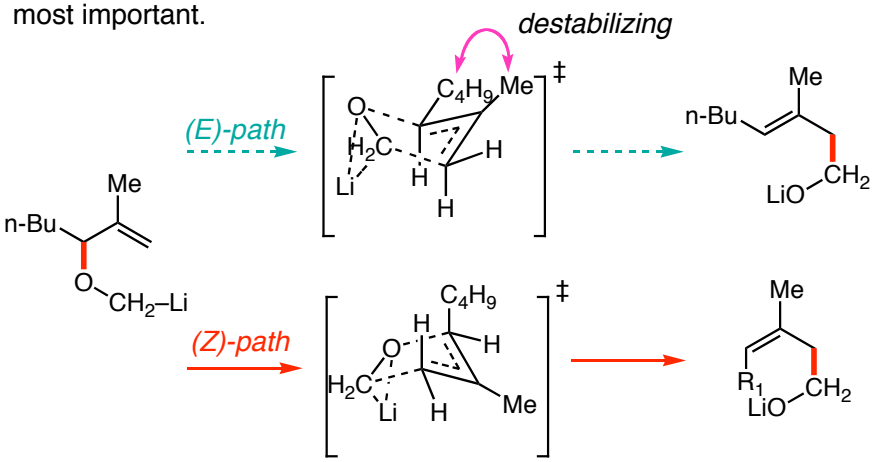

■ (Z) selectivity has also been observed by others: Sato JACS **1990**, *112*, 1999.

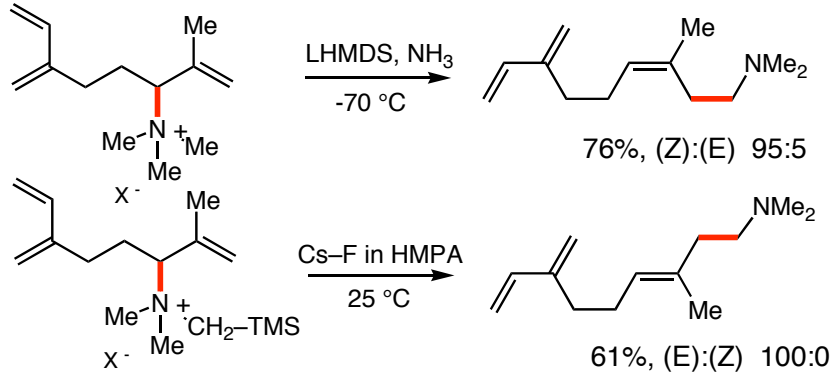

Trisubstituted olefins via [2,3]-rearrangement of sulfoxides:

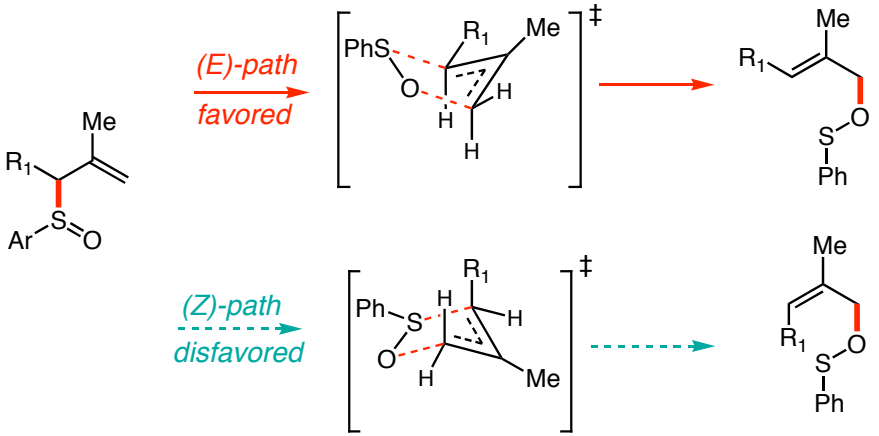

■ In contrast to the previous cases exhibiting (Z) selectivity rearrangements (E)-selective rearrangments has been observed:

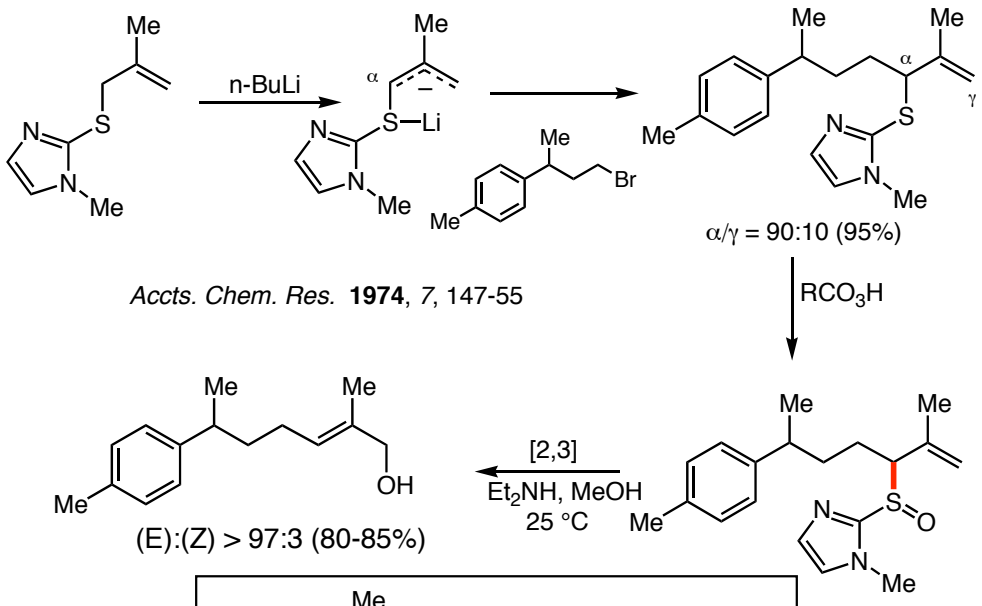

Accts. Chem. Res. **1974**, *7*, 147-55

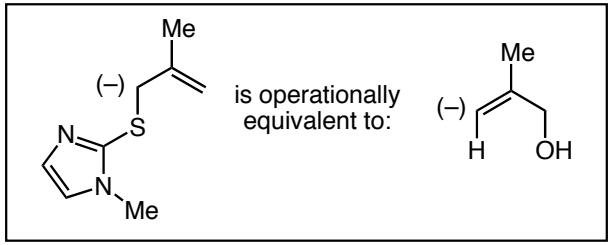

Trisubstituted olefins via [2,3]-rearrangement of sulfonium ylides:

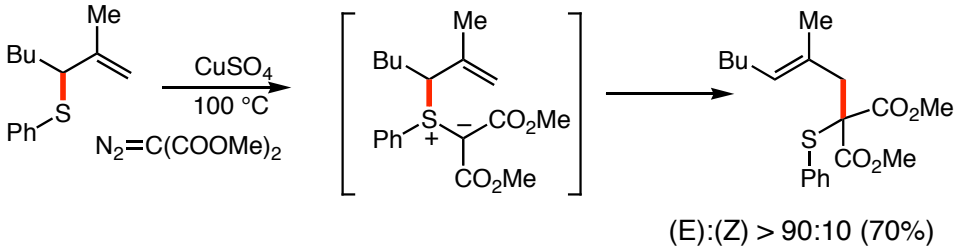

A general procedure for the direct synthesis of sulfur ylides:

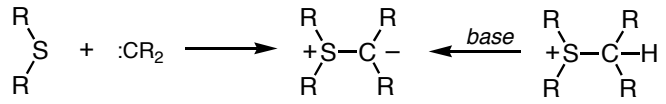

Trisubstituted olefins via Wittig [2,3]-rearrangement:

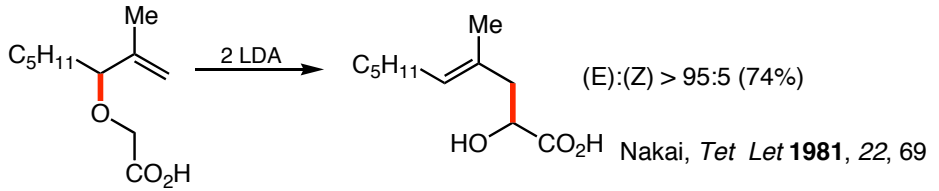

Nakai, *Tet Let* **1981**, *22*, 69

However, this reaction is not general:

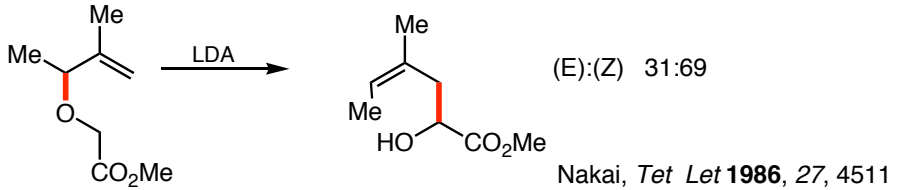

Nakai, *Tet Let* **1986**, *27*, 4511

[2,3]-Sigmatropic Rearrangements: Olefin Geometry

■ Trisubstituted olefins via [2,3]-rearrangement:

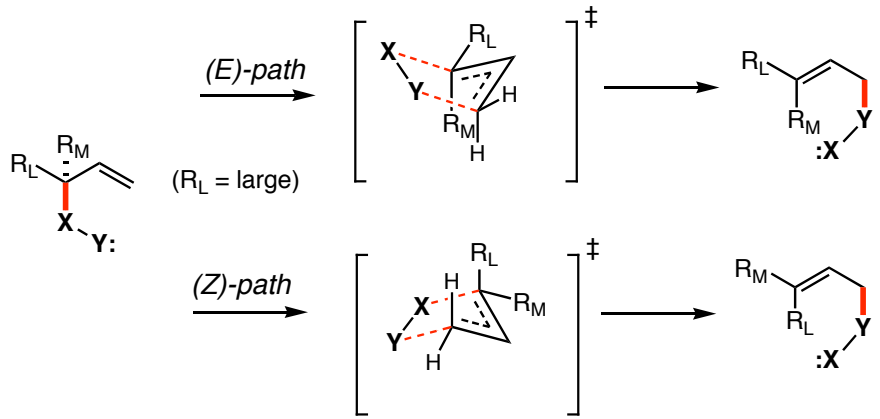

One might project that the (E) path will be moderately favored with selectivity depending on size difference between R_L & R_M

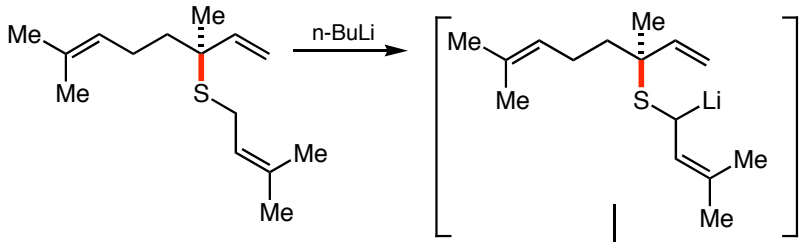

Rautenstrauch, *Helv. Chim Acta* **1971**, *54*, 739

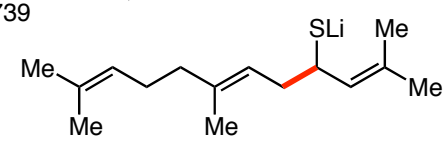

(E):(Z) = 3:2

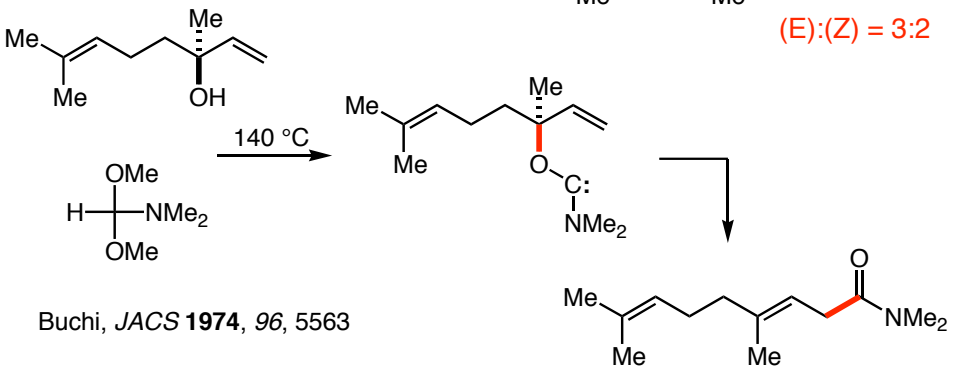

Buchi, *JACS* **1974**, *96*, 5563

poorly selective

An elegant squalene synthesis **Ollis, *Chem. Commun* 1969, 99**

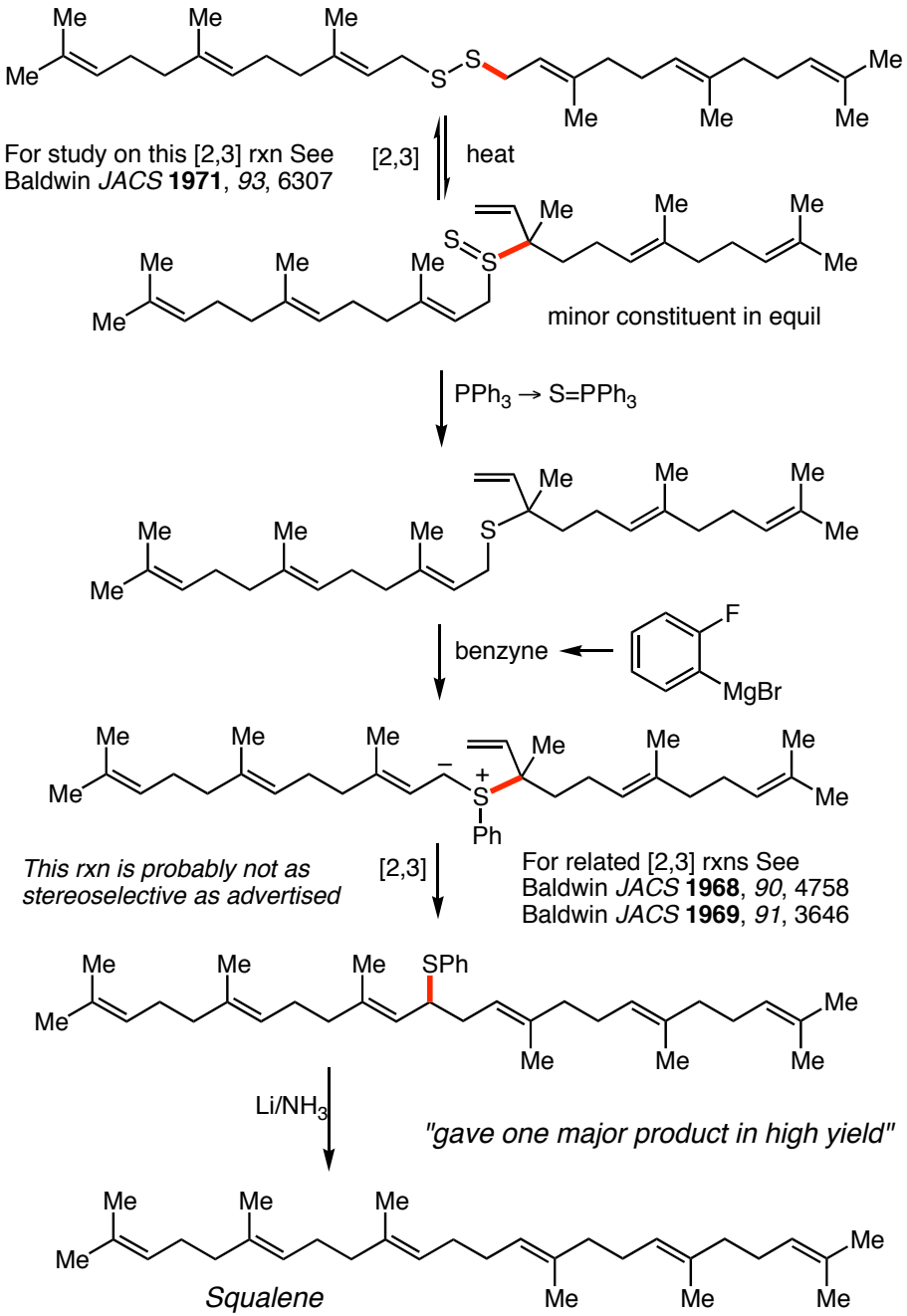

[2,3] Sulfur Ylide Rearrangement Using a Chiral Auxiliary

Kurth JOC **1990**, *55*, 2286 and TL **1991**, *32*, 335

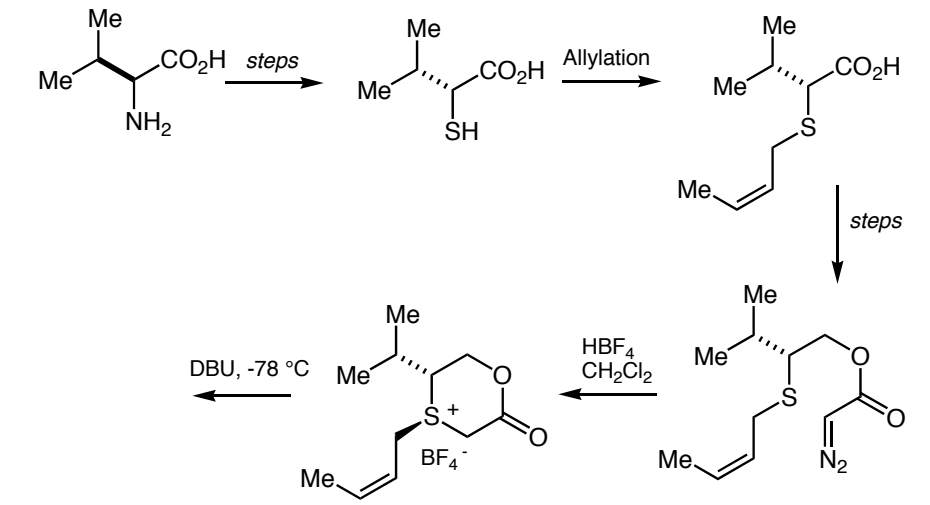

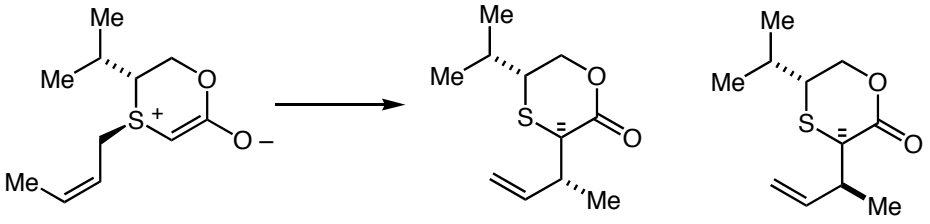

66%, 94:4

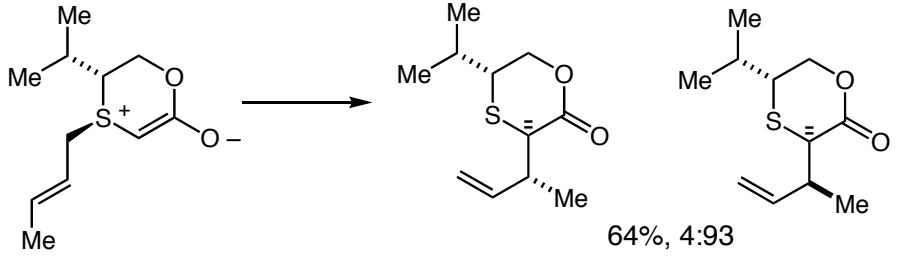

64%, 4:93

Chiral Auxiliaries can also be used in the Wittig Rearrangement

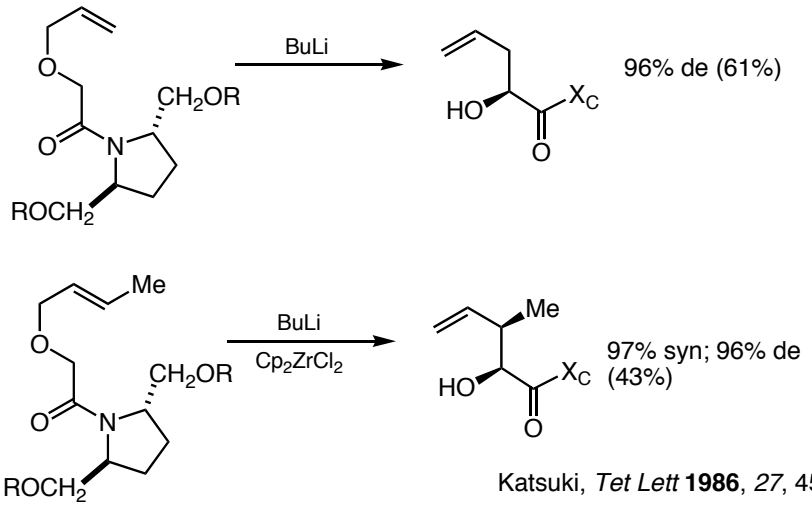

Katsuki, *Tet Lett* **1986**, *27*, 4577

Internal Relay of Stereochemistry in C–C Constructions

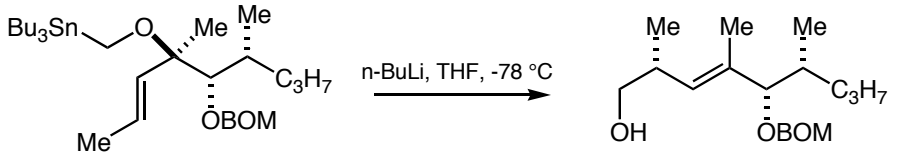

diastereoselection > 100:1 (57%)

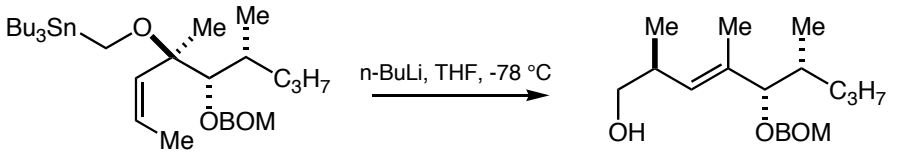

Kallmerten TL **1988**, *29*, 6901.

diastereoselection > 100:1 (64%)

See these papers for other applications
- Kallmerten TL **1993**, *34*, 753.
- Kallmerten TL **1993**, *34*, 749.
- Kallmerten SynLet **1992**, 845.

Internal Relay of Stereochemistry in C–O Constructions

Tandem [4+2] & [2,3] Process: Evans, Bryan, Sims *J. Am. Chem. Soc.* **1972**, 2891.

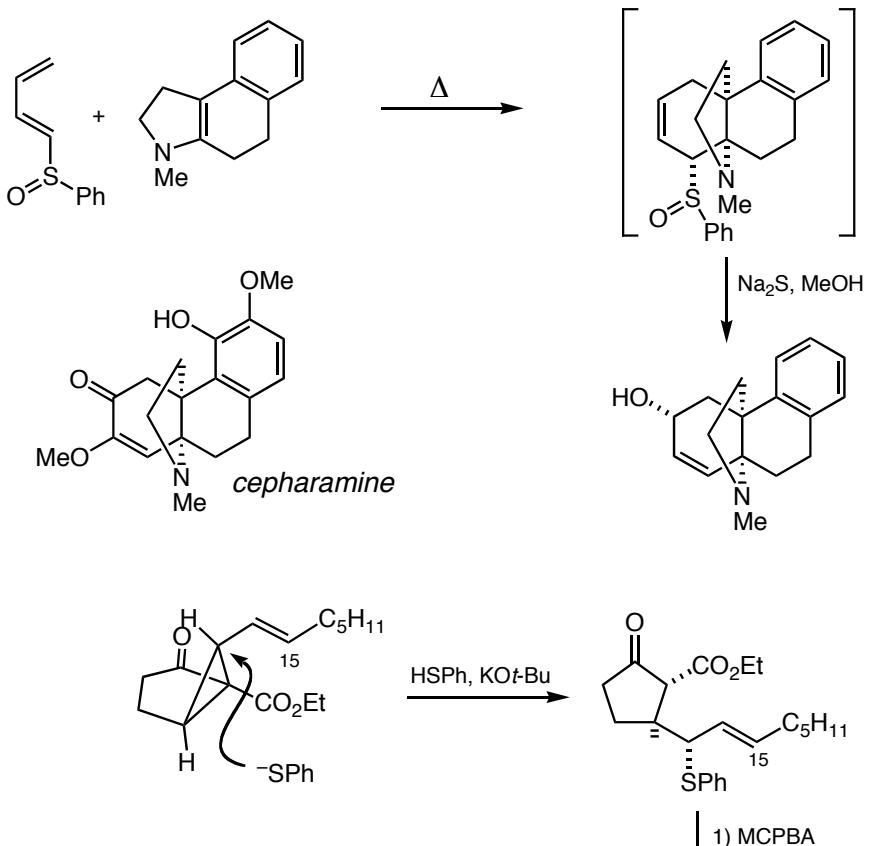

Taber *J. Am. Chem. Soc.* **1977**, *99*, 3513.
Kondo *Tet. Lett.* **1978**, 3927.

Cases where the chirality is exocyclic to the rearrangement

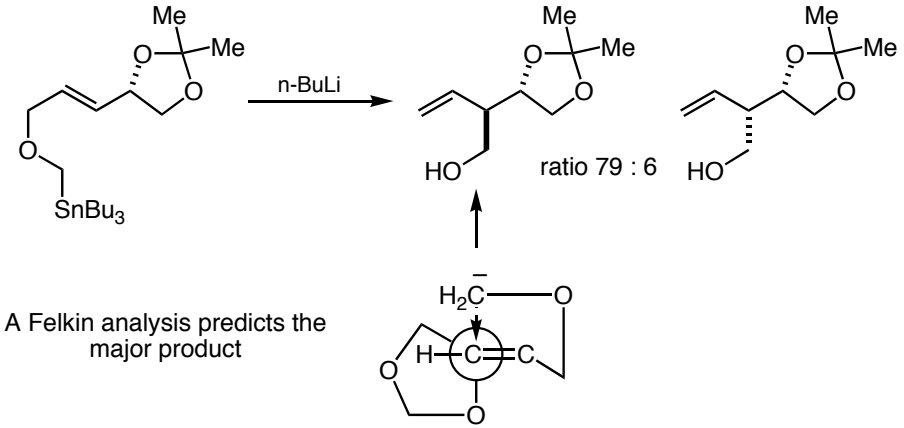

A Felkin analysis predicts the major product

Bruckner, *Angew. Chem. Int. Ed.* **1988**, *27*, 278

Allylic Ethers to Make Three Contiguous Stereocenters

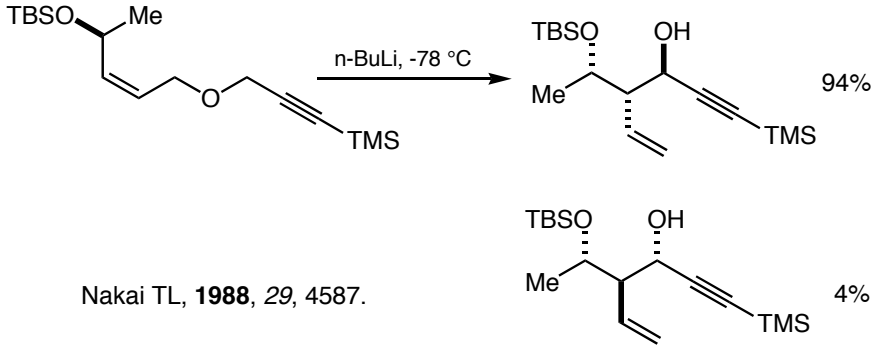

Nakai TL, **1988**, *29*, 4587.

Can you rationalize the stereochemical outcome of this reaction?

The Synthesis of Bakkenolide-A (*Evans JACS* **1977**, *99*, 5453)

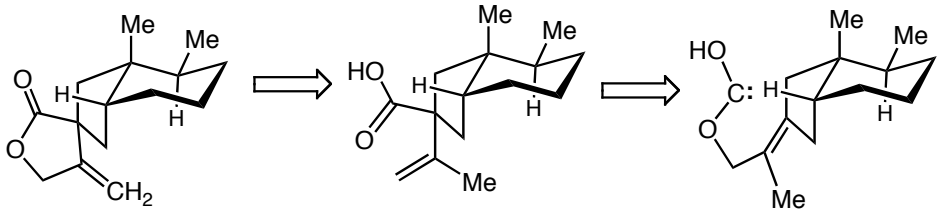

■ Candidate processes:

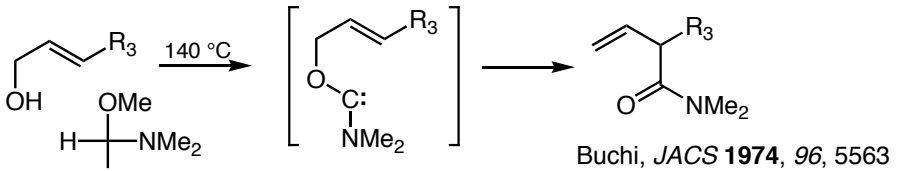

Buchi, *JACS* **1974**, *96*, 5563

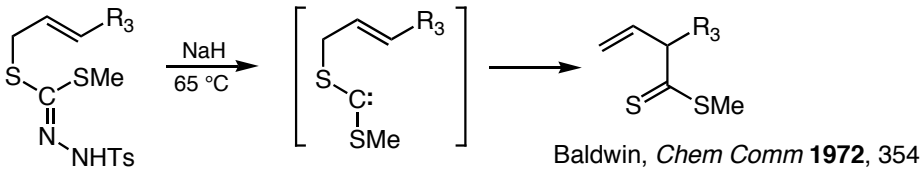

Baldwin, *Chem Comm* **1972**, 354

■ The synthesis:

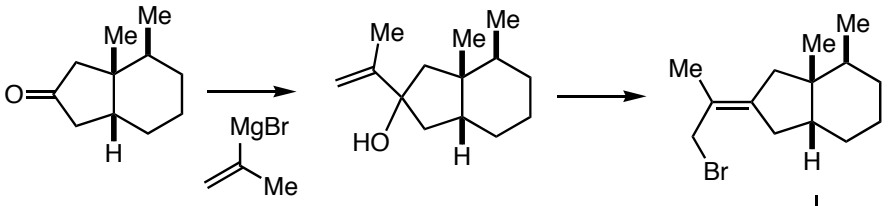

Note that rearrangement is not required to proceed via the carbenoid. propose altenate mechanism

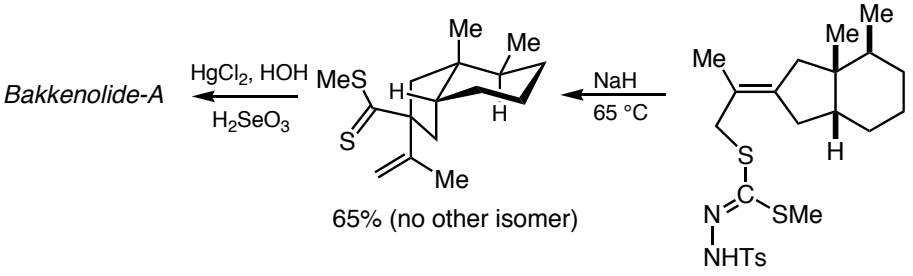

65% (no other isomer)

[2,3] Sigmatropic rearrangements respond to subtile steric effects

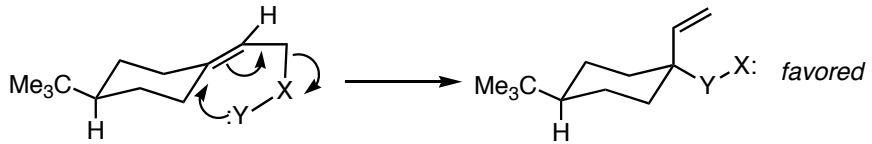

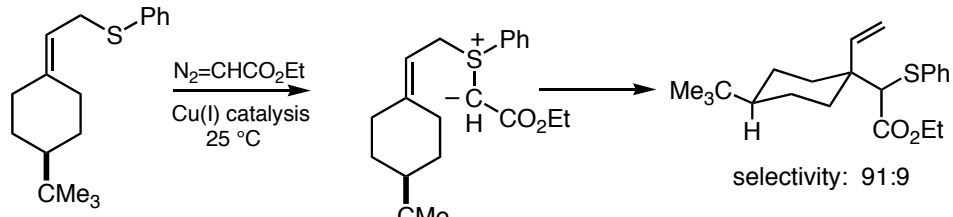

selectivity: 91:9

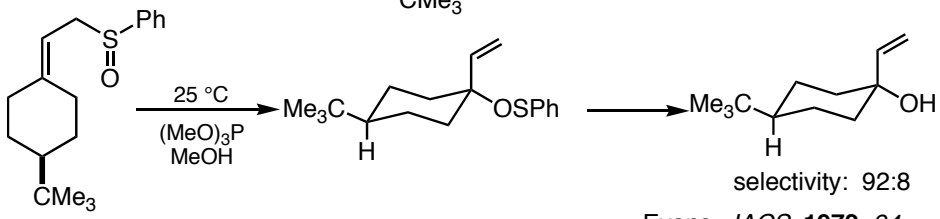

selectivity: 92:8

Evans, *JACS*, **1972**, *94*, 3672

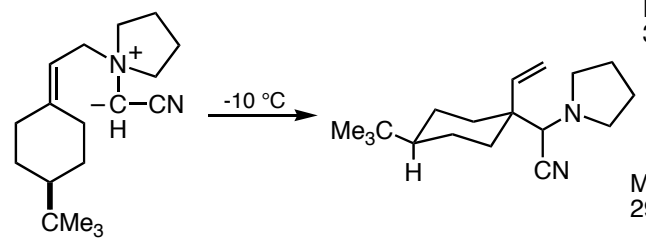

selectivity: 90:10

Mander, *JOC*, **1973**, *38*, 2915

■ The comparison of analogous [2,3] & [3,3] rearrangements:

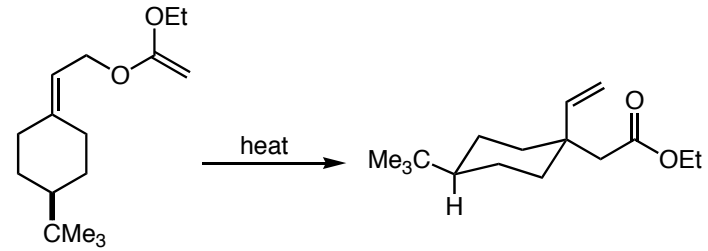

selectivity: 52:48

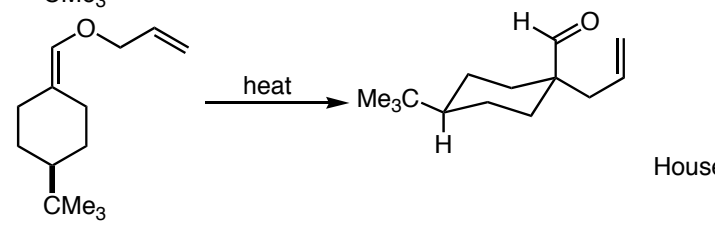

selectivity: 75:25

House, *JOC* **1975**, *40*, 86

Ring expansion reactions have been investigated

Methods based on sulfur ylides: (review) Vedejs, *Accts. Chem. Res.* **1984**, *17*, 358

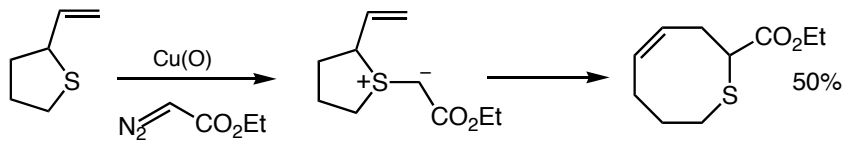

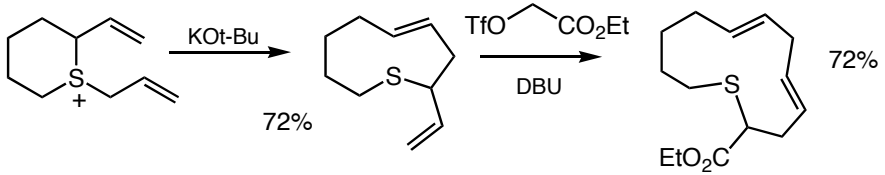

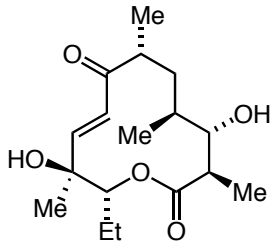

Methynolide has been synthesized by Vedejs using this ring-expansion methodology

Vedejs, *JACS* **1989**, *111*, 8430

An early ring expansion using the Sommelet-Hauser Rearrangement

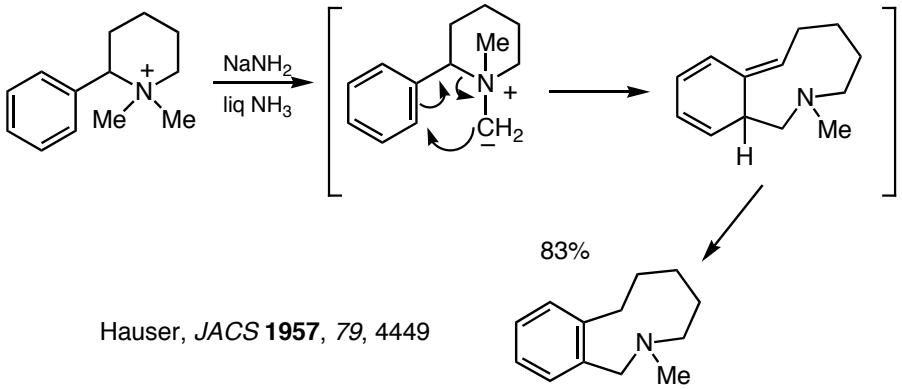

Hauser, *JACS* **1957**, *79*, 4449

A ring contraction using the Wittig Rearrangement

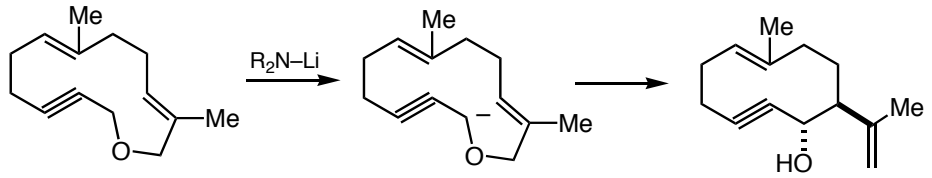

With chiral amide bases induction is observed!

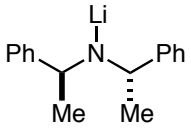

82%, 69% ee

Aristolactone

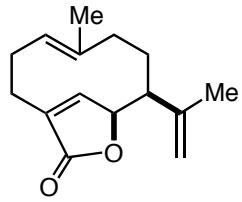

Marshall, *JACS* **1988**, *110*, 2925

A ring contraction using the Stevens Rearrangement

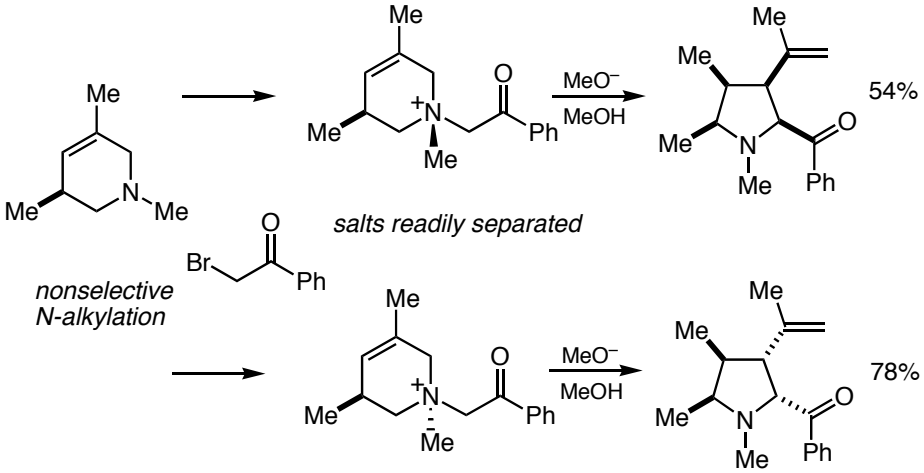

Both rearrangements afford a single isomer

http://www.courses.fas.harvard.edu/colgsas/1063

Chemistry 206

Advanced Organic Chemistry

Lecture Number 14

Pericyclic Reactions–4

- [3,3] Sigmatropic Rearrangements: Introduction
- Cope Rearrangements & Variants
- Claisen Rearrangements & Variants

Reading Assignment for week:

Carey & Sundberg: **Part A**; Chapter 11
Concerted Pericyclic Reactions

K. Houk, *Transition Structures of Hydrocarbon Pericyclic Rxns*
Angew Chem. Int. Ed. Engl. **1992**, *31*, 682-708

K. Houk, *Pericyclic Reaction Transition States: Passions & Punctilios, Accts. Chem. Res.* **1995**, *28,* 81-90
Angew Chem. Int. Ed. Engl. **1992**, *31*, 682-708

D. A. Evans

Friday,
October 20, 2006

Other Reading Material:

[3,3] Sigmatropic Rearrangements

Trost, Ed., *Comprehensive Organic Synthesis* **1992**, Vol 5,
Chapter 7.1: (Cope, oxy-Cope, Anionic oxy-Cope)
Chapter 7.2, Claisen

S. J. Rhoades, *Organic Reactions* **1974**, *22*, 1 (Cope, Claisen)

S. R. Wilson, *Organic Reactions* **1993**, *43*, 93 (oxy-Cope)

T. S. Ho, *Tandem Organic Reactions* **1992**, *Chapter 12* (Cope, Claisen)

Paquette, L. A. (1990). "Stereocontrolled construction of complex cyclic ketones by oxy-Cope rearrangement." Angew. Chem., Int. Ed. Engl. 29: 609.

Problems of the Day:

Predict the stereochemical outcome of this Claisen rearrangement

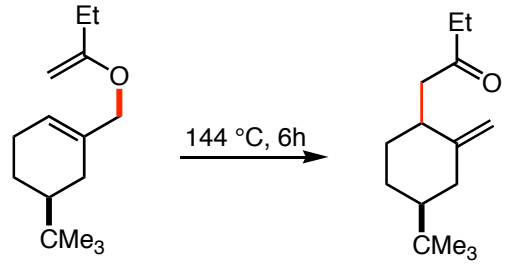

diastereoselection
>87:13

Ireland, *JOC* 1983, *48*, 1829

Provide a mechanism for the indicated fransformation

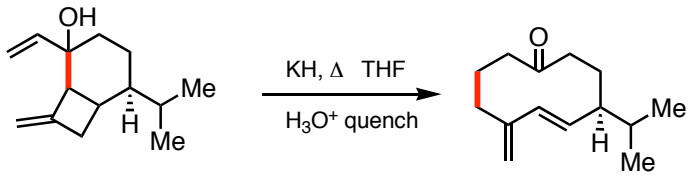

Schreiber, *JACS* **1984**, *106,* 4038

Database Problem number 117: Key words: Rearrangement + Claisen

In a recent article, MacMillan and Yoon (*JACS* **2001**, *123*, 2448) reported the complex rearrangement illustrated below.

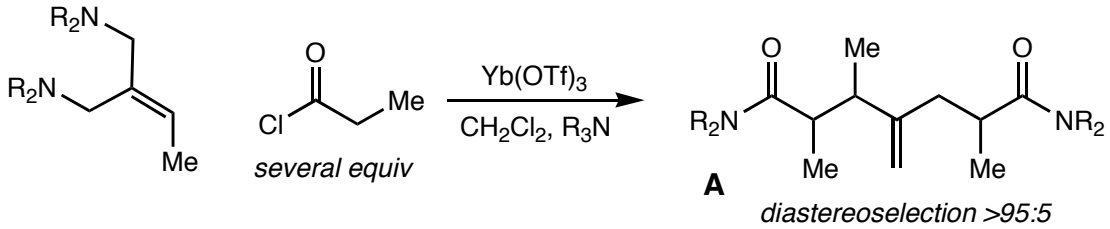

Part A. Provide a mechanism for this overall transformation. In answering this question, you should illustrate those transition states where stereocenters are generated and where stereochemcal information is relayed.

Part B. From your answer in Part A, illustrate the stereochemical relationships in the diamide product **A**.

Database Problem number 195: Key words: Rearrangement + Claisen

Provide a mechanism for the indicated transformation that accounts for the observed stereochemical outcome (*JACS*, **1984**, 7643).

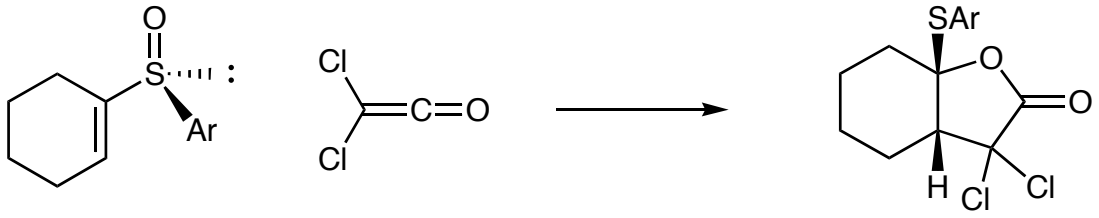

General Reviews:

S. J. Rhoades, *Organic Reactions* **1974**, *22*, 1 (Cope, Claisen)
S. R. Wilson, *Organic Reactions* **1993**, *43*, 93 (oxy-Cope)
T. S. Ho, *Tandem Organic Reactions* **1992**, *Chapter 12* (Cope, Claisen)
Trost, Ed., *Comprehensive Organic Synthesis* **1992**, Vol 5,
Chapter 7.1: (Cope, oxy-Cope, Anionic oxy-Cope)
Chapter 7.2, Claisen

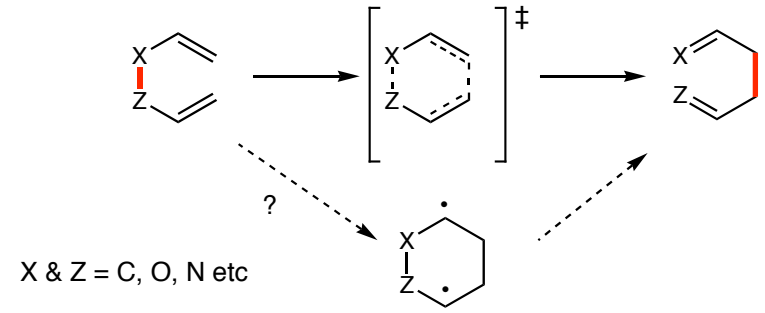

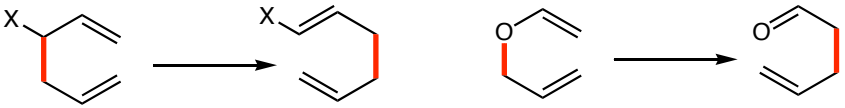

Cope Rearrangement, Ea = 33.5 kcal/mol *Claisen Rearrangement Ea = 30.6 kcal/mol*

The Reaction Energetics Goldstein, *JACS* **1972**, *94*, 7147

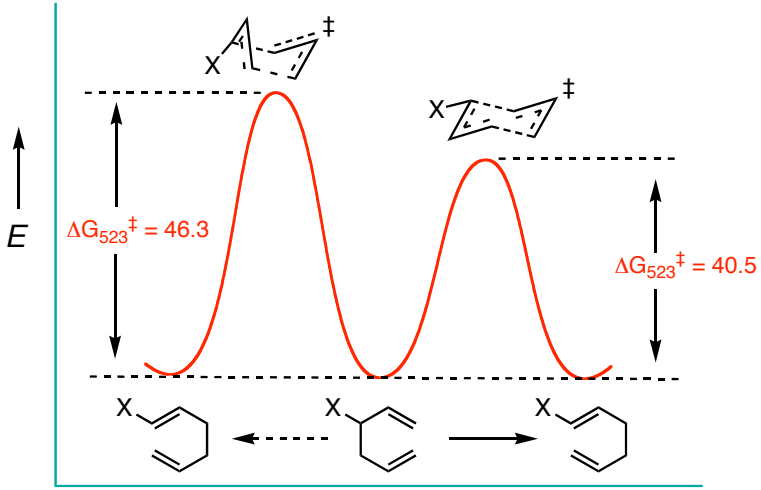

The CopeTransition States

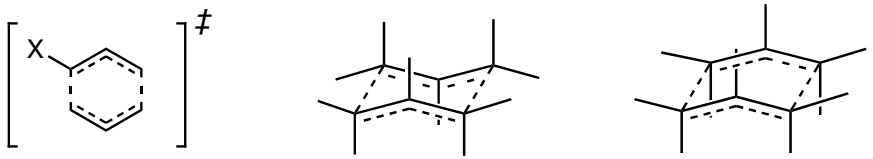

	CHAIR	*BOAT*
Relative Energy $\Delta\Delta G^{\ddagger}$:	0	+ 5.8 kcal/mol

	CHAIR	*BOAT*
Relative Energy $\Delta G°$:	0	+ 5.3 kcal/mol

The Boat and Chair geometries for these transition structures are well defined.

The FMO Analysis (Fleming page 101)

Bring two allyl radicals together to access for a possible bonding interaction between termini.

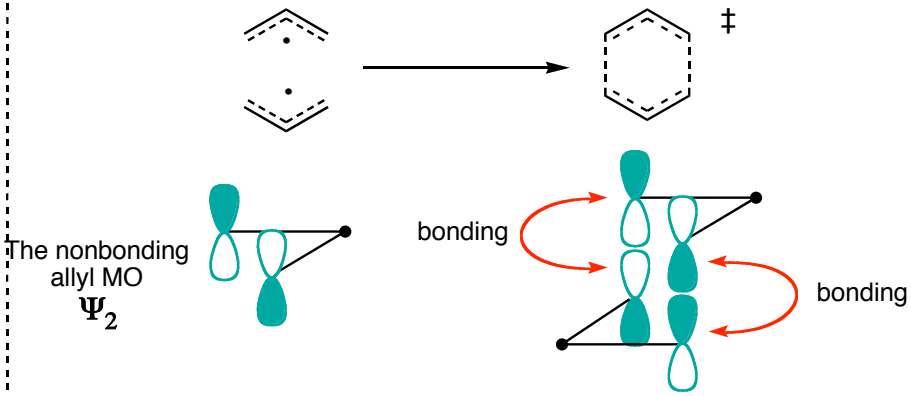

It is evident that synchronous bonding is possible in this rearrangement

Doering/Roth Experiments: *Tetrahedron* 18, 67, (1962):

The Geometry of the transltion state (boat vs chair) can be analyzed via the rearrangement of substituted 1,5-dienes:

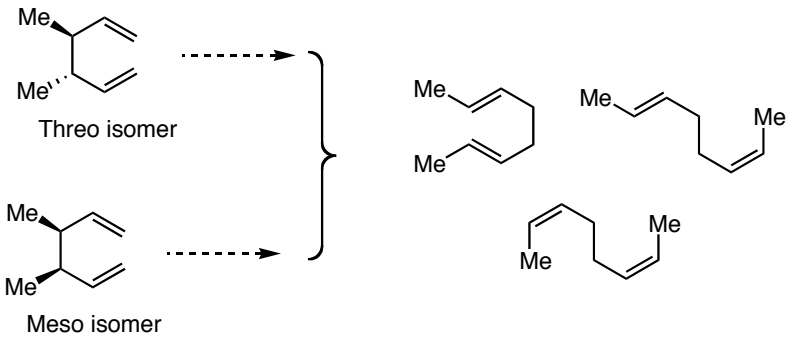

■ Measure product composition from rearrangement of each diene isomer

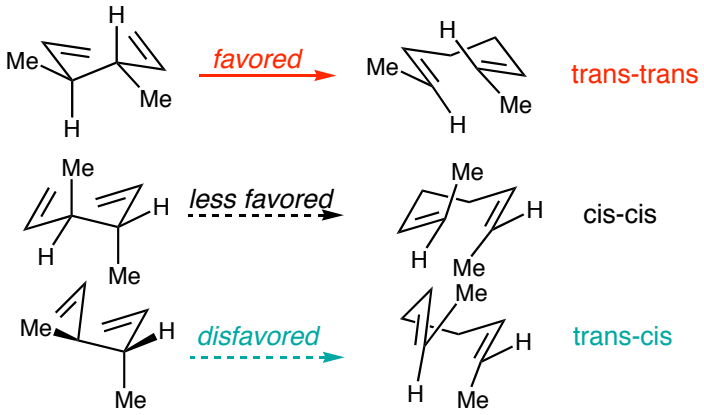

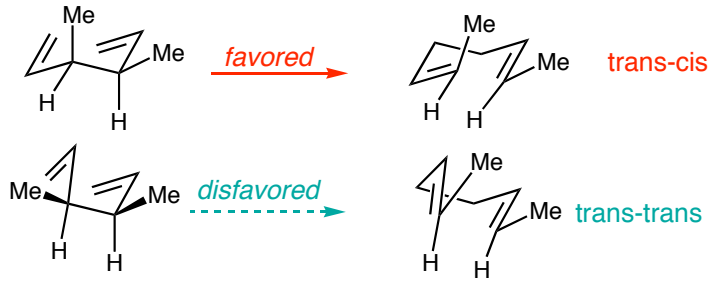

The Results

Results:
***Threo* isomer**

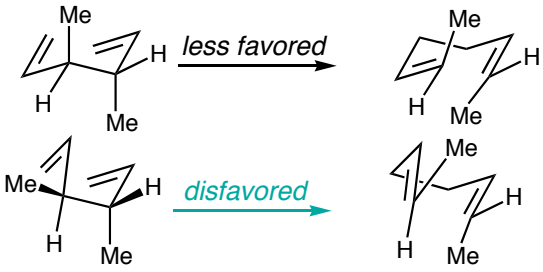

Results:
***Meso* isomer**

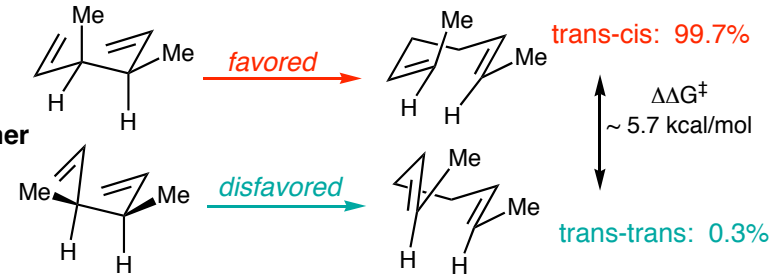

The CopeTransition States

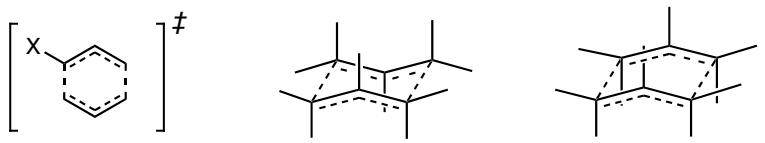

	CHAIR	*BOAT*
Relative Energy ΔΔG‡:	0	+ 5.8 kcal/mol

	CHAIR	*BOAT*
Relative Energy ΔG°:	0	+ 5.3 kcal/mol

The Boat and Chair geometries for these transition structures are well defined.

Ring Strain can be employed to drive the Cope process:

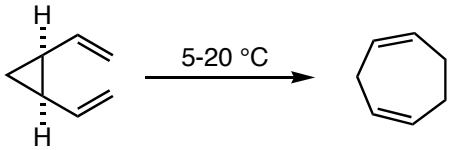

Brown *Chem. Commun.* **1973**, 319

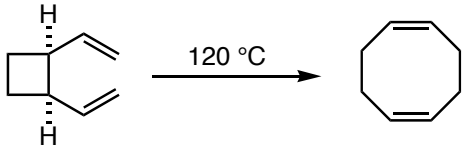

Vogel *Annalen* **1958**, *615*, 1

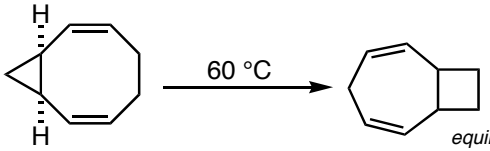

Reese *Chem. Commun.* **1970**, 1519

equilibrium stongly favors this isomer

Ring Strain can be employed to drive the Cope process:

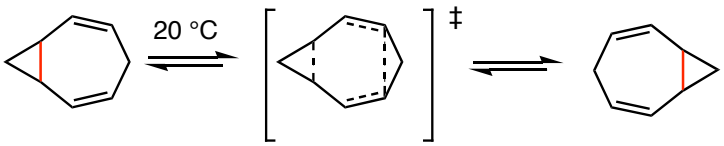

W. von E. Doering's Bullvalene

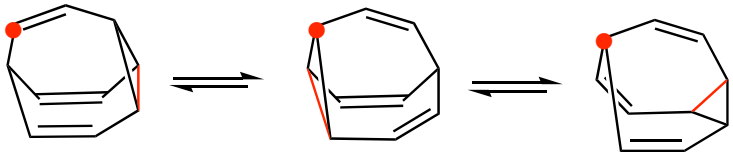

Bullvalene: Ea = 13.9 kcal/mol

At 100 °C one carbon is observed in nmr spectrum

Carey, Vol 1, page 630–631

■ Ring extension via divinylcyclopropane rearrangement

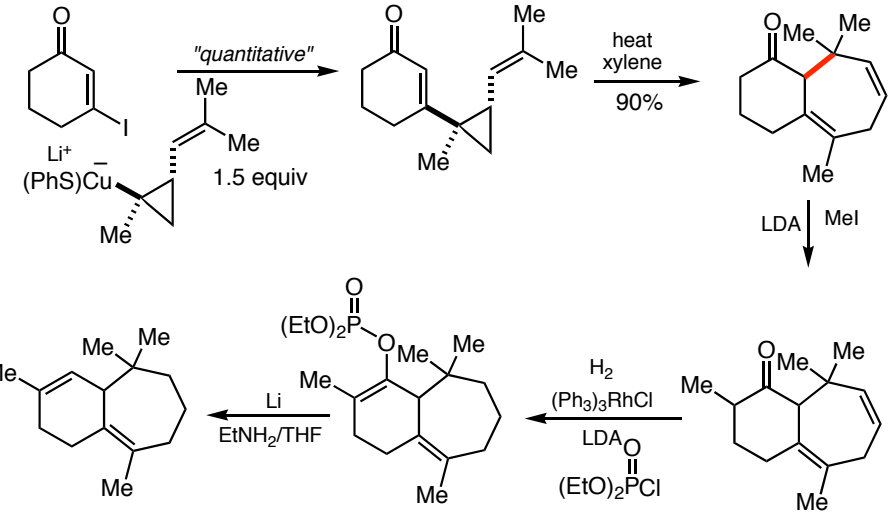

β-himachalene

Piers, *Can J. Chem.* **1983**, *61*, 1226, 1239

■ Position of Equilibrium dictated by ring strain issues:

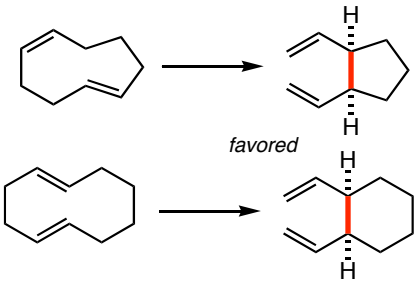

Vogel *Angew. Chem. Int. Ed.* **1963**, *2*, 739

Wharton *J. Org. Chem.* **1973**, *38*, 4117

■ However, tautomerism can shift the equilibrium:

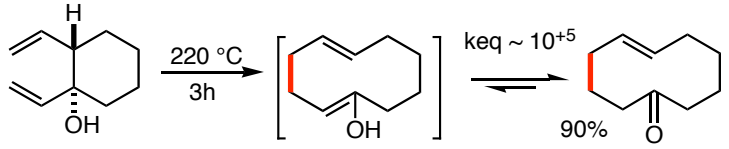

Marvell, *Tet. Lett.* **1970**, 509

Energetically, how much does tautomerization give you?

Accelerated Cope Rearrangements

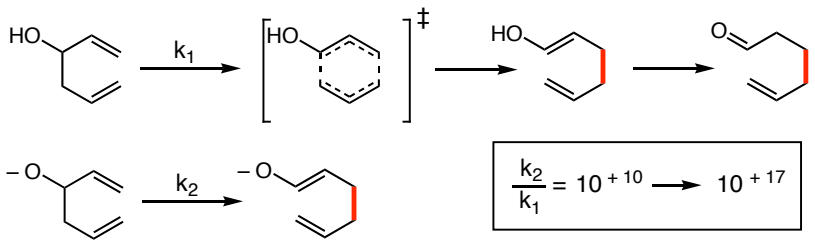

Evans, Golob, *JACS* **1975**, *97*, 4765.

Trost, Ed., *Comprehensive Organic Synthesis* **1992**, Vol 5, Chapter 7.1: (Cope, oxy-Cope, Anionic oxy-Cope)
"Recent applications of anionic oxy-Cope rearrangements."
Paquette, L. A. *Tetrahedron* **1997**, *53*, 13971-14020

A priori Estimate of the Acceleration (DAE)

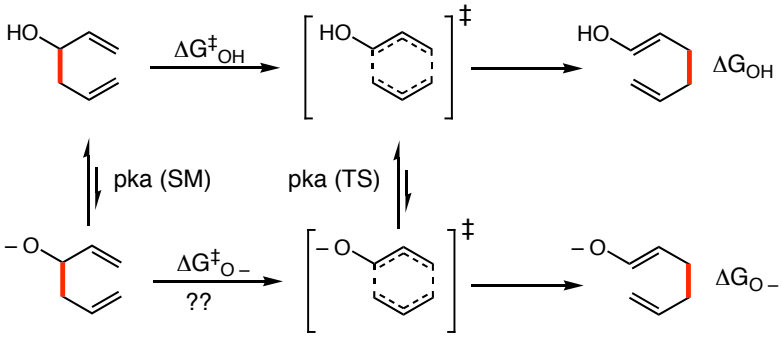

$$\Delta G^{\ddagger}_{O-} = \Delta G^{\ddagger}_{OH} + 2.3RT\,[\,pka_{TS} - pka_{SM}]$$

$\Delta G^{\ddagger}_{O-} = \Delta G^{\ddagger}_{OH} + 2.3RT\,[18 - 29]$ (in DMSO)

$\Delta G^{\ddagger}_{O-} = \Delta G^{\ddagger}_{OH} + 1.4\,[-11]$

$\Delta G^{\ddagger}_{O-} = \Delta G^{\ddagger}_{OH} - 15$ kcal/mol at 298 K (in DMSO)

Documentation of Alkoxy Substituent Effect

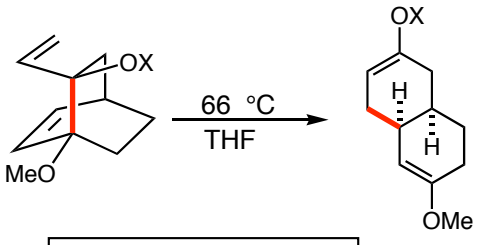

–OX	Half-life	
–OH	(66 yrs)	66 °C
–OLi	no rxn	
–ONa	1.2 hrs	
–OK	1.4 min	
–OK	11 hrs	10 °C
(HMPT) –O⁻ ⁺K	4.4 min	

10^{+12} rate acceleration

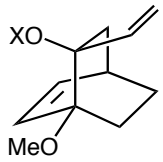

$\Delta\Delta G^{\ddagger}_{estimate} = 15$ kca mol $^{-1}$

$\Delta\Delta G^{\ddagger}_{experiment} = 13$ kca mol $^{-1}$

Origin of the Rate Effect

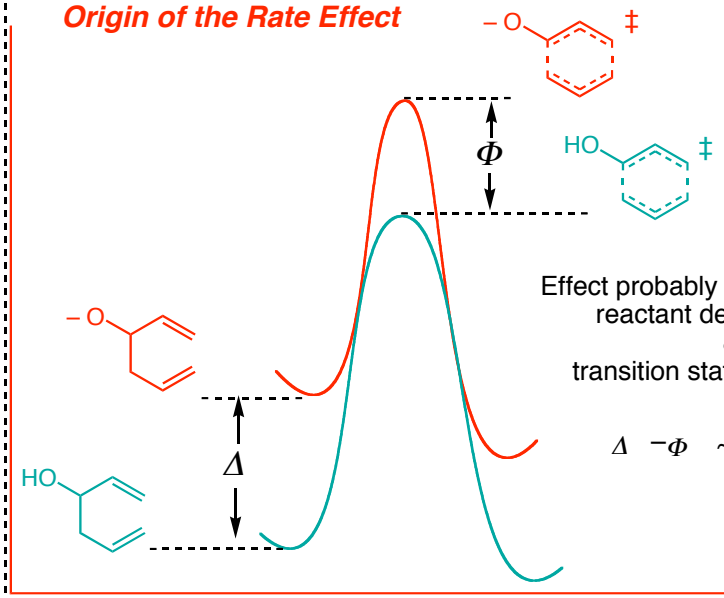

Effect probably comes from both reactant destabilization & transition state stabilization

$\Delta - \Phi \sim 15$ kcal/mol

Maximal rates are observed under conditions where reactant is maximally destabilized

Substituent Effects in Bond Homolysis

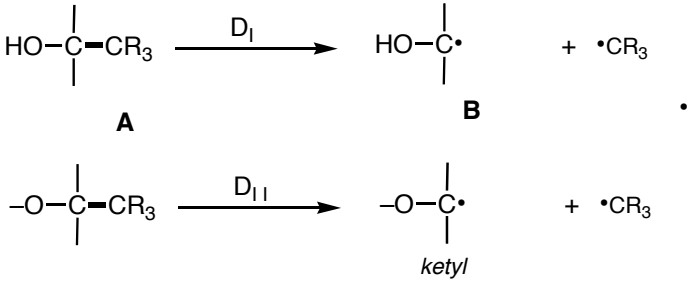

$$D_I - D_{II} = 2.3\ RT\ [pka\ (\mathbf{A}) - pka\ (\mathbf{B})]$$

Acidities of these radicals are known in H_2O, Hayon, *Accts. Chem. Res.* **1974**, *7*, 114

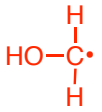

(H_2O) pKa = 10.7

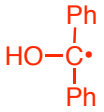

pKa = 9.2

In DMSO, $\Delta D = 2.3\ RT\ [29 - 18] \sim 15$ kcal/mol

■ Substituent Effect based on ab initio calculations

(Evans, Goddard, *JACS* **1979**, *101*, 1994)

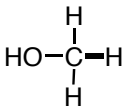

BDE = 90.7
(BDE = 91.8 expt)

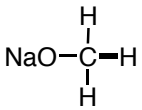

BDE = 80.6

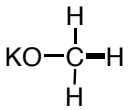

BDE = 79.0

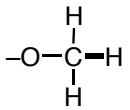

BDE = 74.2

ΔD
+16.5 kcal/mol

Substituent Effects in Molecular Rearrangements

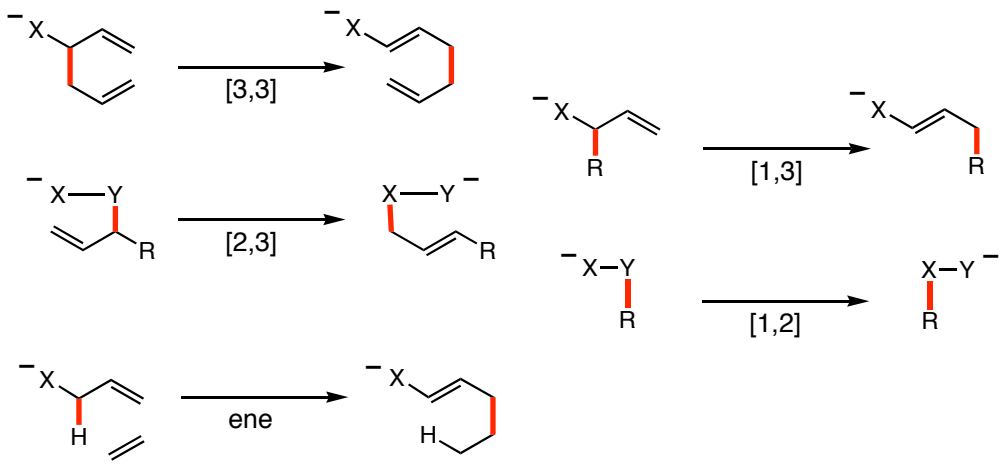

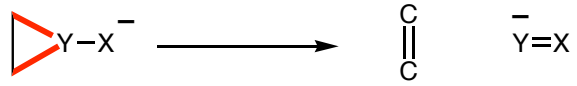

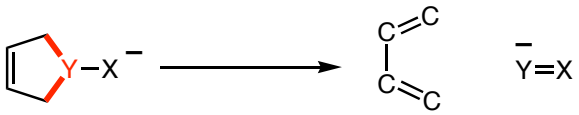

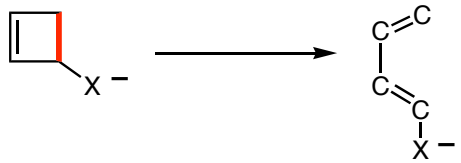

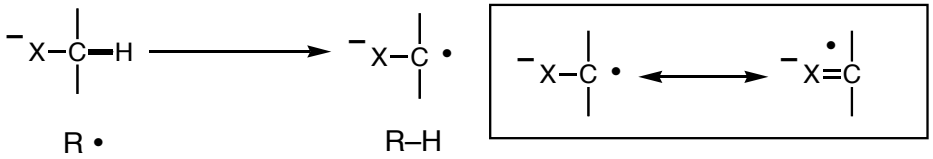

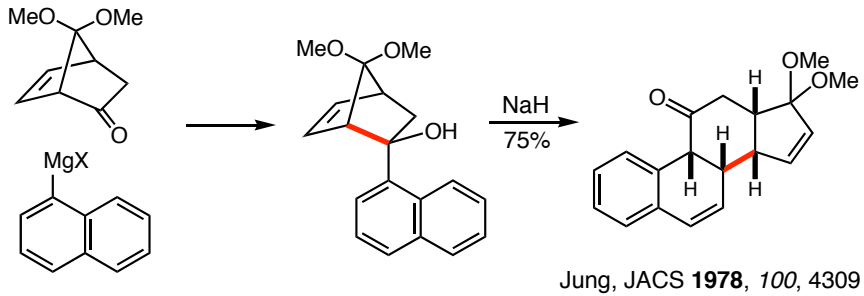

Jung, JACS **1978**, *100*, 4309
Jung, JACS **1980**, *102*, 2463

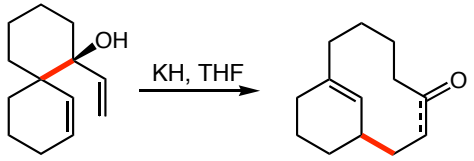

Levine, JOC **1981**, *46*, 2199

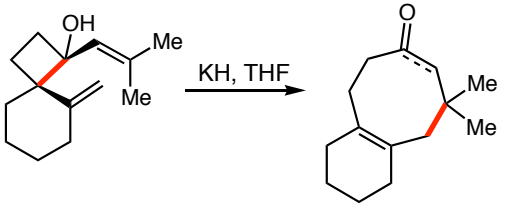

Gadwood, *JOC*, **1982**, *47*, 2268

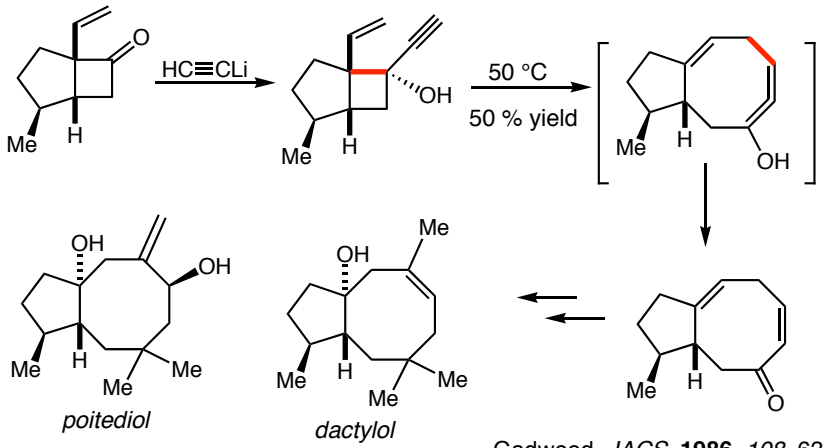

poitediol

dactylol

Gadwood, *JACS*, **1986**, *108*, 6343

Periplanone-B Synthesis

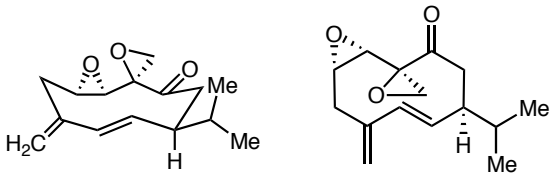

200 μg from 75,000 virgin female cockroaches

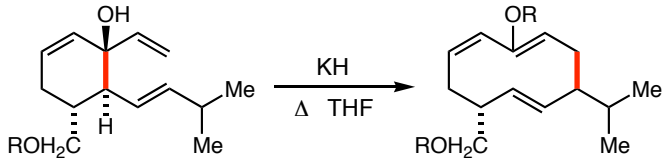

Still, *JACS* **1979**, *101*, 2493

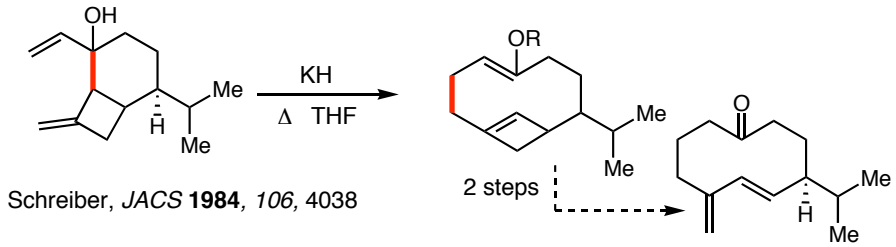

Schreiber, *JACS* **1984**, *106*, 4038

Synthesis of (+)-CP-263,114: Shair, *JACS* **2000**, *122*, 7424-7425.

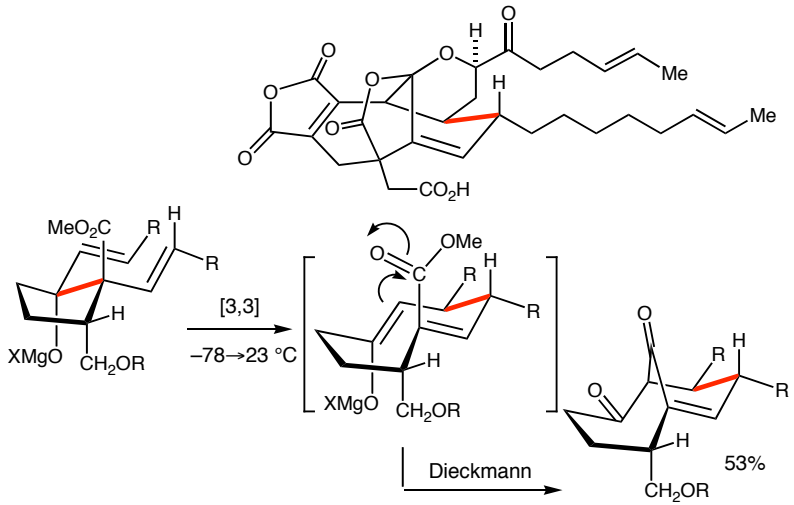

General Reviews:

S. J. Rhoades, *Organic Reactions* **1974**, *22*, 1 (Cope, Claisen)
Trost, Ed., *Comprehensive Organic Synthesis* **1992**, Vol 5, Ch 7.2
Ziegler, *Accts. Chem. Res.* **1977**, *10*, 227 (Claisen)
Bennett, *Synthesis* **1977**, 589 (Claisen)
Blechert, *Synthesis* **1989**, 71 (HeteroCope)
R. K. Hill, *Asymmetric Synthesis* vol 3, Ch 8, p503 (chirality transfer)
Ziegler, *Chem Rev.* **1989**, *89*, 1423 (Claisen)

The Reaction:

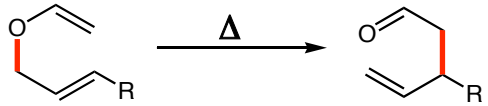

There is good thermodynamic driving force for this reaction.
Bonds Broken: C-C_π (65 kcal mol^{-1}) & C-O_σ (85 kcal mol^{-1})
Bonds Made: C-O_π (85 kcal mol^{-1}) and C-C_σ (85 kcal mol-$^{-1}$)

Themodynamics of Claisen Variants:

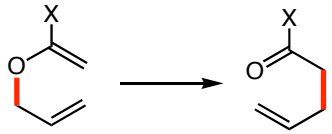

Substituent	ΔH (kcal mol^{-1})
X = H	–16
X = OH	–31
X = NH_2	–30

(Benson estimates)

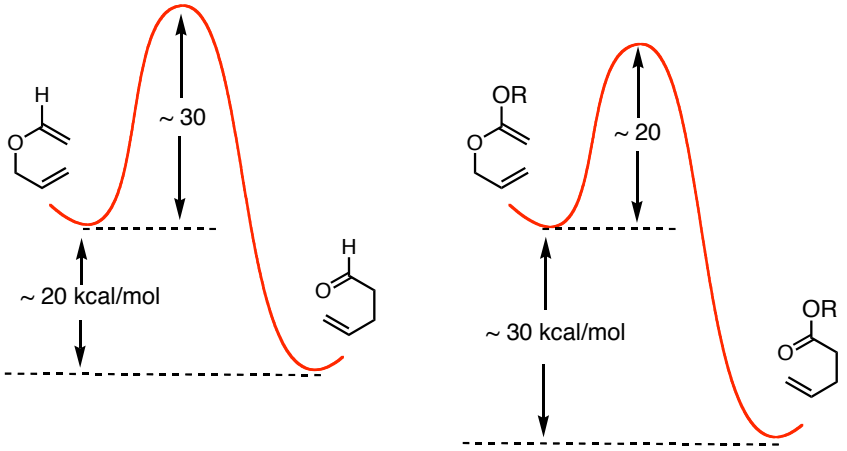

Heteroatom substitution at the indicated position increases exothermicity as well as reaction rate

Recognition Pattern for Organic Synthesis: An Enforced SN2'

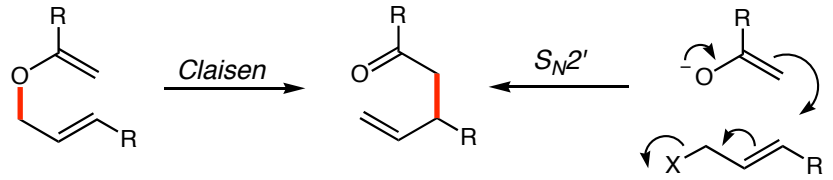

Stereochemical outcome is syn and controlled by hydroxyl stereocenter

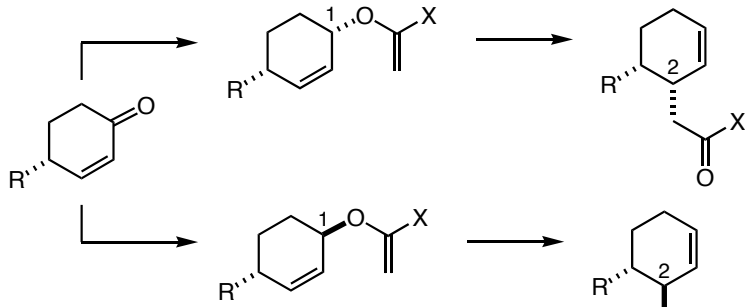

Control of stereocenter 2 evolves into a decision how to establish the hydroxyl-bearing stereocenter

Rearrangements of Aryl Allyl Ethers: Traditional Applications

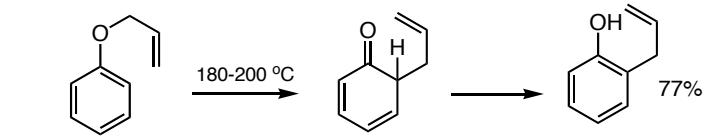

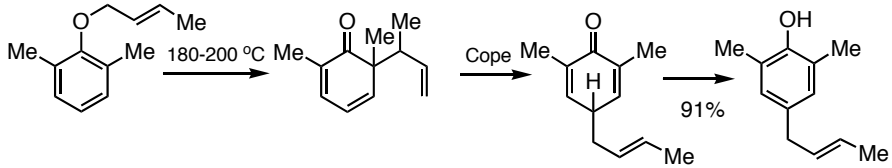

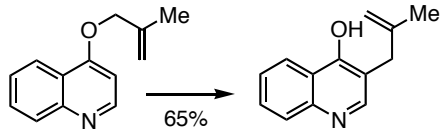

■ Endocyclic Olefins: Ireland, *JOC* 1983, *48*, 1829

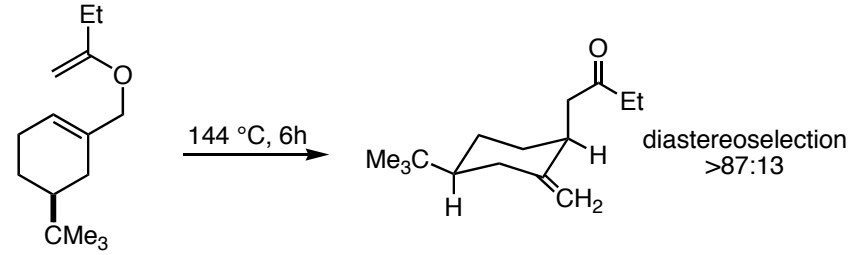

For endocyclic olefins, overlap between developing sigma and pi bonds required. Best overlap for forming chair geometry. As shown below, bring a radical up to either face of the allylic radical. As the bond is formed, overlap must be maintained. **Path A** evolves into a **chair** conformation while **Path B** evolved into a **boat** conformation.

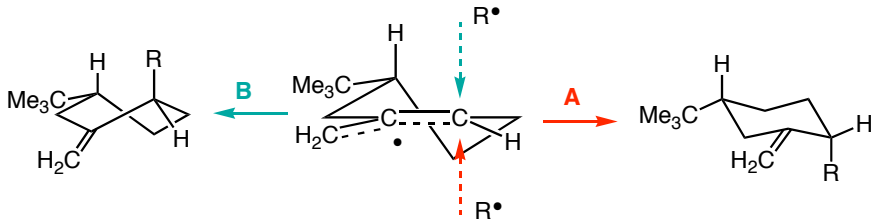

■ Exocyclic Olefins: House, *JOC* 1975, *40*, 86

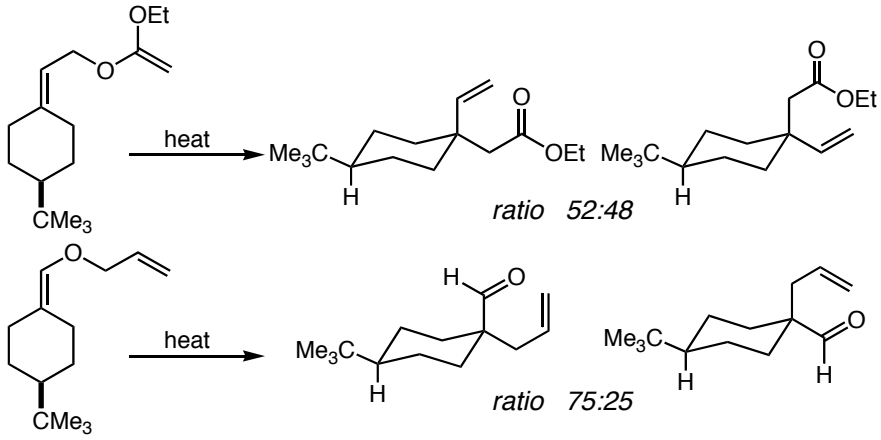

for exoocyclic olefins, overlap between developing sigma and pi bonds is equally good from either olefin diastereoface. In this instance, steric effects dominate & this system shows a modest preference for "equatorial attack." A related case is provided below.

Synthesis of Allyl Vinyl Ethers

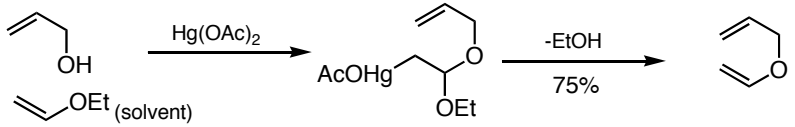

Watanabe, Conlon, *JACS* **1957**, *79*, 2828
Bronsted acids can also serve as catalysts

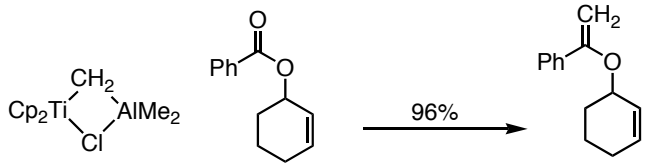

Use of Tebbe's Reagent: Evans, Grubbs, *J. Am. Chem. Soc.* **1980**, *102*, 3272.
(review) S. H. Pines, *Organic Reactions* **1993**, *43*, 1

The Ireland approach to the bicyclic acid A: *JOC* 1962, *27*, 1118

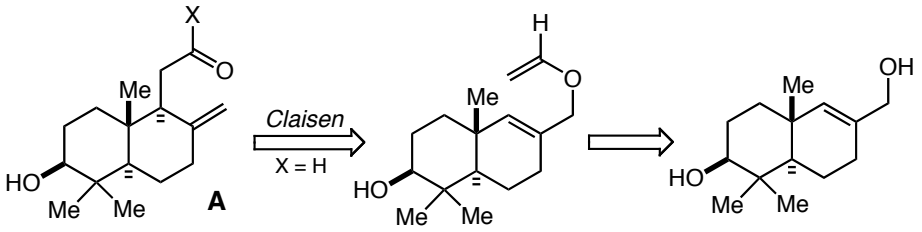

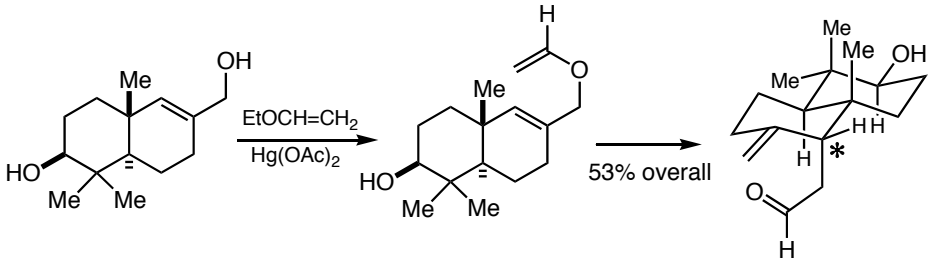

The new stereocenter (⁎) introduced via the rearrangement had the wrong configuration!

Claisen Rearrangement as vehicle for stereoselective olefin synthesis

Consider the following rearrangement:

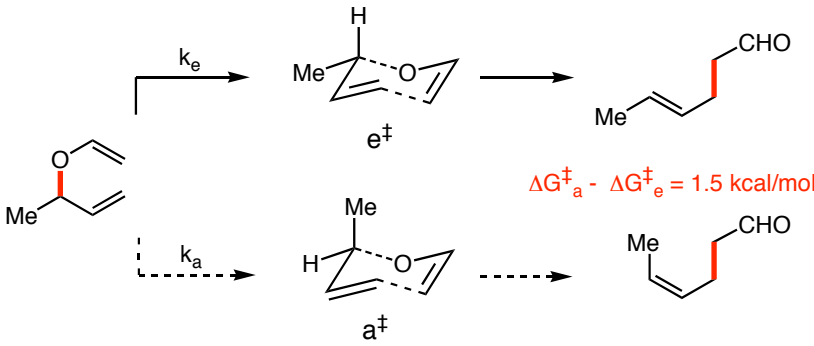

Faulkner & Perrin (Tet. Lett. 2783 (**1969**) have made the correlation between $\Delta\Delta G^{\ddagger}$ for rearrangement & ΔG° for the corrresponding cyclohexane# equilibria:

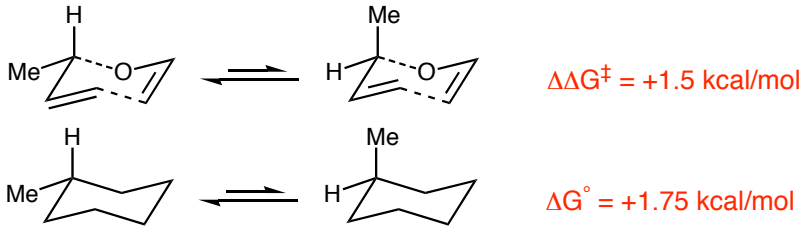

#Note: The A-value of 2-methyl-tetrahydropyran is +2.86 kcal/mol (Lecture No. 6)

They then suggest that there is a good correlation between cyclohexane "A-values" & $\Delta\Delta G^{\ddagger}$ for the rearrangement process. Their case is fortified by the following expamples:

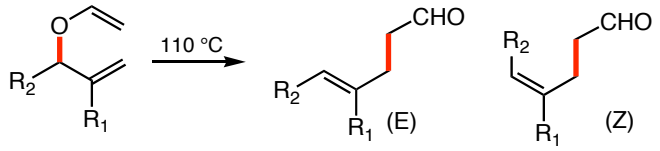

R_1	R_2	(E):(Z) found	(E):(Z) predicted
Me–	Et–	90:10	91:9
Me–	iPr–	93:07	94:6
Et–	Et–	90:10	91:9

Faulkner, *JACS* **1973**, *95*, 553

Faulkner suggests that the installation of other substituents on Claisen transition states will lead to enhanced reaction diastereoselection:

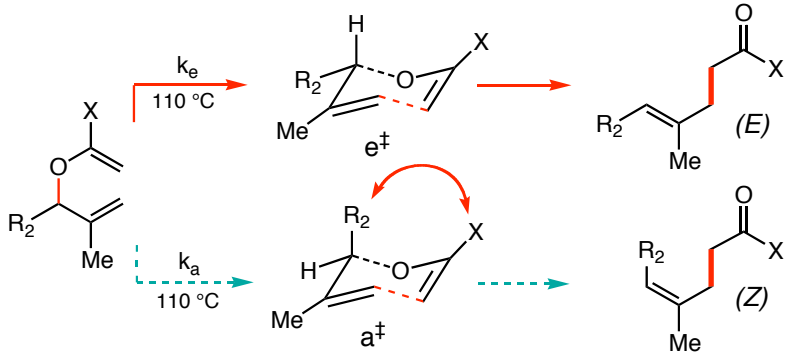

The $R_2 \leftrightarrow X$ interaction should destabilize a‡ as X gets progressively larger.

	X	(E):(Z) found
For R_2 = Et	H–	90:10
	Me–	>99:1
	MeO–	>99:1
	Me_2N–	>98:2

Faulkner, *Tet Let* **1969**, 3243
Faulkner, *JACS* **1973**, *95*, 553
Johnson, *JACS* **1970**, *92*, 741

■ Another comparison: (DAE) M. DiMare, Ph. D. Harvard University, 1988

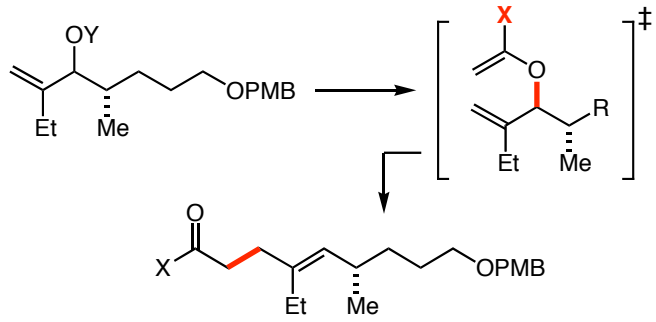

procedure	conditions	X	T, °C	(E):(Z) ratio
Y = Ac, Ireland	LDA, TMSCl	TMSO–	-78→+55	97:3
Y = H, Johnson	$HC(OMe)_3$, H^+	MeO–	130	94:6
Y = H, Eschenmoser	$MeC(OMe)_2NMe_2$	Me_2N–	80	97.5:2.5

Catalyzed Olefin Isomerization Leading to Highly Stereoselective Claisen Rearrangements of Aliphatic Allyl Vinyl Ethers

Scott G. Nelson,* Christopher J. Bungard, and Kan Wang

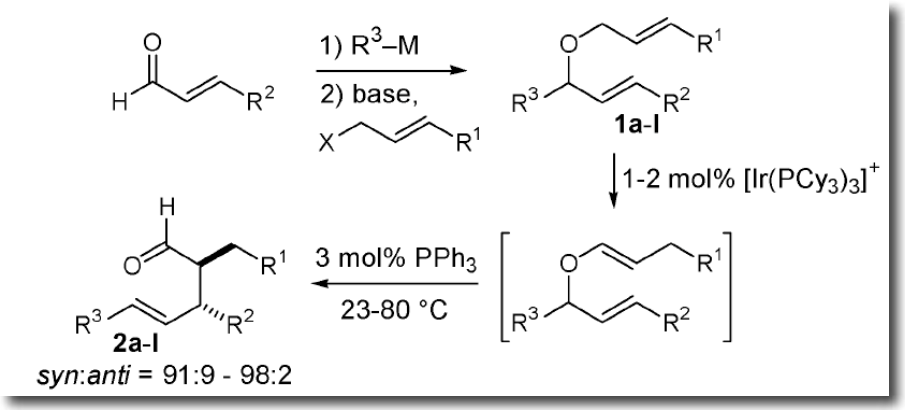

13000 ■ J. AM. CHEM. SOC. 2003, *125*, 13000−13001

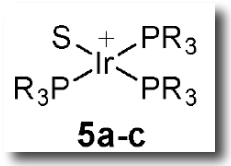

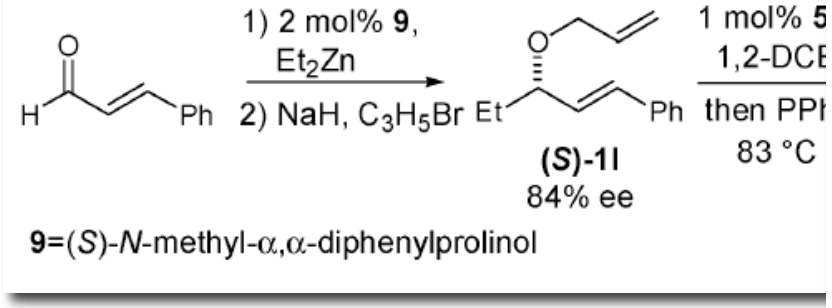

Table 1. ICR Reactions of Substituted Bis(allyl) Ethers **1** (Figure 1)

entry	bis(allyl) ether **1**[a]	syn:anti[b]	% yield[c]
a	$R^1 = H$, $R^2 = CH_3$, $R^3 = Ph$ (**1a**)	94:6	80
b	$R^1 = H$, $R^2 = R^3 = Ph$ (**1b**)	98:2	92
c	$R^1 = H$, $R^2 = {}^i Pr$, $R^3 = Ph$ (**1c**)	95:5	93
d	$R^1 = H$, $R^2 = {}^n Pr$, $R^3 = Ph$ (**1d**)	97:3	70
e	$R^1 = CH_3$, $R^2 = R^3 = Ph$ (**1e**)	95:5	84
f	$R^1 = H$, $R^2 = CH_3$, $R^3 = CH_2SiMe_3$ (**1f**)	93:7	84
g	$R^1 = H$, $R^2 = Ph$, $R^3 = CH_2SiMe_3$ (**1g**)	96:4	93
h	$R^1 = H$, $R^2 = CH_3$, $R^3 = {}^t Bu$ (**1h**)	92:8	86
i	$R^1 = R^2 = CH_3$, $R^3 = {}^t Bu$ (**1i**)	93:7	62
j	$R^1 = H$, $R^2 = CH_3$, $R^3 = {}^n Bu$ (**1j**)	86:8[d]	85
k	$R^1 = H$, $R^2 = Ph$, $R^3 = {}^n Bu$ (**1k**)	96:4	62
l	$R^1 = H$, $R^2 = Ph$, $R^3 = CH_2CH_3$ (**1l**)	95:5	93

[a] Claisen rearrangement conducted at 23 °C (entries b,e), 39 °C (entries

http://www.courses.fas.harvard.edu/colgsas/1063

Chemistry 206

Advanced Organic Chemistry

Lecture Number 15

Pericyclic Reactions–5

■ Claisen Rearrangements & Variants

■ Reading Assignment for week:

Carey & Sundberg: **Part A**; Chapter 11
Concerted Pericyclic Reactions

Carey & Sundberg: **Part B**; Chapter 6
Cycloadditions, Unimolecular Rearrangements
Thermal Eliminations

Wipf, P. *Claisen Rearrangements.*; Trost, B. M. and Fleming, I., Ed.; Pergamon Press: Oxford, 1991; Vol. 5, pp 827. **(handout)**

D. A. Evans

Monday
October 23, 2006

■ Other Reading Material:

Enders, D.; Knopp, M.; Schiffers, R. "Asymmetric [3.3]-sigmatropic rearrangements in organic synthesis." *Tetrahedron: Asymmetry* **1996**, *7*, 1847-1882
Ziegler, F. E. "The Thermal Aliphatic Claisen Rearrangement." *Chem. Rev.* **1988**, *88*, 1423.
Gajewski, J. J. "The Claisen rearrangement. Response to solvents and substituents: The case for both hydrophobic and hydrogen bond acceleration in water and for a variable transition state." *Acc. Chem. Res.* **1997**, *30*, 219-225.
Tietze, L. F. "Domino reactions in organic synthesis." *Chem. Rev.* **1996**, *96*, 115-136.
Parsons, P. J.; Penkett, C. S.; Shell, A. J. "Tandem reactions in organic synthesis: Novel strategies for natural product elaboration and the development of new synthetic methodology." *Chem. Rev.* **1996**, *96*, 195-206.

■ Problems of the Day:

Propose a mechanism for this transformation

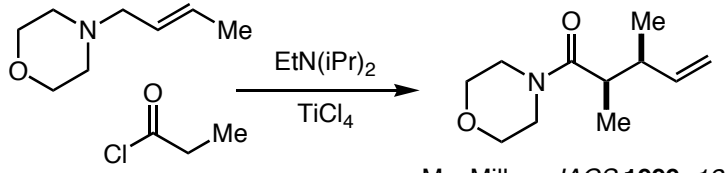

MacMillan, *JACS* **1999**, *121*, 9726

Problem 816. As part of a program directed toward the synthesis of the pinnatoxins, Pelc and Zakarian reported the single-pot conversion of sulfone **A** into cyclohexene **B** (*OL*, **2005**, *7*, 1629). Using clear three-dimensional representations please provide a concise mechanism for this transformation and predict the stereochemical outcome.

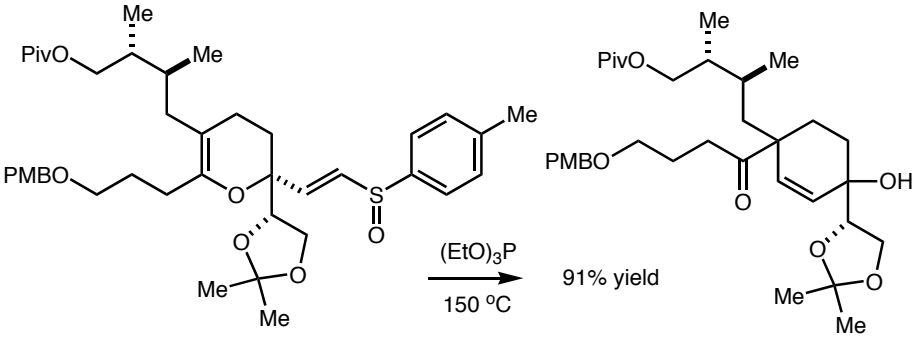

Propose a mechanism for this transformation

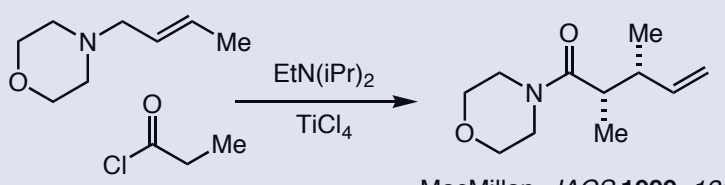

MacMillan, *JACS* **1999**, *121*, 9726

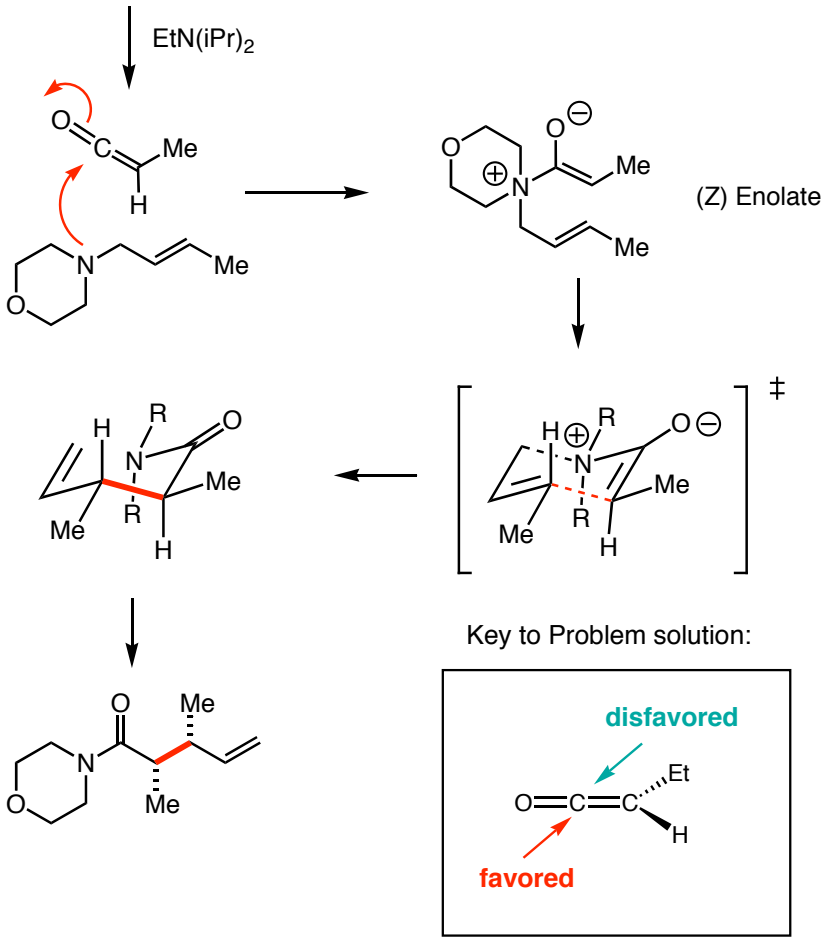

Problem 816. As part of a program directed toward the synthesis of the pinnatoxins, Pelc and Zakarian reported the single-pot conversion of sulfone **A** into cyclohexene **B** (*OL*, **2005**, *7*, 1629). Using clear three-dimensional representations please provide a concise mechanism for this transformation and predict the stereochemical outcome.

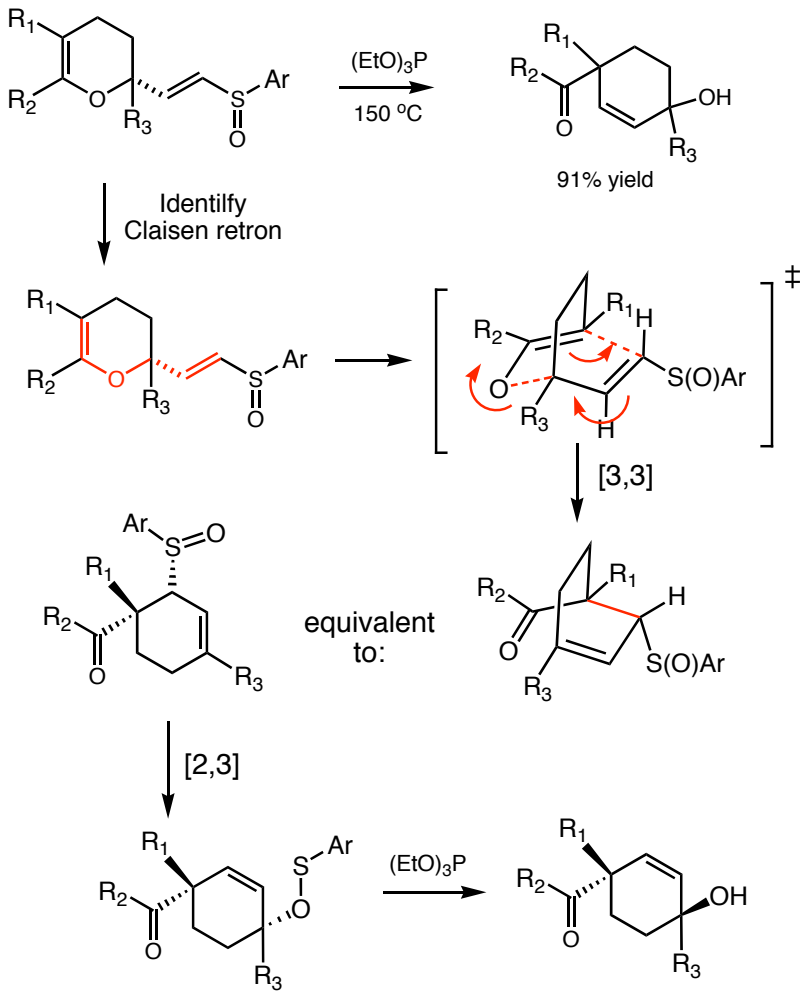

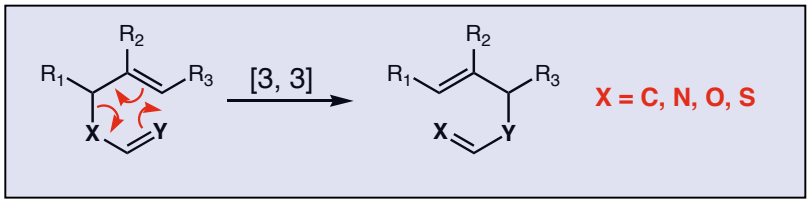

X = O; Y = N:

The Trichloroacetimidate Rearrangement, Overman, *JACS* **1974**, *96*, 597

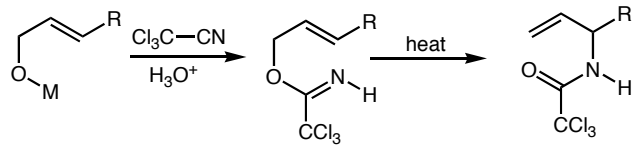

This reaction is also catalyzed by Hg(II) ion

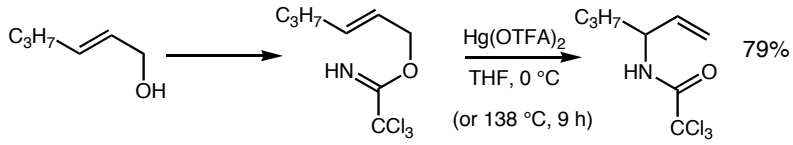

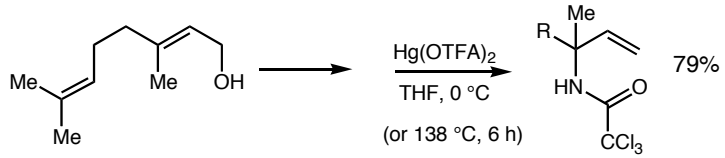

For an excellent review see: Overman, *Angew. Chem. Int. Ed.* **1984**, *23*, 579

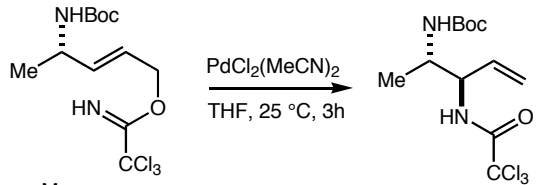

99% anti (45-62%)

Gonda, *Synthesis* **1993** 729

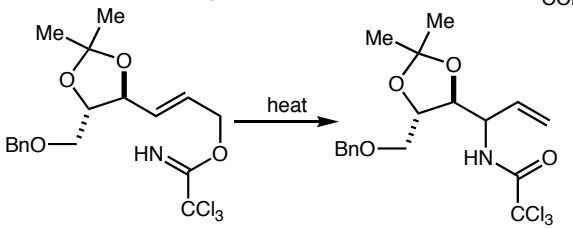

a 1:1 mixture was obtained

Saksena, *JOC* **1986** *51*, 5024

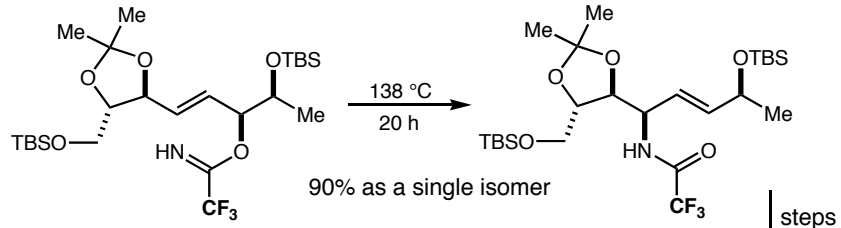

Thomas, *Chem. Commun* **1989** 717

steps

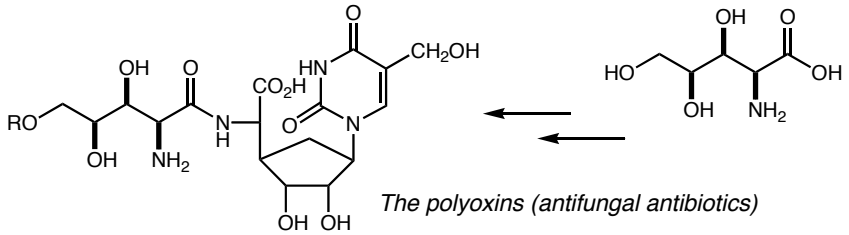

The polyoxins (antifungal antibiotics)

The "Burgess Reagent" is normally used for alcohol dehydration

however, rearrangement is obsteved with allylic alcohols

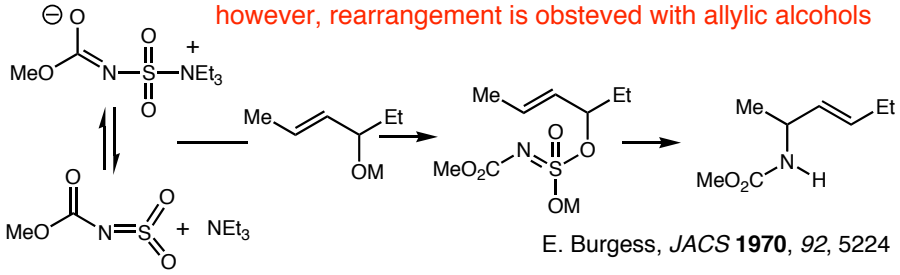

E. Burgess, *JACS* **1970**, *92*, 5224

A new approach to the synthesis of α-amino acids

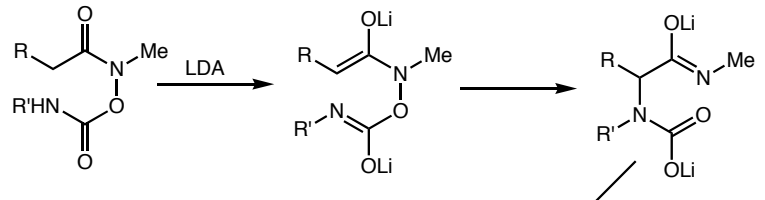

Endo, *SynLett* **1991** 649

This may not be a concerted process

moderate yields

Problem 108. The fumagillin natural products possess several interesting biological properties including antibiotic activity against *Staphylococcus auereus*. In Sorensen's recent synthesis of fumagillol (*Angew. Chem, Int. Ed.* **1999**, *38*, 971), intermediate **1** was transformed into its a-oxygenated counterpart **3** through the indicated reaction sequence.

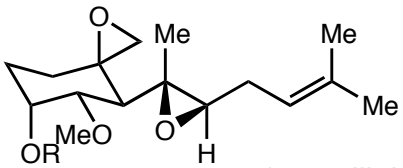

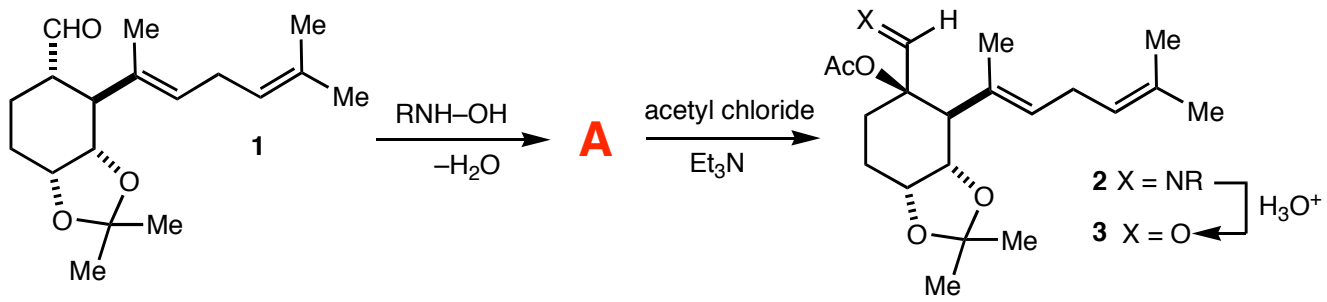

In the space below, identify the structure of intermediate **A** and provide a mechanism for the transformation of **1** into **2**.

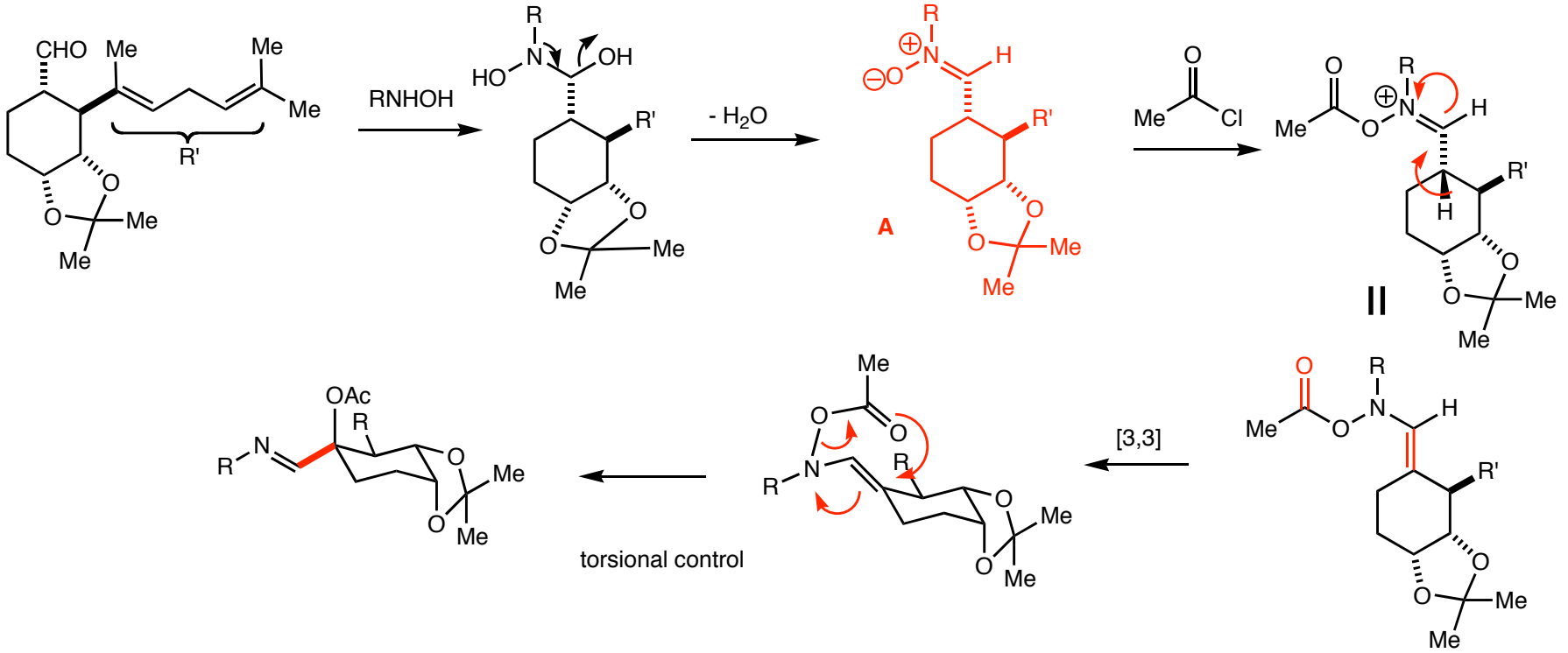

Johnson Orthoester Claisen

■ Lead paper: Johnson, Faulkner, Peterson, *JACS* **1970**, *92*, 741

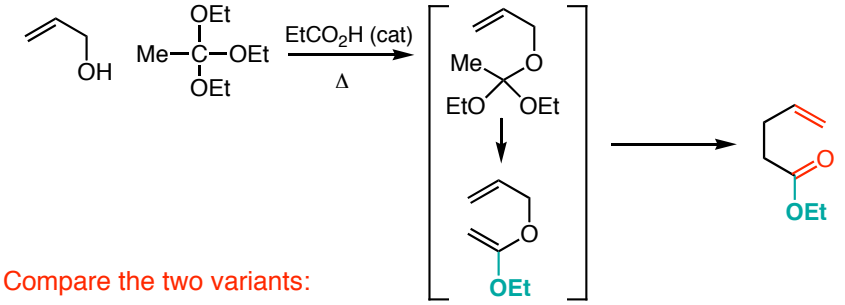

■ Compare the two variants:

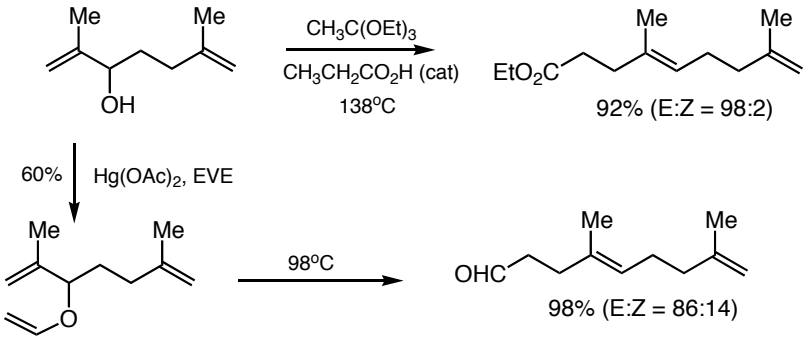

The Saucy Marbet Alternative

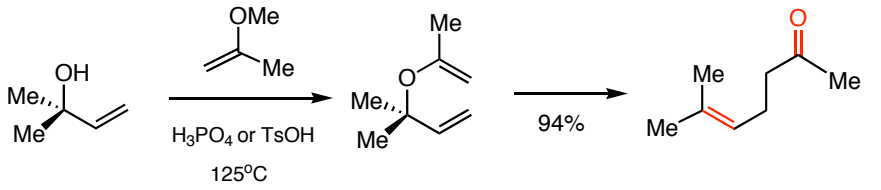

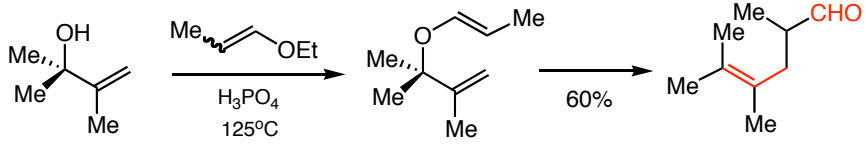

Saucy, Marbet, *Helv. Chim. Acta* **1967**, *50*, 2091,2095

Eschenmoser-Claisen

Eschenmoser, A. *Helv. Chem. Acta* **1964**, *47*, 2425; *Helv. Chim.Acta* **1969**, *52*, 1030.

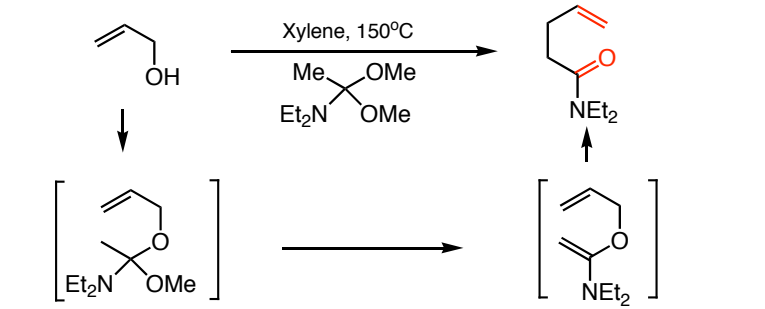

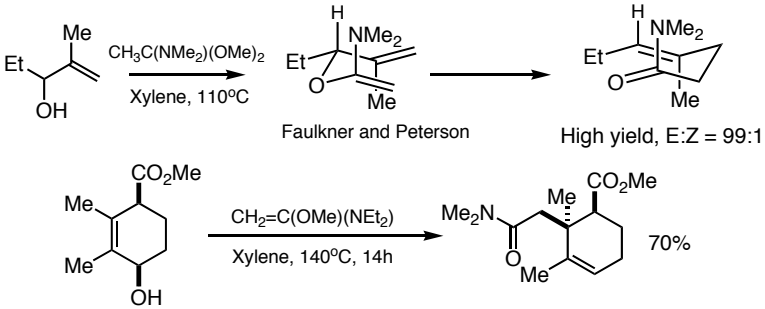

■ Synthesis of Amide Acetals

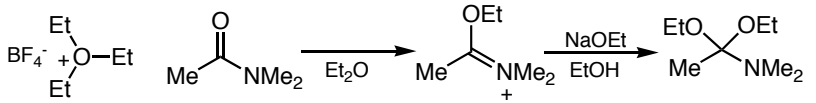

■ Reactions to ponder:

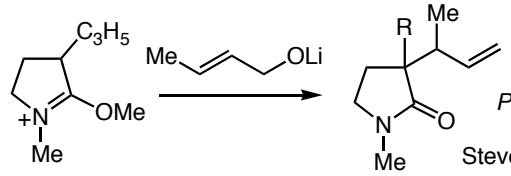

diastereoselection 6:1
Predict the major diastereomer

Stevenson, *Tet. Let.* **1991**, *32*, 4199

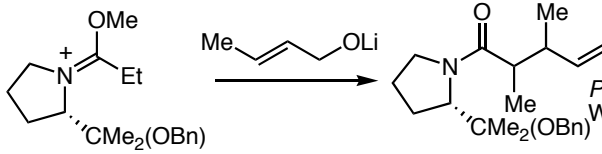

Predict the major diastereomer

Welch, *JACS* **1987**, *109*, 6716

The Johnson Squalene Synthesis: JACS 1970, 92, 741

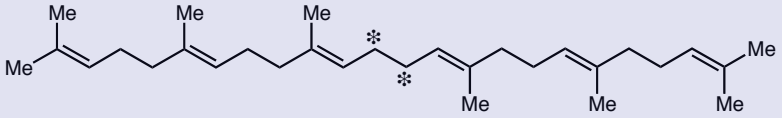

Observations: Molecule contains an obvious symmetry plane
The trisubstituted C=C's are the issue

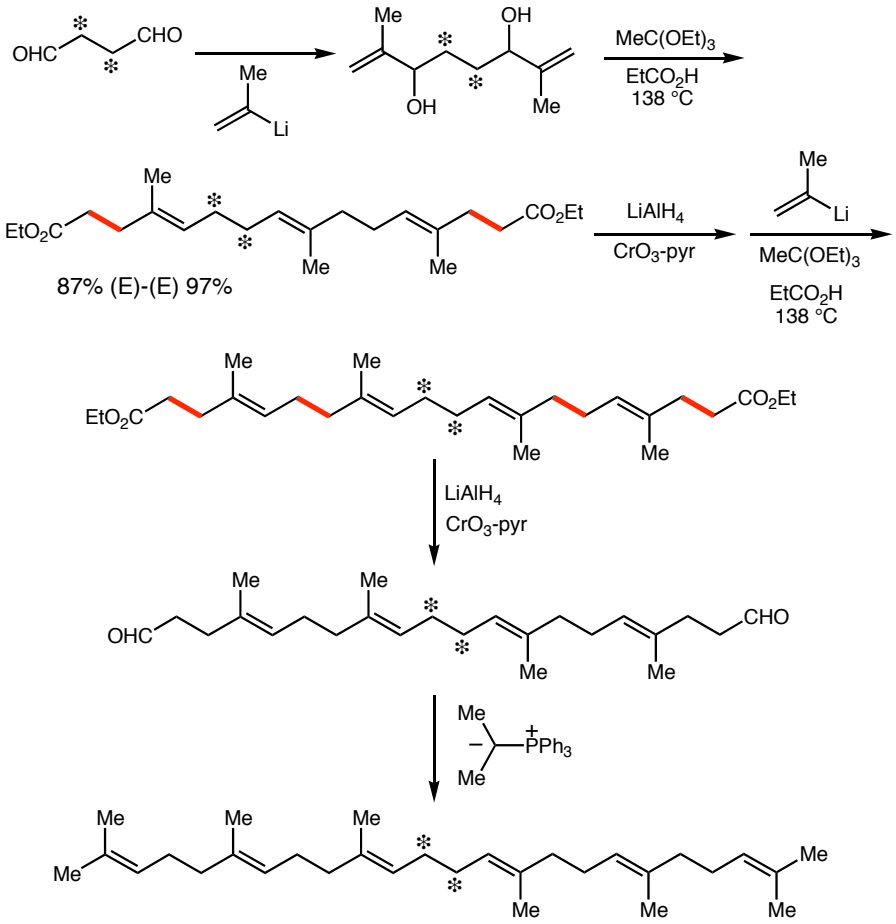

*The Faulkner Juvenile Hormone Synthesis: JACS **1973**, 95, 553*

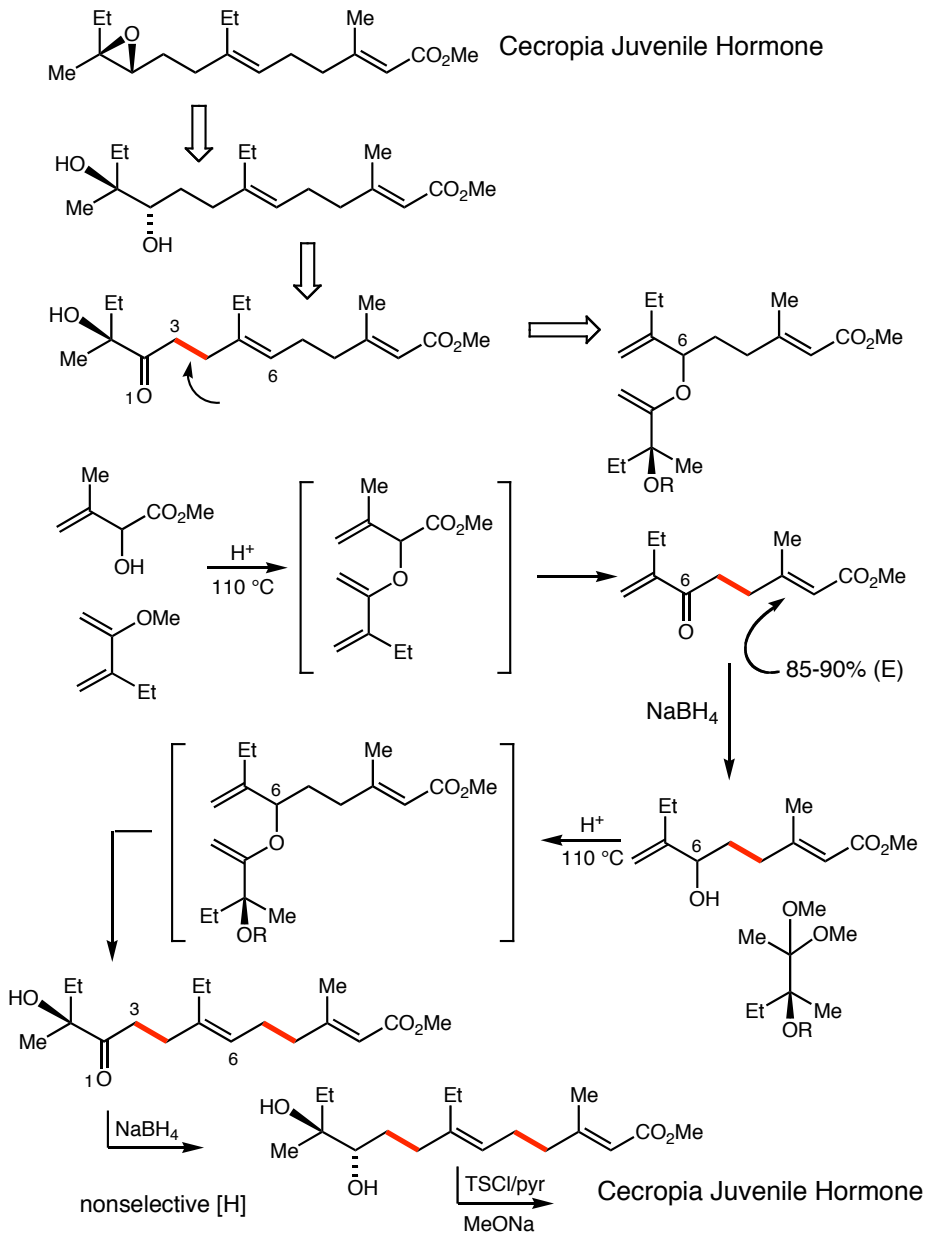

Chirality transfer via the Claisen rxn is an integral aspect of the general utility of process

R. K. Hill, *Asymmetric Synthesis* vol 3, Ch 8, p503 (chirality transfer)

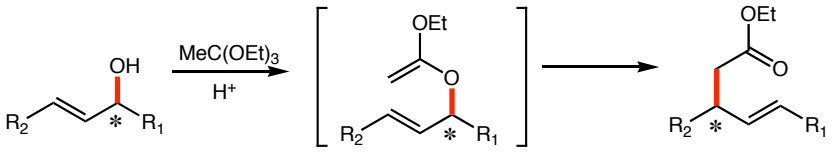

Such chirality permutation processes are only as stereoselective as the energy difference between diastereomeric chair transiltion states:

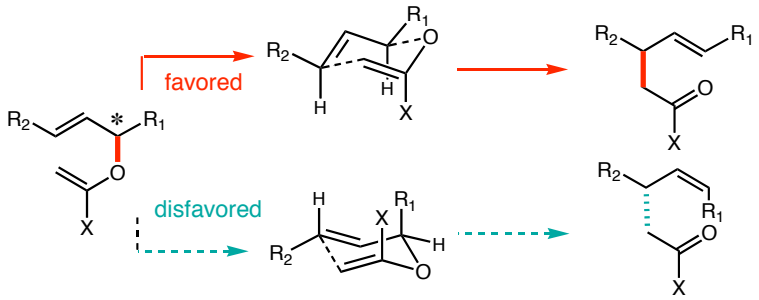

Note that chirality transfer is coupled to olefin geometry in product. Prior arguments (Faulkner) imply that the X substituent will play significant role in promoting selectivity.

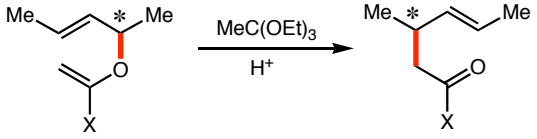

ee > 90%
(E)-selection > 90%

R. K. Hill
JOC **1972**, *37*, 3737

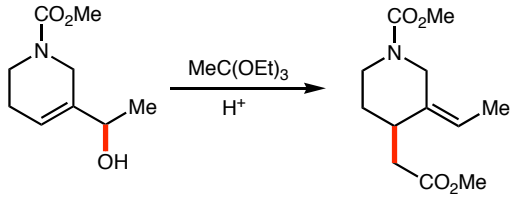

68% enantiomerically pure

Uskokovic,
JACS **1979**, *101*, 6742

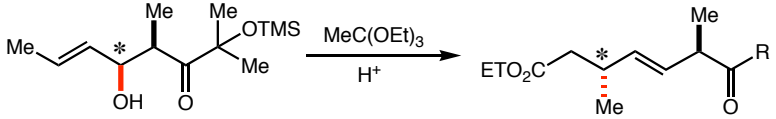

Heathcock
JOC **1988**, *53*, 1922

Sense of Asymmetric induction may be controlled by olefin geometry

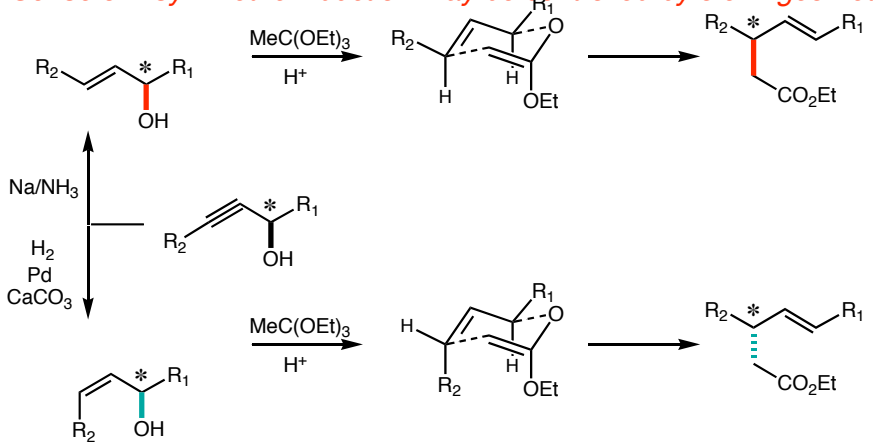

Since stereoselection in reduction of acetylenes is >98%, either product accessible tocopherol (Vitamin E) Cohen *JOC* **1976**, *41*, 3497

JACS **1979**, *101*, 6710

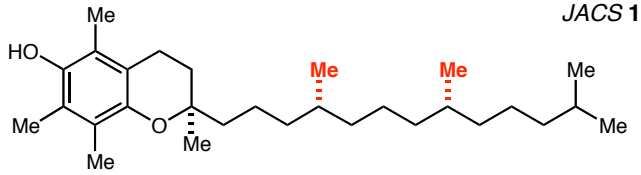

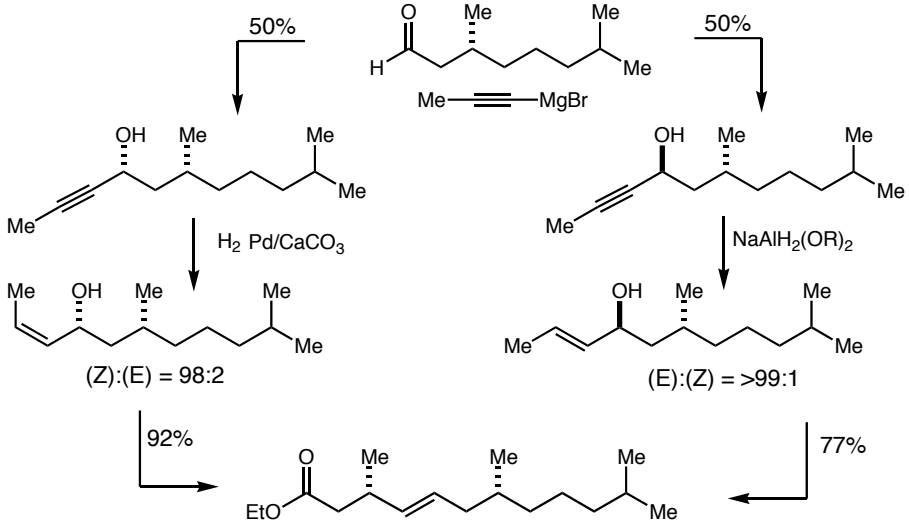

diastereoselection ~ 99% from both routes

Ireland-Enolate Claisen

Recent Review: *Tetrahedron* **2002,** *58,* 2905-2928

Ireland, R. E.; Mueller, R. H.; Willard, A. K. *J. Am. Chem. Soc.* **1976**, *98*, 2868

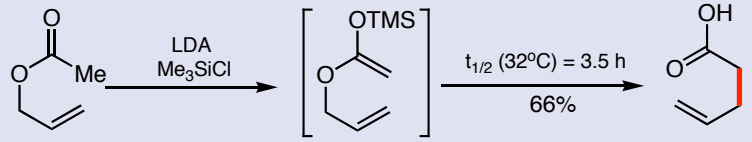

■ Enolization: Amide Bases

Stereoelectronic Requirements: The α-C-H bond must be able to overlap with π* C–O

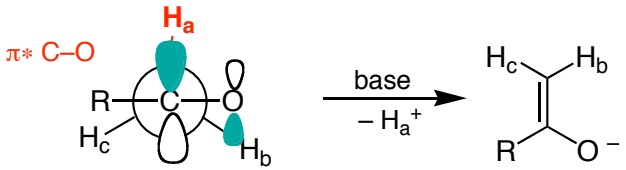

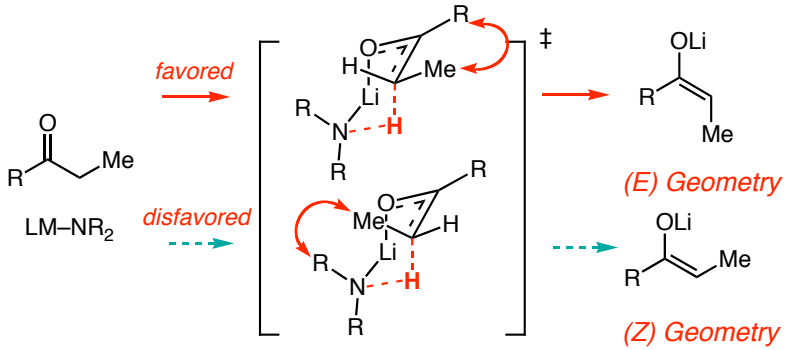

The Ireland Model (*JACS* **1976**, *98*, 2868)
Narula, Tetrahedron Lett. **1981**, *22*, 4119
more recent study: Ireland, *JOC* **1991**, *56*, 650

Substituted enolates afford an additional stereocenter

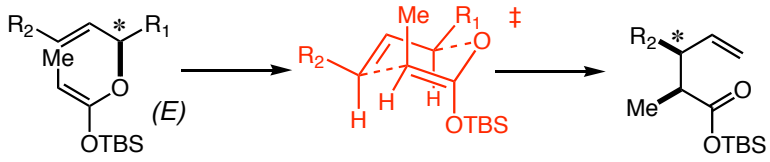

LDA, TBSCl
LDA, TBSCl DMPU

	conditions	(E):(Z)	control
Et, OEt	LDA, TBSCl	94:6	kinetic
	LDA, TBSCl DMPU	7:93	thermo

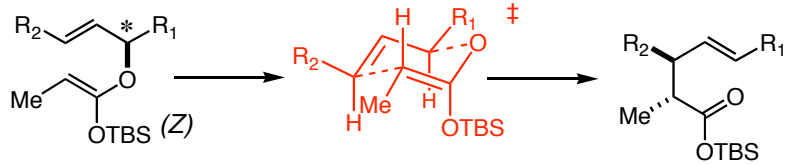

key study: Ireland, *JOC* **1991**, *56*, 650 and earlier cited papers

Double Claisen Rearrangements are also possible

Paterson, *Tet Lett* **1991**, *32*, 7601

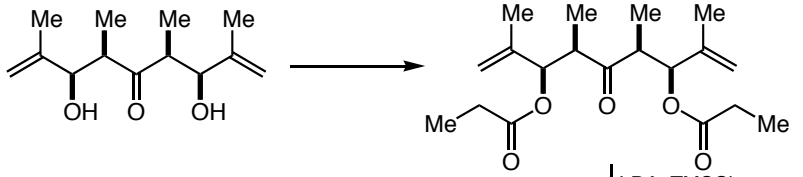

LDA, TMSCl
Et_3N

1,2 syn aldol relation permuted into
1,5 syn relationship via Claisen rearrangement

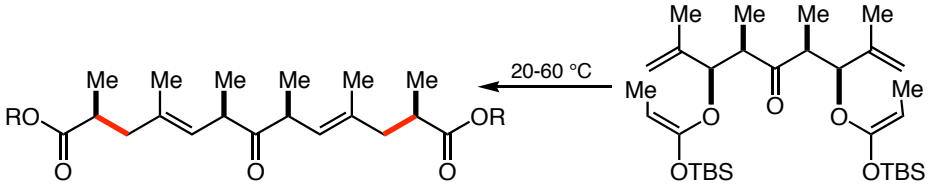

63% yield (diastereoselection 86%)

Consider the prostaglandin nucleus

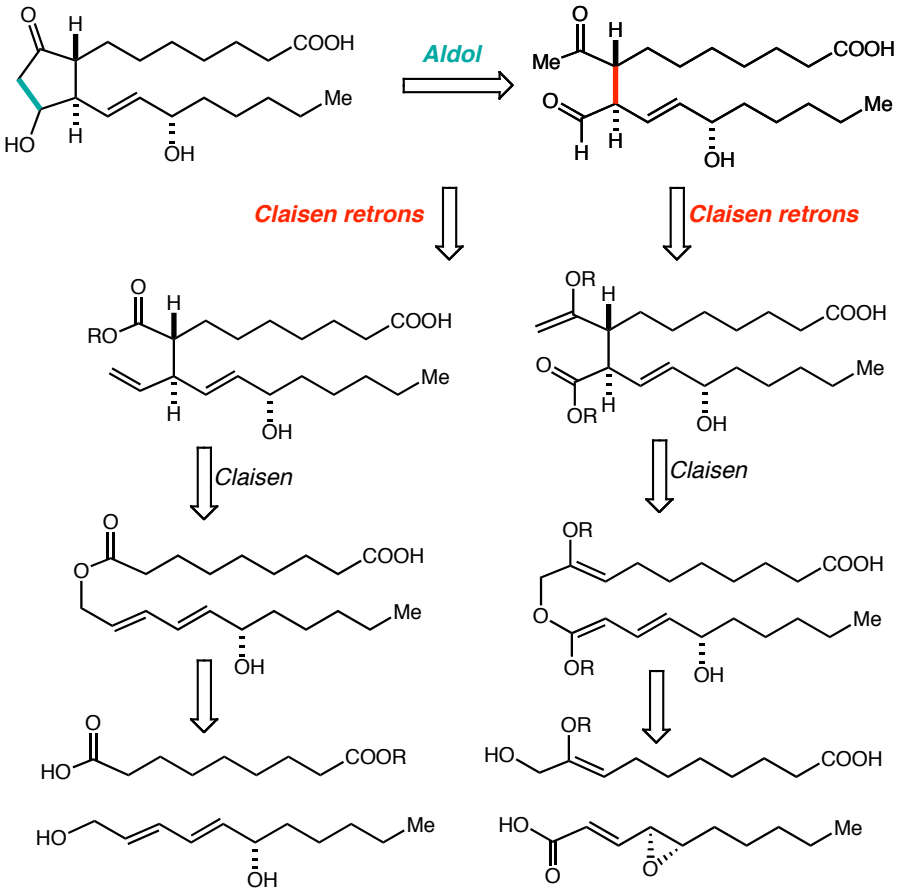

Unrealized plan to generate the required enolate

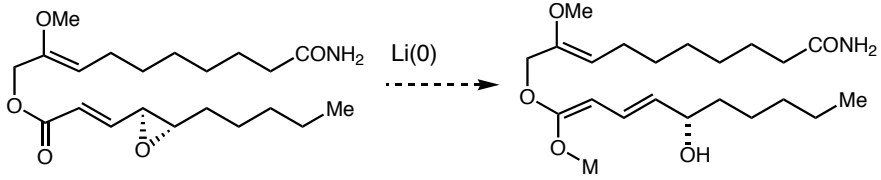

An Application PGA_1: Ireland *JOC* **1976**, *41*, 986; *Aldrichimica Acta* **1988**, *21*, 59

PP-A2 Synthesis, G. Stork, JACS **1976**, *98*, 1583

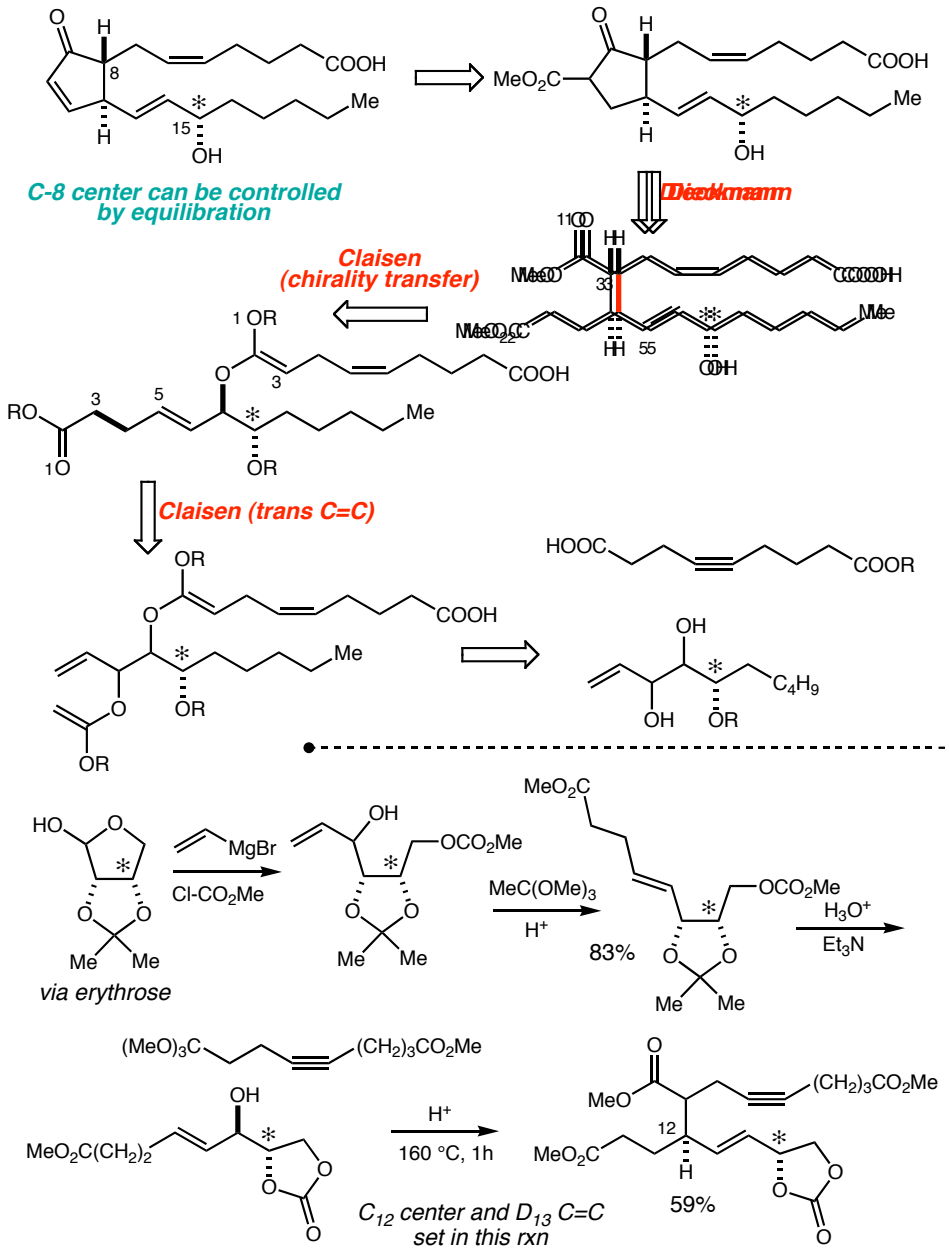

Boat transition states more accessible in Claisen than in Cope rearrangements

A case where the chair-boat preference depends on enol geometry

Factors controlling diastereoselection
Enolate geometry
Chair vs Boat transition states

Bartlett, *JOC* **1981**, *46*, 3896
Ireland, *JACS* **1991**, *56*, 3572

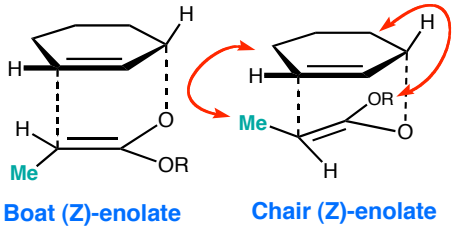

Ireland study supports Bartlett's conclusions

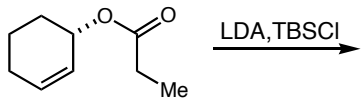

LDA,TBSCl

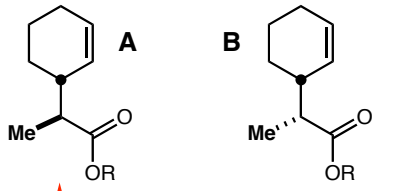

conditions	(E):(Z)	A:B	TS
LDA,THF	83:17	84:16	(E)-chair
LDA,THF DMPU	04:96	72:28	(Z)-boat

Boat geometies can be favored in these and related systems

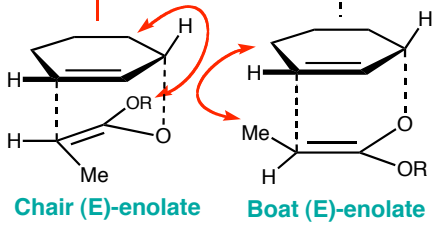

In this case the boat geometry is preferred from either enol geometry

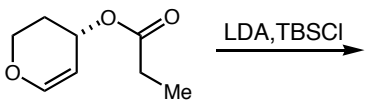

LDA,TBSCl

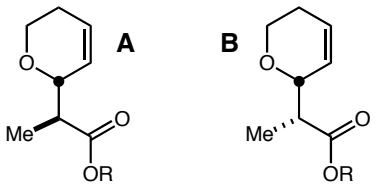

conditions	A:B	TS
LDA,THF	29:71	(E)-boat
LDA,THF DMPU	86:14	(Z)-boat

The analysis:

Ireland, *JACS* **1991**, *56*, 3572

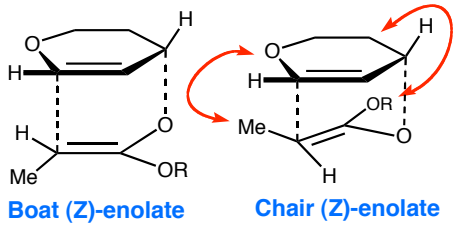

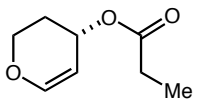

LDA,TBSCl

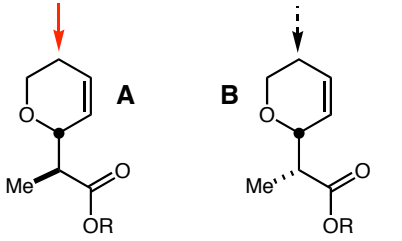

conditions	A:B	TS
LDA,THF	29:71	(E)-boat
LDA,THF DMPU	86:14	(Z)-boat

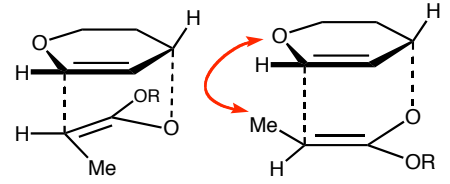

A further example:

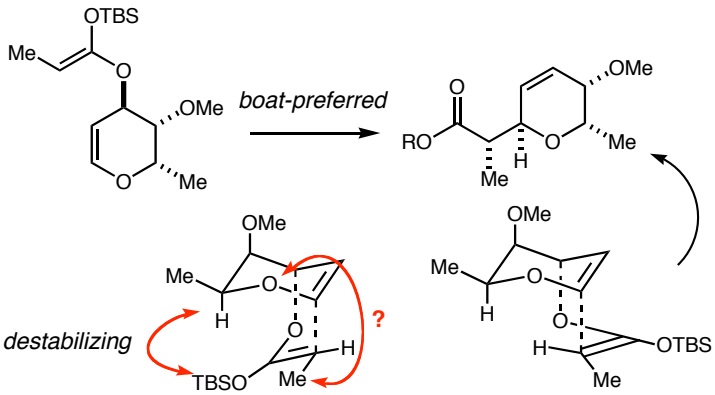

It appears that both of the indicated interactions contribute to the destabilization of chair geometry

Ireland lasalocid synthesis: JACS **1983**, *105,* 1988

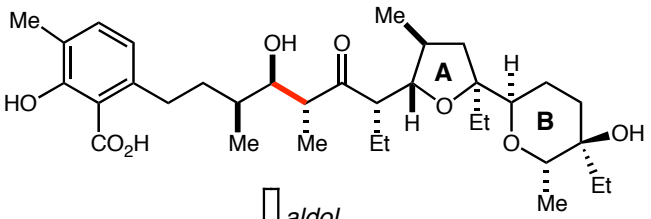

aldol

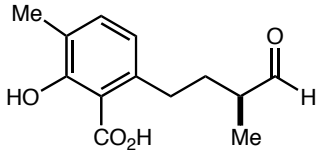

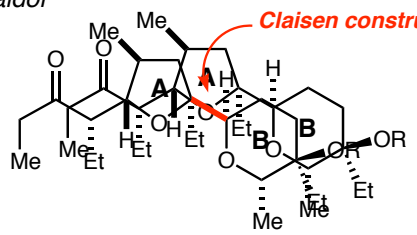

Note that neither retron for Claisen exists in this intermediate

add Claisen retrons

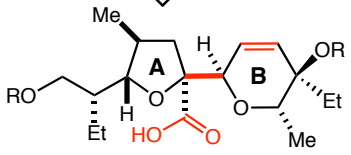

Claisen

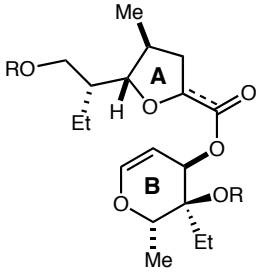

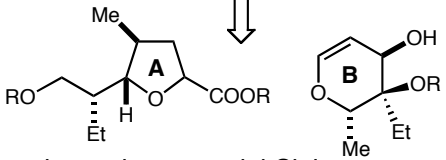

enolate face selectivity is anticipated problem. This results in CO_2H epimers

Here is another potential Claisen construction

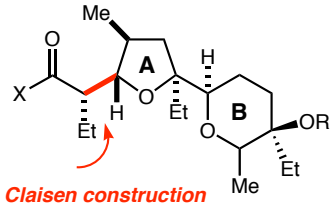

Methyl-bearing stereocenter to be established by selective reduction

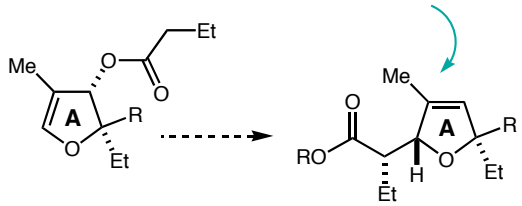

The relevant rearrangements:

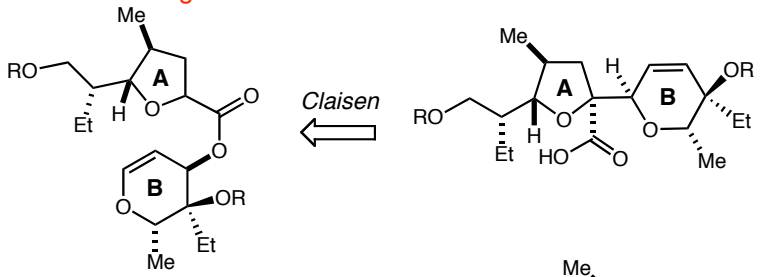

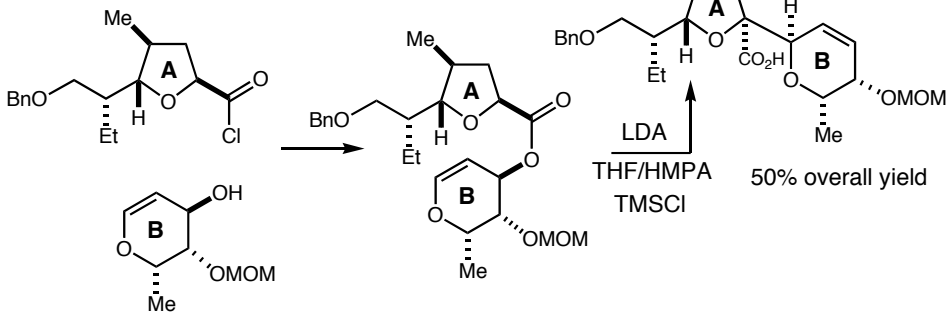

The Ireland monensin synthesis:

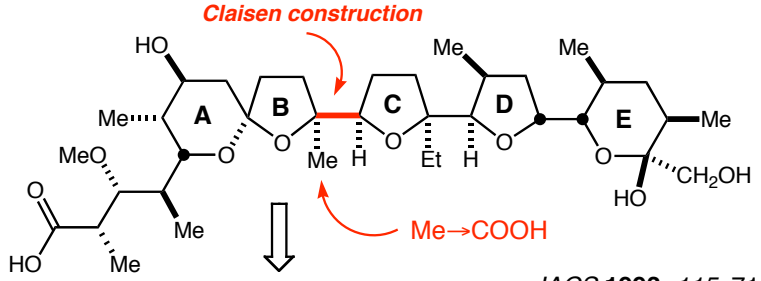

JACS **1993**, *115,* 7152-65

JACS **1993**, *115,* 7166-72
(and previously cited papers)

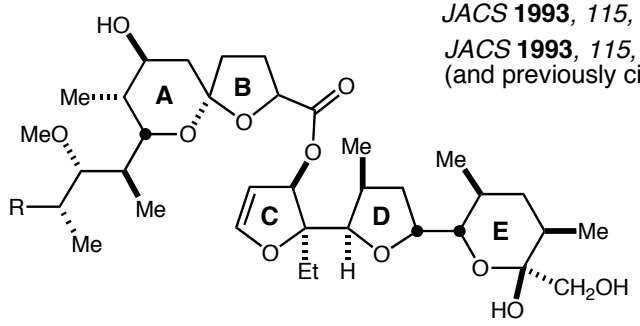

Ireland Claisen Rearrangements: Cyclic Enolates

The previous cases were derived from a connection between R_2 &R_3

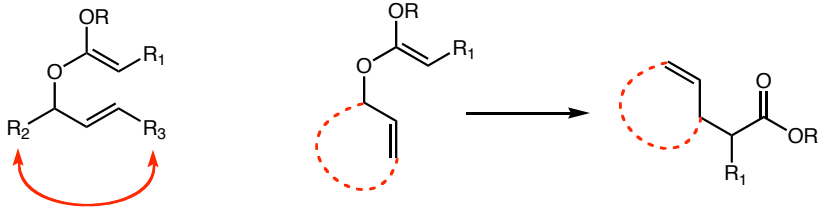

Consider consequence of connecting R_1 &R_2

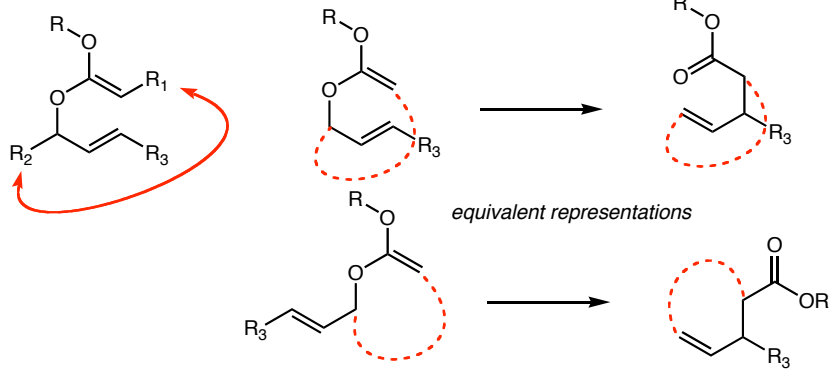

Examples:

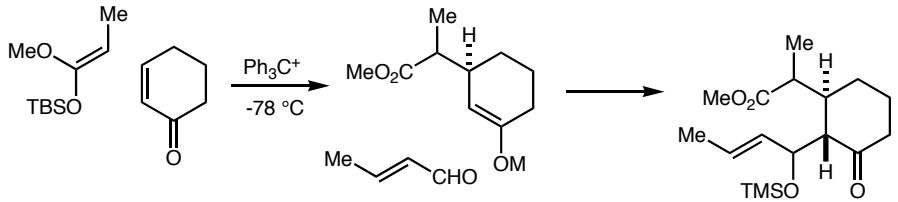

Danishefsky, *Tet. Let 29*, 1371 (1988)

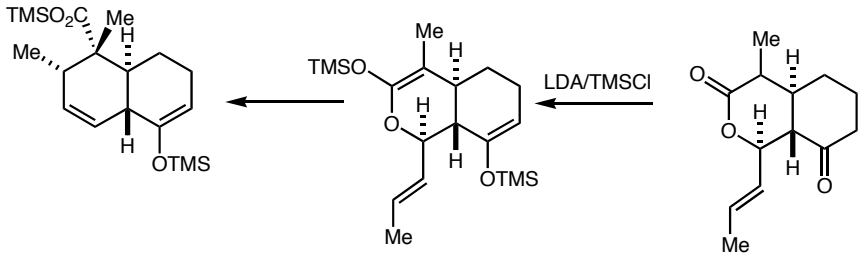

see also Danishefsky, *JACS* **1980**, *102*, 6889, 6891

The Indanomycin Synthesis,
Burke, Tet. Lett. ***1985****, 26, 1163; ibid,* ***1986****, 27, 6295*

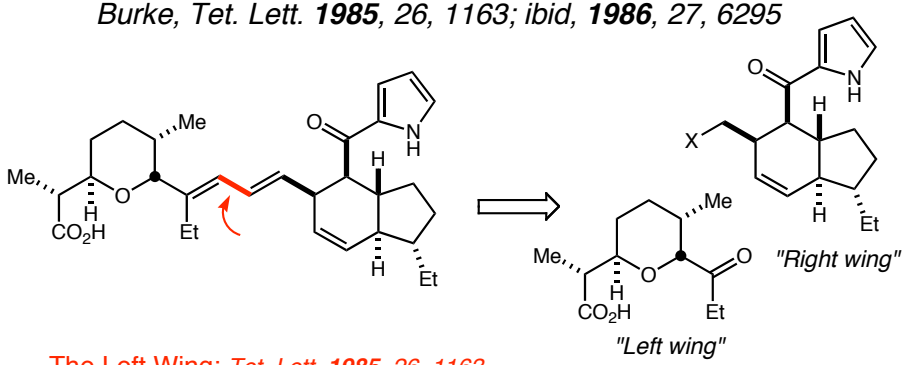

The Left Wing: *Tet. Lett.* ***1985****, 26, 1163*

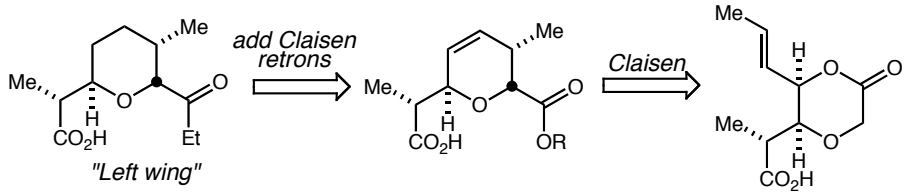

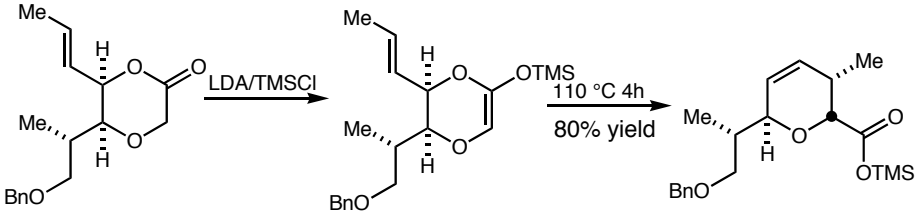

The Right Wing: *Tet. Lett.* ***1986****, 27, 6295*

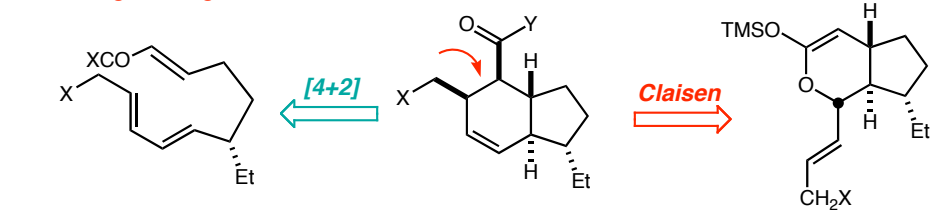

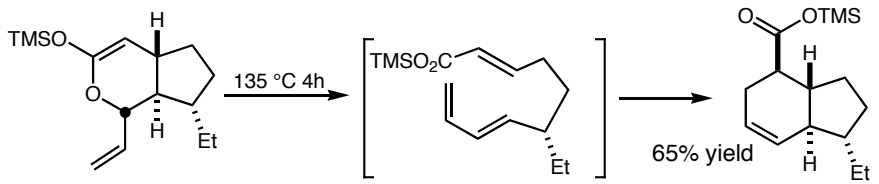

The "apparent" Claisen process is more complicated than anticipated.

Ireland Claisen Rearrangements: Cyclic Enolates

The FK 506 application

Schreiber Synthesis *JACS* **1990**, *112*, 5583

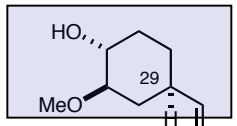

FK 506

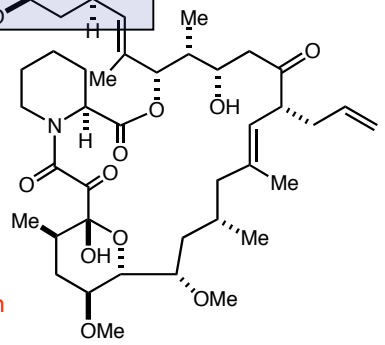

The Schreiber Route:

Claisen disconnection

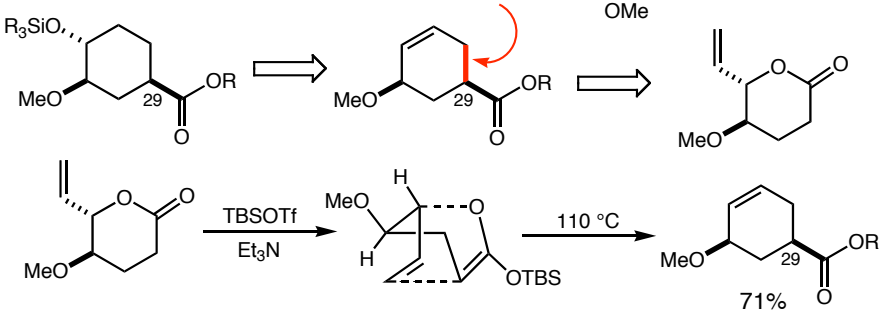

The previous cases were derived from a connection between R_2 &R_3

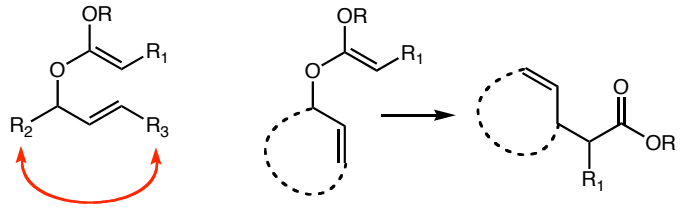

and R_1 &R_2

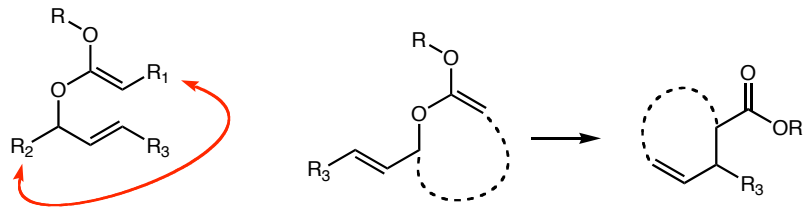

Now connect R_1 &R_3

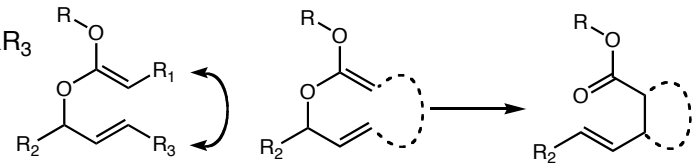

Examples: Funk, *JACS* **1982**, *104*, 4030

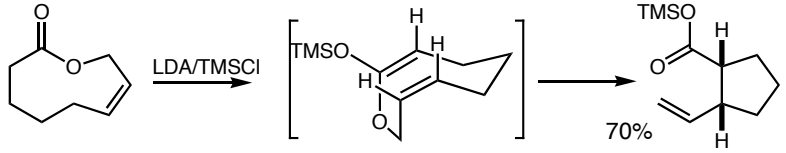

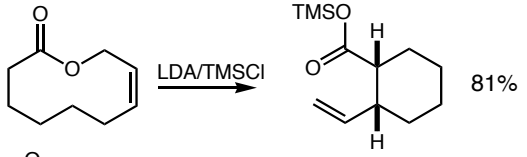

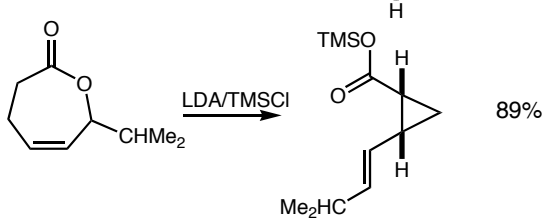

Recent improvments: Funk, *JACS* **1993**, *115*, 8847

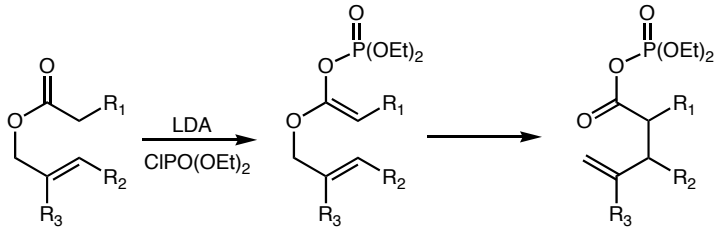

chrysanthemic acid application

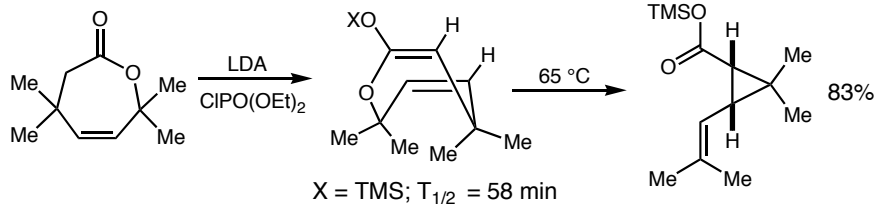

X = TMS; $T_{1/2}$ = 58 min

X = $PO(OEt)_2$; $T_{1/2}$ = 10 min

Claisen Rearrangements: Acyclic Cases with Stereoinduction

Exocyclic Stereochemical Issues

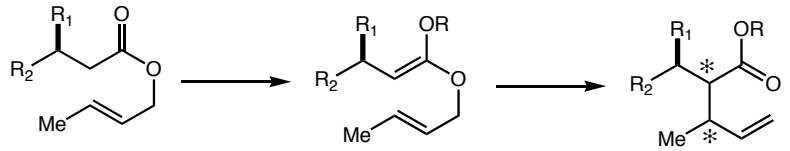

These rearrangements present many of the same issues which were encountered during our discussion of carbonyl addition with regrad to assymmetric induction.

Chelate Control: β-Hydroxy ester enolates: Kurth, *JOC* **1985**, *50*, 1840

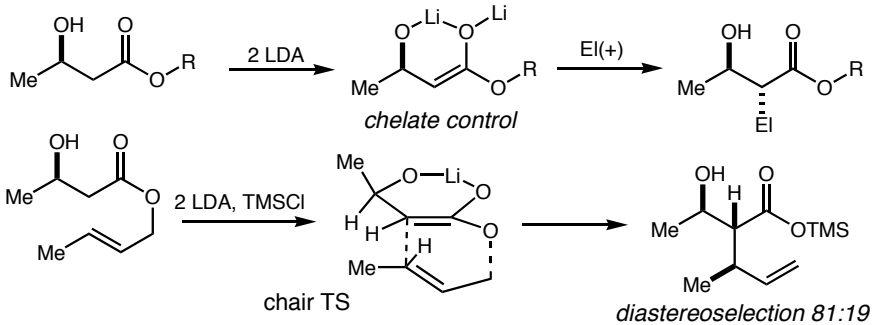

We again see the consequence of chelate-organized asymmetric induction

Felkin Control ?: Cha, *Tet. Lett.* **1984**, *25*, 5263

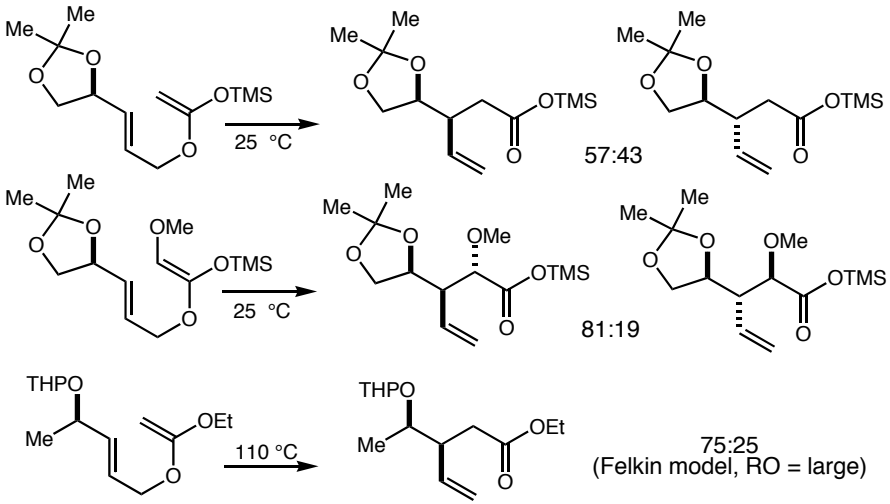

Takano, *Tet. Lett.* **1985**, *26*, 865

N-Allylketene-*N*-*O*-Acetals: Kurth, *JACS* **1985**, *107*, 443

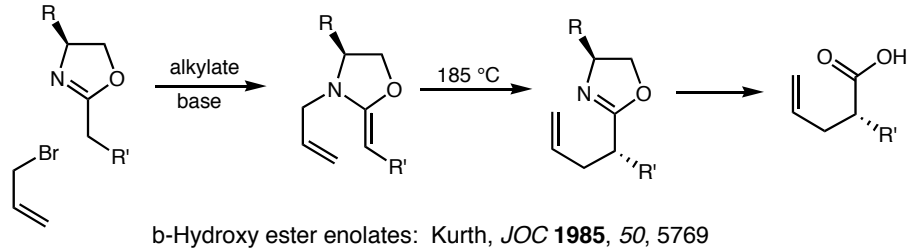

b-Hydroxy ester enolates: Kurth, *JOC* **1985**, *50*, 5769

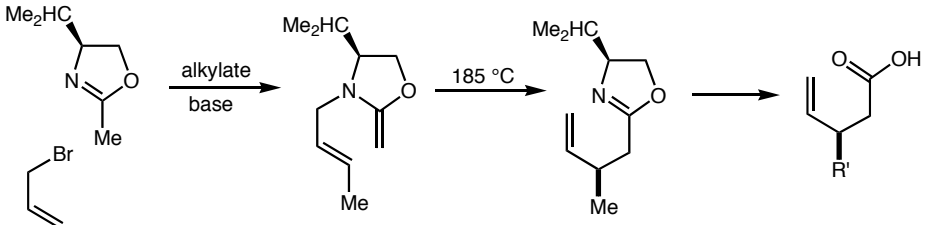

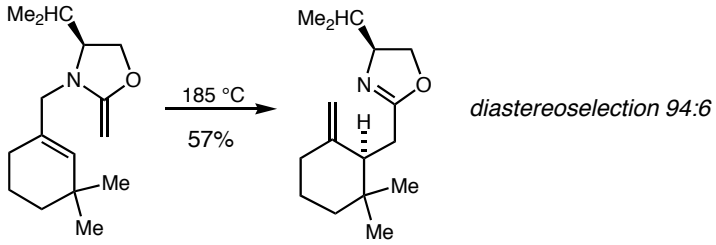

The Claisen Rearrangement is subject to acid catalysis

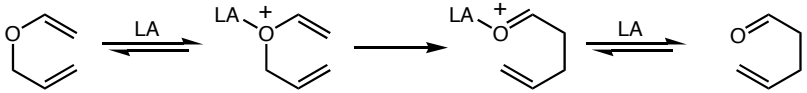

BF_3-HOAc: Bryusova, *J. Gen. Chem. (USSR)* **1941**, *11*, 722

BCl_3: Gerrard, *Proc. Chem. Soc.* **1957**, 19;
Schmid, Helv. Chem. Acta 1973. 56, 14

Et_2AlCl: Sonnenberg, *J. Org. Chem.* **1970**, *35*, 3166

$TiCl_4$: Mukaiyama, *Chem. Lett.* **1975**, *35*, 1041

$(RO)_2AlMe$: Yamamoto, *JACS.* **1988**, *110*, 7922

$(RO)_2AlMe$: Yamamoto, *Tet. Lett.* **1989**, *30*, 1265

$(RO)_2AlMe$: Yamamoto, *JACS.* **1990**, *112*, 316

$LiClO_4$: Reetz, *Tetrahedron.* **1993**, *49*, 6025

Catalyzed Claisen Rearrangement of Allyl-phenyl Ethers

$(RO)_2AlMe$: Yamamoto, *Tet. Lett.* **1990**, *31*, 377

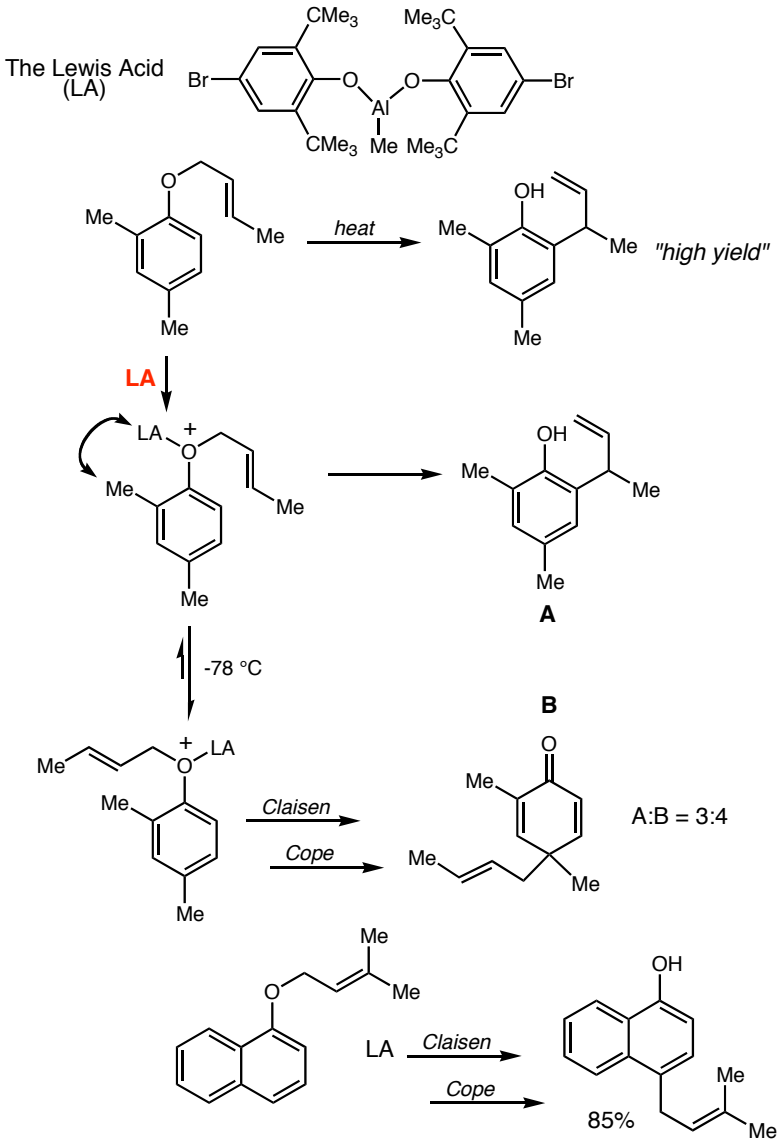

The hindered Lewis acid will alter the partitioning of the Claisen process to the two ortho positions

Catalyzed Claisen Rearrangement of Allyl-vinyl Ethers

$(RO)_2AlMe$: Yamamoto, *JACS.* **1990**, *112*, 316

The thermal process

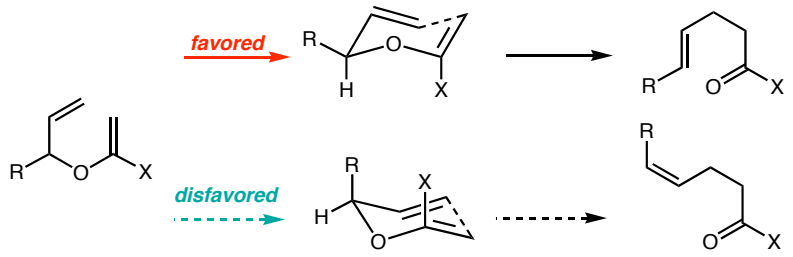

The catalyzed process

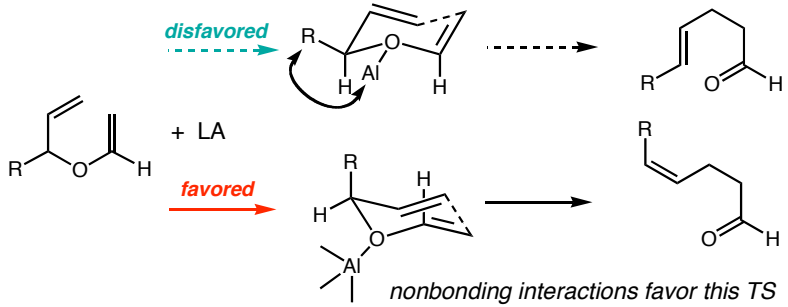

nonbonding interactions favor this TS

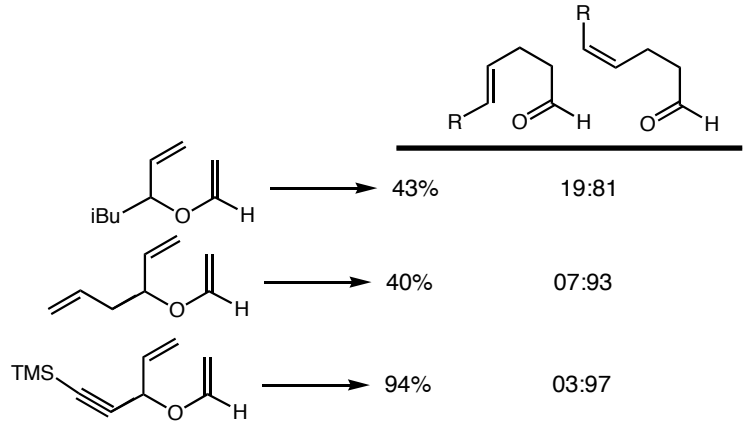

Chiral Lewis Acid Promoted Claisen Rearrangements

Yamamoto, *JACS.* **1990**, *112*, 7791
Yamamoto, *Tet. Asymmetry* **1991**, *2*, 647-662

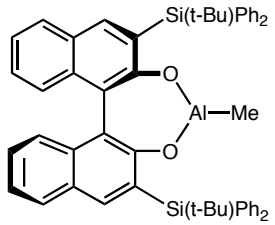

(R)-**1**

Note that these reactions are not catalytic

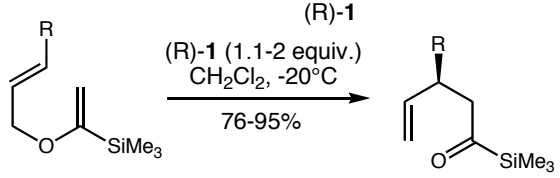

R	**% ee**
Ph	88%
C_6H_{11}	71%

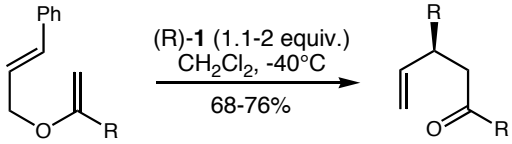

R	**% ee**
$SiMe_2Ph$	90%
$GeMe_3$	93%

Enantioselective Claisen Rearrangements: Metal-Centered Chirality

Corey, *JACS.* **1991**, *113*, 4026

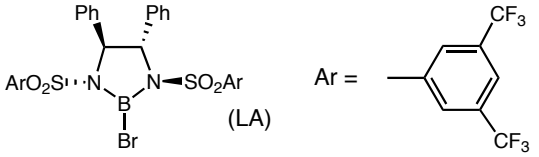

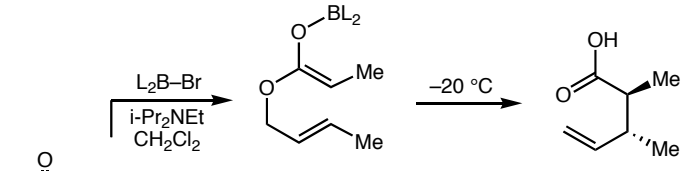

Threo: erythro 99:1
>97% ee (75%)

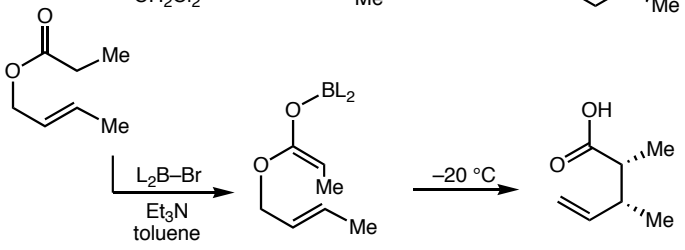

Threo: erythro 10:90
96% ee (65%)

8 cases reported

Allylic rearrangements may be included as a subset of other sigmatropic processes:

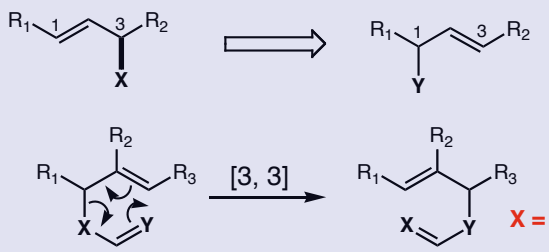

X = C, N, O, S

X = O; Y = S Faulkner, *Synthesis* **1971** 175 (see pg 183)

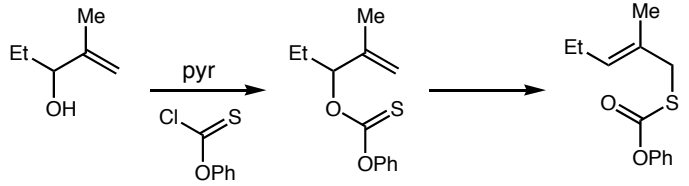

(E) selectivity: 96.5%

A stereochemically related case Johnson, *JACS* **1970** *92*, 735

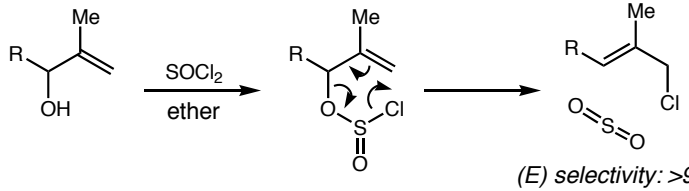

(E) selectivity: >98%

X = O; Y = N

Roberts, *JACS* **1960** *82*, 1950

Hill, *JOC* **1968** *33*, 1111

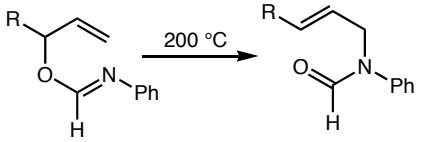

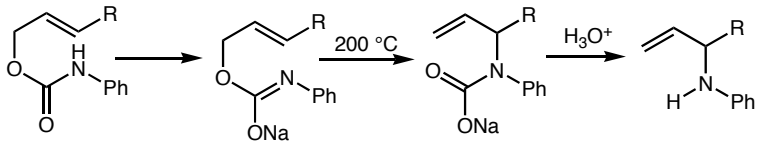

http://www.courses.fas.harvard.edu/colgsas/1063

Chemistry 206

Advanced Organic Chemistry

Lecture Number 16

Cycloaddition Reactions-1

- **Cycloadditions: Introduction**
- **Ketene Cycloadditions**
- **The Diels-Alder Reaction**

Reading Assignment for week:

Carey & Sundberg: **Part A**; Chapter 11
Concerted Pericyclic Reactions

Carey & Sundberg: **Part B**; Chapter 6
Cycloadditions, Unimolecular Rearrangements
Thermal Eliminations

D. A. Evans

Wednesday,
October 25, 2006

The Diels-Alder Cycloaddition Reactions

"Diels-Alder Reactions". Evans, D. A.; Johnson J. S. In Comprehensive Asymmetric Catalysis, Jacobsen, E. N.; Pfaltz, A.; and Yamamoto, H. Editors; Springer Verlag: Heidelberg, **1999**; Vol III, 1178-1235 **(electronic handout)**

The Diels-Alder Reaction in Total Synthesis, K. C. Nicolaou, *Angew Chem. Int. Ed.* **2002**, *41*, 1668-1698 **(electronic handout)**

Catalytic Enantioselective Diels–Alder Reactions: Methods, Mechanistic Fundamentals, Pathways, and Applications, E. J. Corey, *Angew Chem. Int. Ed.* **2002**, *41*, 1650-1667 **(electronic handout)**

Chemistry and Biology of Biosynthetic Diels–Alder Reactions Emily M. Stocking and Robert M. Williams, *Angew Chem. Int. Ed.* **2003**, *42*, 3078-3115 **(electronic handout)**

Problem of the Day:

Rationalize the sense of asymmetric induction for this Diels-Alder Reaction reported by MacMillan, *JACS*, **2000**, 122, 4243. **(pdf)**

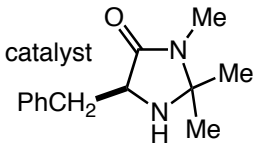

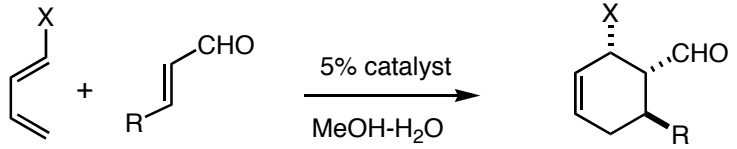

The carbonyl ene reaction is a very powerful transformation that I want to introduce to you. Accordingly, I have prepared a series of problems taken from the Problems Database to familiarize you with this reaction. **Problem 210** is provided as an introduction to the FMO analysis for the process. Subsequent problems have the ene reaction imbedded in reaction cascades.

Problem 210. Question and Answer. The carbonyl ene reaction is illustrated below. Using FMO analysis, evaluate the transition state of this reaction. Your answer should include: a transition state drawing; clear orbital depictions and HOMO-LUMO assignments; an indication of the number of electrons from each segment; and indication of whether the reaction is thermally allowed.

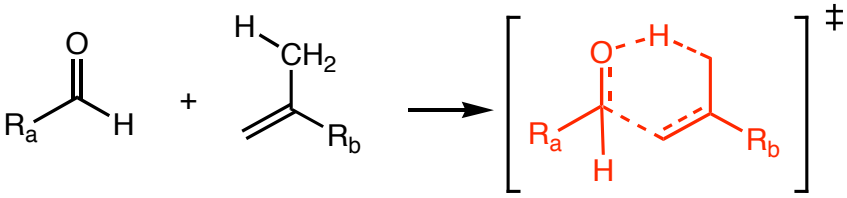

Answer

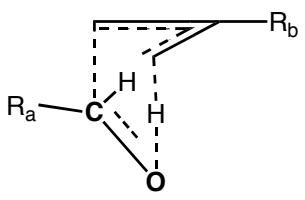

The ene transition state

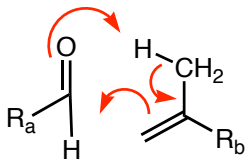

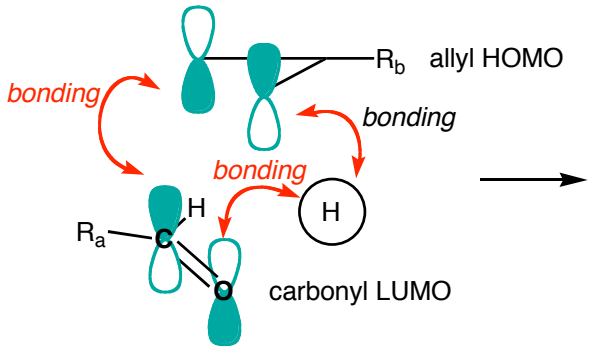

View the ene TS as a 3-component cycloaddition

One possible analysis:
allyl anion: 4 e⁻
Proton
carbonyl: 2 e⁻

[2πs + 2πs +2σs]

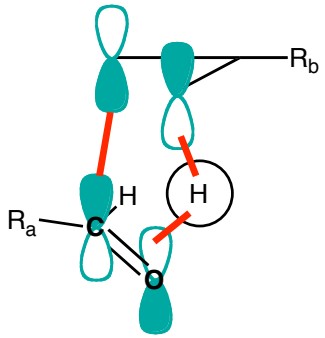

6πe⁻ "cycloaddition"

suprafacial

thermally allowed

Cycloaddition Reactions-1

Why does maleic anhydride react easily with 1,3-butadiene, but not with ethylene? So what are the "rules"?

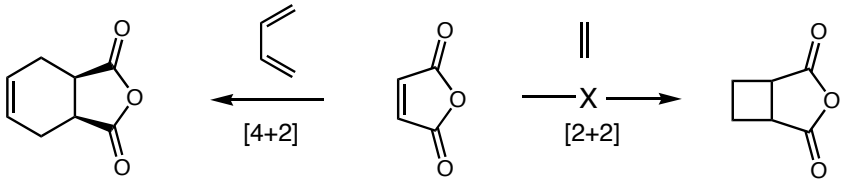

■ The related reaction of 2 ethylenes is nonconcerted: [2 + 2] cycloaddition

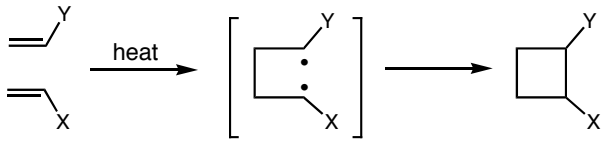

■ We also know that the photochemical variant is concerted

The frontier orbitals of the reacting species must have the proper symmetries

■ Nomenclature

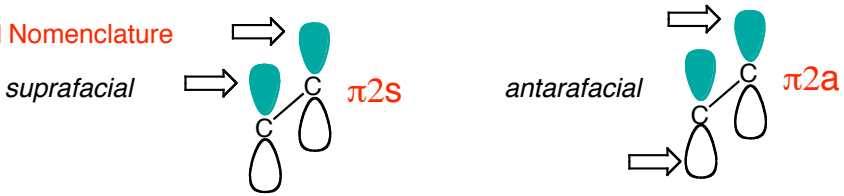

Using this nomenclature, the Diels-Alder reaction is a π4s + π2s cycloaddition

■ Consider [2 + 2] cycloaddition: Thermal activation [π2s + π2s]

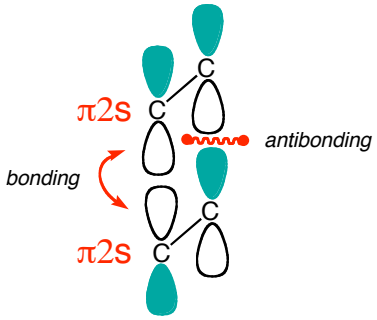

[π2s + π2s] "forbidden"

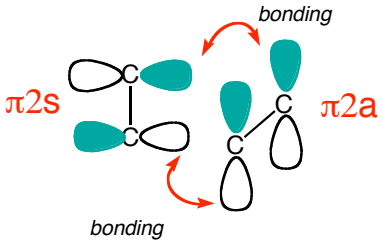

[π2s + π2a] "allowed"

■ Consider [2 + 2] cycloaddition: Photochemical activation [π2s + π2s]

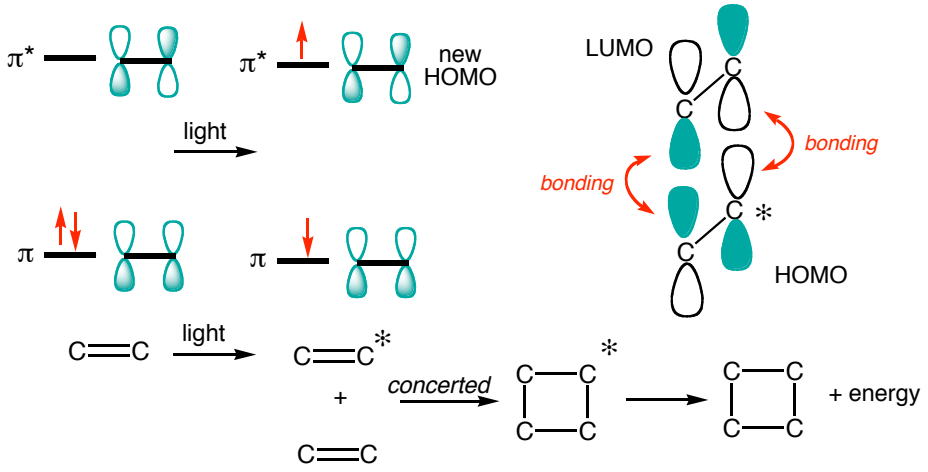

[2+2] Cycloaddition - Examples

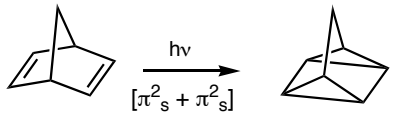

Quadricyclane Dauben, *Tet.* **1961**, *15*, 197.

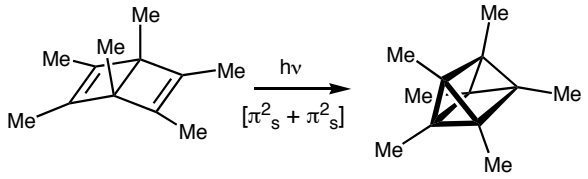

Dewar benzene-Derivative

Prismane-Der.

Schäfer, *AC* **1967**, *79*, 54.

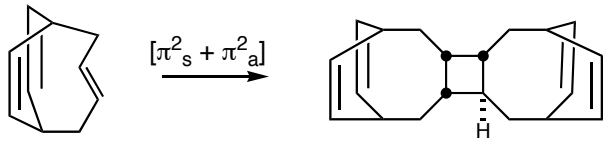

must be antarafical for indicated stereochem

TL **1967**, 4357, 4723.

Summary of Ketene Cycloadditions

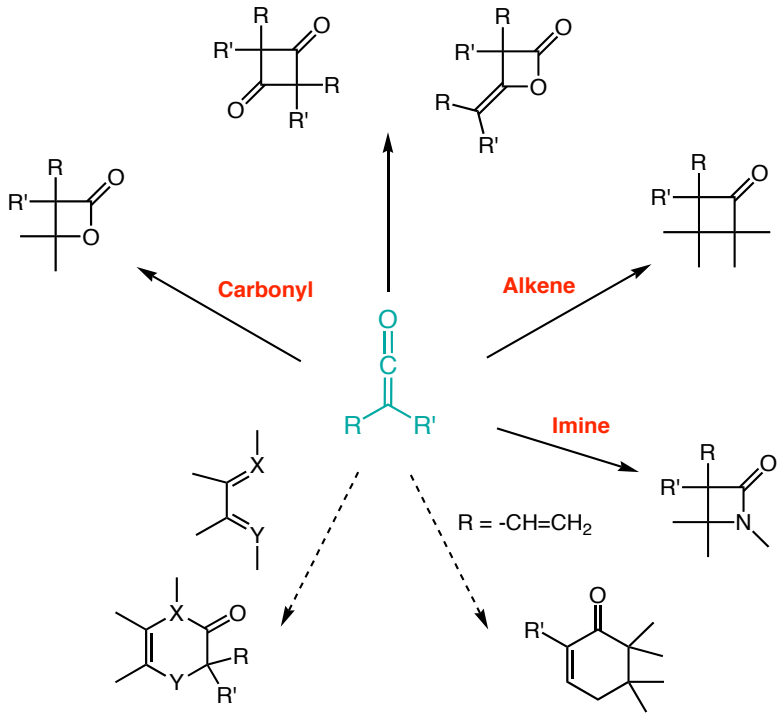

Ketene Preparation

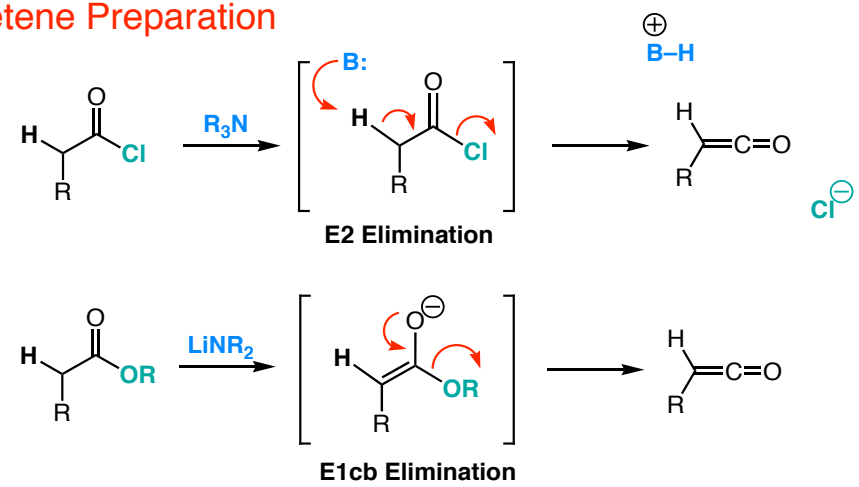

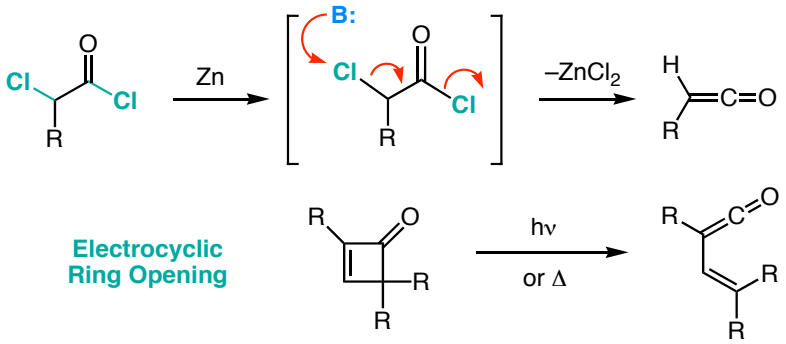

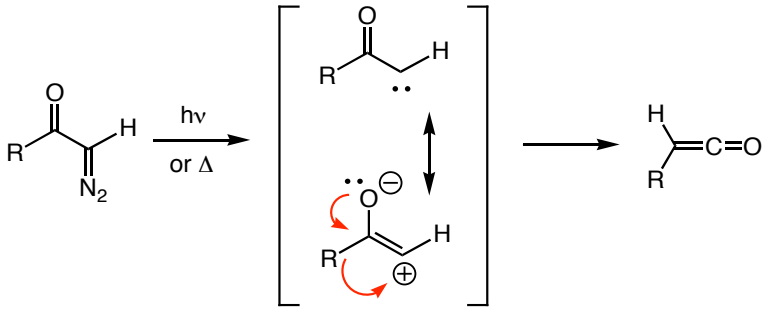

Cycloaddition: FMO Analysis

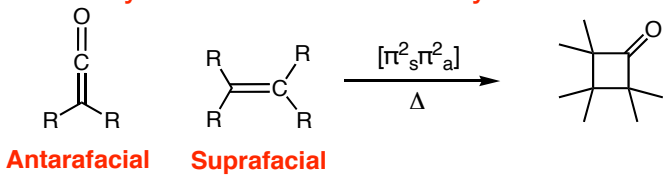

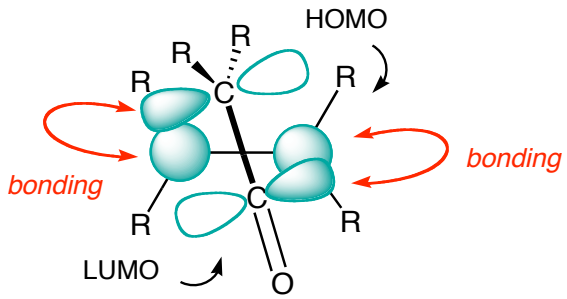

[2+2]: Stepwise Versus Concerted

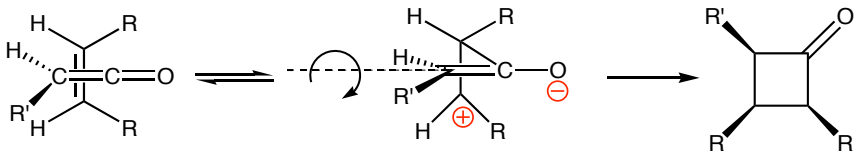

Stepwise

- Very large polar effects
- E olefins yield a mixture of *cis* and *trans* products
- Solvent effects observed, but it could merely be a ground state effect
- KIE seen for many reactions support stepwise mechanism
- Calculations show a highly asynchronus transition state.
- Stereochemical consequence can be rationalized by stepwise mechanism

Concerted

- Ketenes add stereoselectively to Z alkenes.
- Z olefins are much more reactive than E olefins

Ketene-Alkene [2+2]

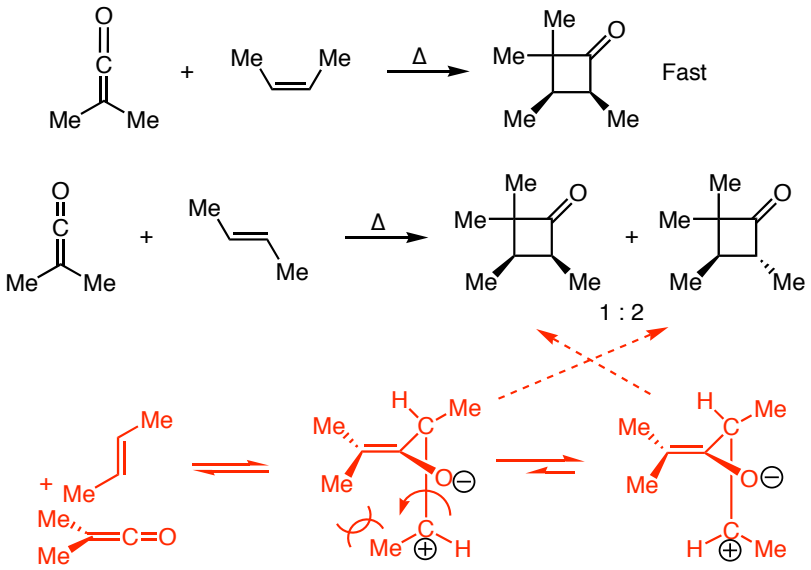

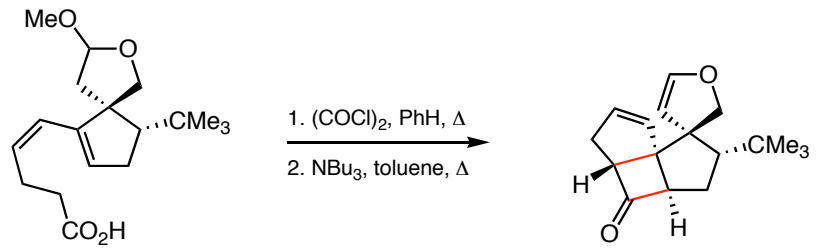

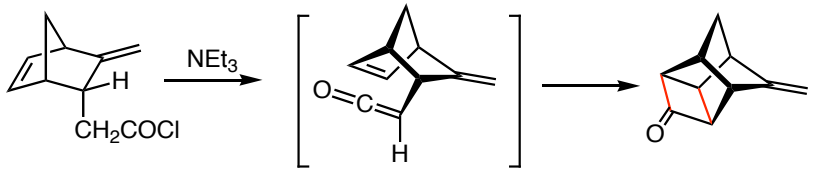

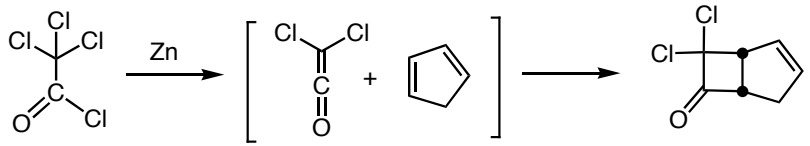

Ketenes + Aldehydes Afford β-Lactones

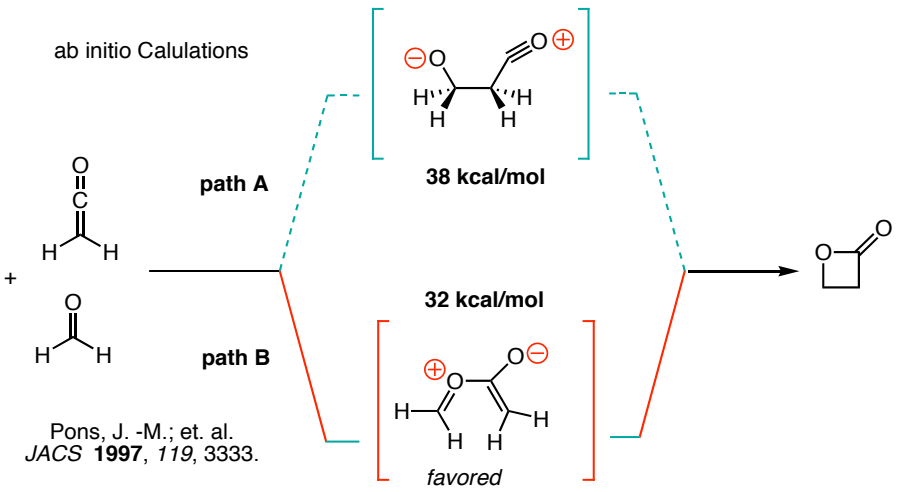

Pons, J. -M.; et. al.
JACS **1997**, *119*, 3333.

Transformations of β-Lactones

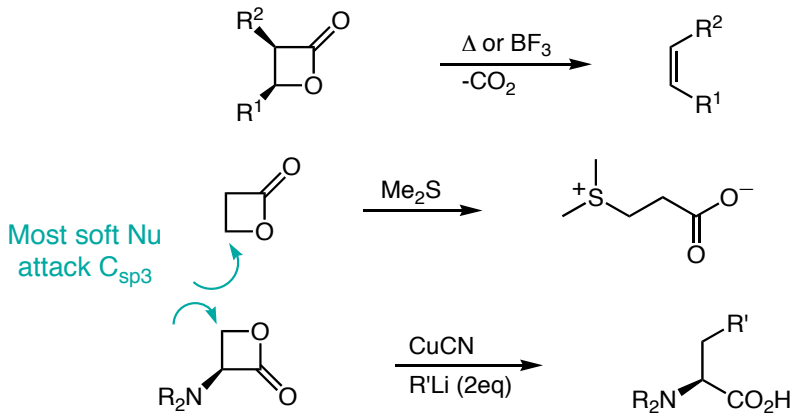

Vederas et al *JACS* **1987**, *107*, 4649.

The Staudinger Reaction

In this process, the illustrated ketene, generated *in situ* from an acid chloride, undergoes reaction with the indicated substrates to form β-lactams in a stereoselective process. When the azo-methine (RN=CHR) geometry in the reactant is (Z) the product stereochemistry is trans (eq 1). In a complementary fashion, the (E) imine affords the cis-substituted product (eq 2). While this transformatlion could be viewed as a [2s+2a] cycloaddition, it is felt that this reaction is stepwise.

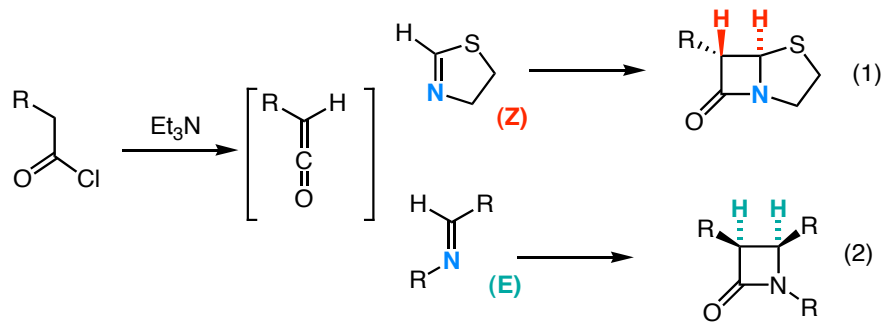

The stepwise mechanism,,,,

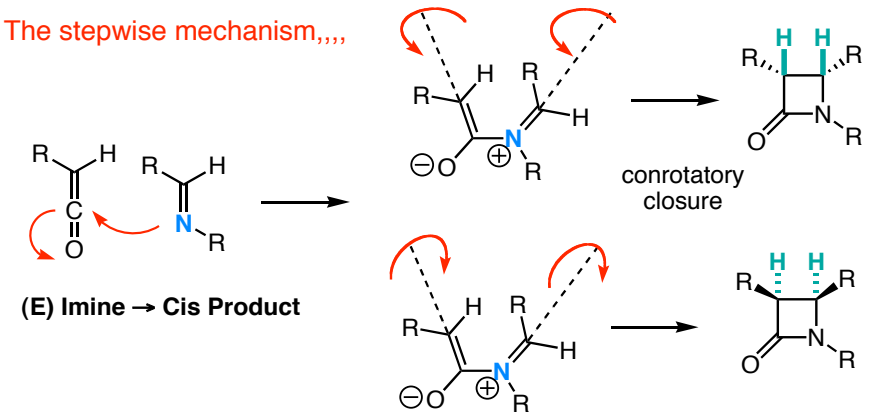

(E) Imine → Cis Product

(Z) Imine → Trans Product

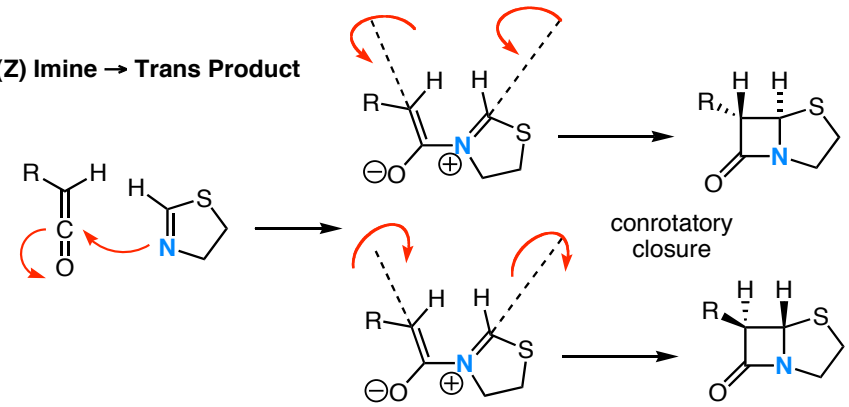

There are two contortaory modes. If you control the conrotatory mode, you control the absolute stereochemistry of the reaction:

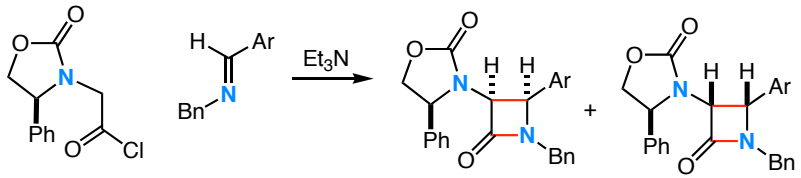

Evans, Sjogren *Tet. Lett.* **1985**, *26*, 3783, 3787.
See also Evans, Williams, *Tet. Lett.* **1988**, *29*, 5065.

diastereoselection > 95:5
80-90% yields

Enantioselective Ketene-Aldehyde Cycloaddiitons

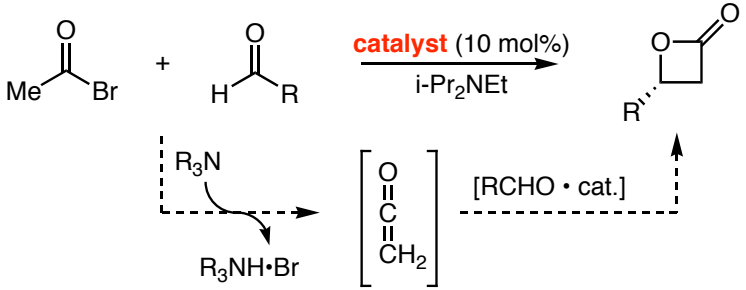

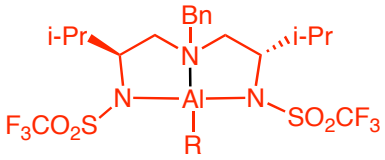

cat. = **5a**: R = Me
5b: R = Cl

entry	Aldehyde **2** (R)	catalyst [time (h), temp (°C)]	% yield	% ee **3** (configuration)
a	$BnOCH_2-$	**5b** (8, -40)	91	92 (*R*)
b	$PhCH_2CH_2-$	**5a** (16, -50)	93	92 (*S*)
	$PhCH_2CH_2-$	**5a** (72, -78)	89	95 (*S*)
c	$CH_2CH(CH_2)_8-$	**5b** (16, -50)	91	91 (*S*)
d	Me_2CHCH_2-	**5a** (24, -50)	80	93 (*S*)
e	$BnOCH_2CH_2-$	**5b** (16, -40)	90	91 (*S*)
f	$TBDPSOCH_2-$	**5b** (16, -40)	74	89 (*R*)
g	$BnOCH_2-C\equiv$	**5a** (16, -50)	86	93 (*R*)
h	$Me_3C-C\equiv$	**5a** (16, -50)	91	85 (*R*)
i	$C_6H_{11}-$	**5b** (24, -40)	56	54 (*R*)

Nelson, S. G.; Peelen, T. J.; Wan, Z. *JACS*, **1999**, 121, 9742-9743

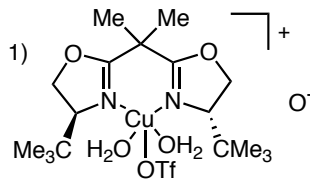

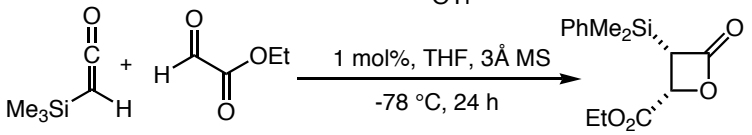

77% yield, 93% ee

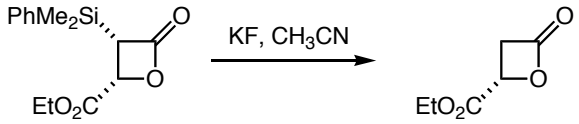

3: >99% yield, 92% ee

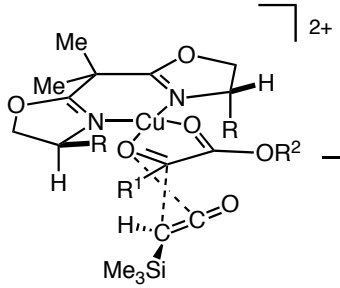

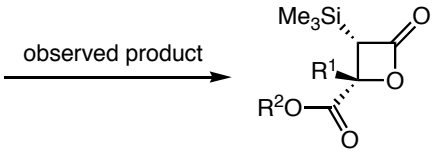

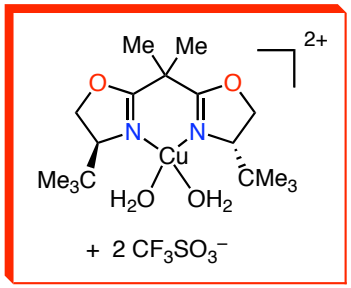

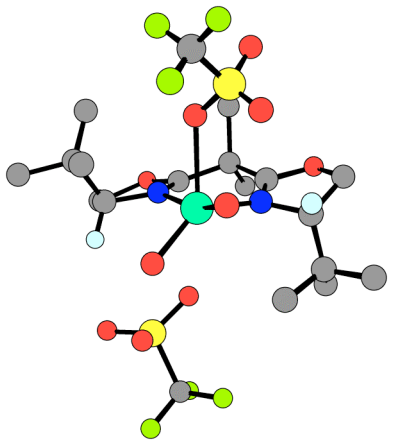

with J. Janey, *Org. Lett.* **2001**, *3*, 2125-2128

Articles and monographs of Significance

"Diels-Alder Reactions". Evans, D. A.; Johnson J. S. In Comprehensive Asymmetric Catalysis, Jacobsen, E. N.; Pfaltz, A.; and Yamamoto, H. Editors; Springer Verlag: Heidelberg, **1999**; Vol III, 1178-1235 **(pdf)**

The Diels-Alder Reaction in Total Synthesis, K. C. Nicolaou, *Angew Chem. Int. Ed.* **2002**, *41*, 1668-1698 **(pdf)**

Catalytic Enantioselective Diels–Alder Reactions: Methods, Mechanistic Fundamentals, Pathways, and Applications, E. J. Corey, *Angew Chem. Int. Ed.* **2002**, *41*, 1650-1667 **(pdf)**

Chemistry and Biology of Biosynthetic Diels–Alder Reactions
Emily M. Stocking and Robert M. Williams, *Angew Chem. Int. Ed.* **2003**, *42*, 3078-3115 **(pdf)**

Recent Advances in Natural Product Synthesis by Using Intramolecular Diels-Alder Reactions, Tadano et al. *Chem Rev.* **2005,** *105,* ASAP **(pdf)**

■ The Reaction:

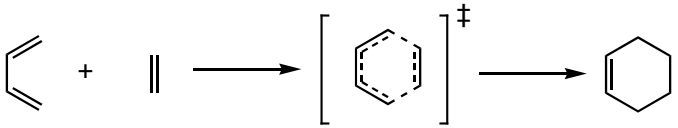

■ Representative natural products displaying the Diels-Alder retron:

These natural products could well have incorporated the DA rxn into the biosynthesis

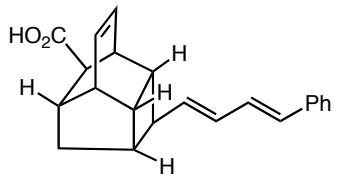

Endiandric Acid C

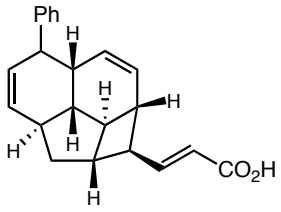

Endiandric Acid B

(Syntheses)
Nicolaou, *JACS* **1982**, *104*, 5555-5562

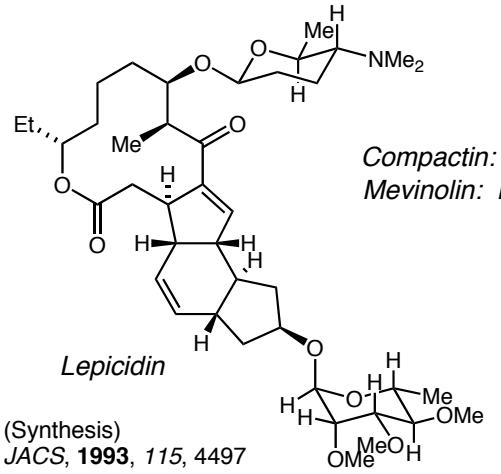

Lepicidin

(Synthesis)
JACS, **1993**, *115*, 4497

Compactin: R = H
Mevinolin: R = Me

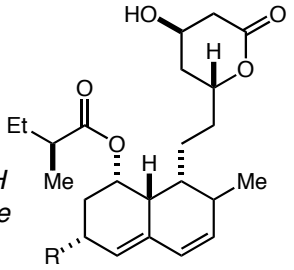

(Biosynthesis) *JACS* **1985**, *107*, 3694
Clive, *JACS* **1988**, *110*, 6914
Kozikowski, *JOC* **1987**, *52*, 3541
Keck, *JOC* **1986**, *51*, 2487
Grieco, *JACS* **1986**, *108*, 5908
Heathcock, *JACS* **1985**, *107*, 3731
Girotra, *Tet. Let.* **1983**, *24*, 3687
Hirama, *JACS* **1982**, *104*, 4251

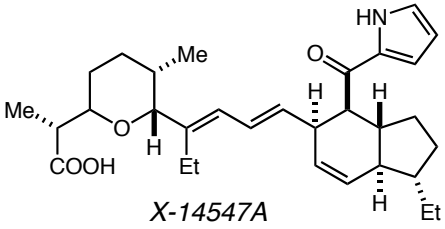

X-14547A

Roush *JOC* **1984**, *49*, 3429
Nicolaou *JOC* **1985**, *50*, 1440
Ley *Chem. Commun.* **1983**, 630

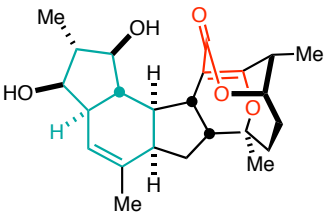

ent-FR182877 (WS9885B)
J. Antibiotics **2000**, *53*, 204

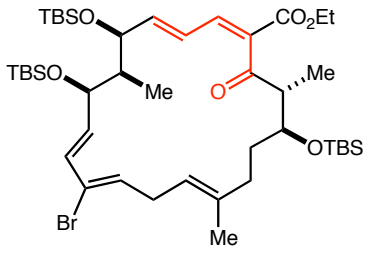

DA
Het DA

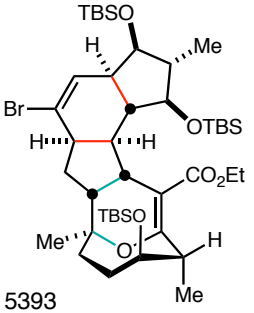

Sorensen, *JACS* **2003,** *125,* 5393
Evans, *JACS* **2003,** *125,* 13531

The Alder Endo Rule

The following observation illustrates an example of the Alder Rule which will be defined below.

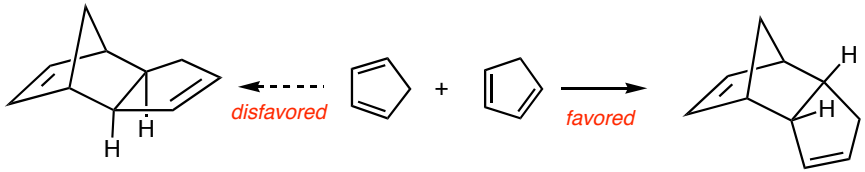

"Exo product" "Endo product"

Observation: The endo Diels-Alder adduct is formed faster even though the exo product is more stable. There is thus some special stabilization in the transition state leading to the endo product which is lacking the exo transition state.

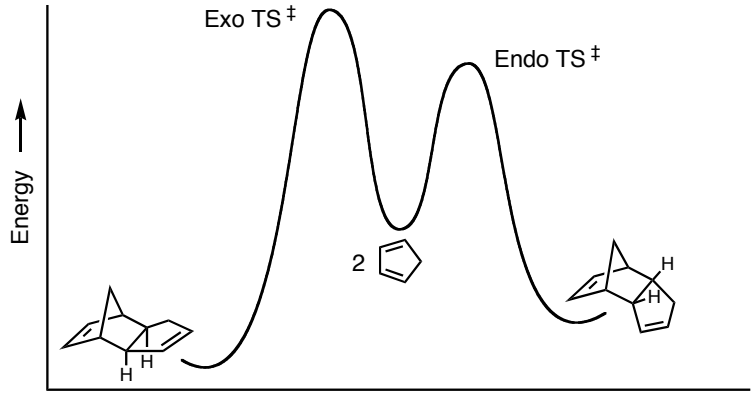

■ Of the two possible transition states, the one having the "greatest accumulation of interacting double bonds will be preferred" (the Alder Endo Rule). Secondary orbital overlap is noted below.

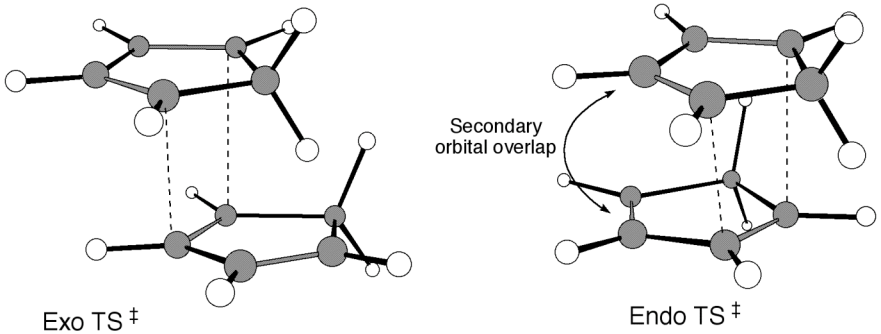

Orbital Symmetry Considerations for Diels Alder Reaction

If the symmetries of the frontier MO's of reacting partners are "properly matched" the reaction is referred to as "symmetry-allowed". The Diels-Alder reaction is such a case. As illustrated, the HOMO and LUMO of both the diene and dienophile, which in this case are the same, will constructively overlap as indicated in formation of both sigma bonds.

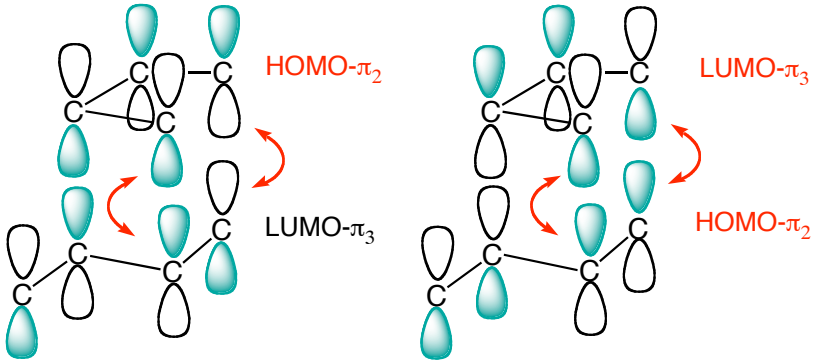

Frontier MO Explanation for the Endo Rule

■ Secondary (transient) orbital overlap can also occcur in the stabilization of certain transition state geometries. Such a transient stabilizing interaction can occur in the endo, but not exo, transition state:

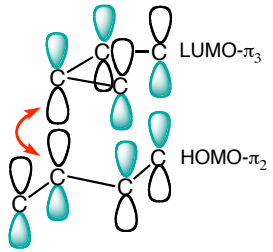

The Other Dimerization Possibility for Butadiene

Does the possibility for the following concerted dimerization exist?

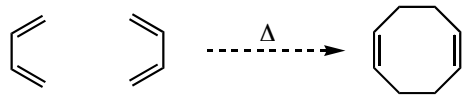

■ Note that the termini only match at one end for the HOMO-LUMO pairing. Hence we say that the symmetry requirements for the reaction in question are not met. This does not mean that the reaction will not occur, only that the reaction will not be concerted. Such reactions are called "symmetry-forbidden".

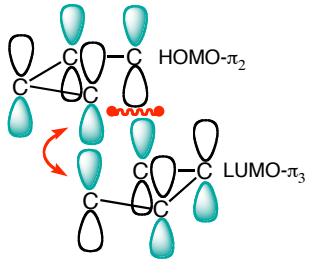

Transition State Modelling is Coming of Age

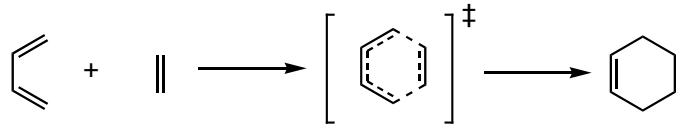

■ The lengths of the forming C–C bonds are Ca. 1.5 times the normal bond distance. This factor comes out of the *ab initio* work of Jorgensen & Houk

leading references: Jorgensen, *JACS* **1993**, *115*, 2936-2942
Houk, Jorgensen, *JACS* **1989**, *111*, 9172

Transition Structures of Hydrocarbon Pericyclic Reactions
Houk *Angew. chem. Int. Ed.* **1992**, *31*, 682-708

■ Bond formation is not synchronus with substituted dienophiles (Jorgensen)

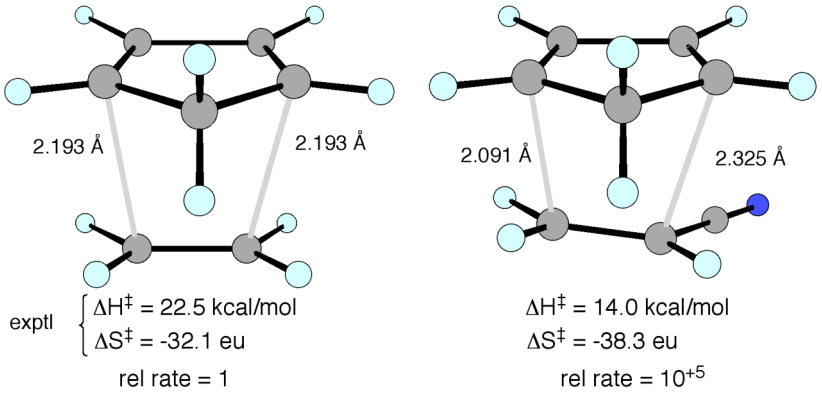

■ Diene Reactivity as measured against Maleic anhydride

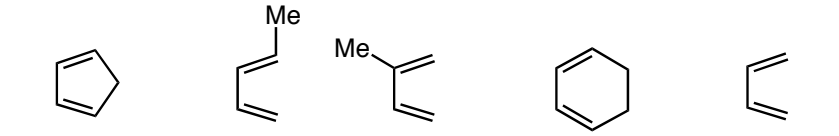

log k = 4.96 log k = 2.36 log k = 2.19 log k = 2.12 log k = 1.83

Sauer, *Angew. Chem. Int. Ed.*, **1980**, *19*, 779-807

■ Lewis Acid Catalysis of the reaction is possible: Yates & Eaton, *JACS* **1960**, *82*, 4436

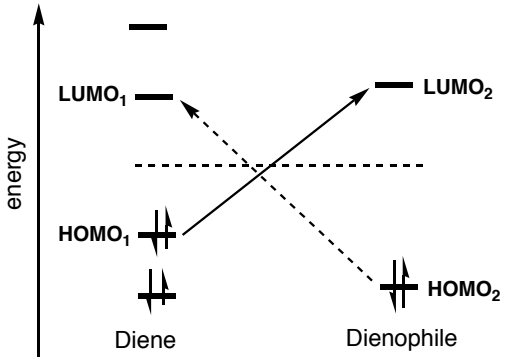

The Critical Energy Difference:
E(LUMO$_1$) - **E**(HOMO$_2$)
or
E(LUMO$_2$) - **E**(HOMO$_1$)

■ The closer the two orbitals are in energy, the better they interact
■ As ΔE decreases for the relevant ground state FMOs, rxn rates increase

Ethylene & Butadiene Vs Butadiene & Acrolein

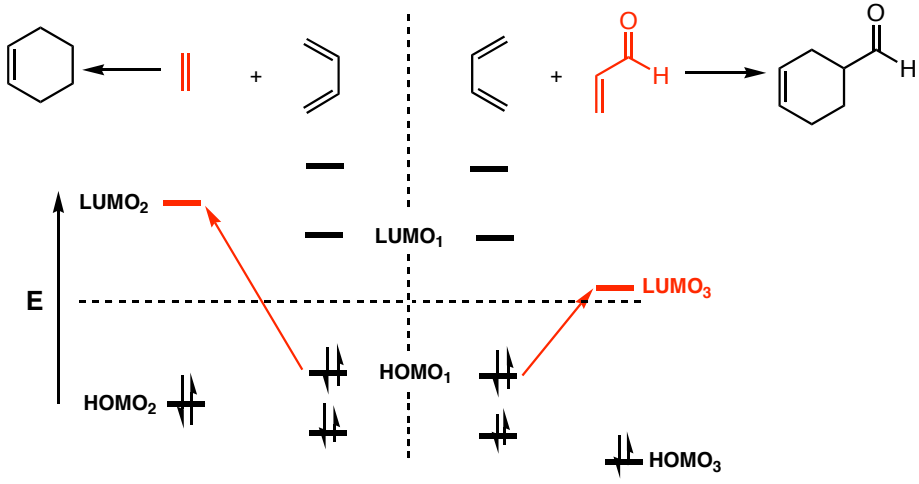

ΔE (LUMO$_3$-HOMO$_1$) < ΔE (LUMO$_2$-HOMO$_1$) ⟹ *Rate Acceleration*

Lewis acid catalysis not only dramatically increases rates by ca 10^{+6} it also improves reaction regiochemistry & endo diastereoselectivity

Orientation of Reacting Partners

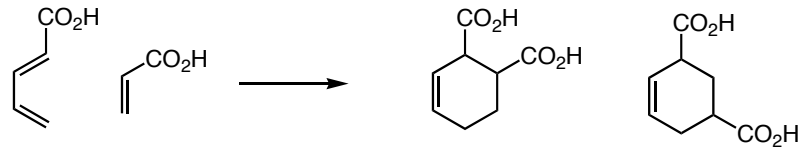

favored *disfavored*

4.5 : 01 @ 100 °C

Lewis acid catalysis improves orientation

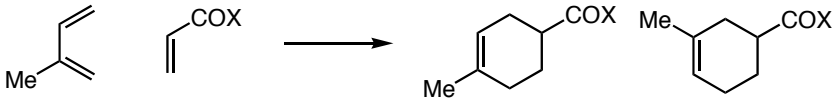

favored *disfavored*

toluene, 120 °C	59 : 41
C_6H_6, $SnCl_4$, 25 °C	96 : 04

*In general, 1-substituted dienes are more regioselective than their 2-substituted counterparts: Sauer, Angew. Chem. Int. Ed., **1967**, 6, 16-33*

Lewis acid catalysis improves endo diastereoselection

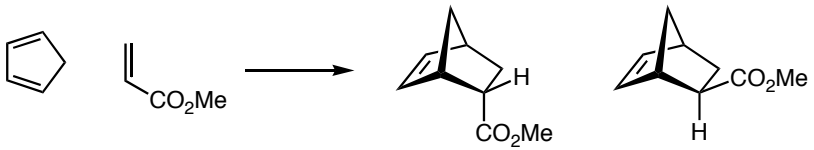

favored *disfavored*

CH_2Cl_2, 0 °C	80 : 20
C_6H_6, $SnCl_4$, 25 °C	95 : 05

DA Reactions Part II: The Reaction Mechanism, Sauer, *Angew. Chem. Int. Ed.*, **1967**, *6*, 16-33

Here is an interesting problem in reaction design

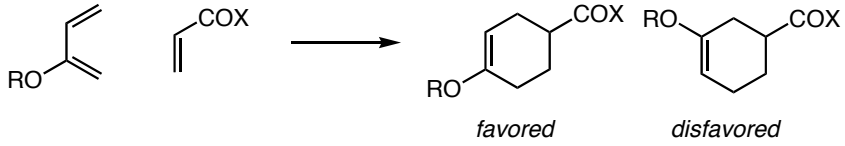

favored *disfavored*

However, what if you need the disfavored product?

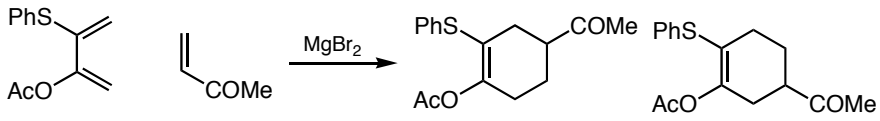

Trost, *JACS* **1980**, *102*, 3554 *disfavored* *favored*

By employing a removable substituent, it is possible to access the normally disfavored product diastereomer

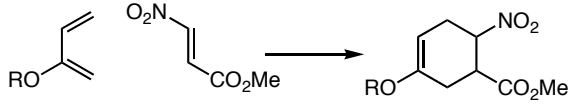

Danishefsky, *JACS* **1978**, *100*, 2918: The NO_2 FG completely dominates directivity

It then can be removed by elimination

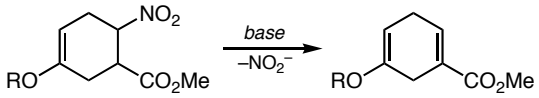

or by reduction Ono, *Tet.* **1985**, 4013

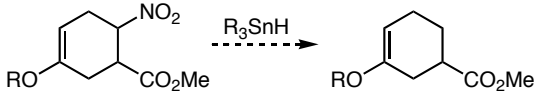

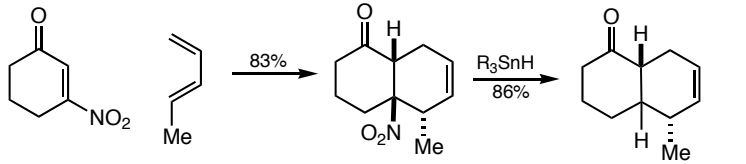

Ono, *Chem. Commun.* **1982**, 33-34

mixture of ring-fusion isomers

Instructive Issues of Regiocontrol with Quinone Dienophiles

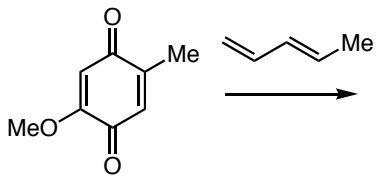

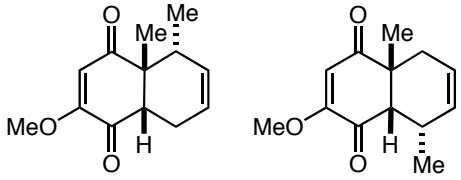

Orientation of Reacting Partners controlled by Lewis acid structure

Reusch *JOC* **1980**, *45*, 5013

Conditions	Ratio
thermal (100 °)	50 : 50
BF_3•OEt_2 (-20 °)	80 : 20
$SnCl_4$ (-20 °)	<5 : 95

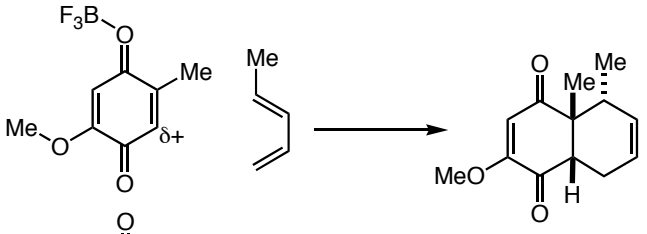

selection 80 : 20

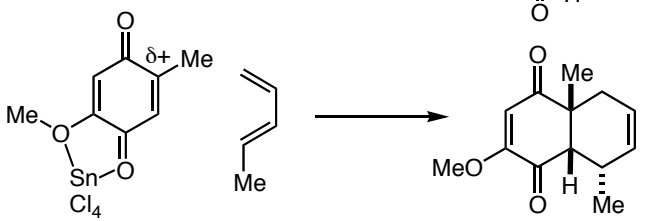

selection >95 :5

Similar results provided by Stoodley *Chem. Comm.* **1982**, 929

Kelly *Tet. Let.* **1978**, 4311

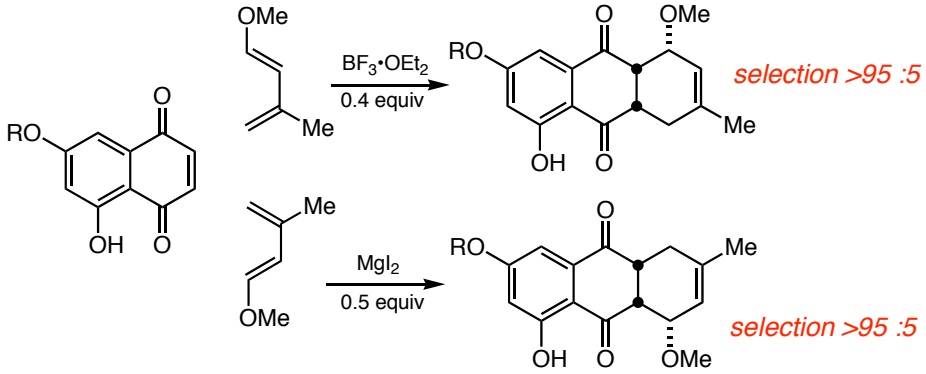

selection >95 :5

selection >95 :5

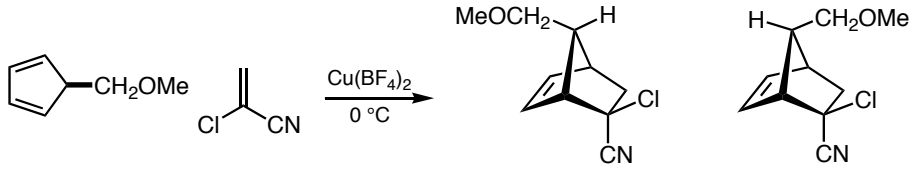

Corey, *JACS* **1969**, *91*, 5675

Ratio: 90 : 10

Diels-Alder Reactions with Chiral Dienes

Comprehensive Organic Synthesis, Vol. 5, Trost, Ed. **1991**

4.1 Intermolecular Diels-Alder Reactions, W. Oppolzer, See page 347

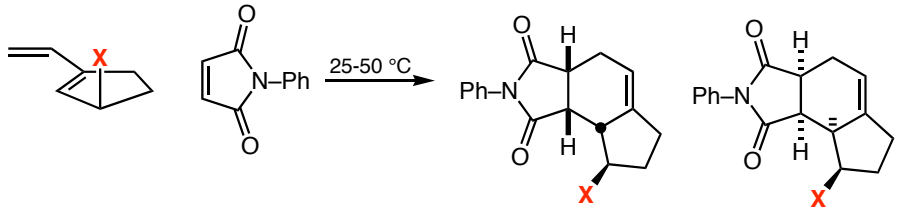

X =	Ratio
–OH	36 : 64
–Me	83 : 17
–OMe	>97 : 3

Overman, *JACS* **1988**, *110*, 4625

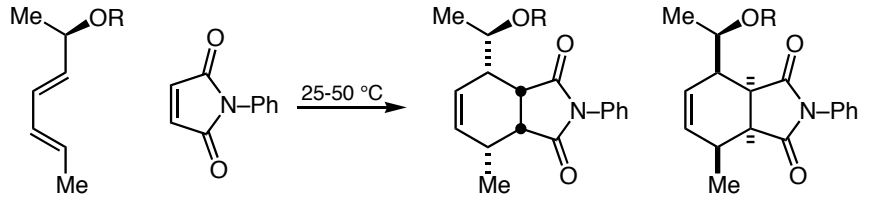

Franck, *Tet. Lett.* **1985**, *26*, 3187

Franck, *JACS* **1988**, *110*, 3257

R = Me: Ratio; 83 : 17

R = Me_3Si: Ratio; 88 : 12

Comments on the Transition State

- Avoid Eclipsing allylic substituents
- better donor (Me) anti to forming bond
- avoid gauche OR interaction

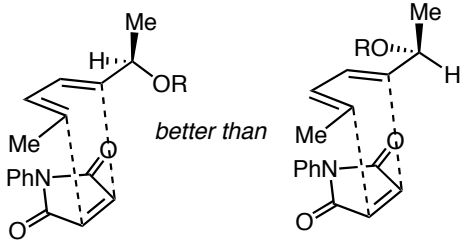

Problem 76, Bodwell has disclosed an interesting thermally initiated reaction cascade that was designed to cuminate in a formal synthesis of strychnine(*Angew. Chem. Int. Ed* **2002**, *41*, 3261). One of his reported transformations is illustrated below.

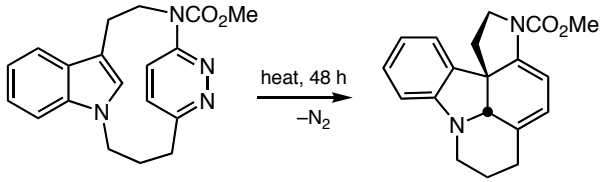

Provide a detailed mechanism for this reaction cascade. Your answer should include three-dimensional structures that accurately depict ground and transition state representations.

Problem 86. In 1983 Masamune introduced a new family of chiral controllers for the Diels-Alder reaction (*J. Org. Chem.* **1983**, *48*, 4441).

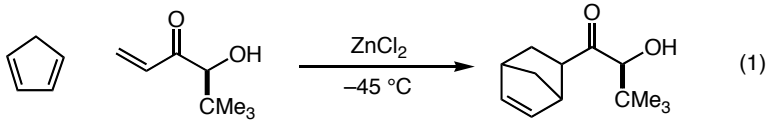

(1)

exo:endo = 94:6
endo diastereoselection >99:1

Please provide a mechanism for the reaction shown in equation 1. Be sure to include clear transition state drawings in your answer, and predict the stereochemistry of the major product diastereomer.

Problem 112. In a recent article, Roush reported the highly endo-selective, Lewis acid catalyzed Diels-alder reaction illustrated below (*Org. Lett* **2001**, *3*, 957). Using your knowledge of Diels-Alder transition states, draw the transition state of this reaction, and from this drawing, predict the relative stereochemical relationships that are to be anticipated in the product.

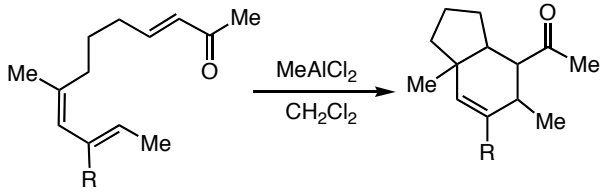

diastereoselection >99:1

Problem 157. A short reaction sequence that results in the rapid assemblage of the taxane skeleton has been reported by Winkler (*Tetrahedron Lett.***1995**, *36*, 687). This transformation is illustrated below wherein intermediate **A** is subsequently induced to react with divinyl ketone.
Provide a concise mechanism for this reaction. For full credit, the relative stereochemical relationships at the indicated stereocenters must be provided.

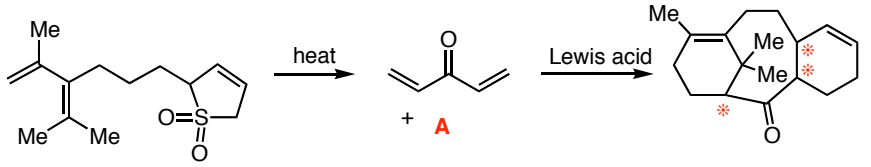

Problem 739. The rapid assembly of the bicyclo[5.3.1]undecane core of penostatin F was recently reported by Barriault and coworkers (*Org. Lett.* **2004**, *6*, 1317). In this remarkable transformation dihydropyran **1** is converted to the highly complex tricycle **3** in only two operations. Please provide a detailed mechanism for this reaction sequence. Be sure to indicate all pericyclic reactions.

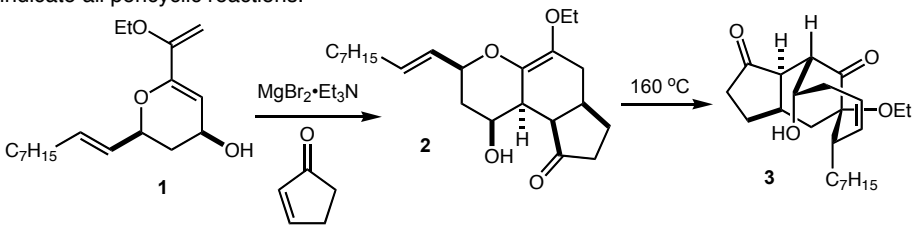

Problem 778. Boger and co-workers recently reported the synthesis of the indole alkaloid minovine (**1**). This pivotal transformations leads to the construction of the minovine skeleton. Provide plausible mechanisms for this transformation.

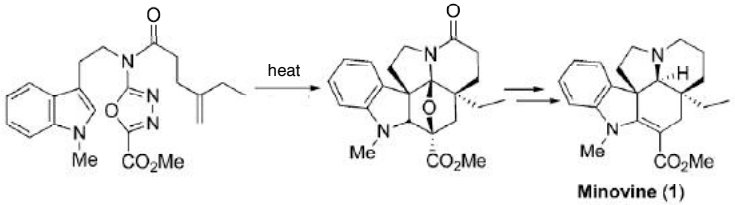

Minovine (1)

Problem 794. Doering and Rosenthal reported the interesting conversion of Nenitzescu's hydrocarbon (**1**) to dihydro-naphthalene (**2**). Provide a mechanistic rationalization for this transformation. (Reference: Doering, W.v.E.; Rosenthal, J.W., *JACS* **1966**, *88*, 2078)

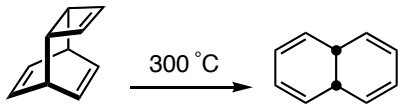

1 **2**

http://www.courses.fas.harvard.edu/colgsas/1063

Chemistry 206

Advanced Organic Chemistry

Lecture Number 17

Cycloaddition Reactions-2

The Diels-Alder Reaction: Absolute Stereocontrol

■ Reading Assignment for week:

Carey & Sundberg: **Part A**; Chapter 11
Concerted Pericyclic Reactions

Carey & Sundberg: **Part B**; Chapter 6
Cycloadditions, Unimolecular Rearrangements
Thermal Eliminations

"Diels-Alder Reactions". Evans, D. A.; Johnson J. S. In Comprehensive Asymmetric Catalysis, Jacobsen, E. N.; Pfaltz, A.; and Yamamoto, H. Editors; Springer Verlag: Heidelberg, **1999**; Vol III, 1178-1235 **(pdf)**

D. A. Evans

Friday,
October 27, 2006

Diels-Alder Must-Read List

The Diels-Alder Reaction in Total Synthesis, K. C. Nicolaou, *Angew Chem. Int. Ed.* **2002**, *41*, 1668-1698 **(pdf)**

Catalytic Enantioselective Diels–Alder Reactions: Methods, Mechanistic Fundamentals, Pathways, and Applications, E. J. Corey, *Angew Chem. Int. Ed.* **2002**, *41*, 1650-1667 **(pdf)**

Chemistry and Biology of Biosynthetic Diels–Alder Reactions
Emily M. Stocking and Robert M. Williams, *Angew Chem. Int. Ed.* **2003**, *42*, 3078-3115 **(pdf)**

Recent Advances in Natural Product Synthesis by Using Intramolecular Diels-Alder Reactions, Tadano et al. *Chem Rev.* **2005,** *105,* 4779-4807 **(pdf)**

Problem 894. Roush and Sciotti have reported the illustrated complex Diels-Alder reaction in conjunction with their synthesis of chlorothricolide (*JACS* **1998**, *120*, 7411). In prior studies, they had documented that the dienophile was highly exo-selective. The absolute stereochemical relationships in the reactants are as indicated. Predict the sense of asymmetric induction for both cycloadditions and assign all stereochemical relationships in the product. Comment on the significance of the vinyl-silicon substituent.

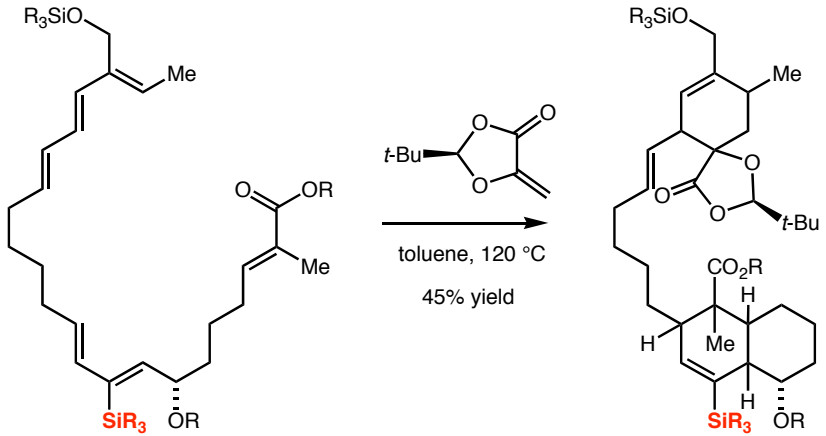

We will cover this case in lecture today.

Review:
Oppolzer in *Comprehensive Organic Synthesis* 1992, *Vol. 4*, 315-399.

■ Ester-Type Chiral Auxiliaries

Corey *JACS* **1975**, *97*, 6908.

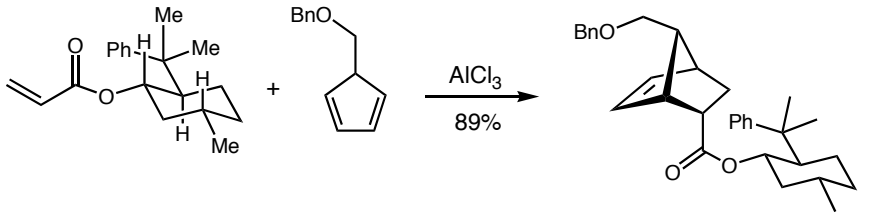

Diastereomer Ratio Not Given

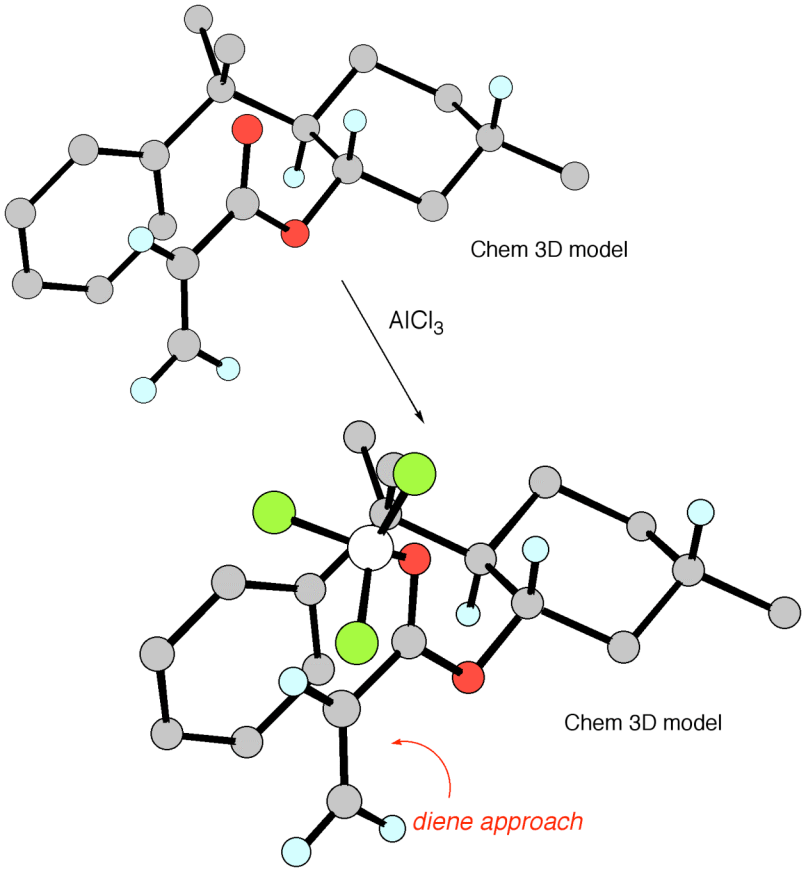

Non-Chelate Ester-Type Chiral Auxiliaries

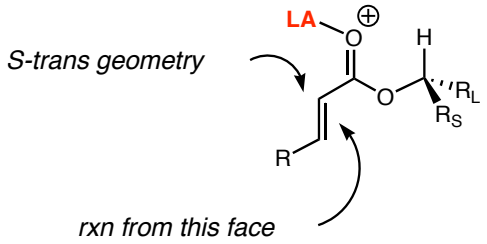

Lewis Acid-Ester Complex Conformation Dictates Diastereoselection

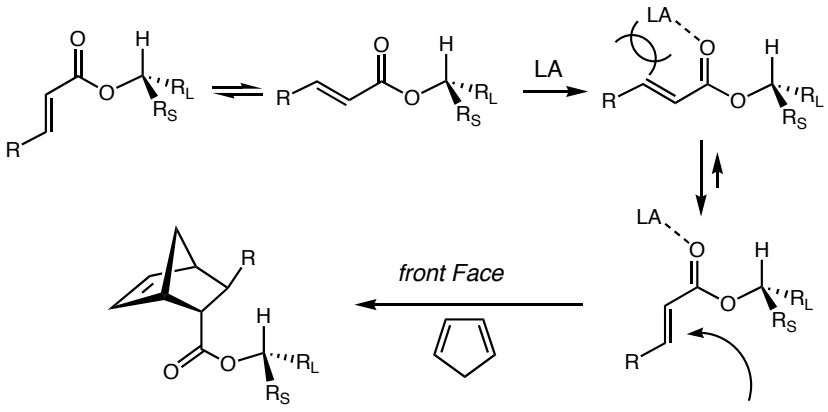

See Oppolzer *ACIEE* **1984**, *23*, 876.

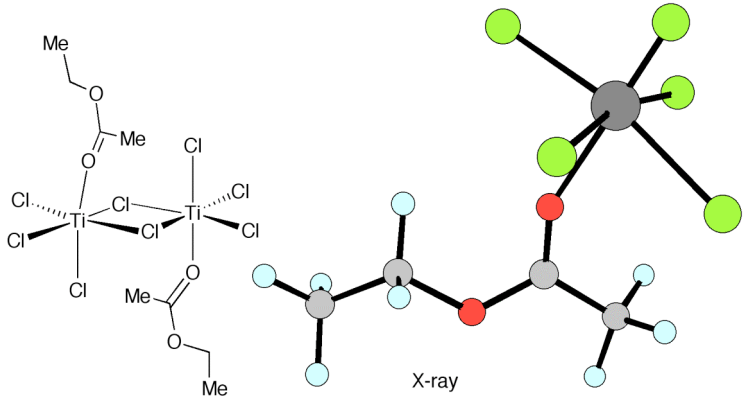

Representative η_1–titanium complexes with organic compounds

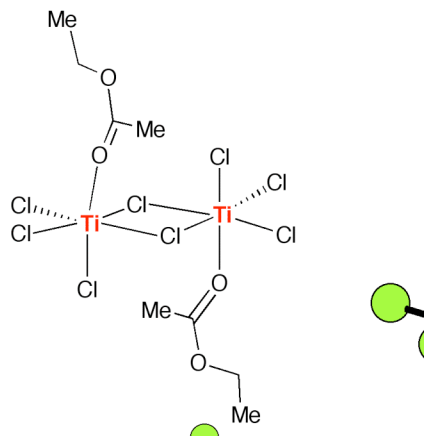

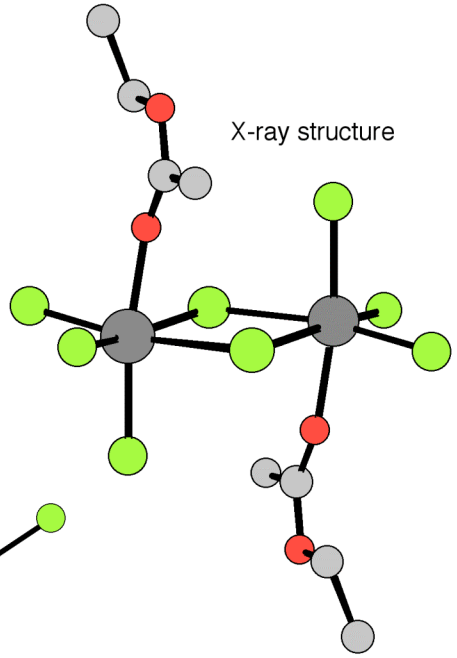

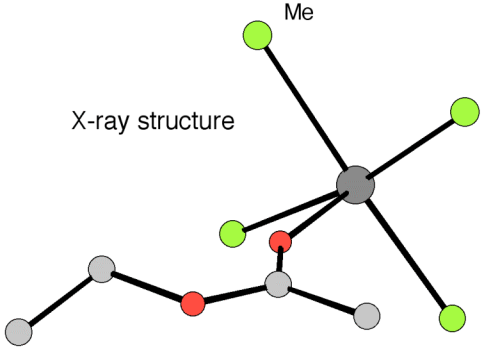

Side view of in-plane Ti coordination: Ti-O-C-C = 2.86°

Ti–O–C angle = 152 °

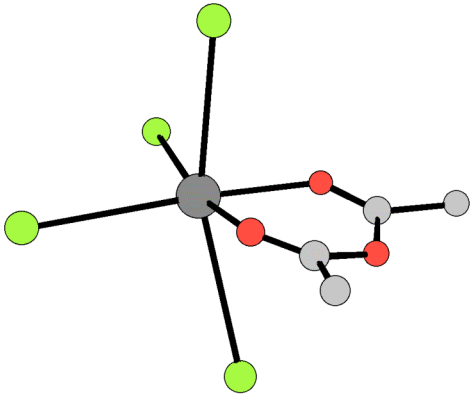

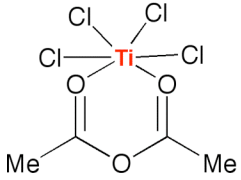

Representative η_1–titanium complexes with organic compounds

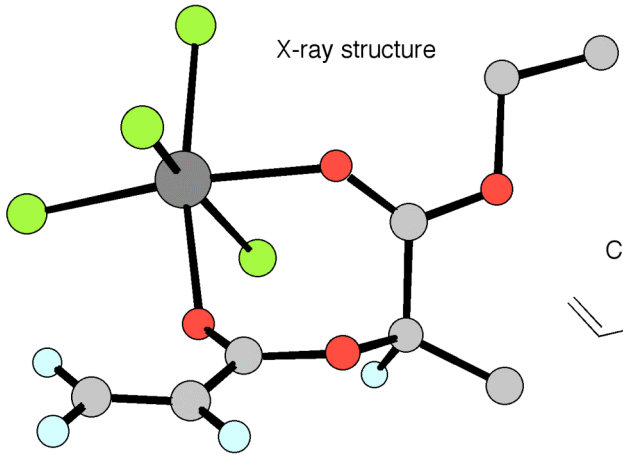

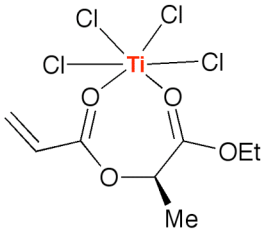

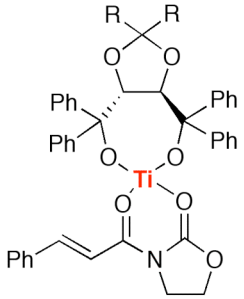

Narasaka *JACS*, **1989**, *111*, 5340

A. Jorgensen, *JACS*, **1995**, *117*, 4435

X-ray structure

Ester-Type Chiral Auxiliaries: Chelating Dienophiles

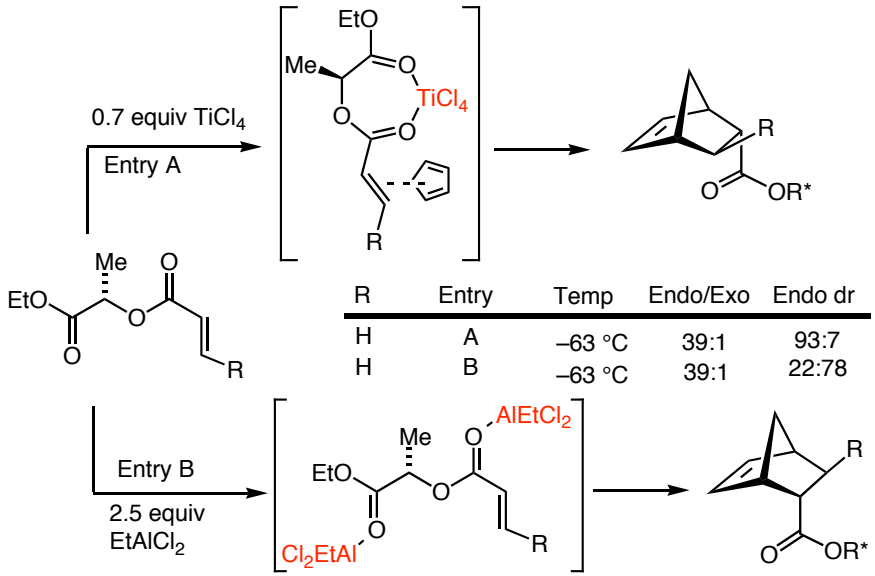

R	Entry	Temp	Endo/Exo	Endo dr
H	A	–63 °C	39:1	93:7
H	B	–63 °C	39:1	22:78

Helmchen *Tetrahedron Lett.* **1984**, *25*, 2191.
ACIEE **1985**, *24*, 112. *Tetrahedron Lett.* **1985**, *26*, 3095.

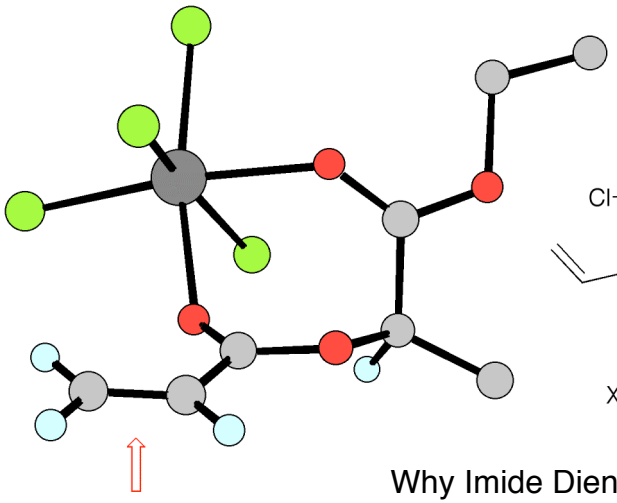

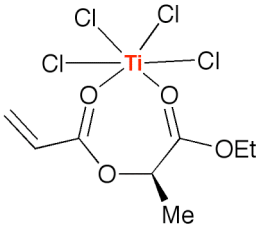

X-ray structure

Why Imide Dienophiles??
They are ~ 100-1000X more reactive

Chelating Imide-type Chiral Auxiliaries
Metal ion Dependent Diastereoselection

Evans *JACS*, **1984**, *106*, 4261.
Evans *JACS*, **1988**, *110*, 1238.

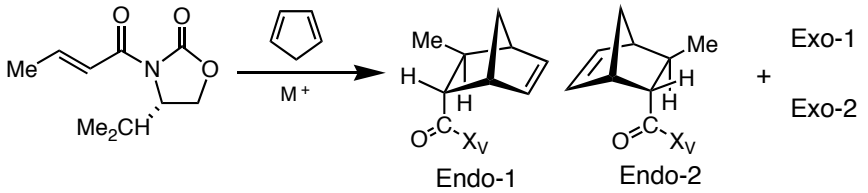

Lewis Acid (1.2 equiv)	Temp.	Endo-1 / Endo-2	Σ Endo / Exo
$SnCl_4$	25	2.7	92 : 8
$SnCl_4$	–78	3.1	93 : 7
$TiCl_4$	–78	2.6	91 : 9
$AlCl_3$	–78	1.5	80 : 20
(2.0 equiv) **Et_2AlCl**	–78	**15.7**	**>99 : 1**
(0.7 equiv) **Et_2AlCl**	–78	**4.4**	**92 : 8**

Binding Mode Dictates Diastereoselectivity

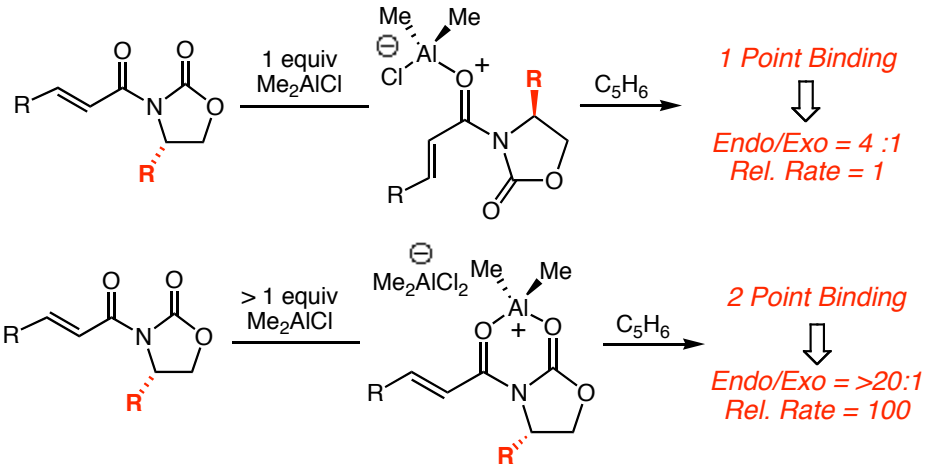

A Case for Π-Stacking: *Angew Chem, Int Ed.* **1987**, *26*, 1184

Compare the alkylation rxn which is dominated by steric effects with the DA rxn which may be controlled by both steric and electronic effects

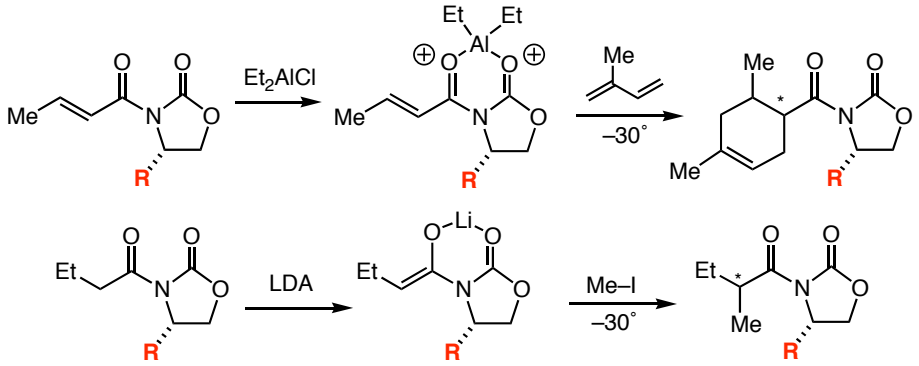

$\Delta\Delta G^{\ddagger} = 2.3\ RT\ Log\ P_1/P_2$

PLOT $\Delta\Delta G^{\ddagger}$ FOR EACH RXN AS A FUNCTION OF THE SUBST., R.

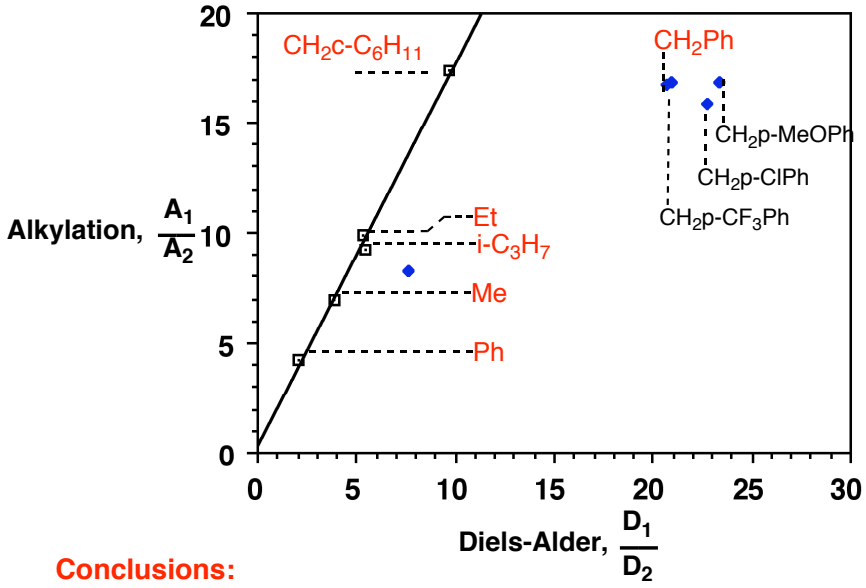

Conclusions:

Steric effects correlate well for the two reactions

Added electronic effects from Bn group enhance facial bias

The Chiral Dienophile

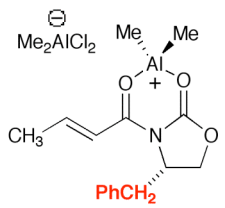

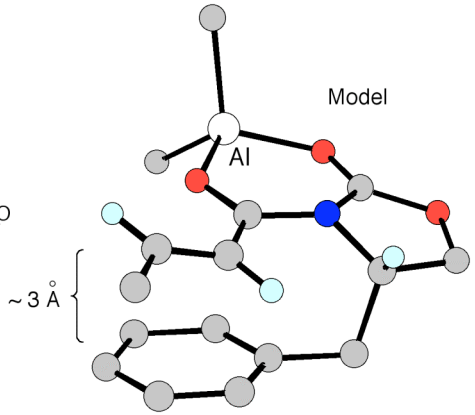

A Complex Application

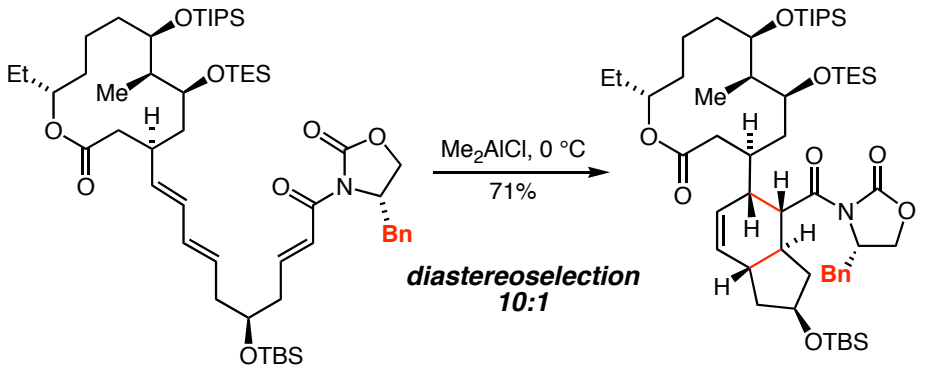

diastereoselection 10:1

The control experiment with no chiral auxiliary:

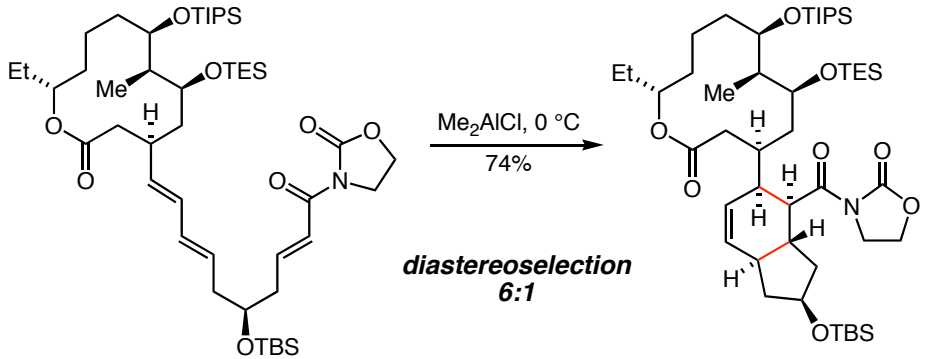

diastereoselection 6:1

Evans, BlackLepicidin Synthesis, *JACS*, **1993**, *115*, 4497

A Complex DA Application: The Synthesis of Chlorothricolide

Roush, Sciotti *J. Am. Chem. Soc.* **1998**, *120*, 7411-7419.

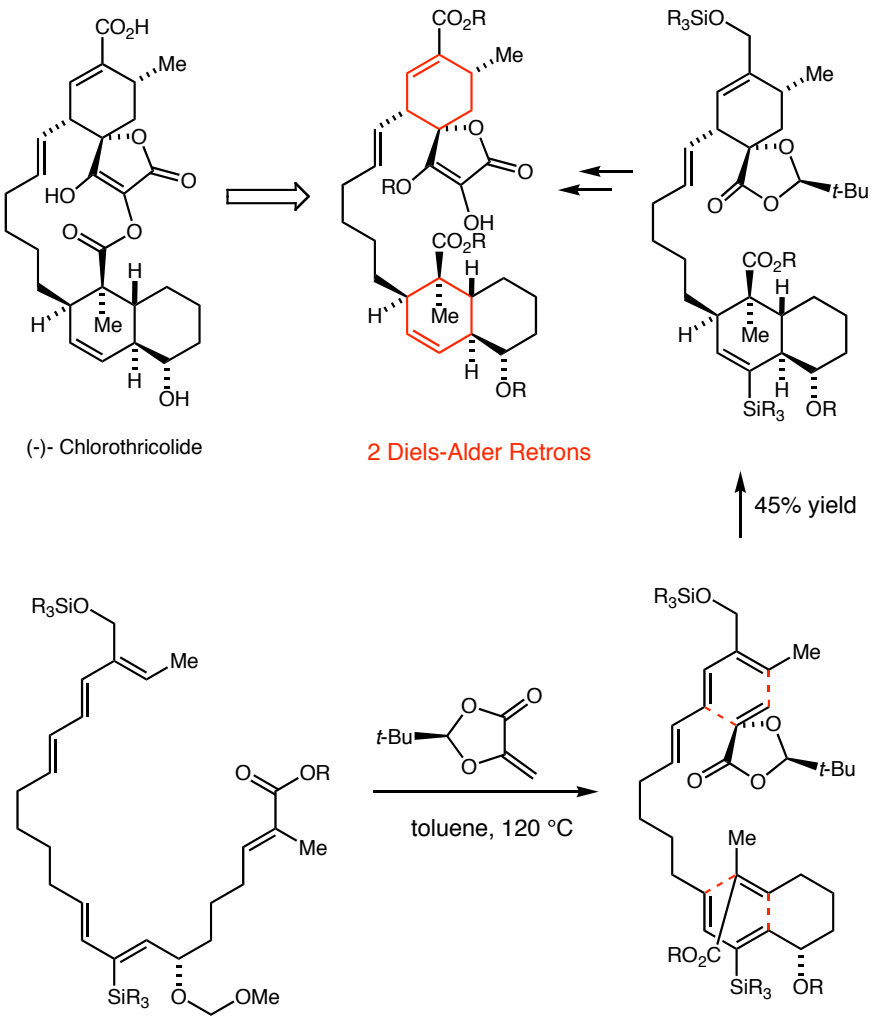

The Intramolecular Diels-Alder Reaction

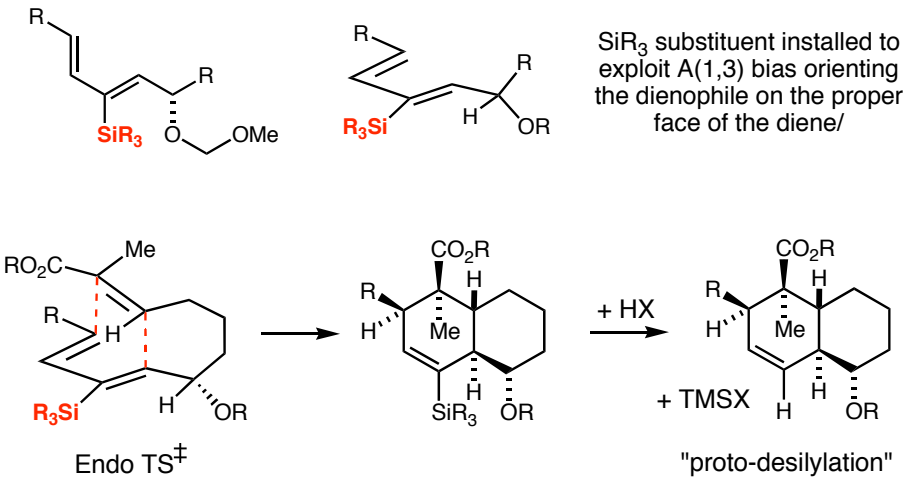

The Bimolecular Diels-Alder Reaction

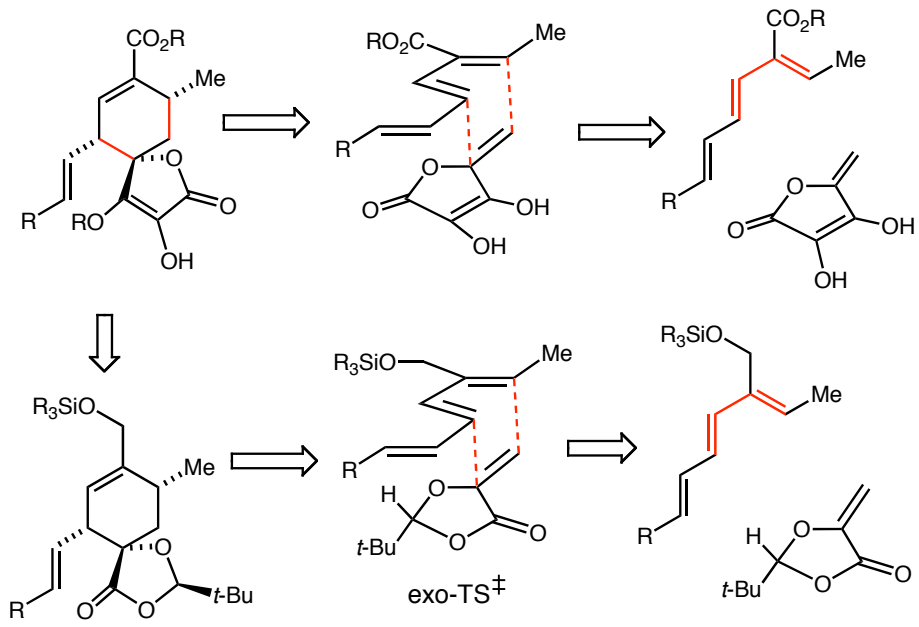

Roush had earlier shown that this dienophile is quite exo-selective

Structures of FR182877 & Hexacyclinic acid

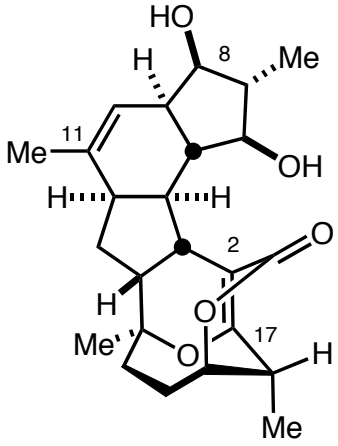

(—)-FR182877

isolated from *Streptomyces sp.#9885*

cytotoxic (IC_{50} <73 ng/ml): MCF-7, A549, HT-29, Jurkat, P388, B16.
Sato, B. *J. Antibiot.* **2000**, 123, 204, 615.
Corrected Structure: *J. Antibiot.* **2002**, C-1.

Structural Differences:

Acylation at C_8 hydroxyl

Oxidation at C_{11}

endo vs. *exo* Diels-Alder retron

Hydration across C_2-C_{17} double bond

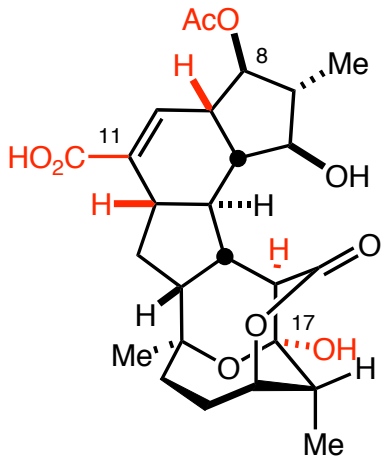

Hexacyclinic Acid

isolated from *Streptomyces cellulosae* (strain S1013)

14 μmol/L cyctotoxicity (HMO2, HEPG2, and MCF7)
Hofs, R., et al. *Angew. Chem. Int. Ed.* **2000**, *39*, 3258.

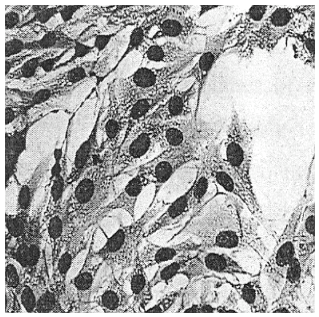

BHK cells: Control

FR182877

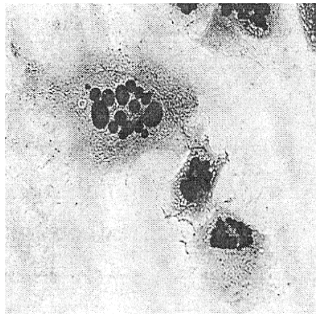

Taxol

Hypothesis: A Transannular Diels-Alder Cycloaddition Cascade

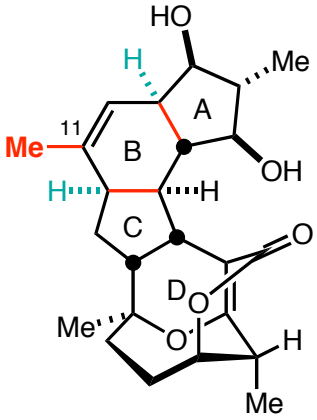

FR182877

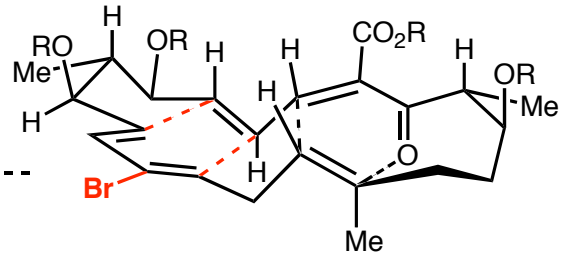

endo-TS‡

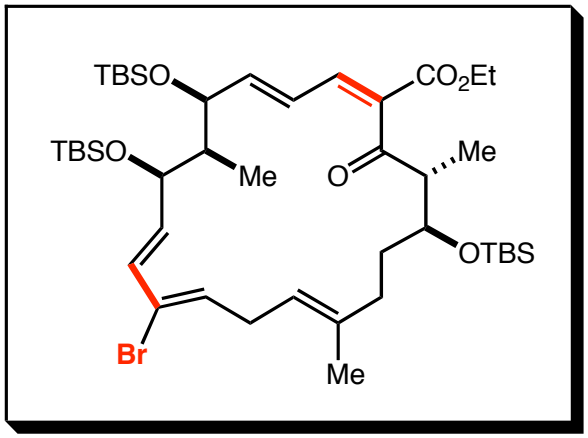

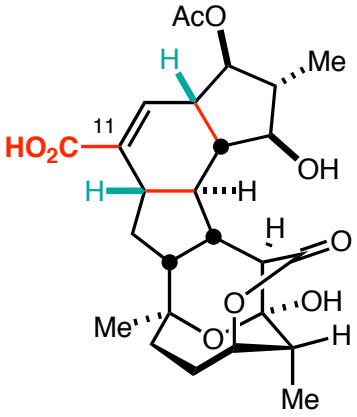

Hexacyclinic acid

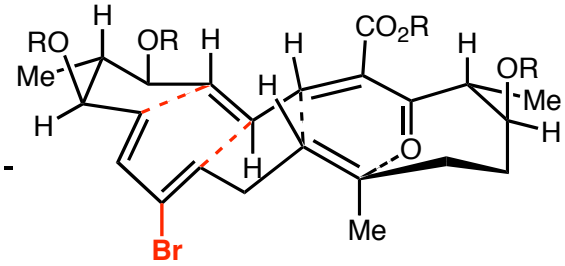

exo-TS‡

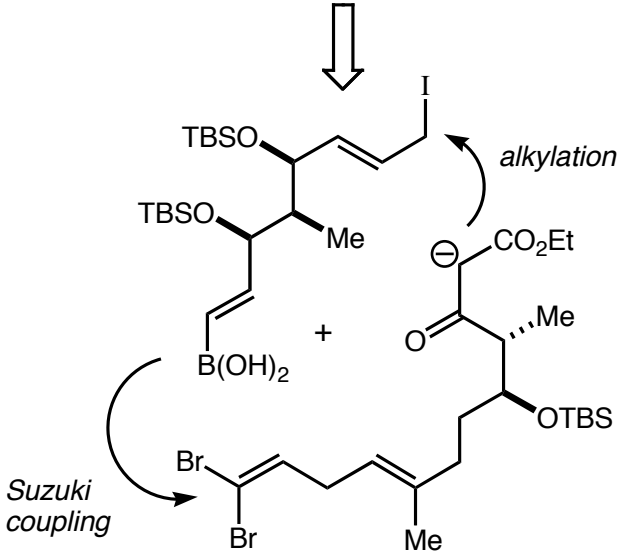

Evans & Starr, JACS **2003,** *125, 13531*

Sorensen, JACS **2003,** *125, 5393*

Diels-Alder Cycloaddition Cascade Stereochemical Options

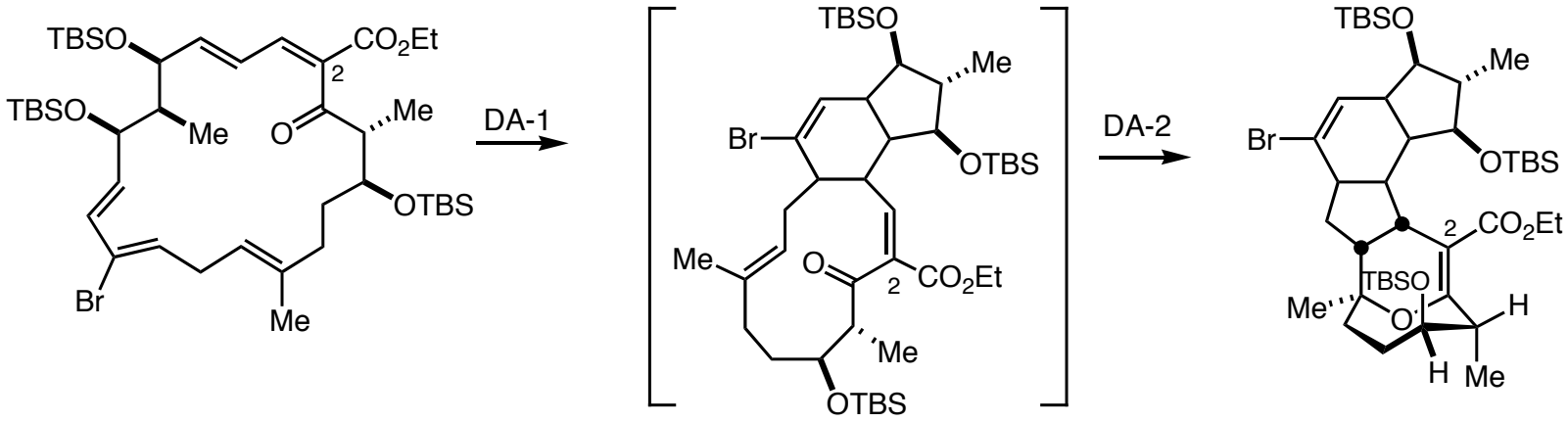

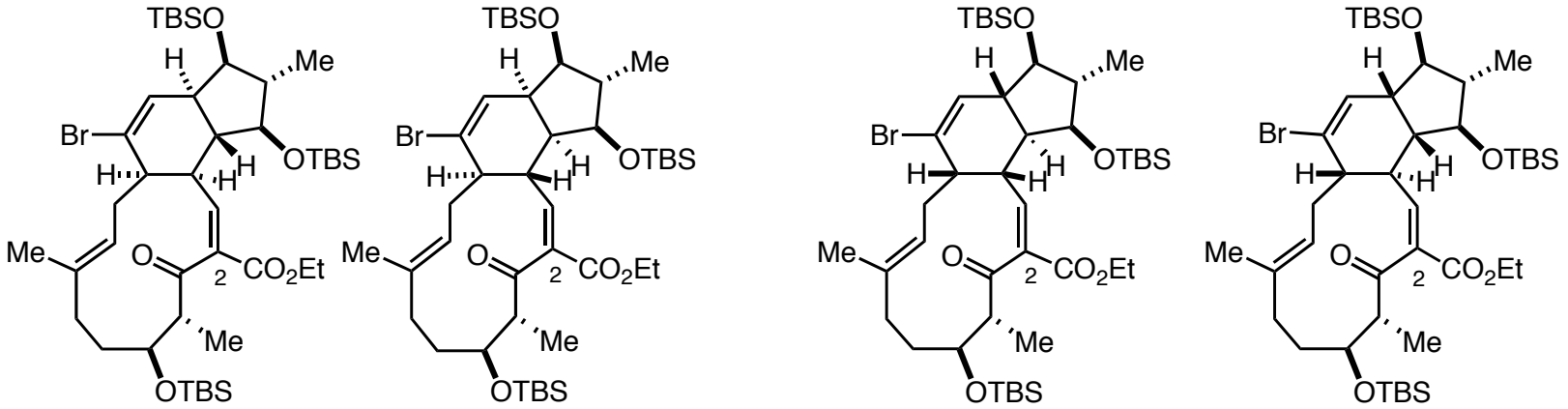

The first cycloaddition must be diastereoselective!!

Analysis of Face Selectivities of the Cycloaddition Steps

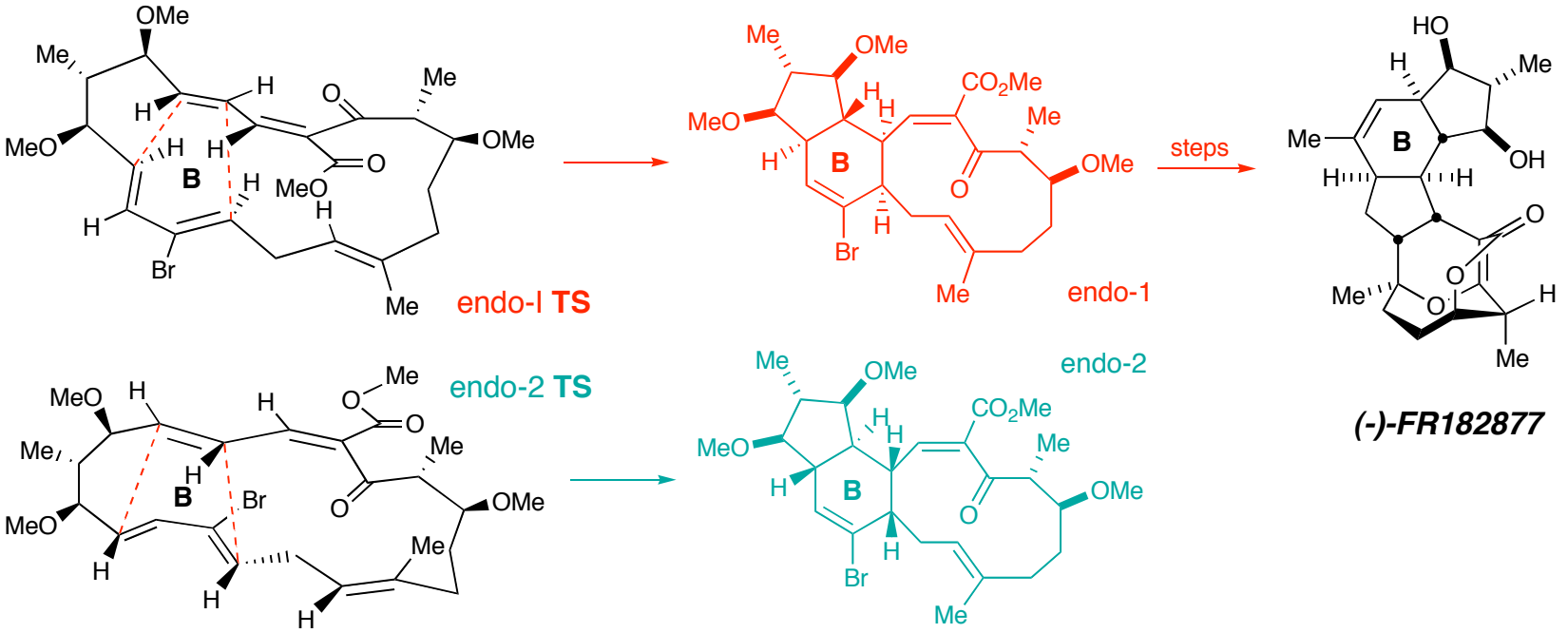

Analysis Procedure: Carry out semi-empirical calculations on transition structures where the forming bonds are varied from 2.9 → 2.1Å. For this analysis, a symmetrical transition state is presumed.

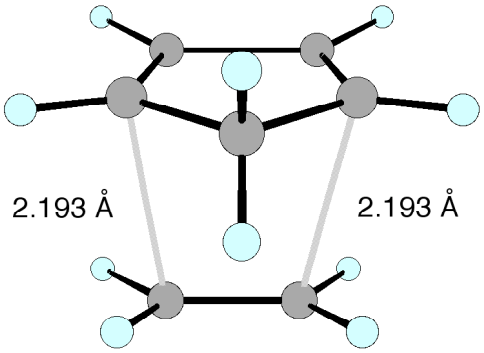

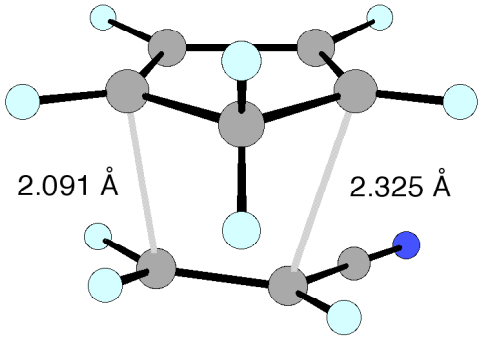

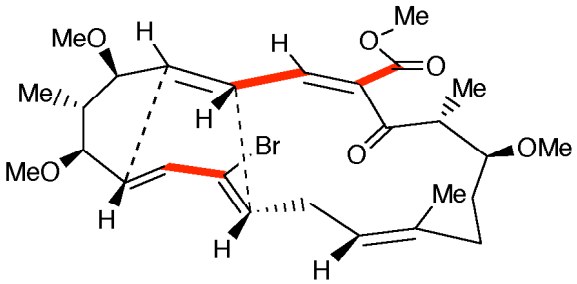

dihedral angle restrictions employed in calculations

Houk *Angew. chem. Int. Ed.* **1992**, *31*, 682-708

Analysis of Face Selectivities of the Cycloaddition Steps

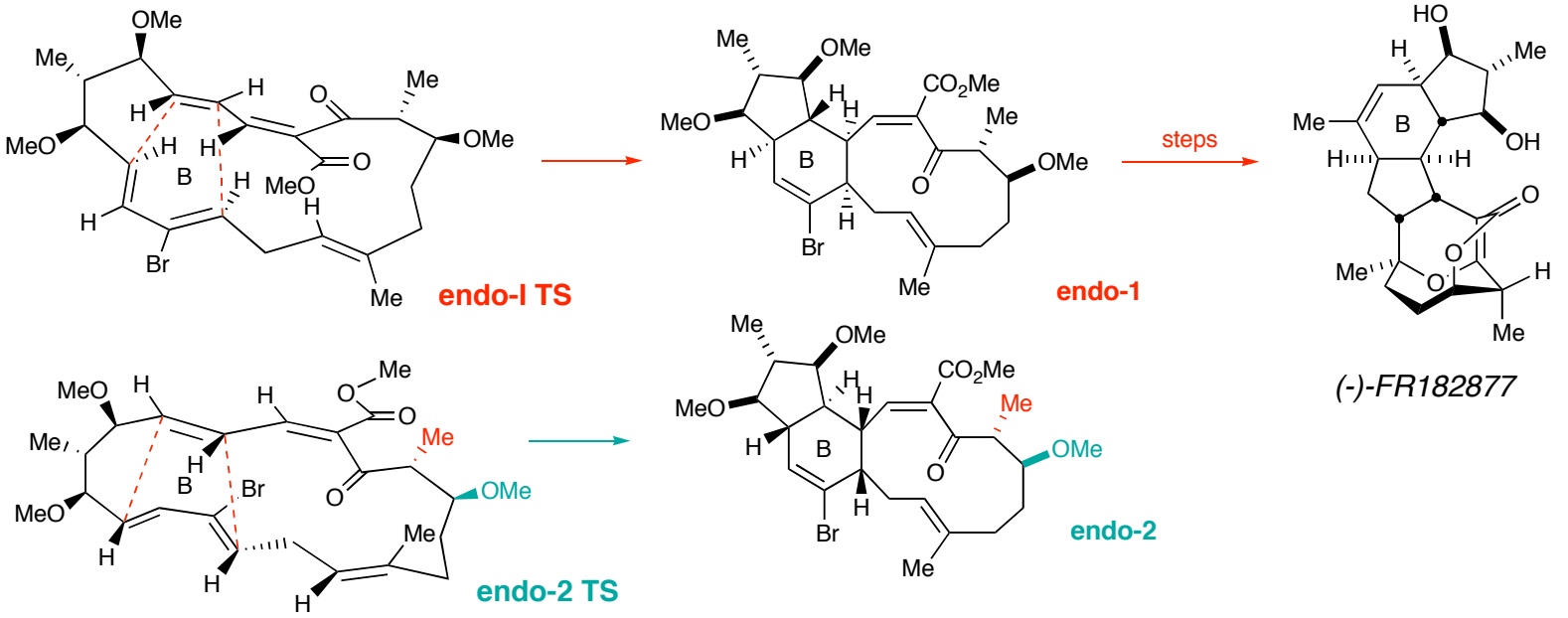

Semi-empirical calculations (PM3) carried out on all of the indicated macrocycles

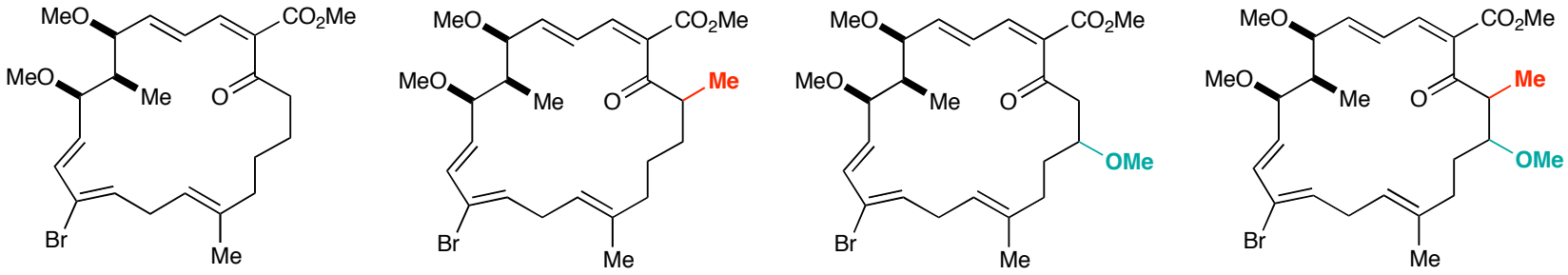

control

endo-I TS ~ **endo-2 TS**

(19R), (19S)

(18R), (18S)

all 4 diastereoisomers

Evans & Starr, JACS **2003,** *125, 13531*

DA face selectivity controlled by by C_{18}–C_{19} stereocenters

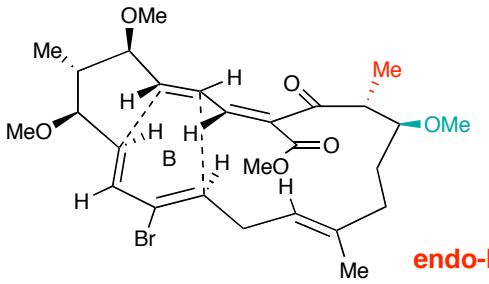

endo-I TS

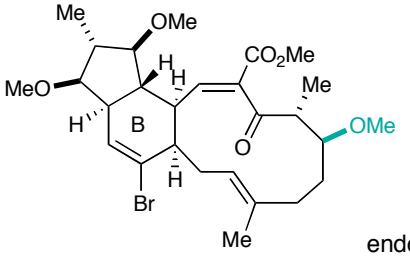

endo-1

steps

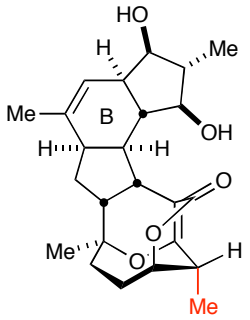

(-)-FR182877

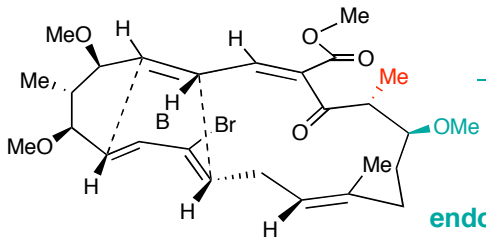

endo-2 TS

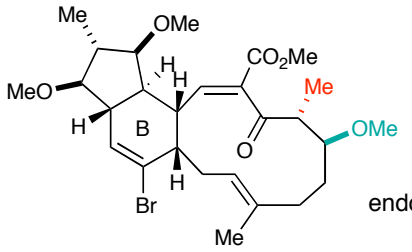

endo-2

$\Delta\Delta E^{\ddagger}$ = 5–9 kcal/mol @ 2.1 Å

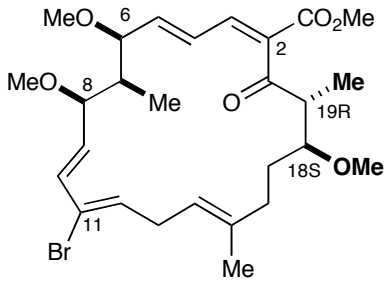

(natural configuration)

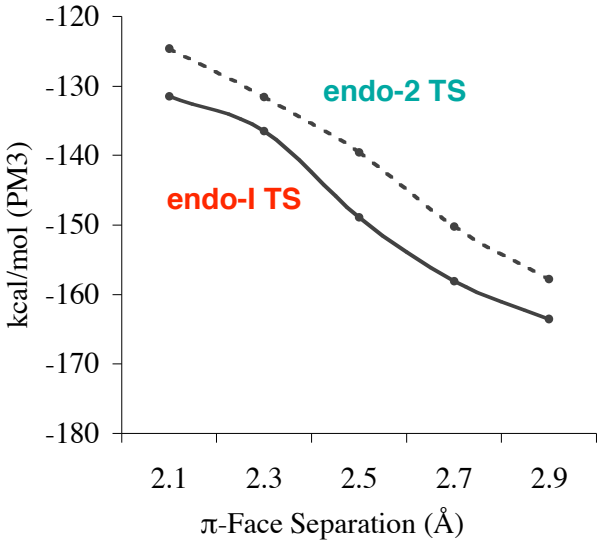

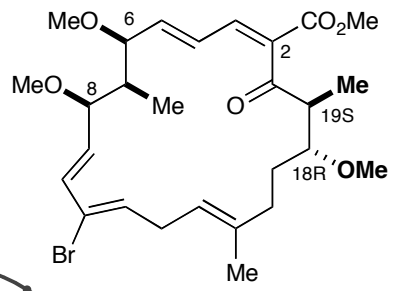

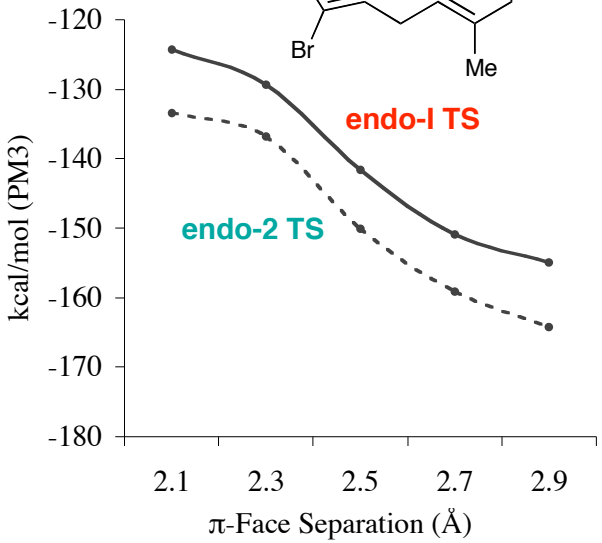

The Transannular Diels-Alder Step

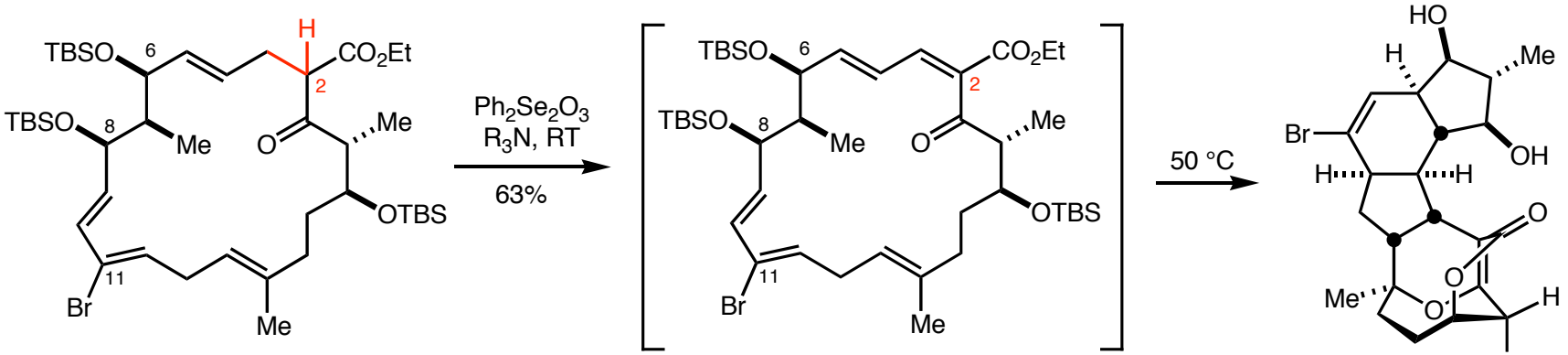

Intermediate

Selenium byproducts removed by hexane precipitation.
Intermediate heated at 50 °C

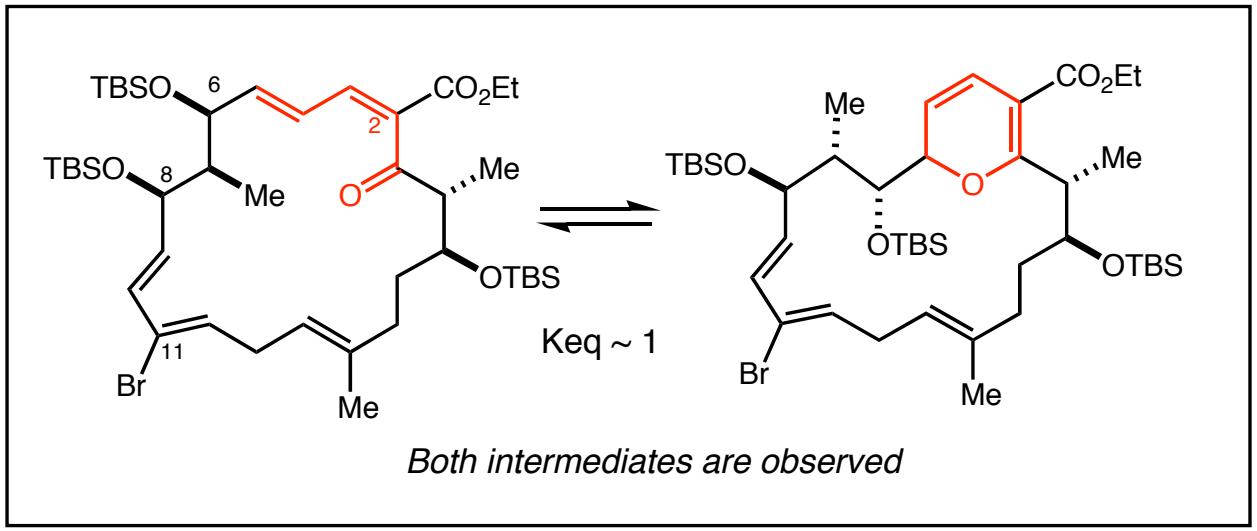

Both intermediates are observed

Summary of Cycloaddition Cascade

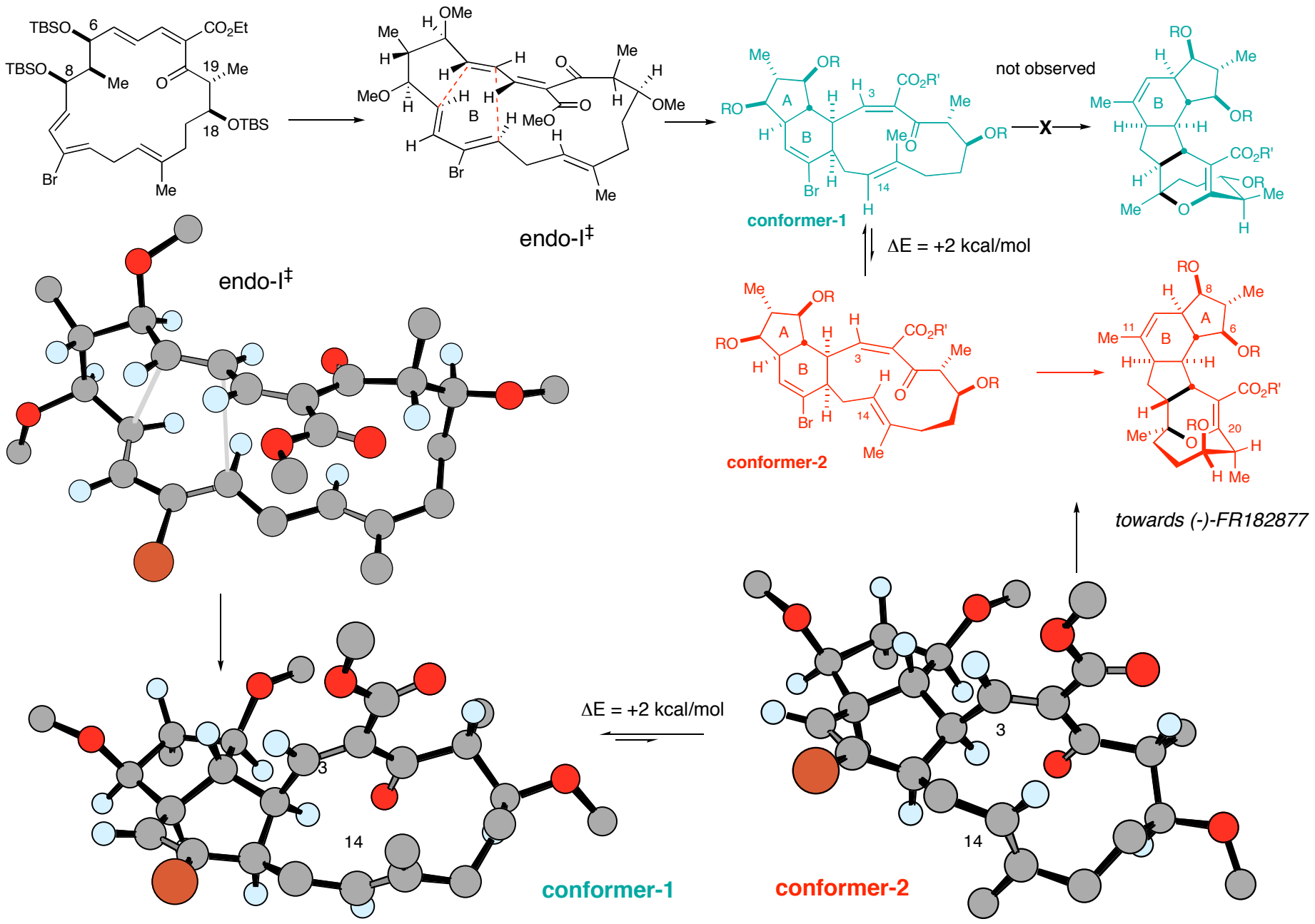

Hypothesis: A Transannular Diels-Alder Cycloaddition Cascade

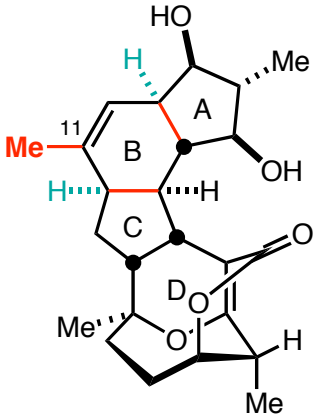

FR182877

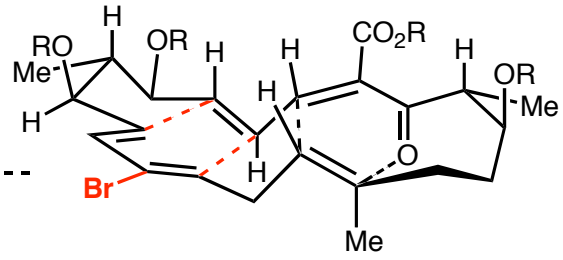

endo-TS‡

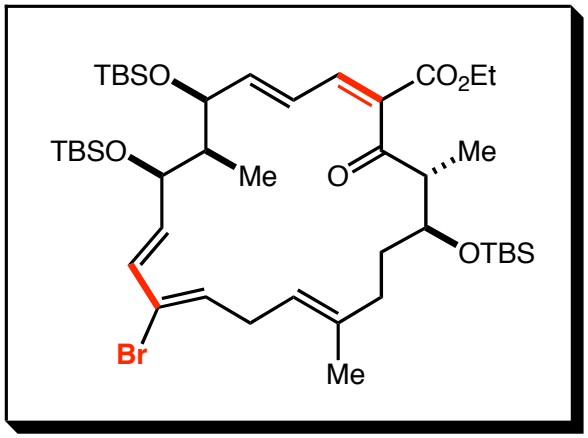

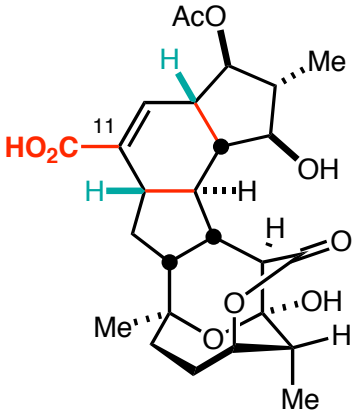

Hexacyclinic acid

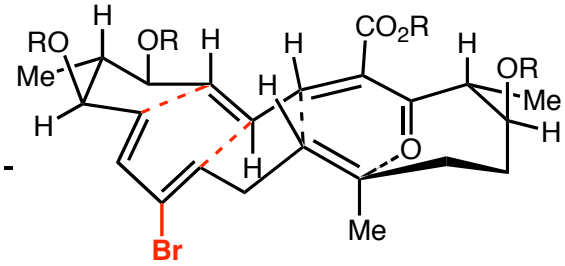

exo-TS‡

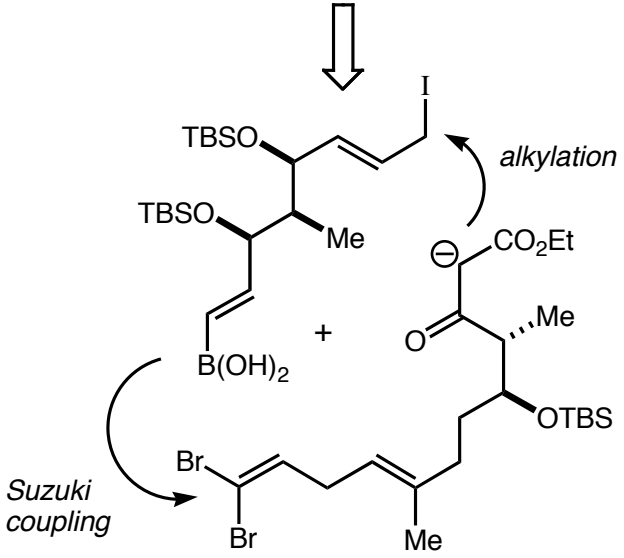

Evans & Starr, JACS **2003,** *125, 13531*

Sorensen, JACS **2003,** *125, 5393*

http://www.courses.fas.harvard.edu/colgsas/1063

Chemistry 206

Advanced Organic Chemistry

Lecture Number 18

Cycloaddition Reactions-3

■ **The Diels-Alder Reaction**
Enantioselective Processes

■ Reading Assignment for week:

Carey & Sundberg: **Part A**; Chapter 11
Concerted Pericyclic Reactions

Carey & Sundberg: **Part B**; Chapter 6
Cycloadditions, Unimolecular Rearrangements
Thermal Eliminations

"*Chiral Bis(oxazoline) Copper (II) Complexes: Versatile Catalysts for Enantioselective Cycloaddition, Adol, Michael and Carbonyl Ene Reactions*". Johnson, J. S.; Evans, D. A. *Acc. Chem. Res.* **2000**, *33*, 325-335. **(handout)**

The formyl C–H…O hydrogen bond as a critical factor in enantioselective Lewis-acid catalyzed reactions of aldehydes, Corey, Lee, *Chem Commun.* **2001,** 1321 **(handout)**

New Strategies for Organic Catalysis: The First Highly Enantioselective Organocatalytic Diels-Alder Reaction, MacMillan, D. *JACS* **2000**, *122*, 4243 **(handout)**

D. A. Evans

Monday
October 30, 2006

The Diels-Alder Cycloaddition Reactions

"Diels-Alder Reactions". Evans, D. A.; Johnson J. S. In Comprehensive Asymmetric Catalysis, Jacobsen, E. N.; Pfaltz, A.; and Yamamoto, H. Editors; Springer Verlag: Heidelberg, **1999**; Vol III, 1178-1235 **(pdf)**

The Diels-Alder Reaction in Total Synthesis, K. C. Nicolaou, *Angew Chem. Int. Ed.* **2002**, *41*, 1668-1698 **(pdf)**

Catalytic Enantioselective Diels–Alder Reactions: Methods, Mechanistic Fundamentals, Pathways, and Applications, E. J. Corey, *Angew Chem. Int. Ed.* **2002**, *41*, 1650-1667 **(pdf)**

Chemistry and Biology of Biosynthetic Diels–Alder Reactions
Emily M. Stocking and Robert M. Williams, *Angew Chem. Int. Ed.* **2003**, *42*, 3078-3115 **(pdf)**

Chiral Lewis Acids in Catalytic Asymmetric Reactions, Narasaka, *Synthesis*, **1991**, 1-11 **(pdf)**

Carbonyl-Lewis Acid Complexes Schreiber, *Angew. Chem. Int. Ed.*, **1990**, *29*, 256-272 **(pdf)**

Problem 363. The C_2-symmetric cationic Cu(II) complex **1** is a chiral Lewis acid catalyst that exhibits good chelating potential. Palomo has reported the utilization of **1** in the catalyzed Diels-Alder reaction is illustrated below (*JACS*, **2003**, *125*, 3943). Provide the absolute stereochemistry of the product of this reaction. Provide a 3-dimensional drawing of the transition state for this reaction.

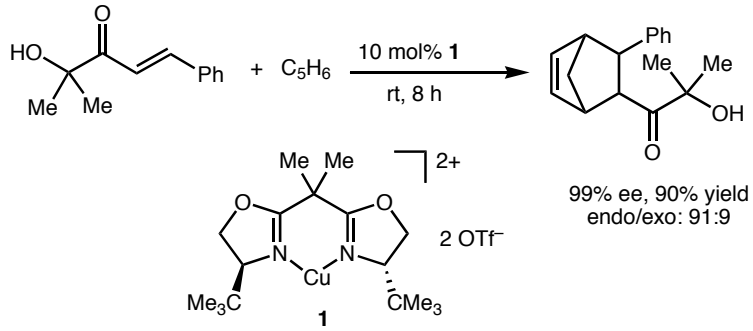

The Design of Enantioselective Diels-Alder Catalysts

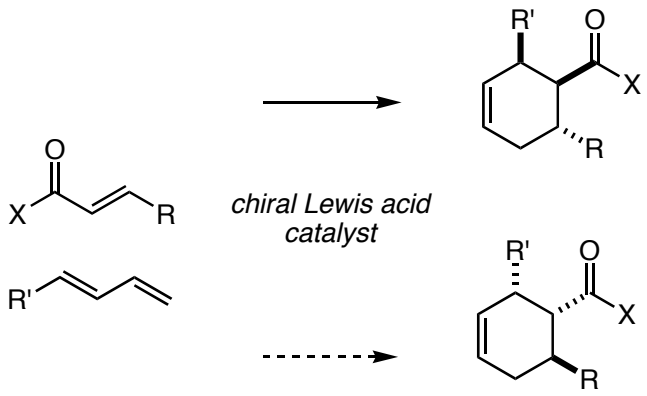

Problem A: Reacting conformation of the dienophile

The S-cis versus S-trans dienophile conformation is coupled to the geometry of the Lewis acid-dienophile complex & both issues determine face selection

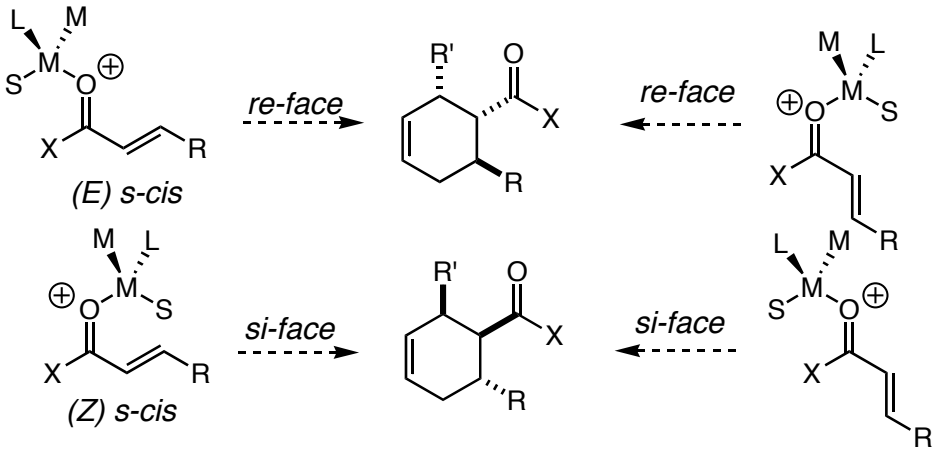

Theoretical Studies on Conformations of Acrolein & Methyl Acrylate & their Lewis Acid Complexes
Houk, *JACS*, **1987**, *109*, 14-23

Problem B: Design of a well-defined Dienophile-LA Complex

Early Empirical Studies

Chiral Lewis Acids in Catalytic Asymmetric Reactions
Narasaka, *Synthesis*, **1991**, 1-11 **(pdf)**

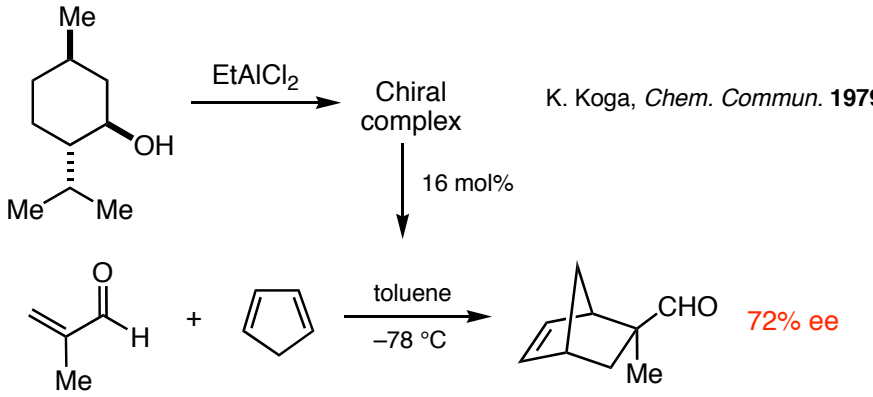

K. Koga, *Chem. Commun.* **1979,** 437

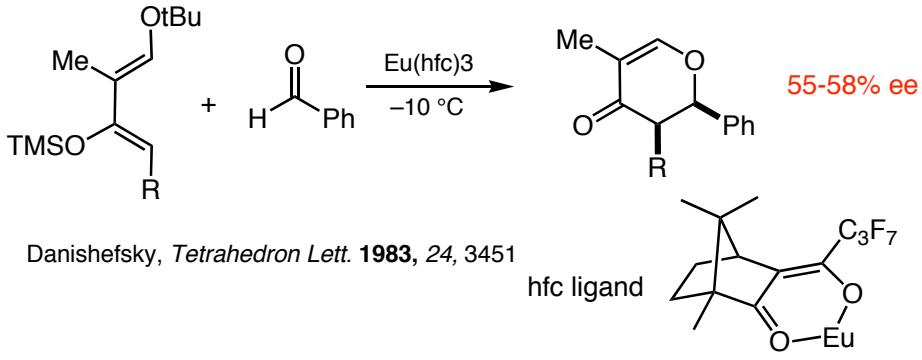

Danishefsky, *Tetrahedron Lett.* **1983,** *24,* 3451

Transition from Chiral Auxiliary Control to Asymmetric Catalysis

with Chapman, Bisaha, *JACS*, **1984**, *106*, 4261, *JACS*, **1988**, *110*, 1238

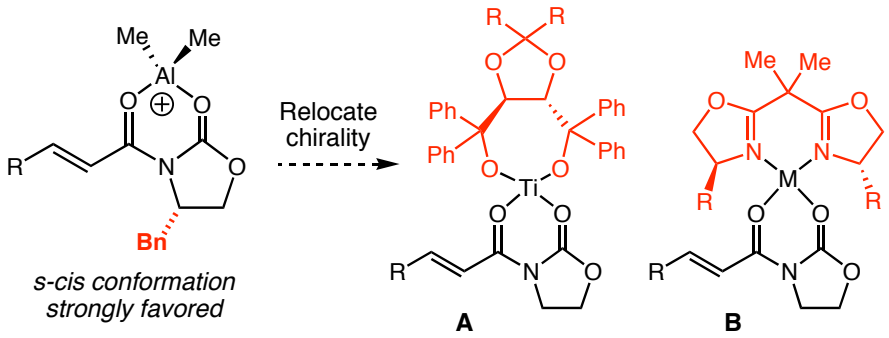

s-cis conformation strongly favored

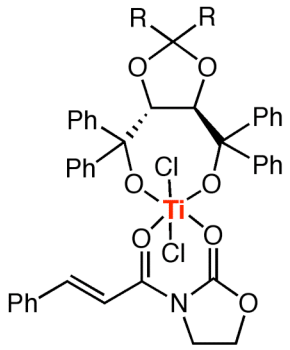

A. Jorgensen, *JACS*, **1995**, *117*, 4435

X-ray structure

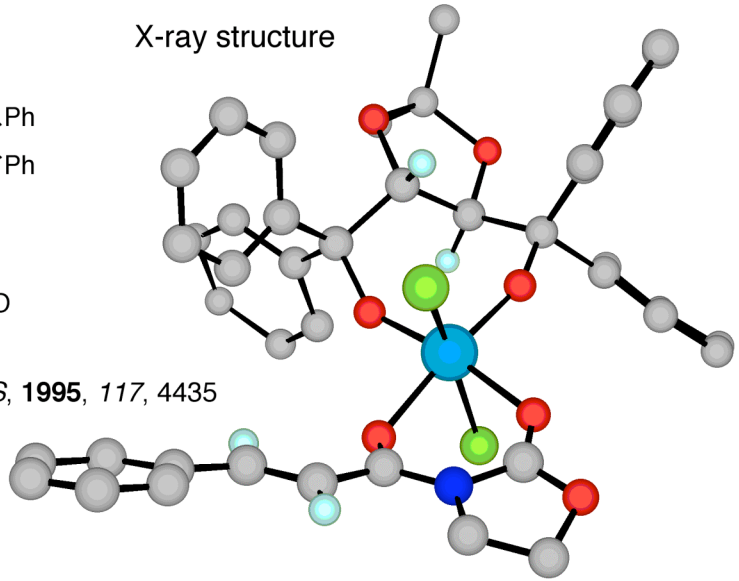

Narasaka *JACS*, **1989**, *111*, 5340

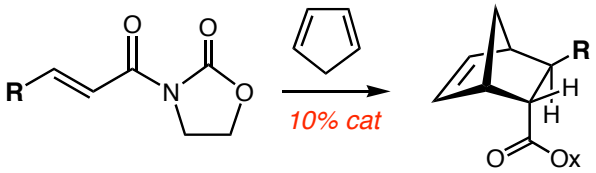

"Endo **4**"

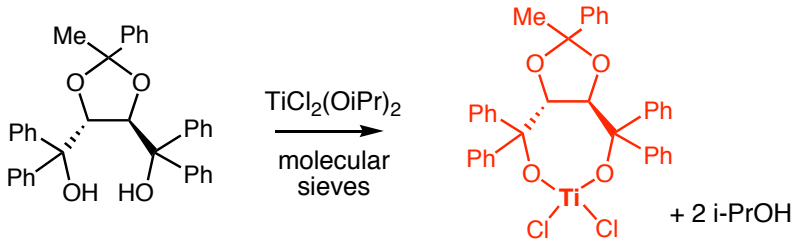

+ 2 i-PrOH

Table III. Asymmetric Diels–Alder Reaction Using a Catalytic Amount of Titanium Reagent

R	reaction temp/°C	endo/exo[a] **4**:**5**	% yield	optical purity of **4**/% ee[b]
Me	0	92:8	87	91
Ph	room temp	88:12	72	64
n-Pr	0	91:9	79	72
H	−40	96:4	93	64

The hunt for the "best" catalytic metal center has begun!

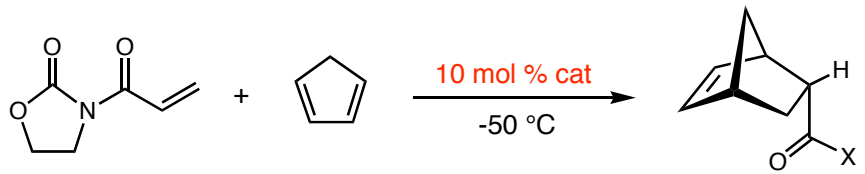

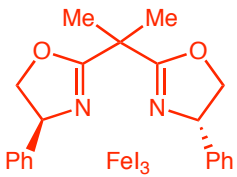

76% ee

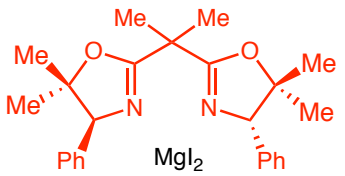

86% ee

Fe(3+) Corey *JACS*, **1991**, *113*, 728; Mg(2+) Corey *Tet. Lett.* **1992**, *45*, 6807

These catalysts are superior for unsubstituted dienophiles

The Diels-Alder Reaction: Enantioselective Catalysis

Cu(II) Lewis Acids: Evans, Miller, Lectka, *JACS* **1993**, *115*, 6460.

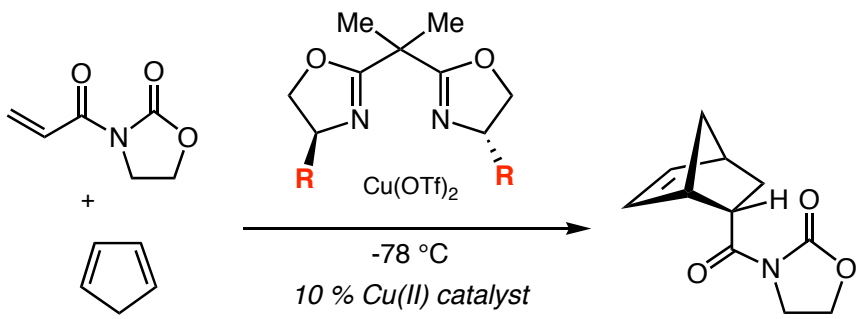

Catalyst (R)	Endo ee
R = Ph	30%
R = $CHMe_2$	58%
R = CMe_3	>98%

Temp	Endo ee
–50 °C	98%
0 °C	92%
25 °C	86%

Bis(oxazoline)Cu(OTf)$_2$•2H$_2$O X-ray Structure

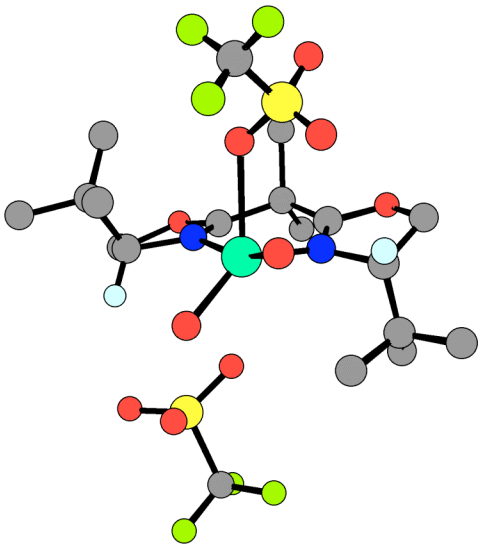

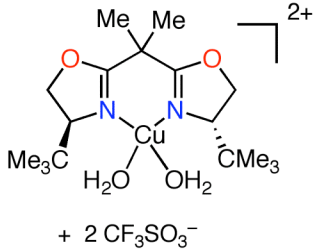

Bis(oxazoline)Cu(SbF$_6$)$_2$•2H$_2$O X-ray Structure

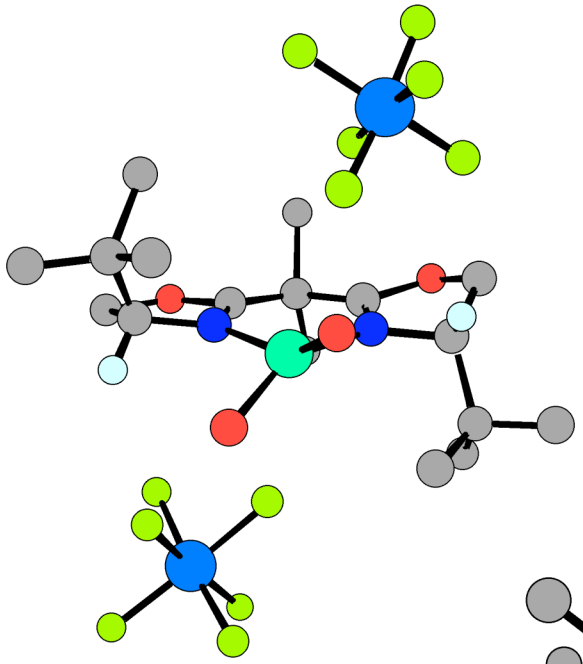

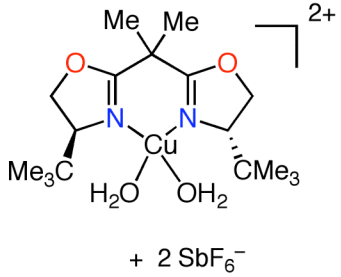

Computer generated complex
PM3

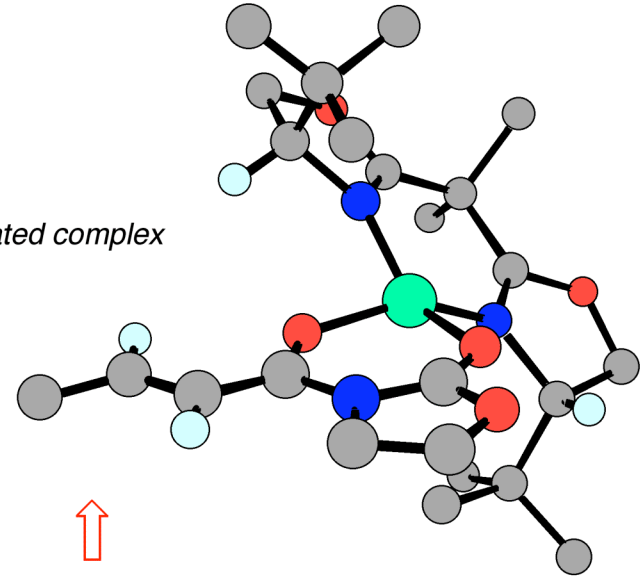

All reactions occur from this face

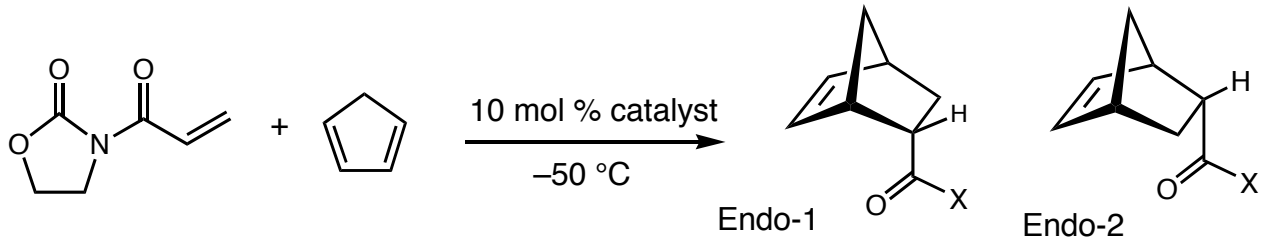

Endo/Exo = 94:6	Endo/Exo = 95:5	Endo/Exo = 97:3
Endo ratio = 88:12 (Endo-2)	Endo ratio = 93:7 (Endo-2)	Endo ratio = 99:1 (Endo-1)

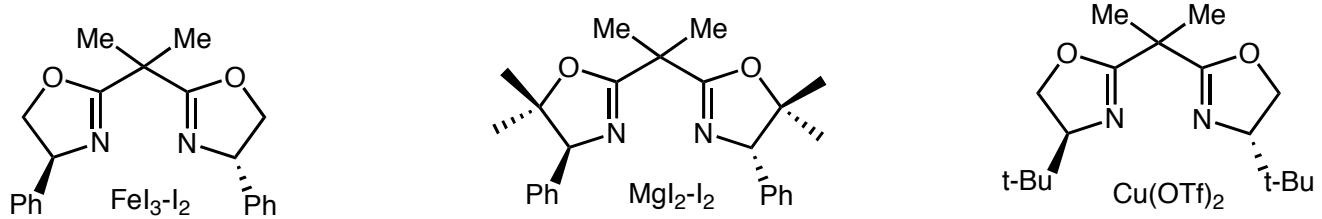

Endo/Exo = 76:24	Endo/Exo = 80:20	Endo/Exo = 96:4
Endo ratio = 66:34	Endo ratio = 50:50	Endo ratio = 98:2

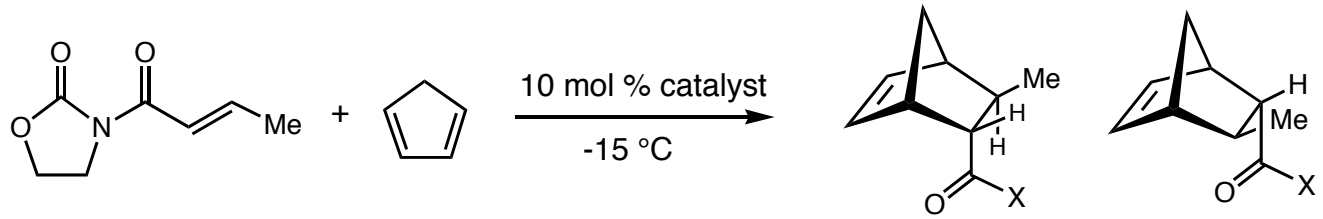

with S. Miller, JACS **1999,** *121,* 7559-7573

Computer generated structures of the Cu(t-bu-box)(2+) & Zn(Ph-box)(2+)-dienophile complexes

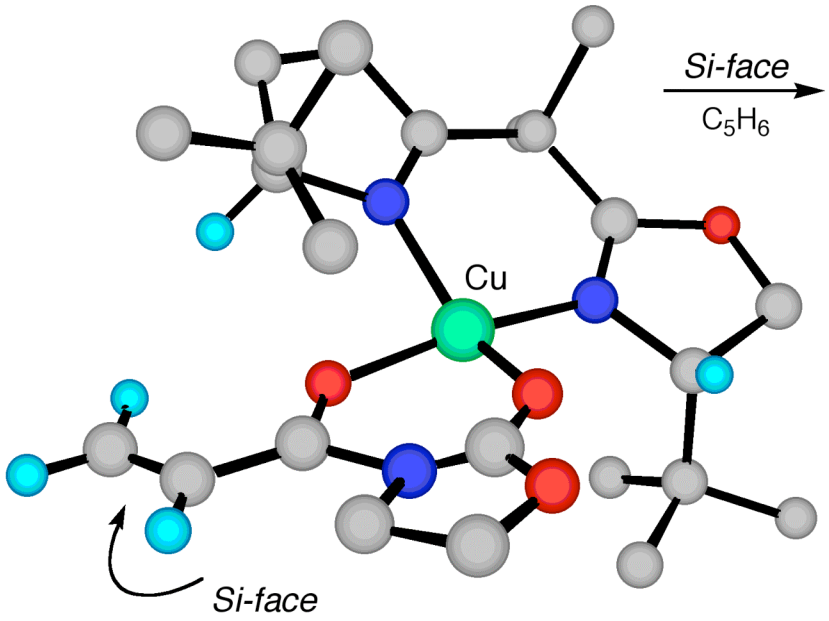

Optimal ligand for Square planar geometry

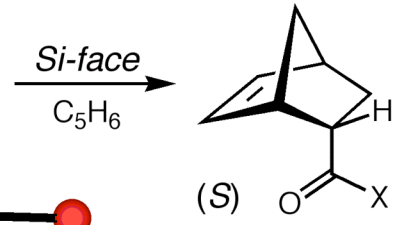

Endo-1

Endo-2

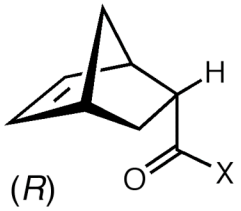

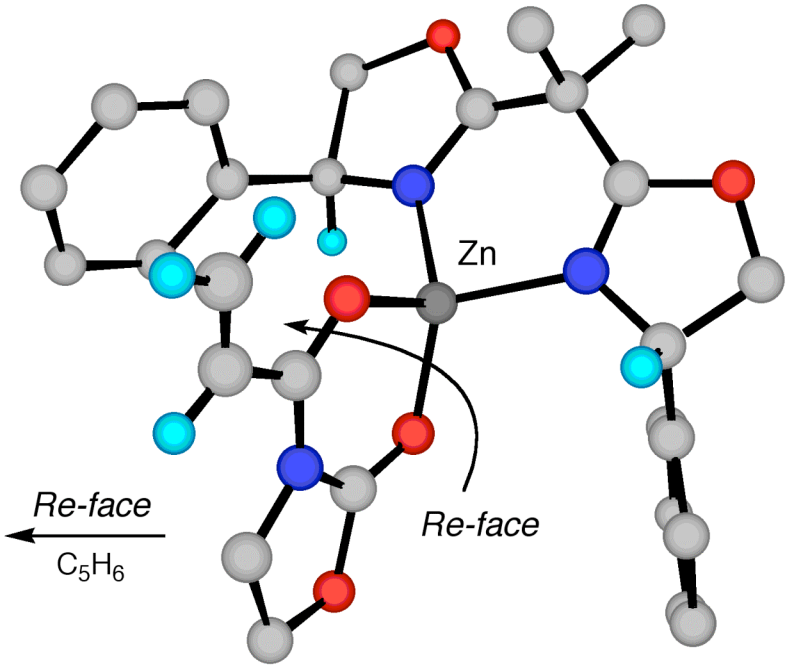

Optimal ligand for tetrahedral geometry

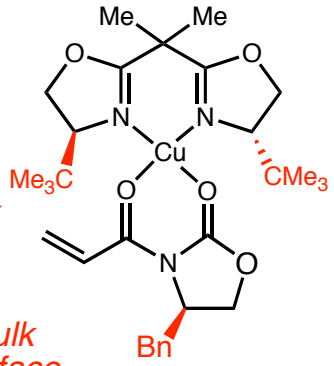

steric bulk on same face

C_5H_6, -78 °C

Matched case if Cu center square-planar

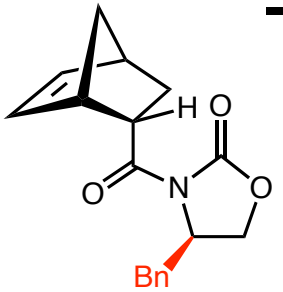

Expected Outcome

highly diastereoselective

catalyst control

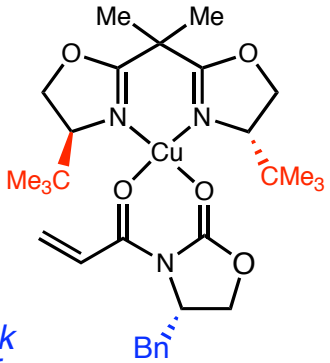

steric bulk on opposite faces

C_5H_6, -78 °C

Mismatched case if Cu center square-planar

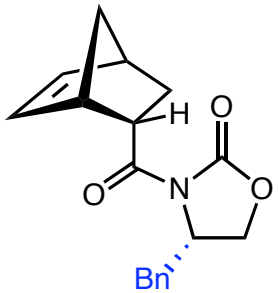

poorly diastereoselective

slow reaction

torsional pressure

Tetrahedral Complex

C_5H_6, -78 °C

Matched case if Cu center Tetrahedral

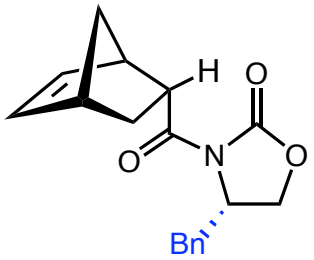

substrate control

This test for torsional rigidity may be applied to any catalyst-substrate complex

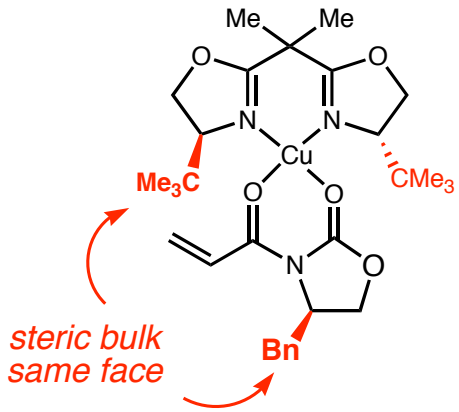

C_5H_6, -78 °C

Matched case if Cu center square-planar

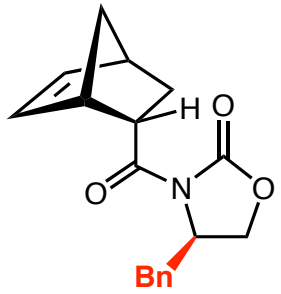

Outcome

Endo(1): *Endo*(2) ≥ 99:1

100% conversion

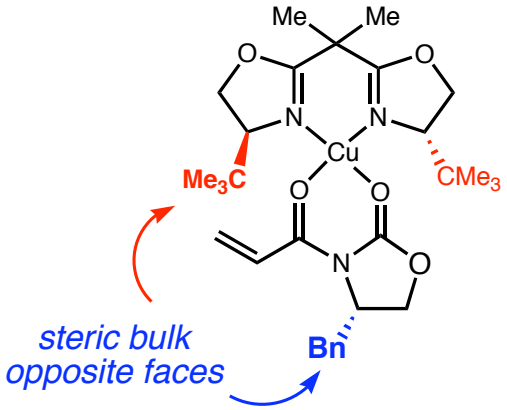

C_5H_6, -78 °C

Mismatched case if Cu center square-planar

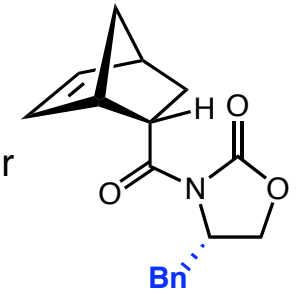

Endo(1): *Endo*(2) = 68:32

20% conversion

Catalyst control

Cu(II) strongly resists distortion from square planar to tetrahedral. Other metals such Mg(II), Fe(III), and Zn(II) succumb to internal stereochemical "pressure."

JACS **1999,** *121,* 7559-7573; *JACS* **1999,** *121,* 7582-7594

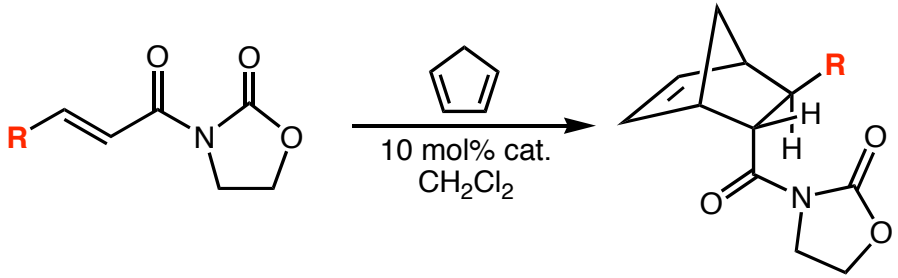

	counterion	time	endo ee	yield
R = Me, +25 °C	X = TfO^-	8 h	94% ee	95%
	X = SbF_6^-	8 h	96% ee	98%

	counterion	time	endo ee	yield
R = Ph, +25 °C	X = TfO^-	24 h	90% ee	85%
	X = SbF_6^-	24 h	96% ee	95%

	counterion	time	endo ee	yield
R = Cl, +25 °C	X = TfO^-	24 h	53% ee	----
	X = SbF_6^-	18 h	94% ee	95%

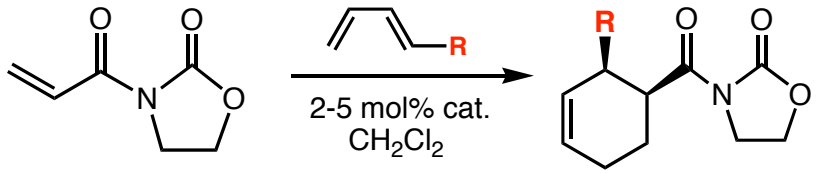

	counterion	time	endo ee	yield
R = Me, +25 °C	X = TfO^-	12 h	86% ee	72%
	X = SbF_6^-	12 h	94% ee	89%

	counterion	time	endo ee	yield
R = Ph, -20 °C	X = TfO^-	12 h	86% ee	72%
	X = SbF_6^-	24 h	97 % ee	95%

	counterion	time	endo ee	yield
R = OAc, 0 °C	X = SbF_6^-	24 h	97 % ee	100%

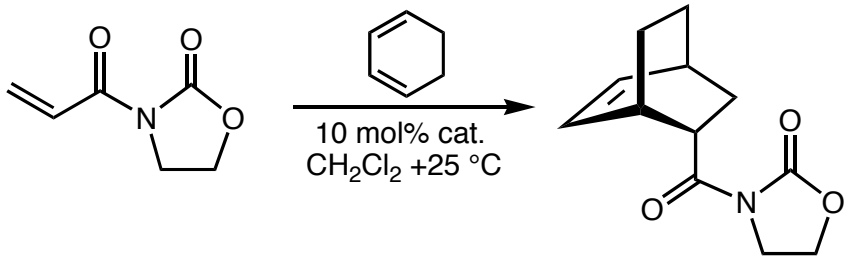

counterion	time	endo ee	yield
X = TfO^-	48 h	82% ee	90%
X = SbF_6^-	5 h	93% ee	90%

JACS **1999**, 121, 7559-7573; *JACS* **1999**, 121, 7582-7594

Extensions may be made to Heterodienes

Jnoff & Ghosez, *JACS* **1999**, *121*, 2617

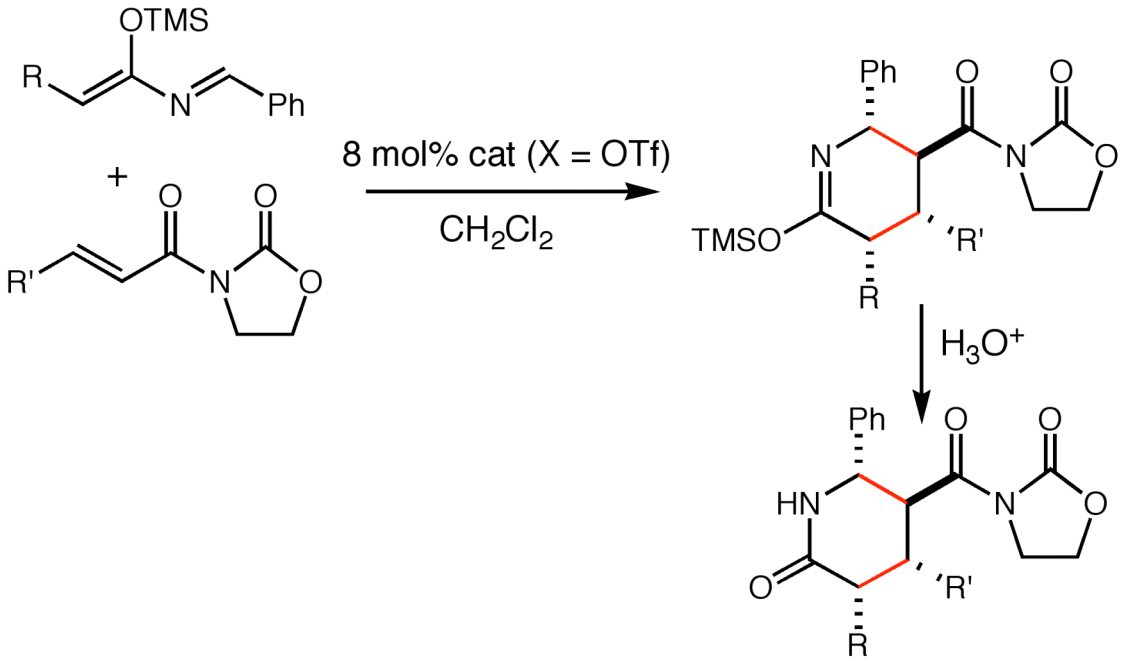

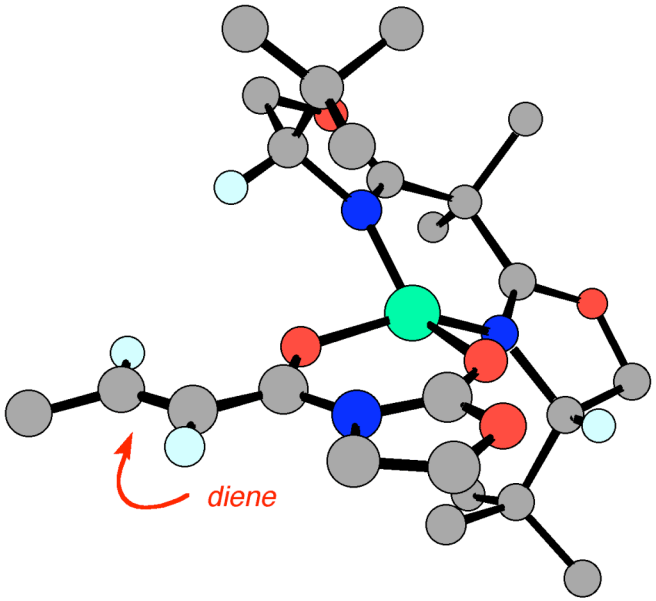

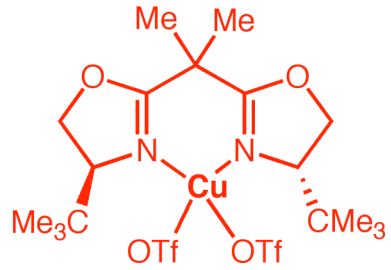

The Catalyst (2-5 mol %)

R	R'	T °C	*endo*/*exo*	yield (%)	% ee
Me	Me	-45	>99:1	80	**95**
Me	Me	rt	>99:1	96	**94**
H	H	-45	6:1	83	**98**
Me	H	-45	>99:1	96	**98**
H	Me	rt	>99:1	80	**93**

Extensions may be made to other Dienophiles

C. Palomo et al., *JACS* **2003**, *125*, 13942-13943

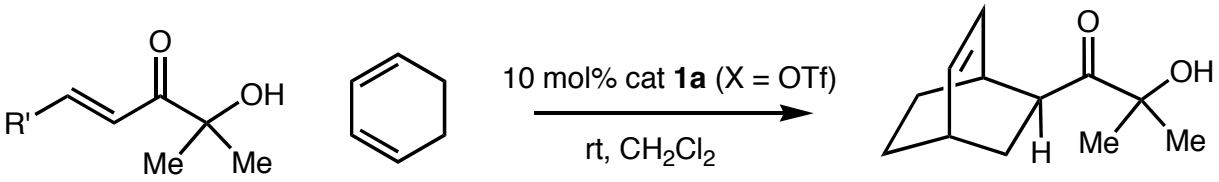

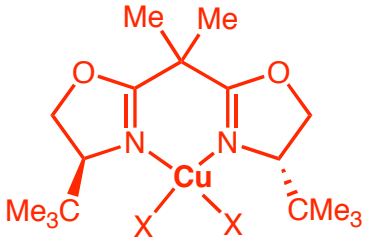

catalyst **1a**: X = OTf
catalyst **1d**: X = SbF_6

endo: exo >99:1
>98% ee, 93% yield

diene	cat.	T, °C	t, h	isom. ratio[b]	*endo:exo*[c]	product	yield, %	ee %[d]
	**1a**	−78	2.5	--	>99:1	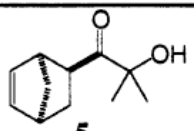 **5**	99	>99
	**1a**	25	2	--	>99:1	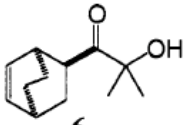 **6**	93	≥98
	**1a**	25	1.5	99:1	--	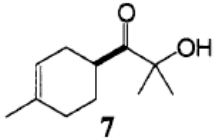 **7**	88	81
	1a	−20	30	>99:1	--		87	88
	1d	−20	14	>99:1	--		85	94
	1d	−20	20	>99:1	--		85	90[e]
	**1a**	−20	20	--	--	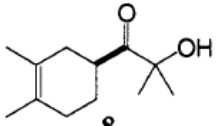 **8**	75	89
	1d	−20	13	--	--		80	94
	1d	−20	20	--	--		90	90[e]
	**1a**	25	8	50:50	--	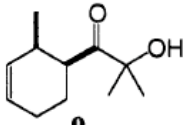 **9**	--	nd
	1d	25	2	76:24	--		--	nd
	1d	−10	15	88:12	--		95	>99

Stereochemical Model

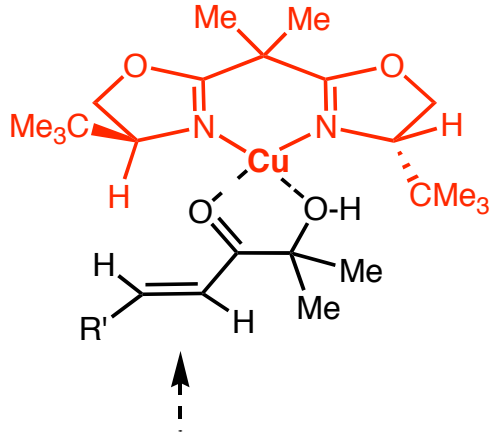

Diene Approach

Cu(box) and Cu(pybox) catalyst-substrate complexes implicated in enantioselective reactions.

"Chiral Bis(oxazoline) Copper (II) Complexes: Versatile Catalysts for Enantioselective Cycloaddition, Adol, Michael and Carbonyl Ene Reactions". Johnson, Evans, *Acc. Chem. Res.* **2000**, *33*, 325-335. **(pdf)**

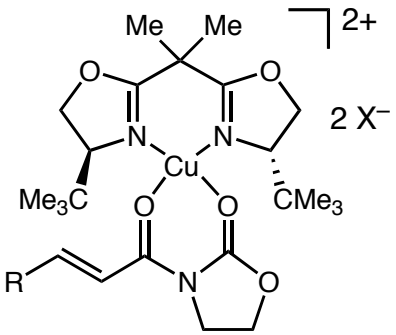

Cycloaddition Reactions
Michael Reactions

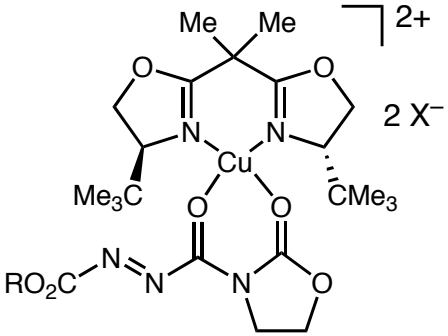

Enol Amination Reactons

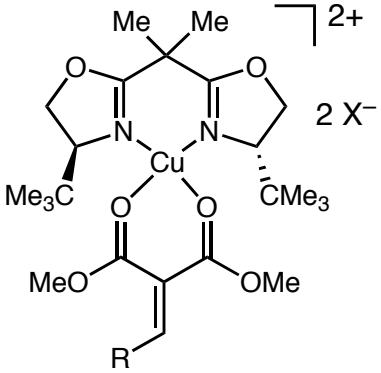

Michael Reactions

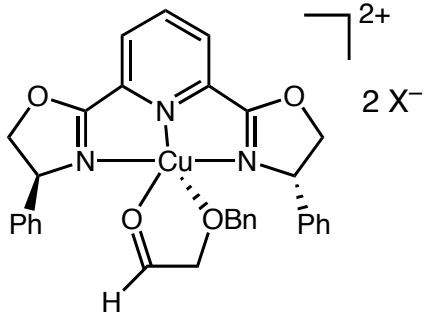

Aldol Reactions

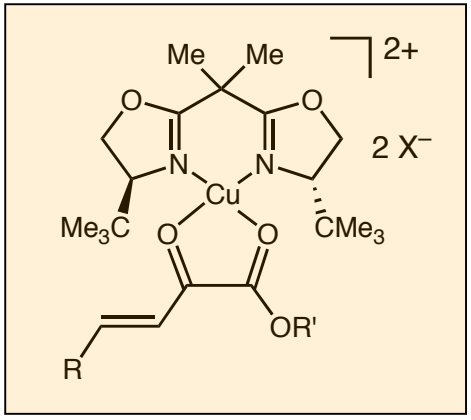

Hetero Diels-Alder Reactions

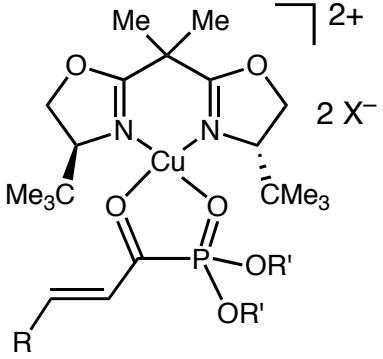

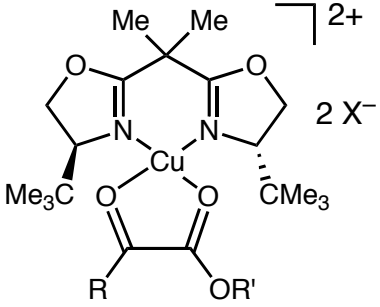

R = H, Cycloaddition Reactions
Ene Reactions

R = Alkyl, Cycloaddition Reactions
Aldol Reactions

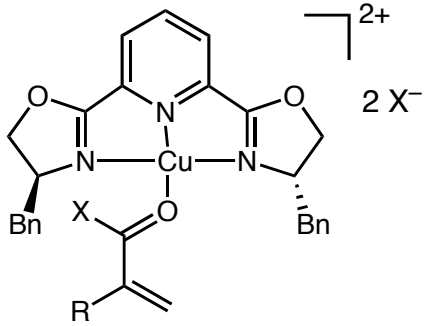

Diels-Alder Reactions

Unsaturated α-Keto Esters in Hetero-Diels-Alder Reactions

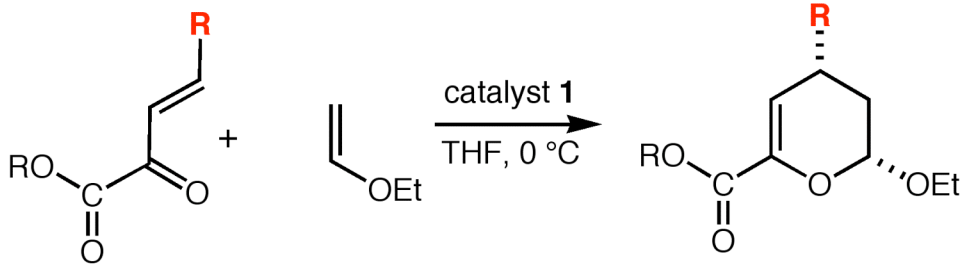

R = Me, Ph, $CHMe_2$, OR, SR,

>95% ee
endo diastereoselection >20:1

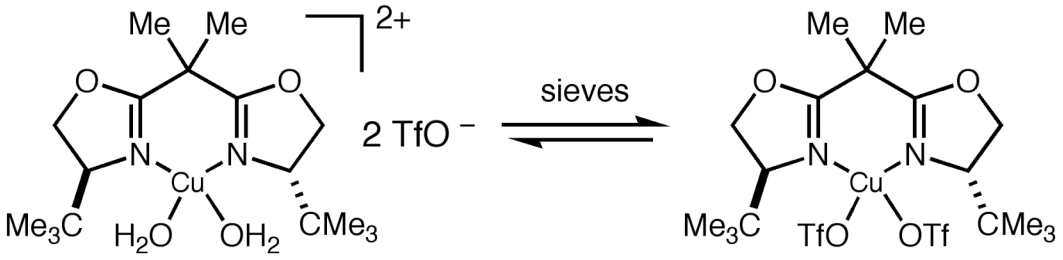

1 (aquo) **1**

The bench-stable aquo complex may be used in the presence of sieves at 2 mol %.

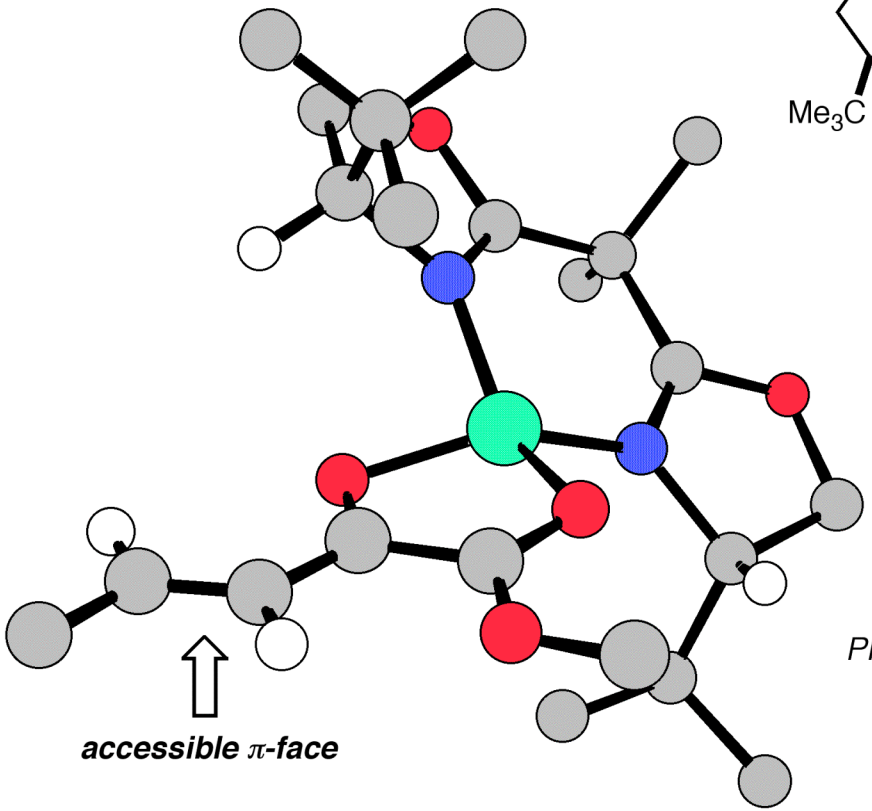

PM3 Structure

with Jeff Johnson & Ed Olhava, *JACS*, **2000**, *122*, 1635

Temperature–Enantioselection Profile for [Cu((S,S)-t-Bu-box)](X)$_2$ Catalysts

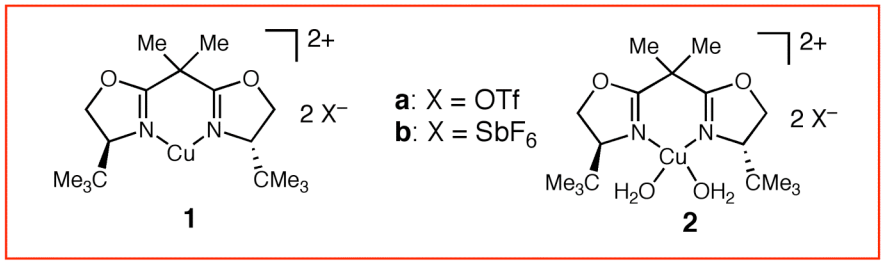

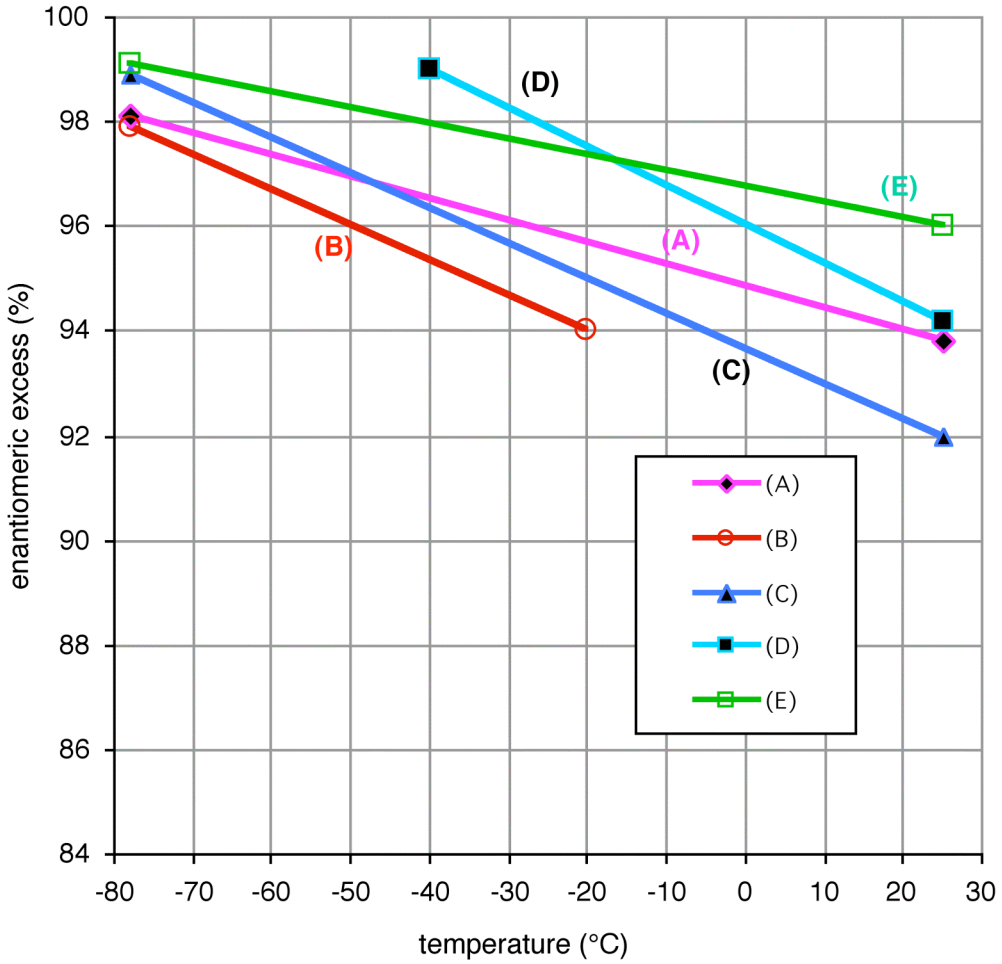

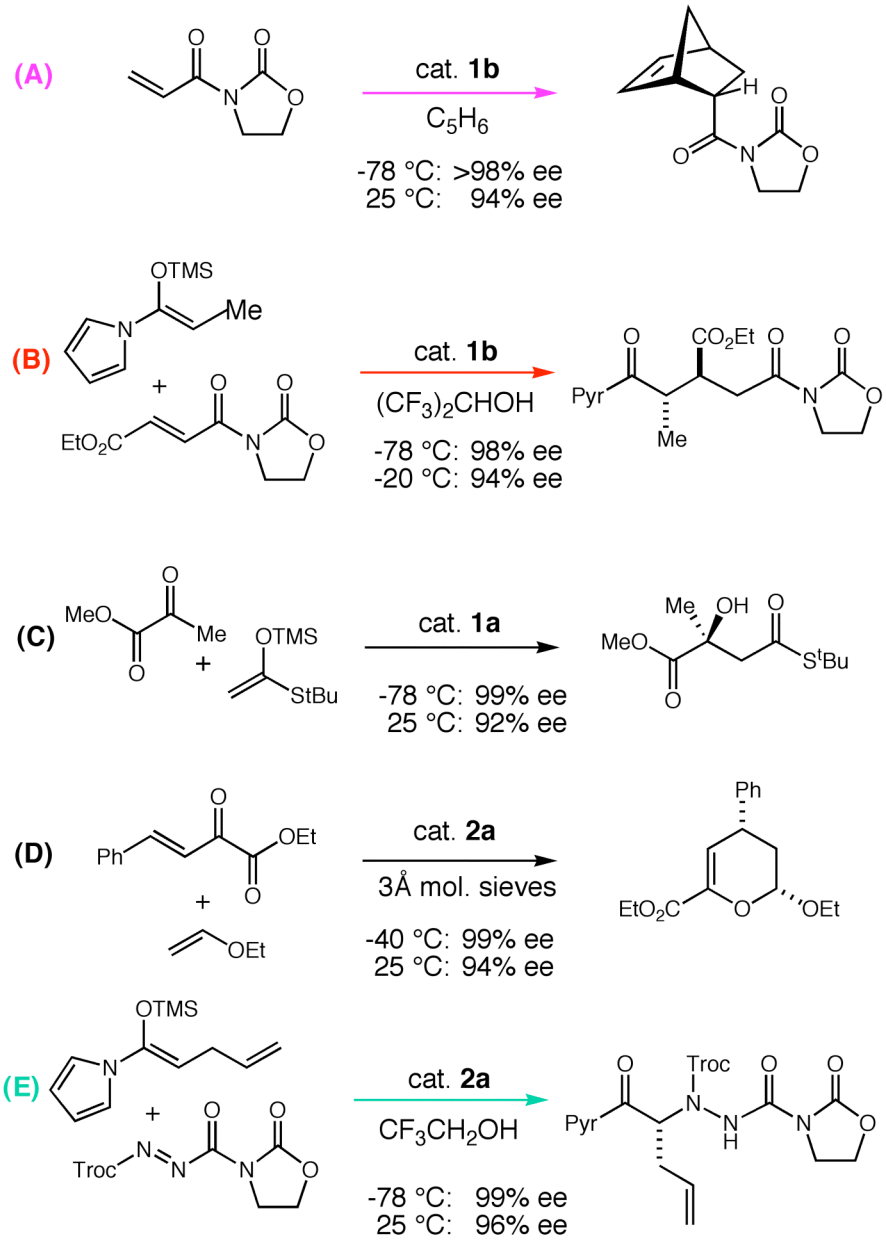

"Chiral Bis(oxazoline) Copper (II) Complexes: Versatile Catalysts for Enantioselective Cycloaddition, Adol, Michael and Carbonyl Ene Reactions". Johnson, Evans, *Acc. Chem. Res.* **2000**, *33*, 325-335. **(pdf)**

Boron-Based Catalyst: Hawkins *JACS* 1991, *113*, 7794

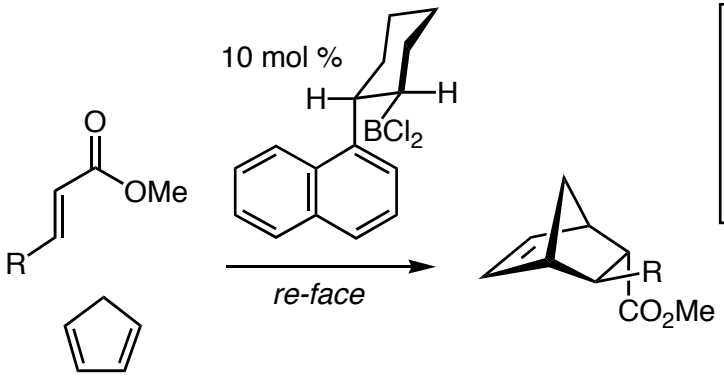

R	Temp (°C)	Endo ee
H	-78	97 %
Me	-20	91 %
CO_2Me	-78	92 %

Endo/Exo Ratios not provic

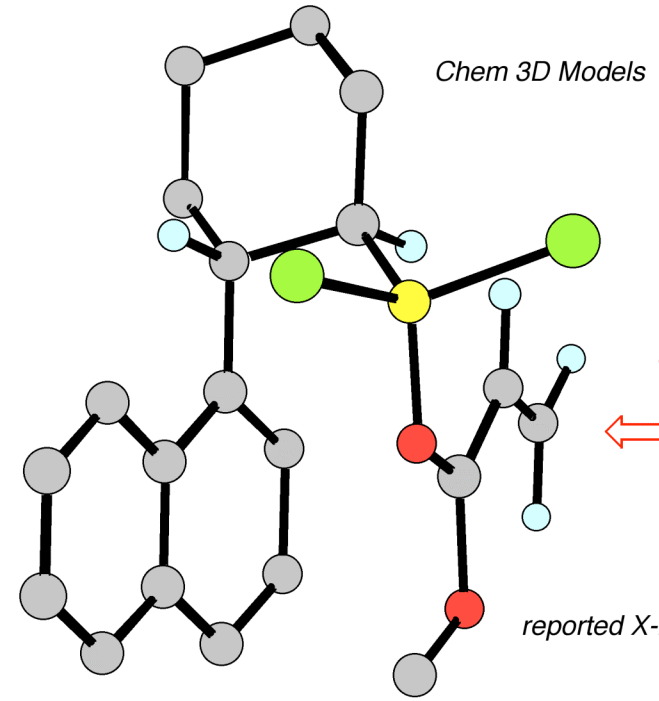

reported X-ray similar to this model

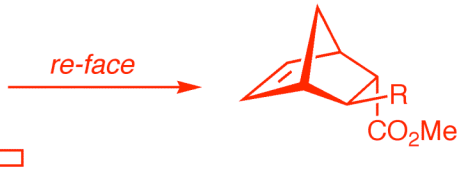

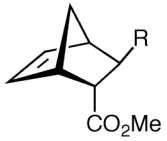

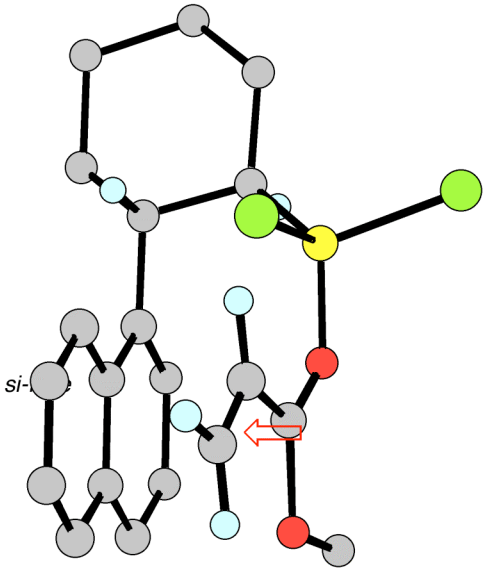

The pragmatic Issue:
The cost of producing the chiral catalyst

A New Hydrogen Bonding Motif

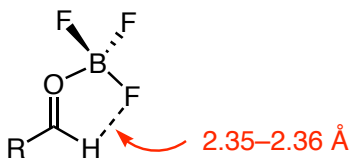

sum of the van der Waals radii:
2.67 Å (H = 1.20 Å and F = 1.47 Å).

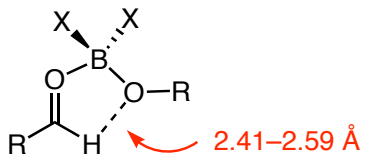

sum of the van der Waals radii:
2.72 Å (H = 1.20 Å and O = 1.52 Å).

The formyl C–H…O hydrogen bond as a critical factor in enantioselective Lewis-acid catalyzed reactions of aldehydes, Corey, Lee, *Chem Commun.* **2001,** 1321 **(pdf)**

"There may also be a contribution from an anomeric effect in which electrons from the noncomplexed lone pair on aldehyde oxygen delocalize into the σ*orbital of the eclipsed B–F or B–O bond. The authors of one study[1] attributed a value of 6 kJ mol to the anomeric effect and 9 kJ mol21 to the formyl hydrogen bond.[4]

(1) M. D. Mackey and J. M. Goodman, *Chem. Commun.*, **1997,** 2383

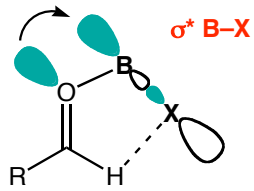

A possiible anomeric effect

Furuta, K.; Miwa, Y.; Iwanaga, K.; Yamamoto, H. *JACS* **1988,** *110,* 6254.

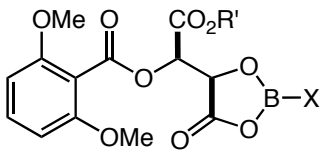

R' = H or Alkyl
X = H or Acyloxy

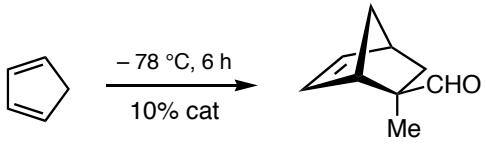

89:11(*exo:endo*)
96% ee

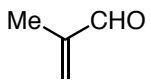

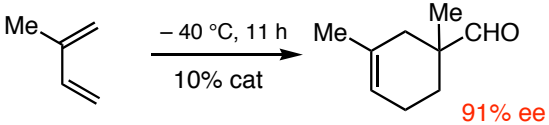

91% ee

dienophile	diene	isomers,[c] endo/exo	ee,[d] %
		11/89	96[e]
		10/90	96[g]
			97
		97/3[h]	93
		98/2[h]	91
		93/7	82
		88/12	84[e]
		>99/1	80[i]
			84[j]
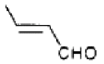		90/10	2[k]
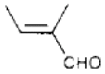		3/97	90

Yamamoto et al. *J. Org. Chem.* **1992,** *57,* 1951-1952

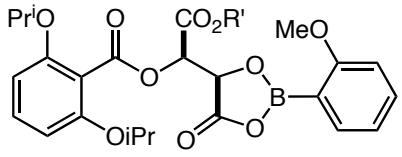

Note modifications to catalyst

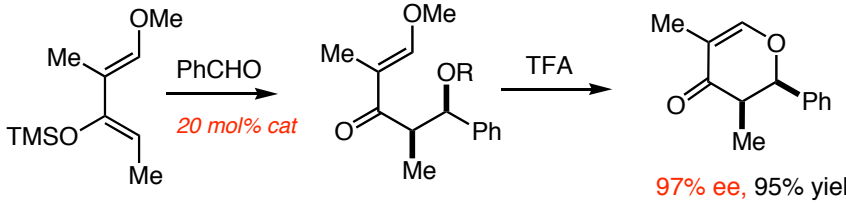

97% ee, 95% yield

Oxazaborolidine Catalysts: Corey *JACS* 2002, *124*, 3808.

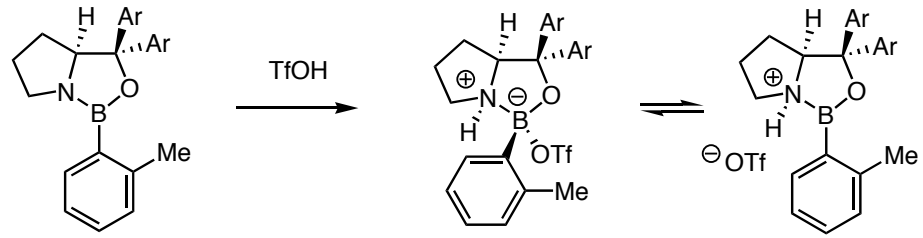

Ar = Ph or 3,5- Me_2-Ph

active catalyst

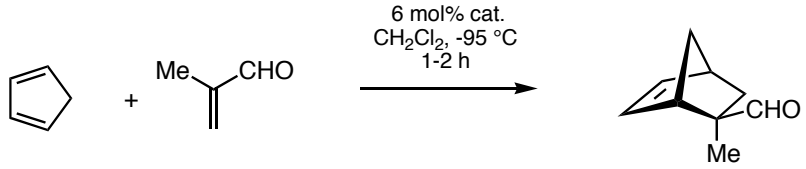

99% yield 89:11(*exo:endo*) 96% ee

Organized formyl CH–O hydrogen bonded complex
Aryl groups screen back face of dienophile
Π– stacking may also be involved
exo or *endo* selectivity varies with the diene

Stereochemical Model:

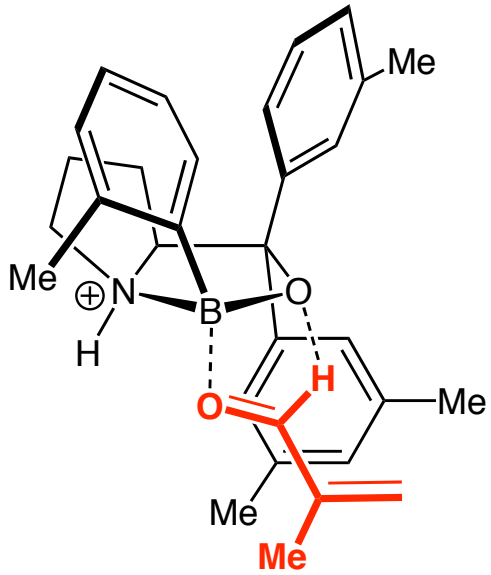

dienophile = 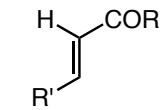

R= H, alkyl OH, OR

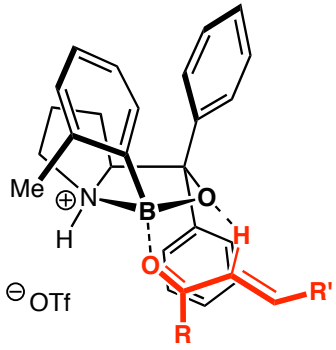

Alkene CH - O interaction may organize complex

Aryl groups screen back face of dienophile

Π– stacking may also be involved

endo product is observed* Note the opposite facial selectivity

Examples: Corey *JACS* **2002** *124*, 9992.

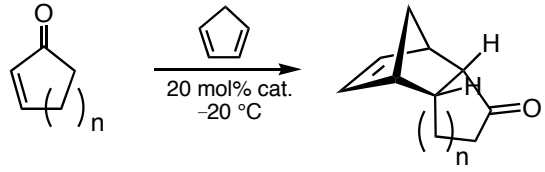

n	time	endo ee	yield
n = 1	14 h	96% ee	92%
n = 2	15 h	96% ee	95%
n = 3	22 h	94% ee	93%

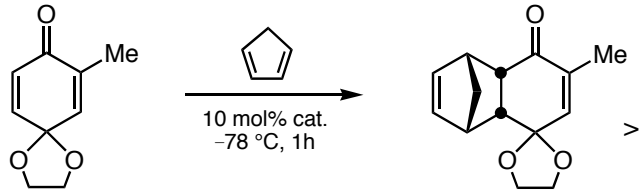

80% yield
> 98:2 *endo:exo*
92% ee

Switching the counterion from triflate OTt(–) to triflamide $(Tf)_2N(–)$ expands dienophile scope: Corey *JACS* **2003**, *125*, 6388.

Chromium (III) Schiff-Base Catalysts:

Jacobsen *Angew. Chem. Int. Ed.* 1999, *38*, 2398.

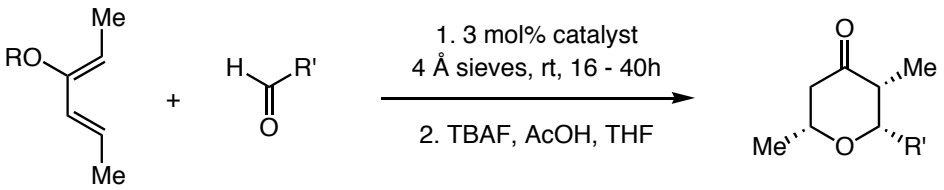

R = TMS, TES, TBS

R' = aryl, alkyl, heteroaromatic

> 95% de
(all cis)
90-99% ee
72-97% yield

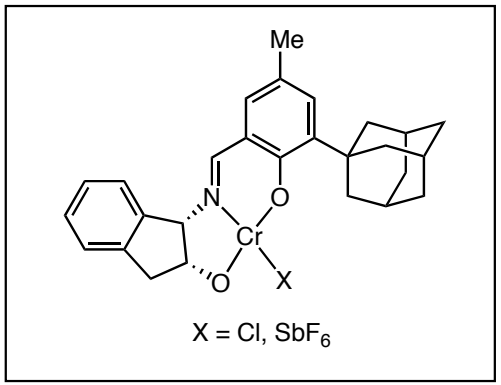

X = Cl, SbF_6

The catalyst is a water-bridged dimer

Sieves may be needed to open up a binding site for the aldehyde

Single-point binding to the aldehyde

A variety of mono- and di-oxygenated dienes are good substrates

Catalyst-Controlled Diastereoselective HDA:

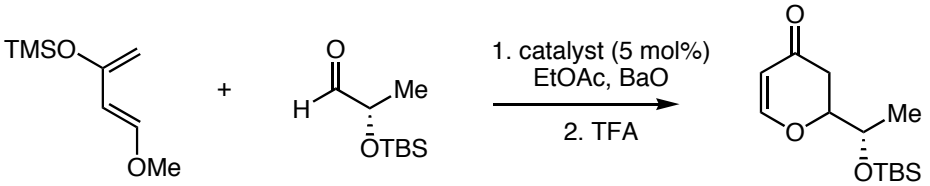

catalyst	yield	dr	ee
achiral catalyst	81%	1:2.0	nd
(1*R*,2*S*)-Cl	96%	1:12	>99%
(1*S*,2*R*)-Cl	97%	15:1	>99%

Org. Lett. **2002**, *4*, 1795.

Stereochemical Model:

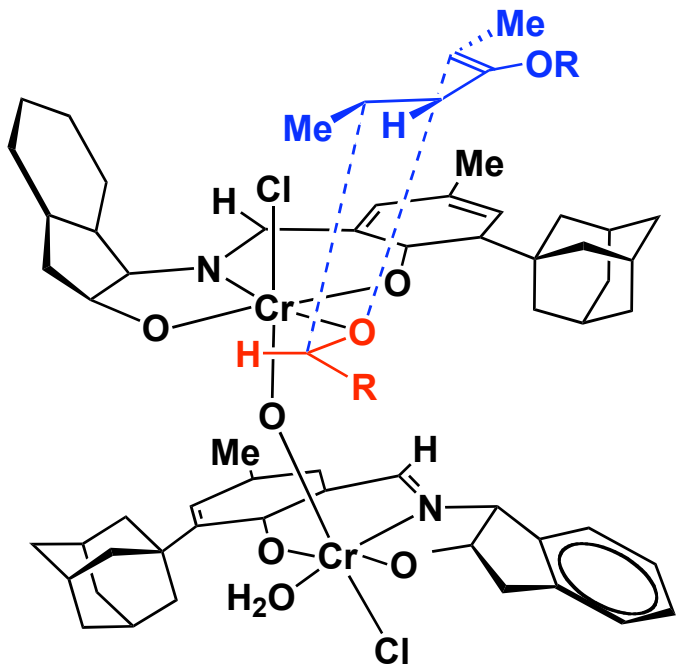

HDA

Hetero-Ene Reaction:

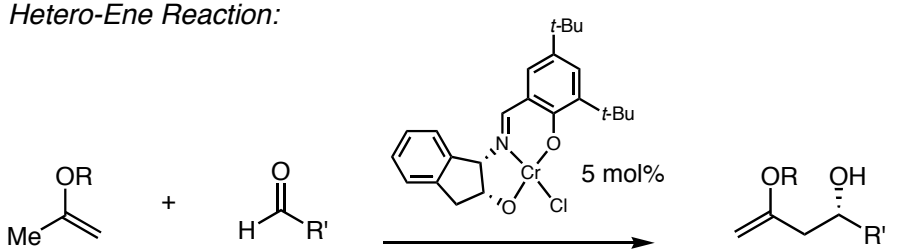

R = TMS, Me

R' = Ar, alkyl

70 - 96% ee
77 - 97% yield

JACS, **2002**,*124*, 2882.; *Angew. Chem. Int. Ed.* **2003**, *42*, 4771.

MacMillan introduces a new catalyst:

MacMillan, D. *JACS* **2000**, *122*, 4243.

■ **C=X Polarization**

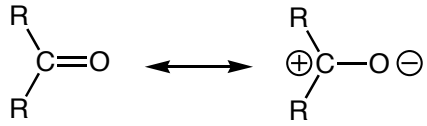

Partial Charge: As the familiar polar resonance structure above indicates, the carbonyl carbon supports a partial positive charge due to the polarization of the sigma and pi system by the more electronegative heteroatom. The partial charges for this family of functional groups derived from molecular orbital calclulations (ab initio, 3-21(G)*, HF) are illustrated below:

LUMO Lowering →

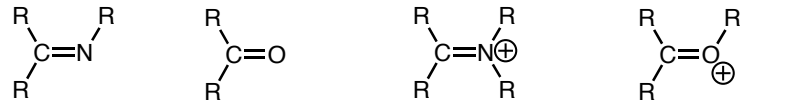

→ *electrophilic reactivity*

Diels-Alder Catalysis via chiral Iminium Ions

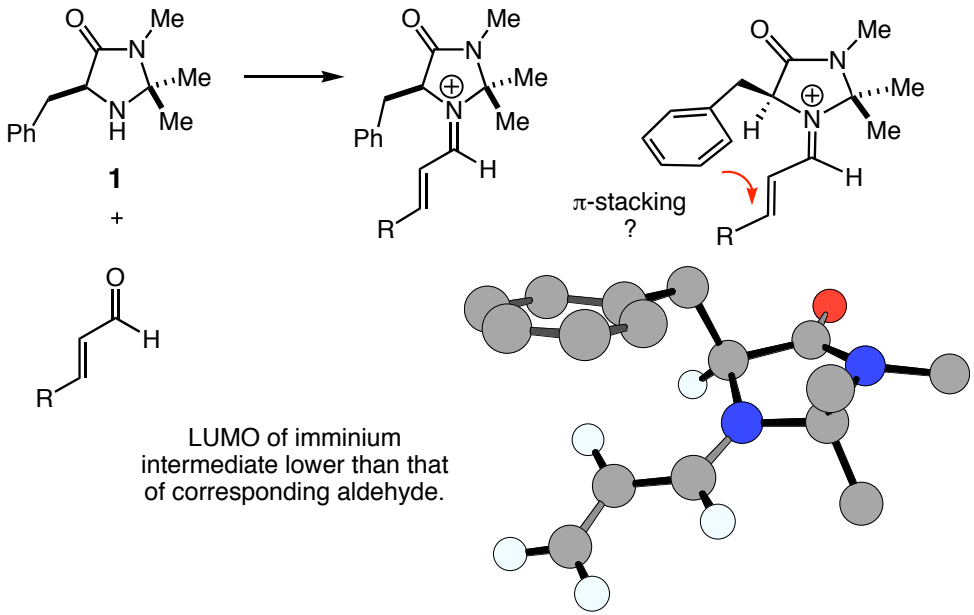

The Catalytic Cycle

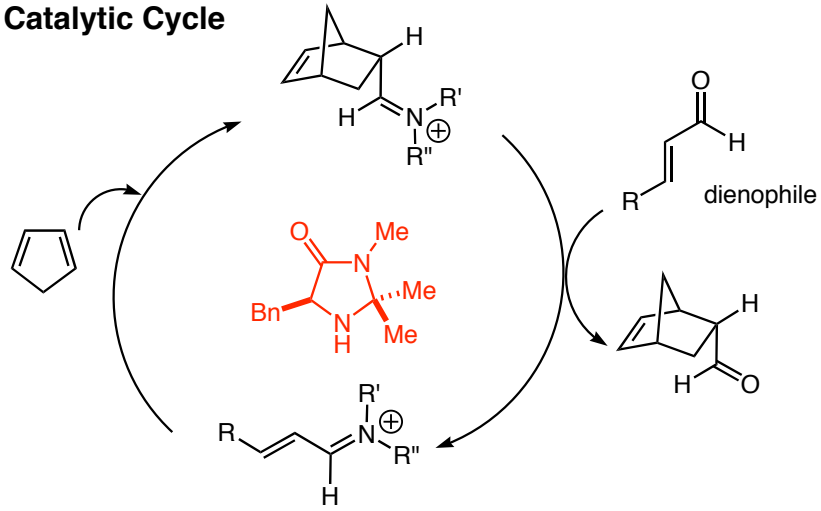

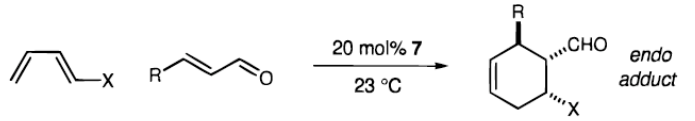

entry	diene	R	product	yield	*exo:endo*	% ee[a]
1	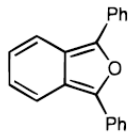	Me	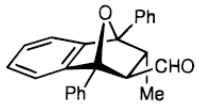	75	35:1	96[c]
2		H	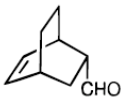	82	1:14	94[d]
3		H	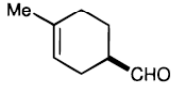	84	--	89
4		H	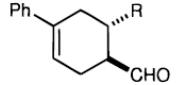	90	--	83
5		Me		75	--	90
6	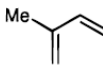	H	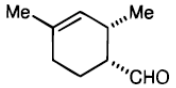	75	1:5	90
7	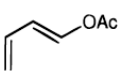	H	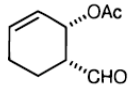	72	1:11	85

http://www.courses.fas.harvard.edu/colgsas/1063

Chemistry 206

Advanced Organic Chemistry

Lecture Number 19

Dipolar cycloaddition Reactions

Merged Cycloaddition–Cycloreverion Processes, G. Borg, Evans Group Seminar **(Handout)**

"The Concerted Nature of 1,3-Dipolar Cycloadditions and the Question of Diradical Intermediates," R; Huisgen, *J. Org. Chem.* **1976,** *41,* 403 **(Handout)**
"Asymmetric 1,3-Dipolar Cycloaddition Reactions", Jorgensen, *Chem Rev*. **1998,** *98,* 863-909 **(pdf)**

"Total Synthesis of (-)-Colchicine via a Rh-Triggered Cycloaddition Cascade'" Schmalz, *Org. Lett*. **2005,** *7*, 4317 **(pdf)**

D. A. Evans

Wednesday
November 1, 2006

Dipolar Cycloaddition Reactions

General References
Carruthers, W. *Cycloaddition Reactions in Organic Synthesis*.; Pergamon: Elmsford, NY, **1990**.

Padwa, A. *1,3-Dipolar Cycloaddition Chemistry*, John Wiley, **1984,** Volumes 1 & 2,

Padwa, A. Generation and utilization of carbonyl ylides via the tandem cyclization-cycloaddition method." *Acc. Chem. Res.* **1991**, *24*, 22. **(pdf)**

Confalone, P. N.; Huie, E. M. *The [3+2] Nitrone-Olefin Cycloaddition Reaction Org. React. (N.Y.)* **1988**, *36*, 1.

S. Kanemasa, *Metal Assisted 1,3-Dipolar Cycloaddition Reactions,* SynLett **2002**, 1371-1387 **(pdf)**

"Intramolecular Dipolar Cycloaddition Reactions of Azomethine Ylides", Coldham, *Chem Rev*. **2005,** *105,* 2765-2809 **(pdf)**

"The Firestone Papers, *J. Org. Chem.* **1972,** *37,* 2181; *J. Org. Chem.* **1976,** *41,* 2212. **(Handout)**

Problem of the Day (Database Problem 4

Provide a plausible mechanism for this transformation in the space below. *In attacking this question, it is important that you are aware of the transformation that transpires when terminal acetylenes are treated with Cu(I) or Ag(I) in the presence of an amine base.*

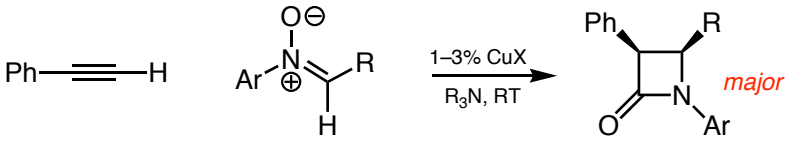

In 1995 Miura and co-workers reported the remarkable reaction illlustrated below (*J. Org. Chem.* **1995**, *60*, 4999). Recently, Fu has reported an enantioselective variant of this transformation (*J. Am. Chem. Soc.* **2002**, *124*, 4572). In most instances, the cis adduct is formed in large excess (>90%). There is really no thoughtful mechanism in the literature for this transformation. You will be graded on "reasonability"

Handout 18A

Merged Cycloaddition–Cycloreversion Processes

Evans Group Seminar
May 3, 2002
Mr. George Borg

[3 + 2]–r[3 + 2] Reactions of Sydnones

- Reactions of sydnones with alkenes produce 2-pyrazolines:

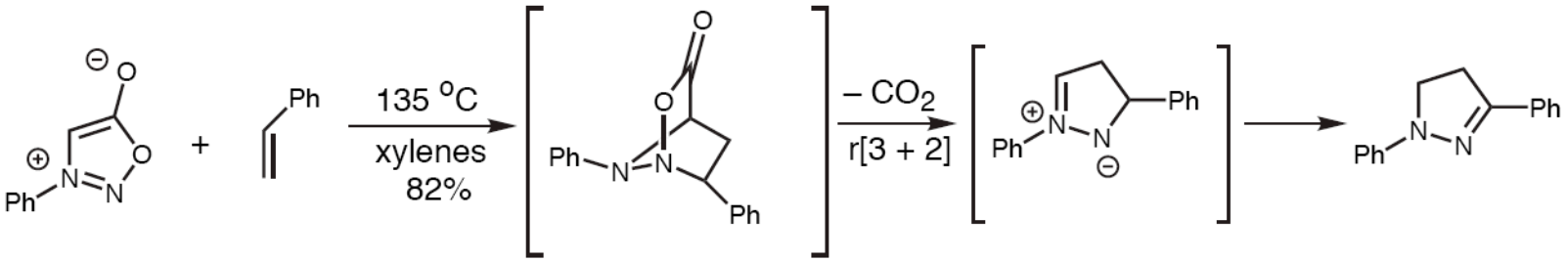

Huisgen, *Chem. Ber.* **1968**, *101*, 552-563.

The General Reaction Family

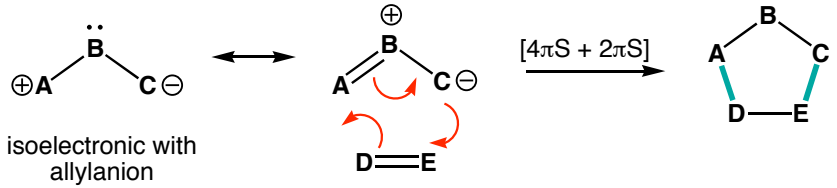

FMO Analysis

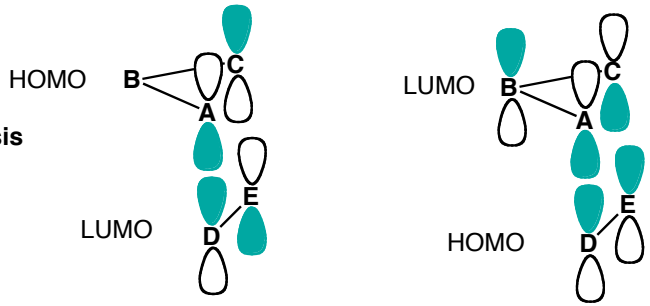

The specific set of reaction partners, will define the dominant frontier orbitals

Reaction Stereospecificity: The Dipolariphile (Padwa, Vol 1, pp 61-90)

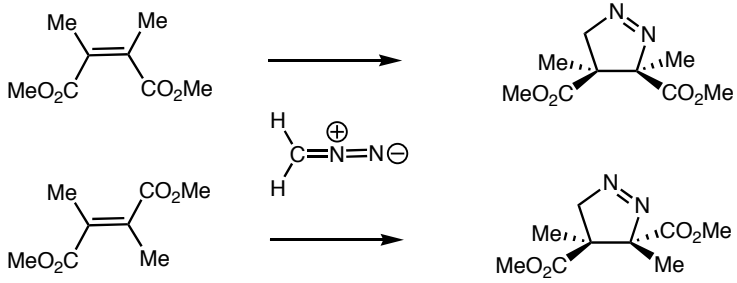

Rinehart, *JACS* **1962**, *84*, 3736

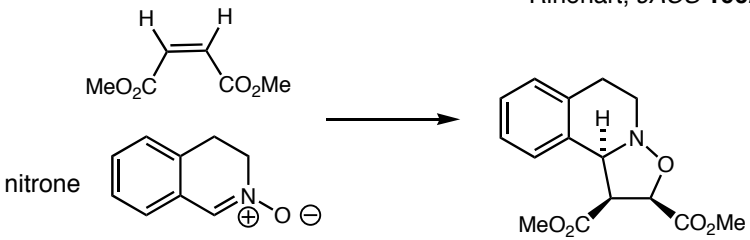

Fumarate gives trans cycloadduct

Huisgen, *Chem. Ber.* **1969**, *102*, 736

Classification of 1,3-Dipoles Containing C, N, & O Atoms

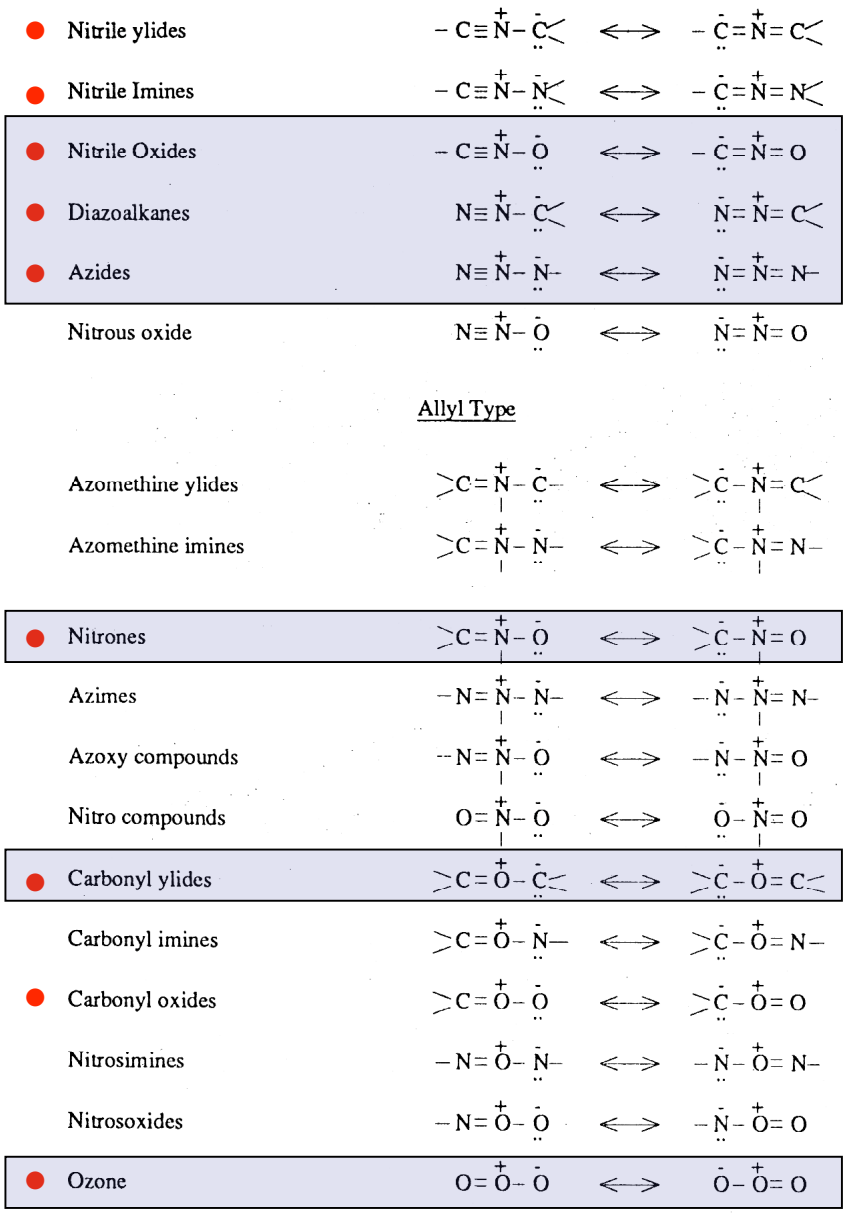

(After R.Huisgen, J.Org.Chem., 1976, 41, 403.)

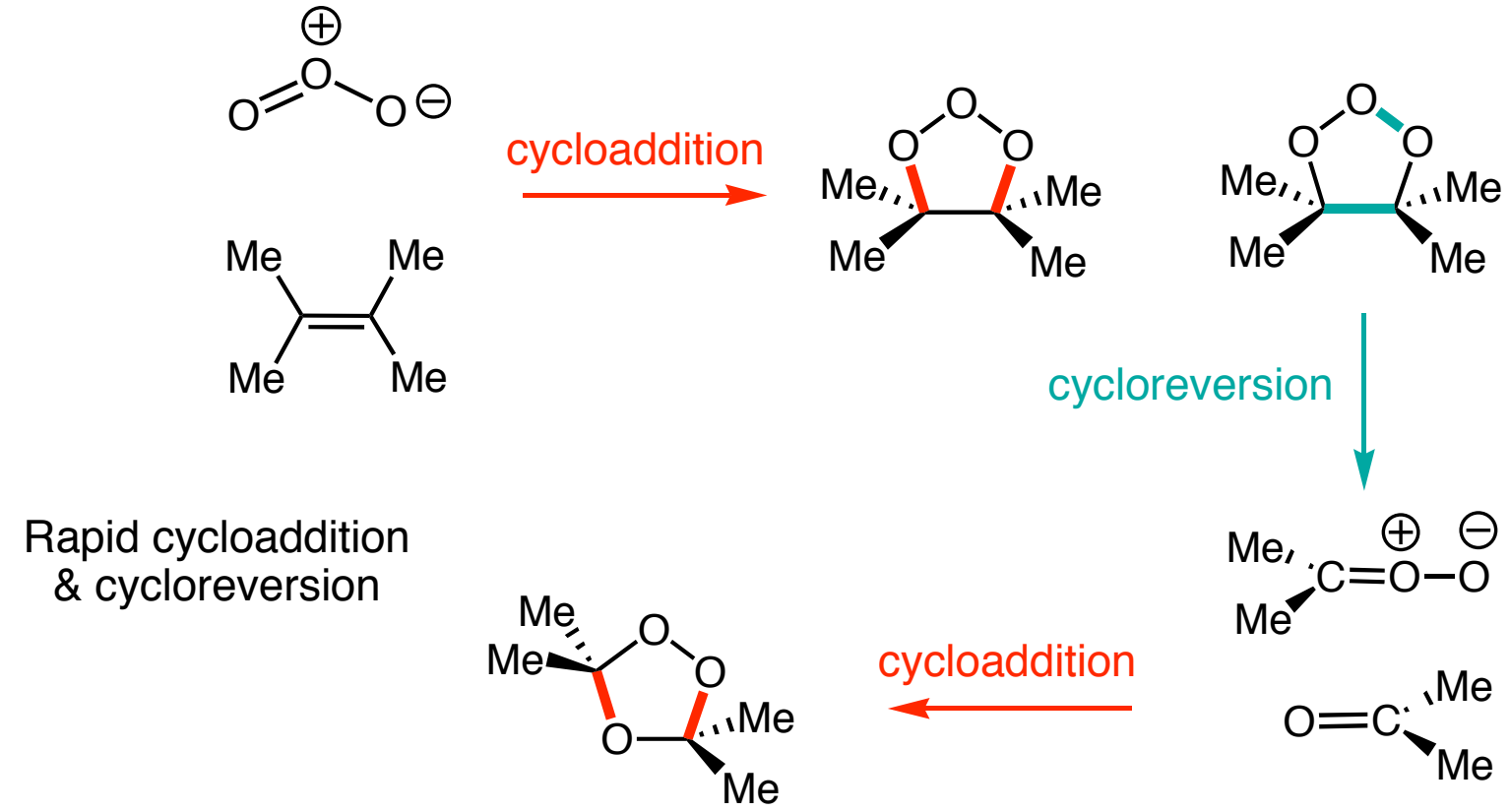

Criegee, R. "Mechanism of Ozonolysis." *Angew. Chem., Int. Ed.* **1975** *14,* 745.

Reaction Stereospecificity: Dipolariphile continued

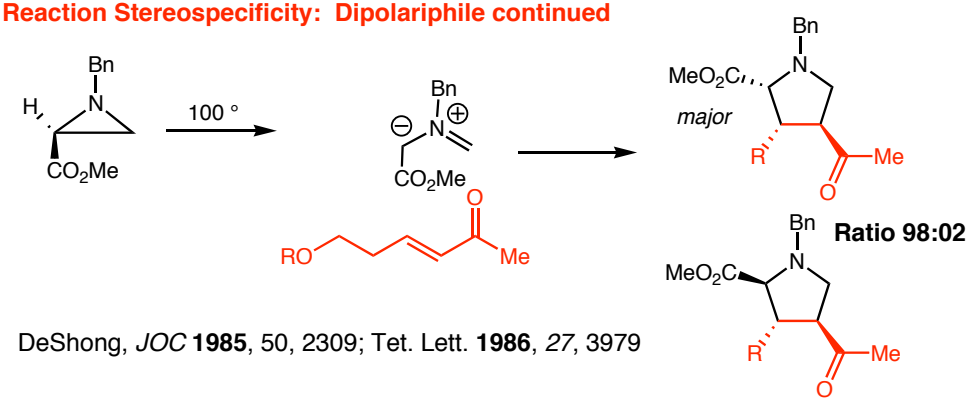

DeShong, *JOC* **1985**, 50, 2309; Tet. Lett. **1986**, *27*, 3979

We will return to the other stereochemical element of this reaction shortly

Reaction Regiochemistry (Padwa, Vol 1, pp 135)

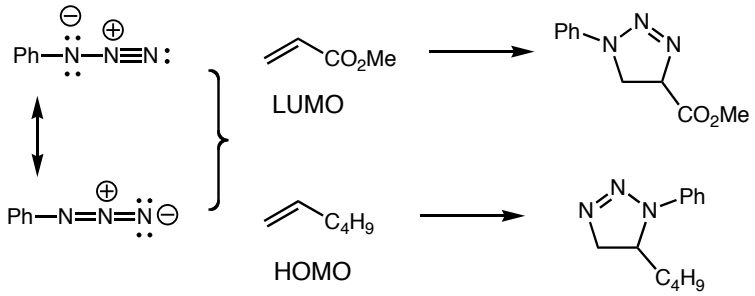

The specific set of reaction partners, will define the dominant frontier orbitals

Steric effects will frequently alter regioselectivity (Padwa, Vol 1, pp 144)

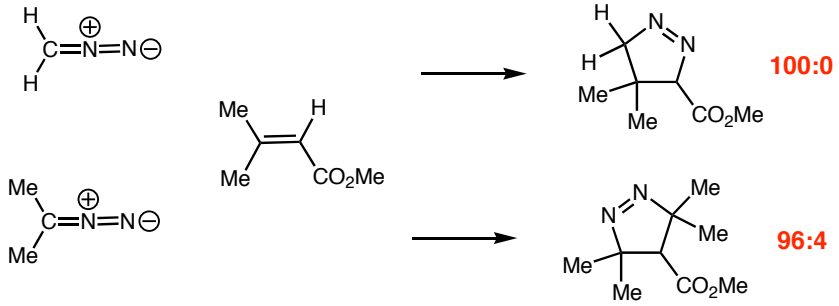

Steric effects are also important considerations in reaction regiochemistry

Ring strain factors may control regioselectivity

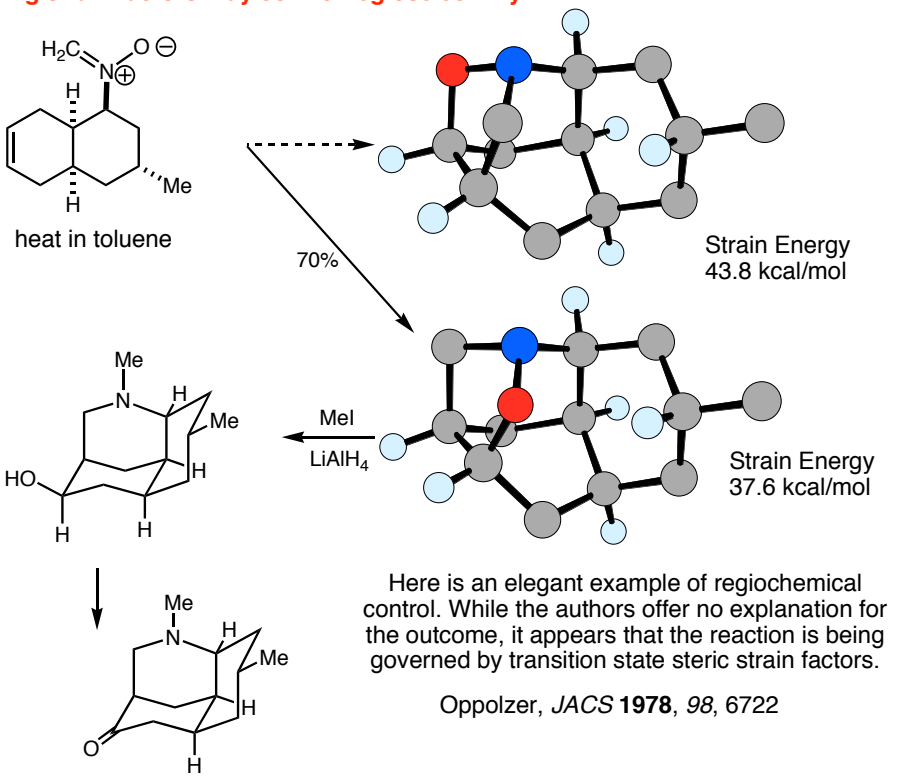

Here is an elegant example of regiochemical control. While the authors offer no explanation for the outcome, it appears that the reaction is being governed by transition state steric strain factors.

Oppolzer, *JACS* **1978**, *98*, 6722

Reaction Diastereoselectivity

Huisgen et al, *Angew.Chem. Int. Ed.* **1969**, *8*, 604

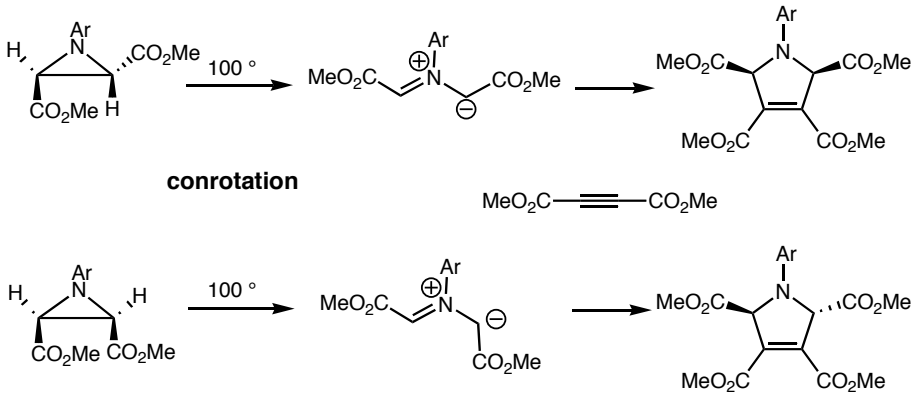

Relative Orientation of Reaction Partners

DeShong, *JOC* **1985**, 50, 2309; Tet. Lett. **1986**, *27*, 3979

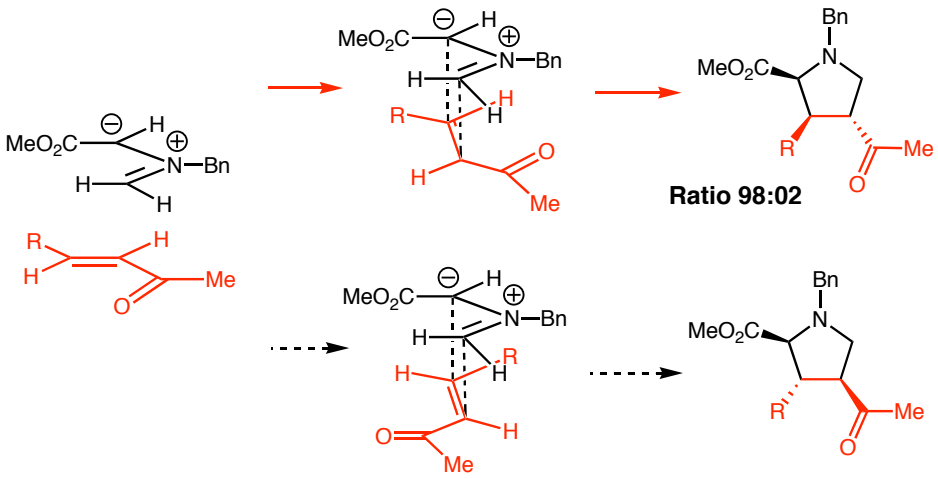

The above analysis is clouded by the fact that the geometry of the 1, 3-dipole is not fixed.

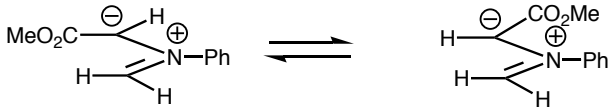

Monosubstituted Olefins.

In the following study, 1,3-dipole isomerism is not an issue

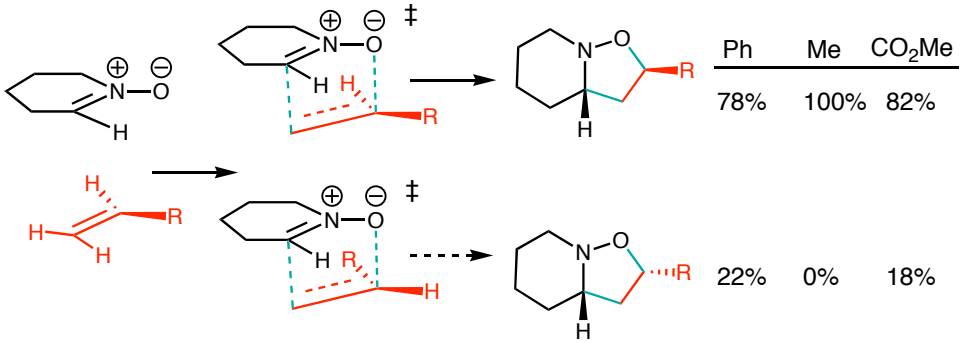

Ph	Me	CO_2Me
78%	100%	82%
22%	0%	18%

Diastereoselection appears to be dictated by steric effects

Tufariello, *Accounts. Chem. Res.* **1979**, *12*, 396-1403

Cis Disubstituted Olefins.

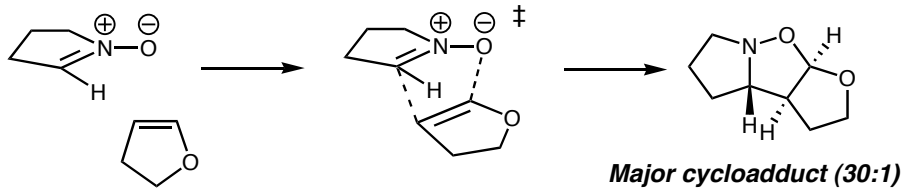

Major cycloadduct (30:1)

The preceding trend appears to be reinforced by cis disubstitution

I. Washita et al, *Chem lett* **1979**, 1337

Intramolecular Reaction Variants

N. LeBel et al, *JACS* **1964**, *86*, 3759

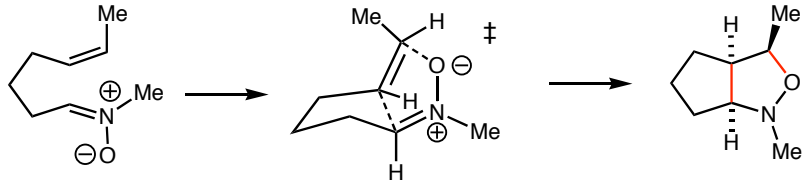

Orientation probably driven by ring strain as in Oppolzer case (previous page)

"highly diastereoselective"

Intramolecular Reaction Variants

P. Confalone et al, Tet. Lett. **1984**, *25*, 4613

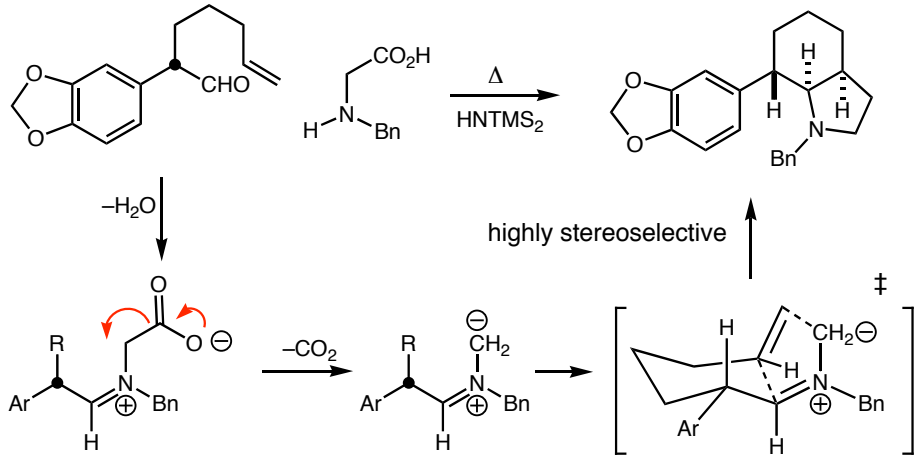

Conclusions on Reaction Diastereoselection

In general reaction diastereoselection appears to be dictated by steric and torsional rather than electronic factors

The Basic Reactions

Padwa, A. *1,3-Dipolar Cycloaddition Chemistry*, John Wiley, **1984,** Vol 1, Chapter 3

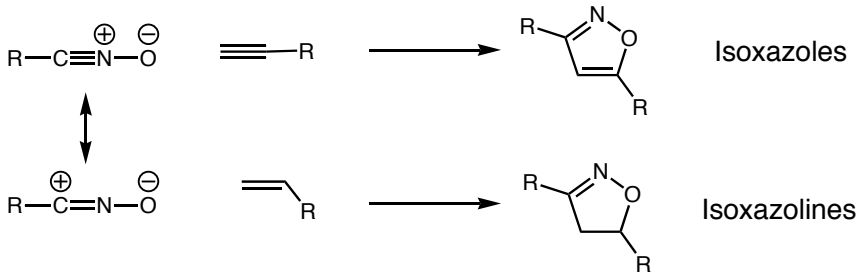

Methods of Generation

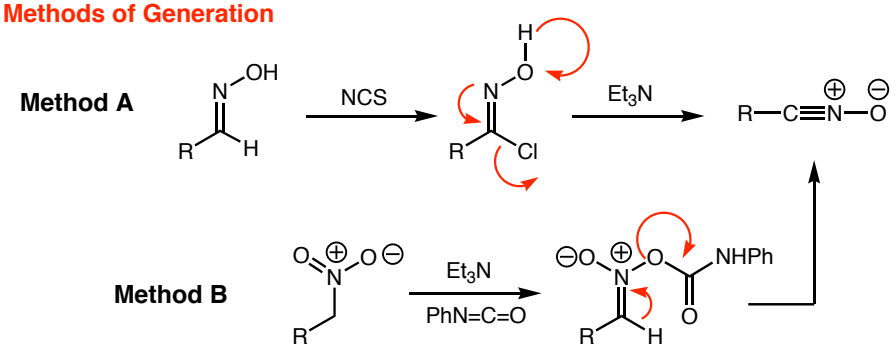

Stability Nitrile oxides are usually prepared in the presence of the olefin or acetylene acceptor. These intermediates are generally unstable and will dimerize if not given an alternative reaction course

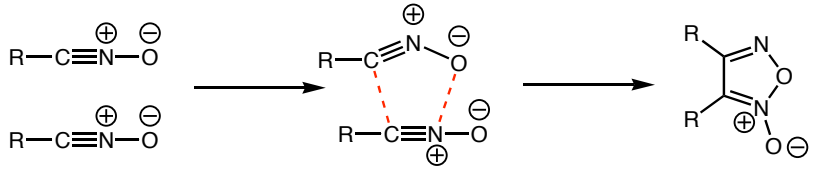

Regioselectivity Nitrile oxide cycloadditions with olefins and acetylenes are usually quite regioselective and in the direction as illustrated above.

DeShong, *JOC* **1985**, 50, 2309; Tet. Lett. **1986**, *27*, 3979

Reactions with olefins are stereospecific

Carruthers, W. *Cycloaddition Reactions in Organic Synthesis.*; Pergamon: Elmsford, NY, **1990**.Chapter 6, pp 269–298

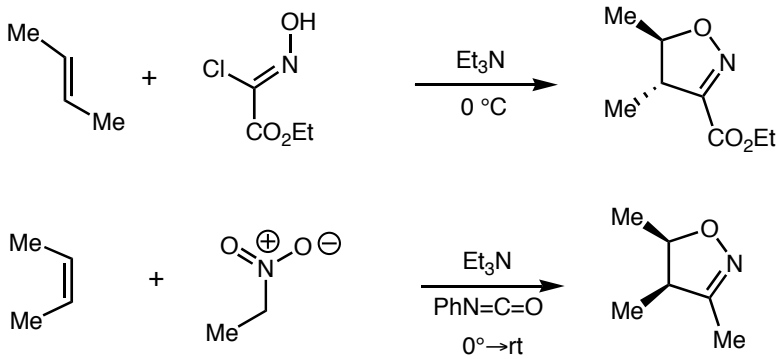

Oxazoline Cleavage

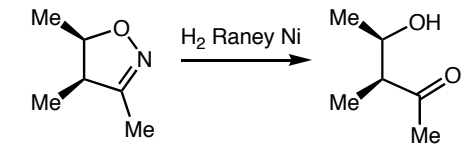

Non-aldol approach to aldol adducts

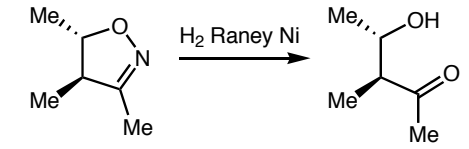

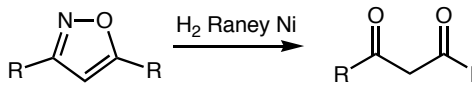

Non-aldol approach to 1,3-dicarbonyls

Preferred method for reducing oxazoles and oxazolines:
Nittta et al, *Chem. Comm.* **1982**, 877-878: $Mo(CO)_6$ MeCN

Miyakolide Synthesis: with David Ripin & David Halstead, *JACS* **1999**, *121*, 6816-6826

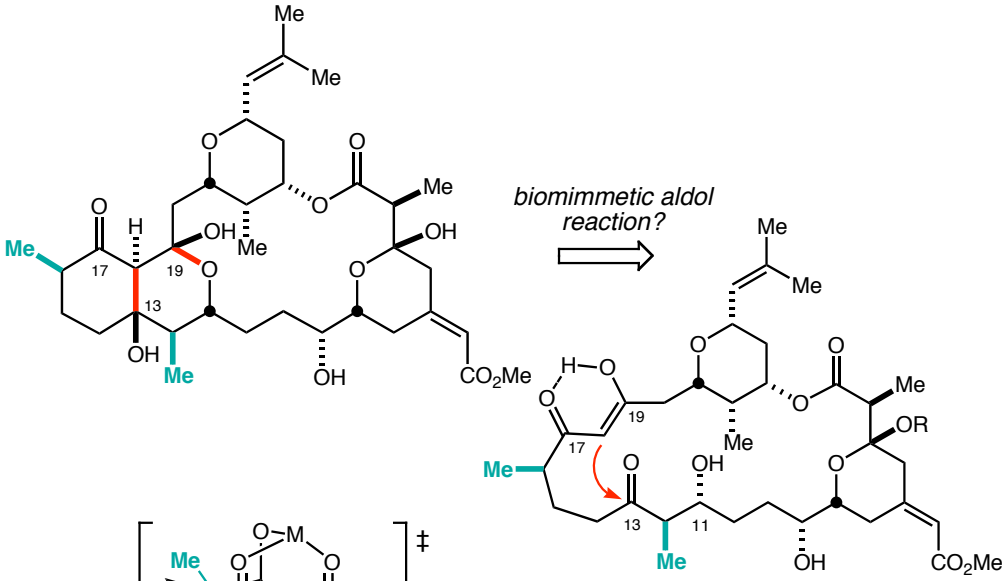

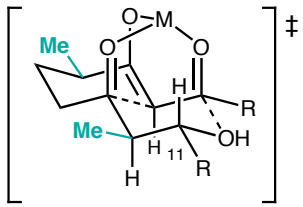

Transannular Aldol

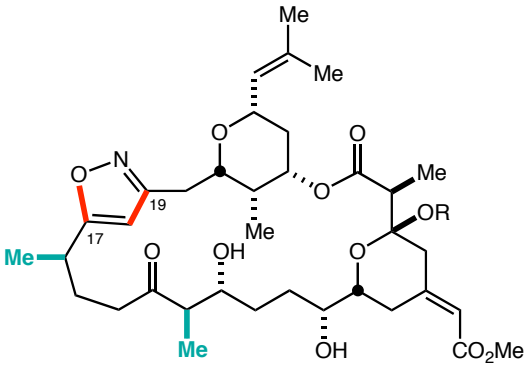

Competing olefin chlorination eliminated this approach to the nitrile oxide precursor

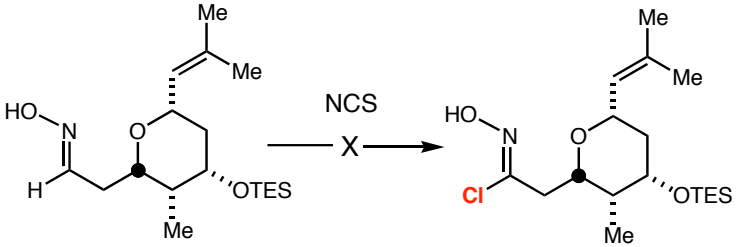

The Intermolecular Case

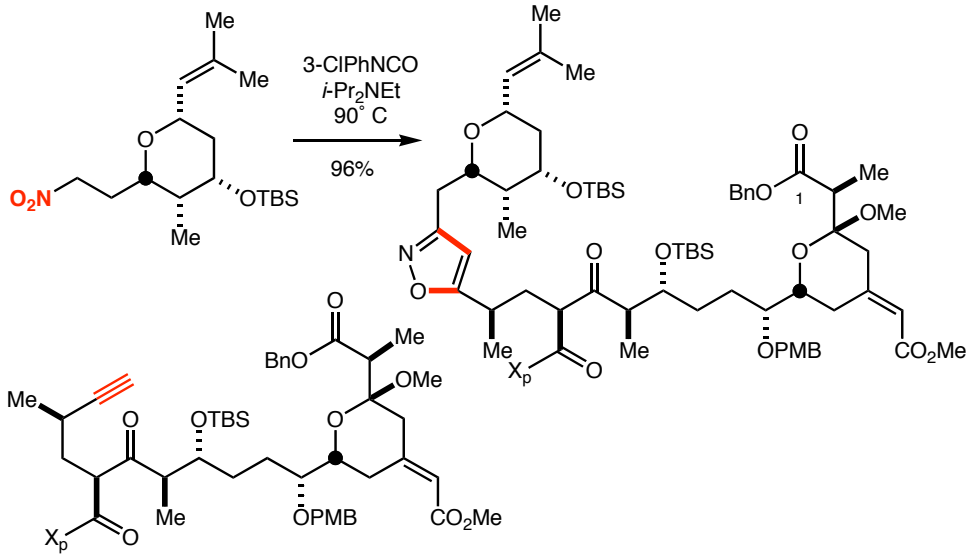

The Intramolecular Case

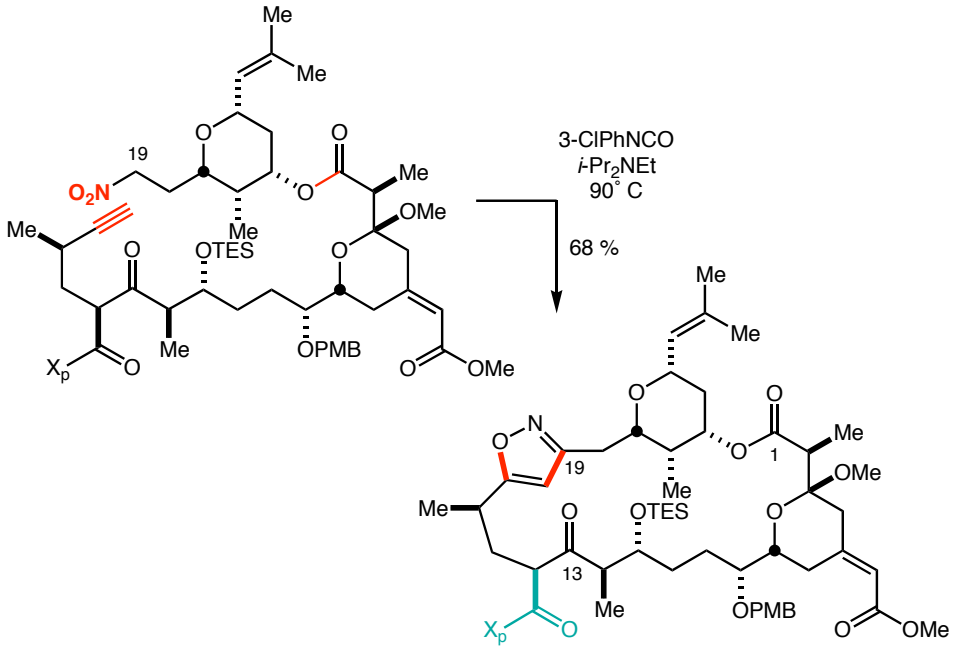

Development of Directed Cycloadditions

Kanemasa at al, *JACS* **1994**, *116*, 2324-2339 **(electronic handout)**
Kanemasa at al, Metal-Assisted Stereocontrol of 1,3-Dipolar Cycloaddition Reactions *SynLett* 2002, 1371-1387 **(electronic handout)**

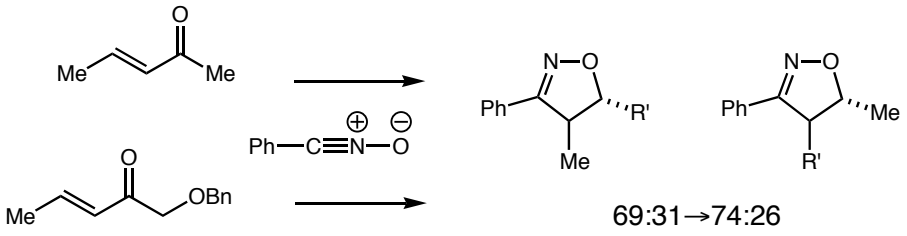

conditions; no cat, ZnI_2, $Ti(OiPr)_4$

While lewis acid activation is known, no change in regiochemistry was noted under above conndditions

Magnesium alkoxides found to effect regiochemical control

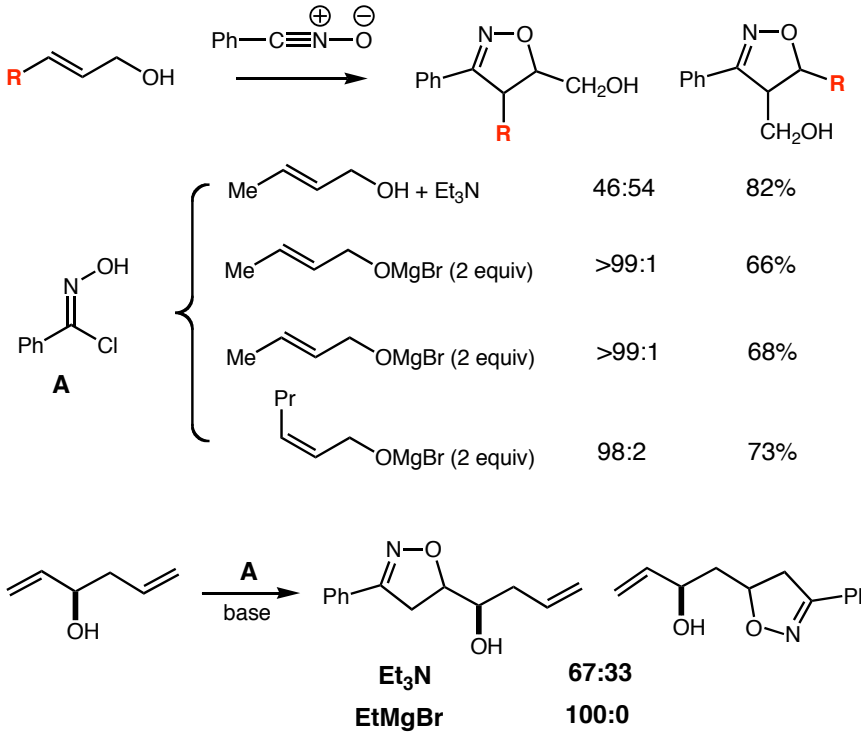

Reaction Diastereoselectivities

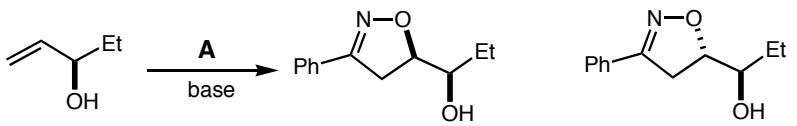

Et_3N	**67:33**	**60%**
EtMgBr	**95:5**	**75%**

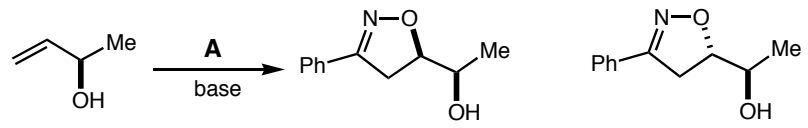

Et_3N	**61:39**	**60%**
EtMgBr	**96:4**	**75%**

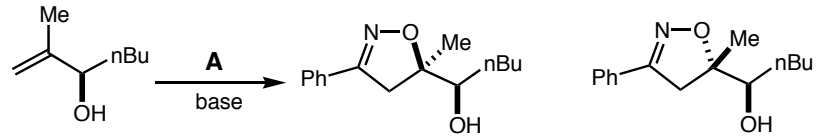

Et_3N	**60:40**	—
EtMgBr	**96:4**	**85%**

Stereochemical Rationale

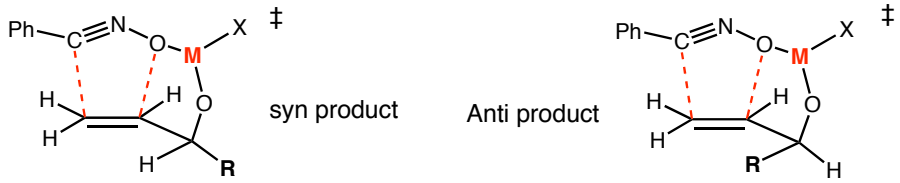

Rate acceleratons

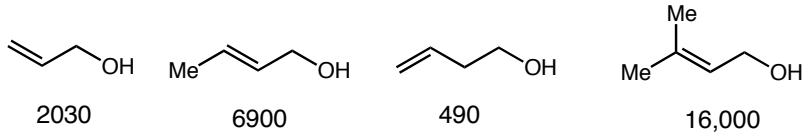

Applications in Polypropionate Synthesis

Carreira at al, *Angew. Chem. Int. Ed.* **2001**, *40*, 2082–2085

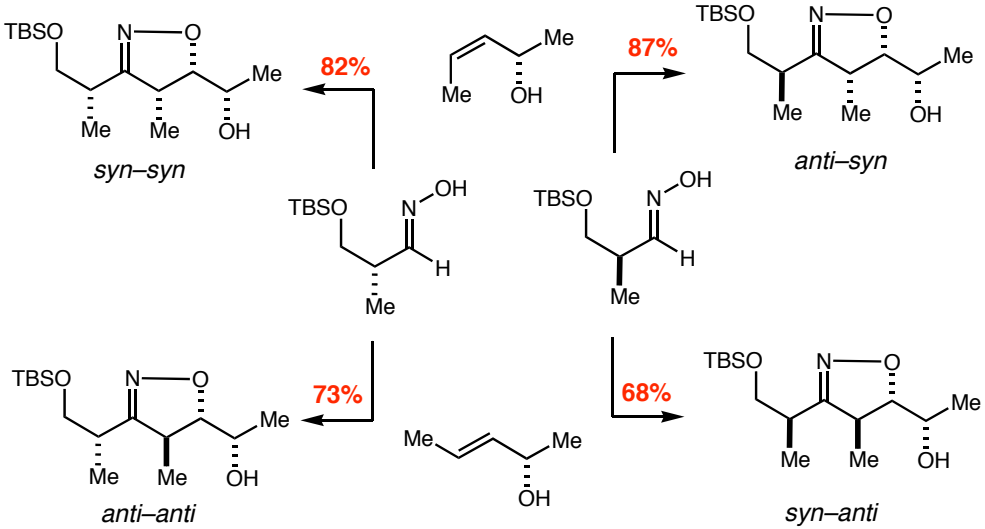

a, Oxime Chlorination: t-BuOCl; b, 3 Equiv EtMgBr, room temp, 12 h

Oxazoline Reduction

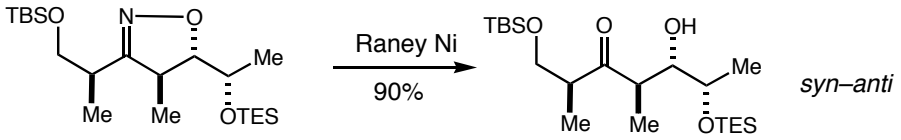

Lit Conditions: Curran, *JACS* **1983**, *105*, 5826; *JOC* **1984**, *49*, 3474

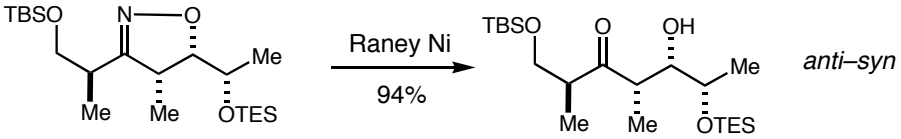

See also, Carreira et al. *Org. Lett.* **2004**, *6,* 2485-2488

Applications to the Synthesis of Epothilones A, B

Carreira & Bode *JACS* **2001**, *123*, 2082–2085

Epothilone A: R = H
Epothilone B: R = Me

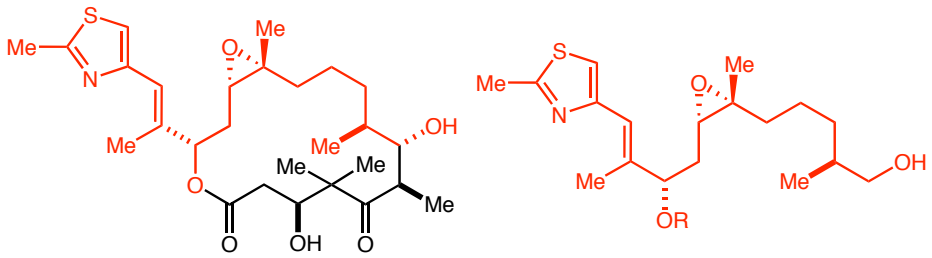

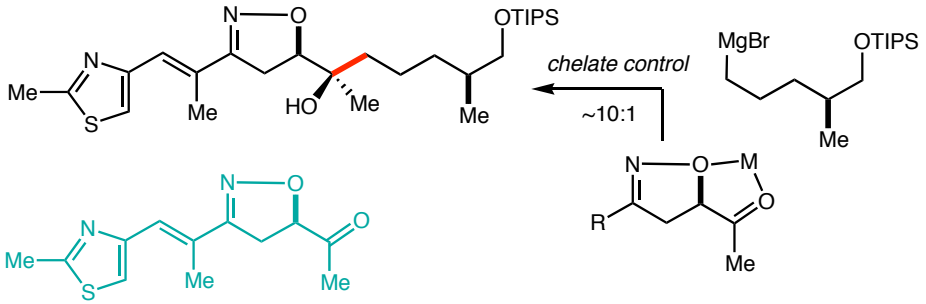

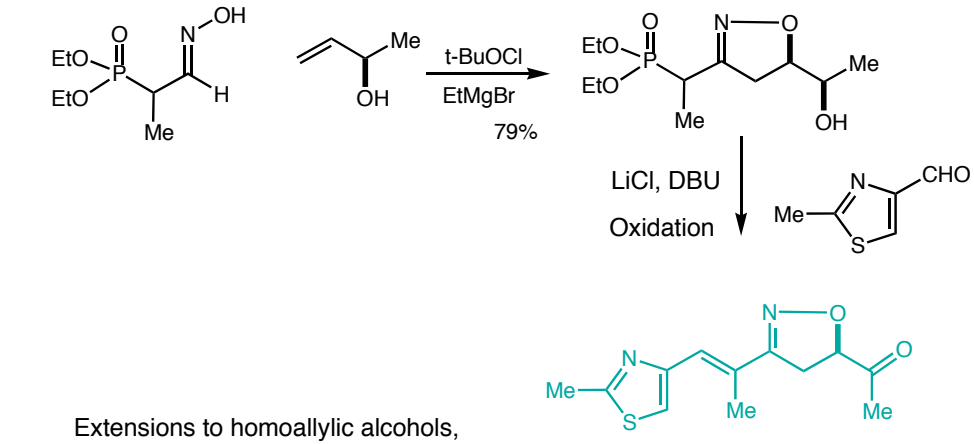

Extensions to homoallylic alcohols,
Carreira et al. *Org. Lett.* **2005**, *7,* 2011-2014

The Basic Reactions

Reviews - Ylides

Padwa, A.; Hornbuckle, S. F. *Chem. Rev.* **1991**, *91*, 263-309.
Padwa, A.; Krumpe, K. E. *Tetrahedron.* **1992**, *48*, 5385-5483.
Padwa, A. *Acc. Chem. Res.* **1991**, *24*, 22-28.

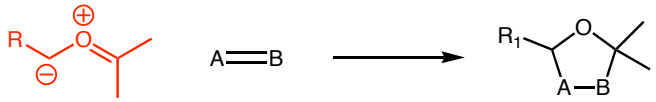

Stabilized (Isolable) Carbonyl Ylides

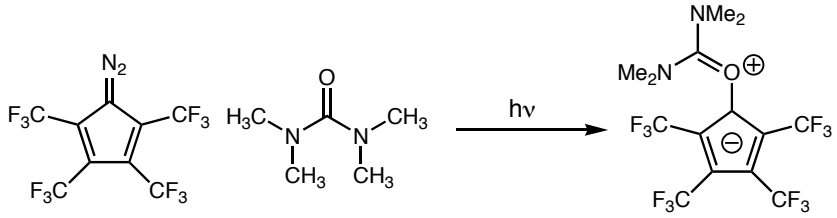

Arduengo, A. J., III; Janulis, E. P., Jr. *J. Am. Chem. Soc.* **1983**, *105*, 5929-5930

Hamaguchi, M.; Ibata, T. *Tetrahedron Lett.* **1974**, 4475-4476.

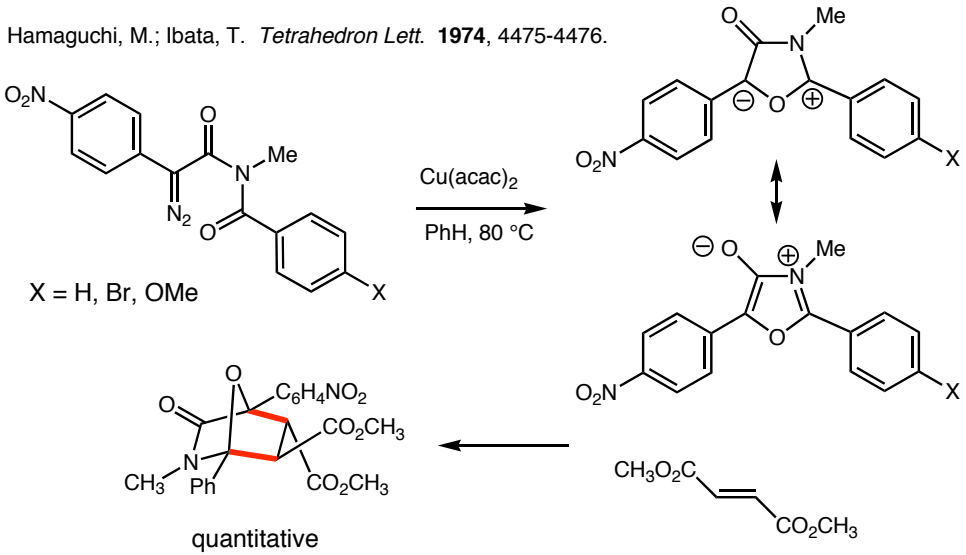

Hamaguchi, M.; Ibata, T. *Chem. Lett.* **1975**, 499-502.

Carbenes Plus Carbonyl Groups

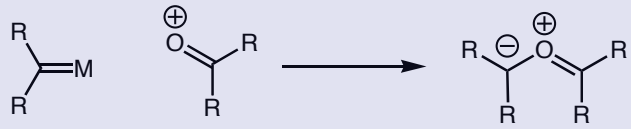

Tandem Intramolecular Cyclization–Intermolecular Cycloaddition

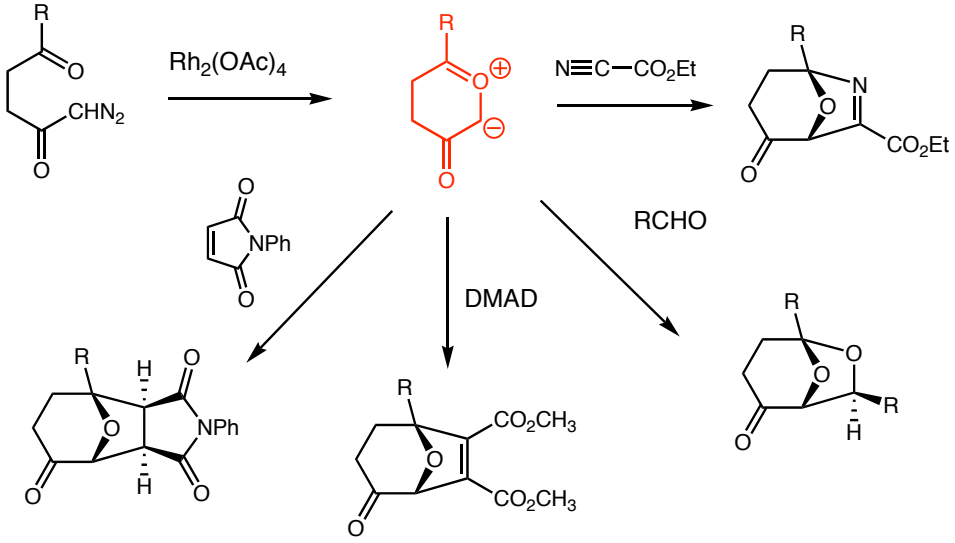

Padwa, A.; Hornbuckle, S. F.; Fryxell, G. E.; Stull, P. D. *J. Org. Chem.* **1989**, *54*, 817-824.

Intramolecular Variants

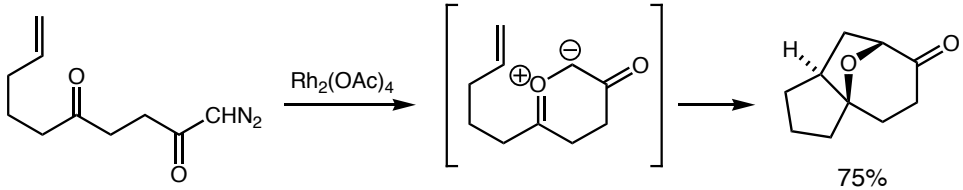

Can make 5-7 membered rings

Carbonyl Ylide Cycloadditions of Diazoimides

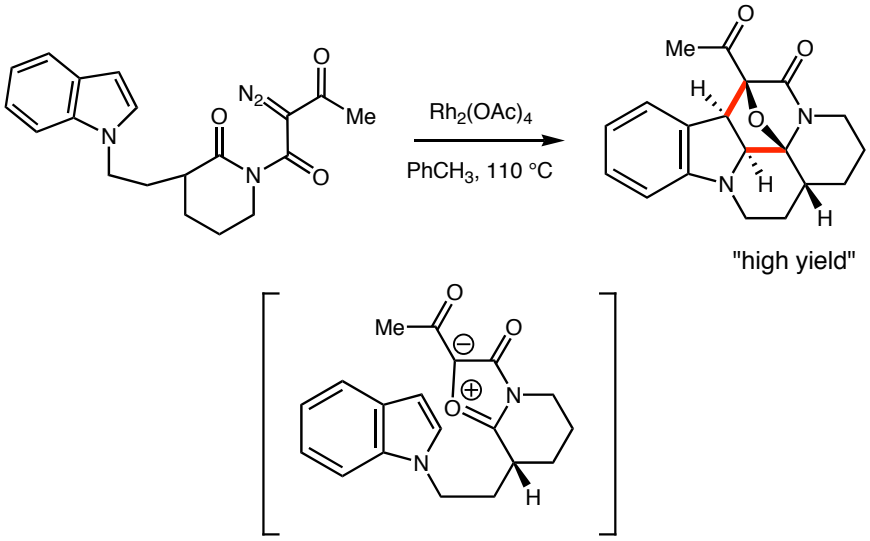

Hertzog, D. L.; Austin, D. J.; Nadler, W. R.; Padwa, A. *Tetrahedron Lett.* **1992**, *33*, 4731-4734.

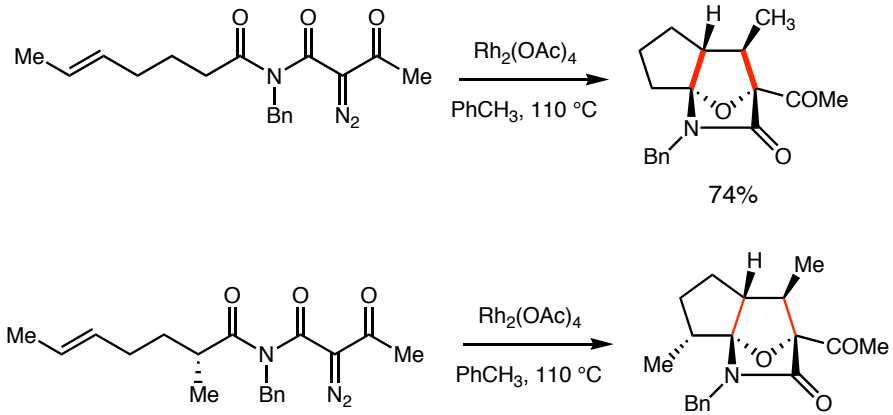

Maier, M. E.; Evertz, K. *Tetrahedron Lett.* **1988**, *29*, 1677-1680.

Cycloadditions with Oxidopyrylium Ylides

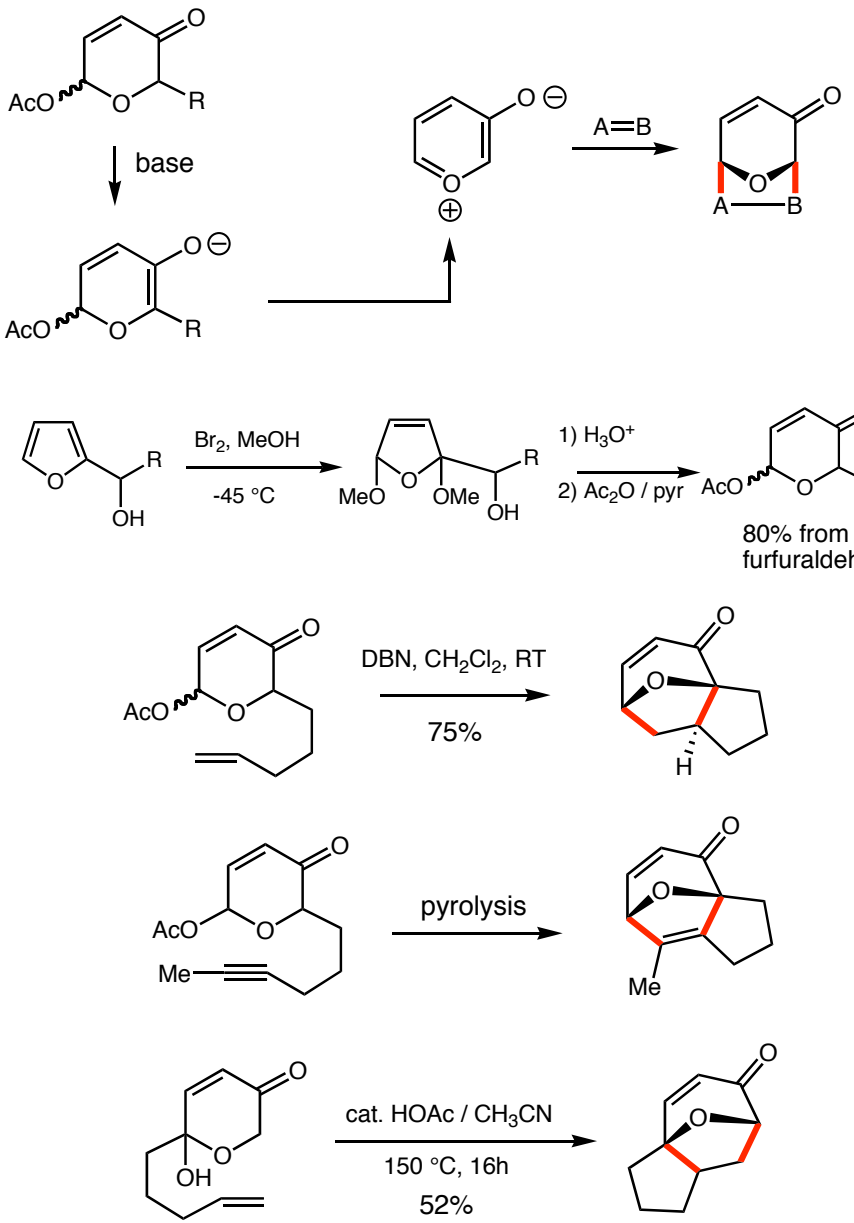

Sammes, P. G.; Street, L. J. *J. Chem. Soc., Chem. Commun.* **1982**, 1056-1057

Total Synthesis of (−)-Colchicine via a Rh-Triggered Cycloaddition Cascade

Timm Graening, Virginie Bette, Jörg Neudörfl, Johann Lex, and Hans-Günther Schmalz*

Universität zu Köln, Greinstrasse 4, D-50939 Köln, Germany

schmalz@uni-koeln.de

Received June 6, 2005

ORGANIC LETTERS

2005
Vol. 7, No. 20
4317−4320

Abstract

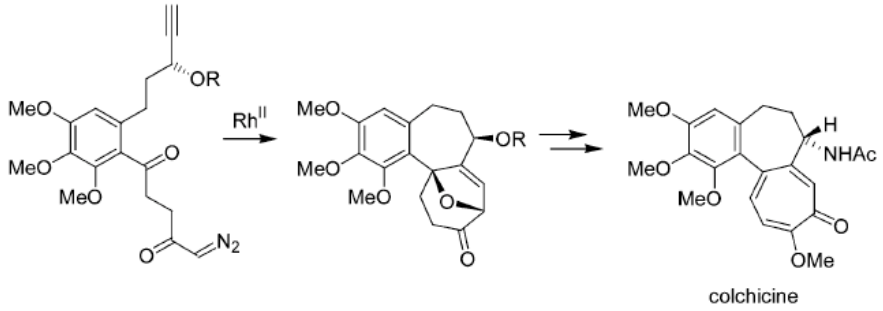

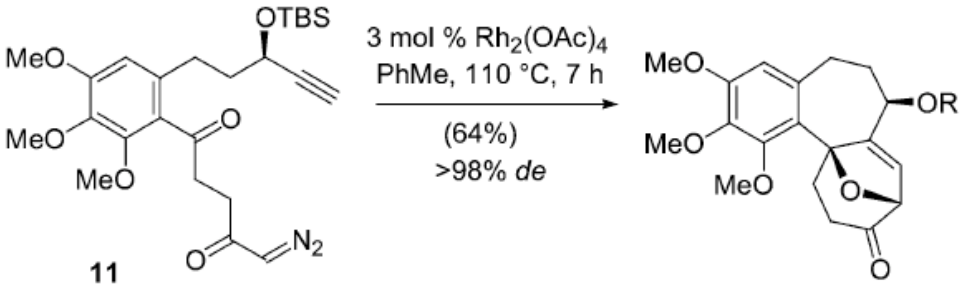

Scheme 1. Retrosynthetic Analysis

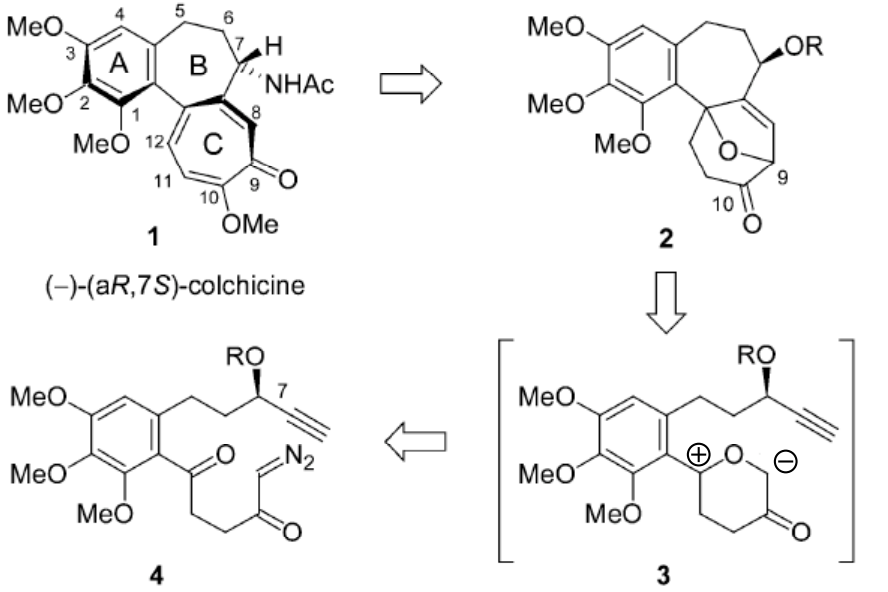

Cyclizations with 5-Hydroxy-4-Pyrones

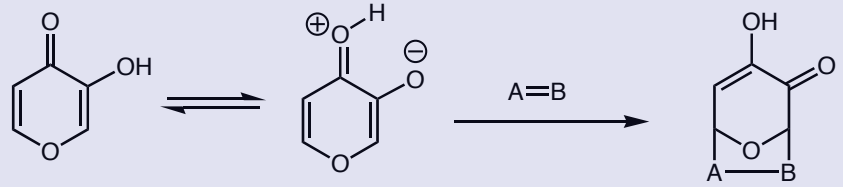

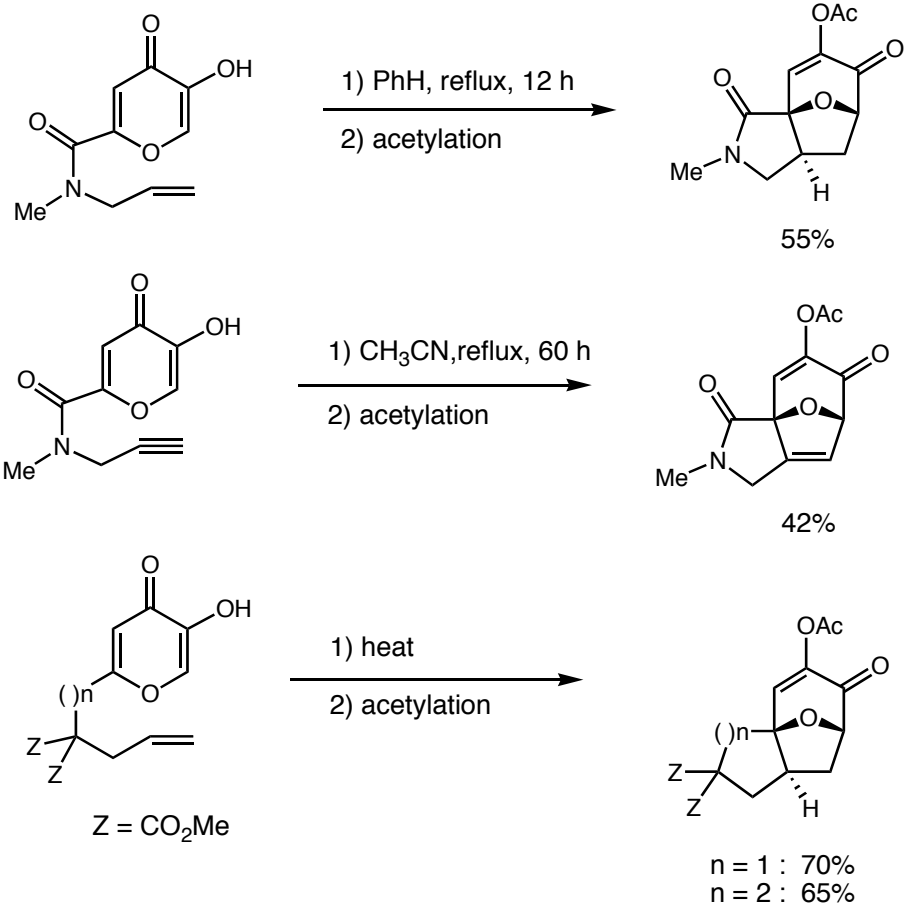

Garst, M. E.; McBride, B. J.; Douglass, J. G. III. *Tetrahedron Lett.* **1983**, *24*, 1675-1678.

Phorbol: The Hydroxypyrone Approach

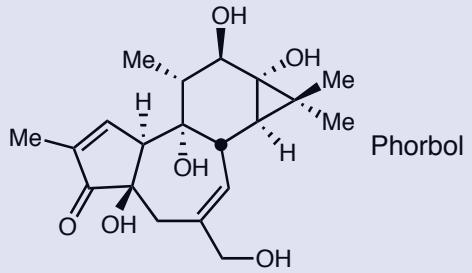

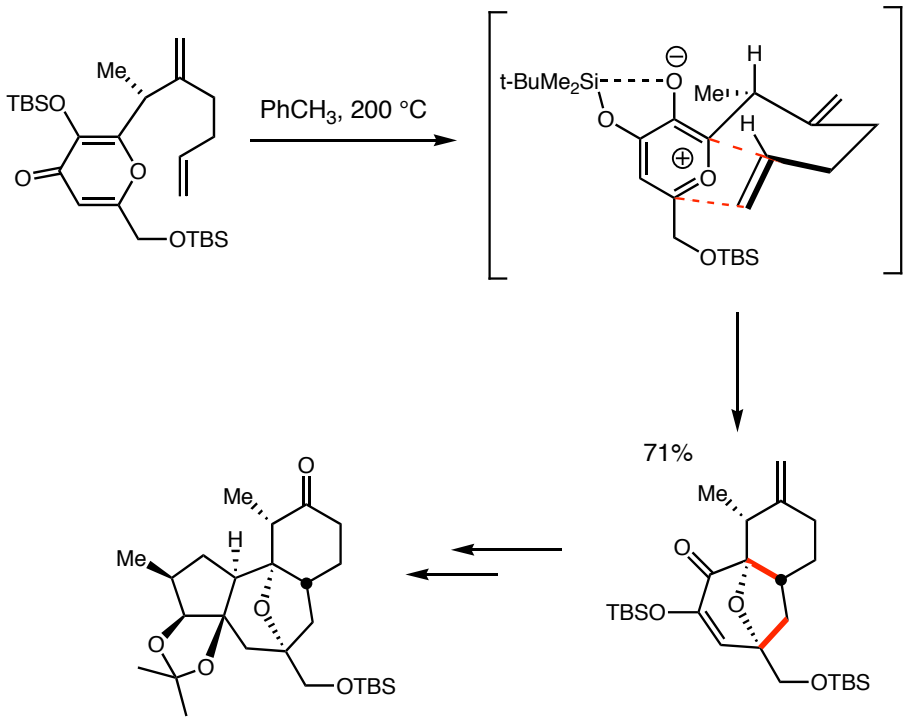

Wender, P. A.; McDonald, F. E. *J. Am. Chem. Soc.* **1990**, *112*, 4956-4958

Database Problem 189

This question is taken from recent work reported by Jack Baldwin (*Org. Lett.*, **1999**, 1933 and 1937).

Part A. Provide a mechanism for the conversion of **I** to **II**.

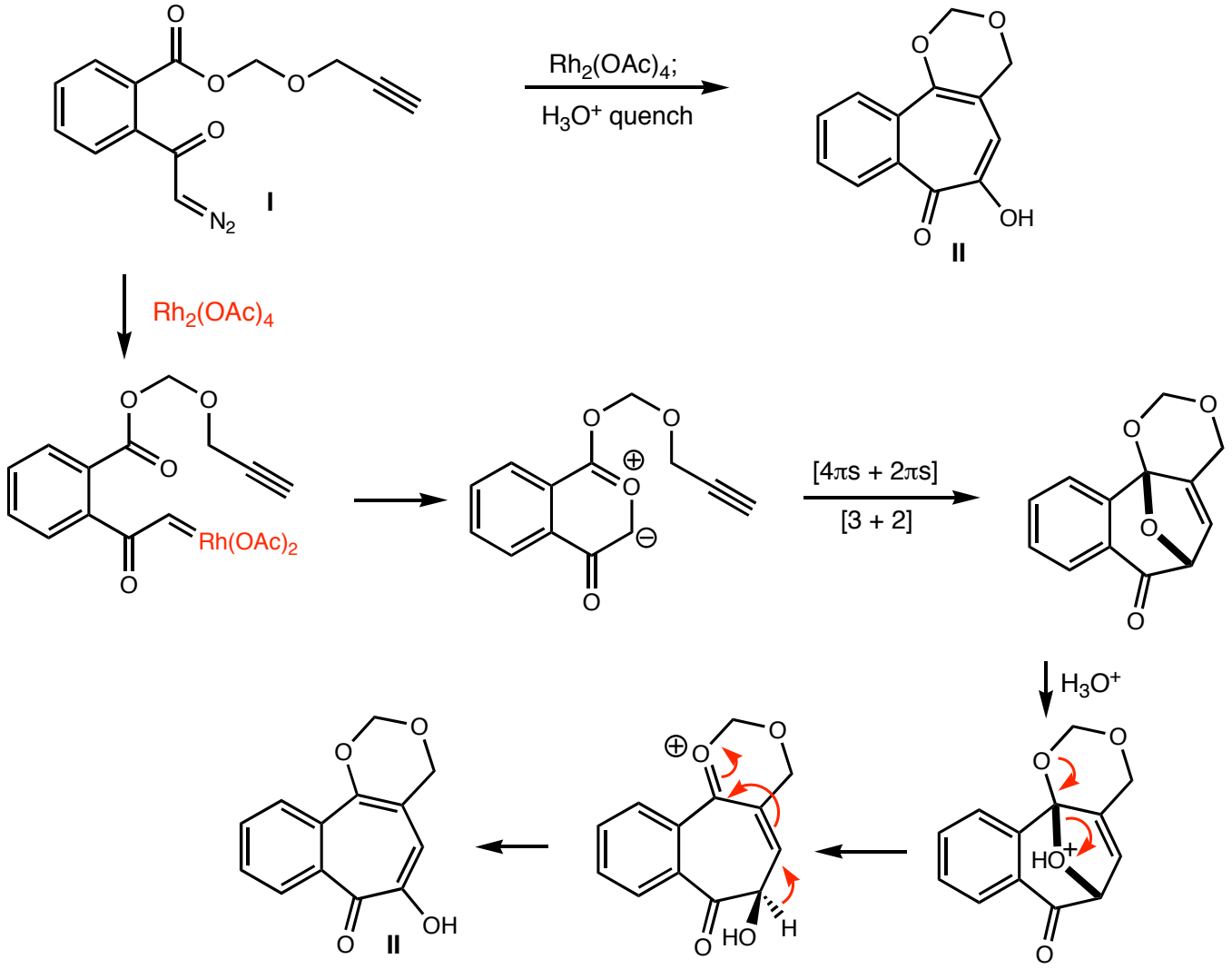

Database Problem 189

This question is taken from recent work reported by Jack Baldwin (*Org. Lett.*, **1999**, 1933 and 1937).

Part B. Compound **II** is protected as its methyl ether **III** and then transformed to **IV**. Provide a mechanism for the conversion of **III** to **IV**. Predict the relative stereochemistry at the starred (*) carbon atoms.

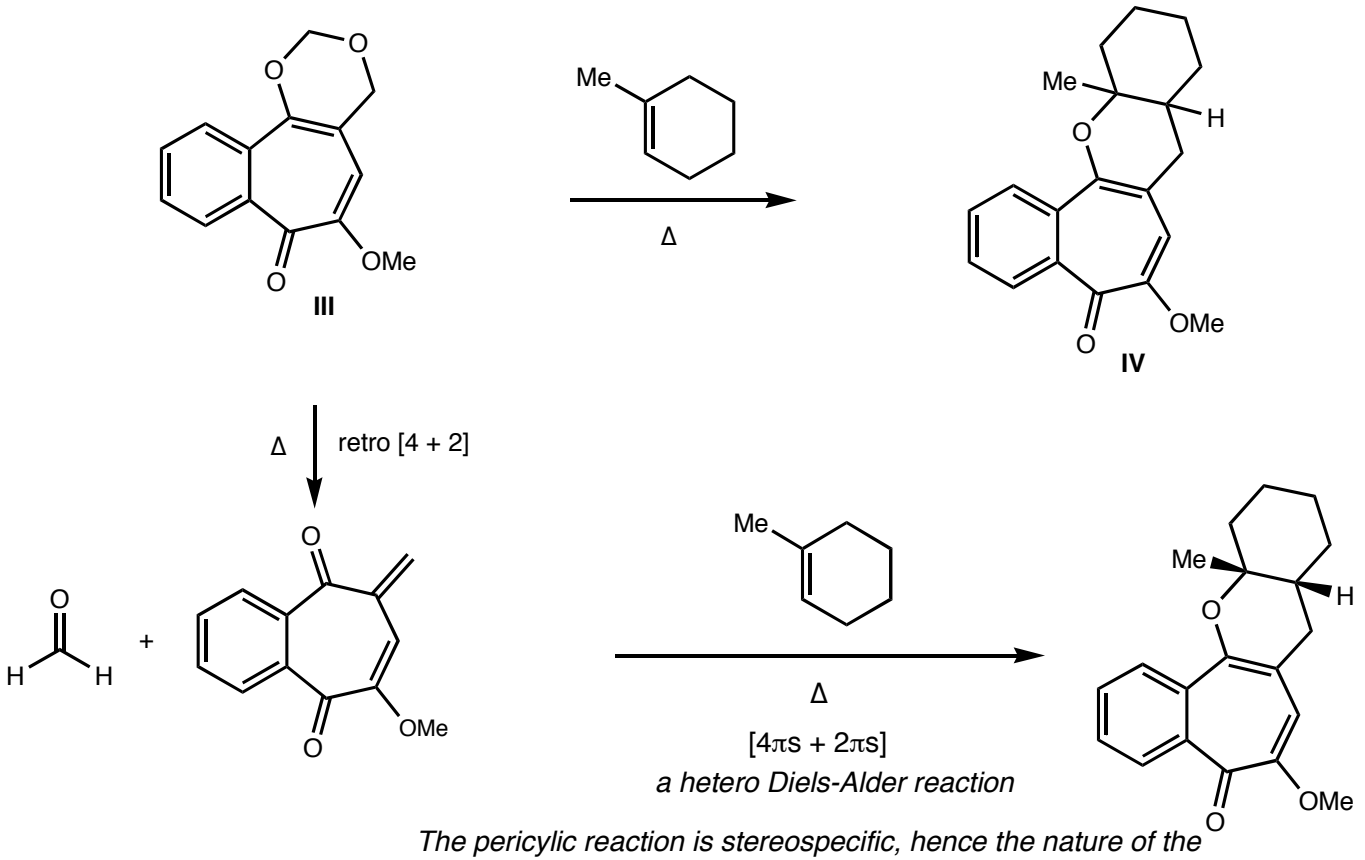

The pericylic reaction is stereospecific, hence the nature of the starting olefin defines the geometry observed in the product.

Problem 53. Williams recently reported an approach to the synthesis of quinocarcinamide (**1**) (*J. Org. Chem.* **1995**, *60*, 6791). The pivotal process that establishes the tetracyclic nucleus is the two-step transformation shown below (eq 1).

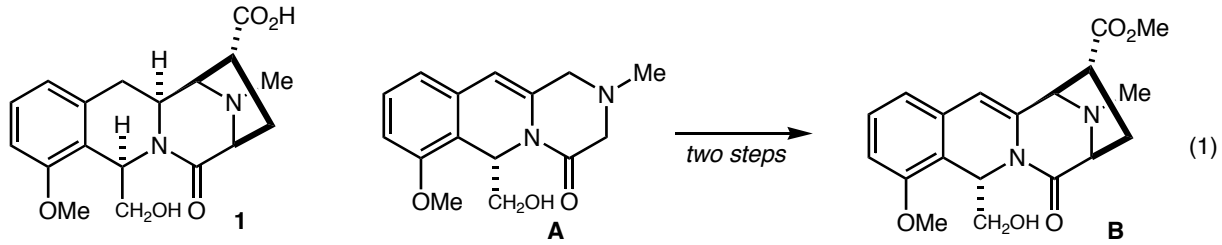

(1)

Devise a strategy for transforming A into B and clearly illustrate your answer in the space below. Full credit will be awarded to concise answers.

Problem 55. The following transformation was recently reported by Heathcock during studies directed toward the synthesis of sarain A
(*Tetrahedron Lett.* **1995**, *6*, 2381). From your knowledge of the functionality present in the starting material, deduce the structure (including stereochemistry) of the reaction product which has the same molecular weight as the starting material. Hint. the 1H NMR spectrum of the product reveals that the olefinic resonances have disappeared.

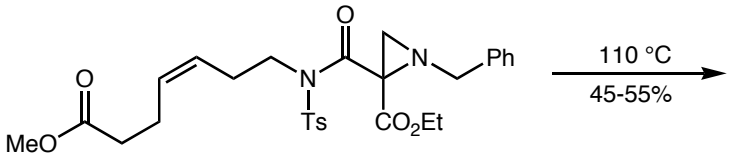

product structure

Problem 65. The following stereoselective nitrile oxide cycloaddition has been reported by Kozikowski (*Tetrahedron Lett.* **1982**, *23*, 2081;
J. Org. Chem. **1984**, 49, 2762). Provide the stereostructure of the major product and rationalize the stereochemical outcome as indicated in the directions.

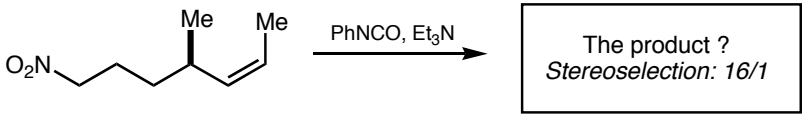

product structure

Problem 87. The illustrated transformation has been utilized by Coldham *(Chem. Commun.* **1999**, 1757) to construct the core ring system of the manzamines.

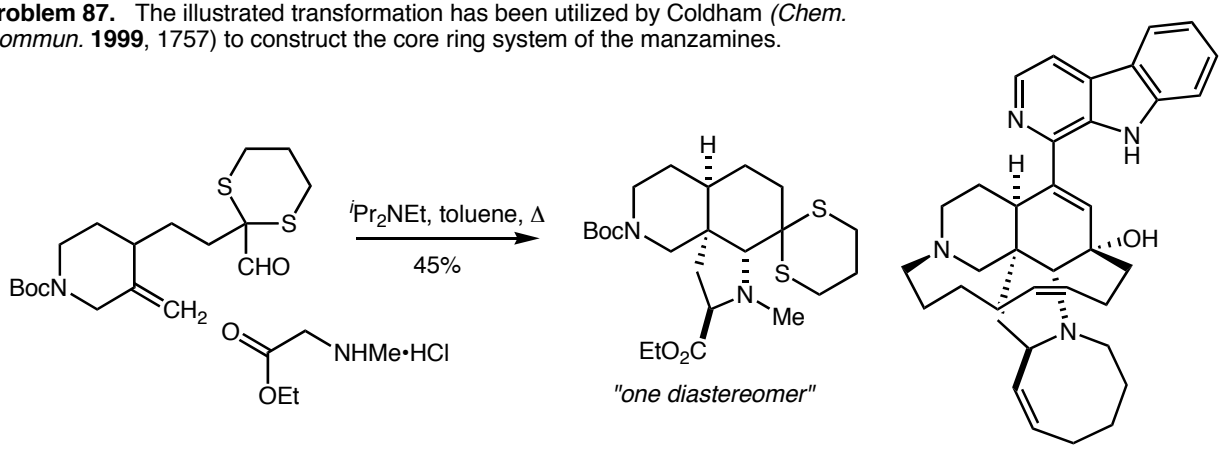

Problem 90. Padwa and co-workers recently disclosed the illustrated multistep polycyclisation as a possible route to the strychnine core (*Org. Lett.* **2001**, ASAP)

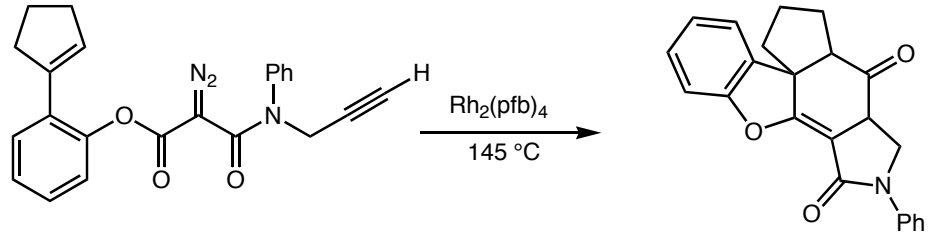

In the space below, provide a mechanism for the indicated transformation. *Hint: The management suggests that a carefull bidirectional analysis might help you to arrive at a sollution of this question.*

Problem 136. A recent paper by Harwood and Park highlights the rapidity which whch one may assemble complex architecture in a single chemical operation (*Tetrahedron Lett.* **1999**, *40*, 2907 and earlier cited references). The transformation in question is illustrated below. You are asked to address two aspects of this transformation.

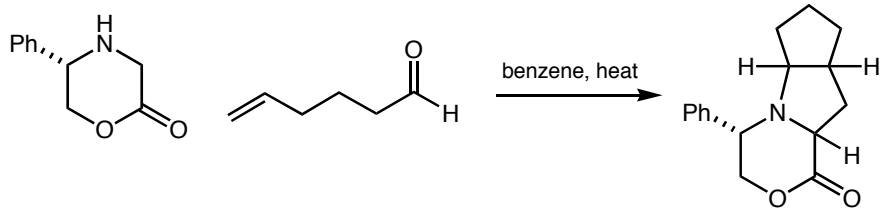

Part A. Provide a concise mechanism for the indicated transformation. For now, ignore the stereochemical aspects of the reaction.

Part B. Predict the stereochemical outcome of the reaction at the three new stereocenters, and provide a three-dimensional drawing of the transition state wherein these centers are produced.

Problem 171. A recent paper by Dolle (*Tetrahedron Lett.* **1999**, *40*, 2907) highlights the rapidity which whch one may assemmble complex architecture in a single chemical operation. The transformation in question is illustrated below.

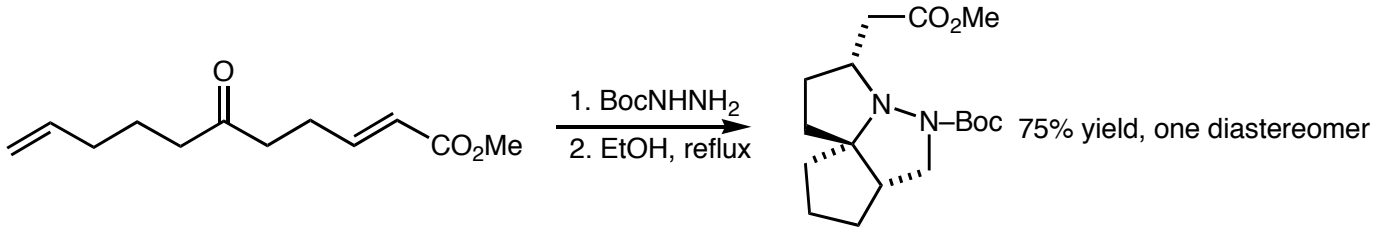

Provide a concise mechanism for the indicated transformation. In that step where the complex stereochemical relationships are established, a carefully rendered three dimensional illustration is requested.

Problem 189. This question is taken from recent work reported by Jack Baldwin (*Org. Lett.*, **1999**, 1933 and 1937). Provide a mechanism for the conversion of **I** to **II**.

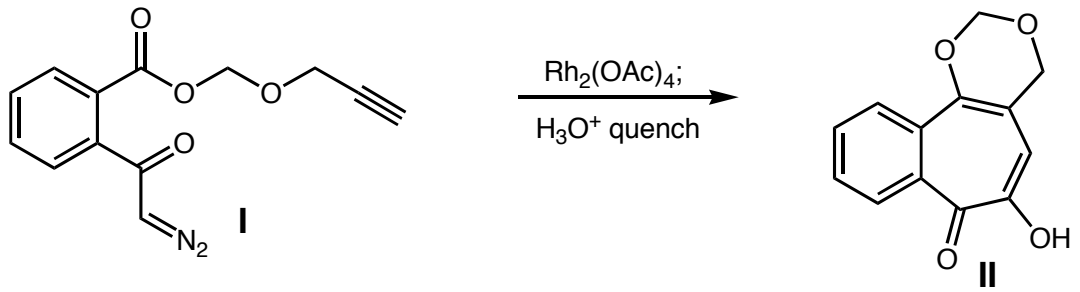

http://www.courses.fas.harvard.edu/colgsas/1063

Chemistry 206

Advanced Organic Chemistry

Lecture Number 20

Acid-Base Properties of Organic Molecules

- Bronsted Acidity Concepts in the Activation of Organic Structures
- Medium Effects on Bronsted Acidity
- Substituent & Hybridization Effects on Bronsted Acidity
- Kinetic & Thermodynamic Acidity of Ketones
- Kinetic Acidity: Carbon vs. Oxygen Acids
- Tabulation of Acid Dissociation Constants in DMSO

Reading Assignment for this Lecture:

Carey & Sundberg: **Part A**; Chapter 7
Carbanions & Other Nucleophilic Carbon Species

"Equilibrium acidities in DMSO Solution", F. G. Bordwell.
Acc. Chem. Res. **1988**, *21*, 456-463. (**handout**)

D. A. Evans

Friday
November 3, 2006

Here is a website containing Bordwell pKa data

http://www.chem.wisc.edu/areas/reich/pkatable/index.htm

Problems of the Day:

Explain why **1** and **3** are ~4 pKa units more acidic than their acyclic counterparts **2** and **4**. (*J. Org. Chem.* **1994**, *59*, 6456)

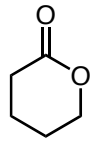

1

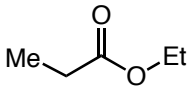

2

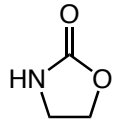

3

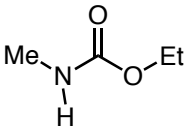

4

The thermodynamic acidities of phenol and nitromethane are both ~10; however, using a common base, phenol is deprotonated 10^{+6} times as fast. Rationalize

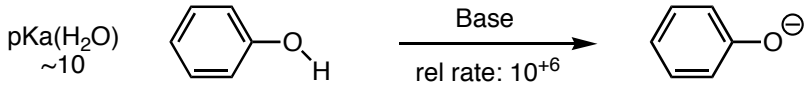

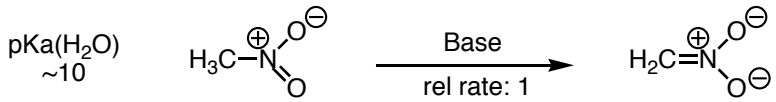

Activation of Organic Molecules

Base Activation

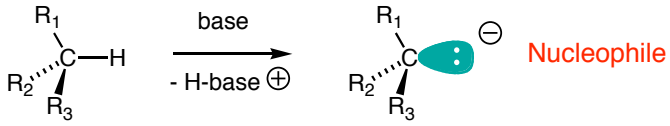

pK_a , describes quantitatively a molecule's propensity to act as an acid, i.e. to release a proton.

- Medium effects
- Structural effects (influence of substituents R_1)

Acid Activation

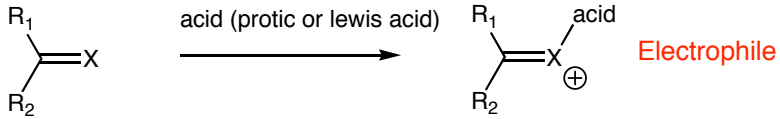

X = e.g. O, NR ...

The Aldol Example

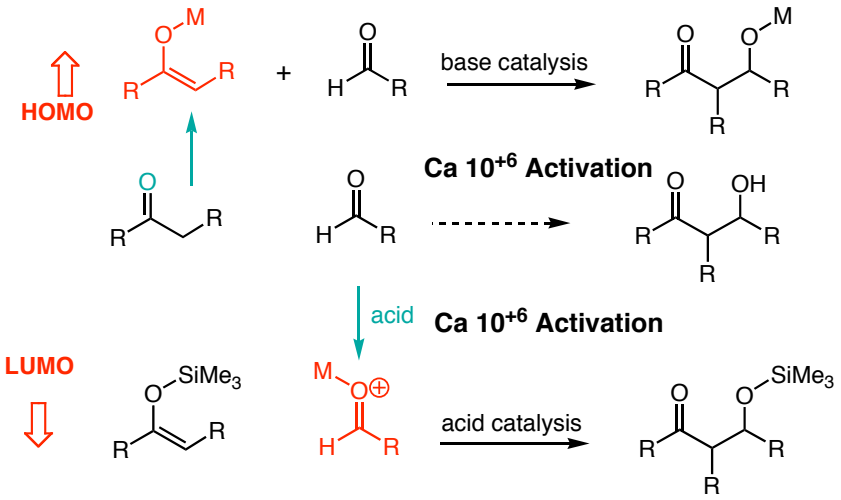

Definition of Ka

Let H–X be any Bronsted acid. In water ionization takes place:

$$H\text{–}X + HOH \rightleftharpoons H_3O^+ + X^-$$

where $K_{eq} = \dfrac{[H_3O^+]\,[X^-]}{[H\text{–}X]\,[HOH]}$ **where [HOH] = 55.5 mol L^{-1}** (A)

Since [HOH] is, for all practical purposes, a constant value, the acid dissociation constant K_a is defined without regard to this entity. e.g.

$$H\text{–}X \rightleftharpoons H^+ + X^- \quad \text{where } H^+ = H_3O^+$$

Hence $$\mathbf{K_a = \dfrac{[H^+]\,[X^-]}{[H\text{–}X]}} \qquad \mathbf{(B)}$$

From the above definitions, K_a is related to K_{eq} by the relation:

$$\mathbf{K_a(H\text{–}X) = 55.5\ K_{eq}(H\text{–}X)} \qquad \mathbf{(C)}$$

Autoionization of water

$$HOH + HOH \rightleftharpoons H_3O^+ + HO^-$$

$K_{eq} = 3.3 \times 10^{-18}$

From Eq C: $K_a = 55.5\ K_{eq} = 55.5(3.3 \times 10^{-18})$

Hence $K_a = 1.8 \times 10^{-16}$

Since pK_a is defined in the following equation:

$$\mathbf{pK_a = -\log_{10}[K_a]}$$ The pK_a of HOH is + 15.7

Keep in mind that the strongest base that can exist in water is HO^-.

Lets now calculate the acid dissociation constant for hydronium ion.

$$H_3O^+ + H_2O \rightleftharpoons H_3O^+ + H_2O$$

obviously: $K_{eq} = 1$

$K_a = [HOH] \times K_{eq}$ hence $K_a = 55.5$

$pK_a = -\log_{10} K_a = -1.7$

The strongest acid that can exist in water is H_3O^+.

The Gibbs Relationship

$$\Delta G^\circ = -RT \ln K$$

or $\Delta G^\circ = -2.3\,RT \log_{10} K$

2.3 RT = 1.4 at T = 298 K in kcal · mol^{-1}

$$\Delta G^\circ_{298} = -1.4 \log_{10} K_{eq}$$

$$\Delta G^\circ_{298} = 1.4\ pK_{eq} \approx 1.4\ pK_a \qquad \text{with } pK = -\log_{10} K$$

Hence, pK_a is proportional to the free energy change

K_{eq}	pK_{eq}	ΔG°
1	0	0
10	–1	–1.4
100	– 2	–2.8 kcal/mol

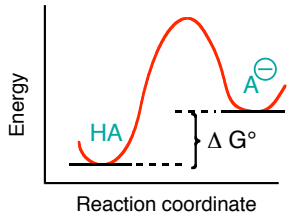

Medium Effects

Consider the ionization process:

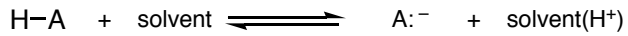

In the ionization of an acid in solution, the acid donates a proton to the medium. The more basic the medium, the larger the dissociation equilibrium. The ability of the medium to stabilize the conjugate base also plays an important role in the promotion of ionization. Let us consider two solvents, HOH and DMSO and the performance of these solvents in the ionization process.

	The Protonated Solvent	Conjug. Base Stabiliz.
Water		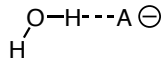
DMSO	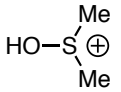	No H-bonding Capacity

As shown above, although HOH can stabilize anions via H-bonding, DMSO cannot. Hence, a given acid will show a greater propensity to dissociate in HOH. As illustrated below the acidity constants of water in HOH, DMSO and in a vacuum dramatically reflect this trend.

Medium Effects on the pKa of HOH

** The gas phase ionization of HOH is endothermic by 391 kcal/mol !!!

HOH pKa	Medium
15.7	HOH
31	DMSO
279 (est)**	Vacuum

Representative pKa Data

Substrate	DMSO	HOH	Δ pKa
HOH	31.2	15.7	15.5
HSH	14.7	7.0	7.7
MeOH	29.0	15.3	13.7
C_6H_5OH	18.0	9.9	8.1
$O_2N–CH_3$	17.2	10.0	7.2
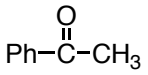	24.6	17	7.6

The change in pKa in going from water to DMSO is increasingly diminished as the conjugate base becomes resonance stabilized (Internal solvation!).

Substrate	DMSO	HOH	Δ pKa
	18.1	16.0	2.1
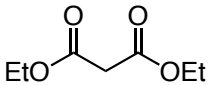	16.4	13.3	3.1
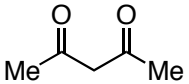	13.3	8.9	4.5
	11.1	11.2	0

Substituent Effects

Electronegativity e.g. Compare Carboxylic Acids vs. Ketones

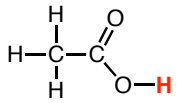

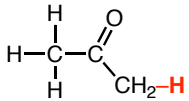

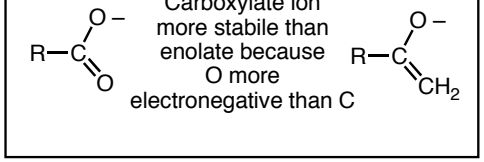

(H_2O) $pK_A = 4.8$ $pK_A \approx 19$

(DMSO) $pK_A = 12.3$ $pK_A \approx 26.5$

Hybridization - S-character of carbon hybridization

Remember:

sp^3-orbitals 25% s-character

sp^2-orbitals 33% s-character

sp-orbitals 50% s-character

Carbon Acids

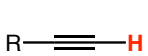

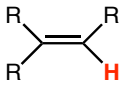

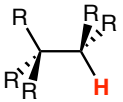

Hybridzation	sp	sp^2	$\approx sp^2$	sp^3
Bond Angle	180°	120°	≈ 120	109°
pK_a(DMSO)	23	≈ 44	≈ 39	≈ 60

Electrons in 2S states "see" a greater effective nuclear charge than electrons in 2P states.

This becomes apparent when the radial probability functions for S and P-states are examined: The radial probability functions for the hydrogen atom S & P states are shown below.

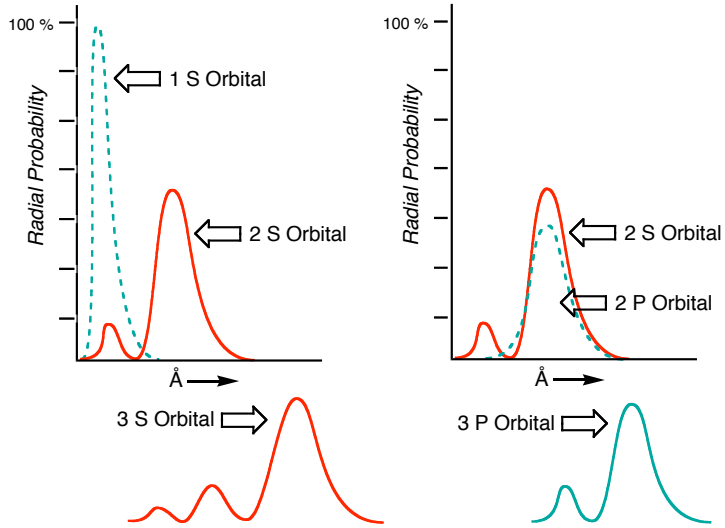

S-states have greater radial penetration due to the nodal properties of the wave function. Electrons in s states see a higher nuclear charge. The above observation correctly implies that the stability of nonbonding electron pairs is directly proportional to the % of S-character in the doubly occupied orbital.

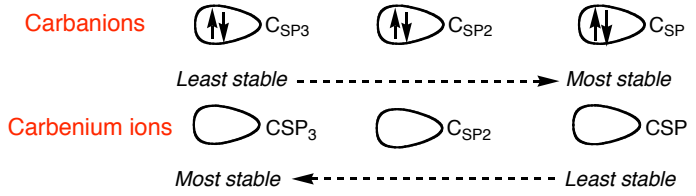

The above trends indicate that the greater the % of S-character at a given atom, the greater the electronegativity of that atom.

Hybridization vs Electronegativity

There is a linear relationship between %S character & Pauling electronegativity

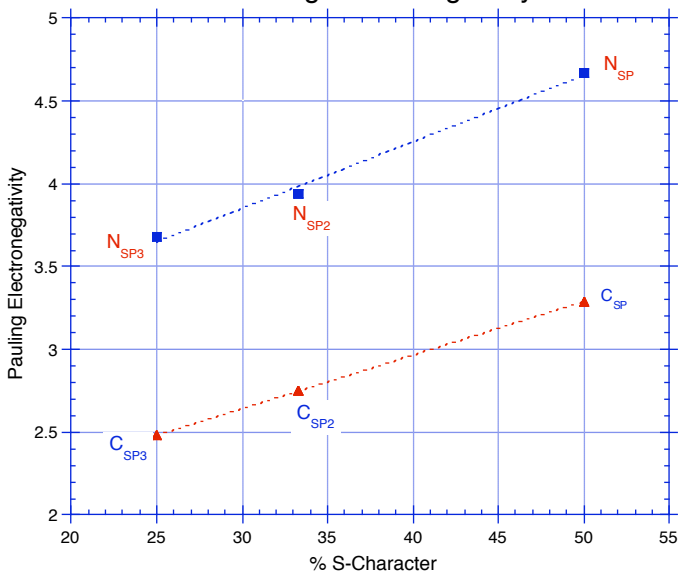

There is a direct relationship between %S character & hydrocarbon acidity

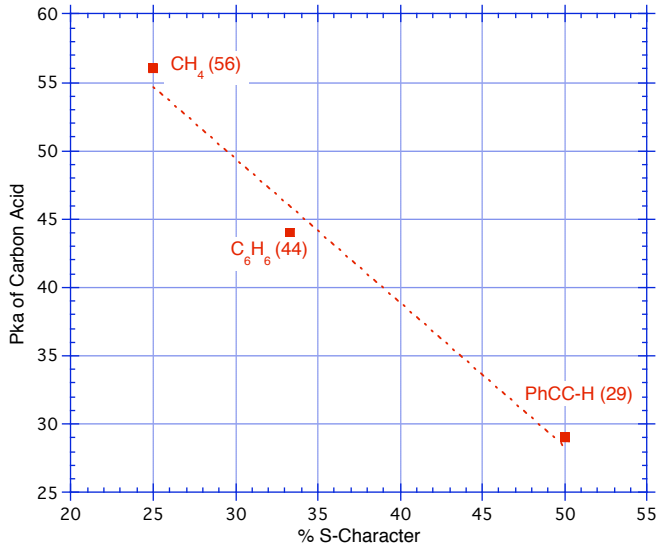

Substituent Effects

Alkyl Substituents on Localized Carbanions are Destabilizilng:

Steric hinderance of anion solvation

Compare: (*JACS* **1975**, *97*, 190)

	pK_A (DMSO)		pK_A (DMSO)
$PhSO_2$-CH(H)-H	29	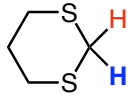	31.1
$PhSO_2$-CH(H)-Me	31	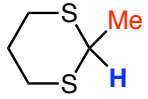	38.3

Heteroatom-Substituents: - 1st row elements of periodic table

	pK_A (DMSO)	
$PhSO_2$-CH(H)-OCH_3	30.7	Inductive Stabilization versus Lone Pair Repulsion (-I vs +M -Effect)
$PhSO_2$-CH(H)-OPh	27.9	
$PhSO_2$-CH(H)-$\overset{\oplus}{N}Me_3$	19.4	Inductive Stabilization

Heteroatom-Substituents: - 2nd row elements of periodic table

Strong carbanion stabilizing effect

	pK_A (DMSO)		pK_A (DMSO)
$PhSO_2$-CH(H)-H	29	$PhSO_2$-CH(H)-SO_2Ph	12.2
$PhSO_2$-CH(H)-SPh	20.5	$PhSO_2$-CH(H)-PPh_2	20.5

■ Carbanion Stabilization by 2rd–Row Atoms: SR, SO_2R, PR_3 etc

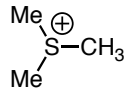

18.2 (DMSO)

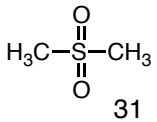

31

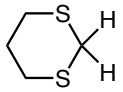

31

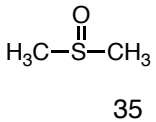

35

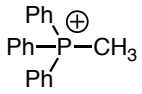

22.5

(*JACS* **1976**, *98*, 7498; *JACS* **1977**, *99*, 5633; *JACS* **1978**, *100*, 200).

The accepted explanation for carbanion stabilization in 3rd row elements is delocalization into vicinal antibonding orbitals

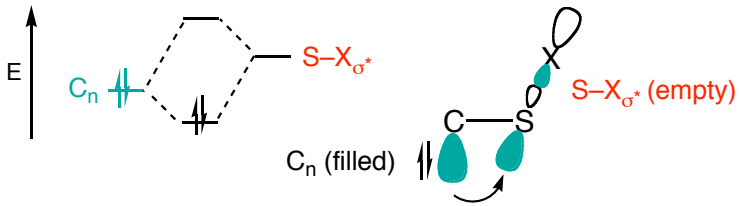

This argument suggests a specific orientation requirement. This has been noted:

Anti (or syn) periplanar orientation of Carbanion-orbital and σ* orbital mandatory for efficient orbital overlap.

Rates for deprotonation with *n*-BuLi

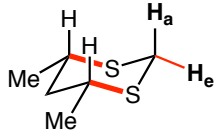

$H_e : H_a = 8.6$ (*JACS* **1974**, *96*, 1811)

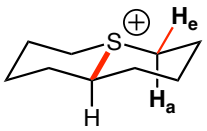

$H_e : H_a = 30$ (*JACS* **1978**, *100*, 200)

■ Conjugative Stabilization of Conjugate Base

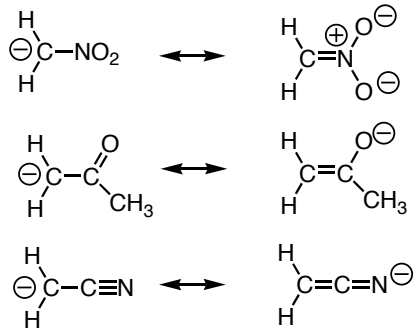

17.2 pK_A (DMSO)

26.5

31.5

For efficient conjugative stabilization, rehybridization of carbanion orbital from n_{sp3} to n_p is required for efficient overlap with low-lying π*-orbital of stabilizing group. However, the cost of rehybridization must be considered.

■ Stereoelectronic Requirement for Carbanion Overlap: Enolization of Carbonyl Compounds

Stereoelectronic Requirements: The α-C-H bond must be able to overlap with π* C–O

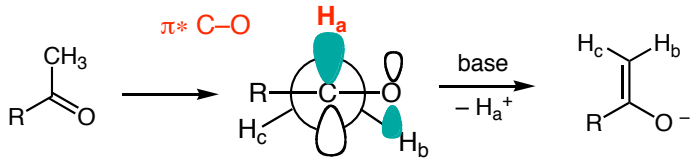

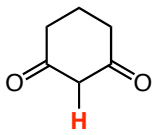

pK_A 5.2

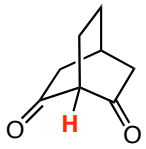

C-H acidity not detectable

Ph_3C–H pK_A (DMSO) 31.5

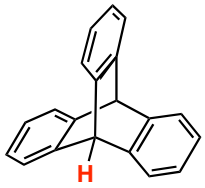

47.7

Phenol Acidity: An Analysis of Resonance & Inductive Effects

Phenol Acidity:

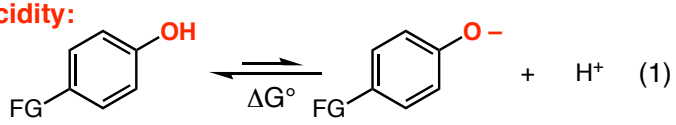

This topic has a number of take-home lessons. Most importantly, is is a useful construct on which to discuss the role of FG's in influencing the acidity of this oxygen acid.

How does one analyze the impact of structure on pKa of a weak acid (pKa > 0) ?

The Approach:

For equilibria such as that presented above, analyze the effect of stabilizing (or destabilizing) interactions on the more energetic constituent which in this case is the conjugate base.

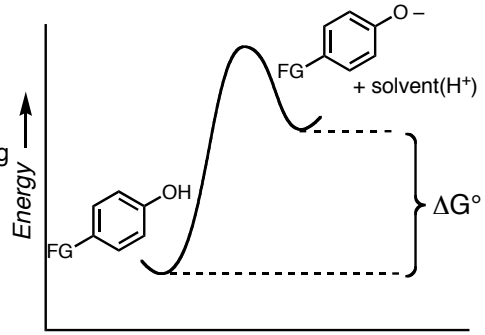

Why is phenol so much more acidic than cyclohexanol?

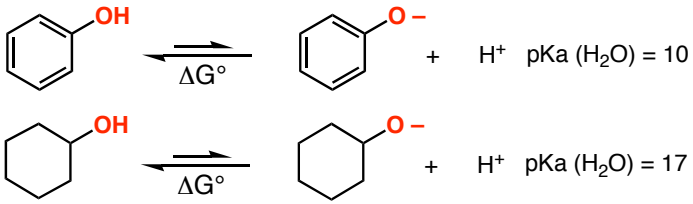

Loudon (pg 730): "The enhanced acidity of phenol is due largely to stabilization of its conjugate base by resonance."

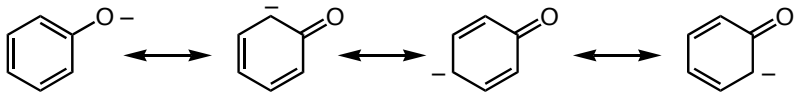

Really!!

Is the benzene ring somehow special. i.e "larger resonance space."

Acetone enol:

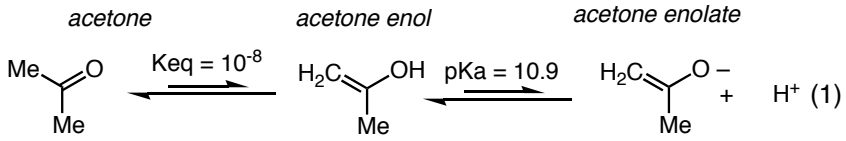

The surprising facts is that the acetone enol has nearly the same pKa as phenol. Hence, the answer to the above question is no!

How important are inductive effects in the stabilization of $C_6H_5O^-$?

Consider the following general oxygen acid X–OH where X can only stabilize the conjugate base through induction:

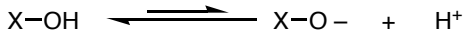

As the electronegativity of X increases the acidity of X–OH increases.

X–OH	pKa(H_2O)
CH_3–OH	15.5
CF_3CH_2–OH	12.4
Cl–OH	7.5

If you take the calculated electronegativity of an SP_2 carbon (2.75) you can see that there is a linear correlation between the electronegativity of X and the pKa of X–OH.

This argument suggests that the acidity of acetone enol is largely due to inductive stabilization, not resonance.

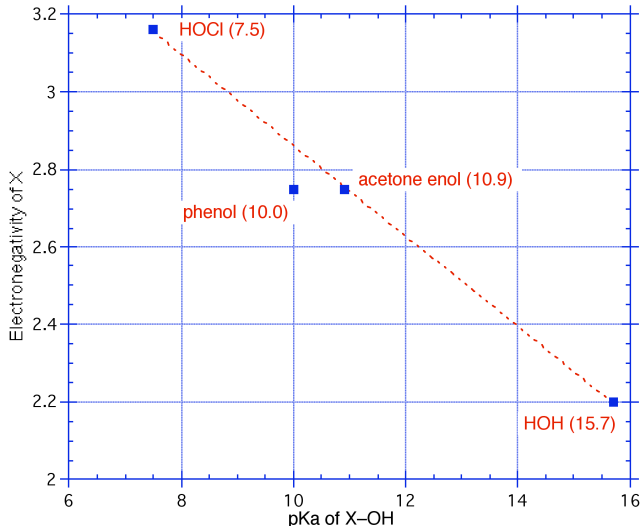

Ionization of a weak acid (pKa > 0)

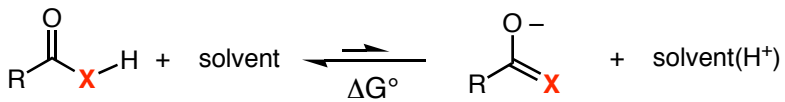

Variables:
X = O (carboxylic acid)
X = NH (amide)
X = CH_2 (Ketone/ester)

R = CR_3
R = OR
R = NR_2

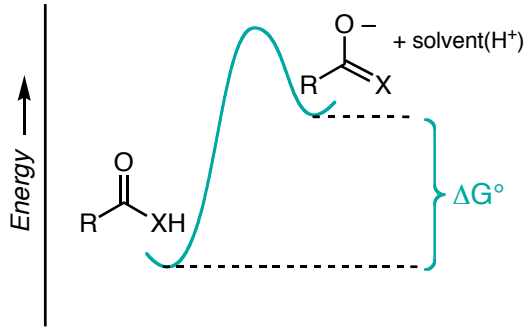

- The Question: How does one analyze the impact of structure on pKa ?
- The Approach:

  For equilibria such as that presented above, analyze the effect of stabilizing (or destabilizing) interactions on the more energetic constituent which in this case is the conjugate base.

Case I: Carboxylic Acids: Inductive Effects

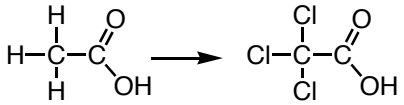

pKa = 4.8 pKa = 0.6

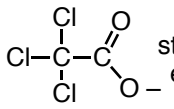

Carboxylate ion stabilized by increased electron-withdrawing CCl_3 group.

Case II: Carboxylic Acids: Inductive Effects & Carbon Hybridization

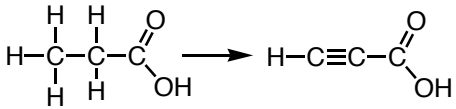

pKa = 4.9 pKa = 1.9

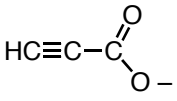

Carboxylate ion stabilized by increased electron-withdrawing SP-hybridized carbon

Case III: Carboxylic Acids vs Ketones:

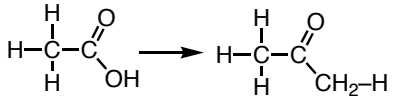

pKa = 4.8 pKa ~ 19

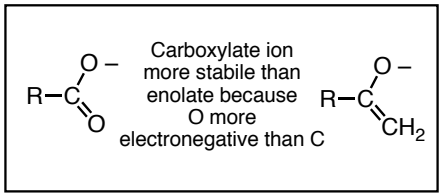

Case IV: Carboxylic Acids, Esters, Amides & Ketones:

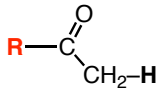

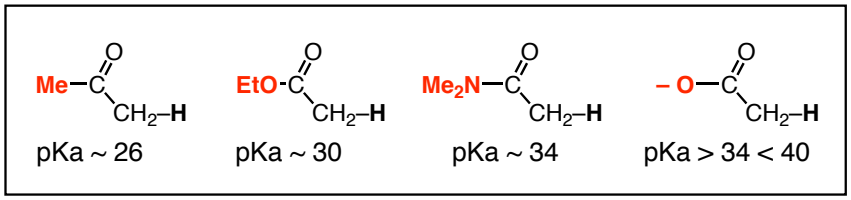

pKa ~ 26 pKa ~ 30 pKa ~ 34 pKa > 34 < 40

The Analysis:

In this series of compounds, there are two variables to consider:

- Inductive Effect: OEt > Me_2N > H_3C but (O–?)
- Resonance Effect:

  The degree to which substituent X: "contributes" electron density into enolate represents a destabilizing interaction:

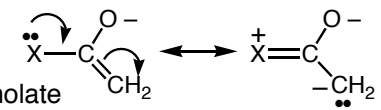

  Trend: O– > Me_2N > OEt
- Resonance donation dominates inductive electron withdrawal as indicated by the data.

Substituents on the α-carbon: Stabilization by either resonance, induction, or both is observed:

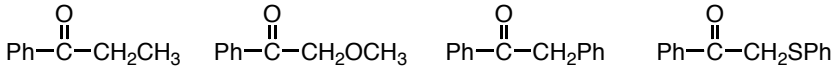

pKa = 24.4 pKa = 22.9 pKa = 17.7 pKa = 17.1

Kinetic Acidity: Rates of proton removal

Consider enolization of the illustrated ketone under non-equilibrating conditions:

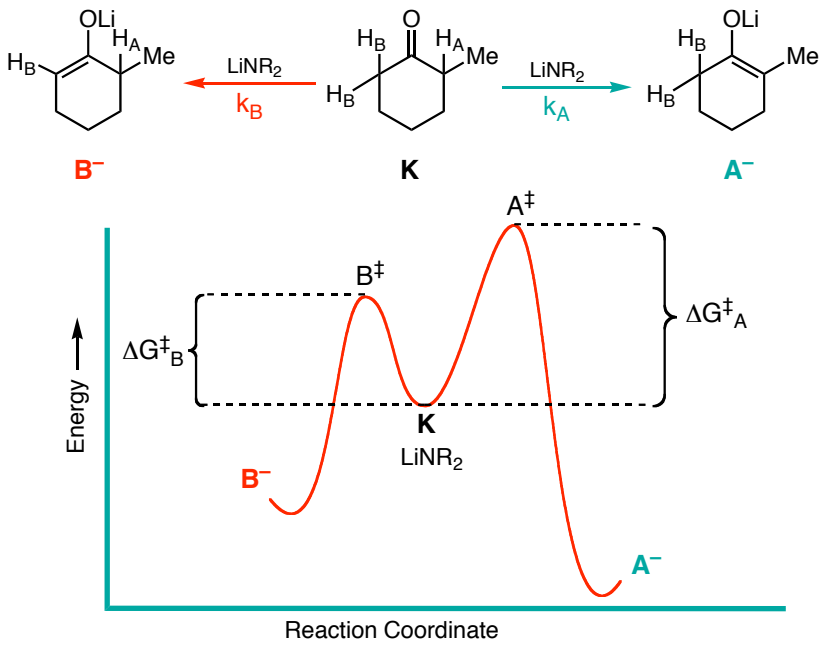

Kinetic acidity refers to the rate of proton removal. e.g. kA vs kB. For example, in reading the above energy diagram you would say that HA has a lower kinetic acidity than HB. As such, the structure of the base (hindered vs unhindered) employed plays a role in determining the magnitude of kA and kB. For the case shown above, $\Delta G^{\ddagger}$**A** will increase more than $\Delta G^{\ddagger}$**B** as the base becomes more hindered since the proton HA resides in a more sterically hindered environment. The example below shows the high level of selectivity which may be achieved with the sterically hindered base lithium diisopropylamide (LDA).

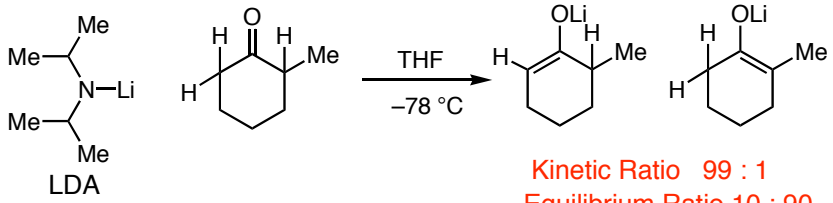

Kinetic Ratio 99 : 1
Equilibrium Ratio 10 : 90

Kinetic & Equilibrium Ratios of Enolates Resulting from Enolization with LDA & Subsequent Equilibration

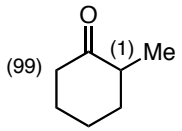

Kinetic Ratios

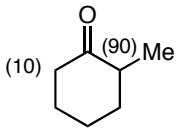

Equilibrium Ratios

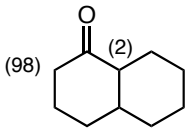

Kinetic Ratios

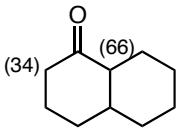

Equilibrium Ratios

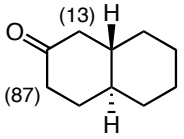

Kinetic Ratios

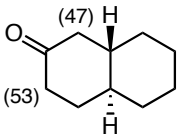

Equilibrium Ratios

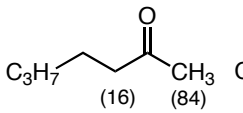

Kinetic Ratios

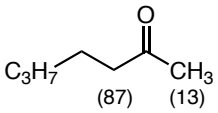

Equilibrium Ratios

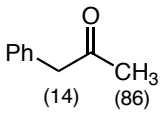

Kinetic Ratios

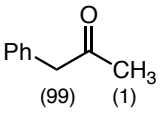

Equilibrium Ratios

Note that alkyl substitution stabilizes the enolate (Why??). This effect shows up in the equilibrium ratios shown above.

Hence, enolization under "kinetic control with LDA allows you to produce the less-substituted enolate while subsequent equilibration by simply heating the enolate mixture allows equilibration to the more substituted enolate.

Kinetic Acidity

Observation: The thermodynamic acidities of phenol and nitromethane are both approximately 10; however, using a common base, phenol is deprotonated 10^{+6} times as fast.

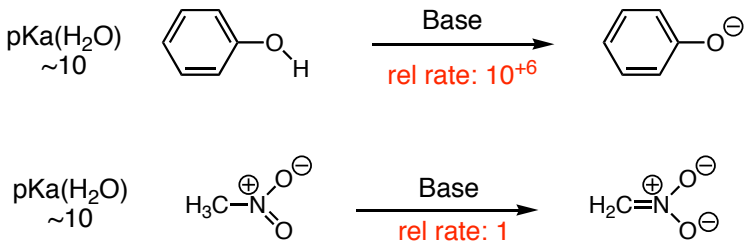

Proton transfers from C-H Bonds are slow.

Why???

Carbon acids are stabilized by resonance. Hence, significant structural reorganization must accompany deprotonation.

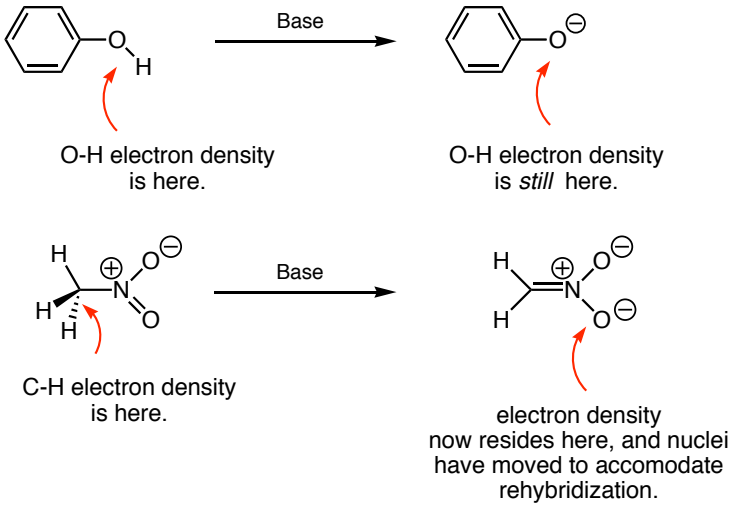

The greater the structural reorganization during deprotonation, the lower the kinetic acidity

Kinetic Acidity vs. Leaving Group Ability: E1cb Elimination

Stirling, *Chem. Commun.* **1975**, 940

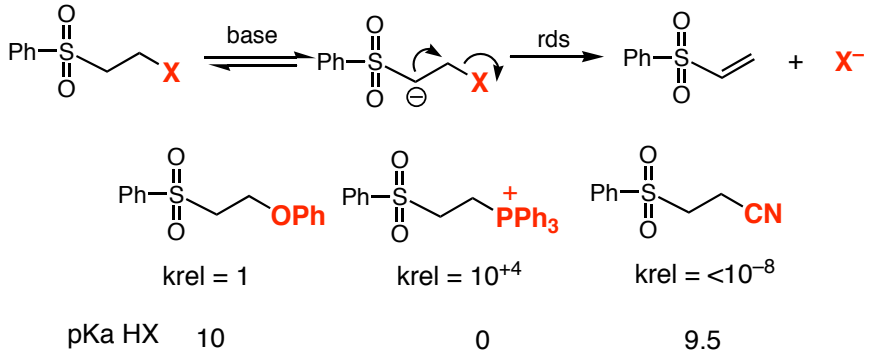

The greater the structural reorganization of leaving group during elimination, the slower the rate of elimination.

Protonation of Conjugate bases

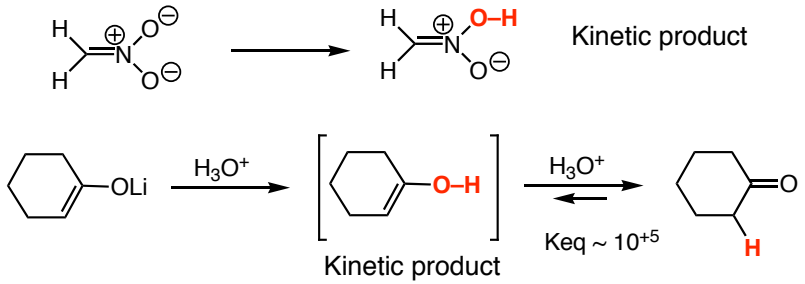

Jack Hine: Least Motion Principle (*Adv. Phys. Org. Chem.* **1977**, *15*, 1) Lowry & Richardson, 3rd Edition, pp 205-206

Those elementary reactions that involve the least change in atomic posiitons will be favored

Please explain

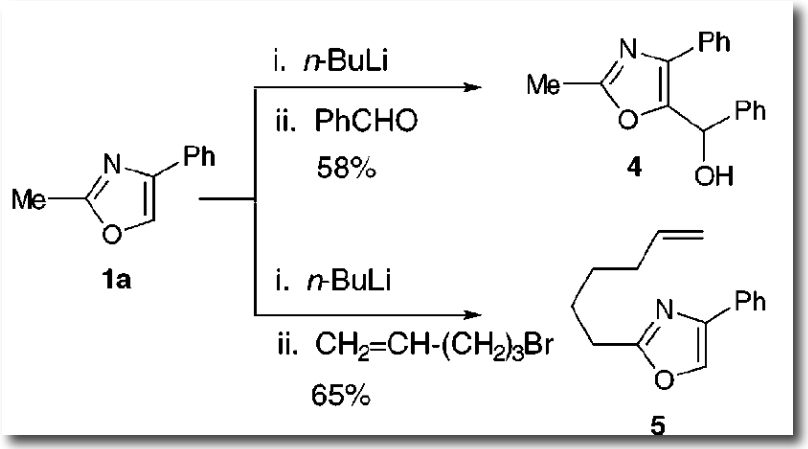

ORGANIC LETTERS

1999
Vol. 1, No. 1
87−90

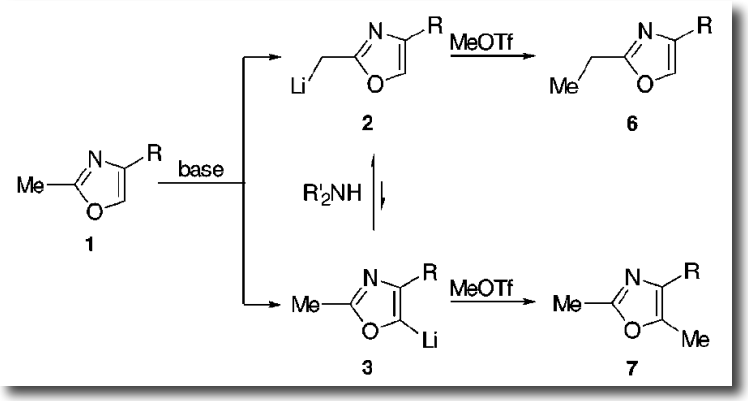

Table 1. Survey of Methods for the Selective Alkylation of Oxazoles and Thiazoles[a]

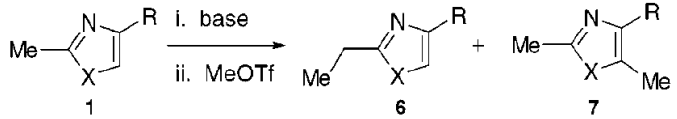

substrate	X	R	base (6:7)[b]		
			n-BuLi[c]	LiN^iPr_2	$LiNEt_2$
1a[d]	O	Ph	9:91	9:91	99:1

Table 3. Selective Lithiation of 2,4-Lutidine

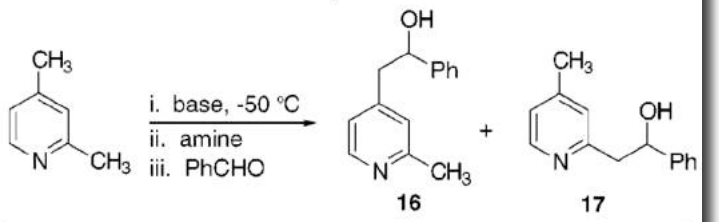

entry	base	amine	**16:17**	yield (%)
1	$LiNEt_2$	-	>95:5	95
2	*n*-BuLi	-	<5:95	86
3	*n*-BuLi	Et_2NH	>95:5	87

Substrate	pKa H_2O	(DMSO)
INORGANIC ACIDS		
H_2O	15.7	(32)
H_3O^+	-1.7	
H_2S	7.00	
HBr	-9.00	(0.9)
HCl	-8.0	(1.8)
HF	3.17	(15)
HOCl	7.5	
$HClO_4$	-10	
HCN	9.4	(12.9)
HN_3	4.72	(7.9)
HSCN	4.00	
H_2SO_3	1.9, 7.21	
H_2SO_4	-3.0, 1.99	
H_3PO_4	2.12, 7.21, 12.32	
HNO_3	-1.3	
HNO_2	3.29	
H_2CrO_4	-0.98, 6.50	
CH_3SO_3H	-2.6	(1.6)
CF_3SO_3H	-14	(0.3)
NH_4Cl	9.24	
$B(OH)_3$	9.23	
HOOH	11.6	

Substrate	pKa H_2O	(DMSO)
CARBOXYLIC ACIDS		
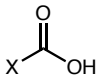		
X= CH_3	4.76	(12.3)
CH_2NO_2	1.68	
CH_2F	2.66	
CH_2Cl	2.86	
CH_2Br	2.86	
CH_2I	3.12	
$CHCl_2$	1.29	
CCl_3	0.65	
CF_3	-0.25	
H	3.77	
HO	3.6, 10.3	
C_6H_5	4.2	(11.1)
o-$O_2NC_6H_4$	2.17	
m-$O_2NC_6H_4$	2.45	
p-$O_2NC_6H_4$	3.44	
o-ClC_6H_4	2.94	
m-ClC_6H_4	3.83	
p-ClC_6H_4	3.99	
o-$(CH_3)_3N^+C_6H_4$	1.37	
p-$(CH_3)_3N^+C_6H_4$	3.43	
p-$OMeC_6H_4$	4.47	
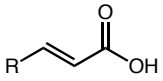		
R= H	4.25	
trans-CO_2H	3.02, 4.38	
cis-CO_2H	1.92, 6.23	

Substrate	pKa H_2O	(DMSO)
ALCOHOLS		
HOH	15.7	(31.2)
MeOH	15.5	(27.9)
i-PrOH	16.5	(29.3)
t-BuOH	17.0	(29.4)
c-hex_3COH	24.0	
CF_3CH_2OH	12.5	(23.5)
$(CF_3)_2CHOH$	9.3	(18.2)
C_6H_5OH	9.95	(18.0)
m-$O_2NC_6H_4OH$	8.4	
p-$O_2NC_6H_4OH$	7.1	(10.8)
p-$OMeC_6H_4OH$	10.2	(19.1)
2-napthol		(17.1)
OXIMES & HYDROXAMIC ACIDS		
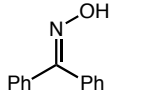	11.3	(20.1)
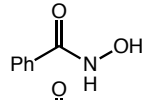	8.88 (NH)	(13.7)
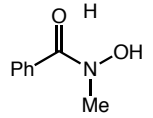		(18.5)
PEROXIDES		
MeOOH	11.5	
CH_3CO_3H	8.2	

Substrate	pKa H_2O	(DMSO)
PROTONATED SPECIES		
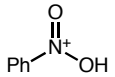	-12.4	
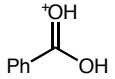	-7.8	
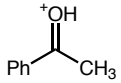	-6.2	
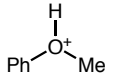	-6.5	
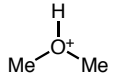	-3.8	
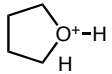	-2.05	
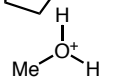	-2.2	
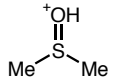	-1.8	
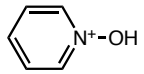	0.79	(+1.63)
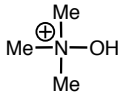		(+5.55)
SULFINIC & SULFONIC ACIDS		
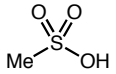	-2.6	
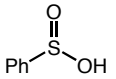	2.1	

*Values <0 for H_2O and DMSO, and values >14 for water and >35 for DMSO were extrapolated using various methods.

For a comprehensive compilation of Bordwell pKa data see: **http://www.chem.wisc.edu/areas/reich/pkatable/index.htm**

Substrate	pKa H_2O	(DMSO)
PROTONATED NITROGEN		
N^+H_4	9.2	(10.5)
EtN^+H_3	10.6	
$i\text{-}Pr_2N^+H_2$	11.05	
Et_3N^+H	10.75	(9.00)
PhN^+H_3	4.6	(3.6)
$PhN^+(Me)_2H$	5.20	(2.50)
$Ph_2N^+H_2$	0.78	
2-napthal-N^+H_3	4.16	
$H_2NN^+H_3$	8.12	
HON^+H_3	5.96	
Quinuclidine 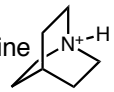	11.0	(9.80)
Morpholine 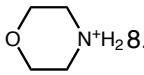	8.36	
N-Me morpholine	7.38	
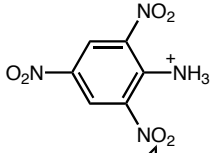	-9.3	
DABCO 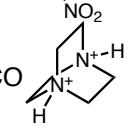	2.97, 8.82 (2.97, 8.93)	
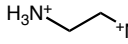	6.90, 9.95	
Proton Sponge 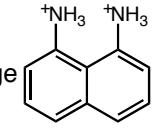	-9.0, 12.0 (--, 7.50)	
$PhCN^+H$	-10	

Substrate	pKa H_2O	(DMSO)
AMINES		
HN_3	4.7	(7.9)
NH_3	38	(41)
$i\text{-}Pr_2NH$	(36 THF))	
TMS_2NH	26(THF)	(30)
$PhNH_2$ (30.6)		
Ph_2NH (25.0)		
$NCNH_2$ (16.9)		
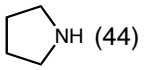	(44)	
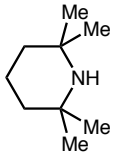	(37)	
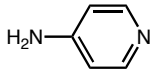	(26.5)	
AMIDES & CARBAMATES		
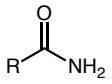	R= H	(23.5)
	CH_3 15.1	(25.5)
	Ph	(23.3)
	CF_3	(17.2)
(urea)	NH_2	(26.9)
	OEt	(24.8)
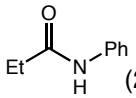	(21.6)	
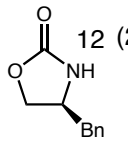	12	(20.5)
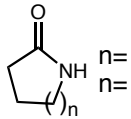	n= 1 (24.1) n= 2 (26.4)	
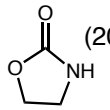		(20.8)
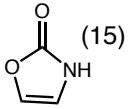	(15)	
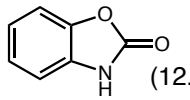		(12.1)

Substrate	pKa H_2O	(DMSO)
IMIDES		
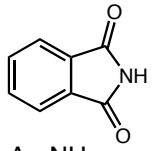	8.30	
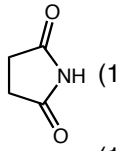		(14.7)
Ac_2NH		(17.9)
SULFONAMIDE		
RSO_2NH_2	R = Me	(17.5)
	Ph	(16.1)
	CF_3 6.3	(9.7)
$MeSO_2NHPh$		(12.9)
GUANIDINIUM, HYRDAZONES,- IDES, & -INES		
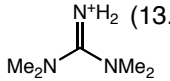	(13.6)	
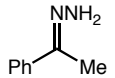		(21.6)
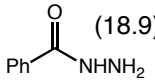	(18.9)	
$PhSO_2NHNH_2$		(17.2)
PhNHNHPh		(26.1)
PROTONATED HETEROCYCLES		
DBU 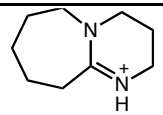	(12) (estimate)	
DMAP 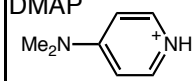	9.2	
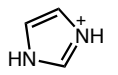	6.95	
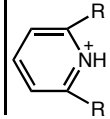	R= H (PPTS)	5.21 (3.4)
	t-Bu	4.95 (0.90)
	Me	6.75 (4.46)
	Cl, H	0.72

Substrate	pKa H_2O	(DMSO)
HYDROXAMIC ACID & AMIDINES		
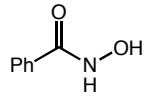	8.88 (NH)	(13.7)
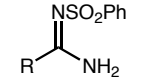	R= Me	(17.3)
	Ph	(15.0)
HETEROCYCLES		
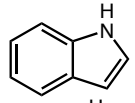		(20.95)
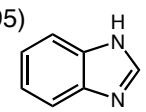		(16.4)
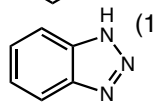		(11.9)
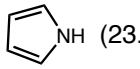		(23.0)
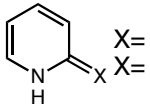	X= O (24) X= S (13.3)	
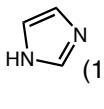		(18.6)
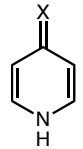	X= O (14.8) X= S (11.8)	
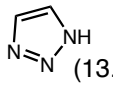		(13.9)
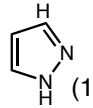		(19.8)
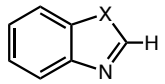	X= O (24.4) X= S (27.0)	
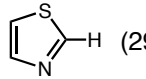		(29.4)
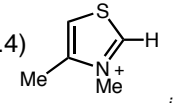		(16.5)
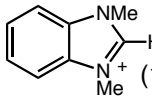		(18.4)
		(24)

*Values <0 for H_2O and DMSO, and values >14 for water and >35 for DMSO were extrapolated using various methods.

For a comprehensive compilation of Bordwell pKa data see: **http://www.chem.wisc.edu/areas/reich/pkatable/index.htm**

HYDROCARBONS

Substrate	pKa H_2O	(DMSO)
$(Me)_3CH$	53	
$(Me)_2CH_2$	51	
$CH_2{=}CH_2$	50	
CH_4	48	(56)
△	46	
$CH_2{=}CHCH_3$	43	(44)
PhH	43	
$PhCH_3$	41	(43)
Ph_2CH_2	33.5	(32.2)
Ph_3CH	31.5	(30.6)
HCCH	24	
PhCCH	23	(28.8)
$XC_6H_4CH_3$		
X= *p*-CN		(30.8)
p-NO_2		(20.4)
p-COPh		(26.9)
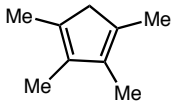		(26.1)
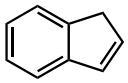	20	(20.1)
	15	(18.0)
H_2	~36	

ESTERS

Substrate	pKa H_2O	(DMSO)
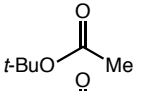	24.5	(30.3)
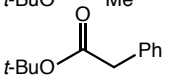		(23.6)
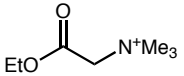		(20.0)
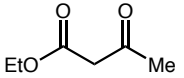	11	(14.2)
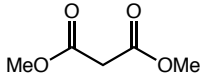	13	(15.7)
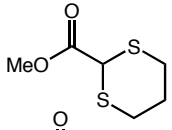		(20.9)
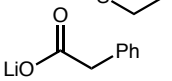		[30.2 (THF)]

AMIDES

Substrate	pKa H_2O	(DMSO)
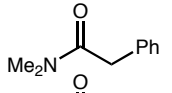		(26.6)
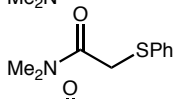		(25.9)
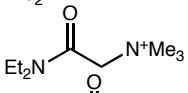		(24.9)
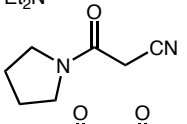		(17.2)
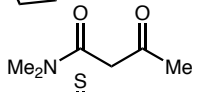		(18.2)
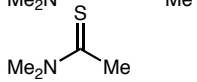		(25.7)

KETONES

Substrate	pKa H_2O	(DMSO)
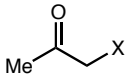		
X= H		(26.5)
Ph		(19.8)
SPh		(18.7)
$COCH_3$	9	(13.3)
SO_2Ph		(12.5)
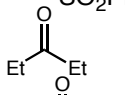	19-20	(27.1)
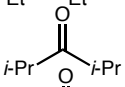		(28.3)
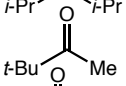		(27.7)
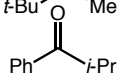		(26.3)
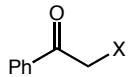		
X= H		(24.7)
CH_3		(24.4)
Ph		(17.7)
$COCH_3$		(14.2)
COPh		(13.3)
CN		(10.2)
F		(21.6)
OMe		(22.85)
OPh		(21.1)
SPh		(16.9)
SePh		(18.6)
NPh_2		(20.3)
N^+Me_3		(14.6)
NO_2		(7.7)
SO_2Ph		(11.4)

Substrate	pKa H_2O	(DMSO)
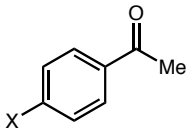		
X= H		(24.7)
OMe		(25.7)
NMe_2		(27.5)
Br		(23.8)
CN		(22.0)
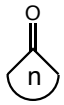		
n= 4		(25.1)
5		(25.8)
6		(26.4)
7		(27.7)
8		(27.4)
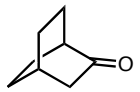		(28.1)
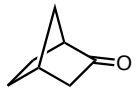		(29.0)
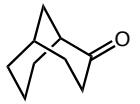		(25.5)
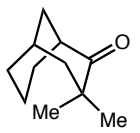		(32.4)

*Values <0 for H_2O and DMSO, and values >14 for water and >35 for DMSO were extrapolated using various methods.

For a comprehensive compilation of Bordwell pKa data see: **http://www.chem.wisc.edu/areas/reich/pkatable/index.htm**

NITRILES

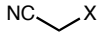

X=	H_2O	(DMSO)
H		(31.3)
CH_3		(32.5)
Ph		(21.9)
COPh		(10.2)
$CONR_2$		(17.1)
CO_2Et		(13.1)
CN	11	(11.1)
OPh		(28.1)
N^+Me_3		(20.6)
SPh		(20.8)
SO_2Ph		(12.0)

HETERO-AROMATICS

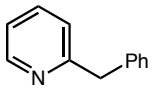
(28.2)

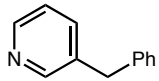
(30.1)

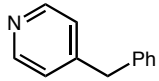
(26.7)

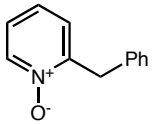
(25.2)

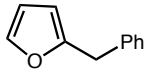
(30.2)

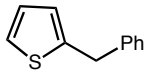
(30.0)

SULFIDES

$PhSCH_2X$

X=	H_2O	(DMSO)
Ph		(30.8)
CN		(20.8)
$COCH_3$		(18.7)
COPh		(16.9)
NO_2		(11.8)
SPh		(30.8)
SO_2Ph		(20.5)
SO_2CF_3		(11.0)
$POPh_2$		(24.9)

$MeSCH_2SO_2Ph$ (23.4)

$PhSCHPh_2$ (26.7)

$(PhS)_3CH$ (22.8)

$(PrS)_3CH$ (31.3)

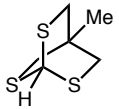
(30.5)

$(PhS)_2CHPh$ (23.0)

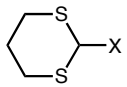

X=	H_2O	(DMSO)
Ph		(30.7)
CO_2Me		(20.8)
CN		(19.1)

$RSCH_2CN$

R=	H_2O	(DMSO)
Me		(24.3)
Et		(24.0)
i-Pr		(23.6)
t-Bu		(22.9)

$PhSCH=CHCH_2SPh$ (26.3)

BuSH 10-11 (17.0)

PhSH ≈7 (10.3)

SULFOXIDES

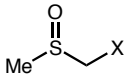

X=	H_2O	(DMSO)
H		(35.1)
Ph		(29.0)
SPh		(29.0)

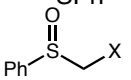

X=	H_2O	(DMSO)
H		(33)
Ph		(27.2)
SOPh		(18.2)

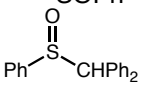
(24.5)

SULFONIUM

$Me_3S^+=O$ (18.2)

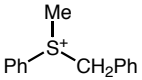
(16.3)

SULFIMIDES & SULFOXIMINES

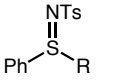

R=	H_2O	(DMSO)
Me		(27.6)
i-Pr		(30.7)

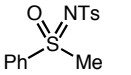
(24.5)

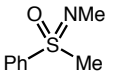
(33)

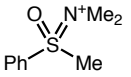
(14.4)

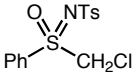
(20.7)

SULFONES

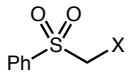

X=	H_2O	(DMSO)
H		(29.0)
CH_3		(31.0)
t-Bu		(31.2)
Ph		(23.4)
$CH=CH_2$		(22.5)
CH=CHPh		(20.2)
CCH		(22.1)
CCPh		(17.8)
COPh		(11.4)
COMe		(12.5)
OPh		(27.9)
N^+Me_3		(19.4)
CN		(12.0)
NO_2		(7.1)
SMe		(23.5)
SPh		(20.5)
SO_2Ph		(12.2)
PPh_2		(20.2)

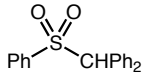
(22.3)

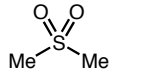
(31.1)

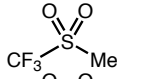
(18.8)

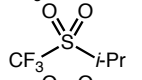
(21.8)

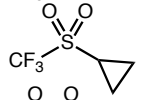
(26.6)

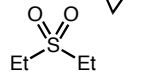
(32.8)

$(PhSO_2)_2CH_2Me$ (14.3)

*Values <0 for H_2O and DMSO, and values >14 for water and >35 for DMSO were extrapolated using various methods.

Substrate	pKa H_2O	(DMSO)
ETHERS		
CH_3OPh		(49)
$MeOCH_2SO_2Ph$		(30.7)
$PhOCH_2SO_2Ph$		(27.9)
$PhOCH_2CN$		(28.1)
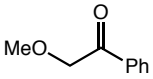		(22.85)
SELENIDES		
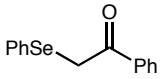		(18.6)
$PhSeCHPh_2$		(27.5)
$(PhSe)_2CH_2$		(31.3)
$PhSeCH_2Ph$		(31.0)
$PhSeCH{=}CHCH_2SePh$		(27.2)
AMMONIUM		
$Me_3N^+CH_2X$		
X= CN		(20.6)
SO_2Ph		(19.4)
COPh		(14.6)
CO_2Et		(20.0)
$CONEt_2$		(24.9)

Substrate	pKa H_2O	(DMSO)
PHOSPHONIUM		
P^+H_4	-14	
MeP^+H_3	2.7	
Et_3P^+H	9.1	
$Ph_3P^+CH_3$		(22.4)
Ph_3P^+*i*-Pr		(21.2)
$Ph_3P^+CH_2COPh$		(6.2)
$Ph_3P^+CH_2CN$		(7.0)
PHOSPONATES & PHOSPHINE OXIDES		
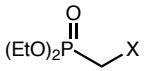		
X= Ph		(27.6)
CN		(16.4)
CO_2Et		(18.6)
Cl		(26.2)
$SiMe_3$		(28.8)
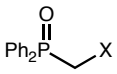		
X= SPh		(24.9)
CN		(16.9)
PHOSPHINES		
$Ph_2PCH_2PPh_2$		(29.9)
$Ph_2PCH_2SO_2Ph$		(20.2)

Substrate	pKa H_2O	(DMSO)
NITRO		
RNO_2		
R= CH_3	≈10	(17.2)
CH_2Me		(16.7)
$CHMe_2$		(16.9)
CH_2Ph		(12.2)
CH_2Bn		(16.2)
CH_2SPh		(11.8)
CH_2SO_2Ph		(7.1)
CH_2COPh		(7.7)
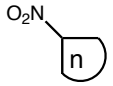		
n= 3		(26.9)
4		(17.8)
5		(16.0)
6		(17.9)
7		(15.8)
IMINES		
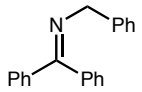		(24.3)

Oxime ethers are ~ 10 pka units less acidic than their ketone counterparts
Streitwieser, JOC 1991, 56, 1989

REFERENCES

DMSO:

JACS 97, 7007 (1975)
JACS 97, 7160 (1975)
JACS 97, 442 (1975)
JACS 105, 6188 (1983)
JOC 41, 1883 (1976)
JOC 41, 1885 (1976)
JOC 41, 2786 (1976)
JOC 41, 2508 (1976)
JOC 42, 1817 (1977)
JOC 42, 321 (1977)
JOC 42, 326 (1977)
JOC 43, 3113 (1978)
JOC 43, 3095 (1978)
JOC 43, 1764 (1978)
JOC 45, 3325 (1980)
JOC 45, 3305 (1980)
JOC 45, 3884 (1980)
JOC 46, 4327 (1981)
JOC 46, 632 (1981)
JOC 47, 3224 (1982)
JOC 47, 2504 (1982)
Acc. Chem. Res. 21, 456 (1988)
Unpublished results of F. Bordwell

Water:

Advanced Org. Chem., 3rd Ed.
J. March (1985)
Unpublished results of W. P. Jencks

THF:
JACS 110, 5705 (1988)

See cited website below for additional data

*Values <0 for H_2O and DMSO, and values >14 for water and >35 for DMSO were extrapolated using various methods.

For a comprehensive compilation of Brodwell pKa data see: **http://www.chem.wisc.edu/areas/reich/pkatable/index.htm**

DMSO Acidities of Common Heterocycles

Bordwell, ACR, **1988**, *21*, 456
Bordwell http://www.chem.wisc.edu/areas/reich/pkatable/index.htm

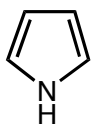

23.0

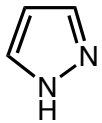

19.8

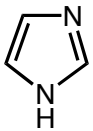

18.6

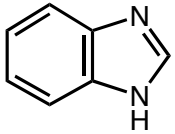

16.4

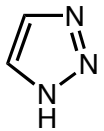

13.9

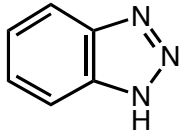

11.9

18.0

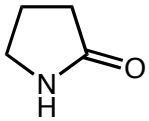

24.0

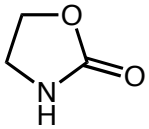

20.8

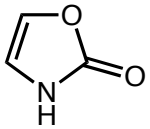

15.0

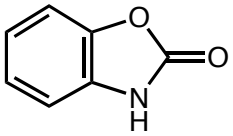

12.1

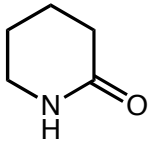

26.4

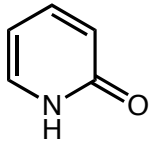

24.0

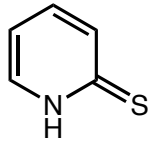

13.3

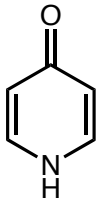

14.8

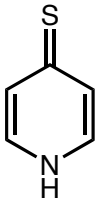

11.8

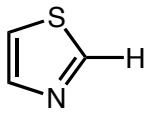

29.4

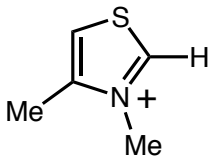

16.5

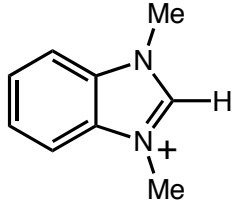

18.4

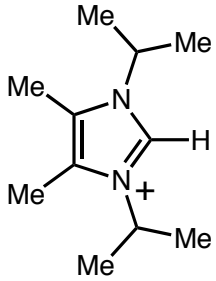

24

http://www.courses.fas.harvard.edu/~chem206/

Chemistry 206

Advanced Organic Chemistry

Lecture Number 21

Carbonyl and Azomethine Electrophiles-1

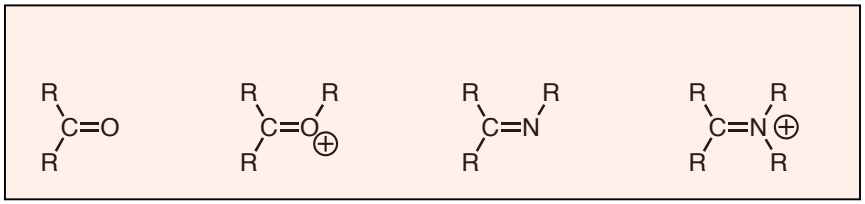

- Reactivity Trends
- C=X Stereoelectronic Effects
- Carbonyl Addition: Theoretical Models
- The Felkin-Anh-Eisenstein Model for C=O Addition
- Diastereoselective Ketone Reduction

Reading Assignment for this Week:

Carey & Sundberg: **Part A**; Chapter 8
Reactions of Carbonyl Compounds

Carey & Sundberg: **Part B**; Chapter 2
Reactions of Carbon Nucleophiles with Carbonyl Compounds

Carey & Sundberg: **Part B**; Chapter 5
Reduction of Carbonyl & Other Functional Groups

D. A. Evans

Monday
November 7, 2005

Additional Reading Material Provided

Additions to 5- & 6-Membered oxocarbenium Ions:

Woerpel etal. *JACS* **1999**, *121*, 12208 **(pdf)**
Woerpel etal. *JACS* **2000**, *122*, 168 **(pdf)**
Woerpel etal. *JACS* **2003**, *125*, 15521 **(pdf)**
Woerpel etal. *JACS* **2003**, *125*, 14149 **(handout)**
Woerpel etal. *JACS* **2005**, *125*, 10879 **(handout)**

"From Crystal Statics to Chemical Dynamics", *Accounts Chem. Research* **1983**, *16*, 153. **(pdf)**
"Theoretical Interpretation of 1,2-Asymmetric Induction. The Importance of Antiperiplanarity", N. T. Anh, O. Eisenstein *Nouv. J. Chem.* **1977**, *1*, 61-70. **(pdf)**

"Around and Beyond Cram's Rule" A. Mengel & O. Reiser, Chem Rev. 1999, 99, 1191-1223 **(pdf)**

Relevant Dunitz Articles

"Geometrical Reaction Coordinates. II. Nucleophilic Addition to a Carbonyl Group", *JACS* **1973**, *95*, 5065.

"Stereochemistry of Reaction Paths at Carbonyl Centers", *Tetrahedron* **1974**, *30*, 1563

"From Crystal Statics to Chemical Dynamics", *Accounts Chem. Research* **1983**, *16*, 153. **(Electronic Handout)**

"Stereochemistry of Reaction Paths as Determined from Crystal Structure Data. A Relationship Between Structure and Energy.", Burgi, H.-B. *Angew. Chem., Int. Ed. Engl.* **1975**, *14*, 460.

The Set of Functional Groups:

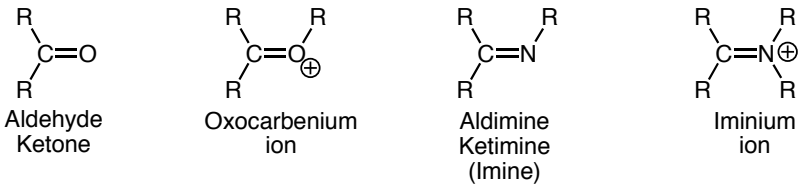

These functional groups are among the most versatile sources of electrophilic carbon in both synthesis and biosynthesis. The ensuing discussion is aimed at providing a more advanced discussion of this topic.

C=X Polarization

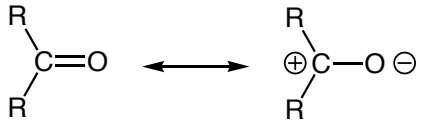

Partial Charge: As the familiar polar resonance structure above indicates, the carbonyl carbon supports a partial positive charge due to the polarization of the sigma and pi system by the more electronegative heteroatom. The partial charges for this family of functional groups derived from molecular orbital calclulations (ab initio, 3-21(G)*, HF) are illustrated below:

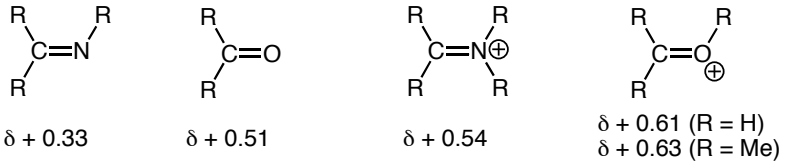

electrophilic reactivity →

Proton Activation of C=X Functional groups

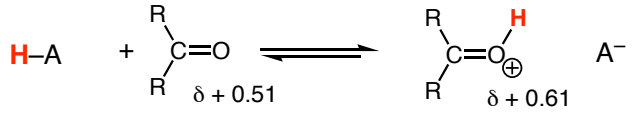

The electrophilic potential of the C=O FG may be greatly increased by either Lewis acid coordination of by protonation. The magnitide of this increase in reactivity is ~ 10^{+6}. Among the weakest Bronsted acids that may be used for C=O actilvation (ketalization) is pyridinium ion (pKa = 5). Hence, the Keq below, while quite low, is still functional.

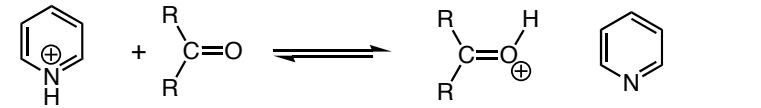

Stereoelectronic Considerations for C=O Addition

LUMO is π* C–O; **HOMO** Provided by Nu:

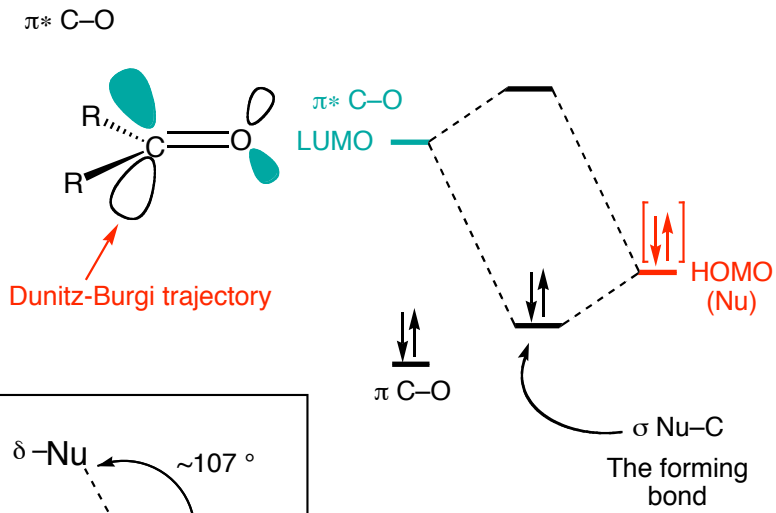

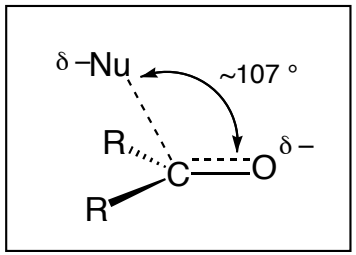

What about C=O vs C=O-R(+)?

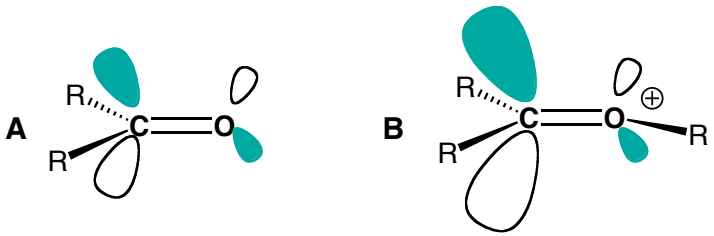

The LUMO coefficient on carbon for **B** will be considerably larger than for **A**. Does this mean that there is a lower constraint on the approach angle for the attacking nucleophile? There is no experimental proof for this question; however, it is worthy of consideration

What was the basis for the Dunitz-Burgi analysis?

Relevant Dunitz Articles

"Geometrical Reaction Coordinates. II. Nucleophilic Addition to a Carbonyl Group", *JACS* **1973**, *95*, 5065.

"Stereochemistry of Reaction Paths at Carbonyl Centers", *Tetrahedron* **1974**, *30*, 1563

"From Crystal Statics to Chemical Dynamics", *Accounts Chem. Research* **1983**, *16*, 153.

"Stereochemistry of Reaction Paths as Determined from Crystal Structure Data. A Relationship Between Structure and Energy.", Burgi, H.-B. *Angew. Chem., Int. Ed. Engl.* **1975**, *14*, 460.

Dunitz Method of Analysis

A series of organic structures containing both C=O and Nu FG's disposed in a geometry for mutual interaction were designed. These structures positioned the interacting FGs an increasingly closer distances. The X-ray structures of these structures were determined to ascertain the direction of C=O distortion. The two families of structures that were evaluated are shown below.

1,8-Disubstituted Naphthalenes. Substituents located at these positions are strongly interacting as illustrated by the MM2 minimized di-methyl-naphthalene structure shown below.

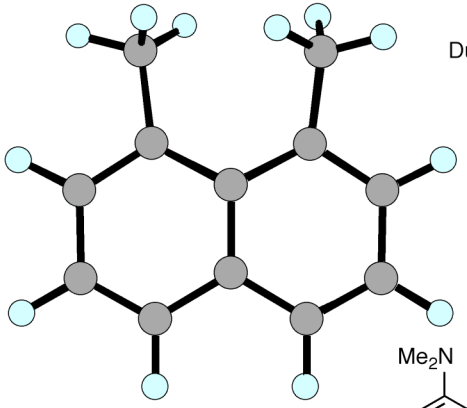

Dunitz, *Helv. Chem. Acta* **1978**, *61*, 2783

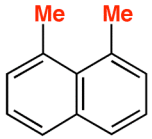

~ 7.6 kcal/moll
Lecture 4

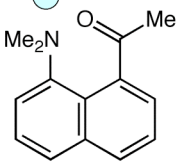

A (shown)

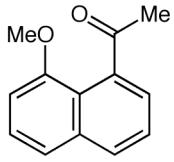

B

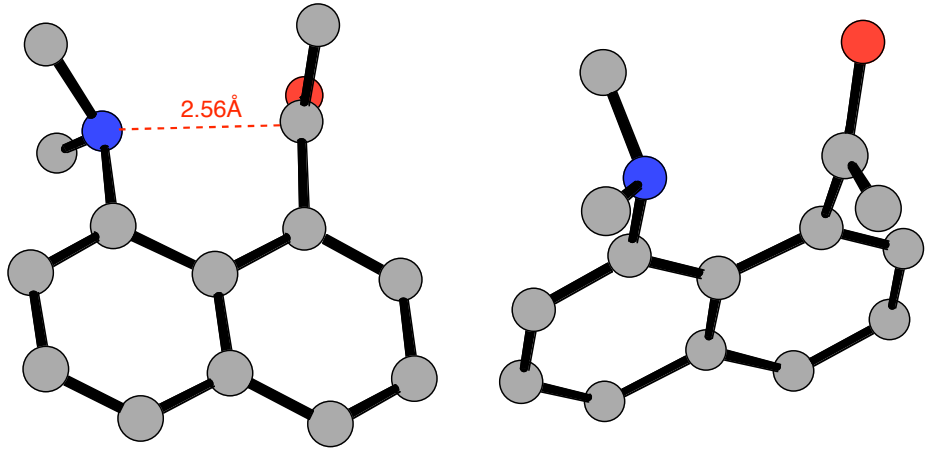

In this structure (**A**), at 2.56Å the C=O is starting to pyramidalize

Cyclic aminoketones. Medium-ring ketones of various ring sizes were analyzed for the interaction of amine an C=O FGs. One example is shown below.

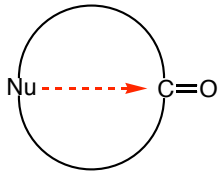

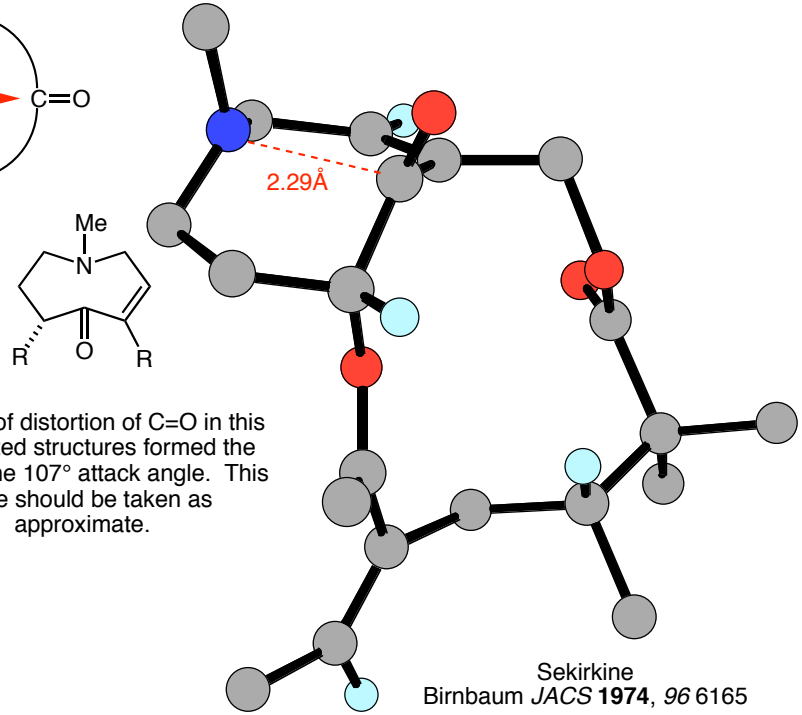

Analysis of distortion of C=O in this and related structures formed the basis of the 107° attack angle. This value should be taken as approximate.

Sekirkine
Birnbaum *JACS* **1974**, *96* 6165

The Dunitz-Burgi Trajectory for C=O Addition

Cyclic aminoketones. Medium-ring ketones of various ring sizes were analyzed for the interaction of amine an C=O FGs. Two examples are shown below.

Sekirkine
Birnbaum *JACS* **1974**, *96* 6165

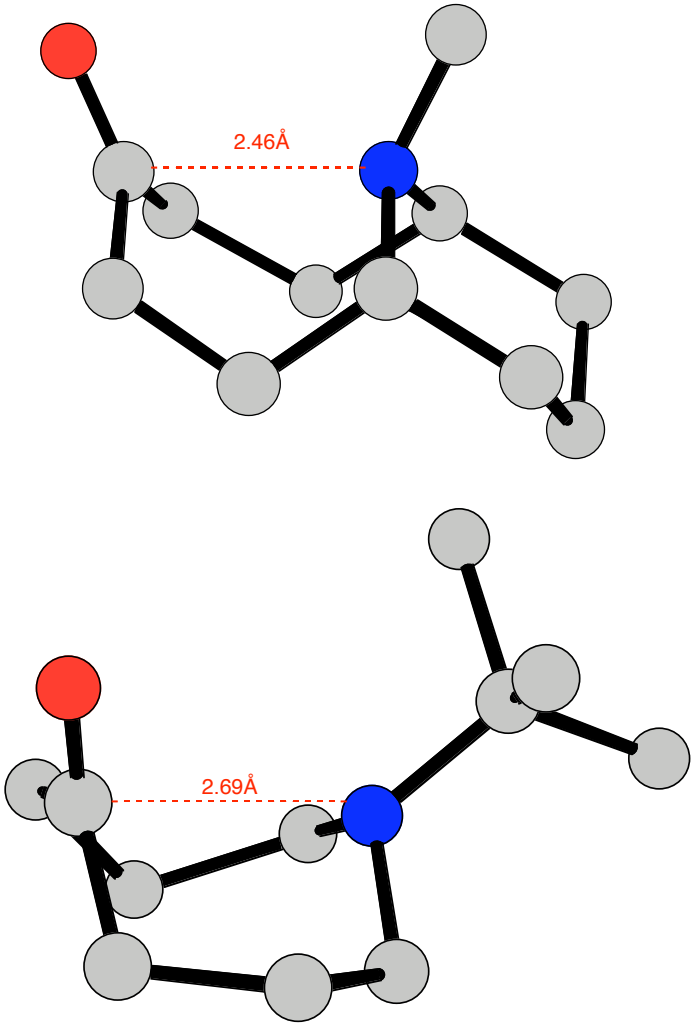

Should these crystallographic date be relevant to the addition to complexed C=O & Iminium Ions?

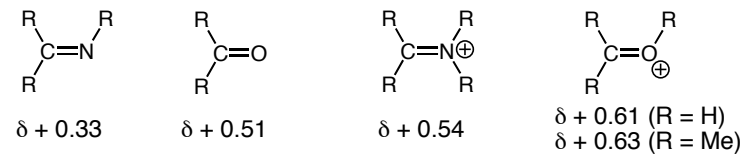

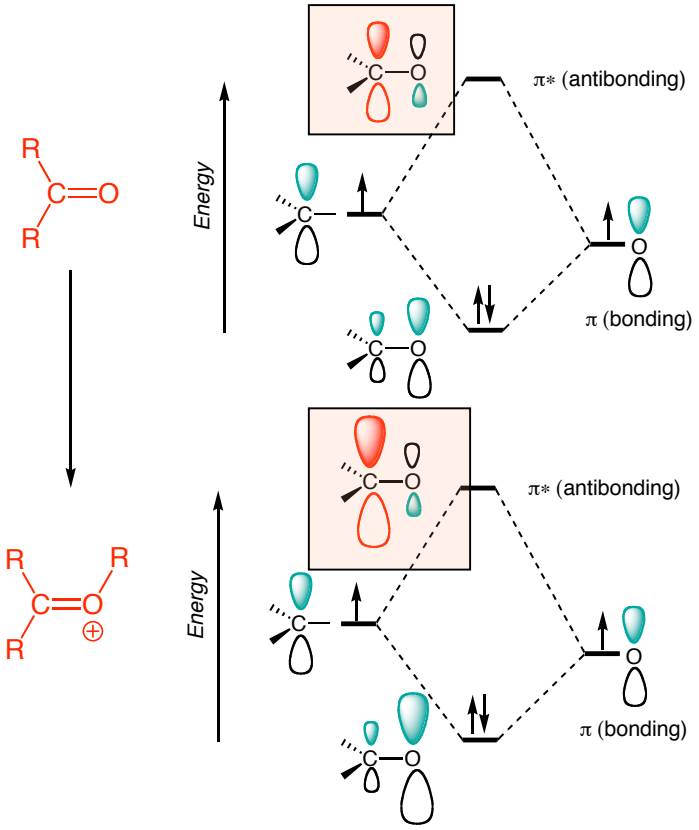

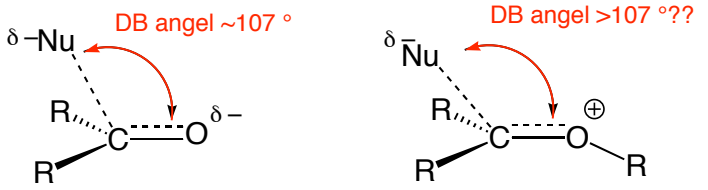

Pivotal Articles

R. V. Stevens in
"Strategies and Tactics in Organic Synthesis", Vol. 1.
On the Stereochemistry of Nucleophilic Additions to Tetrahydropyridinium Salts: a Powerful Heuristic Principle for the Stereorationale Design of Alkaloid Synthesis.;
Lindberg, T., Ed.; Academic Press, 1984;

Eliel etal. , *JACS* **1969**, *91*, 536
Kishi etal. , *JACS* **1982**, *104*, 4976-8

The Proposal for Oxo-carbenium Ions (Eliel, Kishi)

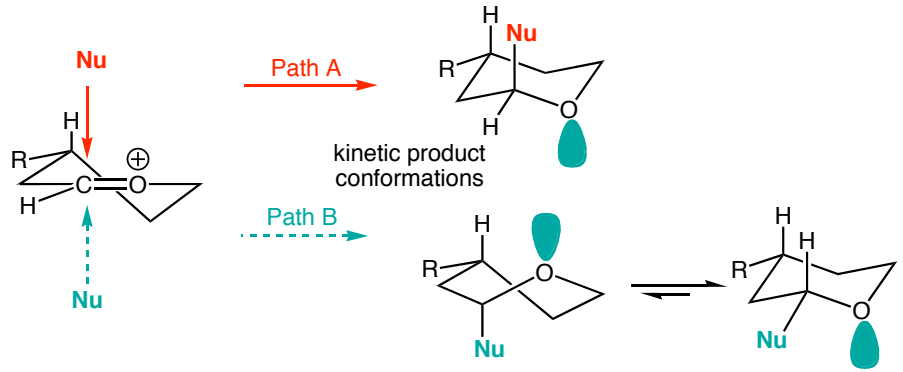

The Proposal for Iminium Ions (Stevens)

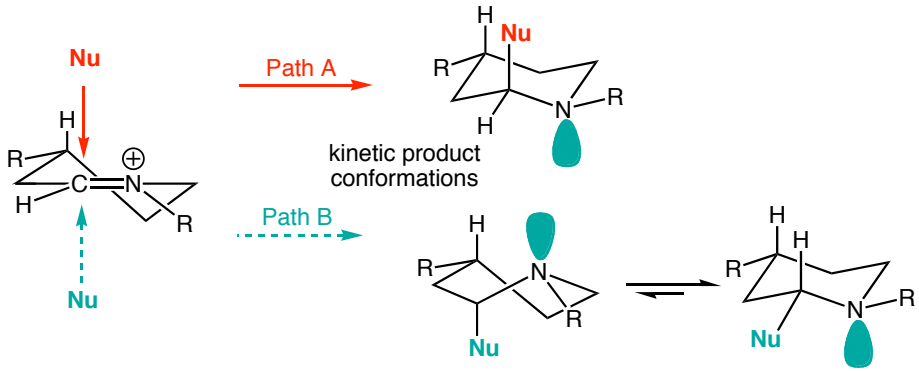

It was proposed that chair-axial addition would be preferred as a consequence of the intervention of a transition state anomeric effect (Path A). Attack through Path B would necessitate the generation of the twist-boat kinetic product conformation thus destabilizing attack from the equatorial diastereoface. While Stevens espoused this concept for iminium ions in the late 70's, his untimely death at the age of 42 significantly delayed his cited publication.

An early example from Eliel; *JACS* 1969, *91*, 536

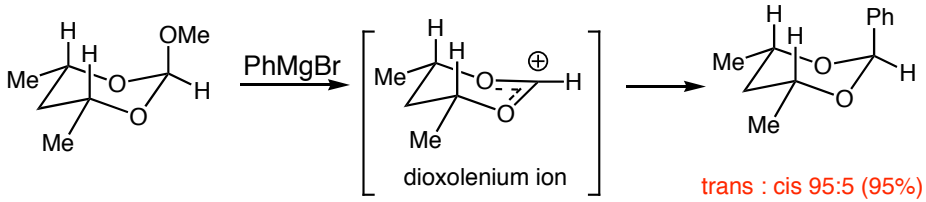

trans : cis 95:5 (95%)

Eliel was the first to attibute stereoelectronic factors to the addition of nucleophiles to cyclic oxo-carbenium ions.

Kishi Examples; *JACS* 1982, *104*, 4976-8

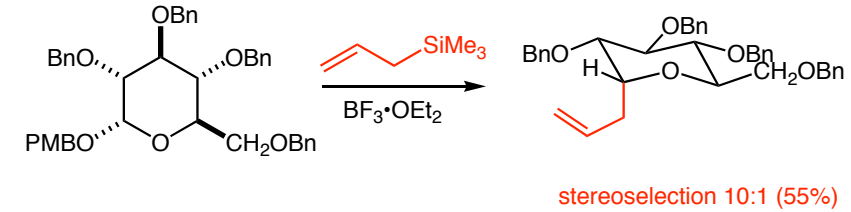

stereoselection 10:1 (55%)

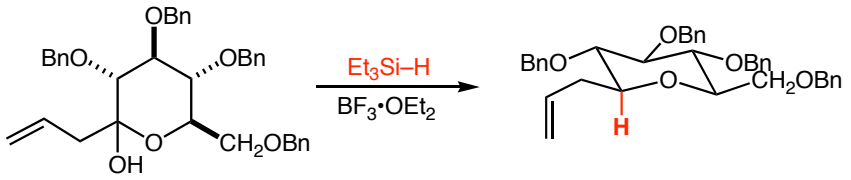

stereoselection 10:1 (55%)

Chair-aixal attack on oxo-carbenium ion occurs for both carbon and hydride nucleophiles

Iminium Ions (Stevens) *cited reference*

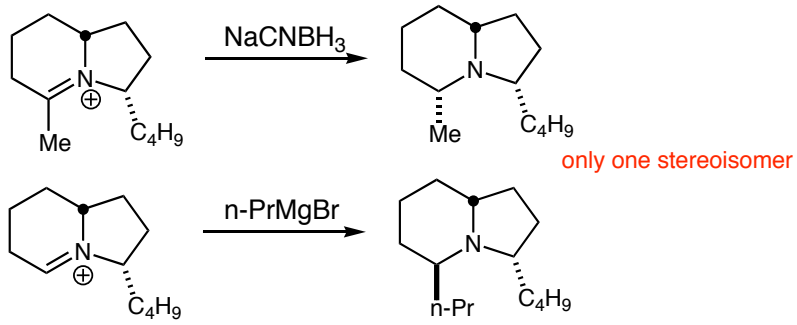

only one stereoisomer

The Eliel Proposal: "Stereoelectronic Factors are involved!"

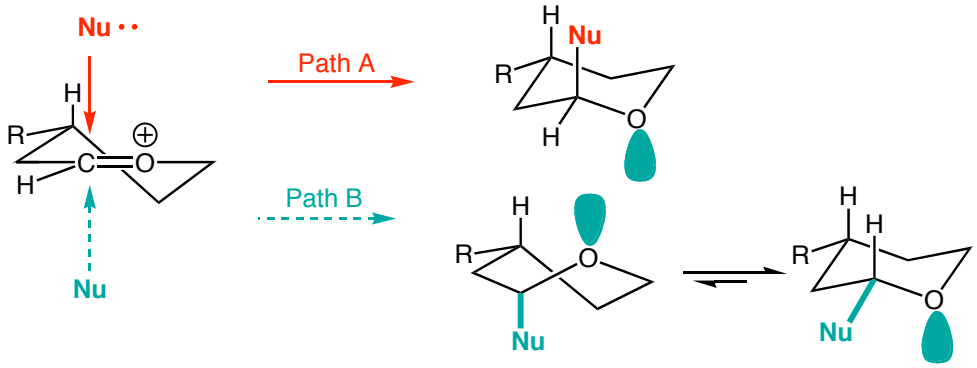

The HOMO: Forming C–Nu bond
The LUMO: π* C=O
Stereoelectronic Effect: the forming C–Nu bond and developing Oxygen lone pair are oriented antiperiplanar

So what is the dominant HOMO–LUMO interaction in the addition of nucleophiles to C=O's?

The Felkin-Anh Hypothesis suggests:

The HOMO: Forming C–Nu bond
The LUMO: π* C=O
Additional transition state stabilization may be achieved by hyperconjugative stabilization of the forming bond through delocalization with the resident *antiperiplanar antibonding C*–R_L bond.

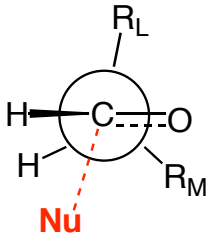

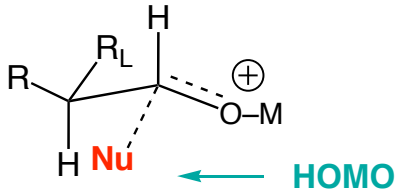

5-Membered oxocarbenium Ions: Woerpel etal. *JACS* 1999, *121,* 12208. *JACS* 2003, *125,* 14149. *JACS* 2005, *127,* 10879.

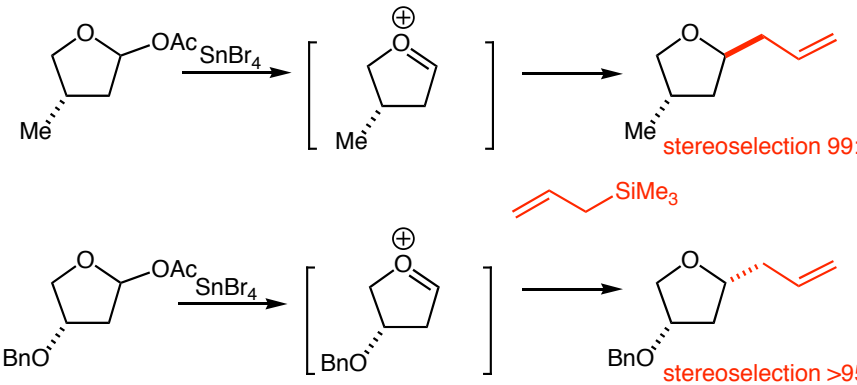

These cases provide dramatic evidence for the importance of electrostatic effects in controlling face selectivity.

6-Membered oxocarbenium Ions: Woerpel etal. *JACS* 2000, *122,* 168 *JACS* 2003, *125,* 15521

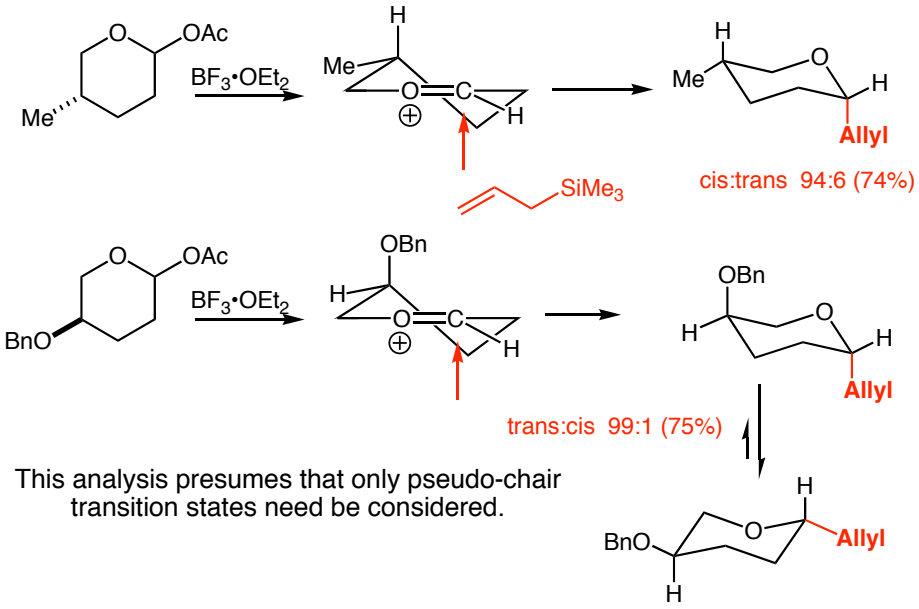

This analysis presumes that only pseudo-chair transition states need be considered.

Woerpel's model states that axial attack from the most stable chair conformer predicts the major product.

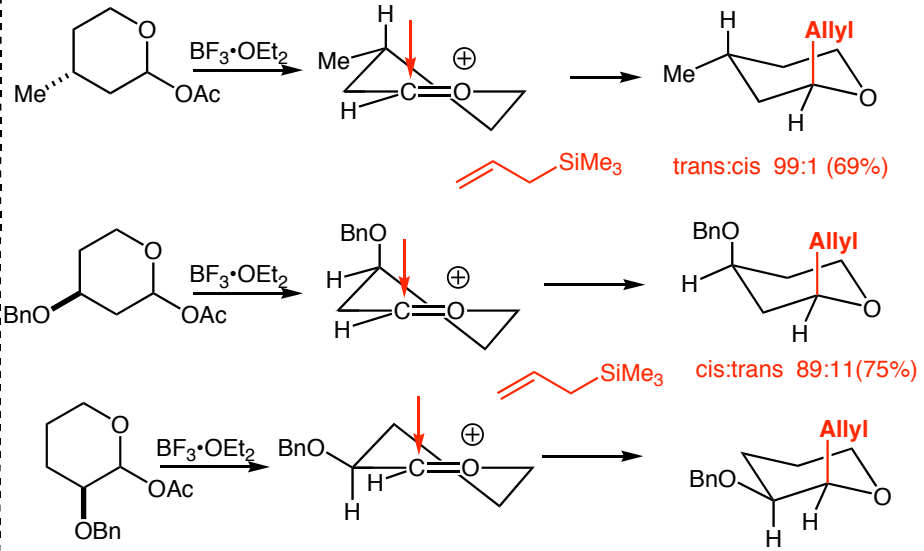

These cases provide dramatic evidence for the importance of electrostatic effects in controlling face selectivity.

Are the preceding addition reactions somehow related to the apparently contrasteric reactions shown below??

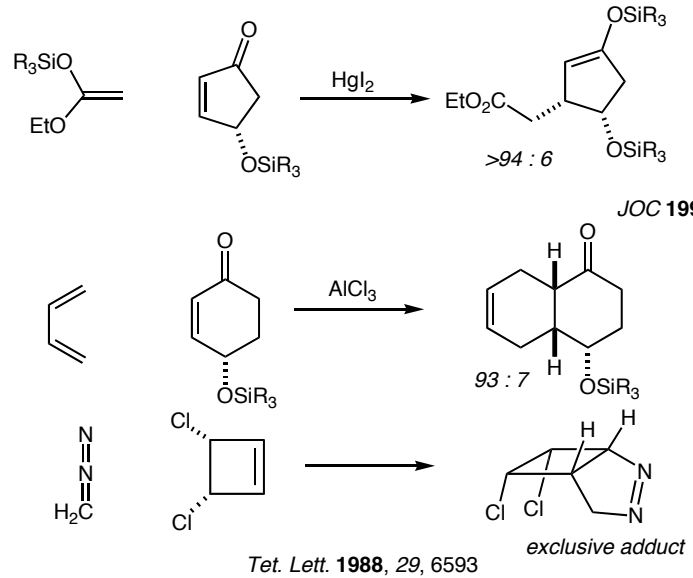

Tet. Lett. **1988**, *29*, 6593

Phorboxazole B

Evans, Fitch, Smith, Cee, *JACS* ***2000***, *122, 10033*

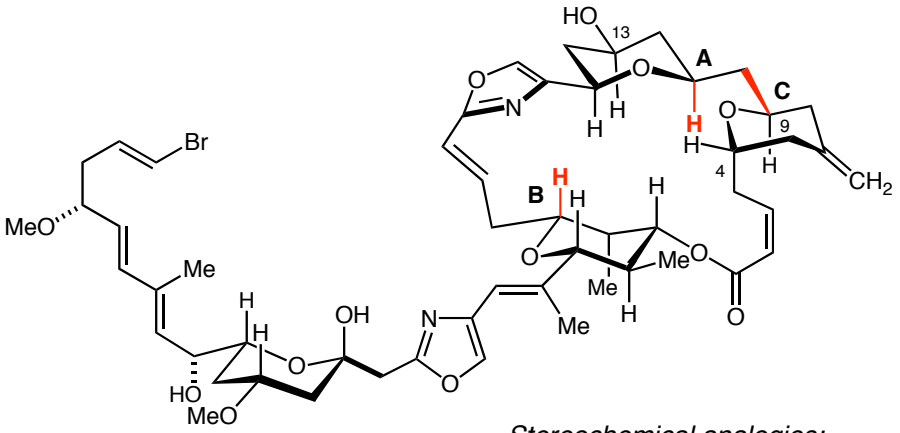

Stereochemical analogies:
Kishi et. al.: *JACS* **1982**, *104*, 4976-8

A: The C-11 Reduction

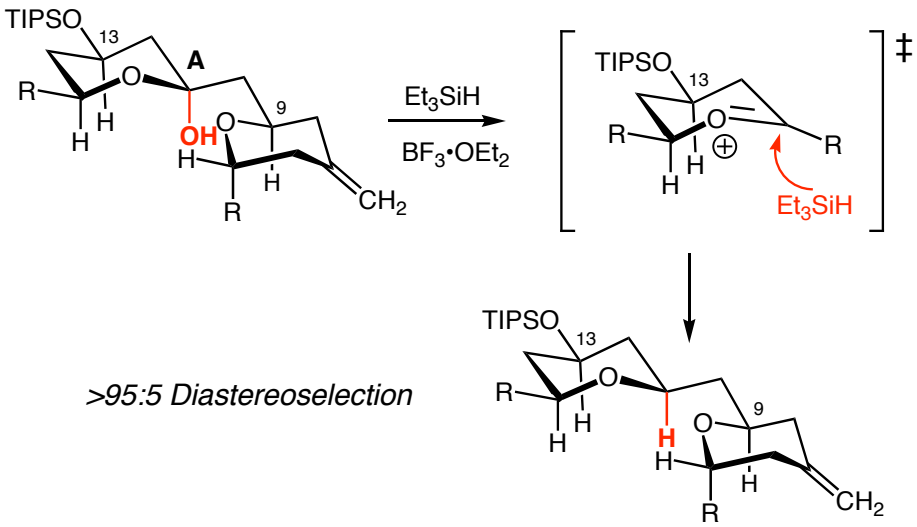

>95:5 Diastereoselection

B: The C-22 Reduction

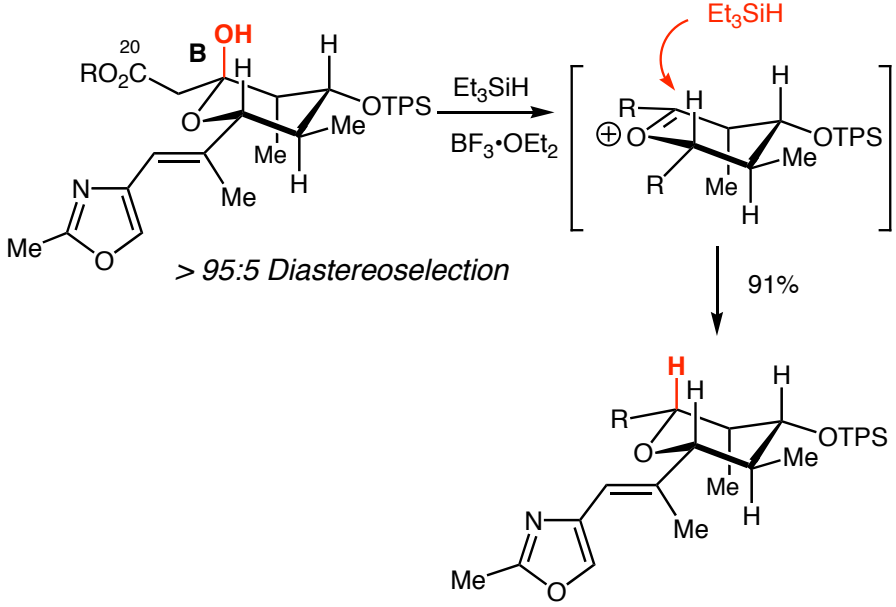

> 95:5 Diastereoselection

C: The C-9 C–C Bond Construction

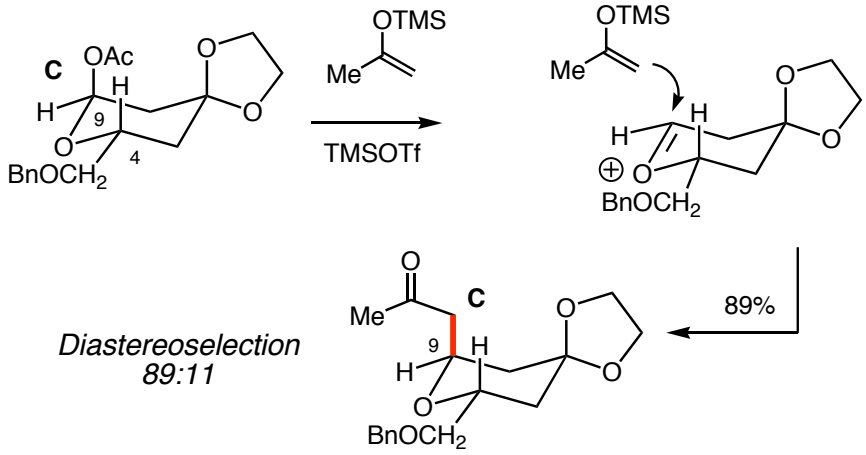

Diastereoselection 89:11

4- vs 6-Membered Transition Structures for C=O Addition

Consider carbonyl hydration:

$H_2C{=}O + n\ HOH \longrightarrow H_2C(OH)_2 + (n\text{-}1)\ HOH$

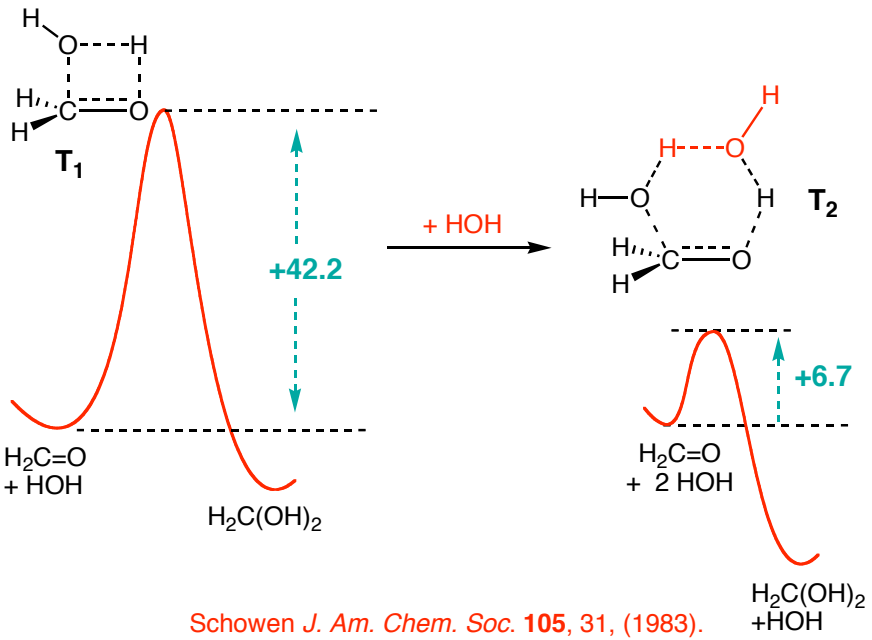

Schowen *J. Am. Chem. Soc.* **105**, 31, (1983).

Overall Process: The valure of the proton shuttle

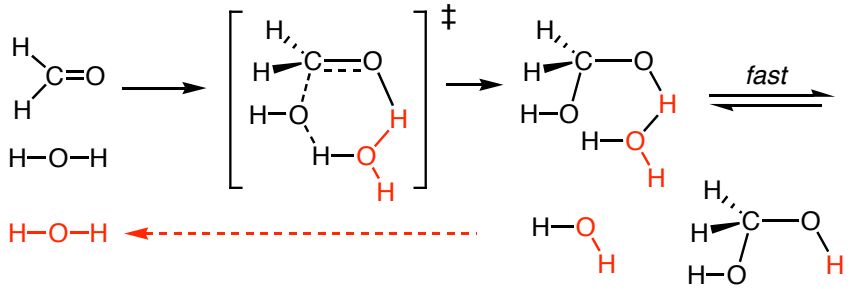

Transiton structure T_2 ~40 kcal/mol more stable than transition structure T_1.

Do these results relate to "real" reactions? Yes!

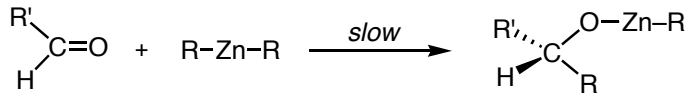

Observation: catalytic amounts of **ZnI_2** dramatically catalyze addition process.

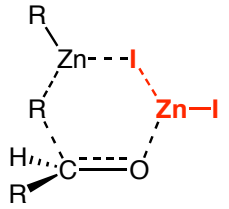

bimetallic transition state

4– Versus 6–Center Transition States for Boron

4-Centered

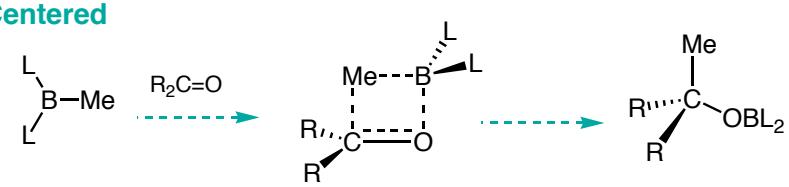

disfavored : rxn does not proceed!)

6–Centered

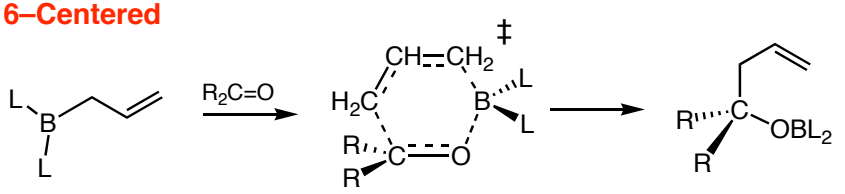

favored

6–Centered

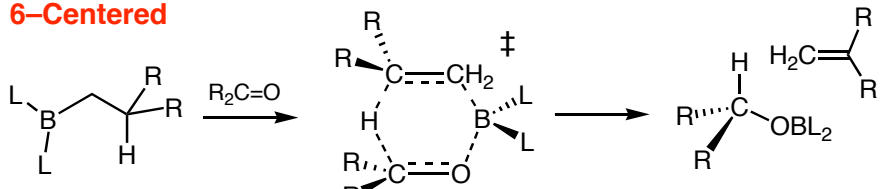

favored

Carbonyl Addition: 4– Versus 6–Center Transition States for Aluminum

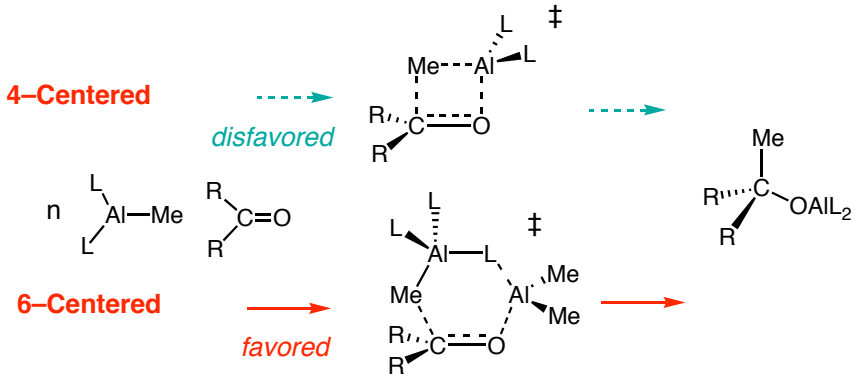

The Bimetallic Transition States are preferred

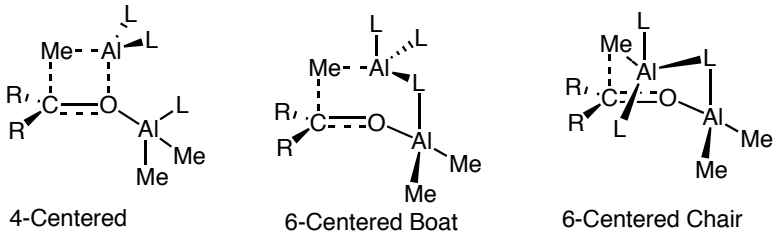

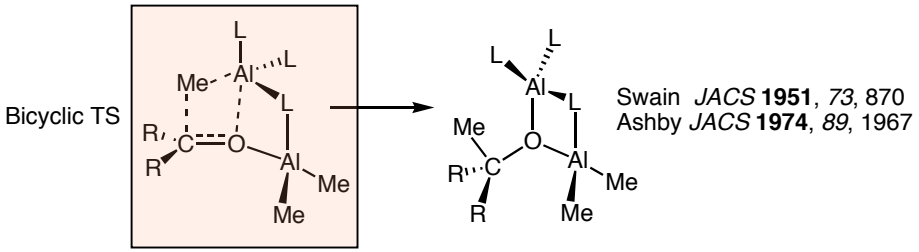

Swain *JACS* **1951**, *73*, 870
Ashby *JACS* **1974**, *89*, 1967

Grignard Reagents:

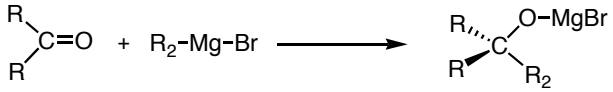

The molecularity and transition structure for this reaction have not been carefully elucidated. The fact that the Grignard reagent is not a single species in solution greatly complicates the kinetic analysis.

The Schlenk Equilibrium

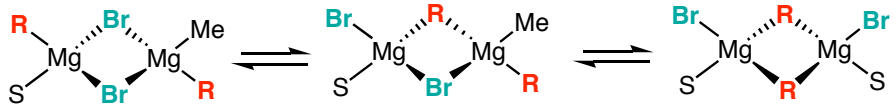

Solution structure of R–MgBr is in dynamic equilibrium through Schlenck equilibration

The Bimetallic (Binuclear) Mechanism for C=O Addition

Recent theoretical study: Yamazaki & Yambe, *J. Org. Chem.* **2002**, *67*, 9346

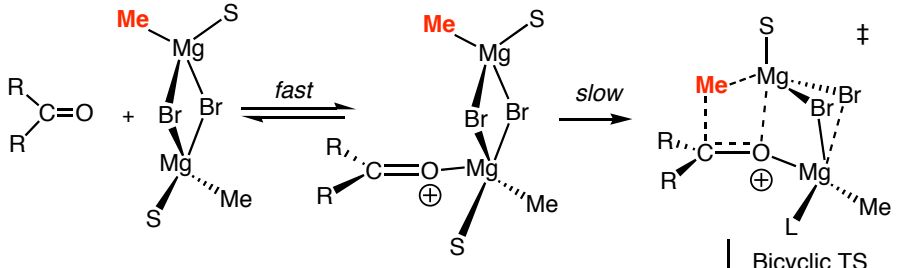

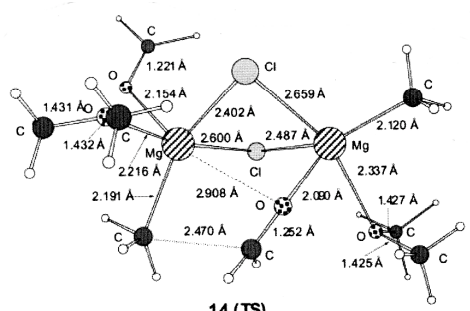

Yamazaki TS **14 (TS)** +0.3 kcal/mol

The Mononuclear Mechanism is now in disfavor

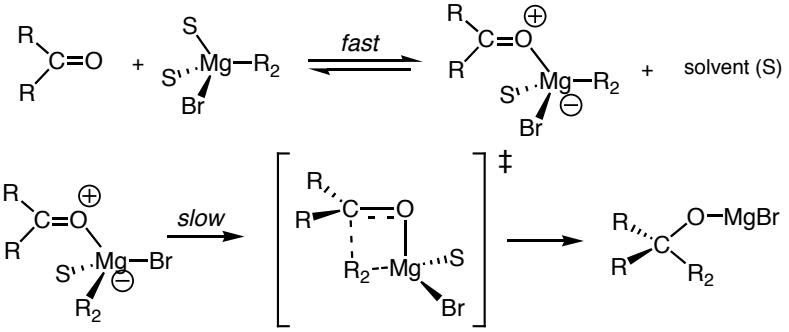

Mengel, A. and O. Reiser, "Around and Beyond Cram's Rule."
Chem. Rev. **1999**, 1191-1223

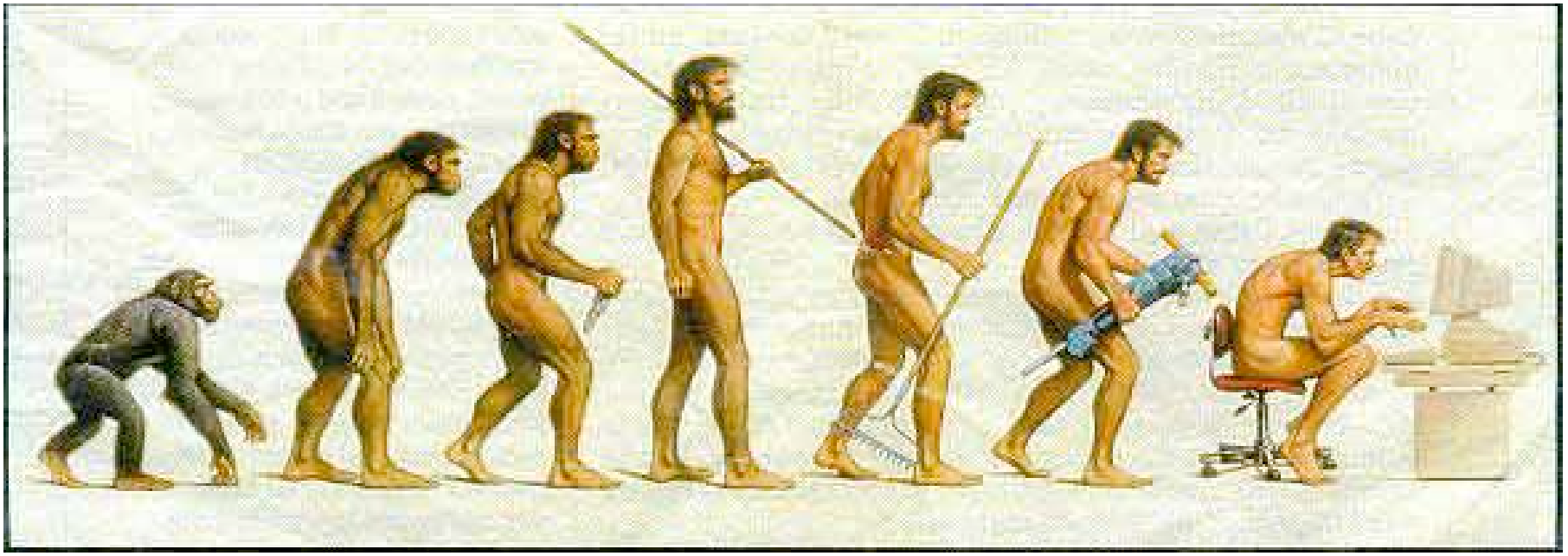

Fischer Cram Cornforth Felkin Anh/Eisenstein Cieplak Tomoda

Humor provided by Sarah Siska

Evolution of a Model for C=O Addition

Product Development & Steric Approach Control:

Dauben, *JACS* **1956**, *78*, 2579

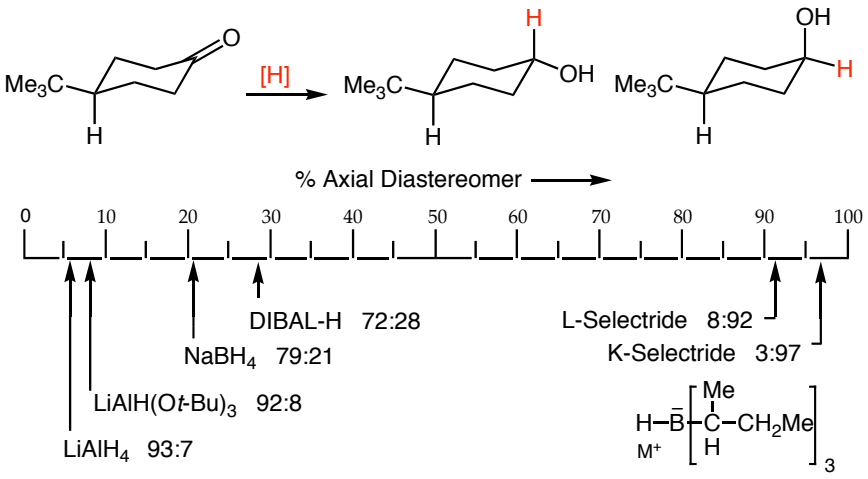

Observation: Increasingly bulky hydride reagents prefer to attack from the equatorial C=O face.

Assumption: Hindered reagents react through more highly developed transition states than unhindered reagents

Carbonyl Addition: Evolution of Acyclic Models

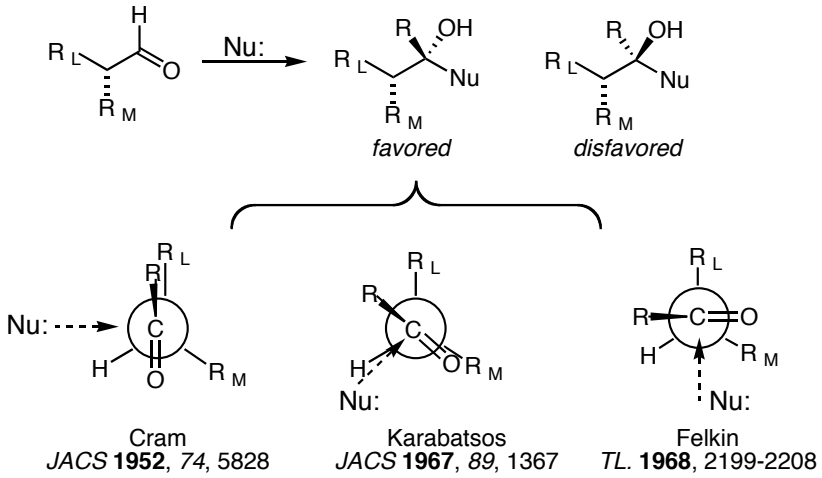

Recall discussion in Lecture 7.

Assumptions in Felkin Model:

- Transition states are all reactant-like rather than product-like.
- Torsional strain considerations are dominant.
  Staggered TS conformations preferred
- The principal steric interactions are between Nu & R.

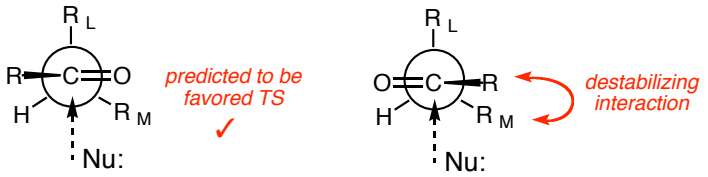

The flaw in the Felkin model: A problem with aldehydes!!

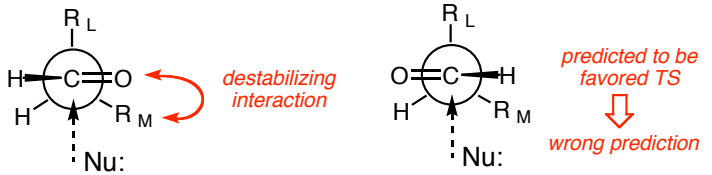

Stereoelectronic Effect: The HOMO-LUMO interaction dictates the following reaction geometry:

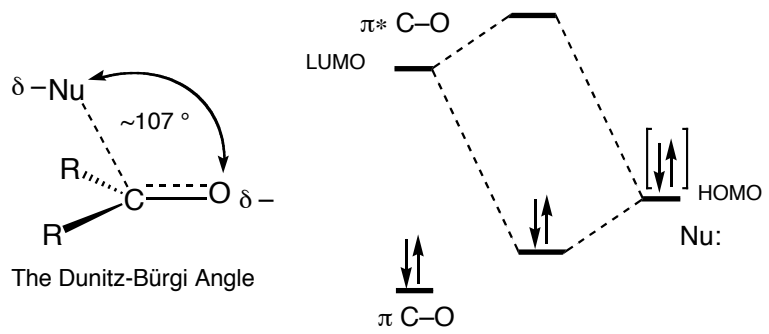

attack angle greater than 90 °; estimates place it in the 100–110 ° range

Burgi, Dunitz, *Acc. Chem. Res.* **1983**, *16*, 153-161

The Felkin-Anh Eisenstein Model

The flaw in the Felkin model: A problem with aldehydes!!

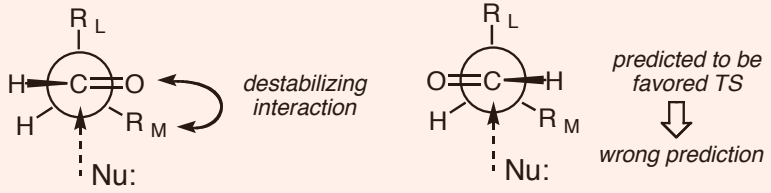

Anh & Eisenstein *Noveau J. Chim.* **1977**, *1*, 61-70
Anh *Topics in Current Chemistry.* **1980**, ***No 88***, 146-162

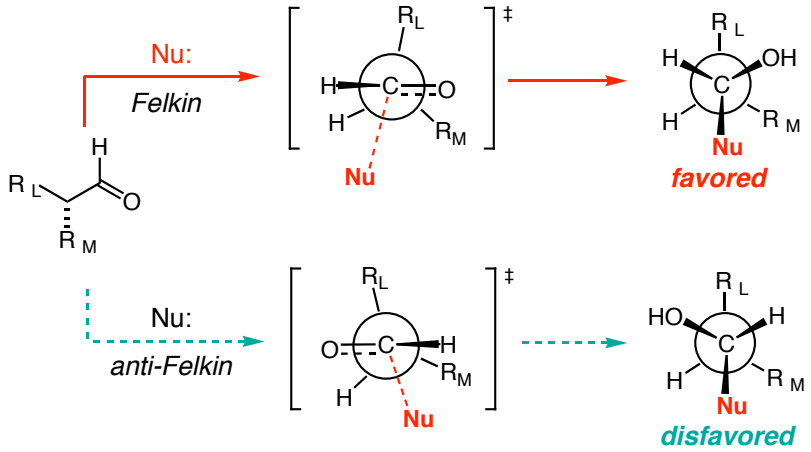

New Additions to Felkin Model:

■ Dunitz-Bürgi C=O–Nu orientation applied to Felkin model.

■ The antiperiplanar effect:
Hyperconjugative interactions between C-R_L which will lower $\pi^*C{=}O$ will stablize the transition state.

Theoretical Support for Staggered Transition states (Lecture 7)

(Read this) Houk, *JACS* **1982**, *104*, 7162-6
(Read this) Houk, *Science* **1986**, *231*, 1108-17

Houk: "The tendency for the staggering of partially formed vicinal bonds is greater than for fully formed bonds"
Lecture–7

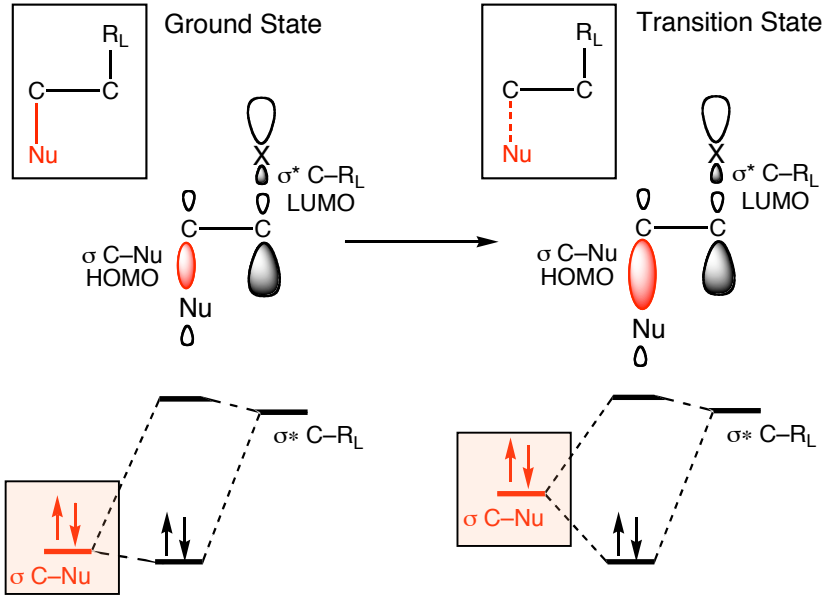

Best acceptor σ* orbital is oriented anti periplanar to forming bond

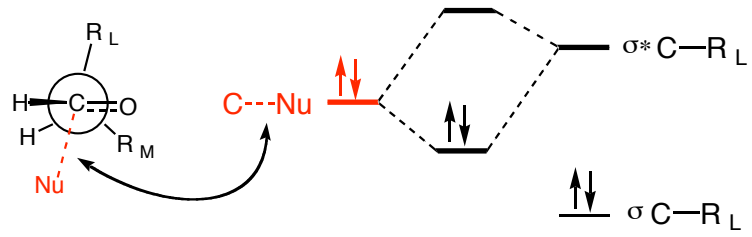

■ **Theoretical support:**

Padden-Row, *Chem. Commun.* **1990**, 456; ibid **1991**, 327
Houk, *J. Am. Chem. Soc.* **1991**, *113*, 5018
Frenking & Reetz, *Tetrahedron* **1991**, *47*, 8091

So what is the dominant HOMO–LUMO interaction in the addition of nucleophiles to C=O's?

The Felkin-Anh Hypothesis suggests:

This case suggests that the dominant HOMO–LUMO interaction is between the forming C–Nu bond (HOMO) and the π*C=O LUMO. The LUMO associated with the resident *antibonding* C–R_L bond may further stabilize TS.

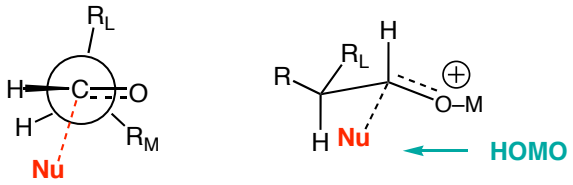

The HOMO: Forming C–Nu bond
The LUMO: π* C=O
Additional transition state stabilization may be achieved by hyperconjugative stabilization of the forming bond through delocalization with the resident *antiperiplanar* a*ntibonding C*–R_L bond.

"Polar" Felkin-Anh Hypothesis suggests:

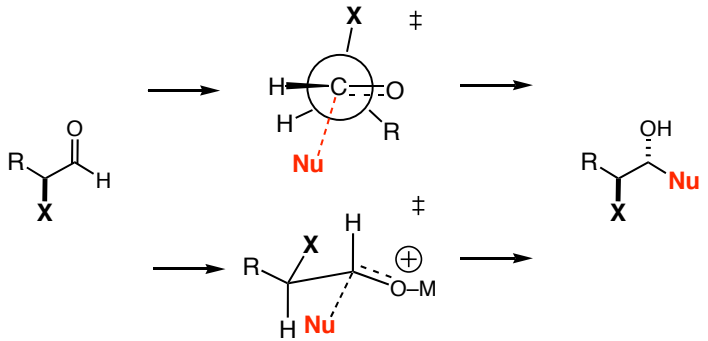

In the polar model, the substituent with the best acceptor antibonding orbital is oriented antiperiplanar to the forming C–Nu bond.

Hierarchy of Donor & Acceptor States

The following trends are made on the basis of comparing the bonding and antibonding states for the molecule CH_3-X where X = C, N, O, F, and H.

σ-anti-bonding States: (C–X)

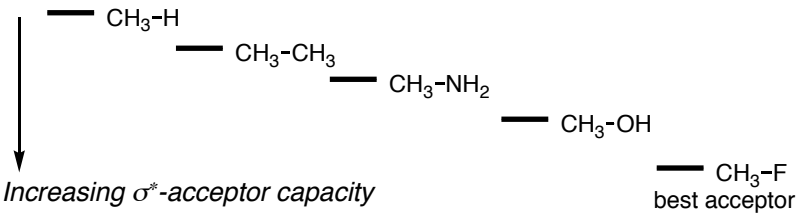

σ-bonding States: (C–X)

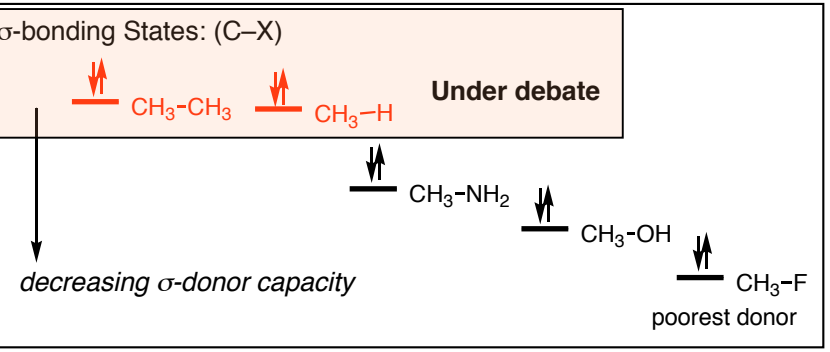

The following are trends for the energy levels of *nonbonding states* of several common molecules. The trend was established by photoelectron spectroscopy.

Nonbonding States

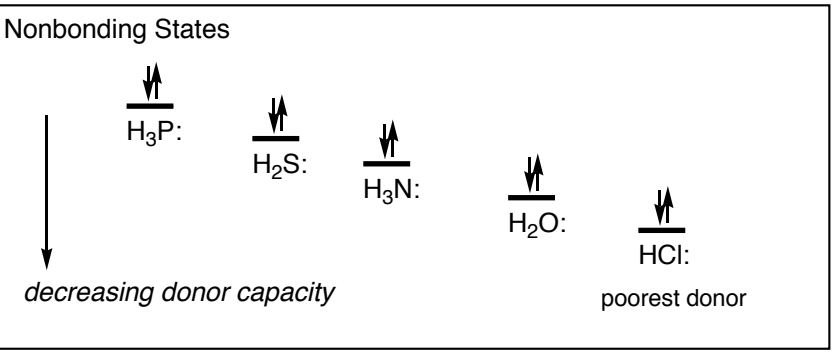

The Felkin-Anh Eisenstein Model: Verification

Addition of Enolate & Enol Nucleophiles

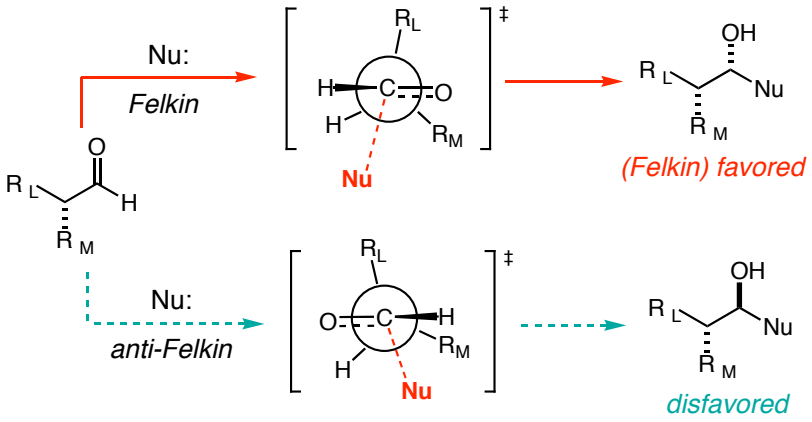

Trend-1: For Li enolates, increased steric hindrance at enolate carbon results in enhanced selectivity

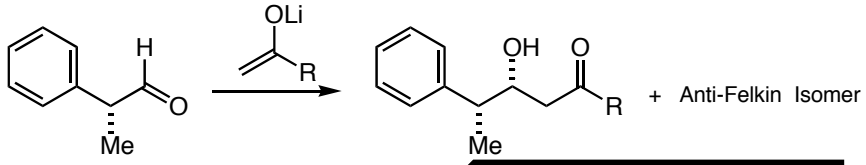

L. Flippin & Co-workers, *Tetrahedron Lett.*. **1985**, *26*, 973.

Enolate (R)	Ratio
R = Me	3 : 1
R = OtBu	4 : 1

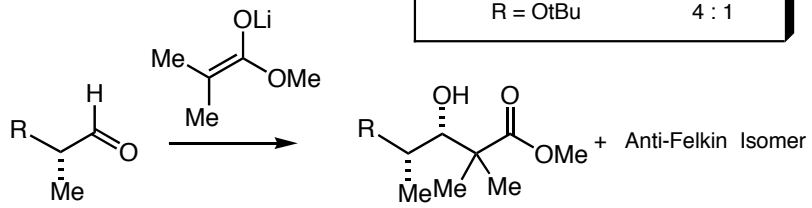

L. Flippin & Co-workers, *Tetrahedron Lett.*. **1985**, *26*, 973.

Ketone (R)	Ratio
R = Ph	>200 : 1
R = c-C_6H_{11}	9 : 1

■ This trend carries over to organometallic reagents as well

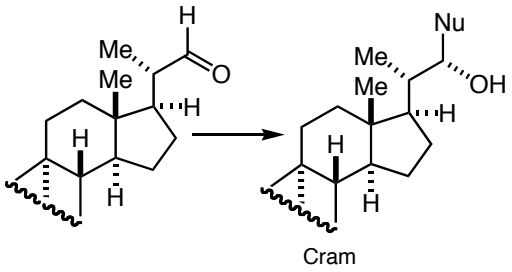

C. Djerassi & Co-workers, *J. Org, Chem.* **1979**, 44, 3374.

Reagent	Ratio
ClMg–C≡CEt	1 : 1
Li, Me, Me	5 : 1

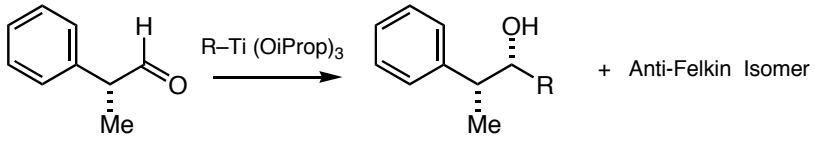

M. Reetz & Co-workers, *Angew Chemie Int. Ed.*. **1982**, *21*, 135.

(R–MgX gives Ca 3:1 ratios)

R-Titanium	Ratio
R = Me	>90 : 10
R = n-Bu	>90 : 10

Trend-2: Lewis acid catalyzed reactions are more diastereoselective

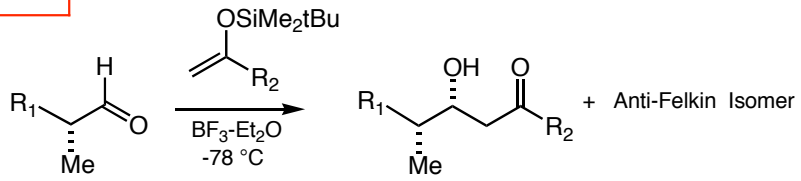

Ketone (R_1)	Enolate (R_2)	Ratio	Ratio Li enolate
R = Ph	R = Me	10 : 1	3 : 1
R = Ph	R = t-Bu	24 : 1	
R = Ph	R = OMe	15 : 1	
R = Ph	R = Ot-Bu	36 : 1	4 : 1
R = c-C_6H_{11}	R = Ot-Bu	16 : 1	

C. Heathcock & L. Flippin *J. Am. Chem. Soc.* **1983**, *105*, 1667.

The Felkin-Anh Eisenstein Model: Ketone Reduction

Addition of Hydride Nucleophiles

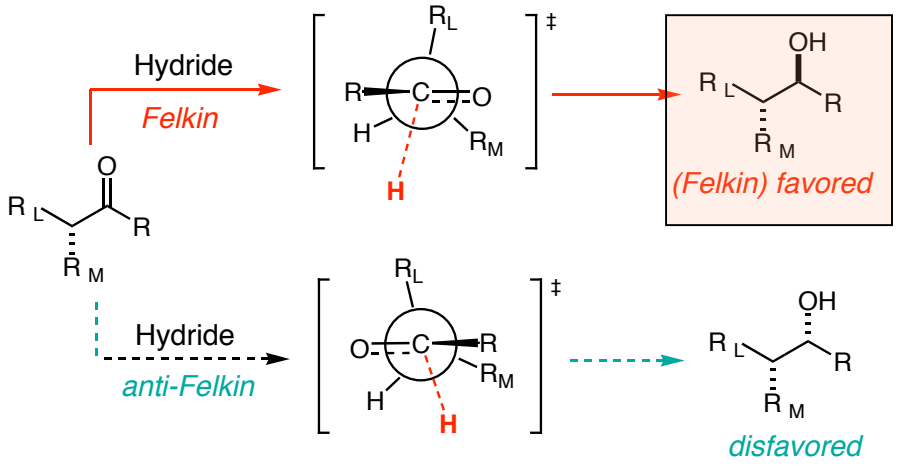

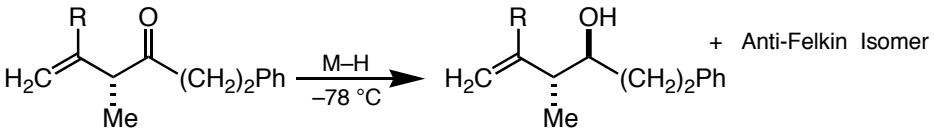

G. Tsuchihashi & Co-workers,
Tetrahedron Lett. **1984**, *25*, 2479.

Ketone (R)	Reagent	Ratio
R = H	$Li^+H–B^–(sec\text{-}Bu)_3$	96 : 4
R = H	DIBAL	47 : 53
R = Me	$Li^+H–B^–(sec\text{-}Bu)_3$	>99 : 1
R = Me	DIBAL	88 : 12

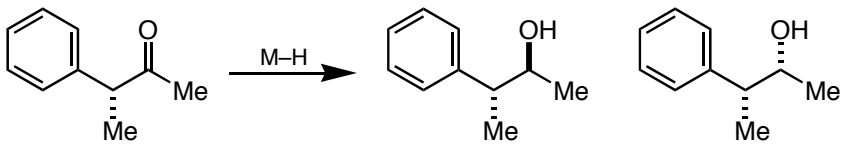

M. M. Midland & Co-workers,
J. Am. Chem. Soc. **1983**, *105*, 3725.

Reagent	Ratio	TS ‡
$Li^+H–B^–(sec\text{-}Bu)_3$	22 : 1	Felkin
$H–B(Sia)_2$	1 : 4	Anti-Felkin

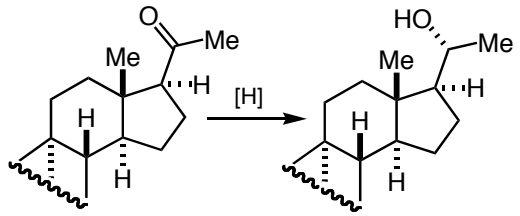

M. M. Midland & Co-workers,
J. Am. Chem. Soc. **1983**, *105*, 3725.

Reagent	Ratio	TS ‡
$Li^+H–B^–(sec\text{-}Bu)_3$	54 : 1	Felkin
$NaBH_4$	5 : 1	Felkin
$LiAlH_4$	3 : 1	Felkin
$H–B(Sia)_2$	1 : 10	Anti-Felkin

Note: Borane reducing agents do not follow the normal trend

Transition States for C=O-Borane Reductions

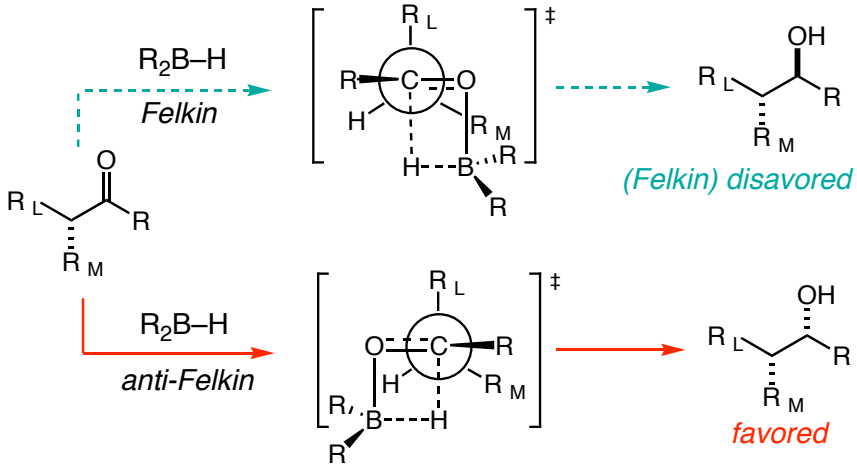

Nonspherical nucleophiles are unreliable in the Felkin Analysis

Exercise: Draw the analogous bis$(R_2BH)_2$ transition structures

The Felkin-Anh Eisenstein Model: A Breakdown

Are there cases not handled by the Anh-Eisenstein Model?

Anh-Eisenstein:
"Best acceptor σ* orbital is oriented anti periplanar to forming bond."

σ* C_{SP3}–C_{SP2} is lower in energy than σ* C_{SP3}–C_{SP3} bond.

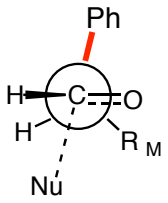

σ* C—Ph

σ C—Ph

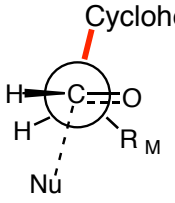

σ* C—Cyclohexyl

σ C—Cyclohexyl

Case I:

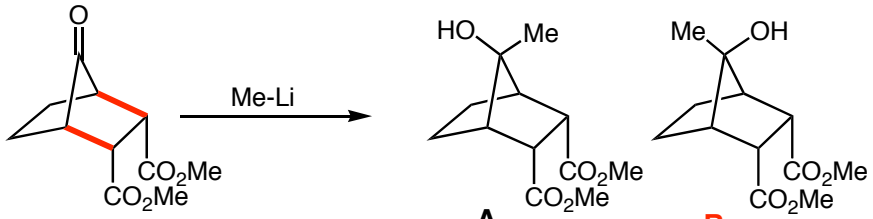

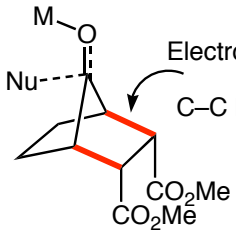

Electronegative -CO_2Me substituent will stabilize both C–C bonding & antibonding states

Felkin-Anh analysis predicts **B**

Felkin-Anh analysis predicts **B** for R = electronegative substituent.

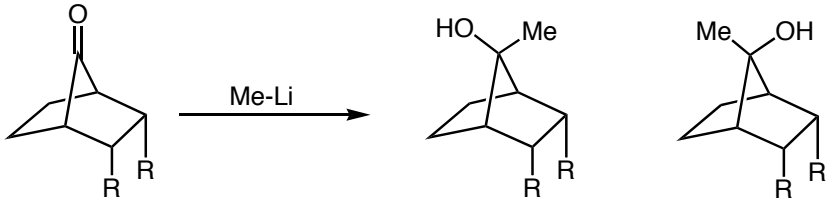

(Felkin-Anh Prediction)

G. Mehta, *JACS* **1990**, *112*, 6140

(R) Substituent	A/B Ratio
—C(=O)—OMe	>90:10
—CH_2OMe	34:66
—$CH{=}CH_2$	27:73
—CH_2–CH_3	17:83

Felkin-Anh analysis predicts the wrong product!

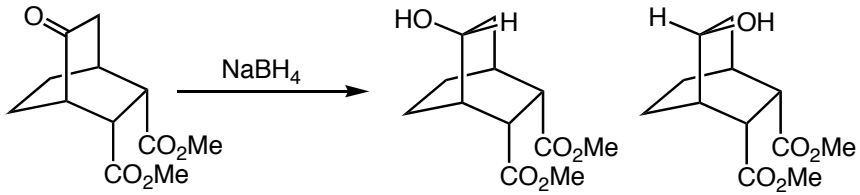

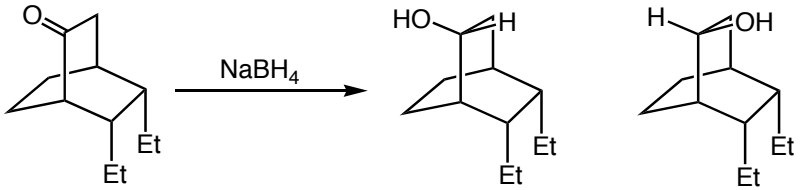

G. Mehta, *Chem. Commun.* **1992**, 1711-2:
"These results can be reconciled in terms of the Cieplak model."

The Felkin-Anh Eisenstein Model: A Breakdown

Case II: The Le Noble Examples Le Noble, *JACS* 1992, *114*, 1916

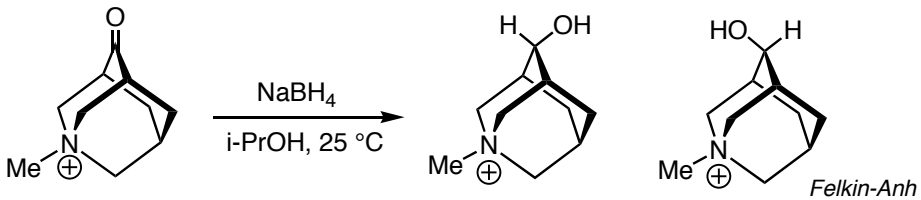

Ratio, ≥ 95:5

Pyramidally distorted C=O ruled out from inspection of X-ray structures.

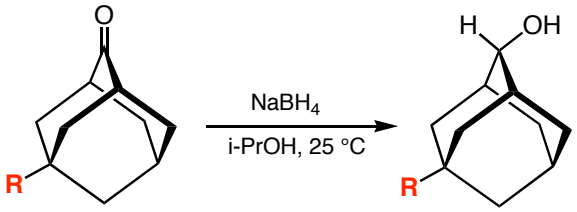

\+ Syn Isomer

(R)	Anti:Syn Ratio
R = F	62:38
R = CO_2Me	61:39
R = $SiMe_3$	45:55
R = OH	43:57

Le Noble, *J. Org. Chem.* **1989**, *54*, 3836

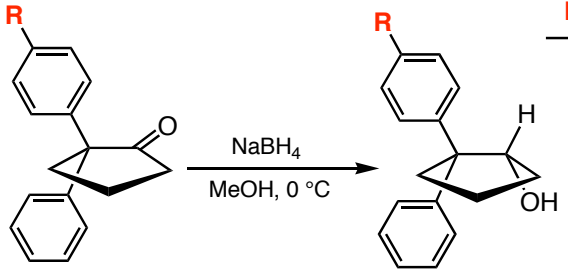

\+ Syn Isomer

(R)	Anti:Syn Ratio
R = NO_2	79:21
R = Cl	63:37
R = OMe	43:57
R = NH_2	36:64

Halterman, *JACS* **1990**, *112*, 6690

Cieplak Model for C=O Addition

Cieplak, *JACS* **1981**, *103*, 4540; Cieplak/Johnson, *JACS* **1989**, *111*, 8447

Point A: TS is stabilized by antiperiplanar allylic bond, but....

Point B: Nature of the stabilizing secondary orbital interactions differ:

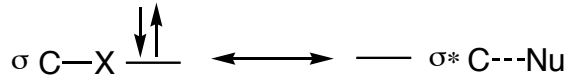

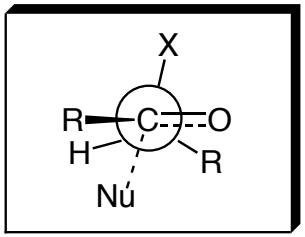

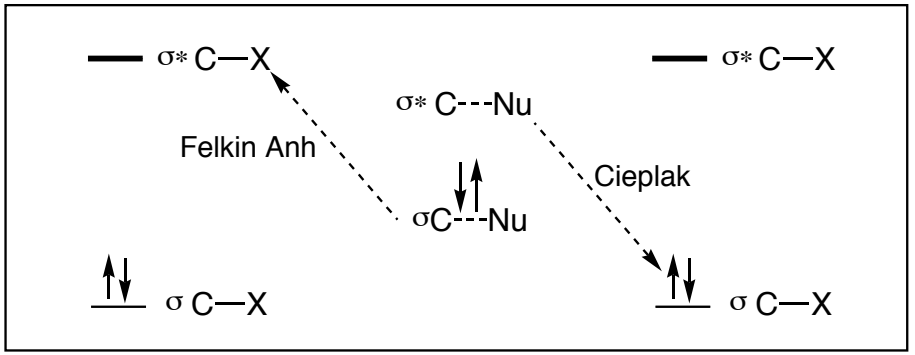

Point C: C–X Electron donating ability follows the order:
C–H > C–C > C–N > C–O
(Houk disputes the ordering of C–H, C–C)

Point D: Importance of torsional effects (Felkin, Anh, Houk, Padden-Row) disputed.

"Structures are stabilized by stabilizing their highest energy filled states. This is one of the fundamendal assumptions in frontier molecular orbital theory." The Cieplak hypothesis is nonsense."

"Just because a hypothesis correlates a set of observations doesn't make that hypothesis correct."

The management

http://www.courses.fas.harvard.edu/~chem206/

Chemistry 206

Advanced Organic Chemistry

Lecture Number 22

Carbonyl and Azomethine Electrophiles-2

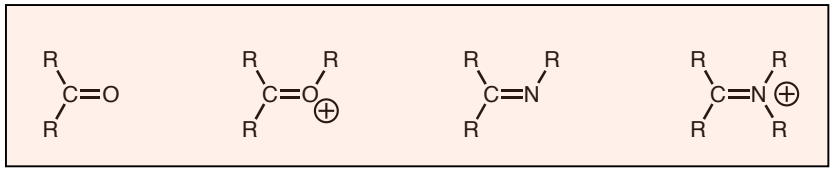

- Breakdown in the Felkin-Anh Model
- Cyclohexanone Revisited
- Diastereoselective Additions to Cyclic Ketones
- Chelate Controlled Carbonyl Additions

Reading Assignment for this Week:

Carey & Sundberg: **Part A**; Chapter 8
Reactions of Carbonyl Compounds

Carey & Sundberg: **Part B**; Chapter 2
Reactions of Carbon Nucleophiles with Carbonyl Compounds

Carey & Sundberg: **Part B**; Chapter 5
Reduction of Carbonyl & Other Functional Groups

D. A. Evans

Wednesday
November 9, 2005

1. "Theoretical Interpretation of 1,2-Asymmetric Induction. The Importance of Antiperiplanarity", N. T. Anh, O. Eisenstein *Nouv. J. Chem.* **1977**, *1*, 61-70. **(pdf)**

2. "Structural, mechanistic, and theoretical aspects of chelation controlled carbonyl addition reactions."Reetz, Acc. Chem. Res. **1993** *26*: 462. **(pdf)**

3. "A Stereochemical Model for Merged 1,2- and 1,3-Asymmetric Induction in Diastereoselective Mukaiyama Aldol Addition Reactions and Related Processes." Evans, et. al. *JACS* **1996**, *118*, 4322-4343. **(pdf)**

4. "The Exceptional Chelating Ability of Dimethylaluminum Chloride and Methylaluminum Dichloride. The Merged Stereochemical Impact of α- and β-Stereocenters in Chelate-Controlled Carbonyl Addition Reactions with Enolsilane and Hydride Nucleophiles". Evans, Allison,Yang, Masse, **2001**, *123*, 10840-10852. **(pdf)**

Me_2AlCl is the most powerful chelating Lewis acid yet documented

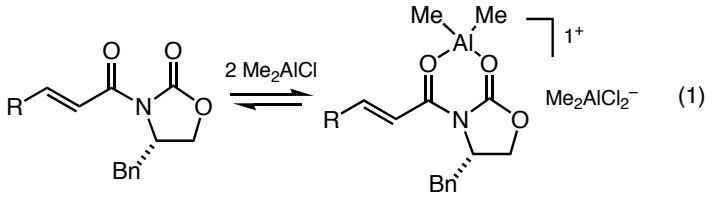

"Asymmetric Diels-Alder Cycloaddition Reactions with Chiral α,β-Unsaturated-*N* Acyloxazolidinones". Evans, D. A.; Chapman, K. T.; Bisaha, J. *J. Am. Chem. Soc.* **1988**, *110*, 1238-1256.

Syn Diastereomer: α & β Centers Reinforcing

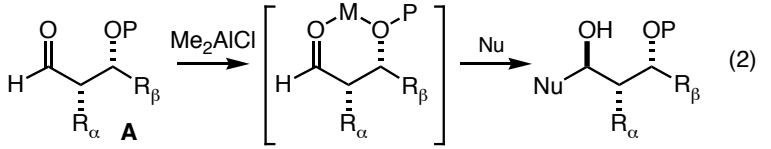

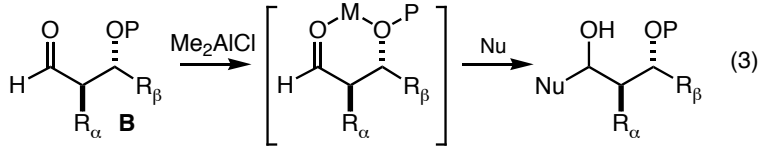

Anti Diastereomer: α & β Centers Opposing

The Cyclohexanone Case Revisited: Frencking & Houk

Observation As R becomes more electronegative, percentage of axial attack increases.

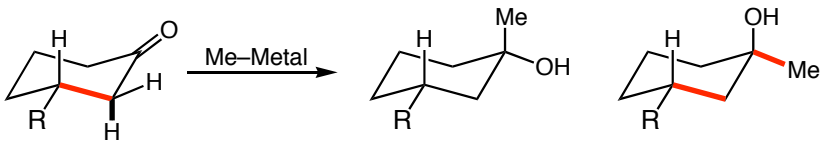

(R) Substituent	% Axial Attack: Me-Li	% Axial Attack: Me_2Cu-Li
R = H	21%	6%
R = C_6F_5	34%	21%
R = CF_3	50%	42%

Felkin-Anh predicts opposite trend.

Cieplak argument consistent with results.

The Frencking Position:

- Cieplak stabilizing interaction is "dubious." Why not stabilize the forming sigma bond?
- Enhanced rate of axial Nu attack on cyclohexanone is caused by better electrostatic interactions of the ketone with the attacking reagent and not by torsional considerations.
- Nonequivalence of the π*C=O LUMO with a greater extension on the axial face dictates stereoselection (Klein, 1973).

"Since interactions between the π C=O & π* C=O and the bonding & anti-bonding (β) C–H & (β) C–C orbitals are all symmetry allowed, it is difficult to predict a priori which interactions are dominant without carrying out quantum mechanical calculations."

Frencking & Reetz, *Angew. Chem.* Int. Ed. **1991**, *30*, 1146

Houk: Electrostatic rather than covalent considerations may be dominant.

Houk: If hyperconjugative interactions are important, equatorial electronegative substituents should interact more strongly with the C(2-3) and C(9-10) bonds than axial substituents.

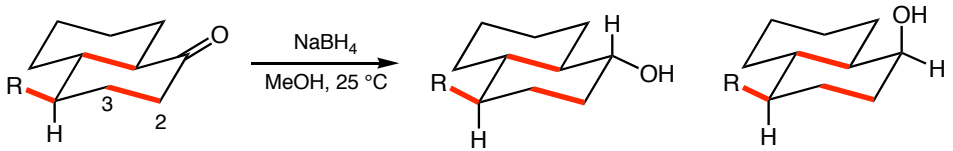

Since there seems to be little effect from the equatorial R substituent, hyperconjugation may not be a major contributor to TS stabilization.

(R) Substituent	Product Ratio
R = H	60:40
R = OAc	71:29
R = Cl	71:29

"**Cieplak:** If nucleophilic addition occurs anti to the better donor bond, the equatorial isomers should have considerably more axial attack than the parent while the axial isomers should have only a slight increase in axial attack."

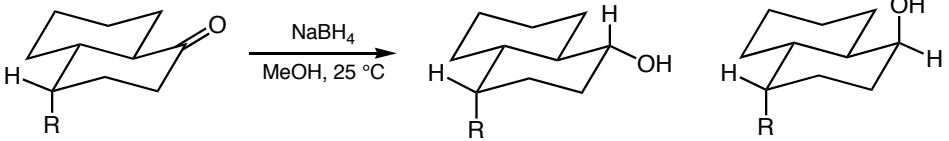

"Nevertheless, exactly the opposite is observed."

(R) Substituent	Product Ratio
R = OAc	83:17
R = Cl	88:12

Houk, "Axial 4-substituents favor axial attack for electrostatic reasons"

"Disfavored"

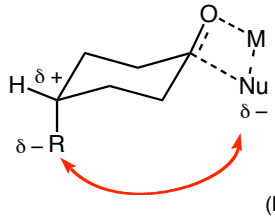

"Favored"

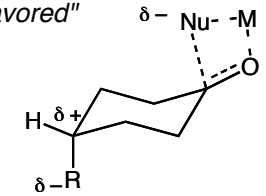

(DAE: Bimetallic transition states were not considered)

K. Houk & Co-workers, *J. Am. Chem. Soc.* **1991**, *113*, 5018

The Felkin-Anh Eisenstein Model: Electronic Effects

Are there electronic effects in the reaction?

Several cases have already been presented which may be relevant

L. Flippin & Co-workers, *Tetrahedron Lett.*. **1985**, *26*, 973.

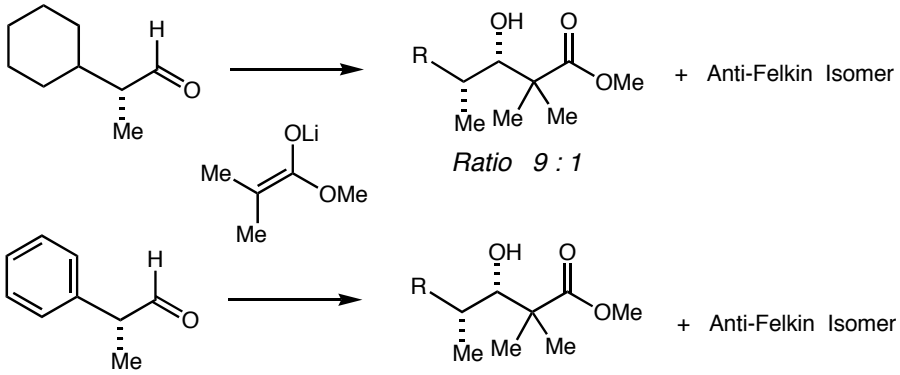

The molecular volume occupied by cyclohexyl acknowledged to be larger than that for phenyl. Because of shape phenyl "can get out of the way."

■ Anh-Eisenstein Explanation based on HOMO-LUMO Analysis:

"Best acceptor σ* orbital is oriented anti periplanar to forming bond."

σ* C_{SP3}–C_{SP2} is lower in energy than σ* C_{SP3}–C_{SP3} bond.

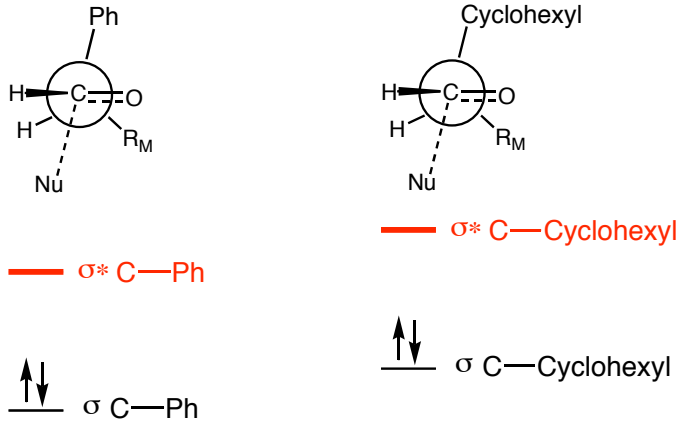

The Polar Felkin-Anh Model

Premise: Transition state **hyperconjugation** between forming bond (HOMO) and best antiperiplanar acceptor (σ* C–**X**, LUMO). Steric effects alre also considered; X = Halogen, OR, SR etc

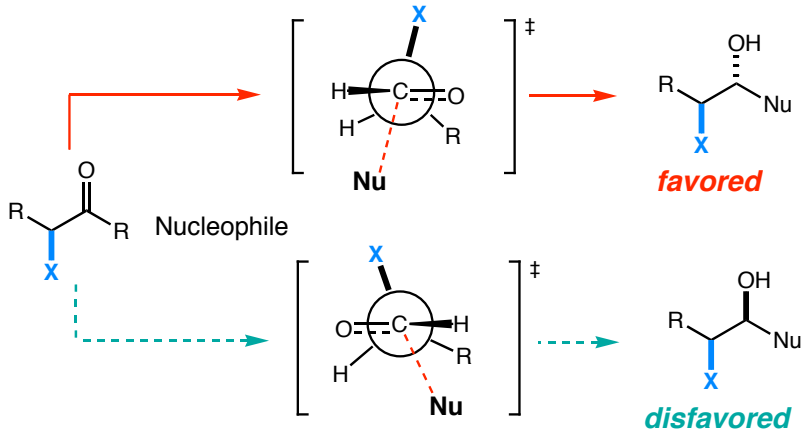

Modified Cornforth Model

Premise: Transition State **dipole minimization** between polar C–X substituent and the transforming carbonyl function dictate preferred TS geometrics. Steric effects alre also considered; X = Halogen, OR, SR etc

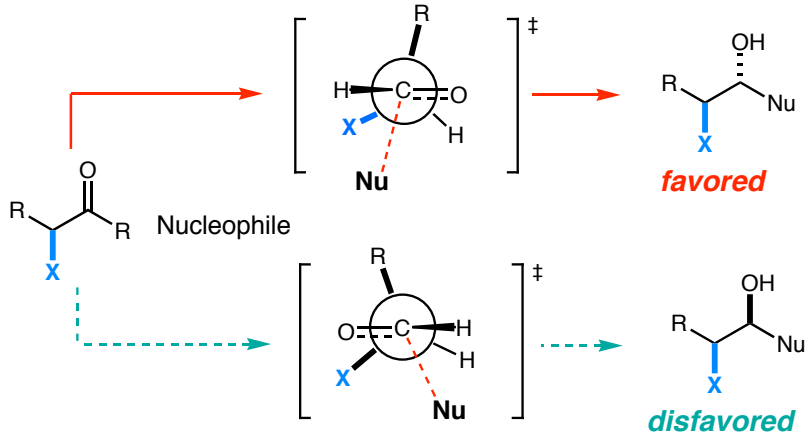

Both models lead to the same stereochemical prediction.

Felkin-Anh vs Cornforth Models

Dialkylborane reductions:
Individual models predict opposite stereochemical outcomes

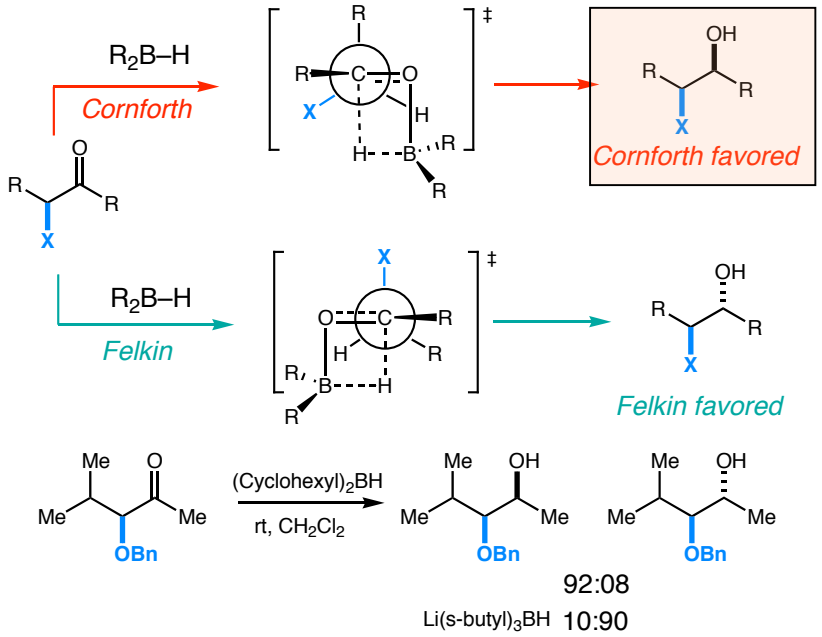

"Resurrecting the Cornforth Model for Carbonyl Addition: Studies on the Origin of 1,2-Asymmetric Induction in Enolate Additions to Heteroatom-Substituted Aldehydes," Evans, D. A.; Siska, S. J.; Cee, V. J. Angew. Chem. Int. Ed., 2003, 42, 1761-1765.

6-Membered oxocarbenium Ions: Woerpel etal. *JACS* 2000, 122, 168.

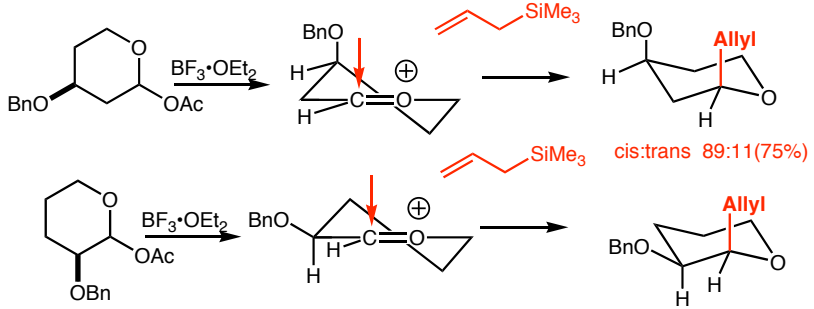

These cases provide dramatic evidence for the importance of electrostatic effects in controlling face selecticity.

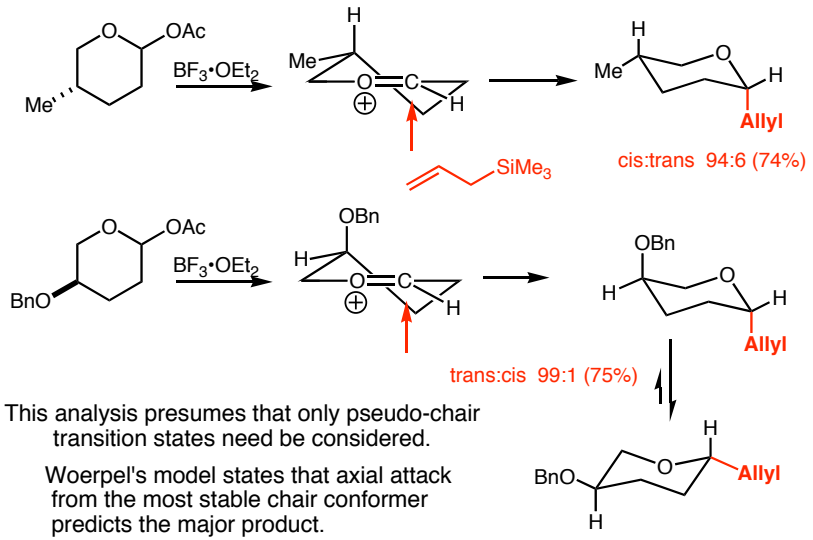

This analysis presumes that only pseudo-chair transition states need be considered.

Woerpel's model states that axial attack from the most stable chair conformer predicts the major product.

The Cornforth Model

Premise: Transition State **dipole minimization** between polar C–X substituent and the transforming carbonyl function dictate preferred TS geometrics. Steric effects alre also considered; X = Halogen, OR, SR etc

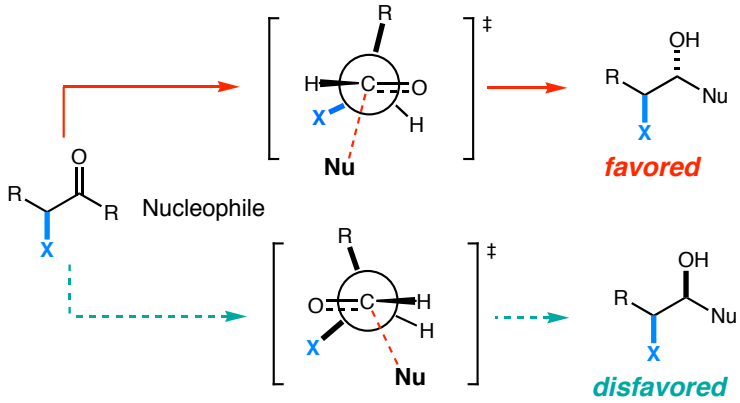

" It is difficult to rationalize the preceding rxns on the basis of the PFA Model. The data are best accomodated by the Cornforth Model.

Carbonyl Addition Reactions: Chelate Organization

Chelate organization also provides a powerful control element in carbonyl addition reactions

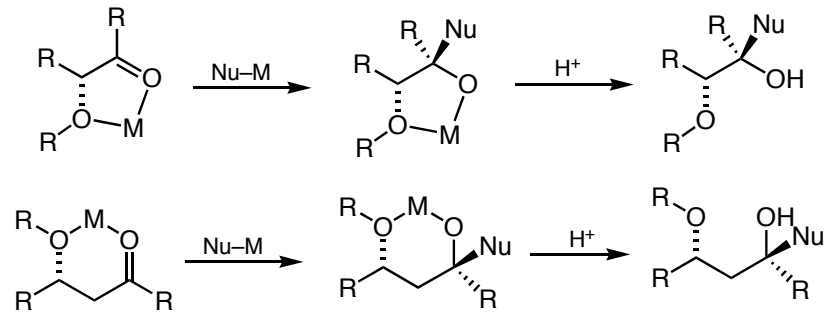

Reviews

Reetz, *Accts. Chem. Res.* **1993**, *26*, 462-468 **(pdf)**
Reetz, *Angew. Chem. Int. Ed.* **1984**, *23*, 556-569

Addition of Carbon Nucleopiles

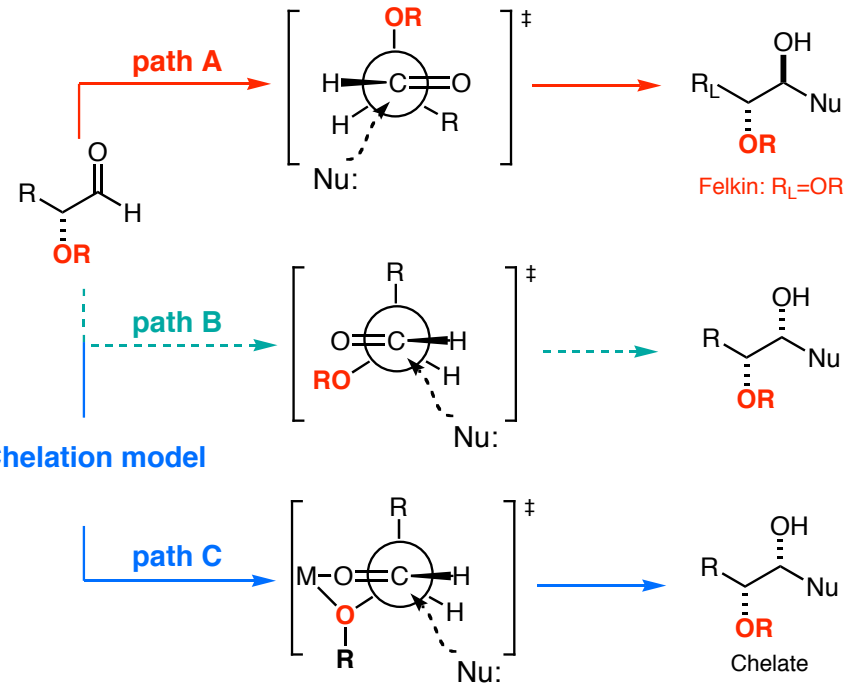

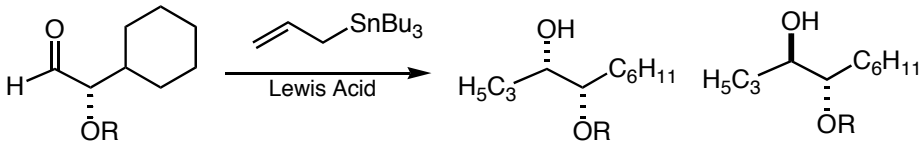

(OR)	Acid	Solv.	Ratio
R = CH_2OBn	$MgBr_2$	THF (0°)	20 : 80
R = CH_2OBn	$MgBr_2$	CH_2Cl_2 (-20°)	>99 : 1
R = CH_2OBn	$TiCl_4$	CH_2Cl_2 (-78°)	>99 : 1
R = $SiMe_2(t)Bu$	BF_3-Et_2O	CH_2Cl_2 (-78°)	5 : 95

G. Keck & Co-workers, *Tetrahedron Lett.* **1984**, *25*, 265

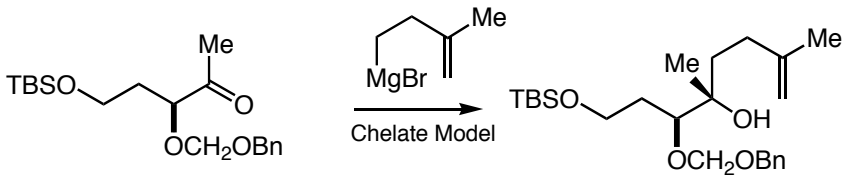

diastereoselection 50 : 1

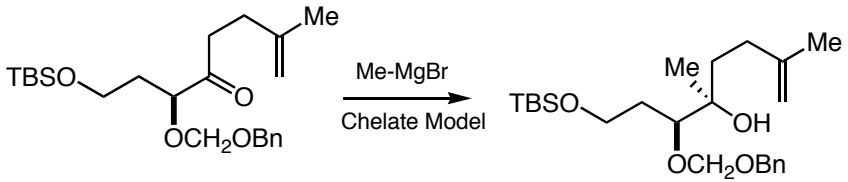

W. C. Still & Co-workers,
Tetrahedron Lett. **1980**, *21*, 1031

diastereoselection >100 : 1

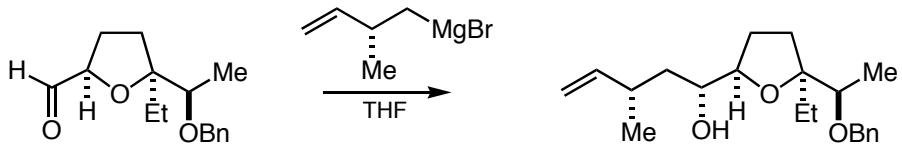

Y. Kishi & Co-workers,
Tetrahedron Lett. **1978**, *19*, 2745

"only one isomer"
Chelate Model

Chelate Organization in C=O Addition

Chelate organization provides a powerful control element in carbonyl addition reactions

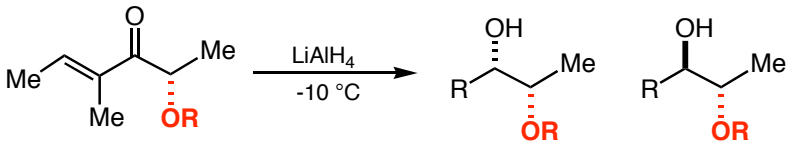

Polar Felkin Anh Chelation

Overman
Tet Lett. **1982**, *23*, *2355*

(OR)	Solv.	Ratio	Model
R = CH_2OBn	THF	30 : 70	Chelate
R = CH_2OBn	Et_2O	2 : 98	Chelate
R = $SiPh_2(t)Bu$	**THF**	**95 : 5**	**F–A: R_L=OR**

Degree of chelate organization may be regulated by choice of solvent and protecting group. Note that $SiPh_2(t)Bu$ group prevents chelation.

Case Study

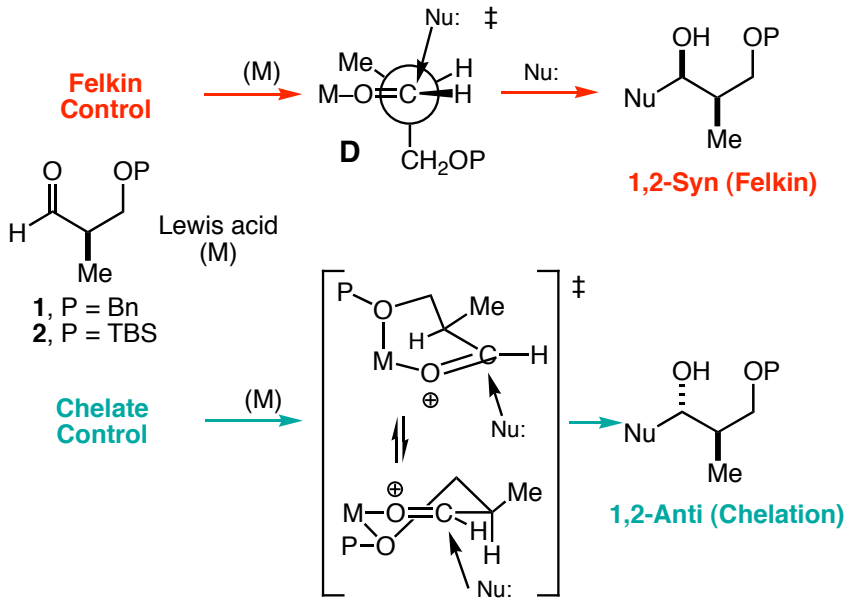

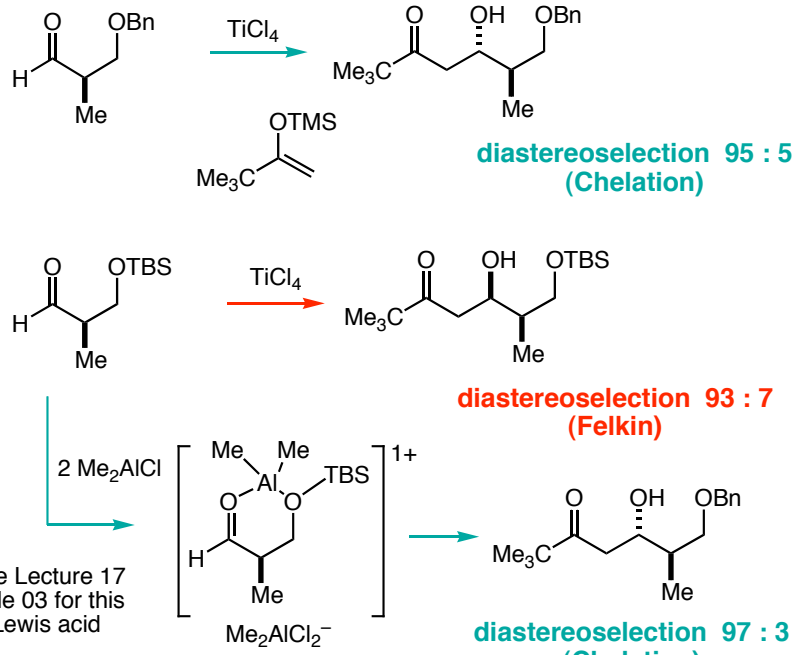

Me_2AlCl & $MeAlCl_2$ only Lewis acids that will chelate strongly to $OSiR_3$ Groups.
Evans, Allison, Yang,Masse, *JACS* **2001**, *123,* 10840–10852

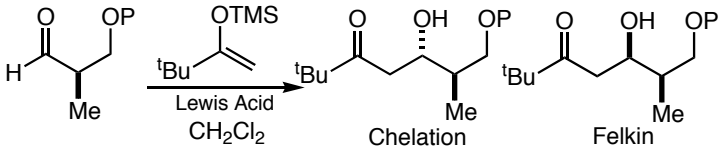

1 P = Bn **9** **10**
2 P = TBS **11** **12**

entry	Lewis acid[b]	**1** P = Bn **9** : **10** (%)	**2** P = TBS **11** : **12** (%)
A	BF_3•OEt_2	26 : 74 (76)	09 : 91 (55)
B	$SnCl_4$	50 : 50 (87)	07 : 93 (41)
C	$TiCl_4$	**97 : 03** (74)	07 : 93 (55)
D	Me_2AlCl	90 : 10 (45)	**97 : 03** (62)[c]
E	$MeAlCl_2$	78 : 22 (70)	77 : 23 (55)

Kinetic Evidence for Chelate-Controlled C=O Additon

Since 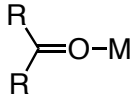 much more reactive than 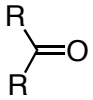

Substrates which can participate in C=O chelation will be more reactive since the effective concentration of chelated intermediate will be higher.

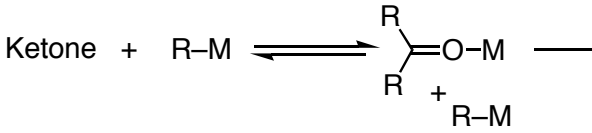

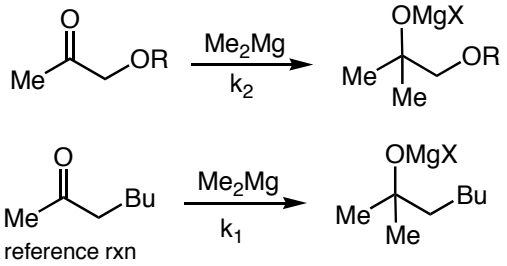

R	rel rate
–Me	213
–Bn	174
–CMe_3	9
–$SiMe_3$	7
–Si-i-Pr_3	1

rxn run inTHF at - 78°C

Eliel, Frye, *JACS* **1992**, *114*, 1778-84 (read)

However, these trends are not transmitted strongly to β-chelation

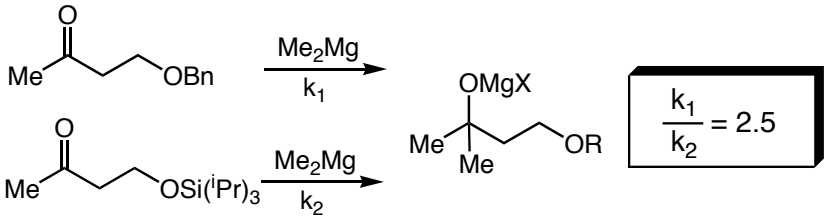

Hence, organization through 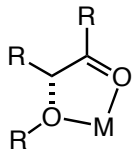 better than 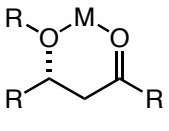

Alpha–Versus Beta-Chelation

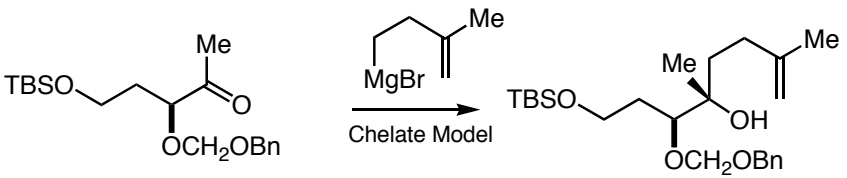

W. C. Still & Co-workers,
Tetrahedron Lett. **1980**, *21*, 1031

diastereoselection 50 : 1

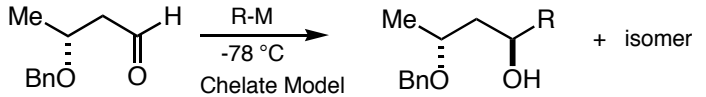

M. T. Reetz & Co-workers
J. Am. Chem. Soc.. **1983**, 105, 4833.

Other nucleophiles reported

R-M	Solv.	Ratio
Me-MgCl	THF	40 : 60
Me-$TiCl_3$	CH_2Cl_2	90 : 10

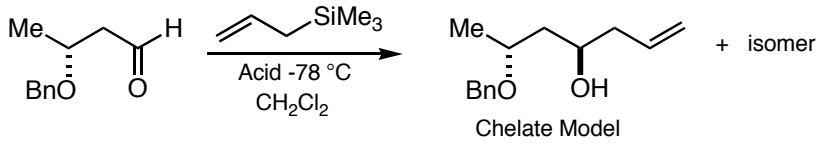

M. T. Reetz & Co-workers
Tetrahedron Lett. **1984**, *25*, 729.

Acid	Ratio
$TiCl_4$	95 : 5
$SnCl_4$	95 : 5
BF_3-OEt_2	85 : 15

- Note that beta chelation can be developed as a control element by varying solvent & Nu.
- Note BF_3 gives "apparent" chelate control

1,3-Stereoinduction Models for Chelate & non-Chelate Rxns

1,3-Stereoinduction Polar Model:

Evans, Dart, Duffy,Yang, *JACS* **1996**, *118,* 4322–4343

1,3-Stereoinduction Chelate Model:

Evans, Allison, Yang,Masse, *JACS* **2001**, *123,* 10840–10852

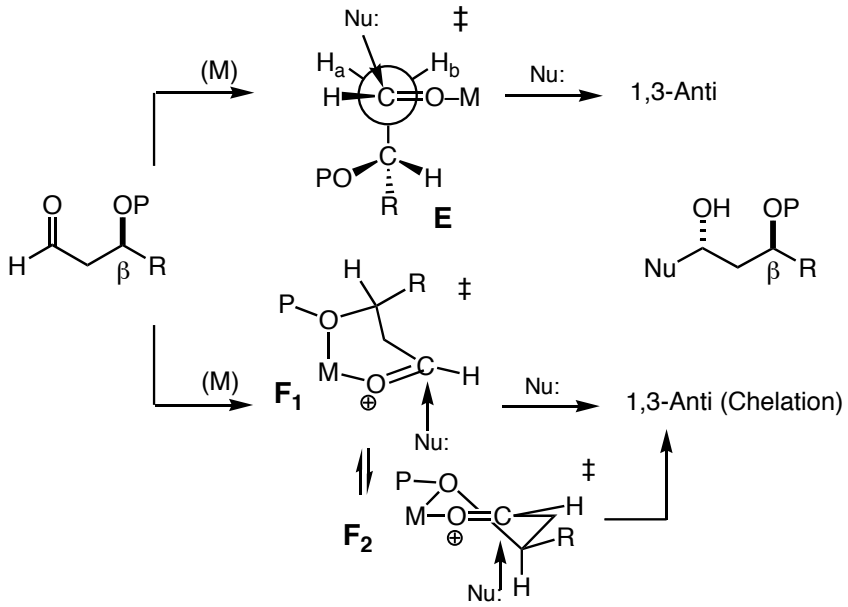

1,3-Anti Relationship is favored by either polar or chelate models

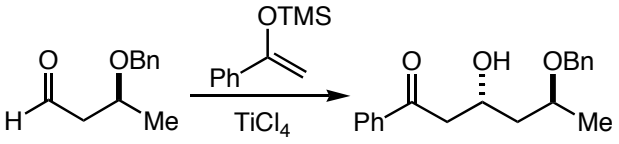

diastereoselection 92 : 8

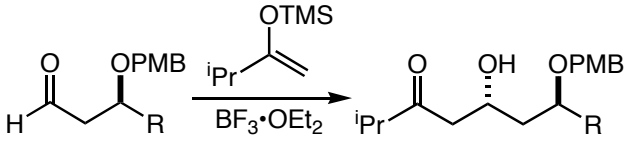

diastereoselection 81 : 19

1,3-Stereoinduction Polar Model:

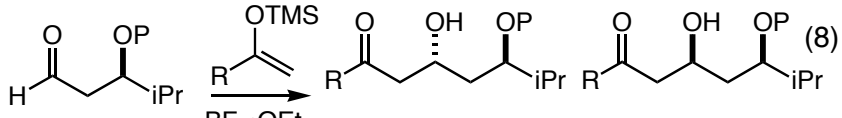

1 P = PMB
2 P = TBS

3 **5** **4** **6**

entry	R	**3** : **4** (P = PMB)	(%)	**5** : **6** (P = TBS)	(%)
A	t-Bu	89 : 11	(82)	84 : 16	(79)
B	i-Pr	92 : 08	(91)	80 : 20	(84)
C	Me	91 : 09	(89)	93 : 07	(87)

Steric effects appear to play a minor role in stereoinduction:

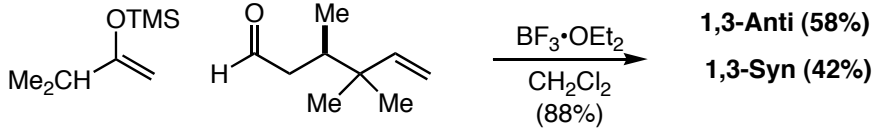

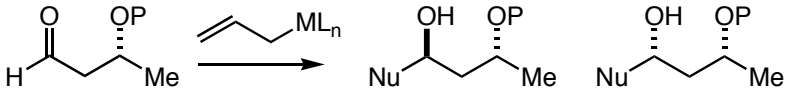

P = Bn (benzy)
P = MOM (methoxymethyl)

entry	conditions	(P = Bn) *anti* : *syn*	(P = MOM) *anti* : *syn*
A	$SiMe_3$ $BF_3•OEt_2$	85 : 15	—
B	$SnPh_3$ $BF_3•OEt_2$	79 : 29	—
C	$SnMe_3$ $BF_3•OEt_2$	—	70 : 30

1,3-Stereoinduction Polar Model

Evans, Dart, Duffy,Yang, *JACS* **1996**, *118,* 4322–4343

Can one develop a Rational model for α & β Stereocenters?

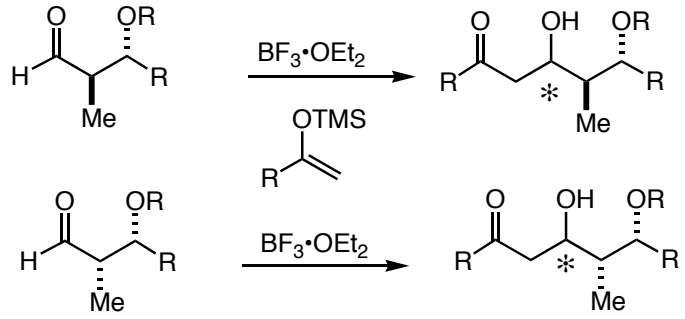

Which of the two stereochemical representations is reinforcing? Non-reinforcing?

Integration of 1,3- Polar Model & Felkin-Anh Model

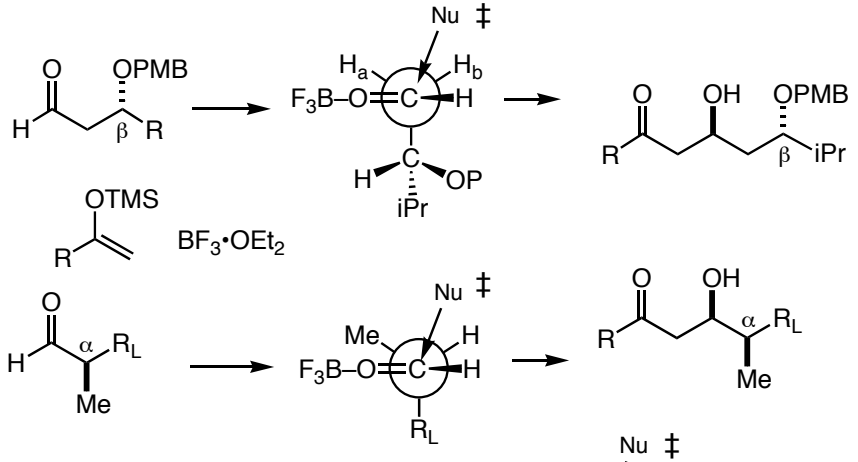

If both models are correct, they should integrate when the two stereocenters are reinforcing

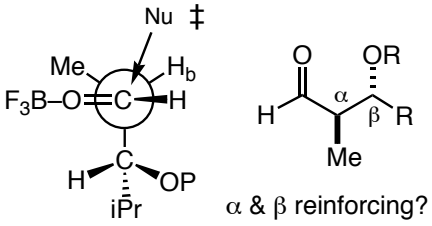

α & β reinforcing?

The Anti Diastereomer

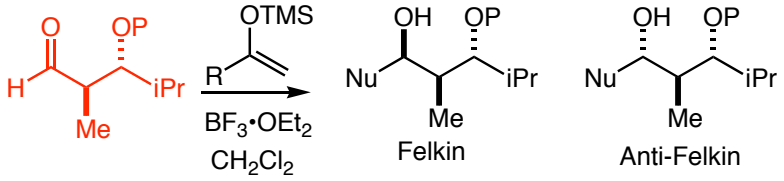

13 P = PMB
14 P = TBS

15
17

16
18

entry	R	**15** : **16** (P = PMB)	**17** : **18** (P = TBS)
A	t-Bu	99 : 01	99 : 01
B	i-Pr	98 : 02	95 : 05
C	Me	97 : 03	71 : 29

The Syn Diastereomer

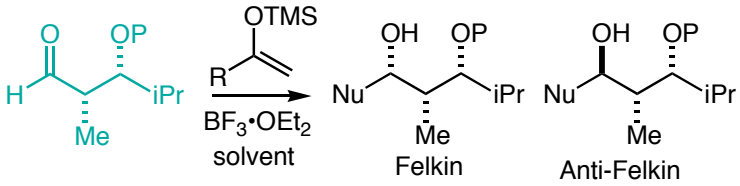

19 P = PMB
20 P = TBS

21
23

22
24

entry	R	Solvent	**21** : **22** (P = PMB)	**23** : **24** (P = TBS)
A	t-Bu	CH_2Cl_2	96 : 04	96 : 04
B	t-Bu	toluene	88 : 12	94 : 06
C	i-Pr	CH_2Cl_2	56 : 44	87 : 13
D	i-Pr	toluene	32 : 68	75 : 25
E	Me	CH_2Cl_2	17 : 83	58 : 42
F	Me	toluene	06 : 94	40 : 60

Conclusions

A: Anti diastereomer is reinforcing. Both models integrate.
B: Syn diastereomer transitions from Felkin control (Large Nu) to 1,3-control (Small Nu).

The Anti Diastereomer: Both Centers Reinforcing

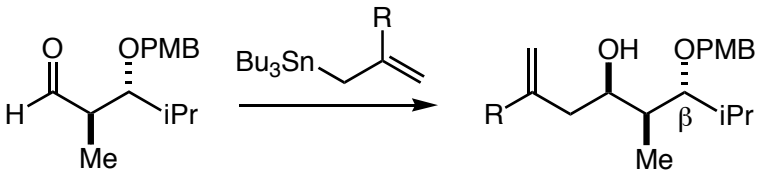

entry	Conditions	R	Felkin : anti-Felkin
A	BF_3•OEt_2, toluene	Me	>99 : 1
B	BF_3•OEt_2, toluene	H	>99 : 1
C	Ph_3CClO_4, CH_2Cl_2	H	>99 : 1

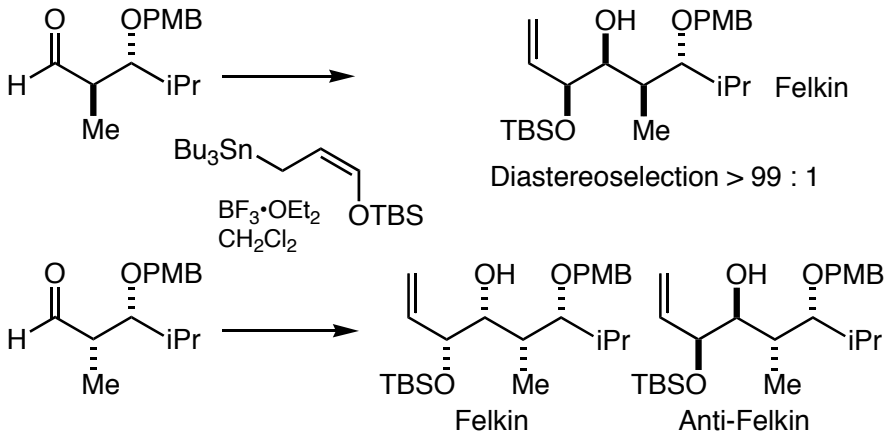

[a]The third unpictured product is the Felkin-3,4-*anti* diastereomer.

The Syn Diastereomer: Stereocenters are Non-reinforcing

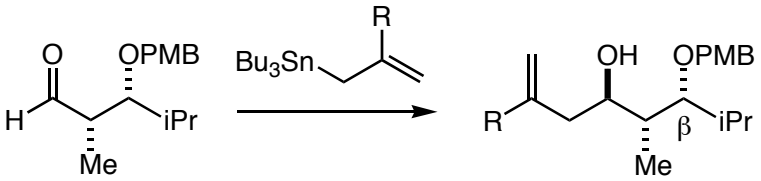

entry	Conditions	R	Felkin : anti-Felkin
A	BF_3•OEt_2, toluene	Me	20 : 80
B	BF_3•OEt_2, toluene	H	13 : 87
C	Ph_3CClO_4, CH_2Cl_2	H	62 : 38

In this example, the OR substituent is the dominant stereo-control element

The Syn Diastereomer: Stereocenters are Non-reinforcing

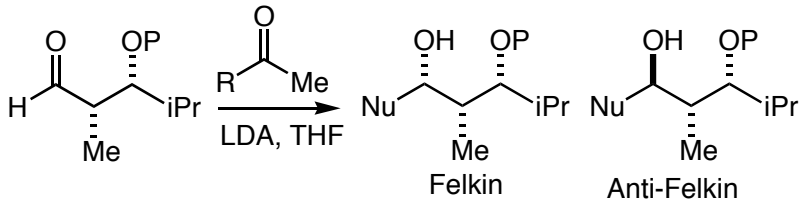

19 P = PMB
20 P = TBS

21 Felkin
22 Anti-Felkin
23 Felkin
24 Anti-Felkin

entry	R	**21** : **22** (P = PMB)	(%)	**23** : **24** (P = TBS)	(%)
A	t-Bu	11 : 89	(71)	08 : 92	(91)
B	i-Pr	14 : 86	(95)	13 : 87	(64)
C	Me	22 : 78	(73)	14 : 86	(88)

Carbonyl Addition Reactions: Chelate Organization

Beta Chelation with Organometals

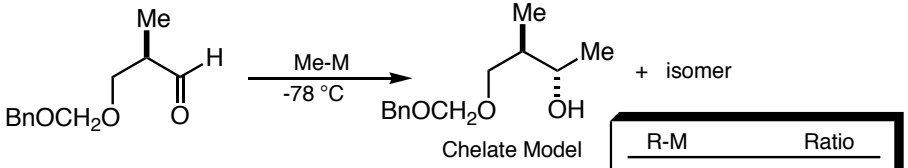

R-M	Ratio
MeMgBr	50 : 50
Me_2CuLi	97 : 3

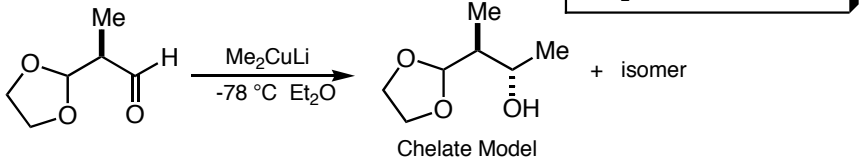

***diastereoselection* > 95 : 5**

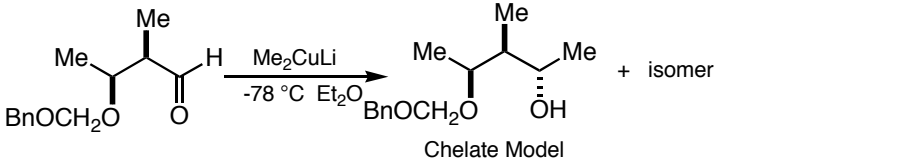

***diastereoselection* > 95 : 5**

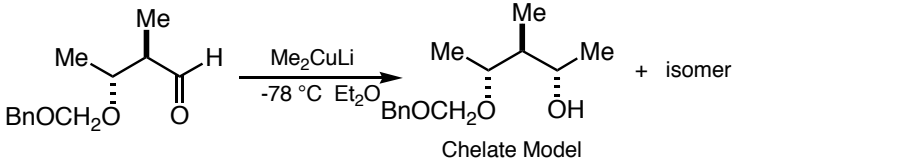

***diastereoselection* 70 : 30**

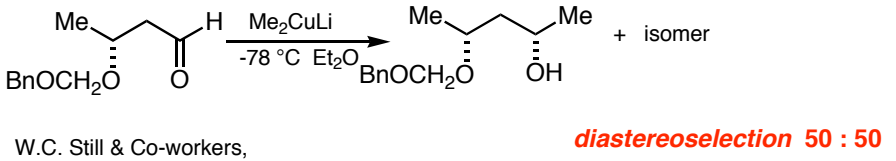

***diastereoselection* 50 : 50**

W.C. Still & Co-workers,
Tetrahedron Lett. **1980**, *21*, 1035.

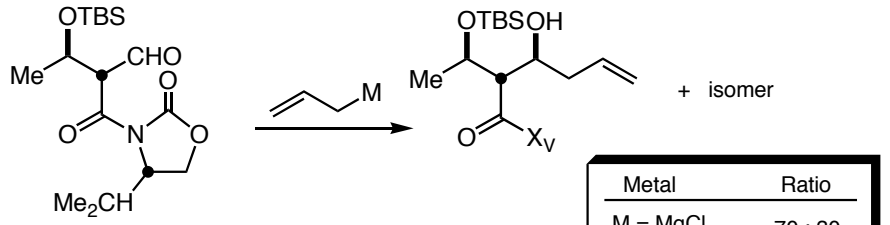

Metal	Ratio
M = MgCl	70 : 30
M = ZnCl	97 : 3

D. A. Evans & E. Sjogren
Tetrahedron Lett. **1986**, *27*, 4961.

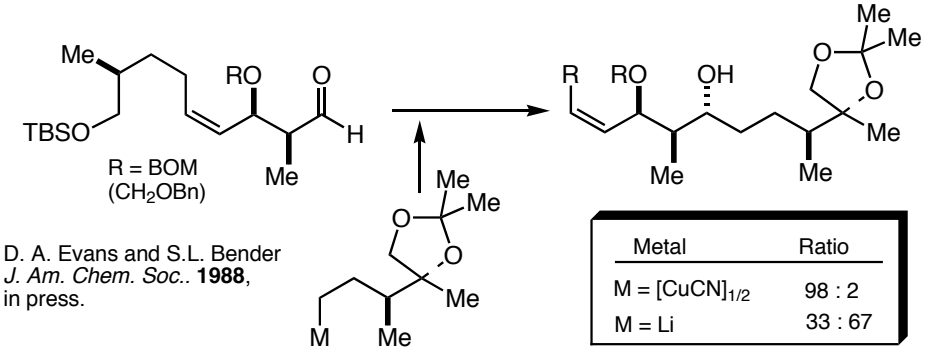

Metal	Ratio
M = $[CuCN]_{1/2}$	98 : 2
M = Li	33 : 67

D. A. Evans and S.L. Bender
J. Am. Chem. Soc.. **1988**,
in press.

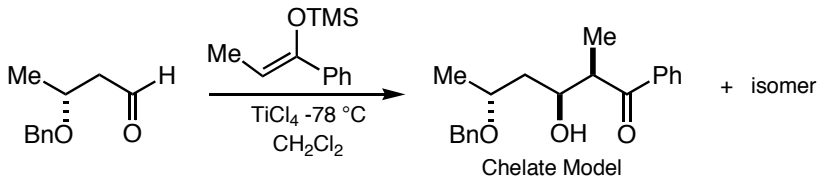

M. T. Reetz & Co-workers
Tetrahedron Lett. **1984**, *25*, 729.

***diastereoselection* >92 %**

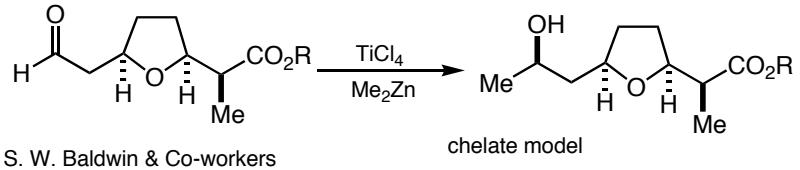

S. W. Baldwin & Co-workers
J. Org. Chem. **1987**, *52*, 320.

***diastereoselection* 96 : 4**

Beta Chelate-Controlled Reduction

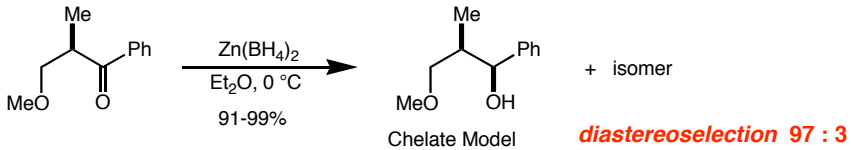

T. Oishi & Co-workers
Chem. Pharm Bull. **1984**, *32*, 1411.

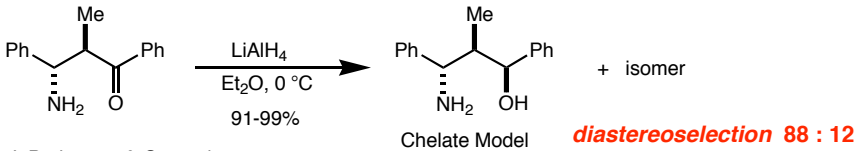

J. Barluenga & Co-workers
J. Org. Chem. **1985**, *50*, 4052.

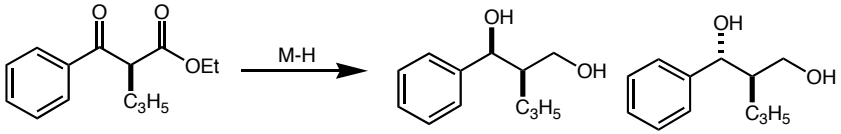

G. R. Brown & Co-workers
Chem. Commun. **1985**, 455.

M-H	Ratio
$Zn(BH_4)_2$ Et_2O	100 : 0
$LiAlH_4$ THF	0 : 100

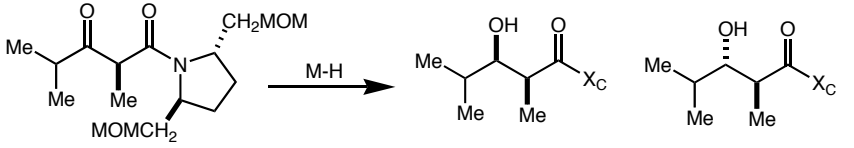

M. Yamaguchi & Co-workers
Tetrahedron Lett. **1985**, *26*, 4643.

T. Oishi & Co-workers
Tetrahedron Lett. **1980**, *21*, 1641
($Zn(BH_4)_2$ on esters.

M-H	Ratio
$Zn(BH_4)_2$ Et_2O	100 : 0
KBH_3H THF	0 : 100

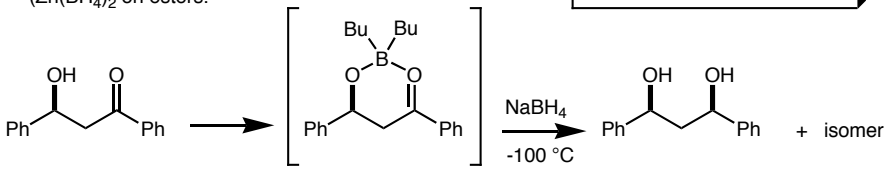

K. Narasaka & Co-workers
Chem. Lett. **1980**, 1415.

diastereoselection 96 : 4

Directed reductions of β-hydroxyketones

Evans, Chapman, Carreira, JACS **110**, 3560 (1988)

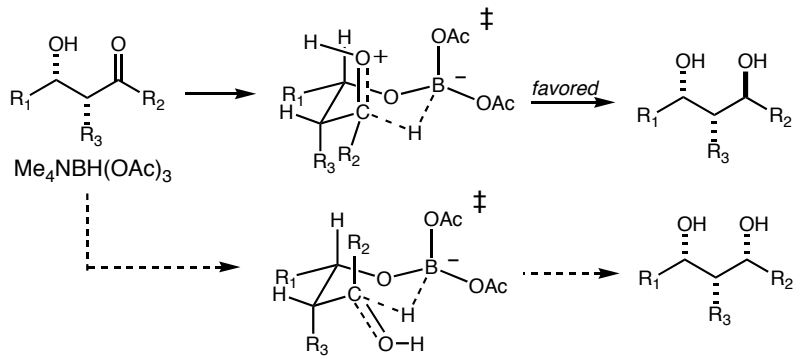

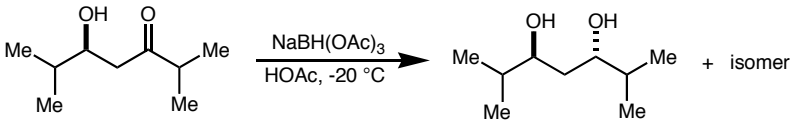

diastereoselection 96 : 4

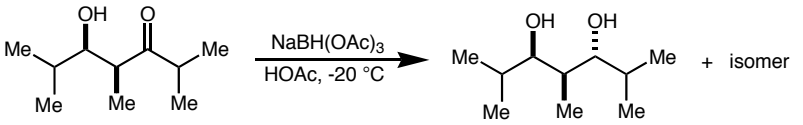

diastereoselection 98 : 2

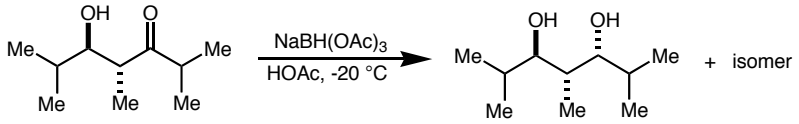

diastereoselection 98 : 2

Propose a mechanism for tihs highly diastereoselective transformation, Evans, Hoveyda JACS **112**, 6447 (1990)

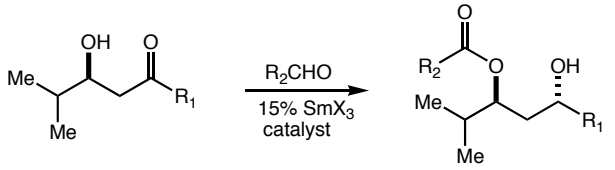

diastereoselection > 100:1

Remote Heteroatom Effects in Carbonyl Addition

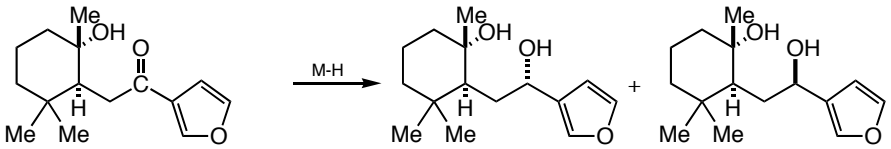

Temp. & Solvent not specified in this study in first three cases

R. Baker & Co-workers
Chem. Commun. **1984,** 74

Reagent	Ratio
Li-AlH$_4$	40 : 60
Na-BH$_4$	50 : 50
Zn-BH$_4$	60 : 40
Li-BHEt$_3$, (THF, -78˚C)	100 : 0

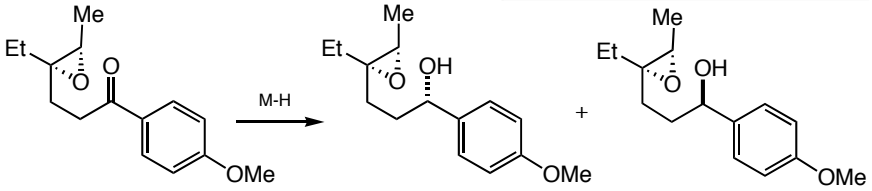

Y. Kishi & Co-workers
Tetrahedron Lett. **1978**, 2741.

* *di-2-(o-toluidinomethyl)pyrrolidine*

Li-BH(R)$_3$, Et$_2$O, 25˚C	1 : 1
LiAlH$_4$, Et$_2$O, 25˚C	3 : 1
LiAlH$_4$-diamine,* -78˚C	11 : 1

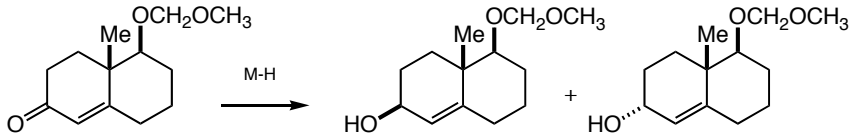

Li-BH(R)$_3$,	73 : 27
LiAlH$_4$	76 : 24

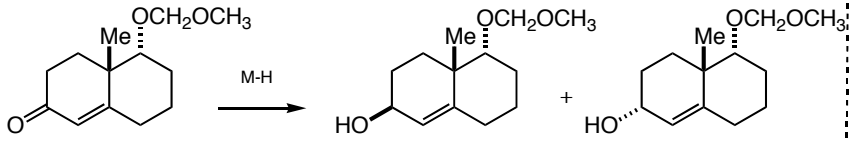

Li-BH(R)$_3$,	28 : 72
LiAlH$_4$	72 : 28

W. G. Dauben & Co-workers
Tetrahedron Lett. **1978**, 2741.

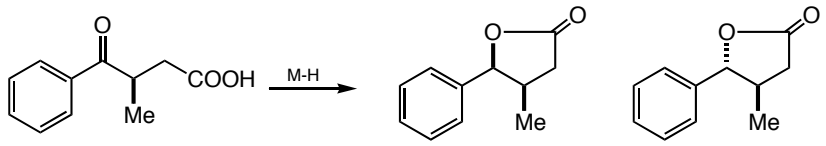

R. Frenette & Co-workers
J. Org. Chem. **52**, 304 (1987)

Reagent	Ratio
NaBH$_2$(OR)$_2$	50 : 50
NaBH$_4$	70 : 30
DIBAL (2.4 equiv)	95 : 5
DIBAL (2.4 equiv) with ZnCl2	99 : 1

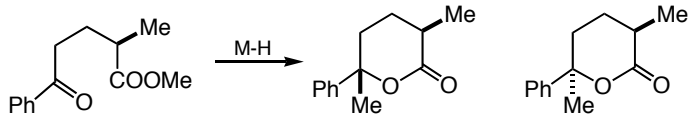

R. Frenette & Co-workers
J. Org. Chem. **52**, 304 (1987)

Solvent	Ratio
THF	50 : 50
C$_6$H$_6$	70 : 30

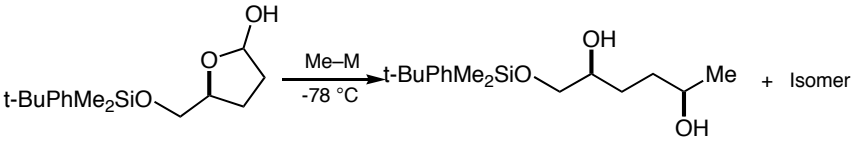

67-87% yields

G. Tsuchihashi & Co-workers
Tetrahedron Lett. **1987**,*28*, 6335.

Reagent	Solvent	Ratio
MeLi	Et$_2$O	1.7 : 1
MeMgBr	THF	1.3 : 1
Me$_3$Al	CH$_2$Cl$_2$	1.1 : 1
MeTiCl$_3$	CH$_2$Cl$_2$	8.4 : 1
MeTi(O-iProp)$_3$	CH$_2$Cl$_2$	12 : 1

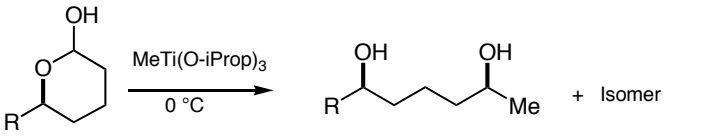

R = Me, Ph(CH$_2$)$_2$

Ratio 4-5.5 : 1

http://www.courses.fas.harvard.edu/colgsas/1063

Chemistry 206

Advanced Organic Chemistry

Lecture Number 23

The Evolution of Stereochemical Models for C=O Addition

■ Reading Assignment for this Week:

Carey & Sundberg: **Part A**; Chapter 8
Reactions of Carbonyl Compounds

Carey & Sundberg: **Part B**; Chapter 2
Reactions of Carbon Nucleophiles with Carbonyl Compounds

Carey & Sundberg: **Part B**; Chapter 5
Reduction of Carbonyl & Other Functional Groups

1. "Theoretical Interpretation of 1,2-Asymmetric Induction. The Importance of Antiperiplanarity", N. T. Anh, O. Eisenstein *Nouv. J. Chem.* **1977**, *1*, 61-70. **(handout)**

D. A. Evans

Friday
November 10, 2006

Additional Electronic handouts

2. "Structural, mechanistic, and theoretical aspects of chelation controlled carbonyl addition reactions."Reetz, Acc. Chem. Res. **1993** *26*: 462. **(pdf)**

3. "A Stereochemical Model for Merged 1,2- and 1,3-Asymmetric Induction in Diastereoselective Mukaiyama Aldol Addition Reactions and Related Processes." Evans, et. al. *JACS* **1996**, *118*, 4322-4343. **(pdf)**

4. "The Exceptional Chelating Ability of Dimethylaluminum Chloride and Methylaluminum Dichloride. The Merged Stereochemical Impact of α- and β- Stereocenters in Chelate-Controlled Carbonyl Addition Reactions with Enolsilane and Hydride Nucleophiles". Evans, Allison,Yang, Masse, *JACS* **2001**, *123*, 10840-10852. **(pdf)**

5. "Resurrecting the Cornforth Model for Carbonyl Addition: Studies on the Origin of 1,2-Asymmetric Induction in Enolate Additions to Heteroatom-Substituted Aldehydes," Evans, D. A.; Siska, S. J.; Cee, V. J. *Angew. Chemie Int. Ed.* **2003,** *42*, 1761-1765 **(pdf)**

5. "Theoretical Investigation of Enolborane Addition to Alpha Heteroatom-Substituted Aldehydes. Relevance of the Cornforth and Polar Felkin-Anh Models for Asymmetric Induction" Cee, V. J.; Cramer, C. C.; Evans, D. A. *JACS* **2006**, *128*, 2920-2930. **(pdf)**

Problem 69. The following stereoselective transformation has been reported by Fujisawa (*Chem.Lett.* **1991**, 1555). Given the stereochemistry of the product, rationalize the stereochemical outcome of the indicated reaction.

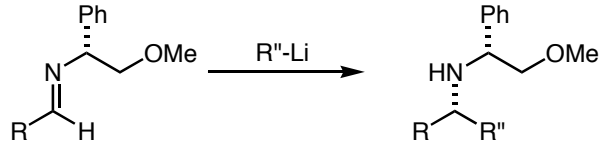

Diastereoselection >97:3

Problem 196. Part A. Provide a mechanism for the following reaction (*Tetrahedron*, **1999**, 8883). Include a clear transition state representation that predicts the major product diastereomer.
Part B. When the reaction is performed in diethyl ether or THF, the diastereoselectivity is significantly lowered. Propose an explanantion for this observation.

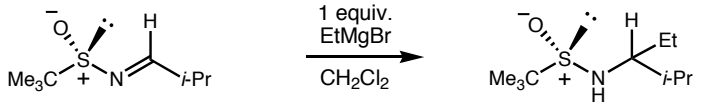

Diastereoselection >90:10

Donald J.Cram (1919–2001)

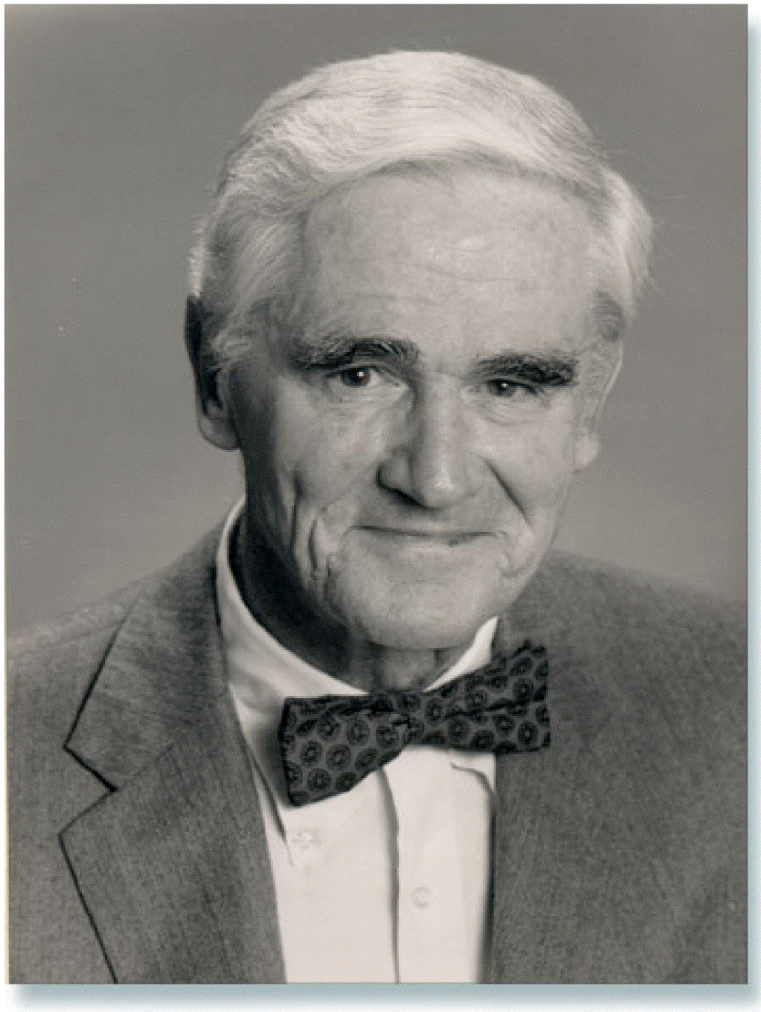

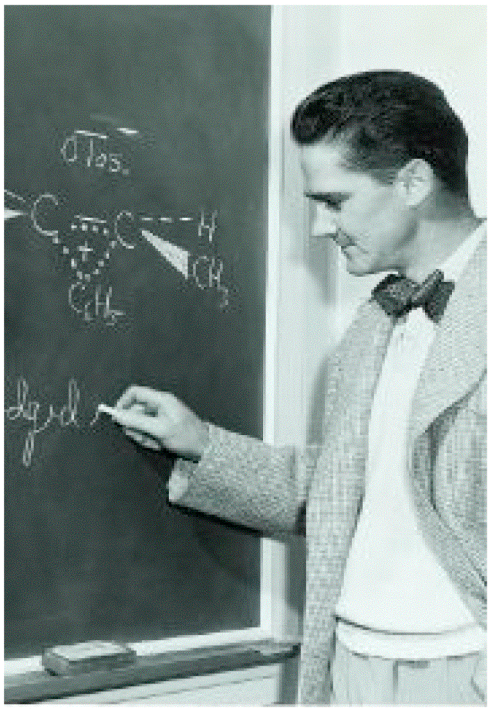

Phenonium Ion Experiments: Cram, *JACS* **1949**, *71*, 3865

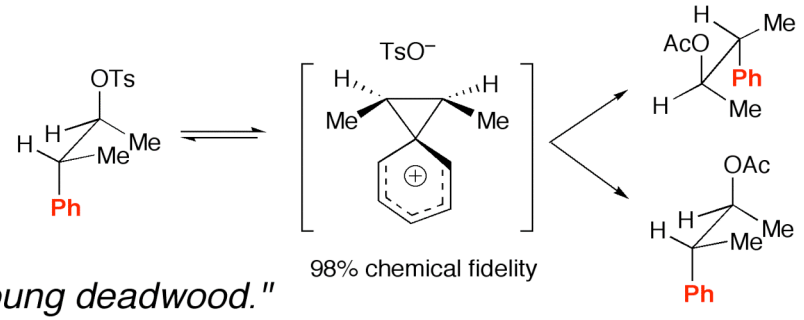

Cram: *"Just remember Dave, old deadwood is better than young deadwood."*

"A View from the Far Side. Memorable Characters and Interesting Places." Evans, D. A. *Tetrahedron* **1999**, *55*, 8589-8608.

Repeating Structural Motifs in Biomolecules

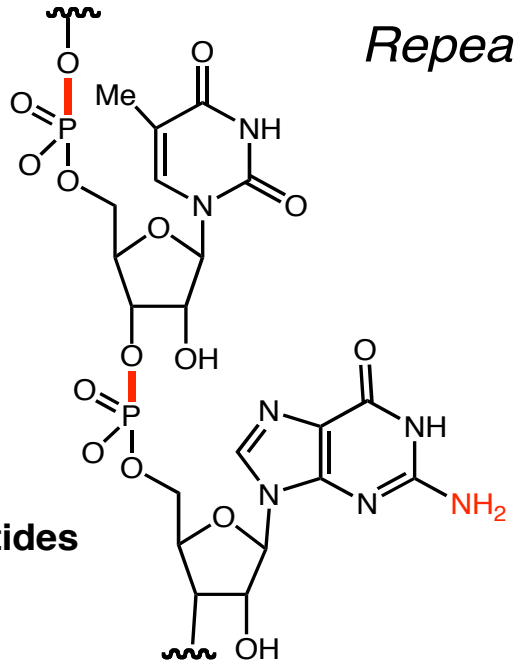

Polynucleotides

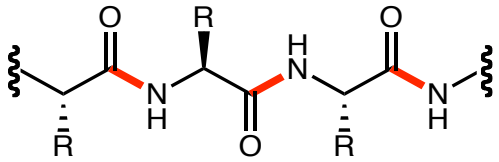

Polypeptides

Coupling occurs at a **nonstereogenic center**

greater complexity

The Diastereomer Problem!!

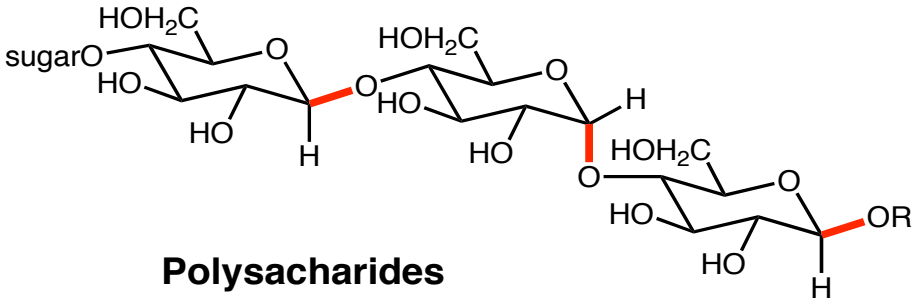

Polysacharides

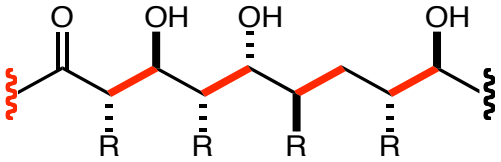

Polyacetates (R = H)
Polypropionates (R = Me)
Carbohydrates (R = OH)

Coupling produces a **new stereogenic center**

Polyketide synthesis via enolate-based bond constructions

The Altohyrtin 1,3-Dioxygen Relationships

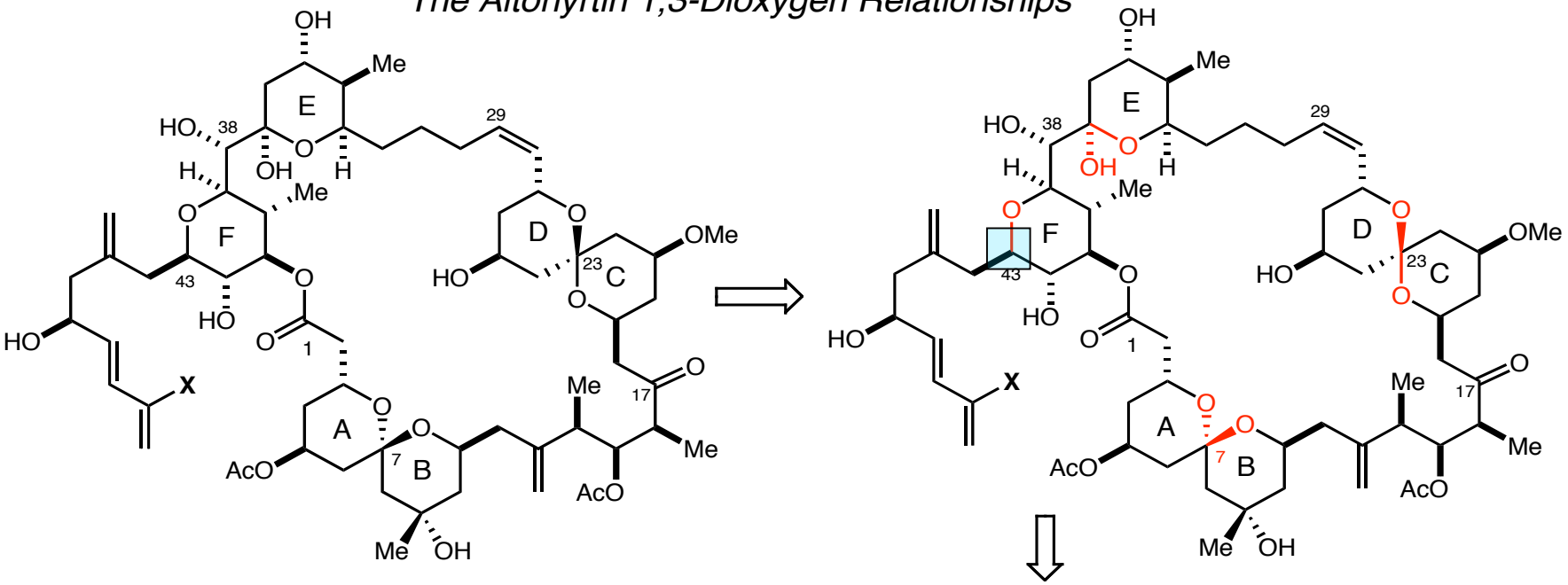

The linear display of the altohyrtin backbone

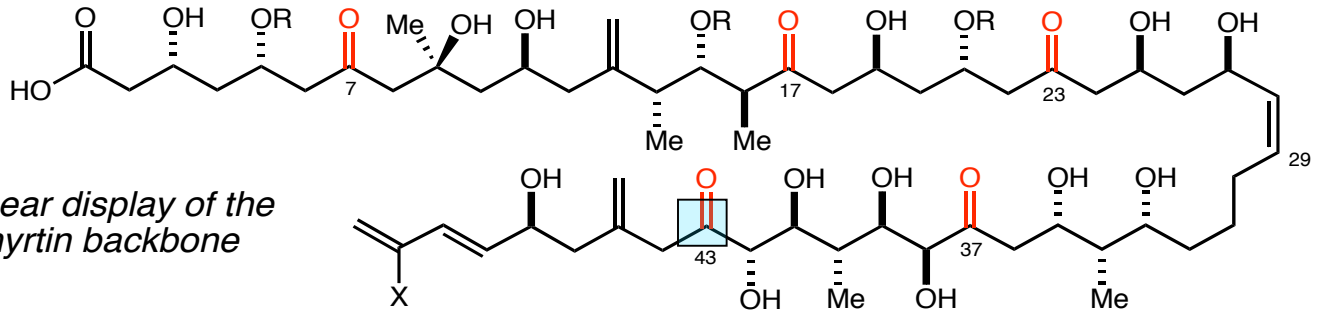

Tetrahedron **1999**, *55*, 8671

The aldol reaction is valuable in the coupling of complex fragments but....

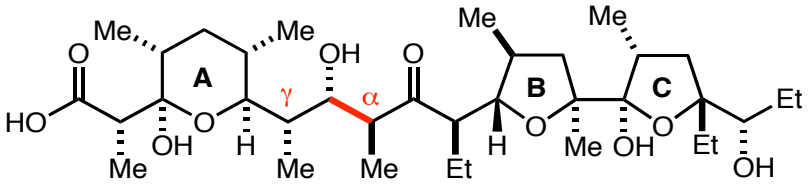

Ferensimycin B

JACS **1991**, *113*, 7613-7630

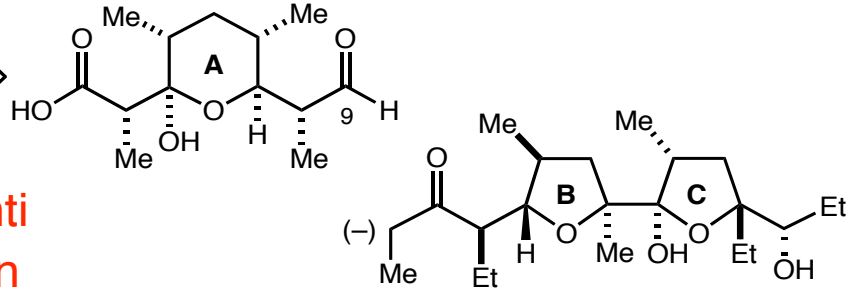

α–β: anti

β–γ: syn

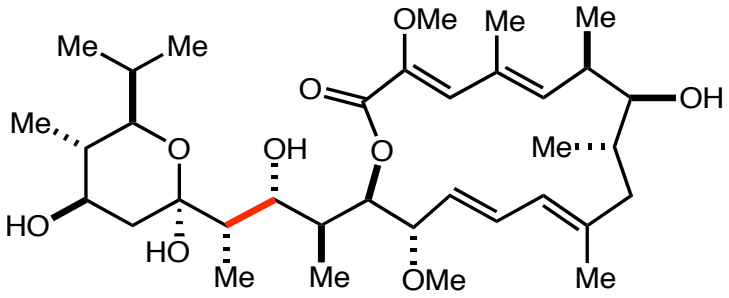

Bafilomycin A_1

Tetrahedron Lett. **1993**, *34*, 6871-6874.

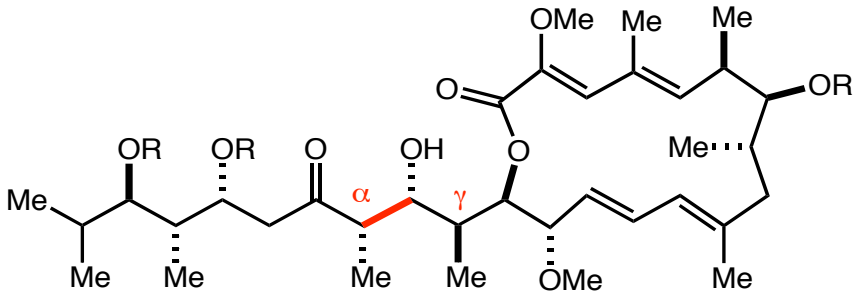

α–β: syn

β–γ: anti

The challenge

To predict how the stereogenic elements in reacting partners might influence the bond construction

Stereochemical Control Elements for Double Stereodifferentiating Aldol Additions

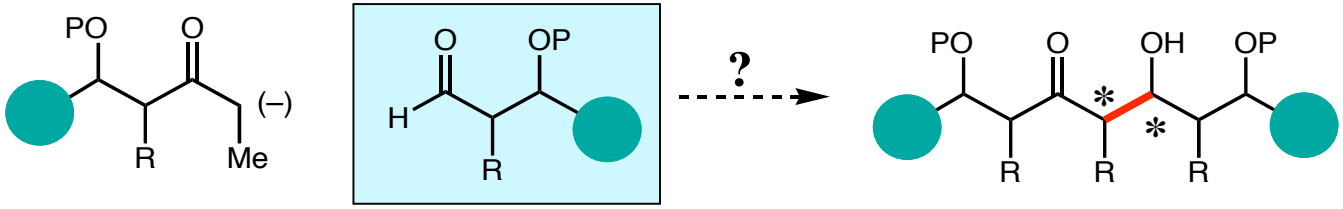

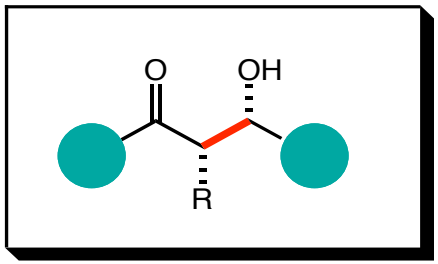

simple diastereocontrol
(enolate geometry)

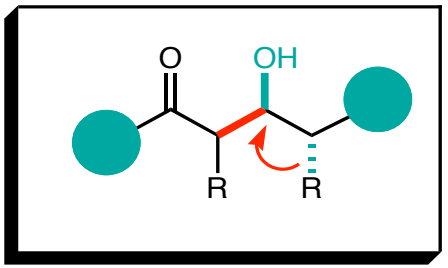

1,2-induction R = Me (Felkin)
R = OR (Polar Felkin)

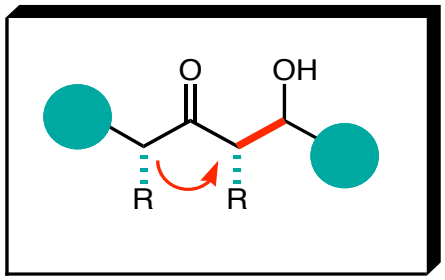

enolate facial bias

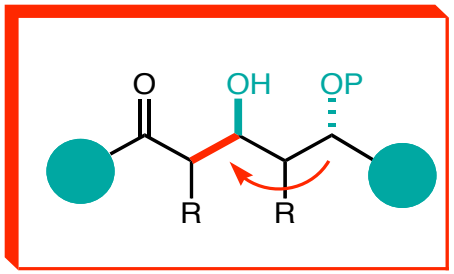

1,3-induction

The Aldehyde Fragment

Effects Governing Face Selectivity at Trigonal Carbon

- Steric Effects — Nonbonding interactions (Van der Waals repulsion) between substituents within a molecule or between reacting molecules

- Electronic Effects (Inductive Effects): — The effect of bond and through-space polarization by heteroatom substituents on reaction rates and selectivities

  Inductive Effects: Through-bond polarization
  Field Effects: Through-space polarization

- Stereoelectronic Effects: — Geometrical constraints placed upon **ground** and **transition states** by orbital overlap considerations.

"Organic chemists are proficient in the analysis of steric effects."

"Organic chemists are frequently unaware of the impact of electronic effects on the stereochemical outcome of reactions."

When steric and electronic (stereoelectronic) effects lead to differing stereochemical consequences

5-Membered oxocarbenium Ions: Woerpel etal. *JACS* **1999**, 121, 12208.

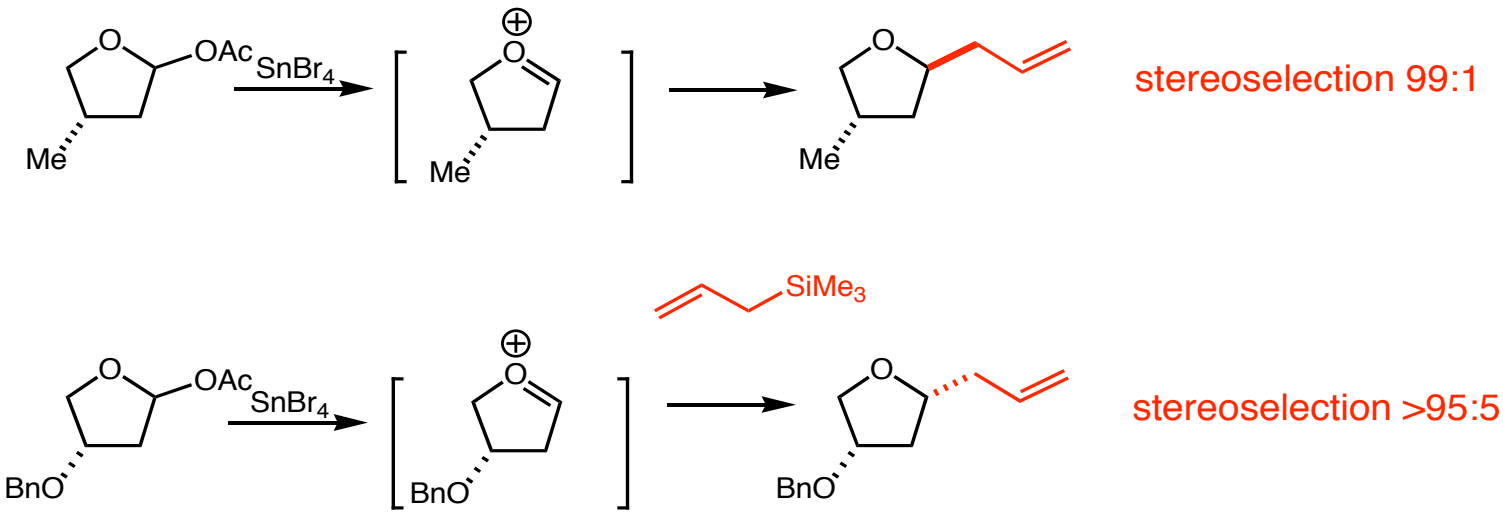

Dramatic evidence of the importance of electrostatic effects in controlling face selecticity.

Effects Governing Face Selectivity at Trigonal Carbon

When steric and electronic (stereoelectronic) effects lead to differing stereochemical consequences

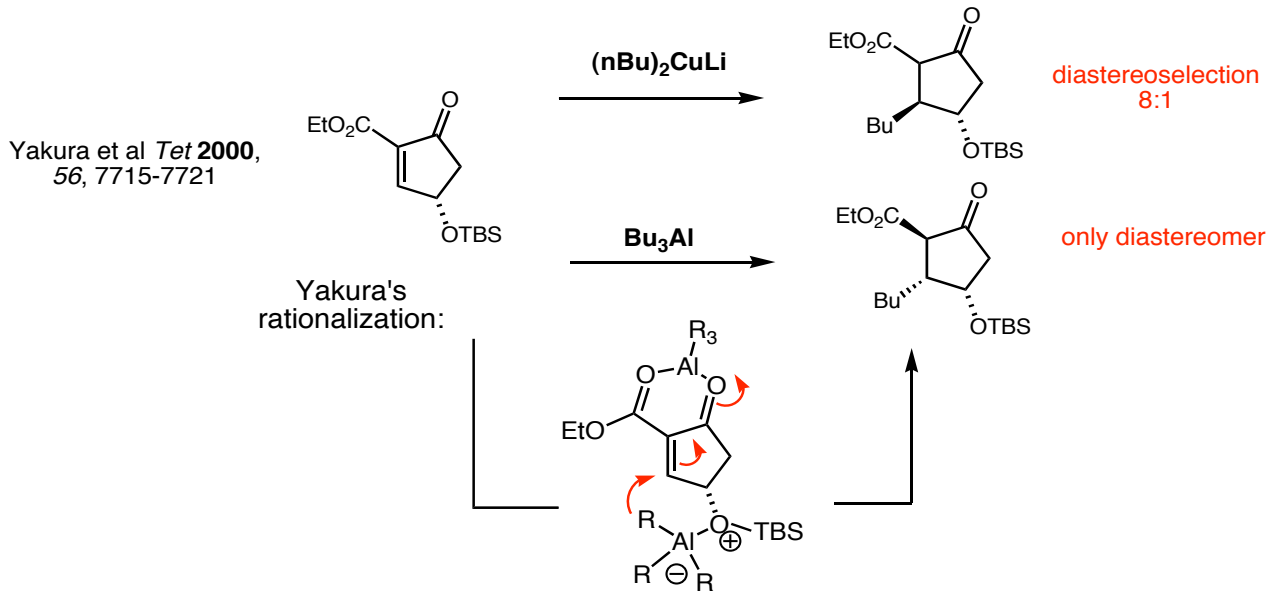

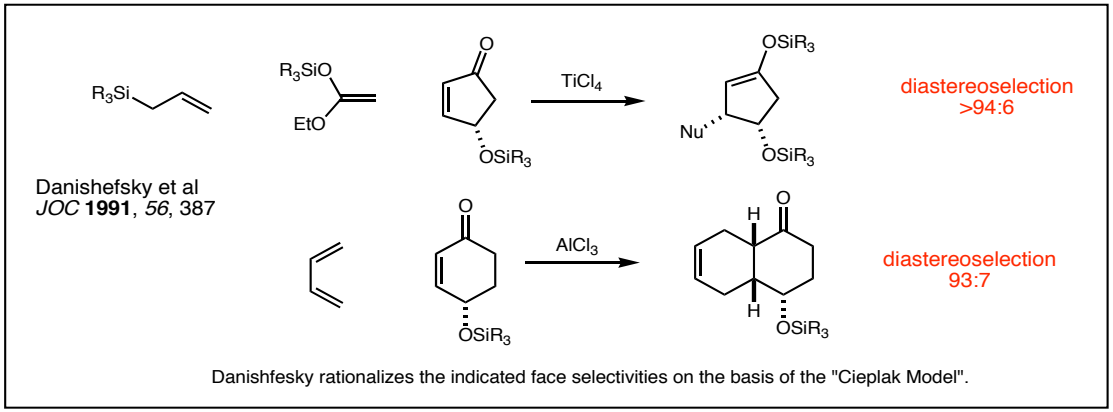

Reaction face selectivities are frequently analyzed incorrectly!

The Evolution of Models for Carbonyl Addition

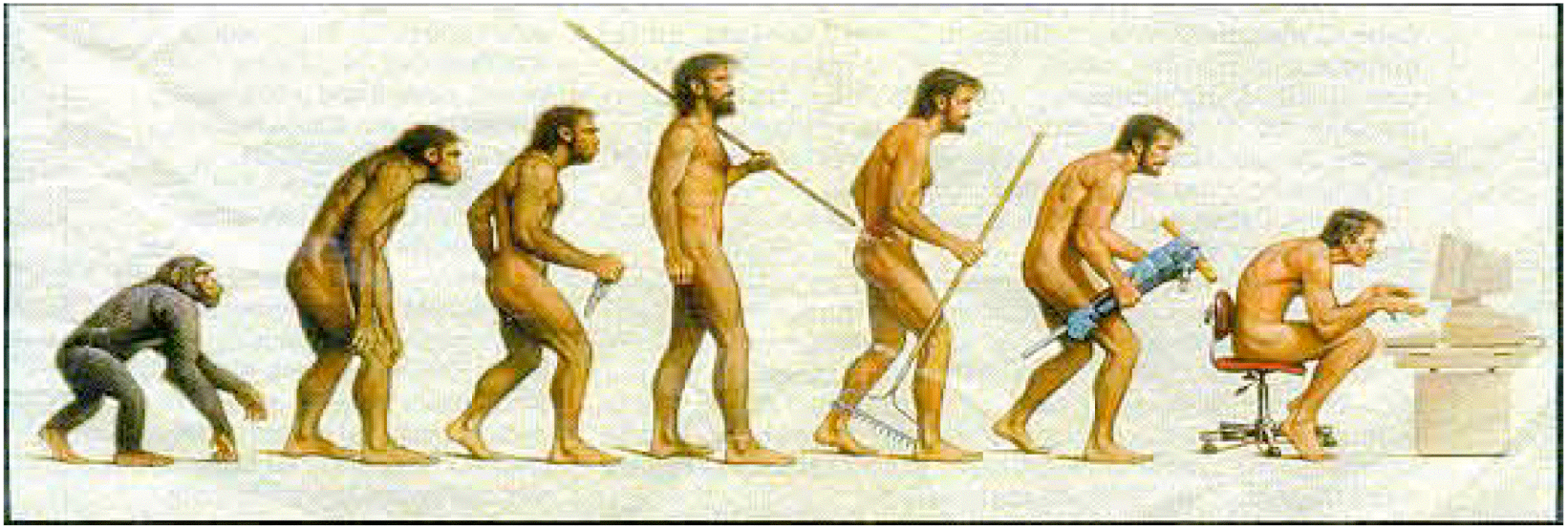

Fischer Cram Cornforth Felkin Anh/Eisenstein Cieplak Tomoda

Humor provided by Sarah Siska

Carbonyl Addition: Evolution of Acyclic Models

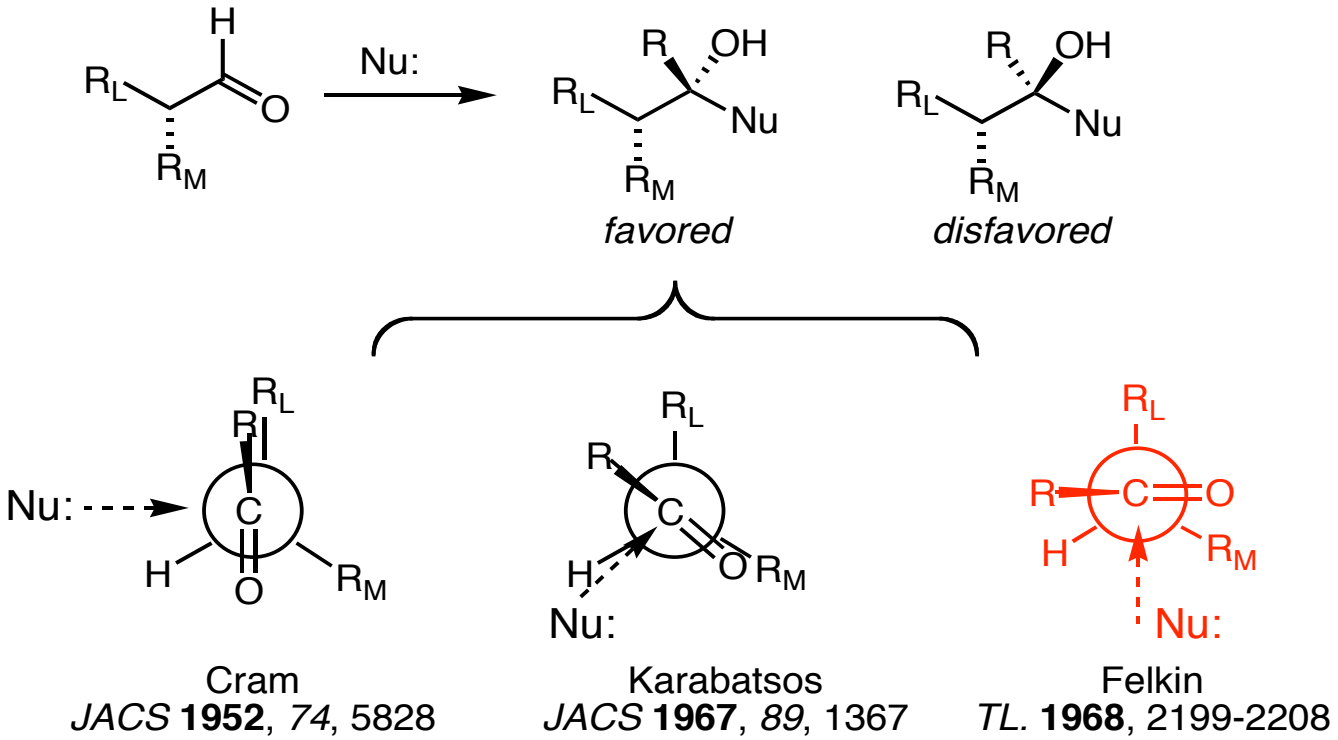

(a) "Torsional strain involving partial bonds. The stereochemistry of the lithium aluminium hydride reduction of some simple open-chain ketones." Felkin, et al. *Tetrahedron Lett*. **1968**, 2199-2204.

(b) "Torsional strain involving partial bonds. The steric course of the reaction between allylmagnesium bromide and 4-t-butylcyclohexanone" *Tetrahedron Lett*. **1968**, 2204-2208.

Assumptions in the Felkin Model:

- Transition states are all reactant-like rather than product-like.
- Torsional strain considerations are dominant.
  Staggered TS conformations preferred.

Houk, *JACS* **1982**, *104*, 7162-6

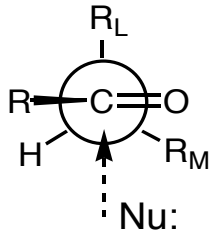

predicted to be favored TS ✓

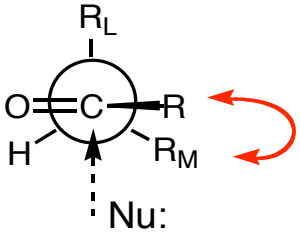

destabilizing interaction

The flaw in the Felkin model: A problem with aldehydes!!

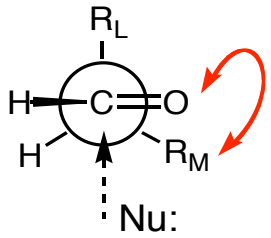

predicted to be disfavored TS

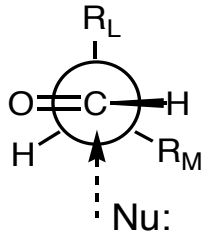

predicted to be favored TS

⇩

wrong prediction

Anh, Eisenstein:
Consider the Dunitz-Bürgi angle

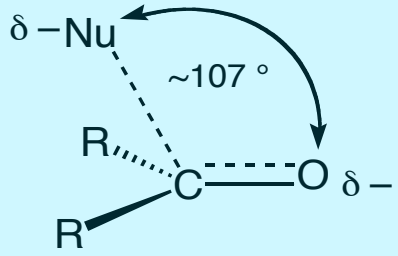

The Dunitz-Bürgi Angle

The Felkin–Anh Model

Anh & Eisenstein *Noveau J. Chim.* **1977**, *1*, 61-70

New Additions to Felkin Model:

- Dunitz-Bürgi C=O–Nu orientation applied to Felkin model.
- The antiperiplanar effect:
Hyperconjugative interactions between σ* C-R_L and forming σ C–N bond which will lower will stablize the transition state.

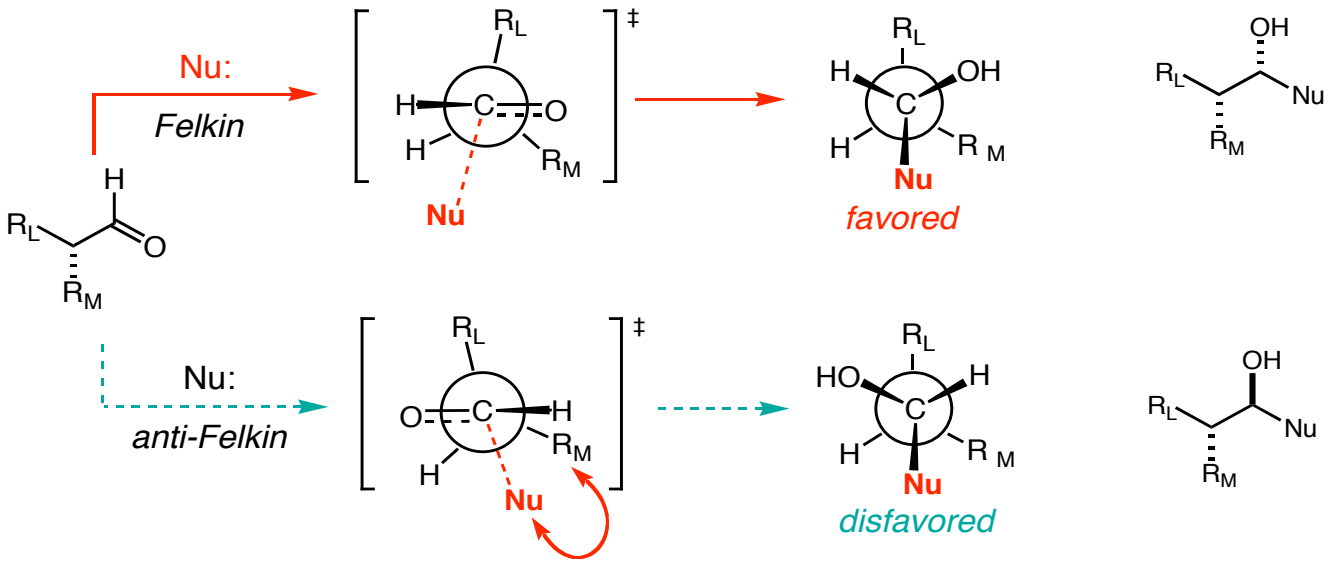

(Felkin): *"Transition state eclipsing interactions are greater than their ground state counterparts."*

(Anh, Eisenstein): *Hyperconjugative interactions between C–R^*_L & C–Nu will stabilize the transition state.*

The Polar Felkin–Anh Model

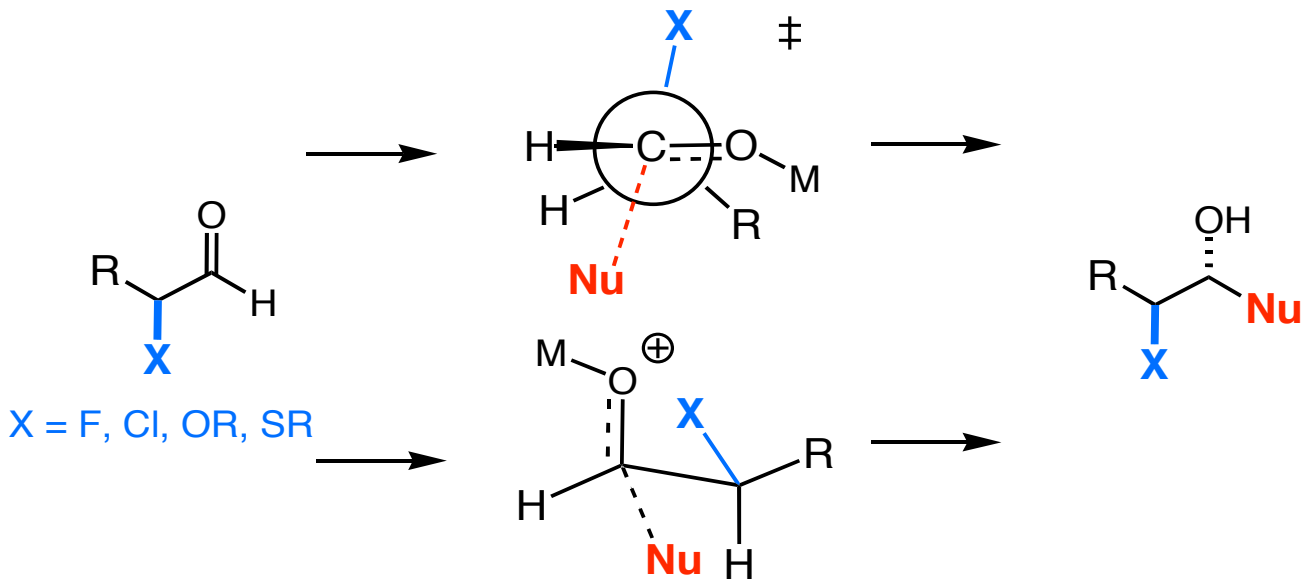

In the polar model, the substituent with the best acceptor antibonding orbital (σ^*C–X) is oriented antiperiplanar to the forming C–Nu bond.

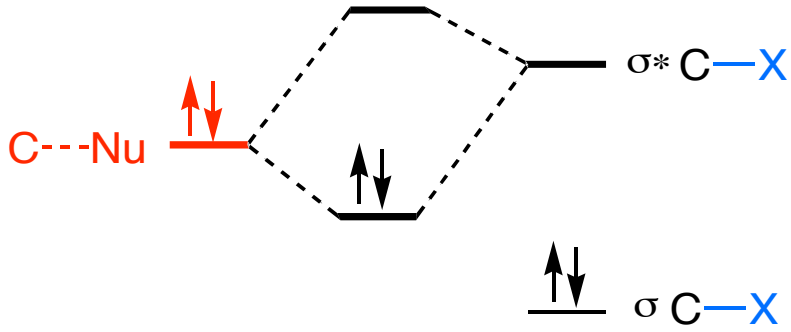

Stereochemical Control Elements for Double Stereodifferentiating Aldol Additions

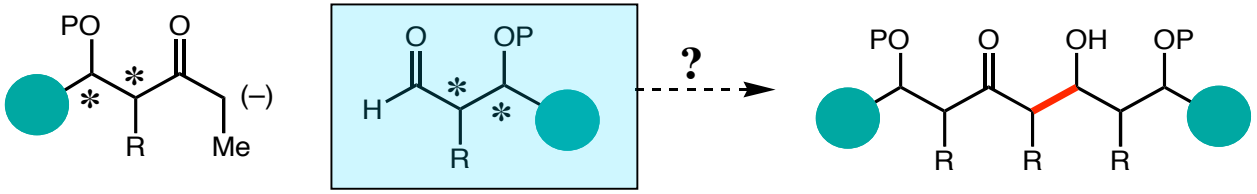

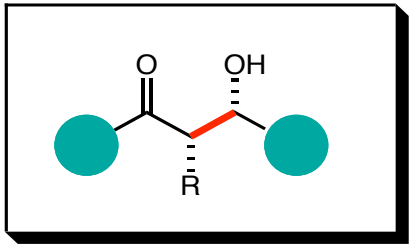

simple diastereocontrol
(enolate geometry)

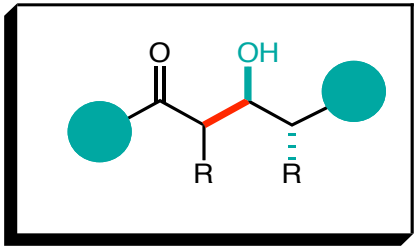

1,2-induction R = Me (Felkin)
R = OR (Polar Felkin)

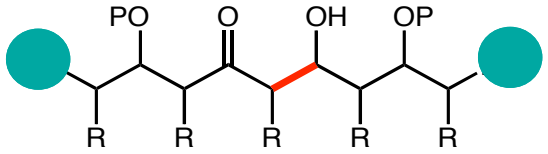

R = H, Me, OR

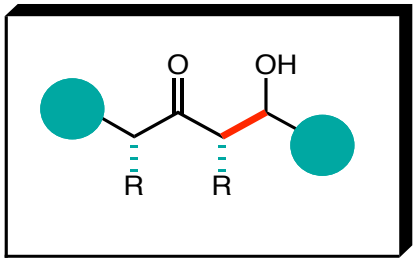

enolate facial bias

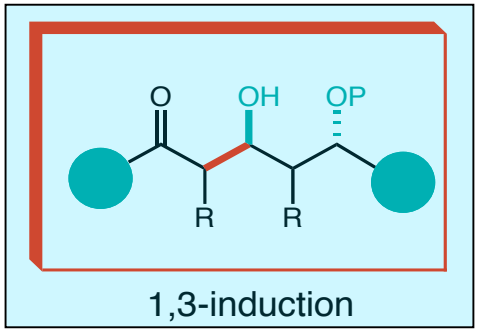

1,3-induction

1,3-Stereoinduction Model

1,3-Stereoinduction Polar Model:
Evans, Dart, Duffy,Yang, *JACS* **1996**, *118,* 4322–4343

1,3-Stereoinduction Chelate Model:
Evans, Allison, Yang,Masse, *JACS* **2001**, *123,* 10840–10852

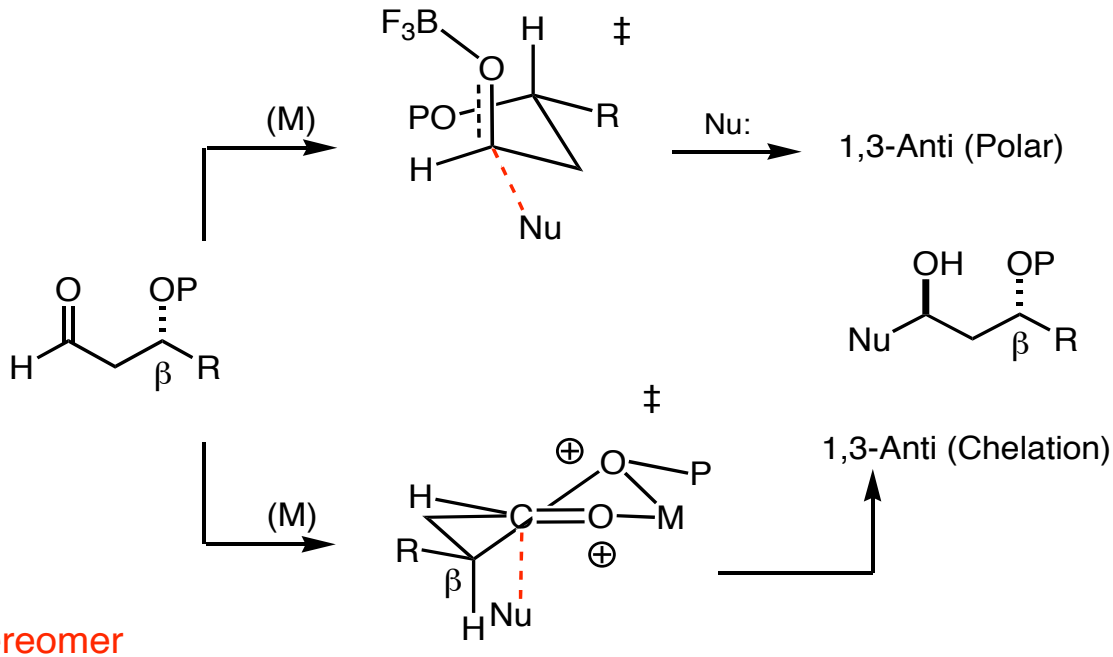

The minor diastereomer

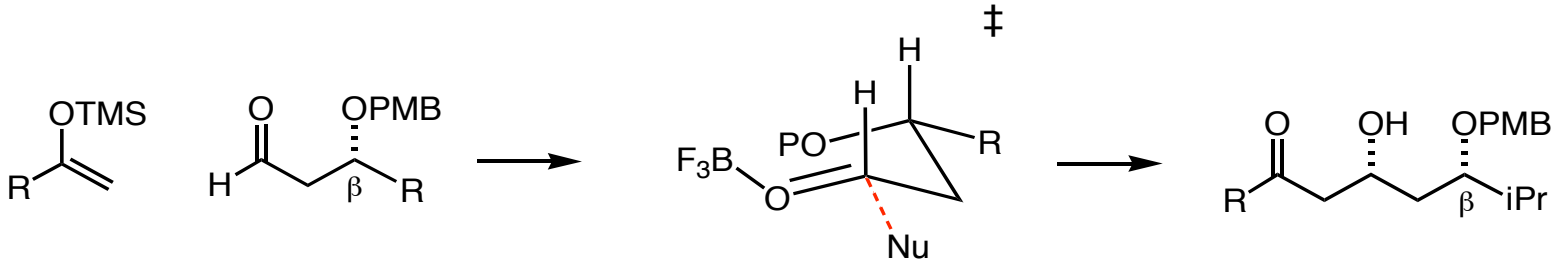

Dipole Destabilization

1,3-Stereoinduction Model

1,3-Anti Relationship is favored by either polar or chelate models

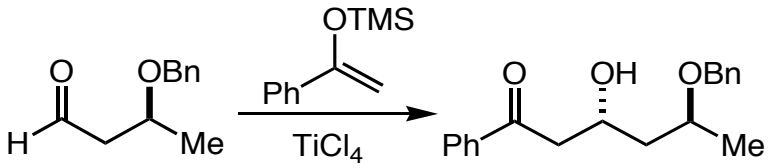

diastereoselection 92 : 8

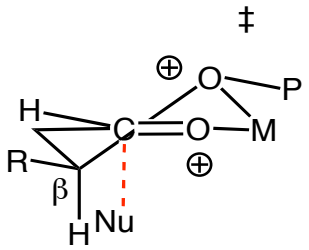

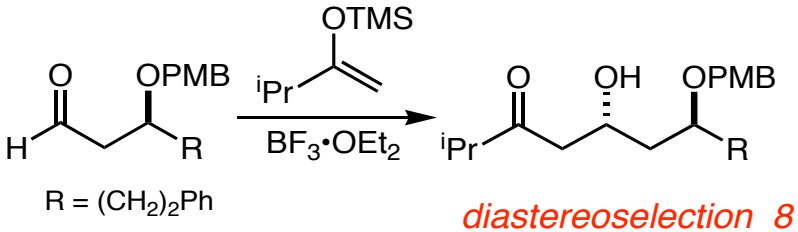

R = $(CH_2)_2Ph$

diastereoselection 81 : 8

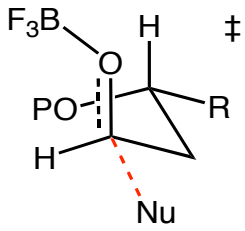

Steric effects appear to play a minor role in stereoinduction:

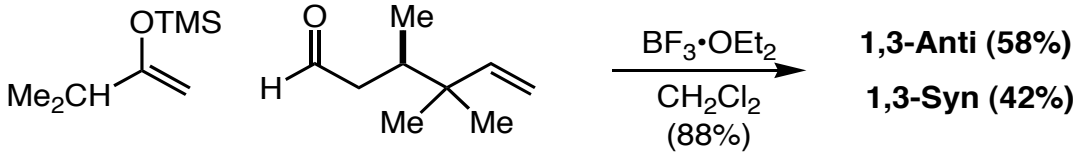

Evans, *JACS* **1996**, *118,* 4322; *JACS* **2001**, *123,* 10840

Electronic rather than steric effects control face selectivity!

A Merged Stereoinduction Model

Can one develop a Rational model for α & β Stereocenters?

α & β reinforcing

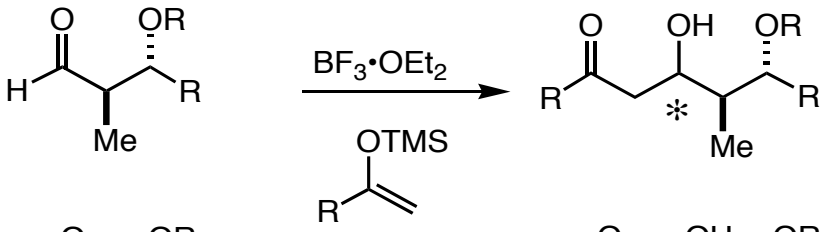

α & β nonreinforcing

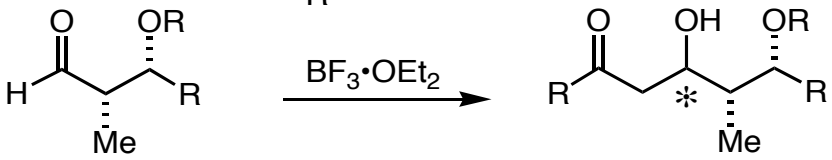

Which of the two stereochemical representations is reinforcing? Non-reinforcing?

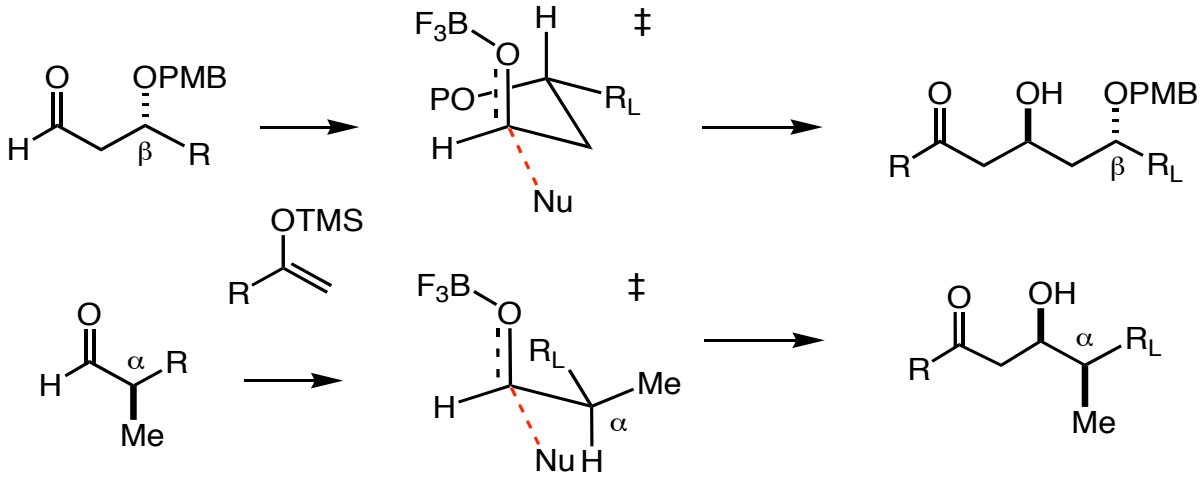

Evans, *JACS* **1996**, *118,* 4322; *JACS* **2001**, *123,* 10840

A Merged Stereoinduction Model

The Anti Diastereomer

α & β reinforcing

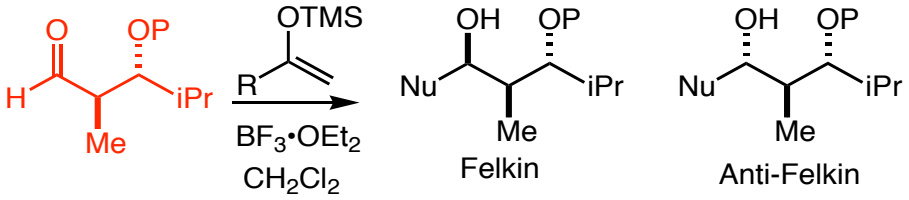

13 P = PMB
14 P = TBS

15 **17** | **16** **18**

entry	R	**15** : **16** (P = PMB)	**17** : **18** (P = TBS)
A	t-Bu	99 : 01	99 : 01
B	i-Pr	98 : 02	95 : 05
C	Me	97 : 03	71 : 29

The Syn Diastereomer

α & β non reinforcing

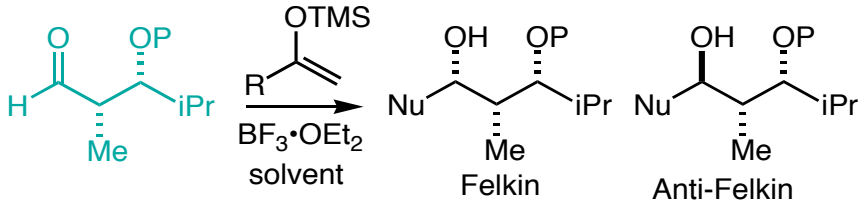

19 P = PMB
20 P = TBS

21 **23** | **22** **24**

entry	R	Solvent	**21** : **22** (P = PMB)	**23** : **24** (P = TBS)
A	t-Bu	CH_2Cl_2	96 : 04	96 : 04
B	t-Bu	toluene	88 : 12	94 : 06
C	i-Pr	CH_2Cl_2	56 : 44	87 : 13
D	i-Pr	toluene	32 : 68	75 : 25
E	Me	CH_2Cl_2	17 : 83	58 : 42
F	Me	toluene	06 : 94	40 : 60

Conclusions

Both models integrate!!

Syn diastereomer transitions from Felkin control (Large Nu) to 1,3-control (Small Nu).

Stereochemical Control Elements for Double Stereodifferentiating Aldol Additions:

Carbohydrate Polyols

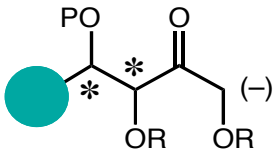

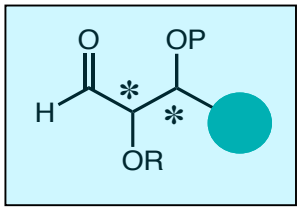

?

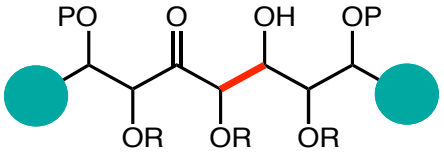

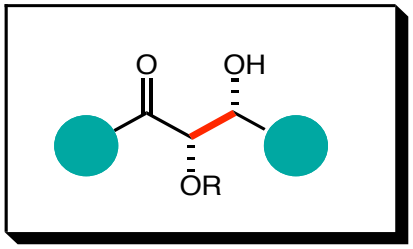

simple diastereocontrol
(enolate geometry)

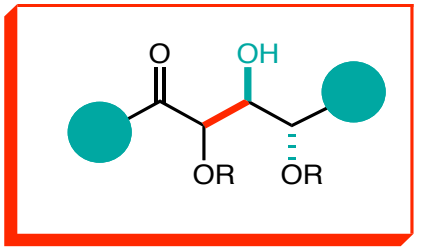

1,2-induction R = OR
(Polar Felkin-Anh)

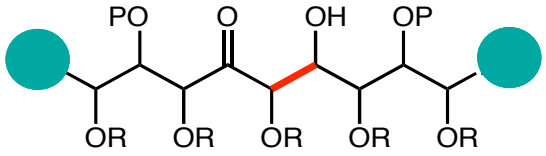

R = H, Me, OR

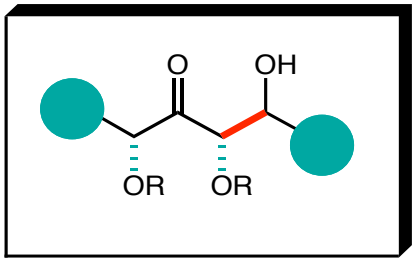

enolate facial bias

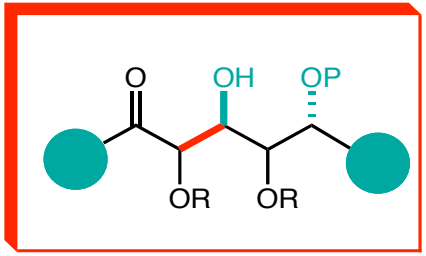

1,3-induction

The Polar Felkin–Anh Model

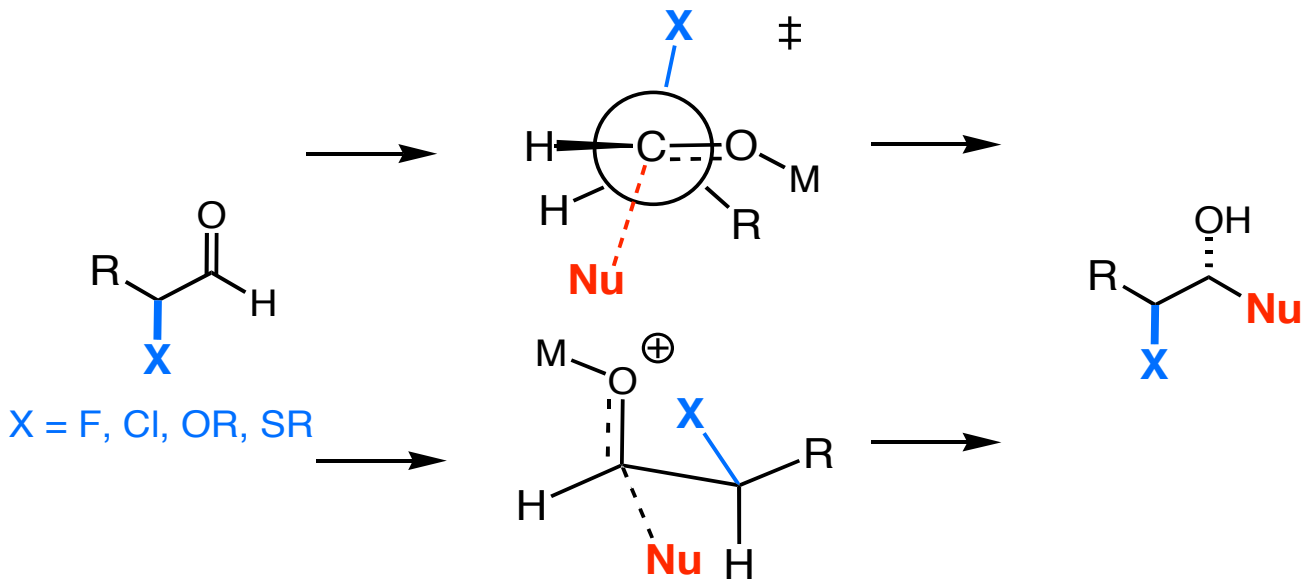

In the polar model, the substituent with the best acceptor antibonding orbital (σ^*C–X) is oriented antiperiplanar to the forming C–Nu bond.

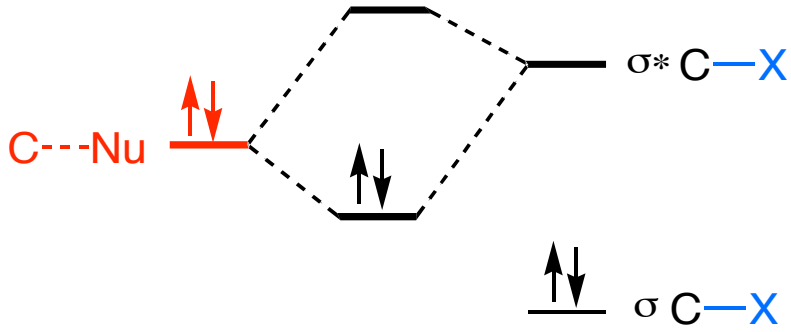

Cornforth Model for C=O Addition

Cornforth, J. W.; Cornforth, R. H.; Mathew, K. K. *J. Chem. Soc.* **1959**, 112

Additions to α-Chloro Carbonyl Derivatives

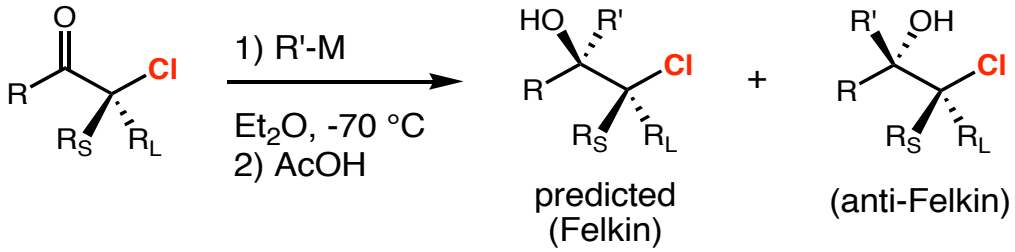

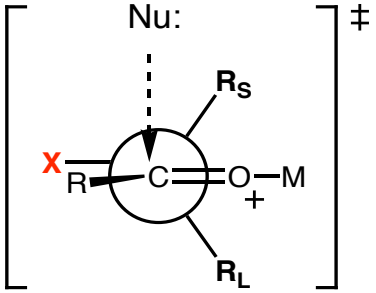

Cornforth model

- argument based on importance of polarization in transition state, and evidence of selectivity in α-chlorocyclohexanone additions
- ". . . where the dipoles are antiparallel, the polarization of the carbonyl group would be easiest," thereby lowering transition state energy
- a modification of Cram's rule for electronegative, non-chelating α-substituents X

How does one distinguish between the Cornforth & Felkin Anh Models for C=O Addition??

Ferlkin-Anh Transition State Hyperconjugation
Cornforth Transition State Electrostatic effects

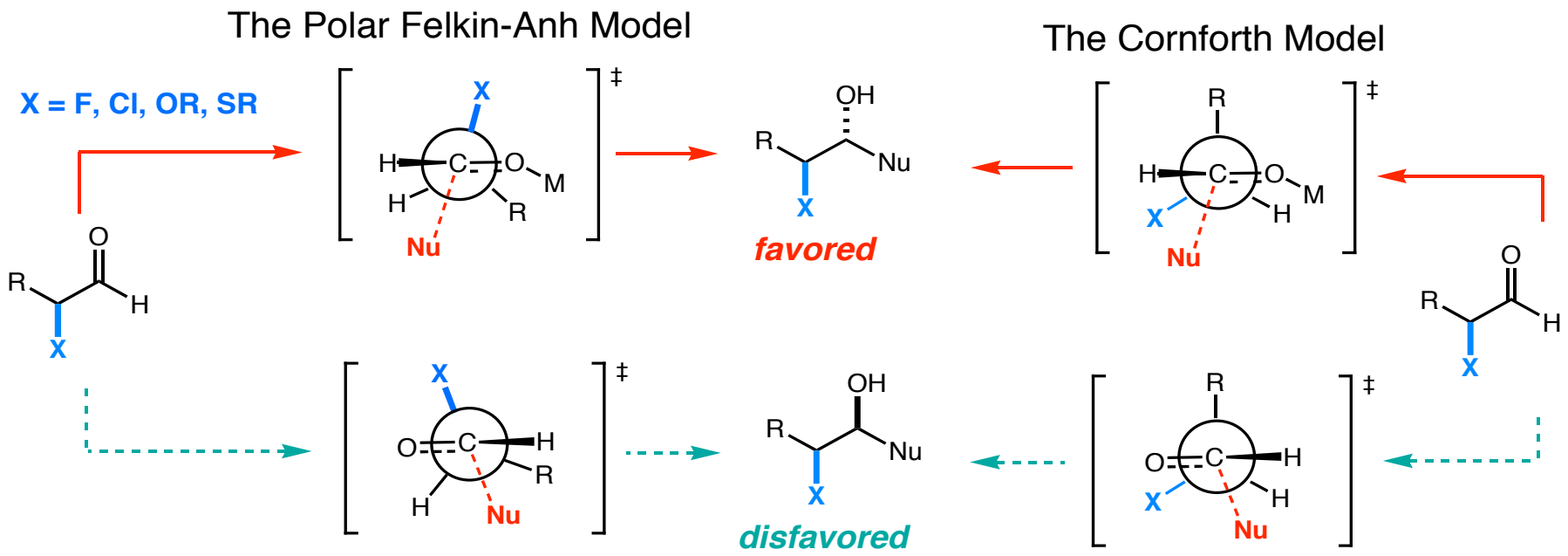

Cases Not Handled by the Felkin-Anh Model

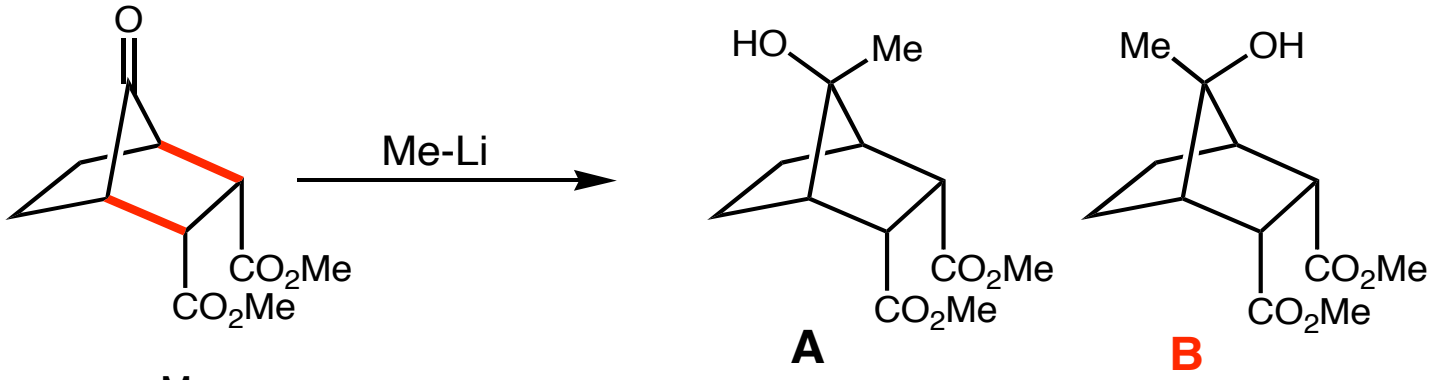

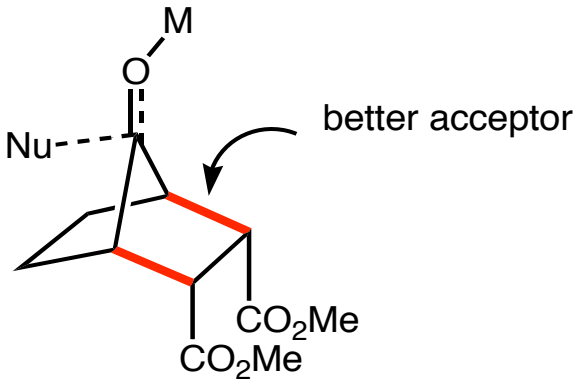

Electronegative -CO_2Me substituent
will stabilize both
C–C bonding & antibonding states

Felkin-Anh analysis
predicts **B**

(R) Substituent	A/B Ratio
—C(=O)—OMe	>90:10
—CH_2OMe	34:66
—$CH{=}CH_2$	27:73
—CH_2–CH_3	17:83

G. Mehta, *JACS* **1990**, *112*, 6140

Effects Governing Face Selectivity at Trigonal Carbon

Le Noble, *JACS* 1992, *114*, 1916

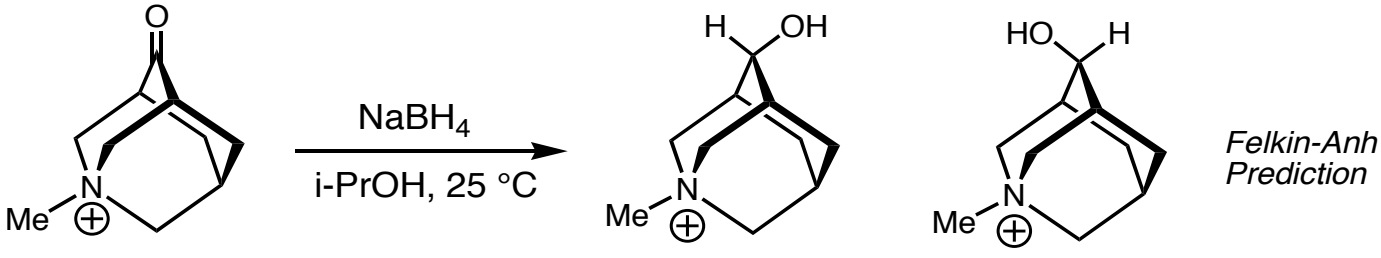

Ratio, ≥ 95:5

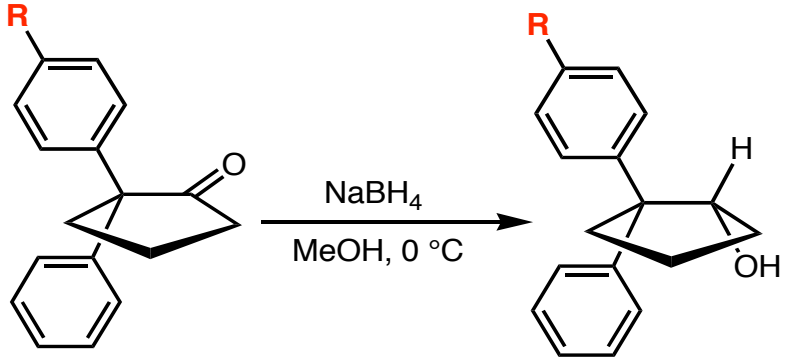

+ Syn Isomer

(R)	Anti:Syn Ratio
R = NO_2	79:21
R = Cl	63:37
R = OMe	43:57
R = NH_2	36:64

Halterman, *JACS* 1990, *112*, 6690

Cieplak Model for C=O Addition

Cieplak, *JACS* **1981**, *103*, 4540; Cieplak/Johnson, *JACS* **1989**, *111*, 8447

Point A: TS is stabilized by antiperiplanar allylic bond, but....

Point B: Nature of the stabilizing secondary orbital interactions differ:

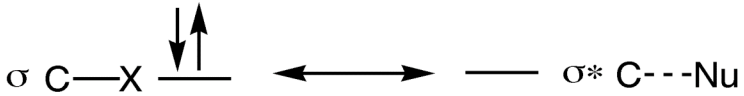

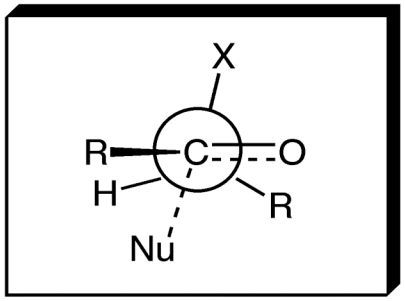

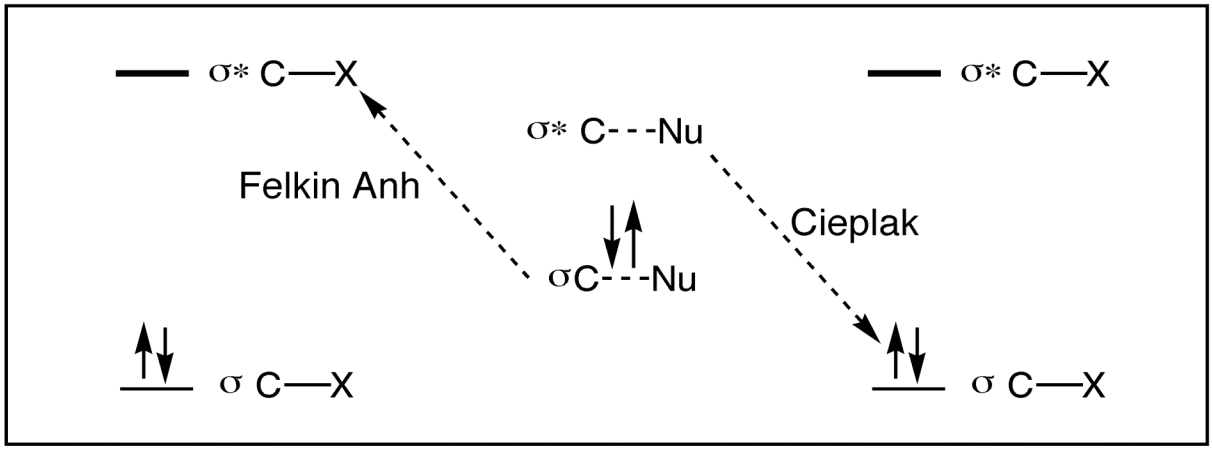

Point C: C–X Electron donating ability follows the order:

C–H > C–C > C–N > C–O

(Houk disputes the ordering of C–H, C–C)

Point D: Importance of torsional effects (Felkin, Anh, Houk, Padden-Row) disputed.

Cieplak Model for C=O Addition

Cieplak, *JACS* **1981**,*103*, 4540; Cieplak/Johnson, *JACS* **1989**, *111*, 8447

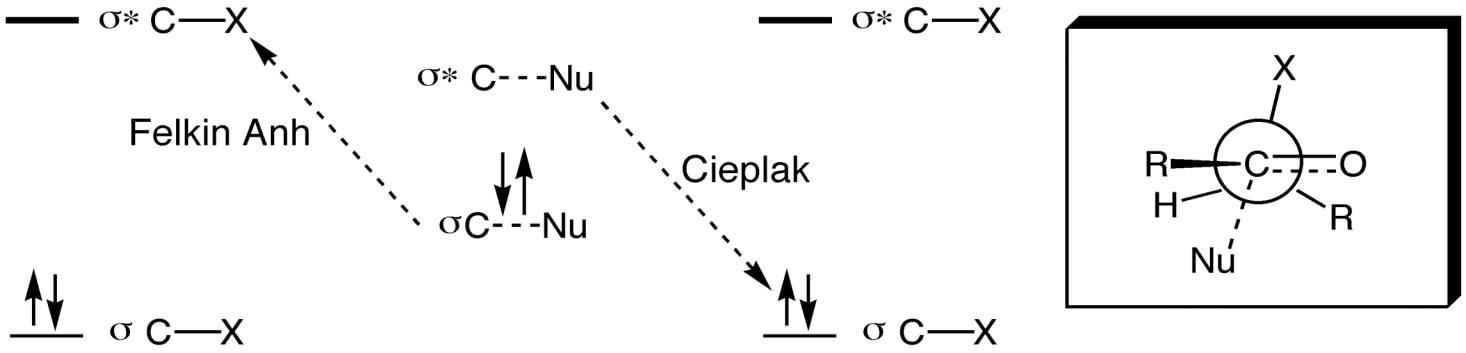

"Structures are stabilized by stabilizing their highest energy filled states. This is one of the fundamendal assumptions in frontier molecular orbital theory." The Cieplak hypothesis is nonsense."

"Just because a hypothesis correlates a set of observations doesn't make that hypothesis correct."

The management

Theoretical Calculations for C=O

Cieplak J. Org. Chem. **1998,** *63,* 521-530

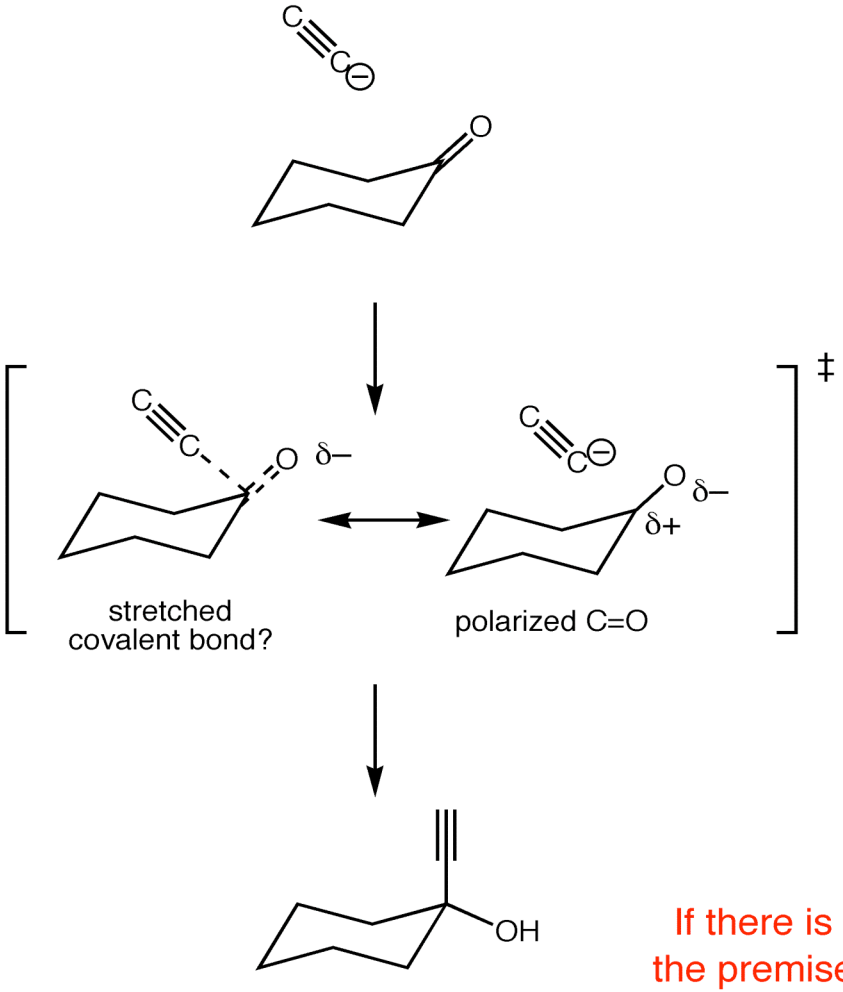

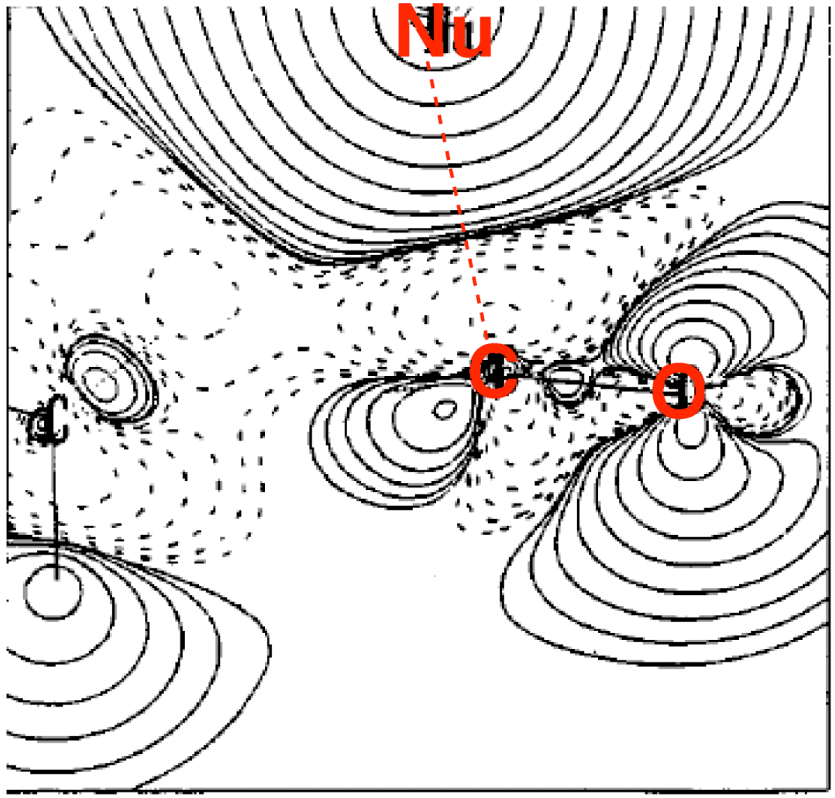

If there is no electron density along the internuclear axis
the premise of the Felkin-Anh model has been invalidated.

Evans: Cieplak Ionic Model for C=O Addition

- There is little or no covalency along Nu....$^{\delta+}$C=O$^{\delta-}$ axis in the transition state (Cieplek)
- Eclipsed transition states are disfavored (Felkin, anh-Eisenstein, Houk)
- Transition state stabilization may be achieved by orienting the best σ-donor perpendicular to polarized C=O (Stereolectronic Effects)

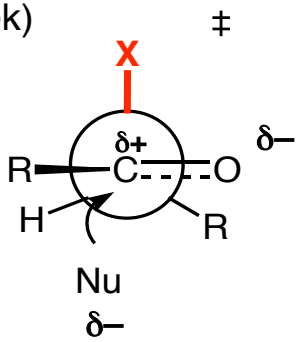

- Transition state stabilization may be achieved by orienting the largest substituent anti, rather than gauche to nucleophile (Steric Effects-1)

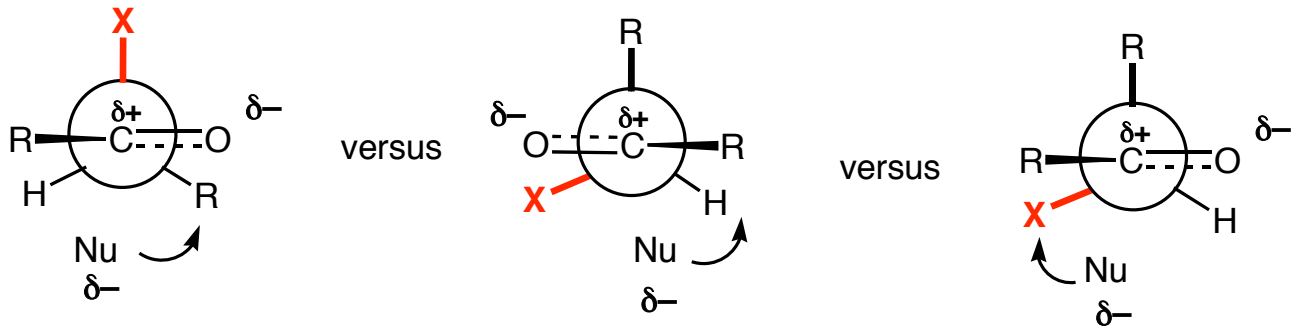

- If the C–X bond is very polar (**X** = F, Cl, OR), electrostatic (dipole) effects may be significant as noted by Cornforth

Cases Not Handled by the Felkin-Anh Model

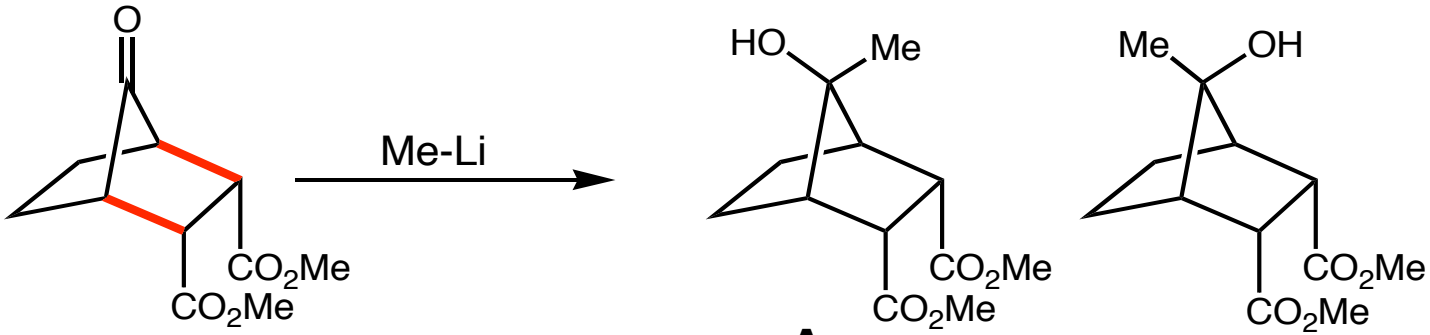

Felkin-Anh analysis predicts **B**

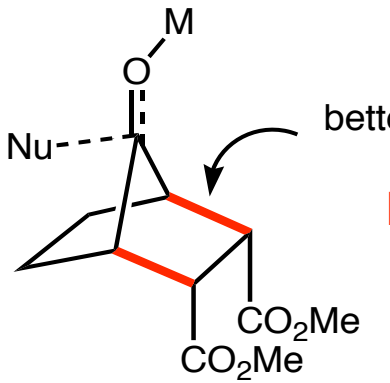

Felkin-Anh

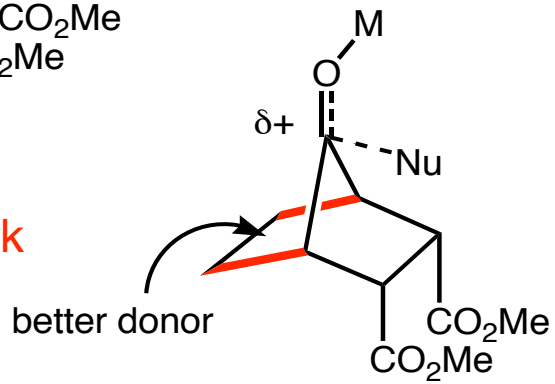

Cieplak

(R) Substituent	A/B Ratio
—C(=O)—OMe	>90:10
—CH_2OMe	34:66
—$CH{=}CH_2$	27:73
—CH_2–CH_3	17:83

G. Mehta, *JACS* **1990**, *112*, 6140

How does one distinguish between the Cornforth & Felkin Anh Models for C=O Addition??

Ferlkin-Anh Transition State Hyperconjugation
Cornforth Transition State Electrostatic effects

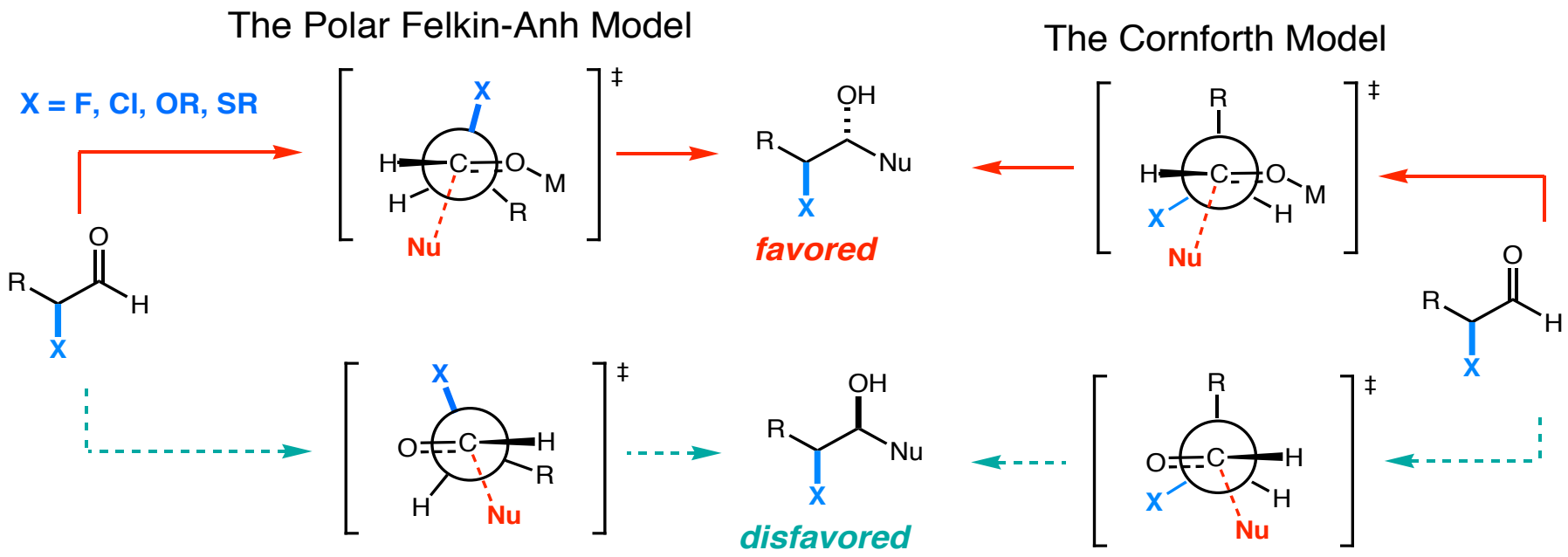

One needs a nucleophile that interacts with the vicinal stereocenter.

Dialkylborane reductions:
Individual models predict opposite stereochemical outcomes

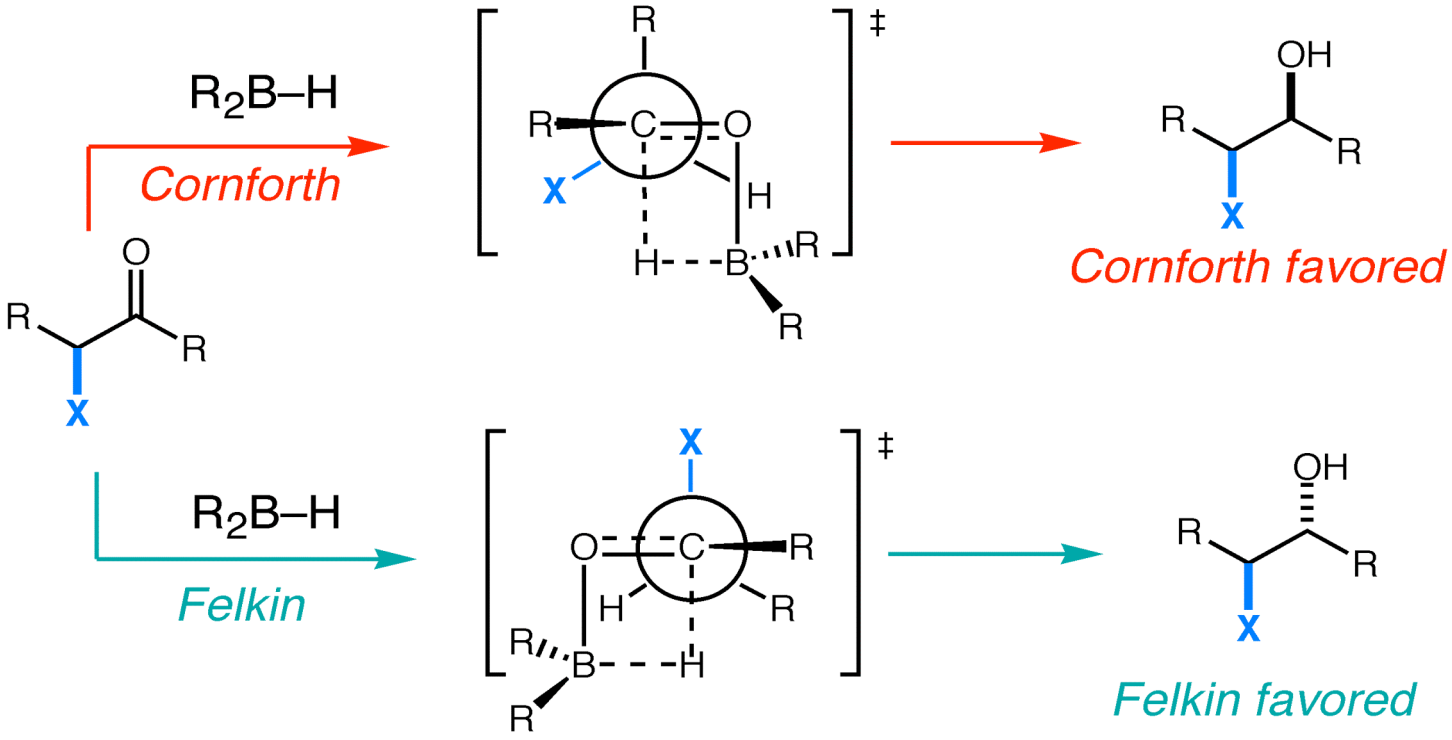

The Cornforth Model Prevails!

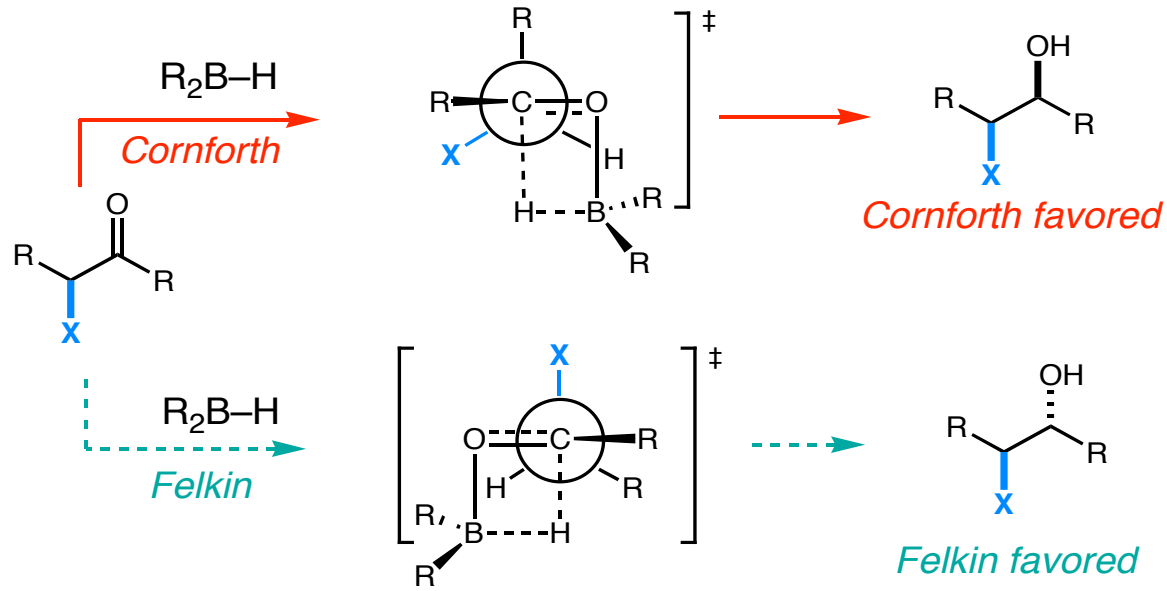

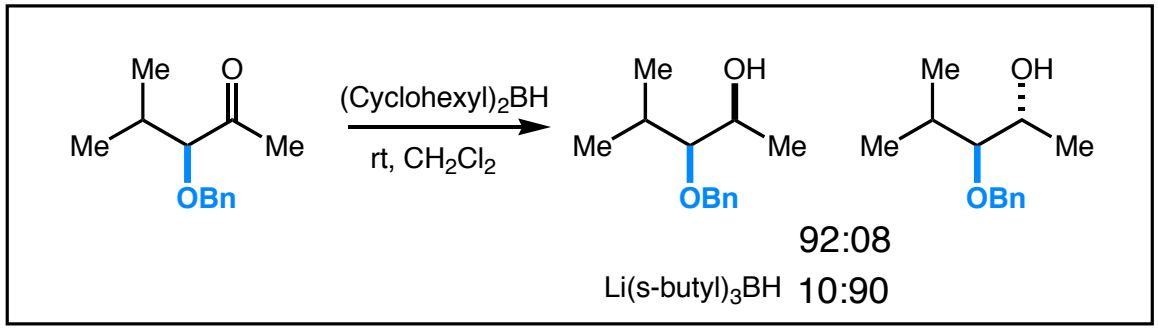

Siska, Cee, Young, *JACS* **2006,** *128,* 9433-9441

Ab Initio Investigation of Enolborane Aldol Reactions

Cee, Cramer, Evans, *JACS* **2006**, *128*, 2920-2930

Problem: Little theoretical support for the Cornforth model
Observation: Majority of prior theoretical studies: $^{-}$CN or $M^{+}H^{-}$

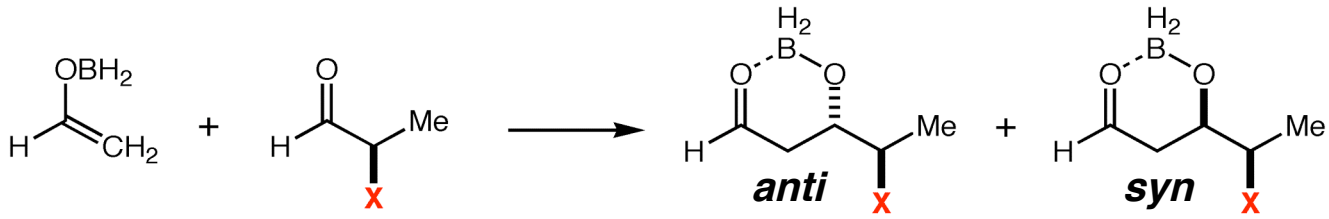

Full Study: X = F, Cl
Partial Study: X = OMe, SMe

I. Theoretical Level: DFT (B3LYP/6-31G*)
II. Find all possible chair-like transition structures
III. Compare energies

Allylation of 2-methoxypropanal: Gung and Xue *Tetrahedron: Asymmetry* **2001**, *12*, 2955-2959

Theoretical Investigation of Transition State Geometries

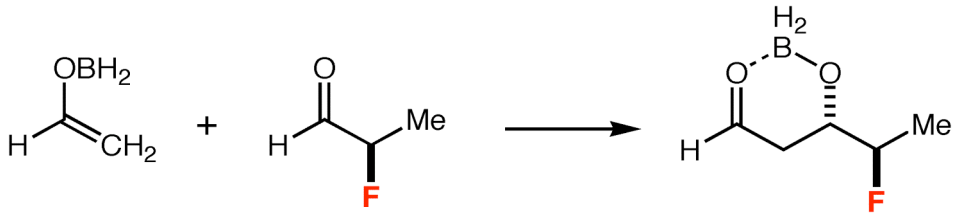

I. Input

guess for transition structure

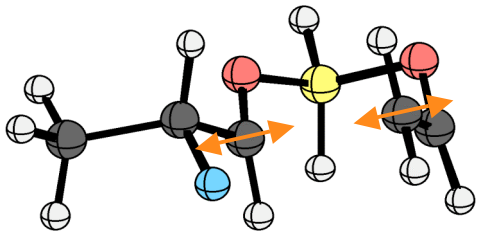

G98

optimized transition structure (E)

II. Characterize

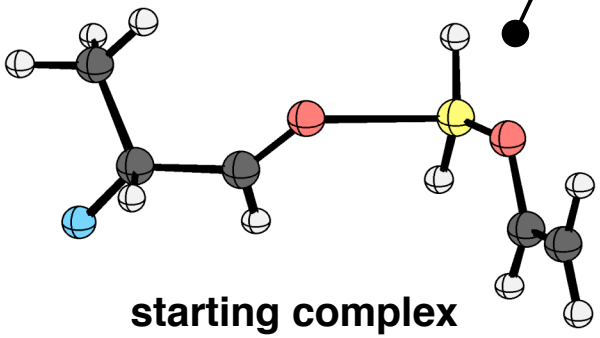

starting complex

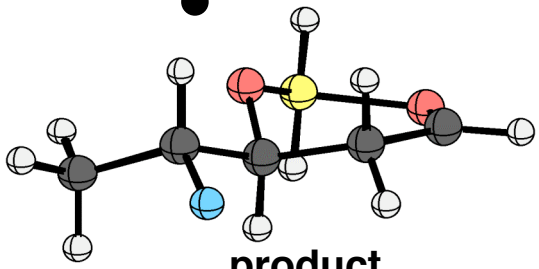

product

III. Rotate C–C, Repeat

Acetaldehyde Enolborane + 2-Fluoropropanal
B3LYP/6-31G (kcal/mol)*

O	F
S	Cl

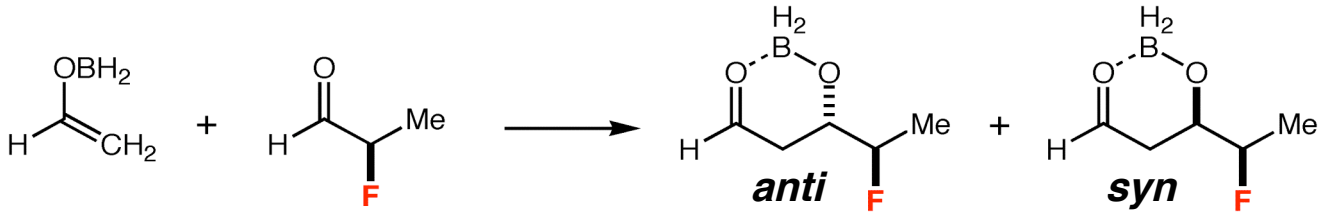

Polar Felkin-Anh **Cornforth**

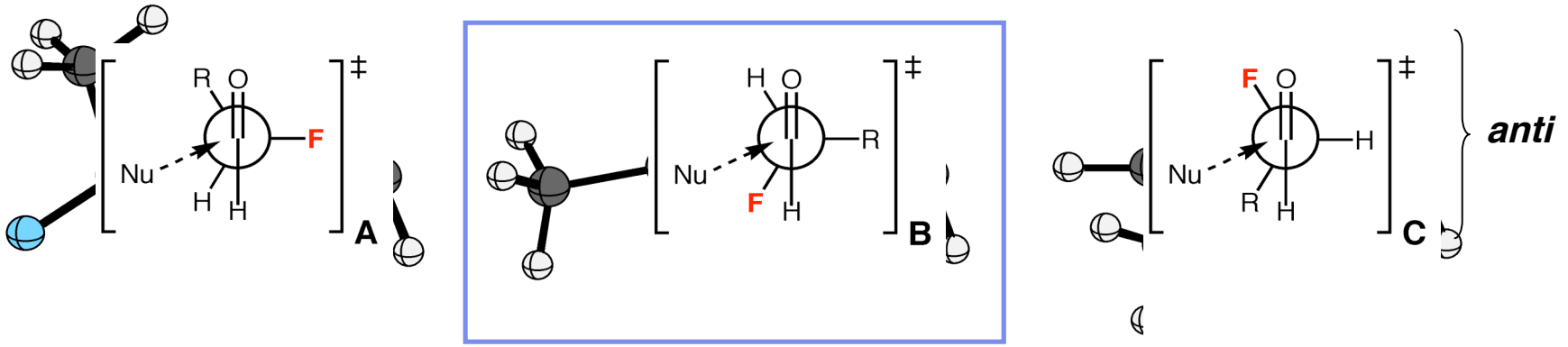

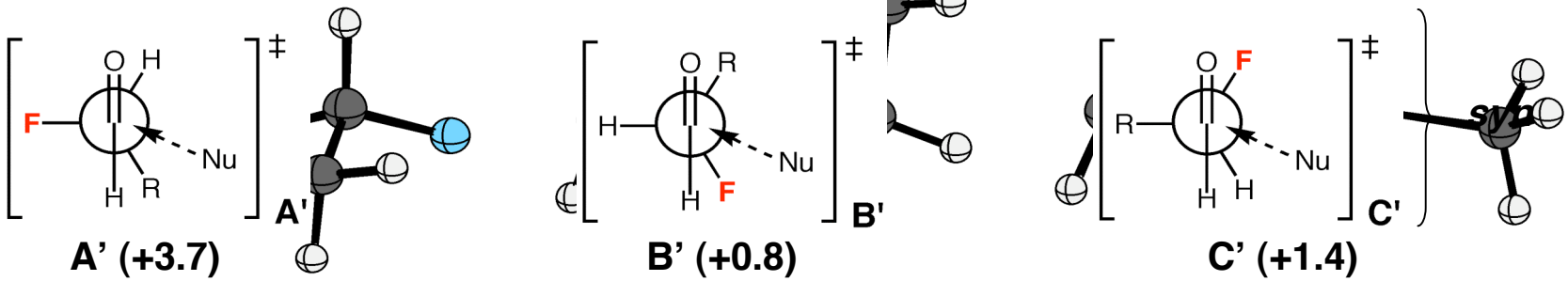

A' (+3.7) **B' (+0.8)** **C' (+1.4)**

Acetaldehyde Enolborane + 2-Chloropropanal
B3LYP/6-31G (kcal/mol)*

O	F
S	Cl

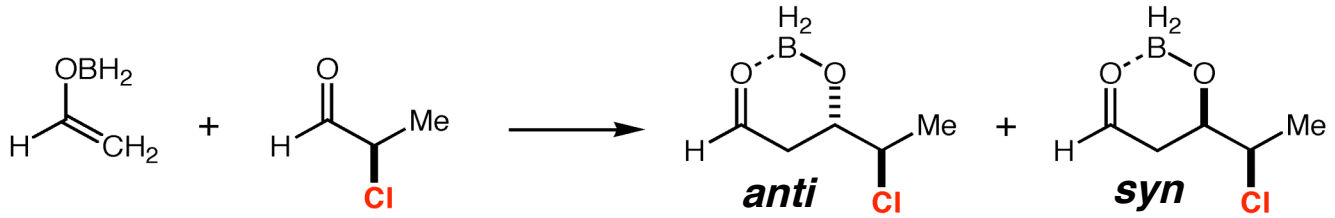

Polar Felkin-Anh

Cornforth

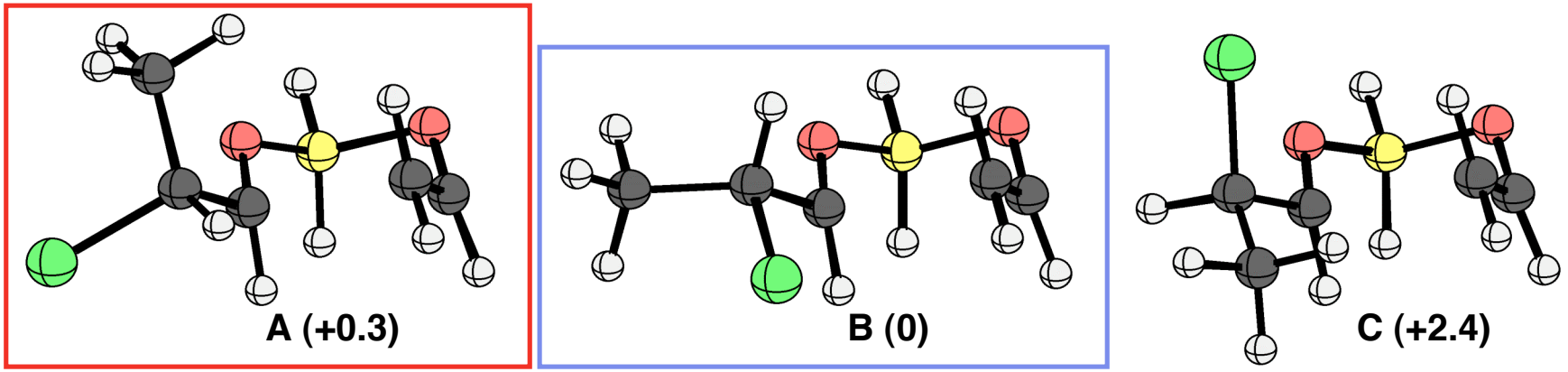

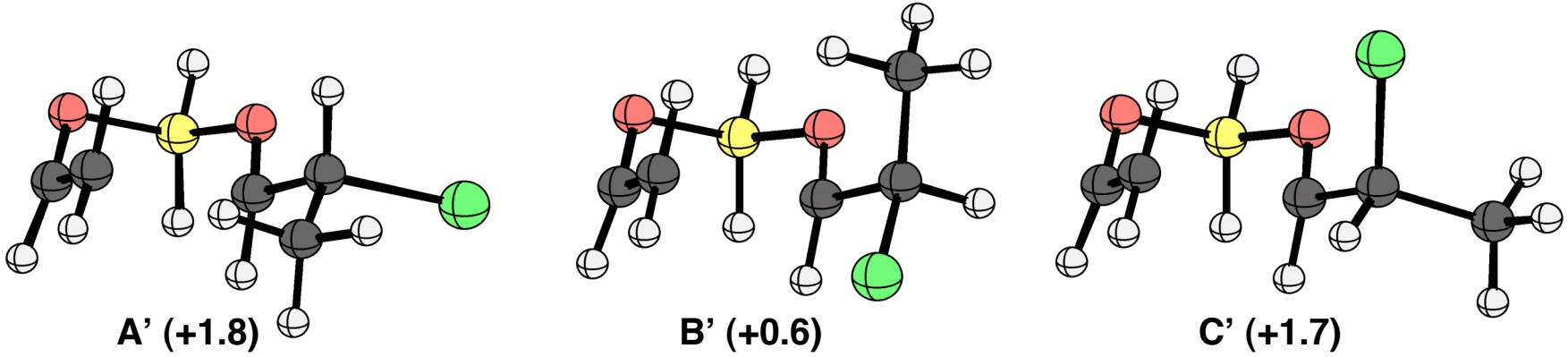

Generality: 2-Methoxypropanal

O	F
S	Cl

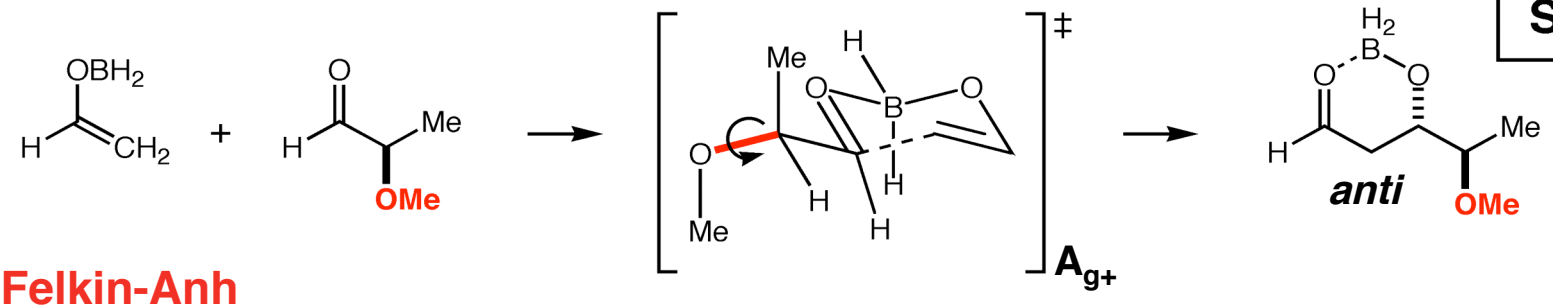

Polar Felkin-Anh

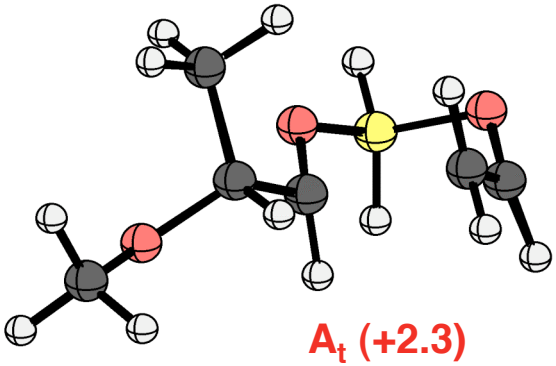

A_t (+2.3)

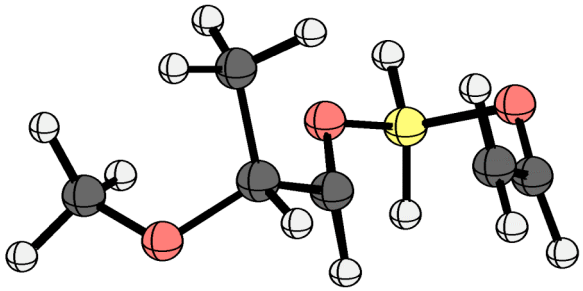

A_{g-} (+2.0)

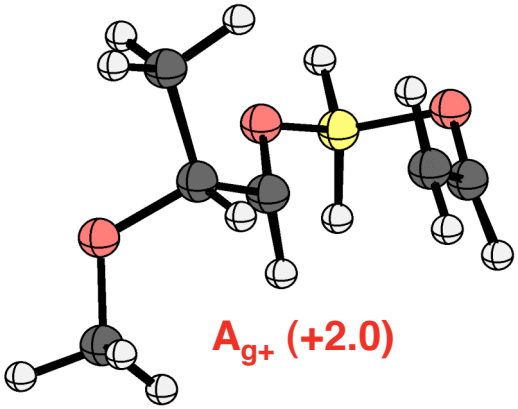

A_{g+} (+2.0)

Cornforth

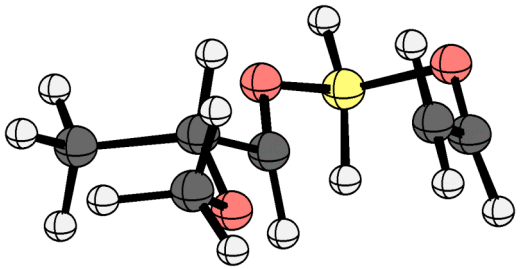

B_t (0)

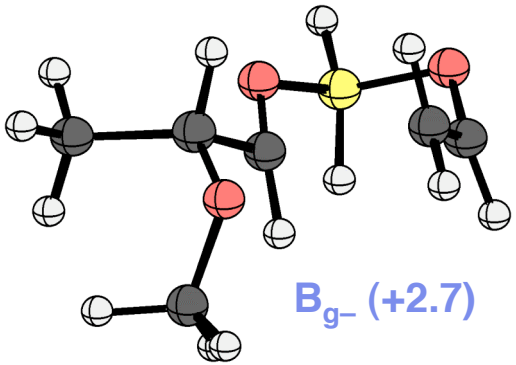

B_{g-} (+2.7)

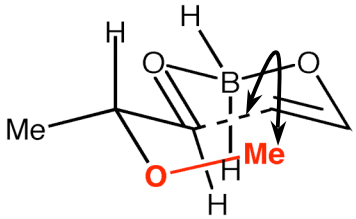

B_{g+}

Generality: 2-Thiomethylpropanal

O	F
S	Cl

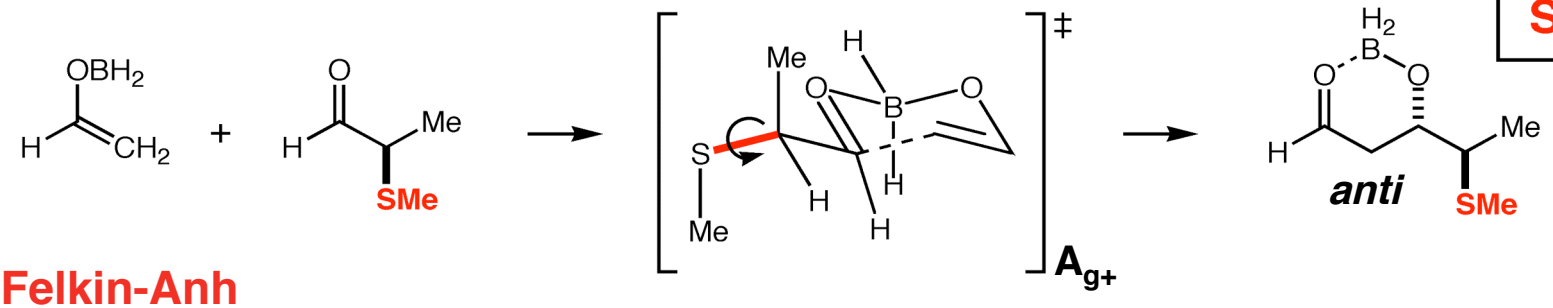

Polar Felkin-Anh

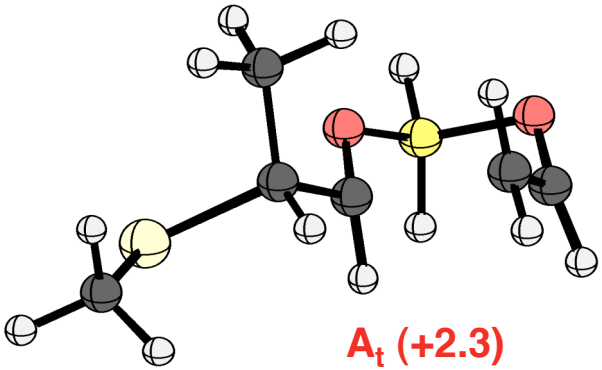

A_t (+2.3)

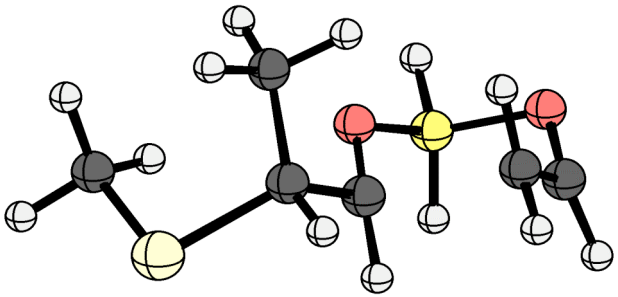

A_{g-} (0)

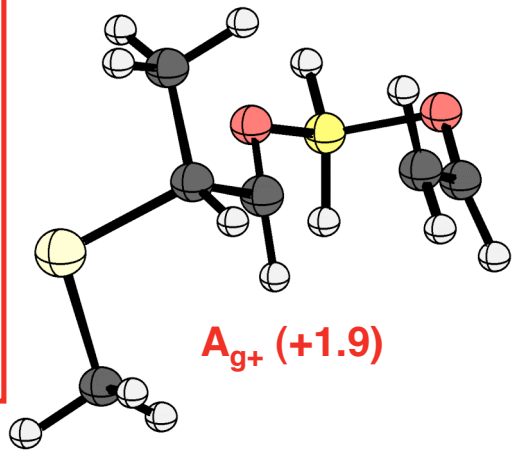

A_{g+} (+1.9)

Cornforth

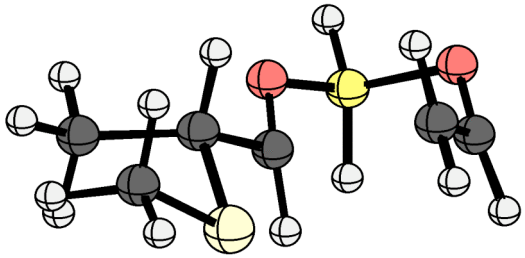

B_t (+3.2)

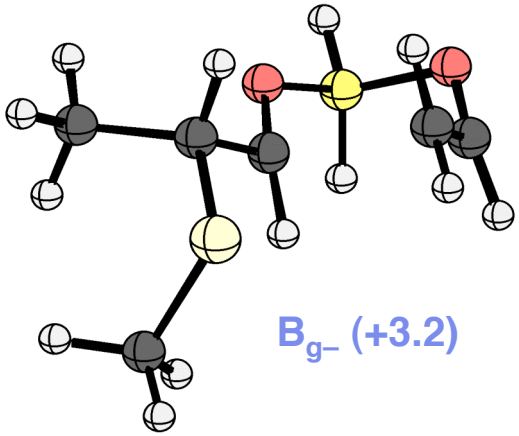

B_{g-} (+3.2)

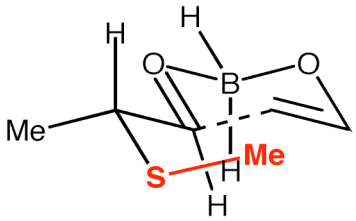

B_{g+}

Periodic/Group Trends: σ^*_{C-X} vs Electronegativity

Trends in C-X:

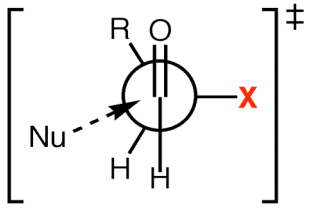

Polar Felkin-Anh

low energy σ^*_{C-X}

MeS Cl MeO F

2nd row 1st row

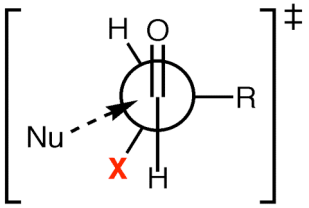

Cornforth

electronegative X

Calculated σ^*_{C-X}:

Polar Felkin-Anh

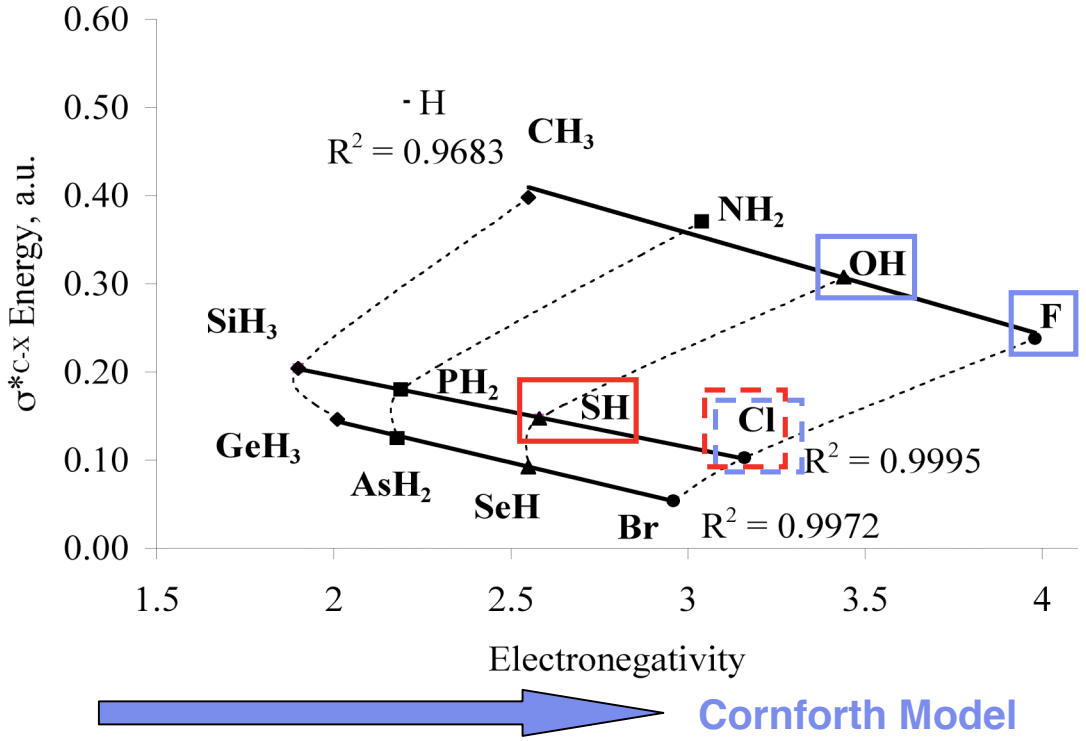

Cornforth Model

Alabugin and Zeidan *J. Am. Chem. Soc.* **2002**, *124*, 3175-3185

How does one distinguish between the Cornforth & Felkin Anh Models for C=O Addition??

Ferlkin-Anh Transition State Hyperconjugation
Cornforth Transition State Electrostatic effects

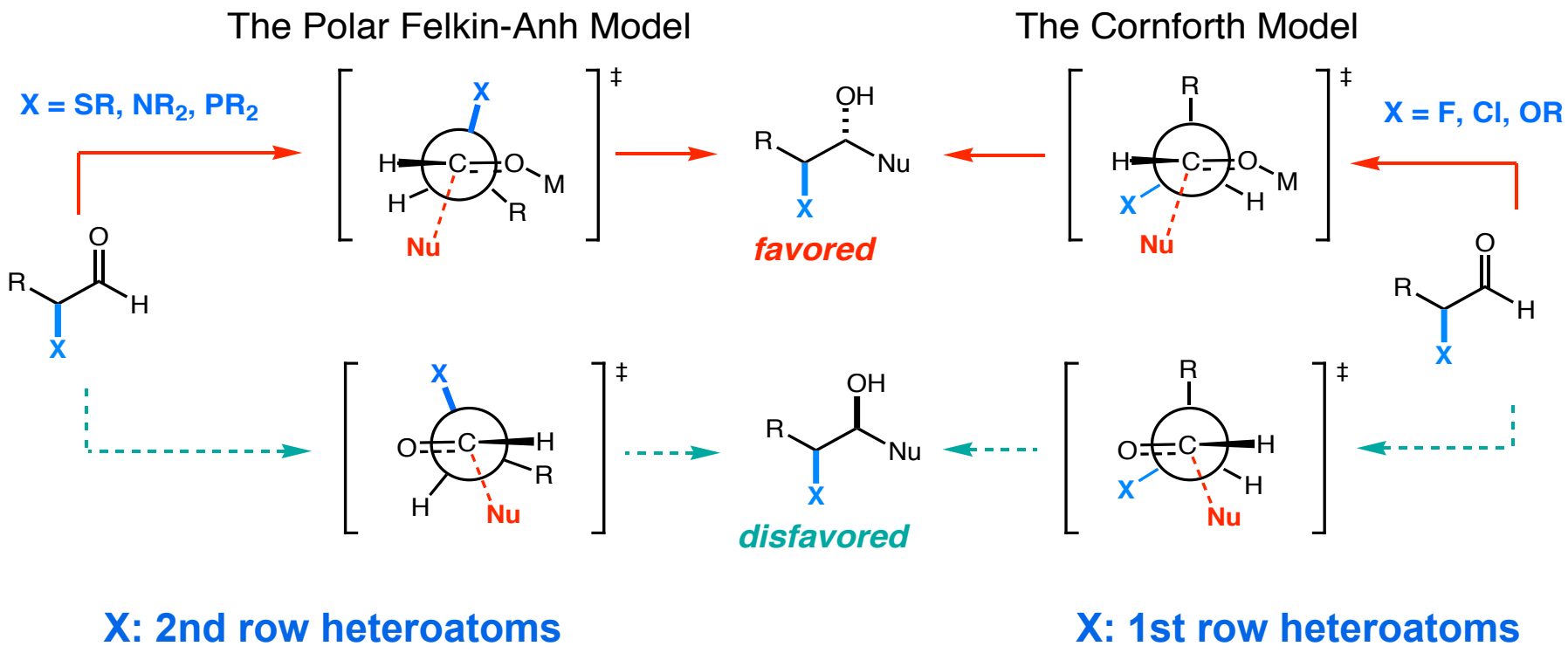

The Stereochemical Demon: Controlling the Reacting Enantioface in C–C Bond Constructions

Electrophilic carbon

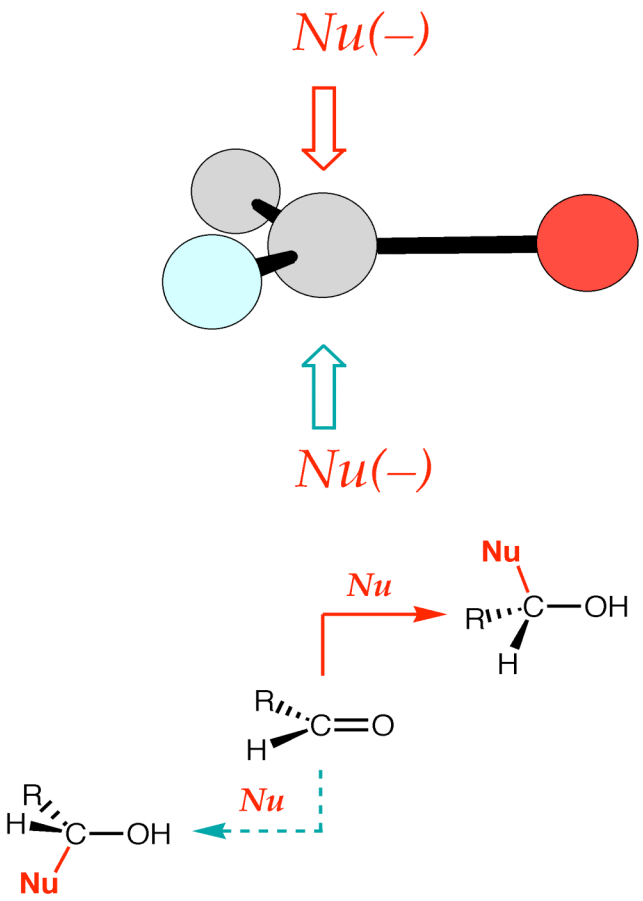

Nucleophilic carbon

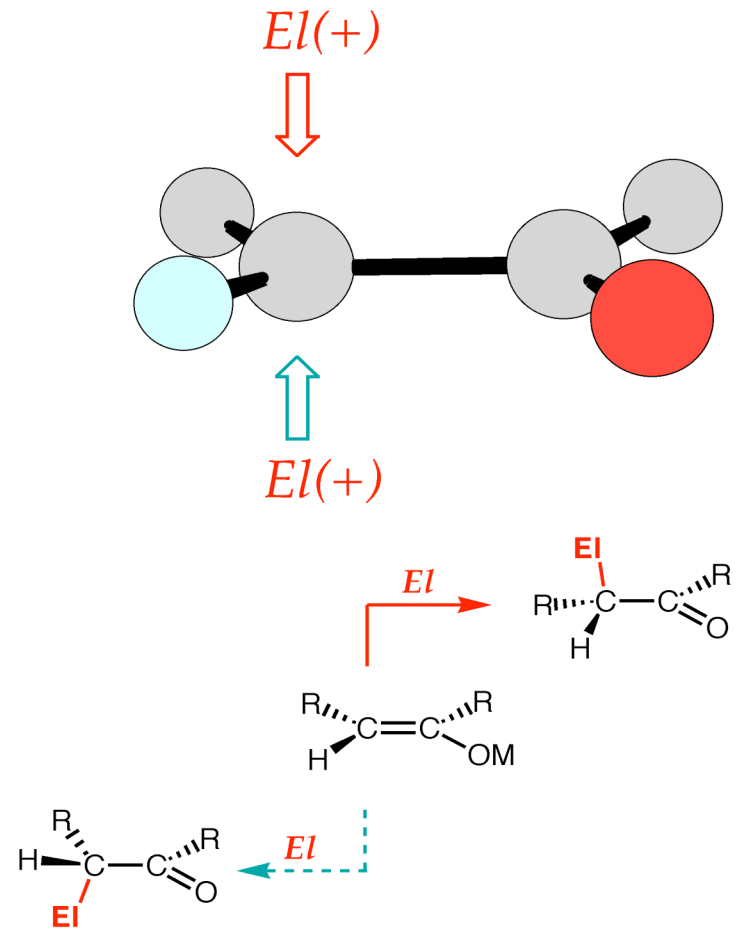

(E) Enolates Exhibit Felkin Aldehyde Diastereoface Selection

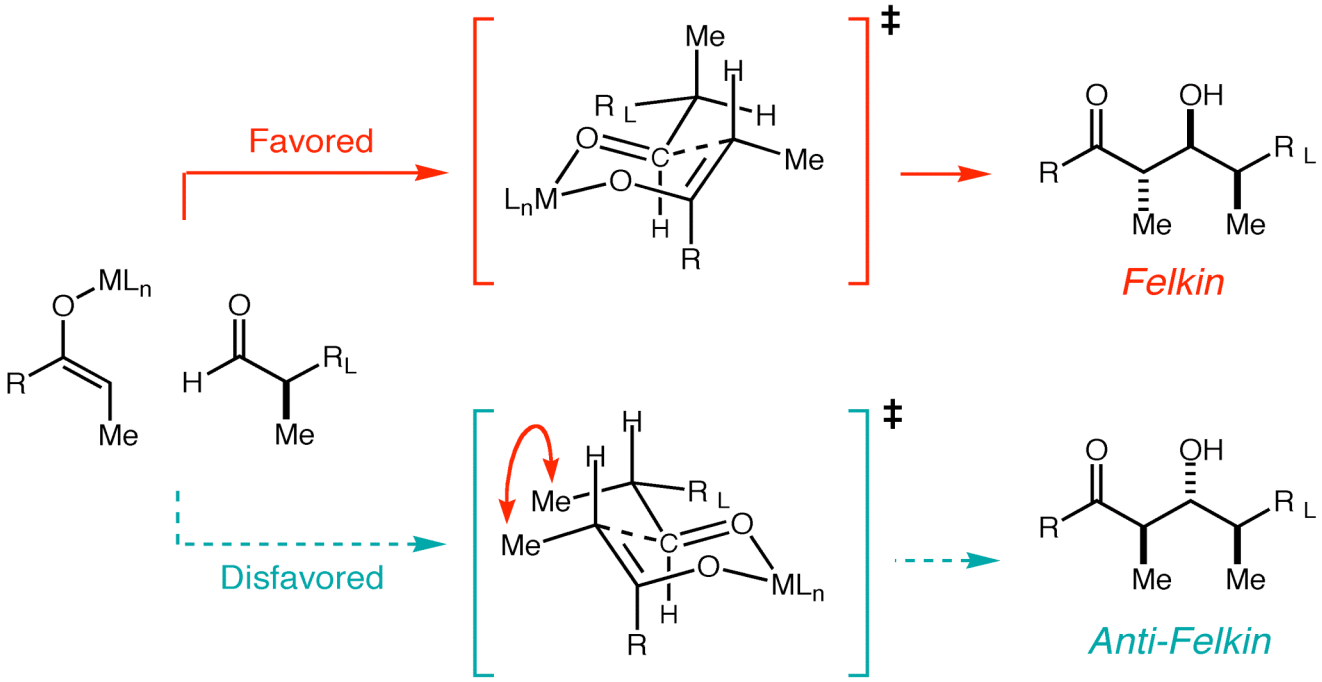

The illustrated syn-pentane interaction disfavors the anti-Felkin pathway.

Evans, Nelson, Taber, *Topics in Stereochemistry* **1982,** *13*, 1-115.
W. R. Roush, *J. Org. Chem.* **1991**, *56*, 4151-4157.

(Z) Enolates Exhibit Anti-Felkin Aldehyde Diastereoface Selection

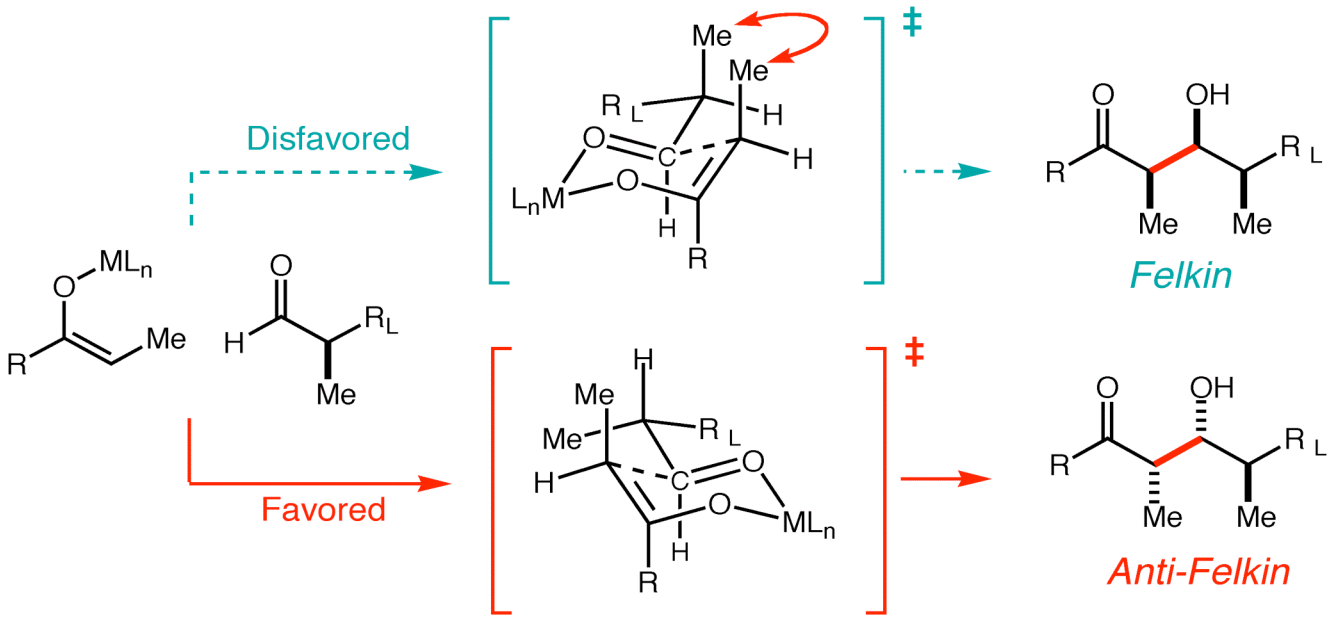

The illustrated syn-pentane interaction disfavors the Felkin pathway.

Evans, Nelson, Taber, *Topics in Stereochemistry* **1982,** *13*, 1-115.
W. R. Roush, *J. Org. Chem.* **1991**, *56*, 4151-4157.

Stereochemical Control Elements for Double Stereodifferentiating Aldol Additions:

Carbohydrate Polyols

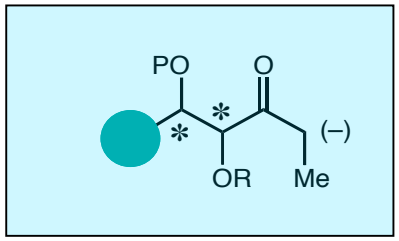

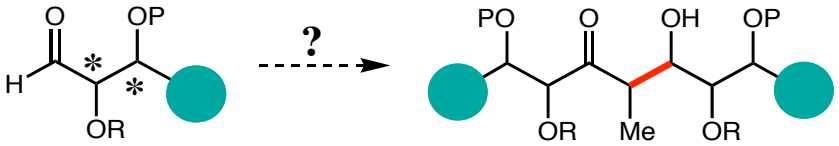

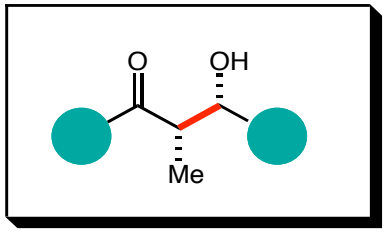

simple diastereocontrol
(enolate geometry)

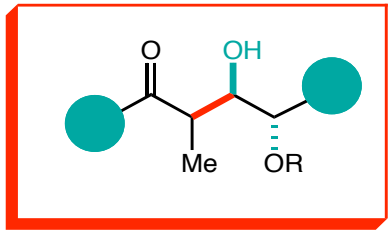

1,2-induction R = OR
(Polar Felkin-Anh)

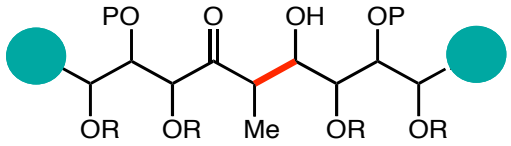

R = H, Me, OR

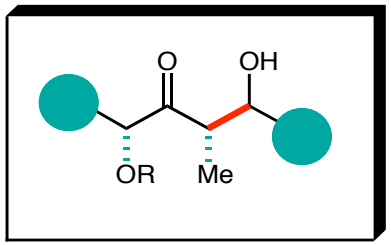

enolate facial bias

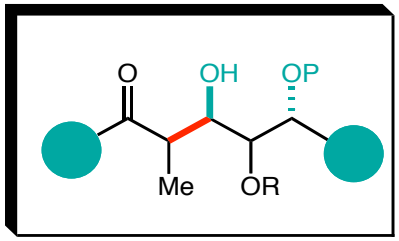

1,3-induction

Transition State Analyses: Polar Felkin-Anh & Cornforth Models.

X = OR

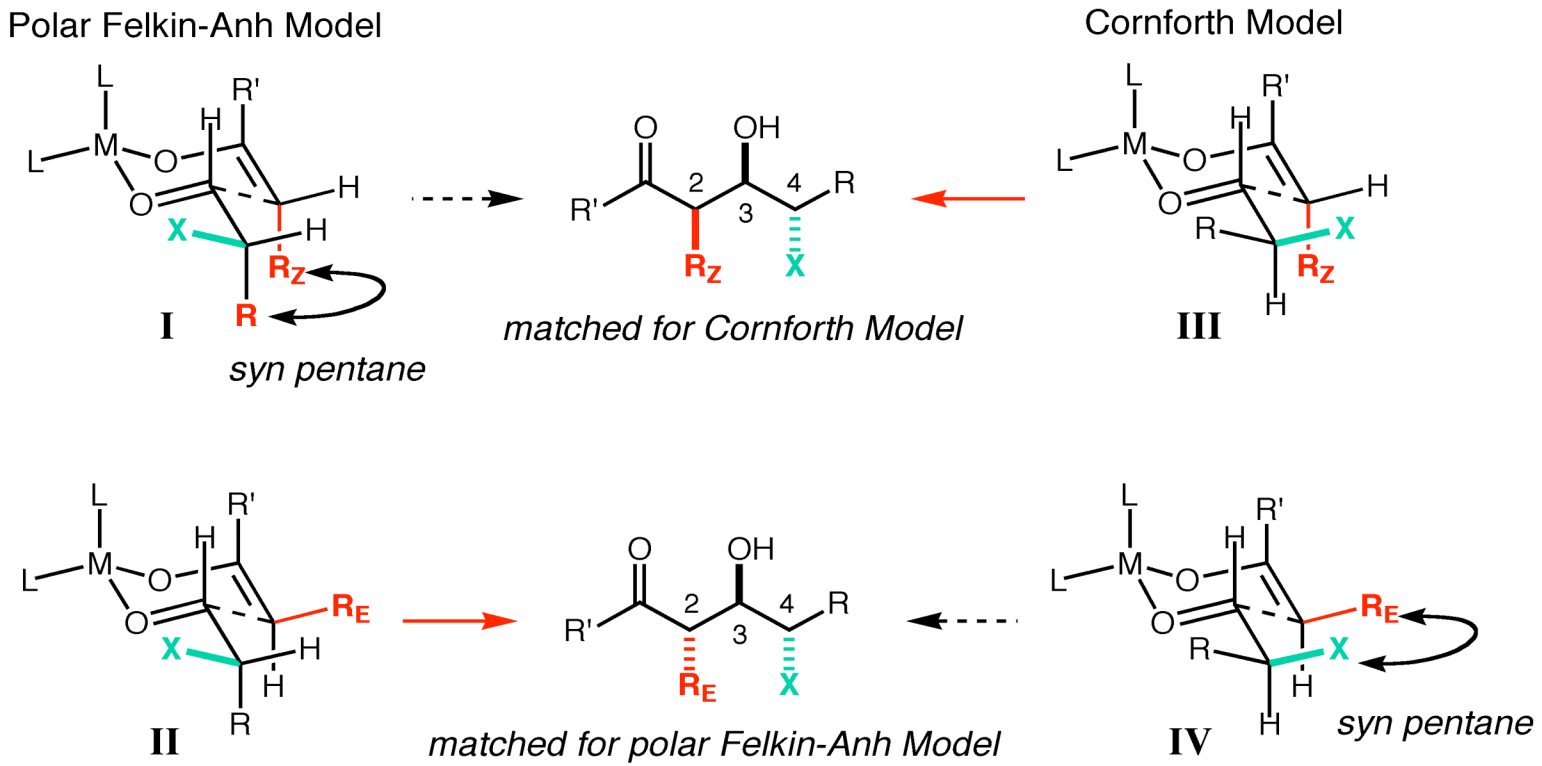

Conforth Model Prediction: (*E*) enolates will exhibit diminished levels of 3,4-anti diastereoselection relative to (*Z*) enolates.

Polar Felkin Model Prediction: (*Z*) Enolates will exhibit diminished levels of 3,4-anti diastereoselection due to reactions through competing transition states relative to the analogous reactons of (*E*) enolates which encounter no such destabilizing syn-pentane interaction.

Evans, Cee, Siska, *Angew Chem Int Ed*. **2003**, *42*, 17661

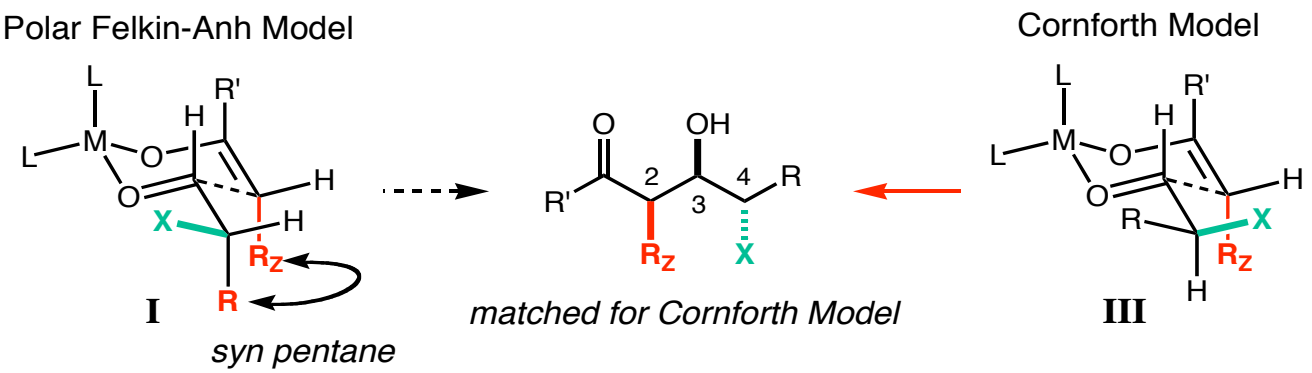

Conforth Model Prediction: (*Z*) enolates will exhibit high levels of 3,4-anti diastereoselection relative to (*E*) enolates.

Polar Felkin Model Prediction: (*Z*) Enolates will exhibit diminished levels of 3,4-anti diastereoselection due to reactions through competing transition states relative to the analogous reactons of (*E*) enolates which encounter no such destabilizing syn-pentane interaction.

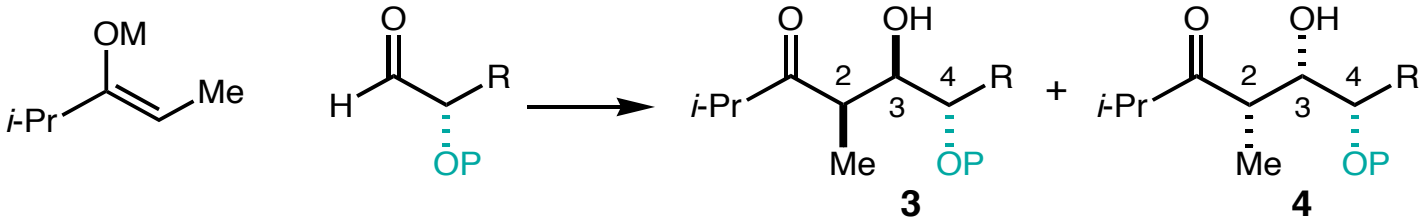

M	P	R	2,3-syn : 2,3-anti	**3** : **4**	yield, %[c]
9-BBN	Bn	Me	95 : 05[b]	89 : 11[b]	95
	Bn	*i*-Pr	95 : 05	98 : 02	73
	TBS	Me	93 : 07	98 : 02	77
	TBS	*i*-Pr	94 : 06	98 : 02	72

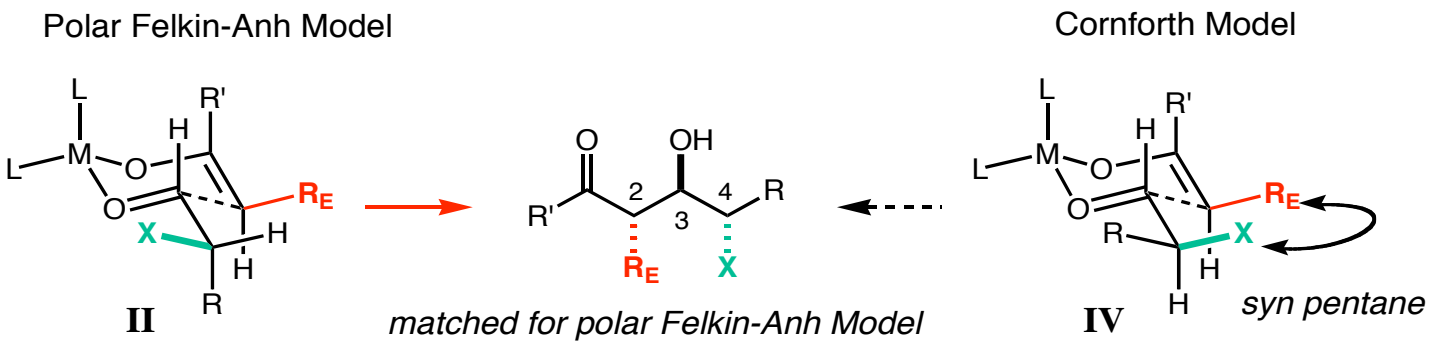

Conforth Model Prediction: (*E*) enolates will exhibit diminished levels of 3,4-anti diastereoselection relative to (*Z*) enolates.

Polar Felkin Model Prediction: (*E*) Enolates will exhibit high levels of 3,4-anti diastereoselection.

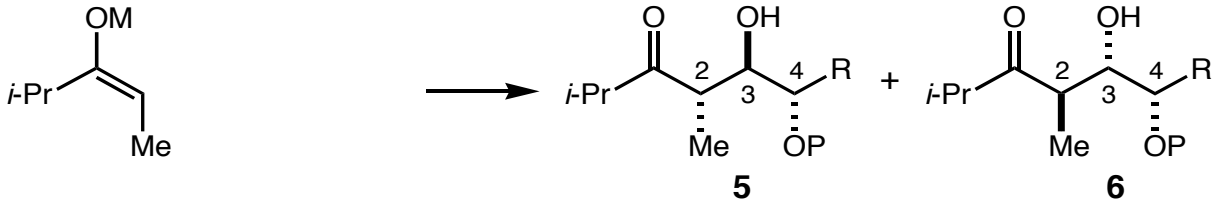

M	P	R	2,3-anti : 2,3-syn	**5** : **6**	yield, %[c]
$(c\text{-Hex})_2B$	Bn	Me	>99 : 01[b]	33 : 67[b]	59
	Bn	*i*-Pr	>99 : 01	67 : 33	77
	TBS	Me	>99 : 01	21 : 79	77
	TBS	*i*-Pr	>99 : 01	43 : 57	85

Evans, Cee, Siska, *Angew Chem Int Ed*. **2003**, *42*, 17661

Cornforth model for C=O addition appears to be a reliable predictor

Conforth Model Prediction: (*E*) enolates will exhibit diminished levels of 3,4-anti diastereoselection relative to (*Z*) enolates.

Polar Felkin Model Prediction: (*Z*) Enolates will exhibit diminished levels of 3,4-anti diastereoselection due to reactions through competing transition states relative to the analogous reactons of (*E*) enolates which encounter no such destabilizing syn-pentane interaction.

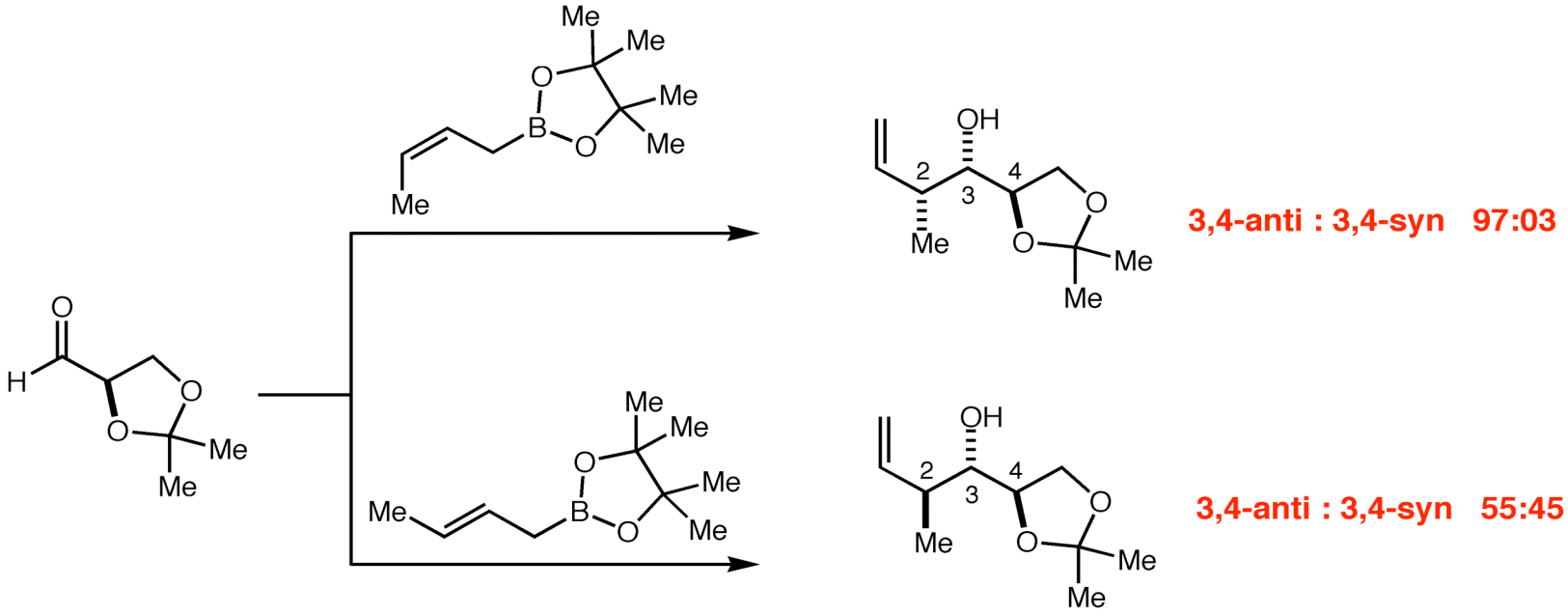

R. W. Hoffmann, *Chem. Scripta* **1985**, *25*, 53; b) R. W. Hoffmann, *Liebigs Ann. Chem.* **1987**, 881
W. R. Roush *J. Am. Chem. Soc.* **1986**, *108*, 3422-3434.

How does one distinguish between the Cornforth & Felkin Anh Models for C=O Addition??

Ferlkin-Anh Transition State Hyperconjugation
Cornforth Transition State Electrostatic effects

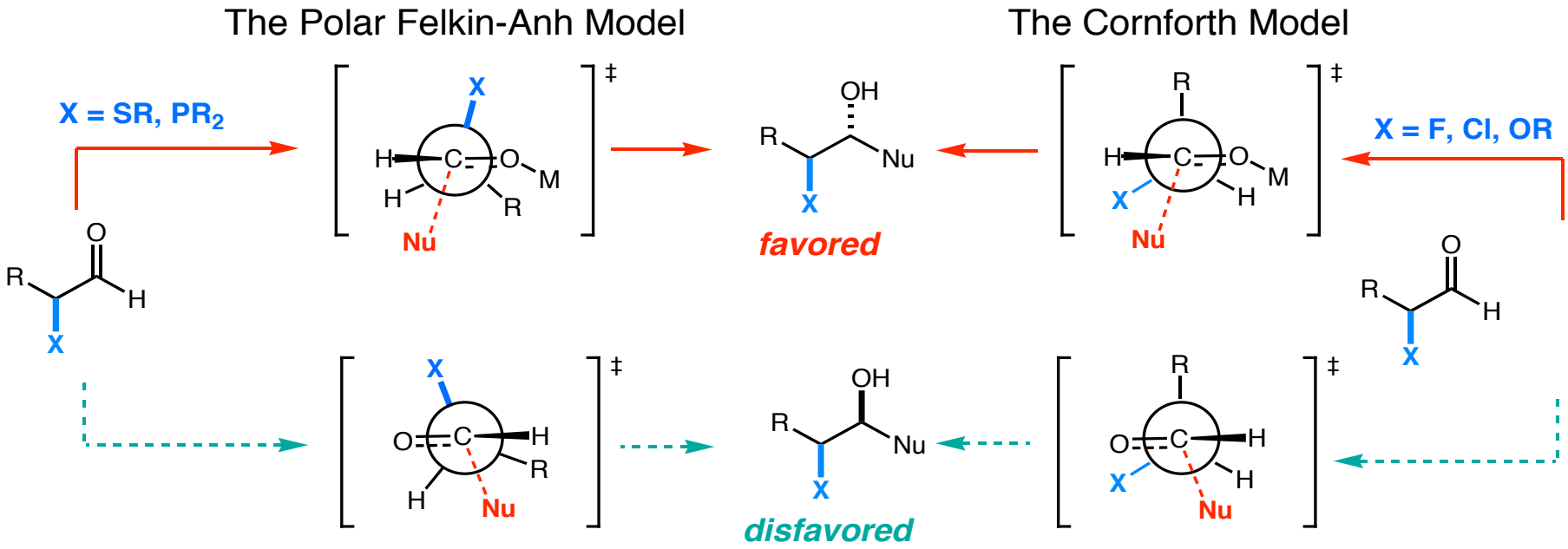

Both enolate and borane nucleophiles implicate the intervention of Cornforth geometries in additions to α-alkoxy aldehydes.

What is the current position for a stereochemical model for alpha alkoxy aldehydes substituted substrates?

Ferlkin-Anh	Transition State Hyperconjugation is now in doubt.
Cornforth	Transition State Electrostatic effects are reasonable
Ionic Model	Best donor substituent perpendicular to pi framework in Cornforth geometry.

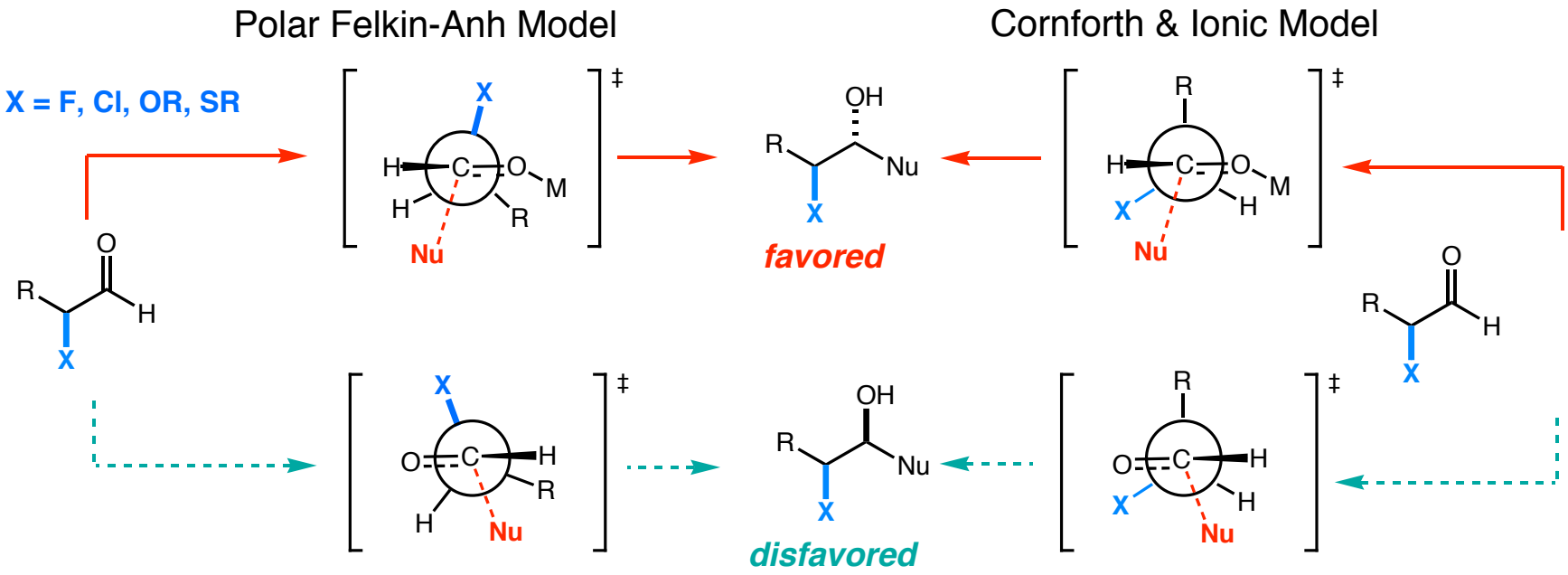

One needs to take seriously the Cieplak sugggestion that there might be any electron density between Nu and C=O in the transition state.

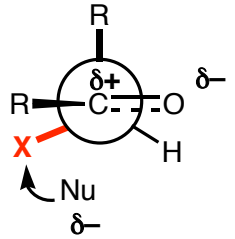

Evans: Cieplak Ionic Model for C=O Addition

- There is little or no covalency along Nu....$^{\delta+}$C=O$^{\delta-}$ axis in the transition state (Cieplek)
- Eclipsed transition states are disfavored (Felkin, anh-Eisenstein, Houk)
- Transition state stabilization may be achieved by orienting the best σ-donor perpendicular to polarized C=O (Stereolectronic Effects)

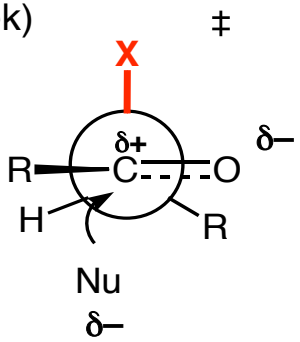

- Transition state stabilization may be achieved by orienting the largest substituent anti, rather than gauche to nucleophile (Steric Effects-1)

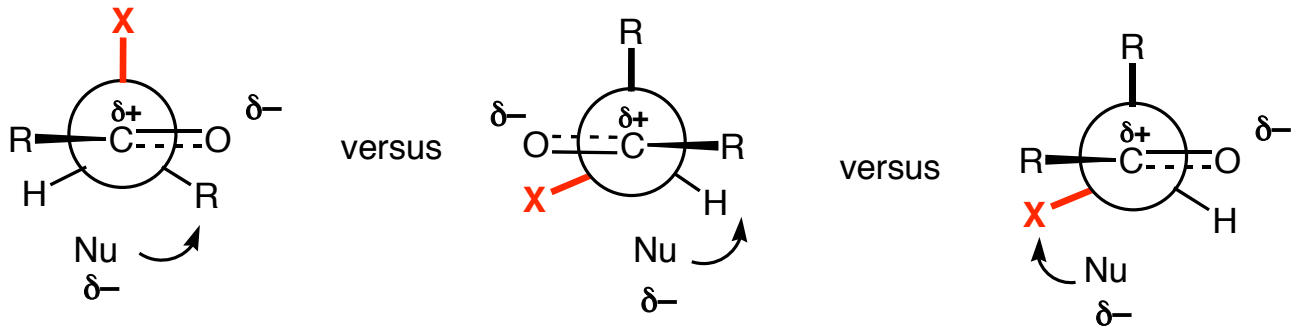

- If the C–X bond is very polar (**X** = F, Cl, OR), electrostatic (dipole) effects may be significant as noted by Cornforth

Effects Governing Face Selectivity at Trigonal Carbon

- Steric Effects — Nonbonding interactions (Van der Waals repulsion) between substituents within a molecule or between reacting molecules

- Electronic Effects (Inductive Effects): — The effect of bond and through-space polarization by heteroatom substituents on reaction rates and selectivities

  Inductive Effects: Through-bond polarization
  Field Effects: Through-space polarization

- Stereoelectronic Effects: — Geometrical constraints placed upon **ground** and **transition states** by orbital overlap considerations.

"Organic chemists are proficient in the analysis of steric effects."

"Organic chemists are frequently unaware of the impact of electronic effects on the stereochemical outcome of reactions."

Acknowledgements

Professor Chris Cramer Dept of Chemistry, Univ. of Minnesota

Jim Gage

Mick Dart

Mike Yang

Joseph Duffy

Joseph Young

Sarah Siska

Victor Cee

http://www.courses.fas.harvard.edu/colgsas/1063

Chemistry 206

Advanced Organic Chemistry

Lecture Number 23 SUPPLEMENT

Enantioselective Carbonyl Addition

- Enantioselective addition of R_2Zn to aldehydes
- Enantioselective Reduction of Ketones & Imines

Reading Assignment:

Carey & Sundberg: **Part A**; Chapter 8
Reactions of Carbonyl Compounds

Carey & Sundberg: **Part B**; Chapter 2
Reactions of Carbon Nucleophiles with Carbonyl Compounds

Carey & Sundberg: **Part B**; Chapter 5
Reduction of Carbonyl & Other Functional Groups

Enantioselective Carbonyl Reduction: Corey *Angew. Chem. Int Ed.* **1998**, *37*, 1986-2012 **(handout)**

Enantioselective Carbonyl Addition (R_2Zn): Noyori *Angew. Chem. Int Ed.* **1991**, *30*, 49-69 **(handout)**

D. A. Evans

Monday
November 13, 2006

Relevant Problems:

Cume Question, 2000: Corey's introduction of chiral oxazaborolidine catalysts **1** in the borane-mediated enantioselective reduction of ketones represents an important advance in asymmetric synthesis (Corey & Helal, *Angew. Chem. Int. Ed.* **1998**, *37*, 1986-2012). Provide a detailed mechanism for the overall transformation. Use 3-dimensional representations to illustrate the absolute stereochemical aspects of the indicated transformation.

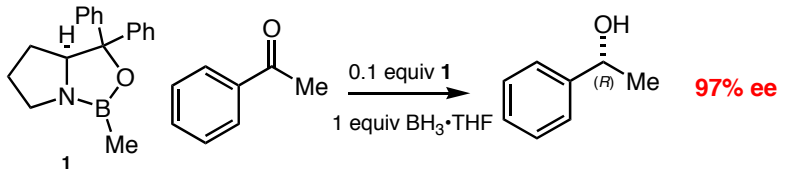

Problem 174: Corey's CBS catalyst for ketone reduction often delivers high yields of enantioenriched secondary alcohols (*ACIE*, **1998**, 1987). Provide a clear clear illustration of the transition state which predicts the absolute stereochemistry of the product obtained in the illustrated reaction. Include an explanation of why the reduction of this practically symmetric ketone is selective.

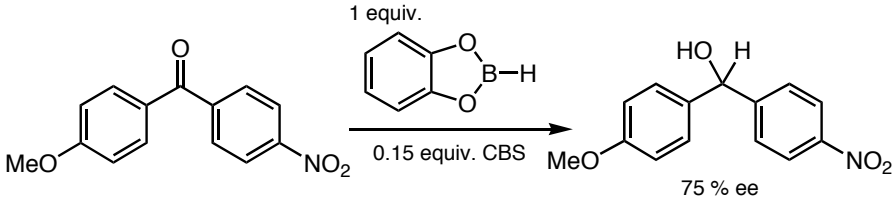

Problem 340: The C_2-symmetric Cu(II) complex is a ciral Lewis acidcatalyst that exhibits good chelating potential. The utilization of **1** in the catalyzed Mukaiyama aldol reaction is illustrated below *(JACS* **1999,** *121*, 686).

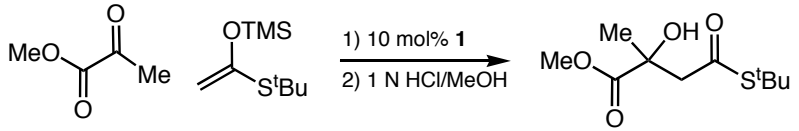

99%ee, 95% yield

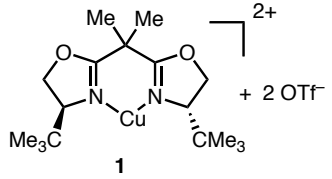

Hint; Remember that Cu(II) complexes strongly prefer a square planar geometry.

Provide the absolute stereochemistry of the product of this reaction.
Provide a 3-dimensional drawing of the transition state for this reaction.

Catalytic Asymmetric Carbonyl Addition

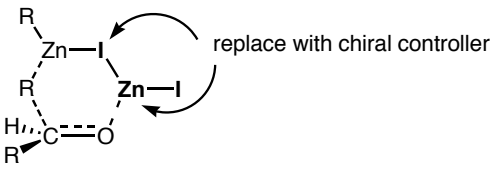

replace with chiral controller

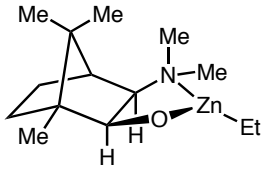

the catalyst

Noyori & co-workers, *J. Am. Chem. Soc.* **1986**, 108, 6072.
J. Am. Chem. Soc. **1989**, 111, 4028.

Review: Noyori *Angew. Chem. Int. Ed.* **1991**, *30*, 49
Review: L. Pu, *Chem. Reviews* **2001**, *101*, 757-824

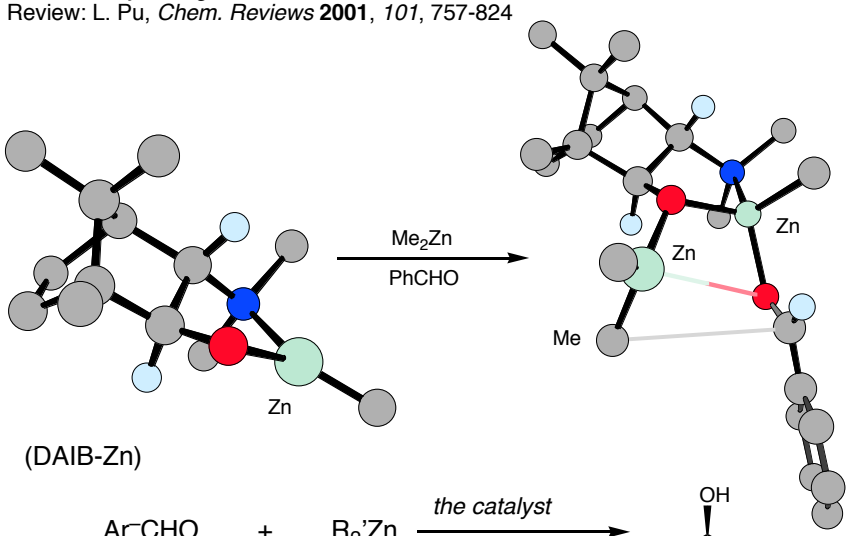

(DAIB-Zn)

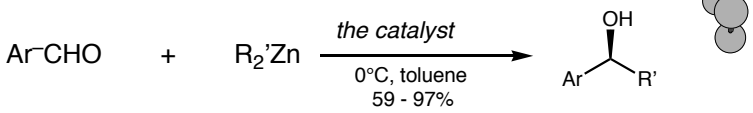

C_6H_5CHO	Et_2Zn	98% e.e.
"	Me_2Zn	91% e.e.
p-ClC_6H_4CHO	Et_2Zn	93% e.e.
p-$MeOC_6H_4CHO$	Et_2Zn	93% e.e.
Cinnamyl	Et_2Zn	96% e.e.
$PhCH_2CH_2CHO$	Et_2Zn	90% e.e.
n-$C_6H_{13}CHO$	Et_2Zn	61% e.e.

- *The method is catalytic in aminoalcohol.*
- *Two zinc species per aldehyde are involved in the alkylation step.*

The Catalytic Cycle

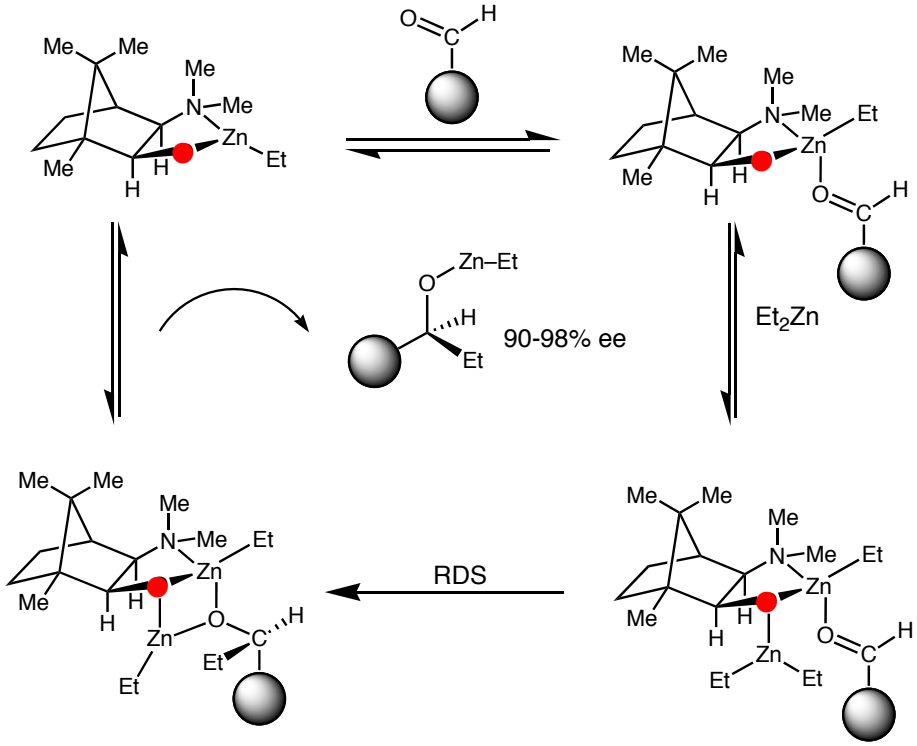

- *Catalyst must be sterically hindered so that association is precluded*

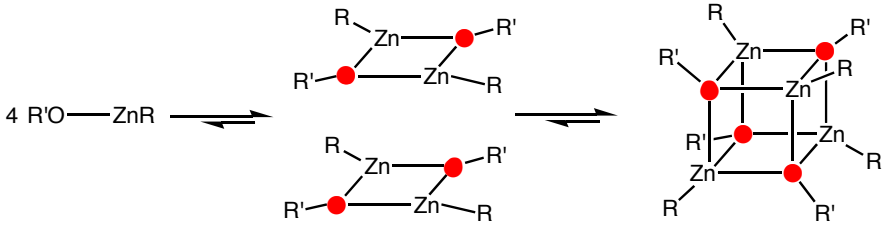

- *Product is taken out of the picture by aggregation*

Enantioselective C=O Addition: Noyori Catalyst-2

Other Catalysts for the R_2Zn Addition Process

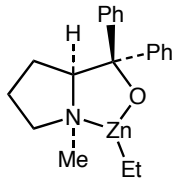

97% e.e. (S)

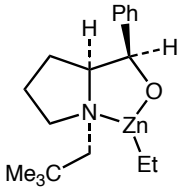

100% e.e. (R)

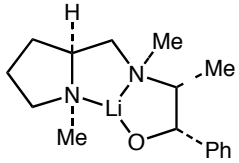

95% e.e. (S)

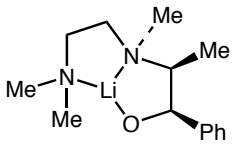

90% e.e. (R)

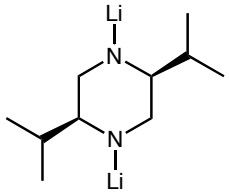

90% e.e. (R)

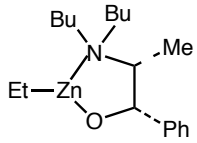

90% e.e. (R)

(Results are cited for the reaction of benzaldehyde and Et_2Zn)

Problem: Rationalize the stereochemical course of each of the catalysts

■ Non-linear effects observed with the Noyori Catalyst (DAIB-Zn)

There is no correlation between catalyst and product ee.

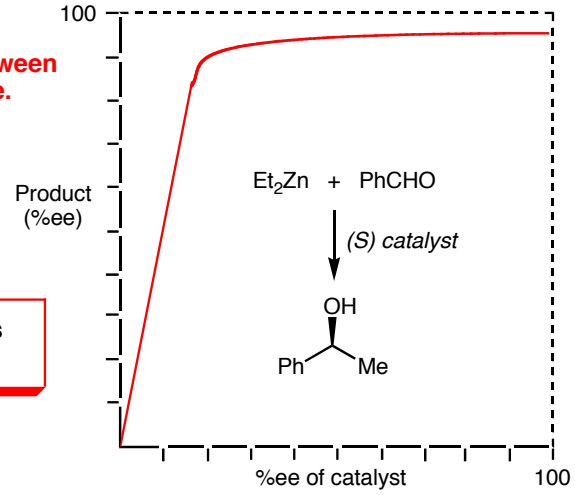

25% ee Catalyst affords product in 95% ee.

Explanation for Nonlinearity of DAIB Catalyst

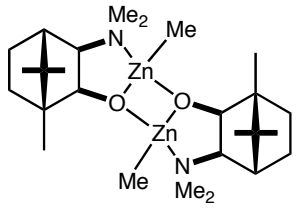

(S,S) dimer

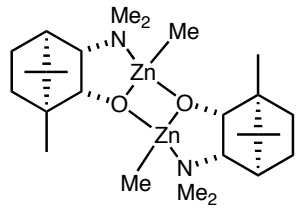

(R,R) dimer

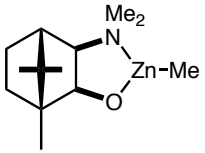

(S) catalyst

+

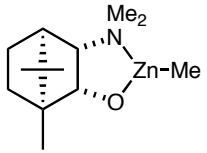

(R) catalyst

(S,R) dimer

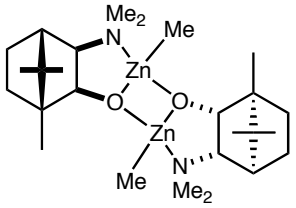

Observations

- (S,S) dimer dissociates upon addition of RCHO & effects catalysis
- (S,R) dimer is overwhelmingly more stable than (S,S) homodimer
- (S,R) dimer is ineffective as a catalyst

Enantioselective C=O Addition: Dialkylzinc Addn Scope

Scope of the DAIB Catalyst

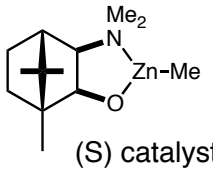

(S) catalyst

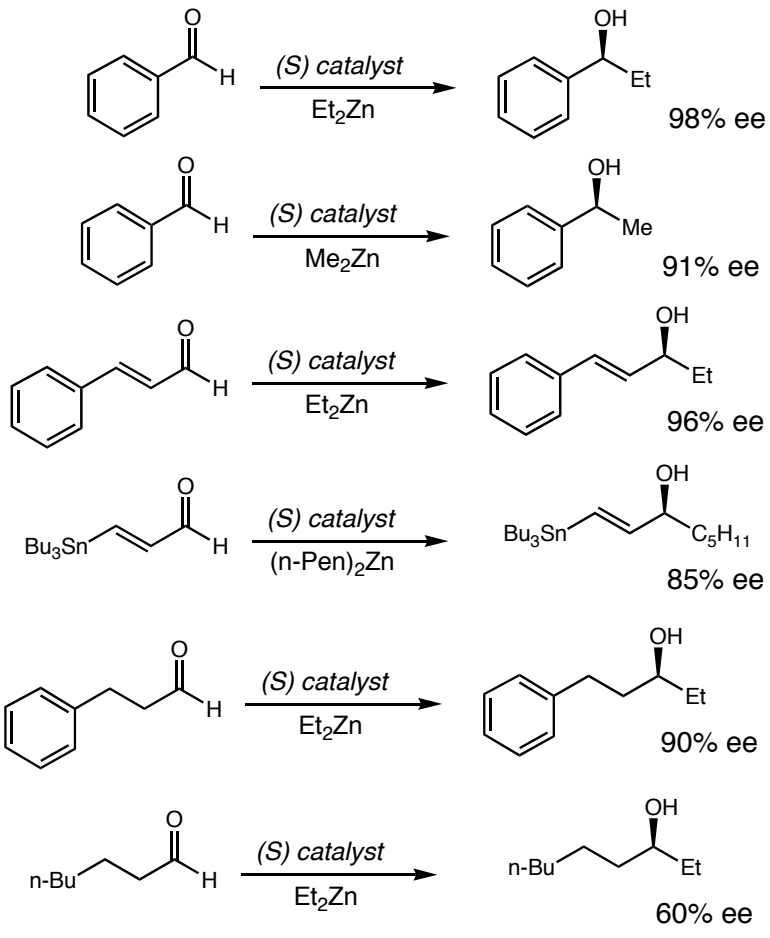

Review: Noyori *Angew. Chem. Int. Ed.* **1991**, *30*, 49

Improved Selectivity with Aliphatic Aldehydes

Soai, *J. Org. Chem.* **1991**, *56*, 4264

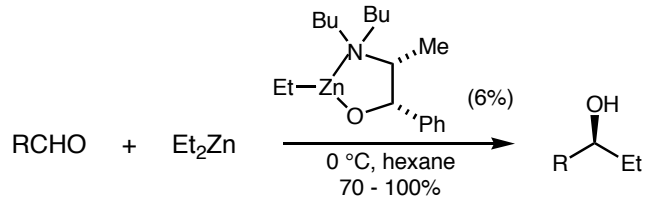

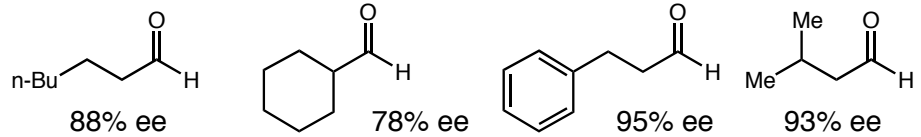

Lepicidin Application: The reaction functions in complex systems

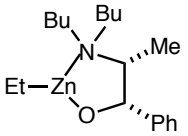

the catalyst

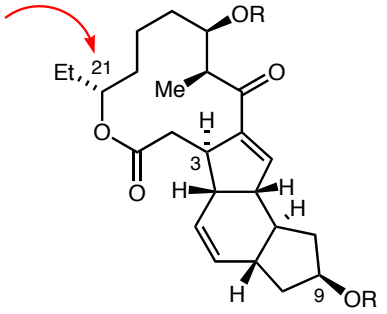

Evans, Black, *JACS* **1993**, *115*, 44974513

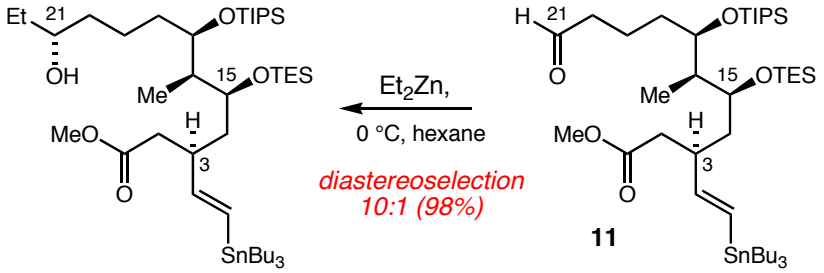

11

Discovery of a Catalytic Process

Enantioselective Carbonyl Reduction: Corey *Angew. Chem. Int Ed.* **1998**, *37*, 1986-2012 **(handout)**

■ The Stoichiometric Process: Itsuno, 1983-1985

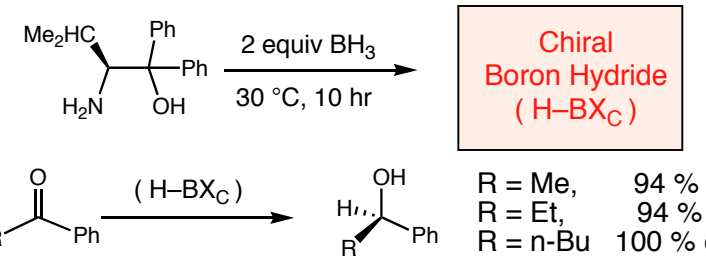

Itsuno, *Chem. Commun.* **1983**, 469

Itsuno, *J. Org. Chem.* **1984**, 49, 555

Itsuno, *J. Chem. Soc. Perkin Trans I.* **1985**, 2615

■ The Catalytic Process: Corey, 1987

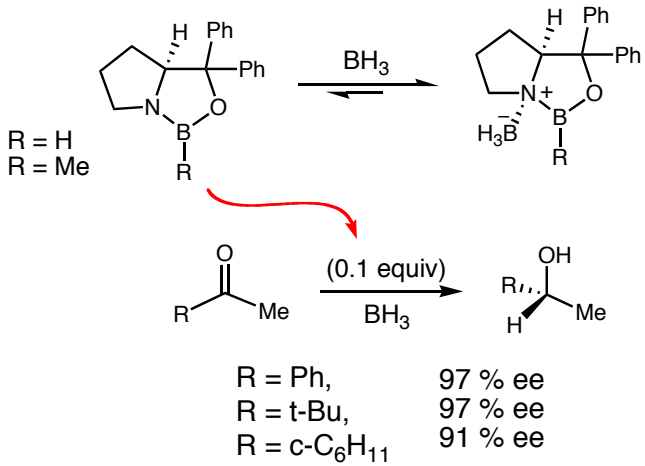

But how does it really work ?

The Catalytic Cycle

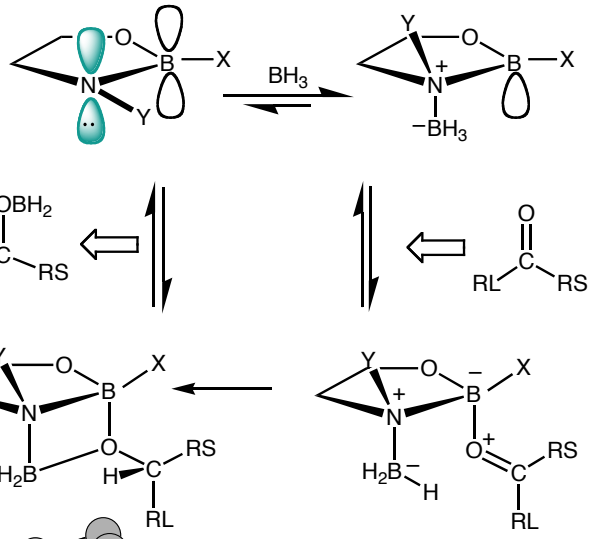

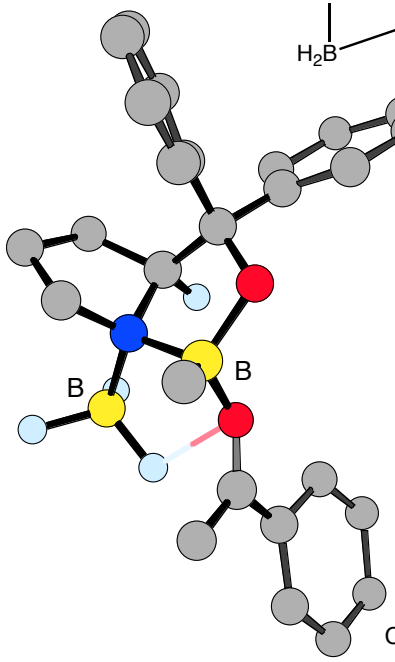

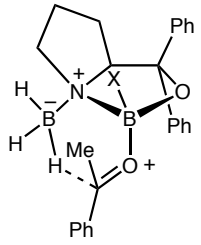

Corey, *JACS* **1987**, *109*, 5551

Corey, *JACS* **1987**, *109*, 7925

Corey, *JOC* **1988**, *53*, 2861

Catalyst X-ray, Corey, *Tet. Let* **1992**, *33*, 3429

Mathre, *JOC* **1993**, *58*, 2880

catalyst prep: Mathre, *JOC* **1993**, *58*, 799

Mathre, *JOC* **1991**, *56*, 751

(Review) Martens, *Tertrahedron Asymmetry* **1992**, *3*, 1475

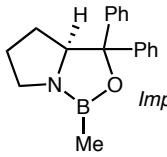

Improved version

Representative Reductions

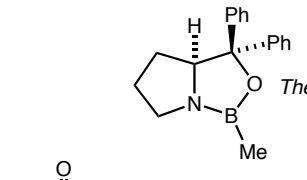

The catalyst

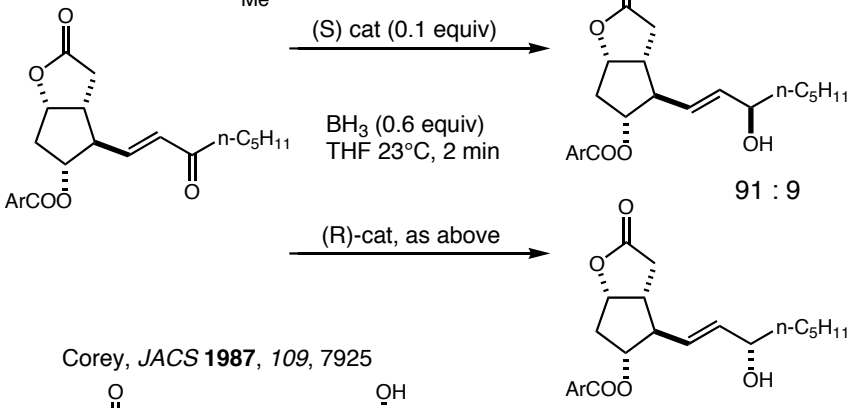

Corey, *JACS* **1987**, *109*, 7925

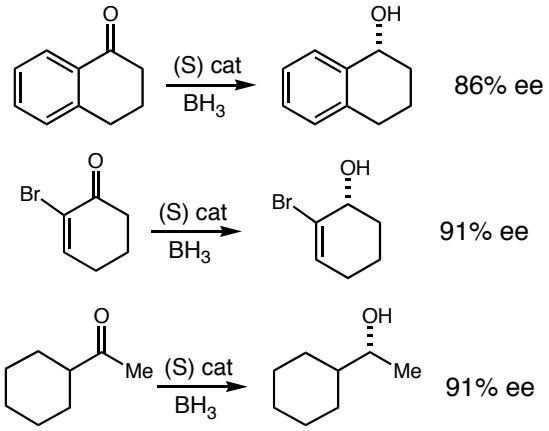

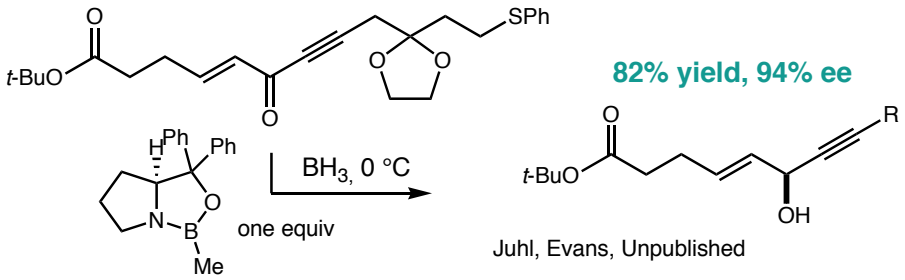

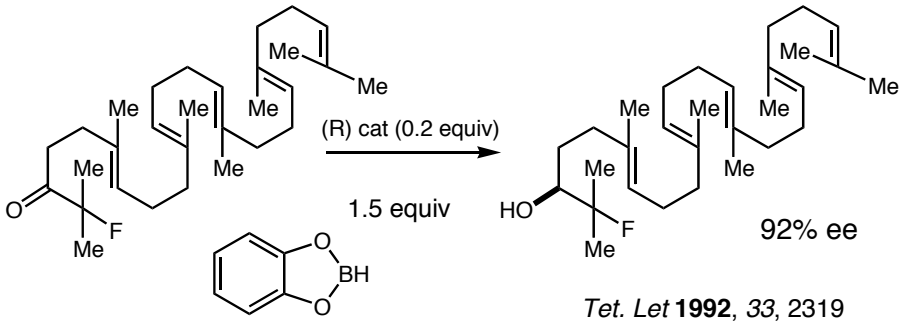

Tet. Let **1992**, *33*, 2319

Fluoxetine (Prozac®) Synthesis

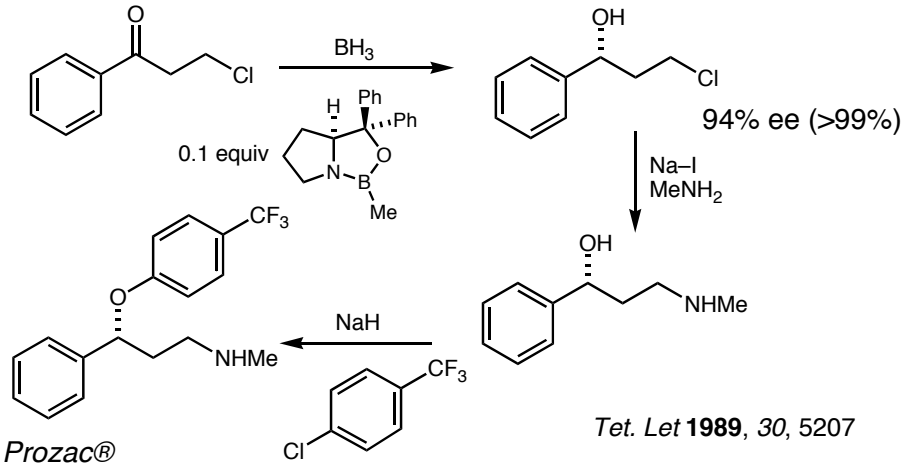

Prozac®

Tet. Let **1989**, *30*, 5207

An α-Amino Acid Synthesis

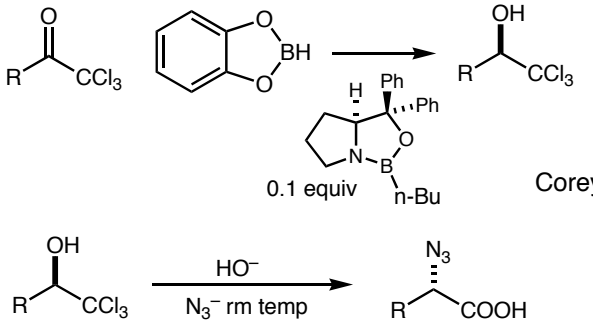

R	ee
n-C_5H_{11}	95%
c-C_6H_{11}	92%
t-C_4H_9	98%

Corey, *JACS* **1992**, *114*, 1906

Tet. Let **1992**, *33*, 3435

Tet. Let **1992**, *33*, 3431

Enantioselective Reducing Agents

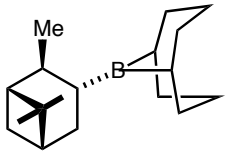

(R)-Alpine Borane

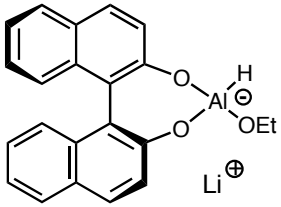

(S)-BINAL-H

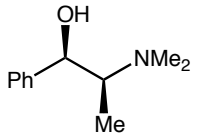

N-Methylephedrine, $LiAlH_4$, $(3,5\text{-xylenol})_2$ $[LiAl(lig)(OAr)_2H]$

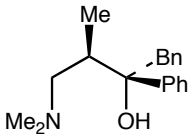

Darvon alcohol, $LiAlH_4$ $[LiAl(lig)_2H]$

Reviews: Midland, *Asymmetric Synthesis*, *Vol 2*, p 45-
Granbois, *Asymmetric Synthesis*, *Vol 2*, p 71-
Brown, *Accts. Chem. Res.* **1992**, *25,* 16-24
Singh, *Synthesis* **1992**, 605-617

Reductions of Representative Carbonyl Compounds

Reagent	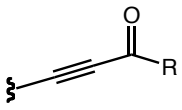	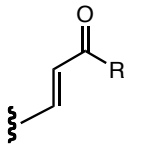	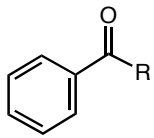
Alpine-Borane	72 - 92% e.e.	59 - 89% e.e.	78% e.e. R=Me 90% e.e. R=CO_2Me
BINAL-H	84 - 96% e.e. (57% ee, R=i-Pr)	>95% e.e.	95 - 100% e.e. (71% ee, R=i-Pr)
Darvon-$LiAlH_4$	34 - 90% e.e.	25% e.e.	15 - 75% e.e.
N-Methylephedrine-$LiAlH_4$	75 - 90% e.e.	78 - 98% e.e. (cyclic ketones)	----

Stoichiometric Chloroborane Reducing Agents

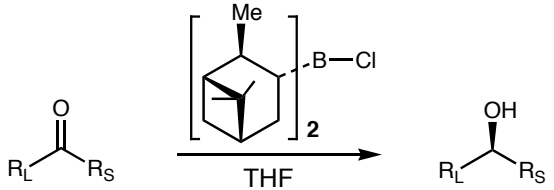

Ketone	Reaction Conditions	% ee
acetophenone	–25 °C	98%
butyrophenone	–25 °C	98%
2,2-dimethylpropiophenone	–25 °C	79%
3,3-dimethyl-2-butanone	25°C, 12 days	95%
2,2-dimethylcyclohexanone	25°C, 2 days	91%

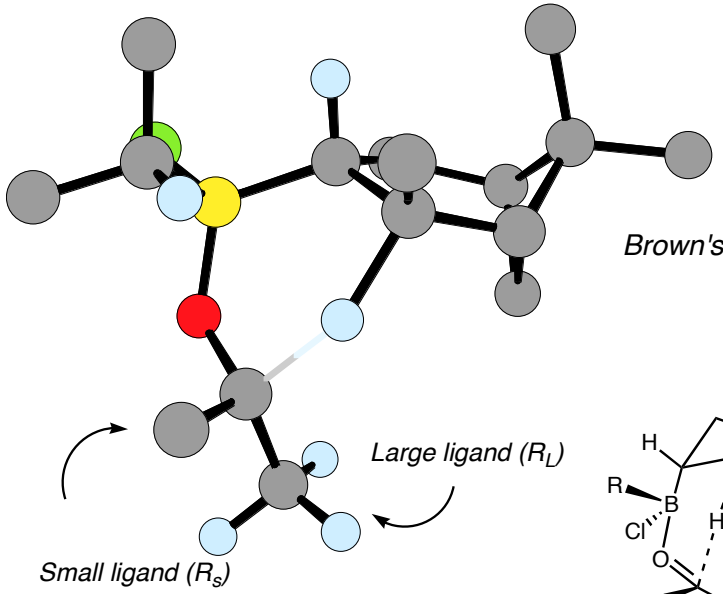

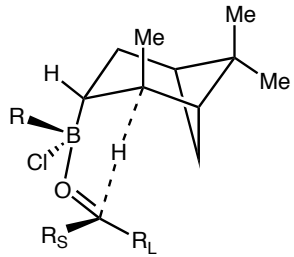

Less hindered aliphatic ketones are not reduced with useful levels of enantioselectivity

Brown, *J. Org. Chem.* **1985**, *50*, 5446
Brown, *J. Org. Chem.* **1986**, *51*, 3394
Brown, *J. Org. Chem.* **1988**, *53*, 2916

http://www.courses.fas.harvard.edu/colgsas/1063

Chemistry 206

Advanced Organic Chemistry

Lecture Number 24

Enolates & Metalloenamines-1

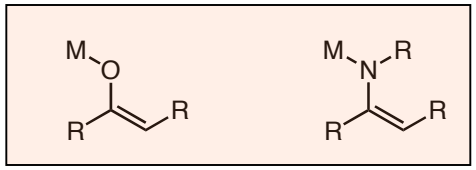

- Mild Methods for Enolate Generation
- Enolate Structure: A Survey of X-ray Structures
- Metallo-Enamine X-ray Structures

Reading Assignment for this Week:

Carey & Sundberg: **Part A**; Chapter 7
Carbanions & Other Nucleophilic Carbon Species

Carey & Sundberg: **Part B**; Chapter 2
Reactions of Carbon Nucleophiles with Carbonyl Compounds

D. A. Evans

Monday,
November 13, 2006

Assigned Journal Articles

"Structure and Reactivity of Lithium Enolates. From Pinacolone to Selective C Alkylations of Peptides. Difficulties and Opportunities Afforded by Complex Structures"
D. Seebach *Angew. Chem. Int. Ed. Engl.*, **27**, 1624 (1988). **(handout)**

"Stereoselective Alkylation Reactions of Chiral Metal Enolates".
D. A. Evans *Asymmetric Synthesis*, **3**, 1 (1984). **(handout)**

"Soft Enolization: A Powerful Method for Diastereoselective Carbon-Carbon Bond Formation",
DA Evans & J. Shaw, Manuscript in preparation **(pdf)**

"Self-Regeneration of Stereocenters (SRS)-Applications, Limitations, & Abandonment of a Synthetic Principle",
D. Seebach et al. *Chem. Int. Ed. Engl.*, **35**, 2708 (1996). **(pdf)**

Other Useful References

"Generation of Simple Enols in Solution". Capon, Guo, Kwok, Siddhanta, and Zucco *Acc. Chem. Res.* **21**, 121 (**1988**).

"Keto-Enol Equilibrium Constants of Simple Monofunctional Aldehydes and Ketones in Aqueous Solution". Keeffe, Kresge, and Schepp *JACS*, 112, 4862 (**1990**).

"pKa and Keto-Enol Equilibrium Constant of Acetone in Aqueous Solution". Chiang, Kresge, and Tang *JACS* **106**, 460 (**1984**).

Database Problem 314. Kawabata and co-workers recently reported the remarkable enolate alkylation illustrated below (*JACS* **2003,** *125***,** 13012). When the indicated α-aminoacid ester is treated with KHMDS in DMF at —60 °C, the derived cyclic amino acid ester is formed in high yield and enantioselectivity. The stereochemical outcome represents a formal retention of configuration. This reaction exhibits some generality as the 4- 5-, 6-, and 7-membered lactams may be obtained in high ee.

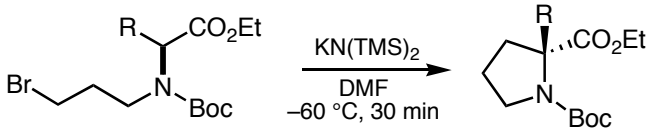

R	ee
Bn	98 (S)
Me_2CH	94 (S)

Provide a rationalization of these results. Three-dimensional drawings are recommended.

Enols & Enolates are the most important nucleophiles in organic & biological chemistry.

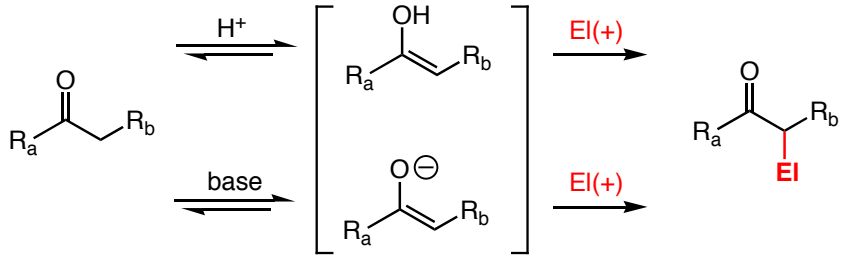

Enamines & metalloenamines, their nitrogen counterparts, are equally important.

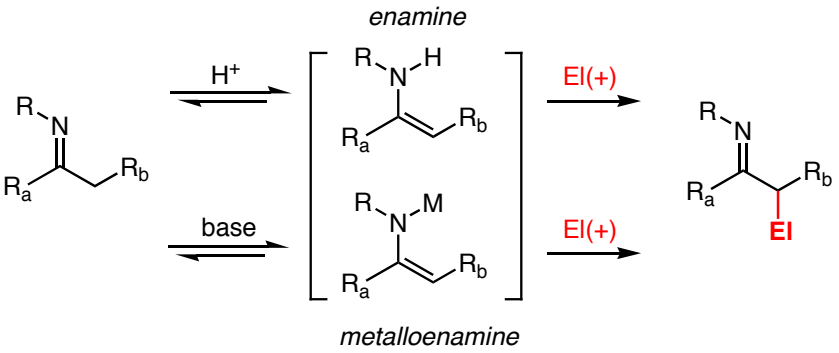

Tautomers: Structural isomers generated as a consequence of the 1,3-shift of a proton adjacent to a X=Y bond. for example:

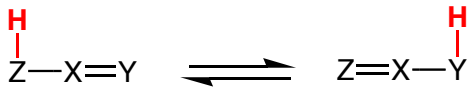

Keto-Enol Tautomers: Tautomerism may be catalyzed by either acids or bases:

base catalysis:

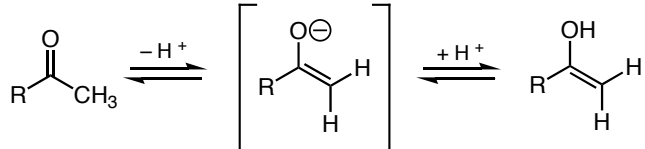

acid catalysis:

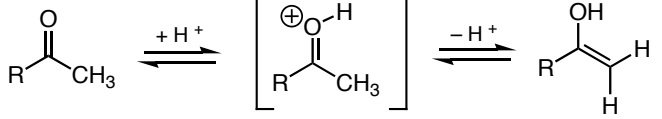

Acidity of Keto and Enol Tautomers: Consider Acetone:

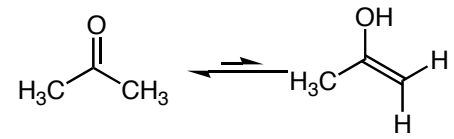

pK = 8.22 (measured)

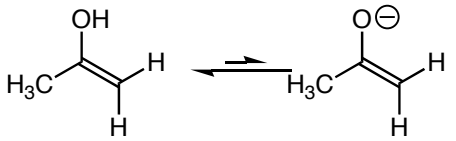

+ H+ pK = 10.94 (measured)

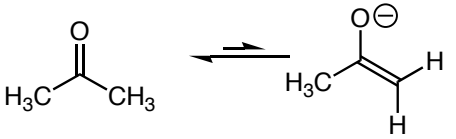

+ H+ pK = 19.16 (calculated)

Kresge, *JACS* **1984**, *106*, 460

On the origin of the acidity of enols: Wiberg, *JACS* **1996**, *118*, 8291-8299

Enolization Kinetics Collum (*J. Org. Chem* **2004**, *69*, 242-249)

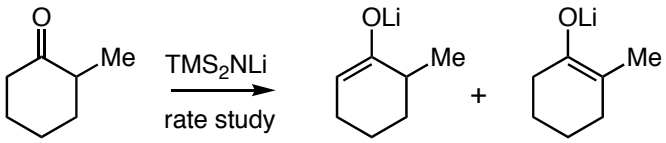

Kinetics suggest $(TMS_2NLi)_2(R_3N)(Ketone)^{‡}$

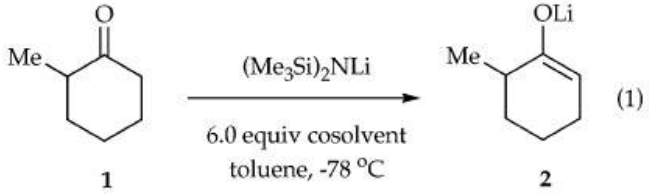

cosolvent:	none	THF	Et_3N
k_{rel}:	1.0	20	3,000

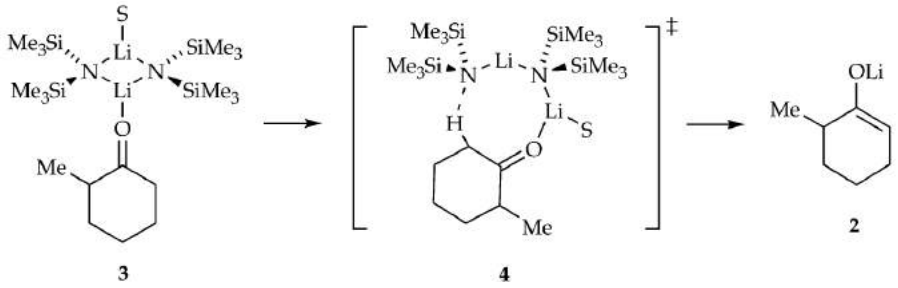

The correlation of high (enolization) rates with solvation of LiHMDS by hindered di- and trialklyamines was traced to steric relief that occurs when the reaction proceeds from the congested dimer-based LiHMDS-ketone complex **3** to the relatively less congested open-dimer-based transition structure **4**.

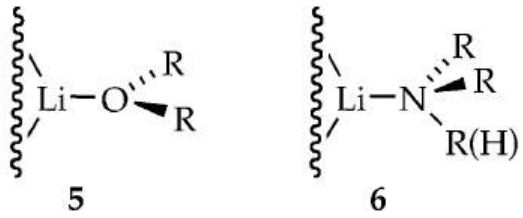

TABLE 2. Relative Rates (k_{rel}) for the Enolization by LiHMDS Solvated by Isostructural Dialkylamines (R_1NHR_2) and Dialkyl Ethers (R_1OR_2)

R_1XR_2	k_{amine}/k_{ether}
$R_1 = R_2 = i$-Bu	2
$R_1 = R_2 = i$-amyl	10
$R_1 = Et$, $R_2 = i$-Pr	35
$R_1 = R_2 = i$-Pr	170
$R_1 = R_2 = s$-Bu	60

In Comparison (Lecture 15)

Enolization: Amide Bases

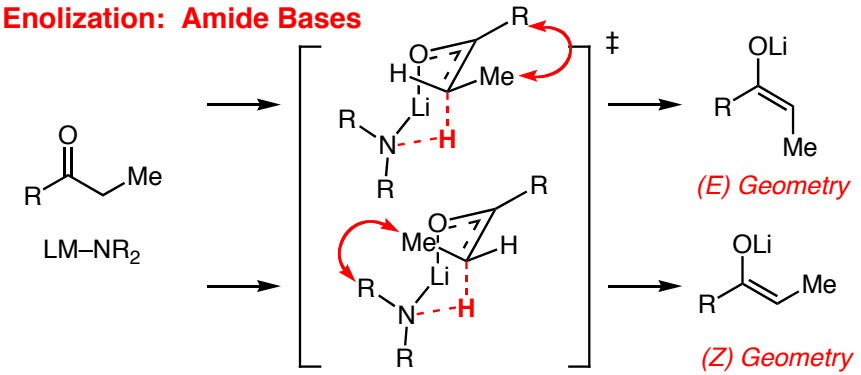

The Ireland Model (*J. Am. Chem. Soc.* **1976**, *98*, 2868)
Narula, Tetrahedron Lett. **1981**, *22*, 4119
more recent study: Ireland, *JOC* **1991**, *56*, 650
For the latest word on this subject see: Xie, *JOC* 1997, *62*, 7516-9

Base Structure

Corey & Co-workers, *Tetrahedron Lett.* **1984**, *25*, 491, 495

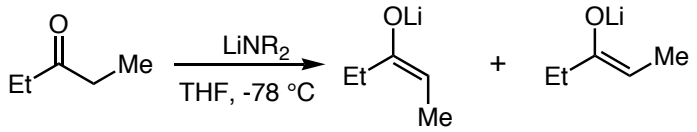

(E) Geometry *(Z) Geometry*

Li–N(i-Pr)$_2$
(LDA) 77 : 23

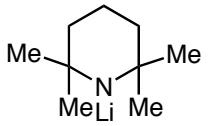

(LiTMP) 86 : 14

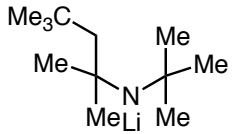

(LOBA) 98 : 2

Lithium Halide Effects

Collum (*J. Am. Chem. Soc.* **1991**, *113*, 9572)
Collum (*J. Am. Chem. Soc.* **1991**, *113*, 9575)
Collum (*J. Am. Chem. Soc.* **1991**, *113*, 5053)

For the latest in the series of Column papers see: *JACS* **2000**, *122*, 2452-2458

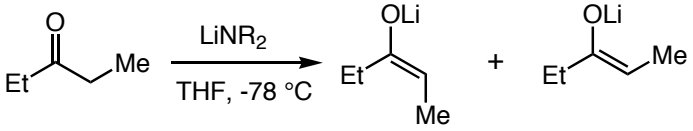

	Ratio, (E):(Z)
LiTMP	86 : 14
LiTMP, 10% LiBr	98 : 2

Enolization in Non-Ethereal Solvents

Collum (*JACS* **2003**, *125*, 14411)

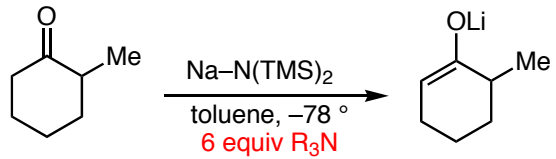

R_3N	none	Me_2NEt	$n\text{-}Bu_3N$	$1\text{-}Bu_3N$
k_{rel}	1	200	3000	1

Reaction kinetics suggest $(TMS_2NLi)_2(R_3N)(Ketone)^{‡}$

Regioselective Enolization

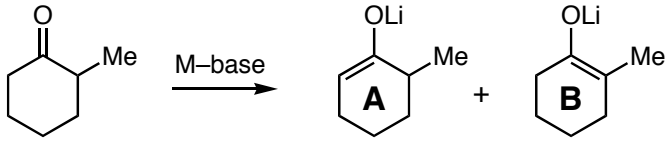

Base	temp	control	Ratio (A:B)
LiN(i-Pr)$_2$	–78 °	kinetic	99:1
LiN(SiMe$_3$)$_2$	–78 °	kinetic	95:5
Ph_3C–Li	–78 °	kinetic	90:10
Ph_3C–Li	heat	thermo	10:90
Na–H	heat	thermo	26:74
K–H	heat	thermo	38:62

A: Alkyl groups stabilize metal enolate

A: As M–O bond becomes more ionic A is attenuated

Kinetic Selection sensitive to structure

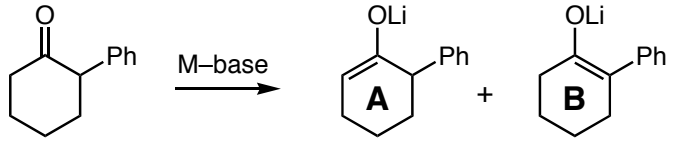

ratio: 99:1

estimated pKa's (Bordwell)

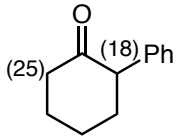

A ⇌ B

pKeq est: 7 (10^{+7})

Unsaturated Ketones

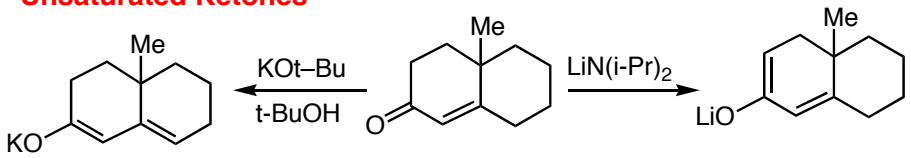

thermodynamic enolate

see kinetic acidity handout for an extensive compilation of cases.

kinetic enolate

Kinetic Selection sensitive to structure

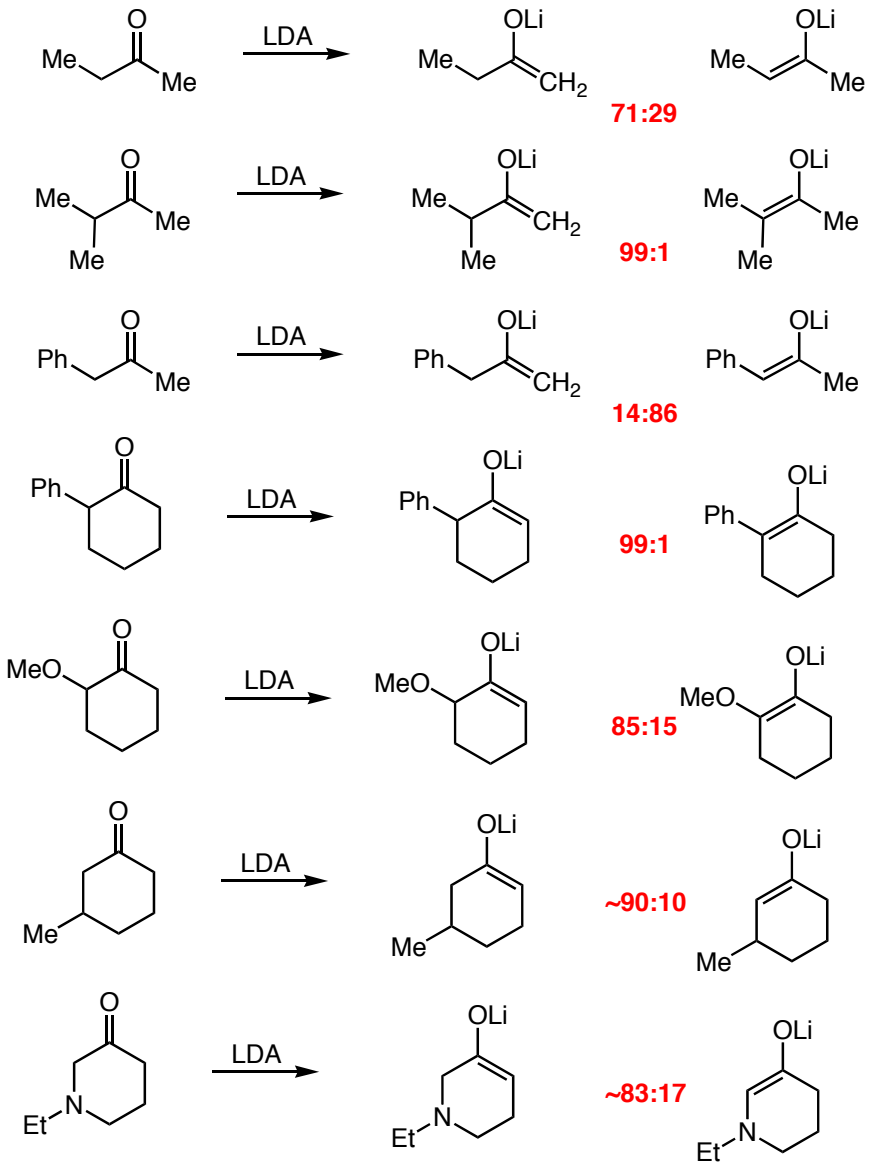

Kinetic Selection in Enolization of Unsaturated Ketones

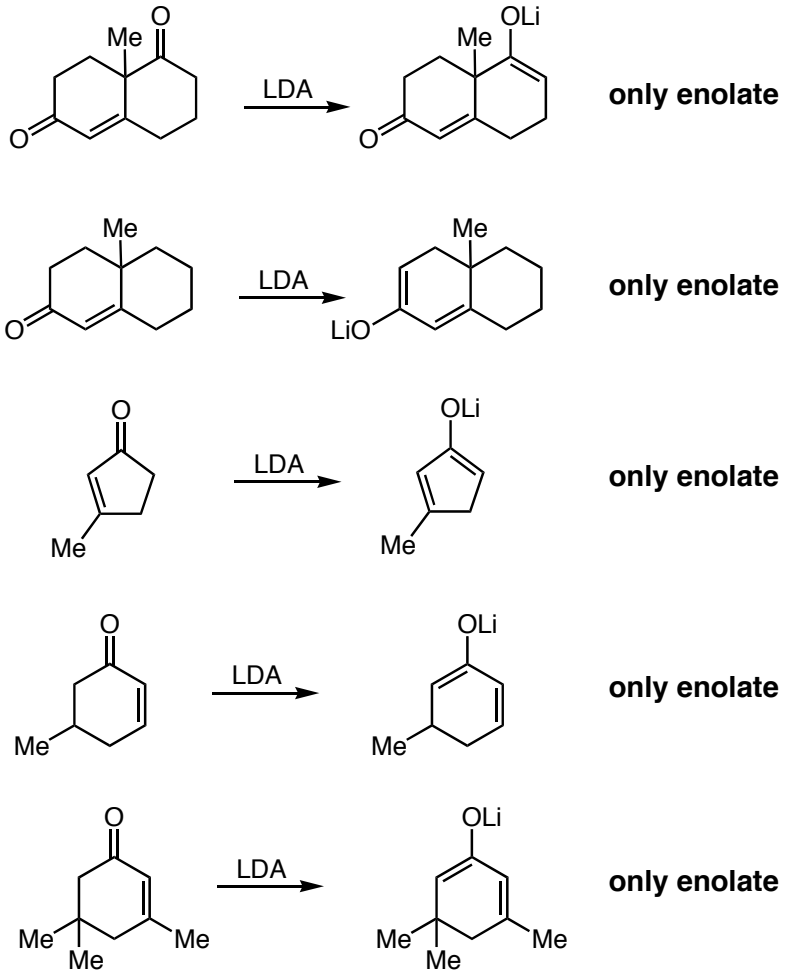

Enolate Structures from X-ray Diffraction

Metal Tautomerism

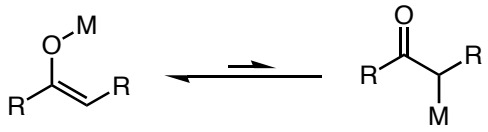

For alkali metal enolates (M = Li, Na, K etc.) the O-metal tautomer is strongly favored. This generalization holds for most alkaline earth enolates (Mg^{+2}) as well. These are the generally useful enolate nucleophiles

For certain metal enolates from heavy metals such as M = Hg^{+2} the C-metal tautomer is sometimes favored.

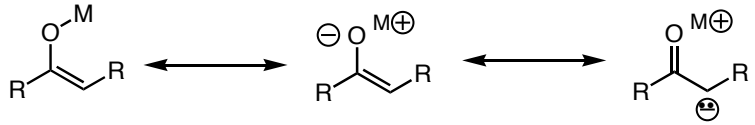

Resonance Structures

O^- resonance structure

C^- resonance structure

Since enolates usually function as carbon nucleophiles, it is therefore of some interest to assess the relative importance of the illustrated contributing polar resonance structures. Within the last decade good X-ray crystal structures of a number of metal enolates have been obtained.

One would predict that as the relative importance of the C^- structure increases, the C–O bond would shorten and the C–C bond would lengthen.

The prediction stated above does hold, but the net change in the C–C bond length is < 2 % !

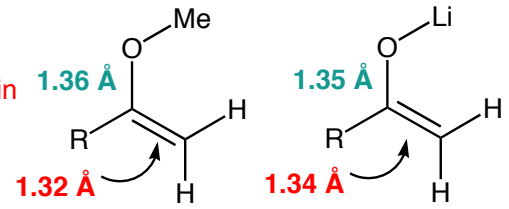

In solution and in the solid state metal enolates have a strong tendency to aggregate into dimers and tetramers to satisfy metal solvation requirements.

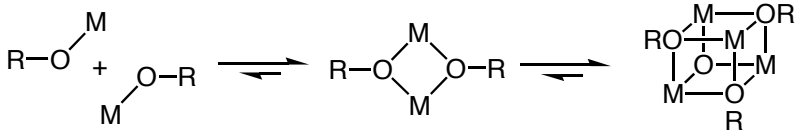

Ab initio calculations (Spartan) indicate that the partial negatilve charge on the alpha carbon is ~ – 0.22 for the Li enolate

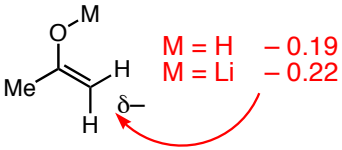

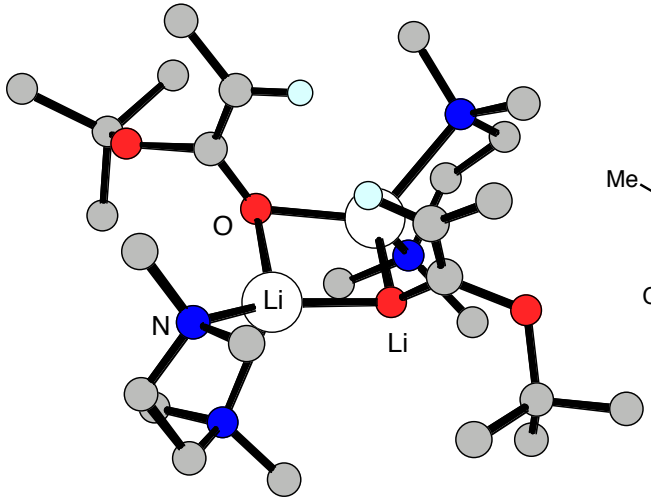

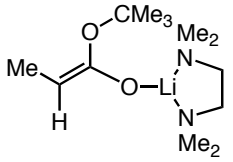

Crystallized as the dimer

Seebach & co-workers, *J. Am. Chem. Soc.* **1985**, *107*, 5403.

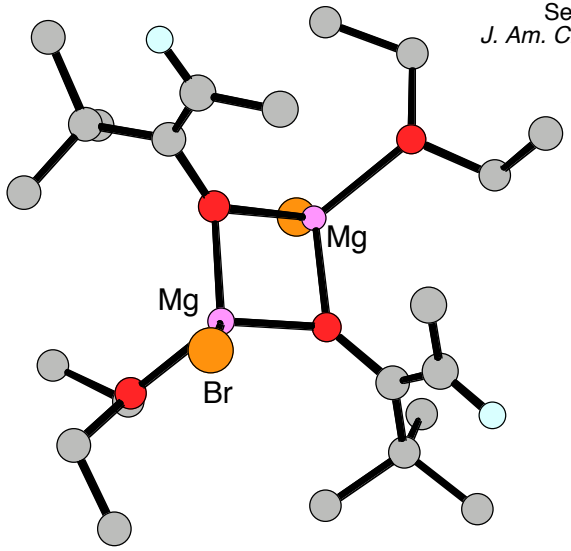

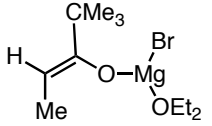

Crystallized as the dimer

Li Enolates

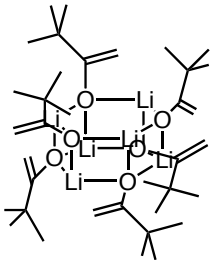

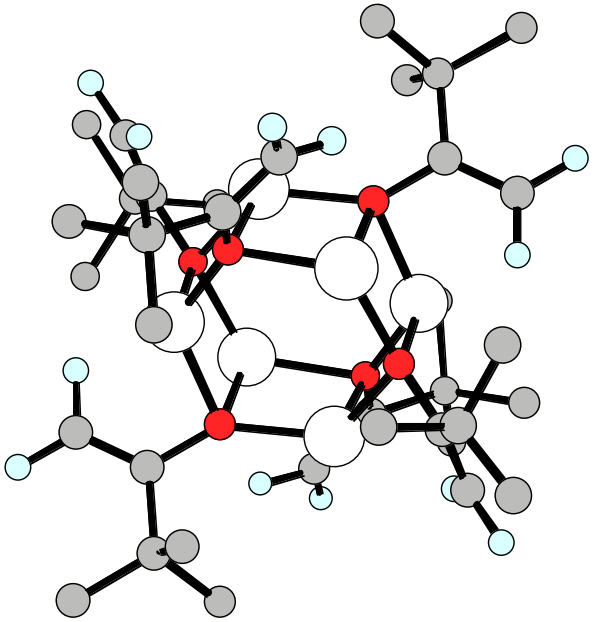

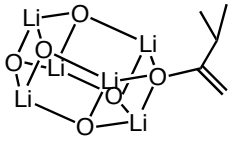

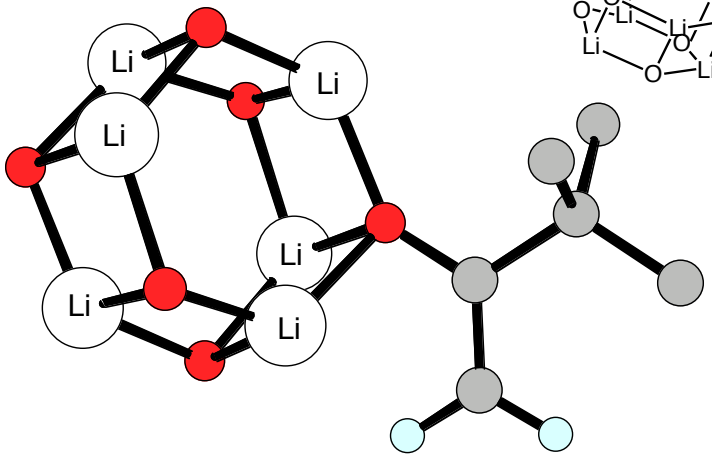

Williard, P. G.; Carpenter, G. B. *J. Am. Chem. Soc.* **1986**, *108*, 462-468.

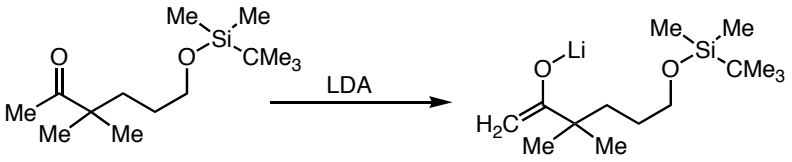

Williard, P. G.; Hintze, M. J. *J. Am. Chem. Soc.* **1987**, *109*, 5539-5541.

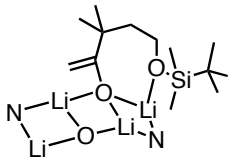

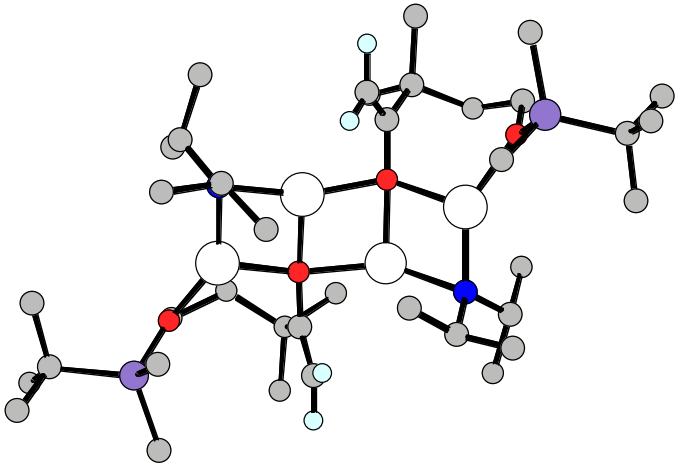

Zn Enolates

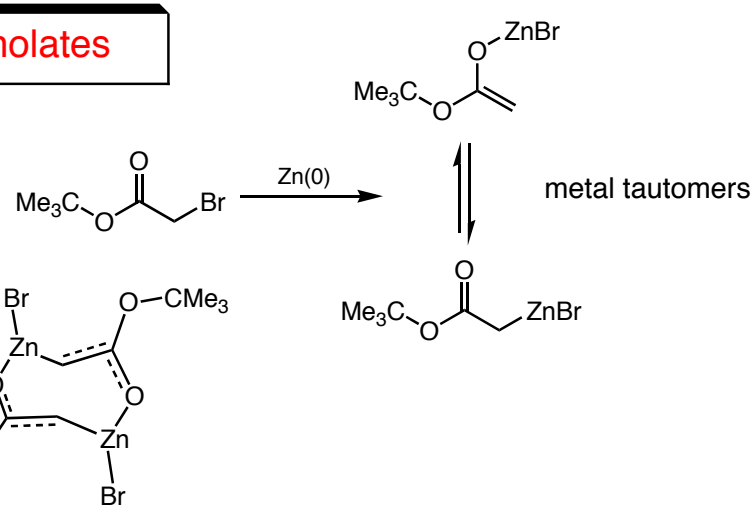

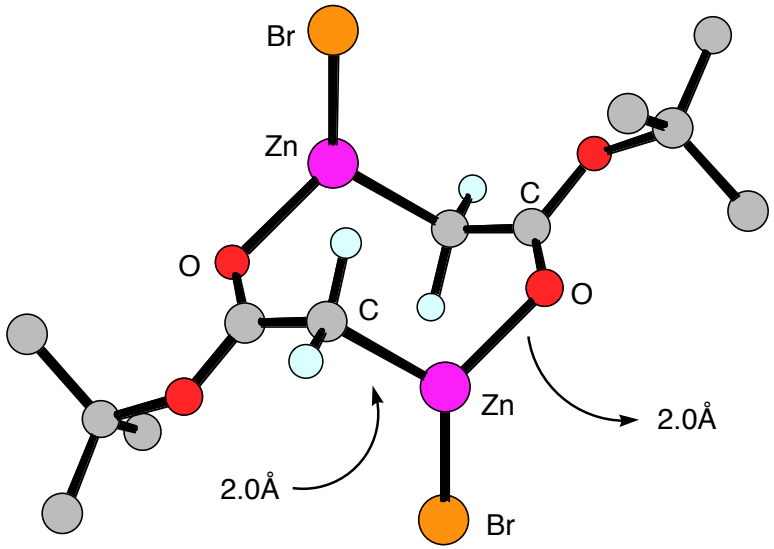

Dekker, J.; Boersma, J.; van der Kerk, G. J. M. *J. Chem. Soc. Chem. Commun.* **1983**, 553.

Dekker, J.; Budzelaar, J.; Boersma, J.; van der Kerk, G. J. M. *Organometallics* **1984**, *3*, 1403.

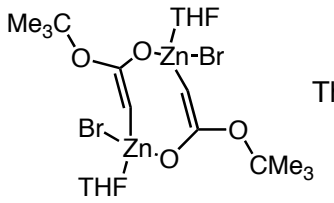

The THF Complex

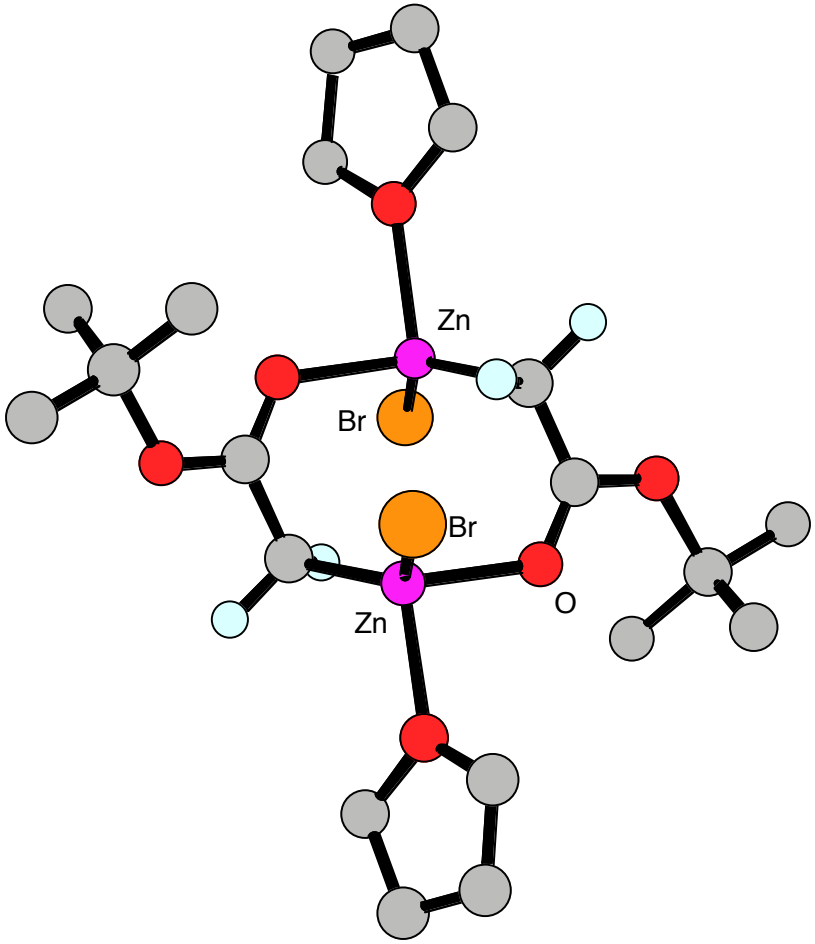

Metalloenamine X-ray Structures

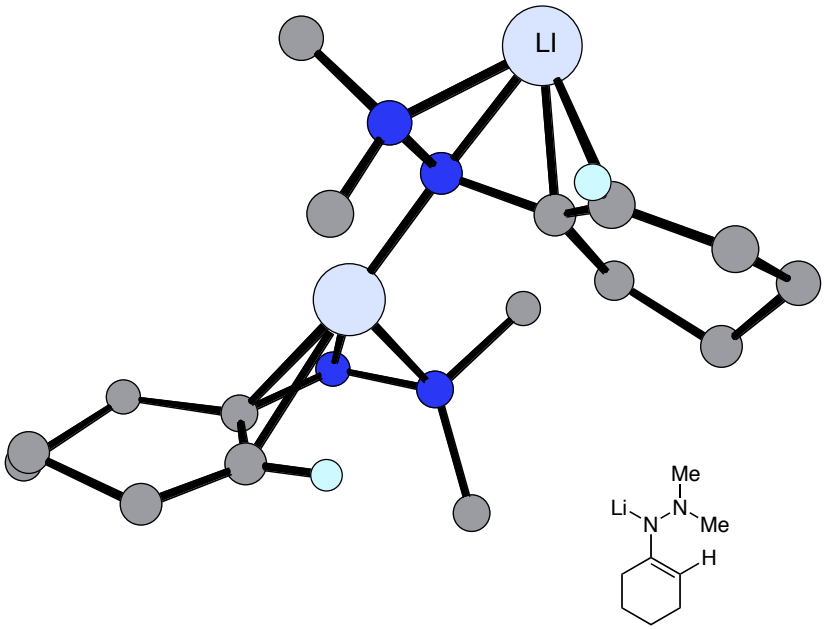

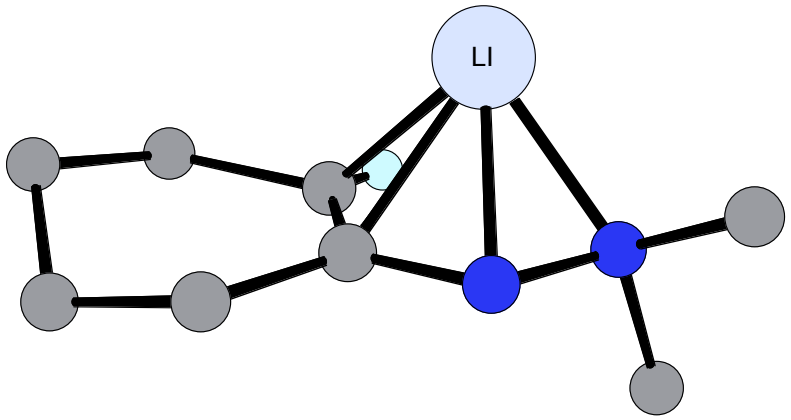

Collum & Clardy, *JACS* **1984**, *106*, 4865

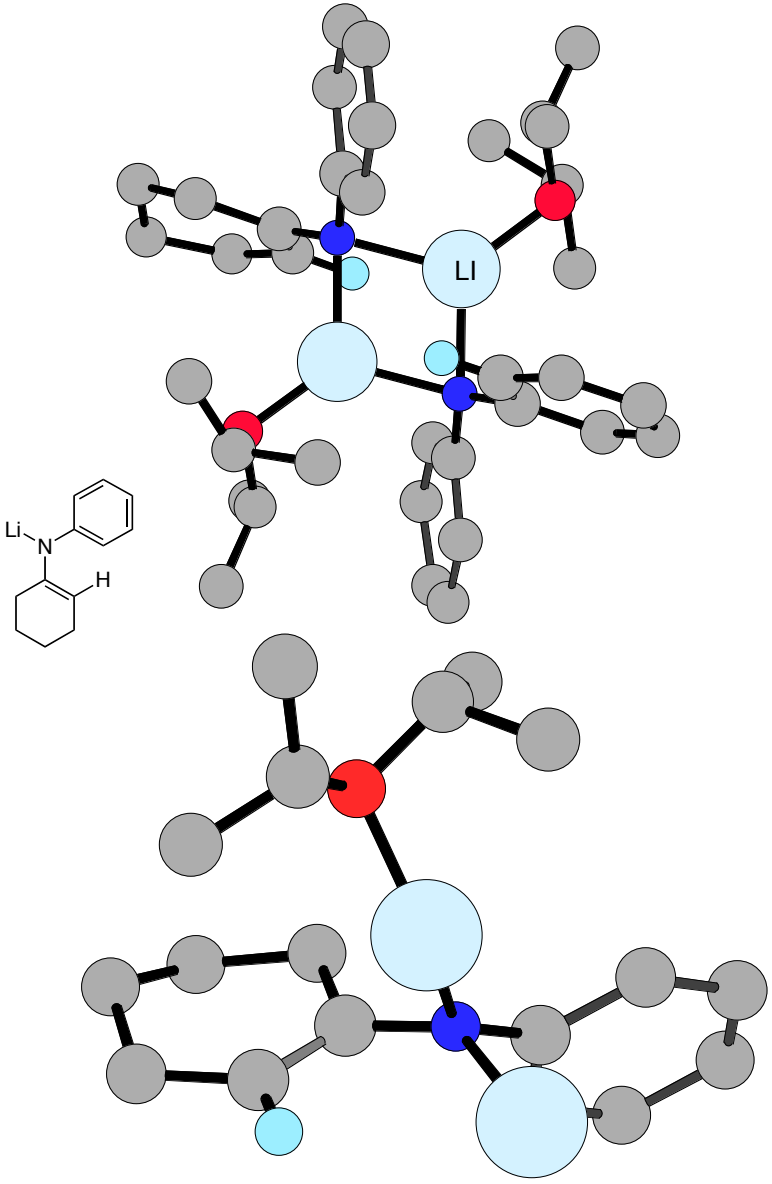

The Reformatsky Reaction

The "Classical" Reformatsky Process

Review: *Comprehensive Organic Synthesis*, **1991**; Vol 2, Chapter 1.8, pp 277-299
Fürstner, A. "Recent Advances in the Reformatsky Reaction." *Synthesis* **1989**, 571.

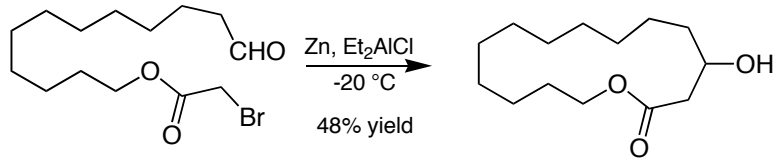

H. Nozaki & Co-workers,
J. Am. Chem. Soc. **197**, *99*, 7705

Both cyclic and acyclic cases studied (11 cases).

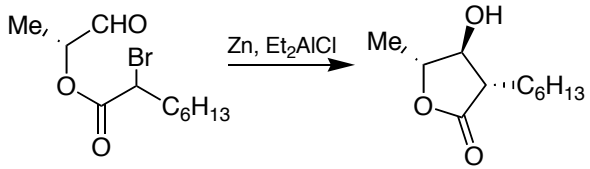

diastereoselection 10:1
55% yield

T. Nishida & Co-workers,
Tetrahedron **1991**, *47*, 6623.

Based on the Nozaki recipe *JACS* **1977**, *99*, 7705

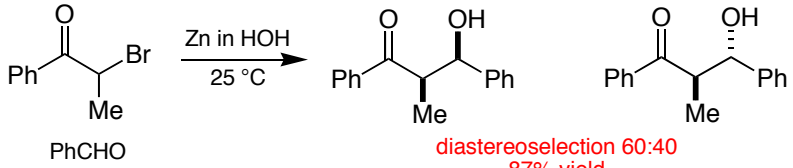

PhCHO

diastereoselection 60:40
87% yield

T. H. Chan & Co-workers,
Chem. Commun. **1990**, 505.

Rxns carried out in water with either activated Zn or Sn.
19 cases reported.

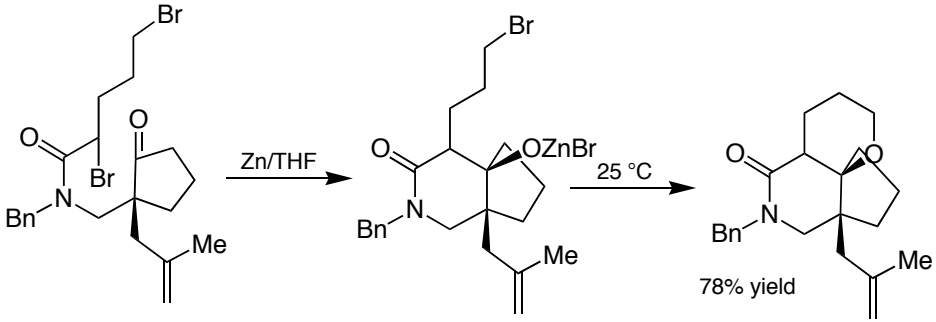

78% yield

C. H. Heathcock & Co-workers,
J. Org. Chem. **1987**, *52*, 5745.

The Samarium(II) Variant

Molander, "Reductions with Samarium (II) Iodide." *Org. Reactions* **1994**, *46*, 211-367.

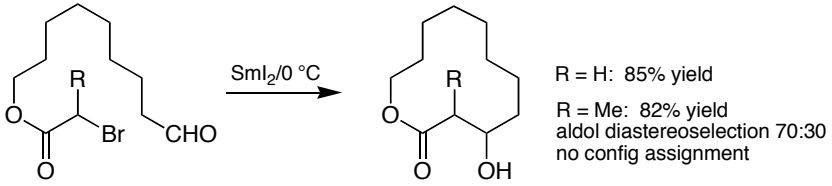

R = H: 85% yield
R = Me: 82% yield
aldol diastereoselection 70:30
no config assignment

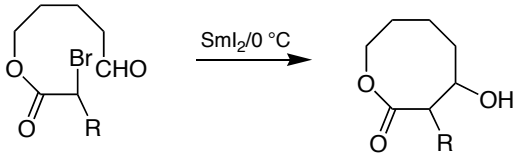

R = H: 76% yield
R = Me: 82% yield
aldol diastereoselection 62:38
no config assignment

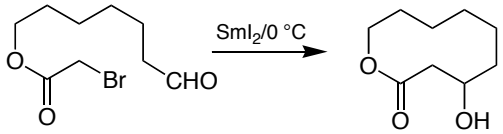

82% yield

Good entry into prior literature

T. Tabushi & Co-workers,
Tetrahedron Lett. **1986**, *27*, 3889.

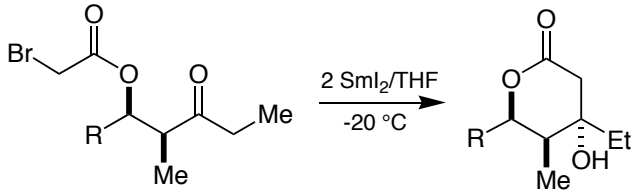

8: 1 diastereoselection
97% yield

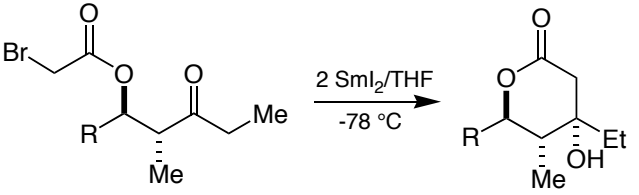

one isomer? 86% yield

G. A. Molander & Co-workers,
J. Am. Chem. Soc. **1987**, *109*, 6556.

Proposed Transition structure

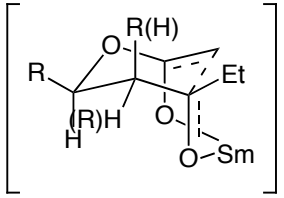

http://www.courses.fas.harvard.edu/colgsas/1063

Chemistry 206

Advanced Organic Chemistry

Lecture Number 25

Enolates & Metalloenamines-2

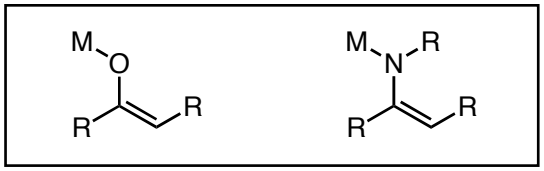

- Concept of Soft Enolization
- Introduction and General Trends
- Enolate Alkylation: Electronic & Steric Control Elements
- Enolate Alkylation: Unusual Cases
- Chiral Amide Enolates
- Chiral Ester Enolates
- Chiral Imide Enolates

Reading Assignment for this Week:

Carey & Sundberg: **Part A**; Chapter 7
Carbanions & Other Nucleophilic Carbon Species

Carey & Sundberg: **Part B**; Chapter 2
Reactions of Carbon Nucleophiles with Carbonyl Compounds

D. A. Evans

Wednesday
November 15, 2006

Assigned Journal Articles

"Structure and Reactivity of Lithium Enolates. From Pinacolone to Selective C-Alkylations of Peptides. Difficulties and Opportunities Afforded by Complex Structures".
D. Seebach *Angew. Chem. Int. Ed. Engl.*, **27**, 1624 (1983). **(handout)**

"Self-Regeneration of Stereocenters (SRS)-Applications, Limitations, & Abandonment of a Synthetic Principle",
D. Seebach et al. *Chem. Int. Ed. Engl.*, **35**, 2708 (1996). **(handout)**

Other Useful References

"Advances in Asymmetric Enolate Methodology" Arya, Qin, *Tetrahedron* **2000**, *56*, 917-947 **(pdf)**

"Stereoselective Alkylation Reactions of Chiral Metal Enolates".
D. A. Evans *Asymmetric Synthesis*, **3**, 1 (1984).

"Generation of Simple Enols in Solution". Capon, Guo, Kwok, Siddhanta, and Zucco *Acc. Chem. Res.* **21**, 121 (1988).

"Keto-Enol Equilibrium Constants of Simple Monofunctional Aldehydes and Ketones in Aqueous Solution". Keeffe, Kresge, and Schepp *JACS*, 112, 4862 (1990).

"pKa and Keto-Enol Equilibrium Constant of Acetone in Aqueous Solution". Chiang, Kresge, and Tang *JACS* **106**, 460 (1984).

Explain why **A** is favored for X = O while **B** is favored for X = NNHR

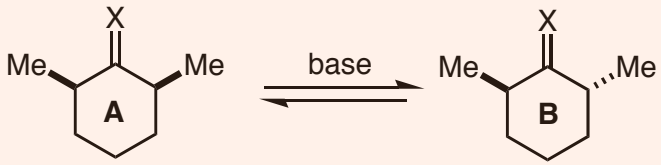

Manuscript for Submission to Angew. Chemie
Provided to you as an electronic handout

Soft Enolization: A Powerful Method for Diastereoselective Carbon-Carbon Bond Formation

David A. Evans[*] and Jared T. Shaw[†]

Strategy

Choose Lewis Acid (LA) which can reversibly associate with amine base (B:).

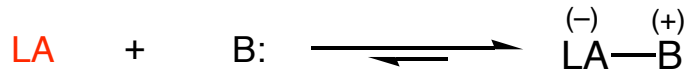

This system has the potential to enolize carbonyl functional groups:

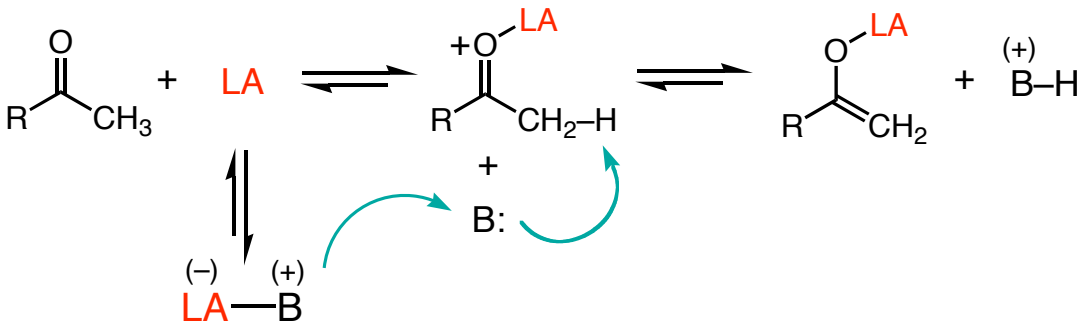

Mild Methods for Forming Enolates

Lewis Acid C=O Complexation Enhances C–H Acidity (Computation)

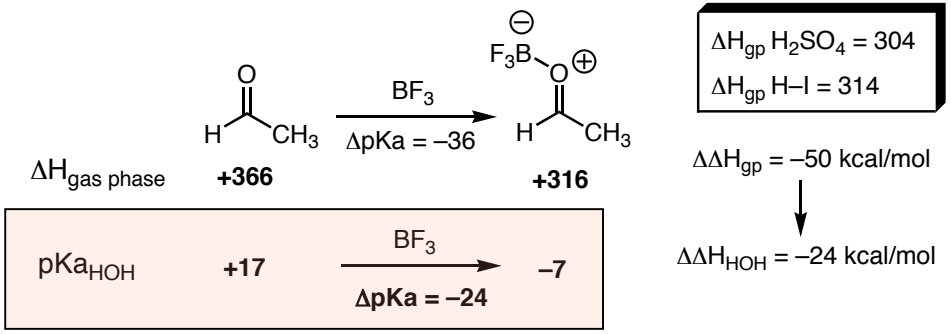

BF_3 complexation generates a "superacid" comparable to the acidity of H_2SO_4

Ren et al, *JACS* **1999**, *121*, 2633-2634 **(pdf)**

Some qualitative observations (Evans Group, Unpublished))

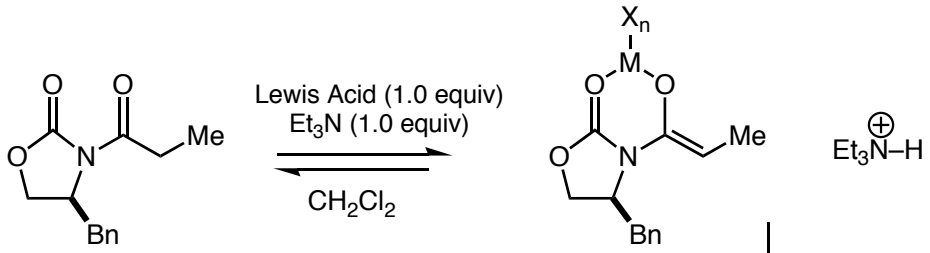

Lewis Acid (MX_n)	% deuterium
$TiCl_4$	100
$TiCl_3(O\textit{i}\text{-Pr})$	100
$TiCl_4{\bullet}(THF)_2$	80
$TiCl_2(O\textit{i}\text{-Pr})_2$	70
$AlCl_3$	70
$MgBr_2{\bullet}OEt_2$*	25
$TiCl(O\textit{i}\text{-Pr})_3$	10
$SnCl_4$, Et_2AlCl, $ZrCl_4$	0

*2.0 equiv required

In these experiments, the Lewis acid was added first followed by the amine.

Some qualitative observations (Evans Group, Unpublished))

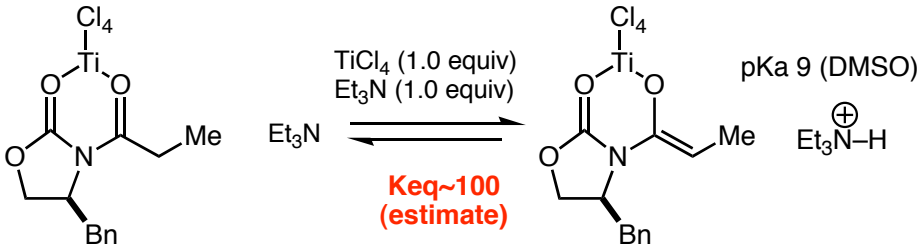

estimated pKa (DMSO)???

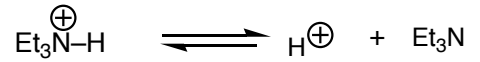

pK

+9

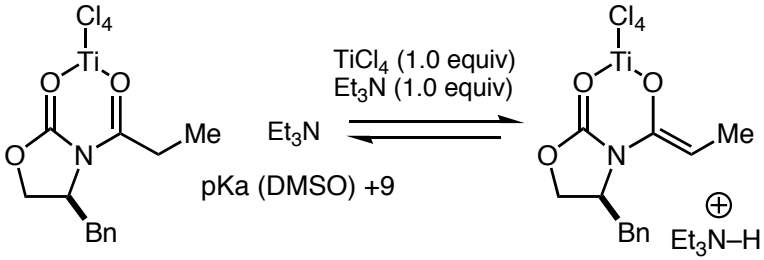

–2

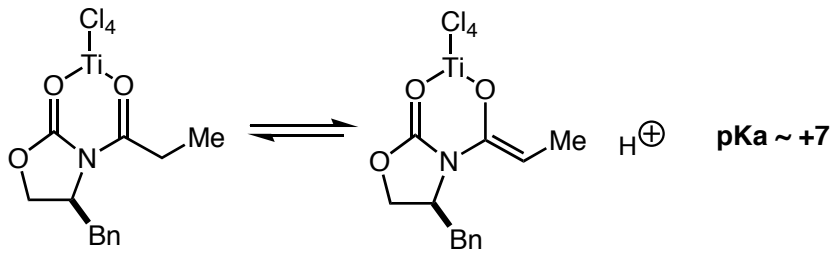

pKa ~ +7

estimated pKa (DMSO) ~ +7

Hence $TiCl_4$ complexation lowers acidity by **~20 pka units.** this number is the same mgnitude as the BF_3–acetaldehyde case just discussed

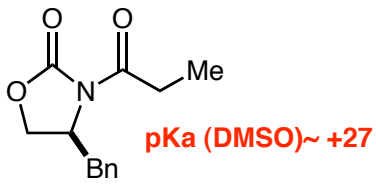

pKa (DMSO)~ +27

Strategy

Choose Lewis Acid (LA) which can reversibly associate with amine base (B:).

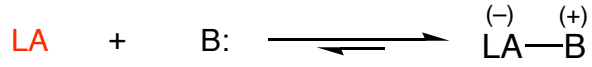

This system has the potential to enolize carbonyl functional groups:

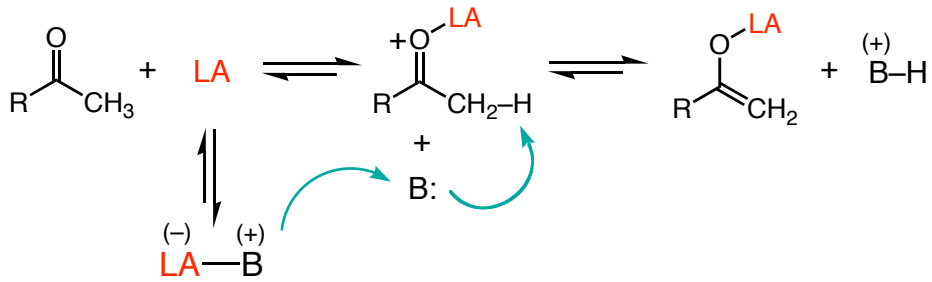

Useful Lewis Acid Pairs Complexation

$^{-}OTf = {}^{-}OSO_2CF_3$

$MgBr_2$ + NEt_3	Reversible
$Li^{-}X$ + NR_3	Reversible
$Sn(OTf)_2$ + NR_3	Reversible (Et_3N, EtNi-Pr_2)
$R_2B^{-}OTf$ + NR_3	Reversible (Et_3N, EtNi-Pr_2)
R_2BCl + NR_3	Reversible (Et_3N, EtNi-Pr_2)
$PhBCl_2$ + NR_3	Reversible (Et_3N, EtNi-Pr_2)
$TiCl_4$ + NR_3	Irreversible (Et_3N, EtNi-Pr_2)
$i^{-}PrOTiCl_3$ + NR_3	Reversible (Et_3N, EtNi-Pr_2)
$(i^{-}PrO)_2TiCl_2$ + NR_3	Reversible (Et_3N, EtNi-Pr_2)
$(i^{-}PrO)_3TiCl$ + NR_3	Reversible (Et_3N, EtNi-Pr_2)

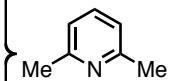

All of the above systems will enolize simple ketones to some extent.

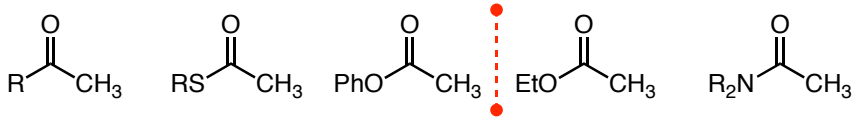

100% enolization for B, Sn, Ti
partial enolization for Li, Mg

Lithium Enolates

Horner-Wadsworth-Emmons Reaction.

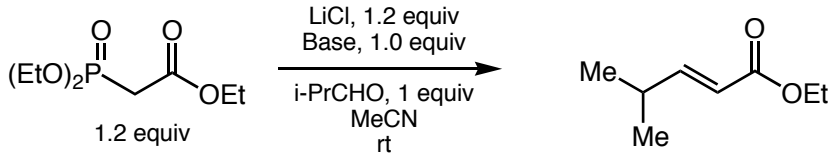

pKa 19.2 (DMSO), K^{+} counterion
pKa 12.2 (Diglyme), Li^{+} counterion

Roush & Masamune, Tet. Lett. 1984, 25, 2183-2186

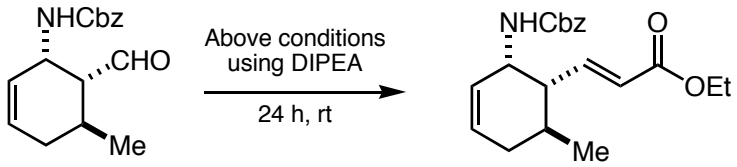

85% + 10% recovered aldehyde

Conventional methods of deprotonation (NaH) resulted in epimerization (Overman *JACS* **1978**, 5179).

Magnesium Enolates

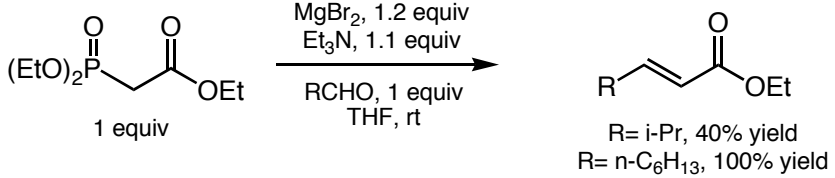

R= i-Pr, 40% yield
R= n-C_6H_{13}, 100% yield

Rathke, Nowak *J. Org. Chem.* **1985**, *50*, 2624-2626.

Magnesium Enolates

Rathke *J. Org. Chem.* **1985**, *50*, 2622-2624.
J. Org. Chem. **1985**, *50*, 4877-4879.
Syn. Comm. **1986**, *16*, 1133-1139.

Diethylmalonate acylations

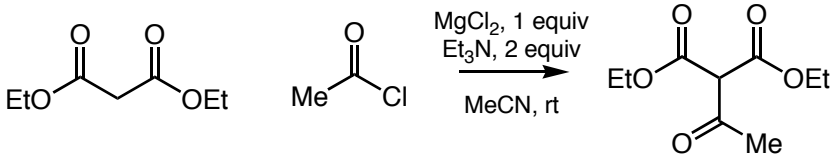

85% yield

Ketone Carboxylation

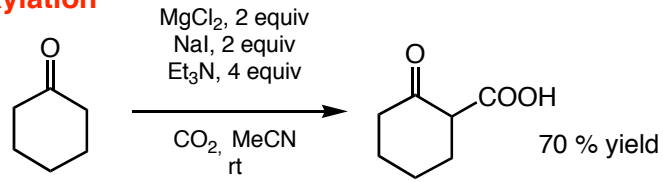

70 % yield

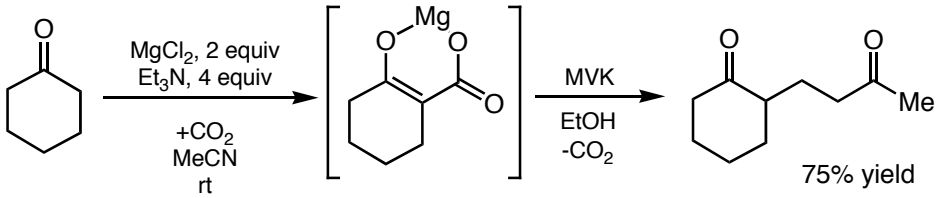

75% yield

Michael reaction

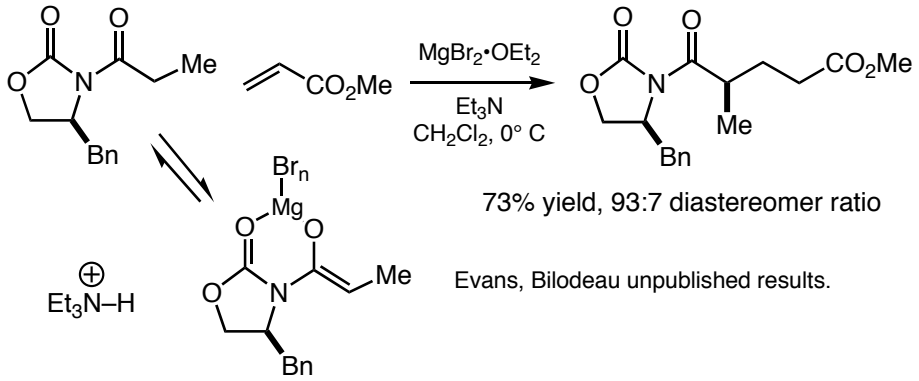

73% yield, 93:7 diastereomer ratio

Evans, Bilodeau unpublished results.

Deuterium quench indicates 25% enolization of *N*-propionyloxazolidinone

Titanium Enolates

The Early Literature

Lehnert, W. *Tetrahedron Lett.* 1970, 4723-4724.

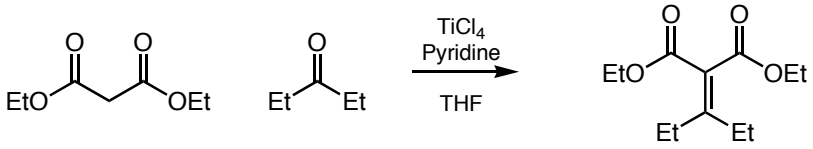

75% yield

Harrison, C. R. *Tetrahedron Lett.* 1987, *28*, 4135-4138.

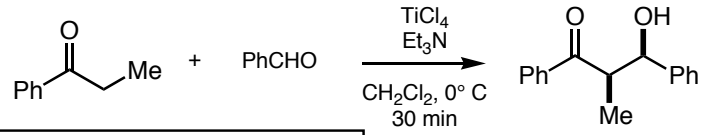

Ketone and aldehyde combined followed by sequential addn of $TiCl_4$ and then amine

91% yield
95:5 syn/anti

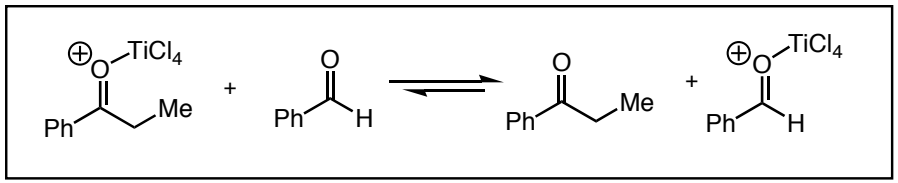

Brocchini, Eberle, Lawton *J. Am. Chem. Soc.* 1988, *110*, 5211-5212.

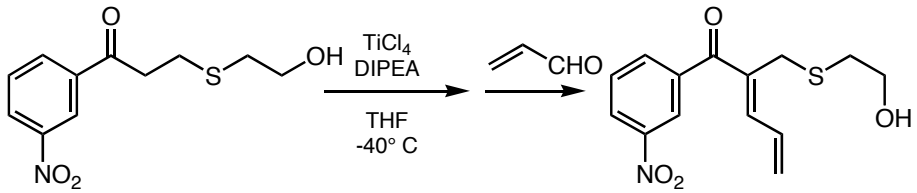

10-15:1 Z/E

Titanium Enolates

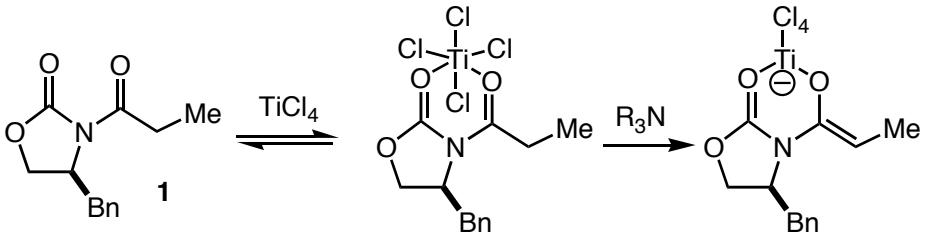

- Enolization process not responsive to tertiary amine structure
- DIPEA, Et_3N, N-Ethylpiperidine all suitable bases.
- DBU and tetramethylguanidine do not provide enolate.
- CH_2Cl_2 is the only suitable solvent for these enolizations.

N-Propionyloxazolidone (**1**)

Lewis Acid	% Enolization
$TiCl_4$	100
i-PrOTiCl$_3$	100
$TiCl_4$•2THF	80
(*i*-PrO)$_2$TiCl$_2$	70
(*i*-PrO)$_3$TiCl	~10

Ethylisopropylketone

Lewis Acid	% Enolization
$TiCl_4$	100
i-PrOTiCl$_3$	80
(*i*-PrO)$_2$TiCl$_2$	50

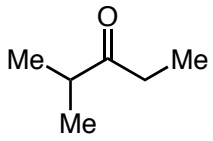

- Order of addition of reagents is important for $TiCl_4$.

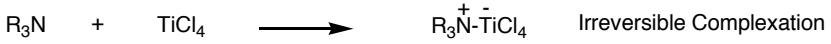

- Order of addition of reagents is not important for *i*-PrOTiCl$_3$ or (*i*-PrO)$_2$TiCl$_2$.

- Enolizable substrates:

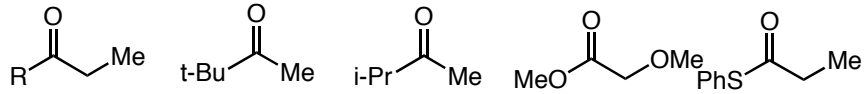

- Substrates Which present problems:

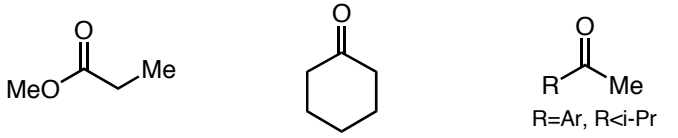

self condensation *self condensation*

Reactions with Representative Electrophiles

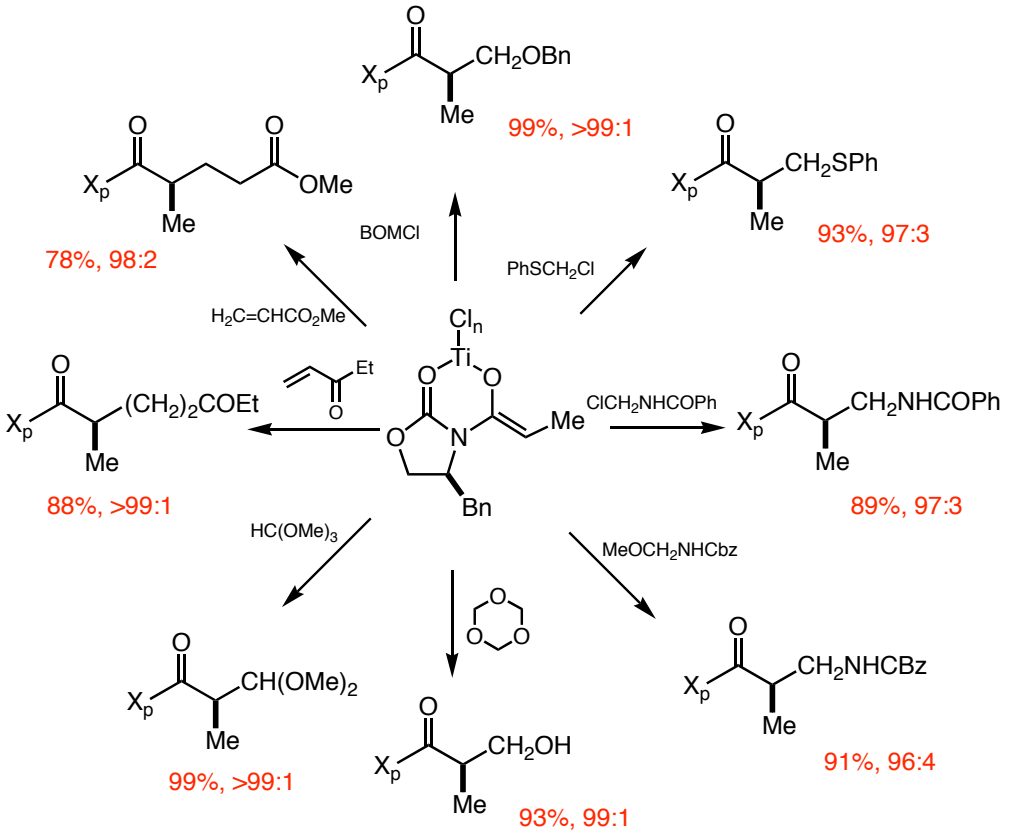

J. Am. Chem. Soc. **1990**, *112*, 8215-8216.; *J. Org. Chem.* **1991**, *56*, 5750-5752.

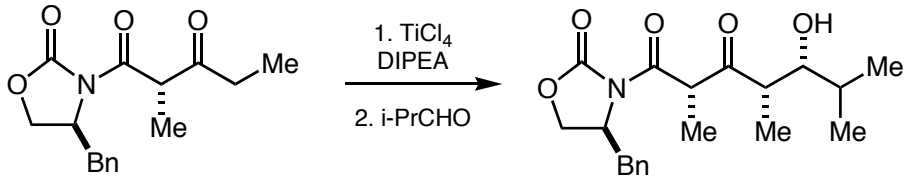

86% yield, >99:1

Evans, Clark, Metternich, Novack, Sheppard *J. Am. Chem. Soc.* **1990**, *112*, 866.

Dialkylboron Triflates

Di-n-butylboron triflate

Mukaiyama, Inoue *Chem. Lett.* **1976**, 559-562.
Bull. Chem. Soc. Jpn. **1980**, *53*, 174-178.

Enolizes ketones with 2,6-lutidine or DIPEA in ethereal solvents.

Diastereoselective Aldol Reactions of Boron Enolates.

Evans, Vogel, Nelson *J. Am. Chem. Soc.* **1979**, *101*, 6120.
Evans, Nelson, Vogel, Taber *J. Am. Chem. Soc.* **1981**, *103*, 3099-3111.
Evans, Bartroli, Shih *J. Am. Chem. Soc.* **1981**, *103*, 2127.
Masamune, S. et. al. *Tetrahedron Lett.* **1979**, 2225, 2229, 3937.
Masamune, S. et. al. *J. Am Chem. Soc.* **1981**, *103*, 1566-1568.

Chiral dialkylboron triflates

Masamune, Sato, Kim, Wollmann
J. Am. Chem. Soc. **1986**, *108*, 8279-8281.

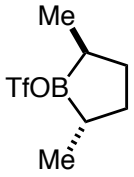

Paterson, I. et. al.

Tetrahedron **1990**, *46*, 4663-4684.
Tetrahedron Lett. **1989**, *30*, 997-1000.
Tetrahedron Lett. **1986**, *27*, 4787-4790.

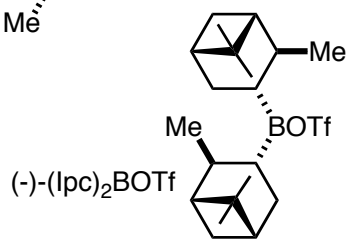

Enolate Stereochemistry

Evans, Nelson, Vogel, Taber *J. Am. Chem. Soc.* **1981**, *103*, 3099-3111.
Goodman, *Tetrahedron Lett.* **1992**, *33*, 7219.
Enolization Model: Paterson, *Tetrahedron Lett.* **1992**, *33*, 7223.

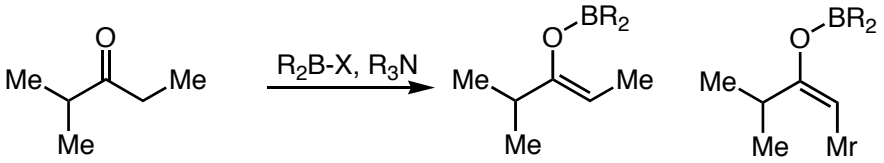

9-BBN-OTf, Et_3N ratio ~ 88: 12

Cy_2B-Cl, Et_3N ratio ~ 3: 97

Brown, *J. Org. Chem.* **1993**, *58*, 147-153

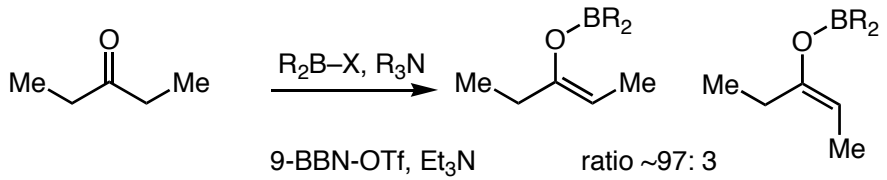

9-BBN-OTf, Et_3N ratio ~97: 3

Cy_2B-Cl, Et_3N ratio 21:79

Bu_2B-OTf, Et_3N ratio ~97: 3

Borane and lutidine or DIPEA form 1:1 complex with L_2B-OTf. Complexation reversible as enolization will occur upon addition of ketone. Less hindered nitrogen bases - pyridine, Dabco, DBU, irreversibly complex with L_2B-OTf.

The Ketone-Boron Complexes as enolate precursors:

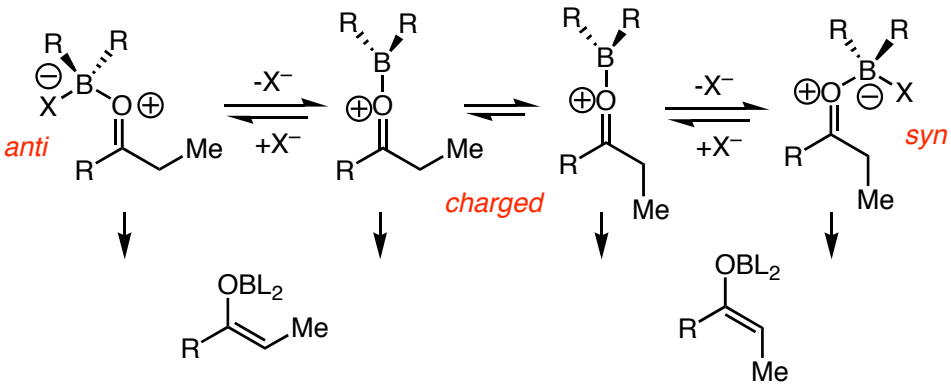

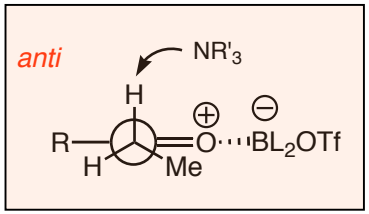

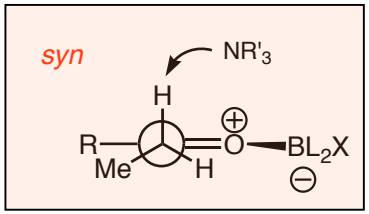

Cy_2BCl-ketone complex may deprotonate through syn complex

R_2BOTf-ketone complex may deprotonate through charged complex with (Z) preference

Question: Why do we generally show enolates reacting with electrophiles at carbon as opposed to oxygen ?? Let's begin the the discussion with an observation:

■ "As electrophile reactivity increases, the percentage of reaction at the enolate oxygen increases." For example, consider the reactions of cyclohexanone enolate with the two electrophiles, methyl iodide and the much more reactive acetyl chloride:

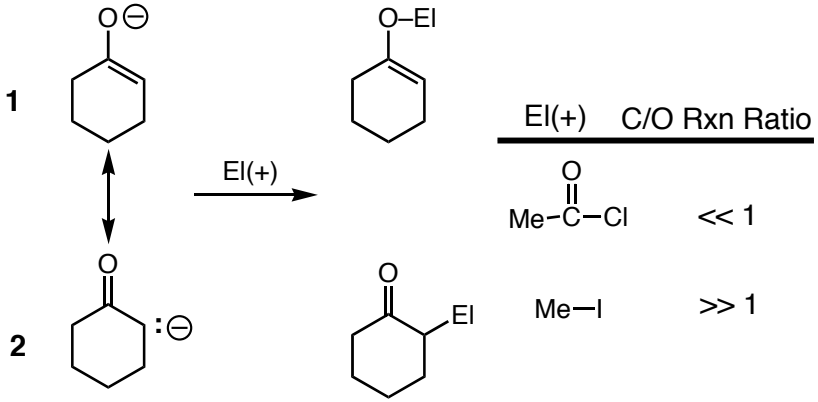

El(+)	C/O Rxn Ratio
Me–C(=O)–Cl	<< 1
Me–I	>> 1

■ The very reactive acid chloride gives almost exclusively the O-acylation product while the less reactive methyl iodide affords the alternate C-alkylation product.

These results may be understood in the context of qualitative statements made by Hammond (**The Hammond Postulate**) and Hine (**The Principle of Least Motion**)

The Principle of Least Motion:
"As reactions become more exothermic, the favored reaction becomes that path which results in the least structural (electronic) reorganization."

See Hine in *Advances in Phys. Org. Chem.* **1977**, *15*, 1-61

Since the X-ray data clearly support the picture that resonance structure **1** best represents the enolate structure, highly reactive electrophiles will favor O-attack according to Hine's generalization.

The Hammond Postulate is also relevant to this issue and is broadly used to make qualitative statements about transition state structure.

Hammond, *JACS* **1955**, *77*, 334 (handout)

■ In attempting to grasp the Hammond Postulate, let's consider two extreme reactions, one which is strongly endothermic and one which is strongly exothermic.

Strongly Exothermic Reactions
$\Delta H^\circ > 20$ kcal/mol

B ⟶ A

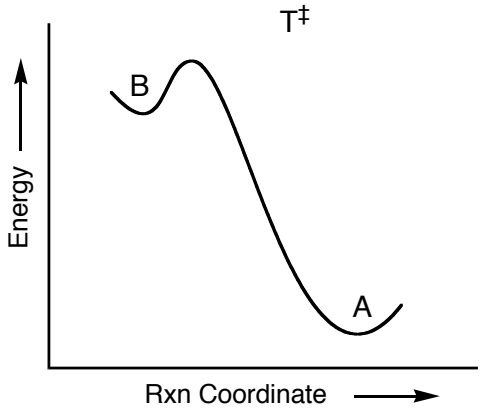

Hammond Postulate
"For strongly exothermic reactions, the transition state T‡ looks like reactant(s) e.g. B."

■ As applied to the enolate-electrophile reaction, for very exothermic reactions, e.g. the reaction with acetyl chloride, the transition state for the process will involve little enolate structural reorganization. Hence in this instance the electrophile heads for the site of highest electron density

Carey & Sundberg: **Part A**; Chapter 4, pp217-220
for discussion of Hammond's Postulate

Based upon the above discussion draw a detailed mechanism for the protonation of cyclohexanone enolate.

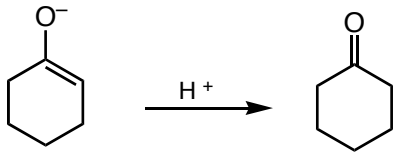

■ Metalloenamines:

Imines may be transformed into their conjugate bases (enolate counterparts) with strong bases:

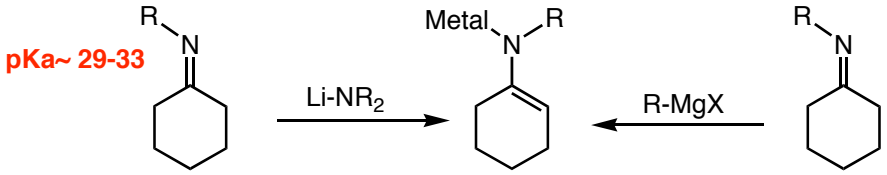

The usual bases employed are either lithium amides (LDA) or Grignard reagents. Note that Grignard reagents do not add to the C=N pi-bond due to the reduced dipole. With this functional group, deprotonation is observed to be the preferred reaction.

■ When to use a metalloenamine:

Metalloenamines are significantly more nucleophilic than ketone or aldehyde enolates. They are used when less reactive electrophiles are under consideration. For example:

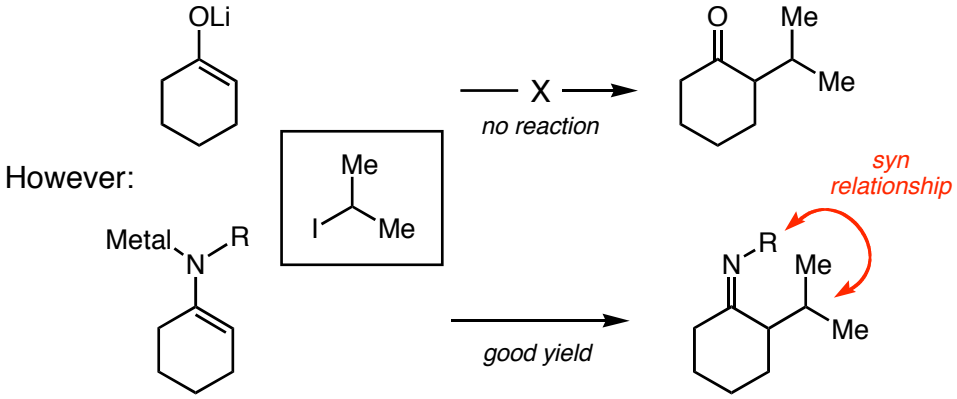

Metalloenamines are reactive enough to open epoxides in good yield. Ketone enolates are only marginally reactive enough for this family of electrophiles.

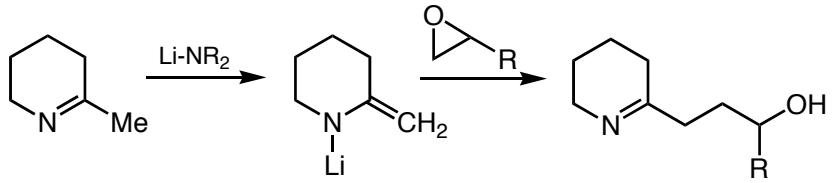

Decreasing Nucleophilicity ------>

Decreasing Electrophilicity ------>

Electrophile \ Nucleophile	⊖NR C=C	⊖O C=C	NR2 C=C	OMe C=C
Br_2, O_3	+	+	+	+
H_3O^+	+	+	+	+
R–C(=O)–Cl	+	+	+	
R–C(=O)–H	+	+	+	
R–C(=O)–R	+	+		
Me—I	+	+		
R–C(=O)–OR	+	+		
H_2C–O–CH_2	+			
Me_2CH—I	+			
R–C(=O)–NR_2				

■ Nature uses enamines, "stabilized" enolates, and enol derivatives in C–C bond constructions extensively.

Enolate Alkylation: Stereoelectronic Control Elements

Review Evans, D. A. *Stereoselective Alkylation Reactions of Chiral Metal Enolates.*; Morrison, J. D., Ed.; AP: New York, 1984; Vol. 3, pp 1-110.

Stereoelectronic Issues

- Enolization: Breaking C–H bond must overlap with π* C–O in TS‡
- Alkylation: Forming C–El bond must overlap with π* C–O in TS‡

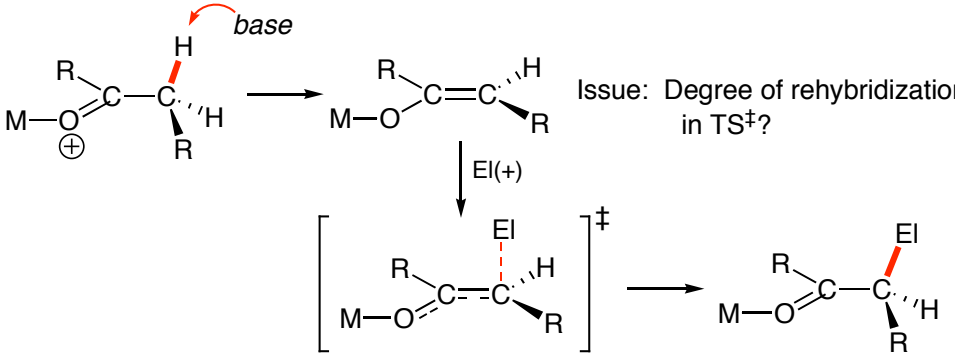

- Cyclohexanone Enolate:

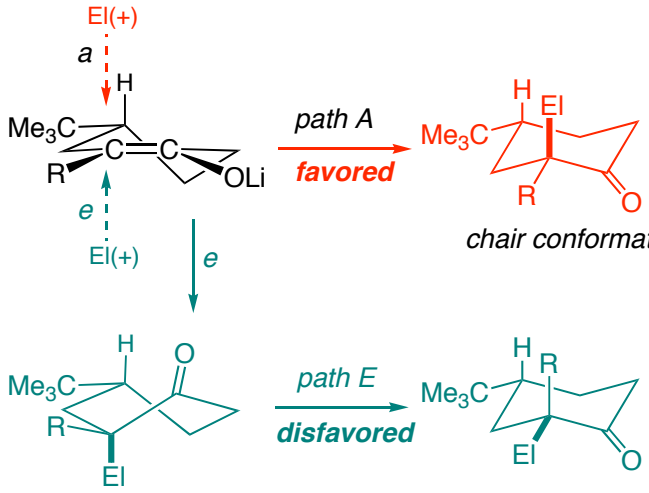

Metal	R-substituent	Electrophile	Ratio, a:e
Li	Me	CD_3I	70:30
Li	CO_2Me	Me-I	83:17

Chair vs boat geometries not stongly reflected in diastereomeric TS‡s. The transition states is early and enolate-like.

Examples where stereoelectronic factors are dominant

Pilli, *Tetrahedron*, **1999**, *55*, 13321

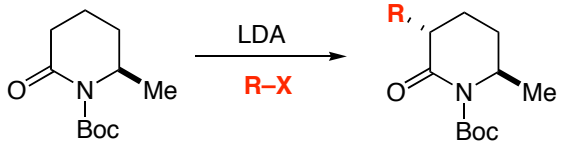

R–X	ratio
Bn–Br	>99:1
Allyl–Br	93:7

good illustration of the impact of allylic strain

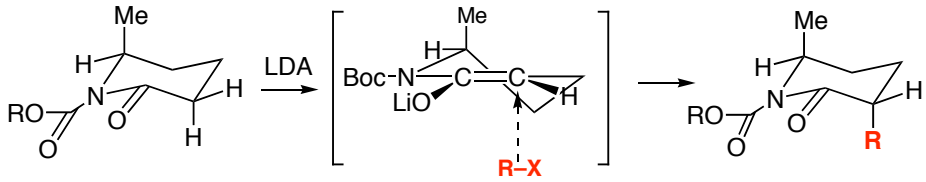

The C_{19} Angular Methyl Group in the steroid nucleus

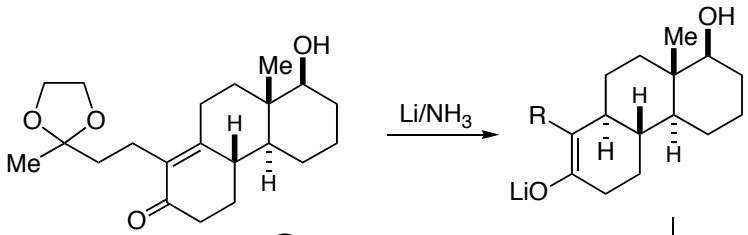

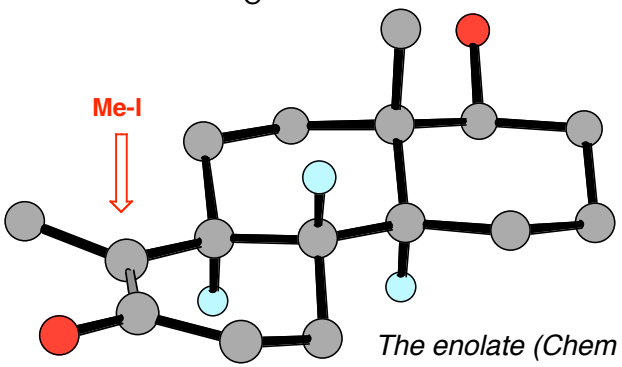

The enolate (Chem 3D)

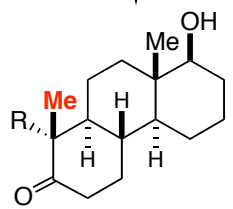

(90%) one isomer

As illustrated in this summary, there is a common thread to addition reactions to 6-membered, endocyclic pi-bonds as contained in oxo-carbenium ions, iminium ions, and enolates. In all instances, stereoelectronic considerations favor **"axial-chair"** transition states over the **"boat"** transition state alternatives. The stereoelectronic requirements for the SN2 reaction impose a related bias in the nucleopilic ring opening of epoxides and bromonium ions.The "diaxial" predisposition for the nucleophilic ring-opening of epoxides is known as the Furst-Plattner Rule.

6-Membered Oxo-carbenium Ions

Stereoelectronic Effect: The geometrical constraint imposed by the forming bond and the obligatory antiperiplanar orientation of the developing lone pair

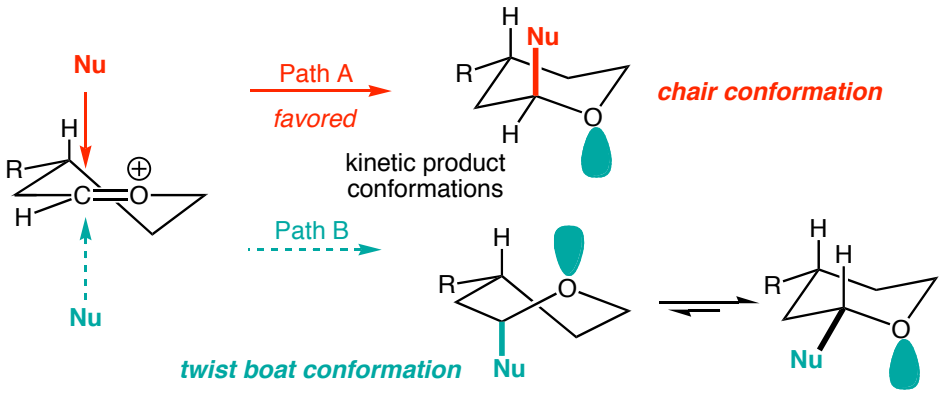

6-Membered Iminium Ions

Stereoelectronic Effect: The geometrical constraint imposed by the forming bond and the obligatory antiperiplanar orientation of the developing lone pair

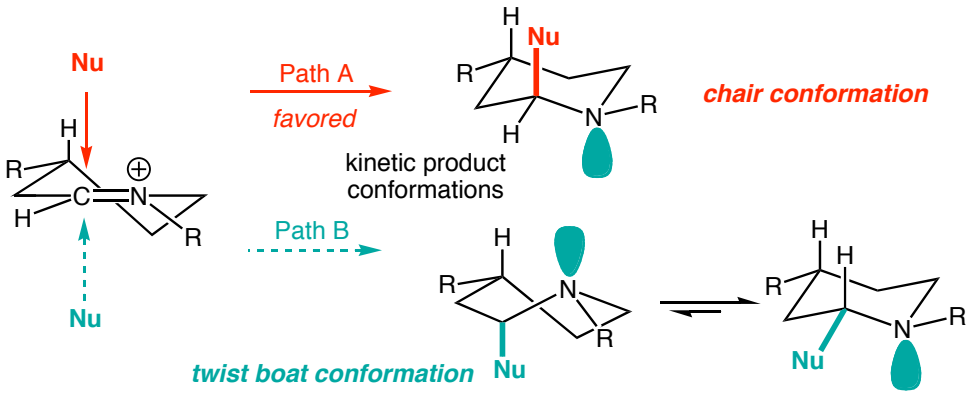

Cyclohexene Epoxides (*FÜRST-PLATTNER RULE*)

Stereoelectronic Effect: The anti geometrical constraint imposed by the forming bond and the leaving group in the indicated S_N2 reaction. The preference for "diaxial ring opening" preference of 6-membered epoxides also extends to bromonium ions and other olefin sigma complexes.

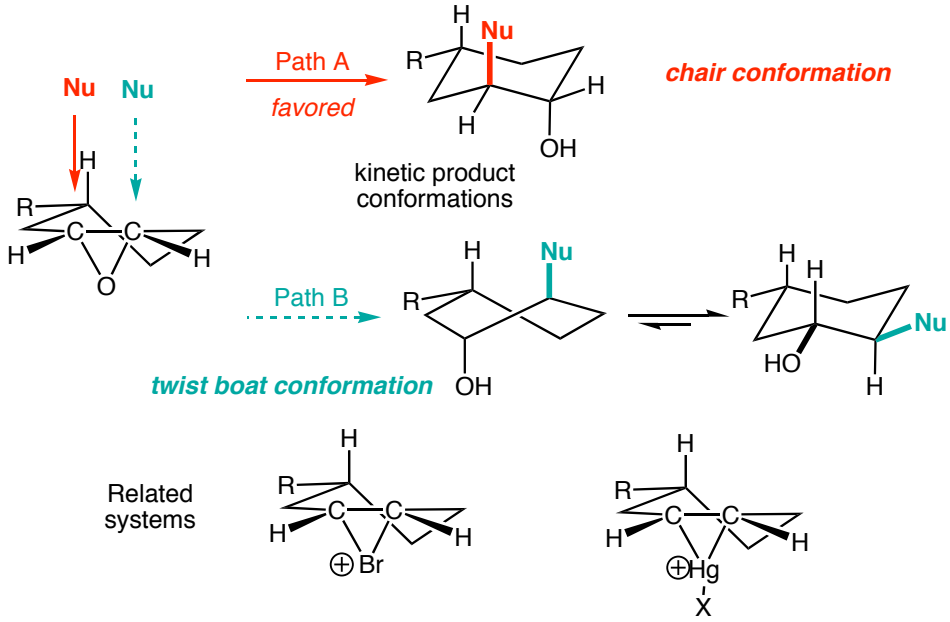

Cyclohexanone Enolates

Stereoelectronic Effect: The geometrical constraint imposed by the forming bond and the obligatory overlap with the developing carbonyl.

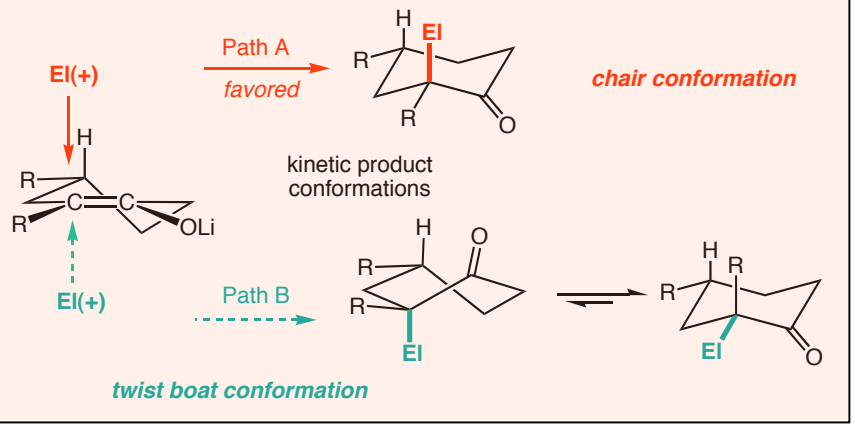

Enolate Alkylation: Steric Control Elements

Steric Effects

In this case, both e and a paths are stereoelectronically equivalent. Diastereoselectivity is now determined by the differential steric effects encountered in the two TS‡s.

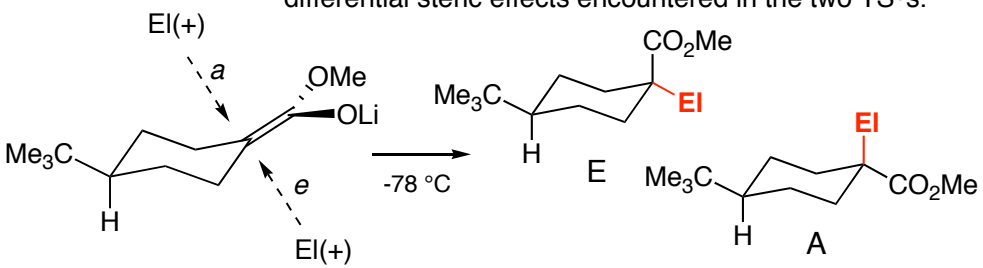

Electrophile	Ratio, E:A
Me-I	84:16
n-Bu-Br	87:13

Representative cases

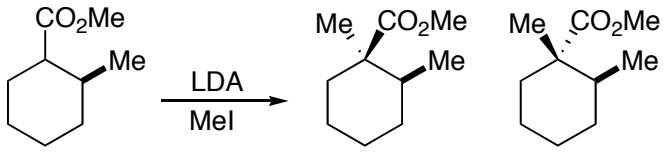

Ratio, 80 : 20

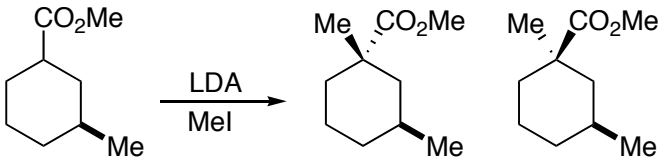

Ratio, 90 : 10

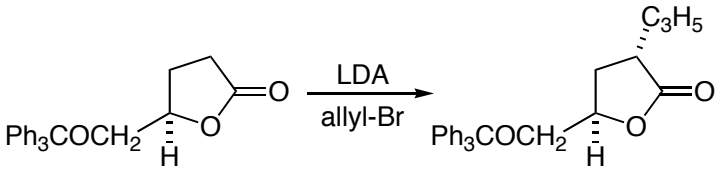

Ratio, >97 : 3

diastereoselectivity depends stongly on O-protecting group

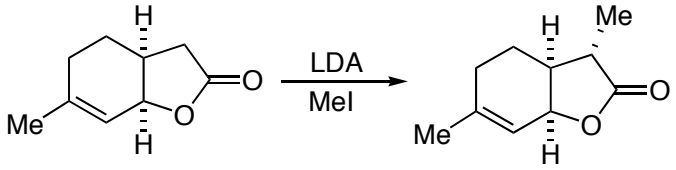

Ratio, >97 : 3

Cases with Opposed steric & electronic effects

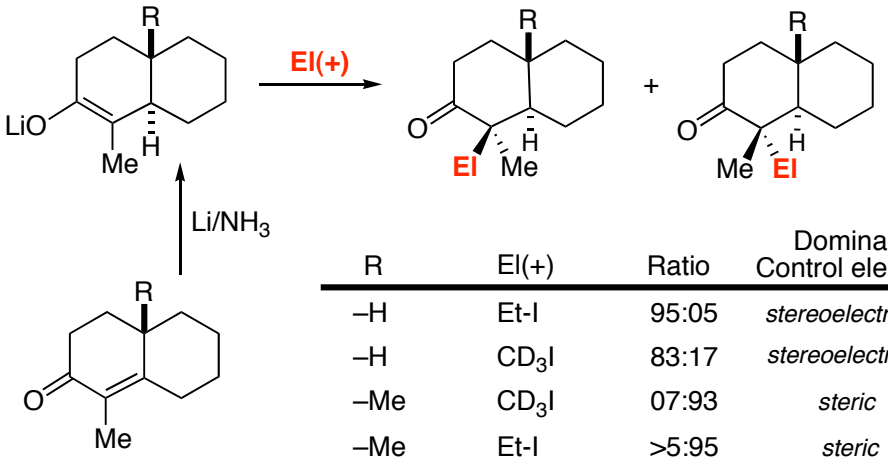

R	El(+)	Ratio	Dominant Control element
–H	Et-I	95:05	*stereoelectronic*
–H	CD_3I	83:17	*stereoelectronic*
–Me	CD_3I	07:93	*steric*
–Me	Et-I	>5:95	*steric*

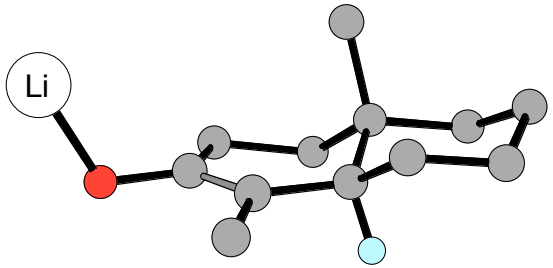

The enolate R = Me (Chem 3D)

Based on above data, this case is reasonable:

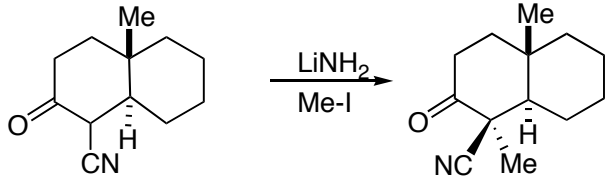

(58%) >90 : 10

However

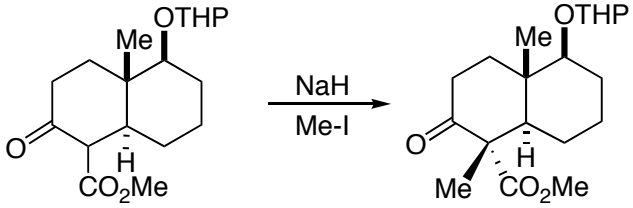

(67%) 93 : 7

http://www.courses.fas.harvard.edu/colgsas/1063

Chemistry 206

Advanced Organic Chemistry

Lecture Number 26

Enolates-3

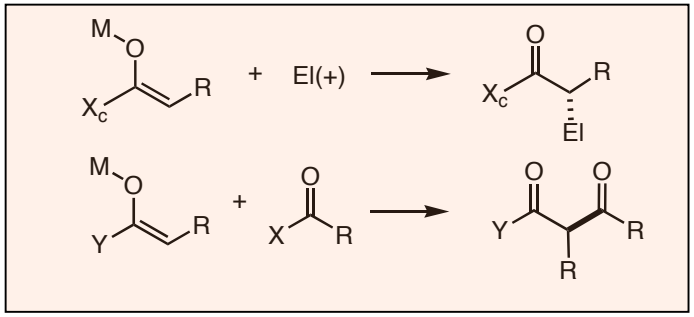

- Chiral Enolates
- Claisen Condenstaion
- Mander Reagent
- Weinreb Amides
- Dieckmann Cyclization

■ Reading Assignment for this Week:

Carey & Sundberg: **Part A**; Chapter 7
Carbanions & Other Nucleophilic Carbon Species

Carey & Sundberg: **Part B**; Chapter 2
Reactions of Carbon Nucleophiles with Carbonyl Compounds

D. A. Evans

Friday
November 17, 2006

Polypropionate Biosynthesis

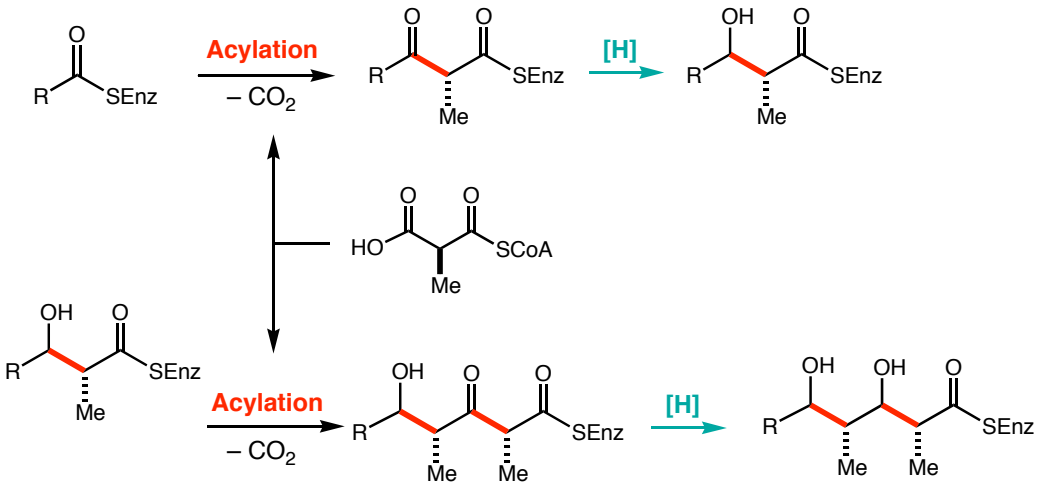

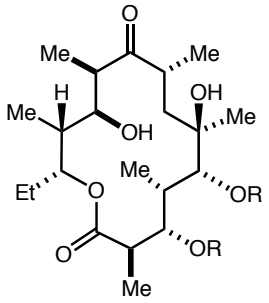

Erythromycin B

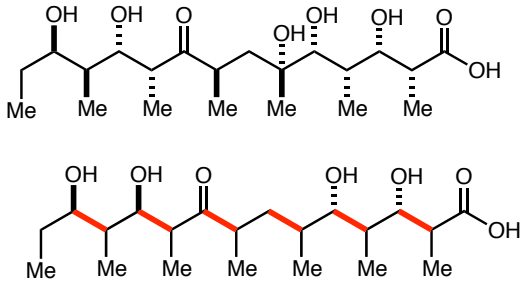

The 7 Propionate Subunits

"Erythromycin, with all of our advantages, looks at present quite hopelessly complex, particularly in view of its plethora of asymmetric centers."

R. B. Woodward, 1956

Chiral Enolate Design Requirements Circa 1978

Overall enantioselection will be the sum total of the defects introduced through:

- **Enolization selectivity**
- **Enolate-electrophile face selectivity**
- **Racemization attendant with X_c removal**

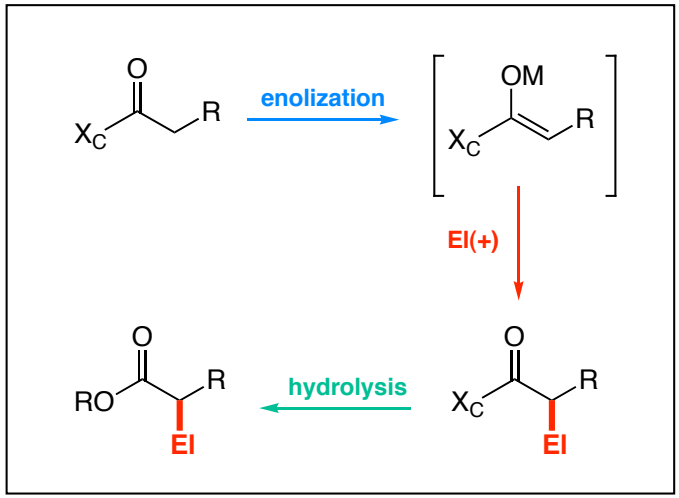

Enolization selectivity: Ester-based chiral controllers X_C limited by enolization selectivity (Lecture 23)

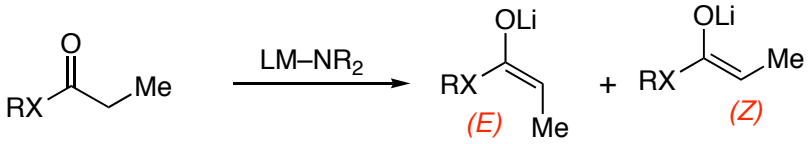

Base	R-Substituent	Ratio, (E):(Z)
LDA (THF)	-OMe, O-t-Bu	95 : 5
LDA (THF)	-S-t-Bu	95 : 5

Enolization selectivity: Amide-based controllers X_C limited by enolization selectivity (Lecture 22)

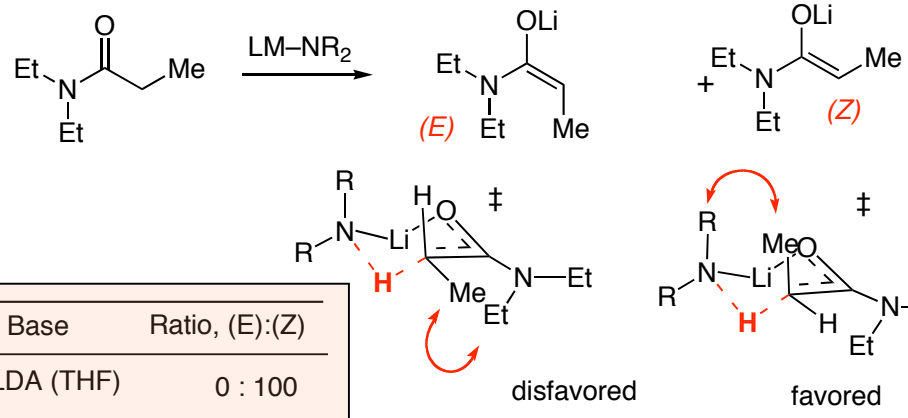

Base	Ratio, (E):(Z)
LDA (THF)	0 : 100
s-BuLi (THF)	25 : 75

Amide Based Chiral Auxiliaries

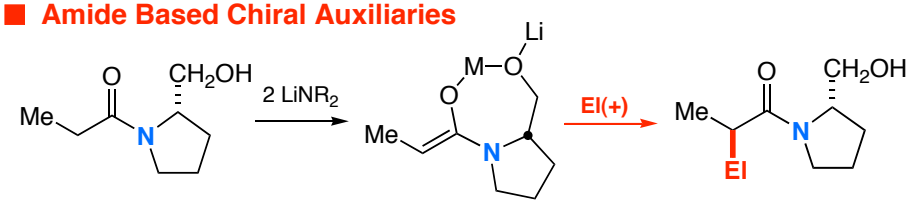

With Takacs, *Tetrahedron Lett.* **1980**, 4233 *diastereoselection Ca 95 %*

Allylic Strain controls Enolate Geometry:

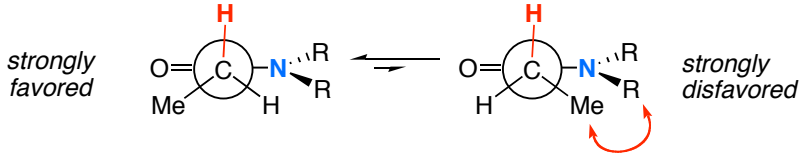

Allylic Strain Prevents Product Enolization:

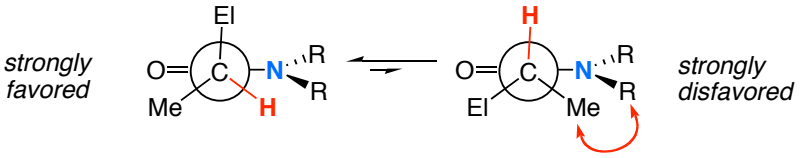

Chiral Amide Enolates

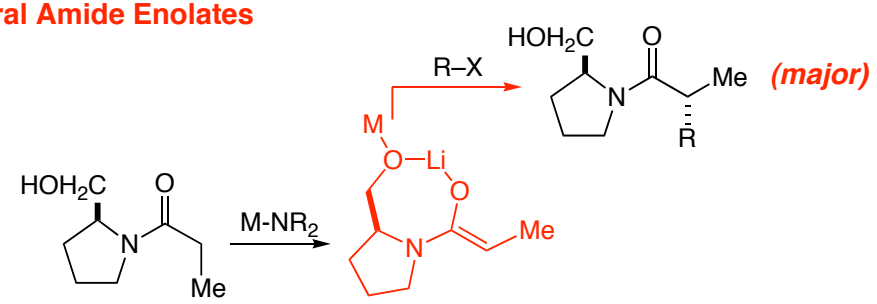

Evans, Takacs,
Tet. Lett. **1980**, *21*, 4233-4236

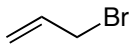

96:4 (98%)

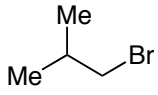

98:2 (84%)

Chem 3D model

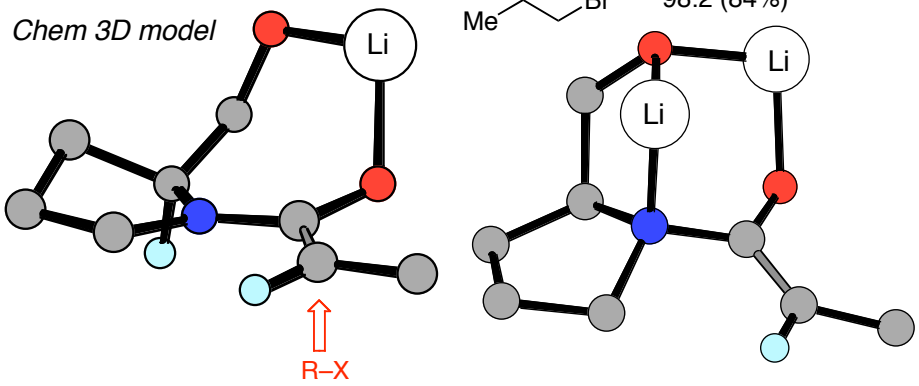

Nature of enolate chelation is ambiguous. Nitrogen chelation is a real possibility.

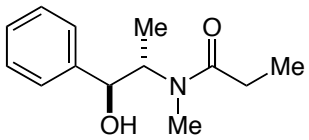

Myers, *JACS* **1997**, *119*, 6496

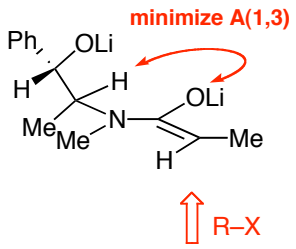

Amide Hydrolysis

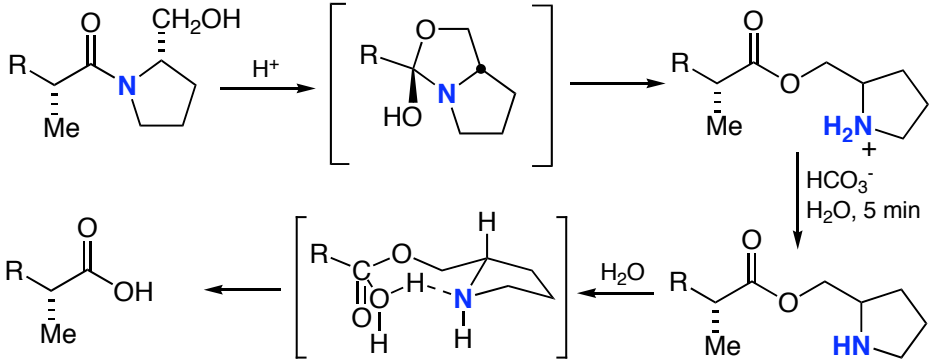

intramolecular general base catalysis

Applications in Ionomycin synthesis

Ionomycin Calcium Complex

JACS **1990,** *112*, 5290-5313

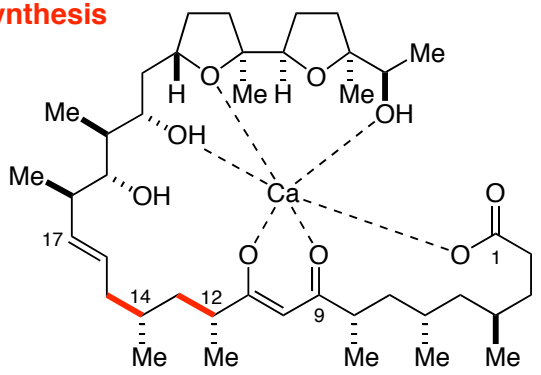

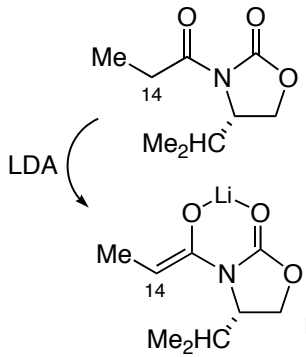

84%

PhCH=CHCH2Br

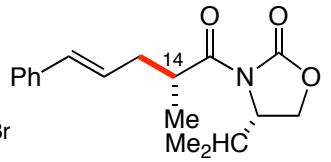

diastereoselection 99:1

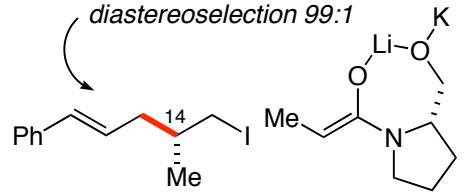

83%

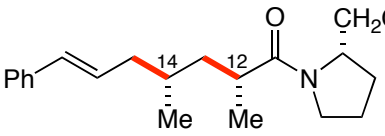

diastereoselection 97:3

Alkali Metal enolates:

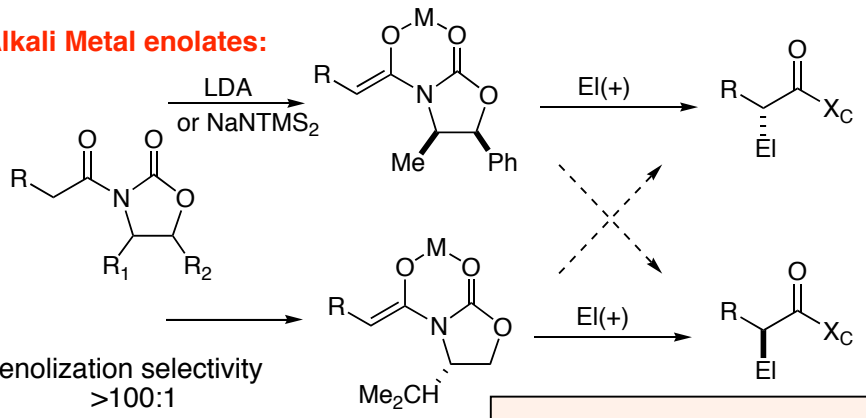

enolization selectivity
>100:1

M = Li, THF < 0 °C
M = Na, THF -78 to 0 °C

marginal reaction

Alkyl Halide	Ratio
$ArCH_2Br$	50-120 : 1
$CH_2C{=}CHCH_2Br$	50 : 1
$ArCH_2OCH_2Br$	50 : 1
CH_3CH_2I	25 : 1
CH_3I	13 : 1

JACS. **1982**,*104*, 1737.

Enolate Acylation

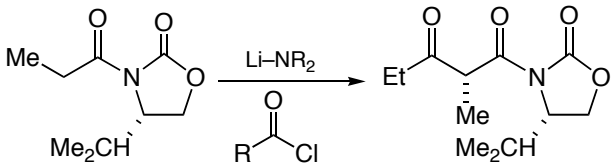

JACS ***1984****, 106, 1154.*

Diastereoselection ~ 97 : 3

New stereocenter not lost through enolization

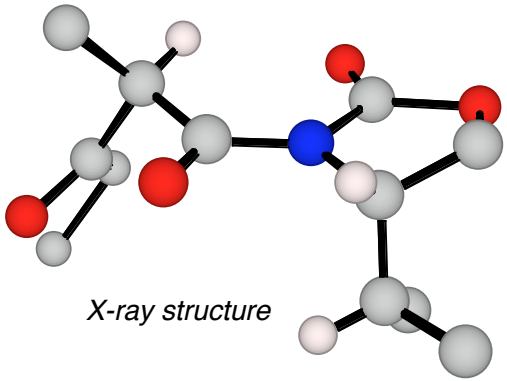

X-ray structure

Enolate Amination

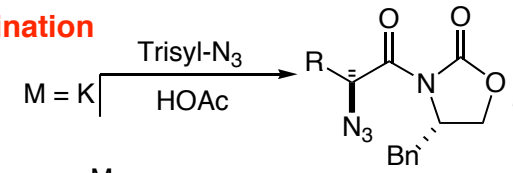

JACS **1987**,*109*, 6881.
JACS **1990**,*112*, 4012-4030

diastereoselection 91-99+ %

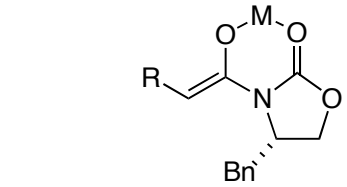

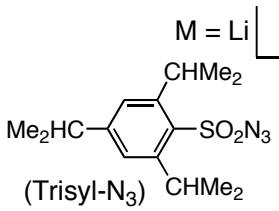

JACS **1986**,*108*, 3695.
Tet. **1988**, *44*, 5525-40

diastereoselection 97-99+ %

Enolate Hydroxylation

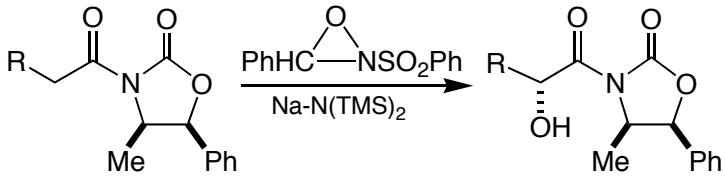

Na enolate is required.
Why?

Imide (R)	Ratio	Yield *
$PhCH_2$-	94 : 6	86 %
$CH_2{=}CHCH_2$-	95 : 5	91 %
$MeO_2CCH_2CH_2CH_2$-	96 : 4	68 %
Ph-	90 : 10	77 %
Me_3C-	>99 : 1	94 %

JACS. **1985**,*107*, 4346.

For all indicated rxns, as the R on the enolate grp increases in size enolate-El face selectivity increases. Explain.

Chiral Ester Enolates

Helmchen, *Angew. Chem. Int.Ed.* **1981**, *20*, 207-208

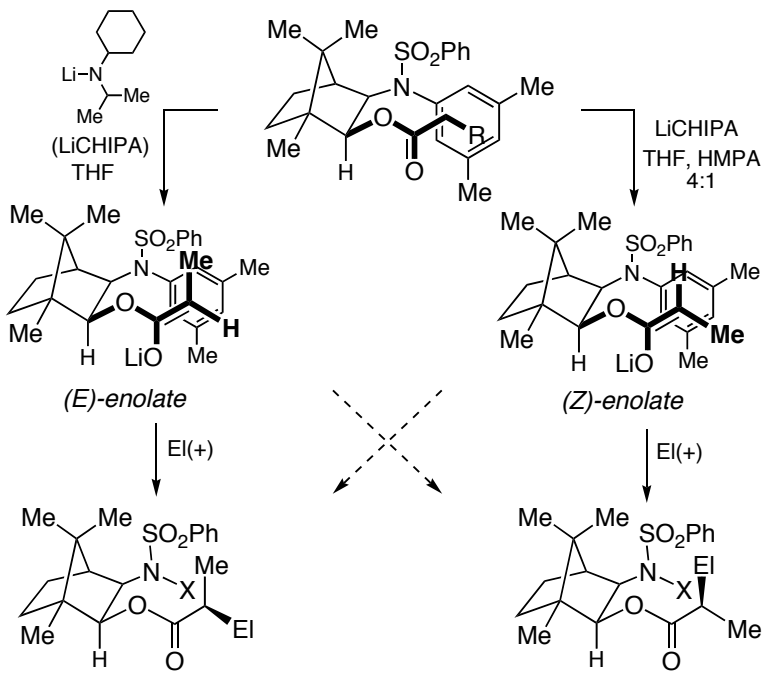

enolate	El(+)	Ratio
(E)	n-$C_{14}H_{29}$–I	98.5:1.5
(Z)	n-$C_{14}H_{29}$–I	06:94

enolate contamination

Helmchen, *Angew. Chem. Int.Ed.* **1984**, *23*, 60-61
Helmchen, *Tet. Lett.* **1983**, *24*, 1235-1238
Helmchen, *Tet. Lett.* **1983**, *24*, 3213-3216

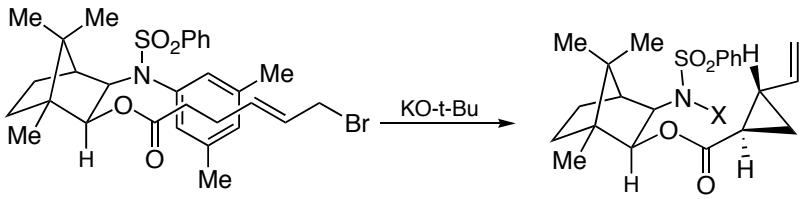

Ratio, 93:7 (74%)

Helmchen, *Tet. Lett.* **1985**, *26*, 3319-3322

Chiral β-Keto Ester Enolates

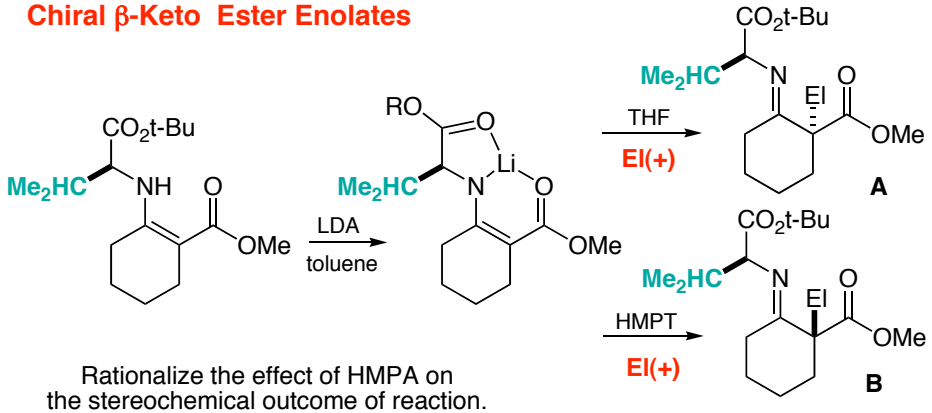

Rationalize the effect of HMPA on the stereochemical outcome of reaction.

Koga, *JACS* **1984**, *106*, 2718-2719

El(+)	addend	Yield	Ratio (A:B)
Me–I	THF	63%	96:04
Me–I	HMPT	57%	01:99
Bn-Br	THF	48%	99:01
Bn-Br	HMPT	77%	15:85

The Rationale:

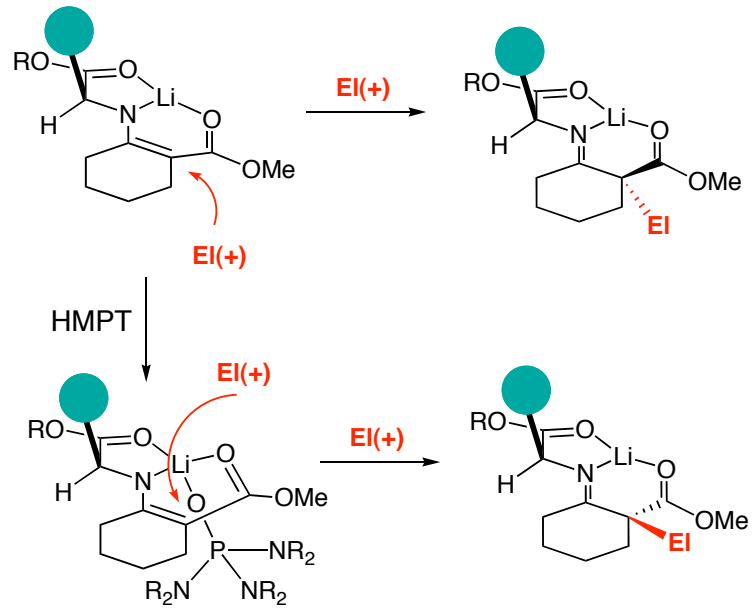

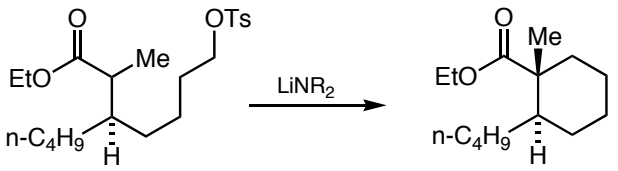

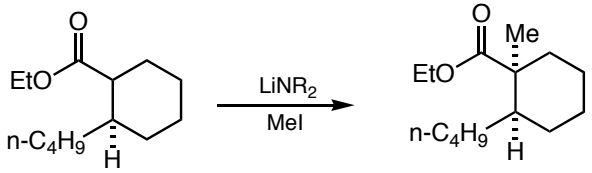

D. Kim, *Tetrahedron Lett.* **1986**, *27*, 943.

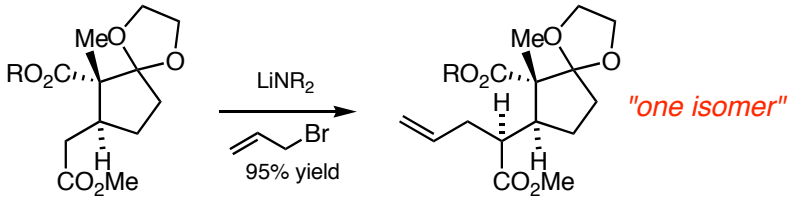

G. Stork, *Tetrahedron Lett.* **1987**, *28*, 2088.

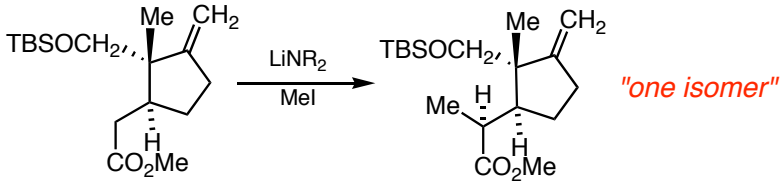

T. Money, *Chem. Commun.* **1986**, 288.

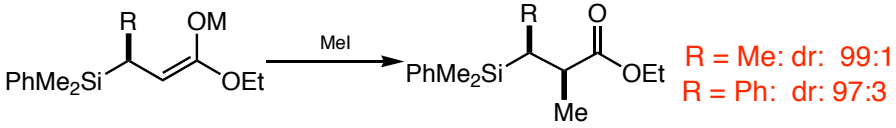

I. Fleming, *Chem. Commun.* **1984**, 28.

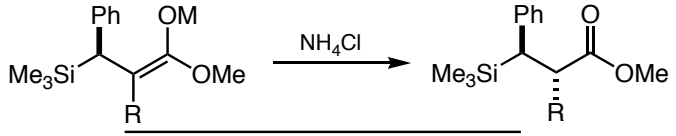

R-substituent	*diastereoselection*
R = Me	87:13
R = Et	80:20
R = $CHMe_2$	40:60 major diastereomer opposite to that shown

I. Fleming & Co-workers, *Chem. Commun.* **1985**, 318.
Y. Yamamoto & Co-workers, *Chem. Commun.* **1984**, 904.

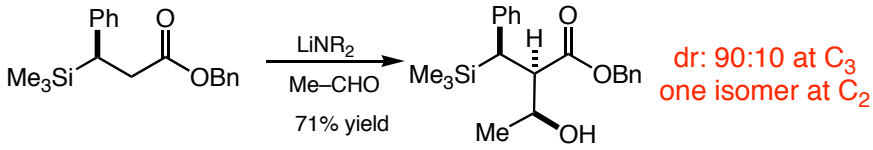

I. Fleming, *Chem. Commun.* **1986**, 1198.

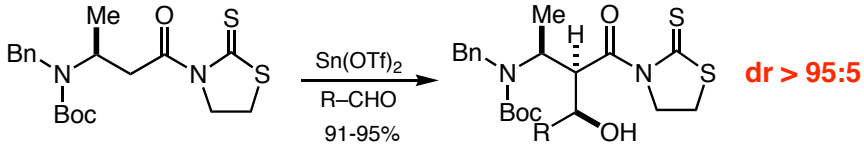

T. Mukaiyama, *Chem. Letters* **1986**, 637

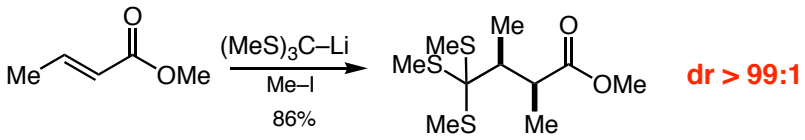

K. Koga, *Tetrahedron Letters* **1985**, *26*, 3031.

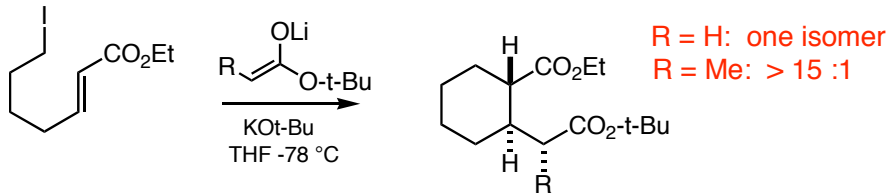

Y. Yamaguchi, *Tetrahedron Letters* **1985**, *26*,1723.

Seminal Paper: Stork & Dowd, *JACS*, **1963**, *85*, 2178-2180

Reviews:

Martin in *Comprehensive Organic Synthesis*, **1991**; Vol 2, Chapter 1.16, pp 475-502

Whitesell *Synthesis*, **1983**, 517-535

Bregbreiter in *Asymmetric Synthesis*, **1983**; Vol 2, Chapter 9, pp 243-273

Enders in *Asymmetric Synthesis*, **1984**; Vol 3, Chapter 4, pp 275-339

Generation & Structure:

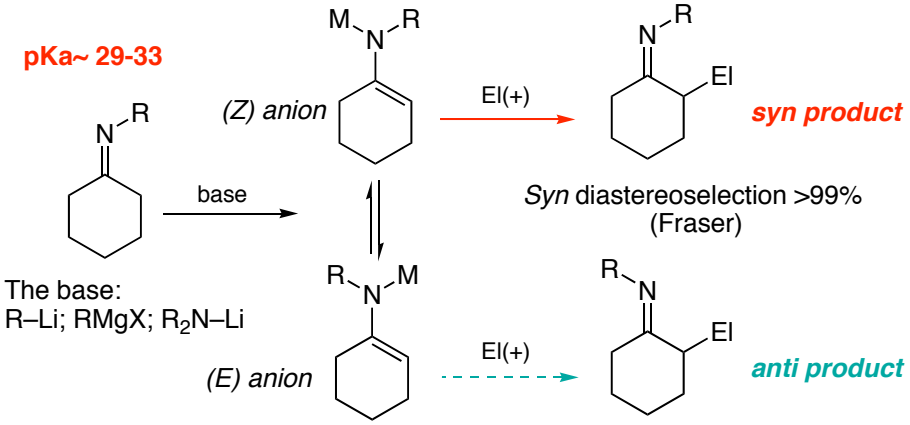

Acidity Measurements: (Streitwiser, *JOC* **1991**, *56*, 1989; Fraser, *ibid.* **1985**, *50*, 3234):

Kinetic product geometry strongly favored the *syn* isomer (>99%) (Fraser)

Fraser, *JACS* ***1978***, *100*, 7999
Fraser, *Chem. Commun.* ***1979***, 47

Solid State & Solution Structure:

X-ray structure reveals the following:

- Anion geometry is (Z)
- For M = Li, anion is delocalized rather than localized as pictured

Collum, *JACS* ***1984***, *106*, 4865-4869
Collum, *JACS* ***1985***, *107*, 2078-2082
Collum, *JACS* ***1986***, *108*, 3415-3422
Collum, *JACS* ***1993***, *115*, 789-790

Geometry Rationalization:

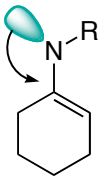

nonbonding N-lone pair may be stabilized by delocalization into antibonding orbital of C=C.

Remember, (Z) geometry also favored for enol ethers

Representative Reactions:

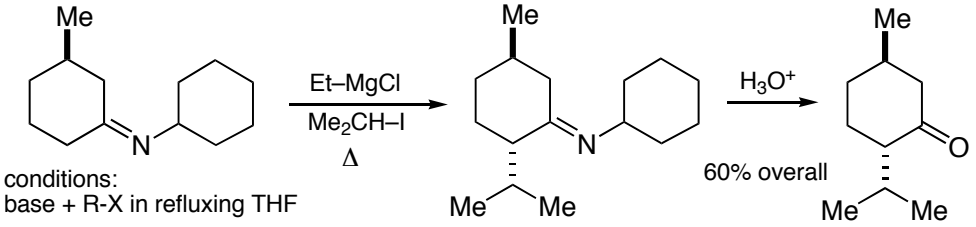

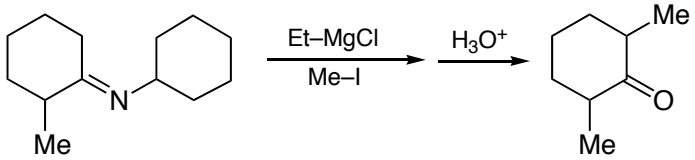

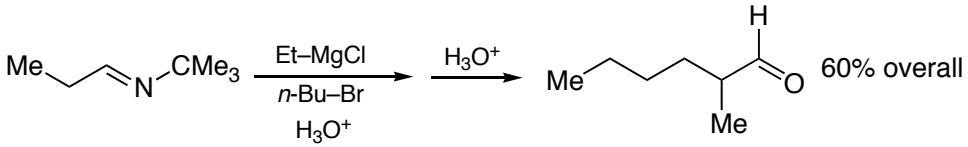

Stork & Dowd, *JACS*, **1963**, *85*, 2178-2180

Nature of N-substituent, base, and solvent additive can play a role in deprotonation regioselectivity: Hosomi, JACS, 1982, 104, 2081-2082

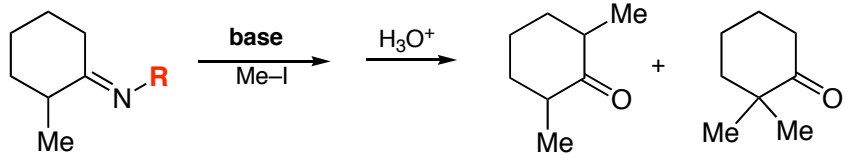

R	base	ratio
–cyclohexyl	*s*-BuLi	10:90
–NMe_2	*s*-BuLi	100:0

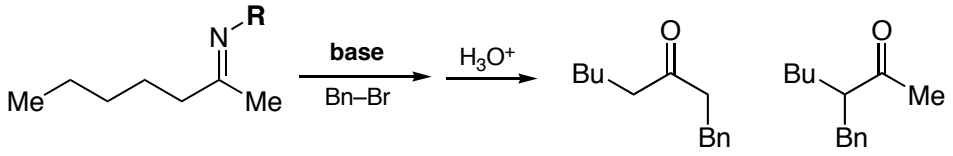

R	base	ratio
–cyclohexyl	*s*-BuLi	74:26
–cyclohexyl	*s*-BuLi	100:0

+ 1 equiv HMPA

Stereoelectronic Issues:

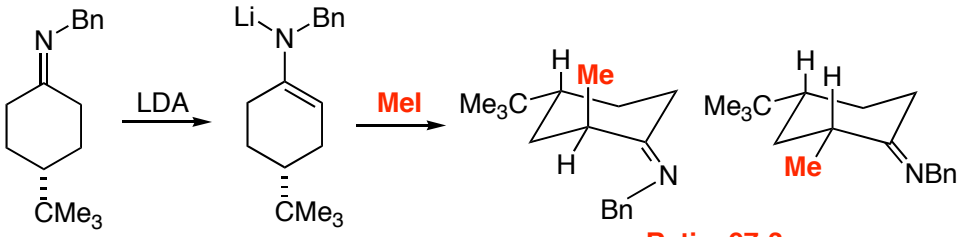

Fraser, *JACS* ***1978***, *100,* 7999 **(handout)**

Tendency for axial-chair alkylation is significantly greater that for ketones

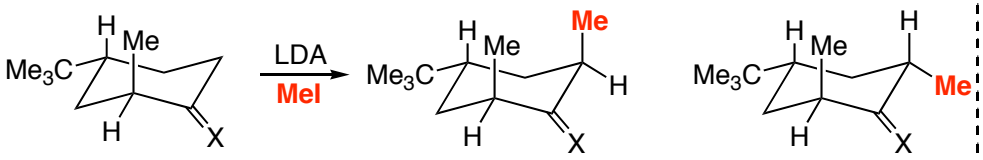

Fraser, *JACS* ***1978***, *100,* 7999 **(handout)**

X	Ratio
X = N-Bn	94:06
X = O	60:40

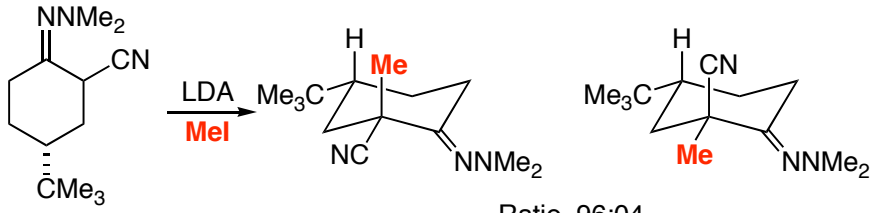

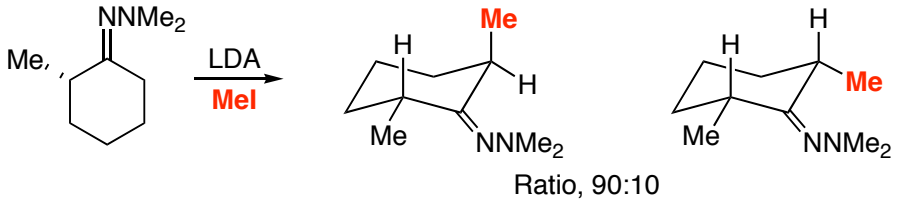

Collum, *JACS* ***1984***, *106,* 4865-4869 **(handout)**

Chiral Metalloenamines:

early papers:
- Meyers, *J. Am. Chem. Soc* ***1976***, *98,* 3032
- Whitesell, *J. Org. Chem.* ***1978***, *42,* 377-378

full papers:
- Meyers, *J. Org. Chem* ***1978***, *43,* 892
- Meyers, *J. Am. Chem. Soc* ***1981***, *103,* 3081
- Meyers, *J. Am. Chem. Soc* ***1981***, *103,* 3088

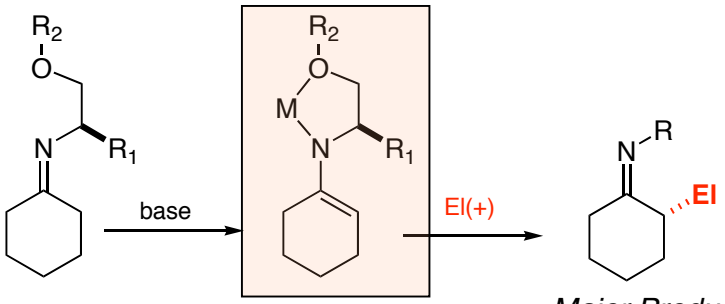

The base:
R–Li; RMgX; R_2N–Li

Major Product

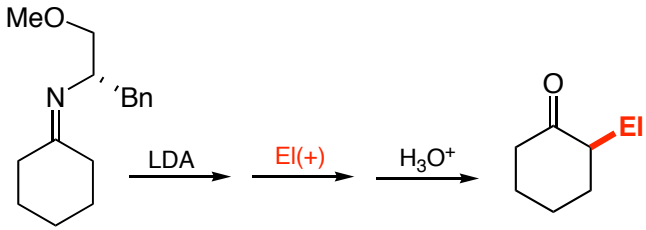

R–X	ee
Me–I	87
Et–I	94
n-Pr–I	99

Meyers, *J. Am. Chem. Soc* ***1981***, *103,* 3081

Chiral Metallated Hydrazones

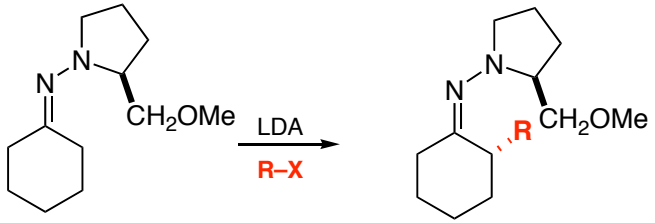

Enders in *Asymmetric Synthesis*, **1984**; Vol 3, Chapter 4, pp 275-339

The Reaction:

Acylation

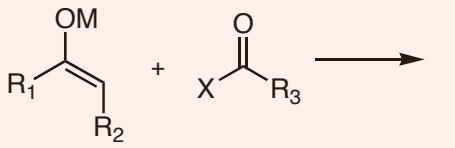

Carboalkoxylation

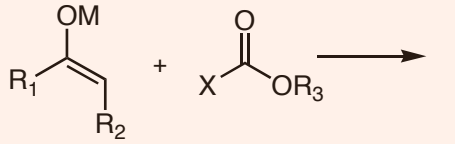

Situations where the reaction is employed:

■ Acyl moiety is a constituent of the target structure:

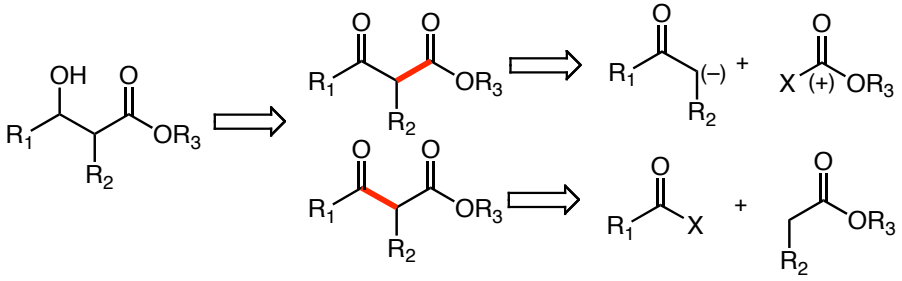

■ Acyl moiety employed in assisting bond construction but not part of the target structure:

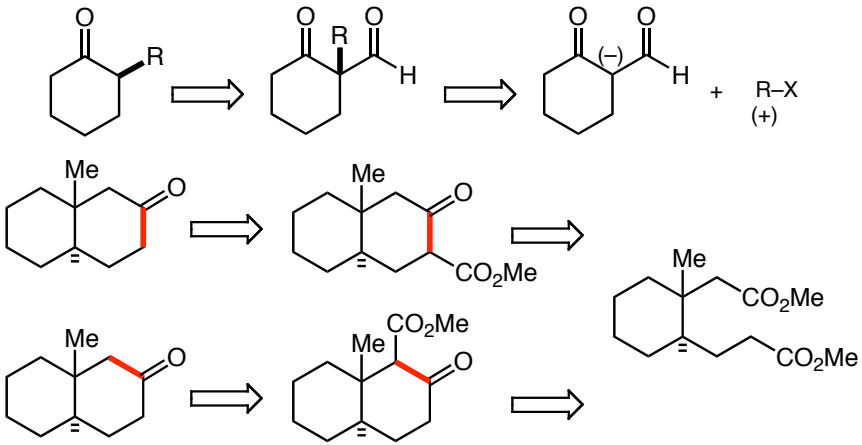

Deacylation: When an acyl residue is employed in the one of the illustrated bond constructions, it may then be removed by nucleophilic deacylation: Several examples are provided.

Deformylation:

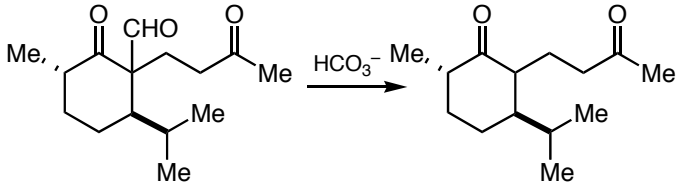

competitive ring cleavage not a problem due to more electrophilic formyl C=O

Decarboxylation:

■ Alkyl-Oxygen Cleavage: *tert*-butyl esters

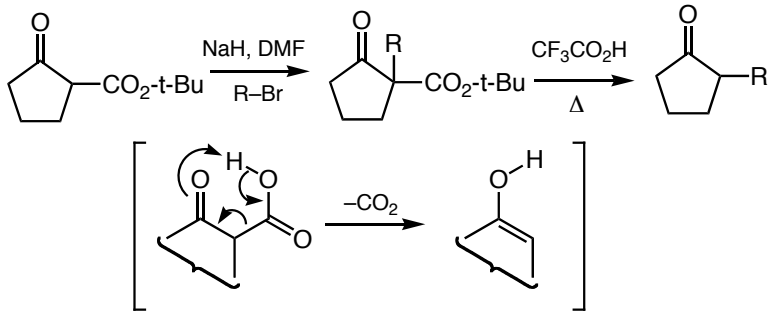

Decarboxylation in this system is a sigmatropic rearrangement involving C=O participation

representative procedure: Henderson, *Synthesis* **1983**, 996

■ Alkyl-Oxygen Cleavage: Methyl esters

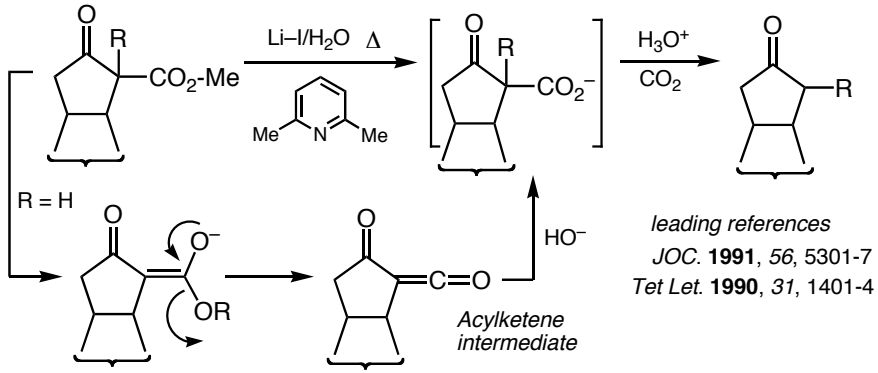

leading references

JOC. **1991**, *56*, 5301-7

Tet Let. **1990**, *31*, 1401-4

Claisen Condensation & Related Processes

Claisen Condensation: Condensation of 2 esters

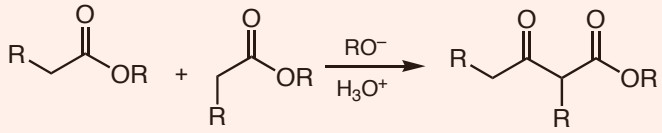

Intramolecular Variant: Dieckmann Condensation

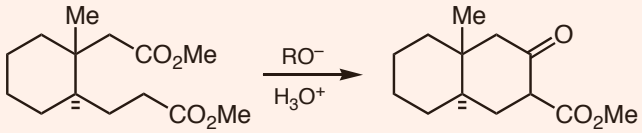

Strictly speaking, the Claisen and Dieckmann condensations are defined as condensations between ester enolates & ester electrophiles.
In this discussion, we choose to liberalize the classifcation to include ketone enolates as well.

Reaction Thermodynamics: Overall Keq ~ 1

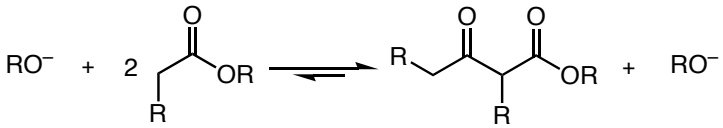

Final enolization Step: Keq ~ 10^{+4}

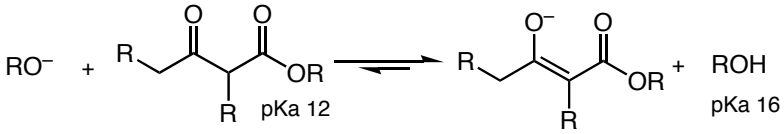

Contrary to popular belief, final enolization step does not render the process irreversible

Reaction Control Elements: These reactions can be manipulated to give either kinetic or thermodynamic control:

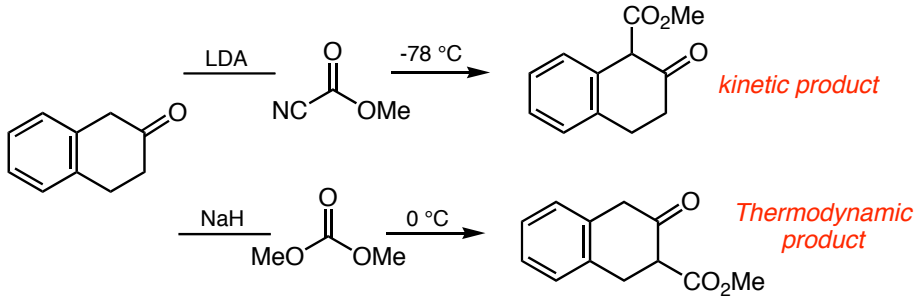

Analysis of the two processes:

Conventional Carbomethoxylation: Equilibrium achieved between all species

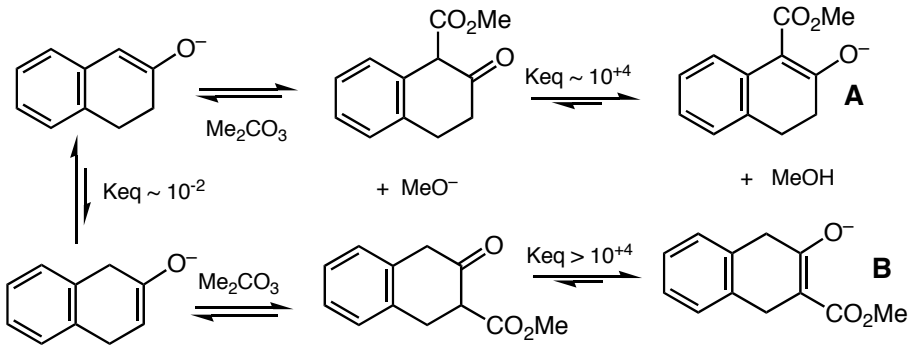

Critical issue: Product enolate **A** is significantly destabilized by peri-interaction with aromatic ring disrupting the required planarity of the delocalized enolate. Hence, the greater stability of **B** dictates the product.

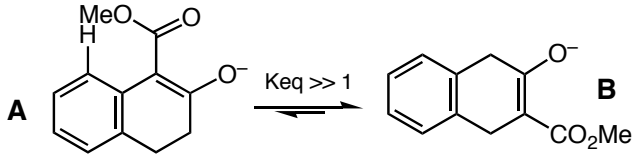

This type of control is general:

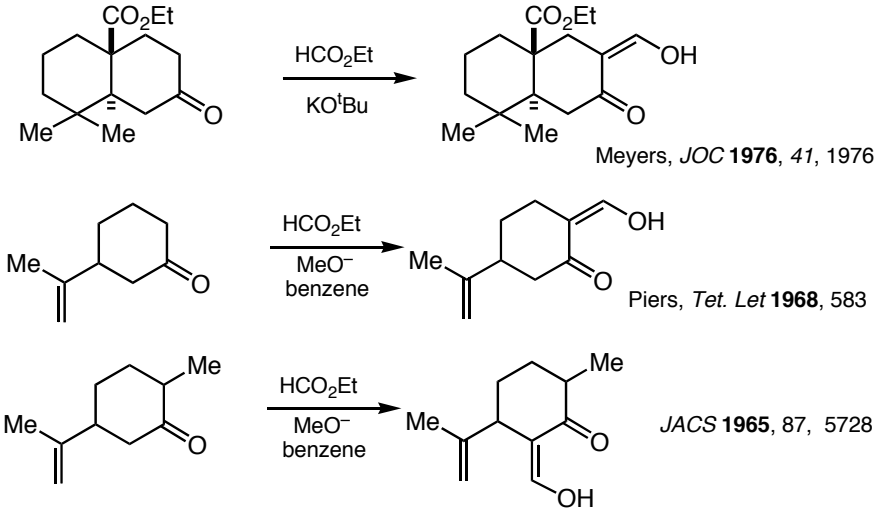

Kinetic Acylation: Methyl Cyanoformate (1):

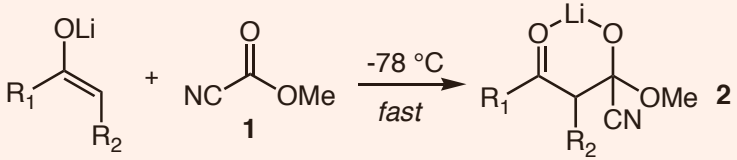

Enolate acylation with **1** is fast

Intermediate **2** breaks down to product more slowly than the acylation step

Under these conditions, proton transfer from product to enolate does not occur.

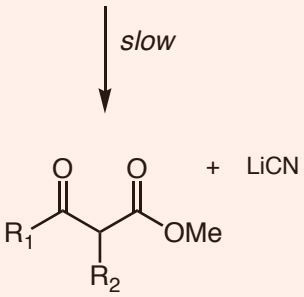

Examples:

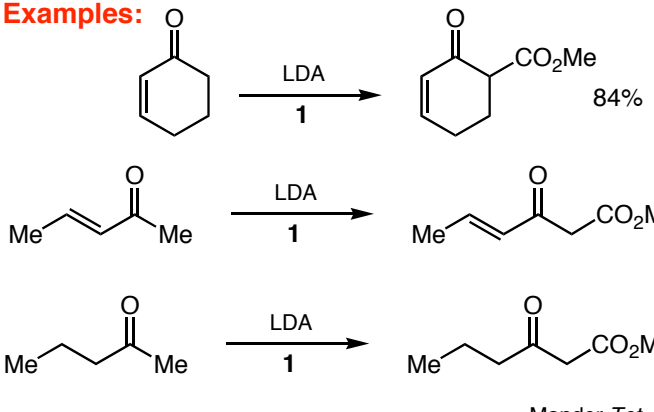

Mander *Tet. Lett.* **1983**, *24*, 5425

Mander, *SynLett.* **1990**, 169

Hashimoto, *Chem. Lett.* **1989**, 1063

The Tetrahedral Intermediate 2; Why is it so stable?

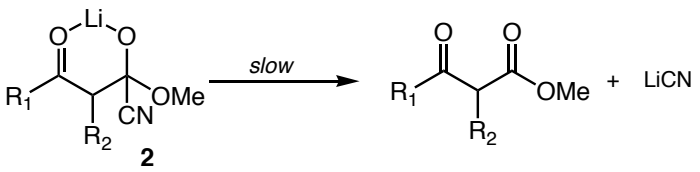

Consider this process in the broader context of elimination reactions of the E1cb classification where:

Y might be either C or some heteroatom
X might be various leaving groups such as CN, OR etc.

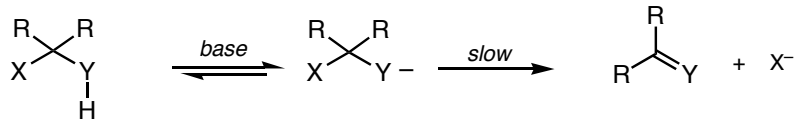

Data is available for the case where X = CN, OR & Y = carbanion:

Stirling, *Chem. Commun.* **1975**, 940-941

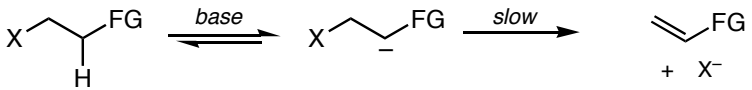

leaving grp (X)	pKa H–X	$\log\left[\frac{k_X}{k_{OPh}}\right]$
–OPh	10	1
–CN	9.5	<-7
$-C(Me)_2-NO_2$	~10	<-9
–OMe	16	-3.9

Above data makes the point that CN is a poor LG but it also leads one to the faulty conclusion that **2** should partition to acyl cyanide rather than methyl ester!

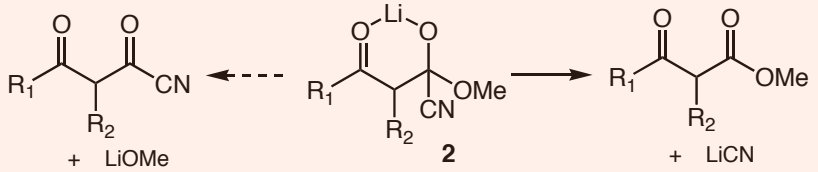

Kinetic Enolate Acylation: Acyl-Benztriazoles

N-Acylbenztriazoles: Excellent Acylating Agents

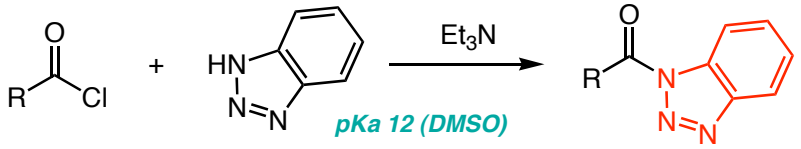

A. Katritzky, *SynLett* **2005,** 1656-1665
Chem. Eur. J. **2003,** *9*, 4586-4593

Compounds nicely crystalline & bench stable

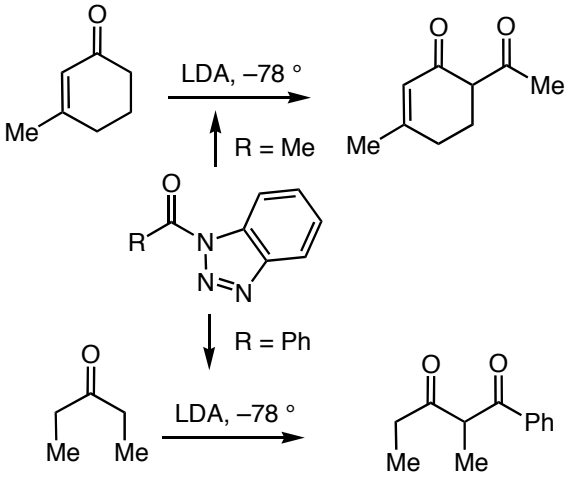

94% yield
Ideal stoichiometry employed

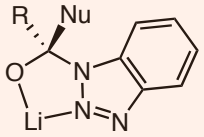

stabilized tetrahedral intermediate

86% yield

Katritzky, *J. Org. Chem.* **2000,** 65, 3679

The only complex application to date

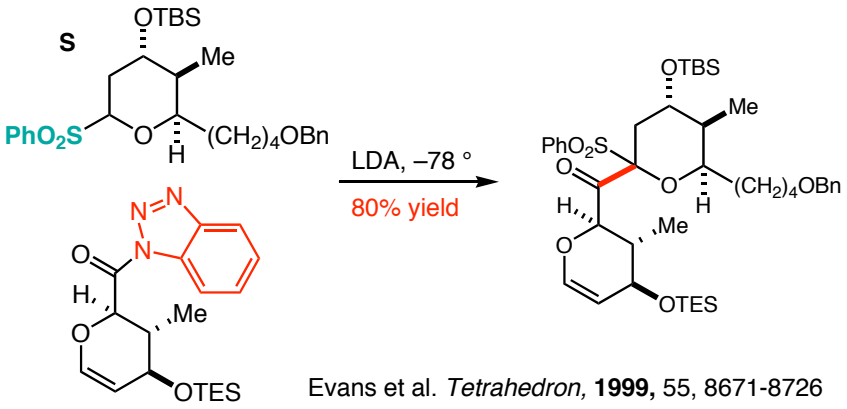

Evans et al. *Tetrahedron,* **1999,** 55, 8671-8726

N-AcylPyrroles: Exceptionally Stable Tetrahedral Intermediates

Evans et al. *Angew. Chem. Int. Ed.*, **2002,** *41*, 3188.

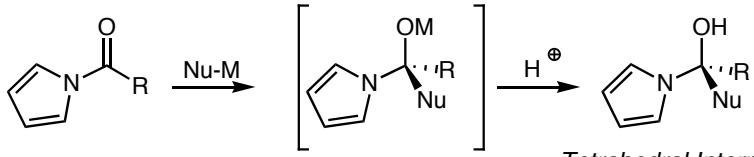

Tetrahedral Intermediates may be Isolated

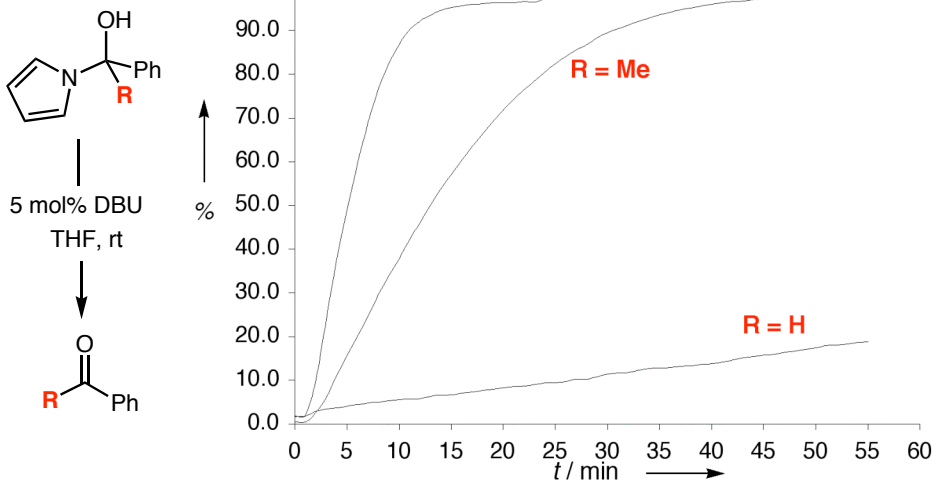

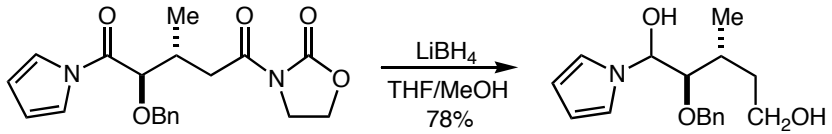

Decreasing Electrophilicity

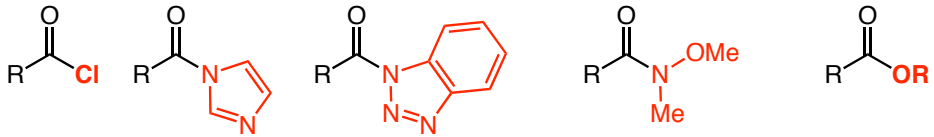

Carbon Acylation with *N*-Methoxy-*N*-methylamides

Acylating agents can be desiged where the tetrahedral intermediate exhibits exceptional stability:

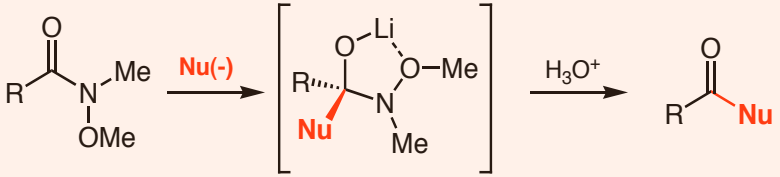

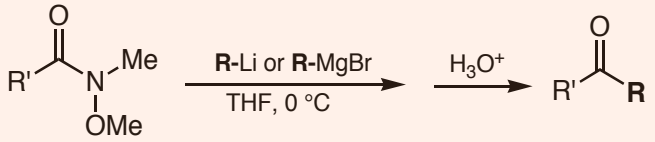

R = Me, n-Bu, or Ph; yields > 90%

Weinreb *Tet. Lett.* **1981**, *22*, 3815.

Nucleophiles:

Acceptable	Unacceptable
R–Li, R–MgX R—≡—Li(MgX)	R–ZnX & other colalent metal alkyls
DIBAL $LiAlH_4$ $LiB(R)_3H$	other colalent metal enolates
	Weak hydride reagents: $NaBH_4$

An excellent review on all aspects of Weinreb amide chemistry:
M. Sibi, *Organic Preparations and Procedures Int.*, **1993**, *25 (1)*, 15-40.

Representative Organometals:

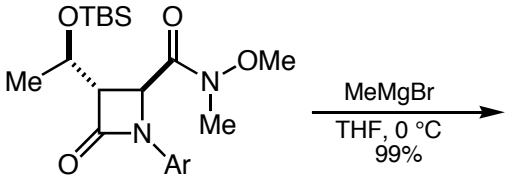

Several other examples reported.

J. Prasad and L. Liebeskind
Tetrahedron Lett. **1987**, *28*, 1857.

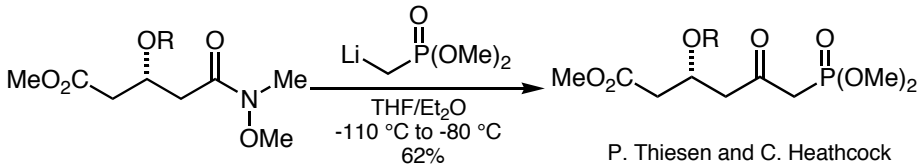

P. Thiesen and C. Heathcock
J. Org. Chem. **1988**, *53*, 2374.

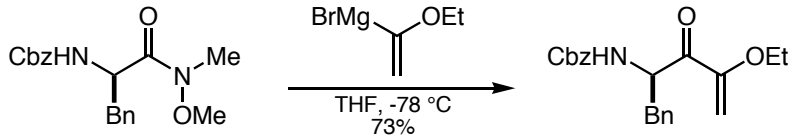

M. Angelastro, N. Peet and P. Bey
J. Org. Chem. **1989**, *54*, 3913.

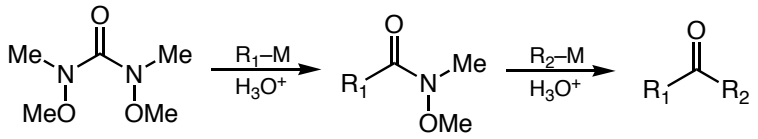

W. Wipple, H. Reich
J. Org. Chem. **1991**, *56*, 2911-2.

Enolates and Metalloenamines:

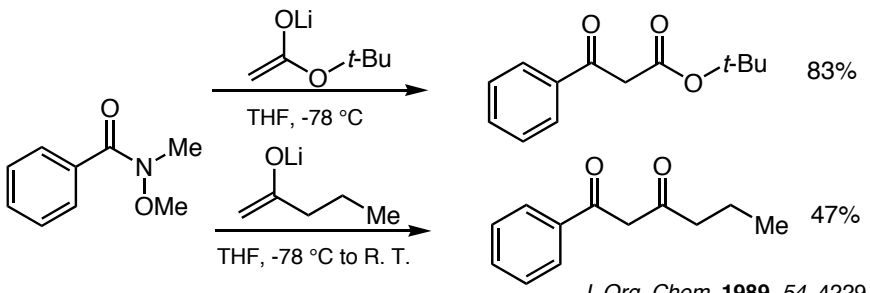

J. Org. Chem. **1989**, *54*, 4229.

Hydride Reductions:

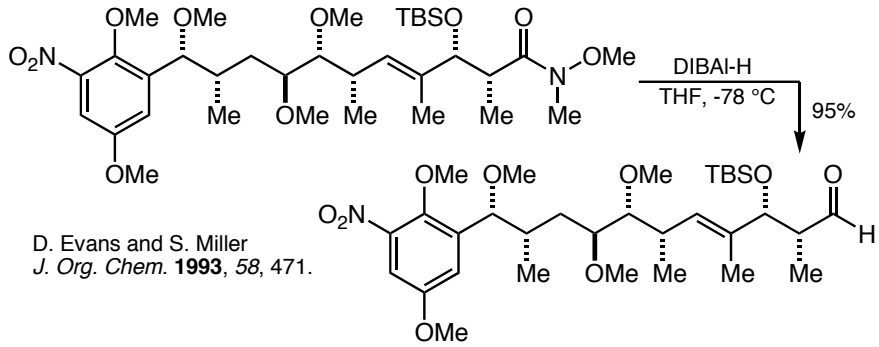

D. Evans and S. Miller
J. Org. Chem. **1993**, *58*, 471.

Carbon Acylation with *N*-Methoxy-*N*-methylamides-2

The Rutamycin B Synthesis, . *JACS.* **1993**, *115*, 11446-11459

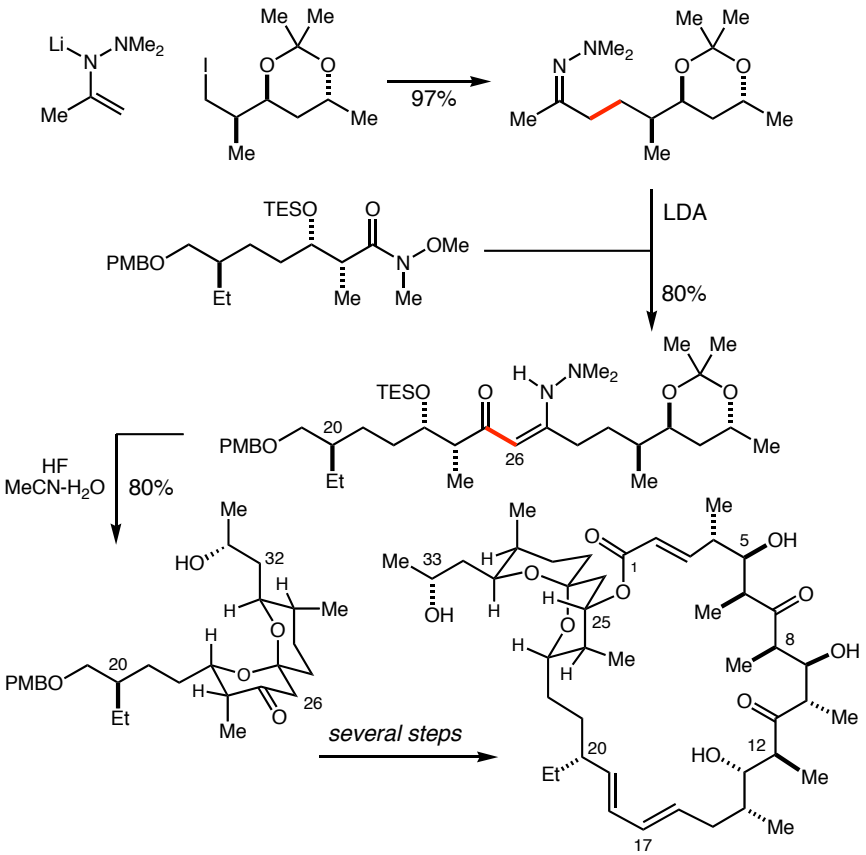

The X-206 Synthesis, *S. L. Bender, Ph. D. Thesis, Harvard University, 1986*

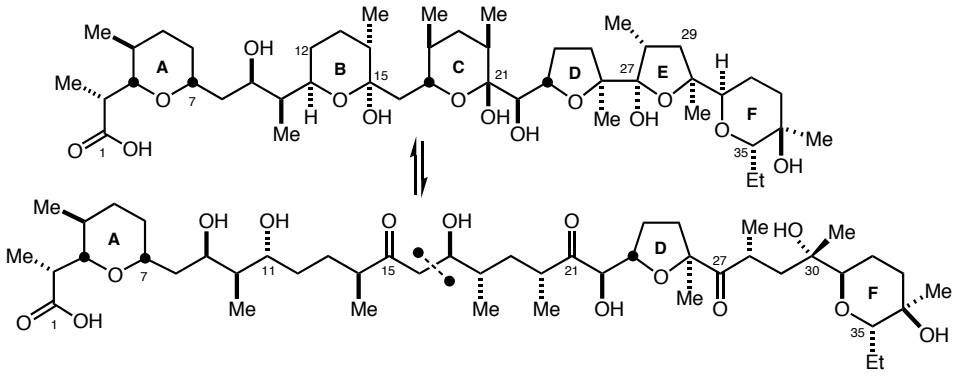

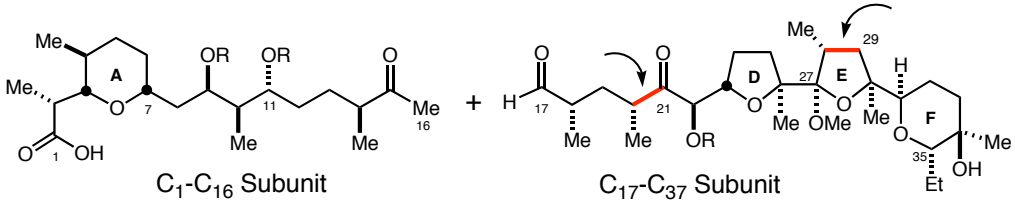

Problem is to control C=O reactivity on central D-fragment

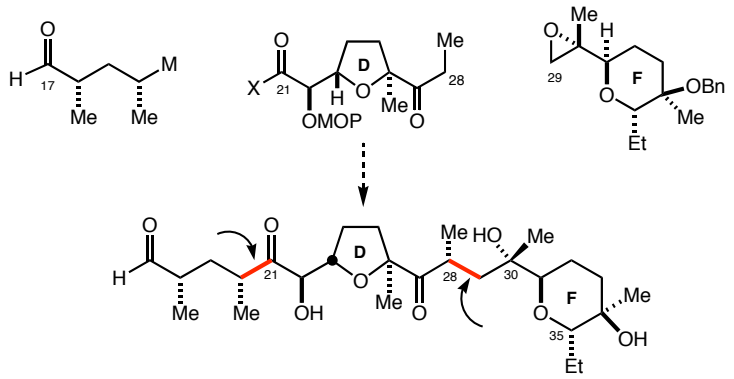

The Solution:

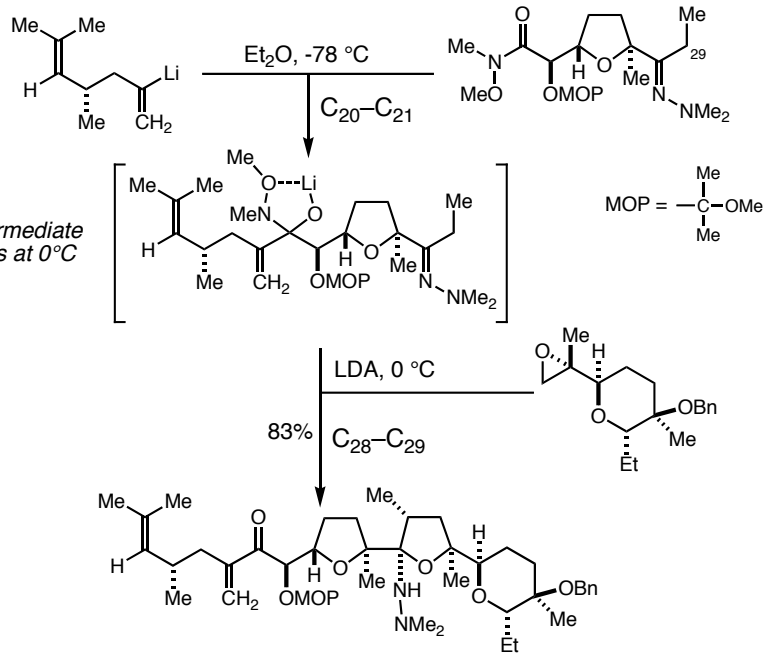

Evans, Bender, Morris J. Am. Chem. Soc. **1988**, *110*, 2506.

Weinreb Amide Coupling Studies

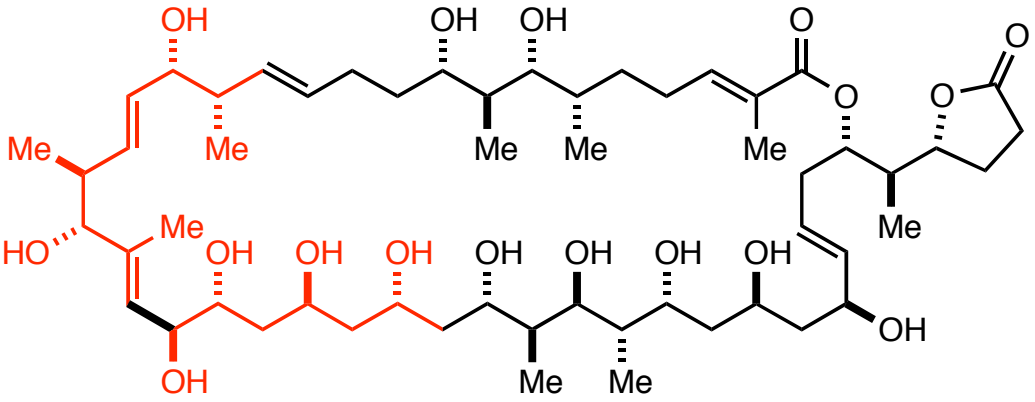

Oasomycin

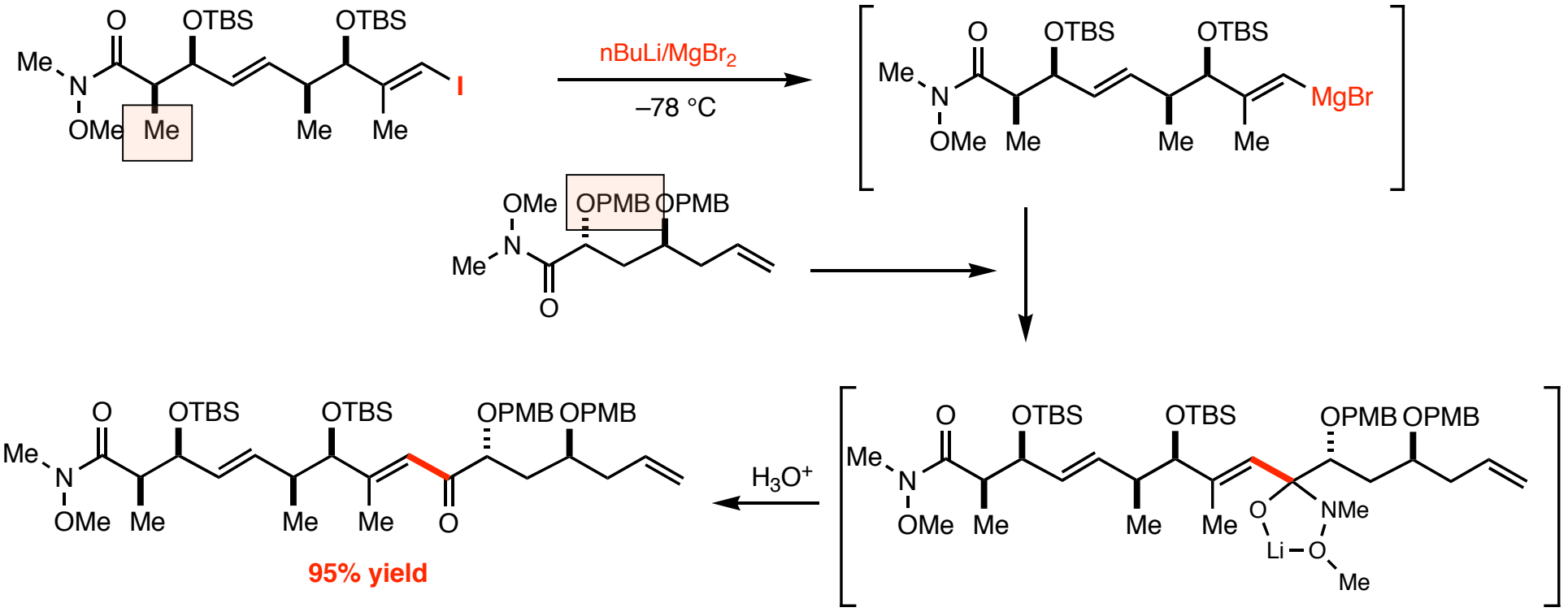

Pavel Nagorny, Angew. Chem. Int Ed, in Press

The Dieckmann Condensation

Reviews: Schaefer, Bloomfield, *Organic Reactions* **1967**, *15*, 1.
Davis & Garratt, *Comprehensive Organic Synthesis* **1991**, *2*, 806-829

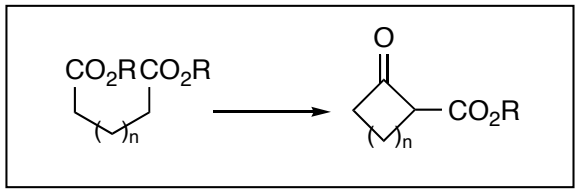

Accesible Ring Sizes

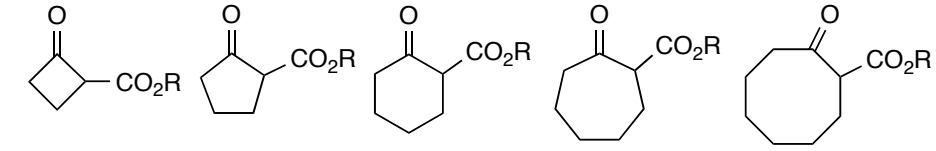

not viable | excellent | excellent | acceptable | situation dependent high dilution required

The individual steps:

Enolization:

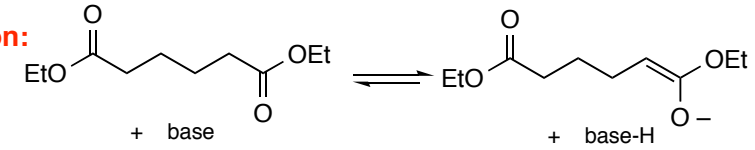

A variety of bases may be considered for the enolization step.
Either alkoxide or a non-nucleophilic base such as NaH are commonly used.
Choice of base can be important (Vide infra).

Ring Closure:

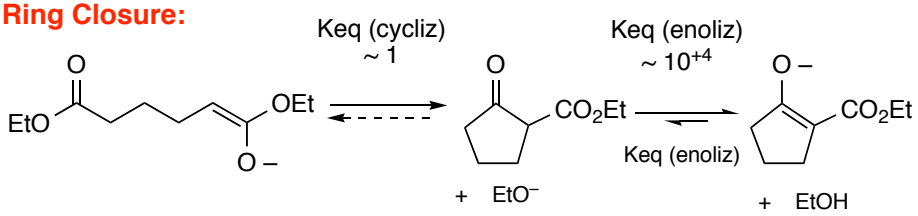

Statements claiming that the final enolization step renders the process irreversible are simply incorrect.

Regioselectivity:

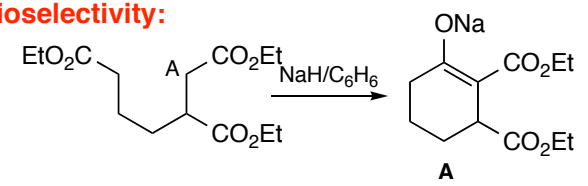

Kinetic Control?

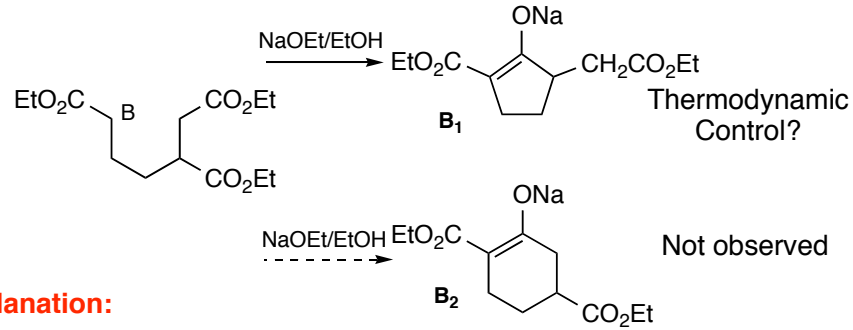

Thermodynamic Control?

Not observed

Explanation:

Enolization at (A) preferred on basis of inductive effects. Hence, Path A preferred in kinetically controlled situation

Enolates (B1) and (B2) both more stable than enolate (A)

Under equilibrating conditions (B1) appears to be preferred over (B2)

The effect of beta heteroatoms: classical kinetic vs. thermodynamic control

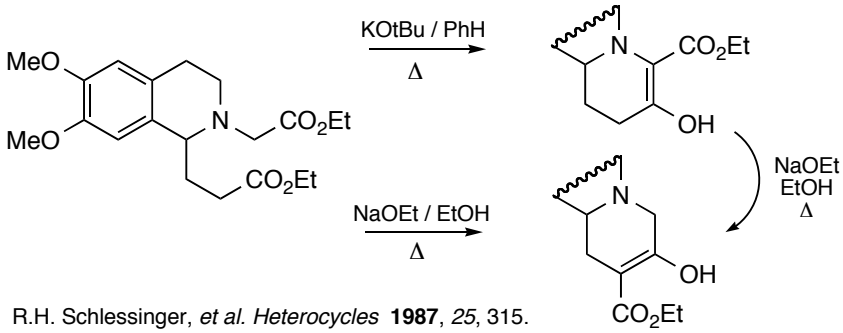

R.H. Schlessinger, *et al. Heterocycles* **1987**, *25*, 315.

Miscellaneous Dieckmann Reactions of Potential Interest

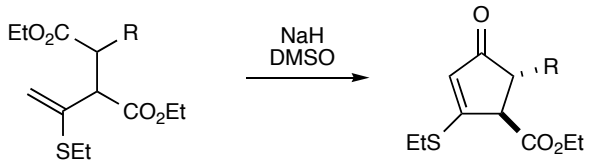

R.Danieli, *J.Org.Chem.* **1983**, *48*, 123.

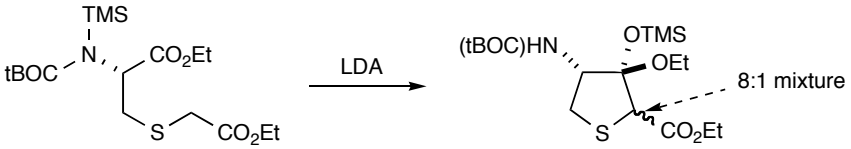

J.L. Adams, *J.Org.Chem.* **1985**, *50*, 2730.

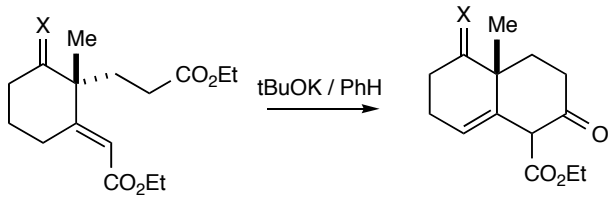

Peterset, *Recl.Trav.Chim.Pays-Bas* **1977**, *96*, 219.

Deduce the mechanism of this multistep process.

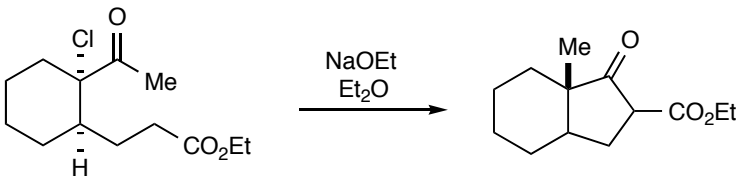

G.Stork and Co-workers, *J.Am.Chem.Soc.* **1960**, *82*, 4315.

Intramolecular Ketone Acylation

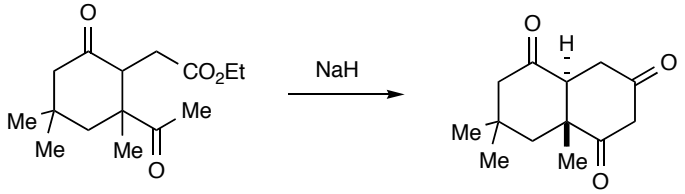

H.-J. Liu and Co-workers, *Tet.Lett.* **1982**, *23*, 295.

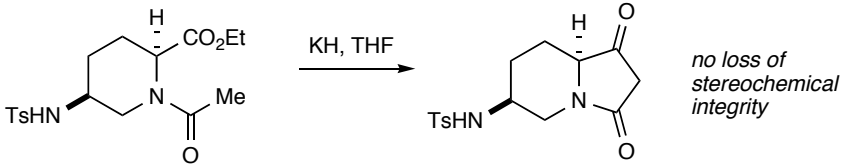

T.M. Harris and Co-workers, *J.Org.Chem.* **1984**, *49*, 3681.

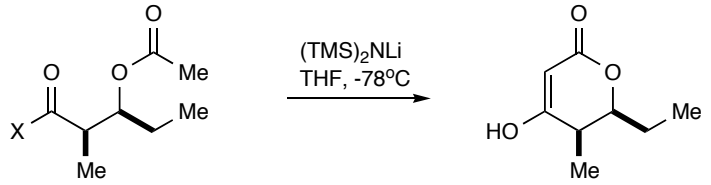

When X = NR_2, this is a good reaction, but when X = OR, it is a poor reaction.

S.Brandawge and Co-workers, *Tet.Lett.* **1992**, *33*, 3025.

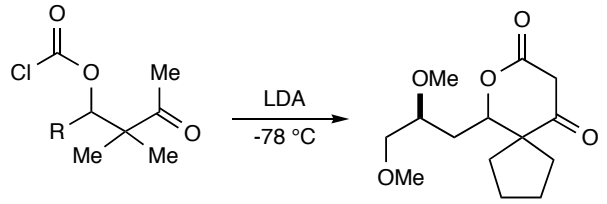

Kocienski and Co-workers, *Tet.* **1990**, *46*, 1716

Intramolecular Enolate Acylation–Dieckmann Condensation

Kinetically controlled Cyclizations

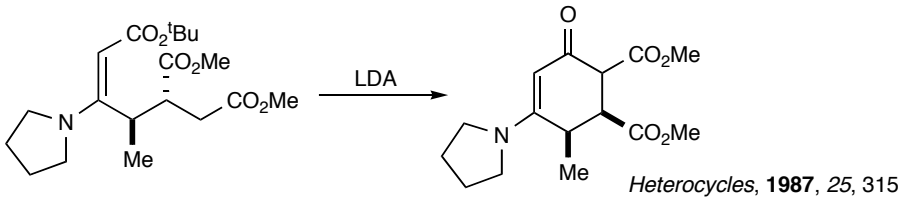

Heterocycles, **1987**, *25*, 315

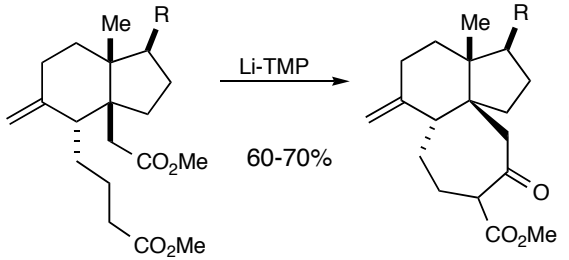

JACS, **1979**, *101*, 5060

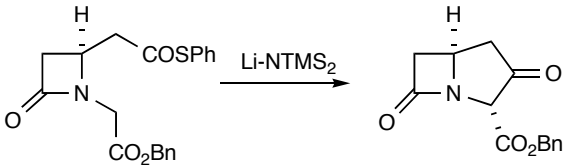

Tet. Let, **1981**, *22*, 3883

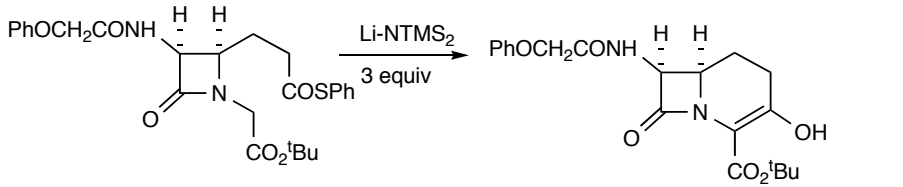

Hatanaka, *Tet. Let*, **1983**, *24*, 4837

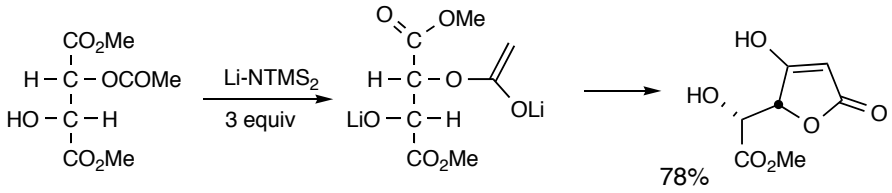

Brandange, *JOC*, **1984**, *49*, 927

Multistep Condensations

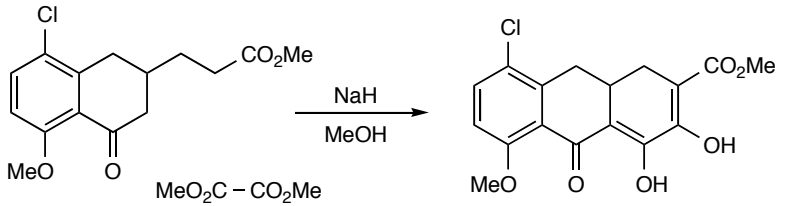

Woodward, *JACS*, **1962**, *84*, 3222

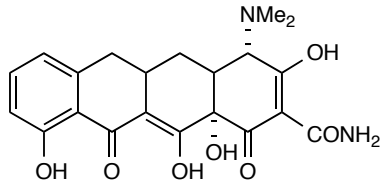

6-demethyl-6-deoxy-tetracycline

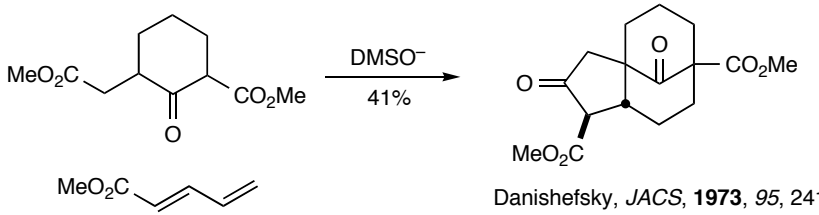

Danishefsky, *JACS*, **1973**, *95*, 2410

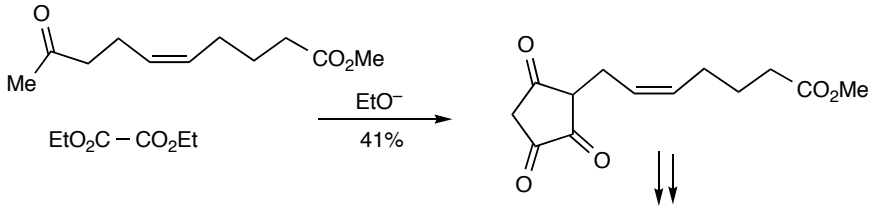

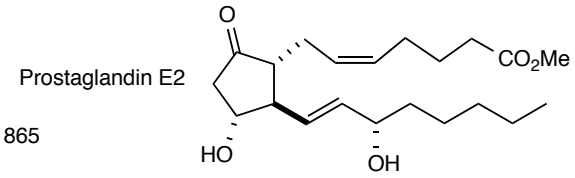

Prostaglandin E2

Sih, *JACS*, **1975**, *97*, 865

The Eschenmoser Coupling Reaction

Key Bond Construction Needed for the B12 Synthesis:

The Problem:

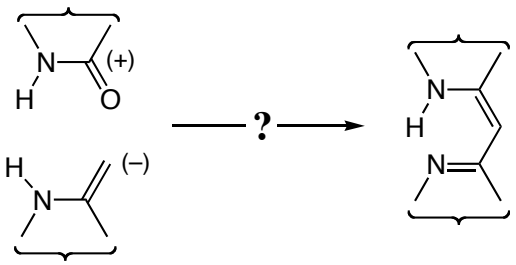

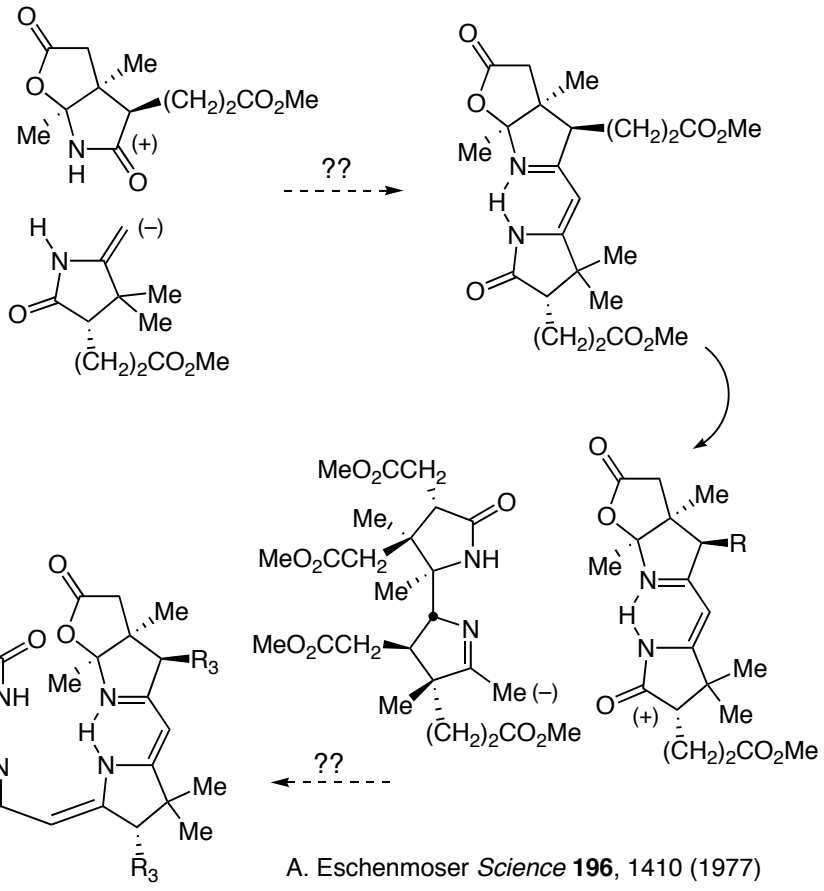

A. Eschenmoser *Science* **196**, 1410 (1977)

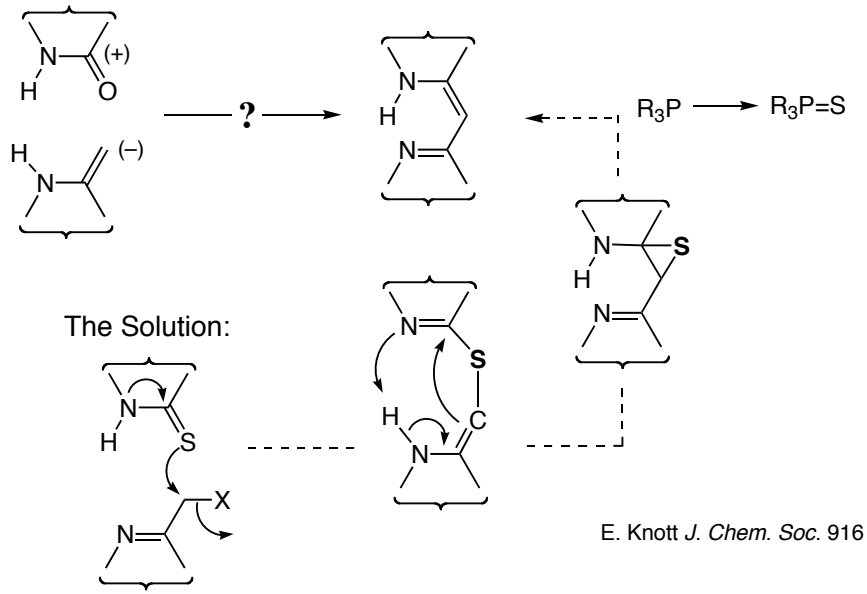

E. Knott *J. Chem. Soc.* 916 (1955)

The General Reaction: Acylation of an Amide C=O

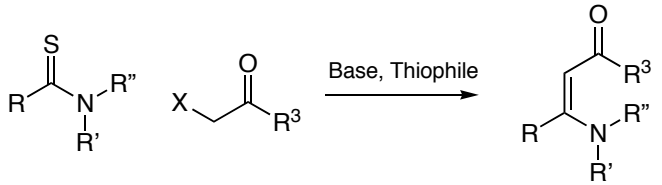

Key papers:

A. Eschenmoser *Helv. Chim. Acta.* **54**, 710 (1971)
A. Eschenmoser *Angew. Chem., Int. Ed. Engl.* **6**, 866 (1967)
A. Eschenmoser *Angew. Chem., Int. Ed. Engl.* **8**, 343 (1969)
Review: Trost *Comp. Org. Synth.* Vol. 2, Ch. 3.7 (1991)

The Thioamide component:

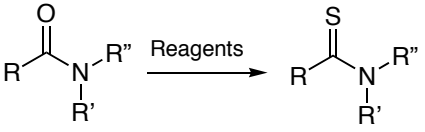

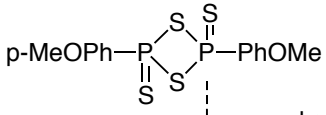

P_4S_{10}	JOC 46, 3558 (1981), Synthesis 149 (1973)
Lawesson's Reagent	Bull. Chim. Soc. Belg. 87, 229 & 293 (1978)
P_4S_{10}, Et_3N or $NaHCO_3$	Indian J. Chem., Sect. B 14, 999, (1976) JACS 102, 2392 (1980)
$RCS_2R' + R_2NH \rightarrow$ Thioamide	Chem. Ind. (London) 803 (1974)
Imidate $+H_2S \rightarrow$ Thioamide	Angew. Chem. 79, 865 (1967)

The Eschenmoser Coupling Reaction-2

Reagents for the Reaction:

Bases:
Inorganic: $MHCO_3$, MOH, MH, MOR
Organic: R_3N, N-methylmorpholine, buffered solutions

Thiophiles: Ar_3P, R_3P, $(RO)_3P$

Combination:

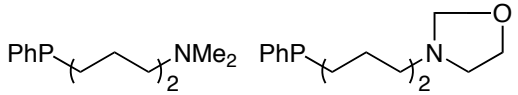

H. Rapoport *J. Org. Chem.* **46**, 3230 (1981)
A. Eschenmoser *Helv. Chim. Acta.* **54**, 710 (1971)

A. Eschenmoser *Science* **196**, 1410 (1977)

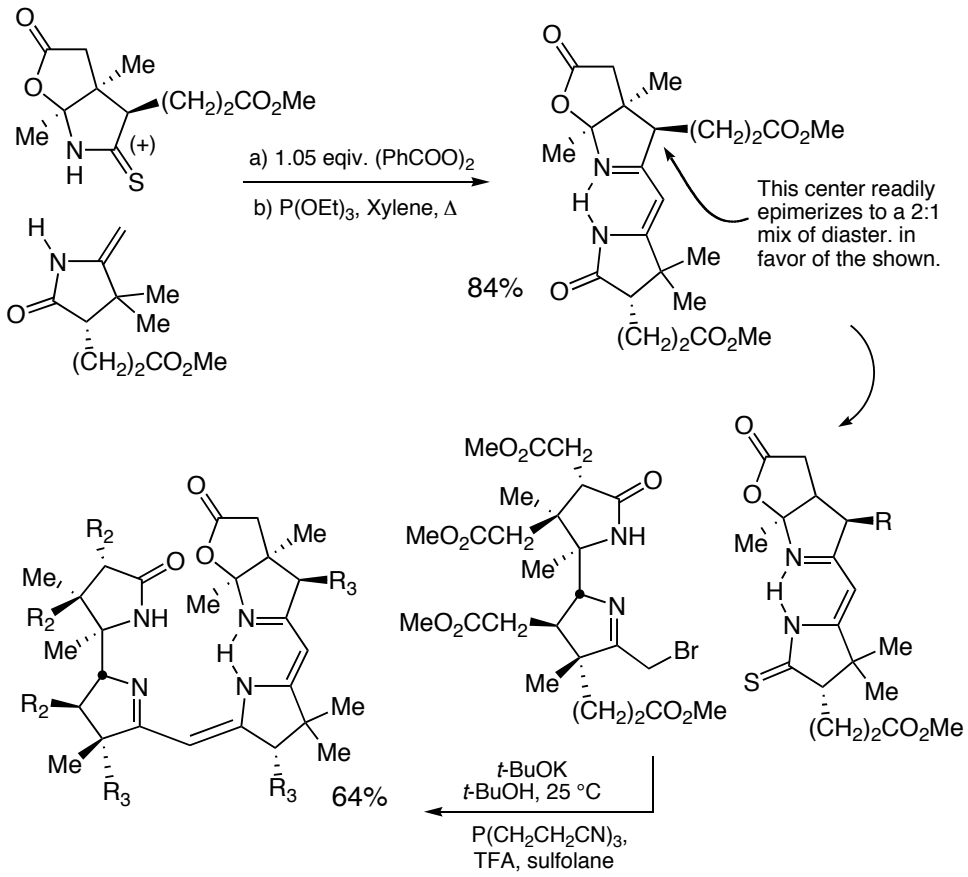

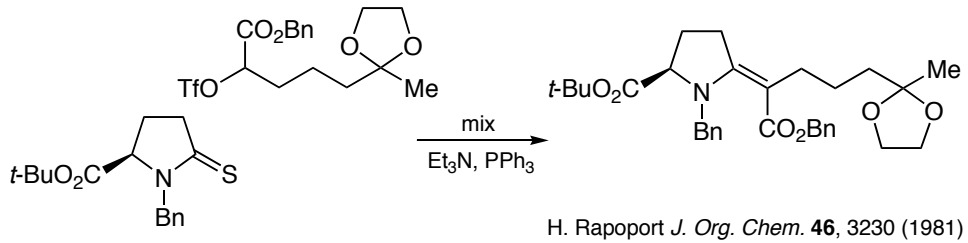

H. Rapoport *J. Org. Chem.* **46**, 3230 (1981)

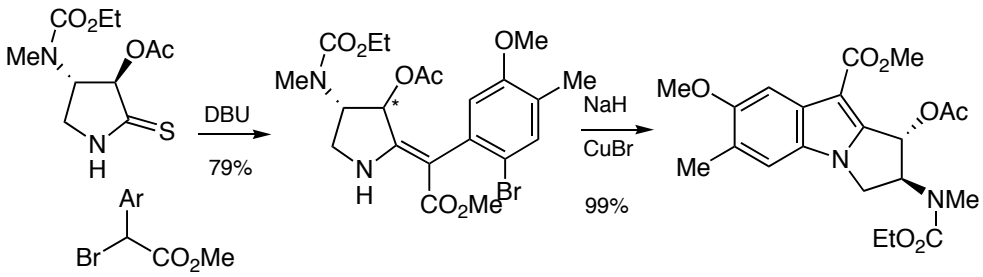

T. Kametani *J. Chem. Soc., Perkin Trans. I* 1607 (1980)

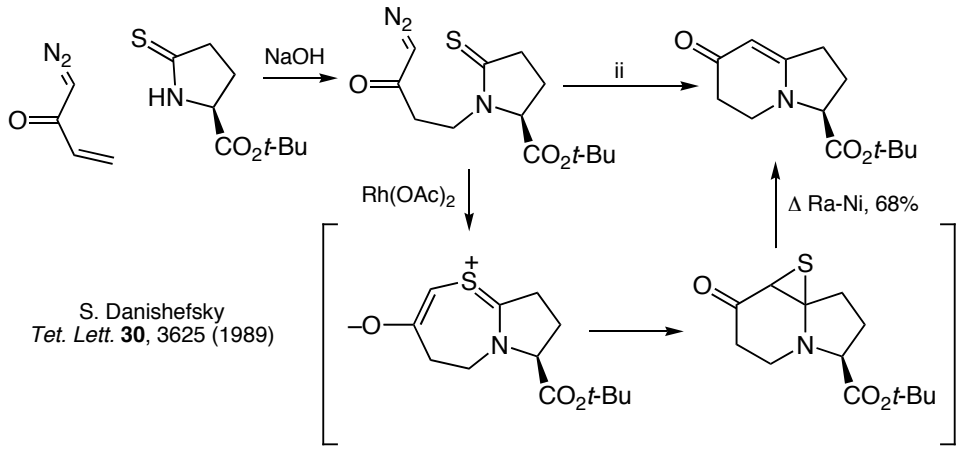

S. Danishefsky
Tet. Lett. **30**, 3625 (1989)

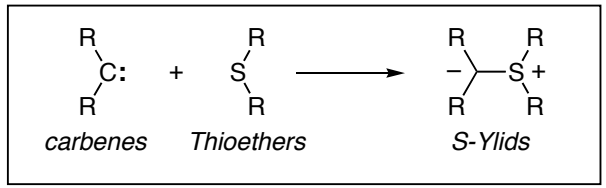

http://www.courses.fas.harvard.edu/colgsas/1063

Chemistry 206

Advanced Organic Chemistry

Lecture Number 27

The Aldol Reaction–1

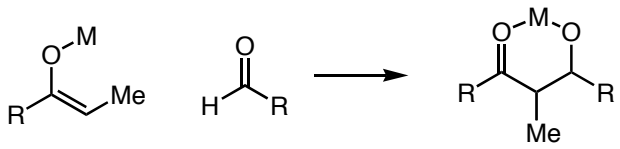

- Polyketide Biosynthesis
- Historical Perspective on the Aldol Reaction
- Aldol Diastereoselectivity
- Enolate Diastereoface Selectivity
- Absolute Control in the Aldol Process

Reading Assignment for this Week:

Carey & Sundberg: **Part A**; Chapter 7
Carbanions & Other Nucleophilic Carbon Species

Carey & Sundberg: **Part B**; Chapter 2
Reactions of Carbon Nucleophiles with Carbonyl Compounds

D. A. Evans

Monday
November 27, 2006

Suggested Reading

Stereoselective Aldol Reactionsw in the Synthesis of Polyketide natural Products, I. Paterson et al. in Modern Carbonyl Chemistry, pp 249-297, J. Otera, Ed. Wiley VCH, **2000**

Ager, D. J., I. Prakash, et al. (**1997**). "Chiral oxazolidinones in asymmetric synthesis." Aldrichimica Acta 30(1): 3-12

Other Useful References

Evans, D. A., J. V. Nelson, et al. (**1982**). "Stereoselective Aldol Condensations." Top. Stereochem. 13: 1.

Heathcock, C. H. (**1984**). The Aldol Addition Reaction. Asymmetric Synthesis. Stereodifferentiating Reactions, Part B. J. D. Morrison. New York, AP. 3: 111.

Oppolzer, W. (**1987**). "Camphor Derivatives as Chiral Auxiliaries in Asymmetric Synthesis." Tetrahedron **43**: 1969.

Heathcock, C. H. (**1991**). The Aldol Reaction: Acid and General Base Catalysis. Comprehensive Organic Synthesis. B. M. Trost and I. Fleming. Oxford, Pergamon Press. 2: 133.

Heathcock, C. H. (**1991**). The Aldol Reaction: Group I and Group II Enolates. Comprehensive Organic Synthesis. B. M. Trost and I. Fleming. Oxford, Pergamon Press. 2: 181.

Kim, B. M., S. F. Williams, et al. (**1991**). The Aldol Reaction: Group III Enolates. Comprehensive Organic Synthesis. B. M. Trost and I. Fleming. Oxford, Pergamon Press. 2: 239.

Franklin, A. S. and I. Paterson (**1994**). "Recent Developments in Asymmetric Aldol Methodology." Contemporary Organic Synthesis 1: 317-338.

Cowden, C. J. and I. Paterson (**1997**). "Asymmetric aldol reactions using boron enolates." Org. React. (N.Y.) 51: 1-200.

Nelson, S. G. (**1998**). "Catalyzed enantioselective aldol additions of latent enolate equivalents." Tetrahedron: Asymmetry 9(3): 357-389.

Mahrwald, R. (**1999**). "Diastereoselection in Lewis-acid-mediated aldol additions." Chem. Rev. 99(5): 1095-1120.

The Aldol Reaction: Polypropionate Biosynthesis

"Nature, it seems, is an organic chemist having some predilection for the aldol and related condensations."
J. W. Cornforth

J. W. Cornforth
Nobel Prize, 1975

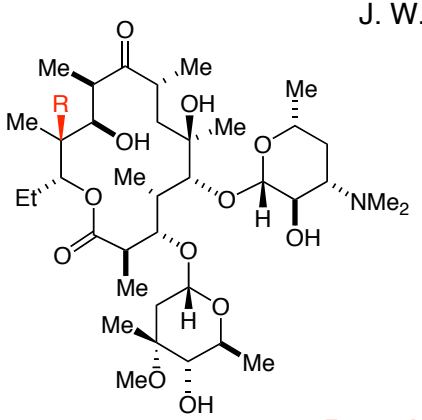

Erythromycin A, R = OH
Erythromycin B, R = H

Retro-biosynthesis: Erythromycin A

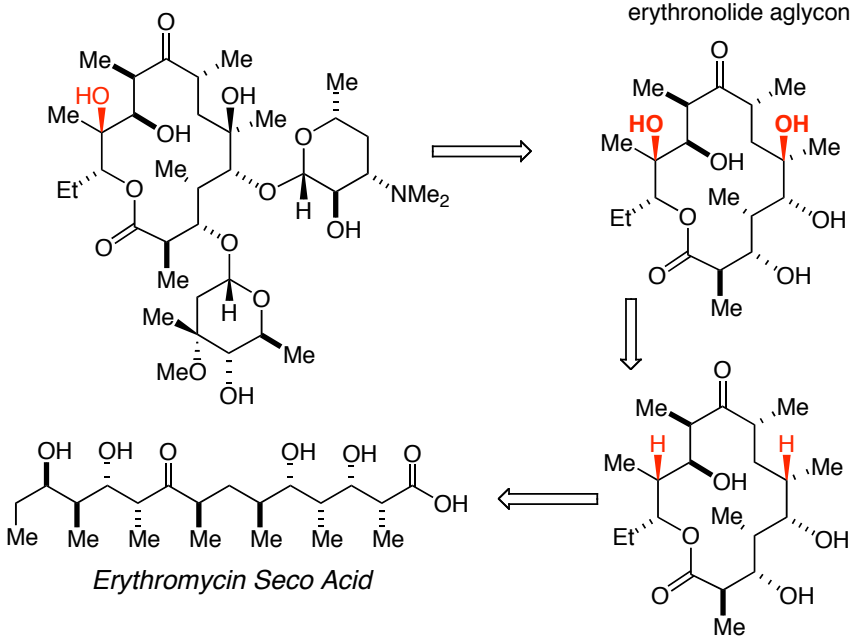

Erythromycin Seco Acid

Recent overview: Staunton, "Polyketide biosynthesis: a millennium review." *Nat. Prod. Rep.* **2001**, *18*, 380-416.

Polypropionate Biosynthesis: The Elementary Steps

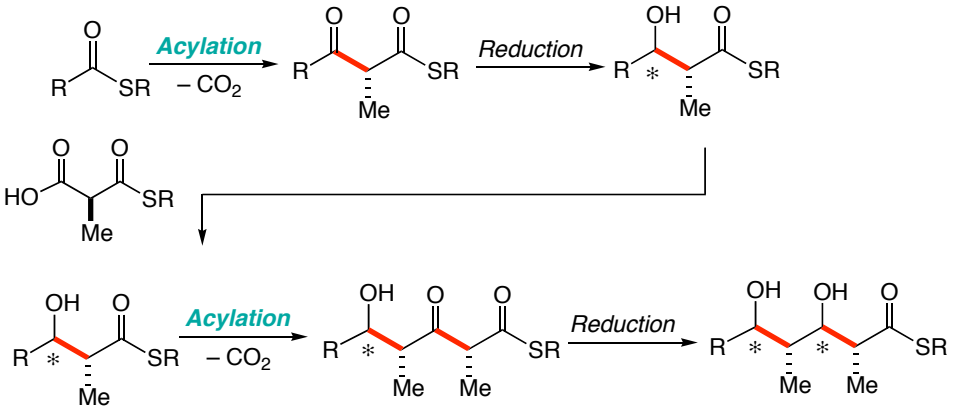

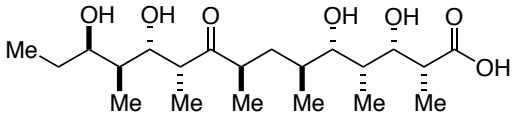

Erythromycin Seco Acid

The 7 Propionate Subunits

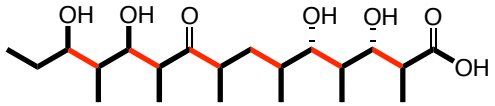

Acylation Event

The timing of the decarboxylation event is not yet known

Concerted option is popular view.

Stepwise alternative makes chemical sense

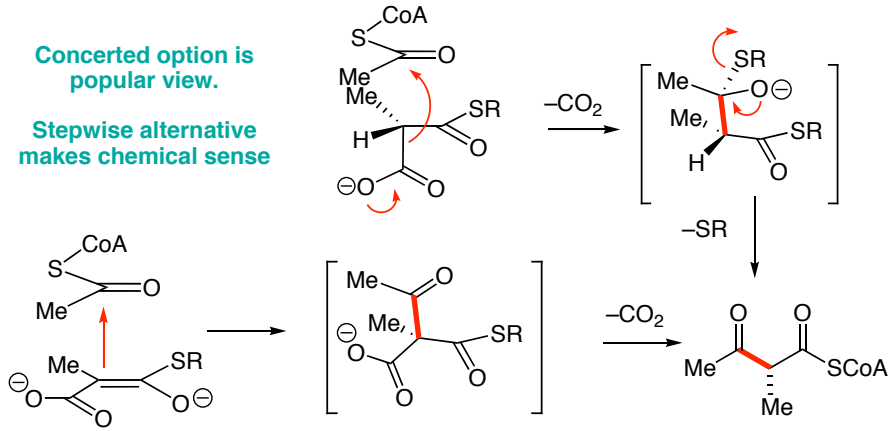

See Lecture 24; page 24-08 for first laboratory example

Polypropionate & Polyacetate Biosynthesis: Develop a Laboratory Simulation

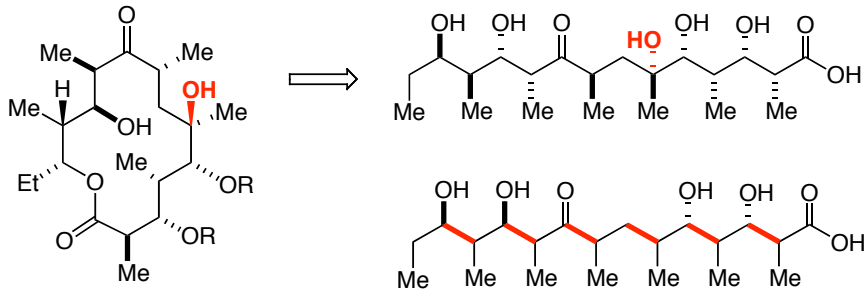

Erythrolide B

The 7 Propionate Subunits

Polypropionate Biosynthesis: The Elementary Steps

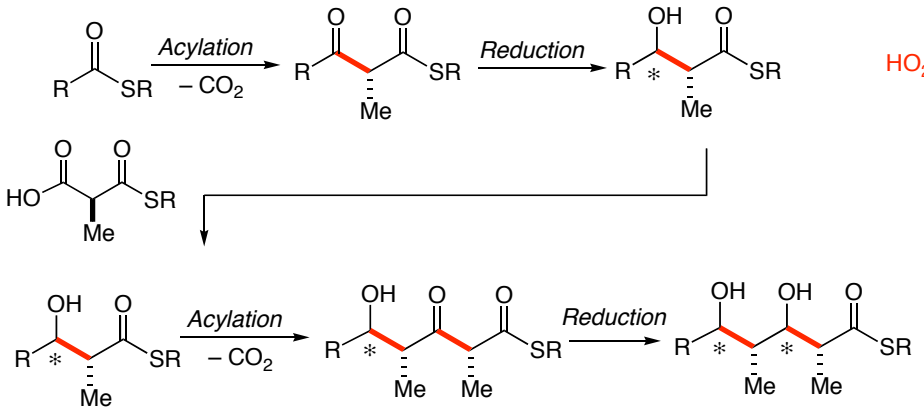

The Laboratory Mimic:

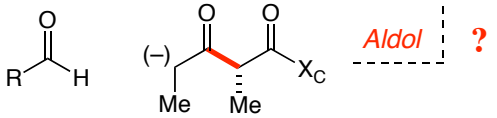

Dipropionyl Synthon

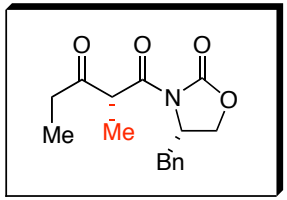

See Lecture 26; page 4:
with M. Ennis JACS ***1984****, 106, 1154.*

Latter Stages of Lonomycin Biosynthesis

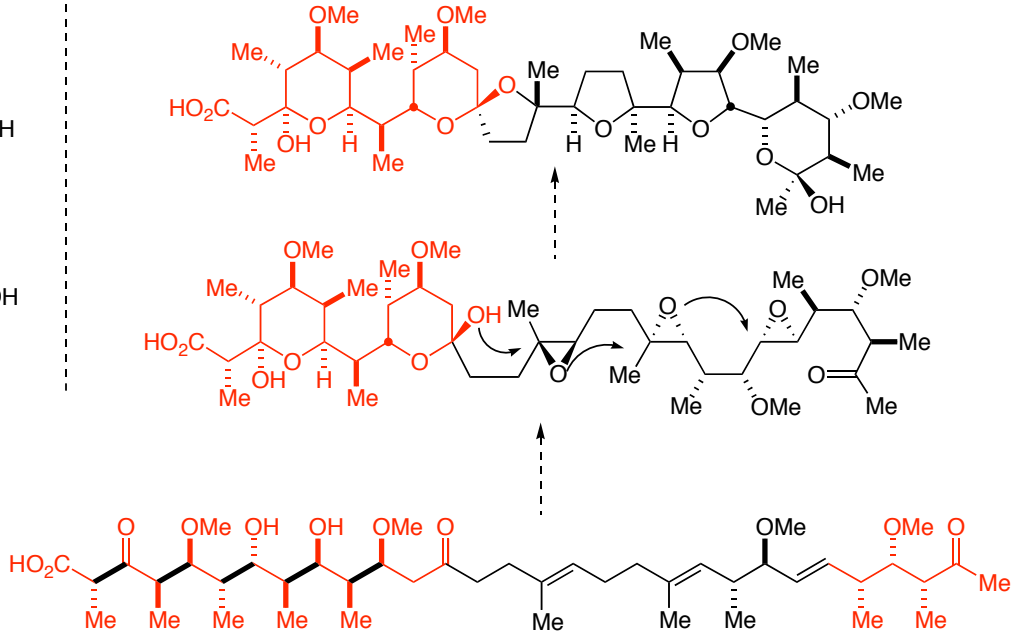

Cane, Celmer, Westley *JACS* **1983**, *105*, 3594

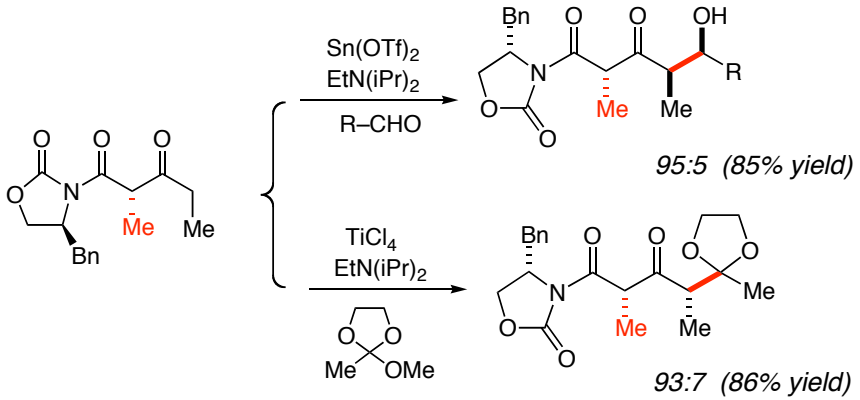

with Ratz, Huff, & Sheppard, *JACS* **1995**, *117*, 3448

General Reviews of the Aldol Literature:

Mukaiyama in *Organic Reactions*, **1982**; Vol 28, pp 203-331
Evans in *Topics in Stereochemistry*, **1982**; Vol 13, pp 1-115
Heathcock in *Asymmetric Synthesis*, **1984**; Vol 3, pp 111-212

Comprehensive Organic Synthesis, **1991**; Vol 2

Group I & II metal enolates: Heathcock; Chapter 1.6, pp 181
Group III metal enolates: Masamune; Chapter 1.7, pp 239
Transition metal enolates: Paterson; Chapter 1.9, pp 301

Control relative stereochemical relationships

Zimmerman 1957:

Proposed chair-like geometry for the Ivanov Reaction

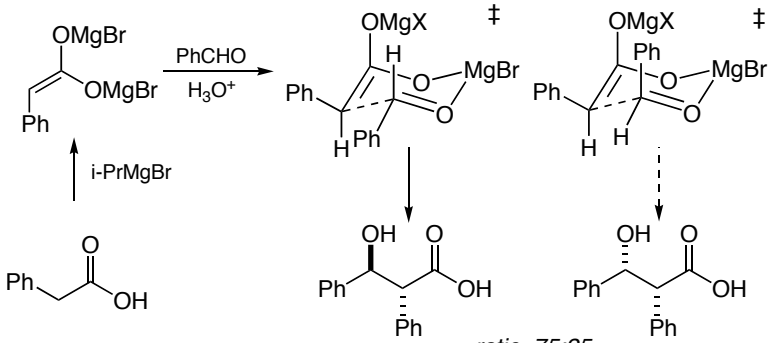

Zimmerman recognized that diastereoselection should be a function of the relative sizes of the substituents on the carbonyl component.

He also speculated on the role that the metal center might play in controlling the process.

The only flaw in the study was that he failed to determine whether the aldol adducts were stable to the reaction conditions.

Zimmerman, *J. Am. Chem. Soc* ***1956***, *79,* 1920 **(handout)**

DuBois 1965-67:

Rough correlation between enolate stucture & product stereochemistry for alkali and alkaline earth enolates

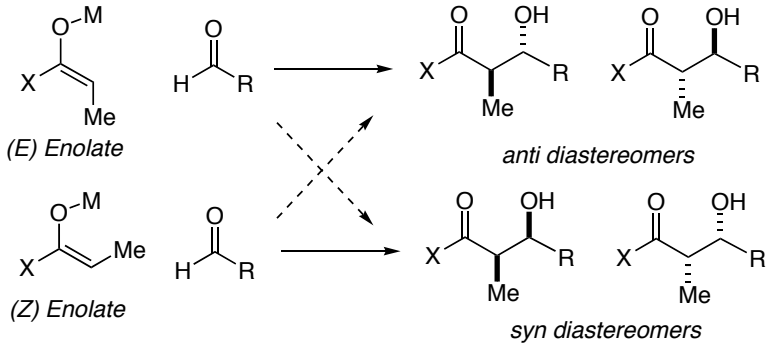

Zimmerman-Traxler Model for *(Z)* Enolates

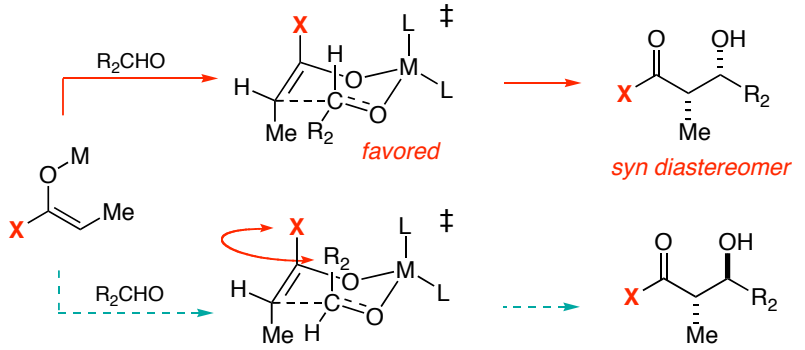

X = CMe_3	M = Li	> 98 : 2	Heathcock 1977
	M = MgBr	> 95 : 5	DuBois 1972
X = C_6H_5	M = Li	80 : 20	
	M = Li	48 : 52	
	M = $AlEt_2$	50 : 50	House 1971

Stereocontrol optimal for "large" X; the reaction is not general.

Why Boron?

To tighten up the transition state. Design TS where control can come exclusively from metal center

M–O	B–O	M–C	B–C
1.9-2.2 Å	1.4-1.5 Å	2.0-2.2 Å	1.5-1.6 Å

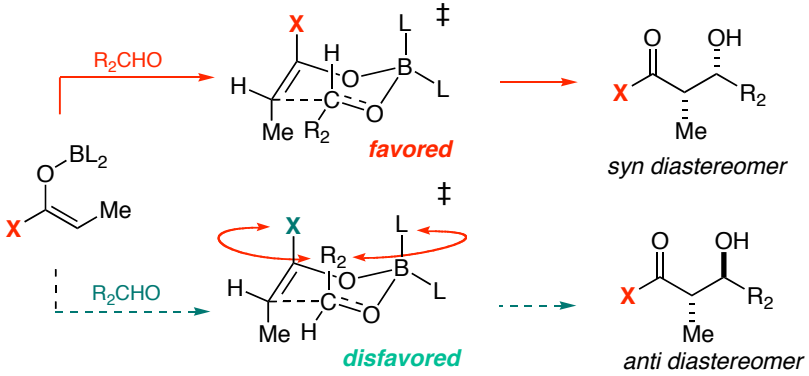

		syn:anti	
X = CMe_3	M = Li	> 98 : 2	Heathcock 1977
	M = MgBr	> 95 : 5	DuBois 1972
	M = BBu_2	> 97 : 3	DuBois 1972
X = C_6H_5	M = Li	80 : 20	Evans, Masamune 1979-81
	M = BBu_2	> 97 : 3	
X = Et	M = Li	80 : 20	
	M = BBu_2	> 97 : 3	
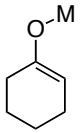	M = Li	48 : 52	House 1971
	M = $AlEt_2$	50 : 50	Yamamoto 1977
	M = BBu_2	33 : 67 (ether)	
	M = BBu_2	17 : 83 (pentane)	
	M = BCy(thex)	6 : 94 (CH_2Cl_2)	
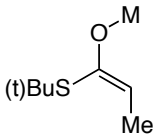	M = $B(Cyp)_2$	<5 : 95 (pentane)	

Evans et al. *JACS* ***1979****, 101,* 6120-6123; *JACS* ***1981****, 103,* 3099-3111

Masamune*, Tet. Lett* ***1979****,* 1665, 2225, 2229, 3937

Are (E) enolates intrinsically less diastereoselective?

Now that there are good methods for preparing (E) enolates, it appears that both enolate geometries are nearly equivalent.

Dialkylboron chlorides (Brown)

JACS. **1989**, *111*, 3441-3442.
J. Org. Chem. **1992**, *57*, 499-504.

J. Org. Chem. **1992**, *57*, 2716-2721.
J. Org. Chem. **1992**, *57*, 3767-3772.
J. Org. Chem. **1993**, *58*, 147-153.

JACS. **1989**, *111*, 3441-3442.

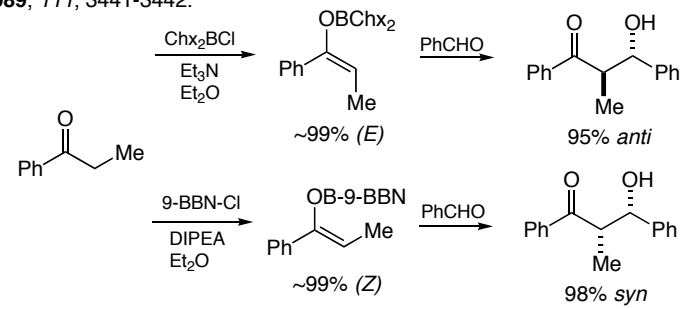

It appears that there is not a great difference in aldol diastereoselectivity

Dissection of the Aldol Problem: Select for one product diastereomer

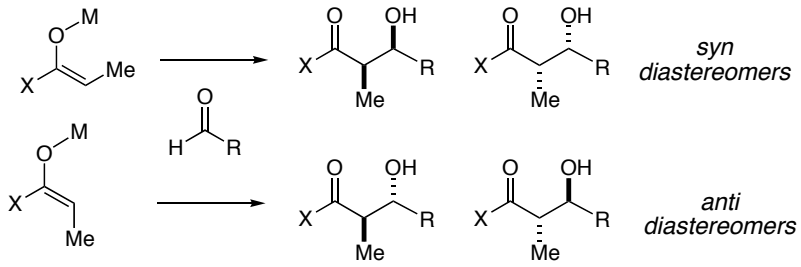

Control attack on the two enolate enantiofaces

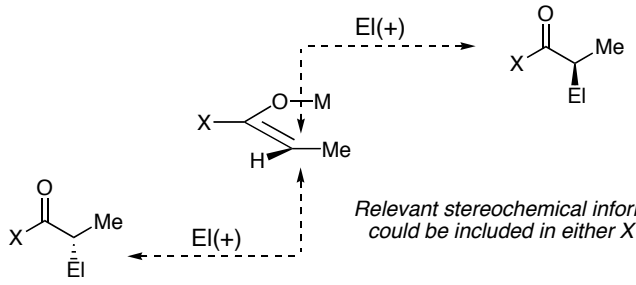

Relevant stereochemical information could be included in either X or M

Imide Enolates: The problem of enolate face selectivity

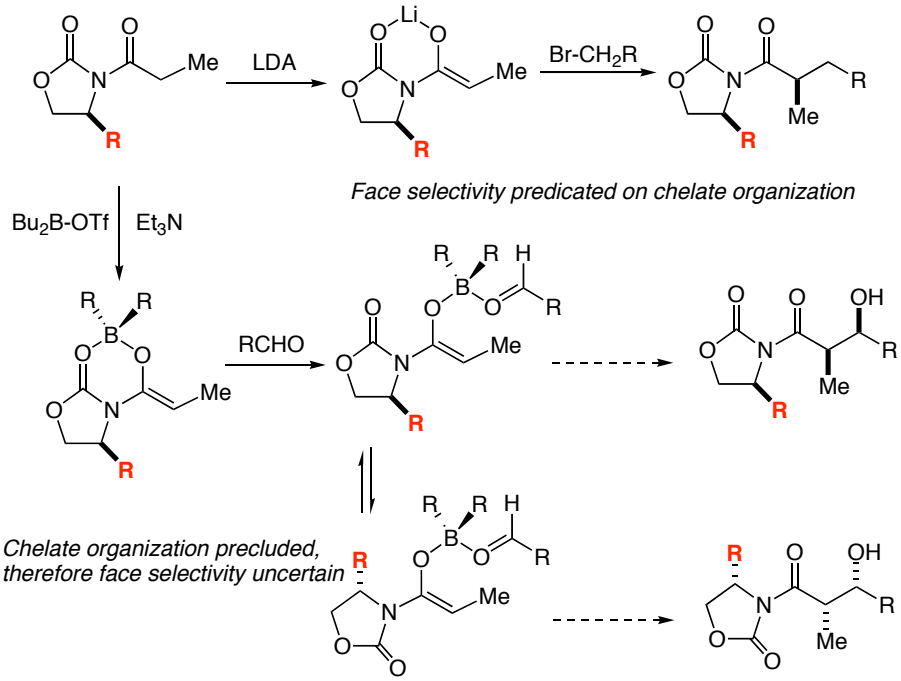

The aldol reaction selects for the opposite enolate diastereoface

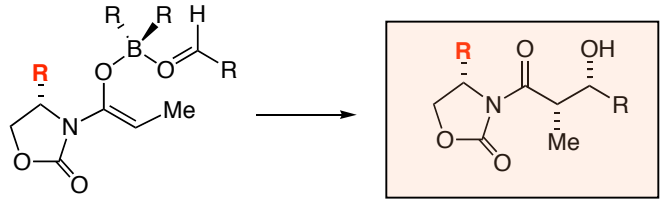

Result discovered but not predicted

diastereoselection > 98%

J. Am. Chem. Soc ***1981****, 103,* 2127-2129 **(Handout)**

The Alpha substituent, X, plays pivotal role in aldol diastereoselection

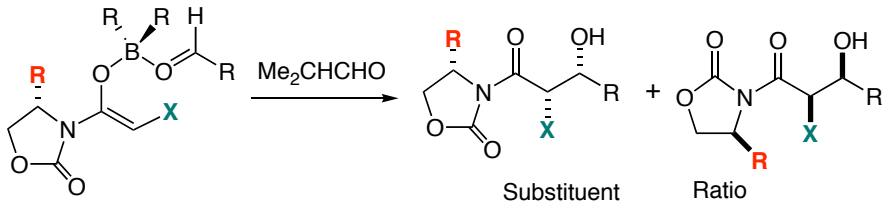

Substituent	Ratio
X = Me	> 300 : 1
X = SMe	60 : 1
X = H	1 : 1

How can we rationalize these data ?

Model for Asymmetric Induction (unpublished)

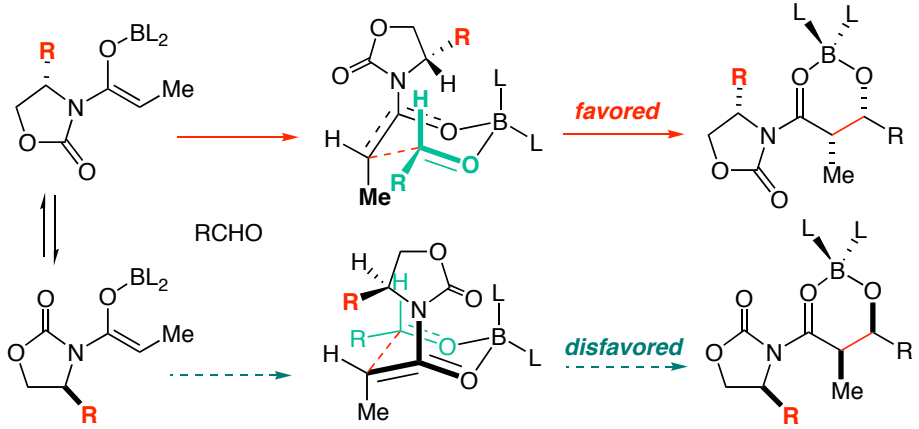

$\Delta\Delta G^{\ddagger}$ (273 K) ~ 2.6 kcal mol $^{-1}$

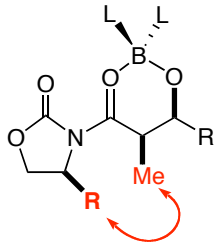

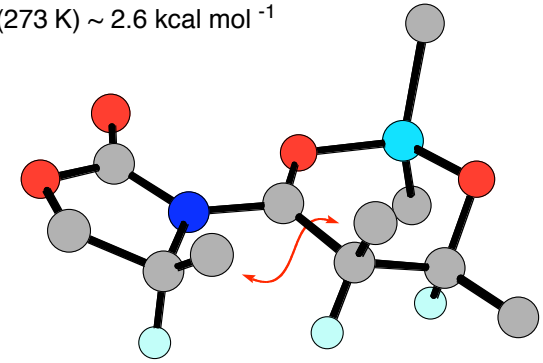

disfavored product diastereomer: The destabilizing interaction?

Aldol Reactions: A Third Reaction Variant

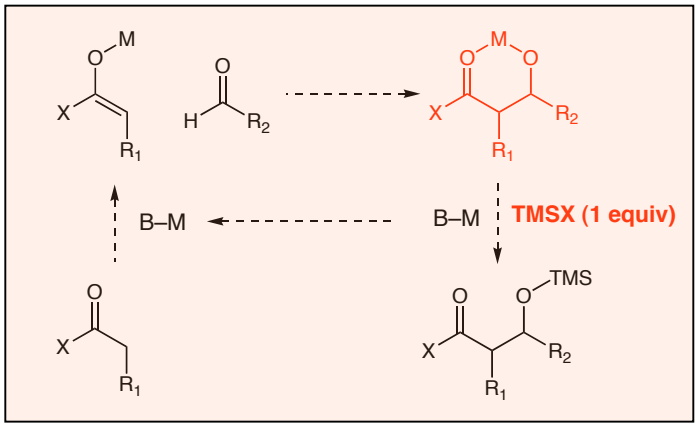

Requirement: **TMS–X must silylate aldolate but not enolate**

Anti Aldol Reactions from (Z) Enolates

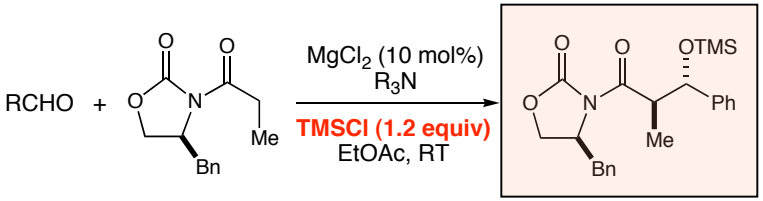

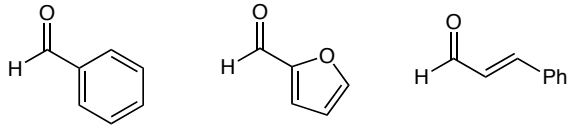

dr = 44:1 (91%) dr = 6:1 (80%) dr = 21:1 (92%)

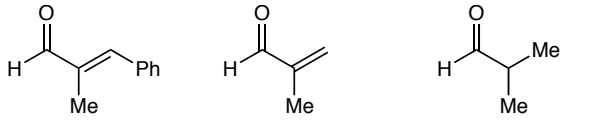

dr = 28:1 (92%) dr = 16:1 (77%) dr = 30:1 (65%)

Magnesium Enolates: with Tedrow, Shaw, Downey, *JACS* **2001**, *124*, 392

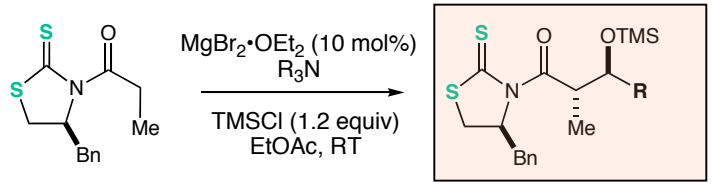

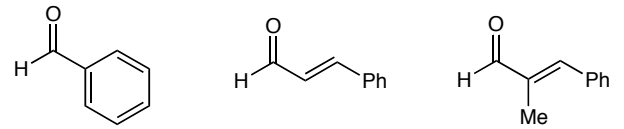

dr = 19:1 (85%) dr = 10:1 (87%) dr = 19:1 (90%)

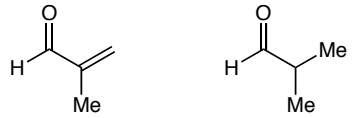

dr = 7:1 (56%) dr = 16:1 (77%)

Magnesium Enolates: with Tedrow, Shaw, Downey, *Org. Lett.* **2002**, *4*, 1127

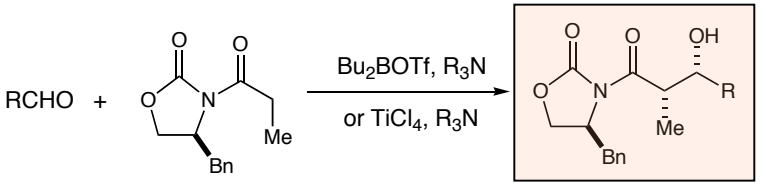

Boron with Bartroli & Shih *JACS* **1981**, *103*, 2127 **Titanium** *JACS* **1990**, *112*, 8215

Summary of Aldol Diastereoselection

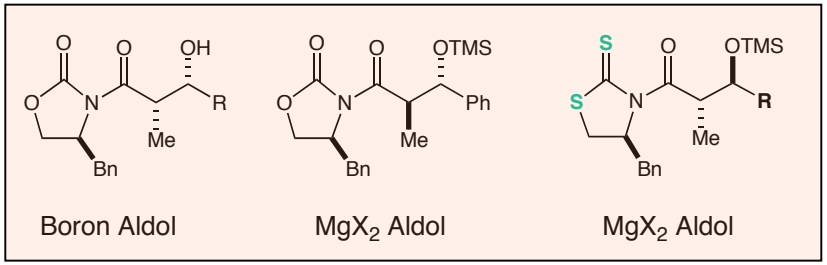

Proposed Boat-Preferred Aldol Transition States

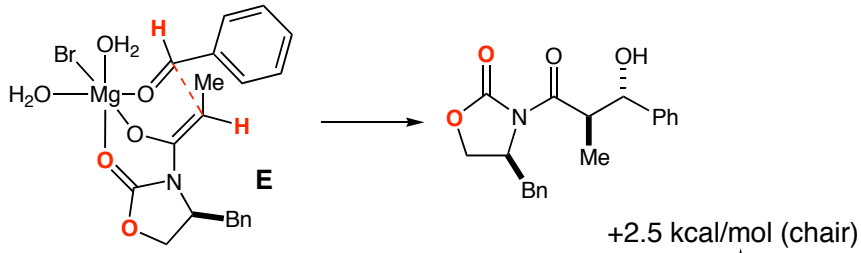

+2.5 kcal/mol (chair)

Tedrow, Shaw, Downey *Org. Lett.* **2002**, *4*, 1127

0 kcal/mol (boat)

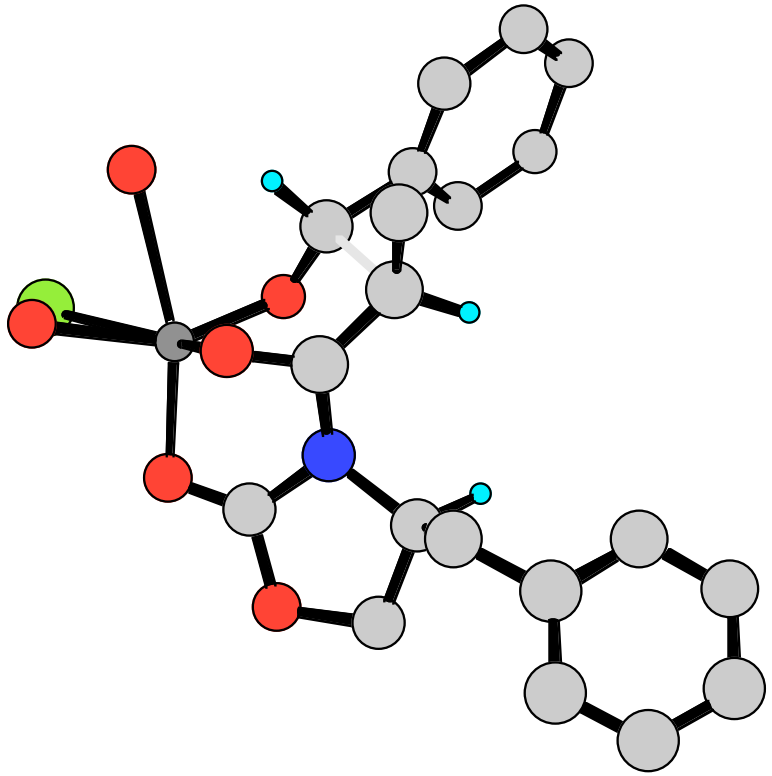

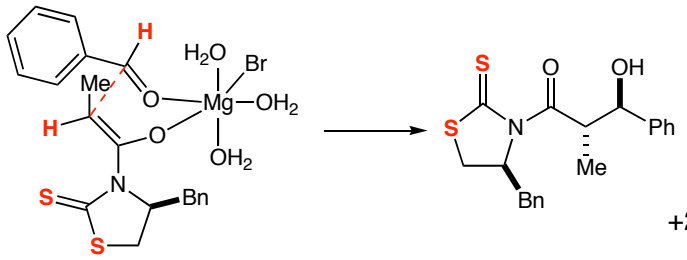

+2.8 kcal/mol (chair)

Tedrow, Shaw, Downey *Org. Lett.* **2002**, *4*, 1127

0 kcal/mol (boat)

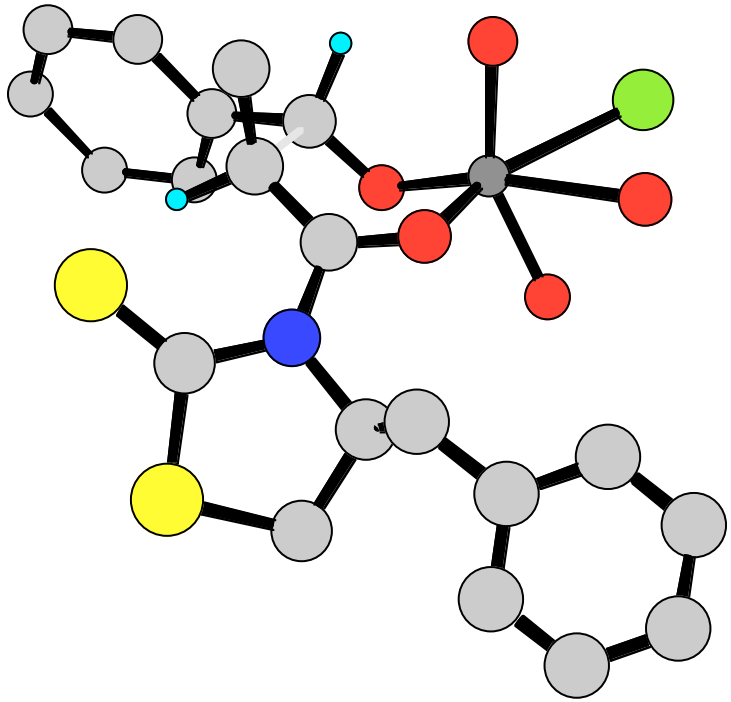

Boat transition states preferred for octahedral metals?

Imide Hydrolysis

Imides may suffer attack at either of the two C=O functions (eq 1, eq 2)

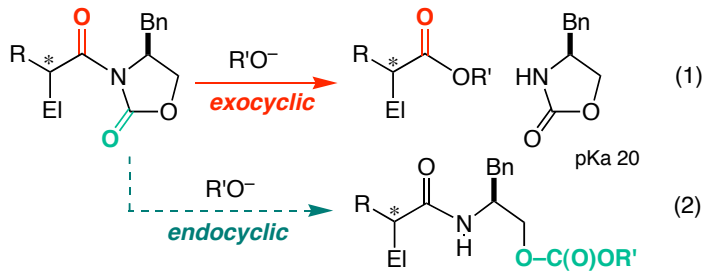

Product distribution a function of attacking nucleophile (*Tet. Lett.* ***1987****, 28,* 6141)

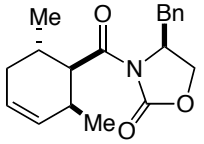

Substrate	Reagent	Exo:Endo Ratio
	LiOH	0 : 100
	LiOOH	76 : 16

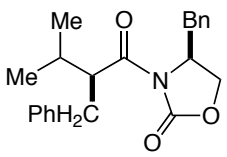

Substrate	Reagent	Exo:Endo Ratio
	LiOH	06 : 89
	LiOOH	96 : 04

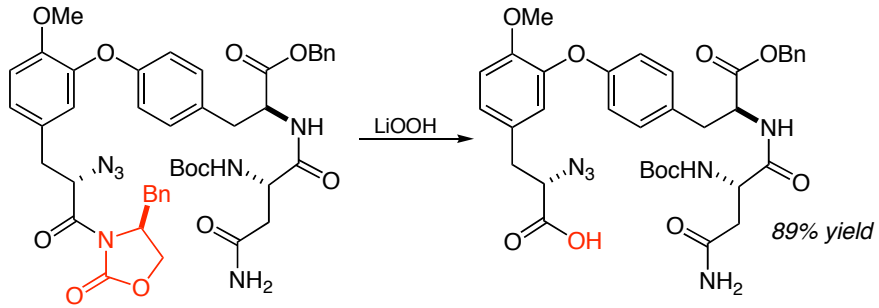

(OF-4949 Synthesis) JACS ***1989****, 111,* 1063

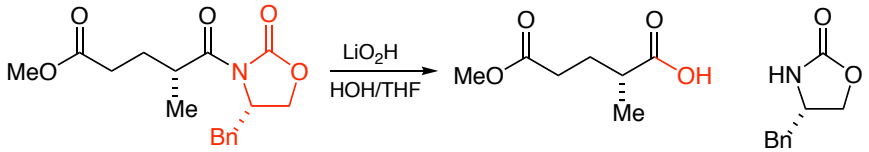

M. Bilodeau, unpublished results

complete hydroytic selectivity possible

Trans-esterification

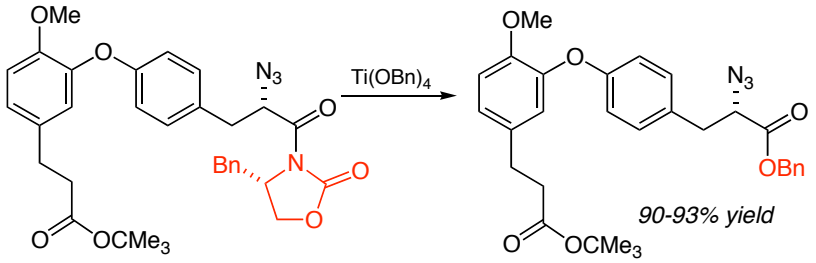

(OF-4949 Synthesis) JACS ***1989****, 111,* 1063

Trans-thioesterification:

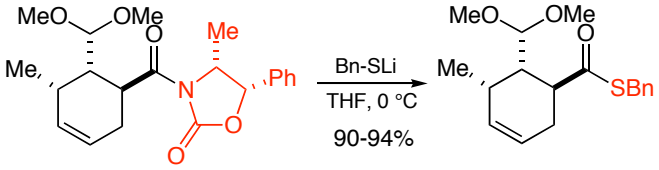

Damon, *Tet. Lett.* ***1990****, 31,* 2849-2852

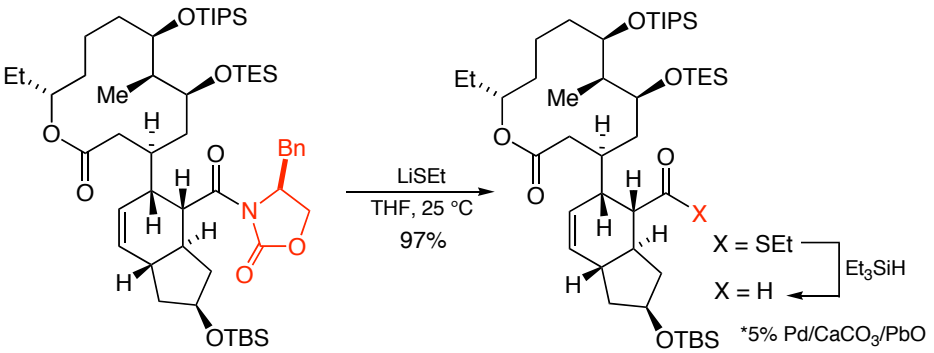

(Lepicidin Synthesis) J. Am. Chem. Soc ***1993****, 115,* 4497-4513

RCOSR ⟶ RCHO Fukuyama, *J. Am. Chem. Soc* ***1990****, 112,* 7050-7051

Transamination to Weinreb Amides (see Handout 24A)

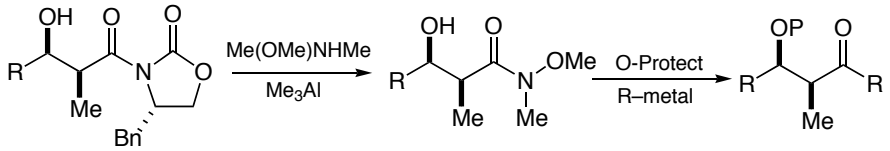

for recent examples see, *J. Am. Chem. Soc* ***1992****, 114,* 9434-9453

The Aldol Reaction: Syn Aldol Rxns of Chiral Ethyl Ketones

General Reaction for Syn Aldols: M = B, Ti

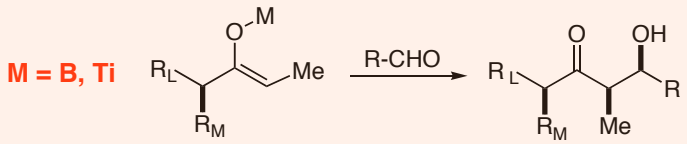

The Transition States:

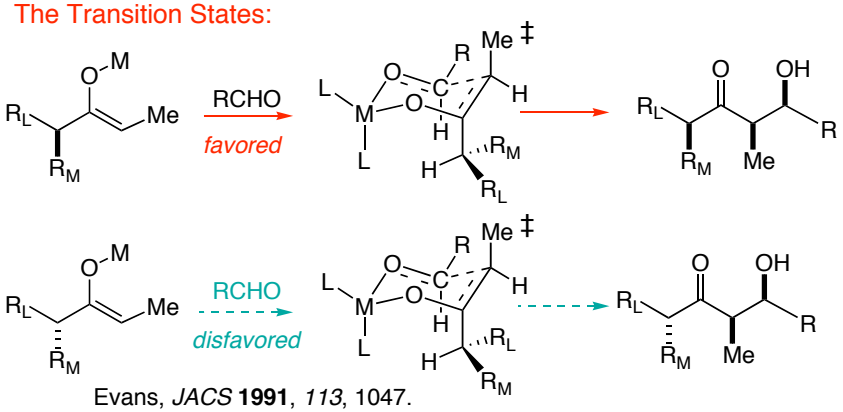

Evans, *JACS* **1991**, *113*, 1047.

Examples:

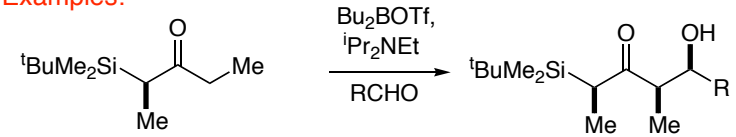

Enders *ACIEE* **1988**, *27*, 581.

Diastereoselection = 96-98%

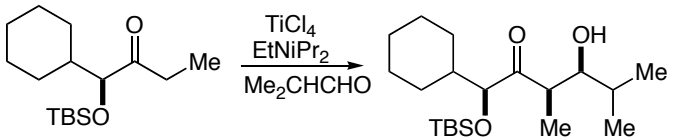

Evans, *JACS* **1991**, *113*, 1047.

Diastereoselection: 99:1 (81%)

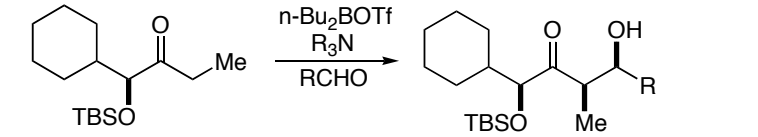

TBS = $SiMe_2{}^tBu$

Masamune, *JACS* **1981**, *103*, 1566.

R	Diastereoselection
Ph	97:3
Et	98:2
$BnOCH_2CH_2$	96:4
Me_2CH	>99:<1

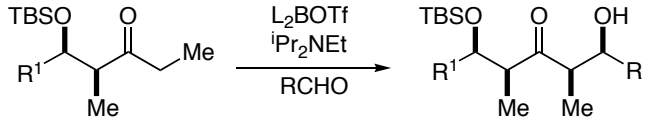

This system does not give a completely clean (Z) enolate

L	Diastereoselection
Bu	63:37 - 84:16
9-BBN	83:17 - 85:15
(-)-Ipc	72:28
(+)-Ipc	91:9 - 94:6

Paterson, McClure, *Tet.Lett.* **1987**, *28*, 1229.

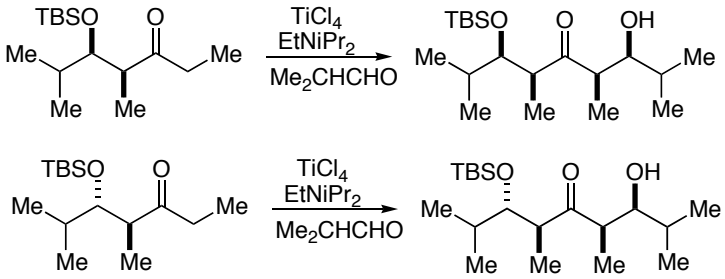

Evans, *JACS* **1991**, *113*, 1047.

Diastereoselection: 95:5 (80-90%)

The Aldol Reaction: Anti Aldol Rxns of Chiral Ethyl Ketones

General Reaction for Syn Aldols:

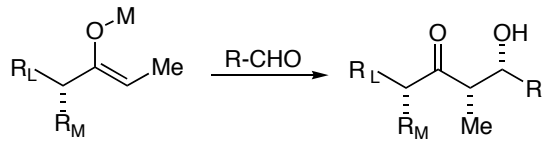

General Reaction for Anti Aldols:

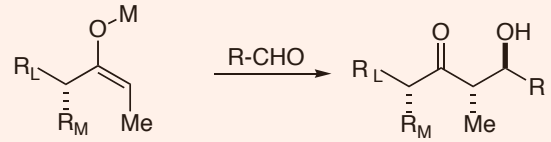

Examples:

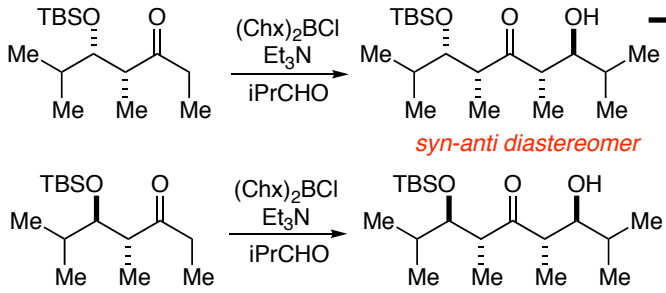

The Transition States:

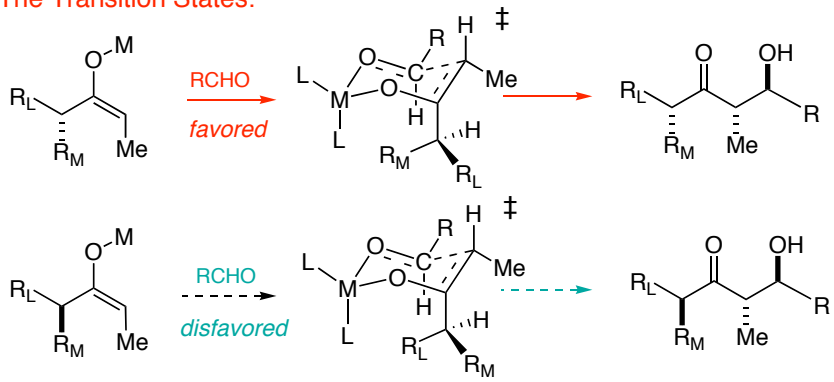

Evans, *JACS* **1991**, *113*, 1047.

(E) Enolate Facial Bias

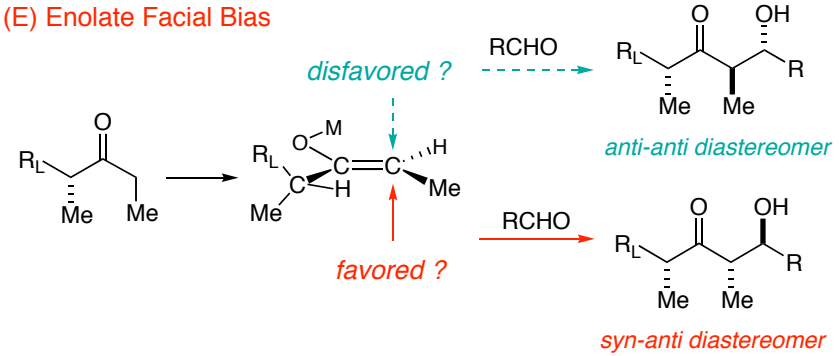

However, the preceding precedent does not extend to these systems:

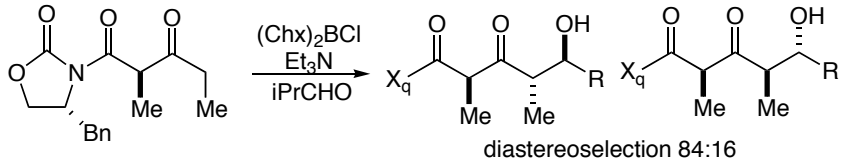

D. A. Evans, H. P. Ng, J. S. Clark, D. L. Rieger *Tetrahedron*, **1992**, *48*, 2127-2142.

An analogous case:

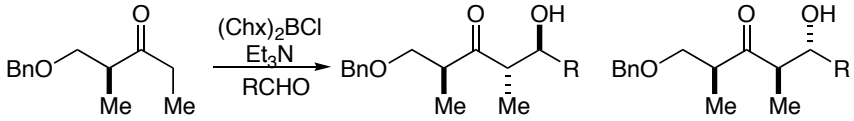

I. Patterson, J. M. Goodman, M. Isaka *Tetrahedron Lett.* **1989**, *30*, 7121-7124

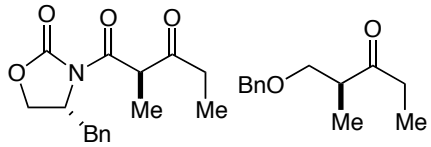

These enolates do not comply with steric analysis: → electronic effects?

Tetrahedron, **1992**, *48*, 2127-2142.

Masamune, Sato, Kim, Wollmann *J. Am. Chem. Soc.* **1986**, *108*, 8279-8281.

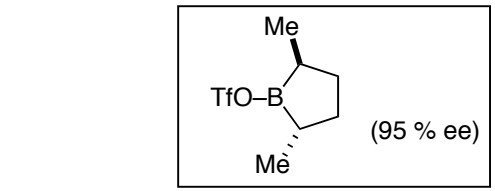

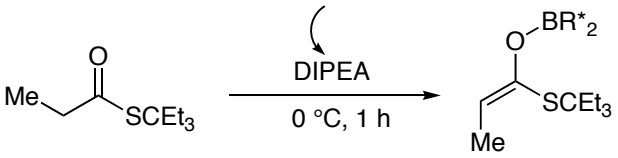

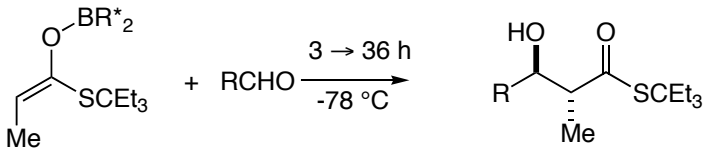

RCHO	Yield, %	anti/syn	ee % (corrected)
n-PrCHO	91	33:1	93 (98)
i-PrCHO	85	30:1	95 (99)
t-BuCHO	95	30:1	96 (99.9)
c-C_6H_{11}CHO	82	32:1	93 (98)
PhCHO	(71)	33:1	96 (99.8)

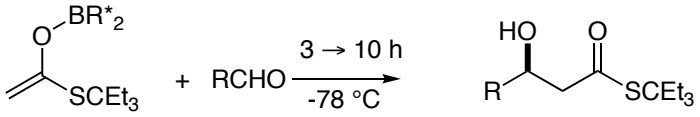

RCHO	Yield, %	ee % (corrected)
n-PrCHO	82	87 (91)
i-PrCHO	81	87 (92)
t-BuCHO	71	94 (98)
c-C_6H_{11}CHO	95	86 (90)
PhCHO	78	88 (92)

See analogous study by Reetz

Reetz *Tetrahedron Lett.* **1986**, 4721

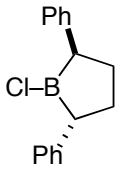

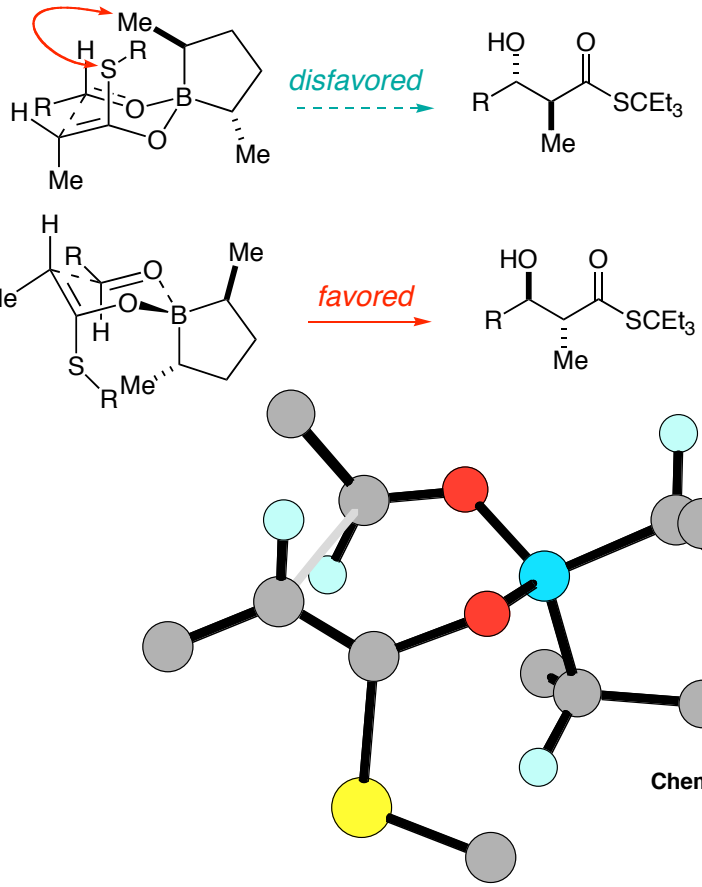

Analogous Carbonyl Allylation

Masamune, Sato, Kim, Wollmann *J. Org. Chem.* **1987**, *52*, 4831

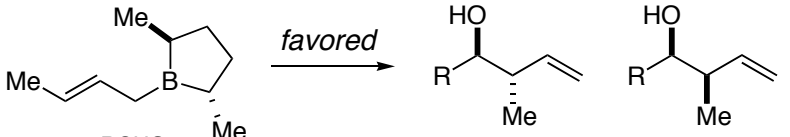

syn:anti, 96:4

enantioselection: 95-97%

Masamune-Reetz Analogy:

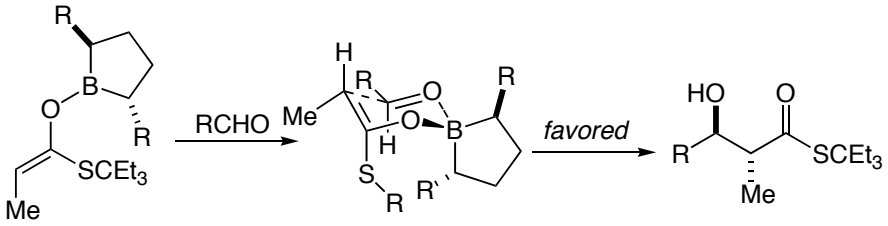

■ Metal-Based Chiral Auxilliary:

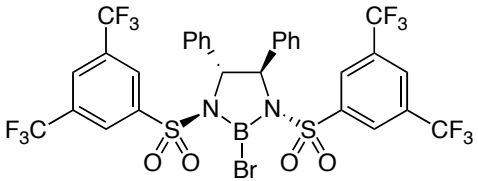

1

References:

(Corey) JACS. **1989**,*111*, 5494
(Corey) JACS. **1990**,*112*, 4977
(Corey) TL. **1991**,*32*, 2857
(Corey) TL. **1993**,*34*, 1737.

Does this reagent perform in accord with the Masamune-Reetz analogy?
Note: The sulfonamide nitrogens are pseudo-tetrahedral

■ Enolization:

Either enolate geometry possible with proper choice of base, solvent, and substrate.

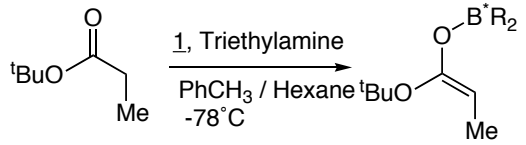

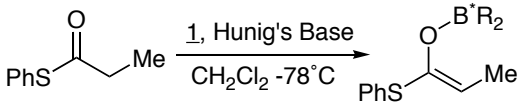

A mechanistic proposal for enolization control is presented in paper

(Corey) JACS. **1989**,*111*, 5494

■ Chiral Anti Aldol Reaction: *JACS* **1990**,*112*, 4977; *TL* **1991**,*32*, 2857.

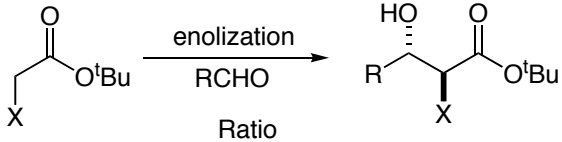

(R)	(X)	Ratio syn:anti	% ee	Yield
Ph-	Me	2 : 98	94	93 %
*c*hex-	Me	6 : 94	75	82 %

(R)	(X)	Ratio syn:anti	% ee	Yield
Ph-	Br	2 : 98	96	86 %
*c*hex-	Br	2 : 98	91	65 %

■ Chiral Syn Aldol Reaction *JACS* **1989**,*111*, 5494.

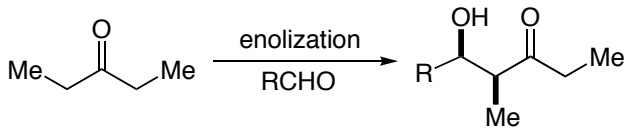

(R)	Ratio syn:anti	% ee	Yield
Ph-	94 : 6	97	86 %
Me_2CH-	98 : 2	95	91 %
$MeCH_2$-	>98 : 2	>98	68 %

■ Chiral Acetate Aldol Reaction *JACS* **1989**,*111*, 5494.

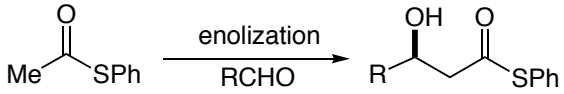

(R)	% ee	Yield
Ph-	91	84 %
Me_2CH-	83	82 %

The Aldol Reaction: Chelate vs Steric Control

Reference Rxn

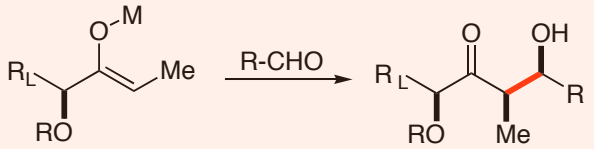

Chelate-Organized Variant

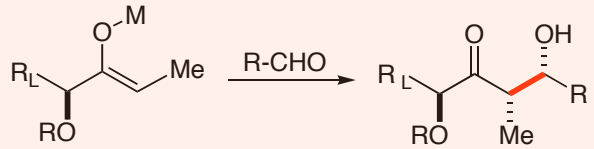

Nonchelate Reaction

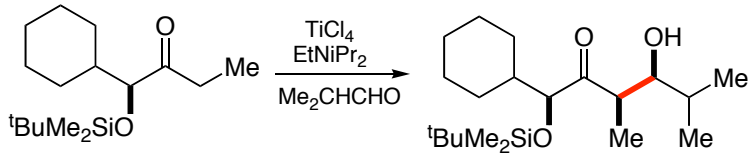

Masamune, *JACS* **1981**, *103*, 1566 (boron enolate)
Evans, *JACS* **1991**, *113*, 1047 (titanium enolate)

Diastereoselection: 99:1

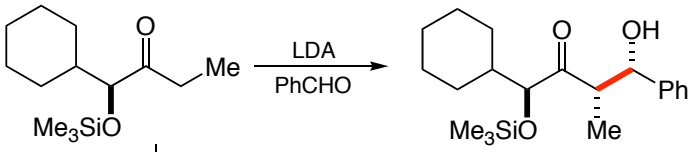

Diastereoselection: 90:10

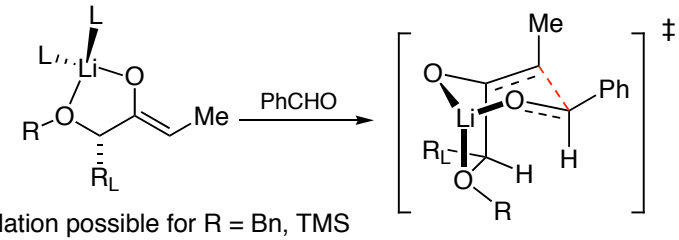

Chelation possible for R = Bn, TMS but marginal for TBS

Thorton, *Tet. Let.* **1990**, *31*, 6001

Complimentary aldol reactions may be obtained by changing metal as well as enolate geometry

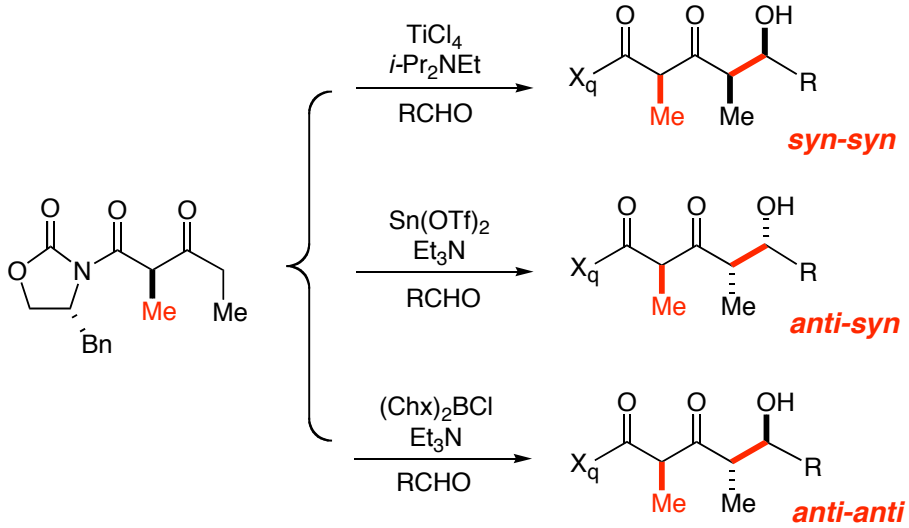

JACS, **1990**, *112*, 866; *Tetrahedron*, **1992**, *48*, 2127-2142.

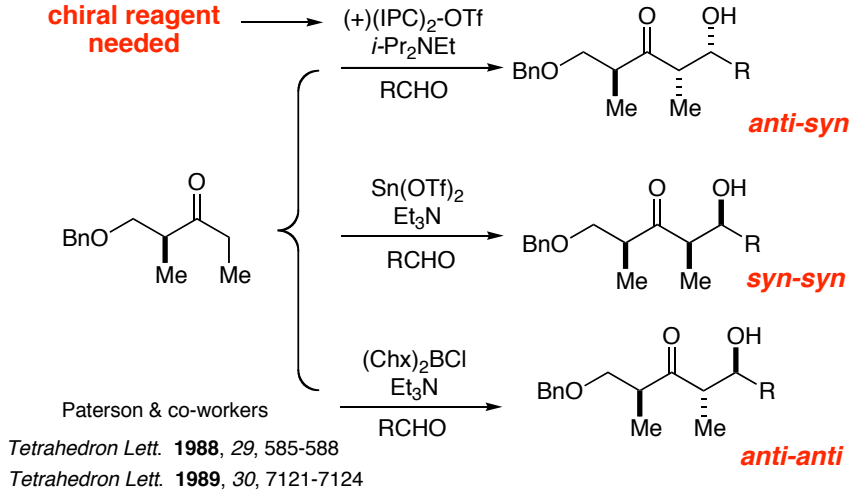

Paterson & co-workers

Tetrahedron Lett. **1988**, *29*, 585-588
Tetrahedron Lett. **1989**, *30*, 7121-7124
Tetrahedron Lett. **1992**, *33*, 4233-4236

Reviews: Oppolzer, *Tetrahedron 1987, 43,* 1969-2004

Oppolzer, *J. Am. Chem. Soc* ***1990****, 112,* 2767

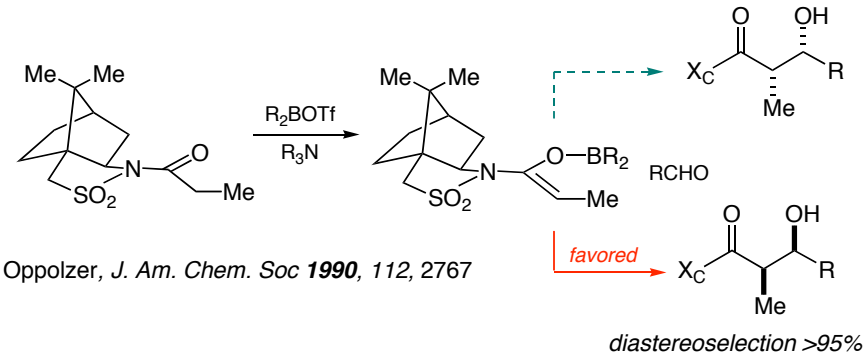

Oppolzer, *J. Am. Chem. Soc* ***1990****, 112,* 2767

diastereoselection >95%

Chelate-controlled alternative

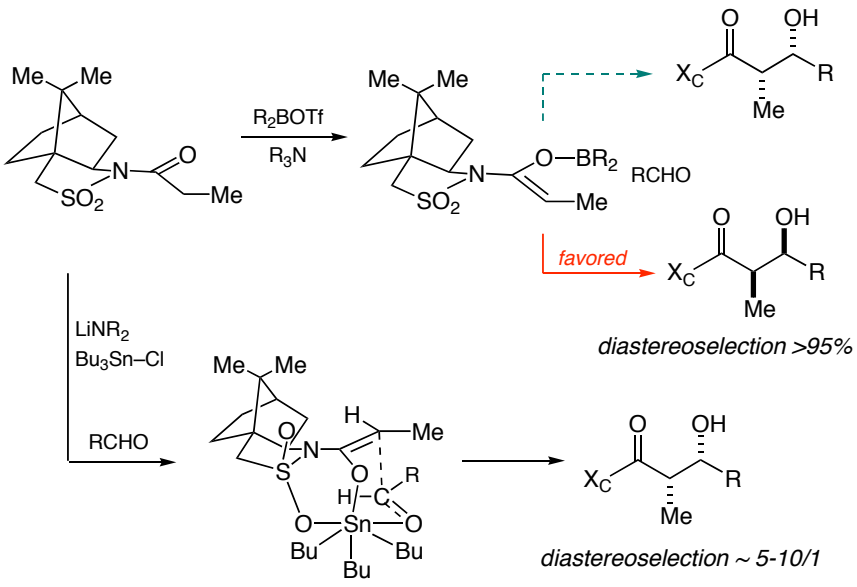

diastereoselection >95%

diastereoselection ~ 5-10/1

X-ray Structures of the Sultam Auxiliary

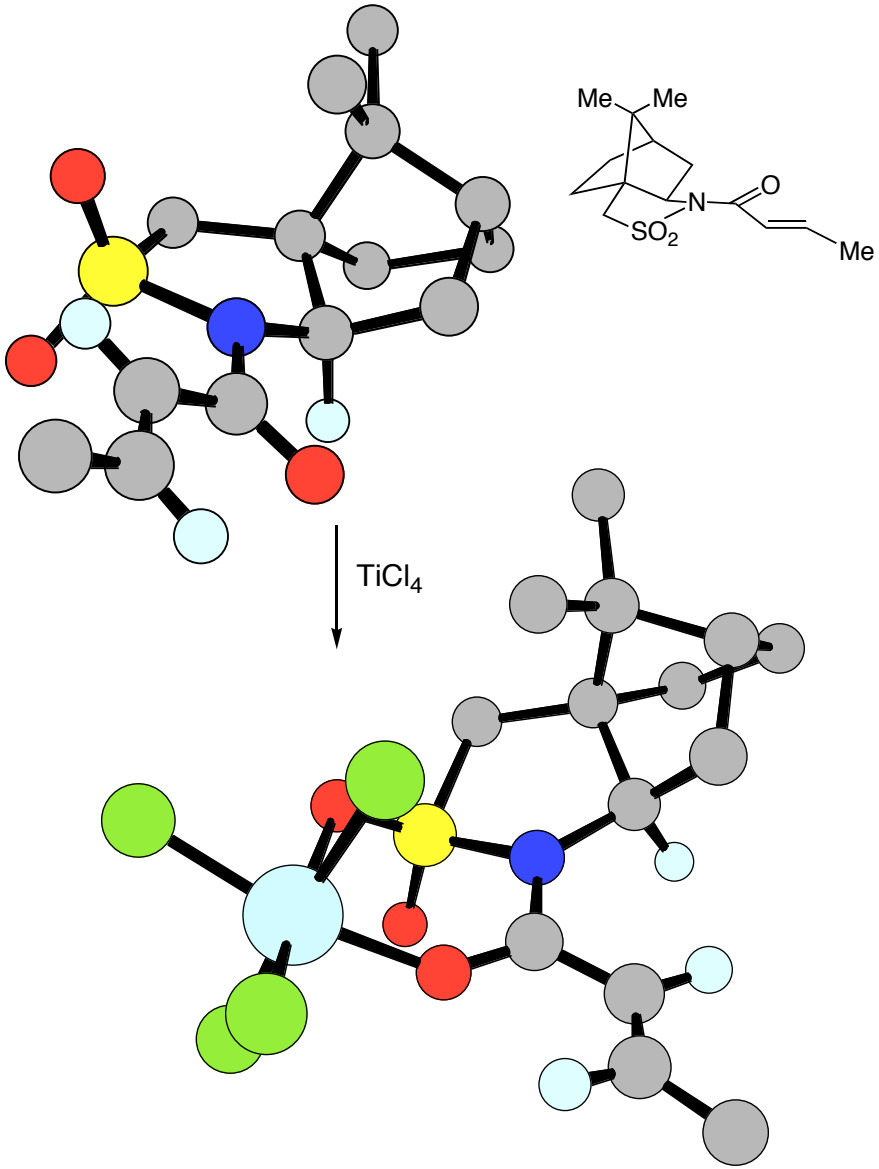

http://www.courses.fas.harvard.edu/~chem206/

Chemistry 206

Advanced Organic Chemistry

Lecture Number 28

The Aldol Reaction–2

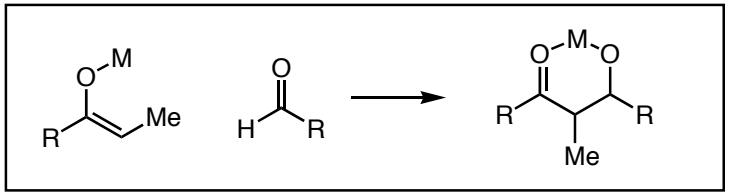

- (E) & (Z) Enolates: Felkin Selectivity
- Double Stereodifferentiating Aldol Reactions
- The Mukaiyama Aldol Reaction Variant
- Allylmetal Nucleophiles as Enolate Synthons

Reading Assignment for this Week:

Carey & Sundberg: **Part A**; Chapter 7
Carbanions & Other Nucleophilic Carbon Species

Carey & Sundberg: **Part B**; Chapter 2
Reactions of Carbon Nucleophiles with Carbonyl Compounds

D. A. Evans

Wednesday
November 29, 2006

Assigned Reading

Concerning the Diastereofacial Selectivity of the Aldol Reactions of α-Methyl Chiral Aldehydes and Lithium and Boron Enolates
W. R. Roush, *J. Org. Chem.* **1991**, *56*, 4151-4157. **(handout)**

Other Useful References

Evans, D. A., J. V. Nelson, et al. (**1982**). "Stereoselective Aldol Condensations." Top. Stereochem. 13: 1.

Heathcock, C. H. (**1984**). The Aldol Addition Reaction. Asymmetric Synthesis. Stereodifferentiating Reactions, Part B. J. D. Morrison. New York, AP. 3: 111.

Oppolzer, W. (**1987**). "Camphor Derivatives as Chiral Auxiliaries in Asymmetric Synthesis." Tetrahedron **43**: 1969.

Heathcock, C. H. (**1991**). The Aldol Reaction: Acid and General Base Catalysis. Comprehensive Organic Synthesis. B. M. Trost and I. Fleming. Oxford, Pergamon Press. 2: 133.

Heathcock, C. H. (**1991**). The Aldol Reaction: Group I and Group II Enolates. Comprehensive Organic Synthesis. B. M. Trost and I. Fleming. Oxford, Pergamon Press. 2: 181.

Kim, B. M., S. F. Williams, et al. (**1991**). The Aldol Reaction: Group III Enolates. Comprehensive Organic Synthesis. B. M. Trost and I. Fleming. Oxford, Pergamon Press. 2: 239.

Franklin, A. S. and I. Paterson (**1994**). "Recent Developments in Asymmetric Aldol Methodology." Contemporary Organic Synthesis 1: 317-338.

Cowden, C. J. and I. Paterson (**1997**). "Asymmetric aldol reactions using boron enolates." Org. React. (N.Y.) 51: 1-200.

Nelson, S. G. (**1998**). "Catalyzed enantioselective aldol additions of latent enolate equivalents." Tetrahedron: Asymmetry 9(3): 357-389.

Mahrwald, R. (**1999**). "Diastereoselection in Lewis-acid-mediated aldol additions." Chem. Rev. 99(5): 1095-1120.

(E) Enolates Exhibit Felkin Aldehyde Diastereoface Selection

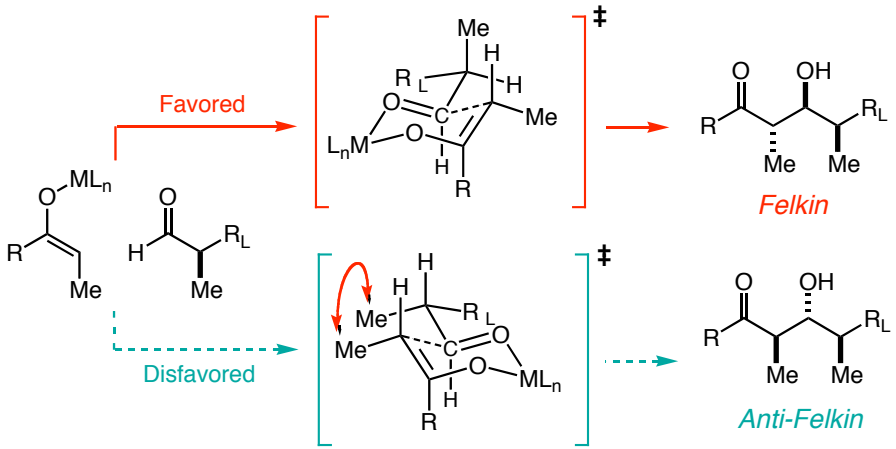

■ The illustrated syn-pentane interaction disfavors the anti-Felkin pathway.

Evans, Nelson, Taber, *Topics in Stereochemistry* **1982,** *13*, 1-115.
W. R. Roush, *J. Org. Chem.* **1991**, *56*, 4151-4157 **(handout).**

Background Information: The influence of β-OR substituents on RCHO

Evans, *JACS* **1996**, *118*, 4322-4343

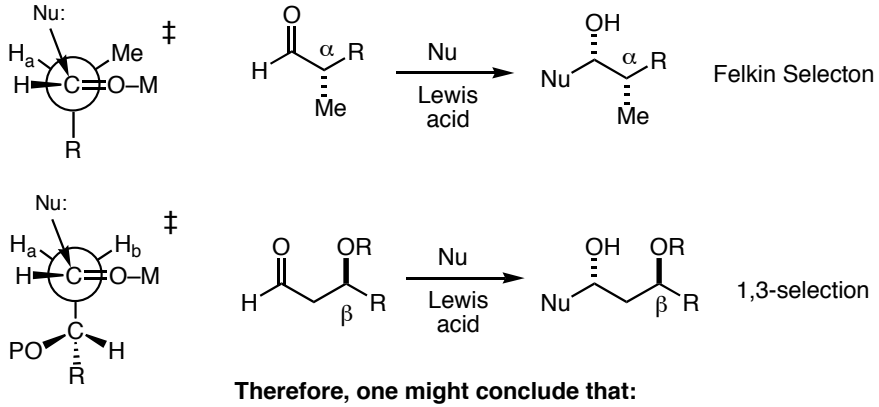

Therefore, one might conclude that:

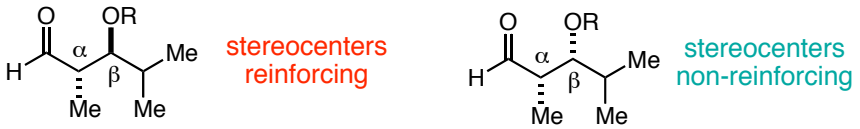

The Non-Reinforcing syn- RCHO is the most Interesting Dependence of the Selectivity of Felkin-controlled Reactions on Nu Size

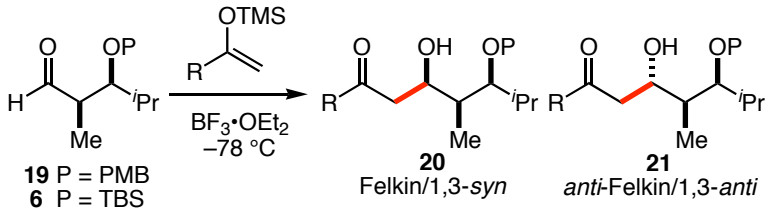

	P = PMB	P = TBS
R	**20** : **21**	**20** : **21**
t-Bu	96 : 04	94 : 06
i-Pr	56 : 44	75 : 25
Me	17 : 83	40 : 60

α-substituent dominates for Large Nu

β-substituent dominates for small Nu

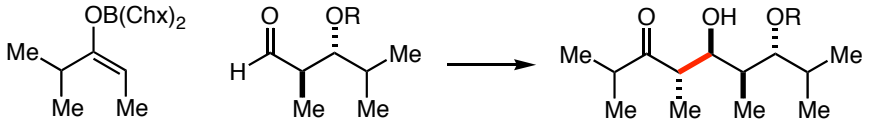

both centers reinforcing

	major : Σ minors	
R = TBS	99 : 1	(77% yield)
R = PMB	93 : 7	(84% yield)

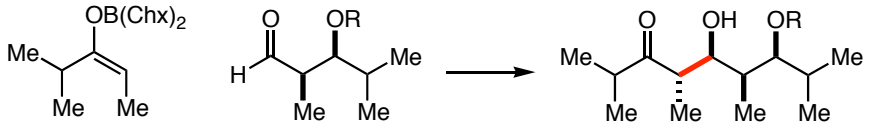

centers non-reinforcing

	major : Σ minors	
R = TBS	94 : 6	(79% yield)
R = PMB	74 : 26	(82% yield)

Achiral (*E*) enolates preferentially add to the Felkin diastereoface
High *anti*:*syn* diastereoselectivity (≥ 97 : 3) is observed in all cases

Evans etal. *JACS* ***1995****, 117,* 9073

(Z) Enolates Exhibit Anti-Felkin Aldehyde Diastereoface Selection

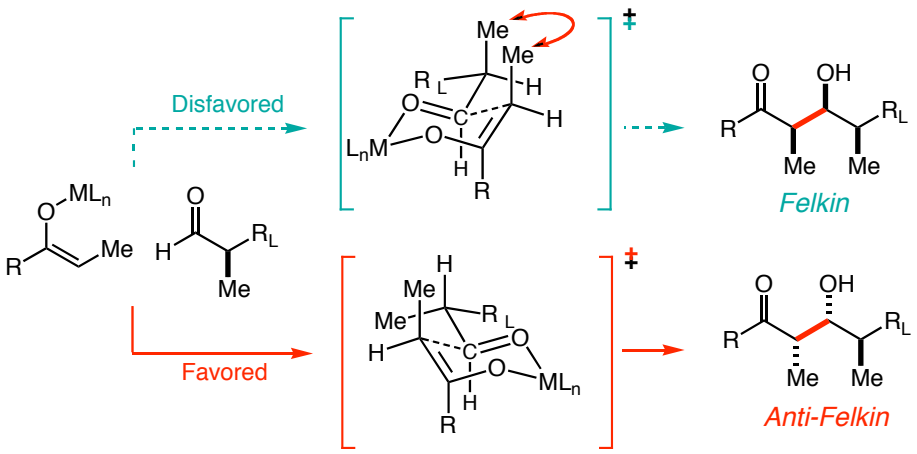

The illustrated syn-pentane interaction disfavors the Felkin pathway.

Evans, Nelson, Taber, *Topics in Stereochemistry* **1982,** *13*, 1-115.
W. R. Roush, *J. Org. Chem.* **1991**, *56*, 4151-4157 **(handout).**

An Early study rationalized results through chelated transition states:

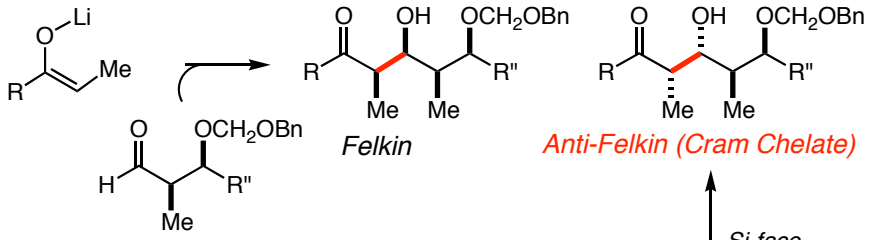

(R)	(R")	Felkin : Anti-Felkin
Et	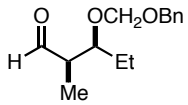	17 : 83
C_6H_{11}		10 : 90
Et	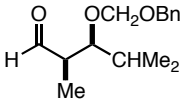	13 : 87
C_6H_{11}		8 : 92

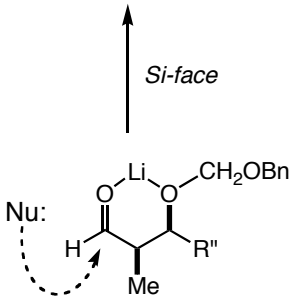

Masamune
JACS ***1982****, 104,* 5526

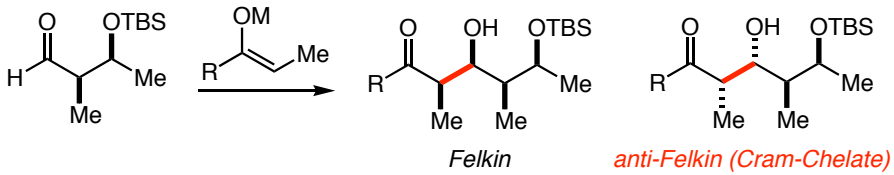

D. W. Brooks & Co-workers
Tetrahedron Lett. **1982**, *23*, 4991-4994.

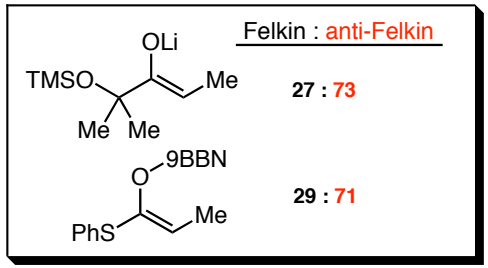

- The bulky OTBS group disfavors chelation. (see Keck, *JACS* **1986**, *108*, 3847.)
- The boron and lithium enolates display nearly equal levels of anti-Felkin selectivity.

Titanium enolates exhibit the same trend

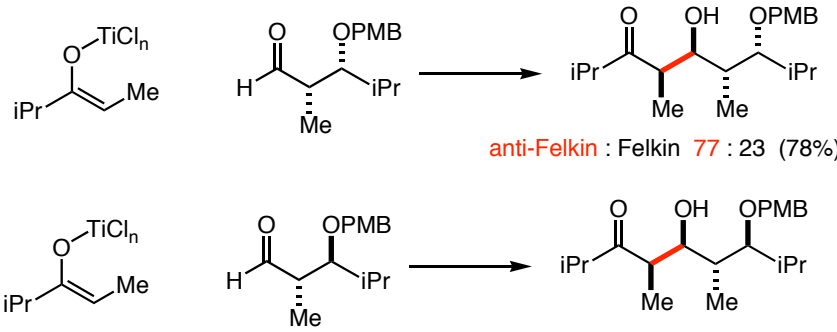

Evans etal. *JACS* ***1995****, 117,* 9073

Double Stereodifferentiating Aldol Bond Constructions

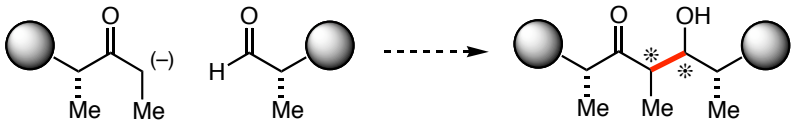

Stereochemical Control Elements

Enolate geometry

Enolate facial bias ⇨ Product Stereochemistry ⇦ **Aldehyde facial bias**

The Issue: Can one reliably take the diastereoselectivites of the individual reaction partners and use this information in the illustrated extrapolation:

The model reactions:

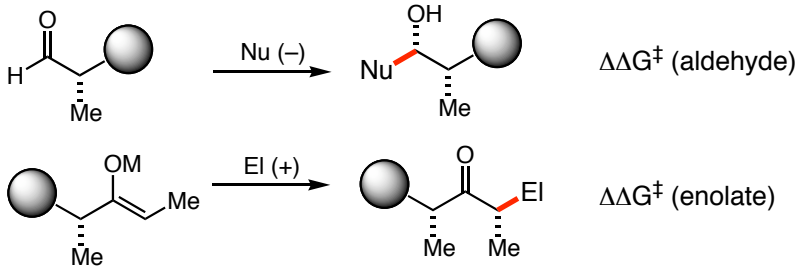

The extrapolation:

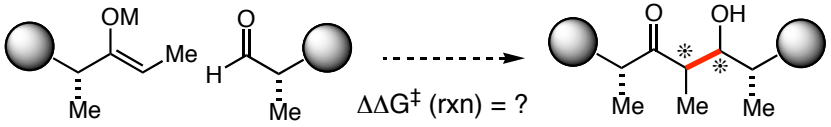

Masamune, *Angew. Chem. Int. Ed.* **1985**, *24*, 1-76

Matched reactant pair: Stereo-induction from both partners reinforcing

The reference reactions:

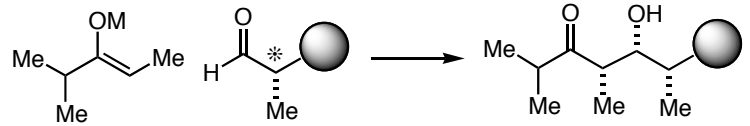

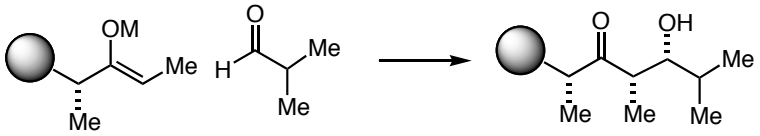

■ The double stereodifferentiating situation: Stereoselectivity?

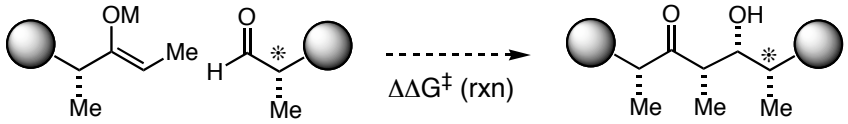

■ The assumption: (Masamune, Heathcock)

It is presumed that useful information can be obtained from related achiral enolate & RCHO addition reactions and that the free energy contributions will be additive:

$$\Delta\Delta G^{\ddagger}\ (\text{Rxn}) \sim \Delta\Delta G^{\ddagger}\ (\text{enolate}) + \Delta\Delta G^{\ddagger}\ (\text{RCHO})$$

$$\log [\text{Product ratio}] \sim \log [\text{enolate ratio}] + \log [\text{aldehyde ratio}]$$

[Product ratio] ~ [enolate prod ratio] x [aldehyde prod ratio]

■ Hence, for the case at hand: [Product ratio] ~ [10] x [10] ~ 100

Mismatched reactant pair: Stereo-induction from partners nonreinforcing

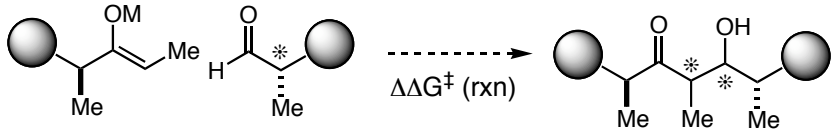

$$\Delta\Delta G^{\ddagger}\ (\text{Rxn}) \sim \Delta\Delta G^{\ddagger}\ (\text{enolate}) - \Delta\Delta G^{\ddagger}\ (\text{RCHO})$$

Double Stereodifferentiating Bond Constructions-2

The Masamune-Heathcock generalizations hold to a point:

(E)-Boron Enolates: The reference reactions

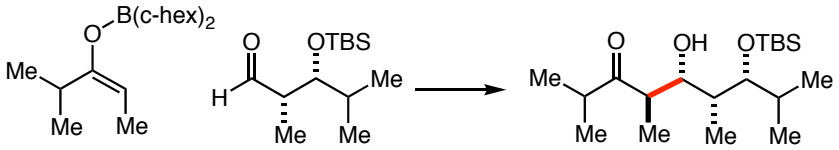

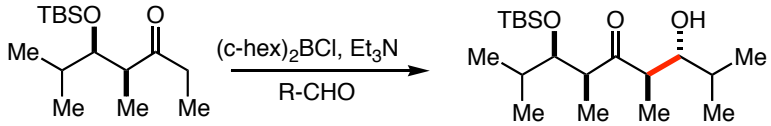

(E)-Boron Enolates: The matched cases

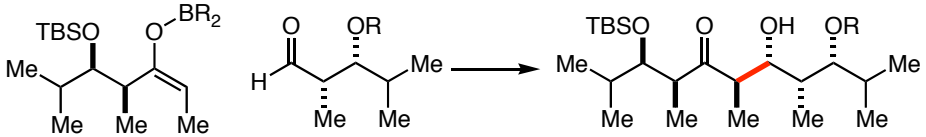

diastereoselection: anti : Σ others

R = TBS: >99 : 1 (85% yield)

R = PMB: >99 : 1 (84% yield)

(E)-Boron Enolates: The mismatched cases

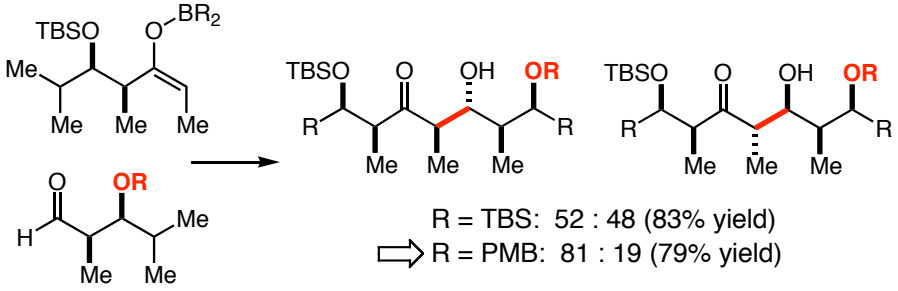

R = TBS: 52 : 48 (83% yield)

⇨ R = PMB: 81 : 19 (79% yield)

β-center on RCHO can play a significant role in this marginal situation

(Z)-Titanium Enolates: The reference reactions

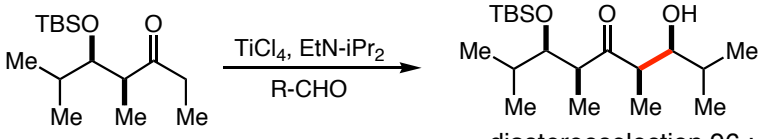

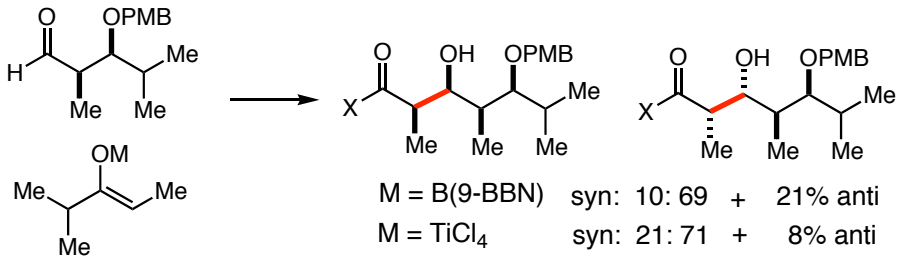

(Z)-Titanium Enolates: The matched cases

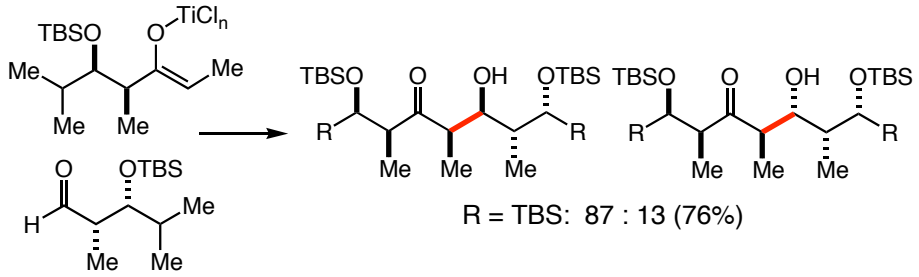

(Z)-Titanium Enolates: The mismatched cases

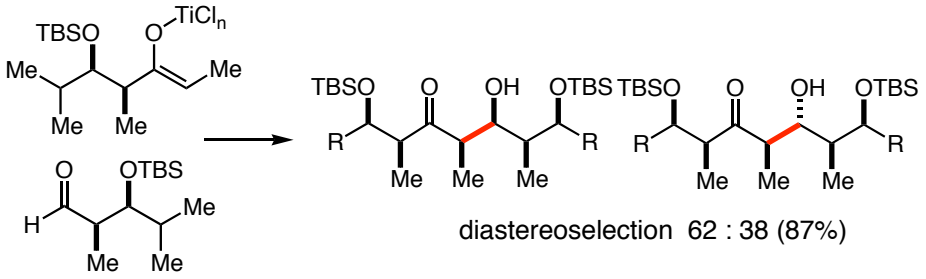

"Double Stereodifferentiating Aldol Reactions. The Documentation of "Partially Matched" Aldol Bond Constructions". Evans, D. A.; Dart, M. J.; Duffy, J. L.; Rieger, D. L. *JACS* **1995**, *117*, 9073-9074.

Synthesis of Polyketide chains

Given a polyprpionate chain of alternating Me & OH substitutents, select a disconnection point sectioning the fragments into subunits of comparable complexity by adding C=O as illustrated.

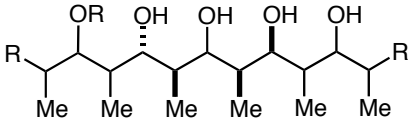

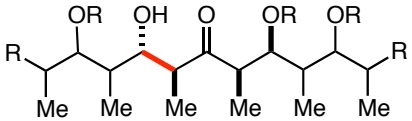

T1$_A$

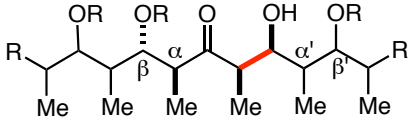

T1$_B$

aldol

Focusing on the =O FG, there are 2 1st-order aldol disconnections highlighted. Let's proceed forward with **T1$_B$**. Carry out the dissconnection to subunits **2$_K$** and **2$_A$**.

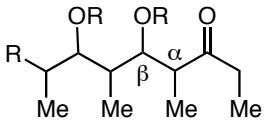

2$_K$

α center important
β center ignore

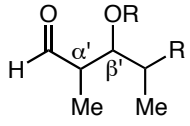

2$_A$

Both centers important

For substituted enolate and enolsilane-based processes, there are at least three identifiable **stereochemical determinants** that influence reaction diastereoselectivity (eq 1). Two of these determinants are associated with the local chirality of the individual reaction partners. For example, enolate (enolsilane) chirality influences the absolute stereochemistry of the forming methyl-bearing stereocenter, and in a similar fashion, aldehyde chirality controls the absolute stereochemical outcome of the incipient hydroxyl-bearing stereocenter. The third determinant, the pericyclic transition state, imposes a relative stereochemical relationship between the developing stereocenters. This important control element is present in the aldol reactions of metal enolates (M = BR_2, TiX_3, Li, etc.), but is absent in the Lewis acid catalyzed (Mukaiyama) enolsilanes aldol variants that proceed via open transition states.

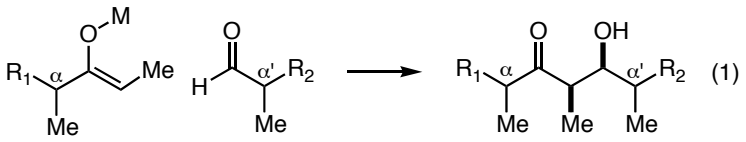

(1)

Stereochemical Determinants	M = BR_2	M = SiR_3
enolate facial bias	✔	✔
aldehyde facial bias	✔	✔
pericyclic transition state	✔	✘

The Lonomycin Synthesis: An example of polypropionate assembage

Evans, Ratz, Huff, Sheppard *JACS* **1995**, *117*, 3448

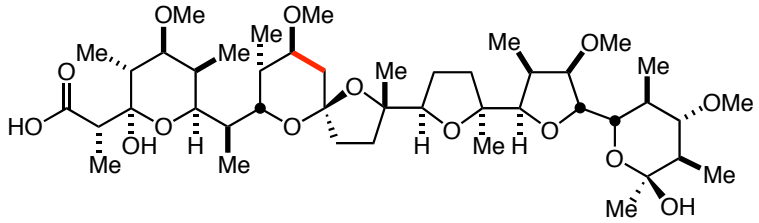

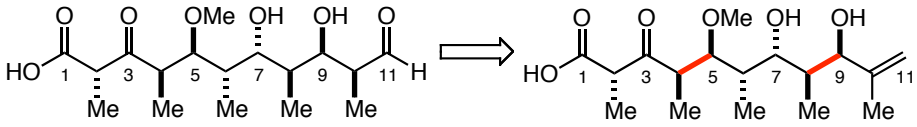

BH_3 Transform: See Lecture No. 8

C_1–C_{11} Assemblage

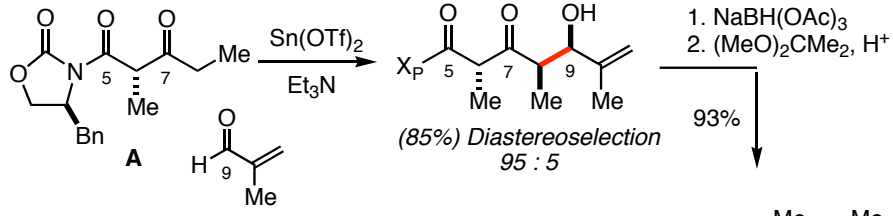

A

(85%) Diastereoselection 95 : 5

JACS, **1990**, *112*, 866

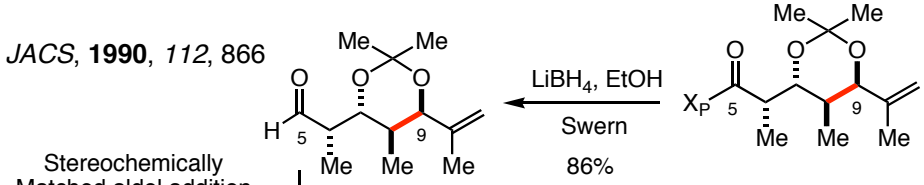

Stereochemically Matched aldol addition

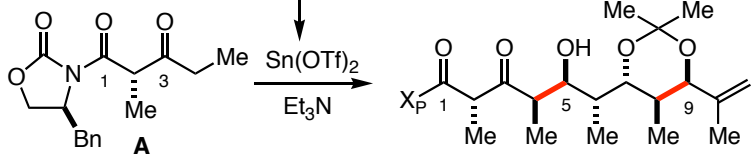

A

Anti-Felkin Adduct Diastereoselection >95 : 5 (86%)

The $Sn(OTf)_2$ aldol reaction of A: see this lecture + *JACS*, **1990**, *112*, 866

The Altohyrtin Synthesis: An example of polypropionate assembage

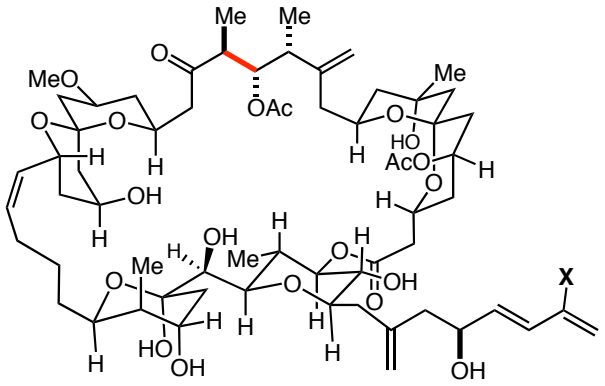

Evans, Trotter, Coleman, Côté, Dias, Rajapakse, *Tetrahedron* **1999**, *55*, 8671-8726.

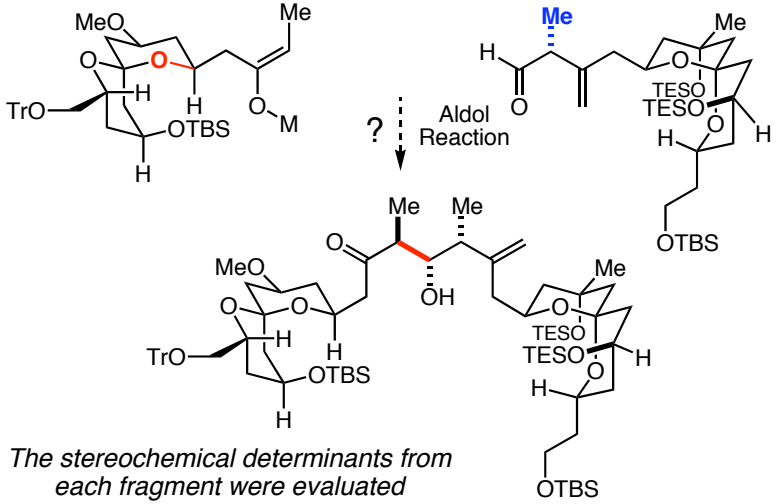

The stereochemical determinants from each fragment were evaluated

Model Studies

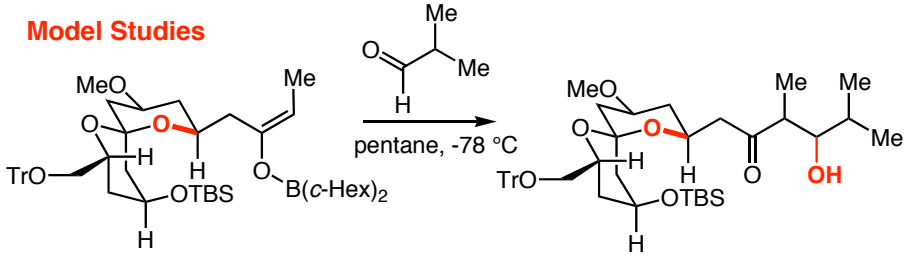

2:1 mixture of diastereomers

Model Studies

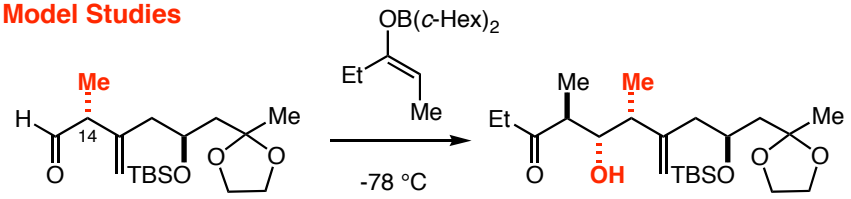

Diastereoselection 97:3

Background

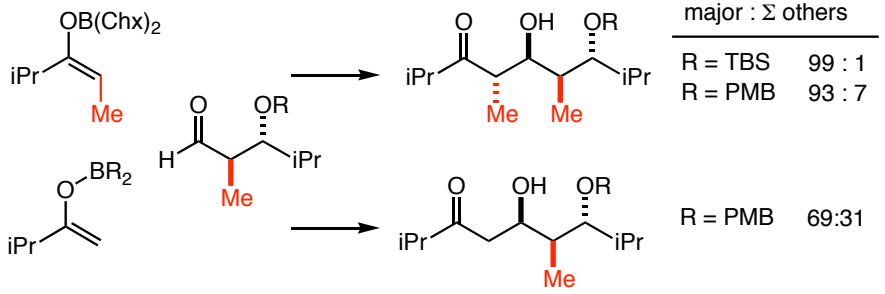

The Aldol Fragment Coupling

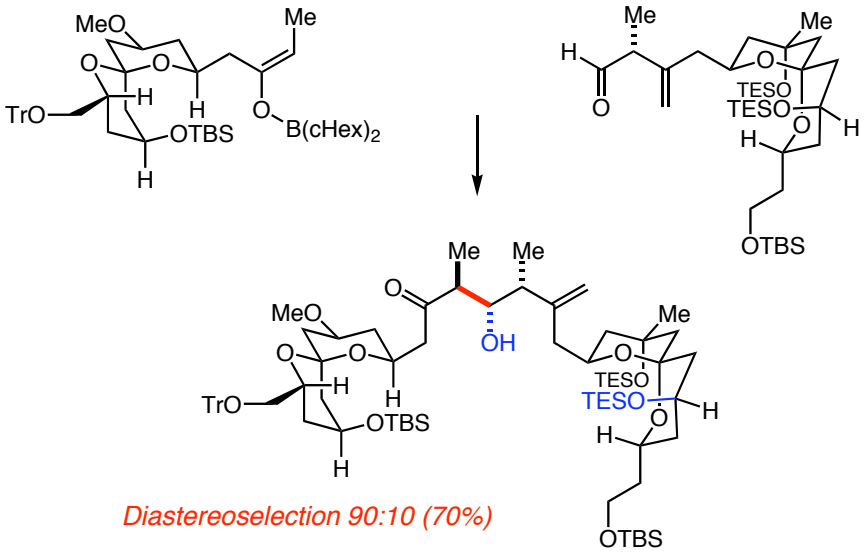

Diastereoselection 90:10 (70%)

Bafilomycin A_1 Synthesis: An example of polypropionate assembage

Evans, Calter, *Tetrahedron Lett.* **1993**, 34, 6871

Bafilomycin A_1

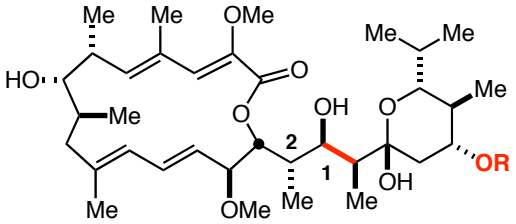

Critical Aldol Disconnection

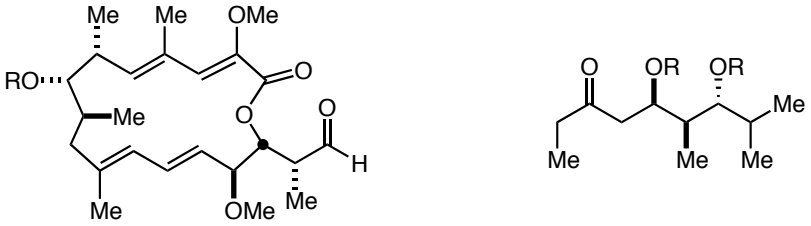

Required: Syn aldol addition

Aldehyde Frag: Target contains syn aldol retron wilth anti-Felkin relationship at 1 & 2

Enolate Frag: Can the needed enolate facial bias be built into the reaction??

Aldol Model Studies

Enolization Conditions: $PhBCl_2$, *i*-Pr_2NEt, CH_2Cl_2, -78 °C.

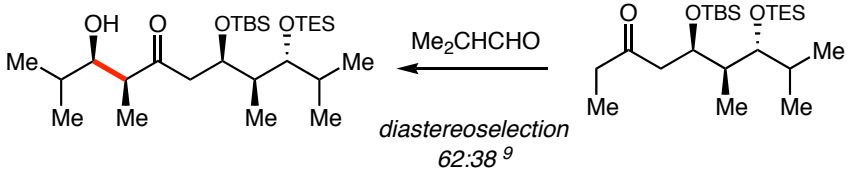

The Critical Observation

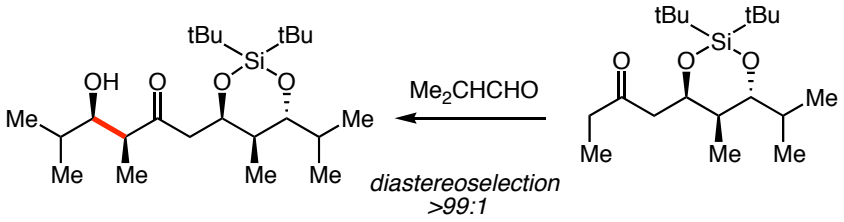

Enolization Conditions: $PhBCl_2$, *i*-Pr_2NEt, CH_2Cl_2, -78°C.

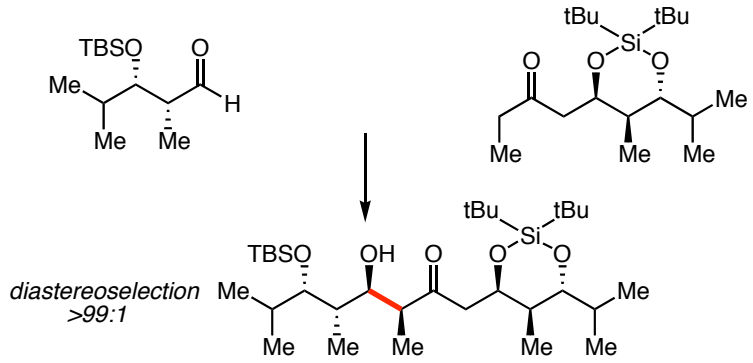

Critical Aldol Disconnection

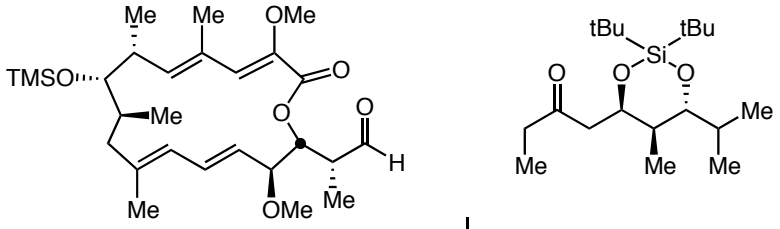

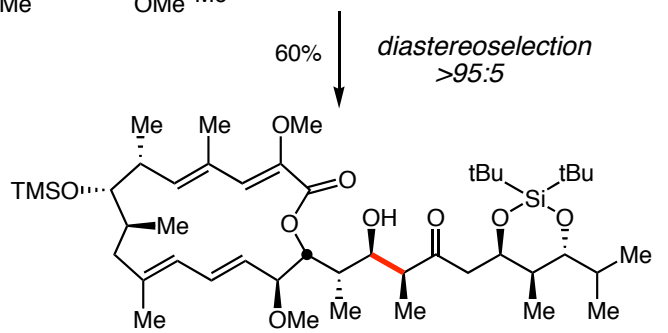

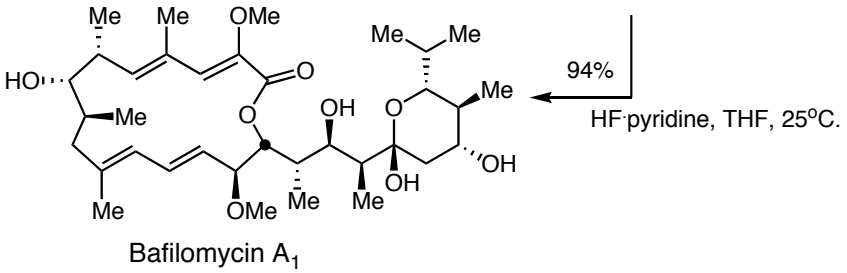

Bafilomycin A_1

Roxaticin, A Typical Polyacetate Natural Product

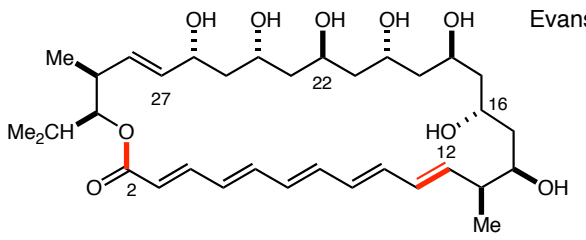

Evans et al. *JACS* **2003**, *125*, 10899

*(+)-Roxaticin (**1**)*

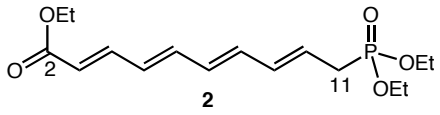

2

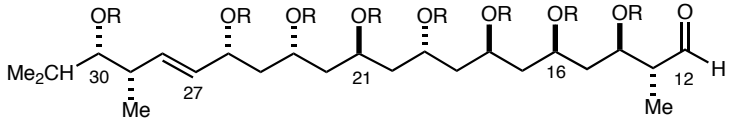

Relevant Chemistry

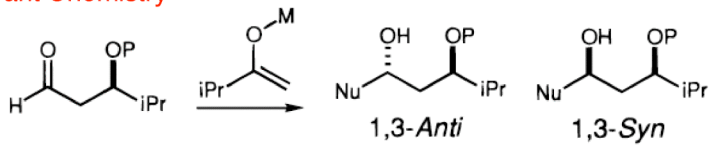

1 P = PMB
2 P = TBS

entry	metal	**3**:**4** (P = PMB) (yield, %)	**5**:**6**[b] (P = TBS) (yield, %)
A	$TMS/BF_3{\cdot}OEt_2$	92:08 (91)	80:20 (84)
B	Li	71:29 (99)	76:24 (91)
C	$TiCl_n$	60:40 (98)	58:42 (88)
D	9-BBN	42:58 (82)	52:48 (79)

[a] Reactions were carried out in CH_2Cl_2 or THF (entry B) at −78

JACS **1996,** *118*, 4322-4343

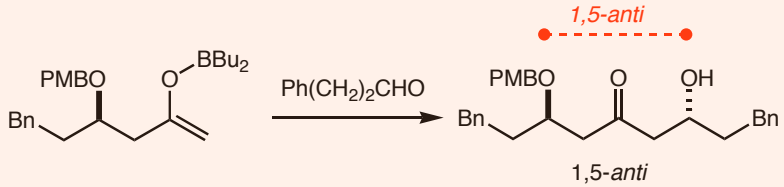

Paterson, et al. *Tet. Lett.* **1996,** *37*, 8585.
Evans, et al. *J. Org. Chem.* **1997,** 788.
Evans et al. *JACS* **2003**, *125*, 10893

>95:5 diastereoselectivity

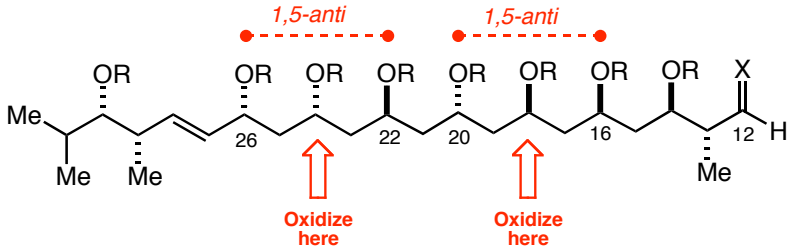

Relevant Reductions

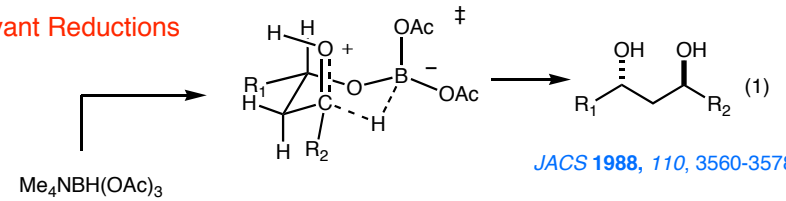

JACS **1988,** *110*, 3560-3578

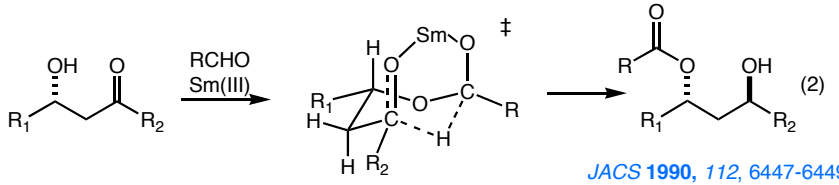

JACS **1990,** *112*, 6447-6449

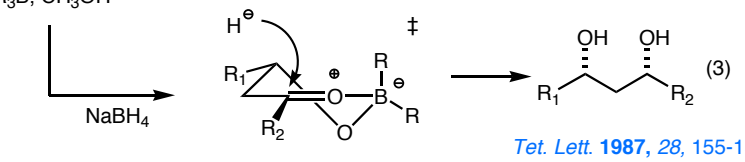

Tet. Lett. **1987,** *28*, 155-158

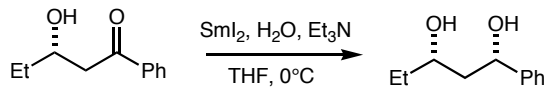

syn/anti ~ 100:1

Org. Lett. **2005,** *7*, 119

Type I Aldol Reaction: Metal Aldol Process

This reaction may be run with either a stoichiometric or catalytic amount of base.

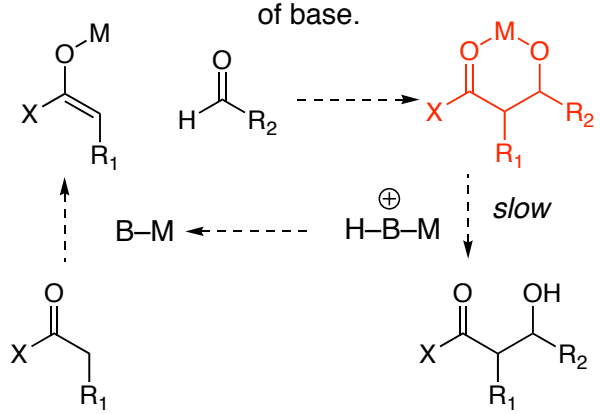

Catalytic Version: Slow step in the catalytic variant is protonation of the intermediate metal aldolate

Type II Aldol Reaction: Mukaiyama Aldol Process

This reaction may be run with either a stoichiometric or catalytic amount of Lewis acid.

The minimalist mechanism: MX = Lewis acid

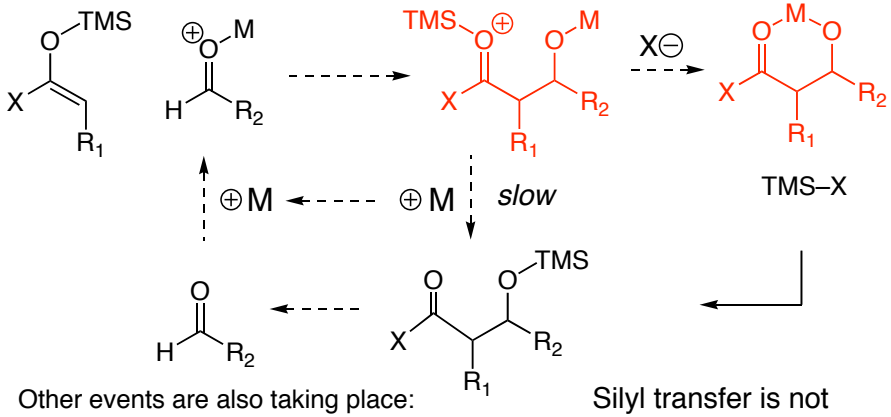

Other events are also taking place:
Carreira *Tet. Lett* **1994**, *35*, 4323

Silyl transfer is not necessarily intramolecular

Recent Reviews

R. Mahrwald, *Diatereoselection in Lewis Acid Mediated Aldol Additions*, *Chem. Rev.* **1999**, *99*, 1095-1120

S. G. Nelson, *Catalyzed enantioselective aldol additions of latent enolate equivalents Tetrahedron: Asymmetry* **1998**, *9*, 357-389.

Mukaiyama Aldol Reaction, E. Carreira In Comprehensive Asymmetric Catalysis, Jacobsen, E. N.; Pfaltz, A.; and Yamamoto, H. Editors; Springer Verlag: Heidelberg, **1999**; Vol III, 998-1059.

Reaction Mechanism: "Closed" versus "Open" Transition States

The Mukaiyama aldol reaction proceeds through an "open" transition state. The two illustrated competing TS orientations do not differ significantly in energy. For most reactions in this family there is not a good understanding of reactant-pair orientation. There is a prevalent view that the anti-periplanar TS is favored on the basis of electrostatic effects.

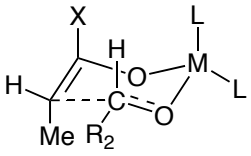

Metal aldolate TS
"Closed"

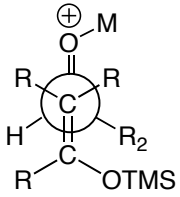

anti-periplanar TS
"Open"

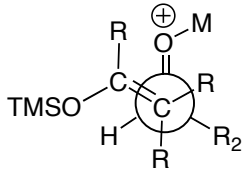

synclinal TS
"Open"

The Mukayama Aldol Reaction-2

Denmark has designed a nice substrate to distinguish between synclinal and anntiperiplanar transition states:

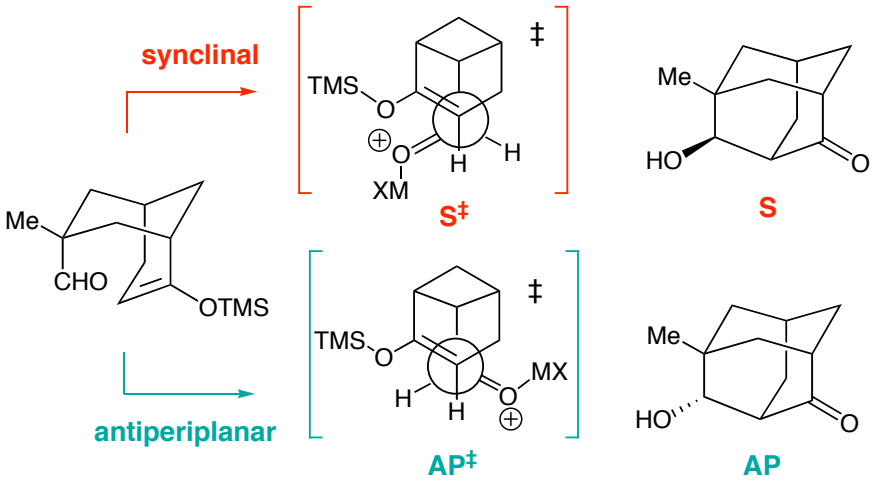

Lewis Acid	S : AP
$TiCl_4$	21:79
$SnCl_4$	18:82
BF_3•OEt_2	29:71
$TrClO_4$	27:73
$SnCl_2$	78:22

conclusion: there is a modest preference for the antiperiplanar TS

Denmark, *J. Org. Chem.* **1994**, *59*, 707-709

Syn-Anti Aldol Diastereoselection

Heathcock: *J. Org. Chem* **1986**, *51*, 3027

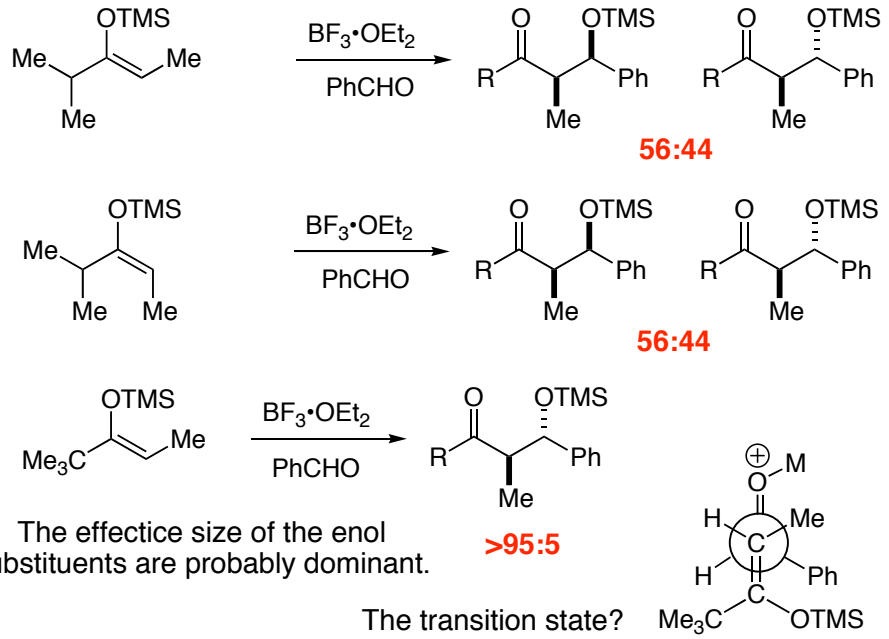

The effectice size of the enol substituents are probably dominant.

The transition state?

These reactions "exhibit little simple diastereoselection except in special cases."....Heathcock

Merged Syn-Anti & Felkin Diastereoselection

Evans: *JACS* **1995**, *117*, 9598

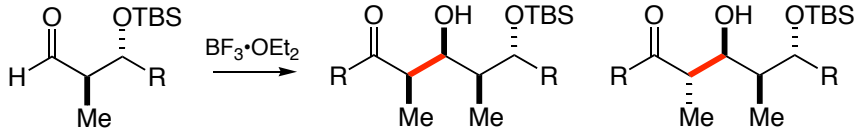

95 : 5 (95%)

Felkin : anti-Felkin > 99 : 1

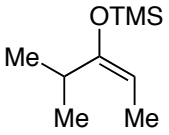

R = iPr

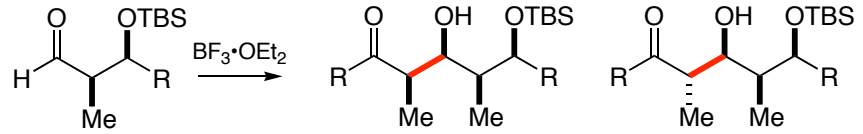

70 : 30 (89%)

Felkin : anti-Felkin 99 : 1

Conclusions:
Moderate to Good syn diastereoselectlion
Excellent Felkin diastereoselectlion

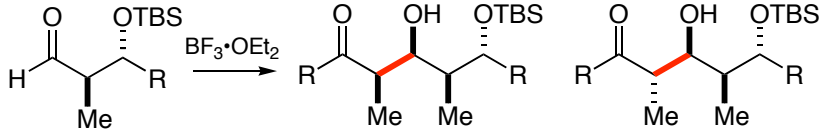

87 : 13 (68%)

Felkin : anti-Felkin > 99 : 1

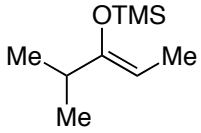

R = iPr

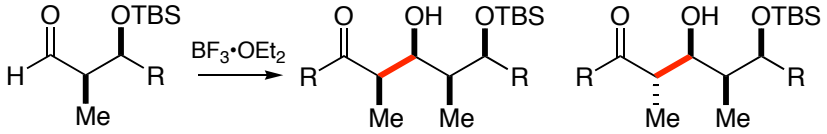

91 : 9 (75%)

Felkin : anti-Felkin 87 : 13

Conclusions:
Moderate to Good syn diastereoselectlion
Excellent Felkin diastereoselectlion

Enolsilane Face Selection

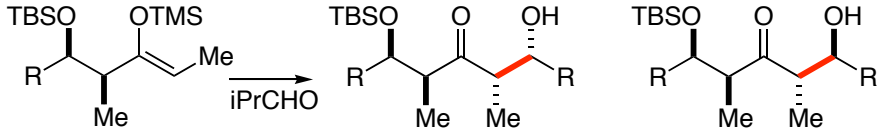

R = iPr

59 : 41 (82%)

Enolsilane Face Selectivity 95 : 5

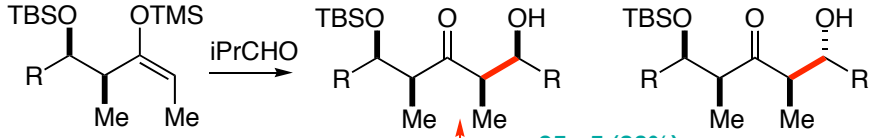

95 : 5 (80%)

Enolsilane Face Selectivity 90 : 10

favored

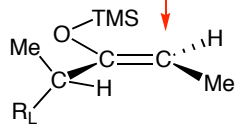

A(1-3) control is good for the (E) enolsilane

Double Stereodifferentiating *Syn* Aldol Rxns with Enolsilanes

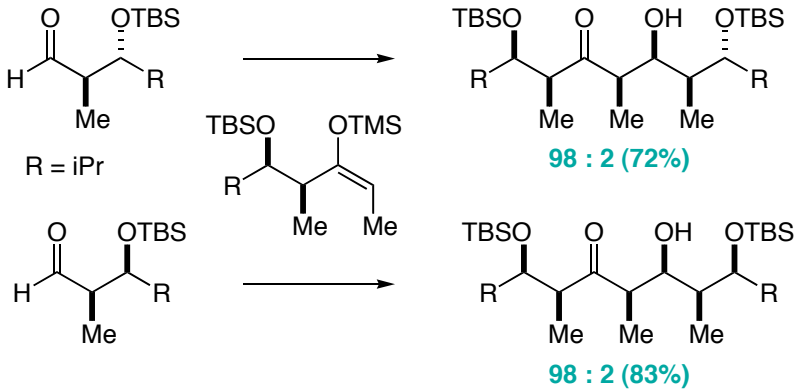

■ General Reviews of Allyl Metal Reagents:
Comprehensive Organic Synthesis, **1991**;Vol. 2.

■ The General Reactions

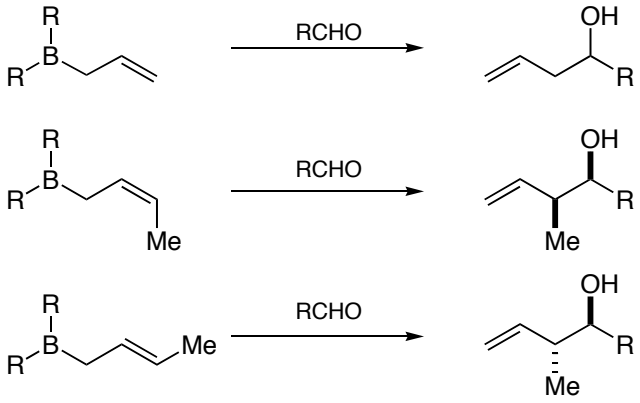

■ The Hoffman Chiral Allylboronic Esters

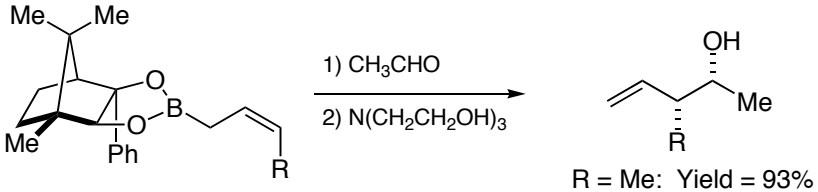

R = Me: Yield = 93%
ee = 60-70%

R = H: Yield = 92%
ee = 65%

R. Hoffman *Tetrahedron Lett.* **1979**, 4653-4656.
ACIEE, **1978**, *17*, 768-769.

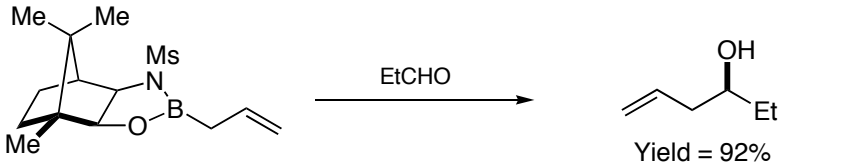

Yield = 92%
ee = 92%

M. Reetz *Chem. Ind. (London)* **1988**, 663-664.

■ The Tartrate-derived Allylboronic Esters

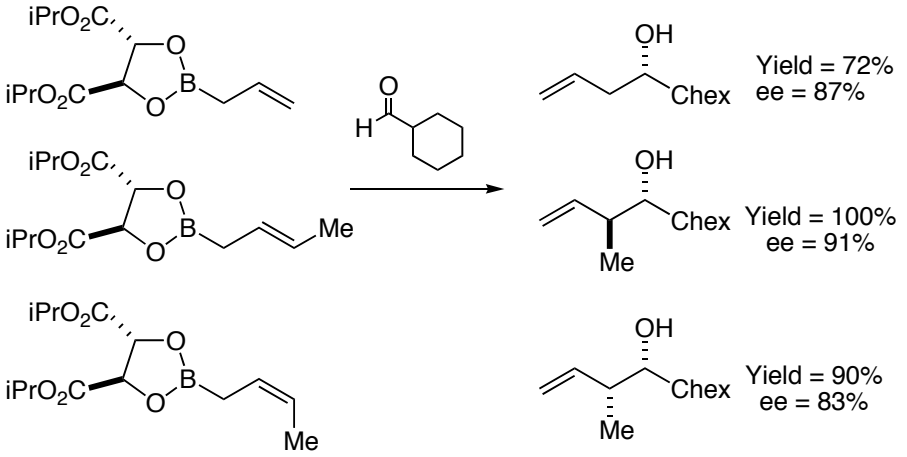

W. Roush, *J. Am. Chem. Soc.* **1985**, *107*, 8186-8190.
Tetrahedron Lett. **1988**, *29*, 5579-5582.

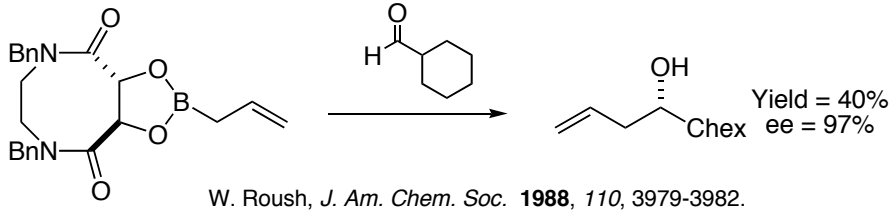

W. Roush, *J. Am. Chem. Soc.* **1988**, *110*, 3979-3982.

■ A Reagent for the Generation of Anti-1,2-Diols

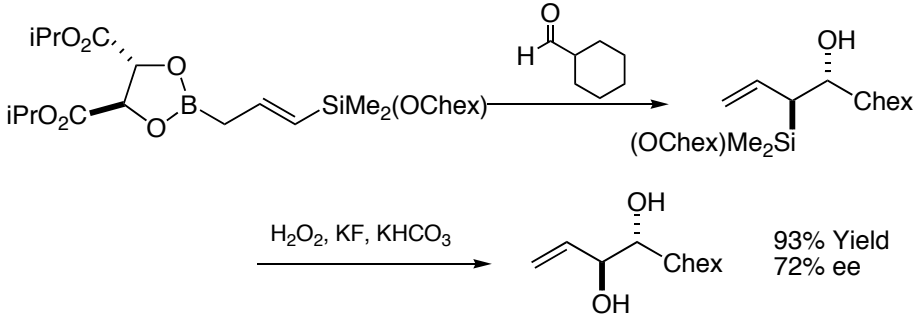

W. Roush, *Tetrahedron Lett.* **1990**, *31*, 7563-7566.

■ Allenylboronic Esters: Tartrate-derived Controllers and Internal Delivery

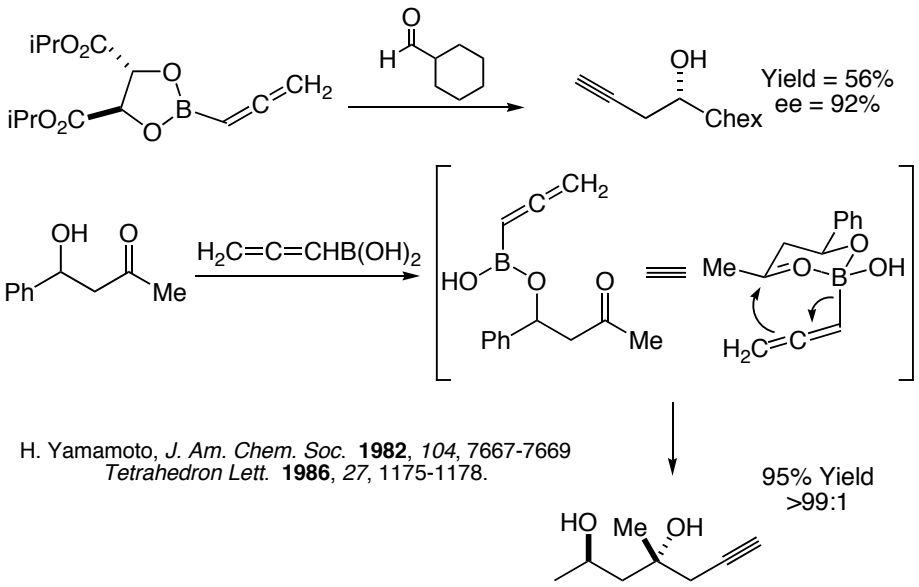

H. Yamamoto, *J. Am. Chem. Soc.* **1982**, *104*, 7667-7669
Tetrahedron Lett. **1986**, *27*, 1175-1178.

■ The Corey Stein Controller

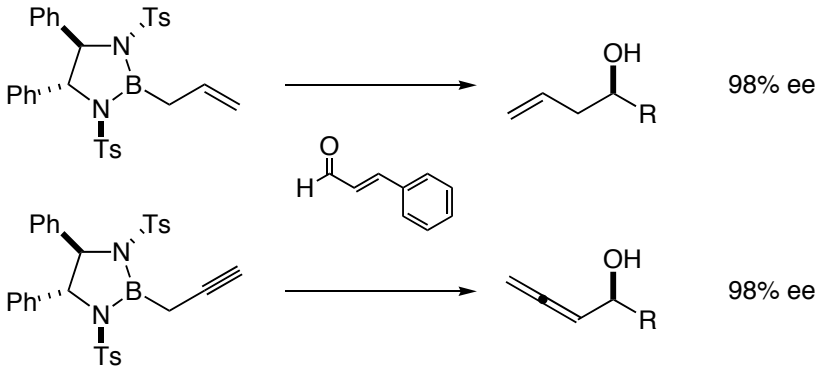

E. J. Corey, *J. Am. Chem. Soc.* **1989**, *111*, 5495-5496.
J. Am. Chem. Soc. **1990**, *112*, 878-879.

■ The Masamune Borolane

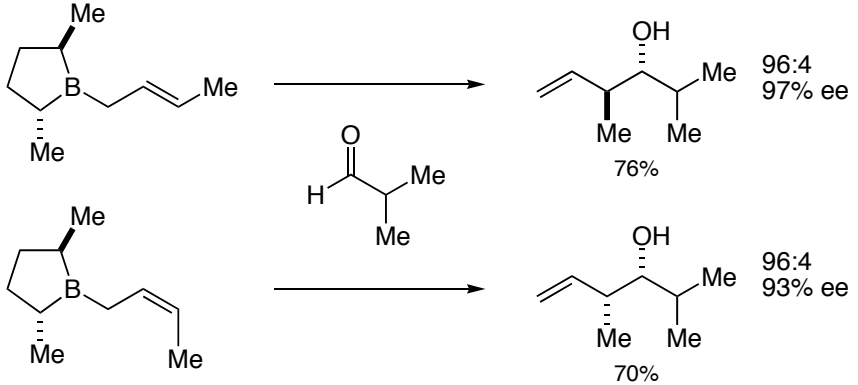

S. Masamune, *J. Org. Chem.* **1987**, *52*, 4831-4832.

■ The Brown IPC Controller

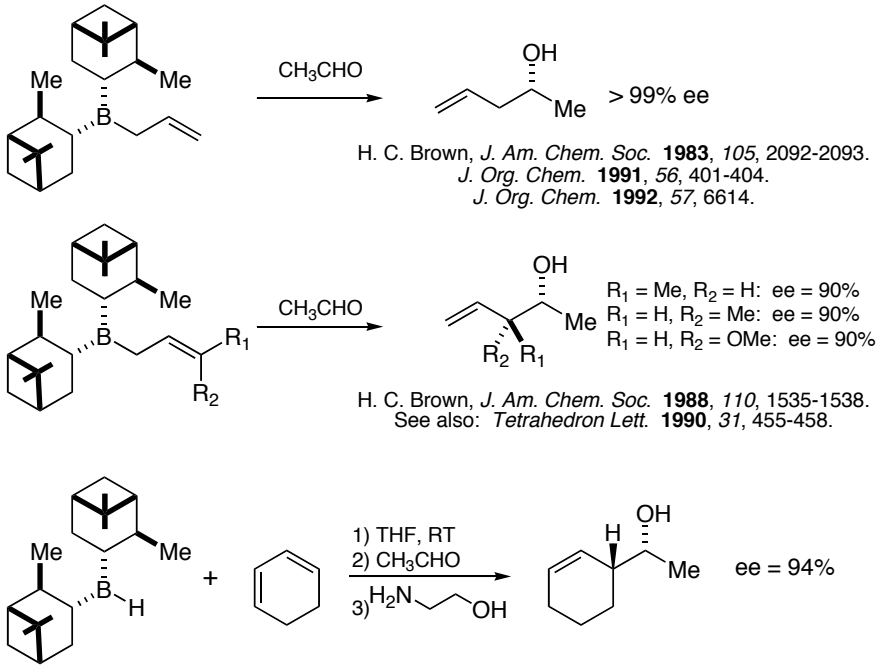

H. C. Brown, *J. Am. Chem. Soc.* **1983**, *105*, 2092-2093.
J. Org. Chem. **1991**, *56*, 401-404.
J. Org. Chem. **1992**, *57*, 6614.

H. C. Brown, *J. Am. Chem. Soc.* **1988**, *110*, 1535-1538.
See also: *Tetrahedron Lett.* **1990**, *31*, 455-458.

H. C. Brown, *J. Chem. Soc., Perkin Trans. 1*, **1991**, 2633.

The Allylboron Reagents Add to Carbonyl Compounds via a Zimmerman-Traxler Transition State

Masamune, Sato, Kim, Wollmann *J. Org. Chem.* **1987**, *52*, 4831

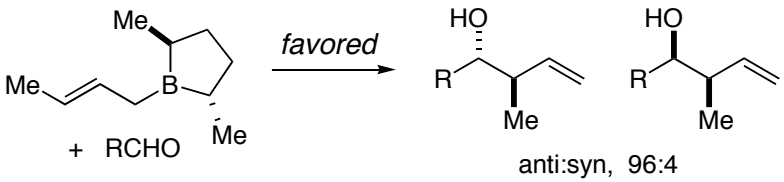

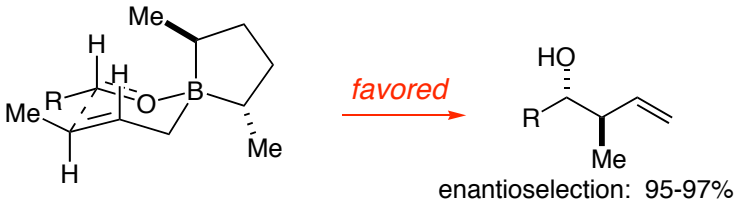

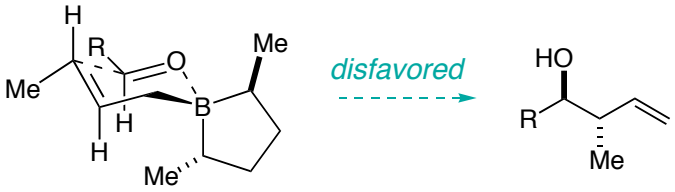

An Enantioselective Allyltitanium Reagent

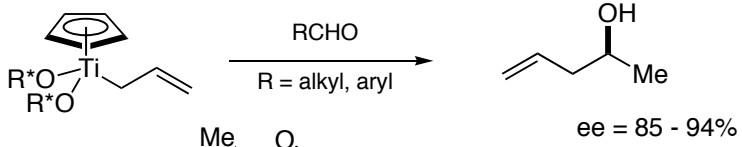

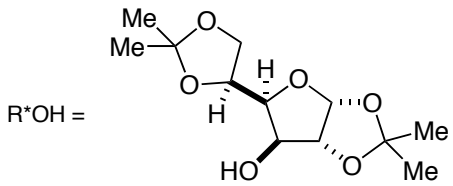

M. Riediker, R. Duthaler, *ACIEE*, **1989**, *28*, 494-495.
In *Organic Synthesis via Organometallics*, **1991**, 285-309.
J. Am. Chem. Soc. **1992**, *114*, 2321-2336.

Duthaler *Chem. Rev.* **1992**, *92*, 807

Another Enantioselective Allyltitanium Reagent

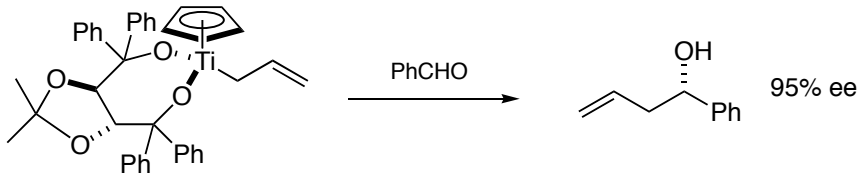

R. Duthaler, *J. Am. Chem. Soc.* **1992**, *114*, 2321-2336.

Chiral α-Substituted Allyl Metal Reagents: Boron

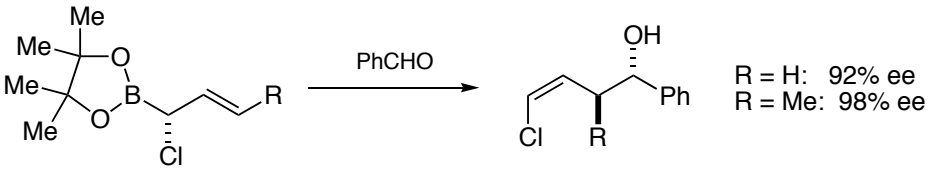

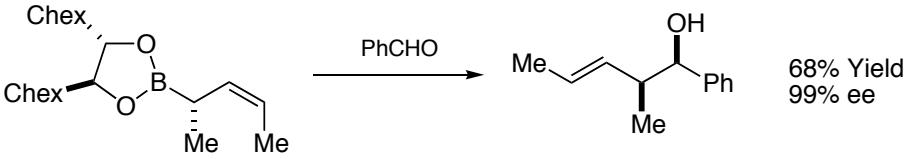

R. Hoffman, *Chem. Ber.* **1986**, *119*, 2013-2024.
Chem. Ber. **1988**, *121*, 1501-1507.
ACIEE, **1986**, *25*, 1028-1030.

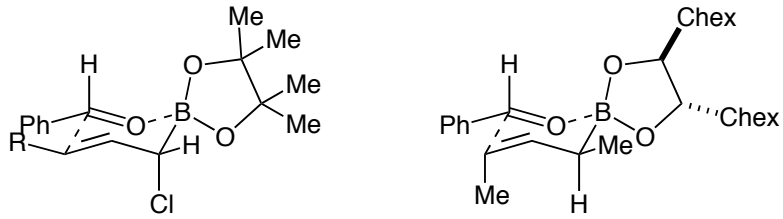

The favored transition states

http://www.courses.fas.harvard.edu/~chem206/

Chemistry 206

Advanced Organic Chemistry

Lecture Number 29

Enamines and Imminium Ions in Organocatalysis

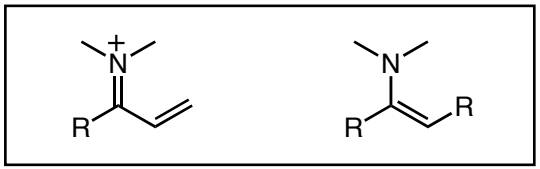

- Introduction and General Trends
- Historical Backgound - The Hajos-Parrish Reaction
- Direct Asymmetric Aldol and Mannich Reactions
- α-Amination and Oxidation Reactions
- Michael Reactions
- Cascade Reactions

Reading Assignment for this Week:

Carey & Sundberg: **Part A**; Chapter 7
Carbanions & Other Nucleophilic Carbon Species

Carey & Sundberg: **Part B**; Chapter 2
Reactions of Carbon Nucleophiles with Carbonyl Compounds

Jonathan F. Lawrence

Friday, December 1, 2006

Assigned Journal Articles

"Theory of Asymmetric Organocatalysis of Aldol and Related Reactions: Rationalizations and Predictions."
K. N. Houk, et al. *Acc. Chem. Res.*, **37**, 558 (2004). **(handout)**

"Enantioselective Organocatalysis",
Dalko, Peter, *ACIEE.* **40**, 3726 (2001). **(electronic handout)**

Other Useful References

"Enamine Catalysis is a Powerful Strategy for the Catalytic Generation and Use of Carbanion Equivalents." List, B. *Acc. Chem. Res.* **37**, 548 (2004).

"Enamine-Based Organocatalysis with Proline and Diamines: The Development of Direct Catalytic Aymmetric Aldol, Mannich, Michael, and Diels-Alder Reactions." Barbas, C., *Acc. Chem. Res.* **37**, 580 (2004).

"Proline Catalyzed Asymmetric Reactions" List, Benjamin, *Tetrahedron,* **58**, 5573 (2002).

"Asymmetric Aminocatalysis", List, Benjamin,*Synlett*, **11**, 1675 (2001).

"Amino Acids and Peptides as Asymmetric Organocatalysts", Miller, Scott *Tetrahedron*, 58, 2481 (2002).

Provide a mechanism that accounts for enantiomerically enriched products.

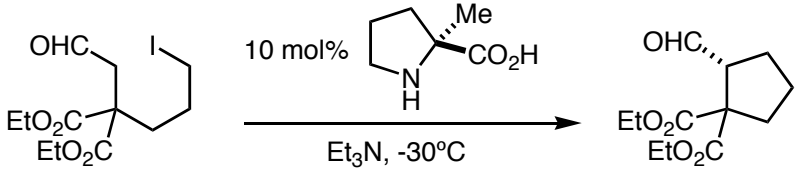

92% yield, 95% ee

List, B. *JACS* **2004**, 126, 450-451.

Properties and Reactivity of Enamines

Tautomeric Equilibria: Ketones vs. Imines

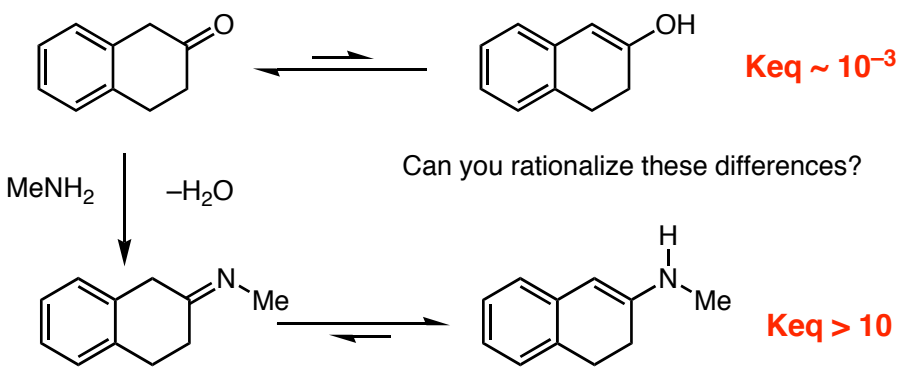

Can you rationalize these differences?

The enamine content in an analogous imine is invariably higher than its carbonyl counterpart. In the case above, ring conjugation now stabilizes the enamine tautomer as the major tautomer in solution.

Representative akylation and acylation reactions of enamines

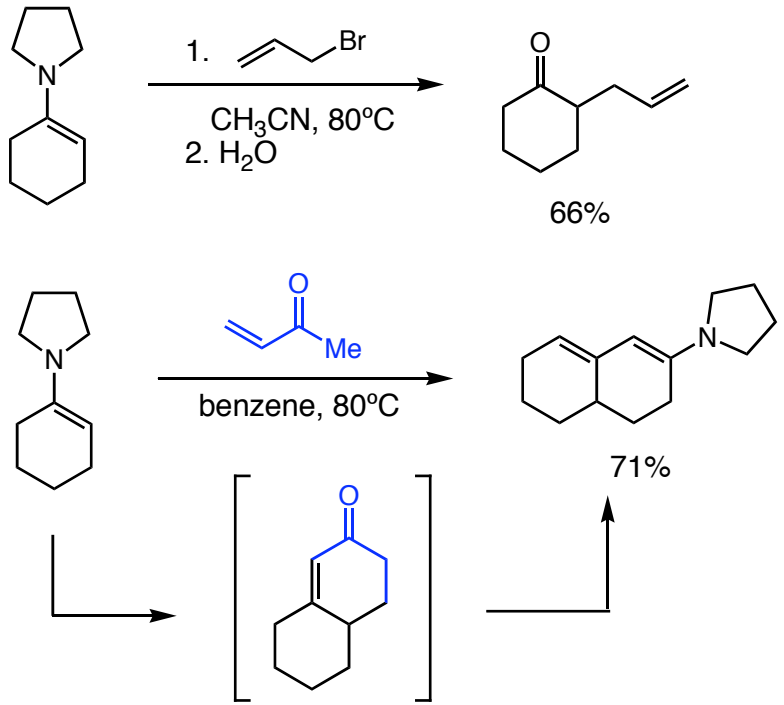

Stork, G. *JACS* **1963**, 85, 207.

Decreasing Nucleophilicity ⟶

Decreasing Electrophilicity ⟶

Electrophile \ Nucleophile	–NR C=C	O– C=C	NR_2 C=C	OMe C=C
Br_2, O_3	+	+	+	+
H_3O^+	+	+	+	+
R–C(=O)–Cl	+	+	+	
R–C(=O)–H	+	+	+	
R–C(=O)–R	+	+		
Me—I	+	+		
R–C(=O)–OR	+	+		
H_2C—O—CH_2	+			
Me_2CH—I	+			
R–C(=O)–NR_2				

■ Nature uses enamines, "stabilized" enolates, and enol derivatives in C–C bond constructions extensively.

Chiral Enamines - The Hajos-Parrish-Eder-Sauer-Weichert Reaction

The First Asymmetric Variant

Yamada, 1969

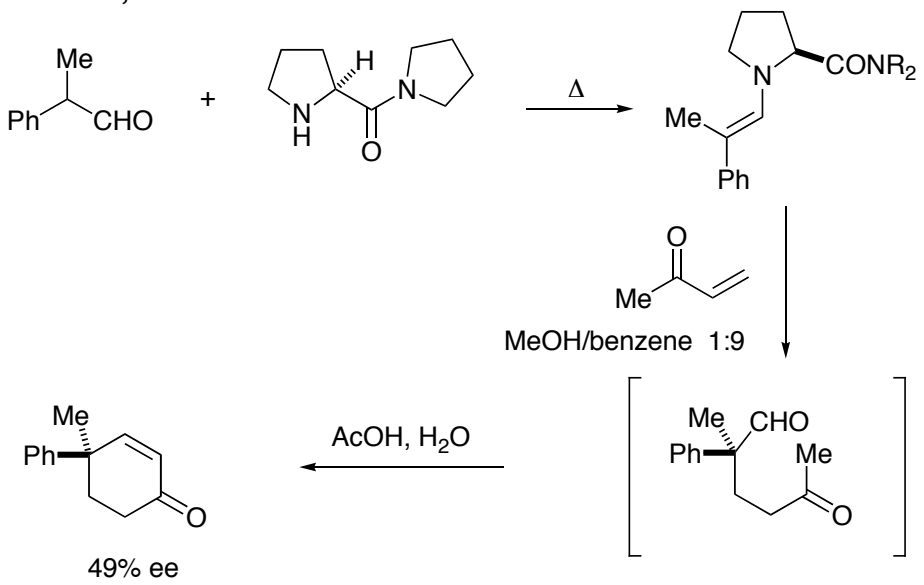

49% ee

Yamada, S. *TL* **1969**, *10*, 4237.

The Seminal Experiments

Hajos and Parrish, 1974

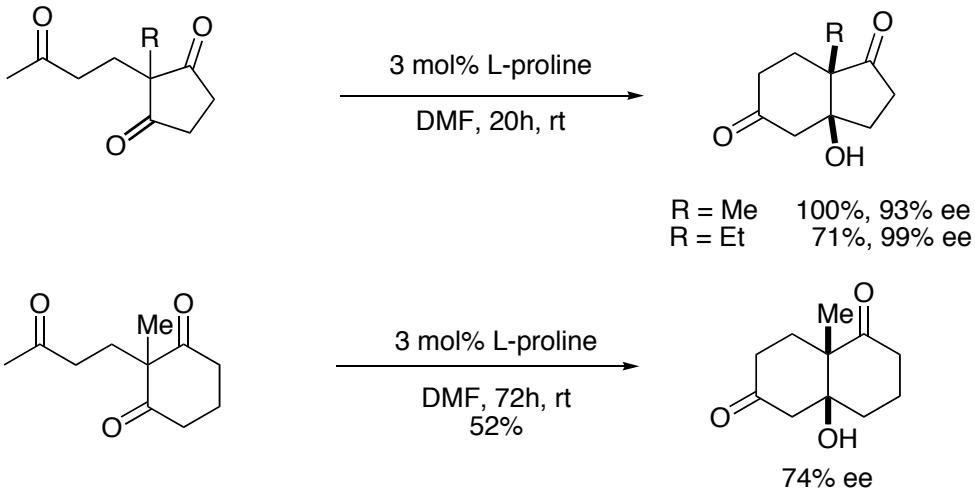

R = Me 100%, 93% ee
R = Et 71%, 99% ee

74% ee

Hajos, J., Parrish, D. *JOC* **1974**, *39*, 1615.
Eder, U., Sauer, G., Weichert, R. *ACIEE* **1971**, *10*, 496.

- the use of protic solvents severly diminished enantioselectivity
- other amino acids as catalysts lead to decreased chemical yield and enantioselectivity
- Eder, Sauer, and Weichert obtained the corresponding aldol condensation product in similar optical purity using 47 mol% L-proline and 1N $HClO_4$

Effect of the Catalyst

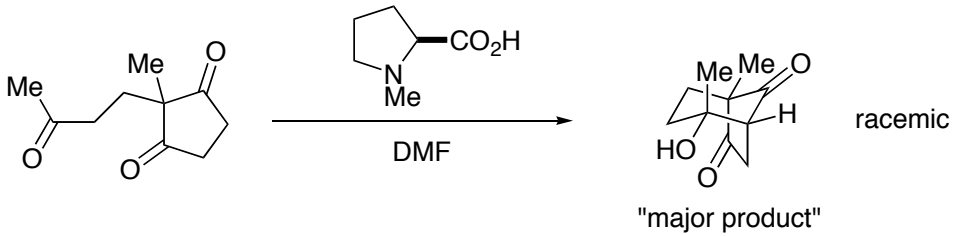

racemic

"major product"

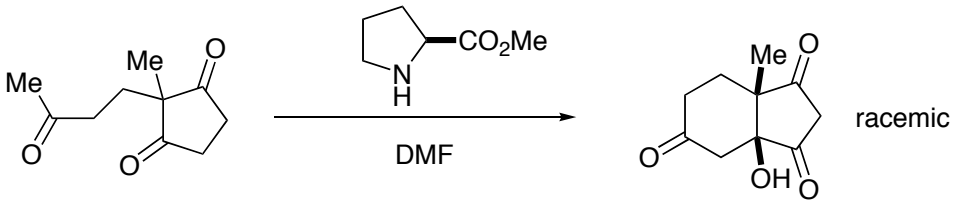

racemic

"major product"

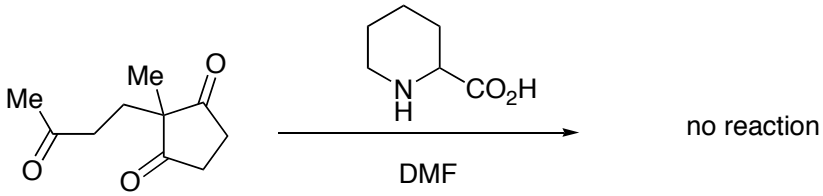

no reaction

Agami, 1984 - 1986

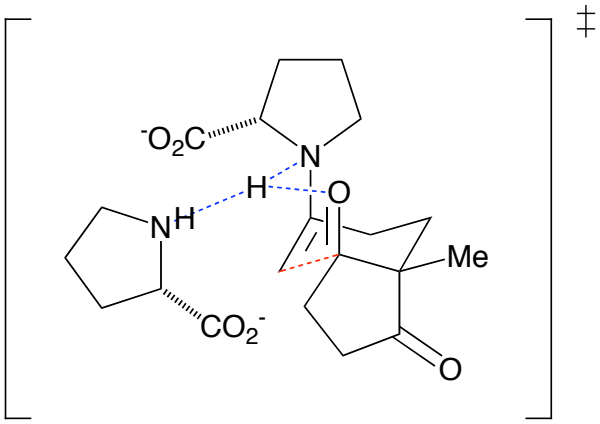

- favorable (enamine) N-H---O hydrogen bond
- N-H *anti* to carboxylate electrostatically favored
- reaction is second-order in proline (non-linear effect observed)
- second proline acts as a proton shuttle, allowing enamine to be nucleophilic

Agami, C. *TL* **1986**, *13*, 1501.

Houk, 2001 - 2003

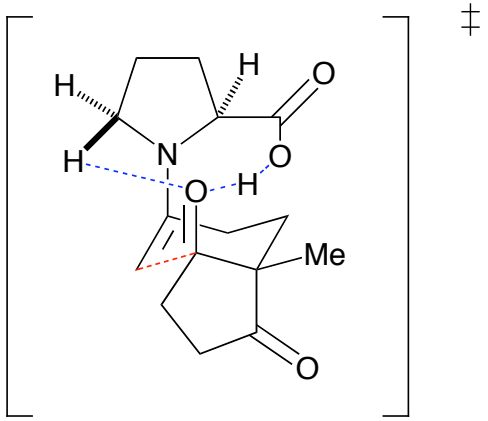

- N-H---O hydrogen bond does not lower energy of transition state
- favorable O-H---O hydrogen bond
- additional NC-H---O hydrogen bond further stabilizes system
- reaction is first order in proline (supported by kinetic data) and no non-linear effect observed

Houk, K. *JACS* **2001**, *123*, 12911.
Houk, K., List, B. *JACS* **2003**, *125*, 16.

general hydrogen bond energies

O -H - - O 3.0-8.0 kcal
C -H - - O 0.5-3.8 kcal

for a discussion on R_3N^+-C-H---O=C bonds, see:
Houk, K. *JACS*, **2002**, *124*, 7163.

The Direct Proline-Catalyzed Aldol Reaction

The initial reaction

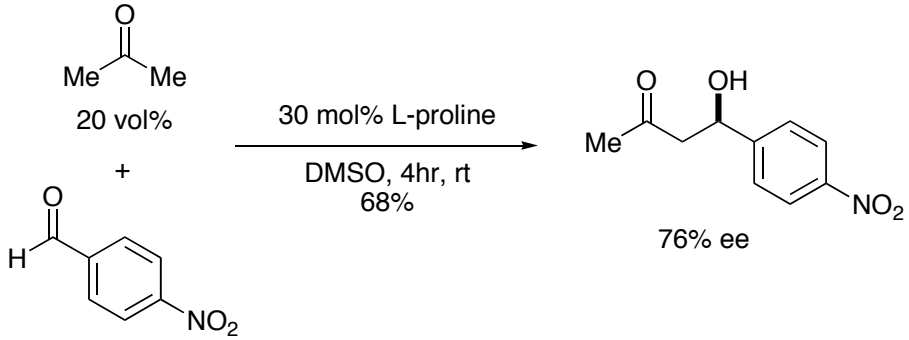

Catalyst Screen

compound	% yield	% ee
(L)-His, (L)-Val (L)-Tyr, (L)-Phe	< 10	--
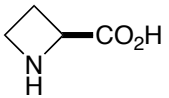	55	40
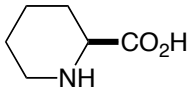	< 10	--
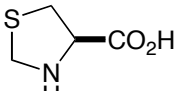	67	73
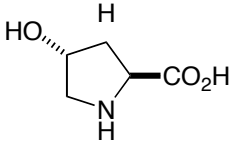	85	78
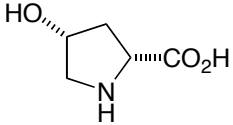	> 50	- 62
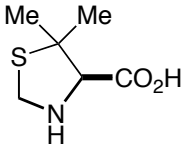	66	86

Aldehyde scope

Catalyst:

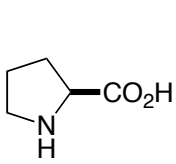

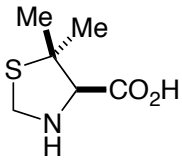

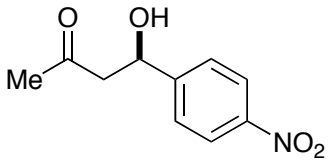

cat. **1**, 68% y., 76% ee
cat. **2**, 60% y., 86% ee

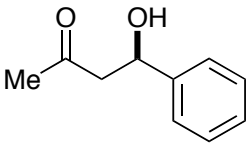

cat. **1**, 62% y., 60% ee
cat. **2**, 60% y., 89% ee

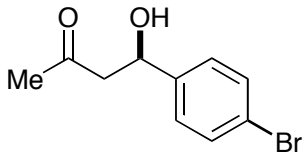

cat. **1**, 74% y., 65% ee
cat. **2**, 65% y., 67% ee

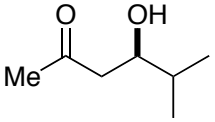

cat. **1**, 97% y., 96% ee
cat. **2**, 61% y., 94% ee

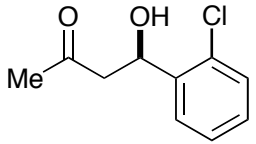

cat. **1**, 94% y., 69% ee
cat. **2**, 71% y., 74% ee

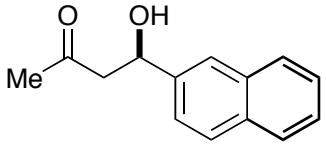

cat. **1**, 54% y., 77% ee
cat. **2**, 60% y., 88% ee

- α–unbranched aldehydes unsuccessful due to self-aldolization

List, B. *JACS*, **2000**, *122*, 2395.
Barbas, C. *JACS*, **2001**, *123*, 5260.

The Direct Proline-Catalyzed Aldol Reation

Conditions which tolerate α–unbranched aldehydes

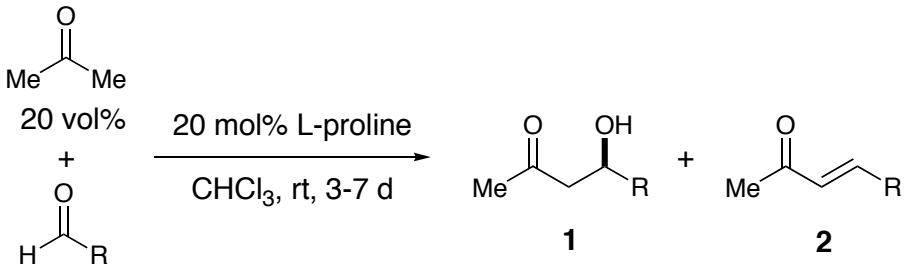

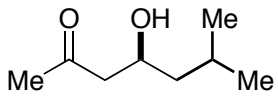

23% yield **1**, 61% ee, 46% yield **2**

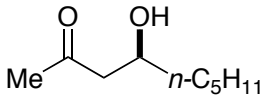

35% yield **1**, 73% ee, 40% yield **2**

List, B. *OL* **2001**, *3*, 573.

Ketone scope

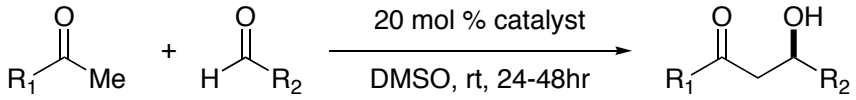

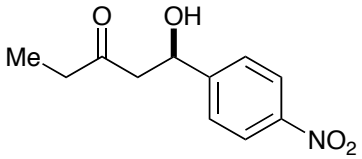

cat. **1**, 65% yield, 77% ee
cat. **2**, 57% yield, 74% ee

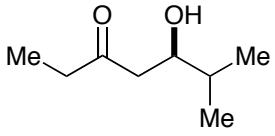

cat. **1**, 60% yield, 80% ee
cat. **2**, <5% yield, ---

Barbas, C. *JACS,* **2001**, *123*, 5260.

Direct Aldol Mechanism

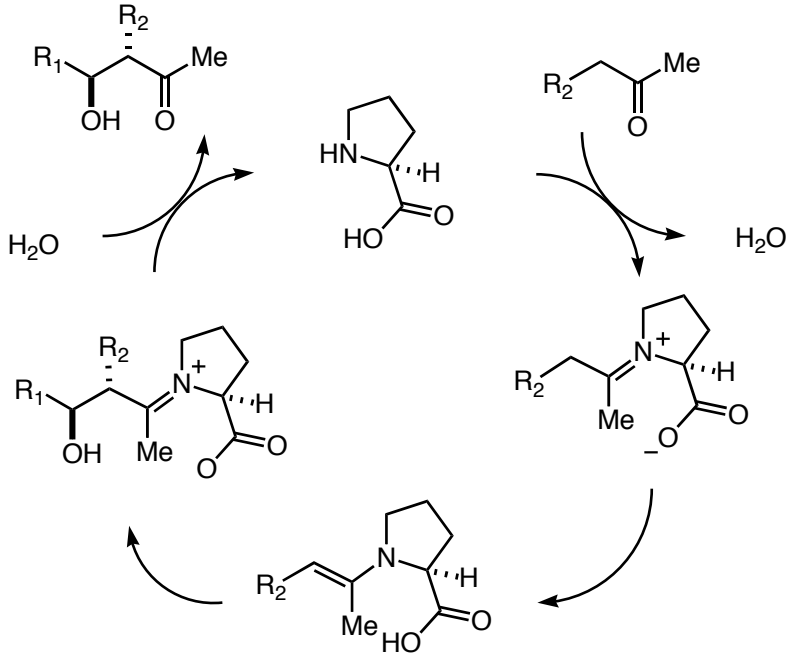

Houk's calculated T.S.:

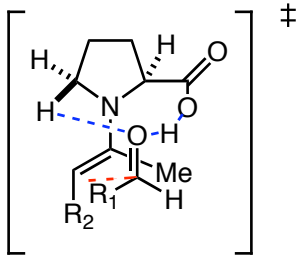

- synclinal approach of aldehyde
- R_1 in pseudo-eqitorial position
- C-H - - O distance ~ 2.4 Å
- DFT calculations in DMSO

Previously Proposed T.S.:

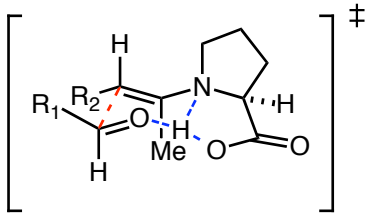

- metal-free Zimmerman-Traxler model

List, B. *JACS* **2000**, *122*, 2395.
List, B., Houk, K. *JACS* **2003**, *125*, 2475.

The Direct Aldol Reaction - Other Applications

Synthesis of 1,2-diols

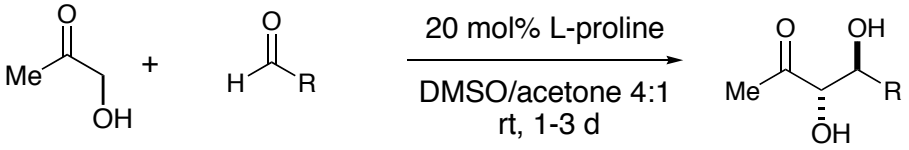

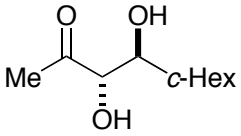

60% yield, >99% ee
>20:1 dr

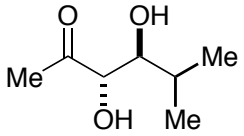

62% yield, >99% ee
>20:1 dr

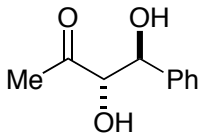

83% yield, 80% ee
1:1 dr
(DMTC cat. gives 95% ee)

Generation of more substituted enamine due to:

- increased acidity of α–proton
- increased stability of enamine due to $O_{n.b.}$ --> π* C=C

List, B. *JACS*, **2000**, *122*, 2395.
Barbas, C. *JACS,* **2001**, *123*, 5260.

Donor scope expanded to include aldehydes

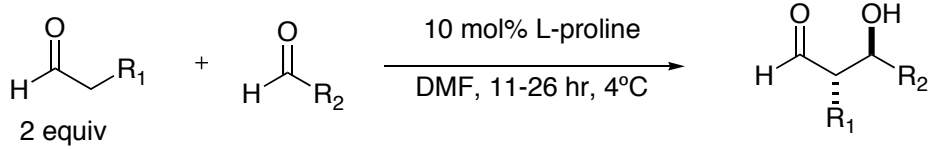

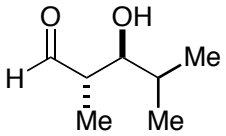

82% yield, >99% ee
24:1 dr

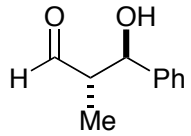

81% yield, 99% ee
3:1 dr

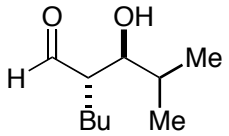

80% yield, 98% ee
3:1 dr

MacMillan, D. *JACS*, **2002**, *124*, 6798.

Synthesis of carbohydrates

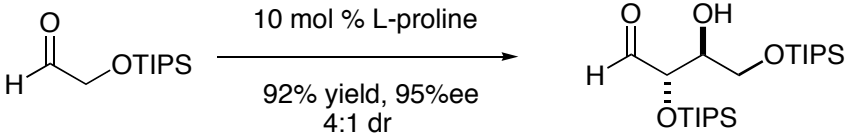

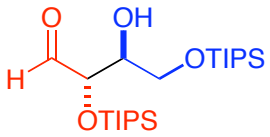

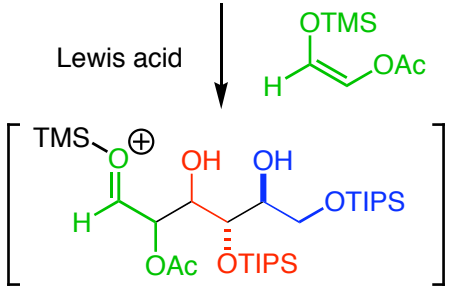

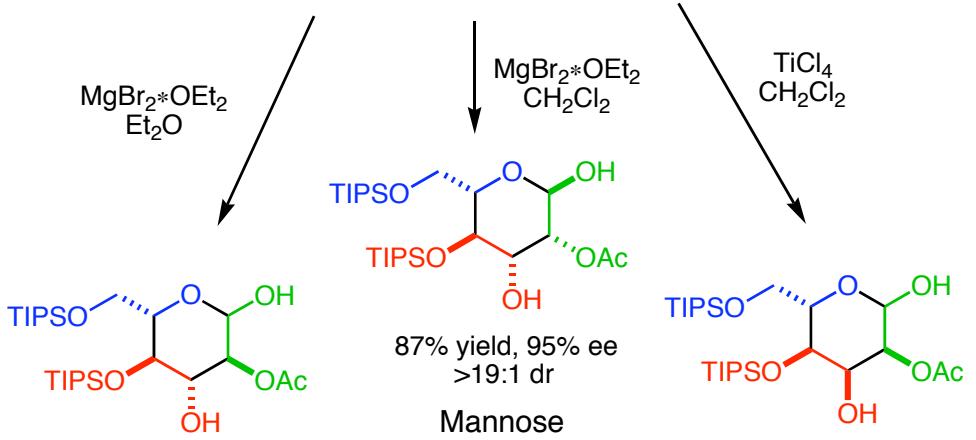

79% yield, 95% ee
10:1 dr
Glucose

87% yield, 95% ee
>19:1 dr
Mannose

97% yield, 95% ee
>19:1 dr
Allose

MacMiillan, D. *Science*, **2004**, 305, 1752.

Other catalysts for the direct aldol reaction

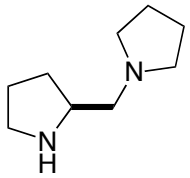

1

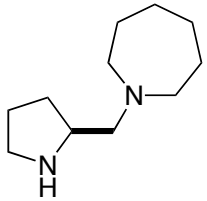

2

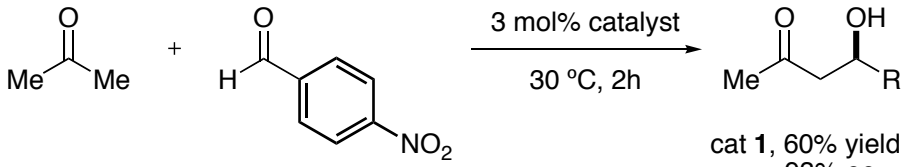

cat **1**, 60% yield
93% ee
cat **2**, 72% yield
93% ee

Yamamoto, *Tet.* **2002**, *58*, 8167.

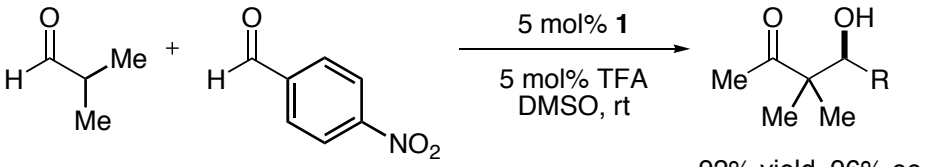

92% yield, 96% ee

- unsymmetrical α,α–disubstituted aldehydes give low diastereoselectivity

Barbas, C., *ACIEE* **2004**, *43*, 2420.

Mannich reaction: First report

Reaction rate considerations

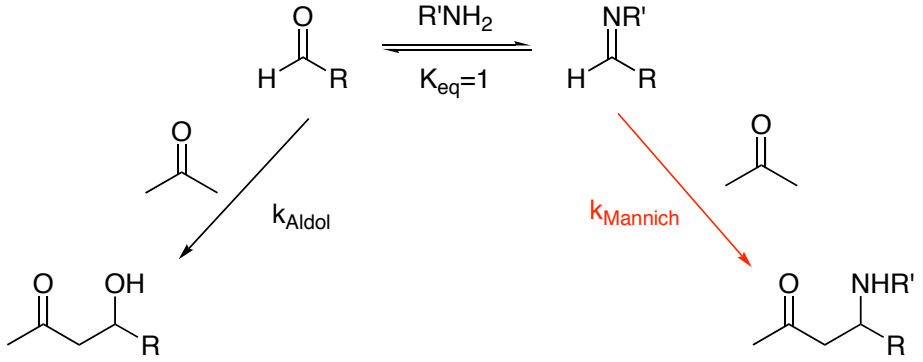

- enamime addition must be faster to the imine than to the corresponding aldehyde ($k_{Mannich} > k_{Aldol}$)
- formation of the aldimine must be faster than aldol addition

Three-component coupling

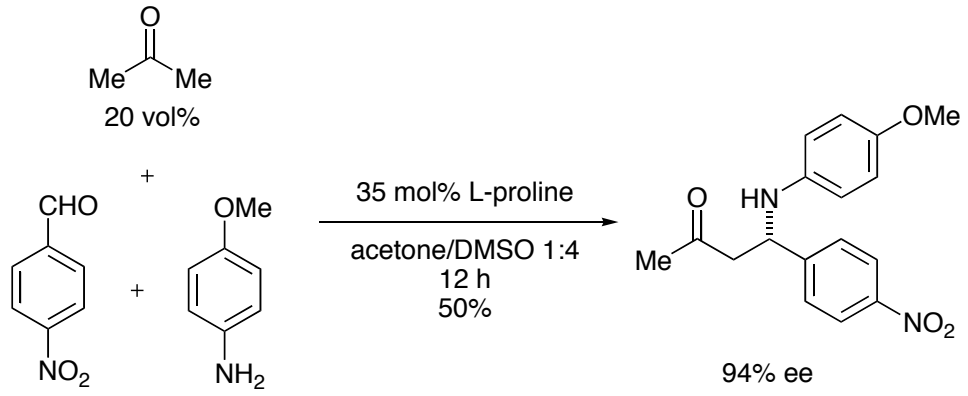

94% ee

(+ <20% aldol product)

List, B. *JACS*, **2000**, *122*, 9336.

The Proline-Catalyzed Direct Mannich Reaction

Substrate Variation

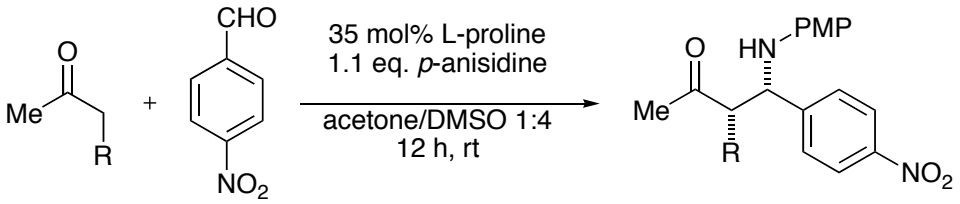

When R = Me

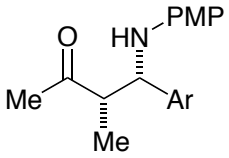

1

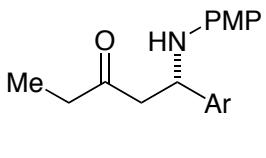

2

95% yield,
ratio**1**:**2** = 2.5:1
1 = 99% ee,
>20:1 dr
2 = 94% ee

When R = OMe, OH

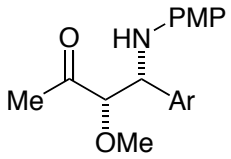

93% yield, 98% ee
>20:1 dr

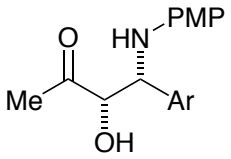

92% yield, >99% ee
>20:1 dr

List, B. *JACS*, **2000**, *122,* 9336.

- aliphatic and aromatic aldehydes are both good substrates
- as electron donationfrom aldehyde increases, enantioselectivity and diastereoselectivity decrease
- proline uniquely effective as Mannich reaction catalyst

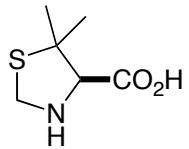

60% y., 16% ee

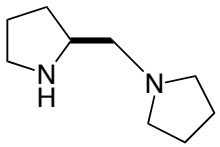

26% y., 0% ee

results for reaction with isovalerylaldehyde

List, B. *JACS* **2002**, *124,* 827.

Transition State comparison

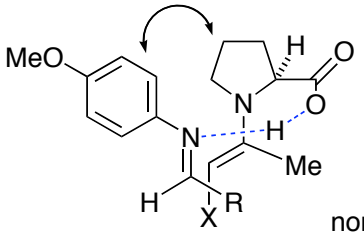

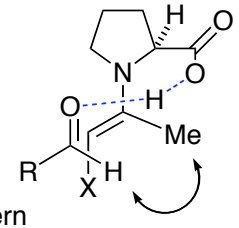

non-bonding interactions govern which diastereoface of electrophile is favored

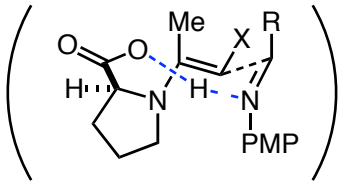

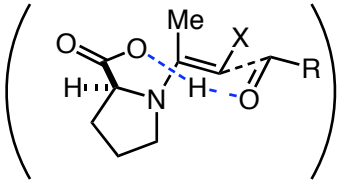

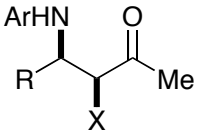

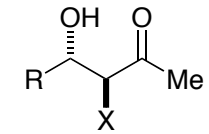

List, B. *JACS* **2002**, *124*, 827.

The Proline-Catalyzed Direct Mannich Reaction

Other electrophiles can be used

α-imino ethyl glyoxylate with ketones:

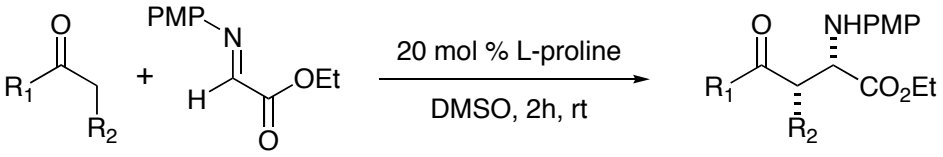

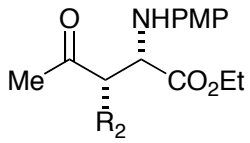

for R_2=Me, allyl, OH
62-79% yield, >99% ee,
>20:1 dr

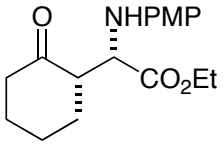

81% yield, >99% ee,
>20:1 dr

Barbas, C. *JACS* **2002**, *124*, 1842

α-imino ethyl glyoxylate with aldehydes:

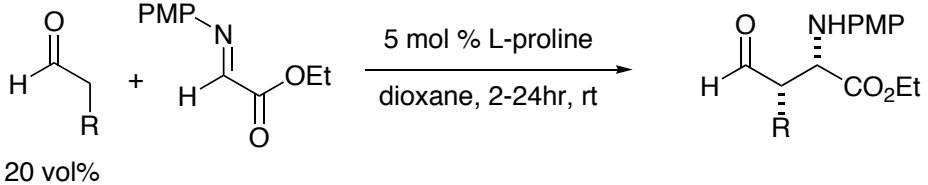

R =	% yield	dr	% ee
Me	72	1.1:1	99
Et	57	1.5:1	99
i-Pr	81	>10:1	93
n-Bu	81	3:1	99
n-Pent	89	>19:1	>99

Barbas, C. *JACS* **2002**, *124*, 1866.

A fortuitous finding: an *anti*-selective Mannich catalyst

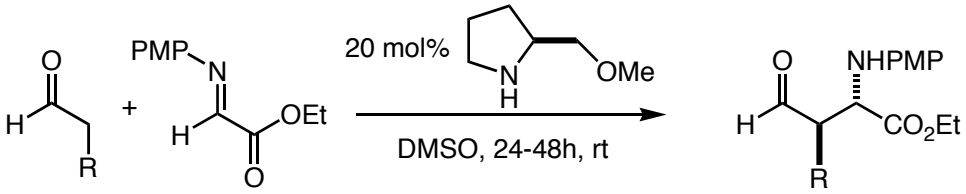

R =	% yield	dr	% ee
Et	44	1:1	75
i-Pr	52	10:1	82
n-Bu	54	10:1	74
t-Bu	57	>10:1	92
n-Pent	78	>10:1	76
n-Hex	68	>19:1	76

transition state:

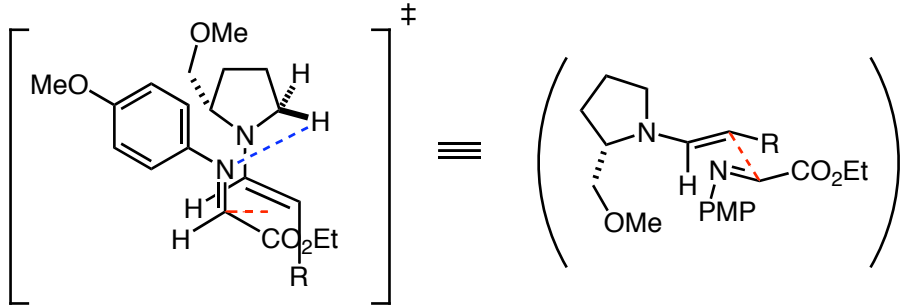

Barbas, C. *TL* **2002**, *43*, 7749.

For a review of SMP use in asymmetric synthesis, see:
Enders, D. *Synthesis* **1996**, 1403.

Amination: a route to α-amino alcohols and ketones

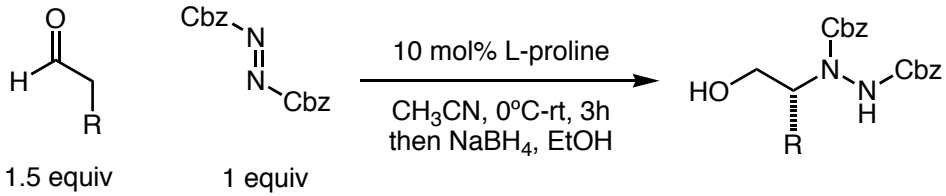

1.5 equiv 1 equiv

R =	% yield	% ee
Me	97	>95
n-Pr	93	>95
n-Bu	94	97
i-Pr	99	96
Bn	95	>95

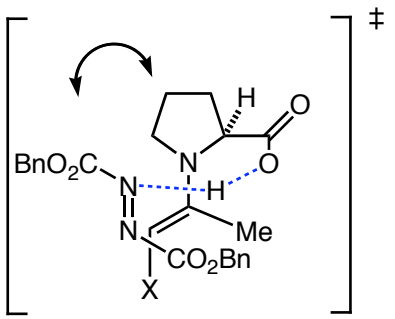

■ longer reaction time leads to epimerization, so aldehyde is reduced *in situ*

List, B. *JACS* **2002**, 124, 5656.

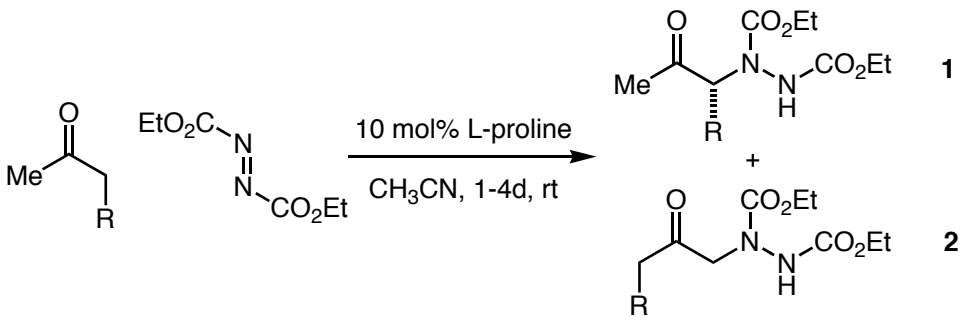

ratio **1**:**2** = 10:1
80% yield, 95% ee

ratio **1**:**2** = 4.5:1
92% yield, 98% ee

Jorgensen, *JACS* **2002**, *124*, 6254.

α-Oxidation of aldehydes with nitrosobenzene

The choice of reaction conditions determines N or O selelctive addition:

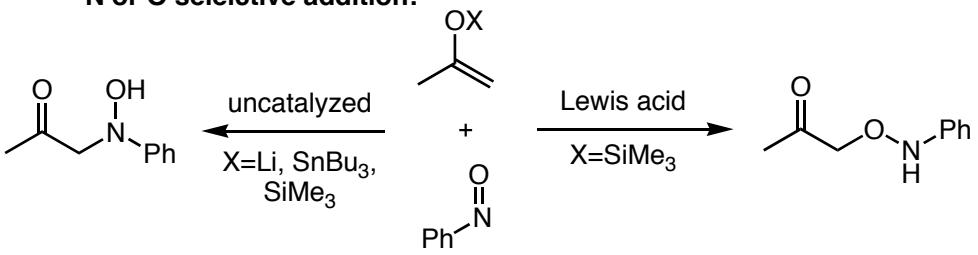

Yamamoto, H. *OL*, **2002**, *4*, 3579.

Larger basicity of nitrogen allows proline to catalyze O-nucleophilic addition:

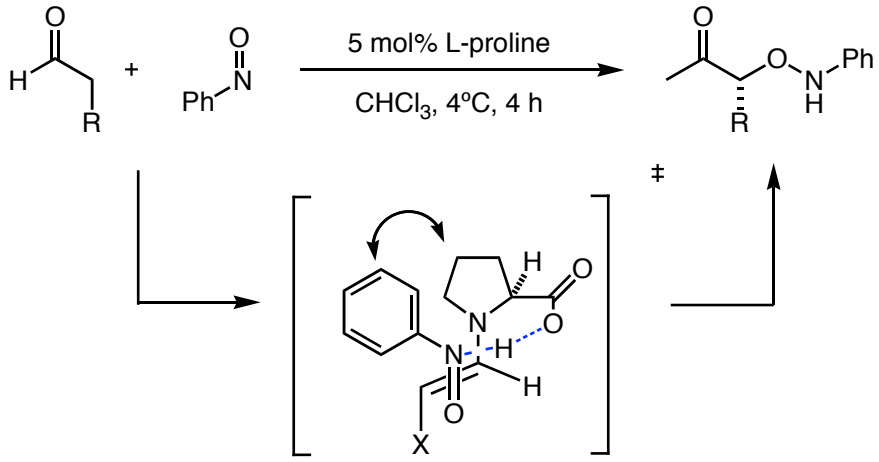

R =	% yield	% ee
Me	88	97
n-Bu	79	98
i-Pr	85	99
$CH_2CH{=}CH_2$	99	96
Bn	95	97
Ph	60	99
$(CH_2)_3OTIPS$	76	98
CH_2-(3'-N-methyl indole)	83	98

MacMillan, D. *JACS* **2003**, *125*, 10808.

Chlorination

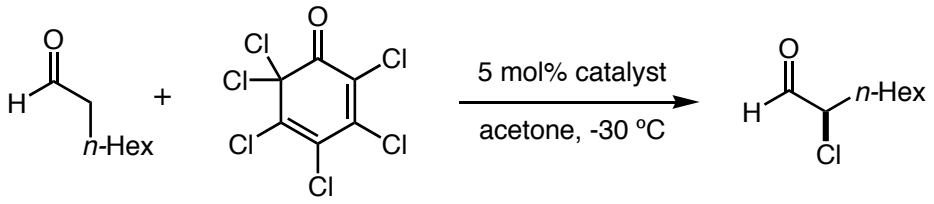

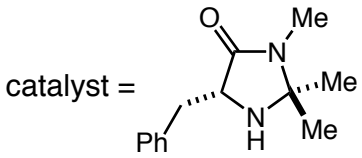

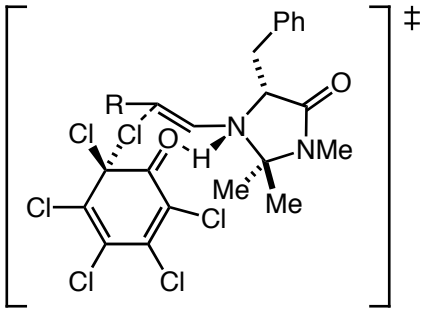

MacMillan, *JACS* **2004**, *126*, 4108.

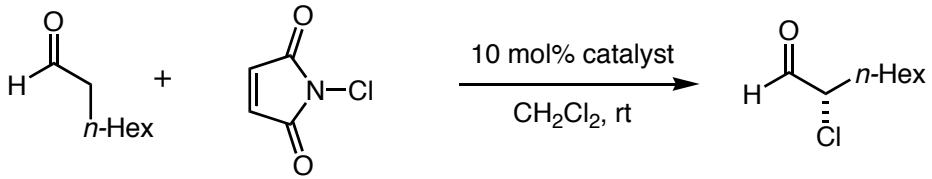

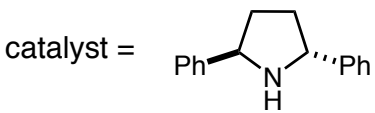

Jorgensen, *JACS* **2004**, *126*, 4790.

Fluorination

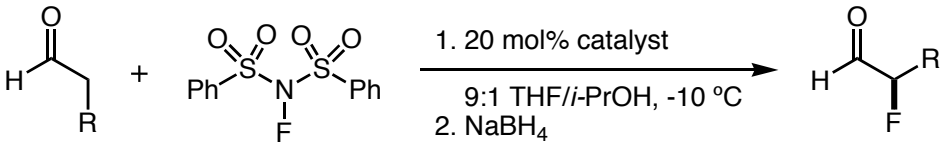

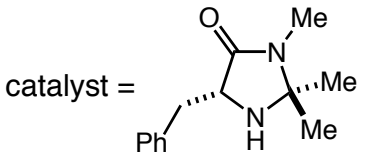

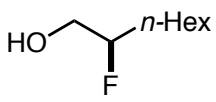

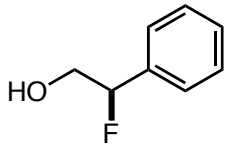

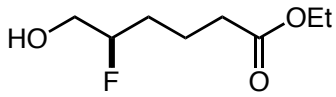

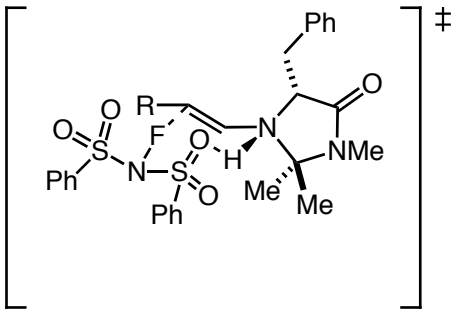

MacMillan, D. *JACS* **2005**, *127*, 8827.

Direct Organocatalytic Michael Reactions

There are two mechanistic possibilities:

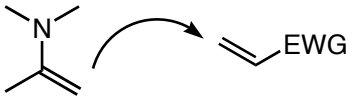

additions to:
- alkylidene malonates
- α,β–unsaturated nitroalkenes

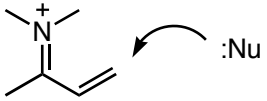

additions of:
- malonate esters
- nitroalkanes
- aromatics (Friedel-Crafts reactions)
- silyloxy furans

Diels-Alder reaction

Dipolar cycloaddition

Enamine examples:

An early attempt:

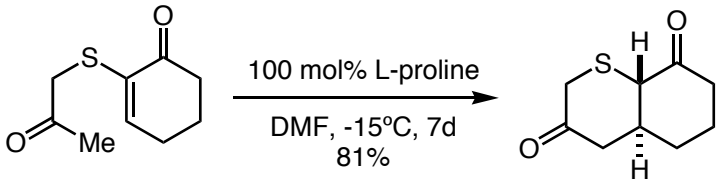

28% ee

Kozikowski, A. *JOC*, **1989**, *54*, 2275.

More recent results with nitroolefins:

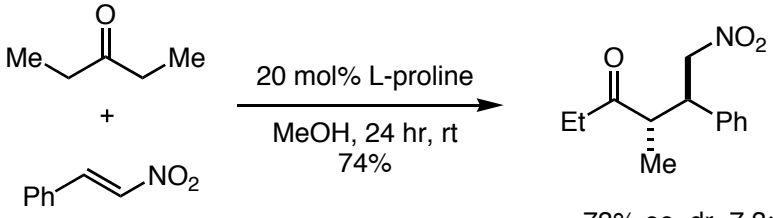

73% ee, dr=7.3:1

■ MeOH required as solvent to obtain high ee

Enders, *Synlett* **2002**, 26.

Use of a diamine catalyst

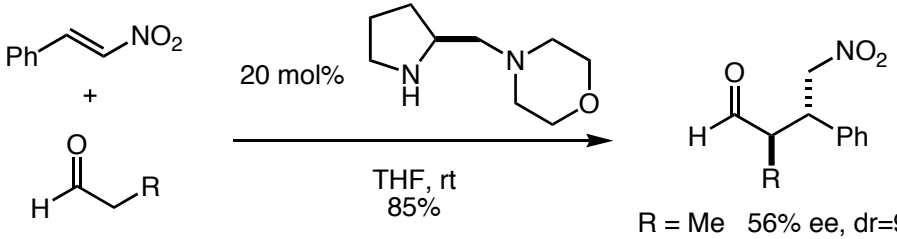

R = Me 56% ee, dr=9:1
R = *i*-Pr 72% ee, dr=11:1

Barbas, C. *OL* **2001**, *3*, 3737.

Contrasting transition states:

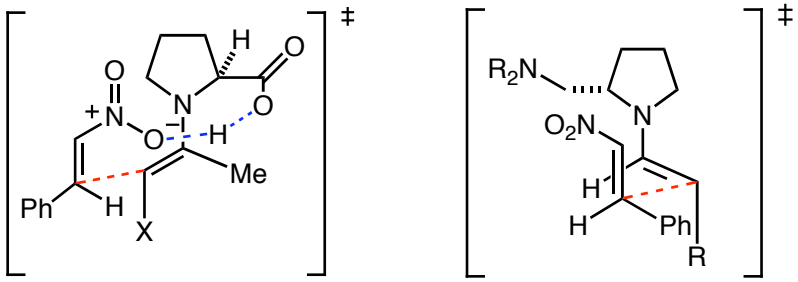

A highly enantioselective system:

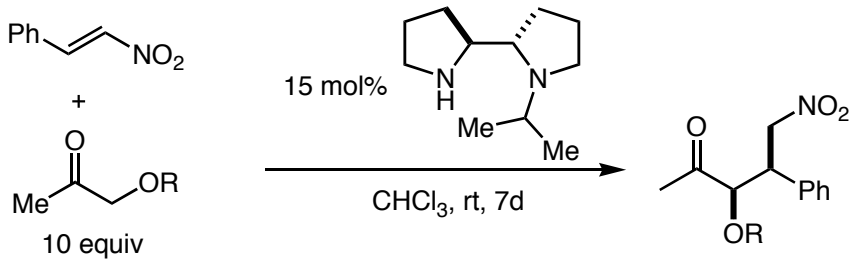

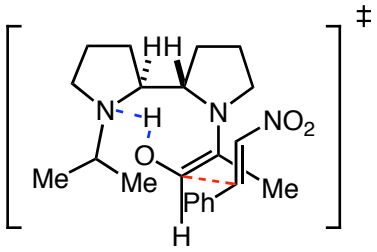

syn/anti

R	yield	dr	ee
Me	75	1:5	69
H	79	5:1	98

Alexakis, A. *OL*, **2003**, *5*, 2559.

Imminium examples

Proline is only mildly successful:

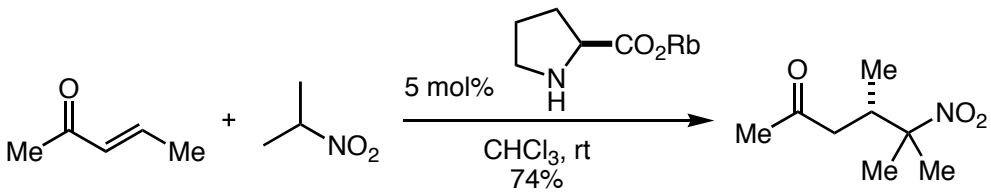

Yamaguchi, *JOC* **1996**, *61*, 3520.

MacMillan introduces a new catalyst:

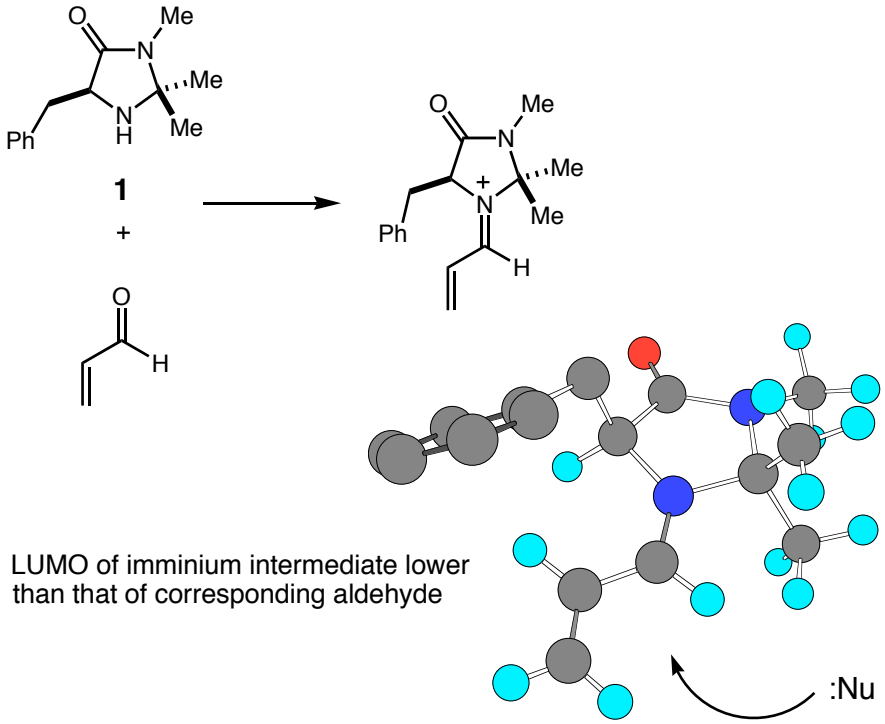

- LUMO of imminium intermediate lower than that of corresponding aldehyde

A listing of reactions catalyzed by MacMillan's imidazolidinone

Diels-Alder reactions:

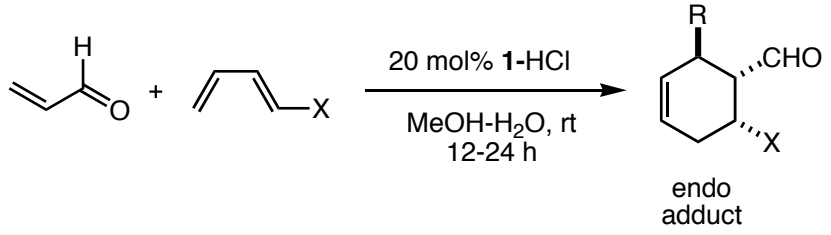

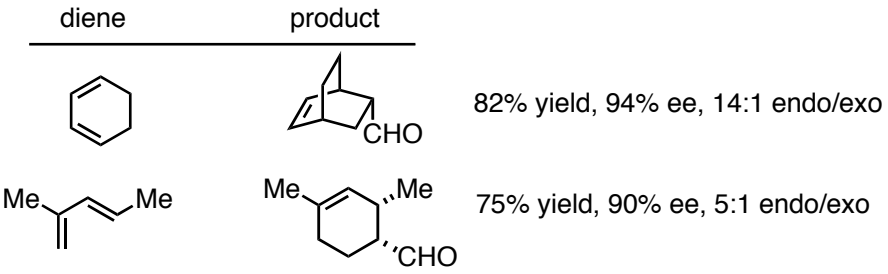

MacMillan, D. *JACS* **2000**, *122*, 4243.

Nitrone cycloadditons:

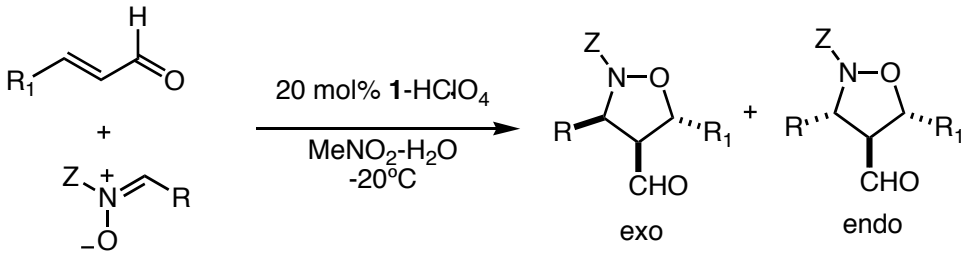

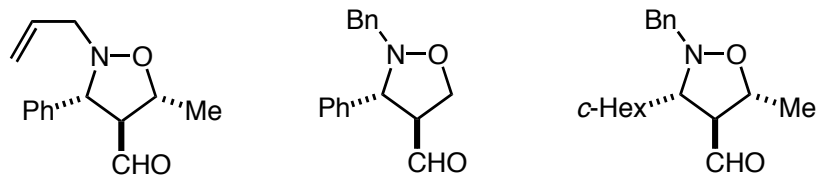

MacMillan, D. *JACS* **2000**, *122*, 9874

Direct Organocatalytic Michael Reaction

More chiral imidazolidinone catalyzed reactions

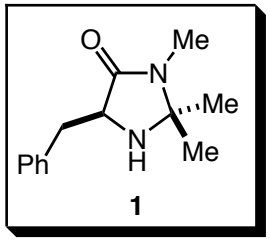

1

Friedel-Crafts reactions:

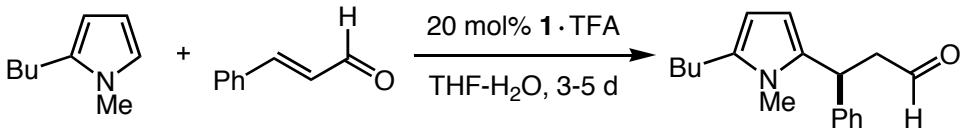

87% y, 90% ee

MacMillan, D. *JACS* **2001**, *123*, 4371.

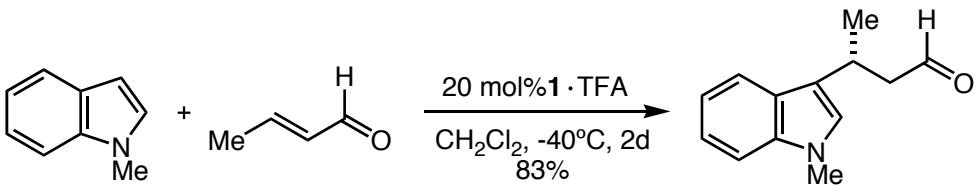

58% ee

- reaction was sluggish with **1**, so a new catalyst was developed

lone pair exposed

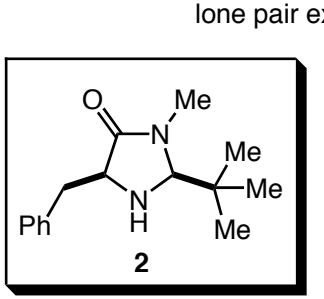

2

≡

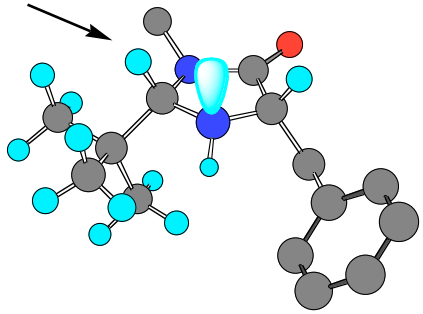

- above reaction now gives 92% ee with **2** due to increased reaction rate and steric shielding from *tert*-butyl group

MacMillan, D. *JACS* **2002**, *124*, 1172.

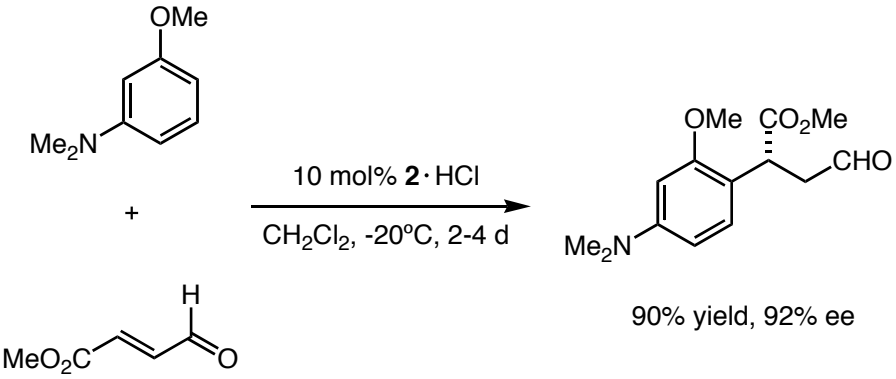

90% yield, 92% ee

MacMillan, D. *JACS* **2002**, *124,* 7894.

IMDA reactions:

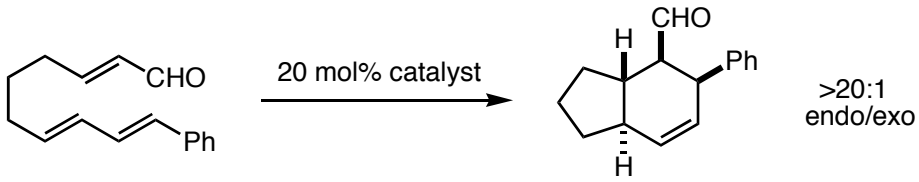

>20:1 endo/exo

catalyst **1**: 84%, 77% ee
2: 85%, 93% ee

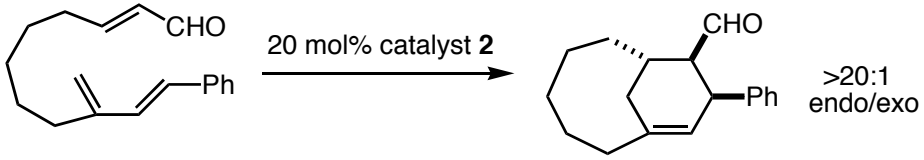

>20:1 endo/exo

65% y, 98% ee

MacMillan, D. *JACS* **2005**, *127,* 11616.

Mukaiyama michael reactions:

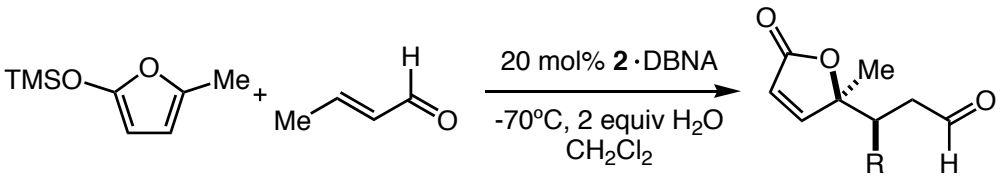

81% yield, 92% ee
22:1 syn/anti

MacMillan, D. *JACS* **2003**, *125*, 1192.

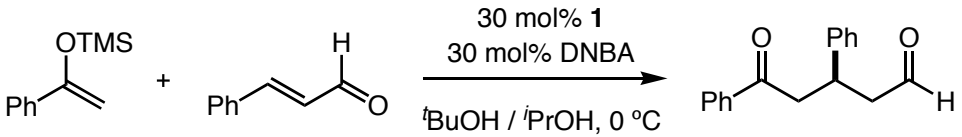

75% yield, 90% ee

Wang, W. *OL* **2005**, *7*, 1637.

■ note that Lewis acid catalysis promotes 1,2 addition with enals

Hydride reductions:

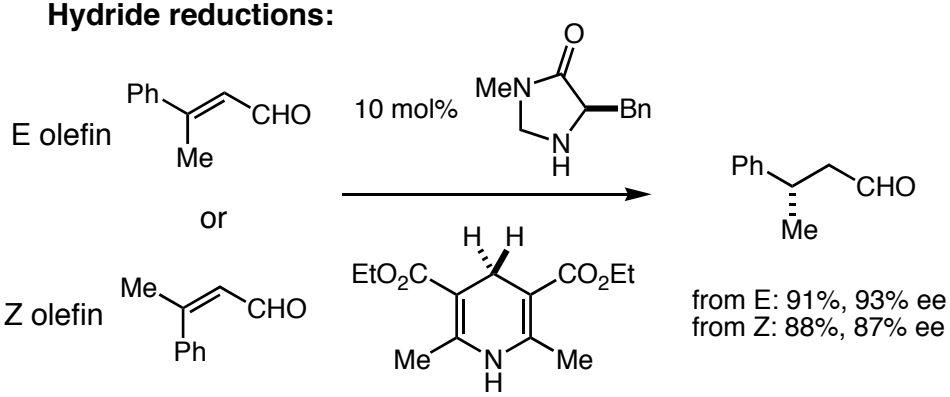

from E: 91%, 93% ee
from Z: 88%, 87% ee

MacMillan, D. *JACS* **2005**, *127*, 32.
see also: List, B. *ACIEE* **2004**, *43*, 6660.

Cascade reactions combine imminium and enamine catalysis

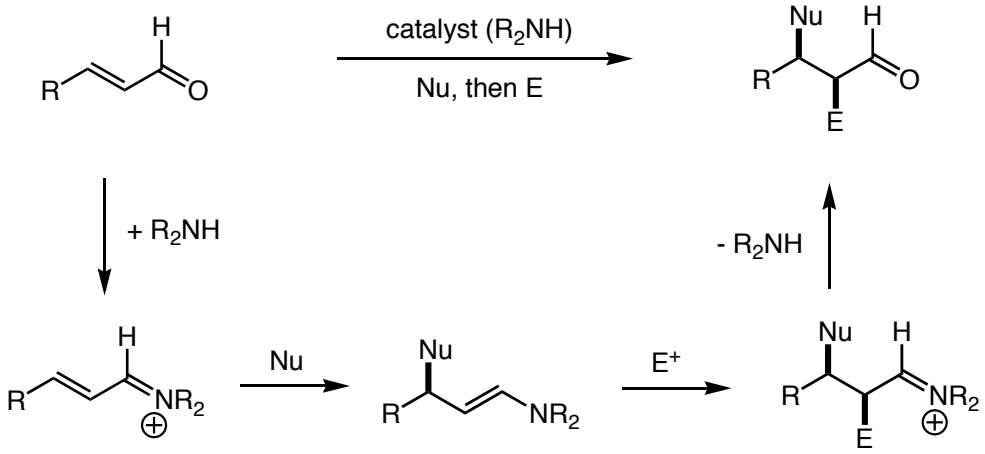

Friedel-Crafts plus chlorination:

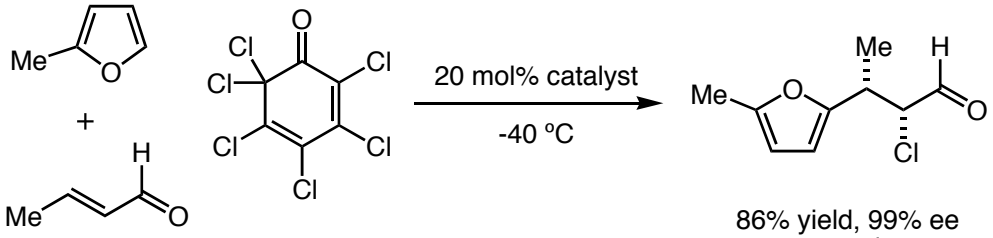

86% yield, 99% ee
14:1 dr

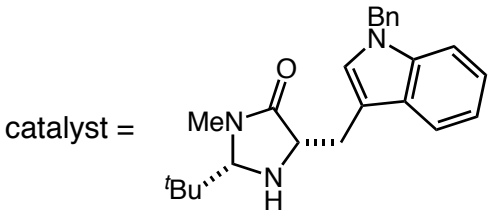

Organocatalytic Cascade Processes

Hydride reduction plus fluorination:

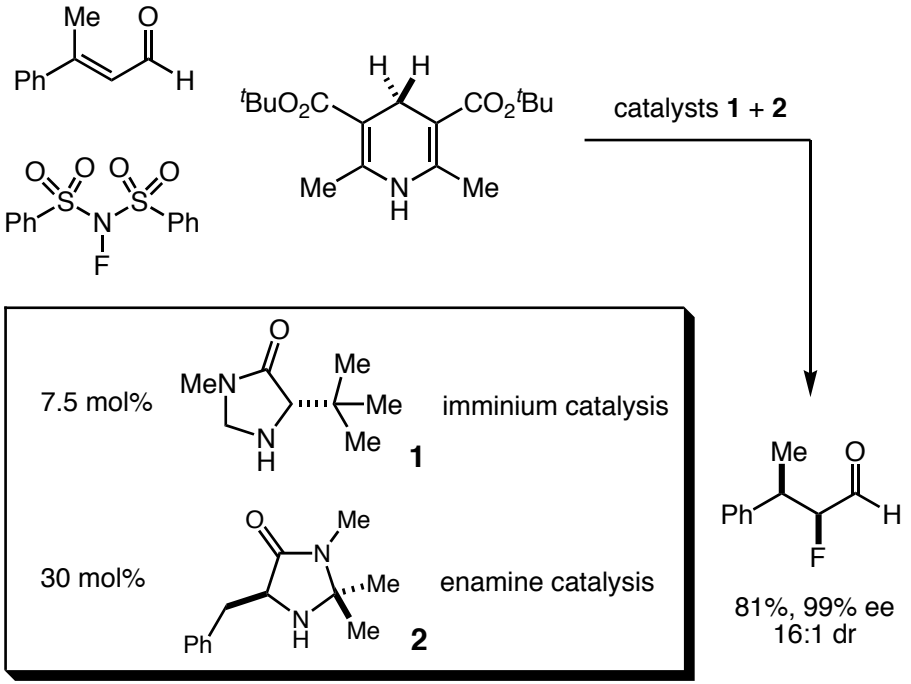

MacMillan, D. *JACS* **2005**, *127*, 15051.

Intramolecular cascade reactions

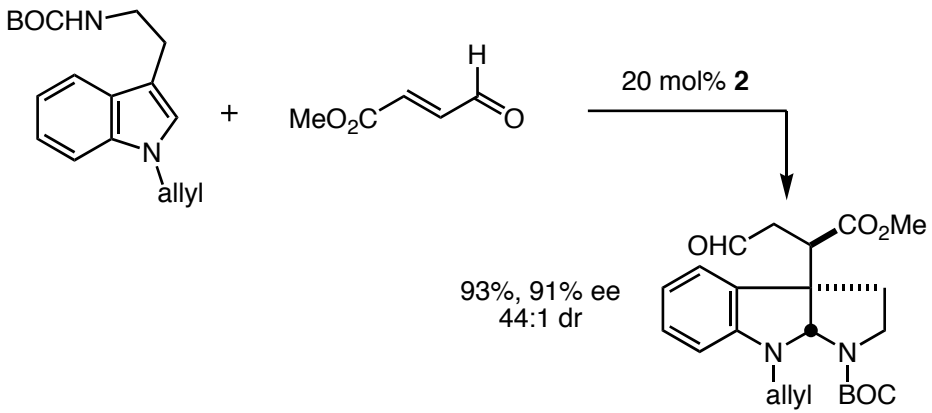

MacMillan, D. *PNAS* **2004**, *101*, 5482.

Epoxidation:

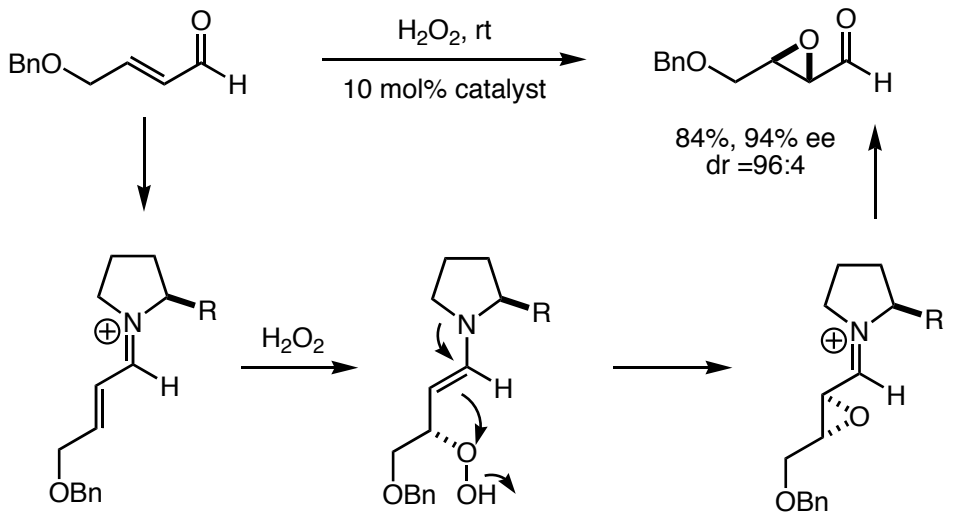

Jorgensen, K. *JACS* **2005**, *127*, 6964.

Cyclopropanation:

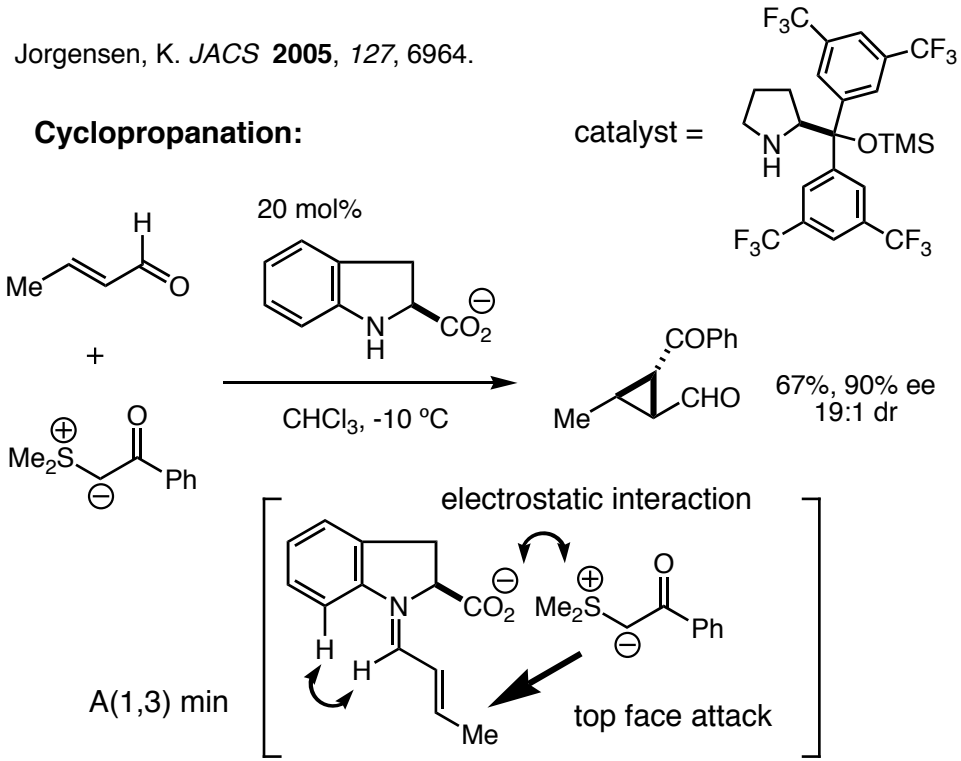

MacMillan, D. *JACS* **2005**, *127*, 3240.

http://www.courses.fas.harvard.edu/colgsas/1063

Chemistry 206

Advanced Organic Chemistry

Lecture Number 30

Functional Group Classification Scheme for Polar Bond Constructions

- Historical Perspective
- Charge Affinity Patterns
- Functional Group Classification Scheme
- The Chemistry of the $-NO_2$ Group
- The Chemistry of the $-N_2$ Group

Reading Assignment for this Week:

"An Organizational Scheme for the Classification of Functional Groups. Applications to the Construction of Difunctional Relationships."
D. A. Evans *Unpublished manuscript.* ***(Handout)***

"Methods of Reactivity Umpolung."
D. Seebach *Angew. Chem. Int. Ed. Engl.* **1979**, *18*, 239. ***(Handout)***

"Nitroaliphatic Compounds–Ideal Intermediates in Organic Synthesis'"
Seebach, D. et. al, *Chimia*, **1979**, *33*, 1-18. ***(Handout)***

D. A. Evans

Monday
December 4, 2006

Papers of Historical Interest:

"Arthur Lapworth: The Genesis of Reaction Mechanism."
M. Saltzman *J. Chem. Ed.* **1972**, *49*, 750. ***(Handout)***

"A Theoretical Derivation of the Principle of Induced Alternate Polarities."
A. Lapworth *J. Chem. Soc.* **1922**, *121*, 416.

"The Electron Theory of Valence as Applied to Organic Compounds."
J. Steiglitz *J. Am. Chem. Soc.* **1922**, *44*, 1293.

Monographs:

Hase, T. A. "Umpoled Synthons. A Survey of Sources and Uses in Synthesis".; John Wiley & Sons, Inc.: New York, 1987.

Ho, T.-L. "Polarity Control for Synthesis"; John Wiley & Sons, Inc.: NY, 1991.

Ono, N., "The Nitro Group in Organic Synthesis", Wiley-VCH, 2001

Several Interesting Problems

Provide a mechanism for the Nef reaction

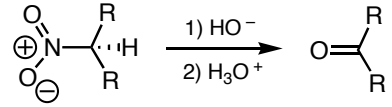

The **von Richter** reaction is illustrated in the accompanying equation. Please provide a plausible mechanism for this transformation taking into account the following observations. (a) If ^{15}N-labeled KCN is used, the N_2 formed is half labeled; (b) 3-bromo-benzonitrile does not form 3-bromo-benzoic acid under the reaction conditions.

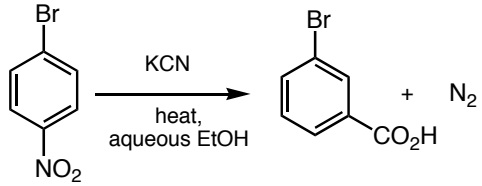

Stoltz and co-workers recently reported the interesting rearrangement illustrated below (*JACS* **2003**, *125*, 13624). Please provide a mechanism for the illustrated transformation. Your answer should include clear 3-D drawings where relevant. the answer may be found in the database.

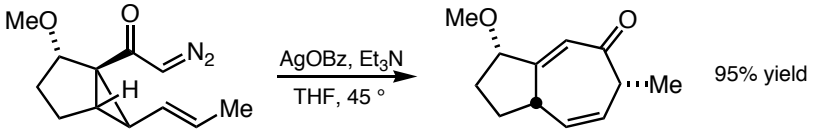

Required Reading:

"An Organizational Scheme for the Classification of Functional Groups. Applications to the Construction of Difunctional Relationships."
D. A. Evans *Unpublished manuscript.*

"Methods of Reactivity Umpolung."
D. Seebach *Angew. Chem. Int. Ed. Engl.* **1979**, *18*, 239.

"Nitroaliphatic Compounds–Ideal Intermediates in Organic Synthesis'"
Seebach, D. et. al, *Chimia*, **1979**, *33*, 1-18.

Papers of Historical Interest:

"Arthur Lapworth: The Genesis of Reaction Mechanism."
M. Saltzman *J. Chem. Ed.* **1972**, *49*, 750.

"A Theoretical Derivation of the Principle of Induced Alternate Polarities."
A. Lapworth *J. Chem. Soc.* **1922**, *121*, 416.

"The Electron Theory of Valence as Applied to Organic Compounds."
J. Steiglitz *J. Am. Chem. Soc.* **1922**, *44*, 1293.

_____

"Displacement of Aliphatic Nitro Groups by Carbon & Heteroatom Nucleophiles." R. Tamura, A. Kamimura, N. Ono *Synthesis* **1991**, 423.

"Functionalized Nitroalkanes as Useful Reagents for Alkyl Anion Synthons." G. Rosini, R. Ballini *Synthesis* **1988**, 833.

"Conjugated Nitroalkenes: Versatile Intermediates in Organic Synthesis."
A. G. M. Barrett, G. G. Graboski *Chem. Rev.* **1986**, *86*, 751.

Monographs:

Hase, T. A. "Umpoled Synthons. A Survey of Sources and Uses in Synthesis".; John Wiley & Sons, Inc.: New York, 1987.

Ho, T.-L. "Polarity Control for Synthesis"; John Wiley & Sons, Inc.: New York, 1991.

Arthur Lapworth (1872–1941)

Lapworth was among the first to understand and conceptualize the effect of heteroatomic substituents on the reactivity of individual carbon centers, and how this effect is propagated through the carbon framework of organic molecules.

Lapworth's Theory of Alternating Polarities:

"Latent Polarities of Atoms and Mechanism of Reaction, with Special Reference to Carbonyl Compounds."
A. Lapworth *Mem. Manchester. Lit. Phil. Soc.* **1920**, *64 (3)*, 1.

"The addition of electrolytes to the carbonyl compound invariably proceeded as if the carbon were more positive than the oxygen atom, and invariably selected the negative ion; for example:"

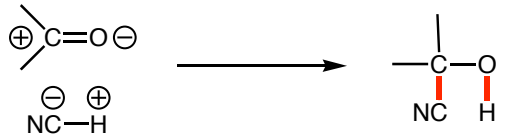

"The extension of the influence of the directing, or "key atom," over a long range seems to require for its fullest display the presence of double bonds, and usually in conjugated positions...."

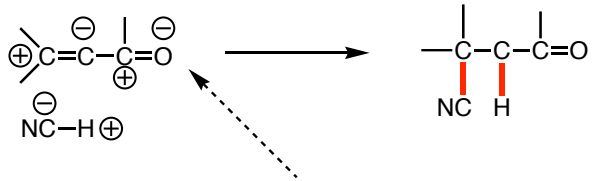

The "key atom" is the one with the most electronegative character, in this case the carbonyl oxygen.

anionoid/cationoid ⇢ nucleophilic/electrophilic

The Lapworth polarity designations can be used to form the basis of a functional group classification scheme.

Martin Saltzman
Providence College
Providence, Rhode Island 02918

Arthur Lapworth

The genesis of reaction mechanism

Lectureship at the University of Manchester. After his arrival in Manchester in 1909, it was a matter of only four years before Lapworth succeeded W. H. Perkin, Jr., as the Professor of Organic Chemistry. This position he held until 1922, when he relinquished it to allow for the promotion of his colleague, Robert Robinson. He then assumed the chair of Physical and Inorganic Chemistry, which carried with it the administrative responsibilities for the University Laboratory. Ill health terminated his active chemical career in 1935.

Lapworth proposed a master plan for classification of reagents in organic chemistry, classifying reagents according to charge. Reagents were anionoid or cationoid according to the definition: "If the formation of a covalent bond in the complex A-B takes place by the union of A− with B+ then A is anionoid and B is cationoid." These terms cationoid and anionoid have been supplanted by the Ingold terminology of electrophilic and nucleophilic, though they are synonymous.

An electronic handout will be provided

Thus in the carbonyl group with oxygen labeled negative and carbon positive in conjunction with the classification of reagents according to charge, the reactions of this functional group follows a logical course. If the concept of latent polarities is extended to all the atoms, an alternation of + and − labels may be assigned. The α-carbon atom in acetaldehyde should carry a latent negative charge.

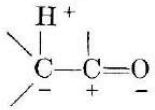

Removal of this α-hydrogen atom by base which adds to carbonyl of another molecule, produces an anion. The whole category of aldol type condensations can now be seen to have a common basis.

As early as 1902 Lapworth was cognizant of the influence that a carbonyl group could have on the reactivity at a carbon atom several times removed. Thus the γ-hydrogen atom in ethyl crotonate had similar properties to the α-hydrogen in the saturated carbonyl compound. Applying the theory of alternating latent polarities, it is evident that this γ-hydrogen should be acidic and easily removed by base

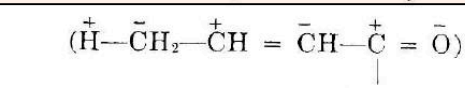

- Polar rxns form the basis set of bond constructions in synthesis
- Generalizations on conferred site reactivity will therefore be important

Given this target 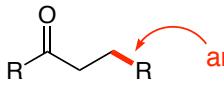 and the desire to form this bond

The functional group =O "dictates" the following bond construction

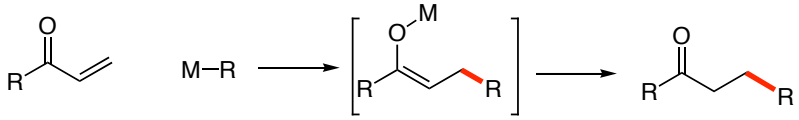

- Conferred site reactivity of =O 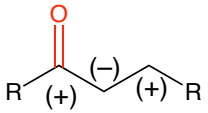

Charge Affinity Patterns

- Use the descriptors (+) and (–) to denote the polar disconnections shown.

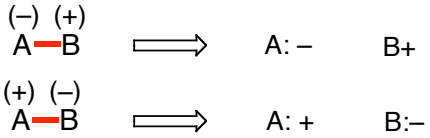

- In the transforms illustrated above, symbols (+) & (–) are used to denote the particular polar transform illustrated.
In the present case there is NO INTRINSIC BIAS in favoring one transform over the other.

Let's now add an OH functional group (FG) to propane at C-2 and see whether one creates a bias in the favoring of one or the other transforms:

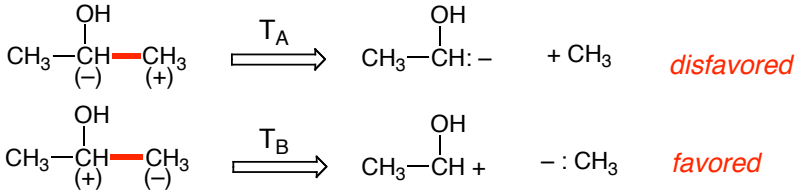

- The actual reaction associated with this transform is the addition of organometals to carbonyl substrates.

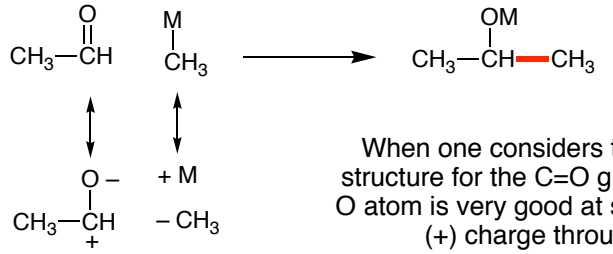

When one considers the polar resonance structure for the C=O group it is clear that an O atom is very good at stabilizing an adjacent (+) charge through resonance.

- Consider polar disconnections of the illustrated β-hydroxy ketone **1**:

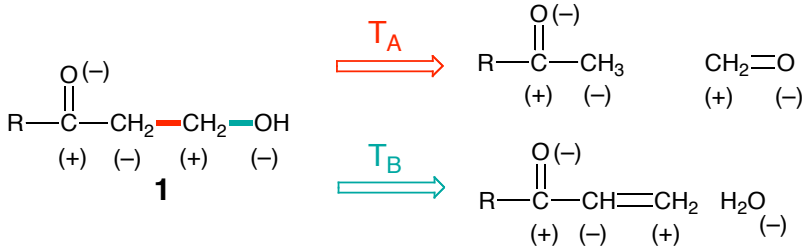

It is evident that the heteroatom functional groups, =O and -OH, strongly bias the indicated polar disconnections.

Charge Affinity Patterns of Common Functional Groups

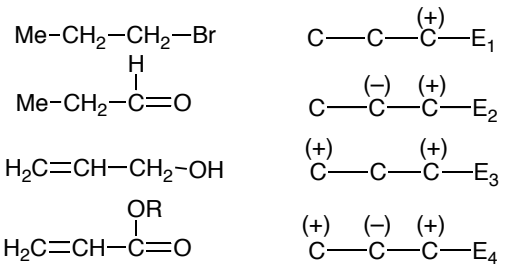

Functional groups activate the carbon skeleton at the point of attachment by either induction & resonance.

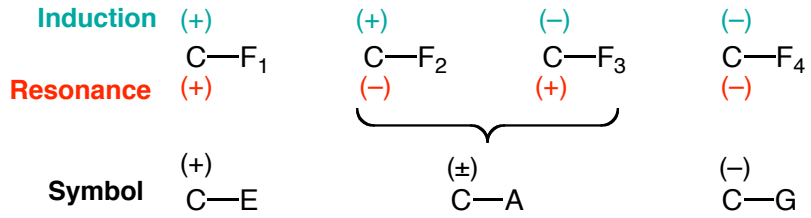

E = electrophilic at the point of attachment
A = ambiphilic at the pont of attachment
G = nucleophilic at the point of attachment

For simplicity, we will designate three FG classes according to the designations provided above.

E & G-Functions:

To organize activating functions into common categories it is worthwhile to define "hypothetical" functional groups E, and G, having the charge affinity patterns denoted below.

Hypothetical E-function

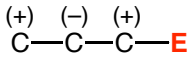

Hypothetical G-function

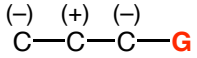

Given the appropriate oxidation state of the carbon skeleton, such functional groups confer the indicated polar site reactivity patterns toward both electrophiles and nucleophiles.

Any FG that conforms either to the ideal charge affinity parrern or a sub-pattern thereof will thus be classified as either an E- or G-function.

Representative E-functions:

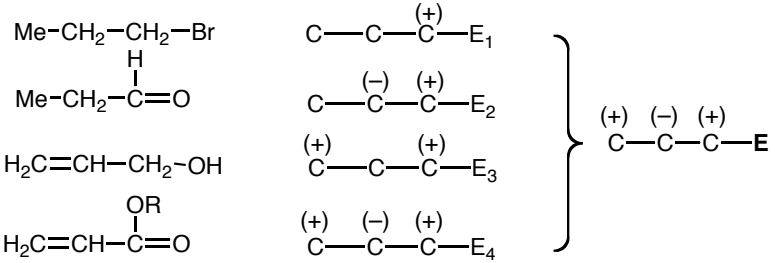

A-Functions:

A 3rd hypothetical FG, designated as A, may be defined that has an unbiased charge affinity pattern as in **1**. Such an idealized FG's activates all sites to both nucleophilic and electrophilic reactions, and as such include those functions classifies as either E– or G–. The importance of introducing this third class designation is that it includes those functional groups having non-alternate charge affinity patterns such as **2–4**.

Hypothetical A-function

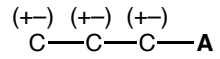

1

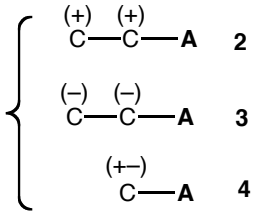

FG-Classification Rules

In the proposed classification scheme the following rules followed in the assignment of class designation of a given FG.

- Activating functions are to be considered as heteroatoms appended to or included within the carbon skeleton.
- Activating functions are inspected and classified according to their observed polar site reactivities.
- Since proton removal and addition processes are frequently an integral aspect of FG activation, the FG, its conjugate acid or base, and its proton tautomers are considered together in determining its class designation.
- The oxidation state of the FG is deemphasized since this is a subordinate strategic consideration.

Common E-Functions: Symbol: (+)C—E

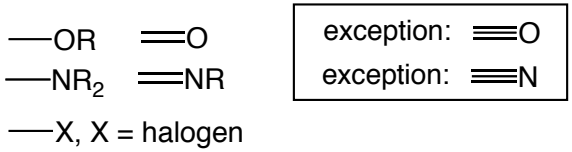

Also consider all combinations of of above FGs; e.g =O + OR

Common G-Functions: Symbol: (–)C—G

Typical G-class functions are the Group I-IV metals whose reactivity patterns, falls into a subset of the idealized G-FG **5**.

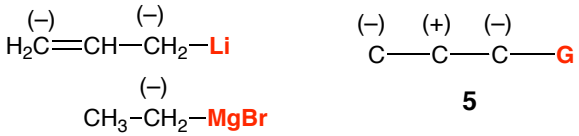

Common A-Functions: Symbol: (±)C—A

A-functions are usually more structurally complex FGs composed of polyatomic assemblages of nitrogen, oxygen and their heavier Group V and VI relatives (P, As, S, Se).

Typical A-functions, classified by inspection, are provided below

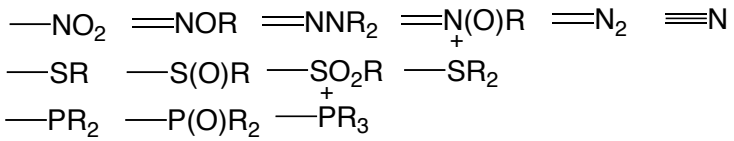

■ These FG's are capable of conferring both (+) and (–) at point of attachment.

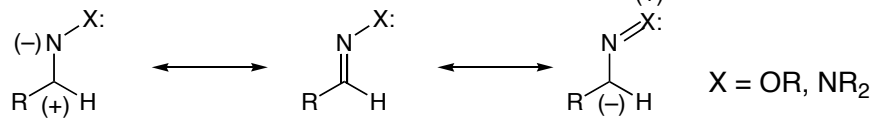

Remarkably, the dual electronic properties of oximes were first discussed by Lapworth in 1924 before the modern concepts of valence bond resonance were developed.

Lapworth, A. *Chemistry and Industry* **1924**, *43*, 1294-1295.

The Nitro Functional Group

As an example, the class designation of the nitro function is determined by an evaluation of the parent function, its nitronic acid tautomer, as well as conjugate acid and base.

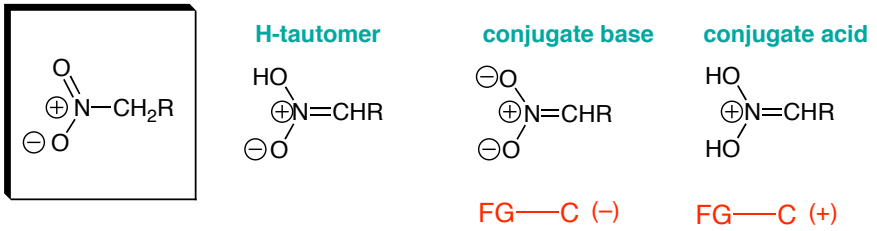

The Reaction:

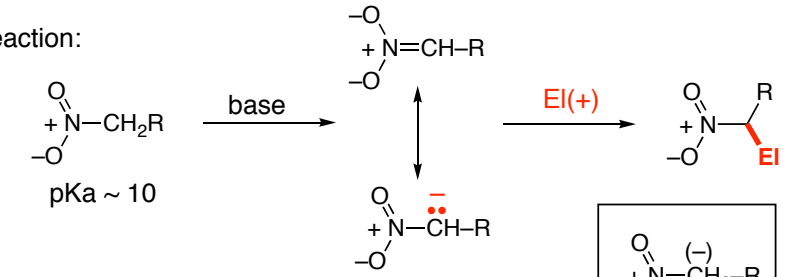

The charge affinity pattern:

■ **This reactivity pattern may be extended via conjugation:**

The Reaction:

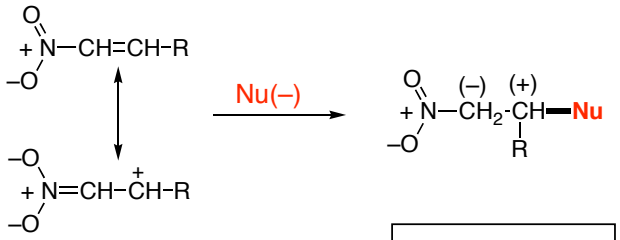

Charge affinity pattern:

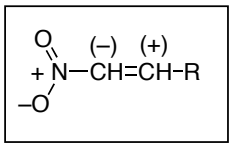

■ **The resonance feature which has been exploited:**

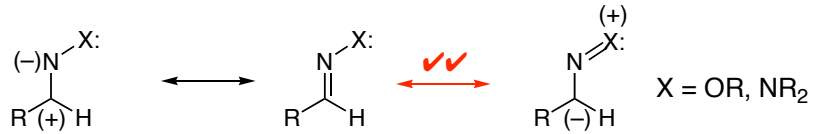

Some Reactions of the Nitro Functional Group

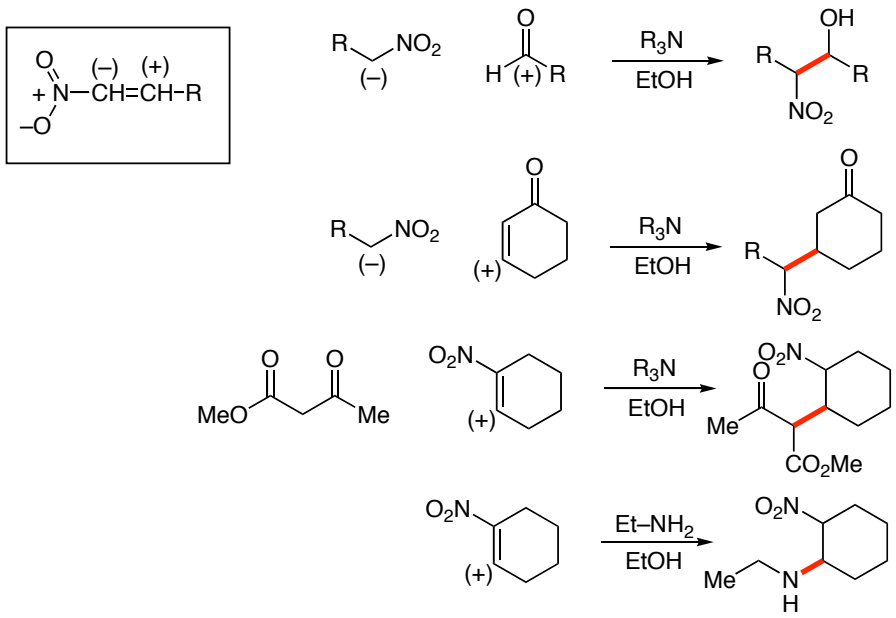

Important Transformations of the –NO_2 Functional Group

■ Reduction:

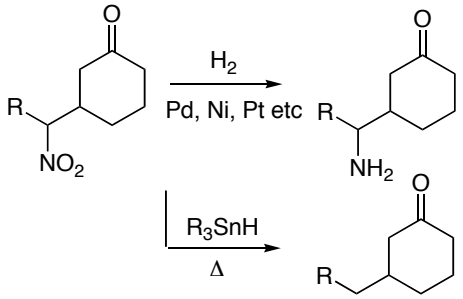

rxn is quite facile

Ono, N.; Kaji, A. *Synthesis* **1986**, 693.

■ Nef Reaction:

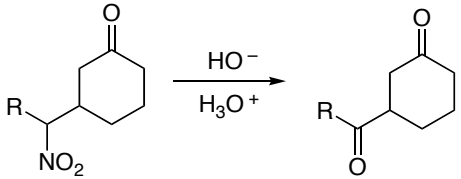

Pinnick, *Org. Reactions* **1990**, *38*, 655

The Nef Reaction

■ **Overall Transformation:**

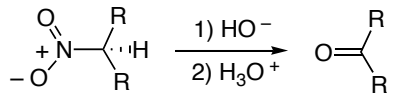

■ Mechanism

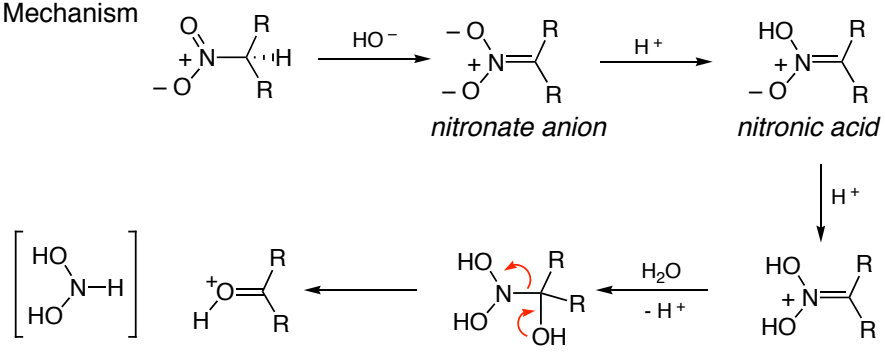

The charge affinity patterns represented

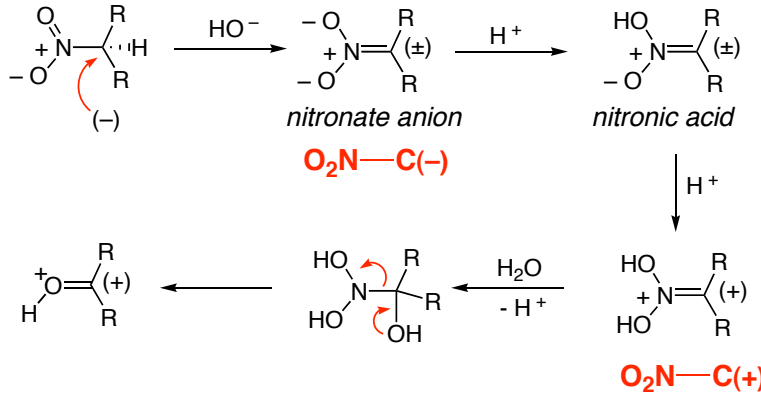

■ **The resonance features which have been exploited:**

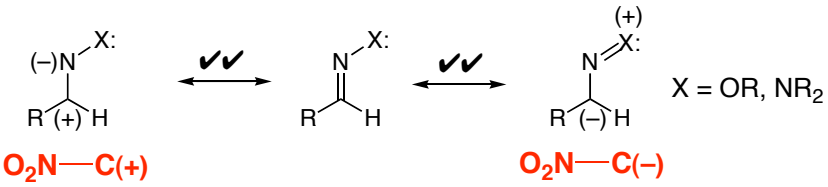

Other Nonalternate Behavior of –NO_2 FG

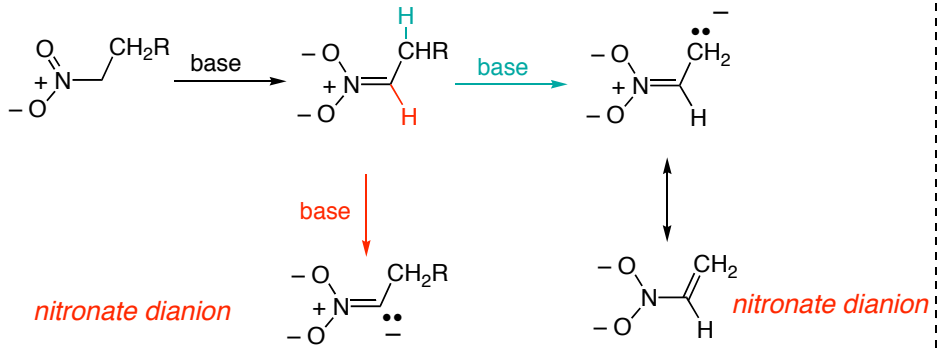

$O_2N-\overset{2(-)}{C}-C$ $\qquad$ $O_2N-\overset{(-)\ (-)}{C}-C$

Reactivity Patterns

Seebach et. al. *Tetrahedron Lett.* **1977**, 1161-1164

Representative examples: $O_2N-\overset{2(-)}{C}-C$

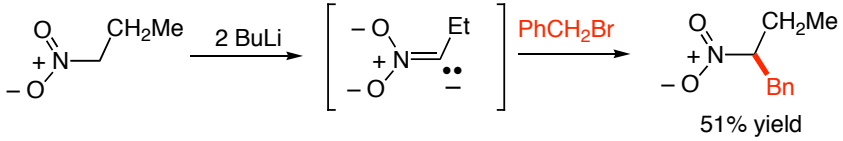

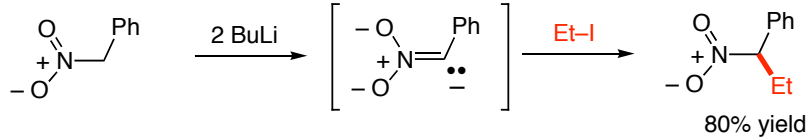

Representative examples: $O_2N-\overset{(-)\ (-)}{C}-C$

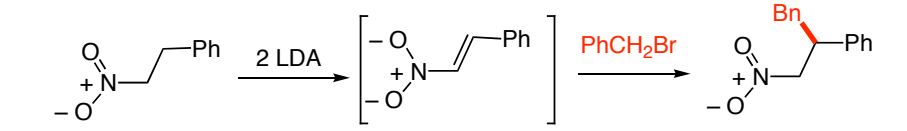

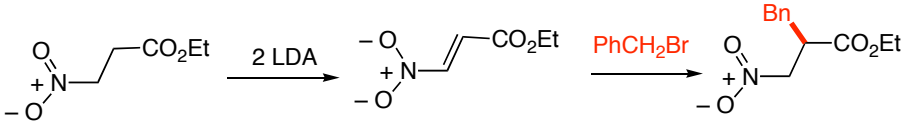

Seebach et. al. *Tetrahedron Lett.* **1977**, 1161-1164

–NO_2 As a Leaving Group

Review: Tamura et. al. *Synthesis* **1991**, 423-434.

"Nitroaliphatic Compounds–Ideal Intermediates in Organic Synthesis"' Seebach, D. etal, *Chimia*, **1979**, *33*, 1-18

Representative examples: $O_2N-C(+)$

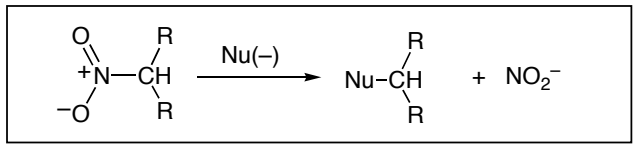

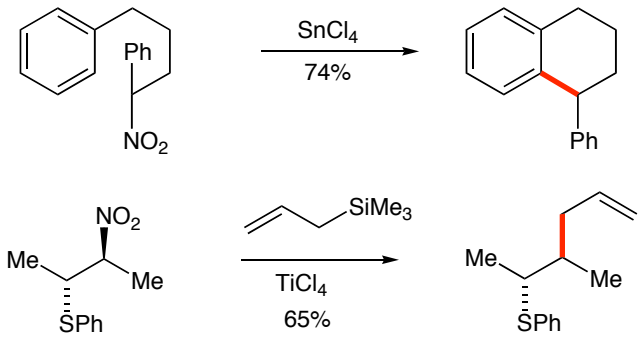

$-NO_2$ As a Leaving Group

Representative examples: $O_2N—C$ (+)

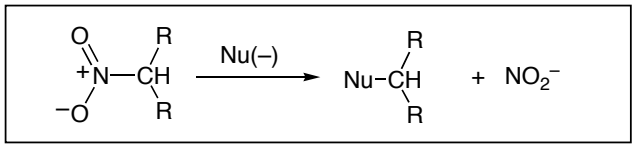

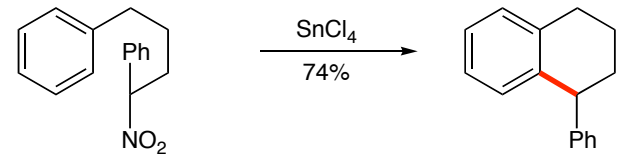

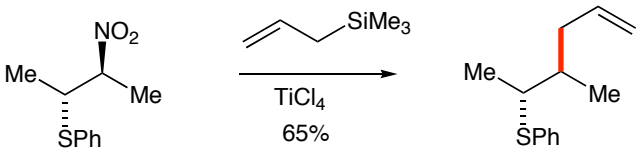

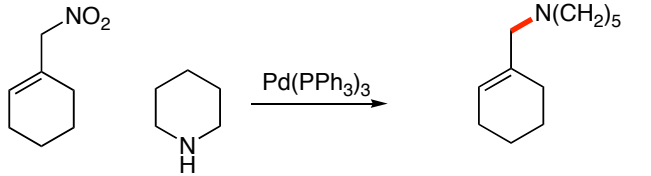

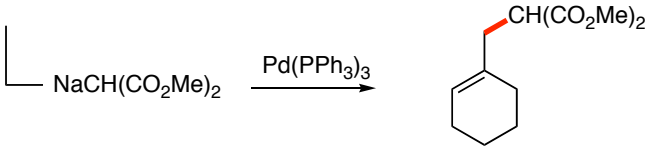

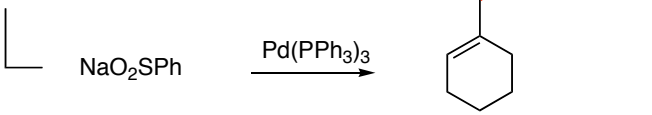

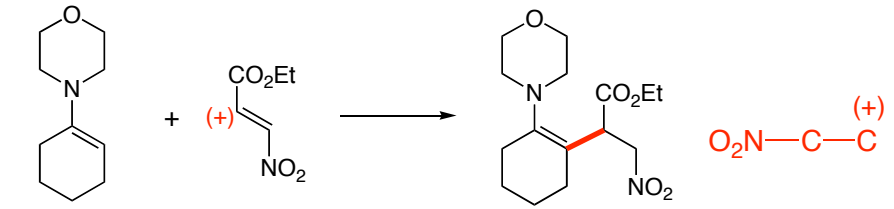

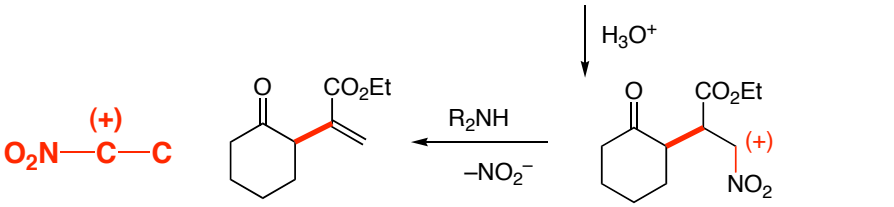

McMurry etal. *Chem Comm.* **1971** 488-489.

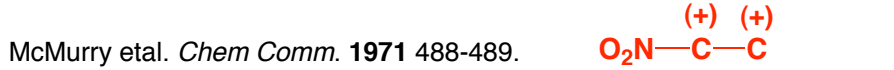

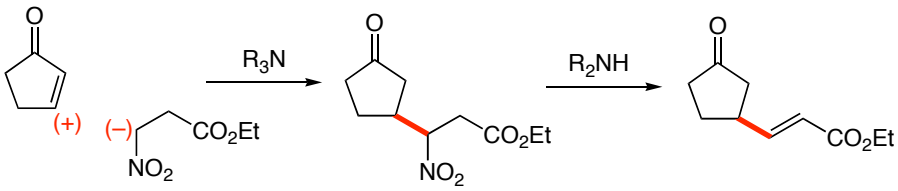

Bakuzis etal. *Tetrahedron Lett.* **1978** 2371.

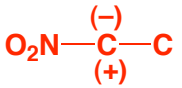

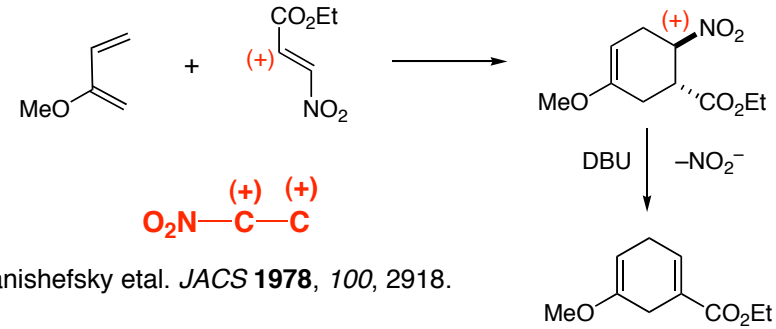

Danishefsky etal. *JACS* **1978**, *100*, 2918.

The Diazo Functional Group

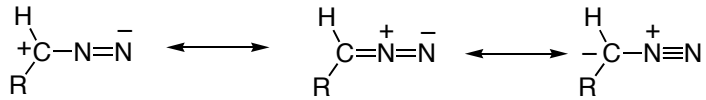

- Both (+) and (–) reactivity patterns suggested by resonance structures

- Rxns with acids:

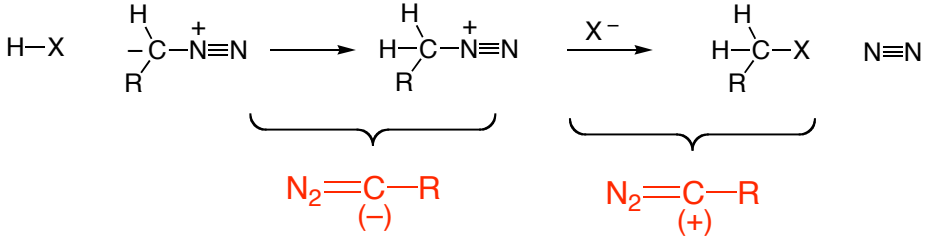

- **Initiating reactivity is (–); subsequent reactivity is (+)**

- **Ring expansion reactions:**

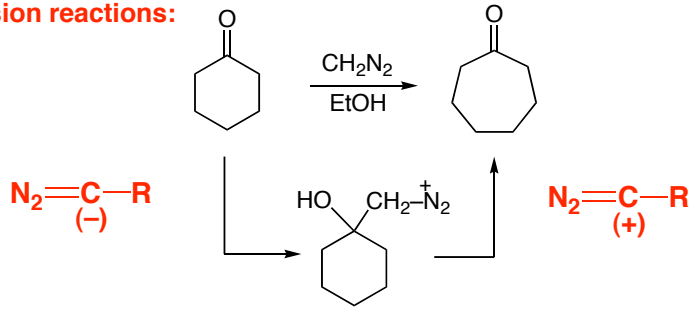

Restriction: Starting ketone must be more reactive than product ketone

- **Precursors to Carbenes:**

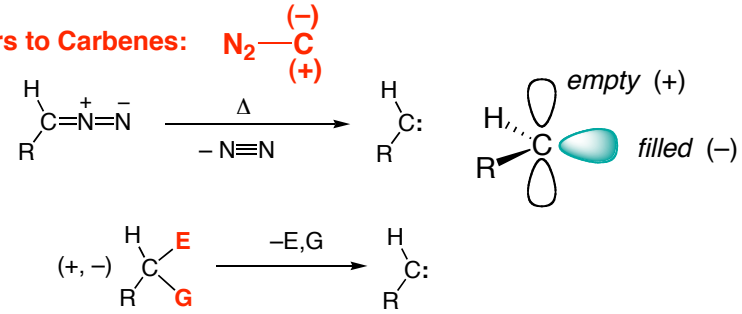

Acid Catalyzed Reactions of Diazo Compounds

Review: Smith, Tet. 1981 2407

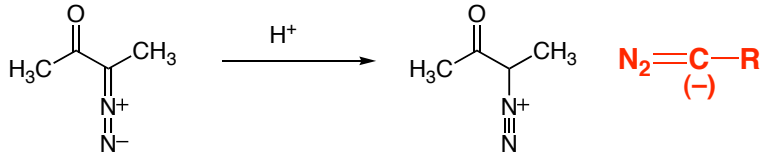

Diazocarbonyl *Diazonium*

Common acids include BF_3•OEt_2, HBF_4, TFA, etc.

Mechanism of activation is unclear for both Lewis and protic acids; activation may occur by protonation on C or O

Acid-Catalyzed Reactions

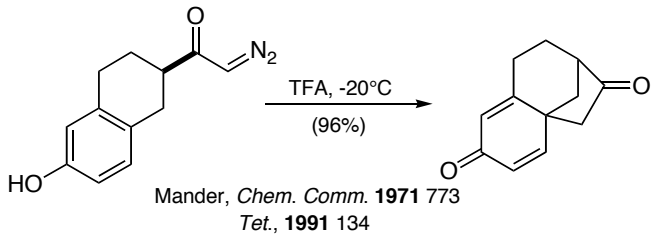

Mander, *Chem. Comm.* **1971** 773
Tet., **1991** 134

"Having become familiar with the peculiarities of diazoketone chemistry while preparing [other compounds] (and, I might add, inured to handling uncomfortably large quantites of diazomethane), it occurred to us that we might be able to substitute a diazo group for bromine."

Lewis Mander

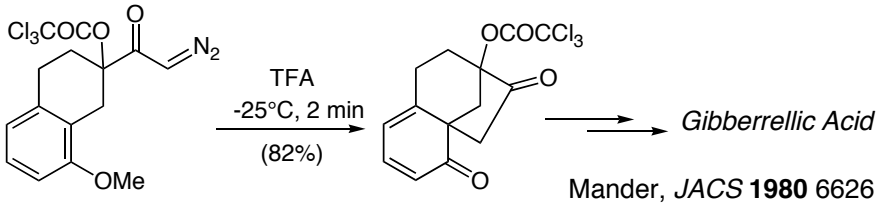

Mander, *JACS* **1980** 6626

Diazo–Carbonyl Insertations:

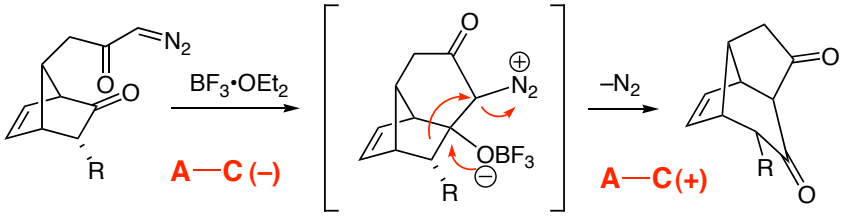

Mander, *Aust. J. Chem.* **1979** 1975

Wolff Rearrangements

Web Problem 332. Stoltz and co-workers recently reported the interesting rearrangement illustrated below (*JACS* **2003**, *125*, 13624).

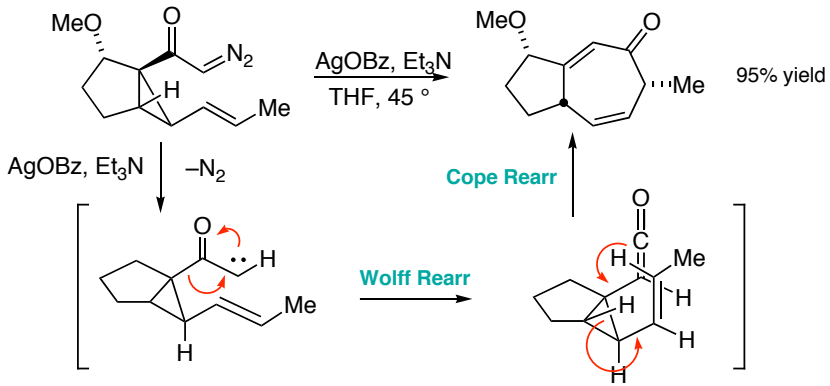

Diazo-mediated Ring Construction:

Evans, Mitch, *JACS* **1980**, *102*, 5956

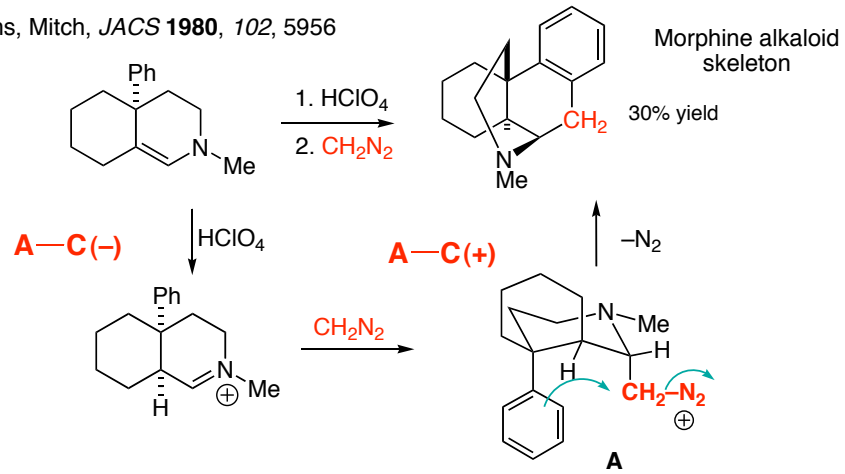

Web Problem 150. Provide a concise mechanism for the indicated reaction in the space below. Key descriptor for answer, "Carbene".

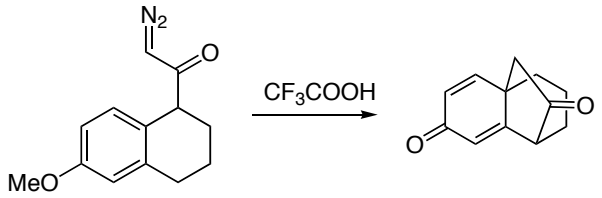

The Answer

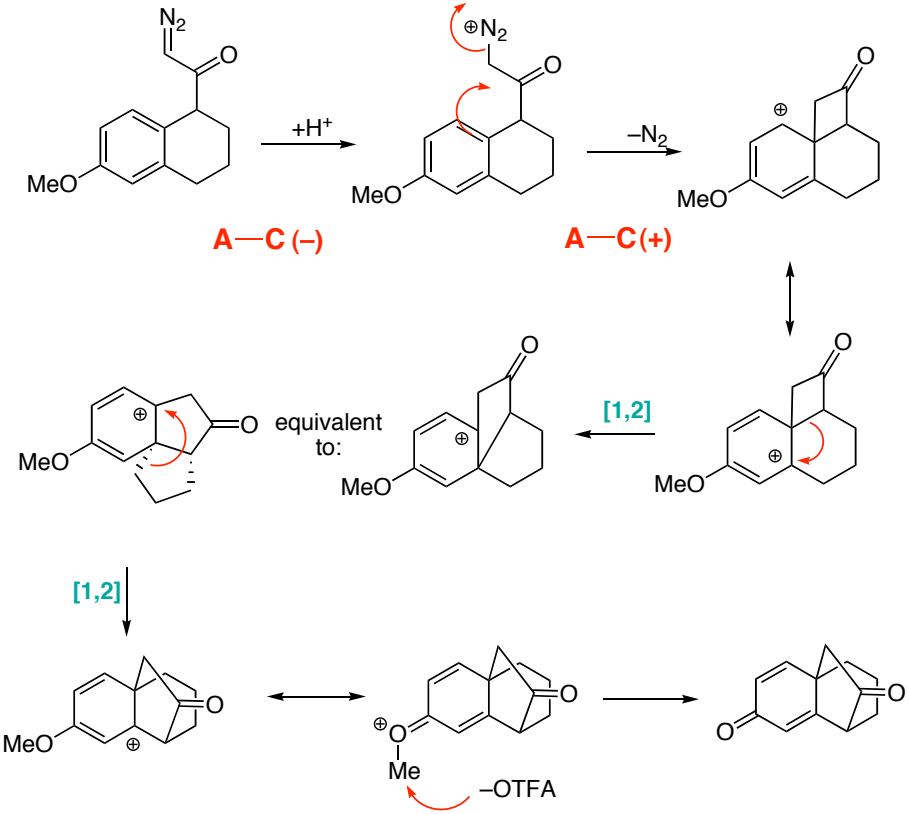

Dipolar Cycloadditions: Carbonyl Ylides

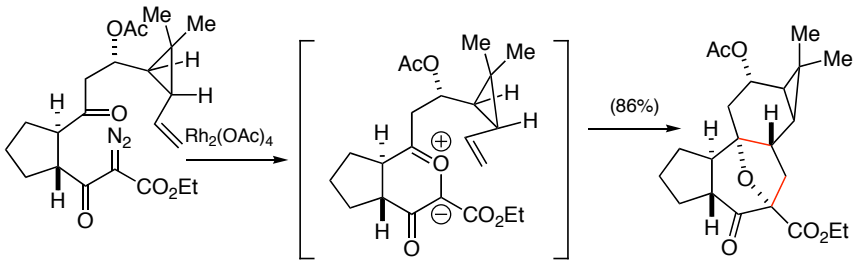

Dauben, *JOC* **1993** 7635 *Tigilane Skeleton*

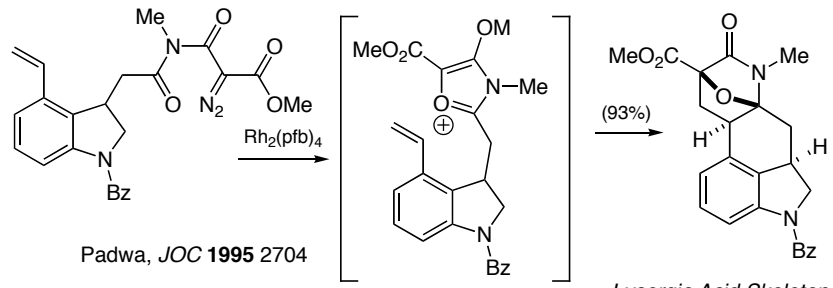

Padwa, *JOC* **1995** 2704 *Lysergic Acid Skeleton*

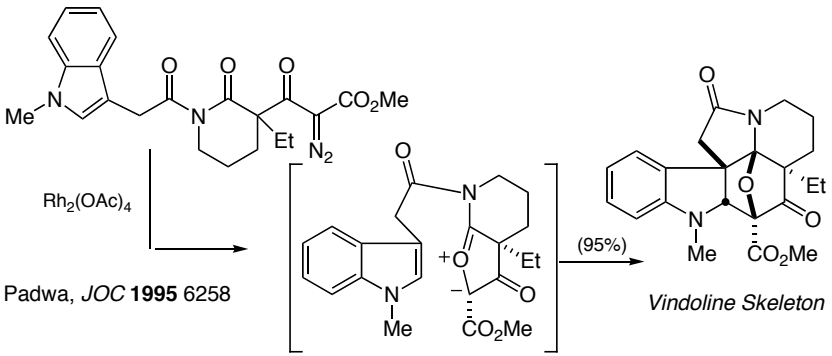

Padwa, *JOC* **1995** 6258 *Vindoline Skeleton*

Web Problem 109. The following is a general reaction for the formation of pyrroles. In this condensation, any of the three reaction constituents may be widely varied. (Ono, "The Nitro Group in Organic Synthesis" Wiley-VCH, **2001**. Chapter 10, pp 326-328). Siince it is not clear what the "inorganic" reaction product is, provide us with anything that is mechanistically sound using the reagents illustrated. Key descriptor for answer, "Nitro".

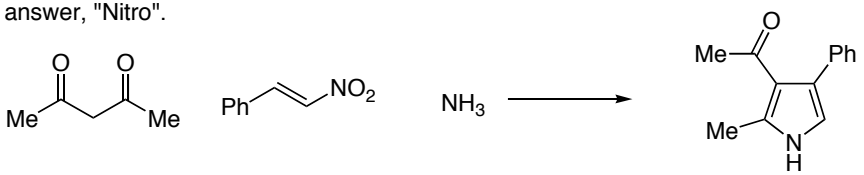

In the space below provide a plausible mechanism for this transformation.

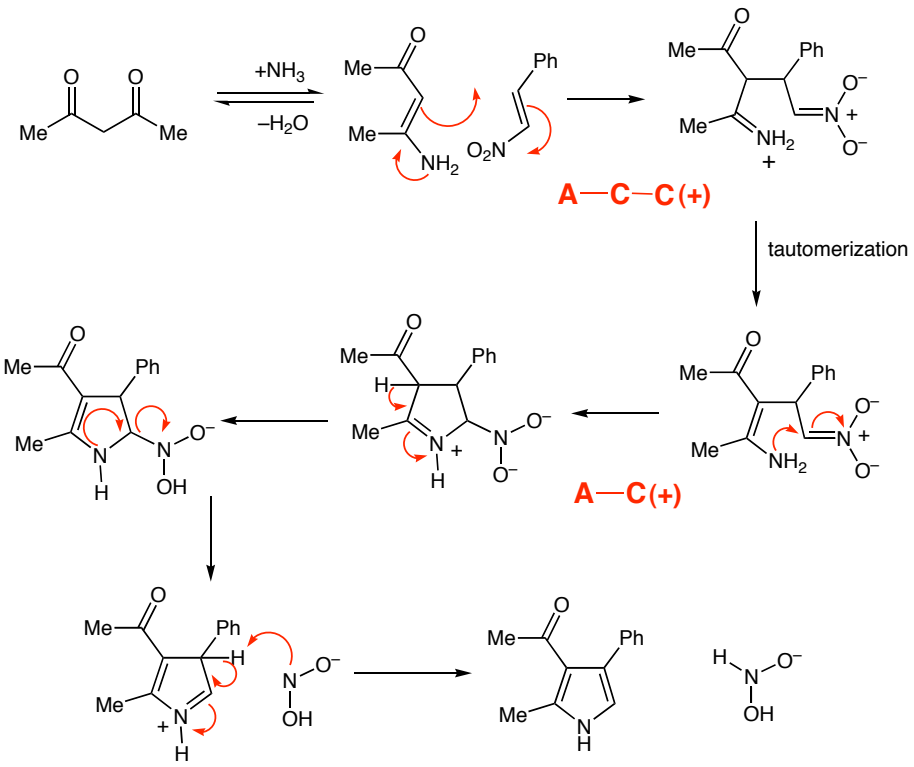

Overall reactivity pattern: **A—C—C** (+) (+)

http://www.courses.fas.harvard.edu/colgsas/1063

Chemistry 206

Advanced Organic Chemistry

Lecture Number 31

Ambiphilic Functional Groups–2
Hydrazone-Based Transformations

- Wolff-Kishner Reduction
- Wharton Rearrangement
- Eschenmoser-Tanabe Fragmentation
- Reduction of Tosyl Hydrazones: "The Alkene Walk"
- Tosyl Hydrazone-Based Fragment Coupling
- TBS-Hydrazones: Superior intermediates
- The Shapiro Reaction
- Bamford-Stevens Reaction

Reading Assignment for this Week:

"The Myers papers" **(handouts)**

Nitroso-Alkenes
T. L. Gilchrist, *Chem. Soc. Rev.* **1983**, *12*, 53-72 **(handout)**

The Synthetic Utility and Mechanism of the Rednctive Deoxygenation of α,β-Unsaturated p-Tosylhydrazones with Sodium Cyanoborohydride
R. O. Hutchins et al. *J. Org. Chem* **1975,** *40*, 923

David A. Evans

Wednesday
December 6, 2006

Relevant Background Reading

Hutchins, R. O. (**1991**). "Reduction of C=X to CH_2 by Wolff-Kishner and Other Hydrazone Methods". *Comprehensive Organic Synthesis*. Trost and Fleming. Oxford, Pergamon Press. 8: 327.

Shapiro, R. H. (**1976**). "Alkenes from Tosylhydrazones." *Org. React.* (N.Y.) 23: 405.

Addlington, R. M. and A. G. M. Barrett (**1983**). "Recent Applications of the Shapiro Reaction." *Acc. Chem. Res*. 16: 55.

Chamberlin, and Bloom (**1990**). "Lithioalkenes from arylsulphonyl-hydrazones." Org. React. (N.Y.) 39: 1.

Bergbreiter, and Momongan (**1991**). "Hydrazone Anions". *Comprehensive Organic Synthesis*. Trost and Fleming. Oxford, Pergamon Press. 2: 503.

Cume Question, November, 2000 and current Problem Set

Sorensen and coworkers recently reported the synthesis of (–)-hispidospermidin (Sorensen *JACS*. **2000**, *122*, 9556). The **Shapiro Reaction**, along with methodology developed by Whitesell, was use in the construction of intermediate **3** from the indicated building blocks **1** and **2** (eq 1).

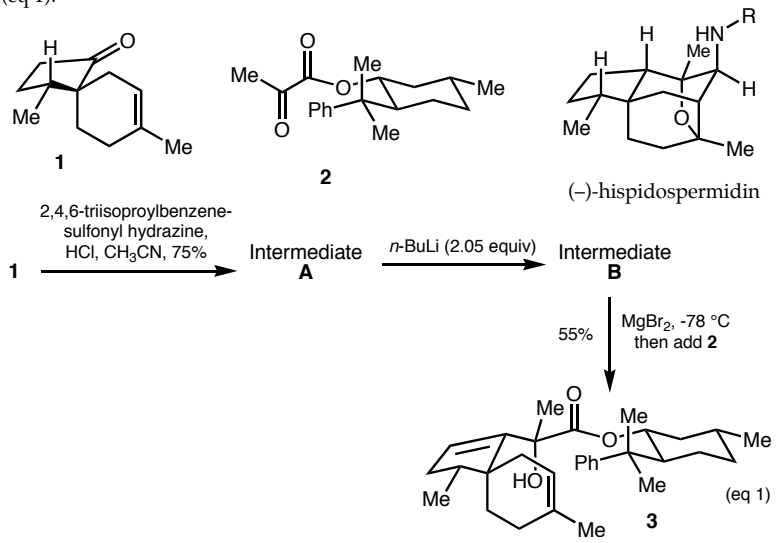

Hydrazone Anions: A useful Reversed Polarity Equivalent

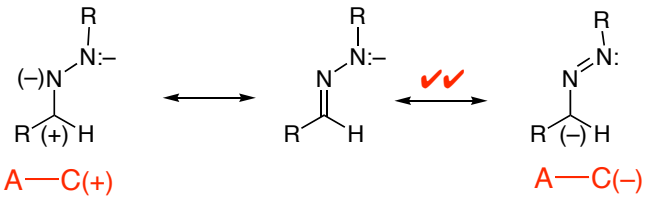

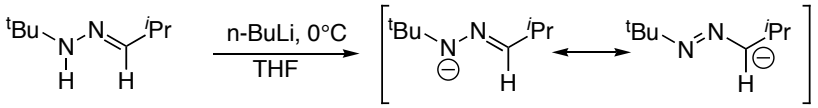

J. E. Baldwin, et al. *JCS Chem. Comm.* **1983**, 1040.

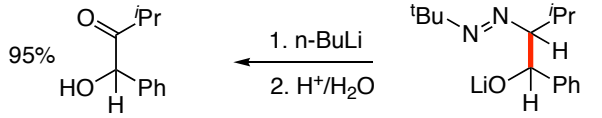

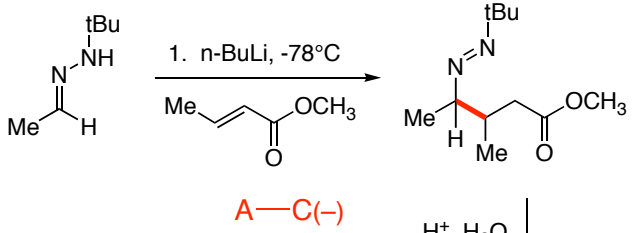

J. E. Baldwin, et al. *JCS Chem. Comm.* **1984**, 1095.

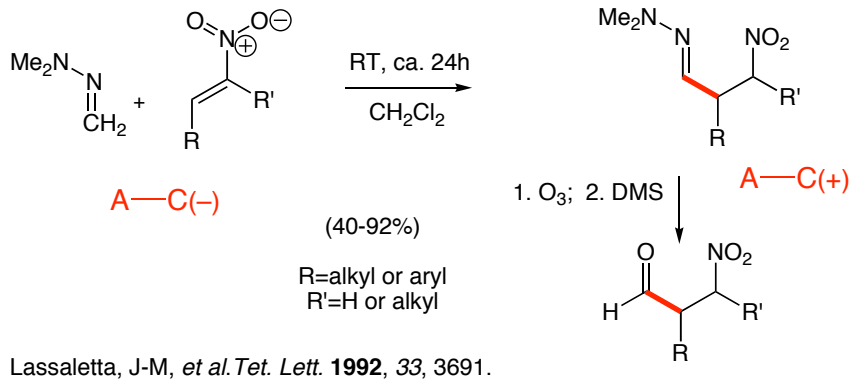

Lassaletta, J-M, *et al.Tet. Lett.* **1992**, *33*, 3691.

Chiral Hydrazones as Carbonyl Anion Equivalents

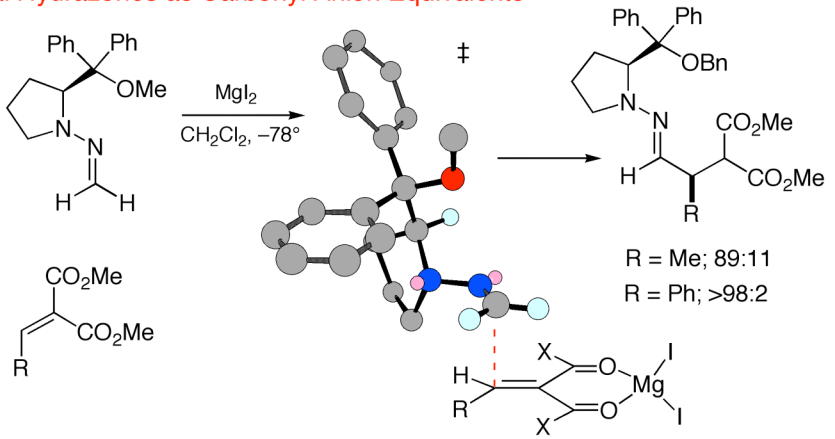

Lassaletta, J-M, *et al. Chem Commun* **2002**, 498-499

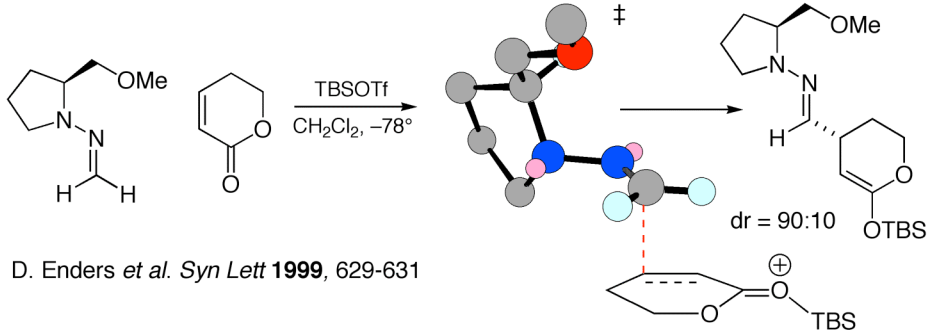

D. Enders *et al. Syn Lett* **1999**, 629-631

Wolff-Kishner Reduction

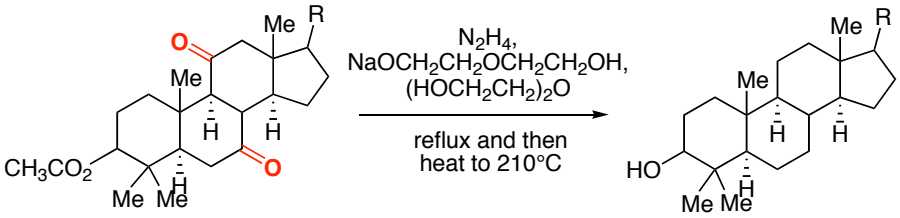

Barton, D. H. R., Ives, D. A. J., and Thomas, B. R. *J. Chem. Soc.* **1955**, 2056.

Mechanism

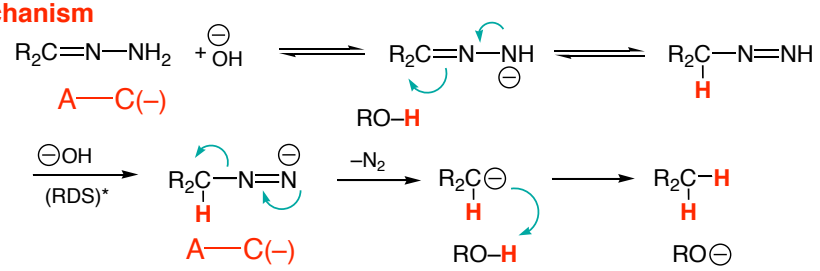

Elimination of α-Leaving Groups

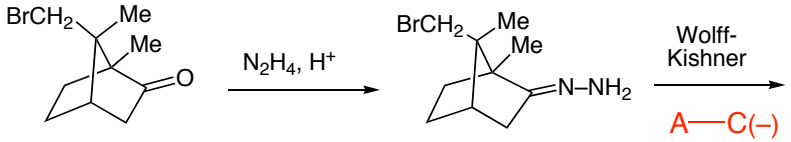

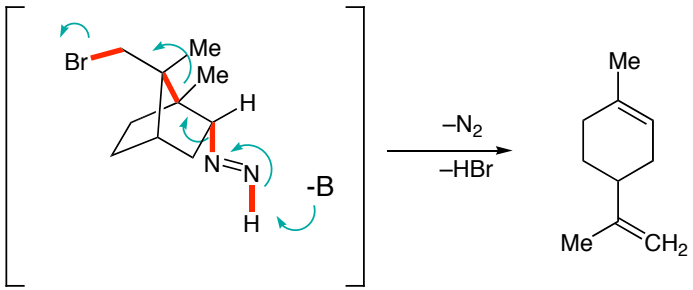

D. H. Gusyafson, W. F. Erman *J. Org. Chem.* **1965**, *30*, 1665.

The Wharton Rearrangement

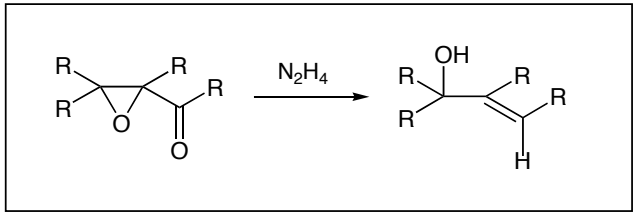

This example illustrates the 2 possible modes for the decomposition of **A**.

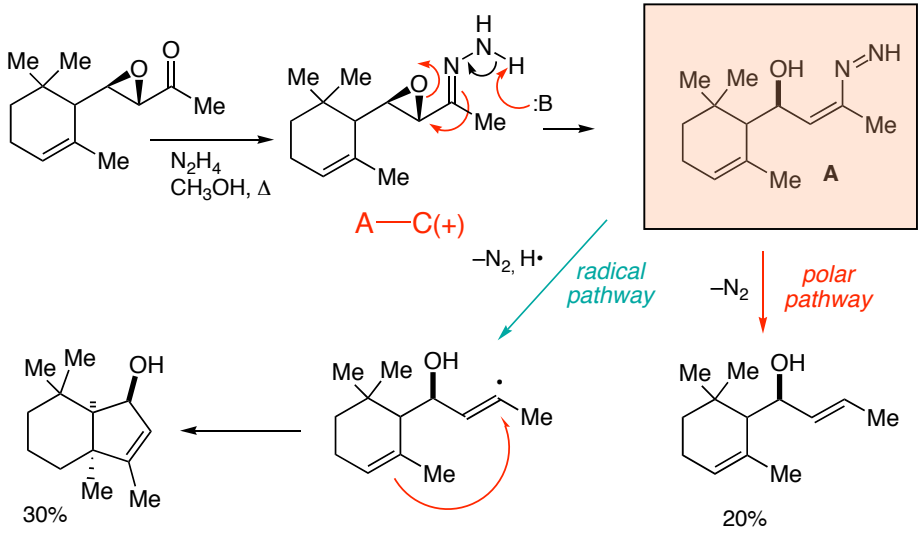

G. Stork et al. *JACS* **1977**, *99,* 7067.

Some procedural improvements:

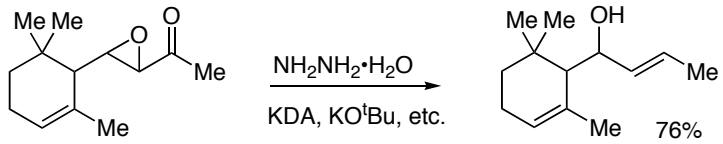

For stable hydrazones, strongly basic conditions favor the ionic pathway.

C. Dupuy, J. L. Luche *Tetrahedron Lett.* **1989**, *44,* 3437.

Tosylhydrazones – Better Than Hydrazones

Tosylhydrazones are isolable, stable, and easily prepared.

The presence of the tosyl leaving group strongly biases the system towards polar reaction pathways under hydridic reducing conditions.

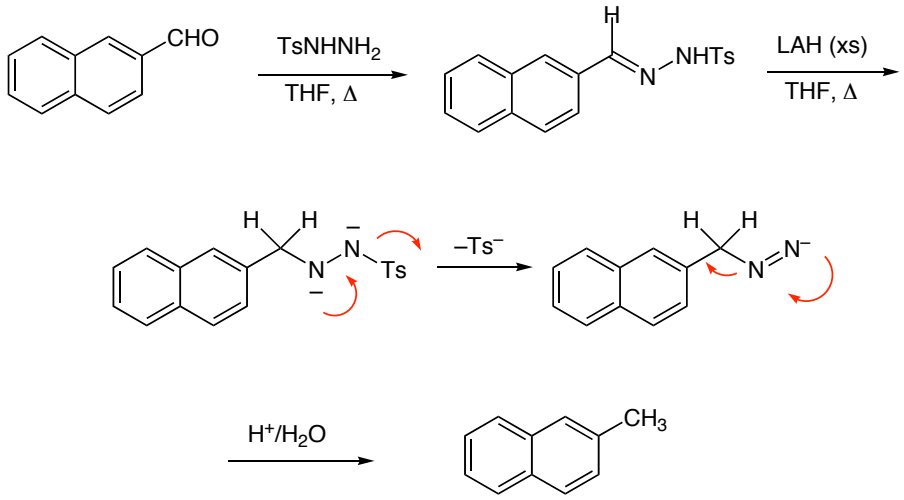

L. Caglioti, M. Magi *Tetrahedron* **1963**, *19*, 1127.

Further Refinements

Very mild reduction with $NaBH_3CN$ under slightly acidic conditions (pH 4-5).
No reduction in the absence of acid; carbonyl, nitro, nitrile FGs unaffected.
Aromatic, sterically hindered carbonyls very poor substrates.

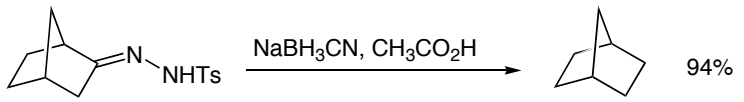

R. O. Hutchins, et al. *JACS* **1973**, *95,* 3662.

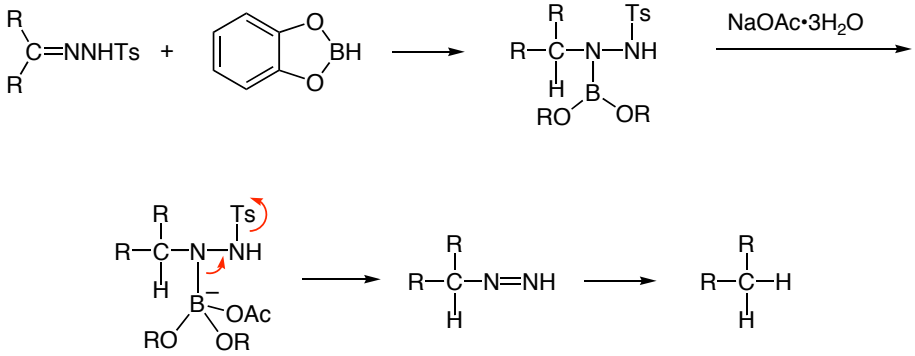

G. W. Kabalka, et al. *J. Org. Chem.* **1975**, *40,* 1834.

Another Interesting Leaving Group

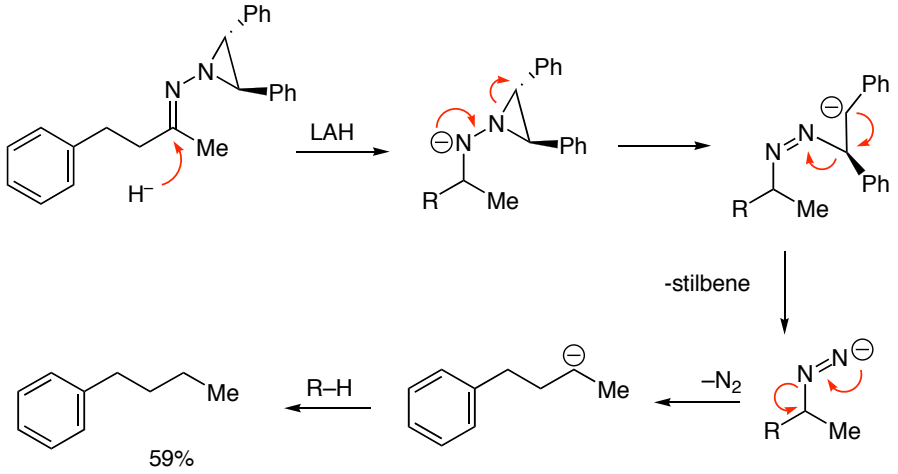

A. R. Chamberlin, et al. *Tetrahedron Lett.* **1991**, *32,* 1691.

The Eschenmoser–Tanabe Fragmentation

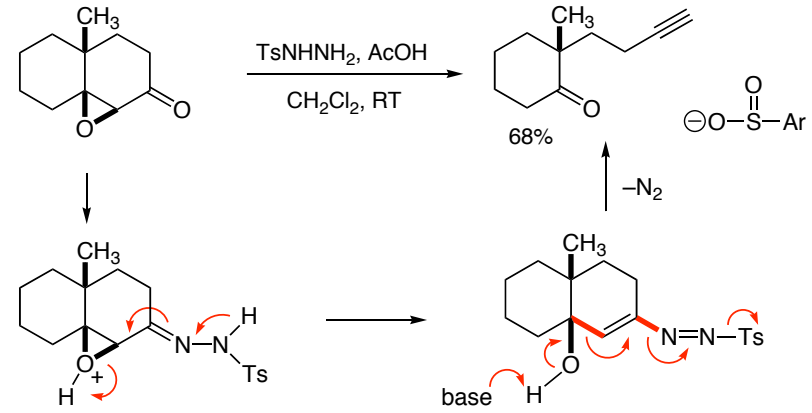

A. Eschenmoser, et al. *Helv. Chem. Acta* **1967**, *50,* 708.

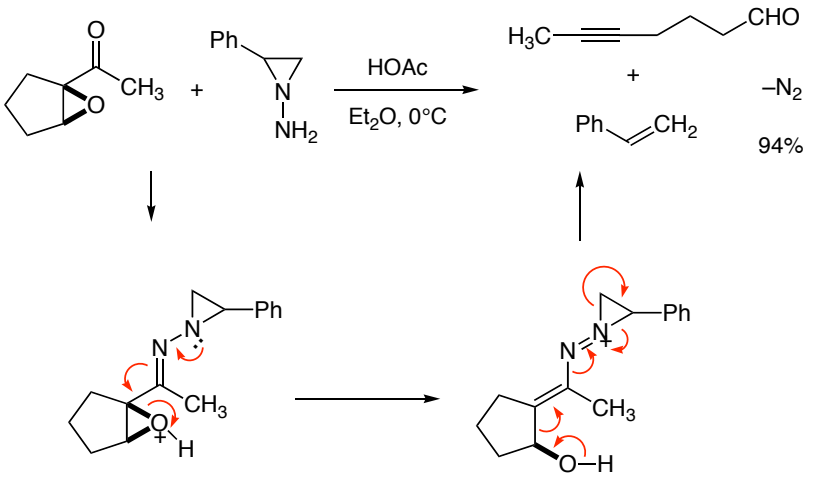

A. Eschenmoser, et al. *Helv. Chem. Acta* **1967**, *50,* 2108.

Tosylhydrazone Reductions: The Alkene Walk

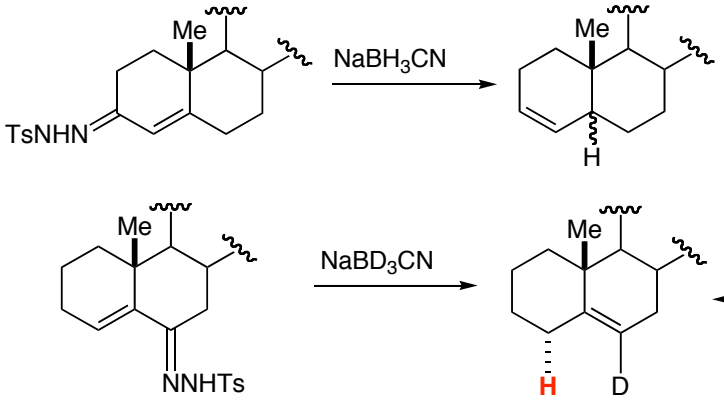

C. Djerassi, et al. *JACS* **1976**, *98,* 2275.

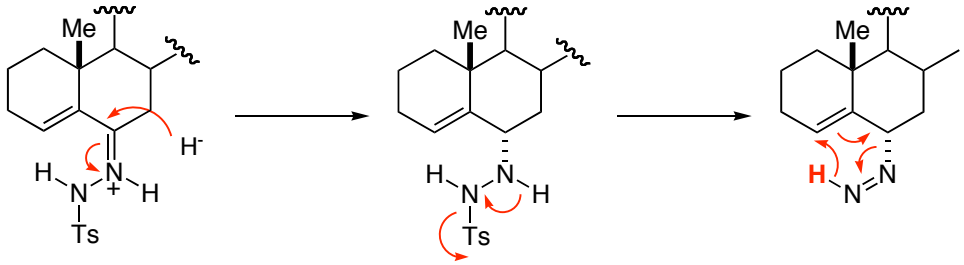

This has been developed into a reliable reduction

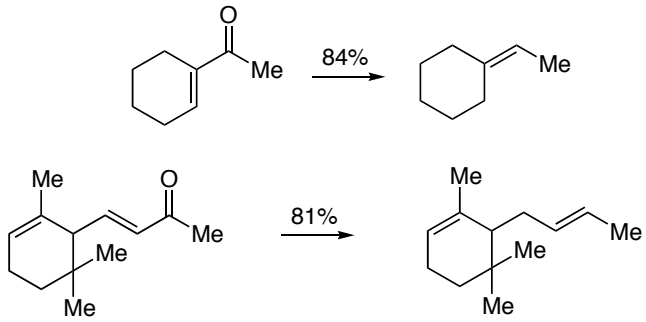

16 cases reported: Hutchins, et al. *JOC* **1975**, *40,* 923

Alkene Walk: Syntheses

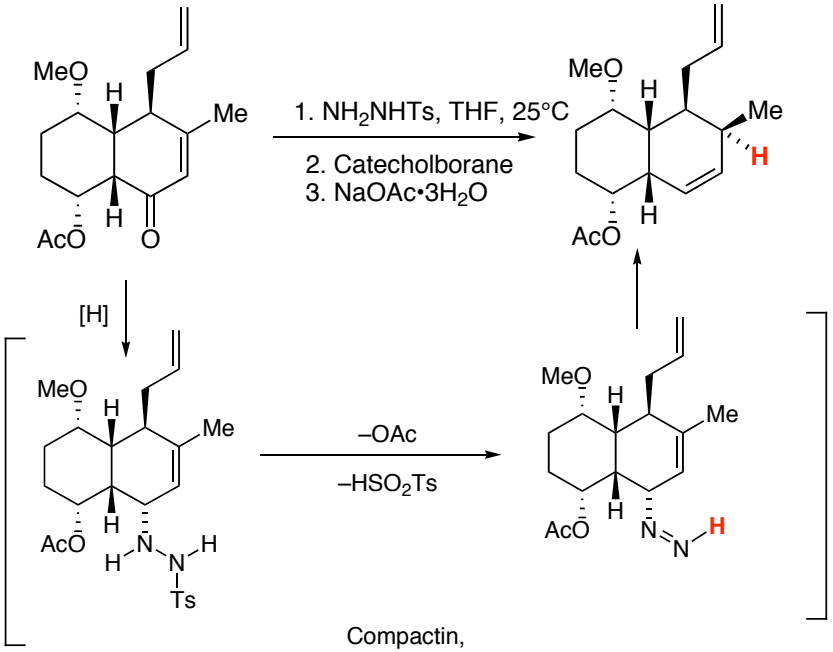

Compactin,
Wendler, N. L., *et al. Tet. Lett.* **1982**, *23,* 5501.

The stereochemical course of the hydrazone reduction may be stereospecifically transferred via the 1, 3-rearrangement

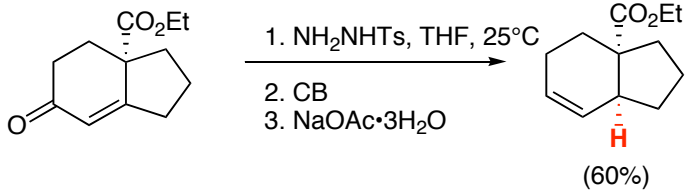

(60%)

Topiramate,
Maryanoff, B. E., *et al. Tet. Lett.* **1992**, *33,* 5009.

Sulfonylhydrazone Reductions: Alcohol Deoxygenation

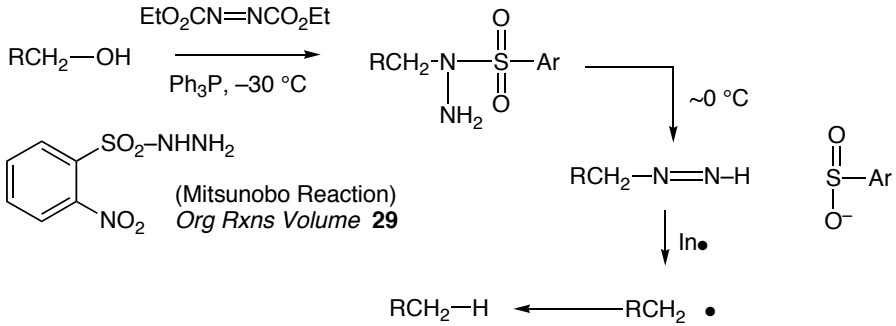

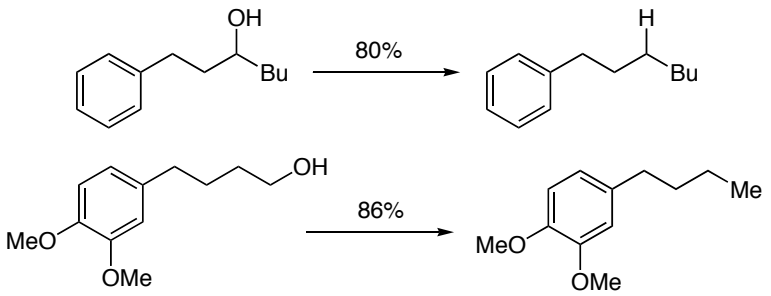

The intervention of radicals has been implicated (again):

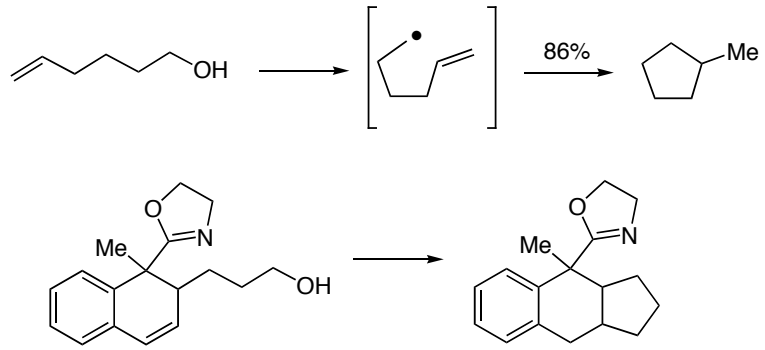

10 cases reported: A. Myers, et al. *JACS* **1997**, *119,* 8572.

Design, Synthesis, and Reactivity of 1-Hydrazinodienes for Use in Organic Synthesis

Glenn M. Sammis, Eric M. Flamme, Hao Xie, Douglas M. Ho, and Erik J. Sorensen*

Department of Chemistry, Princeton University, Princeton, New Jersey 08544-1009

8612 ■ J. AM. CHEM. SOC. 2005, *127*, 8612−8613

Scheme 1. A New Type of Hydrazine-Substituted Diene for Use in Organic Synthesis

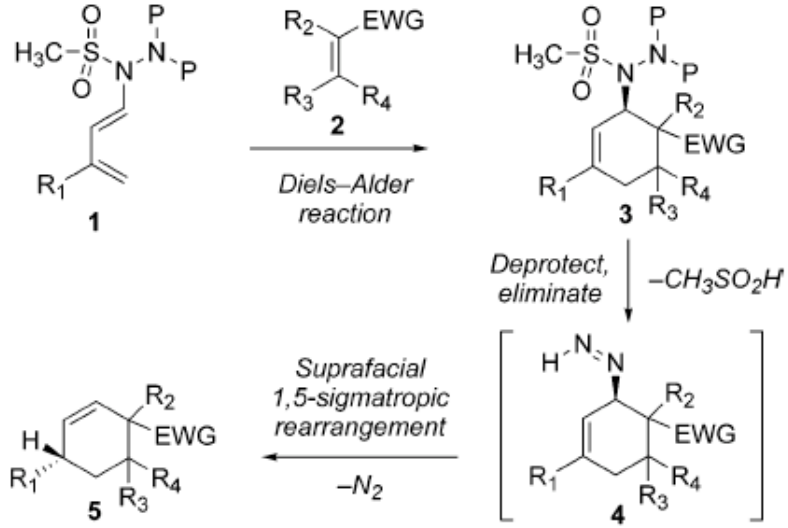

Scheme 2. Synthesis of 1-Hydrazinodiene **7**

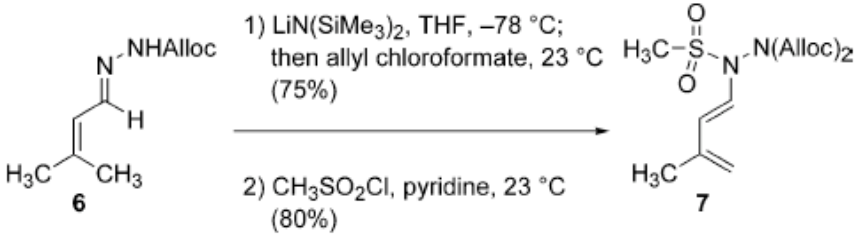

Table 1. Dienophile Scope for the Diels−Alder/1,5-Sigmatropic Rearrangement Process

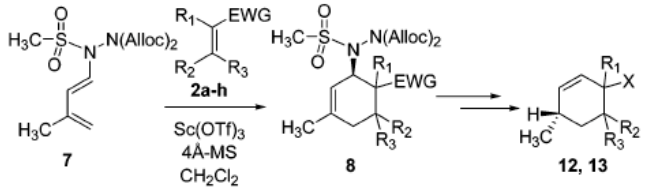

12a-f: X = CH(-OCH$_2$CH$_2$O-); **13a-b**: X = CO_2Et

Dienophile	Sc(OTf)$_3$ (mol%)[a]	dr (*endo*/*exo*)[b]	Yield **8** (%)[c]	Yield **12(13)** (%)
2a	10	83:17 (92:8)[d]	89[e] (81)[d,e]	62[f]
2b	10	25:75	65	60[f]
2c	10	30:70	45	55[f]
2d	10	7:93	72	68[e]
2e	10	33:67	47	54[f]
2f	10	20:80	66	57[f]
2g	30	5:95	76	49[g]
2h	30	10:90	30	13[g]

Tosylhydrazone-Based Fragment Coupling

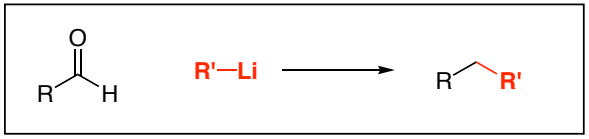

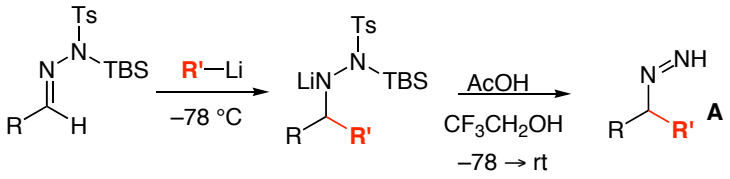

The monoalkyl azene **A** decomposes via a radical pathway

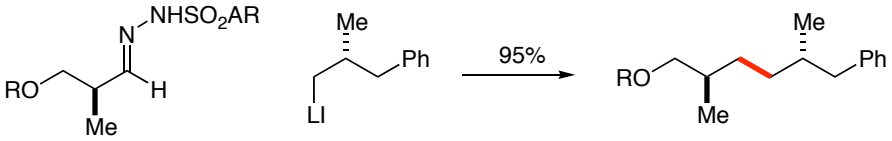

16 cases reported: A. G. Myers etal. *JACS*, **1998**, *120*, 8891.

A Complex Application: A. Smith etal. *JACS* **1999**, *121*, 7423

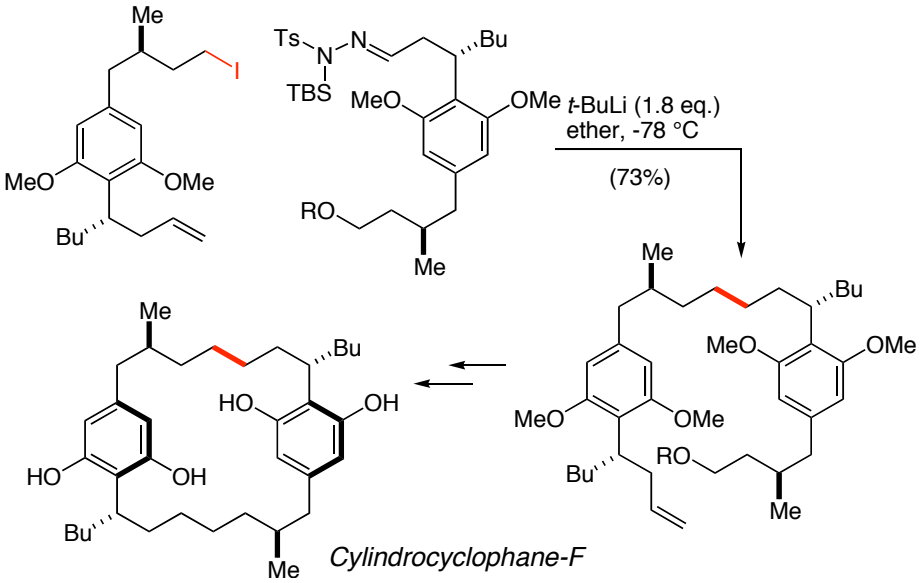

Stereoselective Construction of Trisubstituted Olefins

A. G. Myers, P. J. Kukkola *JACS*, **1990**, *112*, 8208.

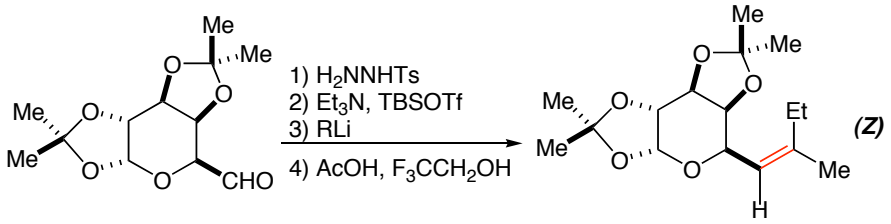

RLi	Ratio *Z*:*E*	Yield
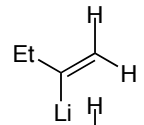	50:50	79%
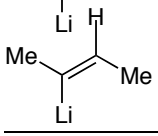	<5:95	81%

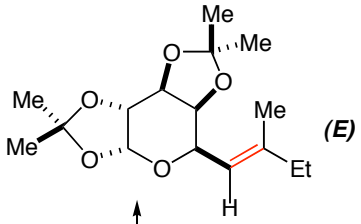

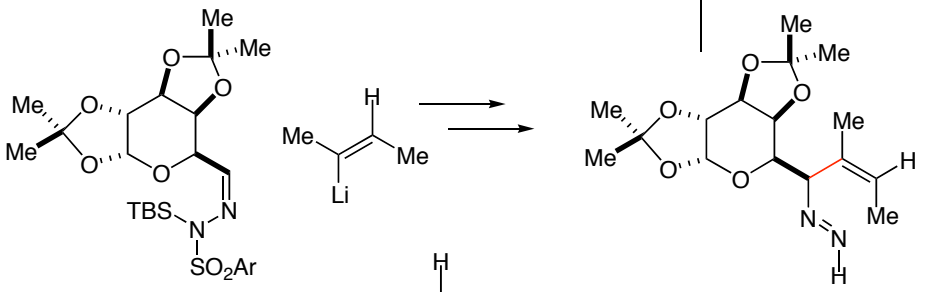

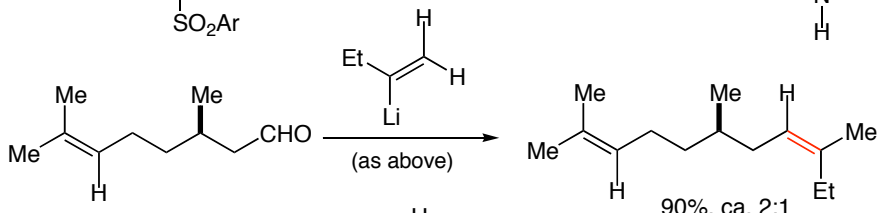

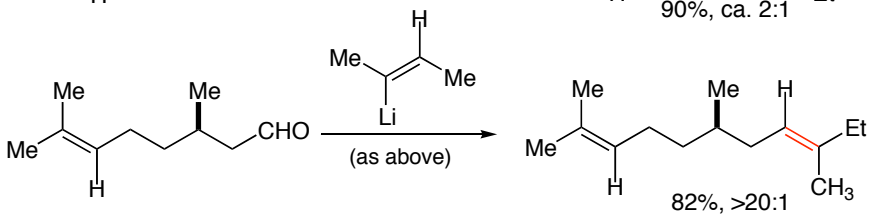

The Constitution of Limonin, Arigoni, Barton, Corey and Jeger, *Experietia*, **1960**, 41

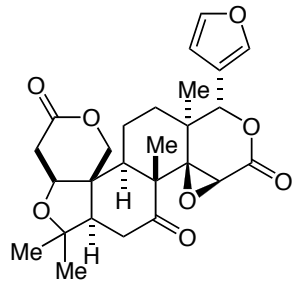

Limonin

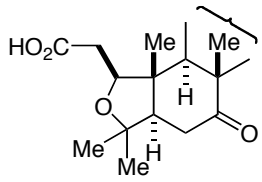

Wolff-Kishner too harsh

Proposed reaction: Barton, *JCS*, **1962**, 470.

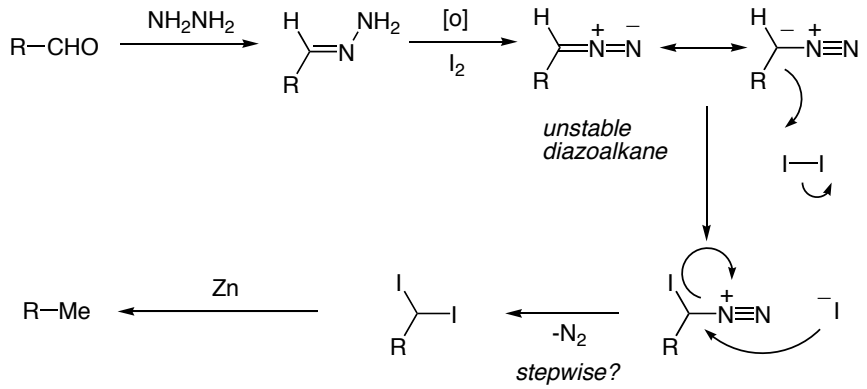

Not very general:

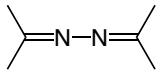

azine is often a major product

Ketones provide vinyl iodides

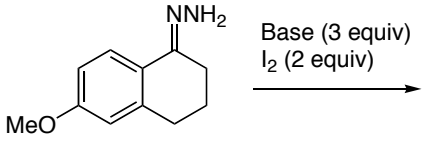

30 - 78% yield

Barton, *Tetrahedron*, **1988**, *44*, 147-162

For a very recent application, see: Theodorakis, *Angew. Chemie Int. Ed.* **2004**, *43*, 793-742

Recent Contributions from the Myers laboratory: bis-TBS Hydrazine : BTBSH

Preparation:

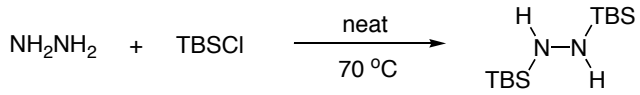

79% (distilled)

Furrow and Myers, *JACS*, **2004**, *126*, 5436

Straightforward condensation:

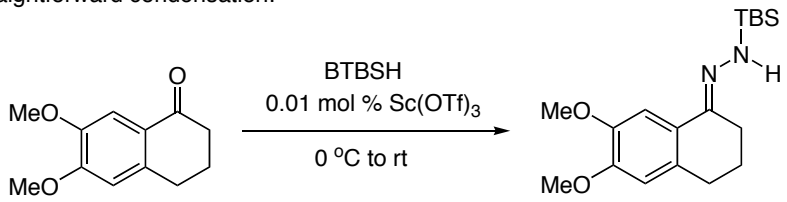

95% yield, 15 examples

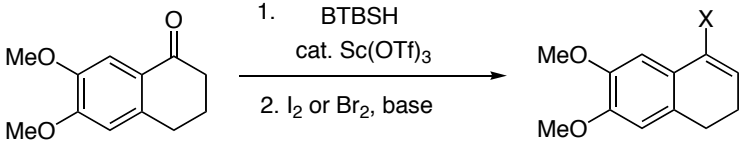

X = I (82%)
X = Br (84%)

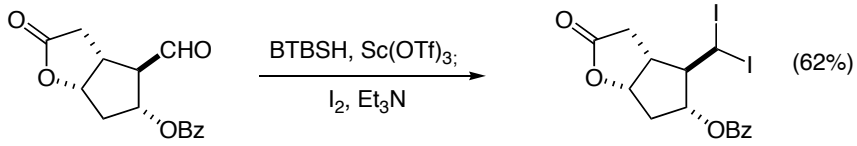

(62%)

The Corey Lactone

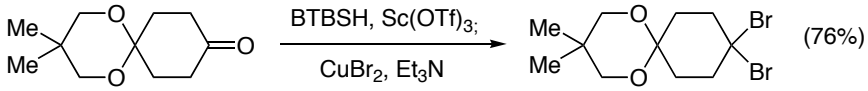

(76%)

Furrow and Myers, *JACS*, **2004**, *126*, 5436

Recent Contributions from the Myers laboratory: bis-TBS Hydrazine : BTBSH

Preparation:

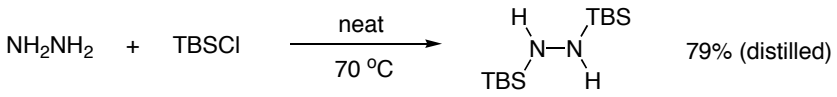

79% (distilled)

Furrow and Myers, *JACS*, **2004**, *126*, 5436

Modified Wolff-Kishner reductions: One-pot, two-step protocol

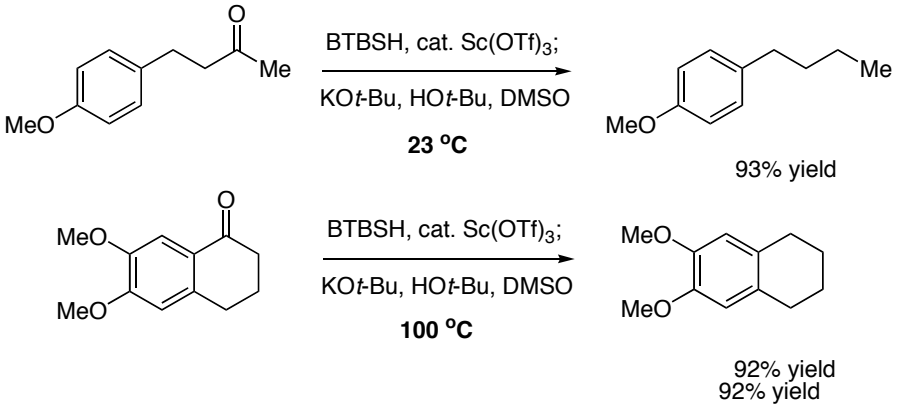

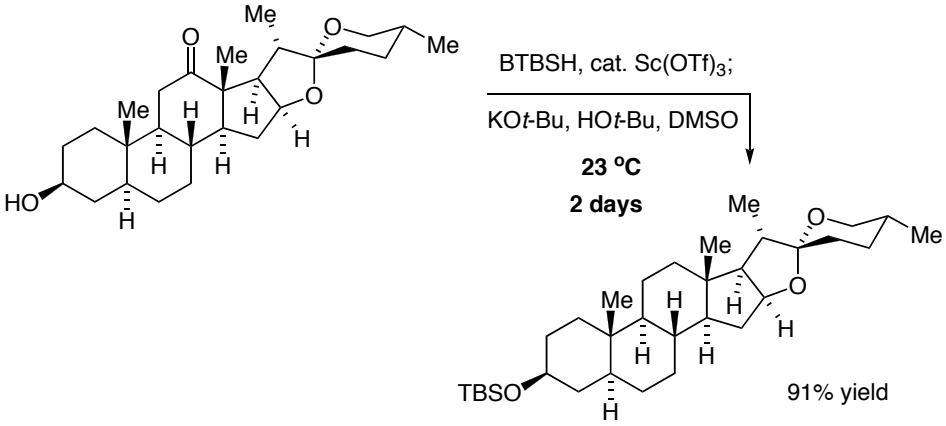

7 examples, *JACS*, **2004**, *126*, 5436

The Generation of Diazoalkanes in Situ from TBS Hydrazones:

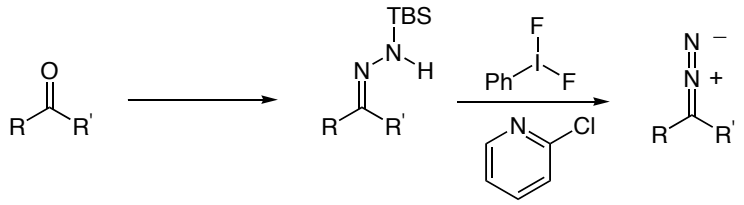

Furrow and Myers, *JACS*, **2004**, *126*, 12223

The generation of unstabilized diazoalkanes is very difficult as usually both the starting materials and products are unstable.

Methods such as the Bamford-Stevens reaction may be hazardous.

Esterification of Carboxylic Acids with Diazoalkanes generated in Situ

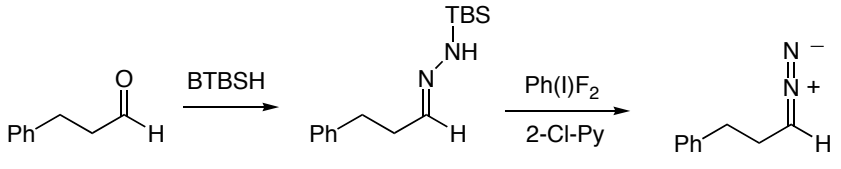

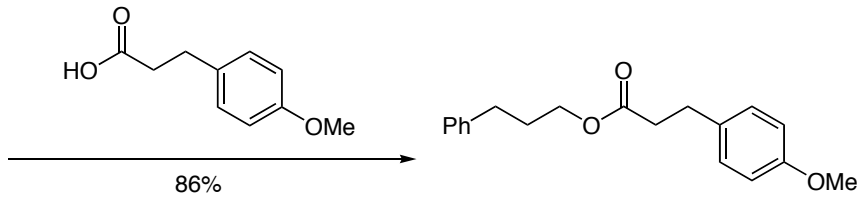

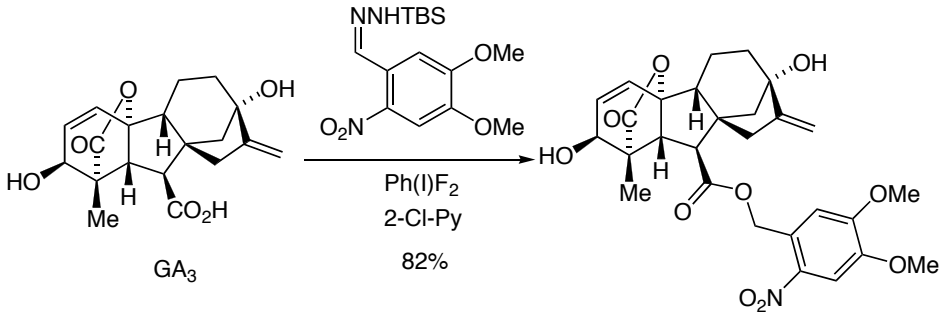

α-Keto Carbonium Ion Equivalents

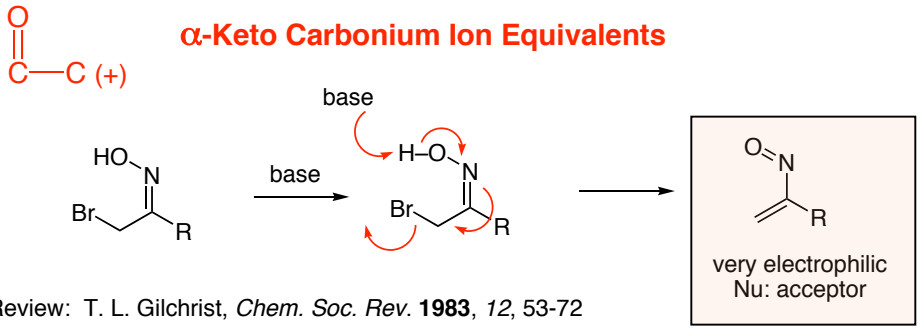

Review: T. L. Gilchrist, *Chem. Soc. Rev.* **1983**, *12*, 53-72

Reactions with Nucleophiles

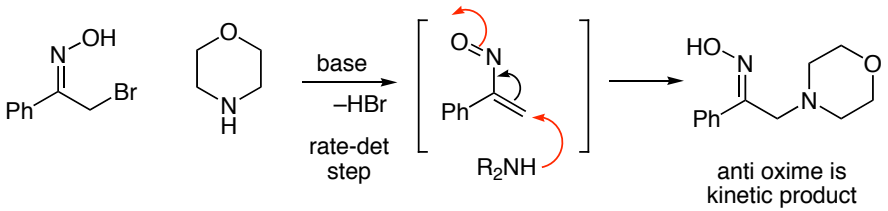

T. Kaiser, *JACS.* **1972**, *94*, 9276-9277

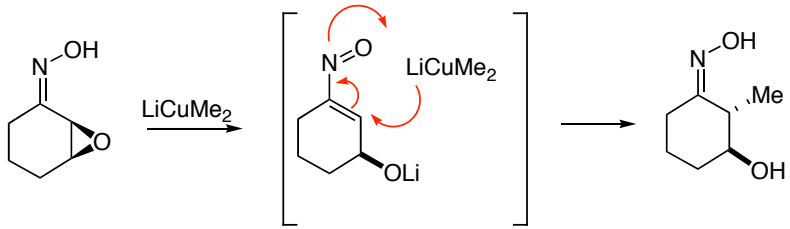

Corey, *Tetrahedron Lett.* **1975**, 3117

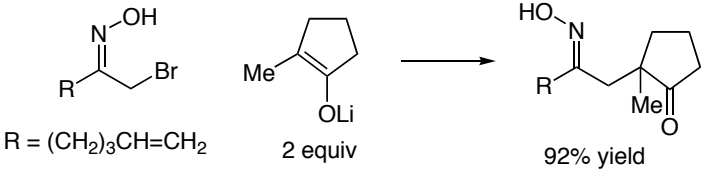

Corey, *Helv. Chem. Acta.* **1977**, *60*, 2964

Cycloadditions

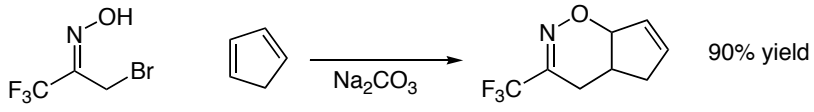

Ressig, *J. Org. Chem.* **1992**, *57*, 339

Stereoelectronic Issues

there is the expected strong chair-axial bias

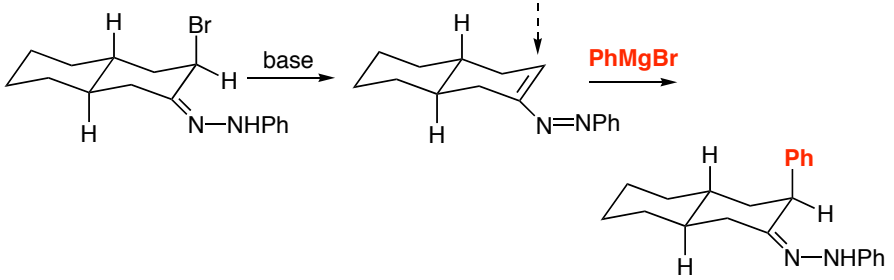

Stereoelectronic vs Steric Issues

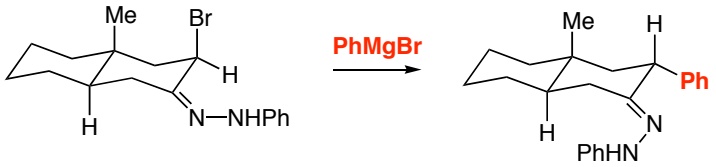

Bozzini, *Tetrahedron* **1982**, 38, 1459

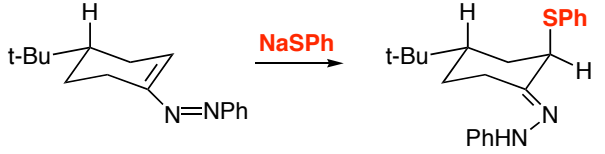

there is the expected strong chair-axial bias

Bozzini, *Tetrahedron* **1982**, 39, 3413

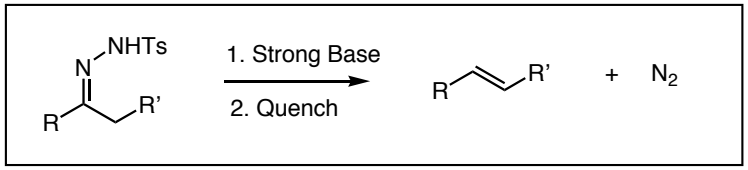

General Reviews:

Trost, Ed., *Comprehensive Organic Synthesis* **1992**, Vol 6, Chapters 4.3 .
Trost, Ed., *Comprehensive Organic Synthesis* **1992**, Vol 6, Chapters 4.6.
Shapiro, *Organic Reactions* **1976**, Vol 23, pp 405-507.

Mechanism:

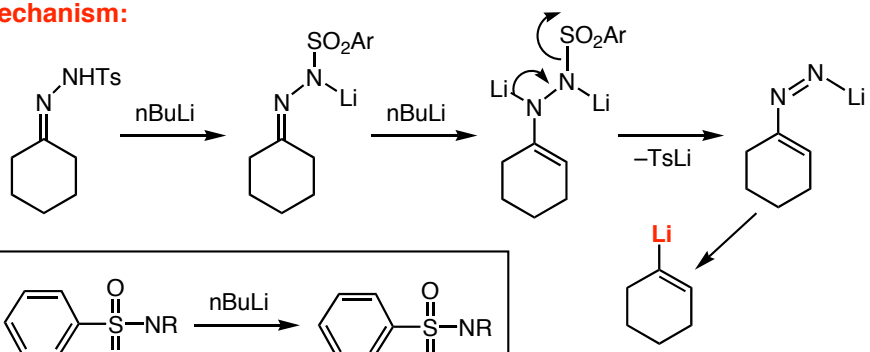

the Triisopropylsulfonyl (Trisyl) group is used (Roberts *Tet. Let.* **1981**, *22*, 4895).

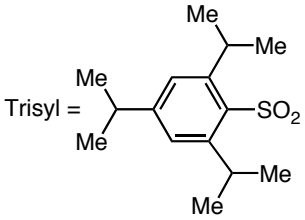

Regiochemistry

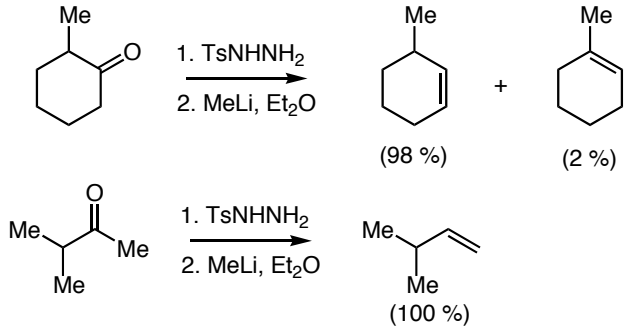

Deprotonation of the monoanion occurs predominantly at the kinetically more acidic site giving, after elimination, the less substituted alkene product.

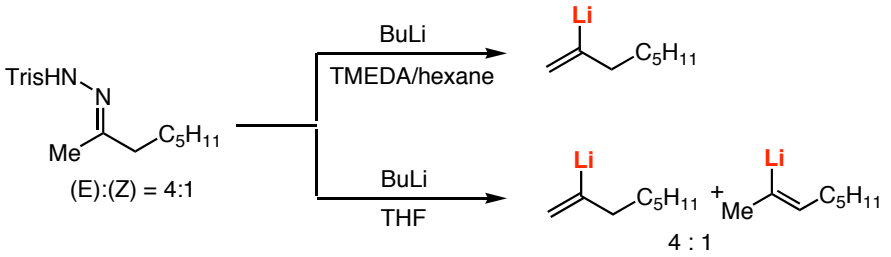

In THF solution regiochemical ratios generally reflect the starting hydrazone geometries

Bond *J. Org. Chem.* **1978**, *43*, 154.

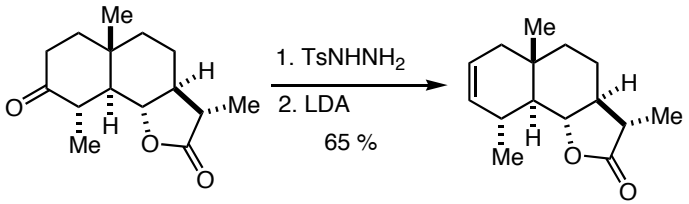

Grieco *J. Org. Chem.* **1977**, *42*, 1717.

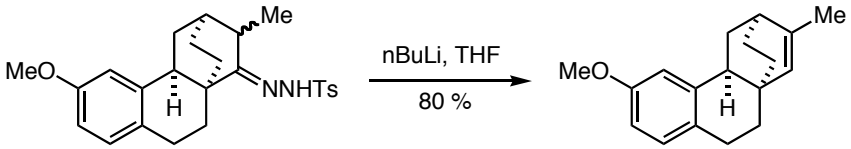

Nemoto *et. al. JCS, Perkin Trans. 1* **1985**, 927.

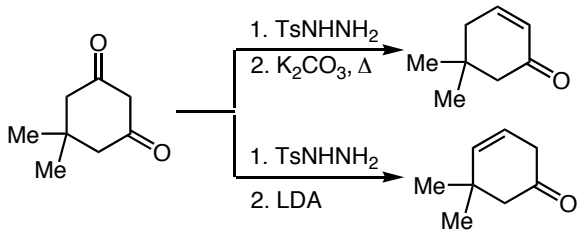

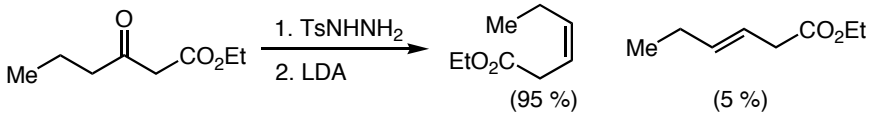

Trapping of the intermediate alkenyllithium

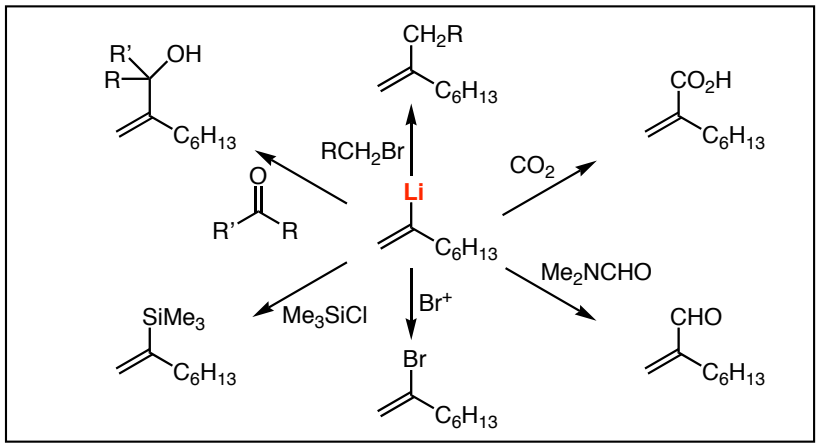

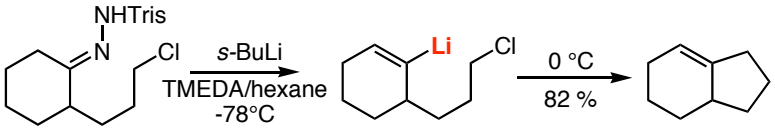

Bloom *Tet Lett.* ***1984***, *25*, 4901

Carbonyl Transposition

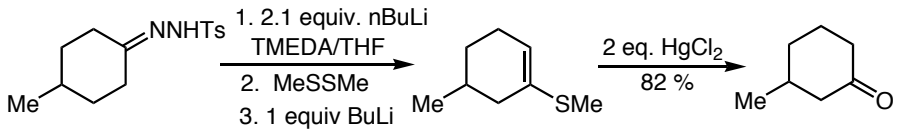

Nakai *Chem. Lett.* **1980**, 1099

Shapiro alternatives

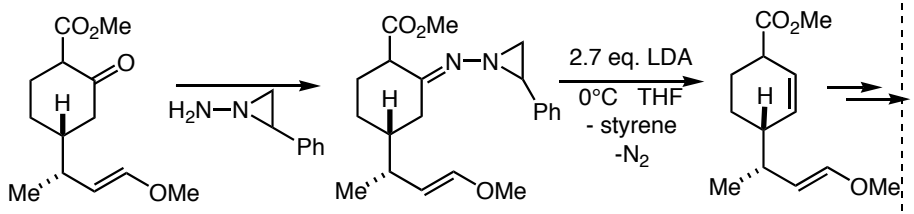

(Juvabione) Evans *J. Am. Chem. Soc.* **1980**, *102*, 774

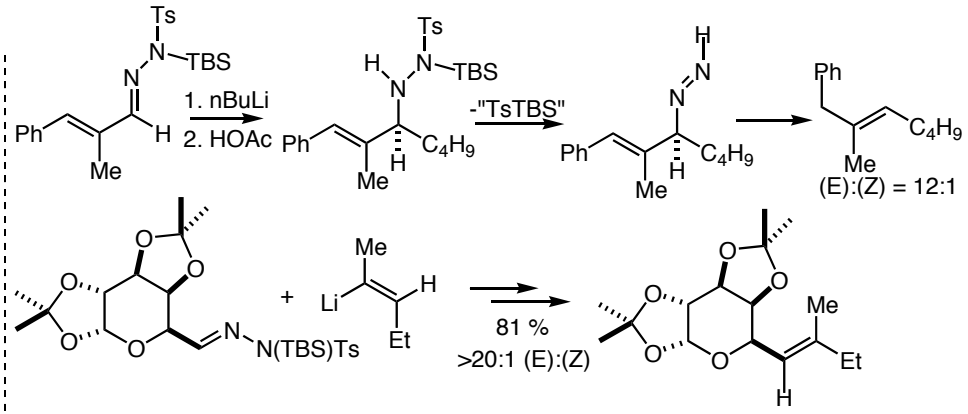

Myers, *J. Am. Chem. Soc.* **1990**, *112*, 8208

Applications

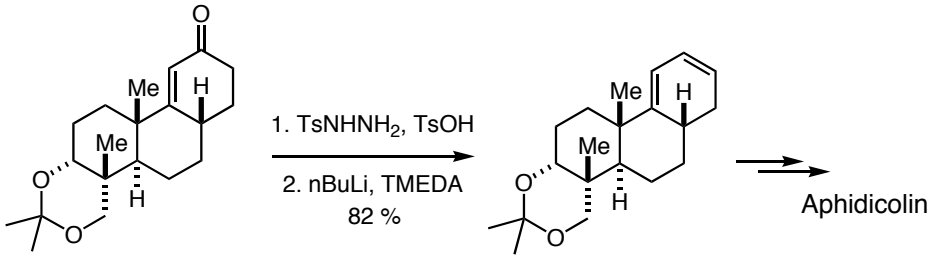

van Tamelen *J. Am. Chem. Soc.* **1983**, *105*, 142.

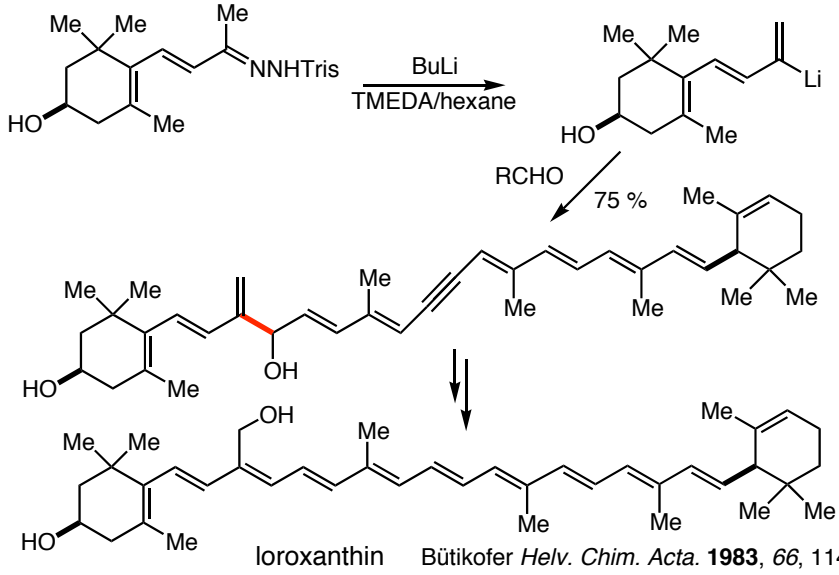

loroxanthin Bütikofer *Helv. Chim. Acta.* **1983**, *66*, 1148

How would you convert A into B?

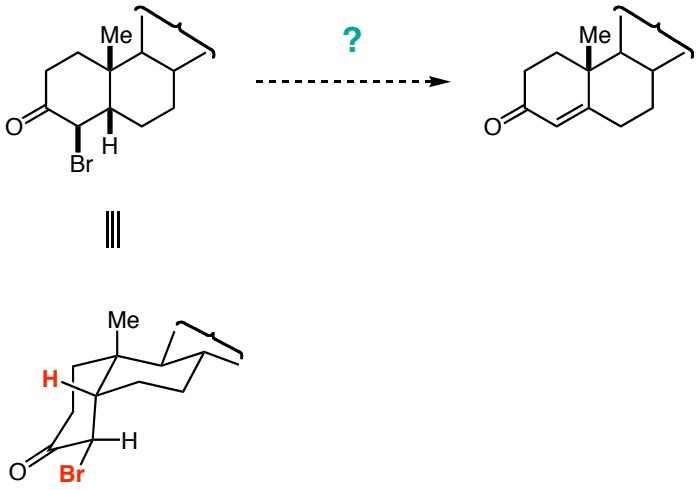

Problem: The syn relationship between Br and H renders the direct dehydrohalogenation with base unfavorable (relative to other potential reactions).

Solution: proceed via the hydrazone.

Mattox-Kendall Dehydrohalogenation (Paquette, *Reagents*, Vol 5, p 3509)

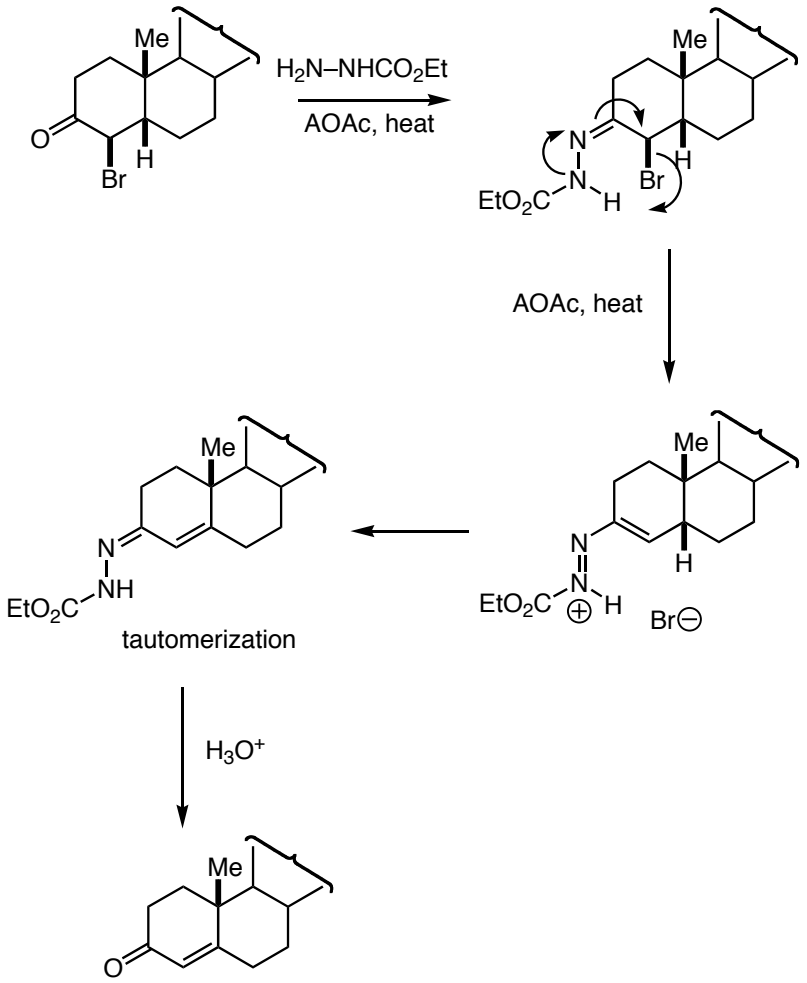

An Alternative Decomposition Pathway for Tosyl Hydrazones

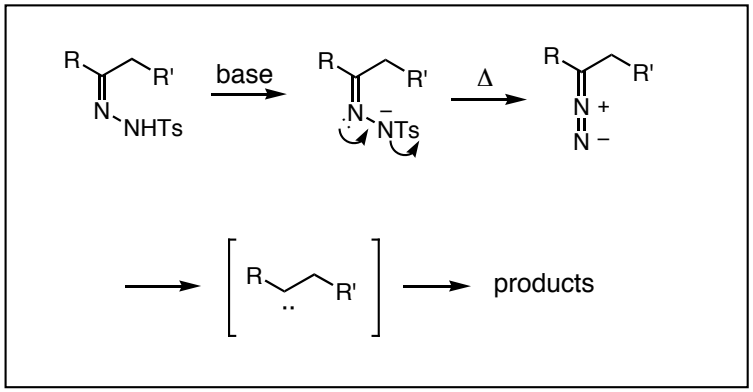

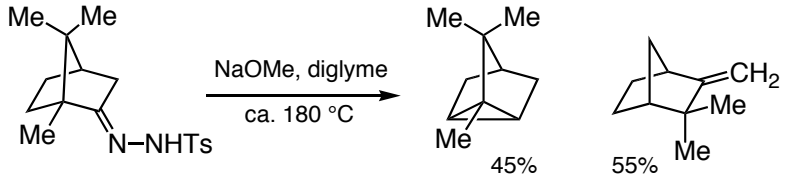

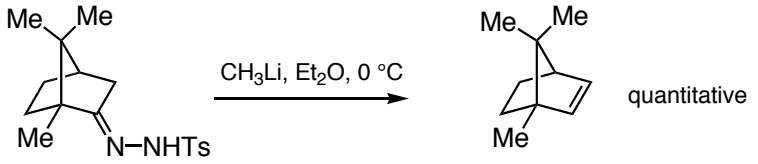

Bamford-Stevens vs. Shapiro

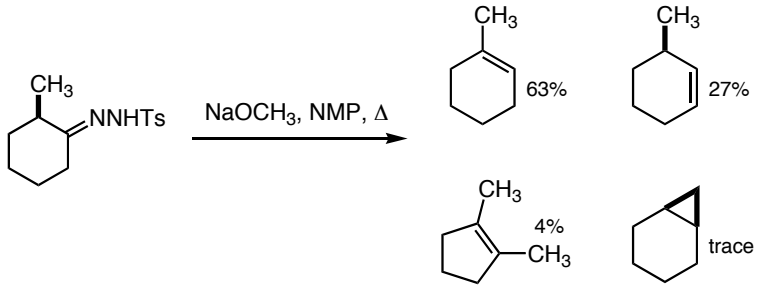

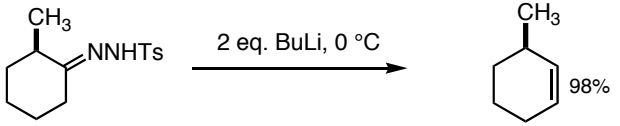

R. H. Shapiro *Org. React.* **1976**, *23*, 405.

Directed Bamford-Stevens

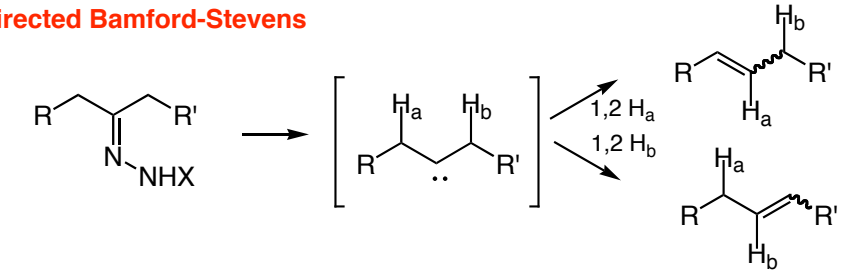

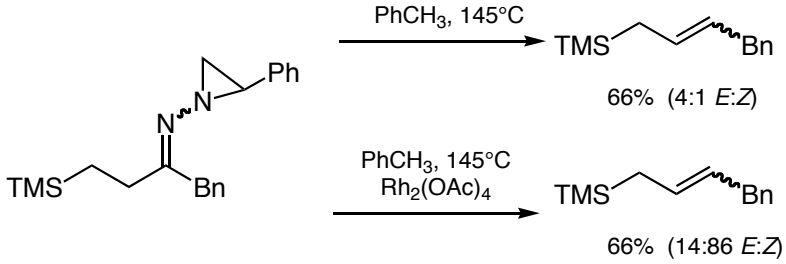

T. K. Sarkar, et al. *JCS Chem. Comm.* **1992**, 1184.

http://www.courses.fas.harvard.edu/colgsas/1063

Chemistry 206

Advanced Organic Chemistry

Lecture Number 32

Ambiphilic Functional Groups–3 Sulfur-Based Activating Groups

- Sulfur-Ylides
- Sulfur-Stabilized Carbanions: Structure
- Sulfone-Based Transformations
- Pummerer Rearrangement

Reading Assignment for this Week:

Carey & Sundberg: **Part A**; Chapter 7
Carbanions & Other Nucleophilic Carbon Species

Carey & Sundberg: **Part B**; Chapter 2
Reactions of Carbon Nucleophiles with Carbonyl Compounds

"Chemical Chameleons: Organosulfones as Synthetic Building Blocks"
B. M. Trost, *Bull. chem. Soc. Japan,* **1988**, *61*, 107-124 **(handout)**

"Evolution of Dithiane-Based Strategies for the Construction of Architecturally Complex Natural Products", *Accounts Chem. Res.* **2004,** *37,* 366-377 **(handout)**

Pummerer Review, A. Padwa, *Synthesis* **1997**, 1353-1377 **(handout)**

D. A. Evans

Friday
December 8, 2006

Relevant Background Reading

General: Simpkins, N.S. *Sulphones in Organic Synthesis*, Pergamon Press, New York, 1993.

General: Magnus, P.D. *Tetrahedron* **1977**, *33*, 2019.

Julia: Blakemore, *J. Chem. Soc. Perkin Trans I.* **2002**, 2563.

Electrophilic Properties: Trost, B.M. *Bull.Chem. Soc. Jpn.* **1988**, *61*, 107.

SO_2 Extrusion: Vogtle, F.; Rossa, L. *ACIEE* **1979**, *18*, 515.

Ramberg-Bäcklund Rxn: Paquette, L.A. *Org. Reactions* **1977**, *25*, 1.

Triflones: Hendrickson, J.B. *Org. Prep. Proc. Int.* **1977**, 175.

Sulfoximides: Johnson, C.R. *Tetrahedron* **1984**, *40*, 1225

Problem 37: The stereoselective construction of trans olefins through carbanion-mediated condensation processes has still not been rendered general. One transformation that may be used in certain circumstances is the "one-step" Julia transformation illustrated below. Provide a mechanism for this transformation.

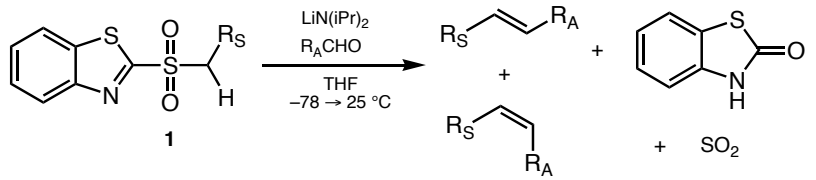

The cruel mechanistic problems that you should be prepared for in Chem 206
Six Pummerer Problems in database.

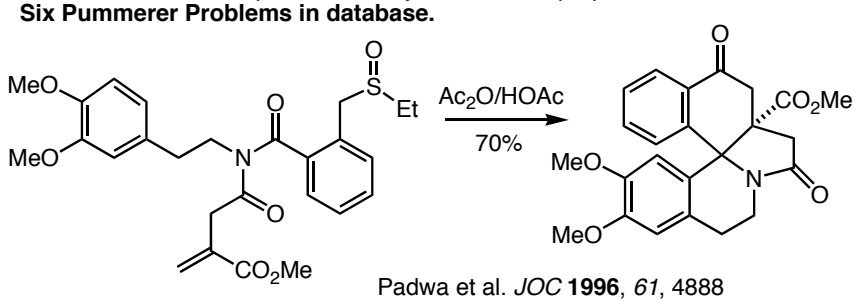

Padwa et al. *JOC* **1996**, *61*, 4888

Acidities of Sulfur-based Functional Groups

Bordwell, F. G.; Zhang, X.-M. *Acc. Chem. Res.* **1993**, *26*, 510-17.

		pKa (DMSO)	
CH_3-S-CH_3	Sulfide	**(45)**	← CH_4 pKa (~56)
			← NH_3 pKa (~41)
$CH_3-S(=O)-CH_3$	Sulfoxide	**~35**	
$CH_3-S(=O)_2-CH_3$	Sulfone	**~ 31**	← HOH pKa 31
$(CH_3)_3S^+$	Sulfonium Salt	**18.2**	pKa of Phenol
$CH_3-S(=O)(CH_3)_2^+$	Oxo-Sulfonium Salt	**< 18**	
Thiazole	Thiazolium Salt	**29.4**	
Thiazolium Salt		**16.5**	

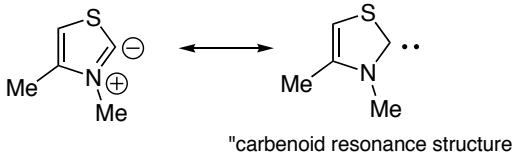

(–)
R_2S-C
(+)
Reactivity Pattern
Nonalternate

Reactions of Sulfonium Ylids

■ Synthesis:

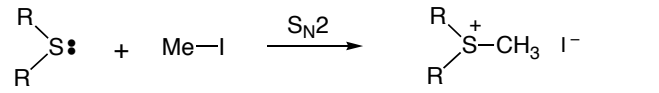

Sulfonium Salt: pKa ~ 18

(+)
R_2S-C

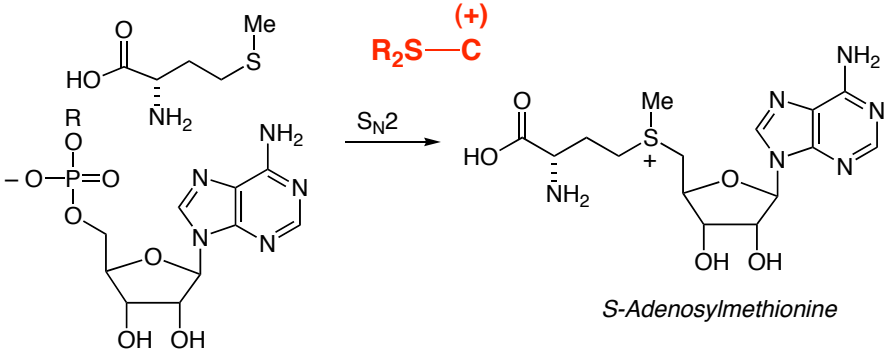

S-Adenosylmethionine

■ Deprotonation:

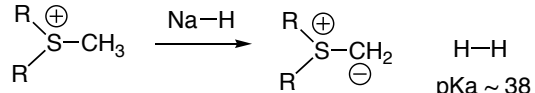

pKa ~ 18 pKa ~ 38

(–)
R_2S-C

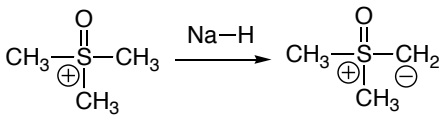

■ **Leaving Group Potential:** $R_2S-C(+)$

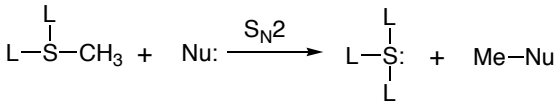

Excellent LG

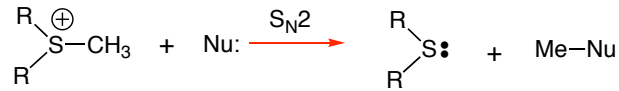

Good LG

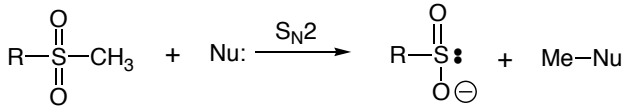

X-ray Structures of Metallated Sulfones & Sulfoxides

Sulfone- & Sulfoxide Based Carbanions: Structure

- Sulfone- and sulfoxide-stabilized carbanions are extremely useful carbon nucleophiles in organic synthesis.

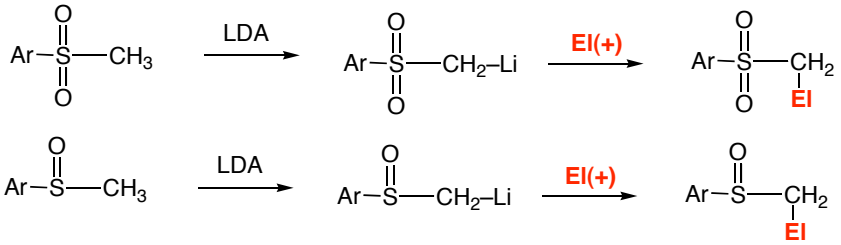

However, until recently little information was available on the solid state structures of these species:

"The Structure of Lithium Coumpounds of Sulfones, Sulfoximides, Sulfoxides, Thioethers, 1,3 Dithianes, Nitriles, Nitro Compounds, and Hydrazones."
Boche, G. *Angew. Chem., Int. Ed. Engl.* **1989**, *28*, 277.

Here are several examples taken from the Boche review:

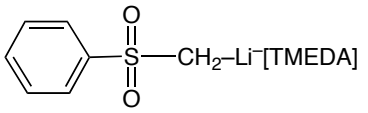

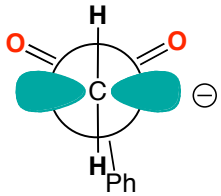

delocalization into sigma* S–O

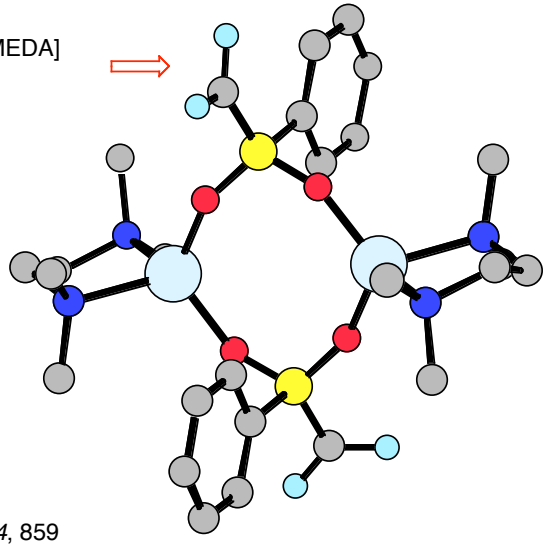

Gais, etal.
Angew. Chem. Int. Ed. **1985**, *24*, 859

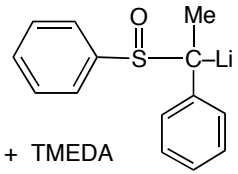

Boche, etal. *Angew. Chem. Int. Ed.* **1986**, *25*, 1101

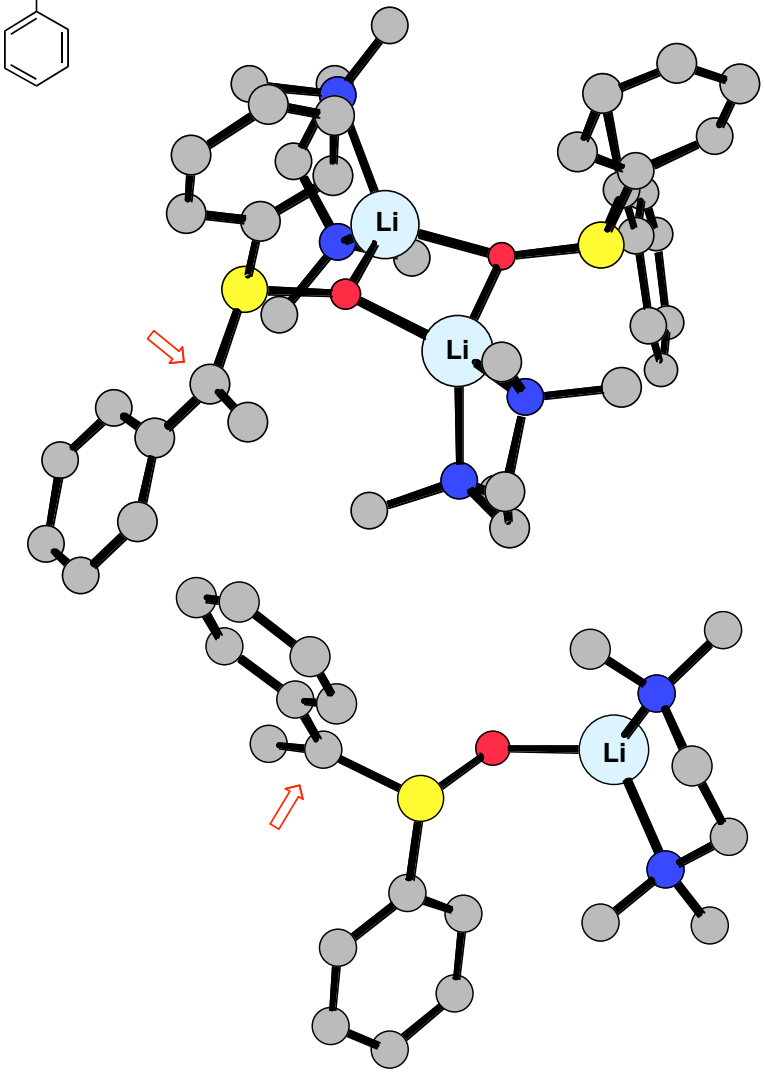

- The Li counterions are not associated with the charged carbon.
- The carbanions are largely trigonal.

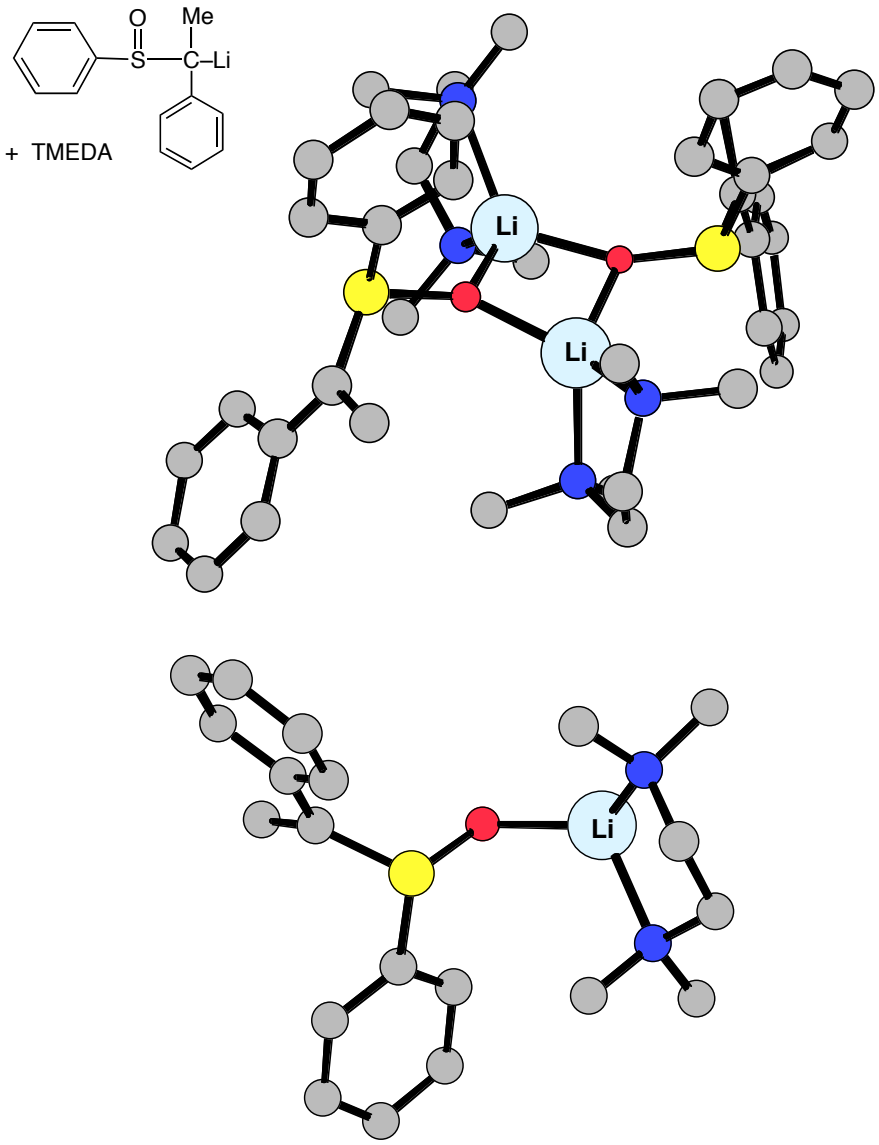

Boche, etal. *Angew. Chem. Int. Ed.* **1986**, *25*, 1101

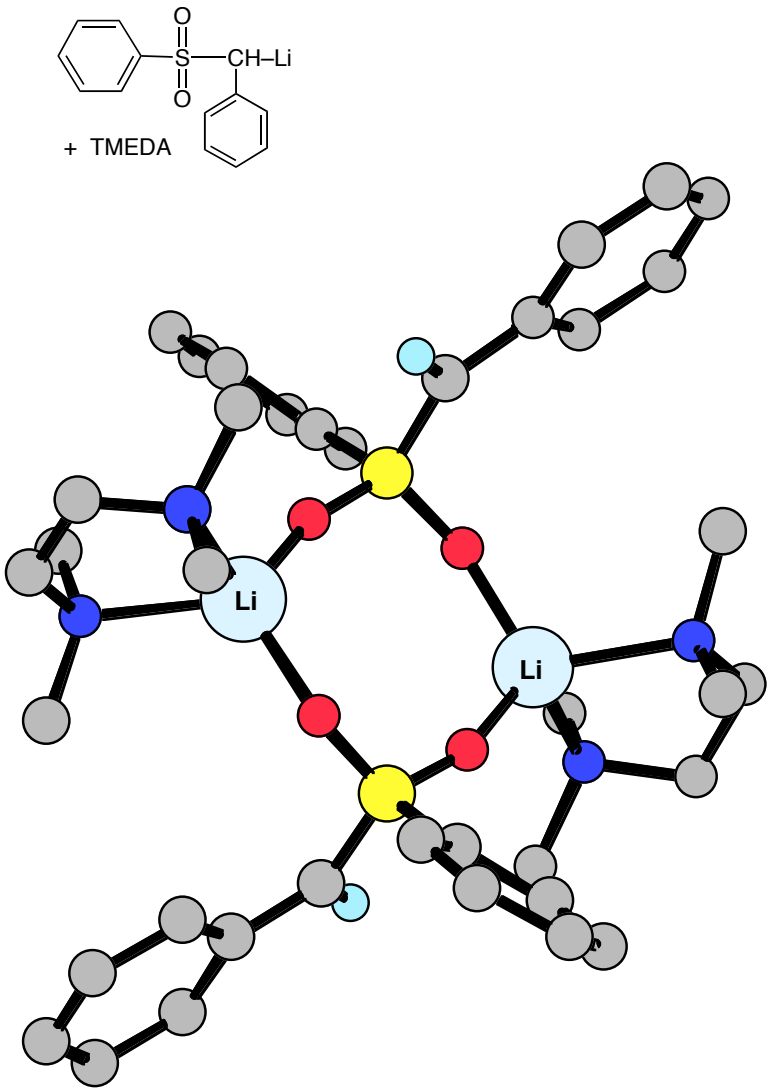

Boche, etal. *Angew. Chem. Int. Ed.* **1985**, *24*, 573

Reactions with ketones: $R_2S-\overset{(\mp)}{C}$ Reactivity Pattern: Nonalternate

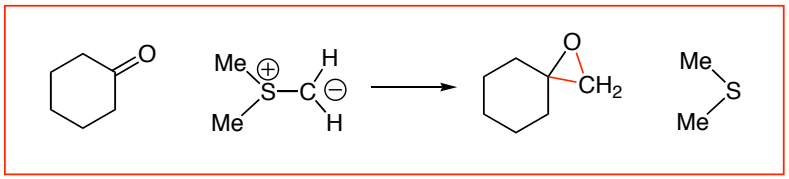

Corey & Chaycovski, *JACS* **1965**, *87*, 1353-1364. **(Handout)**

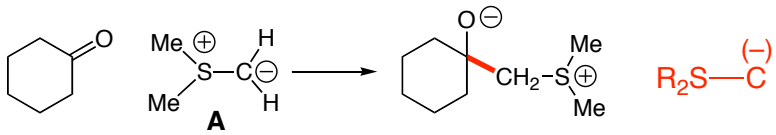

A

$R_2S-\overset{(-)}{C}$

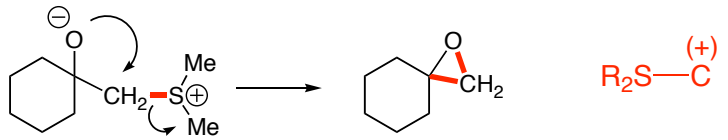

$R_2S-\overset{(+)}{C}$

"Twenty-five Years of Dimethylsulfoxonium Methylide (Corey's Reagent).", Gololobov, Y. G.; Lysenko, V. P.; Boldeskul, I. E. *Tetrahedron* **1987**, *43*, 2609. **(electronic handout)**

Reactions of OxoSulfonium Ylids: Conjugate Addition

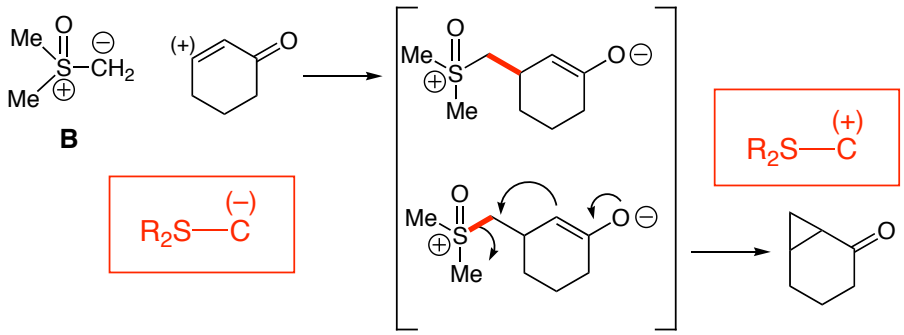

B

$R_2S-\overset{(-)}{C}$

$R_2S-\overset{(+)}{C}$

Nonalternate reactivity pattern revealed in consecutive reactions

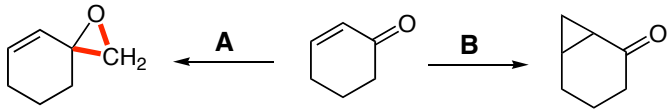

Reactions of Sulfones

Synthesis:

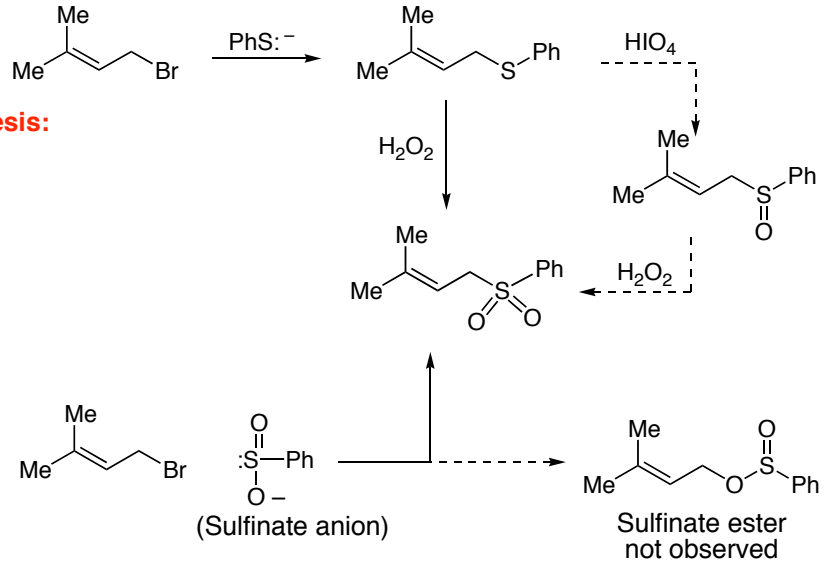

(Sulfinate anion)

Sulfinate ester not observed

Good review article: Magnus, *Tetrahedron* **1977**, *33*, 2019-2045.

Reactions of Sulfones

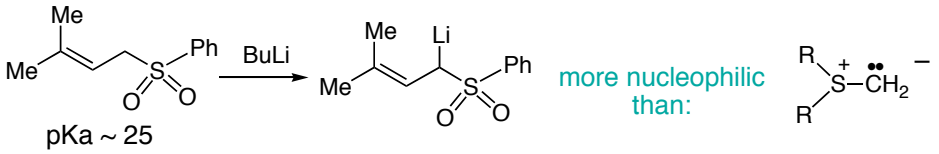

pKa ~ 25

more nucleophilic than:

poorer leaving group than:

$R_2SO_2-\overset{(-)}{C}$

$R_2SO_2-\overset{(+)}{C}$

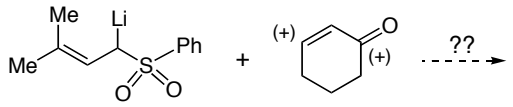

1,2- vs 1,4-addition ??

Will function as LG ??

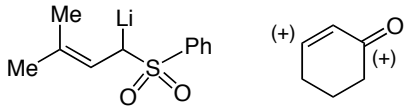

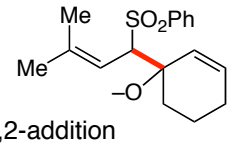

1,2-addition

$R_2SO_2—C^{(-)}$

Alkoxide not sufficiently nucleophilic to displace $PhSO_2^-$ anion.

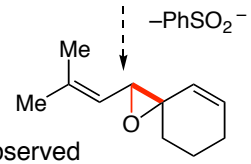

Not observed

However!!

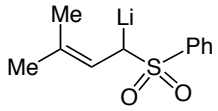

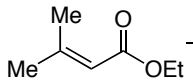

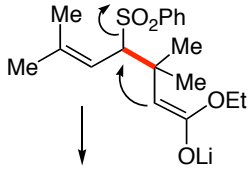

Industrial synthesis developed by M. Julia

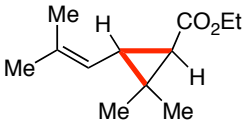

trans chrysanthemic acid

$R_2SO_2—C^{(-)}$ → $R_2SO_2—C^{(+)}$

Synthesis of Vitamin A: Julia & Co-workers, *Bull. Soc. Chim. Fr.* **1985**, 130

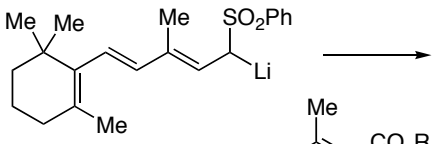

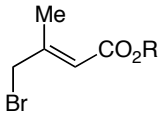

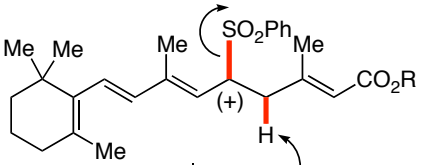

KOH/MeOH

$R_2SO_2—C^{(-)}$

$R_2SO_2—C^{(+)}$

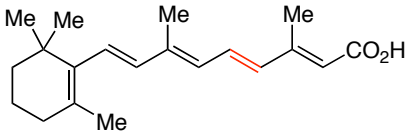

The Sulfone group may also be readily removed reductively:

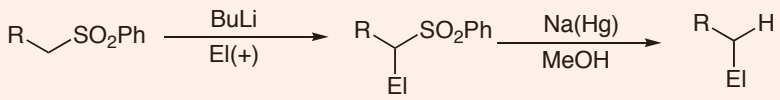

Fragment Coupling with Sulfonyl Carbanions

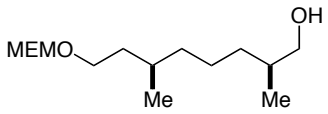

Heathcock, C.H.; *et al.*
J.Org.Chem. **1988**, *53*, 1922.

1. MsCl, TEA
2. PhSLi, THF, RT
3. mCPBA

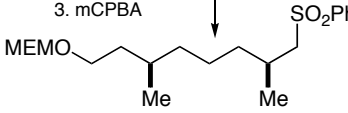

2 eq. nBuLi
THF/HMPA;
then add iodide

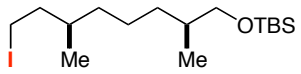

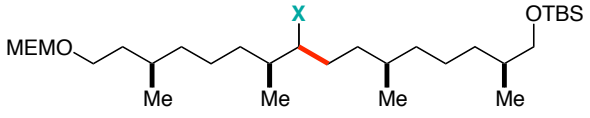

65 - 85% yield

Li wire, Na_2HPO_4
THF/HMPA/tBuOH

X= SO_2Ph

X = H

50% yield

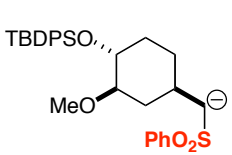

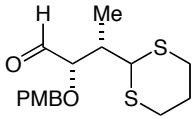

Smith, A.B. III; *et al.*
Tet.Lett. **1989**, *30*, 6963.

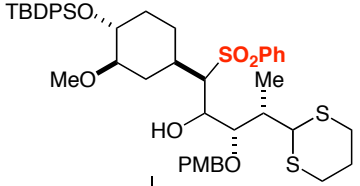

77% yield

TFAA, DMSO; NEt_3
CH_2Cl_2, -78 °C

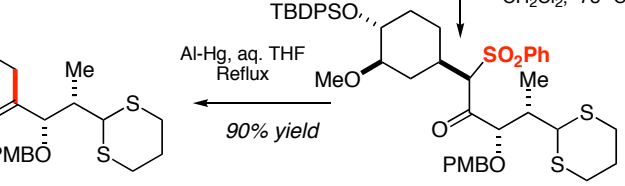

Al-Hg, aq. THF
Reflux

90% yield

Functionalization of cyclic Ethers

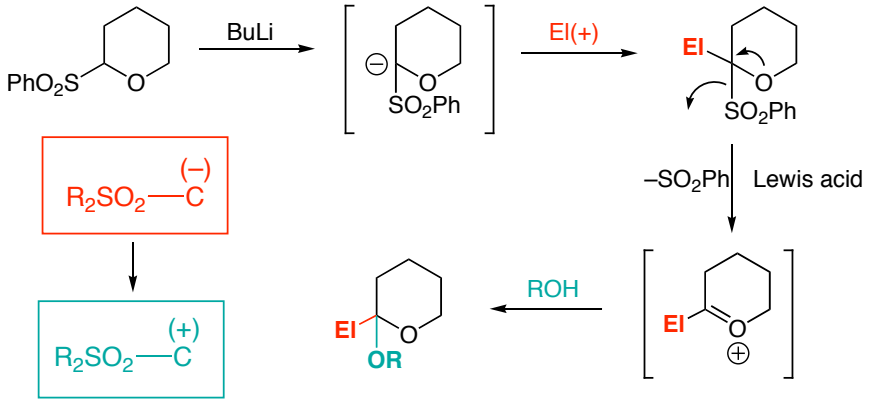

Ley *et al*, *Synlett*, **1992**, 395; Ley *et. al*, *Tetrahedron*, **1992**, *48*, 7899

Total Synthesis of Routiennocin (CP-61,405)

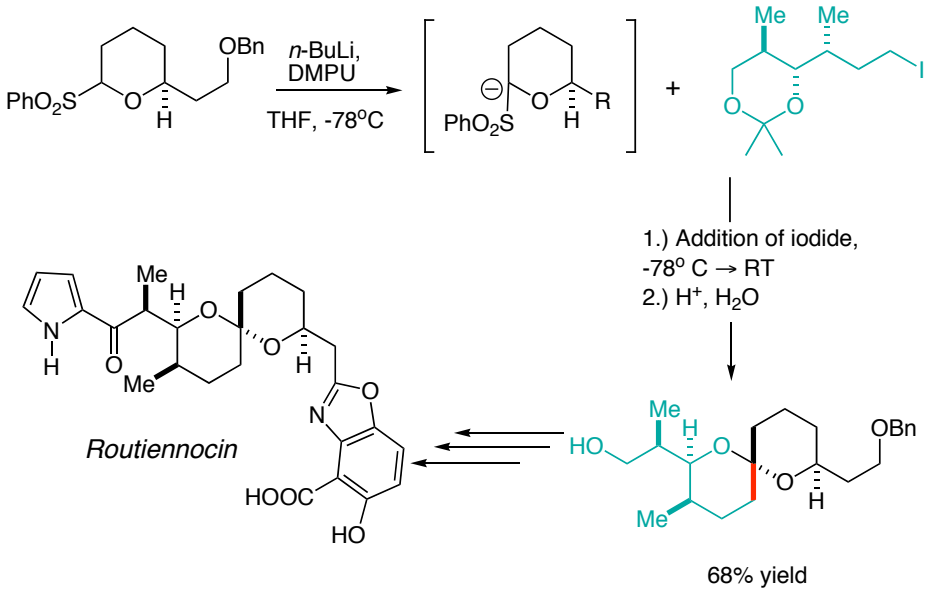

Total synthesis of Okadaic Acid

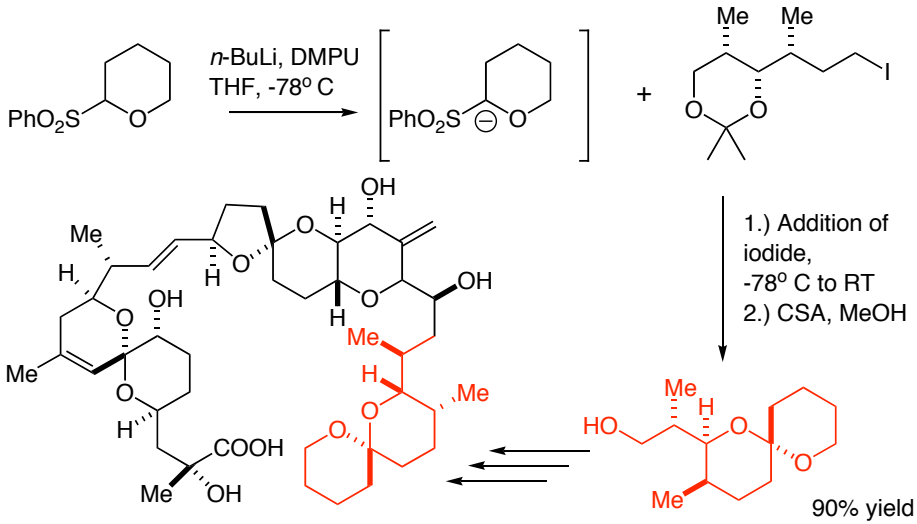

Ley *et al, J. Chem. Soc., Perkin Trans. 1*, **1998**, 3907.

Total synthesis of Bryostatin 2

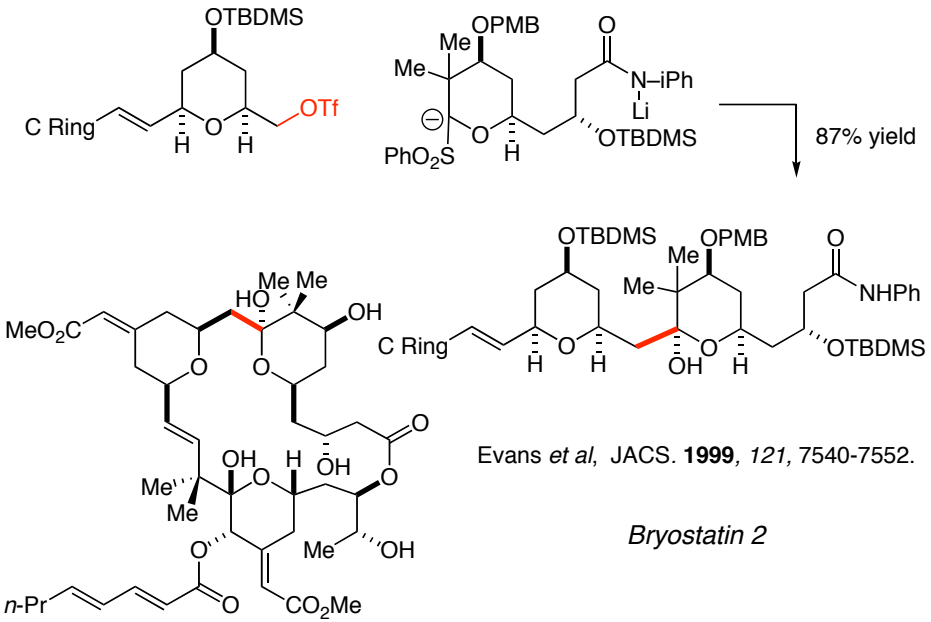

Evans *et al*, JACS. **1999**, *121*, 7540-7552.

First Generation Julia Trans Olefin Synthesis:

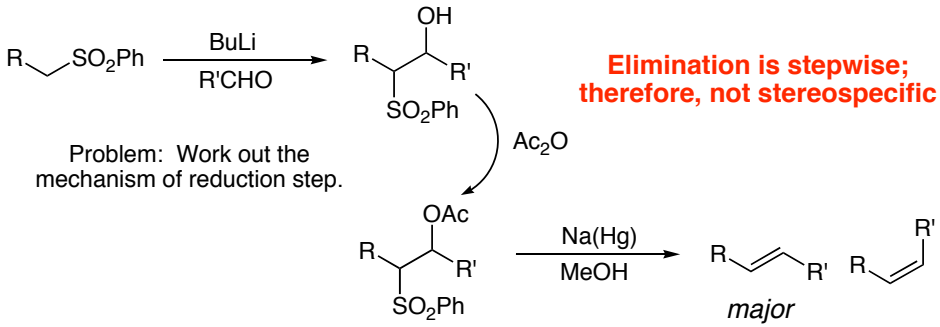

Elimination is stepwise; therefore, not stereospecific

Problem: Work out the mechanism of reduction step.

Good sulfone review: Trost, *Bull Chem. Soc. Japan,* **1988**, *61*, 107-124.

Julia Review,
Blakemore, *J. Chem. Soc. Perkin Trans I.* **2002**, 2563. **(electronic handout)**

The reduction step is not stereosecific

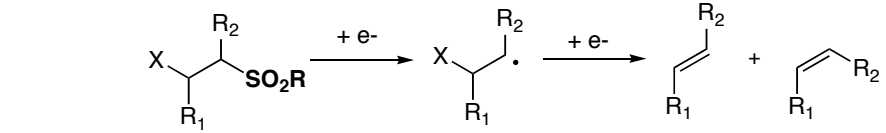

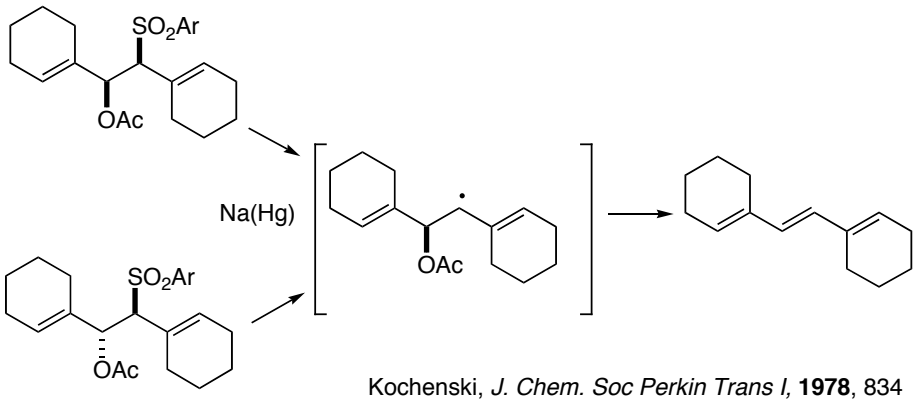

Kochenski, *J. Chem. Soc Perkin Trans I,* **1978**, 834

Julia Olefination - Ionomycin

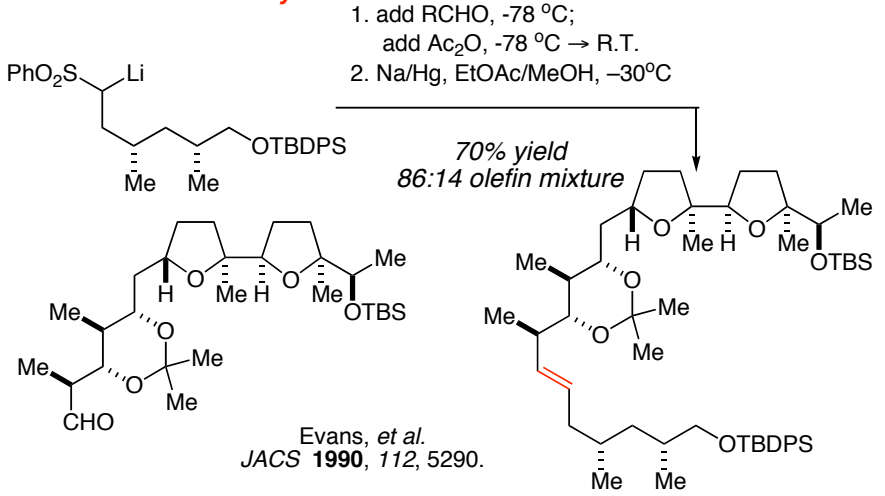

Evans, *et al.*
JACS **1990**, *112*, 5290.

Cytovaricin Synthesis: *JACS* **1990**, *112*, 7001

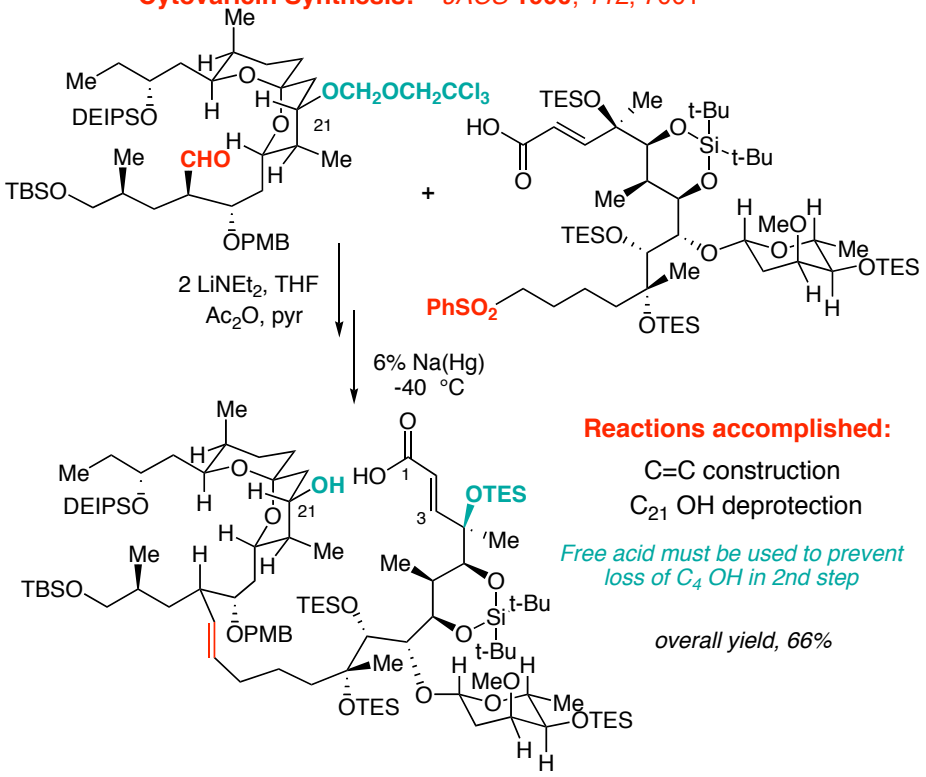

Reactions accomplished:

C=C construction
C_{21} OH deprotection

Free acid must be used to prevent loss of C_4 OH in 2nd step

overall yield, 66%

Phorboxazole B Synthesis

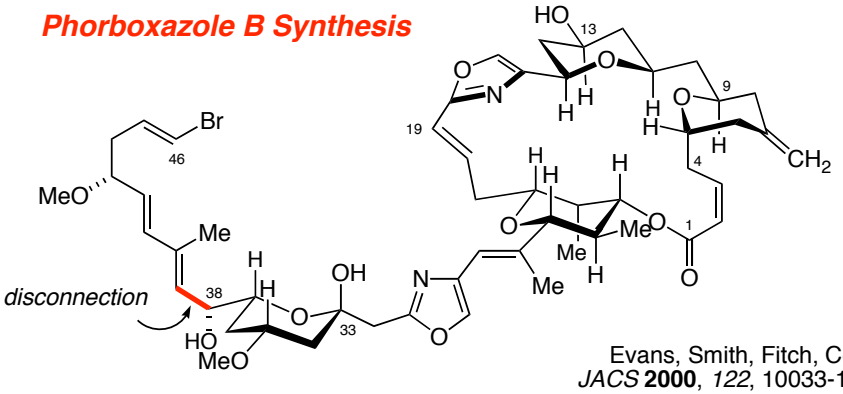

Evans, Smith, Fitch, Cee
JACS **2000**, *122*, 10033-10046.

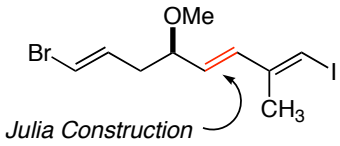

C_{39}–C_{46} Synthon

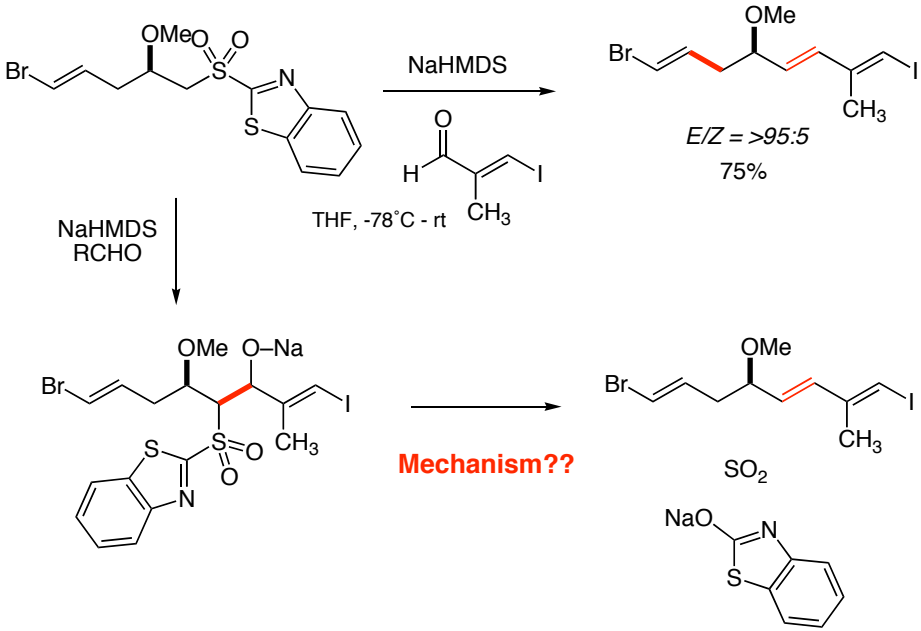

The Mechanism:

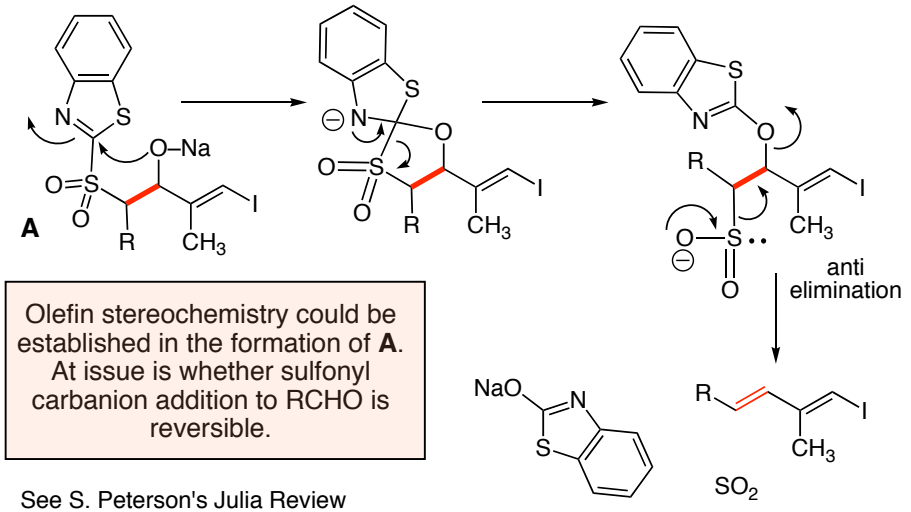

Olefin stereochemistry could be established in the formation of **A**. At issue is whether sulfonyl carbanion addition to RCHO is reversible.

See S. Peterson's Julia Review
(electronic handout)

Recent Modifications of the Julia Process:

Kocienski, *SynLett* **2000**, *3*, 365-366.

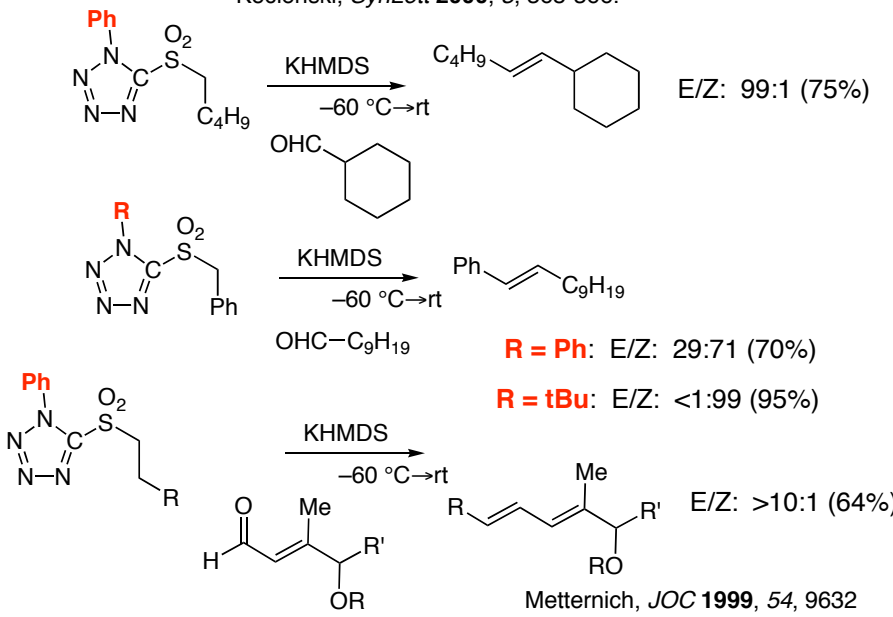

Metternich, *JOC* **1999**, *54*, 9632

Carbonyl Anions: A useful Reversed Polarity Equivalent

Consider the two possible polar disconnections of the C–R_2 bond of the ketone shown below:

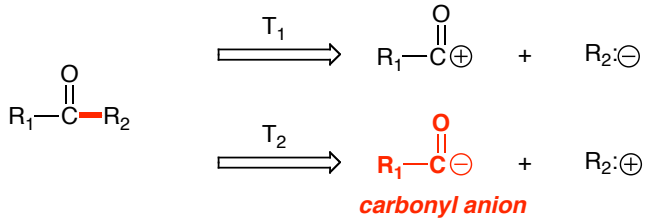

Carbonyl anions are not normally accessible via aldehyde deprotonation

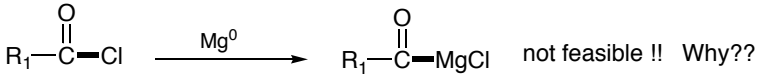

Operational equivalents to the carbonyl anion are useful in synthesis

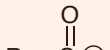

1,3-Dithianes as Carbonyl Anion Equivalents

Dithiane Review:A. B. Smith, *Acc. Chem. Res.* 2004, *37*, 365 (Handout)

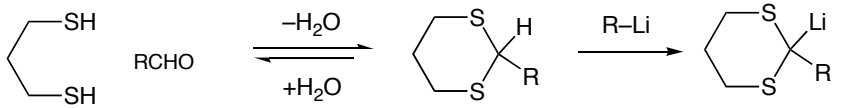

Reactivity Patterns: $(RS)_2$–C(+) $(RS)_2$–C(–)

Latest Innovations: A. B. Smith, *JACS* **2003**, *125*, 14435-14445 (Handout)

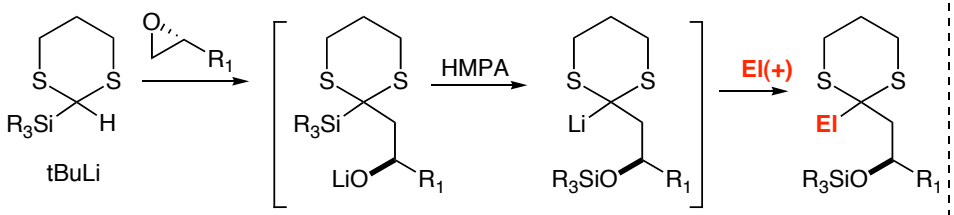

The overall set of reactions which establishes the equivalency of the hypothetical carbonyl anion **1** and its equivalent synthon **2** is shown below:

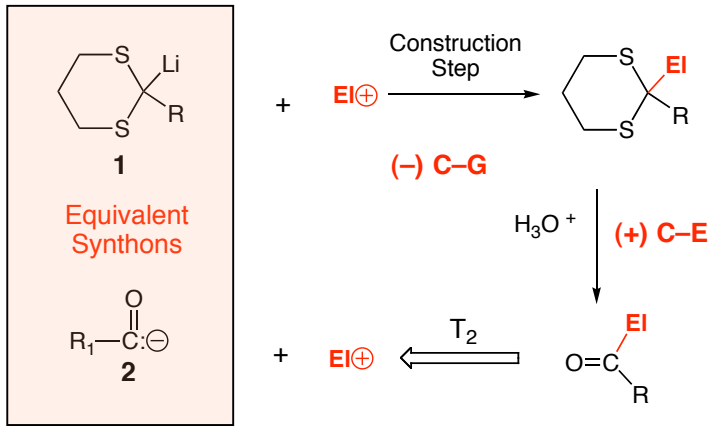

Nitronate Anions are also useful Carbonyl Anions

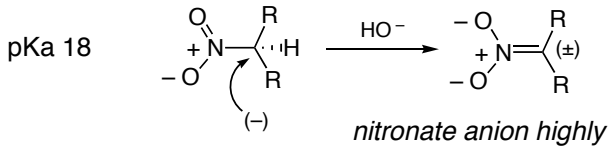

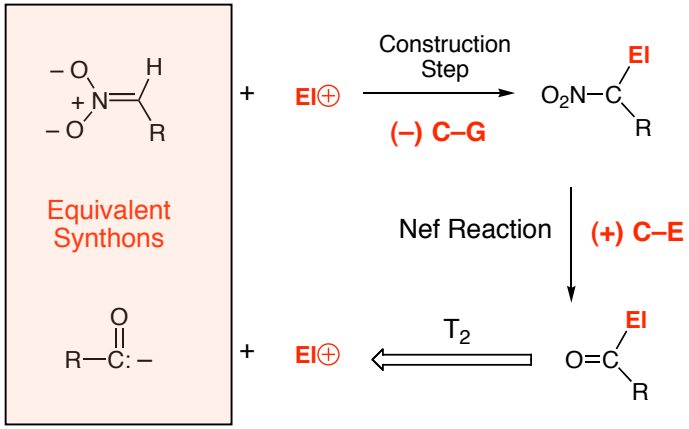

Dithianes anions highly nucleophilic (indiscriminate):
Nitonate anions higly discriminating

Introduction. As you know, transform T_1 conforms to the polar bias mapped on to the carbon skeleton by =O, while transform T_2 does not. Although T_1 is the more common transform, sometimes, because of the presence other functionality in either R_1 or R_2, the "reversed-polarity" transform is more suitable for the particular synthesis at hand.

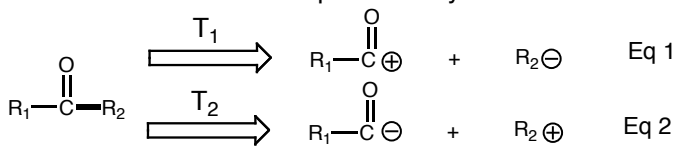

Reversed Polarity Synthon

Ideally, one might visualize a catalytic agent (**Q**) which might react reversibly with an aldehyde in conjunction with inverting its charge affinity pattern. Nature has designed such reagents.

Charge Affininty Inversion Step: The structural constraints on (Q) are that it must be nucleophilic, add reversibly to aldehydes, and stabilize an adjacent carbanionionic center.

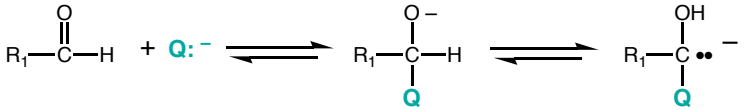

Lets call (Q) a charge affininty inversion operator since in operates on RCHO and reverses the intrinsic polar reactivity of the RCHO carbon from (+) to (–).

Overall Process:

Inversion Operator (**Q**)

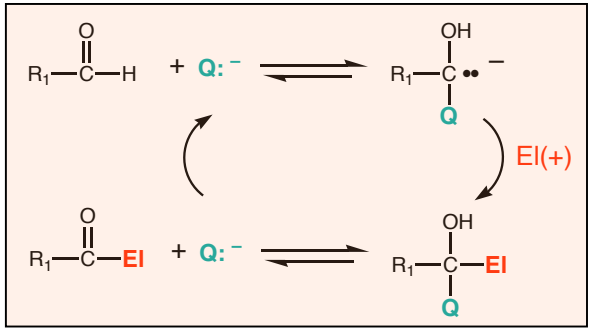

Benzoin Condensation:

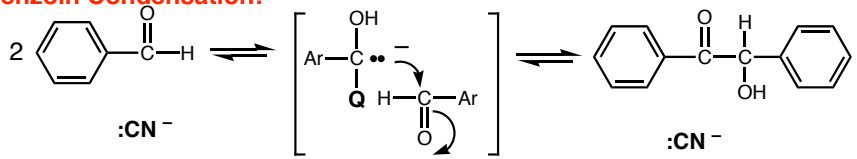

Cyanide ion is the best example of a reagent which functions as an inversion operator. The benzoin reaction is restricted to aromatic aldehydes. Why?

Nature's Inversion Operators

There is a clear need in nature to have both types of polar bond constructions exemplified by Transforms T_1 and T_2 (Eq 1-2). One such reaction is shown below.

This reaction, which is enzyme-catalyzed, requires the cofactor thiamine which functions as the inversion operator in these biological processes.

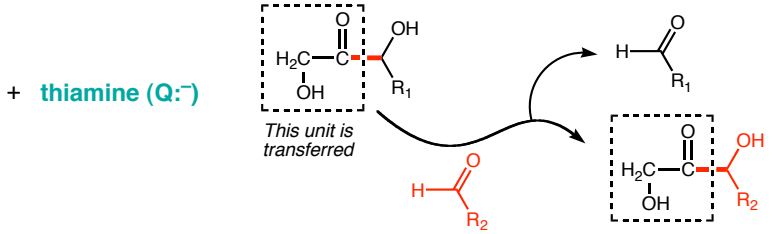

Crucial bond construction:

Related transform:

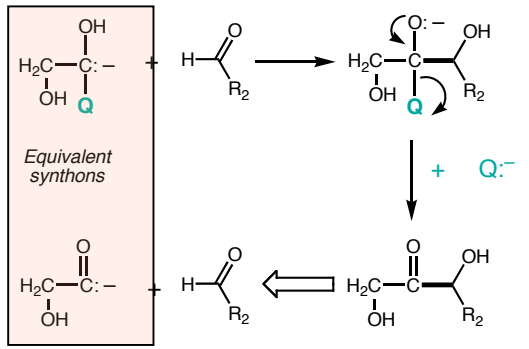

The Thiamine Coenzyme (Virtamin B_1) & how it functions

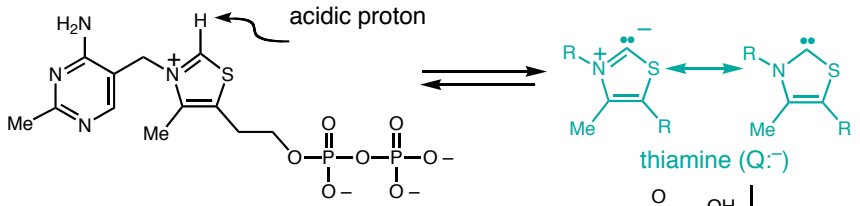

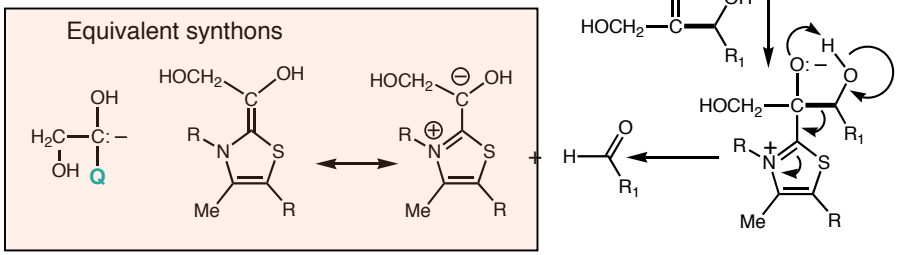

Basic Transformation:

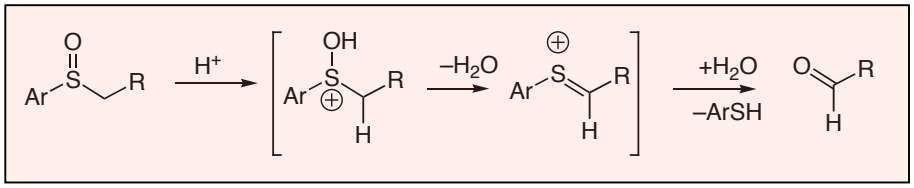

The Pummerer Rearrangement facilitates the transformation of a sulfinyl → aldehyde transformation. The rearrangement may be initiated by either a Bronsted acid or an anhydride such as trifluoroacetic anhydride (TFAA). With the latter reagent, the transformation occurs at room temperature.

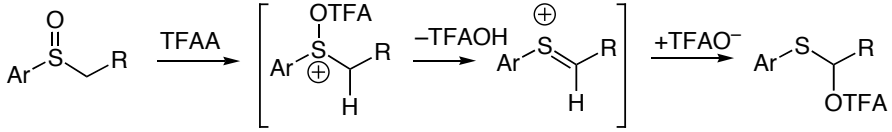

Leading References

De Lucchi, Miotti, et al. (1991). "The Pummerer reaction of sulfinyl compounds." *Organic Reactions* **1991**, *40*: 157.

Grierson, and Husson (**1991**). Polonovski- and Pummerer-type Reactions and the Nef Reaction. *Comprehensive Organic Synthesis*. Trost and Fleming. Oxford, Pergamon Press. *6*: 909.

Padwa, A., D. E. Gunn, et al. "Application of the Pummerer reaction toward the synthesis of complex carbocycles and heterocycles." *Synthesis* **1997** 1353-1377.

Carreno, "Applications of sulfoxides to asymmetric synthesis of biologically active compounds." Chem. Reviews **1995** *95*, 1717-1760.

Kita, Y. and N. Shibata (1996). "Asymmetric pummerer-type reactions induced by O-silylated ketene acetals." Synlett(4): 289-296.

The Related Polonovski Reaction:

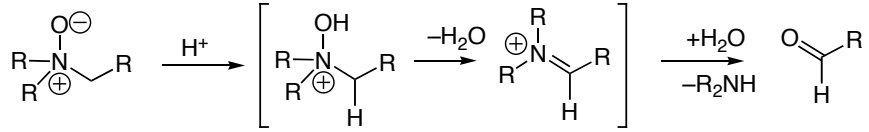

Regioselectivfity: *Depends on the relative kinetic acidy of the α protons*

Transformations Mediated by the Pummer Rearrangement

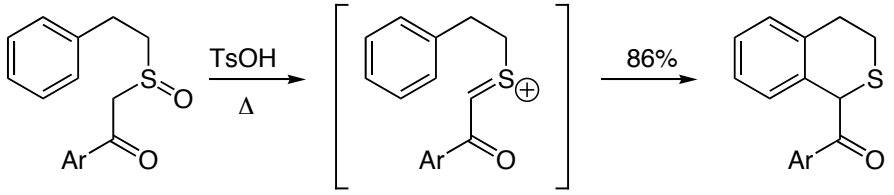

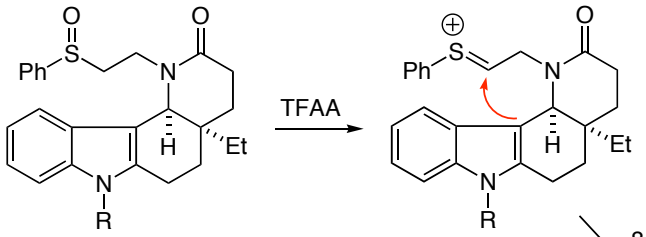

P. Magnus et al. *Accts Chem Res*. **1984**, *17*, 35

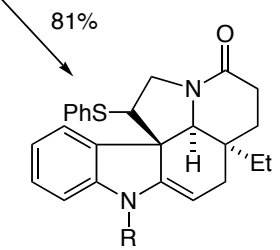

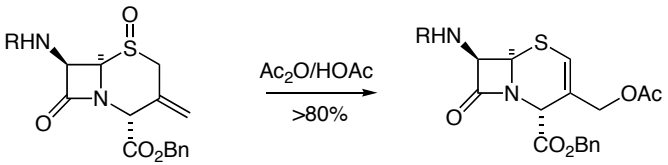

The cruel mechanistic problems that you should be prepared for in Chem 206

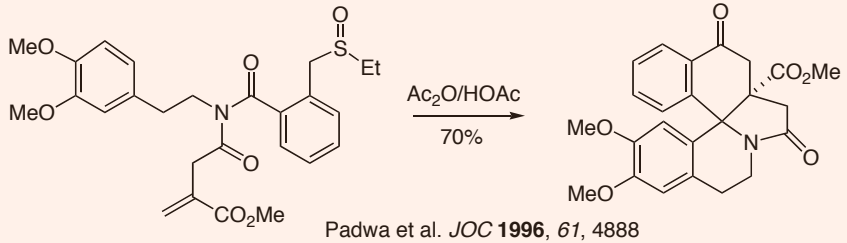

Padwa et al. *JOC* **1996**, *61*, 4888

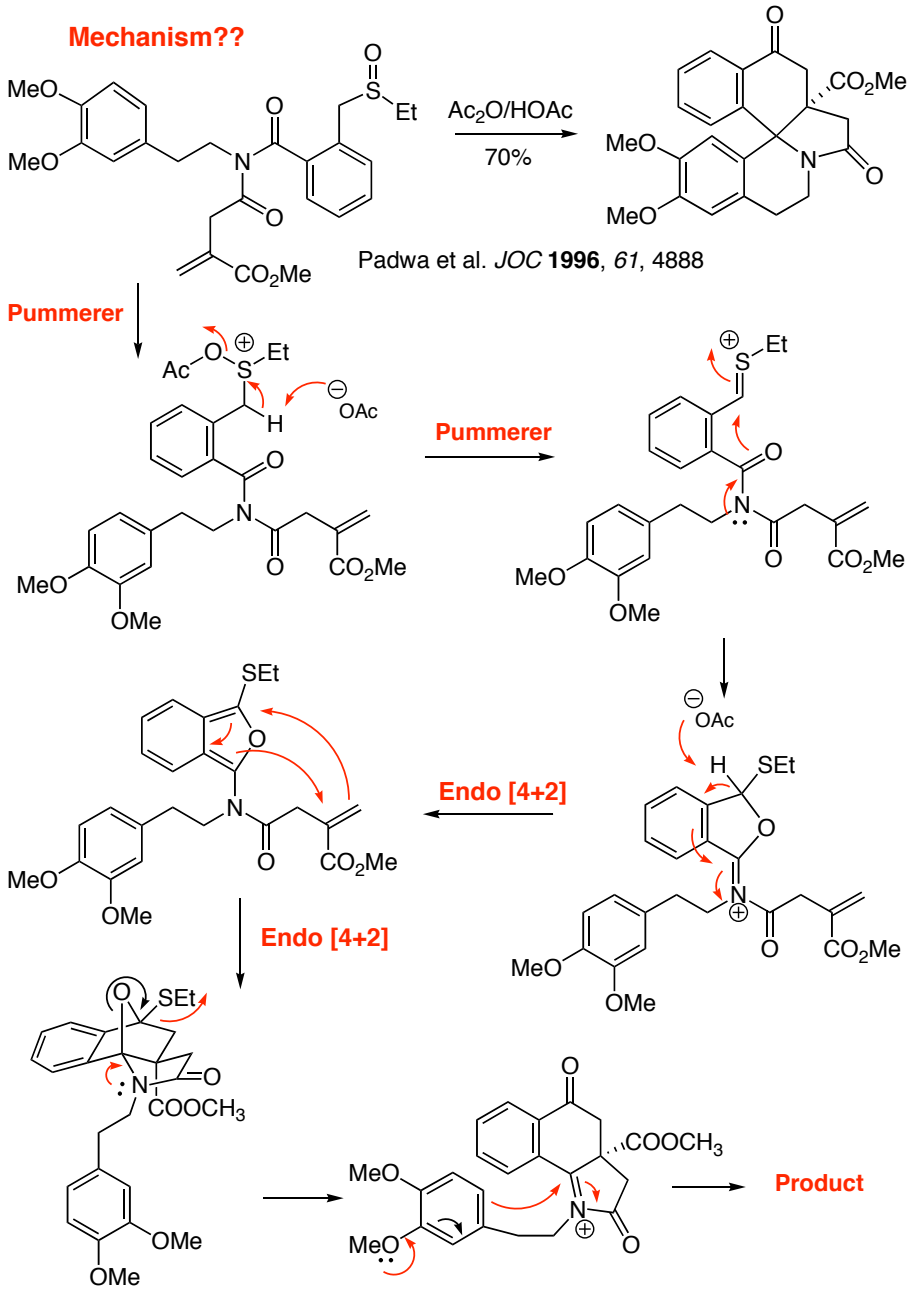

Exam 3, 2000: Question 5 (11 points). An interesting rearrangement which also results in the construction of this same ring system (Question 4) has been reported by Langlois & coworkers (*J.Org. Chem.* **1985**, *50*, 961). This rearrangement is illustrated below. Provide a mechanism for this transformation.

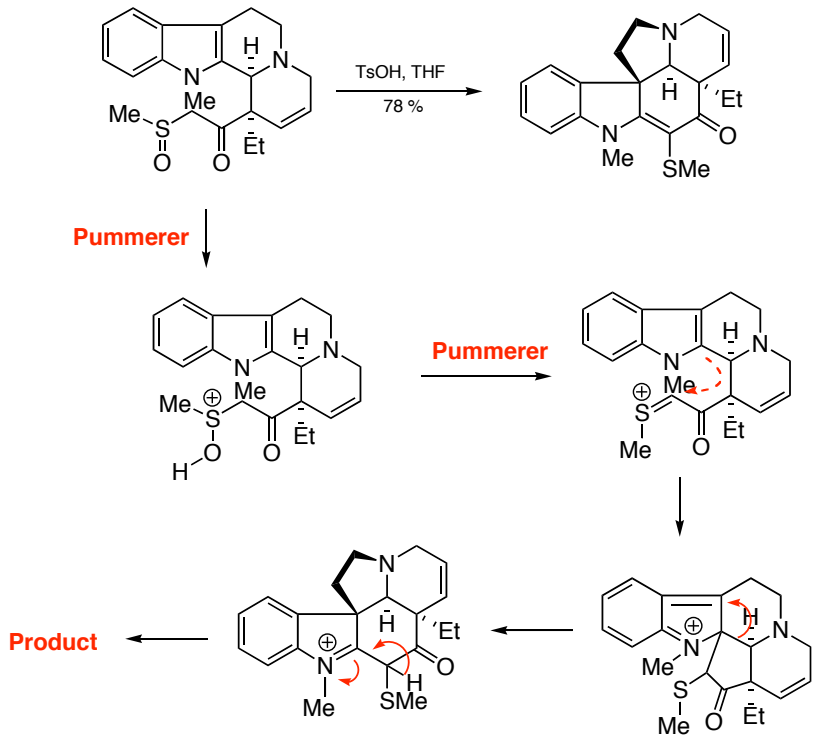

http://www.courses.fas.harvard.edu/colgsas/1063

Chemistry 206

Advanced Organic Chemistry

Lecture Number 33

Introduction to Carbonium Ions

- Carbocation Stabilization
- Carbocation Structures by X-ray Crystallography
- Vinyl & Allyl Carbonium Ions

Reading Assignment for this Lecture:

Carey & Sundberg, *Advanced Organic Chemistry*, 4th Ed. Part A Chapter 5, "Nucleophilic Substitution", 263-350 .

Birladeanu, L. (**2000**). "The Story of the Wagner-Meerwein Rearrangement." *J. Chem. Ed.* **2000**, *77*, 858. **(handout)**

Olah, G. A. (**2001**). "100 Years of Carbocations and their Significance in Chemistry." *J. Org. Chem.* **2001**, *66*, 5944-5957. **(handout)**

Walling, C. (**1983**). "An Innocent Bystander Looks at the 2-Norbornyl Cation." *Acc. Chem. Res.* **1983**, *16*, 448. **(handout)**

Laube (**1995**). "X-Ray Crystal Structures of Carbocations Stabilized by Bridging or Hyperconjugation." *Acc. Chem. Res.***1995**, *28*,: 399 **(electronic pdf)**

D. A. Evans

Monday
December 11, 2006

Other Relevant Background Reading

March, *Advanced Organic Chemistry*, 4th Ed. Chapter 5, pp165-174.
Lowery & Richardson, M*ech. & Theory in Org, Chem.*, 3rd Ed. pp 383-412.
Arnett, Hoeflich, Schriver in *Reactive Intermediates* **Vol 3**, Wiley, 1985, Chapter 5, p 189.

Saunders, M. and H. A. Jimenez-Vazquez (**1991**). "Recent studies of carbocations." Chem. Rev. 91: 375.

Stang, P. J. (**1978**). "Vinyl Triflate Chemistry: Unsaturated Cations and Carbenes." Acc. Chem. Res. 11: 107.

Olah, G. A. and G. Rasul (**1997**). "Chemistry in superacids .26. From Kekule's tetravalent methane to five-, six- and seven-coordinate protonated methanes." Acc. Chem. Res. 30(6): 245-250.

Olah, G. A. (**1995**). "My search for carbocations and their role in chemistry (Nobel lecture)." *Angew. Chem., Int. Ed. Engl.* **34**, 1393-1405

Problem 17: The reaction illustrated below was recently reported by Snider and co-workers (*Org. Lett.* **2001**, *123*, 569-572). Provide a mechanism for this transformation. Where stereochemical issues are present, provide clear three dimensional drawings to support your answer.

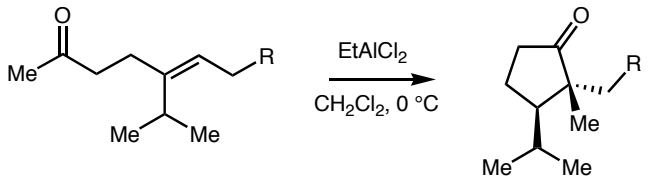

Carey & Sundberg-A, p 337: Provide mechanisms for the following reactions.

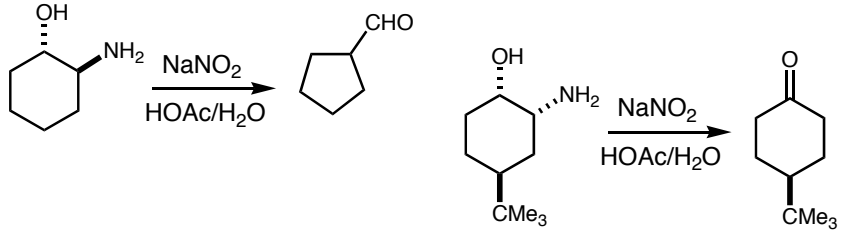

Quotes for the Day

"That man is nothing but a shyster lawyer."

Saul Winstein in reference to H. C. Brown
September, 1969

Winstein, a Canadian by birth, spent most of his professional career at UCLA, where he did research at the forefront of physical organic chemistry. He is best known for probing deeply the mechanisms of organic reactions, among them, allylic rearrangements, replacements and eliminations, using kinetics, stereochemistry, isotopic labelling and other physical methods. He developed concepts such as neighboring group participation, classical and non-classical carbocations, homoallylic and homoaromatic stabilization, tight and solvent-separated ion pairs, anchimeric assistance, and Y-values as a measure of solvent ionizing power. Winstein maintained a prodigious output of work of rigorous quality and perceptiveness, with an emphasis on logic and a search for answers to fundamental questions. He received many honors including, posthumously, the National Medal of Science.

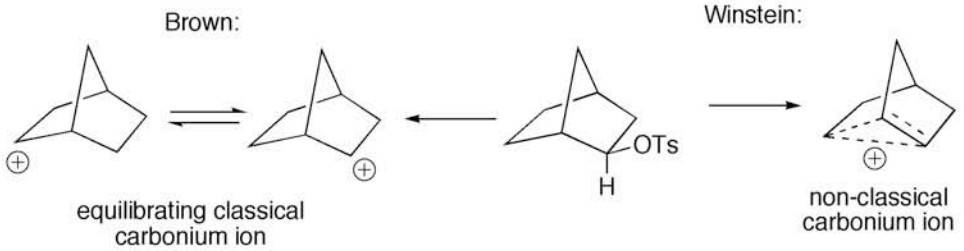

B.A., 1941, University of California (Los Angeles)
Ph.D. 1944, University of California (Los Angeles)

John D. Roberts was born in 1918.

He became Prof. at MIT and then Prof. at Caltech where he is still active. His work has been centered on mechanisms of organic reactions.

One of the joys of being a professor is when an exceptional student comes along and wants to work with you.

J.D. Roberts, The Right Place at the Right Time. p. 63.

John D. Roberts inspecting an early natural-abundance ^{13}C spectrum taken by Frank J. Weigert with the Varian DFS NMR spectrometer in

John D. Roberts graduated from the University of California at Los Angeles where he had received A. B. (hons) degree in 1941 and the Ph. D. degree in 1944. In 1945-1946 he was a National Research Council Fellow and Instructor at Harvard. Later on, he went to MIT in 1946 as an Instructor. He had introduced the terms "nonclassical" carbocations and "benzyne" into organic chemistry. He had won numerous awards; he is a member of the National Academy of Sciences (1956) and the American Philosophical Society (1974). He received the Welch Award (1990, with W. E. Doering), the National Medal of Science (1990), and the ACS Arthur C. Cope Award (1994). Since 1939 his research has been concerned with the mechanisms of organic reactions and the chemistry of small-ring compounds. His current work involves applications of nuclear magnetic resonance spectroscopy to physical organic chemistry.

Roberts made major research and pedagogic contributions to mechanistic organic chemistry. He pioneered the use of 14C and other isotopic labels to follow molecular rearrangements as, for example, in the complex and subtle solvolysis of cyclopropyl-carbinyl systems. He introduced the terms "nonclassical" carbocations and "benzyne" into organic chemistry, and used isotopic labeling to establish the intermediacy of each. Roberts was early to recognize NMR's potential, and used 1H NMR to study nitrogen inversion, long-range spin-spin coupling and conformational isomerism, and later 13C and 15N NMR to study other reactions, including the active sites of certain enzymes. Roberts' superb short books on "Nuclear Magnetic Resonance" (1959), "Spin-Spin Splitting in High Resolution NMR" (1961) and "Notes on Molecular Orbital Calculations" (1961) did much to popularize and clarify these subjects for organic chemists. His highly successful text "Basic Principles of Organic Chemistry" (1964), written with Marjorie Caserio, introduced spectroscopy early to undergraduates. Roberts received many awards, including the Roger Adams (1967) and Priestley (1987) Medals. An excellent photographer, Roberts graciously supplied several of the photographs for the MSU collection.

The Gathering at JDR's 70th Birthday Celebration

1988

Dervan, Ireland, Evans, Bergman, Grubbs, JDR, Myers, Dougherty, Hammond
Recent organic faculty at CIT, present and departed

Carbocation Subclasses

Carbon-substituted **Heteroatom–stabilized**

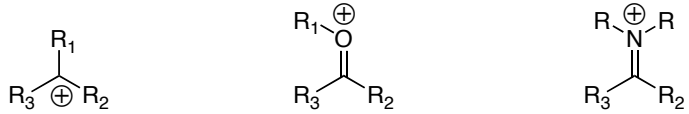

R–R_3 = alkyl or aryl R–R_3 = alkyl or aryl R–R_3 = alkyl or aryl

The following discussion will focus on carbocations unsubstitutred with heteroatoms

Classical vs nonclassical carbonium ions

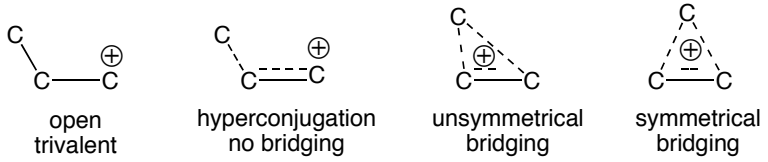

open trivalent | hyperconjugation no bridging | unsymmetrical bridging | symmetrical bridging

increasing nonclassical character →

classical **nonclassical**

Stability: Stabilization via alkyl substituents (hyperconjugation)

Order of carbocation stability: 3°>2°>1°

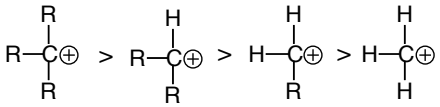

Due to increasing number of substituents capable of hyperconjugation

The relative stabilities of various carbocations can be measured in the gas phase by their affinity for hydride ion.

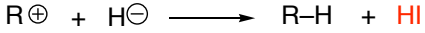

Hydride Affinity = $-\Delta G°$

ΔHI increases → C(+) stability decreases

Note: As S-character increases, cation stability decreases due to more electronegative carbon.

J. Beauchamp, *J. Am. Chem. Soc.* **1984**, *106*, 3917.

	Hydride ion affinities
CH_3^+	314
$CH_3CH_2^+$	276
$(CH_3)_2CH^+$	249
$(CH_3)_3C^+$	231
$H_2C{=}CH^+$	287
$H{-}C{\equiv}C^+$	386
$PhCH_2^+$	239

Carey & Sundberg–**A**, pp 276-

Hydride ion affinities (HI)

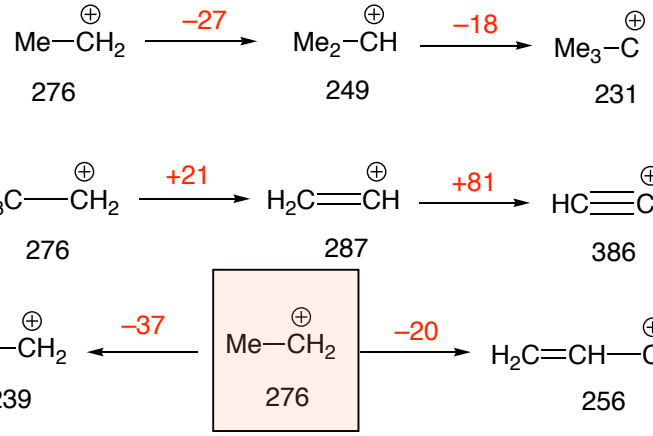

The effect of beta substituents: Rationalize

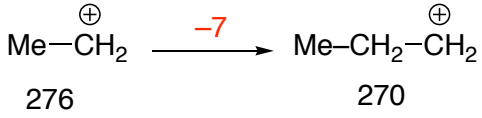

Hydride ion affinities versus Rates of Solvolysis

	$PhCH_2$–Br	CH=CH–CH_2–Br	Me_2CH–Br
rel rate	100	52	0.7
HI	239	256	249
Δ-HI	0	+17	+10

Relative Solvolysis rates in 80% EtOH, 80 °C

A. Streitwieser, *Solvolytic Displacement Reactions*, p75

Conclusion:
Gas phase stabilities do not always correlate with rates of solvolysis

Carbocation Stability: The pK_{R+} value

Definition: $R^+ + H_2O \rightleftharpoons ROH + H^+$

$$K_{R+} = \frac{a_{ROH} \cdot a_{H+}}{a_{R+} \cdot a_{H2O}}$$ a = activity

$$pK_{R+} = -\log K_{R+}$$ Carey & Sundberg, A, p 277

***Table*: pK_{R+} values of some selected carbenium salts**

$(4\text{-MeO-}C_6H_4)_3C^+$	Ph_3C^+	$(3\text{-Cl-}C_6H_4)_3C^+$	Ph_2CH^+	*least stable*
0.82	– 6.63	– 11.0	– 13.3	
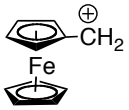	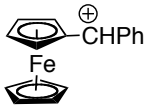	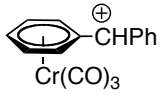	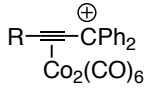	
0.40	0.75	–10.4	–7.4	
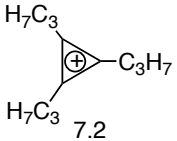		*most stable*		
7.2	4.77			

Carey & Sundberg, A, pp 276-

Carbocation Generation

Hydride abstraction from neutral precursors

$$R_3C{-}H + \text{Lewis-Acid} \longrightarrow R_3C^+$$

$R_3C{-}H$ = 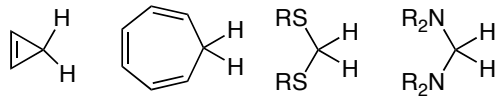 etc.

Lewis-Acid: $Ph_3C^+\ BF_4^-$, BF_3, PCl_5

Removal of an energy-poor anion from a neutral precursor via Lewis Acids

$$R_3C{-}X + \mathbf{LA} \longrightarrow R_3C^+ + LA{-}X^-$$

LA: Ag , $AlCl_3$, $SnCl_4$, $SbCl_5$, **SbF_5**, BF_3, $FeCl_3$, $ZnCl_2$, PCl_3, PCl_5, $POCl_3$ ...
X: F, Cl, Br, I, OR

Acidic dehydratization of *secondary* and *tertiary* alcohols

$$R_3C{-}OH + H{-}X \xrightarrow{-H_2O} R_3C^+ + X^-$$

R: Aryl + other charge stabilizing substituents
X: SO_4^{2-}, ClO_4^-, FSO_3^-, $CF_3SO_3^-$

From neutral precursors via heterolytic dissociation (solvolysis) - First step in S_N1 or E1 reactions

$$R_3C{-}X \xrightarrow{\text{solvent}} R_3C^+ + X^-$$

Ability of X to function as a leaving group:
$-N_2^+ > -OSO_2R' > -OPO(OR')_2 > -I \geq -Br > Cl > OH_2^+$ ...

Addition of electrophiles to π-systems

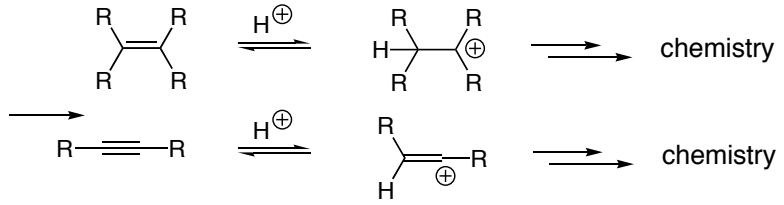

Problem 897: Provide a Mechanism of this transformation

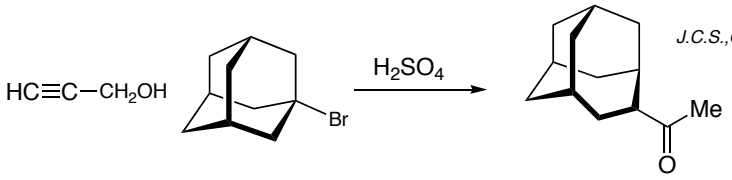

J.C.S.,CC **1971**, 556

Carbocation Stabilization Through Hyperconjugation

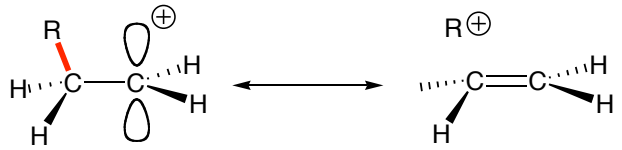

■ **FMO Description**

Take linear combination of σ C–R (filled) and C p_z-orbital (empty):

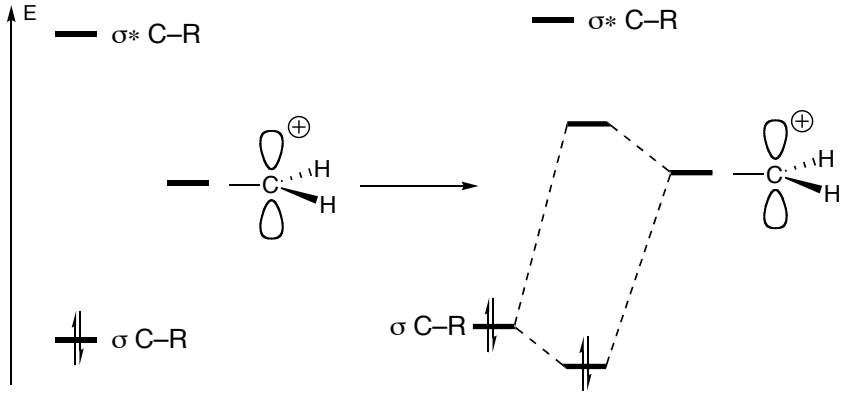

Syn-planar orientation between interacting orbitals

C–H versus C–C Hyperconjugation: The t-Pentyl Cation

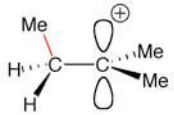

Calculated carbocation agrees with solution structure

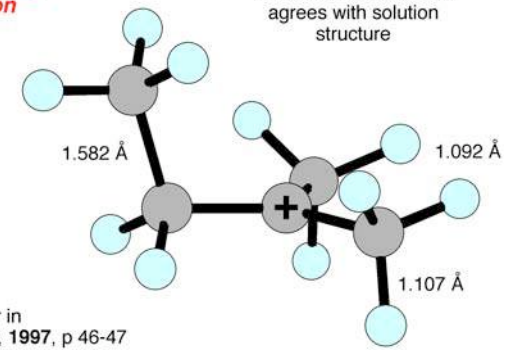

R. P von Schleyer in *Stable Carbocation Chemistry*, **1997**, p 46-47

Physical Evidence for Hyperconjugation: The Adamantyl Cation

Bonds participating in the hyperconjugative interaction, e.g C–R, will be lengthened while the C(+)–C bond will be shortened.

First X-ray Structure of an Aliphatic Carbocation

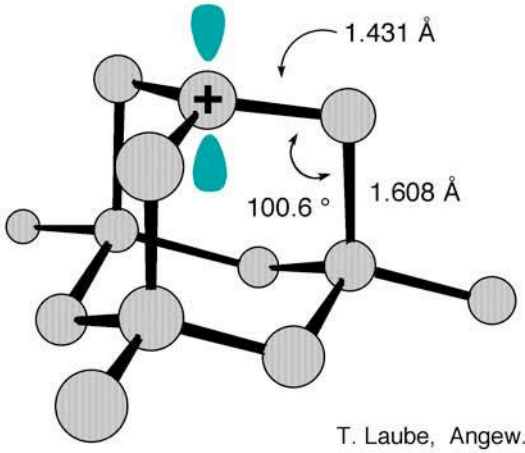

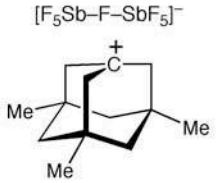

T. Laube, Angew. *Chem. Int. Ed.* **1986**, *25*, 349

The Adamantane Reference (MM-2)

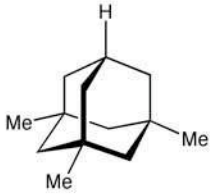

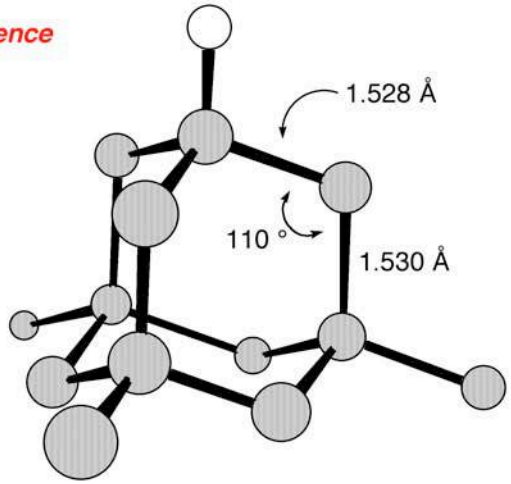

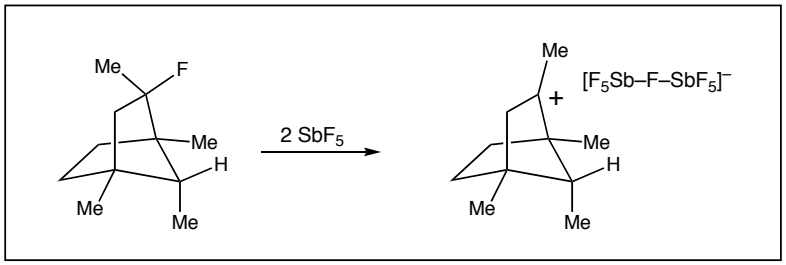

T. Laube, Angew. *Chem. Int. Ed.* **1987**, *26*, 560

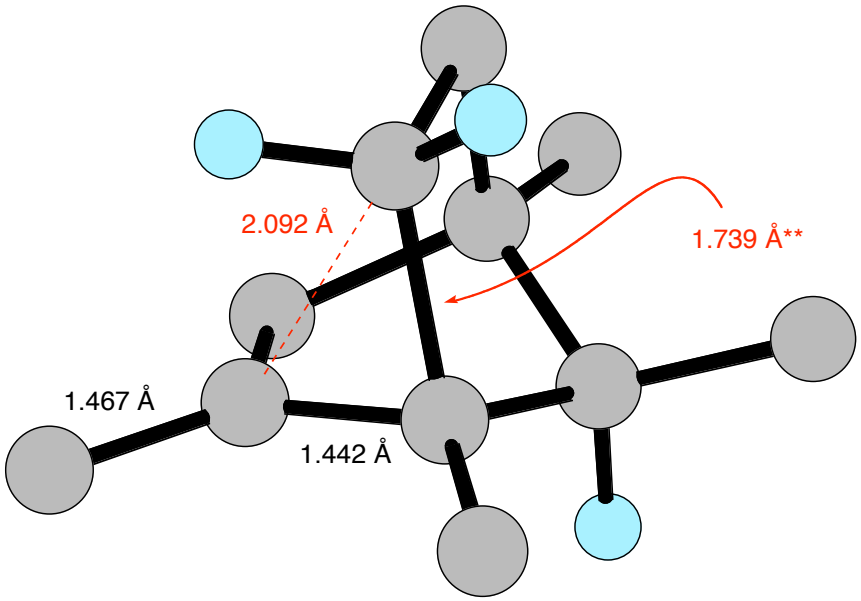

**One of the longest documented C–C bond lengths.

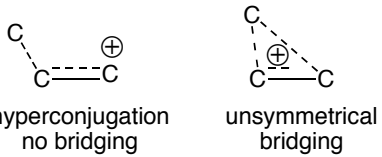

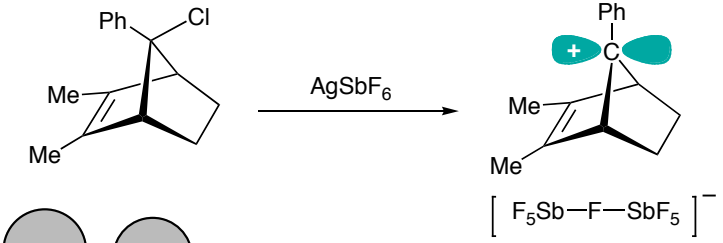

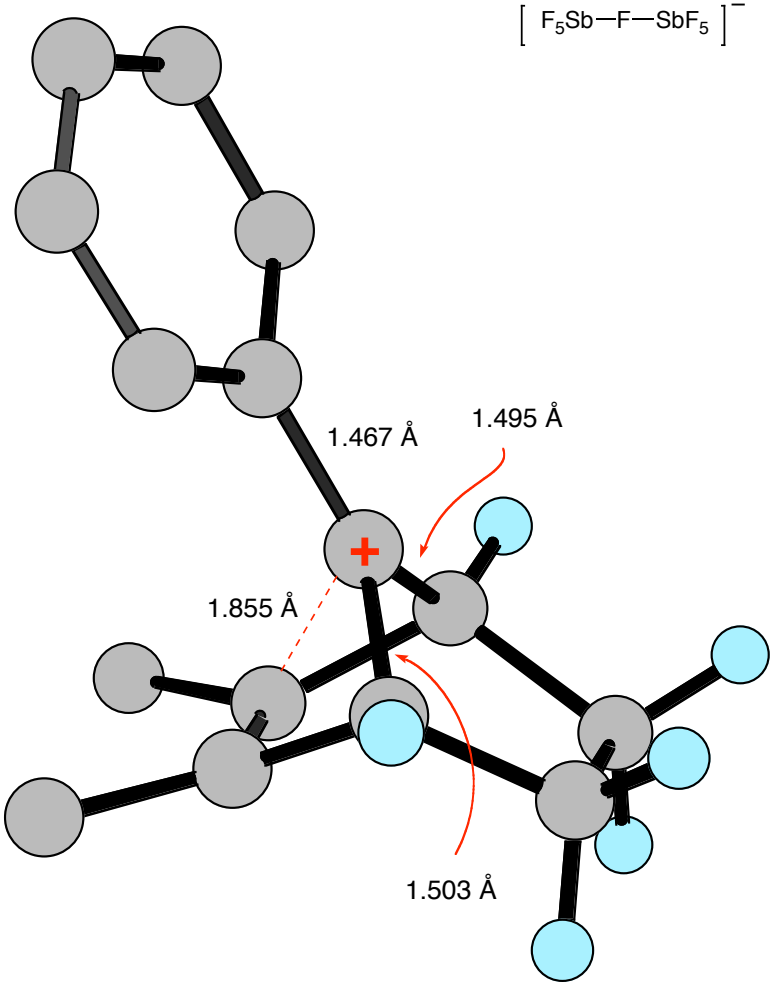

T. Laube, *JACS* **1989**, *111*, 9224

Carbonium Ion X-ray Structures: A Summary

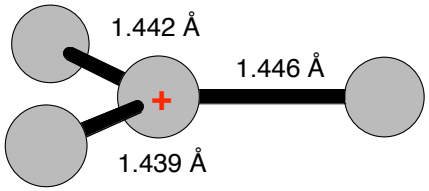

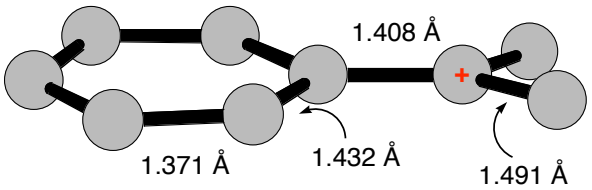

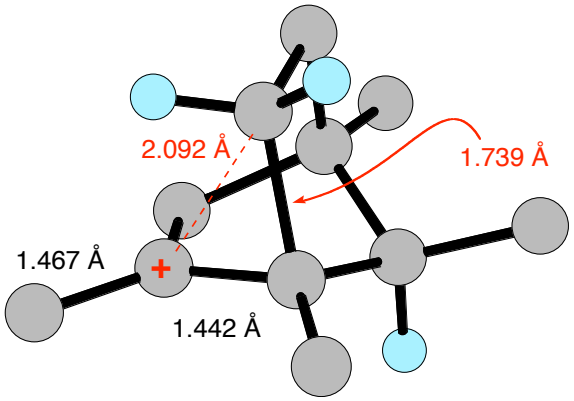

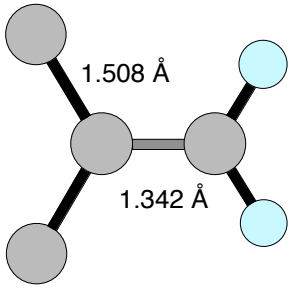

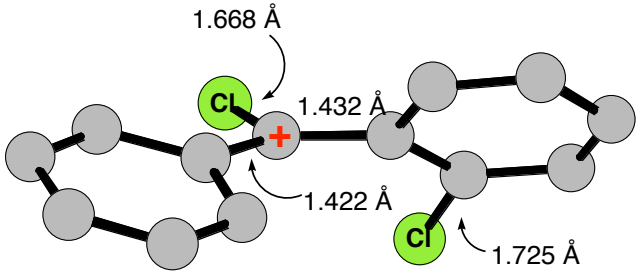

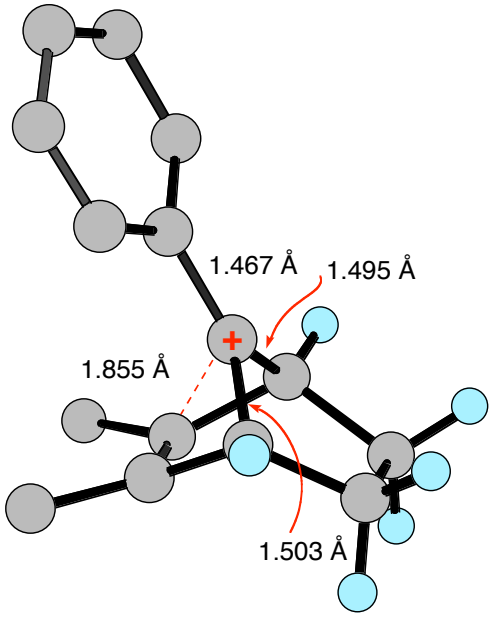

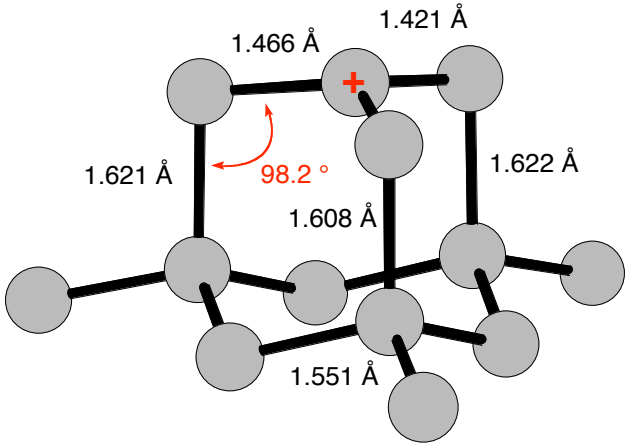

Nomenclature: classical vs nonclassical

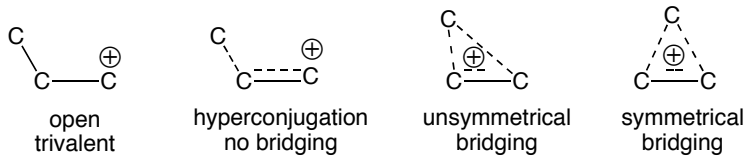

increasing nonclassical character →

classical — **nonclassical**

Substitution Reactions

Substitution (S_N1)

Favorable

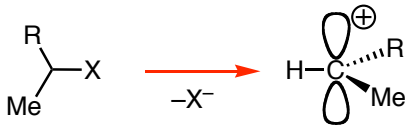

Unfavorable

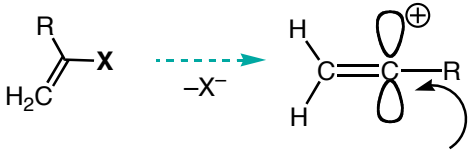

Sp hybridized Carbon
is more electronegative

CSp2 Carbonium Ions do exist!

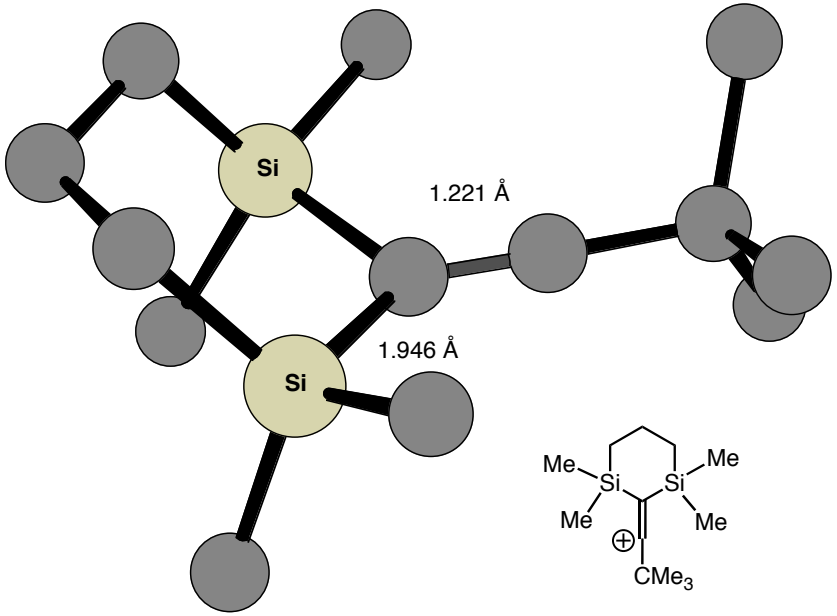

Normal CC triple bond lengths are ~1.21 Å

Angew. Chem. Int. Ed. **2004**, *43*, 1543–1546

Vinyl Cations

The X-ray Structure of a Vinyl Cation**

Thomas Müller, Mark Juhasz, and*
*Christopher A. Reed**

Dedicated to Prof. Yitzhak Apeloig
on the occasion of his 60th birthday.

Vinyl cations,[1] the dicoordinated unsaturated analogues of trivalent carbenium ions, were first detected by Grob and co-workers in the early 1960s in solvolysis reactions of α-aryl vinyl halides.[2] In the 1970s numerous investigations established vinyl cations as reaction intermediates in solvolysis reactions of activated alkenyl halides[3] and in reactions of electrophiles with alkynes.[4] The direct NMR detection of

ture.[5] We report herein the X-ray structure of the β-silyl substituted vinyl cation **1**, which provides the first direct experimental structural information about this important class of reaction intermediates.[6] In addition, the molecular structure of cation **1** gives direct structural evidence for the occurrence of β-silyl hyperconjugation in carbocations.[7]

Vinyl cation **1** was prepared by reaction of the alkynylsilane **2** with trityl ion as described previously for related cations (see Scheme 1).[8] The counterions were either tetra-

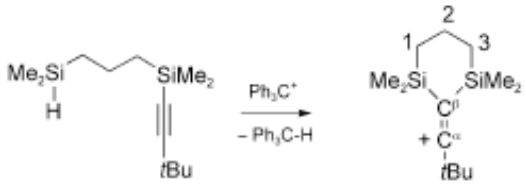

Scheme 1. Synthesis of vinyl cation **1**.

Vinyl & Phenyl Cations: Highly Unstable

Evidence suggests that vinyl cations are linear.

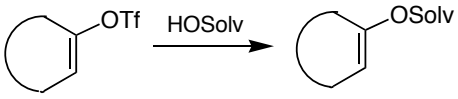

As ring size decreases, the rate of hydrolysis also diminishes. Implying that the formation of the linear vinyl cation is disfavored due to increasing ring strain.

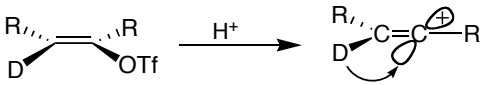

Hyperconjugation

A secondary kinetic isotope effect was measured to be K_H/K_D = 1.5 (quite large) indicating strong hyperconjugation and an orientation of the vacant p orbital as shown above.

P. J. Stang *J. Am. Chem Soc.* **1971**, *93*, 1513; P. J. Stang *J.C.S. PT II* **1977,** 1486.

Hydride ion affinities (HI)

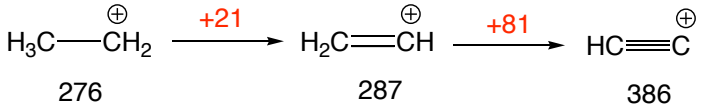

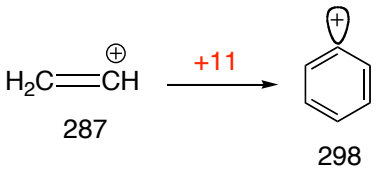

Phenyl Cations

The ring geometry opposes rehybridization (top) so the vacant orbital retains sp^2 character. Additionally, the empty orbital lies in the nodal plane of the ring, effectively prohibiting conjugative stabilization.

Allyl & Benzyl Carbocations

Carbocation Stabilization via π-delocalization

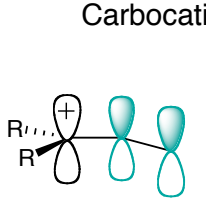

allyl cation

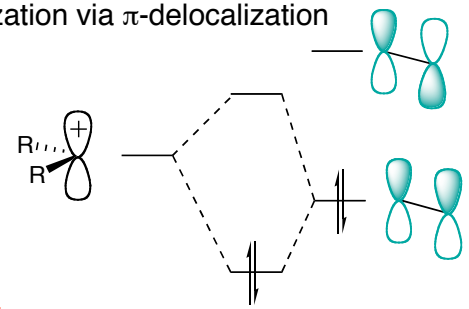

■ Stabilization by Phenyl-groups

The Benzyl cation is approximately as stable as a t-Butylcation.

	ΔH^0_r [kcal/mol]
$(CH_3)_3C^{\oplus}$ + $PhCH_3$ ⇌ $(CH_3)_3CH$ + $PhCH_2^{\oplus}$	3.8
$(CH_3)_3C^{\oplus}$ + $PhCH_2Cl$ ⇌ $(CH_3)_3CCl$ + $PhCH_2^{\oplus}$	– 0.8

Hydride ion affinities (HI)

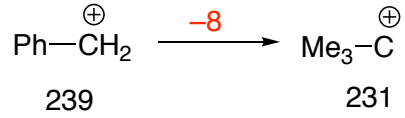

Hydride ion affinities versus Rates of Solvolysis

	$PhCH_2$–Br	Me_2CH–Br	$CH{=}CH{-}CH_2$–Br
	100	0.7	52
HI	239	249	256
Δ-HI	0	+10	+17

Relative Solvolysis rates in 80% EtOH, 80 °C

A. Streitwieser, *Solvolytic Displacement Reactions*, p75

Volkman, Andrews, Johnson, *JACS* 1975, *97*, 4777

The plan (According to Volkman):

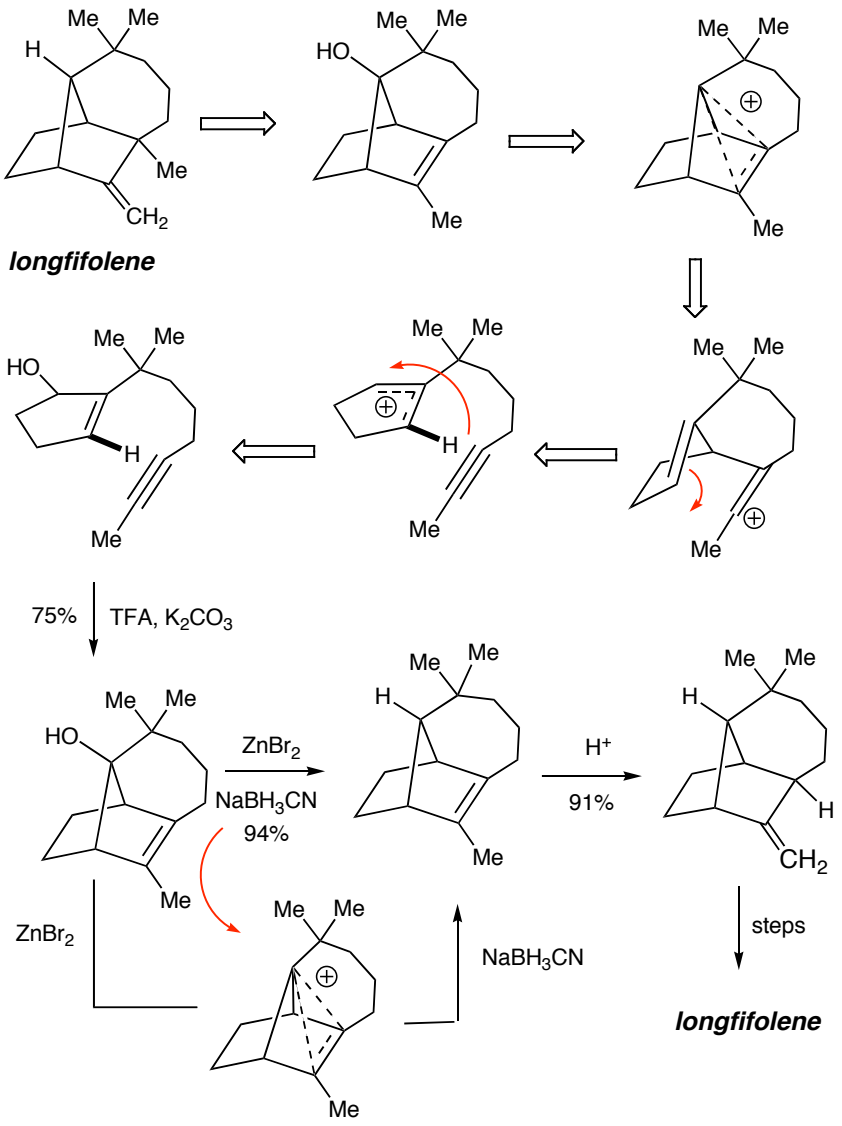

Ho, Nouri, Tantillo, *JOC* 2005, *70*, 5139-5143

The Cationic Cascade Route to Longifolene

W. S. Johnson's total synthesis of the sesquiterpenoid longifolene is a classic example of the power of cationic polycyclizations for constructing complex molecular architectures. Herein we revisit the key polycyclization step of this synthesis using hybrid Hartree-Fock/density functional theory calculations and validate the feasibility of Johnson's proposed mechanism. We also explore perturbations to the 3-center 2 electron bonding array in a key intermediate that result from changing the polycyclic framework in which it is embedded.

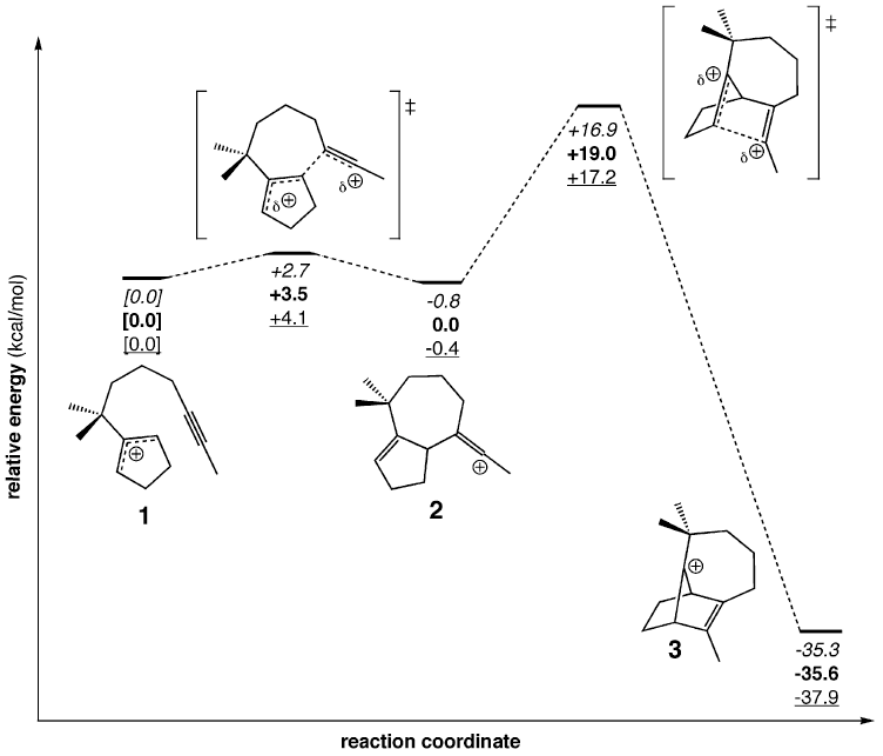

FIGURE 1. Relative energies (kcal/mol) of stationary points for the mechanism shown in Scheme 2 (B3LYP/6-31G(d) zero-point corrected energies in italics, B3LYP/6-31G(d) free energies at 0 °C in bold, and CPCM-B3LYP/6-31G(d) energies in water underlined).

Carbocation Stabilization via Cyclopropylgroups

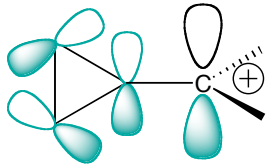

See Lecture 5, slide 5-05 for discussion of Walsh orbitals

A rotational barrier of about 13.7 kcal/mol is observed in following example:

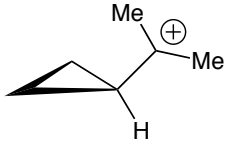

NMR in super acids
$\delta(CH_3)$ = 2.6 and 3.2 ppm

X-ray Structures support this orientation

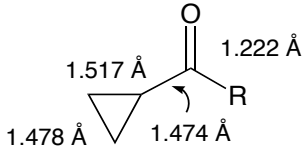

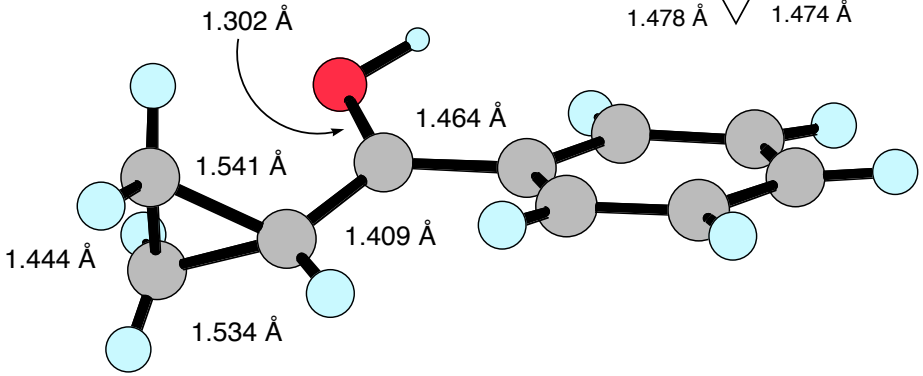

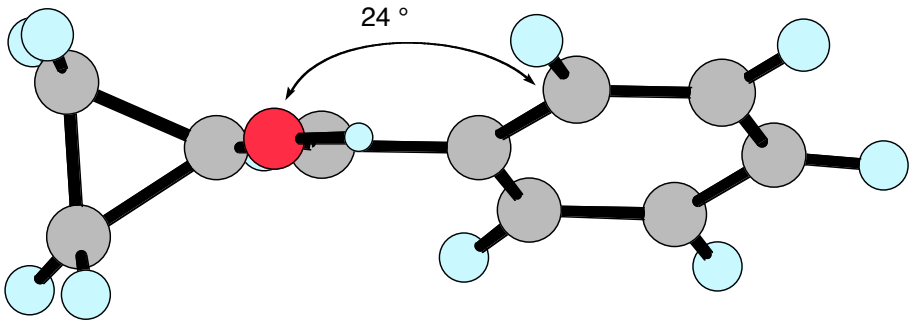

R. F. Childs, *JACS* **1986**, *108*, 1692

Solvolysis rates represent the extend of that cyclopropyl orbital overlap contributing to the stabiliziation of the carbenium ion which is involved as a reactive intermediate:

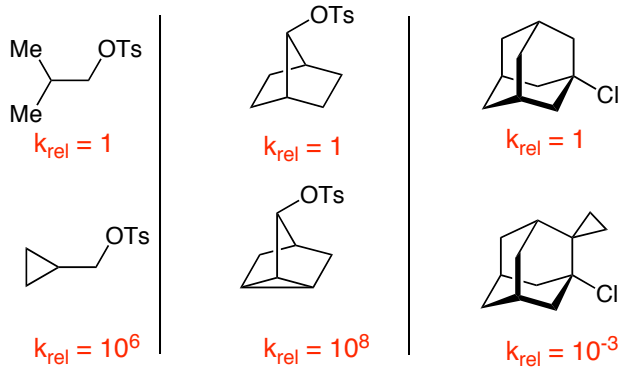

Why??

Carey–A, p 286

Bridgehead Carbocations

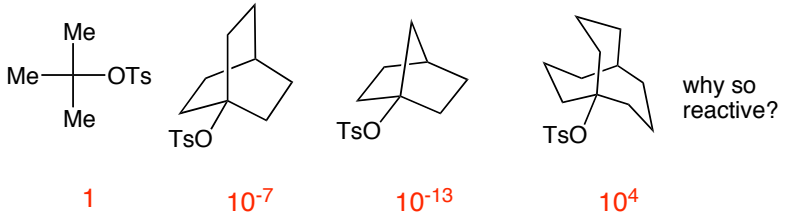

Bridgehead carbocations are highly disfavored due to a strain increase in achieving planarity. Systems with the greatest strain increase upon passing from ground state to transition state react slowest.

why so reactive?

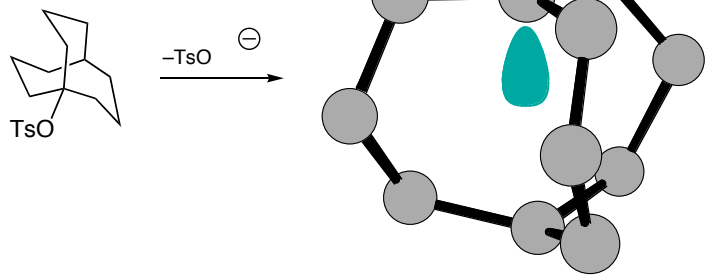

"The Synthesis and Isolation of Stable Hypervalent Carbon Compound (10-C-5) Bearing a 1,8-Dimethoxyanthrecene Ligand"

Akibe, et al. *JACS* **1999**, *121*, 10644-10645

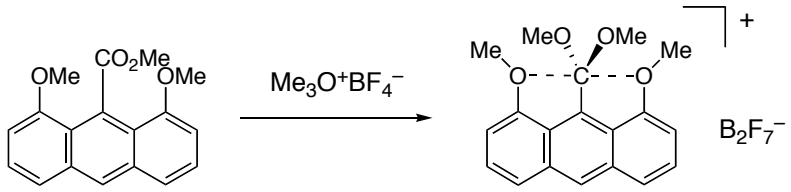

"The relevant C–O distances are longer than a covalent C–O bond (1.43 Å) but shorter than the sum of the van der Waals radii (3.25 Å)."

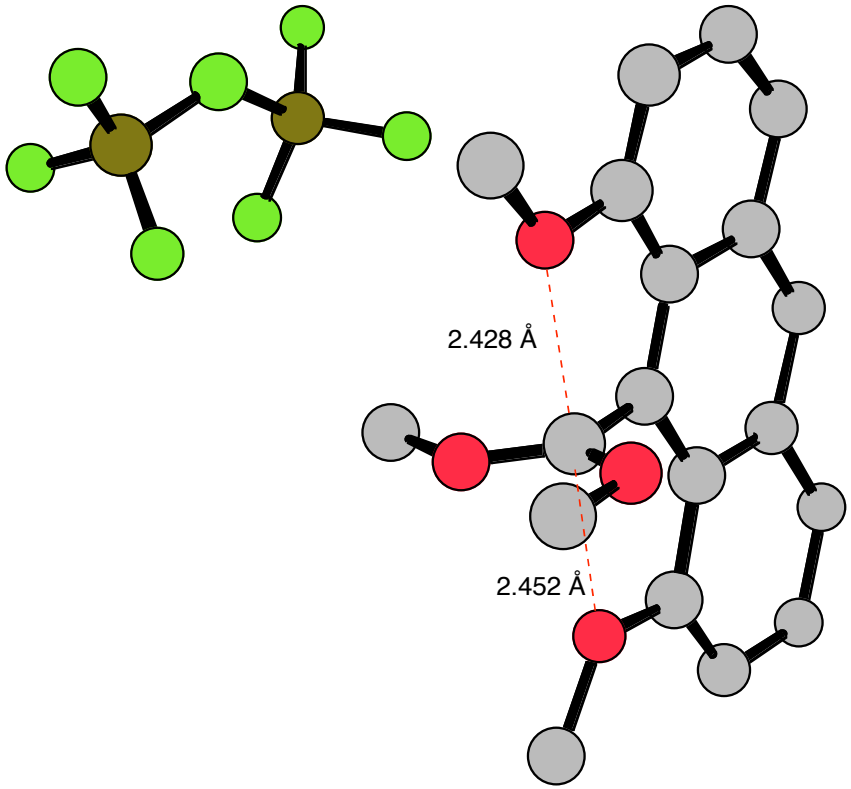

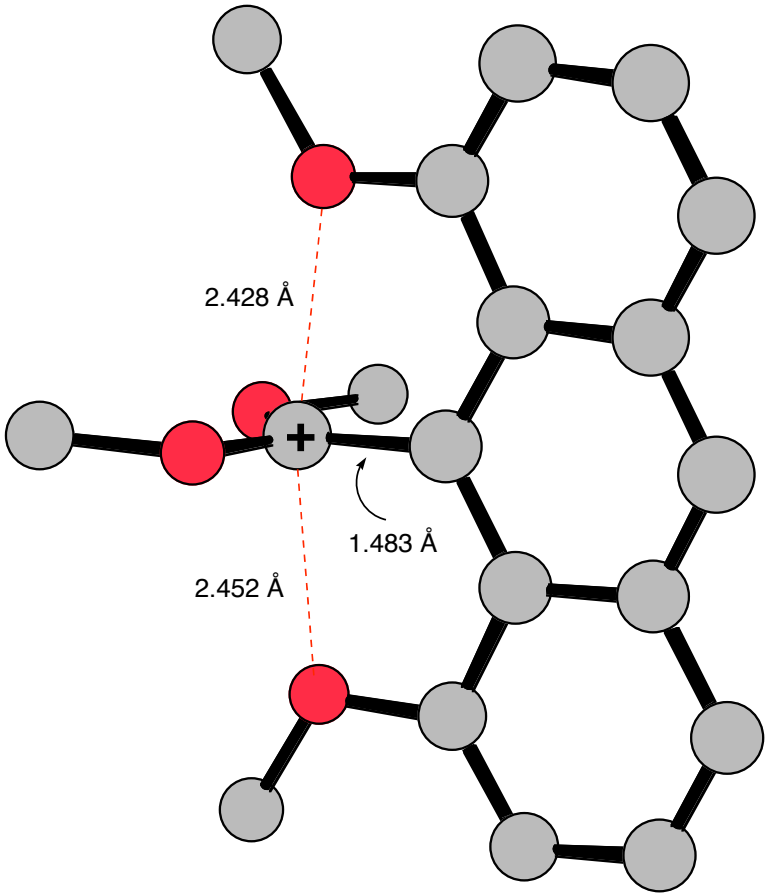

For a recent monograph on hypervalent Compounds see:
"Chemistry of Hypervalent Compounds", K. Akiba, Wiley-VGH, 1999

http://www.courses.fas.harvard.edu/colgsas/1063

Chemistry 206

Advanced Organic Chemistry

Lecture Number 34

Introduction to Carbonium Ions–2

- Allyl- & Vinylsilanes: The β-Silicon Effect
- Carbonium Ion Rearrangements

Reading Assignment for this Lecture:

Carey & Sundberg, *Advanced Organic Chemistry*, 4th Ed. Part A Chapter 5, "Nucleophilic Substitution", 263-350 .

Birladeanu (**2000**). "The Story of the Wagner-Meerwein Rearrangement." *J. Chem. Ed. 77*: 858. **(handout)**

Lambert, (**1999**). "The β effect of silicon and related manifestations of σ conjugation." *Acc. Chem. Res. 32*, 183-190. **(handout)**

Saunders, M. and H. A. Jimenez-Vazquez (**1991**). "Recent studies of carbocations." *Chem. Rev.* 91: 375.

D. A. Evans

Wednesday
December 13 , 2006

Problem 56: Here is a typical carbonium ion question that you should be able to handle by the end of the course. Write out a mechanism for the following transformation.

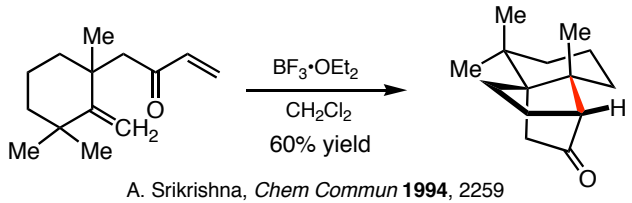

A. Srikrishna, *Chem Commun* **1994**, 2259

Problem 79: In a synthesis of taxusin, the pivotal reaction(s) which generated the bicyclo [5.3.1.] undecane ring system charactertistic of this family of terpenoids are illustrated below. Given the illustrated transformation, what specific reagents would you employ to carry out this process.

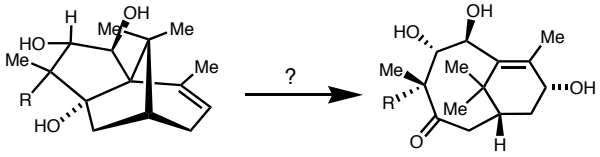

Holton & Co-workers, *JACS*, **110**, 6558 (1988).

Problem 185: **Final Exam, 1999.** During Corey's synthesis of Aspidophytine (*JACS*, **1999**, *121*, 6771), the pivotal intermediate **3** was assembled by the union of **1** and **2** under the specified conditions. Provide a mechanism for this single-pot transformation.

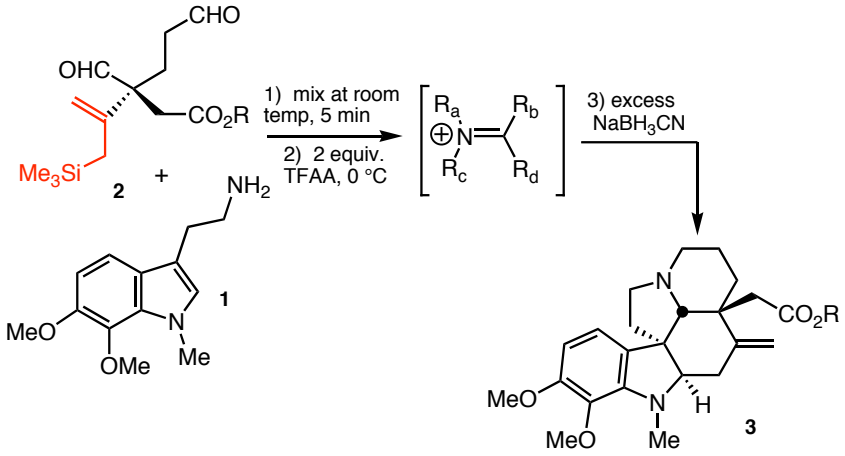

Carbocation [1,2] Sigmatropic Rearrangements

1,2 Sigmatropic shifts are the most commonly encountered cationic rearrangements. When either an **alkyl** substituent or a **hydride** is involved, the term **Wagner-Meerwein shift** is employed to identify this class of rearrangments.

Birladeanu (**2000**). "The Story of the Wagner-Meerwein Rearrangement." J. Chem. Ed. 77: 858. **(handout)**

Stereoelectronic requirement for migration....

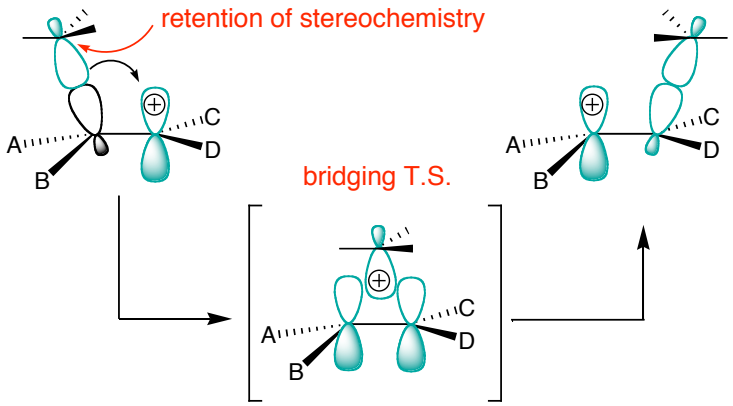

2-electron Huckel transition state

If **migration accompanies ionization**, the migration terminus will be **inverted**. Overlap between the σ C-C (migration origin) and the σ* C-X (migration terminus) will be maximized in an **antiperiplanar** arrangement.

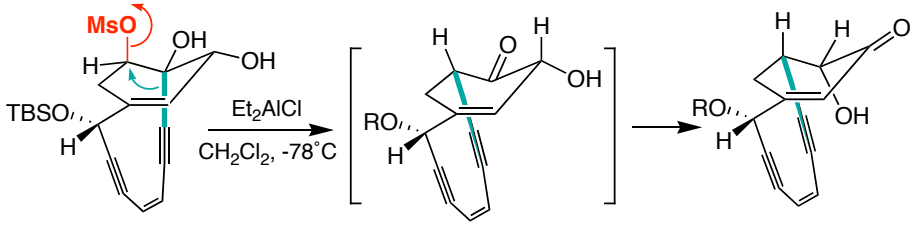

S. L. Schreiber et al *Tetrahedron Lett.* **1989**, *30*, 3765.

Pinacol rearrangement (vicinal diol): Driving force is the gen. of C=O

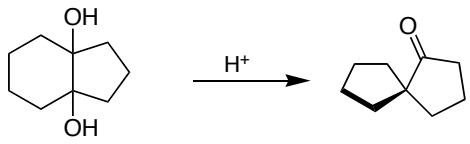

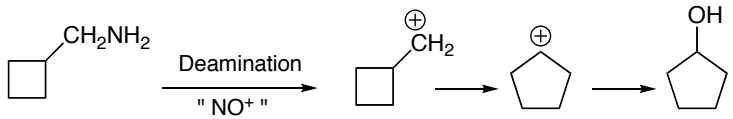

Demjanov-rearrangement (Driving force: relief of ring strain)

Wagner-Meerwein Rearrangements: Application in Total Synthesis

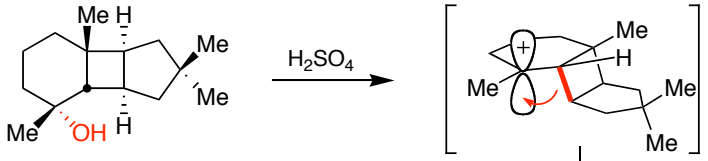

A

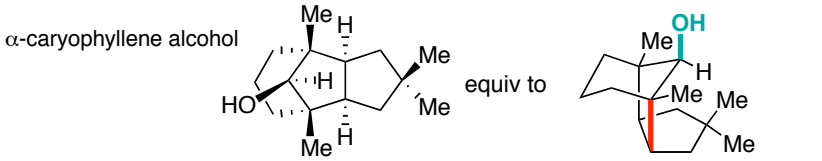

Preparation of A:

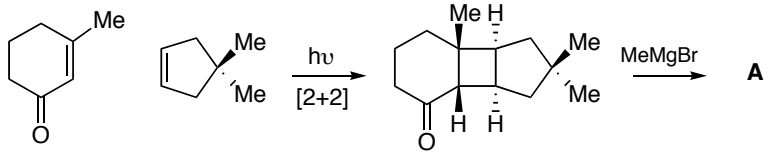

E. J. Corey *JACS* **1964**, *86*, 1652 **(electronic handout).**

Synthesis of (±)-Isocomene: Pirrung, *JACS* **1979**, 7130; *1981*, 82.

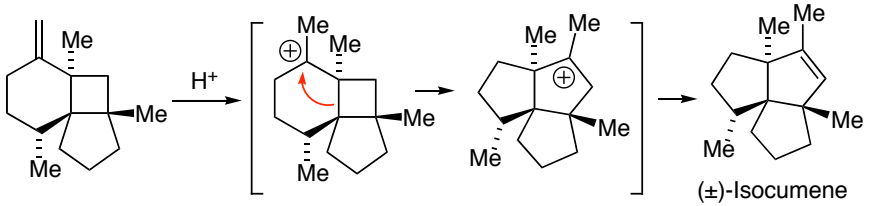

Carbocations: Neighboring Group Participation

Groups with accessable electron density (heteroatoms, arenes) and the correct stereoelectronic orientation (anti-periplanar) can "assist" in the ionization of a leaving group.

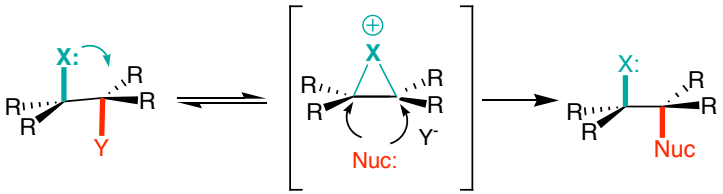

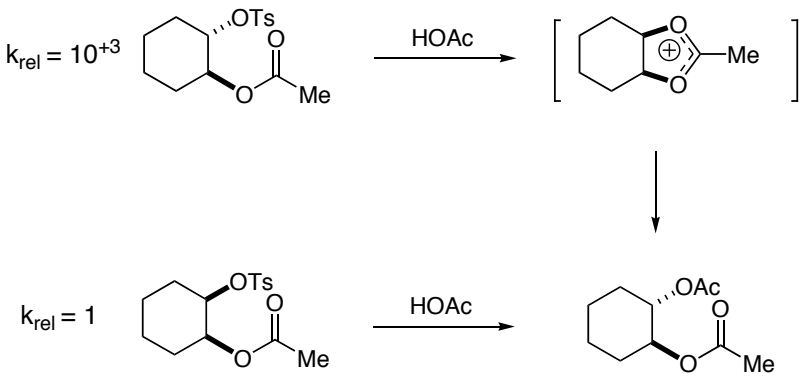

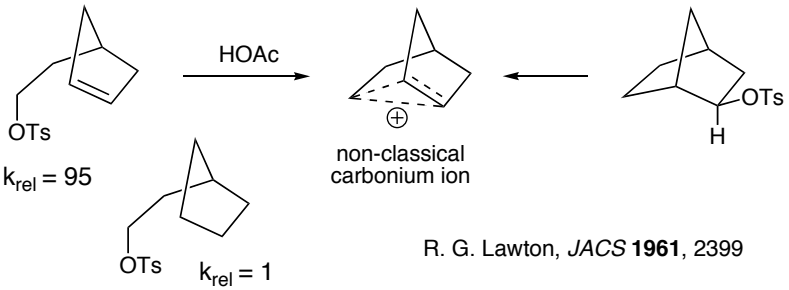

R. G. Lawton, *JACS* **1961**, 2399

The Cram Phenonium Ion Experiments: Cram, *JACS* **1949**, *71*, 3865

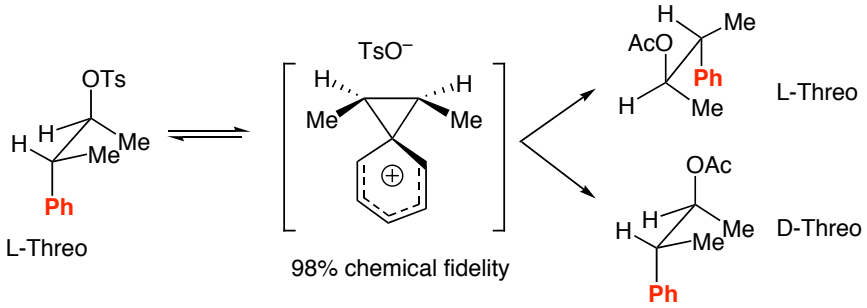

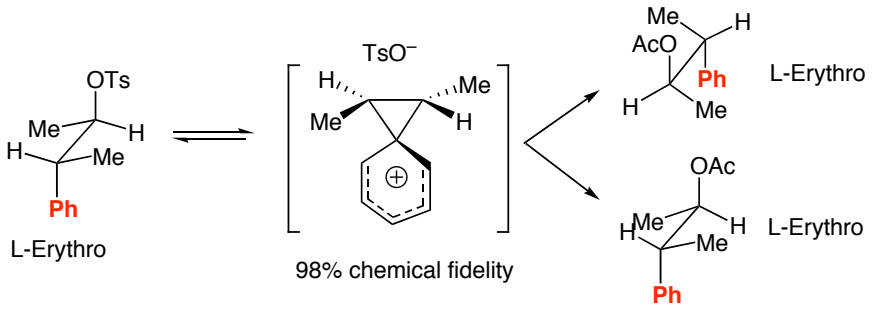

Donald J.Cram (1919–2001)

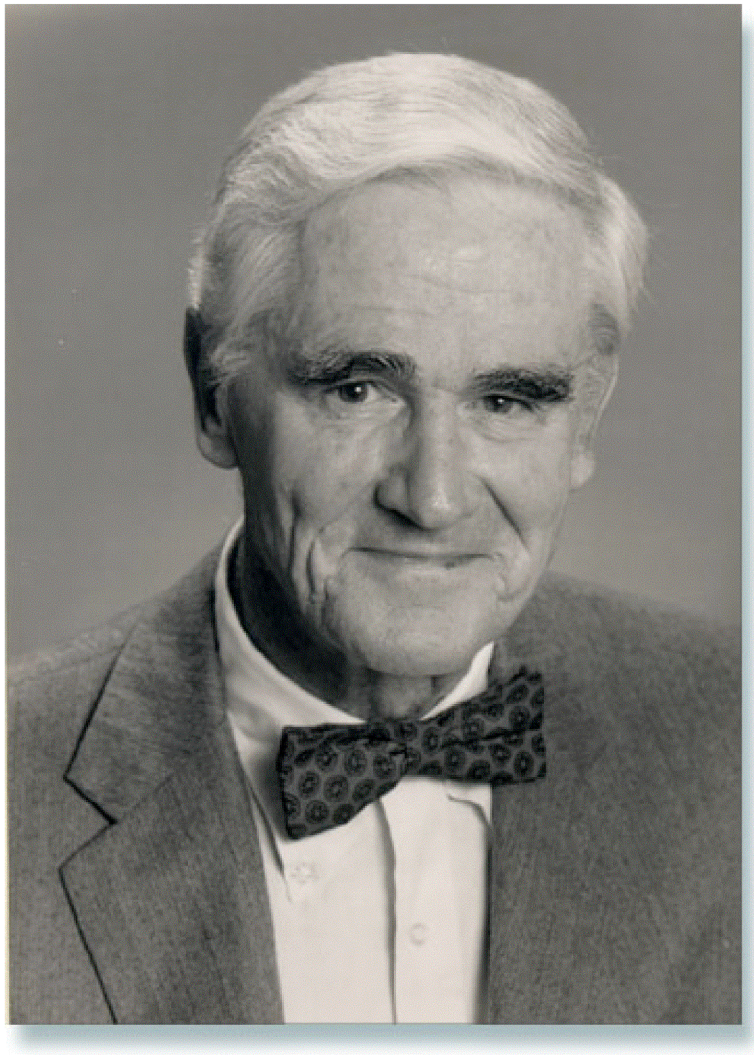

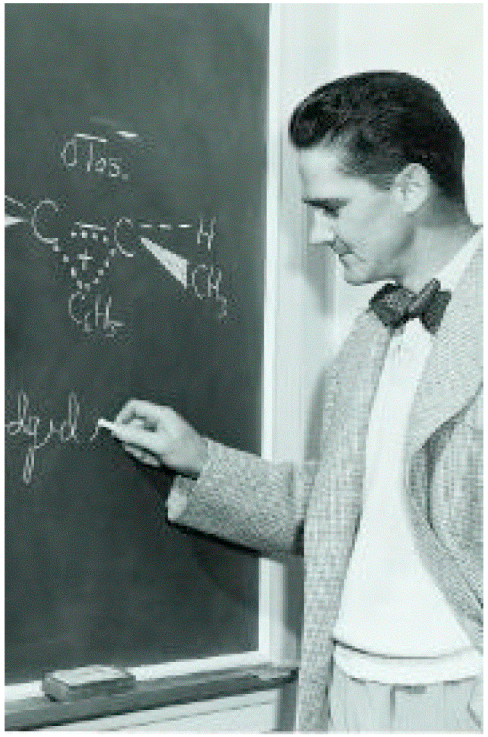

Phenonium Ion Experiments: Cram, *JACS* **1949**, *71*, 3865

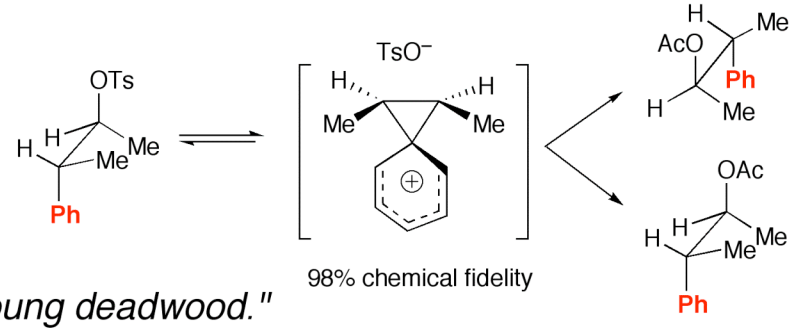

98% chemical fidelity

Cram: *"Just remember Dave, old deadwood is better than young deadwood."*

"A View from the Far Side. Memorable Characters and Interesting Places." Evans, D. A. *Tetrahedron* **1999**, *55*, 8589-8608.

Allyl- & Vinylsilanes: The β-Silicon Effect

References:

Lambert *Acc. Chem. Res.* **1999**, *32*, 183-190
Lambert, *JACS* **1990**, *112*, 8120; **1996**, *118*, 7867.
Fleming, *Organic Reactions* **1989**, *37*, 54.
Fleming, *Chem. Rev.*, **1997**, 2063.

Allyl– & Vinylsilanes react with electrophiles

(trapped by solution Nu)

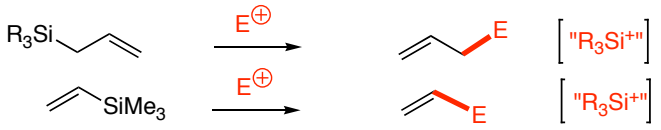

Mechanism - the simple picture: β-Silicon stabilizes carbocation

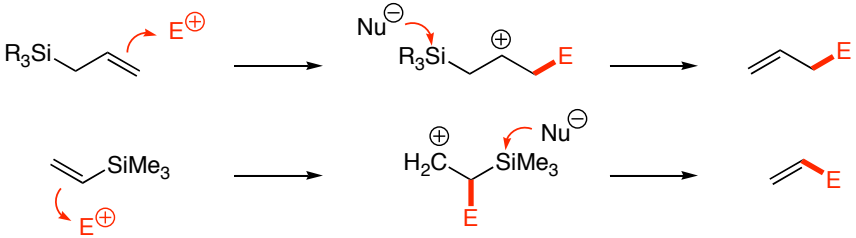

Fleming, *Organic Reactions* **1989**, *37*, 54.

β-Silicon Effect: the origin of regioselectivity

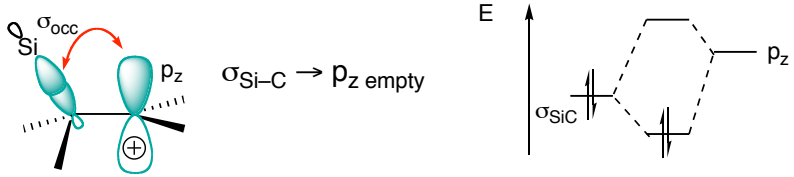

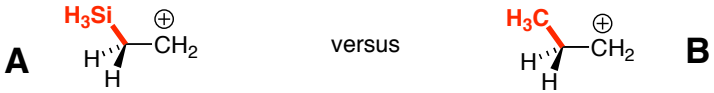

Calculation: A more stable than B by 38 kcal/mol.

Jorgensen *JACS* **1985**, *107*, 1496.

Magnitude of the β-Silicon Effect

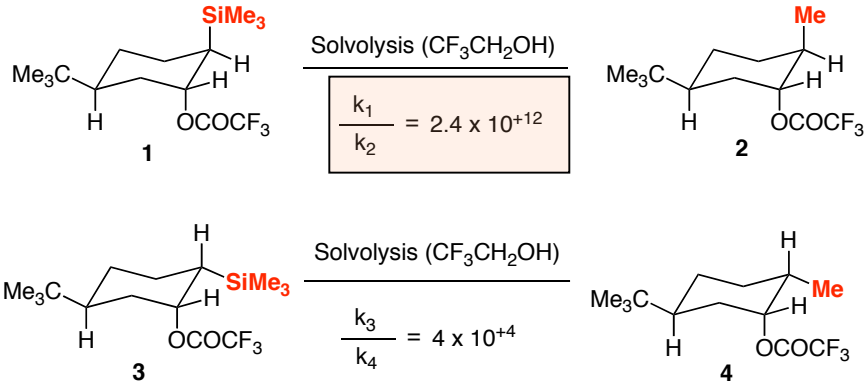

In all instances, the solvolysis product is 1-tert-butylcyclohexene

"These figures established the β-effect as one of the kinetically strongest in organic chemistry": J. Lambert

Data provide no distinction between open and bridged intermediates

Proof for a stepwise mechanism provided the following protodesilylation experiment:

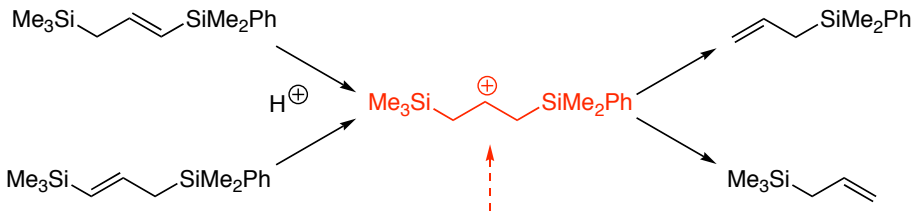

both silanes yield the same product mixture. Hence, the reaction proceeds most likely via a **common intermediate**, a carbeniumion

Allylsilanes are more nucleophilic than alkenes

⇨ HOMO is higher in energy due to ***negative hyperconjugation***

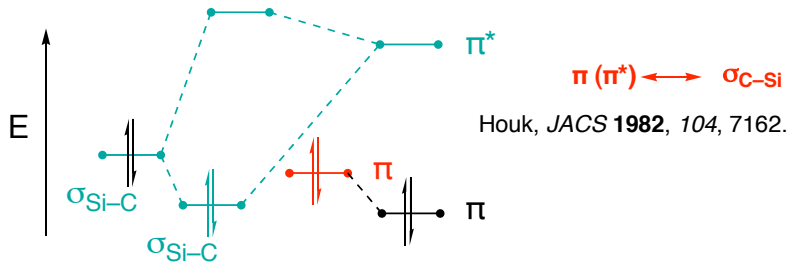

Houk, *JACS* **1982**, *104*, 7162.

Electrophile Addition - Stereoelectronics

anti addition observed

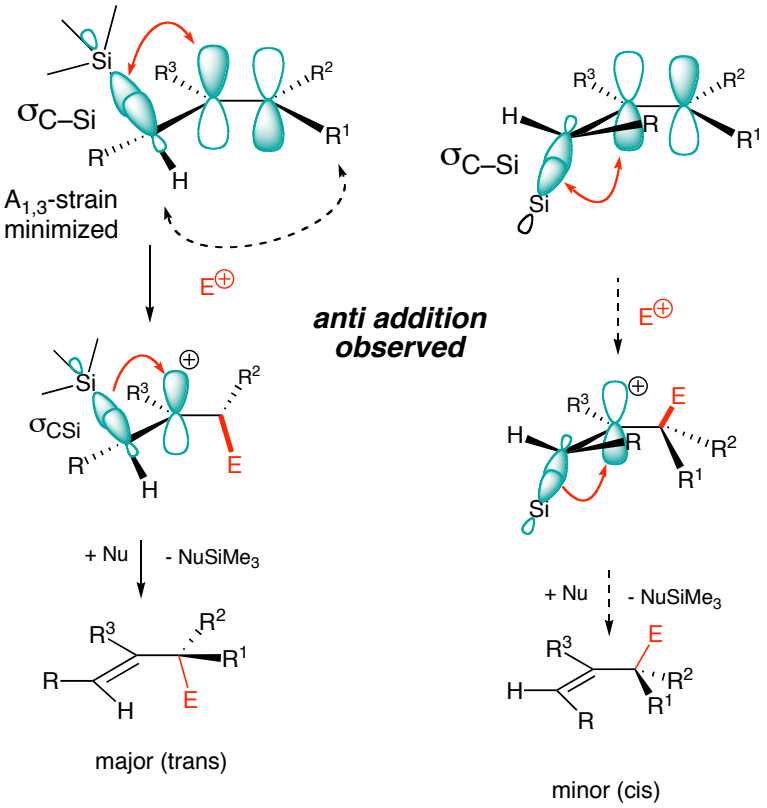

The stereochemical consequences for the major product are:

- ❒ trans-alkene:
- ❒ anti-addition of E^+ with respect to SiR_3

Examples:

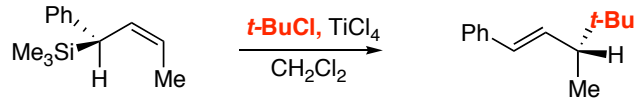

JACS **1982**, *104*, 4962.

But

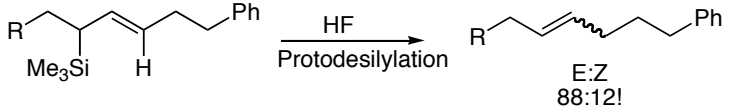

Carbonyl Addition of Allylsilanes: Open Transition States

Me_3Si^- is not sufficiently Lewis acidic to activate C=O through pre-association; however $(RO)_2MeSi^-$ is Lewis acidic enough to activate C=O through pre-association. These allylsilanes add to RCHO througl closed transition states

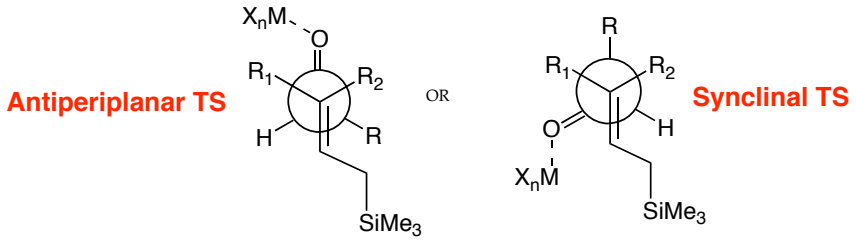

Calculations by Houk et al. show that the relative energy differences between the antiperiplanar and and synclinal transition states are negligible. Both the antiperiplanar and synclinal models predict a ***syn*** selectivity for the newly formed stereogenic centers.

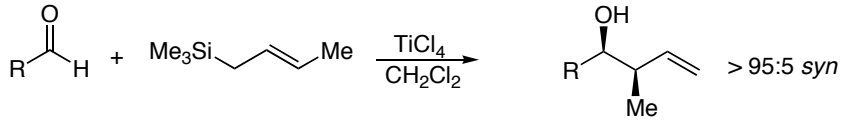

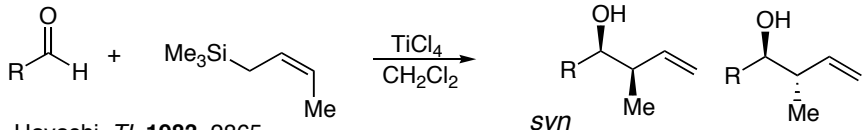

Hayashi, *TL* **1983**, 2865.

Catalytic Enantioselective Addition of Allylic Organometallic Reagents to Aldehydes and Ketones, Denmark and Jiping Fu, *Chem. Rev.* **2003,** *103,* 2763-2793 **(handout)**

Allylsilanes add to aldehydes and acetals under Lewis acid promotion

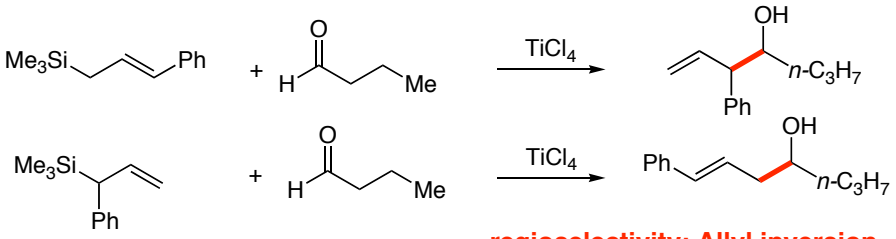

regioselectivity: Allyl inversion

Acetals can be used as well

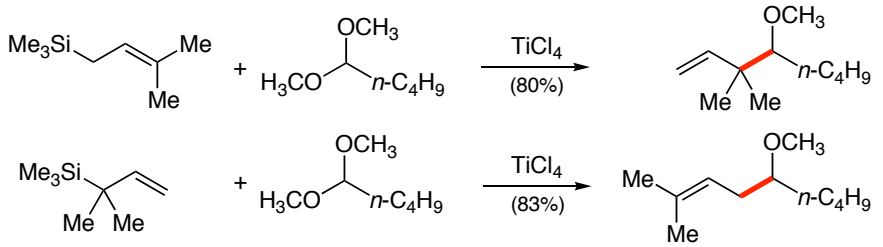

The Sakurai Reaction (Enone Conjugate Addition)

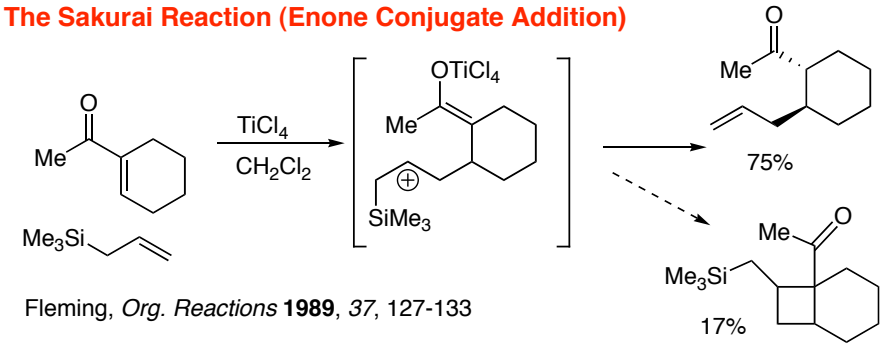

Fleming, *Org. Reactions* **1989**, *37*, 127-133

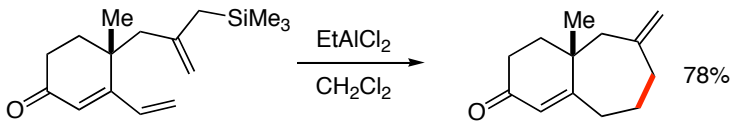

Majetich, *Tetrahedron* **1987**, *43*, 5621

Reactions Proceedilng through Silicon-Migration

Si migration may be promoted by using hindered Si substituents

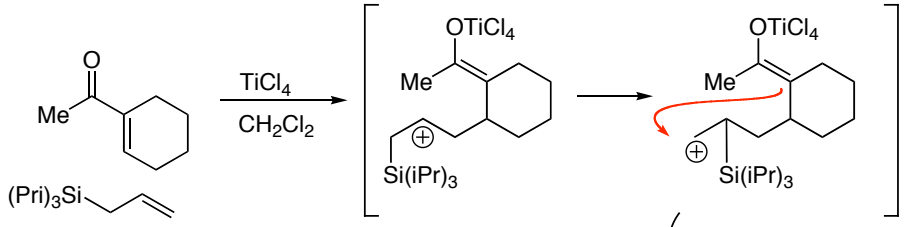

A. I. Meyers, *J. Org. Chem.* **1998**, *63*, 5517

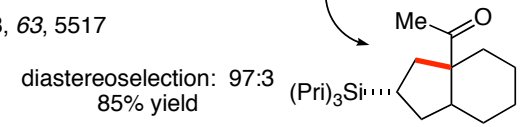

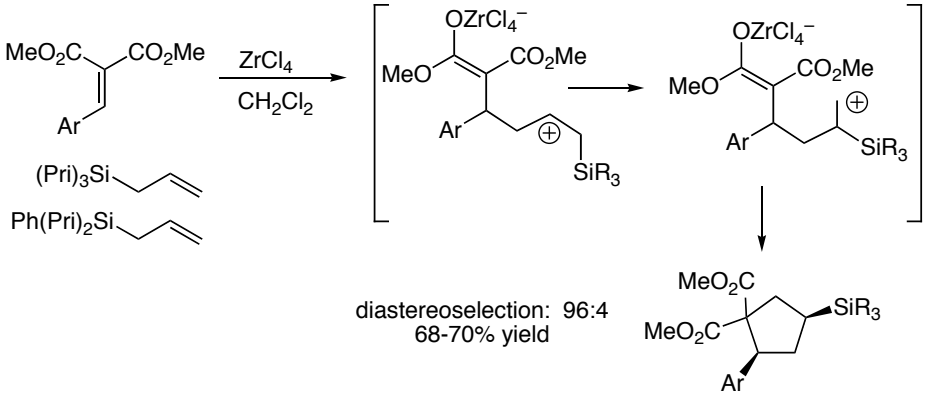

Can you work out the mechanism??

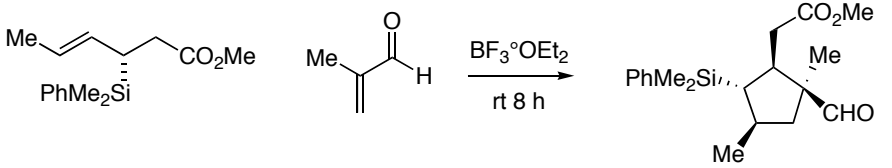

Panek, *J. Org. Chem.* **1993**, *58*, 2345

Stereochemistry of Electrophile Addition to Vinylsilanes

Vinyl/Allylsilanes in Organic Synthesis - Selected Examples

Fleming, *Org. Reactions* **1989**, *37*, 54.

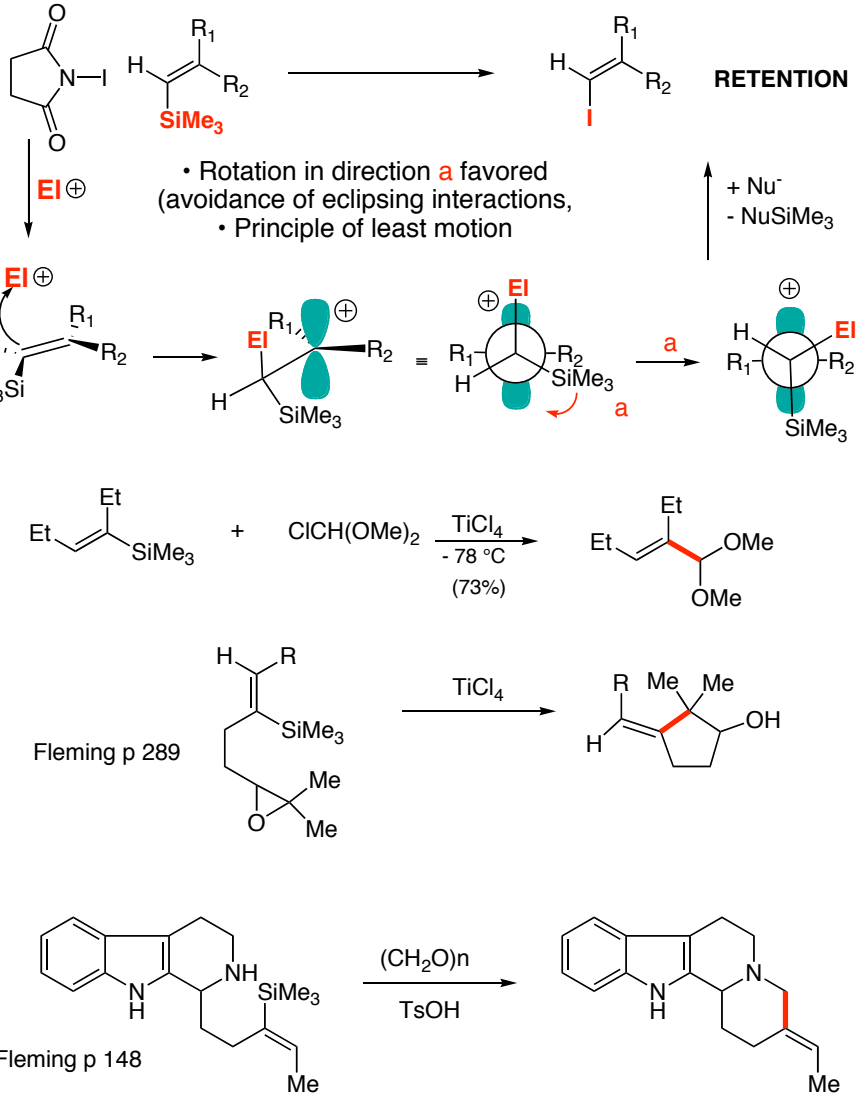

Summary Statements

1. Me_3C^+ is more stable than Me_3Si^+ in spite of the fact that Si is less electronegative than C.

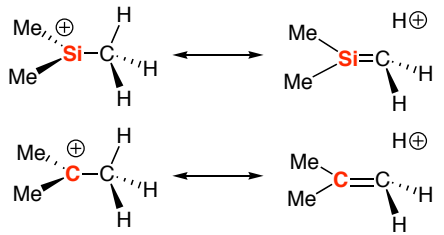

C–Si hyperconjugation is less pronounced than the anaologous C–C hyperconjugation do to the impact of the longer C–Si bond lengths.

2. Carbonium ions α to Si are less stabilized than carbonium ions β to Si.

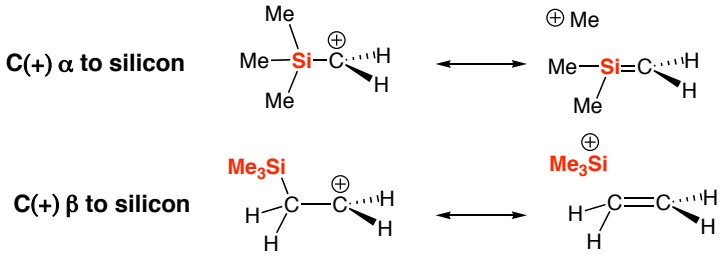

C–Si hyperconjugation is less pronounced than the anaologous C–C hyperconjugation do to the impact of the longer C–Si bond lengths.

3. According to Lambert, silicon has a propensity to stabilize β carbonium ion via hyperconjugation (vertical stabilization) rather than bridging (nonvertical stabilization.

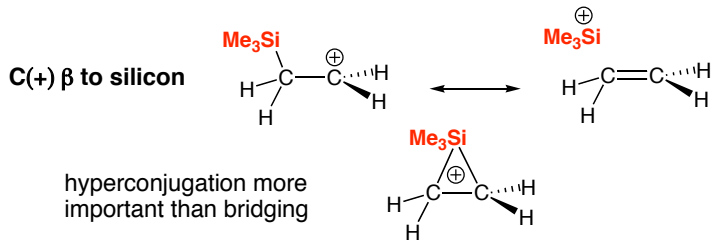

4. Silicon has a lower propensity to undergo Wagner–Meerwein like rearrangements than carbon.

Iminium Ions

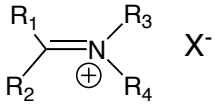

Common Methods of Generation:

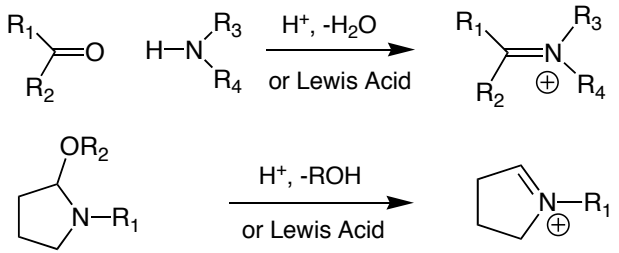

Oxidation of Amines

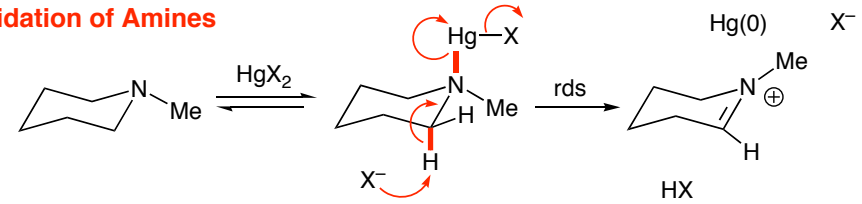

Stereoelectronic Effects on Nu Addition to Iminium Ions

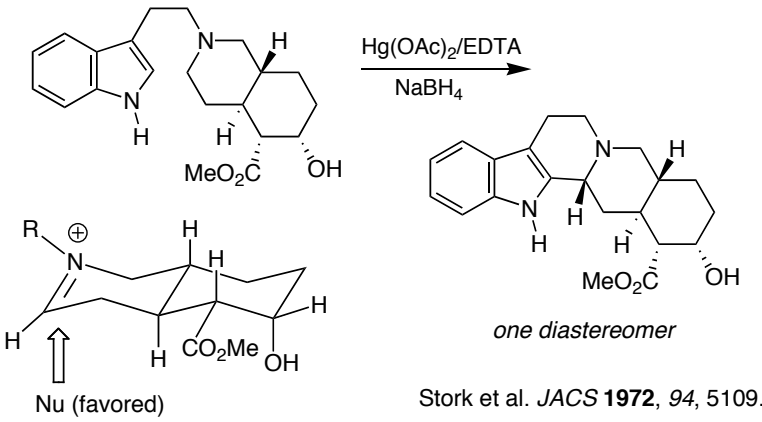

Stork et al. *JACS* **1972**, *94*, 5109.

C=N Stereoelectronic Effects: Lecture 20

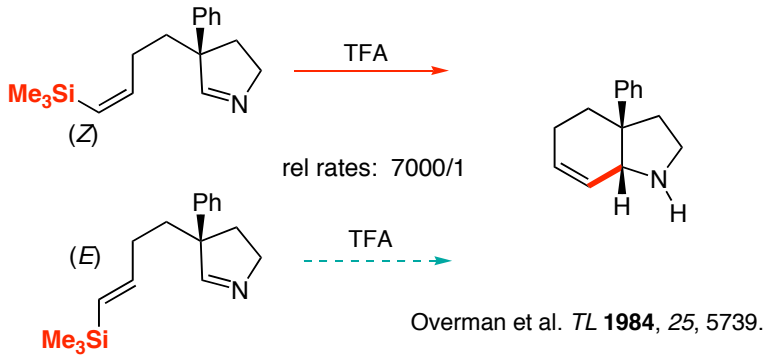

Overman et al. *TL* **1984**, *25*, 5739.

(*Z*) *vinylsilane*) (*E*) *vinylsilane*)

Only in the case of the (Z) vinylsilane is the emerging p orbital coplanar with C-Si bond. Full stabilization of the empty orbital cannot occur with the (E) vinylsilane.....hence the rate difference.

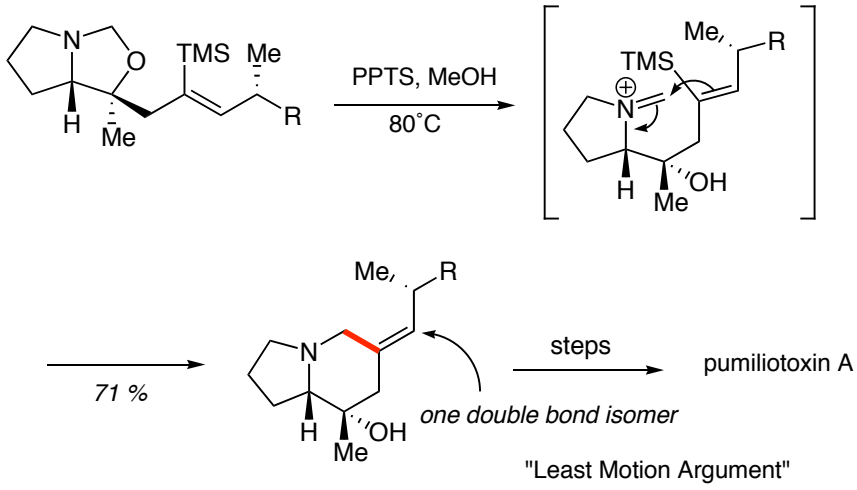

Overman et al. *JOC* **1989**, *54*, 2591.

Review:

Heimgartner, H. In "Iminium Salts in Organic Chemistry"; Bohme, H., Viehe, H., Eds.; Wiley: New York, 1979; Part 2, pp 655-732.

The 3-aza-Cope Rearrangement:

Neutral Variant:

Exothermic as written by ~7-10kcal/mole.

Ammonium Variant:

Even more exothermic than the neutral version, since enamine lacks resonance and iminium salt has stronger p-Bond than imine does.

2-aza-Cope Rearrangement:

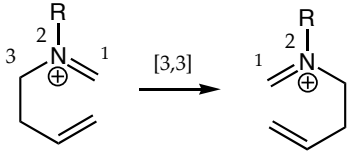

In the simplest case, degenerate. Steric effects, conjugation, or selective trapping of a particular isomer, will drive equilibrium. As with the 3-aza-Cope, the cationic version proceeds under much milder conditions.

1-aza-Cope Rearrangement:

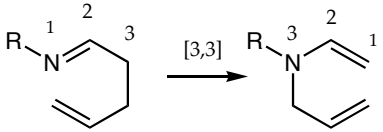

The 3-aza-Cope rearrangement can be driven in reverse by judicious choice of substrates(i.e., incorporating the imine into a strained ring or by making R an acyl group).

The 3-aza-Cope Rearrangement

First Neutral Case: Hill TL **1967**, 1421.

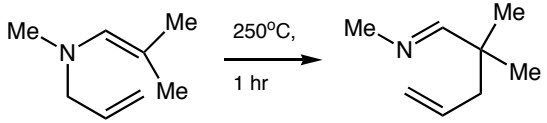

"Practically quantitative", no real yields given.

First Cationic Case: Elkik *Compt. Rend.* **1968**, *267*, 623.

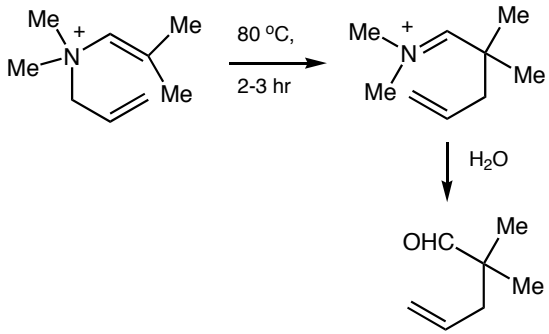

No yields given.

Good way to allylate aldehydes: Opitz *Angew. Chem.* **1960**, *72*, 169.

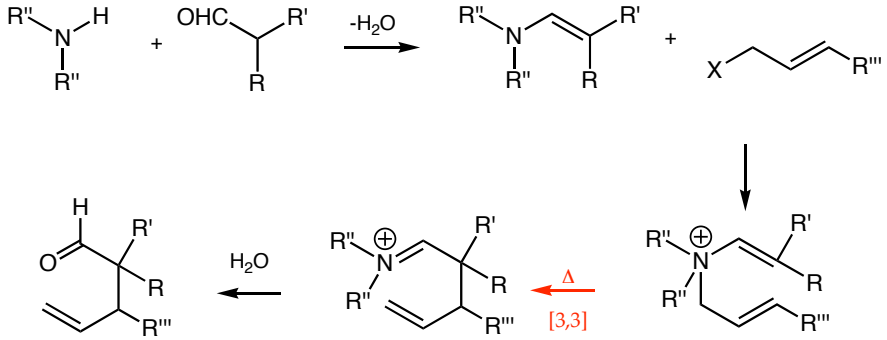

The 2-aza-Cope Rearrangement

First Reported Case: Horowitz JACS 1950, *72*, 1518.

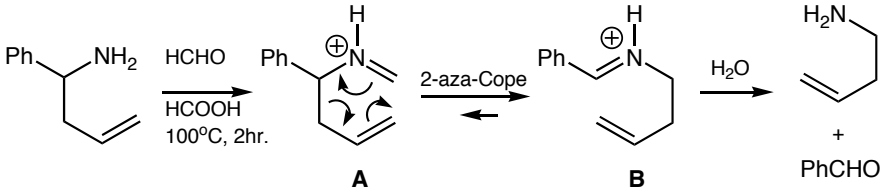

Equilibrium between **A** and **B** driven towards **B** by conjugation of iminium double bond to the aromatic ring in **B**.

Application to Yohimbine Analog Synthesis: Winterfeldt *Chem. ber.* **1968**, *101*, 2938.

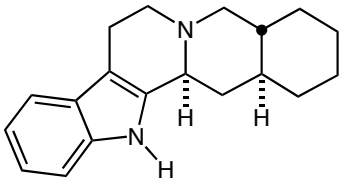

Yohimbane

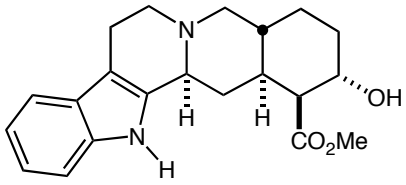

Yohimbine

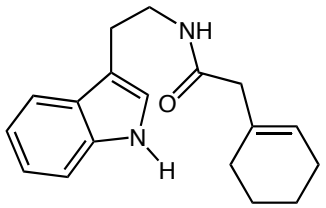

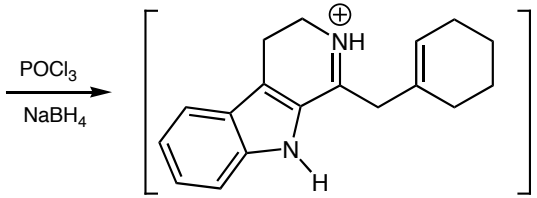

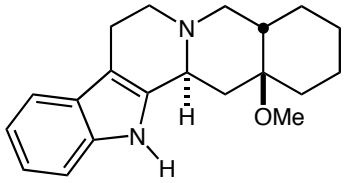

15-Methoxy-isoyohimbane

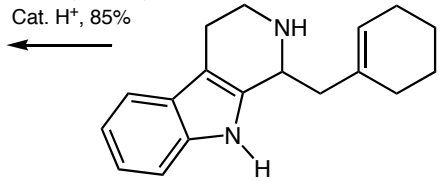

Mechanism for Yohimbane Analog Formation:

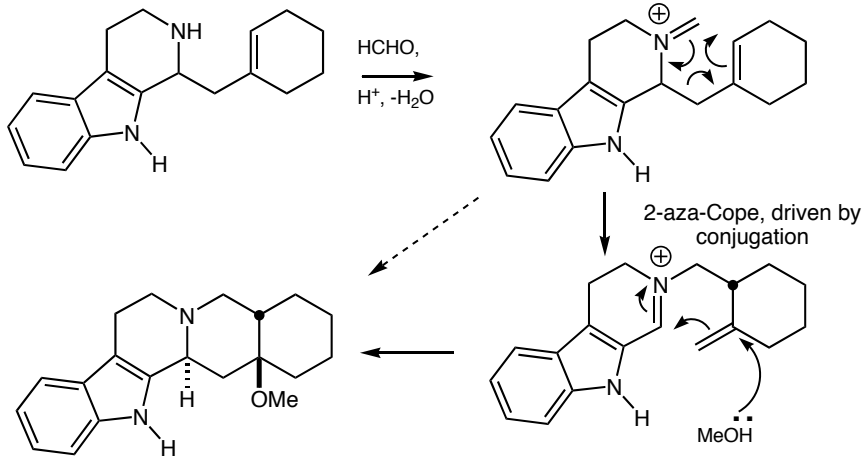

*N-Acyliminium Ion Rearrangements: Hart JOC **1985**, 50, 235.*

Hart observed an unusual product while trapping the intermediates of N-acyliminium olefin cyclizations.

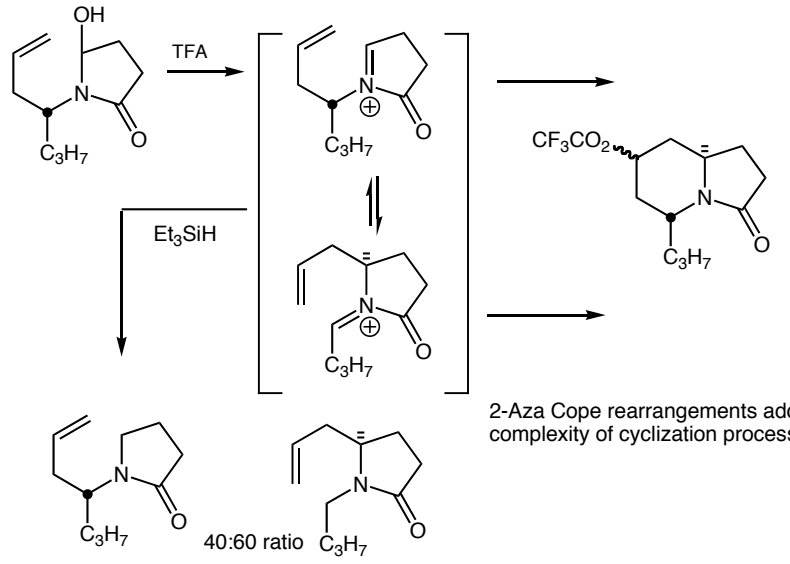

2-Aza Cope rearrangements add to complexity of cyclization process

N-Acyliminium Ion Rearrangements

*Synthesis of (-)-hastanecine: Hart JOC **1985**, 50, 235.*

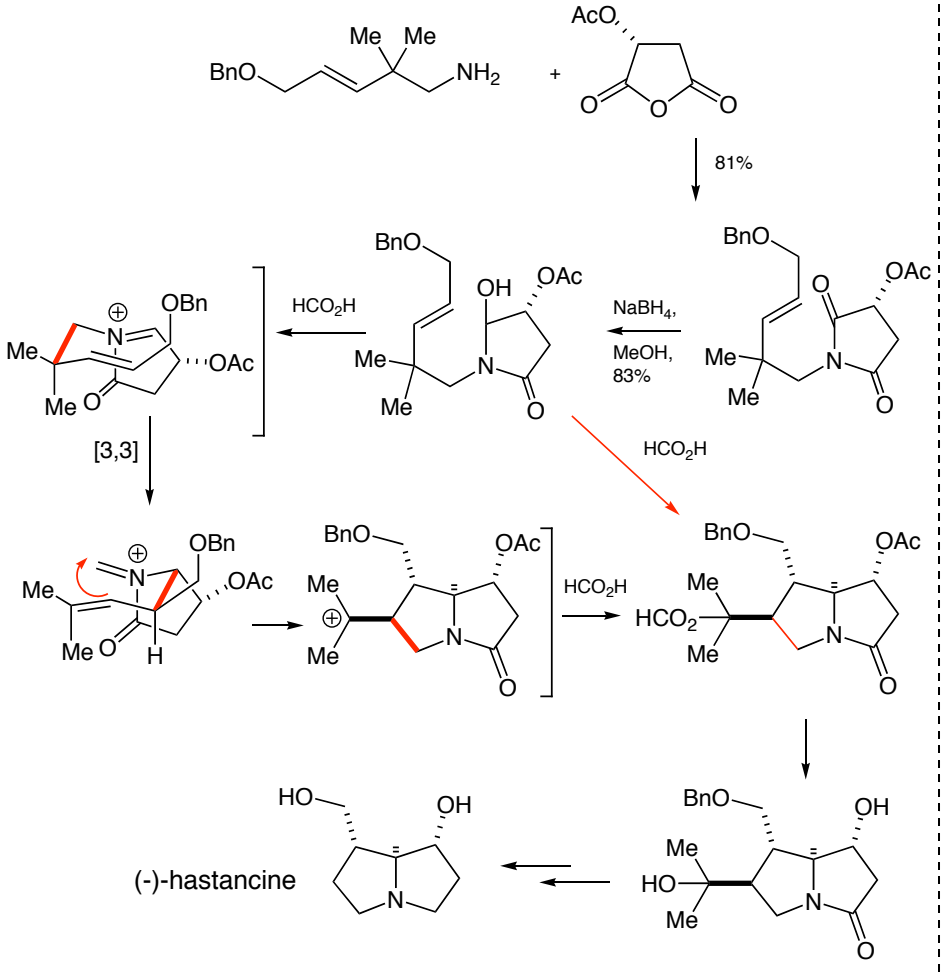

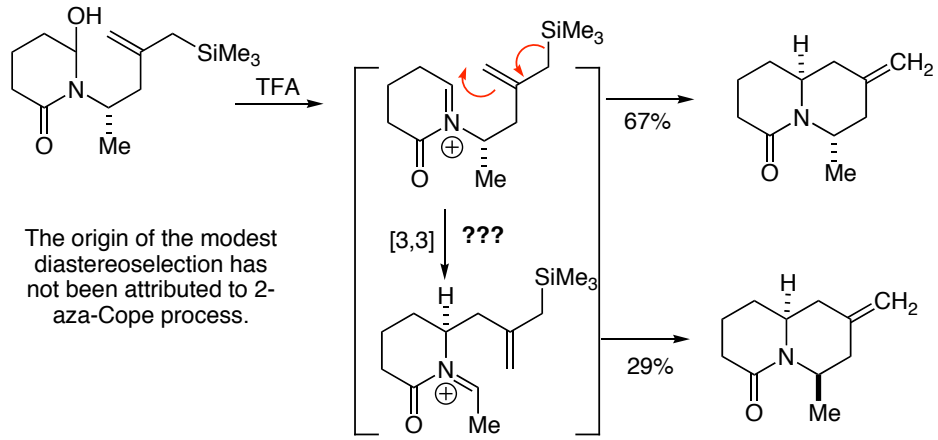

The origin of the modest diastereoselection has not been attributed to 2-aza-Cope process.

Gelas-Mailhe, *Tet. Lett,* **1992**, *33*, 73

Competing 2-Aza-Cope and Pinacol Rearrangements: Which Dominates??

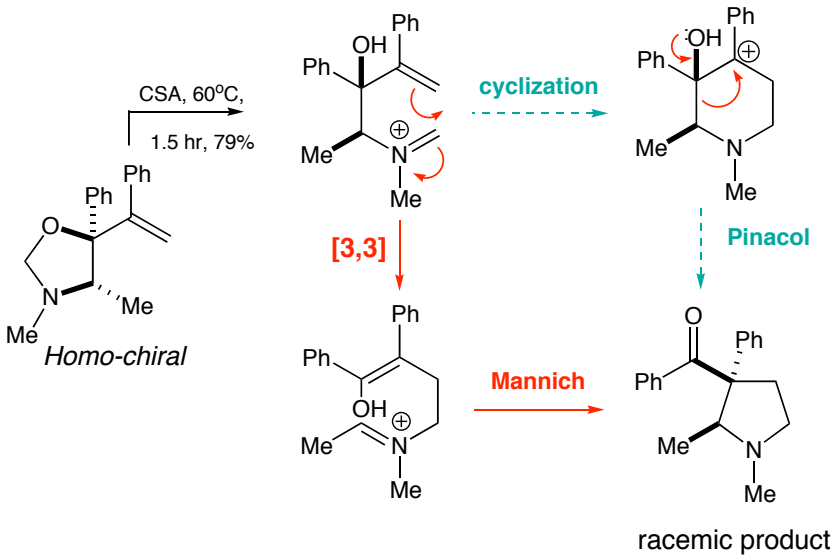

racemic product

2-aza-Cope rearrangements afford a low-barrier to competing processes

2-Aza-Cope-Mannich sequence:

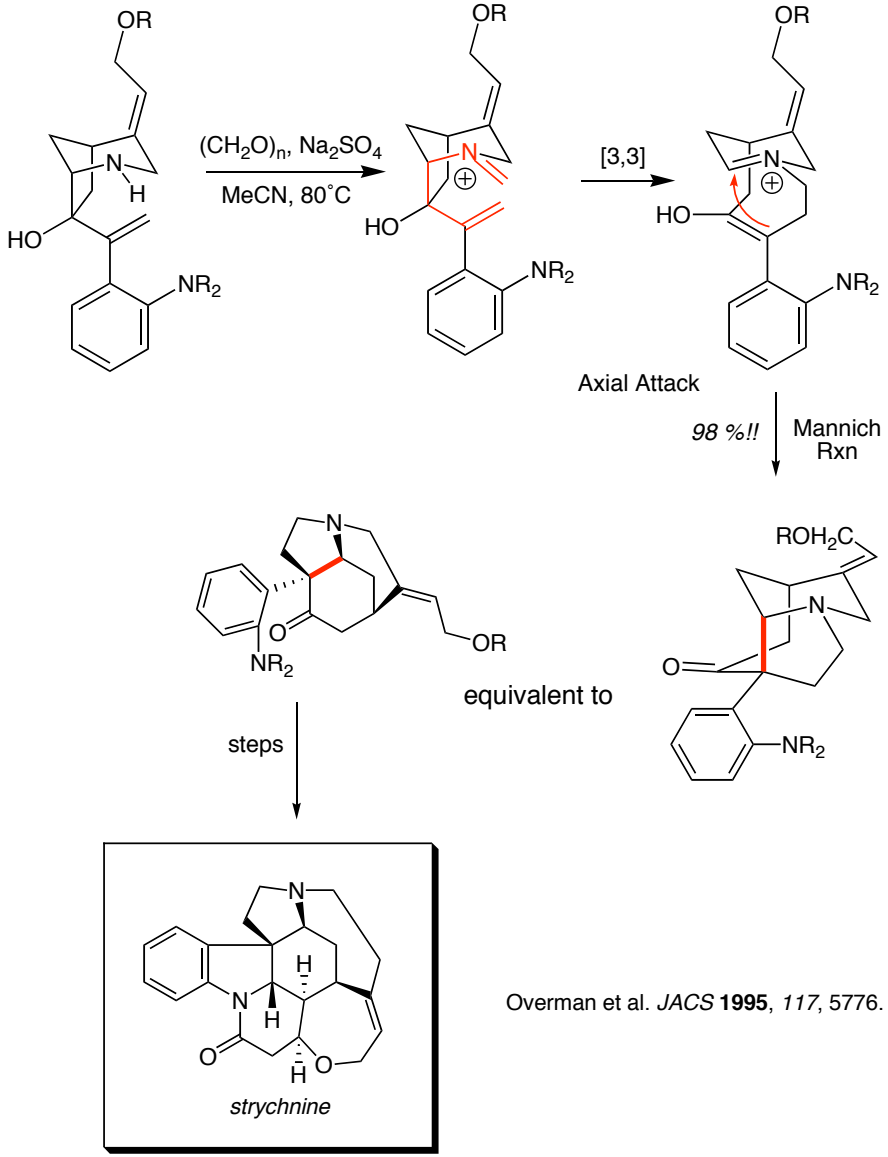

Overman et al. *JACS* **1995**, *117*, 5776.

Another aza-Cope-Mannich sequence:

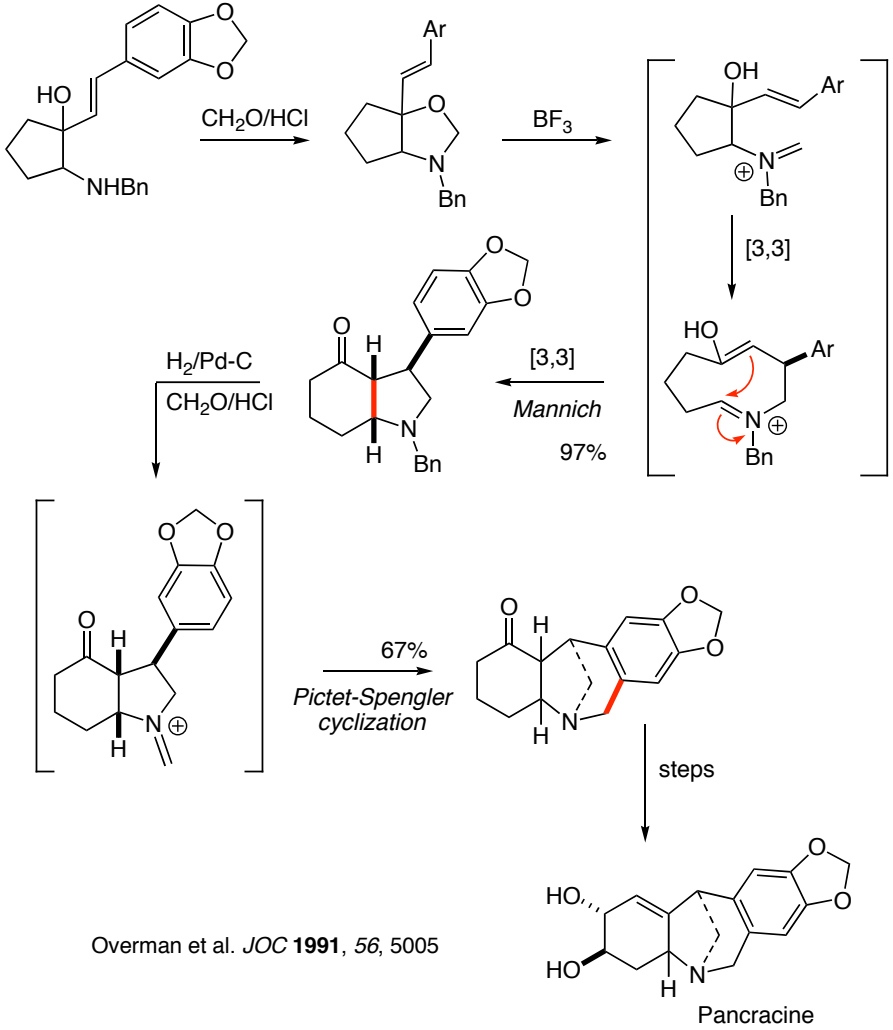

Overman et al. *JOC* **1991**, *56*, 5005

References

Prins reaction: Adams, D.R.; Bhaynagar, S. D. *Synthesis* **1977**, 661
Prins & carbonyl ene reactions: Snider, *Comprehensive Organic Synthesis*, **1991**, *Vol. 2*

The Prins Process:

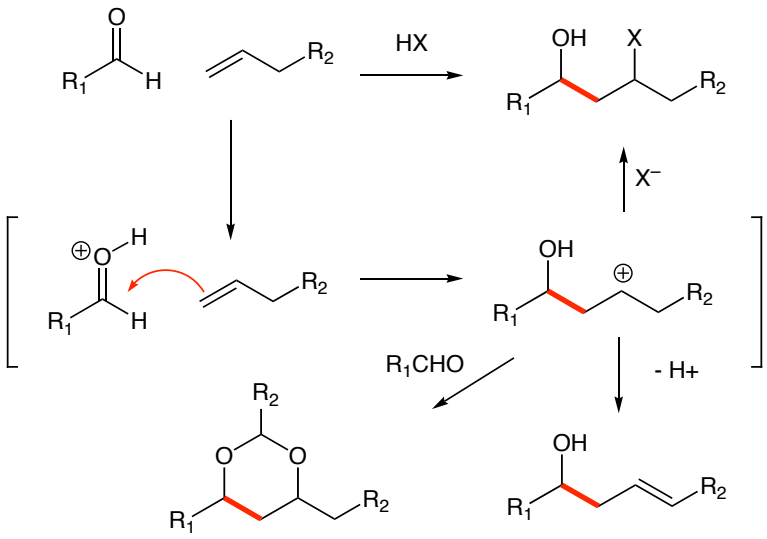

The Prins-Pinacol Variant:

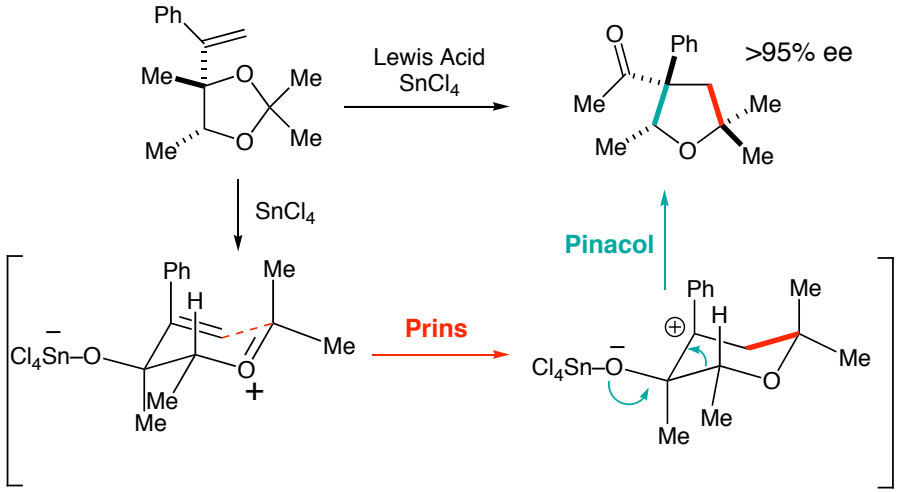

Evidence for Prins-Pinacol Mechanism

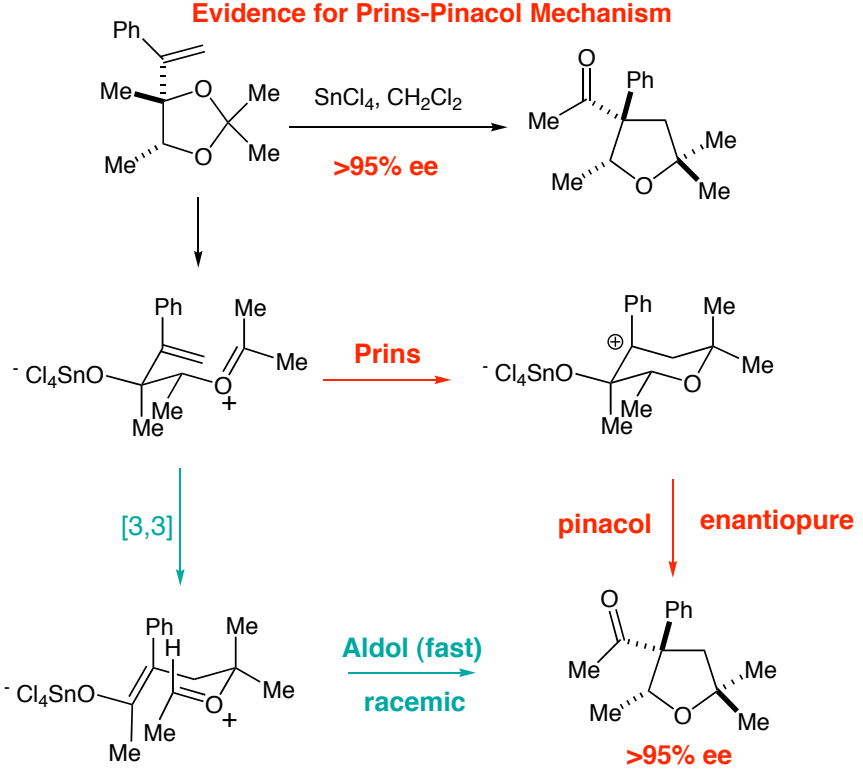

If a [3,3] rearrangement were intervening, the product would be racemic.
Overman, *JACS* **2000**, *122*, 8672
Overman, *Org Lett* **2001**, *3*, 1225

Examples of Stereoselective THF Formation

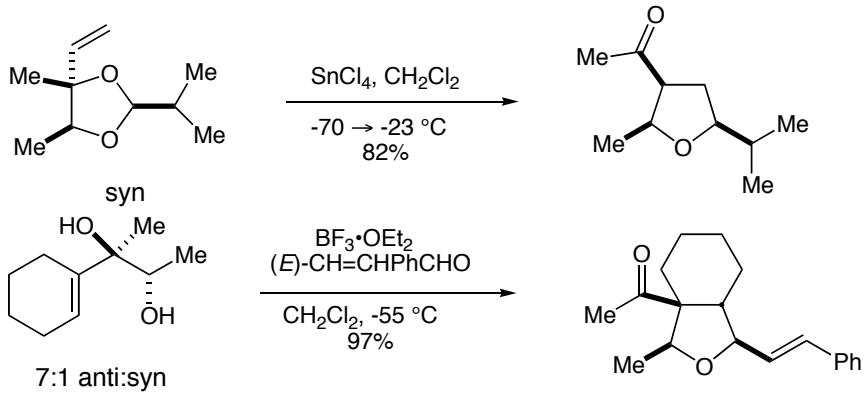

The Prins-Pinacol Reaction

Prins-Pinacol Mechanism

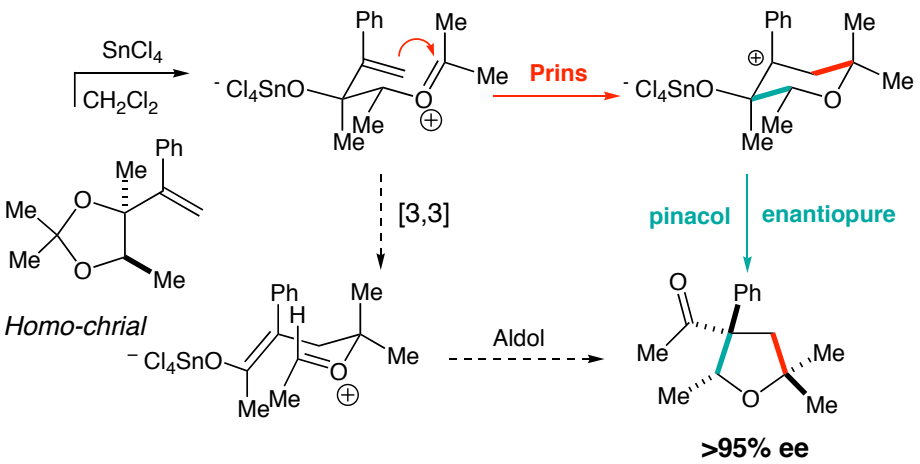

Prins cyclization faster than [3,3] rearrngement

2-aza-Cope vs. Pinacol:

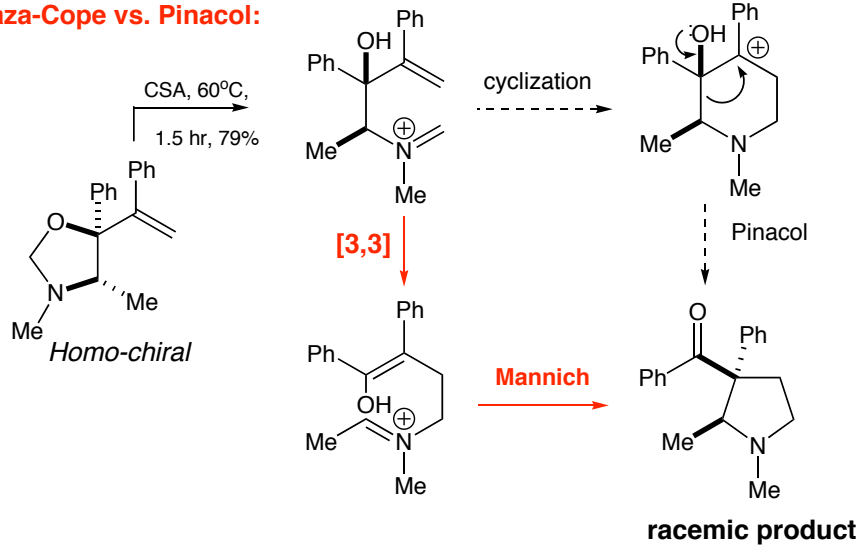

[3,3] rearrngement faster than Mannich cyclization

Overman: Magellanine Synthesis

JACS, **1993**, *115*, 2992

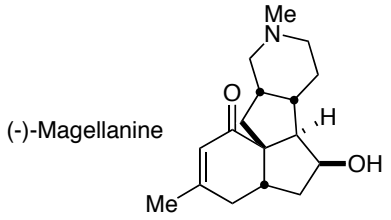

The pivotal transformation

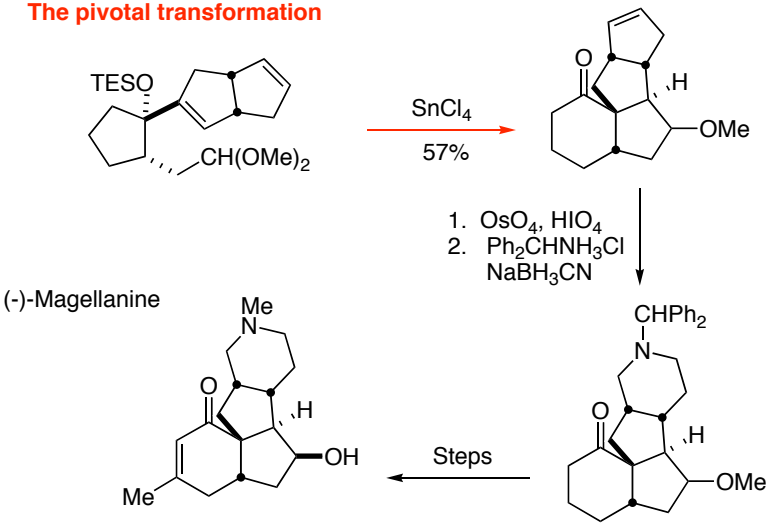

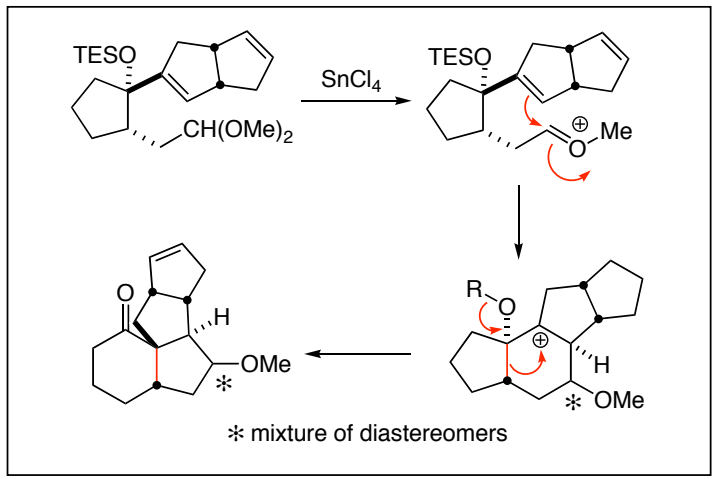

Overman Synthesis of a Eunicellin Diterpene

Overman & MacMillan JACS, **1995**, *117,* 10391

(-)-7-Deacetoxy-alcyoninacetate

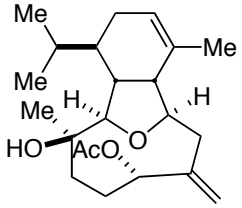

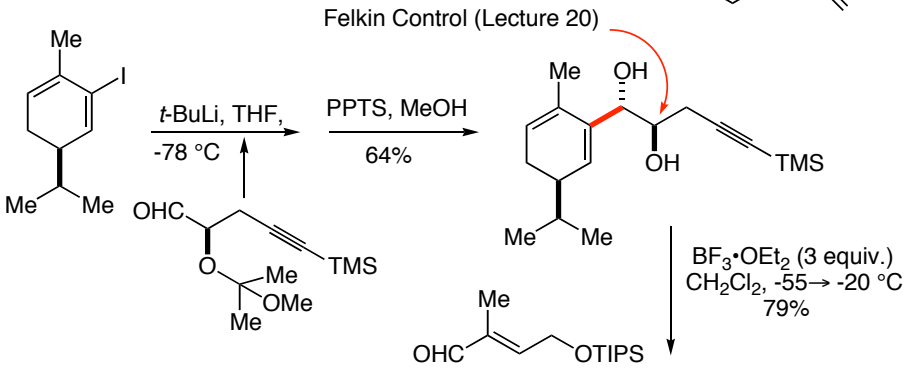

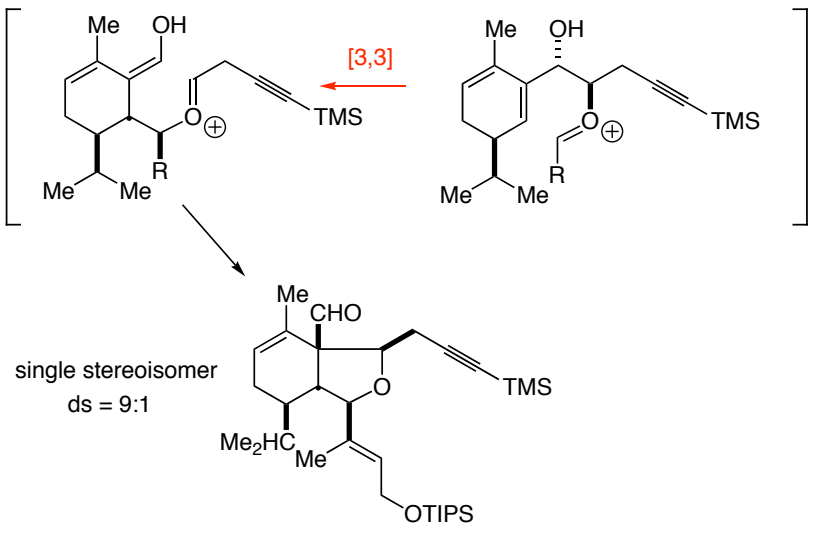

6 steps, 39% yield from (*S*)-carvone

Overman: Synthesis of *trans*-Kumausyne

JACS, **1991**, *113,* 5378

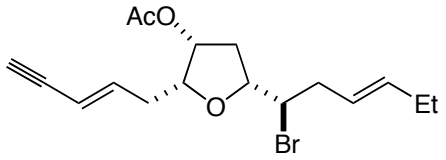

trans-Kumausyne

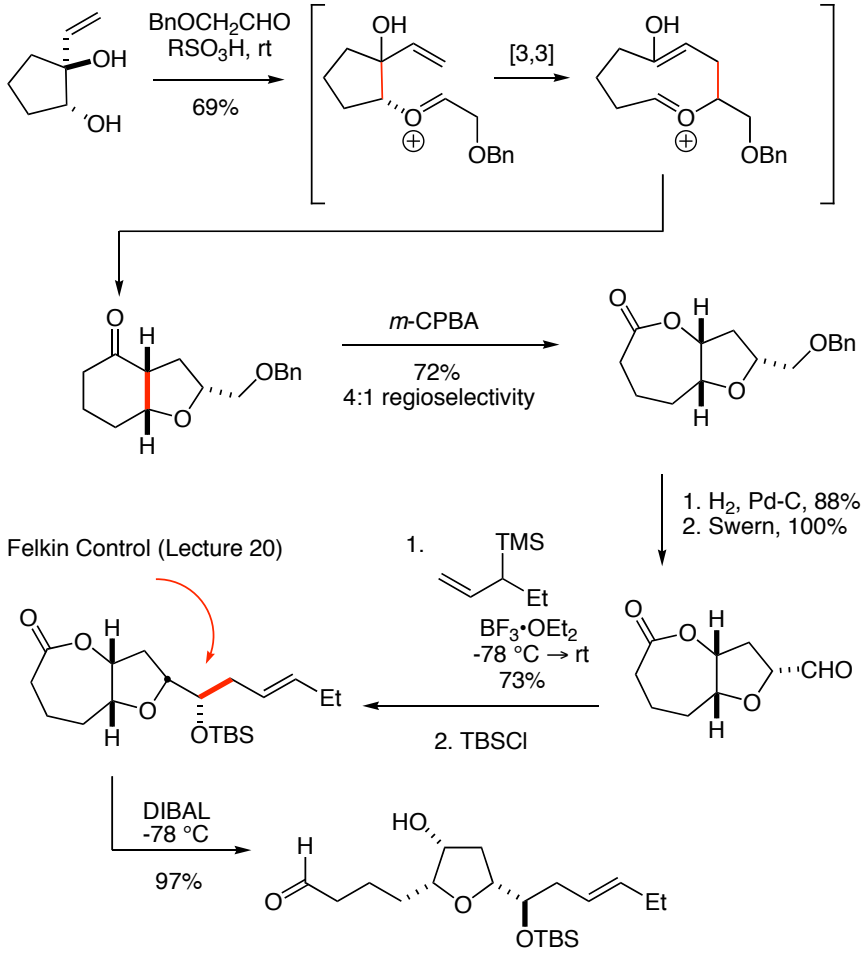

Mukaiyama Aldol–Prins Cascade

Rychnovsky JACS, **2001**, *123,* 8420

The Basic Process

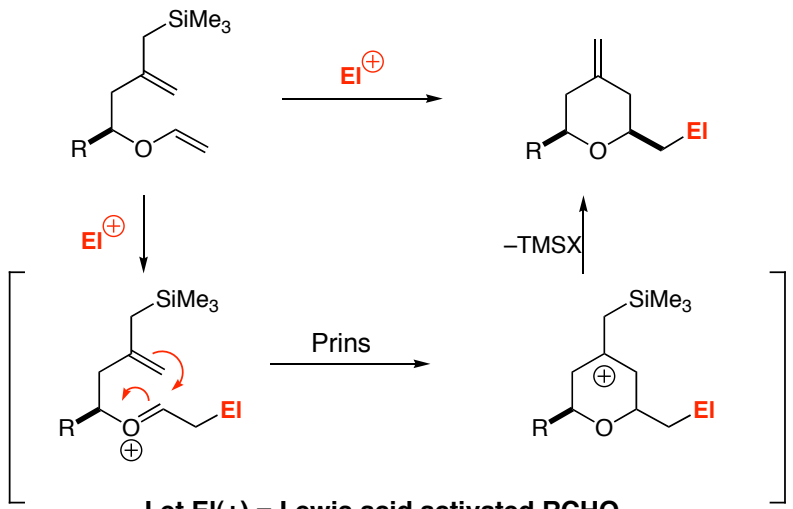

Let El(+) = Lewis acid activated RCHO

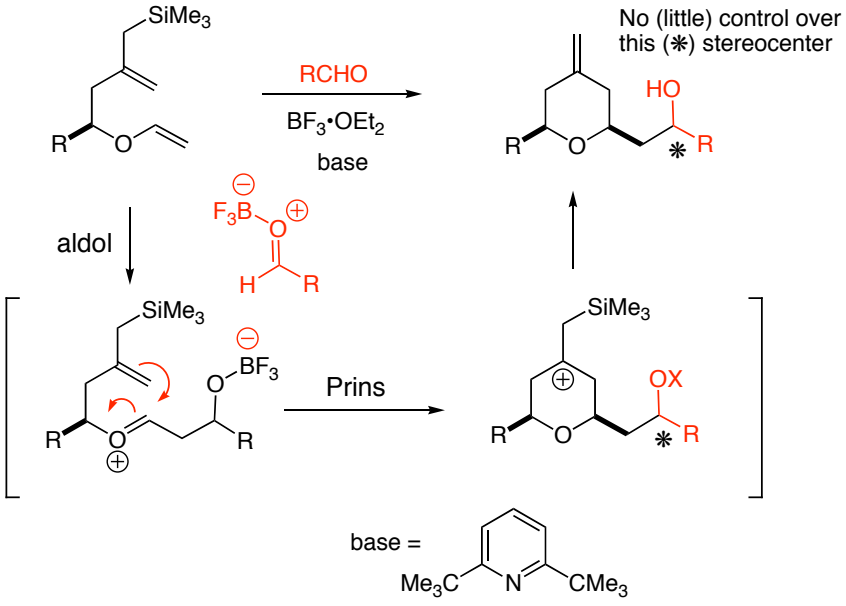

Application to Leucasandrolide

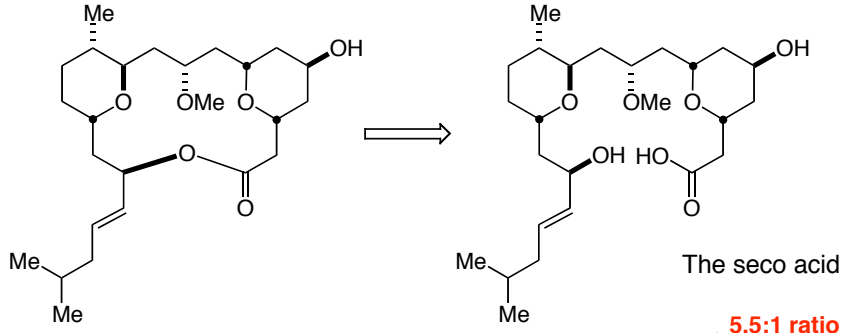

The Pivotal Step:

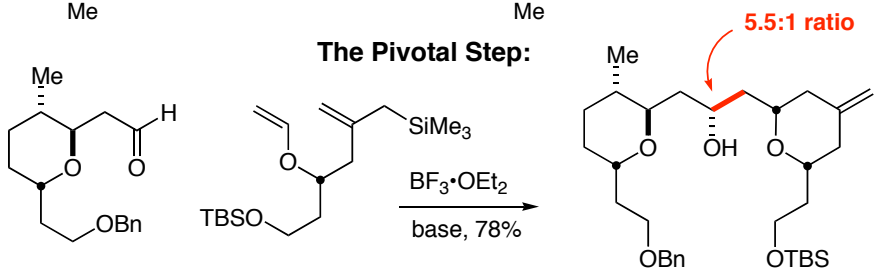

Control of hydroxyl center: see Lecture 20

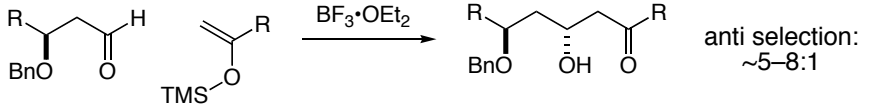

Evans et al., *JACS* **1996**, *116*, 4322

Aldehyde Synthesis

Chiral enolate alkylation: see Lecture 23

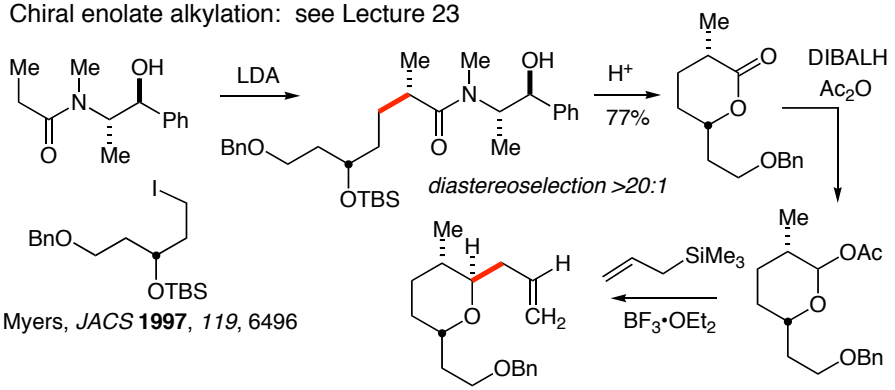

Myers, *JACS* **1997**, *119*, 6496

cyclic oxo-carbenium ion addition: see Lecture 19

http://www.courses.fas.harvard.edu/colgsas/1063

Chemistry 206

Advanced Organic Chemistry

Lecture Number 34

Introduction to Carbenes & Carbenoids-1

- Carbene Structure & Electronics
- Methods for Generating Carbenes
- Simmons-Smith Reaction
- Carbene-Olefin Insertions
- Carbene Rearrangements

Reading Assignment for this Lecture:

Carey & Sundberg, *Advanced Organic Chemistry*, 4th Ed. Part B Chapter 10, "Reactions Involving Highly Reactive Electron-Deficient Intermediates", 595–680.

Chiral DirhodiumCarboxamidates: Catalysts for Highly Enantioselective Syntheses of Lactones and Lactams, *Aldrichchimica Acta*. **1996**, *29*, 3 **(handout)**

Doyle, Catalytic Methods for Metal Carbene Transformations, *Chem. Rev.* **1986**, *86*, 919-939 **(electronic handout)**

McKervey, Organic Synthesis with α-Diazocarbonyl Compounds, *Chem. Rev.* **1994**, *94*, 1091-1160 **(electronic handout)**

Muller, Catalytic Enantioselective Aziridinations & Asymmetric Nitrene Insertions, *Chem. Rev.* **2003**, *103*, 2905-2919 **(electronic handout)**

Problems Database Keywords: Carbenes & Carbenes + rearrangements

D. A. Evans

Friday
December 15 , 2006

Useful References to the Carbene Literature

Books: Modern Catalytic methods for Organic Synthesis with Diazo Compounds; M. P. Doyle, Wiley, 1998.

Provide a mechanism for the following transformations.

Problem 410: Automerization of Naphthalene (The Cume Question from Hell!)

Rationalize

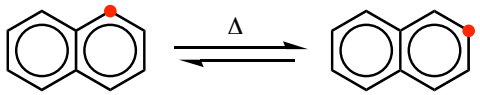

α–^{13}C-labeled $C_{10}H_8$ is isomerized into β–^{13}C-labeled $C_{10}H_8$ at 1035 °C

L. T. Scott, *JACS* **1991**, *113*, 9692.

Problem 411: Provide a Mechanism for this Transformation

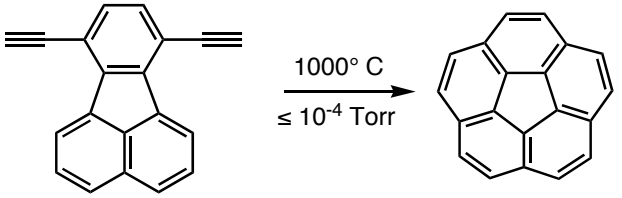

Corannulene 10%

Scott, L.T., et. al., *JACS* **113** 7082 (1991)

Problem 411: While investigating the reactivity of α-diazoketones, Padwa and co-workers (*Tetrahedron Lett.* **1993**, *49*, 7853) discovered the interesting reaction of diazoketone **1** under the conditions shown below. Provide a detailed mechanism for the formation of spirocycle **2**.

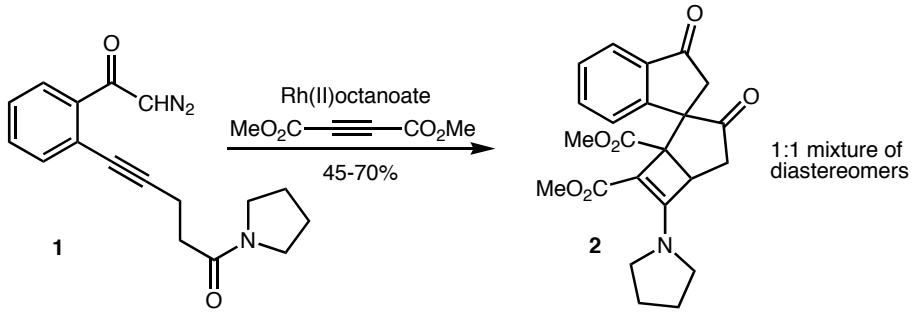

1:1 mixture of diastereomers

Problem 47

Wood recently reported a very clever approach to the synthesis of the indolocarbazole family of natural products (*JACS* **1995**, *117*, 10413). His approach to the indolocarbazole core is the one-pot transformation outlined below.

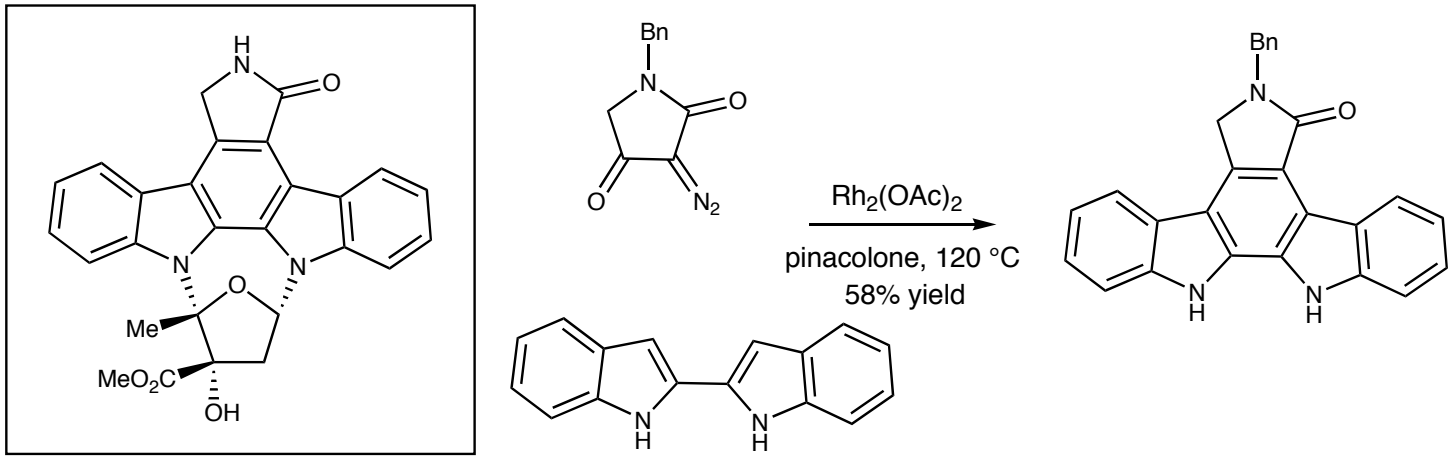

Provide a plausible mechanism for this multi-step transformation in the space below.

Problem 332

Stoltz and co-workers recently reported the interesting rearrangement illustrated below (*JACS* **2003**, *125*, 13624).

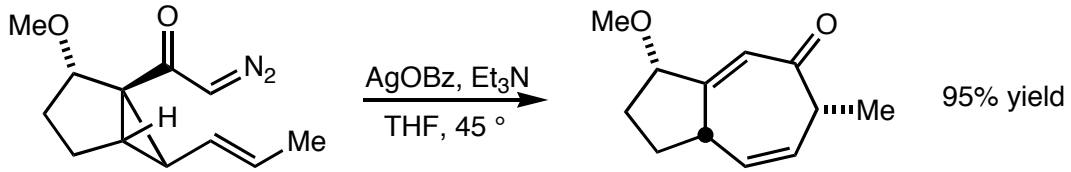

Please provide a mechanism for the illustrated transformation. Your answer should include clear 3-D drawings where relevant and should provide the stereochemistry of the major product diastereoisomer.

Problem 405

Lechner and Christl described this interesting, albeit unintended degradation of **1** upon treatment with methyllithium (*Angew. Chem. Int. Ed.* **1975**, 765). These studies were undertaken en route to tetrahedrane, although the ultimate goal was never realized.

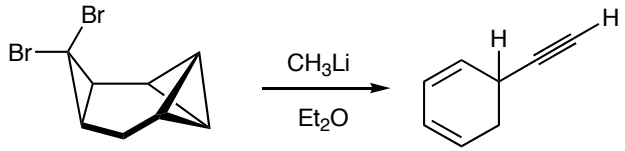

Please provide a mechanism for this transformation.

Suggested Reading:

Doyle, *Chem Rev.* **1988,** *86*, 919.
Kodadek, *Science*, **1992**, *256*, 1544.

Recent Review Article:
Chemistry of Diazocarbonyls: McKervey et al. *Chem Rev.* **1994**, *94*, 1091.

Books:
Modern Catalytic methods for Organic Synthesis with Diazo Compounds; M. P. Doyle, Wiley, 1998.

Carbenes and Nitrenes in "Reactive Molecules: The Neutral Reactive Intermediates in Organic Chemistry", Wentrup, C. W. 1984, Wiley, p. 162.

Rearrangements of Carbenes and Nitrenes in Rearrangements in Ground & Excited States, Academic Press, DeMayo ed., Jones, W. M. 1980, p. 95.

Carbene Chemistry, 2nd ed. Academic Press, Kirmse, W., 1971.

Carbenes: Electronic Structure

■ Carbene Configuration: Triplet vs. Singlet

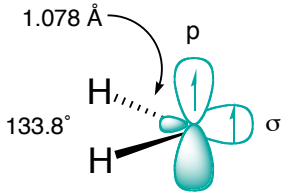

Triplet (two unpaired e⁻)

Often has **radical**-like character

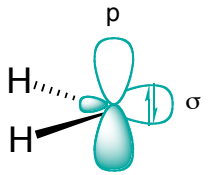

Singlet (all e⁻ paired)

Often has **electrophilic** or **nucleophilic** character: **A**-type (**Ambiphilic)**

■ Nitrene

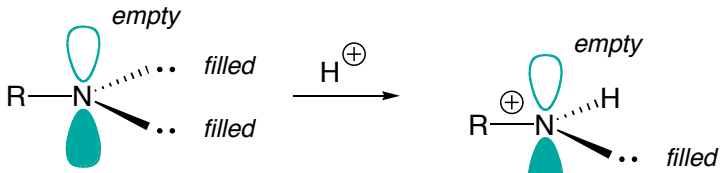

Singlet (all e⁻ paired)

■ Nitrenium ion

■ Carbene Configuration: Triplet vs. Singlet

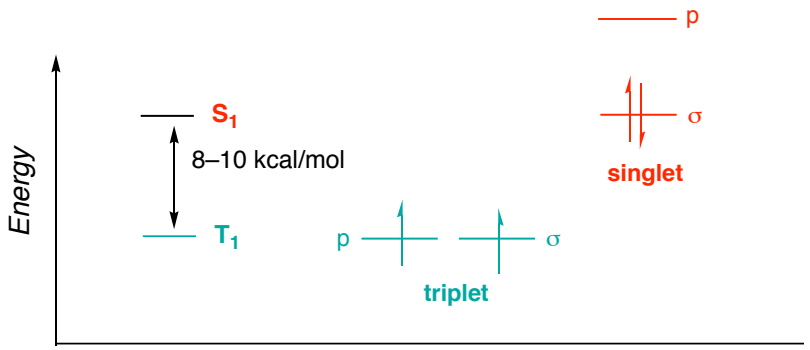

Due to electron repulsion, there is an energy cost in pairing both electrons in the σ orbital. If a **small energy difference** between the σ and p orbitals exists, the electrons will remain **unpaired (triplet)**. If a **large gap** exists between the σ and p orbitals the electrons will **pair** in the σ orbital (**singlet**).

■ the History of the Singlet-Triplet Gap

Year	Method	Author	HCH Angle	Grnd State	S–T Splitting kcal/mol
1932	Qual.	Muliken	90-100°	*singlet*	—
1947	Thermochem	Walsh	180°	*triplet*	*small*
1957	Qual. QM	Gallup	160°	*triplet*	30
1969	Ab initio	Harrison	138°	*triplet*	>33
1971	Kinetics	Hase	—	*triplet*	8–9
1971	SCF	Pople	132°	*triplet*	19
1974	MINDO	Dewar	134°	*triplet*	8.7
1976	Expt	Lineberger	138°	*triplet*	19.5
1976	An Initio	Schaeffer	——	*triplet*	19.7
1978	**Expt**	**Zare**	**——**	***triplet***	**8.1**
1982	**Expt**	**Haydon**	**——**	***triplet***	**8.5**

(Wentrup)

Heteroatom-Substituted Carbenes: Singlets

The p orbital of carbenes substituted with **p-donor atoms** (N, O, halogen) is raised high enough in energy to make the pairing of the electrons in the σ orbital energetically favorable. As a result, these carbenes are often in the **singlet** state.

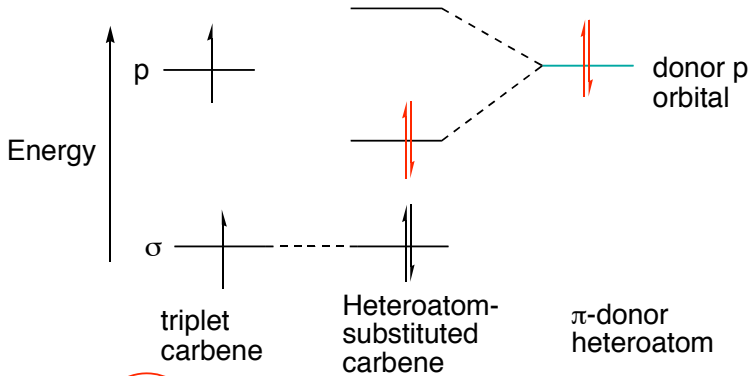

Examples:

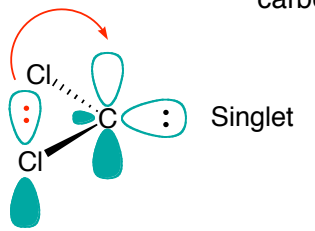

Singlet

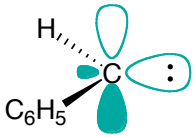

Singlet

Methods of Synthesis

Alkyl Halides:

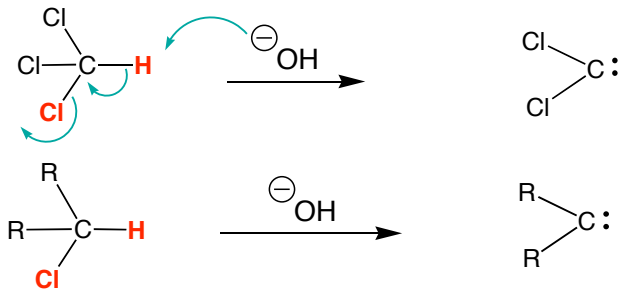

ketenes

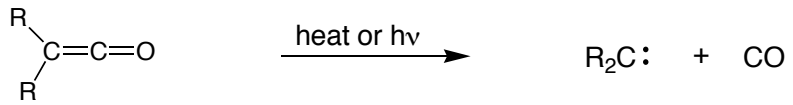

Bamford-Stevens Reaction: See Lecture 31 on Hydrazones

Shapiro *Org. Rxns.* **1976**, *23*, 405.

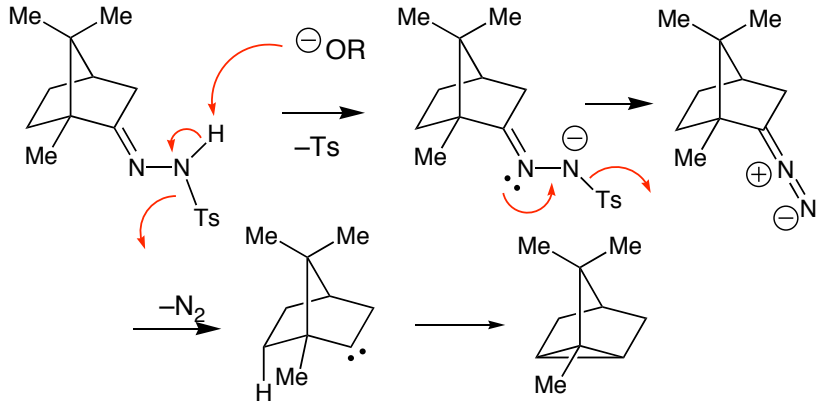

diazo compounds

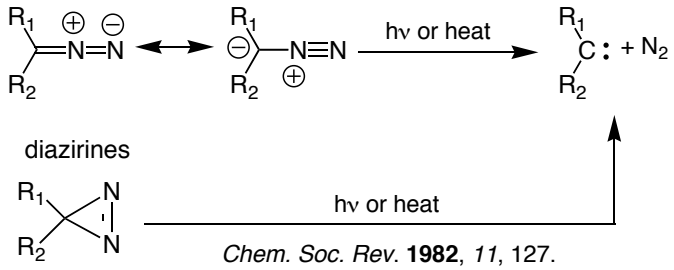

Chem. Soc. Rev. **1982**, *11*, 127.

metal-catalyzed decomposition Doyle *Chem Rev.* **1986**, *86*, 919 **(handout)**

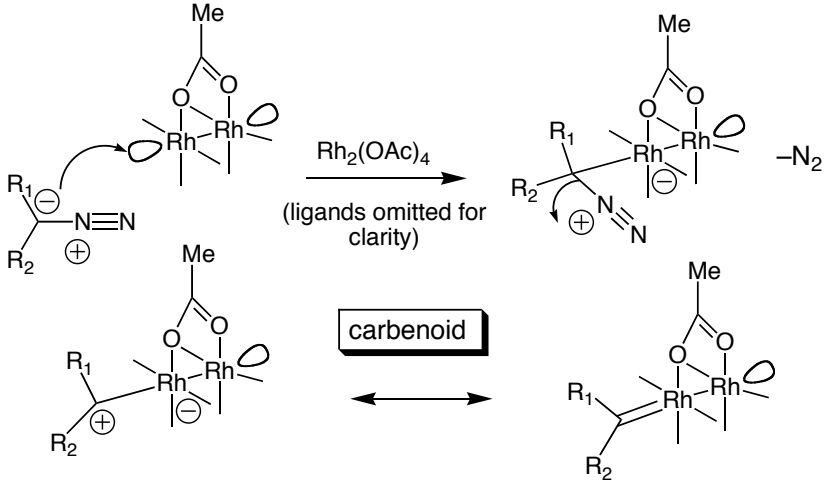

Carfbene–Olefin Cycloaddition: The FMO Analysis

See discussion in Fleming pp 95–96

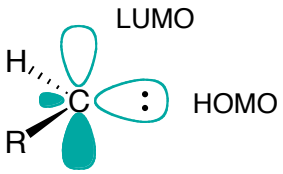

Linear Approach

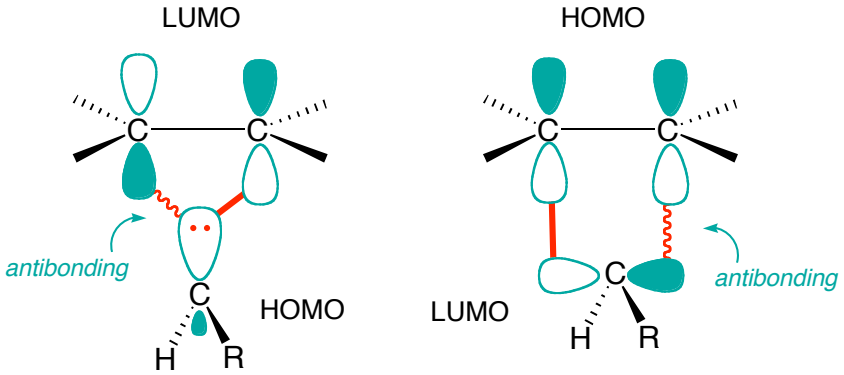

Non-linear Approach

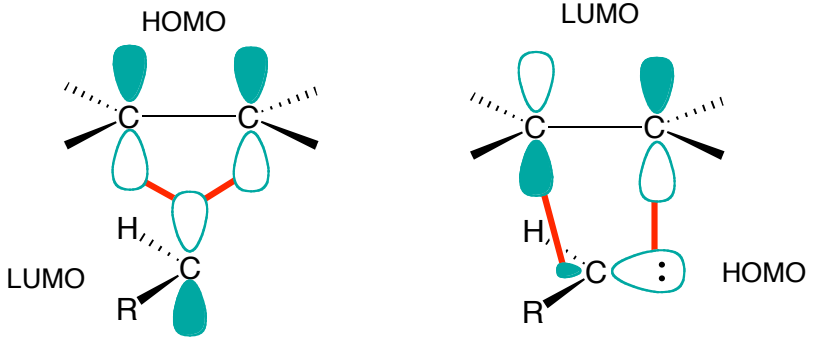

■ Synthetic Applications

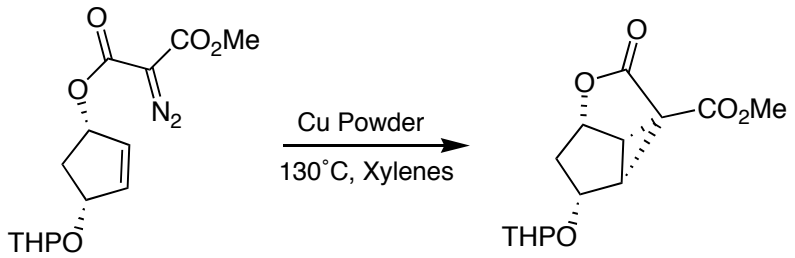

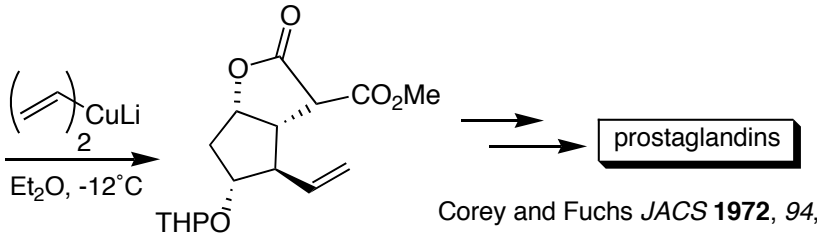

Corey and Fuchs *JACS* **1972**, *94*, 4014.

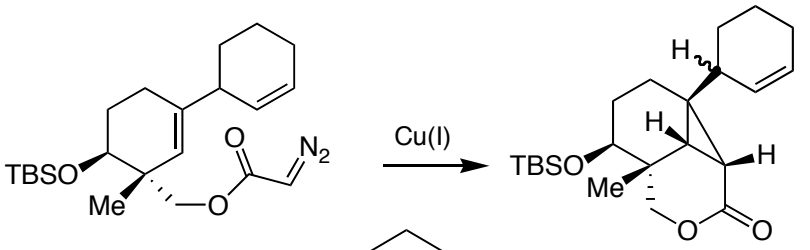

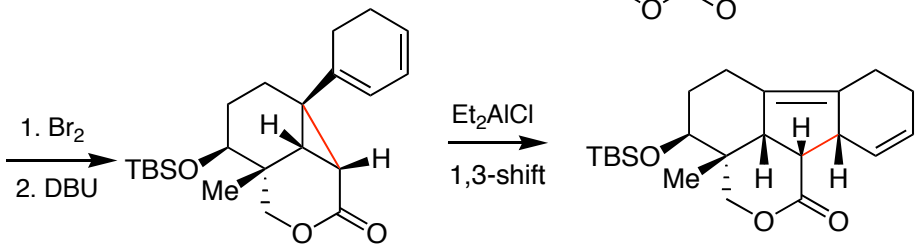

Corey & Myers *JACS* **1985**, *107*, 5574.

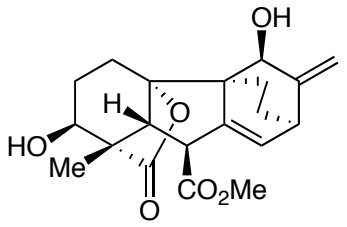

Antheridic Acid

Carbenes from Epoxides

Hodgson and co-workers recently reported the highly diastereoselective cyclopropanation illustrated below (*JACS*, **2004**, *126*, 8664).

This intramolecular cyclopropanation appears to be general for five- as well as six-membered ring fomation.

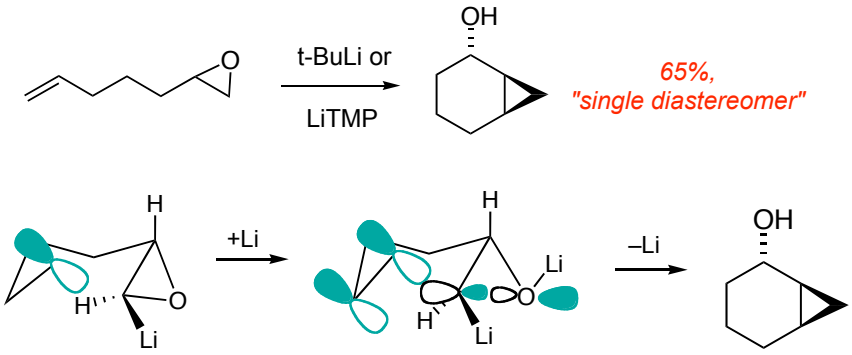

The Simmons-Smith Reaction

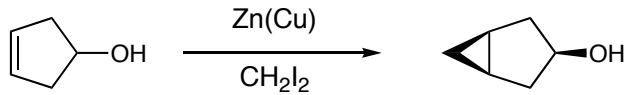

150:1 cis: trans
75% yield

Winstein et al.
JACS, **1961**, *91*,3235

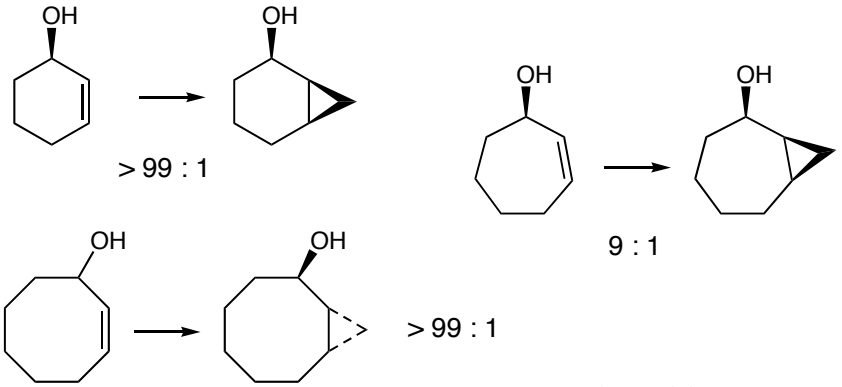

Winstein, S. *JACS* **1969,** *91,* 6892

Hydroxyl directivity is a powerful atribute of the S–S Rxn

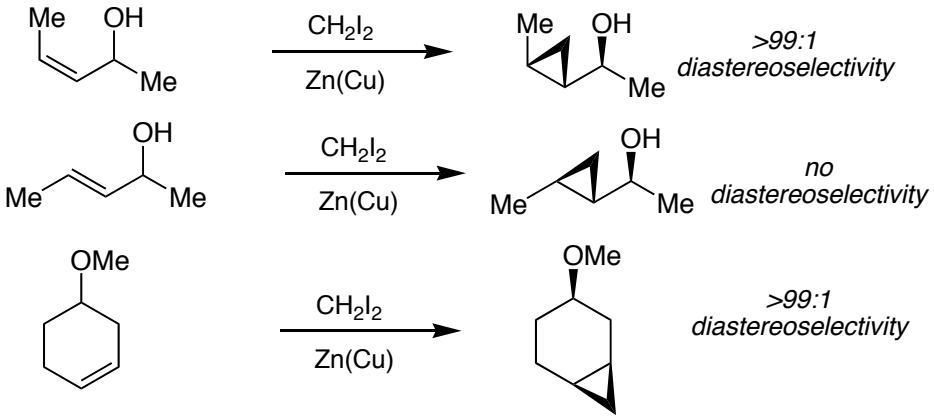

For an review of the directed Simmons-Smith, see:
Evans, D. A.; Hoveyda, A.; Fu, G. *Chem. Rev.* **1993**, *93*, 1307.

The Furakawa Simmons-Smith Variant

For a recent general review of the Simmons-Smith reaction see:
Charette & Beauchemin, *Organic Reactions*, **58**, 1-415 (2001)

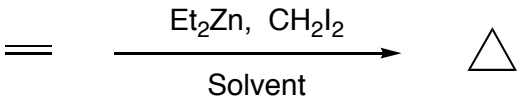

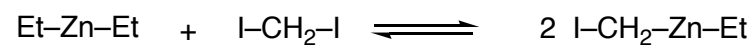

Furukawa, J.; Kawabata, N.; Nishimura, J. *Tetrahedron,* **1968,** *24,* 53
Furukawa, J.; Kawabata, N.; Fujita, T. *Tetrahedron,* **1970,** *26,* 243

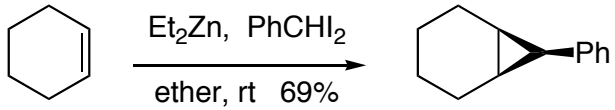

Characterization of metal carbenoid intermediates: not much data!

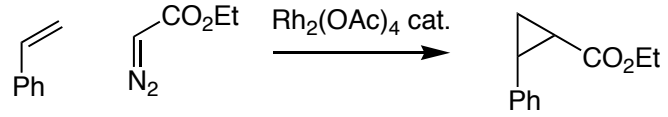

For a detailed mechanistic study which provides supporting evidence for the intermediacy of a Rh carbene, see: Kodakek, *Science*, **1992**, *256*, 1544.

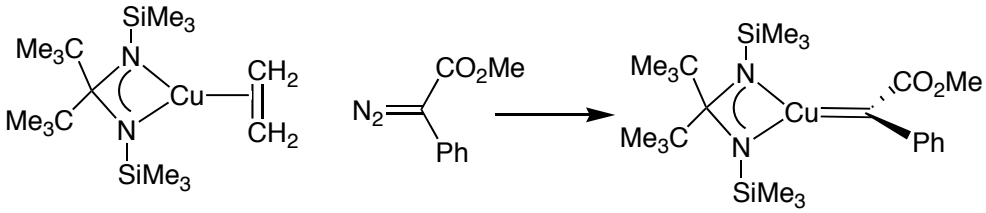

spectroscopically observed

"Copper(I) Carbenes: The Synthesis of Active Intermediates inCu-Catalyzed Cyclopropanation" P. Hoffmann et al, *Angew. Chem. Int. Ed.* **2001**, *40*, 1288-1290

Catalytic Asymmetric Variants: Chiral Cu(I) Complexes

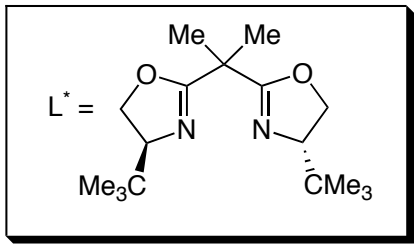

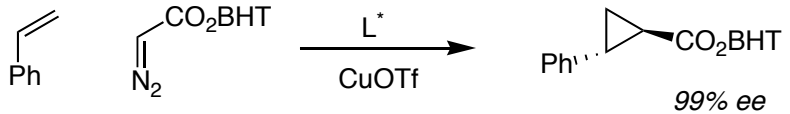

99% ee
94:6 trans/cis

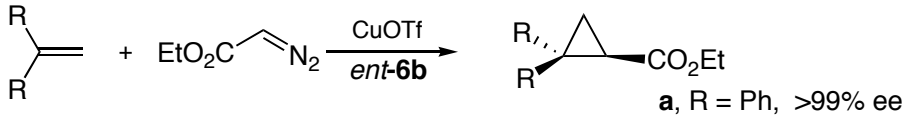

a, R = Ph, >99% ee
b, R = Me, >99% ee

Evans, et al. *J. Am. Chem. Soc.* **1991**, *113*, 726.

Mechanism

There is no definitive evidence for metal-catalyzed cyclopropanation and the possibility that metallacyclobutane intermediates are involved cannot be ruled out.

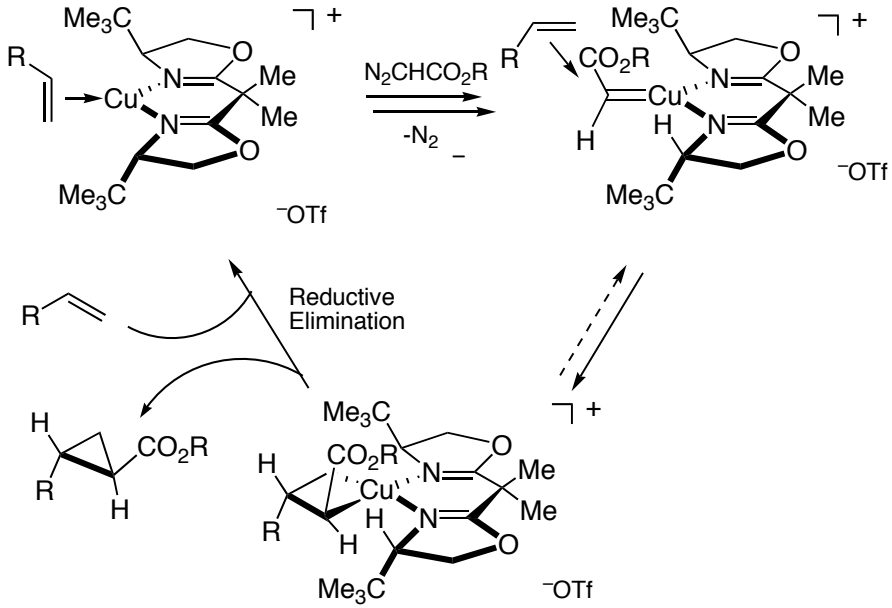

Catalytic Asymmetric Variants:Chiral Rh(II) Complexes

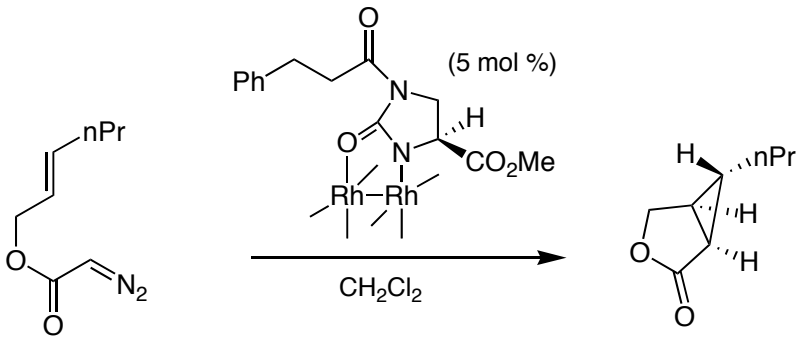

Doyle et al. *Tetrahedron Lett.* **1995**, *36*, 7579.

95% ee

How do these complexes really work??

Catalytic Asymmetric Variants: Chiral Rh(II) Complexes

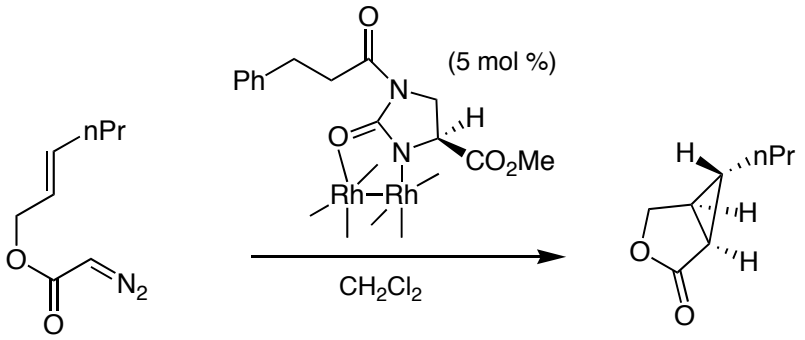

Doyle et al. *Tetrahedron Lett.* **1995**, *36*, 7579.

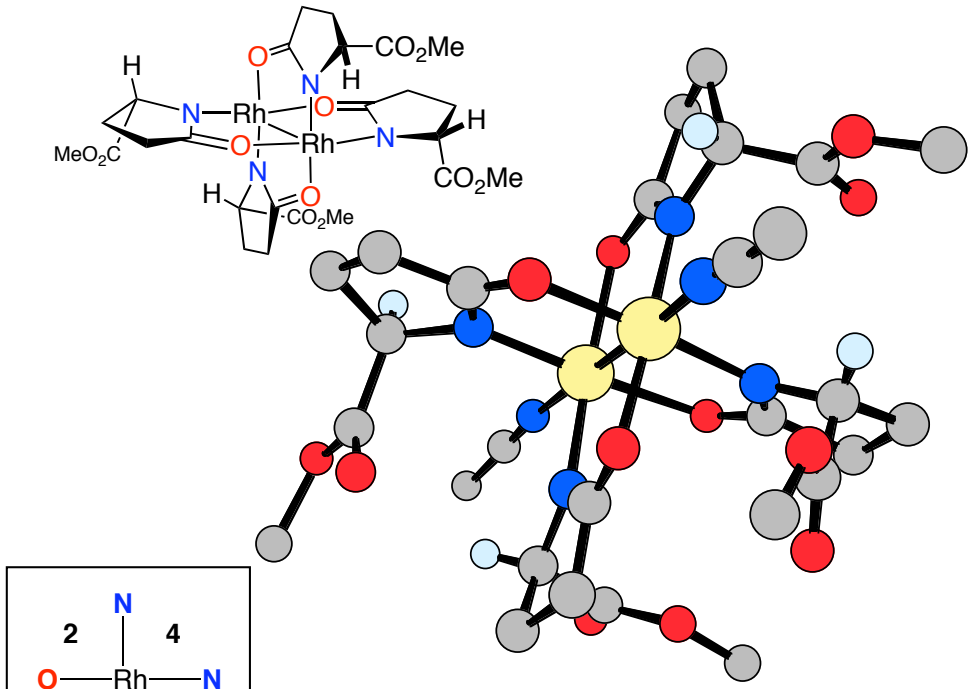

Numbers designate increasing steric hindrance in each quadrant

Doyle, *JACS* **1993**, *115*, 9968

The Carbene Complex

Doyle, *JACS* **1993**, *115*, 9968

Molecular mechanics: favored by 3 kcal/mol

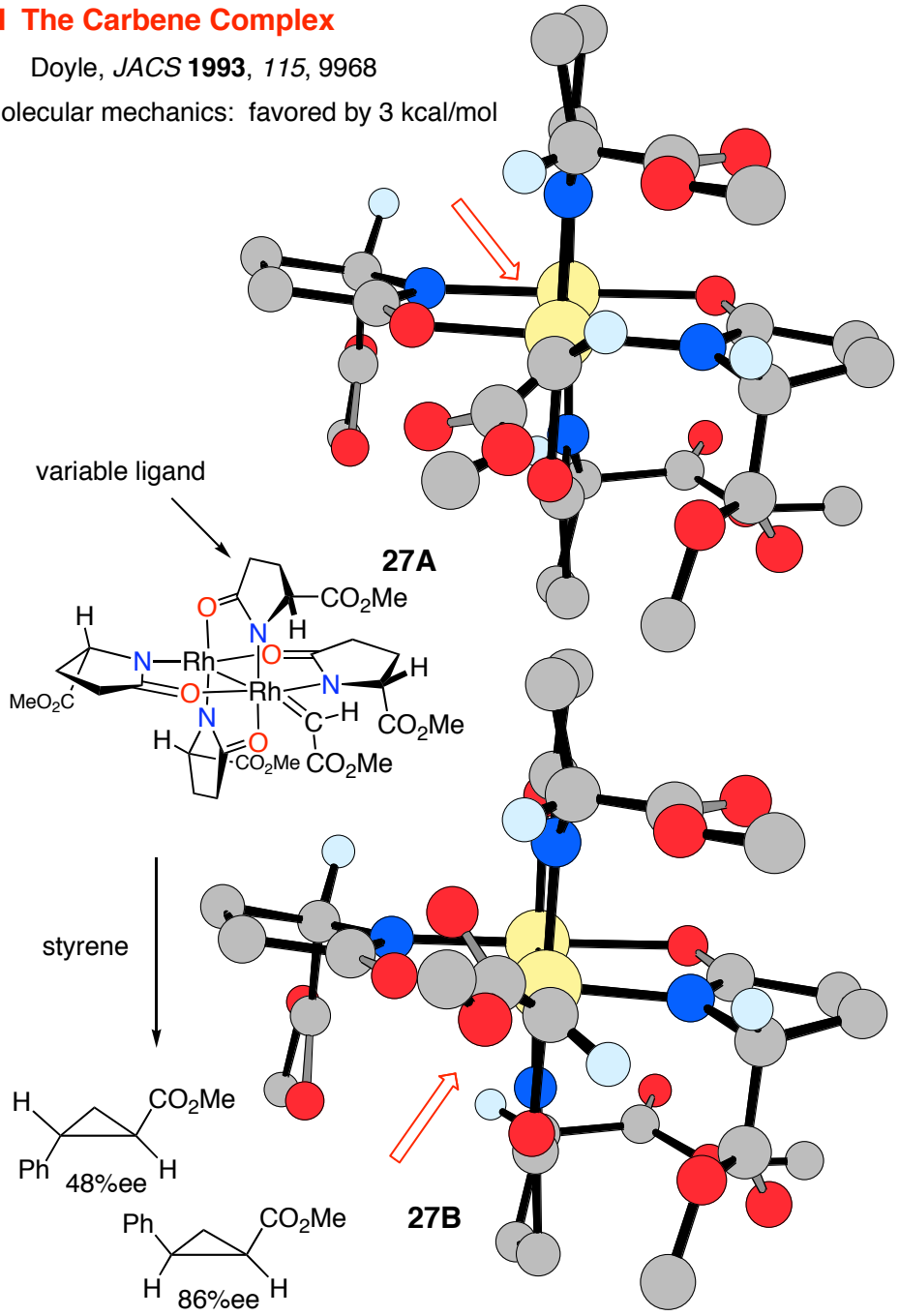

Wolff Rearrangement

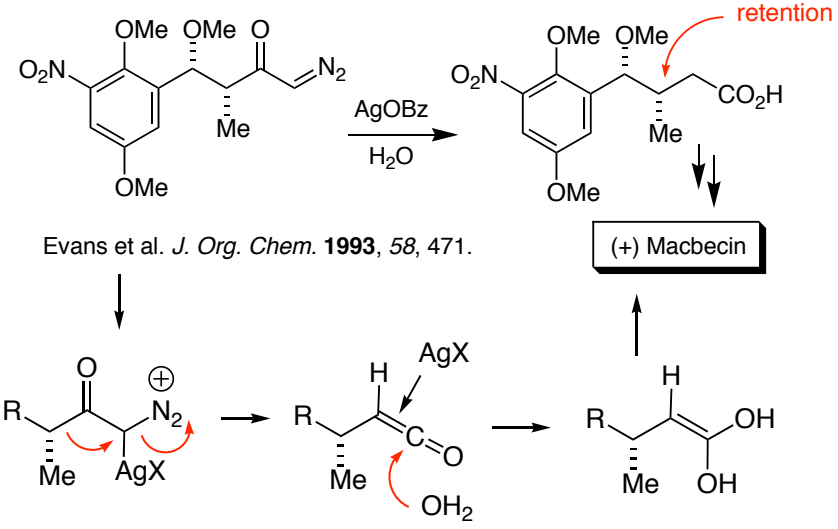

Evans et al. *J. Org. Chem.* **1993**, *58*, 471.

Carbene-Carbene Rearrangements

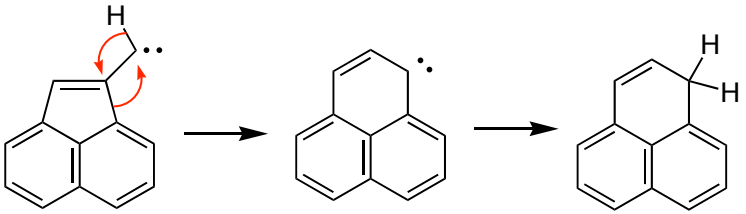

Wu, *Tetrahedron Lett.* **1973**, 3903.

Skattebol Rearrangement

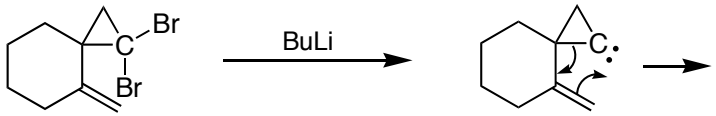

Tetrahedron Lett. **1973**, 2283.

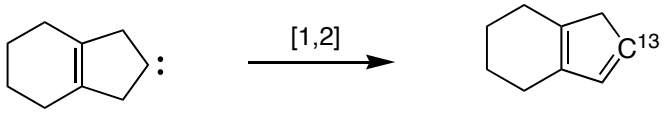

Other Rearrangements

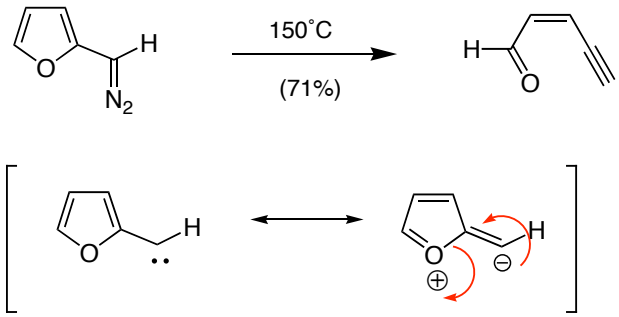

Schecter, *J. Am. Chem. Soc.* **1971**, *93*, 5940.

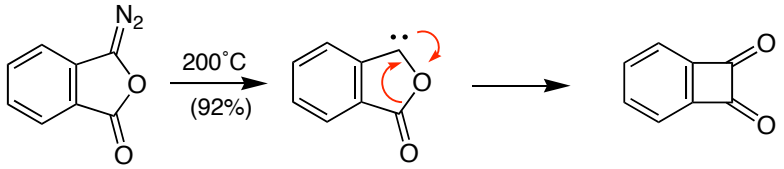

Sammes, *Chem. Comm.* **1975**, 328.

Vinylidenes

Corey-Fuchs: Danishefsky et al. *J. Am. Chem. Soc.* **1996**, *118*, 9509.

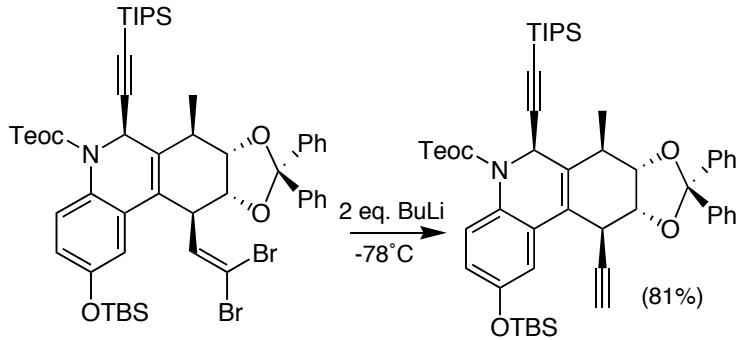

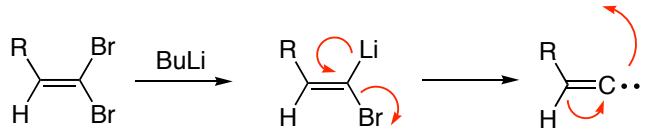

Carbene Rearrangements

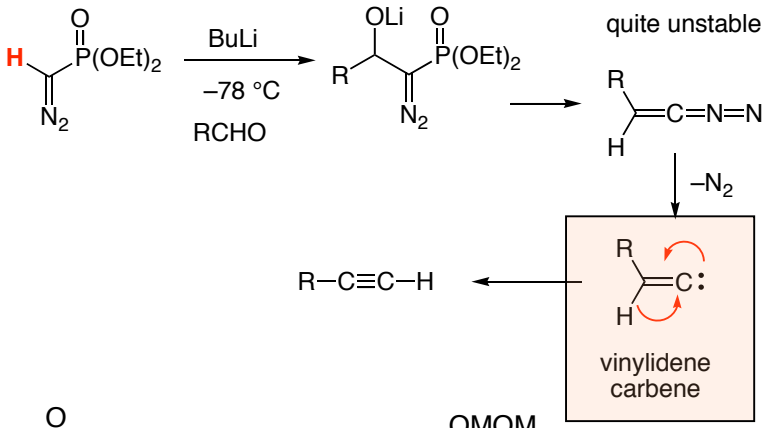

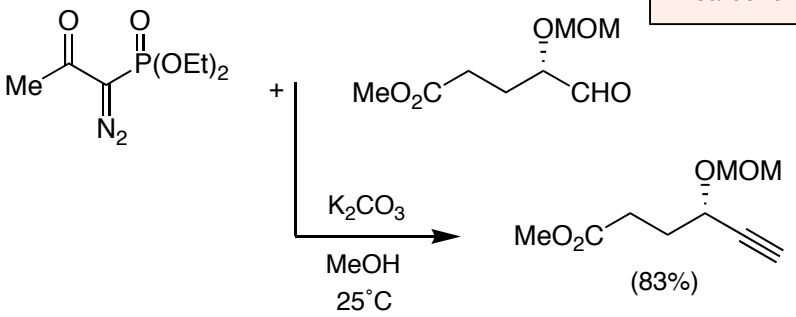

Bestmann, et al. *Synlett* **1996**, 521.

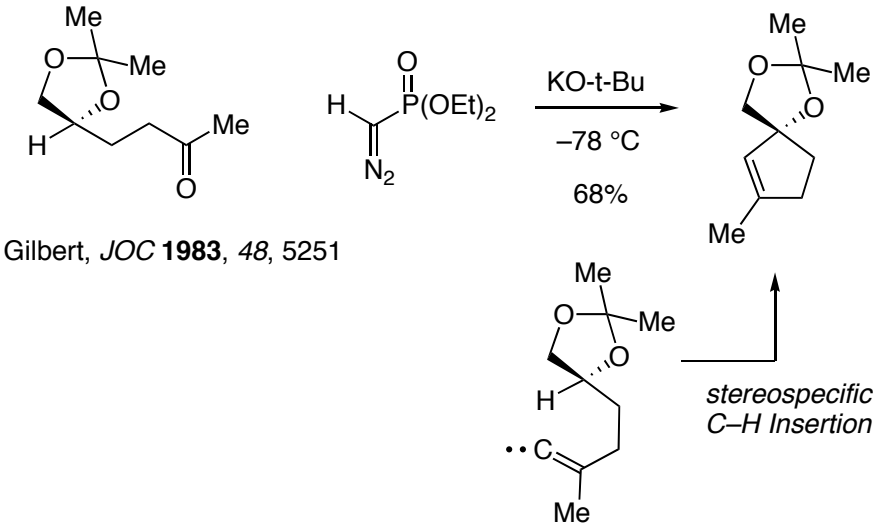

Gilbert, *JOC* **1983**, *48*, 5251

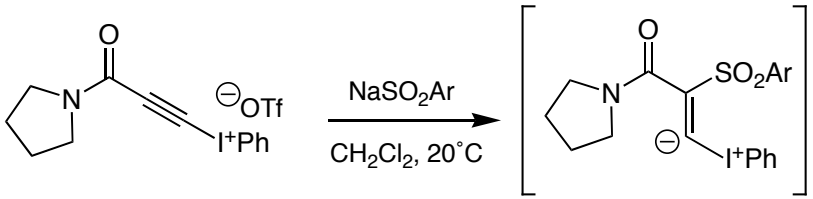

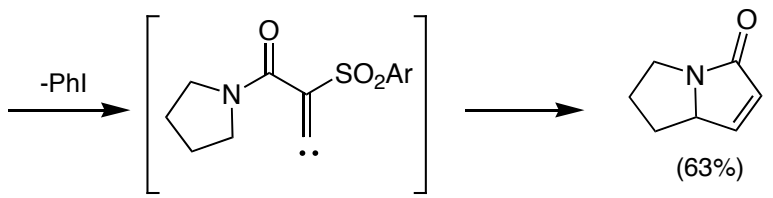

Stang et al. *J. Am. Chem. Soc.* **1994**, *116*, 93.

carbene intermediates are accessible at high temperatures, more later!

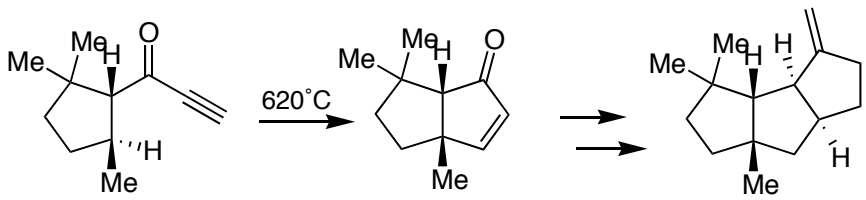

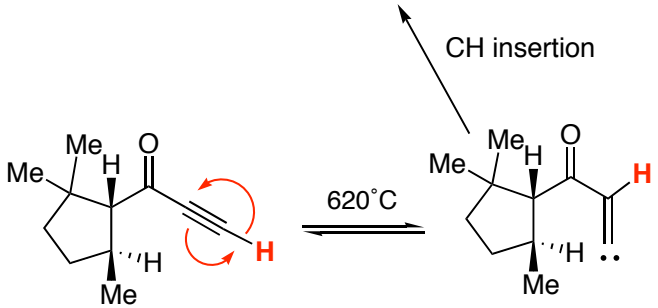

Carbenes are Accessible via Sigmatropic Rearrangement

[1,2] Shifts: Alpha-Alkynone Cyclizations

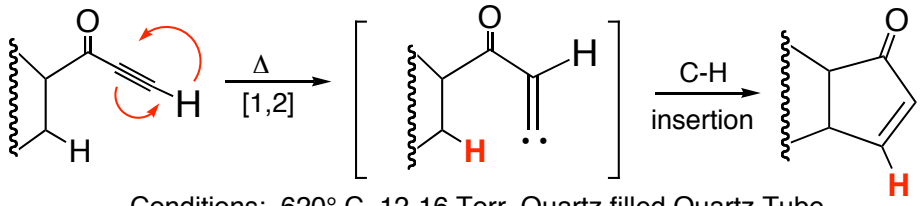

Conditions: 620° C, 12-16 Torr, Quartz filled Quartz Tube

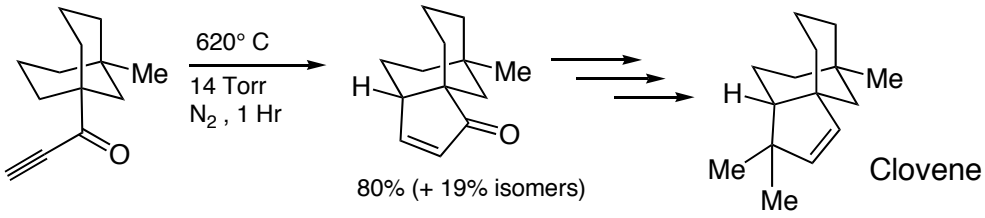

Clovene

Karpf, M., Dreiding, A.S., *Helv. Chim. Acta.* **67** 1963 (1984)

The Automerization of Naphthalene (The Cume Question from Hell!)

Rationalize

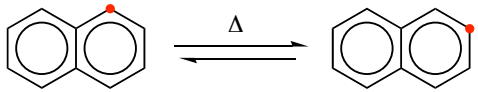

α–^{13}C-labeled $C_{10}H_8$ is isomerized into β–^{13}C-labeled $C_{10}H_8$ at 1035 °C

Mechanism-2,3: L. T. Scott, *JACS* **1991**, *113*, 9692.

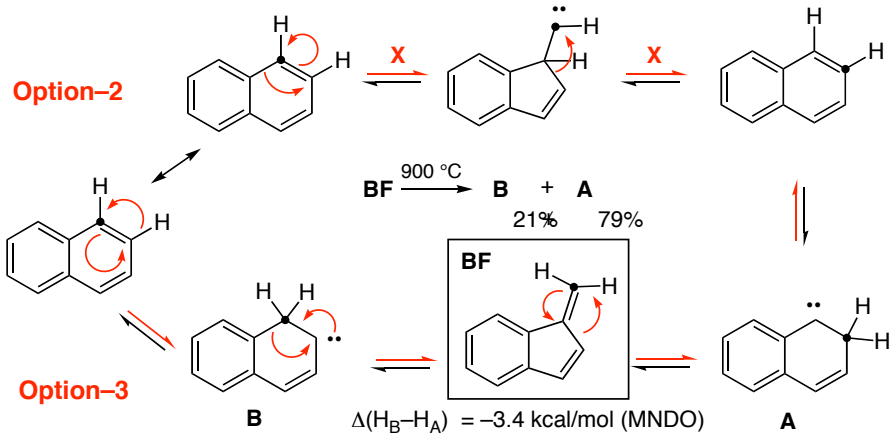

Provide a Mechanism for this Transformation

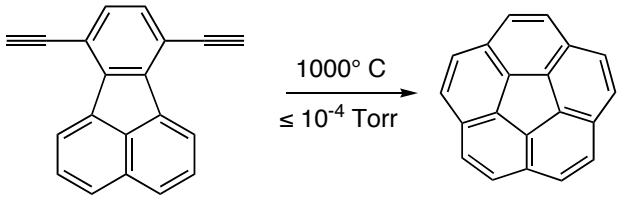

Corannulene 10%

Scott, L.T., et. al., *JACS* **113** 7082 (1991)

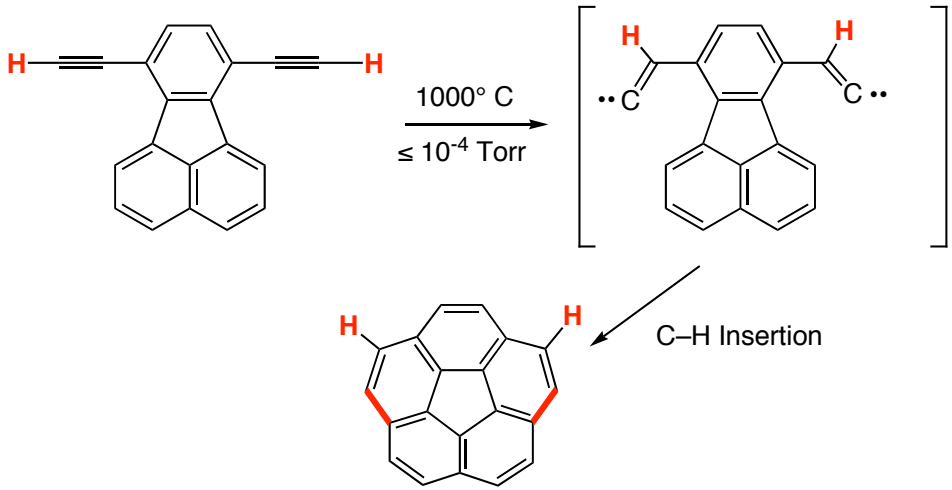

Ylide Formation

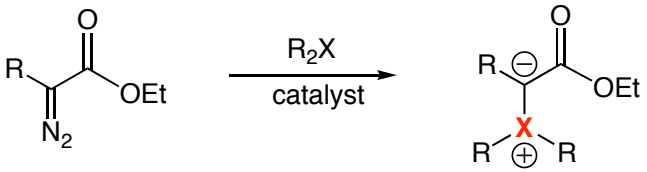

Reviews: Padwa, *Chem. Rev.* **1991** 263
Padwa, *Chem. Rev.* **1996** 223
Barnes, Evening Seminar, March 16, 1993

X is generally S, O or N and can be sp^2 or sp^3 hybridized

Ylides often undergo sigmatropic rearrangements or cycloadditions

[2,3]-Sigmatropic rearrangement:

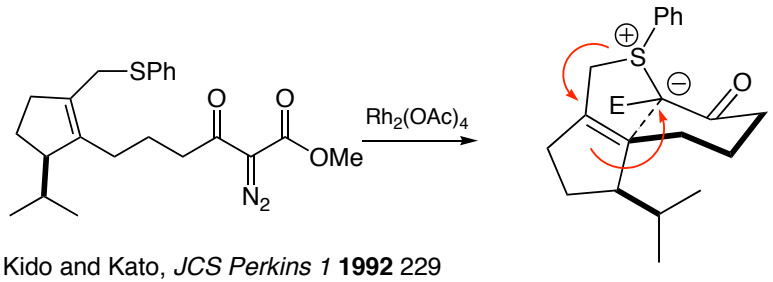

Kido and Kato, *JCS Perkins 1* **1992** 229

Acorenone B

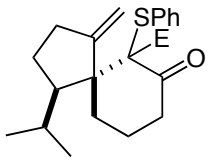

Stevens Rearrangement ([1,2] alkyl shift):

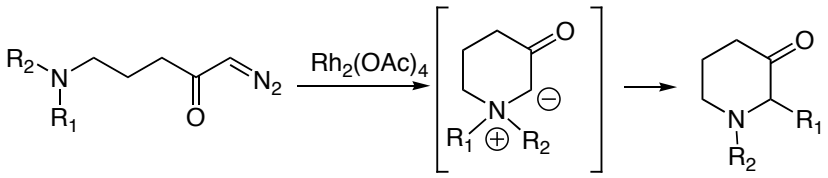

West, *JACS* **1993** 1177

Ring expansion reactions have been investigated

Methods based on sulfur ylides: (review) Vedejs, *Accts. Chem. Res.* **1984**, *17*, 358

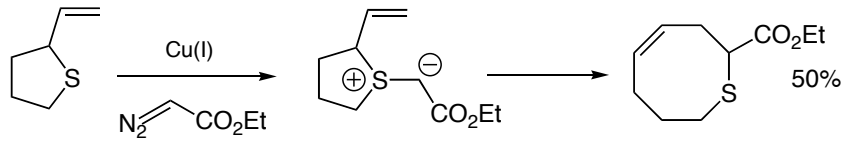

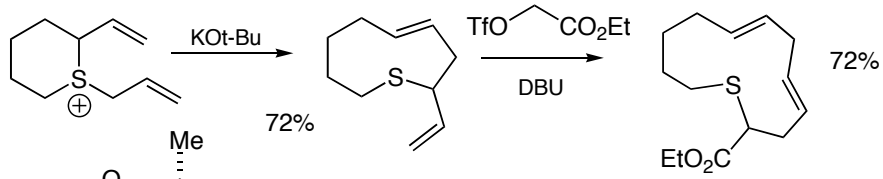

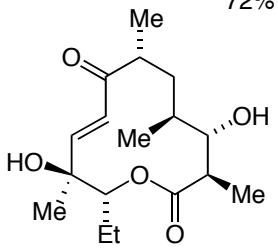

Methynolide has been synthesized by Vedejs using this ring-expansion methodology

Vedejs, *JACS* **1989**, *111*, 8430

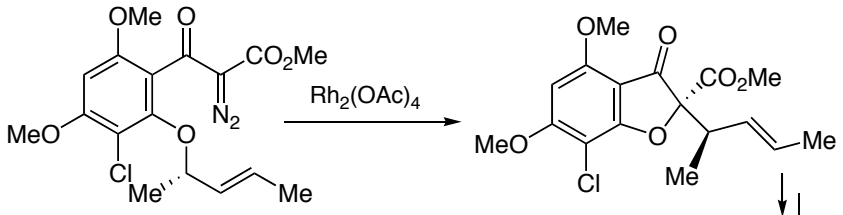

Pirrung et al *JACS*, **1991**, *113*, 8561.

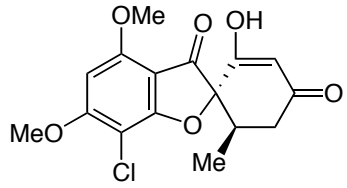

griseofulvin

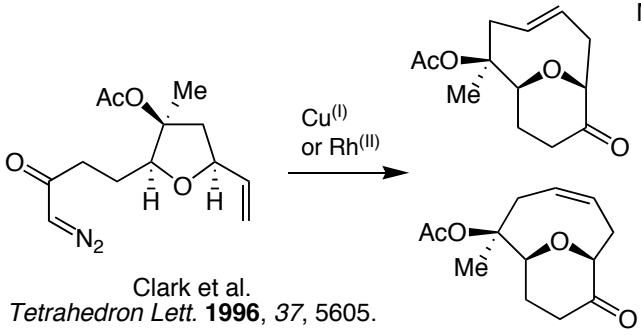

Clark et al.
Tetrahedron Lett. **1996**, *37*, 5605.

Carbenes: Reaction with Heteroatoms

Suggested Reading

Houk and Wu *J. Org. Chem.* **1991**, *56*, 5657.

Padwa and Hornbuckle *Chem. Rev.* **1991**, *91*, 263.

Review Articles

Padwa and Krumpe *Tetrahedron* **1992**, *48*, 5385.

Hoffman, R. W. *Angew. Chem. Int. Ed. Engl.* **1979**, *18*, 563.

McKervey et al. *Chem. Rev.* **1994**, *94*, 1091.

Ylide Formation by the Interaction of Carbeneoids with Carbonyl Lone Pairs

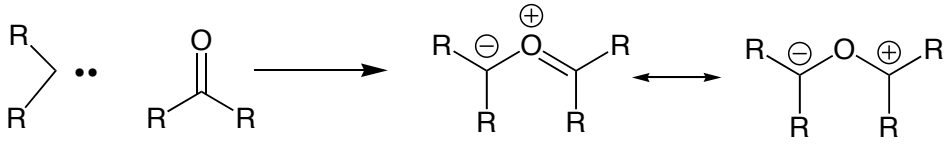

Generally, the carbene precursor of choice is a diazoalkane or, more frequently, an α-diazocarbonyl reagent. These can be decomposed via thermolysis or photolysis. However, the most common method involves catalytic amounts of
transition metals, such as copper or rhodium.

Dipolar Cycloaddition (See Lecture 18)

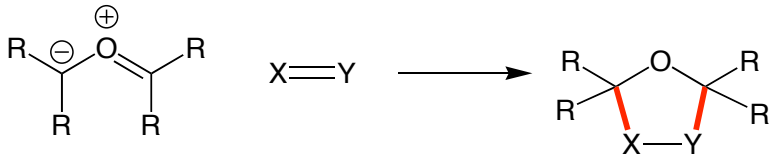

Tandem Intramolecular Cyclization–Intermolecular Cycloaddition (Lecture 18)

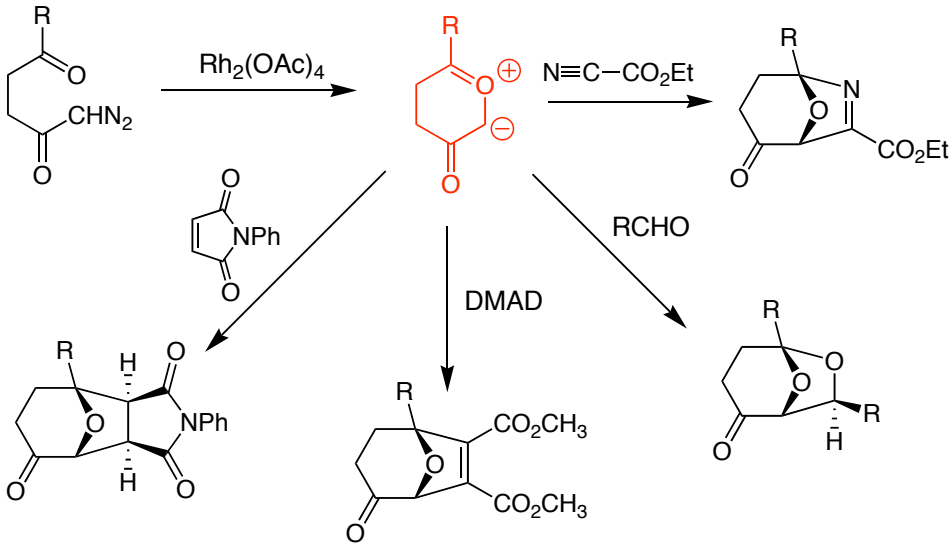

Dipolar-Dipolarophile Cycloadditions: HOMO–LUMO Energies

Carbonyl Ylides have very small HOMO-LUMO gaps

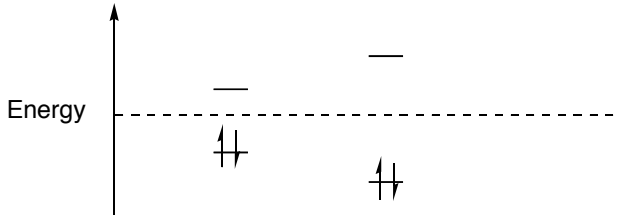

Therefore, either raising the dipolarophile HOMO (electron-donating substituents) or lowering the LUMO (electron-withdrawing) will accelerate the reaction.

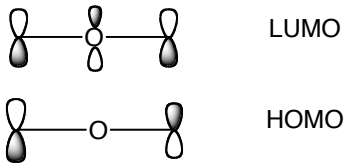

Reactions of Diazoimides: [3+2] addition

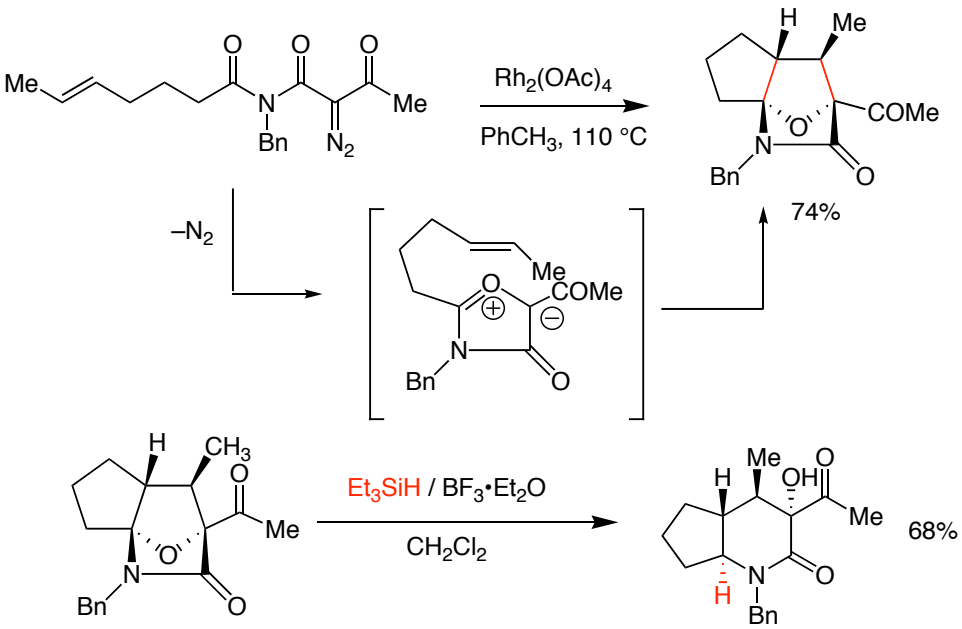

Maier, M. E.; Evertz, K. *Tetrahedron Lett.* **1988**, *29*, 1677-1680.

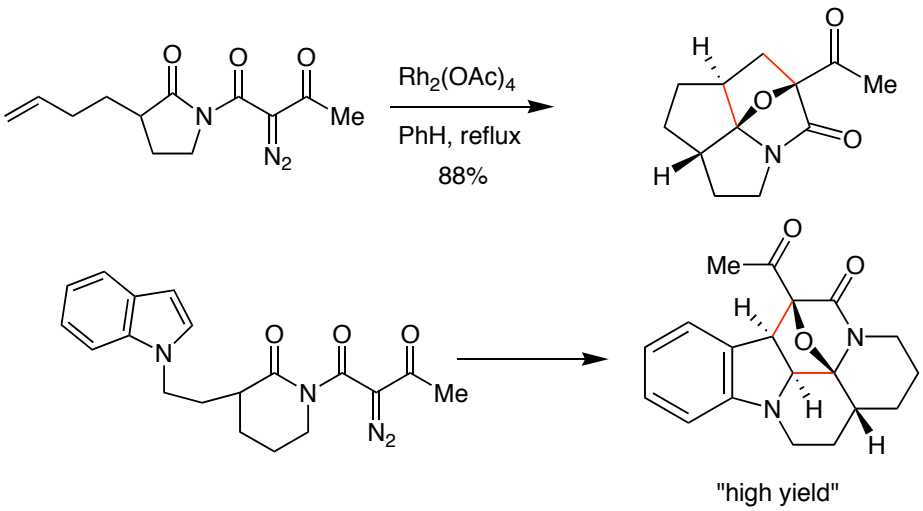

"high yield"

Padwa et. al. *Tetrahedron Lett.* **1992**, *33*, 4731-4734.

Can you propose a rational mechanism for this transformation?

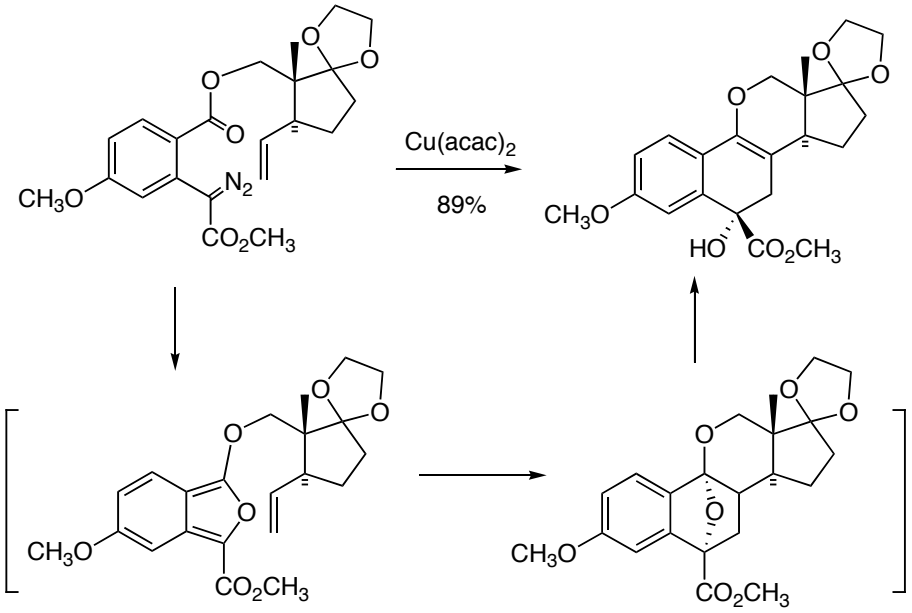

Hildebrandt, *Tetrahedron Lett.* **1988**, *29*, 2045-2046.

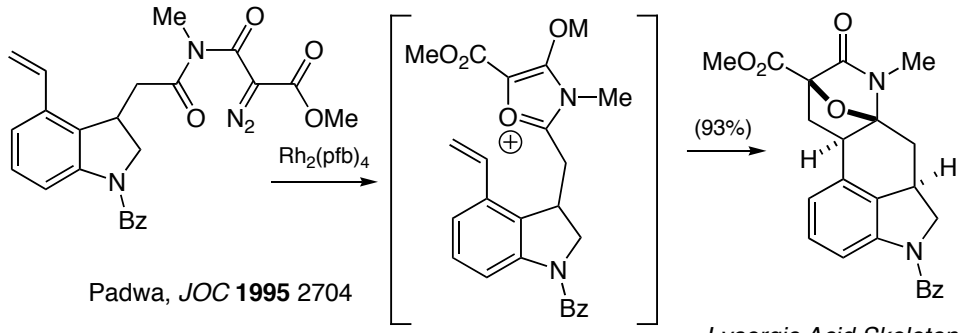

Padwa, *JOC* **1995** 2704

Lysergic Acid Skeleton

INORGANIC ACIDS

Substrate	pKa H_2O	(DMSO)
H_2O	15.7	(32)
H_3O^+	-1.7	
H_2S	7.00	
HBr	-9.00	(0.9)
HCl	-8.0	(1.8)
HF	3.17	(15)
HOCl	7.5	
$HClO_4$	-10	
HCN	9.4	(12.9)
HN_3	4.72	(7.9)
HSCN	4.00	
H_2SO_3	1.9, 7.21	
H_2SO_4	-3.0, 1.99	
H_3PO_4	2.12, 7.21, 12.32	
HNO_3	-1.3	
HNO_2	3.29	
H_2CrO_4	-0.98, 6.50	
CH_3SO_3H	-2.6	(1.6)
CF_3SO_3H	-14	(0.3)
NH_4Cl	9.24	
$B(OH)_3$	9.23	
HOOH	11.6	

CARBOXYLIC ACIDS

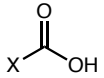

	pKa H_2O	(DMSO)
X= CH_3	4.76	(12.3)
CH_2NO_2	1.68	
CH_2F	2.66	
CH_2Cl	2.86	
CH_2Br	2.86	
CH_2I	3.12	
$CHCl_2$	1.29	
CCl_3	0.65	
CF_3	-0.25	
H	3.77	
HO	3.6, 10.3	
C_6H_5	4.2	(11.1)
o-$O_2NC_6H_4$	2.17	
m-$O_2NC_6H_4$	2.45	
p-$O_2NC_6H_4$	3.44	
o-ClC_6H_4	2.94	
m-ClC_6H_4	3.83	
p-ClC_6H_4	3.99	
o-$(CH_3)_3N^+C_6H_4$	1.37	
p-$(CH_3)_3N^+C_6H_4$	3.43	
p-$OMeC_6H_4$	4.47	

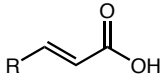

R= H	4.25	
trans-CO_2H	3.02, 4.38	
cis-CO_2H	1.92, 6.23	

ALCOHOLS

HOH	15.7	(31.2)
MeOH	15.5	(27.9)
i-PrOH	16.5	(29.3)
t-BuOH	17.0	(29.4)
c-hex_3COH	24.0	
CF_3CH_2OH	12.5	(23.5)
$(CF_3)_2CHOH$	9.3	(18.2)
C_6H_5OH	9.95	(18.0)
m-$O_2NC_6H_4OH$	8.4	
p-$O_2NC_6H_4OH$	7.1	(10.8)
p-$OMeC_6H_4OH$	10.2	(19.1)
2-napthol		(17.1)

OXIMES & HYDROXAMIC ACIDS

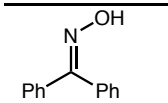

	11.3	(20.1)

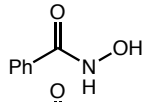

	8.88 (NH)	(13.7)

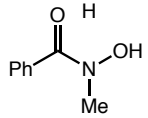

		(18.5)

PEROXIDES

MeOOH	11.5	
CH_3CO_3H	8.2	

PROTONATED SPECIES

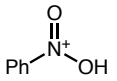

	-12.4	

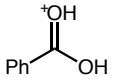

	-7.8	

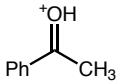

	-6.2	

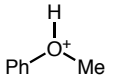

	-6.5	

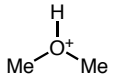

	-3.8	

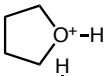

	-2.05	

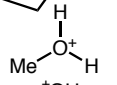

	-2.2	

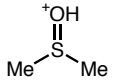

	-1.8	

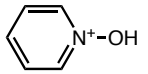

	0.79	(+1.63)

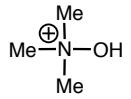

		(+5.55)

SULFINIC & SULFONIC ACIDS

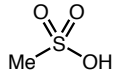

	-2.6	

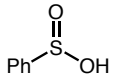

	2.1	

*Values <0 for H_2O and DMSO, and values >14 for water and >35 for DMSO were extrapolated using various methods.

For a comprehensive compilation of Bordwell pKa data see: **http://www.chem.wisc.edu/areas/reich/pkatable/index.htm**

Substrate	pKa H_2O	(DMSO)
PROTONATED NITROGEN		
N^+H_4	9.2	(10.5)
EtN^+H_3	10.6	
i-$Pr_2N^+H_2$	11.05	
Et_3N^+H	10.75	(9.00)
PhN^+H_3	4.6	(3.6)
$PhN^+(Me)_2H$	5.20	(2.50)
$Ph_2N^+H_2$	0.78	
2-napthal-N^+H_3	4.16	
$H_2NN^+H_3$	8.12	
HON^+H_3	5.96	
Quinuclidine 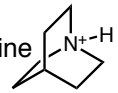	11.0	(9.80)
Morpholine 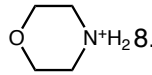	8.36	
N-Me morpholine	7.38	
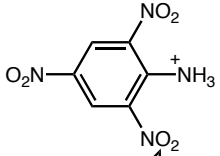	-9.3	
DABCO 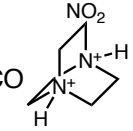	2.97, 8.82 (2.97, 8.93)	
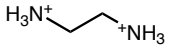	6.90, 9.95	
Proton Sponge 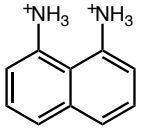	-9.0, 12.0 (--, 7.50)	
$PhCN^+H$	-10	

Substrate	pKa H_2O	(DMSO)
AMINES		
HN_3	4.7	(7.9)
NH_3	38	(41)
i-Pr_2NH	(36 THF))	
TMS_2NH	26(THF)	(30)
$PhNH_2$	(30.6)	
Ph_2NH	(25.0)	
$NCNH_2$	(16.9)	
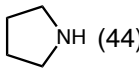	(44)	
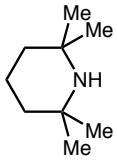	(37)	
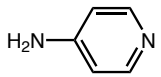	(26.5)	
AMIDES & CARBAMATES		
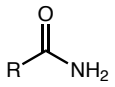 R= H		(23.5)
CH_3	15.1	(25.5)
Ph		(23.3)
CF_3		(17.2)
(urea) NH_2		(26.9)
OEt		(24.8)
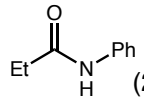	(21.6)	
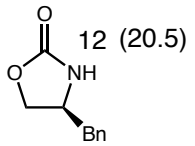	12	(20.5)
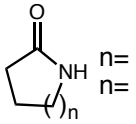 n= 1 (24.1) n= 2 (26.4)		
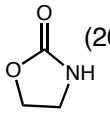		(20.8)
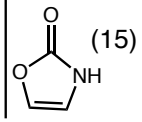	(15)	
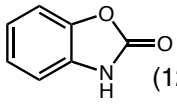		(12.1)

Substrate	pKa H_2O	(DMSO)
IMIDES		
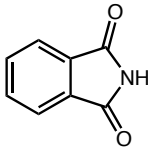	8.30	
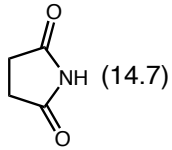		(14.7)
Ac_2NH		(17.9)
SULFONAMIDE		
RSO_2NH_2 R = Me		(17.5)
Ph		(16.1)
CF_3	6.3	(9.7)
$MeSO_2NHPh$		(12.9)
GUANIDINIUM, HYRDAZONES,- IDES, & -INES		
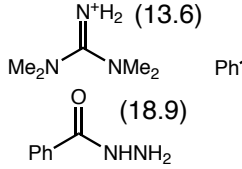	(13.6) (21.6) (18.9)	
$PhSO_2NHNH_2$		(17.2)
PhNHNHPh		(26.1)
PROTONATED HETEROCYCLES		
DBU 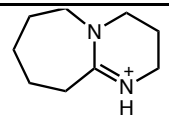		(12) (estimate)
DMAP 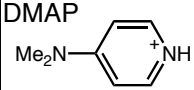	9.2	
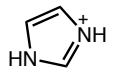	6.95	
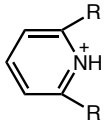 R= H (PPTS)	5.21	(3.4)
t-Bu	4.95	(0.90)
Me	6.75	(4.46)
Cl, H	0.72	

Substrate	pKa H_2O	(DMSO)
HYDROXAMIC ACID & AMIDINES		
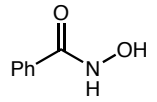	8.88 (NH)	(13.7)
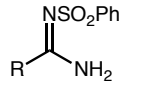 R= Me		(17.3)
Ph		(15.0)
HETEROCYCLES		
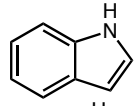		(20.95)
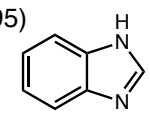		(16.4)
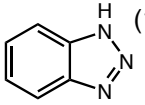		(11.9)
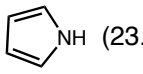		(23.0)
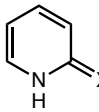 X= O		(24)
X= S		(13.3)
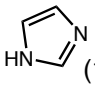		(18.6)
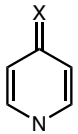 X= O		(14.8)
X= S		(11.8)
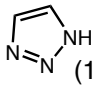		(13.9)
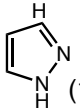		(19.8)
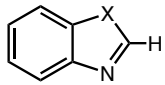 X= O		(24.4)
X= S		(27.0)
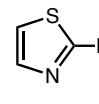		(29.4)
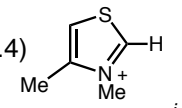		(16.5)
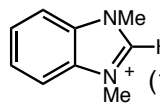		(18.4)
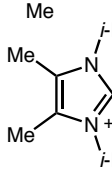		(24)

*Values <0 for H_2O and DMSO, and values >14 for water and >35 for DMSO were extrapolated using various methods.

For a comprehensive compilation of Bordwell pKa data see: **http://www.chem.wisc.edu/areas/reich/pkatable/index.htm**

Substrate	pKa H_2O	(DMSO)
HYDROCARBONS		
$(Me)_3CH$	53	
$(Me)_2CH_2$	51	
$CH_2{=}CH_2$	50	
CH_4	48	(56)
	46	
$CH_2{=}CHCH_3$	43	(44)
PhH	43	
$PhCH_3$	41	(43)
Ph_2CH_2	33.5	(32.2)
Ph_3CH	31.5	(30.6)
HCCH	24	
PhCCH	23	(28.8)
$XC_6H_4CH_3$		
X= *p*-CN		(30.8)
p-NO_2		(20.4)
p-COPh		(26.9)
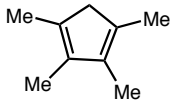		(26.1)
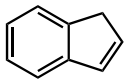	20	(20.1)
	15	(18.0)
H_2	~36	

Substrate	pKa H_2O	(DMSO)
ESTERS		
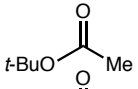	24.5	(30.3)
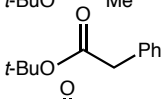		(23.6)
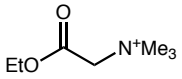		(20.0)
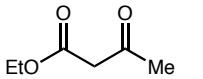	11	(14.2)
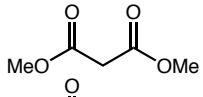	13	(15.7)
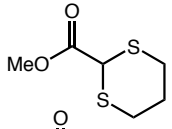		(20.9)
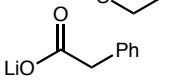		[30.2 (THF)]
AMIDES		
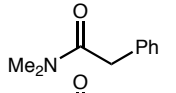		(26.6)
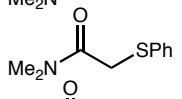		(25.9)
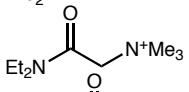		(24.9)
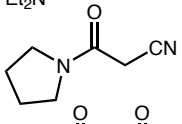		(17.2)
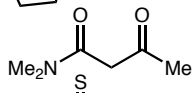		(18.2)
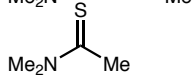		(25.7)

Substrate	pKa H_2O	(DMSO)
KETONES		
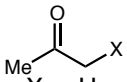		
X= H		(26.5)
Ph		(19.8)
SPh		(18.7)
$COCH_3$	9	(13.3)
SO_2Ph		(12.5)
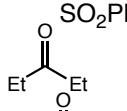	19-20	(27.1)
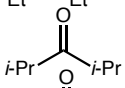		(28.3)
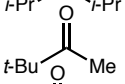		(27.7)
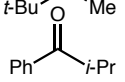		(26.3)
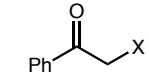		
X= H		(24.7)
CH_3		(24.4)
Ph		(17.7)
$COCH_3$		(14.2)
COPh		(13.3)
CN		(10.2)
F		(21.6)
OMe		(22.85)
OPh		(21.1)
SPh		(16.9)
SePh		(18.6)
NPh_2		(20.3)
N^+Me_3		(14.6)
NO_2		(7.7)
SO_2Ph		(11.4)

Substrate	pKa H_2O	(DMSO)
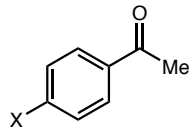		
X= H		(24.7)
OMe		(25.7)
NMe_2		(27.5)
Br		(23.8)
CN		(22.0)
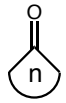		
n= 4		(25.1)
5		(25.8)
6		(26.4)
7		(27.7)
8		(27.4)
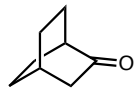		(28.1)
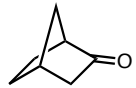		(29.0)
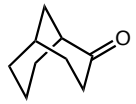		(25.5)
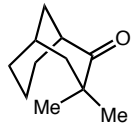		(32.4)

*Values <0 for H_2O and DMSO, and values >14 for water and >35 for DMSO were extrapolated using various methods.

For a comprehensive compilation of Bordwell pKa data see: **http://www.chem.wisc.edu/areas/reich/pkatable/index.htm**

NITRILES

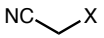

X=		pKa H_2O	(DMSO)
	H		(31.3)
	CH_3		(32.5)
	Ph		(21.9)
	COPh		(10.2)
	$CONR_2$		(17.1)
	CO_2Et		(13.1)
	CN	11	(11.1)
	OPh		(28.1)
	N^+Me_3		(20.6)
	SPh		(20.8)
	SO_2Ph		(12.0)

HETERO-AROMATICS

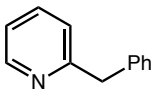

(28.2)

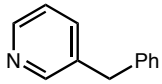

(30.1)

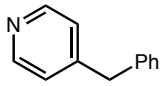

(26.7)

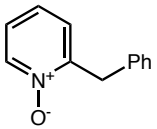

(25.2)

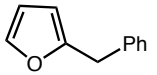

(30.2)

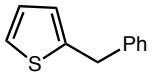

(30.0)

SULFIDES

$PhSCH_2X$

X=		pKa H_2O	(DMSO)
	Ph		(30.8)
	CN		(20.8)
	$COCH_3$		(18.7)
	COPh		(16.9)
	NO_2		(11.8)
	SPh		(30.8)
	SO_2Ph		(20.5)
	SO_2CF_3		(11.0)
	$POPh_2$		(24.9)

$MeSCH_2SO_2Ph$ (23.4)

$PhSCHPh_2$ (26.7)

$(PhS)_3CH$ (22.8)

$(PrS)_3CH$ (31.3)

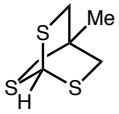

(30.5)

$(PhS)_2CHPh$ (23.0)

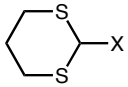

X=		pKa H_2O	(DMSO)
	Ph		(30.7)
	CO_2Me		(20.8)
	CN		(19.1)

$RSCH_2CN$

R=		pKa H_2O	(DMSO)
	Me		(24.3)
	Et		(24.0)
	i-Pr		(23.6)
	t-Bu		(22.9)

$PhSCH=CHCH_2SPh$ (26.3)

BuSH 10-11 (17.0)

PhSH ≈7 (10.3)

SULFOXIDES

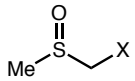

X=		pKa H_2O	(DMSO)
	H		(35.1)
	Ph		(29.0)
	SPh		(29.0)

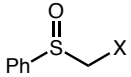

X=		pKa H_2O	(DMSO)
	H		(33)
	Ph		(27.2)
	SOPh		(18.2)

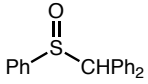

(24.5)

SULFONIUM

$Me_3S^+=O$ (18.2)

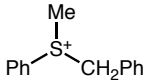

(16.3)

SULFIMIDES & SULFOXIMINES

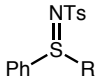

R=		pKa H_2O	(DMSO)
	Me		(27.6)
	i-Pr		(30.7)

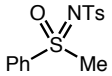

(24.5)

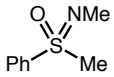

(33)

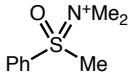

(14.4)

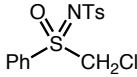

(20.7)

SULFONES

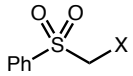

X=		pKa H_2O	(DMSO)
	H		(29.0)
	CH_3		(31.0)
	t-Bu		(31.2)
	Ph		(23.4)
	$CH=CH_2$		(22.5)
	CH=CHPh		(20.2)
	CCH		(22.1)
	CCPh		(17.8)
	COPh		(11.4)
	COMe		(12.5)
	OPh		(27.9)
	N^+Me_3		(19.4)
	CN		(12.0)
	NO_2		(7.1)
	SMe		(23.5)
	SPh		(20.5)
	SO_2Ph		(12.2)
	PPh_2		(20.2)

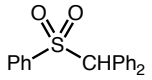

(22.3)

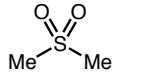

(31.1)

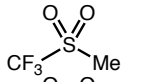

(18.8)

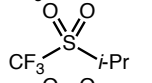

(21.8)

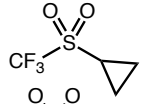

(26.6)

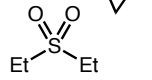

(32.8)

$(PhSO_2)_2CH_2Me$ (14.3)

*Values <0 for H_2O and DMSO, and values >14 for water and >35 for DMSO were extrapolated using various methods.

pKa's of CH bonds at Heteroatom Substituted Carbon & References

Substrate	pKa H_2O	(DMSO)
ETHERS		
CH_3OPh		(49)
$MeOCH_2SO_2Ph$		(30.7)
$PhOCH_2SO_2Ph$		(27.9)
$PhOCH_2CN$		(28.1)
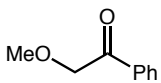		(22.85)
SELENIDES		
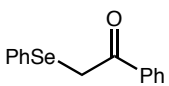		(18.6)
$PhSeCHPh_2$		(27.5)
$(PhSe)_2CH_2$		(31.3)
$PhSeCH_2Ph$		(31.0)
$PhSeCH{=}CHCH_2SePh$		(27.2)
AMMONIUM		
$Me_3N^+CH_2X$		
X= CN		(20.6)
SO_2Ph		(19.4)
COPh		(14.6)
CO_2Et		(20.0)
$CONEt_2$		(24.9)

Substrate	pKa H_2O	(DMSO)
PHOSPHONIUM		
P^+H_4		-14
MeP^+H_3		2.7
Et_3P^+H		9.1
$Ph_3P^+CH_3$		(22.4)
$Ph_3P^+i\text{-}Pr$		(21.2)
$Ph_3P^+CH_2COPh$		(6.2)
$Ph_3P^+CH_2CN$		(7.0)
PHOSPONATES & PHOSPHINE OXIDES		
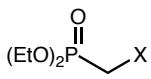		
X= Ph		(27.6)
CN		(16.4)
CO_2Et		(18.6)
Cl		(26.2)
$SiMe_3$		(28.8)
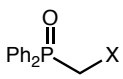		
X= SPh		(24.9)
CN		(16.9)
PHOSPHINES		
$Ph_2PCH_2PPh_2$		(29.9)
$Ph_2PCH_2SO_2Ph$		(20.2)

Substrate	pKa H_2O	(DMSO)
NITRO		
RNO_2		
R= CH_3	≈10	(17.2)
CH_2Me		(16.7)
$CHMe_2$		(16.9)
CH_2Ph		(12.2)
CH_2Bn		(16.2)
CH_2SPh		(11.8)
CH_2SO_2Ph		(7.1)
CH_2COPh		(7.7)
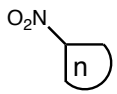		
n= 3		(26.9)
4		(17.8)
5		(16.0)
6		(17.9)
7		(15.8)
IMINES		
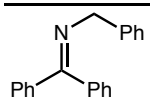		(24.3)

Oxime ethers are ~ 10 pka units less acidic than their ketone counterparts
Streitwieser, JOC 1991, 56, 1989

REFERENCES

DMSO:

JACS 97, 7007 (1975)
JACS 97, 7160 (1975)
JACS 97, 442 (1975)
JACS 105, 6188 (1983)
JOC 41, 1883 (1976)
JOC 41, 1885 (1976)
JOC 41, 2786 (1976)
JOC 41, 2508 (1976)
JOC 42, 1817 (1977)
JOC 42, 321 (1977)
JOC 42, 326 (1977)
JOC 43, 3113 (1978)
JOC 43, 3095 (1978)
JOC 43, 1764 (1978)
JOC 45, 3325 (1980)
JOC 45, 3305 (1980)
JOC 45, 3884 (1980)
JOC 46, 4327 (1981)
JOC 46, 632 (1981)
JOC 47, 3224 (1982)
JOC 47, 2504 (1982)
Acc. Chem. Res. 21, 456 (1988)
Unpublished results of F. Bordwell

Water:

Advanced Org. Chem., 3rd Ed.
J. March (1985)
Unpublished results of W. P. Jencks

THF:
JACS 110, 5705 (1988)

See cited website below for additional data

*Values <0 for H_2O and DMSO, and values >14 for water and >35 for DMSO were extrapolated using various methods.

For a comprehensive compilation of Brodwell pKa data see: **http://www.chem.wisc.edu/areas/reich/pkatable/index.htm**

DMSO Acidities of Common Heterocycles

Bordwell, ACR, **1988**, *21*, 456
Bordwell http://www.chem.wisc.edu/areas/reich/pkatable/index.htm

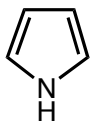

23.0

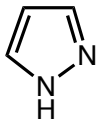

19.8

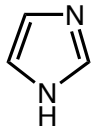

18.6

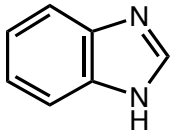

16.4

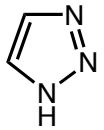

13.9

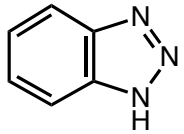

11.9

18.0

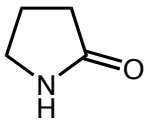

24.0

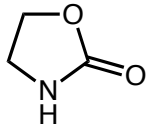

20.8

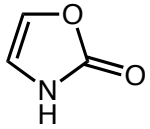

15.0

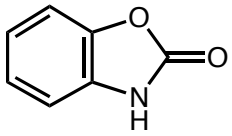

12.1

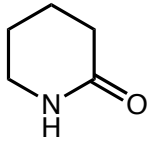

26.4

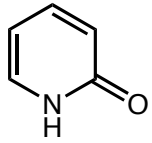

24.0

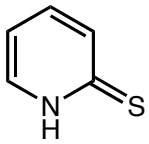

13.3

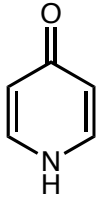

14.8

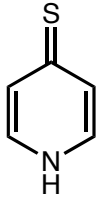

11.8

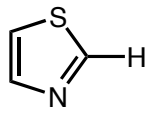

29.4

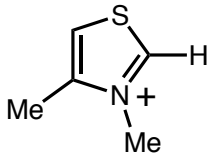

16.5

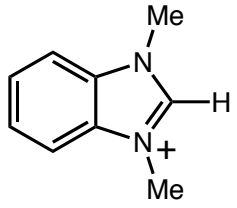

18.4

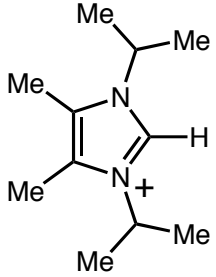

24

pKa Values

INDEX

Inorganic	2	Phenazine	24
Phosphates	3	Pyridine	25
Carboxylic acids	4, 8	Pyrazine	26
Aliphatic	4, 8		
Aromatic	7, 8	Quinoline	27
Phenols	9	Quinazoline	27
Alcohols and oxygen acids	10, 11	Quinoxaline	27
Amino Acids	12	Special Nitrogen Compounds	28
Peptides	13	Hydroxylamines	28
Nitrogen Compounds	14	Hydrazines	28
Aliphatic amines	15, 17, 19	Semicarbazones	28
Cyanoamines	16	Amidoximes	28
Anilines	17, 18, 20	Thiols	29
Nucleosides	21	Carbon Acids	30,31
Special Table Heterocycles	22	Indicators	31
Acridine	23	References	32-34
Benzoquinoline	24		
Cinnoline	23		
Hydantoin	24		
Imidazole	24		

For complex chelating agents, see also reference 77.

Note. This document was compiled by W.P. Jencks and has been added to by F.H. Westheimer

ACIDS

Compound	pK	Ref.
$AgOH$	3.96	4
$Al(OH)_3$	11.2	28
$As(OH)_3$	9.22	28
H_3AsO_4	2.22, 7.0, 13.0	28
$H_2AsO_4^-$	6.98*	77
$HAsO_4$*	11.53*	77
As_2O_3	0	4
H_3AsO_3	9.22*	
H_3BO_3	9.23*	28
$H_2B_4O_7$	4.00	34
HB_4O_7	9.00	34
$Be(OH)_2$	3.7	4
HBr	-9.00	31
$HOBr$	8.7	28
$HOCl$	7.53, 7.46	28, 33
$HClO_2$	2.0	28
$HClO_3$	-1.00	28
$HClO_4$ (70%)	-10.00	31
CH_3SO_3H	-0.6	31
HCN	9.40	34
H_2CO_3	6.37, 6.35*, 3.58	34, 32
HCO_3	10.33*	
H_2CrO_4	-0.98	30
$HCrO_4$	6.50*	2, 30
$HOCN$	3.92	34
HZ	3.17*, 0.59*	77
H_2GeO_3	8.59, 12.72	34, 78
$Ge(OH)_4$	8.68, 12.7	28
HI	-10.0	31
HOI	11.0	28
HIO_3	0.8	28
$H_4IO_6^-$	6.00	34
H_5IO_6	1.64, 1.55, 8.27	34, 28
$HMnO_4$	-2.25	30
NH_3OH*	5.98*	
NH_4*	9.24*	77
HN_3	4.72*	77
HNO_2	3.29	28
HNO_3	-1.3	28
$N_2H_5^+$	7.99*	77
$H_2N_2O_2$	7.05	34
$H_2N_2O_2^-$	11.0	34
H_2OsO_5	12.1	34
H_2O	15.7	none
H_3O^+	-1.7	none
$Pb(OH)_2$	6.48 (10.92)	4 (78)
H_3PO_2	2.0, 2.23*	28
$H_2PO_4^-$	7.21*	77
HPO_4–	12.32*	77
H_3PO_3	2.0	28
$H_2PO_3^-$	6.58*	77
$H_4P_2O_7$	1.52*	77
$H_3\ P_2O_7^-$	2.36*	77
$H_2P_2O_7^=$	6.60*	77
$HP_2O_7^=$	9.25*	77
$HReO_4$	-1.25	30
$HSCN$	4.00	34
H_2SeO_3	2.6, 8.3, 2.62*	28
$HSeO_3$	8.32	77
H_2SeO_4	Strong, 2.0	28
$HSeO_4$	2.00	34
H_3SiO_3	10.0	34
H_2SO_3	1.9, 7.0, 1.76*	28, 77
H_2SO_4	-3.0, 1.9	28
HSO_3	7.21*	77
HSO_4^-	1.99*	77
$H_2S_2O_4$	1.9	29
H_2Se	3.89*	77
HSe^-	11.00*	77
H_2S	7.00*	77
HS^-	12.92*	77
$HSbO_2$	11.0	34
HTe	5.00	34
H_2Te	2.64, 11.0	34, 78
H_2TeO_3	2.7, 8.0	28
$Te(OH)_6$	6.2, 8.8	28
$H_2VO_4^-$	8.95	30
$HVO_4^=$	14.4	30
H_2CrO_4	0.74	77
$HOCN$	3.73	77
$HSCN$	0.85	77
H_3PO_2	1.07	77
H_3PO_4	2.12*	77
$H_2S_2O_3$	0.60*, 1.72*	77
H_3AuO_3	13.3, 16.0	78
H_3GaO_3	10.32, 11.7	78
H_5IO_6	3.29, 6.70, 15.0 (see above!)	78
$H_4V_6O_{17}$	1.96	78
H_2NSO_3H	1.0	80

* *Indicates a thermodynamic value.*

PHOSPHATES AND PHOSPHONATES

Phosphates

Compound	pK	Ref.
Phosphate	1.97, 6.82, 12.5	55
Glyceric acid 2-phosphate	3.6, 7.1	53
Enolpyruvic acid	3.5, 6.4	53
Methyl-	1.54, 6.31	55
Ethyl-	1.60, 6.62	55
n-Propyl-	1.88,6.67	55
n-Butyl-	1.80, 6.84	55
Dimethyl-	1.29	55
Di-n-propyl	1.59	55
Di-n-butyl-	1.72	55
Glucose-3-	0.84, 5.67	56
Glucose-4-	0.84, 5.67	56
α-glycero-	1.40, 6.44	54
β-glycero-	1.37, 6.34	54
3-phosphoglyceric acid	1.42, 3.42	54
2-phosphoglyceric acid	1.42, 3.55, 7.1	
peroxymonophosphoric acid	4.05	69
diphosphoglyceric acid	7.40, 7.99	54
glyceraldehyde-	2.10, 6.75	54
dioxyacetone-	1.77,6.45	54
hexose di-	1.52, 6.31	54
fructose-6-	0.97, 6.11	54
glucose-6-	0.94, 6.11	54
glucose-1-	1.10, 6.13	54
adenylic acid	3.8?, 6.2?	54
inosinic acid	2.4?, 6.4?	54
ADP	2 strong, 6.6	54
ATP	3 strong, 6.6	54
pyrophosphoric acid	0.9, 2.0, 6.6, 9.4	54
phosphopyruvic acid	3.5, 6.38	54
creatine phosphate	2.7, 4.5	54
arginine phosphate	2.8, 4.5, 9.6, 11.2	54
arginine	2.02, 9.0, 12.5	54
amino phosphate	(-0.9), 2.8, 8.2	54
trimetaphosphate	2.05	77

Phosphonates

$H_2O_3P(CH_2)_4PO_3H_2$	<2, 2.75, 7.54, 8.38	57
$H_2O_3P(CH_2)_3PO_3H_2$	<2, 2.65, 7.34, 8.35	57
$H_2O_3PCH_2CH(CH_3)PO_3H_2$	<2, 2.6, 7.00, 9.27	57
$H_2O_3PCH_2PO_3H_2$	<2, 2.57, 6.87, 10.33	57
Methyl-	2.35	57
Ethyl-	2.43	57
n-propyl-	2.45	57
isopropyl-	2.55, 7.75	57
n-butyl-	2.59, 8.19	57
isobutyl-	2.70, 8.43	57
s-butyl-	2.74, 8.48	57
t-butyl-	2.79, 8.88	57
neopentyl-	2.84, 8.65	57
1,1 Dimethylpropyl-	2.88, 8.96	57
n-hexyl-	2.6, 7.9	57
n-dodecyl-	--, 8.25	57
$CH_3(CH_2)_5CH(COOH)$-	1, --	57
CF_3-	1.16, 3.93	57
CCl_3-	1.63, 4.81	57
$NH_3^+CH_2$-	2.35, 5.9	57
$(^-OOCCH_2)_2NH^+CH_2$-	--, 5.57	57
$CHCl_2$-	1.14, 5.61	57
CH_2CI-	1.40, 6.30	57
CH_2Br-	1.14, 6.52	57
$(^-OOCCH_22NH^+(CH_2)_2$-	--, 6.54	57
CH_2I-	1.30, 6.72	57
$NH_3^+CH_2CH_2$-	2.45, 7.00	57
C_6H_5CH=CH-	2.00, 7.1	57
$HOCH_2$-	1.91, 7.15	57
$C_6H_5NH_{2+}(CH_2)_3$-	2.1, --	57
$C_6H_5NH(CH_2)_3$-	--, 7.17	57
$Br(CH_2)_2$-	2.25, 7.3	57
$CH_3(CH_2)_5CH(COO^-)$-	--, 7.5	57
$C_6H_5CH_2$-	2.3, 7.55	57
$NH_3^+(CH_2)_4$)-	2.55, 7.55	57
$NH_3^+(CH_2)_5$-	2.6, 7.6	57
$NH_3^+(CH_2)_{10}$-	--, 8.00	57
$^-OOC(CH_2)_{10}$-	--, 8.25	57
$(CH_3)_3SiCH_2$-	3.22, 8.70	57
$C_6H_5CH_2$-	3.3, 8.4	57
$(C_6H_5)SC$-	3.85, 9.00	57

Arylphosphonic acids

$2X\text{-}RC_6H_3PO_3H_2$

X	R		
Cl	4-O_2N	1.12, 6.14	57
Br	5-O_2N	(a), 6.14	57
Cl	5-Cl	(a), 6.63	57
Cl	H	1.63, 6.98	57
Br	H	1.64, 7.00	57
Br	5-CH_3	1.81, 7.15	57
Cl	4-NH_2	--, 7.33	57
CH_3O	4-O_2N	1.53, 6.96	57
CH_3O	H	2.16, 7.77	57
CH_3O	4-O_2N	--, 8.22	57
HO	4-O_2N	1.22, 5.39	57
O_2N	H	1.45, 6.74	57
F	H	1.64, 6.80	57
I	H	1.74, 7.06	57
NH_2H	--, 7.29	57	
CH_3H	2.10, 7.68	57	
C_6H_5	H	(a), 8.13	57
HOOC	H	1.71, 9.17	57

**These values were obtained in 50% ethanol.
(a) The compounds were not sufficiently soluble.
For graphical plots of a large number of substituted phosphorus compounds see 83.

triphosphate	8.90, 6.26, 2.30	77
tetrametaphosphate	2.74	77

fluorophosphate	0.55, 4.8		56

Phosphonates (Ref. 2)

X	-H	-H	$-NH_3^+$	$-NH_3^+$
$X(CH_2)PO_3H_2$	2.35	7.1	1.85	5.35
$X(CH_2)_2PO_3H_2$	2.45	7.85	2.45	7.00
$X(CH_2)_4PO_3H_2$			2.55	7.55
$X(CH_2)_5PO_3H_2$			2.6	7.65
$X(CH_2)_6PO_2H_2$	2.6	7.9		
$X(CH_2)_{10}PO_2H_2$				8.00

Phosphines in acetonitrile, see ref. 89.

CARBOXYLIC ACIDS

Aliphatic

Compound	pK	Ref.
Acetoacetic	3.58	6
Acetopyruvic	2.61, 7.85 (enol)	6
Aconitic, trans-	2.80, 4.46	6
Betaine	1.84	6
Citric	3.09, 4.75, 5.41	6
Crotonic	4.69	6
Dihydroxyfumaric	1.14	6
Dethylenediamine-	2.00, 2.67	6
tetraacetic	6.16, 10.26	
Formic	3.77*	2
Fumaric	3.03, 4.54	6
Glyceric	3.55	6
Glycollic	3.82	6
Glyoxylic	3.32	6
Homogentistic	4.40	6
α-keto-β-methyl valeric	2.3	6
Lactic	3.86	6
Maleic	1.93, 6.58	6
Malic	3.40, 5.2	6
Oxaloacetic (trans-enol)	2.56	6
+(cis-enol)	2.15, 4.06	6
Protocatechuic	4.48	6
Pyruvic	2.50	6
Tartaric +	2.99, 4.40	6
+ or -	2.89, 4.40	6
meso	3.22, 4.85	6
Vinylacetic	4.42	6

Acetic acids, substituted

H-	4.76*	20
O_2N-	1.68*	20
$(CH_3)_3N^+$-	1.83*	20
$(CH_3)_2NH^+$-	1.95*	20
$CH_3NH_2^+$-	2.16*	20
NH_3^+-	2.31*	20
CH_3SO_2-	2.36*	20
NC-	2.43*	20
$C_6H_5SO_2$-	2.44	20
HO_2C	2.83*	20
C_6H_5SO-	2.66	20
F-	2.66	20
Cl-	2.86*	20
Br-	2.86	20
Cl_2-	1.29	20
F_2-	1.24	20
Br_3-	0.66	20
Cl_3-	0.65	20
F_3-	0.23 (-0.26) (2)	20
$HONC_4$	3.01	20
F_3C-	3.07*	20
N_3-	3.03	20
I-	3.12	20
C_6H_5O-	3.12	20
$C_2H_5O_2C$-	3.35	20
C_6H_5S-	3.52*	20
CH_3O-	3.53	20
NCS-	3.58	20
CH_3CO-	3.58*	20
C_2H_5O-	3.60	20
n-C_3H_7O	3.65	20
n-C_4H_9O	3.66	20
sec.-C_4H_9O-	3.67	20
HS-	3.67*	20
i-C_3H_7O-	3.69*	20
CH_3S-	3.72*	20
i-C_3H_7S-	3.72*	20
$C_6H_5CH_2S$-	3.73*	20
C_2H_5S-	3.74*	20
n-C_3H_7S-	3.77*	20
n-C_4H_9S-	3.81*	20
HO-	3.83*	20
^-O_3S-	4.05	20
$(C_6H_5)_3CS$-	4.30*	20
C_6H_5-	4.31*	20
CH_2-CH-	4.35*	20

** Indicates thermodynamic values.*

Unsaturated acids (25°)

Compound	pK	ref.
trans-CH_3-CH=$CHCO_2H$	4.69*	20
cis-CH_3-CH=$CHCO_2H$	4.44*	2
C_6H_5-$CH_2CH_2CO_2H$	4.66*	2
trans-C_6H_5-CH=$CHCO_2H$	4.44*	2
m-$CH_3OC_6H_4CH_2CH_2CO_2H$	2	4.65*
m-$CH_3OC_6H_4CH$=$CHCO_2H$	4.38*	2
m-$ClC_6H_4CH_2CH_2CO_2H$	4.58*	2

Compound	pK	ref.
H-$CH_2CH_2CO_2H$	4.88*	2
H-CH=$CHCO_2H$	4.25*	2
$C_6H_5CH_2CH_2CO_2H$	4.66*	2
C_6H_5CH=$CHCO_2H$**	4.44*	2
$C_6H_5CH_2CH_2CO_2H$	4.66*	2
C_6H_5CH=$CHCO_2H$**	4.44	2
m-ClC_6H_4CH=$CHCO_2H$**	4.29*	2

Unsaturated acids, *Cis*- and *Trans*-

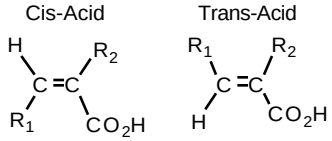

R_1	R_2	cis-acid	trans-acid	Ref.
H-	H-	4.25*	4.25*	2
CH_3-	H-	4.44*	4.69*	2
Cl-	H-	3.32	3.65	2
C_6H_5-	H-	3.88*	4.44*	2
ClC_6H_4	H-	3.91	4.41	2
6-BrC_6H_4	H-	4.02	4.41	2
CH_3-	CH_3-	4.30	5.02	2
C_6H_5-	H-	5.26***	5.58***	2
2,4,6-$(CH_3)_3C_6H_2$-	H-	6.12***	5.70***	2
C_6H_5-	CH_3-	4.98***	5.98***	2

Dicarboxylic acids, unsaturated*

Maleic	1.92, 6.23	2
Citraconic (Dimethylmaleic acid)	2.29, 6.15	2
Acetylenedicarboxylic	1.73, 4.40	2
Δ^1-tetrahydrophthalic	3.01, 5.34	2
Bromomaleic	1.45, 4.62	2
Bromofumaric	1.46, 3.57	2
Chlorofumaric	1.78, 3.81	2
Fumaric	3.02, 4.38	2
Mesaconic (Dimethylfumaric acid)	3.09, 4.75	2
Phthalic	2.95, 5.41	2
Itaconic (1-Propene-2-3-dicarboxylic acid)	3.85, 5.45	2
Chloromaleic	1.72, 3.86	2

Alicyclic Dicarboxylic acids

cis-Caronic(1,1-dimethylcyclopropane-23-dicarboxylic acid	2.34*, 8.31*	2
1,2-trans-cyclopropanedicarboxylic	3.65*, 5.13*	2
trans-caronic	3.82*, 5.32*	2
1,2-cis-cyclopropane-dicarboxylic	3.33*, 6.47*	2

**trans
***in 40% acetone
*thermodynamic

Aliphatic

Alicyclic Dicarboxylic acids

Compound	pK	Ref	Compound	pK	Ref
1,2-trans-Cyclopropane-dicarboxylic	3.65, 5.13	2	cis-Ethyleneoxide-dicarboxylic	1.94, 3.92	2
trans-Ethyleneoxide-dicarboxylic	1.93, 3.25	2	1,3-cis-Cyclobutane-dicarboxylic	4.03, 5.31	2
1,3-trans -Cyclobutanedi-carboxylic	3.81, 5.28	2	1,2-cis-Cyclopentane-dicarboxylic	4.37, 6.51	2
1,2-trans-Cyyclopentane-dicarboxylic	3.89, 5.91	2	1,3-cis-Cyclopentane dicarboxylic	4.23, 5.53	2
1,3-trans-Cyclopentane-dicarboxylic	4.40, 5.45	2	1,2-cisCyclohexane-dicarboxylic	4.34, 6.76	2
1,2-trans-Cyclohexane-dicarboxylic	4.18, 5.93	2	1,3 -cis-Cyclohexane-dicarboxylic	4.10, 5.46	2
1,3-trans-Cyclohexane-dicarboxylic	4.31, 5.73	2	1,4-cis-Cyclohexane di-carboxylic	4.44, 5.79	2
1,4-trans-Cyclohexane-dicarboxylic	4.18, 5.42	2			

Dicarboxylic acids*

oxalic	1.23, 4.19	2	Succinic	4.19, 5.48	2
Malonic	2.83, 5.69	2	O-O'-Dimethyl-	3.77, 5.94	2
Methyl-	3.05, 5.76	2	(high melting)		
Ethyl-	2.99, 5.83	2	O-O'-Dimethyl-	3.94, 6.20	2
n-propyl	3.00, 5.84	2	(low melting)		
i-propyl-	2.94, 5.88	2	O,O'-Diethyl-	3.63, 6.46	2
Dimethyl-	3.17, 6.06	2	(high melting)		
Methylethyl-	2.86, 6.41	2	O,O'-Diethyl-	3.51, 6.60	2
Diethyl-	2.21, 7.29	2	(low melting)		
Ethyl-n-propyl-	2.15, 7.43	2	Tetramethyl-	3.50, 7.28	2
Di-n-propyl-	2.07, 7.51	2			
Glutaric	4.34, 5.42	2	Adipic	4.42, 5.41	2
B-Methyl	4.25, 6.22	2	Pimelic	4.48, 5.42	2
B-Ethyl	4.29, 6.33	2	Suberic	4.52, 5.40	2
B-n-Propyl	4.31, 6.39	2	Azelaic	4.55, 5.41	2
B,B-Dimethyl-	3.70, 6.29	2	DL-1:2-Dichlorosuccinic	1.68, 3.18	20
B,B-Methylethyl-	3.62, 6.70	2	meso-1:2-Dichlorosuccinic	1.74, 3.24	20
B,B-Diethyl-	3.62, 7.12	2	DL-1:2-Dibromosuccinic	1.48, ----	20
B,B-Di-n-propyl	3.69, 7.31	2	meso-1:2-Dibromosuccinic	1.42, 2.97	20
D-Tartaric	3.03, 4.45	20	DL-1:2-Dimethylsuccinic	3.93, 6.00	20
DL-Tartaric	3.03, ----	20	meso-1:2-Dimethylsuccinic	3.77, 5.36	20
meso-Tartaric	3.29, 4.92	20			

**All are thermodynamic values*

Aliphatic

Bicyclo[2.2.2]octane-1-carboxylic acids, 4-substituted

H-	6.75	2
$C_2H_5O_2C$-	6.31	2
NC-	5.90	2
HO-	6.33	2
Br-	6.08	2

Lysergic acid, etc.

ergometrine	6.8, --	2
Dihydroergometrine	7.4, --	2
β-dihydrolysergol	8.2, --	2

Lysergic acid	7.8, 3.3	2
α-dihydrolysergic	8.3, 3.6	2
ergometrinine	7.3, --	2
α-dihydrolysergol	8.3, --	2
6-methylergoline	8.85, --	2
isolysergic acid	8.4, 3.4	2
γ-dihydrolysergic	8.6, 3.6	2

Hydroxycyclohexanecarboxylic acids

Cyclohexanecarboxylic	4.90	2
cis-1,2	4.80	2
cis-1,3	4.60	2
cis-1,4	4.84	2
trans-1,2	4.68	2
trans-1,3	4.82	2
trans-1,4	4.68	2

Aromatic

benzene-CO_3H	4.20*	2
Anthracene-1-COOH	3.69	2
Anthracene-9-COOH	3.65	2
naphthalene-2-COOH	4.17	2
Naphthalene-1-COOH	3.69	2

Substituted benzoic acids (ref. 2)

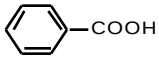

Benzoic acid	**o**	**m**	**p**
H-	4.20*	4.21*	
O_2N-	2.17*	3.45*	3.44
CH_3CO-			
CH_3SO_2-		3.64*	3.52*
CH_3S-			
HS-			
Br-	2.85*	3.81*	4.00*
F-	3.27*	3.87*	4.14*
CH_3O-	4.09*	4.09*	4.47*
n-C_3H_7O-	4.24*	4.20*	4.46*
n-C_4H_9O-		4.25*	4.53*

Benzene Polycarboxylic acids	**Ref. 2**

Acid	**Position of carboxyl**	**pK^I**	**pK^{II}**	**pK^{III}**	**pK^{IV}**	**pK^V**	**pK^{VI}**
Benzoic	1	4.17*					
Phthalic	1,2	2.98*	5.28*				
Isophthalic	1,3	3.46*	4.46*				
Terephthalic	1,4	3.51*	4.82*				
Hemimellitic	1,2,3	2.80*	4.20*	5.87*			
Trimellitic	1,2,4	2.52*	3.84*	5.20*			

C_6H_5O-	3.53*	3.95*	4.52*
CH_3-	3.91*	4.24*	4.34*
$(CH_3)_2CH$-			4.35*
$(CH_3)_3N^+$-	1.37	3.45	3.43
NC-		3.60*	3.55*
HO_2C*	2.95*	3.54	3.51
F_3C-		3.79	
HO-	2.98*	4.08*	4.58*
I-	2.85*	3.86*	
Cl-	2.94*	3.83*	3.99*
$(CH_3)_3Si$-		4.24*	4.27*
C_2H_5O-	4.21*	4.17*	4.45*
i-C_3H_7O-	4.24*	4.15*	4.68*
n-$C_5H_{11}O$-			4.55*
C_6H_5-	3.46*		
CH_3CH_2-	3.77		4.35*
$(CH_3)_3C$-	3.46	4.28	4.40*
$^-HO_3P$-	3.78	4.03	3.95
^-O_3S-		4.15	4.11
H_2N-	4.98	4.79	4.92
$(CH_3)_2N$-	8.42	5.10	5.03
$^-HO_3As$-			4.22
^-O_2C-	5.41**	4.60	4.82
CH_3NH-	5.3	5.10	5.04

*thermodynamic
for complex chelating agents, see also ref. 84.
see also page 9a for more carboxylic acids.

Ortho-substituted benzoic acids

Benzoic acid	**pK**	**Ref.**
2-CH_3-	3.91**	2
2-t-C_4H_9-	3.46	2
2,6-$(CH_3)_2$-	3.21	2
2,3,4,6-$(CH_3)_4$-	4.00	2
2,3,5,6-$(CH_3)_4$-	3.52	2
2-C_2H_5-	3.77	2
2-C_6H_5-	3.46**	2
2,4,6-$(CH_3)_3$-	3.43	2
2,3,4,5-$(CH_3)_4$-	4.22	2

Trimesic	1,3,5	3.12*	3.89*	4.70*		
Mellophanic	1,2,3,4	2.06*	3.25*	4.73*	6.21*	
Prehnitic	1,2,3,5	2.38*	3.51*	4.44*	5.81*	
Pyromellitic	1,2,4,5	1.92*	2.87*	4.49*	5.63*	
Benzenepentacarboxylic	1,2,3,4,5	1.80*	2.73*	3.97*	5.25*	6.46*
Mellitic	1.2,3,4,5,6	1.40*	2.19*	3.31*	4.78*	5.89* 6.96*

**ionic strength 0.03*
***thermodynamic*

Carboxylic Acids	**Ref. 77**
Aminomalonic acid*	3.32, 9.83
N-Butylaminoacetic acid	2.29, 10.07
2-carboxyethyliminodiacetic acid	2.06, 3.69, 9.66
β-carboxymethylaminopropionic	3.61, 9.46
α,α-diaminobutyric	1.85, 8.24, 10.44
Di-(carboxymethyl)-aminomethyl phosphonic acid	2.00, 2.25, 5.57, 10.76
α,β-dimercaptosuccinic	2.40, 3.46, 9.44, 11.82
Ethylenediamine-N,N-diacetic	5.58, 11.05
α-hydroxybutyric	3.65
N-2-hydroxyethyliminodiacetic	2.2, 8.73
3-hydroxypropyliminodiacetic	2.06, 9.24
Iminodipropionic	4.11, 9.61
Isobutyric*	4.86
Mandelic acid	3.41
2-Mercaptoethyliminodiacetic	-2.14, 8.17, 10.79
Methyliminodiacetic	2.81, 10.18
2-Methoxyethyliminodiacetic	2.2, 8.96
2-Methylthioethyliminodiacetic	2.1, 8.91
oxalic acid*	1.25, 4.14
N-n-propylaminoacetic	2.25, 10.03
N-2-sulfoethyliminodiacetic	1.92, 2.28, 8.16
α-Bromobutyric acid	2.97
N-(carbamoylmethyl)-imino-diacetic acid	2.30, 6.60
Cyanomethyliminodiacetic	3.06, 4.34
α,β-diaminopropionic acid	1.23, 6.69
Diethylaminoacetic	2.04, 10.47
Dimethylaminoacetic	2.08, 9.80
N-ethylaminoacetic	2.30, 10.10
Gluconic*	3.86
β-hydroxybutyric	4.39
β-hydroxypropionic	3.73
Iminodiacetic*	2.98, 9.89
β-iodopropionic*	4.04
N-isopropylaminoacetic	2.36, 10.06
α-mercaptobutyric	3.53
N-methylaminoacetic	2.24, 10.01
Nitrilotriacetic	3.03, 3.07, 10.
2-Phosphonoethyliminodiacetic	1.95, 2.45, 6.54, 10.46

**Thermodynamic*

PHENOLS

Compound	pK	Ref.	Compound	pK	Ref.
Chromotropic acid	5.36, 15.6	6	Resorcinol	--, 9.15 (30°)	50
o-Methoxyphenol	--, 9.93	50	p-Methoxyphenol	--, 10.16	50
o-Hydroxybenz-aldehyde	7.95	50	3-Hydroxyanthranilic acid	10.09, 5.20	51
2-Amino-4,5 dimethylphenol hydrochloride	10.4 5.28	51	2-Aminophenol hydrochloride	9.99, 4.86	51
4,5-dihydroxybenzene-1,3 disulphonic acid	7.66 12.6e				
Kojic acid	9.40	77			

Phenol	o	m	p	Phenol	o	m	p
H-	9.95*	9.94*		O_2N-	7.23*	8.35*	7.14*
$(CH_3)_3N^+$-	7.42	8	8	OCH-	6.79	8.00	7.66
CH_3SO_2-		9.33	7.83	NC-		8.61**	7.95
CH_3CO-		9.19	8.05	CH_3O_2C-			8.47*
$C_2H_5O_2C$-			8.50*	n-$C_4H_9O_2C$-			8.47*
$C_3H_5CH_2O_2C$-			8.41*	I-		9.17*	
Br-	8.42*	9.11*	9.34*	Cl-	8.48*	9.02*	9.38*
F-	8.81*	9.28*	9.95*	CH_3S-		9.53	9.53
HO-	9.48	9.44	9.96	$HOCH_2$-	9.92*	9.83*	9.82*
CH_3-	10.28*	10.08	10.19*	C_2H_5-	10.2	9.9	10.0
CH_3O-	9.93	9.65	10.20	H_2N-	9.71	9.87	10.30
^-O_2C-		9.94*	9.39*	^-O_3S-		9.29	9.03
$^{--}O_3P$-		10.2	9.9	$^{--}O_3As$			8.37
C_6H_5-	9.93	9.59	9.51	NO-			6.35**
2-Chloro-4-Nitro-		5.42	79				
2-Nitro-4-Chloro-		6.46	79				

** Thermodynamic*
***Reference 52*

ALCOHOLS and other OXYGEN ACIDS

Alcohols

Compound	pK	Ref.
Choline	13.9	6
Chloral hydrate	9.66, 11.0	61
Trifluoroethanol	12.5	62
CF_3CH_2OH	11.4, 12.43	63
$CF_3CH(OH)CH_3$	11.8	63
$CF_3CH_2(CH_3)3OH$	12.43	10
$C_3F_7CH_2OH$	11.4**	63
$(C_3F_7)_2CHOH$	10.6**	63
$HCCCH_2OH$	13.55	64
$C(CH_2OH))_4$	14.1	64
$HOCH_2CHOHCH_2OH$	4.4	64
$HOCH_2CH_2OH$	14.77	64
CH_3CCH_2OH	14.82	64
CH_3OH	15.54	64
$CH_2=CHCH_2OH$	15.52	64
H_2O	15.74	64
CH_3CH_2OH	16	64

Substituent effects for ionization of RCH_2OH

R			
CCl_3-	12.24,11.80		64,65
CF3-	12.37		64
CHF_2CH_2-	12.74		64
$CHCl_2$-	12.89		64
CHEC-	13.55		64
H_2Cl-	14.31		64
CH_3CCH_2-	14.8		64
$HOCH_2$	15.1		64
H-	15.5		64
$CH_2=CH$-	15.5		64
CH_3-(extrap)	(15.9)		64
$CF_3C(CH_3)_2OH$	11.6		64
$HOCH_2CF_2CH_2OH$	11		64
Primary alcohols=R•CH_2•OH and Secondary alcohols in 50% alcohol			
C_2F_5	11.35		65
C_4F_9	11.35		65
C_5F_{11}	11.37		65
C_7F_{15}	11.35		65
CHF_2	12.00		65
CF_2Cl	11.63		65
CHF_2CF_2	11.34		65
CHF_2 • $(CF_2)_2$	11.35		65
CF3 • CH2	12.7		65
CF_3 • $(CH_2)_2$	12.9		65
CF_3 • CHMe • OH	11.28		65
C_3F_7 • CHMe • OH	11.38		65
C_3F_7CHEt • OH	11.37		65
C_3F_7CHPr • OH	11.37		65
C_3F_7 • $CH(CF_3)$ • OH	10.46		65
C_3F_7•$CH(C_2F_5)$•OH	10.48		65
$(C_3F_7)_2CH$•OH	10.52		65

Carbonium ions

Triphenylmethanols in	H_2SO_4	$HC1O_4$	HNO_3	ref	
4,4,4-Trimethoxy		.82.	.82	.80	66
4,4'-Dimethoxy	-1.24	-1.14	-1.11	66	
4-Methoxy	-3.40	-3.59	-3.41	66	
4-Methyl	-5.41	-5.67		66	
4_Trideuteriomethyl-	5.43	5.67		66	
3,3',3"-Trimethyl-	6.35	-5.95		66	
Unsubstituted triphenyl-					
methanol-	6.63	-6.89	6.60	66	
64 4,4;,4;-Trichloro-			7.74-	8.01	66
64 4_Nitro-			9.15-	9.76	66

CCl_3CH_2OH	11.8***	
CF_3CH_2OH	11.3***	

Hydroxamic acids

Furo-	8.45		72	
Glycine	7.40		72	
Hippuro-	8.80		72	
*iso*Nicotin	7.85		72	
64 p-Methylbenz-		8.90		72
Nicotin-		8.30		72
Nicotin-methiodide	6.46		72	
m-Nitrobenz-	8.07		72	
Picolin	8.50		72	
Pyrimidine-2-carbox-	7.88		72	
Salicyl-	7.43		72	
Tropo-		9.09		72

Other oxygen acids

Trimethylamine-n-oxide	4.6		18	
Dimethylglyoxime (50% dioxane)		12.84		77
O-methyl ether	12.92		77	
Tropolone	12a		77	
α-Bromotropolone	6.95[a]		77	
Acetald hydrate	13.48		91	
Formald hydrate	13.29		91	

[a]50% dioxane
***50 aquaeous ethanol

OTHER OXYGEN ACIDS

Compound	pK	Ref.
Pyridine oxides		
4-Aminopyridine 1-oxide	3.69	67
4-Dimethylaminopyridine 1-oxide	3.88	67
4-Dimethylaminopyridine 1-oxide	3.88	67
4-Dimethylamino-1-methoxypyridinium perchlorate	>11	67
2-Methylaminopyridine 1-oxide	2.61	67
2-Amino-1-methoxypyridinium perchlorate	12.4	67
4-Hydroxypyridine 1-oxide	2.45	67
4-Methoxypyridine 1-oxide	2.05	67
1-Methoxypyridi-4-one	2.57	67
2-Hydroxypyridine 1-oxide	-0.8	67
2-Ethoxypyridine 1-oxide	1.18	67
1-Methoxypyrid-2-one	-1.3	
4-Methylaminopyridine 1-oxide	3.85	67
4-Amino-1-methoxypyridinium perchlorate	>11	67
2-Aminopyridine 1-oxide	2.67	67
2-Dimethylaminopyridine 1-oxide	2.27	67
2-Methylamino-1-methoxypyridinium toluene-p-sulphonate	>11	67
4-Benzyloxypyridine 1-oxide	1.99	67
1-Benzyloxypyrid-4-one	2.58	67
2-Methoxypyridine 1-oxide	1.23	67
1-Benzyloxypyrid-2-one	-1.7	67

Pyridine 1-oxides

R	pK	Ref.
4-CH_3	1.29	47
3-CH_3	1.08	47
3,4-$(CH)_4$	1.01	47
3-$COOC_4H_9$	0.03	47
4-NO_2	-1.7	47
3-NH_2	1.47	47
H	0.79	47
3-COOH	0.09	47
4-COOH	-0.48	47

Peroxides ROOH (Ref. 70)

H	CH_3	C_2H_5	iso-C_3H_7	tert-C_4H_9	iso-C_4H_9
11.6	11.5	11.8	12.1	12.8	12.8

Oximes	ref. 93
benzoquinoline mon-	6.25
3-pyridine-1,2-ethanedione-2-oxime methiodide	7.20
Pyridine-2-aldoxime heptiodide	8.00
Pyridine-4-aldoxime methiodide	8.50
Pyridine-4-aldoxime pentiodide	8.50

Hydroxamic acids		
Aceto-	9.40	68
n-Butyro-	9.48	68
n-Butyro-	9.00	68
p-Methoxybenzo-	9.19	68
N-Hydroxyphthalimide	7.00, 6.10	71, 72
Salicylo	7.32	68
Benzo-	8.88	68
p-Chlorobenzo-	9.59	68
α-Naphtho-	~7.7	68
Propiono-	9.46	68

Oximes		
Benzophenone oxime	11.3	18
Diethyl ketoxime	12.6	18
Isonitrosoacetylacetone (INAA)	7.4	76
5-Methyl-1,2,3-cyclohexanetrione-1,3-dioxime	8.3	76
Acetophenone oxime	11.48	18
Acetoxime	11.42	18
Isonitrosoacetone (INA)	8.3	76
Salicyclaldoxime (SA)	9.2	76
1,2,3-Cyclohexanetrionetrioxime	8.0	76
5-Methyl-1,2,3-cyclohexane-trionetrioxime	8.0	76

Oxygen acids		
sulfinic acids		
p-Toluene-	1.99	73
p-Chlorobenzene-	73	
p-Nitrobenzene-	73	
p-Bromobenzene-	1.89	73
m-Nitrobenzene-	1.88	73
Benzene-	1.84, 2.16	73

Peroxyacids		
Peroxymonosulfuric	9.4	69
Acetic	8.2	70
n-Butyric	8.2	70
Formic	7.1	70
Propionic	8.1	70
peroxydiphosphoric	5.18, 7.8	85
peroxymonophosphoric	4.85	90

4-Pyridine-1,2-ethanedione-2-oxime methiodide	7.1
Pyridine-2-aldoxime methiodide	8.0
Phenylglyoxald-	8.3
Pyridine-4-aldoxime dodeciodide	8.5
Pyridine-3-alkoxime methiodide	9.2

Hydroxamic acids	ref. 93
D-Lysine-	7.93
N-phenylnicotino-	8.00
Chloroaceto-	8.40
Formo-	8.65
p-Chlorophenoxyaceto-	8.75
p-Hydroxybenzo-	8.93
p-Methoxybenzo-	9.00
N-Phenylbenzo-	9.15
o-Aminobenzo-	9.17
L-Tyrosine	9.20
L-Lysine	7.9
p-Nitrobenzo-	8.0
p-Aminobenzo-	9.3
L-Lacti-	9.3
Propiono-	9.4
Phthalo-	9.4
Indole-3-aceto-	9.5
Cyclohexano-	9.7
Hexano-	9.7

Amino Acids

Compound	**pK -COOH**	**-NH_3**	**Ref.**
Alanine	2.35	9.69	6
α-Aminobutyric acid	2.55	9.60	
α-Aminoisobutyric	2.36	10.21	6
Argininosuccinic	>12, 1.62 2.70, 4.26	9.58	6
Aspartic acid	2.09, 3.86	9.82	6
Canaline	10.3, 9.20	11.6 (?)	6
Creatinine	4.84	9.2	6
Cystine	1.65	7.85	6
	2.26	9.85	6
Diidotyrosine	6.48, 2.12	7.82	6
Glutamic acid	2.19, 4.25	9.67	6
Glycine	2.34	9.6	6
Histidine	6.0, 1.82 6		9.17
Hydroxylsine	2.13	8.62 9.67	6
Isoleucine	2.36	9.68	6
Lysine	2.18	8.95 10.53	6
O-Methyl tyrosine		9.27	21
O-Methyltyrosine ethyl ester	7.31		22
octopine	13, 1.36 6 2.40		8.77
Phenylalanine	1.83	9.13	6
2-Pyrrolidoone-5-carboxylic acid (glucamic acid)	3.32		
Serine	2.21	9.15	6
Threonine	2.63	10.43	6
N-Trimethyl tyrosine		9.75	21
Tyrosine	10.07, 2.20	9.11	
Urocanic acid	5.8	3.5	
Valine	2.32	9.62	6
β-Alanine	3.60	10.19	6
γ-Aminobutyric acid	4.23	10.43	6
Arginine 12.48	2.17	9.04	6
Asparagine	2.02	8.8	6
Azaserine	8.55		6
Canavanine	7.40, 9.25	11.50 (?)	6
Creatine	2.67	11.02	6
Cysteine 10.78	1.71	8.33	6
3,4-Dihydroxyphenylalanine	9.88, 2.36 11.68	8.68	6
Glutamine	2.17	9.13	6
Histamine 5.0		9.7	6
β-Hydroxyglutamic acid	2.09 4.18	9.20	6
Hydroxyproline	1.92	9.73	6
Leucine	2.36	9.60	6
Methionine	2.28	9.21	
1-Methylhistidine	6.48, 1.69	8.85	6
Norleucine	2.39	9.76	6
Norvaline	2.36	9.76	6
Ornithine	1.71	8.69 10.76	6
Proline	1.99	10.60	6
Sarcosine	2.23	10.01	6
Taurine 1.5		8.74	6
Thiolhistidine <1.5, 11.4	1.84	8.47	6
Tryptophan	2.38	9.39	6
Tyrosine ethyl ester	7.33	9.80	22
Peptides			
Anserine 7.0	2.65	9.5	6
Carnosine 6.83	--	9.51	6
Cystinyldiglycine	3.12 3.12	6.36 6.95	6
Glycylglycine	3.06	8.13	
Gly-gly-gly	3.26	7.91	23
Glycylproline	2.84	8.55	6
Aspartyl histi-	2.45	7.98	

dine	6.82	3.02		Gly-gly-gly-gly	3.05	7.75	23
Diglycylcystine	2.71	7.94	6	Lysyl-lysine (L,L)	3.01	7.53	6
Glutathione 9.12	2.12	8.66	6		10.05	11.01	
	3.53						

Compound	**-COOH**	**α-NH_2**	**ε-NH_2**	**ε-NH_2**	**ε-NH_2**	**Ref.**
Gly•Ala (L) or (D)	3.17	8.23				27
Ala•Gly (L) or (D)	3.16	8.24				27
Gly•Ala•Ala (LL)	3.38	8.10				27
Gly•Ala•Ala (LD)	3.30	8.17				27
Ala•Ala•OH (DD)	3.30	8.14				27
Ala•Ala•OH (LD)	3.12	8.30				27
H•Ala•Ala•Ala•OH (3L)	3.39	8.03				27
H•Ala•Ala•Ala•OH (LLD)	3.37	8.05				27
H•Ala-Ala-Ala•OH (LDL)	3.31	8.13				27
H•Ala-Ala-Ala•OH (DLL)	3.37	8.06				27
H-Ala-Ala-Ala•OH (3D)	3.39	8.06				27
H•Ala-Ala-Ala-Ala•OH (4L)	3.42	7.94				27
H•Ala-Ala-Ala-Ala•OH (LLDL)	3.24	7.93				27
H•Ala-Ala-Ala-Ala•OH (LDLL)	3.22	7.99				27
H•Ala-Ala-Ala-Ala•OH (DLLL)	3.42	7.99				27
H•Lys-Ala•OH (LL)	3.22	7.62	10.70			27
H•Lys-Ala•OH (LD)	3.00	7.74	10.63			27
H•Ala-Lys-Ala•OH (3L)	3.15	7.65	10.30			27
H•Ala-Lys-Ala•OH (LDL)	3.33	7.97	10.36			27
H•Ala-Lys-Ala•OH (LLD)	3.29	7.84	10.49			27
H•Ala-Lys-Ala-Ala•OH (4L)	3.58	8.01	10.58			27
H•Ala-Lys-Ala•OH (LDLL)	3.32	8.01	10.37			27
H•Ala-Lys-Ala-Ala-Ala•OH (5L)	3.53	7.75	10.35			27
H•Ala-Lys-Ala-Ala-Ala•OH (LDLLL)	3.30	7.85	10.29			27
H•Lys-Lys•OH (LL)	3.01	7.53	10.05	11.01		27
H•Lys-Lys•OH (LD)	2.85	7.53	9.92	10.98		27
H•Lys-Lys•OH (3L)	3.08	7.34	9.80	10.54	11.32	27
H•Lys-Lys-Lys•OH (LDL)	2.91	7.29	9.79	10.54	11.42	27
H•Lys-Lys-Lys•OH (LDD)	2.94	7.14	9.60	10.38	11.09	27

Compound	**pK**			**ref.**
Glutathione	3.59, 8.75, 9.65			77
Glycylserine	8.23			77
Glycylleucine	8.13			77
Leucylglycine	7.96			77
Glycylisoleucine	7.96			77
Leucylglycylglycine	7.66			77
Glycylphenylalanine	8.28			77
Glycyltyrosine	8.22			77
Benzylglutamic acid	3.49, 4.99			77
Glycyltryptophane	8.04			77
Glutathione, oxidized	3.15, 4.03, 8.57, 9.54			77
Alanylalanine (LL)	3.30	8.14		92
Alanylalanine (LD)	3.12	8.30		92
Lysylalanine (LL)	3.22	7.62	10.70	92
Lysylalanine (LD)	3.00	7.74	10.63	92
Leucyltyrosine (LL)	3.46	7.84	10.09	92
Leucyltyrosine (DL)	3.12	8.38	10.35	92

Lysyllysine (LD)	2.85	7.53	9.92	92

NITROGEN COMPOUNDS

Aliphatic Amines	**pK**	**ref.**			
Ammonia	9.21	1	n-Propyl-	10.53	1
Primary Amines			Trimethylsilymethyl-	10.96	1
β-Alanine ester	9.13	1	CH_3ONH_2	4.60	12
Allylamine-	9.69	2	Allyl-	9.49	1
Benzyl	9.34	1	γ-Amino-n-butyric acid ester	9.71	1
n-Butyl-	10.59	1	sec-Butyl-	10.56	1
t-Butyl-	10.55	1	Cyclohexyl-	10.64	1
Cyclohexylmethyl-	10.49	1	β-difluoroethyl-	7.52	1
Ethanol-	9.50	1	Ethyl	10.63	1
Ethylenedi-	9.98, 7.52	1, 77	Glycine ester	7.75	1
Hydrazine	8.10	1	Hydroxyl-	5.97	1
Isopropyl-	10.63	1	Methoxy-	4.60	1
Methyl-	10.62	1	neo-Pentyl-	10.21	1
Phenylamyl-	10.49	2	δ-Phenylbutyl	10.40	2
β-Phenylethyl-	9.83	1	γ-Phenylpropyl-	10.20	1
			Triethylenedi-	8.8*	?

X	**XNH_3^+**	**$XCH_2NH_3^+$**	**$X(CH_2)_2NH_3^+$**	**$X(CH_2)_3NH_3^+$**	**$X(CH_2)_4NH_3^+$**	**$X(CH_2)_5NH_3^+$**	**ref.**
H-	9.25*	10.64*	10.67*	10.58*	10.61*	10.63*	2
HF_2C-		7.52					
RO_2C-		7.75	9.13	9.71	10.15*	10.37	2
HO-	5.96*		9.50*				
C_6H_5-	4.58*	9.37*	9.83*	10.20*	10.39*	10.49*	2
H_2N-	8.12*		9.98*	10.65*	10.84*	11.05*	2
H_2C=CH-		9.69					
CH_3-	10.64*	10.67*	10.58*	10.61*	10.63*	10.64*	2

X	**-H**	**$-NH_3^+$**	**$-CO_2^-$**	**$-SO_3^-$**	**$-PO_3^-$**	2
$X\text{-}NH_3^+$	9.25*	-.88		1	10.25	
$X(CH_2)_2NH_3^+$	10.64		9.77	5.75	10.8	
$X(CH_2)_2NH_3^+$	10.67		10.19	9.20	10.8	
$X(CH_2)_4NH_3^+$	10.61	9.31	10.77	10.65	10.9	
$X(CH_2)_5NH_3^+$	10.63	9.74	10.75	10.95	11.0	
$X(CH_2)_8NH_3^+$	10.65	10.10				
$X(CH_2)_{10}NH_3^+$	10.64			11.35	11.25	
$X(CH_2)_3NH_3^+$	10.58	8.59	10.43	10.05		

Secondary amines					
Dimethyl-	10.64	1	Di-n-butyl-	11.25	1
Di-n-propyl-	11.00	1	Diisobutyl-	10.50	1
Diisopropyl-	11.05	1	α-Ethylpyrroline	7.43	2
t-Butylcyclohexyl-	11.23	1	α-Benzylpyrroline-	7.08	2
α-Cyclohexylpyrroline	7.95	2	2-Methylpiperidine	10.99	2
α-(p-Tolyl)pyrroline	7.59	2	α-Cyclohexylpyrrolidine	10.80	2
α-Ethylpyrrolidine	10.43	2	α-(p-Tolyl)pyrrolidine	10.01	2
α-Benzylpyrrolidine	10.36	2	N,O-dimethylhydroxylamine	4.75	12
N-methylhydroxylamine	5.96	12	Acetanilide	+0.61	4
Diethyl-	10.98	1	**thermodynamic value*		

Aliphatic Amines

1,2-Iminoethane	7.98	7
cis-2,3-Iminobutane	8.72	7
1,2-Imino-2-methylpropane	8.61	7
1,2-Iminobutane	8.29	7
trans-2,3-Iminobutane	8.69	7

Secondary Amines

Allylmethyl-	10.11	1
Benzylethyl-	9.68	1
Morpholine	8.36	1
N-Benzoylpiperazine	7.78	1
Di-sec-butyl-	11.01	1
N-Methylmethoxyamine	4.75	1
Pyrolidine	11.27	1
1-Tosylpiperazine	7.39	
Benzylmethyl-	9.58	1
Piperidine	11.22	1
N-Carbethoxypiperazin	8.28	1
Dietrimethylsilylmethyl-	11.40	1
Diallyl-	9.29	1
N-Methylhydroxyl-	5.96	1
Trimethyleneimine	11.29	1
Cis-2,6-dimethyl-piperidine	10.92	3

Tertiary amines

Trimethyl-	9.76	1
Dimethyldiethyl-	10.29	1
Dimethyl-n-propyl-	9.99	1
Dimethyl-isobutyl-	9.91	1
Dimethyl-sec-butyl-	10.40	1
Tri-n-propyl-	10.65	1
Triallyl-	8.31	1
N-Allylpiperidine	9.69	2
1-Diethylamino-hexane-thiol-(6)		

Cyanoamines

N-piperidine-CH_2CN	4.55	8
Et_2NCN	-2.0	8
$Et_2N(CH_2)_2CN$	7.65	8
$Et_2N(CH_2)_4CN$	10.08	8
$Et_2NC(CH_3)_2CN$	9.13	8
$EtN(CH_2CN)_2$	-0.6	8
$EtN(CH_2CH_2CN)_2$	4.55	8
H_2NCH_2CN	5.34	8
N-Amphetamine-$(CH_2)_2$-CN	7.23	8
N-Norcodeine-$(CH_2)_2CN$	5.68	8
Dimethylcyanimide	1.2	9
Diethylcyanimide	1.2	9
Aminoacetonitrile	5.3	9
Diethylaminoacetonitrile	4.5	9

Methyl-β-diethylamino-ethyl-sulfide		
1,2-Dimethyl-Δ^2-pyrroline	11.94	2
1-methyl-2-n-butyl-Δ^2-pyrroline	11.90	
1-Ethyl-2-methyl-Δ^2-pyrroline	11.92	2
1-n-Butyl-2-methyl-Δ^2-pyrroline	11.90	2
1,2-Dimethyl-Δ^2-tetrahydropyridine	11.57	2
N-Ethyl derivative of: 1,2-Imino-ethane	7.93	7
Trans-2,3-Iminobutane	9.47	7
Trimethylhydroxylamine	3.65	12
Dimethylethyl-	9.99	1
Triethyl-	10.65	1
Dimethyl-n-butyl-	10.02	1
Dimethyl-isopropyl-	10.30	1
Dimethyl-t-butyl-	10.52	1
Tri-n-butyl-	10.89	1
Diallylmethyl-	8.79	1
1-n-Propylpiperidine	10.48	2
10.1	10.1	5
9.8	--	5
1,2-Dimethylpyrrolidine	10.26	2
1-Methyl-2-n-butylpyrrolidin	10.24	2
1-Ethyl-2-methylpyrrolidine	10.64	2
1-n-Butyl-2-methylpyrrolidine	10.43	2
1-Ethyl-2-methylpyrrolidine	10.70	2
1,2-Iminobutane	8.18	7
cis-2,3-Iminobutane	8.56	7
N-dimethylhydroxylamine	5.20	12
Allyldimethyl	8.78	1
1,2-Dimethylpiperidine	10.26	2
1-Ethyl-2-methyl-Δ^2-tetrahydropyridine	11.57	2

2-Amino-2-cyanopropane	5.3	9
β-Isopropylaminopropionitrile	8.0	9
β-Diethylaminopropionitrile	7.6	9
Et_2NCH_2CN	4.55	8
$Et_2N(CH_2)_3CN$	9.29	8
$Et_2N(CH_2)_5CN$	10.46	8
$HN(CH_2CN)_2$	0.2	8
$HN(CH_2CH_2CN)_2$	5.26	8
$N(CH_2CH_2CN)_3$	1.1	8
N-piperidine-$C(CH_3)_2CN$	9.22	8
N-Methamphetamine-$(CH_2)_2CN$	6.95	8
Methyl cyanamide	1.2	9
Ethyl cyanamide	1.2	9
Cyanamide	1.1	9
Dimethylaminoacetonitrile	4.2	9

β-Aminopropionitrile	7.7	9
β-Dimethylaminopropionitrile	7.0	9
β,β"-Dicyanodiethylamine	5.2	9

For complex chelating agents of aliphatic amines, see also ref. 77.

Fluoro-substituted amines

$CF_3CH_2NH_2$	5.7	10
$CF_3CH_2N(CH_3)_2$	4.75	10
$CF_3CH_2NHCH_3$	6.05	10

Phenylethylamines

2-phenylethylamine	9.78	11
N-methyl-2-(3,4-dihydroxyphenyl)-ethylamine	8.78	11
N-methyl-2-phenyl	10.31	11
Epinephrine	8.55	11
Arterenol	8.55	11

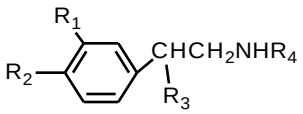

ref. 11

R_1	R_2	R_3	R_4	pK
H	H	H	H	9.78
H	H	OH	H	8.90
H	OH	OH	H	8.81
OH	H	OH	H	8.67
H	OH	H	H	9.22
OH	OH	H	H	8.93
OH	OH	OH	H	8.58
H	H	H	CH_3	10.31
H	H	OH	CH_3	9.31
H	OH	OH	CH_2	8.62
OH	H	OH	CH_3	8.89
H	OH	H	CH_3	9.36
OH	OH	H	CH_3	8.78
OH	OH	OH	CH_3	8.55

Ring amines and imines (in 80% methyl cellosolve) (ref. 2)

Pentamethylene	9.99
Hexamethylene	10.00
Heptamethylene	9.77
Octamethylene	9.39
Nonamethylene	9.14
Decamethylene	9.04
Undecamethylene	9.14
Dodecamethylene	9.31
Tridecamethylene	9.35
Tetradecamethylene	9.35
Hexadecamethylene	9.29
Heptadecamethylene	9.27
Cyclohexyl	9.82
Cycloheptyl	9.99
Cyclooctyl	
Cyclononyl	9.95
Cyclodecyl	9.85
Cycloundecyl	9.71
Cyclododecyl	9.62
Cyclotridecyl	9.63
Cyclotetradecyl	9.54
Cyclopentadecyl	9.54
Cycloheptadecyl	9.57
Cyclooctadecyl	9.54

Amines other

Dimeoone	5.23	18
Phthalimide	8.30	18
Nitrourea	4.57	18
Nitrourethane	3.28	18
Diphenylthiocarbazone	4.5	6
β,β,β"-Triaminotriethylamine	8.42, 9.44, 10.13	87

Anilines Ref. 2

Monosubstituted

Substituent	**o**	**m**	**p**
H-	4.62*	4.64*	4.58*

$(CH_3)_3N^+$-		2.26	2.51
CH_3O_2C-	2.16	3.56	2.30
CH_3SO_2-		2.68*	1.48
CH_3S-		4.05	4.40
Br-	2.60*	3.51*	3.91*
F-	2.96*	3.38*	4.52*
CH_3O-	4.49*	4.20*	5.29*
C_6H_5-	3.78*	4.18	4.27*
$(CH_3)_3C$-	3.78		
^-O_3S-		3.80	3.32
H_3N^+	1.3	2.65	3.29
O_2N-	-0.28*	2.45*	0.98*, 1.11*
HO_2C-	2.04	3.05	2.32
$C_2H_5O_2C$-	2.10		2.38
F_3C-		3.49*	2.57*
HO-	4.72	4.17	5.50
Cl-	2.62*	3.32*	3.81*
$(CH_3)_3Si$-		4.64*	4.36*
C_2H_5O-	4.47*	4.17*	5.25*
CH_3-	4.38*	4.67*	5.07*
$^-HO_3As$	3.77	4.05	4.05
H_2N-	4.47	4.88	6.08

**Thermodynamic*

p-$(CH_3)_3C$-	4.65		
m-Br-	3.08		
m-Cl-	3.09		
p-F-	4.01		
p-$(CH_3)_3Si$-	3.99		
p-CH_3O-	5.14, 5.16		

Dimethyl

H	5.07	52
m-NO_2	2.63	52
m-CN	2.97	52
p-NO_2	0.61	52
p-CN	1.78	52
p-NO	4.54	52

Dimethyl (in 50% ethanol)

Substituent $XC_6H_4N(CH_3)_2$	ref. 2
H-	4.21, 4.09
m-CH_3	4.66
p-C_2H_5-	4.69
o-$(CH_3)_2CH$-	5.05
p-$CH_3CH_2CH_2CH_2$-	4.62
o-$(CH_3)_3C$-	4.26
p-I-	3.43, 2.73
p-Br-	3.52, 2.82
p-Cl-	3.33
m-$(CH_3)_3Si$-	4.41
o-CH_3O-	5.49
o-CH_3	5.15, 5.07
p-CH_3	4.94
p-$CH_3CH_2CH_2$-	4.43
p-$(CH_3)_2CH$-	4.77
p-$(CH_3)_2CHCH_2$-	4.19

Ortho-substituted anilines (in 50% ethanol)

H-	4.25
2-CH_3-	3.98, 4.09
2,3-$(CH_3)_2$-	4.42
2,4-$(CH_3)_2$-	4.61
2,5-$(CH_3)_2$-	4.17, 4.23
2,6-$(CH_3)_2$-	3.42, 3.49
3,5-$(CH_3)_2$-	4.48
2-CH_3-	4.09
2-$(CH_3)_2CH$-	4.06
2-$(CH_3)_2C$-	3.38
2,6-$(CH_3)_2$-4-$(CH_3)_3C$-	3.88
2,4-$(CH_3)_2$-6-$(CH_3)_3$-	3.43
2-CH_3-4,6-$(CH_3)_3C$-	3.31
2,4,6-[$(CH_3)_3C_3$]-	<2

Substituted Naphthylamines

1-NH_2-	3.92*
1-NH_2-2-NO_2-	-1.6
1-NH_2-3-NO_2-	2.22
1-NH_2-4-NO_2-	0.54
1-NH_2-5-NO_2-	2.80
1-NH_2-6-NO_2-	3.15
1-NH_2-7-NO_2-	2.83
1-NH_2-8-NO_2-	2.79
1-NH_2-8-SO_3-	1.71
1-NH_2-3-SO_3-	3.20*
1-NH_2-4-SO_3-	2.81*
1-NH_2-5-SO_3-	3.69*
1-NH_2-6-SO_3-	3.80*
1-NH_2-7-SO_3-	3.66
1-NH_2-8-SO_3-	5.03*
2-NH_2-	4.11*
2-NH_2-1-NO_2-	-1.0
2-NH_2-3-NO_2-	2.93
2-NH_2-4-NO_2-	2.63
2-NH_2-5-NO_2-	3.16
2-NH_2-6-NO_2-	2.75
2-NH_2-7-NO_2-	3.13
2-NH_2-8-NO_2-	2.86
2-NH_2-1-SO_3-	2.35
2-NH_2-3-SO_3-	--
2-NH_2-4-SO_3-	3.70
2-NH_2-5-SO_3-	3.96*
2-NH_2-6-SO_3-	3.74*
2-NH_2-7-SO_3-	3.95*
2-NH_2-8-SO_3-	3.89*

N-substituted anilines*

R	C_6H_5NHR	$C_6H_5N(CH_3)R$	$C_6H_5NR_2$	2-$CH_3C_6H_4NHR$	2-$CH_3C_6H_4NR_2$
H-	4.58	4.85	4.58	4.39	4.39
CH_3-	4.85	5.06	5.06	4.59	5.86
C_2H_5-	5.11	5.98	6.56	4.92	7.18
n-C_3H_7-	5.02	--	5.59	--	
n-C_4H_9-	4.95	--	~5.7	--	
i-C_4H_9-	--	5.20	--	--	
sec-C_4H_9-	--	6.04	--	--	
t-C_6H_{12}-	6.30	--	--	--	
Cyclopentyl-	5.30	6.71	--	5.07	
Cyclohexyl-	5.60	6.35	--	5.34	
t-C_4H_9-	6.95	7.52	--	6.49	

**Thermodynamic*

AMINES ref. 77

Primary amines

2-aminoethylsulphonic acid	9.08
Aminomalonic acid	3.32, 9.83
N-n-butylethylenediamine	7.53, 10.30
2,3-diaminobutane, meso	6.92, 9.97
2,3-diaminobutane, racemic	6.91, 10.00
2,2'-diaminodiethyl sulfide	8.84, 9.64
1,3-diamino-2,2-dimethylpropane	8.18, 10.22
N,N'-Di-(2-aminoethyl)-ethylenediamine	3.32, 6.67, 9.20, 9.92
1,2-diamino-2-methylpropane	6.79, 10.00
1,3-Diaminopropan-2-ol	8.23, 9.68
N,N'-Diglycyethylenediamine	7.63, 8.35
Ethylenediamine-N,N-diacetic acid	5.58, 11.05
Furfurylamine	8.89
2-(2-hydroxypropylamino)-ethylamine	6.94, 9.86
2-(3-hydroxypropylamino)ethylamine	6.78, 9.76
N-Methylaminoacetic acid	2.24, 10.01
Methyl-α-amino-β-mercaptoproionate	6.56, 8.99
N-n-propylethylenediamine	7.54, 10.34
1,2,3-triaminopropane	3.72, 7.95, 9.59
Tris-(hydroxymethyl)-aminomethane	8.10
2-amino-2'-hydroxydiethyl sulfide	9.04
N-(carbamoylmethyl)-iminodiacetic acid	2.30, 6.60
2,2'-diaminodiethylamine	3.58, 8.86, 9.65
2,3-diamino-2,3-dimethylbutane	6.56, 10.13
3,3'-diaminodi-n-propylamine	8.02,9.70, 10.7
1,2-Di-(2-aminoethylthio)ethane	8.43, 9.32
1,2-diaminopropane	7.13, 10.00
N,N-diethylethylenediamine	7.07, 10.02
N,N-dimethylethylenediamine	6.63, 9.53
N-Ethylethylenediamine	7.63, 10.56
N-(2-hydroxyethyl)-ethylenediamine	6.83, 9.82
N-isopropylethylenediamine	7.70, 10.62
2-Methoxyethylamine	9.20
Mercaptoethylamine	8.27, 10.53
N-Methylethylenediamine	7.56, 10.40
2-Methylthioethylamine	9.18
2-thienylmethylamine	8.92
Triaminotriethylamine	8.56, 9.59, 10.29

Secondary amines

N-Butylaminoacetic acid	2.29, 10.07
N,N'-Diethylethylenediamine	7.70, 10.46
2,2'-dihydroxydiethylamine	9.00
N,N'-di-n-propylethylenediamine	8.14, 10.97
Ethylenediamine-N,N'-diacetic acid	6.42, 9.46
Iminodipropionic acid	4.11, 9.61
Piperazine	5.68, 9.82
β-carboxymethylaminopropionic acid	3.61, 9.46
N,N'-Dimethylethylenediamine	7.40, 10.16
N-ethylaminoacetic acid	2.30, 10.10
Iminodiacetic acid	2.98, 9.89
N-isopropylaminoacetic acid	2.36, 10.06
N-n-propylaminoacetic acid	2.28, 10.03

Tertiary amines

4-(2-aminoethyl)morpholine	4.84, 9.45
Di-(2-hydroxyethyl)aminoacetic acid	8.08
Hexamethylenetetramine	5.13
Methyliminodiacetic acid	2.81, 10.18
Diethylaminoacetic acid	2.04, 10.47
Dimethylaminoacetic acid	2.08, 9.80
N-2-hydroxyethyliminodiacetic acid	2.2, 8.73
Triethylenediamine	4.18, 8.19

Ref. 1

Diallylmethyl	8.79
Benzyldimethyl	8.93
N-Allylpiperidine	9.68
N-Allylmorpholine	7.05
Propargyldimethyl	7.05
Propargylethyldimethyl	8.88
N-Methylmorpholine	7.41
N-Methylpyrrolidine	10.46
N,N-Dimethylhydroxylamine	5.20
Allyldimethyl	8.73
Benzyldiethyl	9.48
N-Ethylpiperidine	10.40
N-Ethylmorpholine	7.70
Propargymethyldimethyl	8.33
N-Methylpiperidine	10.08
N-Methyltrimethyleneimine	10.40
Triethanolamine	7.77
N,N-Dimethylmethoxyamine	3.65

Ref. 5

N-Dimethyl-cysteamine	7.95, 10.7
N-Dipropyl-cysteamine	8.00, 10.8
N-β-Mercaptoethyl-morpholine	6.65, 9.8
1-Diethylamino-butan- (4)	10.1
Methyl-[β-diethylamino-ethyl]sulfide	9.8
N-Diethyl-cysteamine	7.8, 10.75
N-β-Mercaptoethyl-piperidine	7.95, 11.05
1-Diethylamino-propan- (3)	8.0, 10.5
1-Diethylamino-hexan- (6)	10.1

ANILINES (Ref. 88)

m-Substituted anilines

m-C_2H_5	4.70			m-$CH(CH_3)_2$	4.67		
-$C(CH_3)_3$		4.66		3,5-$(CH_3)_2$		4.74	
3,5-$[C(CH_3)_3]_2$	4.97			m-$COCH_3$	3.56		
m-CN	2.76			3-Cl,5-OCH_3	3.10		
3-OCH_3.5-NO_2	2.11			3,5-$(OCH_3)_2$	3.82		
3,5-Br_2	2.34						

NAPHTHALAMINES (reference 88)

substituted naphthalamines

2-naphthalamine	**X**			**2-naphthalamine**	**X**		
1-NH_2,3-X	NO_2	2.07		2-NH_2,4-X	NO_2	2.43	
	CN	2.26			CN	2.66	
	Cl	2.66			Cl	3.38	
	Br	2.67			Br	3.40	
	I		2.82		I	3.41	
	$COOCH_3$	3.12			$COOCH_3$	3.38	
	OCH_3		3.26		OCH_3		4.05
	OH	3.30		1-NH_2,6-X	NO_2	2.89	
	CH_3	3.96			Cl	3.48	
	Cl	2.71			OCH_3	3.90	
2-NH_2,5-X	NO_2	3.01			OH	3.97	
	OH	4.07		2-NH_2,7-X	NO_2	3.10	
1-NH_2,5-X	NO_2	2.73			Cl	3.71	
	OH	3.96			OCH_3	4.19	
	Cl	3.34			OH	4.25	
	NH_2	4.21			NH_2	4.66	
1-NH_2,7-X	NO_2	2.55		2-NH_2,6-X	NO_2	2.62	
	Cl	3.48			OCH_3	4.64	
	OCH_3		4.07	2-NH_2,8-X	NO_2		2.73
	OH	4.20		1-NH_2,4-X	NO_2	0.54	
1-NH_2,2-X	NO_2	-1.74			Br	3.21	
1-X,2-NH_2	NO_2	-0.85		2-NH_2,3-X	NO_2	1.48	
1-NH_2,8-X	NO_2	2.79,					

Anilines (in 50% ethanol)

Unhindered	**pK**	**ref.**
Aniline	4.19	40
p-Aminodiphenyl	3.81	40
2-Naphthylamine	3.77	40
3-Phenanthrylamine	3.59	40
m-Aminodiphenyl	3.82	40
2-Aminofluorene	4.21	40
2-Phenanthrylamine	3.60	40
2-Anthrylamine	3.40	40
Hindered		
o-Aminodiphenyl	3.03	40
peri		
1-Naphthylamine	3.40	40
9-Phenanthrylamine	3.19	40
3-Aminopyrene	2.91	40
1-Phenanthrylamine	3.23	40
1-Anthrylamine	3.22	40
meso		
9-Anthrylamine	2.7	40
o-Aminophenols		
3-Hydroxyanthranilic acid	10.09, 5.20	51
2-Aminophenol hydrochloride	9.99, 4.86	51
Indicators		
p-Aminoazobenzene	2.82, 2.76	60
4-Chloro-2-nitroaniline	-1.02, -1.03	60
4,6-Dichloro-2-nitroaniline	-3.61, -3.32	60
6-Bromo-2,4-dinitroaniline	-6.64, -6.71	
2-Amino-4,5-dimethylphenol hydrochloride	5.28	10.40, 51
N,N-Dimethyl-2,4-dinitroaniline	-1.00, --	60
p-Nitrodiphenylamine	-2.4 to -2.9, -2.50	60
4-Methyl-2, dinitroaniline	-3.96, -4.44	60

Heterocyclics

Nucleosides, etc.

Adenine	4.15, 9.80	6
2'-AMP	3.81, 6.17	6
3'-AMP	3.74, 5.92	6
ADP	3.95, 6.3	36
ATP	4.00 (4.1), 6.5	36
Barbital	7.85, 12.7	37
Cytosine	4.45, 12.2	6
Cytosine (deoxy)	4.25	6
3' CMP	4.16-4.31, 6.04	6
CDP	4.44	6
CDP, (deoxy)	4.8, 6.6	6
Guanine	3.3, 9.2, 12.3	6
Guanosine	2.2, 9.5	6
"	1.6, 9.16, 12.5	35
5'-GMP	2.4, 9.4, 6.1	6
GDP	2.9, 9.6, 6.3	6
Hypoxanthine	1.98, 8.94, 12.10	6
5'-IMP	8.9, 1.54, 6.04	6
5-Methylcytosine	4.6, 12.4	6
5-Methylcytosine deoxyriboside 5'-phosphate	4.4	6
3-Methyluracil	9.75	37
3-Methylxanthine	8.5 (8.1), 11.3	38
Adenosine	3.63	6
"	3.3, 12.5	35
5'-AMP	3.3, 6.1	36
	3.74, 6.2-6.4	6
Barbituric acid	3.9, 12.5	37
Cytidine	4.11	6
"	4.22, 12.5	35
2'-CMP	4.3-4.4, 6.19*	6
5'-CMP	4.5, 6.3	6
CTP	4.6, 6.4	6
2,6-Diaminopurine	5.09, 10.77	6
Isoguanine	4.51, 8.99	6
Guanosine (deoxy)	1.6-2.2, 9.16-9.5	6
GMP (2' + 3')	2.3, 9.36, 0.7, 5.9	6
5'-GMP (deoxy)	2.9, 9.7, 6.4	6
GTP	3.3, 9.3, 6.5	6
Inosine	1.2, 8.9	6
"	8.75, 12.5	6
5-Methylcytosine deoxyriboside	4.5, 13.0	6
1-Methyluracil	9.95	37
1-Methylxanthine	7.7, 12.05	38
7-Methylxanthine	8.5 (8.3)	38
9-Methylxanthine	6.3	38
Purine	2.52, 8.90	37
Thymidine	9.8	6
5'-TMP	10.0, 1.6, 6.5	6
Uracil deoxyriboside	9.3	6
5'-UMP	9.5, 6.4	6
UTP	9.5, 6.6	6
Uridine	9.25	6
"	9.17, 12.5	35
Xanthosine	0, 5.5, 13.0	6
Orotic acid	2.8, 9.45, 13	6
Pyrimidine	1.30	37
Thymine	0, 9.9, 713.0	6
Uracil	.5, 9.5, 13.0	6
UMP (2' + 3')	9.43, 1.02, 5.88	6
UDP	9.4, 6.5	6
Uric acid	5.4, 10.3	6
Xanthine	0.8, 7.44, 11.12	6
"	7.2	38

Heterocyclic Bases (Ref. 2)

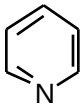

Pyridine 5.14*
pK (20°)

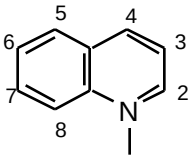

Quinoline 4.85*

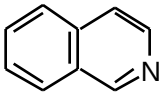

Isoquinoline 5.14*

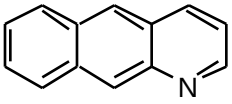

Benzoquinoline 5.05*

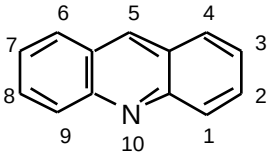

Acridine 5.60

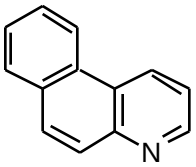

5,6-Benzoquinoline
5.15*

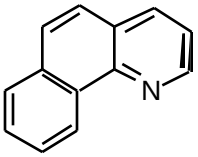

7,8-Benzoquinoline
4.25*

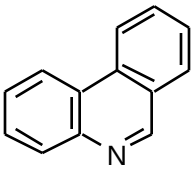

Phenanthridine 3.30[a]

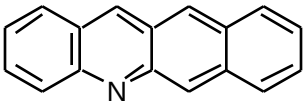

2,3-Benzacridine 4.52[a]

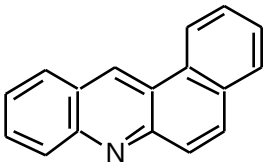

3,4-Benzacridine 4.70*

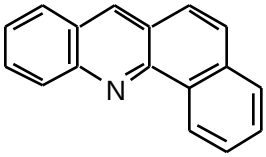

1,2-Benzacridine 3.45[a]

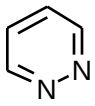

Pyridazine 2.10*

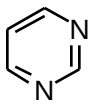

Pyrimidine 1.10*

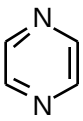

Pyrazine 0.37*

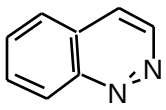

Cinnoline 2.64*

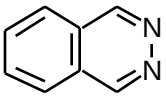

Phthalazine 3.39*

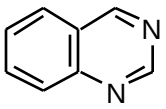

Quinazoline 3.31*

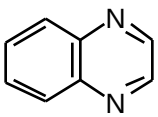

Quinoxaline 0.6*

[a] 50% EtOH

Heterocyclics			3-Hydroxy	8.81, 5.52	39
Aureomycin	3.30, 7.44, 9.27	77	5-Hydroxy (acridone)	--f, -0.32	39
Iridine	--, 5.62	39	5-Methoxy	--, 7	39

Acridine	**1--**	**2--**	**3--**	**4--**	**5--**	**9--**	Ref. 2

H--	5.60*	4.11[a]				
H_2N--	4.40*	8.04*	5.88*	6.04*	9.99*	
	3.59[a]	7.61[a]	5.03[a]	5.50[a]	9.45[a]	
HO--	4.18[a]	4.86[a]	5.52[39]	4.45[a]	-.32[39]	
	10.7[a]	9.9[a]	8.81[39]	9.4*	>12	
CH_3--	3.95[a]		4.60[a]		4.70[a]	
H_2K-(1-CH_3--)--				4.79[a]	9.73[s]	3.22[a]
1,9-$(CH_3)_2$--	2.88[a]					

[a] 50% ethanol; ref. 39

8-amino-1,2-benzacridine	6.72	40
2-amino-4-methyl-5,6-benzoquinoline	7.14	40
3-amino-6,7-benzoquinoline	4.78	40
8-amino-3,4-benzacridine	7.42	40
1'-amino-5,6-benzoquinoline	5.03	40
4'-amino-5,6-benzoquinoline	5.20	40
2-amino-4-methyl-7,8,benzoquinoline	6.74	40
6,7-benzoquinoline	5.05, 3.84[a]	19
5,6-benzoquinoline	5.15, 3.90[a]	19
4-amino-	7.99[a]	19
2-methyl-	4.44[a]	19
4-amino-2-methyl-	8.45[a]	19
2-amino-4-methyl-	7.14, 6.51[a]	19
4'-amino-	5.20, 4.10[a]	19
3'-amino-	4.02[a]	19
1'-amino-	5.03	19
2',4'-diamino-	4.91[a]	19
Benziminazole	5.53	19
2-amino-	7.54	19
Benztriazole	1.6	19
Benzthiazole	1.2, 0.1[a]	19
2-amino-	4.51	19
benzoxazole	(decomp.)	19
2-amino-	3.73	19
2,3-benzacridine	4.52[a]	19
5-amino-	9.72[a]	19
5-acetamido-	4.56[a]	19
7-amino-	5.38[a]	19
5-amino-6:7:8:9-tetrahydro-	9.66[a]	19
Caffeine	0.61	4
cinchonine	7.2	4
Cinnoline	2.70	19
4-amino-	6.84	19
Cocaine	7.6	4
Cinnoline 4-hydroxy	9.27, 0.35	39
6-hydroxy	7.52, 3.65	39
-hydroxy	8.20, 2.74	39

α,α'-dipyridyl	4.43	6
4-amino-	8.75[a]	19
4-amino-2-methyl-	9.45[a]	19
4-amino-2-methyl-8-chloro-	5.95[a]	19
8-chloro-	2.5[a]	19
3,4-diamino-	8.15[a]	19
3-amino-	4.78, 3.73[a]	19
7,8-benzquinoline	4.25, 3.15[a]	19
4-amino-	7.68[a]	19
4-amino-2-methyl-	7.96[a]	19
2-amino-4-methyl-	6.74, 6.02[a]	19
6-amino-2-methyl-	5.23[a]	19
1'-amino-2-methyl-	4.75[a]	19
3,4-benzacridine	4.70, 4.16[a]	19
5-amino	8.41[a]	19
7-amino-	5.03[a]	19
8-amino-	7.42 (6.51)[a]	19
8-acetamido-	4.48[a]	19
8-dimethylamino-	7.31, 6.99	19
1,2-benzacridine	3.45[a]	19
5-amino-	8.13[a]	19
7-amino	4.05[a]	19
8-amino-	6.72, 5.97[a]	19
4',5-diamino-	8.44[a]	19
Cinnoline	--, 0.21	39
3-hydroxy	8.64, 0.21	39
5-hydroxy	7.40, 1.92	39
7-hydroxy	7.56, 3.31	39
4-methoxy	--, 3.21	39

Heterocyclics

o,o'-dipyridyl	4.43	6
hydantoin	9.16	42
5-isopropyl-2-thio-	8.70	42
5,5-pentamethylene2-thio	8.79	42
3,5,5-trimethyl-2-thio	10.80	42
3-methyl-5,5-pentamethylene-2-thio-	11.23	42

Imidazoles

2-Methylimidazole	7.75	43
N-Acetylhistidine	7.05	43
2-Methyl-4-hydroxy-aminobenz-	6.65	43
4-Hydroxymethyl-	6.45	43
2-Methylbenz-	6.1	43
Histamine	6.0	43
4-Hydroxy-6-aminobenz-	5.9	43
4-Hydroxybenz-	5.3 (OH 9.5)	43
4-Methoxybenz-	5.1	43
4-Bromo-	3.7	43
6-Nitrobenz-	3.05, 10.6	43
4-Nitro-	1.5, 9.1	43
isoQuinolines		
1-Hydroxy-	-1.2	44
5-Hydroxy	5.40, 8.45	44
3-Amino-	5.05	40
5-Amino-	5.59	40
Amino-	6.20	40
6-Hydroxy-	5.85, 9.15	44
8-Hydroxy-	5.66, 8.40	44
2-Methylisoquinolone	-1.8	44
Isoquinoline	5.46, 5.14	44, 19
Phenazine	--, 1.23	39
2-Hydroxy-	7.5, 2.6	39
10-Methyl-2-phenazone	--, 3.0	
6-Aminophenanthridine	6.88	40
9-Aminophenanthridine	7.31	40
o-Phenanthroline	4.27[a], 5.2	19
p-Phenanthroline	3.12[a]	19
1,10-Diamino-3,8-Dimethyl-	8.78[a], 6.31[a]	
Phenanthridine	--, 4.65	44
6-Hydroxy-	8.43, 5.35	44
9-Hydroxy (phenanthridone)	<-1.5	44
9-Amino-	7.31, 6.75[a]	19
2,7,9-Triamino-	8.06[a]	19
Phthalazine	3.47	19
1-Amino-	6.60	19
1-Hydroxy-	11.00, -2	39
Picolimic acid	5.52	4
5,5-dimethyl-2-thio-	8.71	42
5,5-Diphenyl-2-thio-	7.69	42
1-Methyl-5,5-pentamethyl-ene-2-thio-	9.25	42
4-Methyl-	7.45	43
Imidazole	6.95	43
4-(2',4'-Dihydroxyphenyl)-	6.45	43
Carbobenzoxy-L-histidyl-L-tyrosine ethyl ester	6.25	43
6-Aminobenz-	6.0 (NH_2 3.0)	
Benzimidazole	5.4	43
Histidine methylester	5.2 (NH_2 7.1)	43
2-Methyl-4-hydroxy-6-nitro-benzimidazole	3.9	43
4-Hydroxy-6-Nitrobenz-	3.05	43
[b]2-Hydroxymethylnaphth(1,2)-	4.44, 12.23	86
[b]2-Hydroxymethylnaphth(2,3)-	4.50, 12.23	86
4-Hydroxy-	4.80, 8.68	44
1-Amino-	7.62	40
4-Amino-	6.28	40
6-Amino-	7.17	40
8-Amino-	6.06	40
7-Hydroxy-	5.70	40
1-Methoxy-	3.05	44
4-NO_2	1.35	88
4-Br	3.31	88
1-Hydroxy-	--, 1.44	39
5-Methyl-1-phenazone	--, 4.9	39
m-Phenanthroline	3.11[a]	19
1-Amino-	ca. 7.3, 7.29[a]	19
2,2'-Dipyridyl	4.23	19
2-Hydroxy-	8.79, 4.82	44
7-Hydroxy-	4.38, 8.68	44
9-Methoxy-	--, 2.38	44
2-Amino-9-methyl-	5.66[a]	19
2,7-Diamino-9-methyl-	6.26[a]	19
6-Amino-	6.88	40
Phenazine	1.23	19
1-Amino-	2.6[a]	19
2-Amino-	4.75, 3.46[a]	19
1,3-Diamino-	5.64[a]	19
2,3-Diamino-	4.74	19
2,7-Diamino-	4.63, 3.9[a]	19
Pteroylglutamic acid	8.26	77
Pyridines		
2-Amino-	6.86	41
4-Amino-	9.17	41
2-Methyl-	5.94[b]	45
2-Vinyl-	4.98	45
2-Chloro-	0.49	45
2,4,6-Trihydroxy-	4,6, 9.0, 13	39
1-Methyl-4-pyridone	3.33	
2-(N-Methylacetamido)-	2.01	46
2-Benzamido-	3.33	
2-(N-Methylbenzamido)-	1.44	
3-(N-Methylacetamod)-	3.52	46
3-(N-Methylbenzamido)-	3.66	46
4-(N-Methylacetamido)-	4.62	46

4-(N-Methylbenzamido)-	4.68	46
4-Benzamido-	5.32	46
3-NO_2	0.81	88
3-COO^-	4.77	47
2,3-Me_2	6.60	48
2,5-Me_2	6.47	48
3,4-Me_2	6.52	48
2,4,6-Me_3	7.48	48
4-OEt	6.67	48
3-Cl	2.84	48
3-CO_2Et	3.35	48
3-COOH	3.13	88
2-Amyl-	6.00[b]	45
2-Hexyl-	5.95[b]	45
2-Benzyl-	5.13	45
2-Bromo-	0.71	45
2,4-Dihydroxy	6.50, 13, 1.37	39
1-Methyl-2-pyridone	0.32	39
2-Acetamido-	4.09	46
1-Methylpyrid-2-one acetylimine	7.12	46
3-Acetamido-	4.46	46
3-Benzamido-	3.80	46
1-Methylpyrid-4-one acetylimine	11.03	46
1-Methylpyrid-4-one benzylimine	9.89	46
4-COO^-	4.90	47
2,4-Me_2	6.72	48
2,6-Me_2	6.77	48
3,5-Me_2	6.14	48
2-Me,5-Et	6.51	48
3-F	3.10	48
3-Br	2.84	48
4-CO_2Et	3.45	48

Pyridine N-oxides (see oxygen acids)

Substituted Pyridines

Pyridine	**2-**	**3-**	**4-**
H-	5.17[b]		
Cl-	0.72[b]	2.84[b]	
I-	1.82[b]	3.25[b]	
CH_3CH_2-	5.97[b]	5.70[b]	6.02[b]
$(CH_3)_3C$-	5.76[b]	5.82[b]	5.99[b]
HO-	0.75	4.86	3.27
	11.62	8.72	11.09
SO_3-[47]		2.9	
CH_3O-	3.28	4.88	6.62
F-	-0.44[b]	2.97[b]	
Br-	0.90[b]	2.84[b]	
CH_3-	5.97[b]	5.68[b]	6.02[b]
$(CH_3)_2CH$-	5.83[b]	5.72[b]	6.02[b]
CH_3CO		3.18[b]	
H_2N-	6.68[b]	5.80[b]	8.96[b]
$CONH_2$[47]		3.40	3.61
NC-[47]		1.45	

Ortho-Substituted Pyridines (in 50% ethanol)

Substituent	**pK**	**ref.**
H-	4.38	2
2-C_2H_5-	4.93	2
2-(CH_3)	4.68	2
2,6-[$(CH_3)_2CH]_2$	3.58	2
2-$(CH_3)_3C$-	4.68	2
2-C_2H_5-6-$(CH_3)_3C$-	4.36	2
2,6-$[(CH_3)_3C]_2$–	3.58	2
2-CH_3-	5.05	2
2-$(CH_3)_2CH$-	4.82	2
2,6-$(CH_3)_2$	5.77	2
2,6-$[(CH_3)_3C]_2$	3.58	2
2-CH_3-6-$(CH_3)_3C$	5.52	2
2-$(CH_3)_2CH$-6-$(CH_3)_3C$-	5.13	2

		pK_{NH}	**35°**	**pK_{OH}**	
Benzimidazole	6.00	5.58	5.36		
2-Methyl	6.96	6.29	6.18	---	
2-Ethyl	6.90	6.27	6.14	--	
2-Hydroxymethyl	---	5.40	---	11.55	ref. 86
1-Methyl-2-hydroxymethyl	---	5.55	---	11.45	

Other (ref. 95)

Thiazolidine	6.31
Methyl thiazolidine-4-carboxylate	4.00
Thiazolidine-4-COOH	1.51, 6.21

(ref. 96)

2-Methyl-Δ^2-oxazoline	5.5
4-Carbamoyl-2-phenyl-Δ^2-oxazoline	2.9
2-Phenyl-Δ^2-oxazoline	4.4

Heterocyclics

Pyrazines	**pK**	**ref**.
Pyrazine	1.1, 0.6	49, 39
2,5-Dimethyl-	2.1	49
2,3,5,6-Tetramethyl-	2.8	49
2-Methoxy-	--, 0.75	39
2-Methyl-	1.5	49
2,6-Dimethyl-	2.5	49
2-Hydroxy-	8.23, 0.1	39
1-Methyl-2-pyrazine	-0.04	39
2-Amino-	3.14	19
Pyrimidine	1.30	19
2-Amino-	3.54	19
5-Amino-	2.83	19
2-Amino-4,6-dimethyl-	4.85	19
2,4,6-Triamino-	6.84	19
2-Hydroxy-	9.17, 2.24	39
Pyridazine	2.33	19
3-Hydroxy-	10.46, -1.8	39
3,6-Dihydroxy-	5,67, -2.2, 13	39
4-Methoxy-	3.70	39
3-Amino-	5.19	19
4-Hydroxy-	8.68, 1.07	39
3-Methoxy-	2.52	39
3,6-Dimethoxy-	1.61	39

For complex chelating agents, see also ref. 77
[b] thermodynamic at 25°.

2,4-Dihydroxy-(Uracil)	9.38, 12	39
4,6-Dihydroxy-	5.4	39
2,4,6-Trihydroxy-(Barbituric acid)	3.9, 12.5	39
2-Methoxy-	<1	39
4-Methoxy-	2.5	39
1-Methyl-2-pyrimidone	2.50	39
3-Methyl-4-pyrimidone	1.84	39
4-Amino-	5.71	19
2-Amino-4-methyl-	4.15	19
2,4-Diamino-	7.26	19
4-Methyl-	1.98	19
4-Hydroxy-	8.59, 1.85	39
4,5-Dihydroxy-	7.48, 1.99, 11.61	39
2,4,5-Trihydroxy-(isoBarbituric acid)	8.11, 11.48	39
4-Hydroxy-5-methoxy-	8.60	1.75 39
1-Methyl-4-pyrimidone	1.8	39

Miscellaneous

4-Hydroxy-2-methylpyridazinium chloride	1.74	44
8-Hydroxy-6-methyl-1,6-naphthyridinium chloride	4.34	44
2-Hydroxyphenazine	2.6	44
4-Hydroxypteridine	-0.17	44
3-Methyl-4-pteridone	-0.47	44
5-Hydroxypyrimidine	1.87, 6.78	44
8-Hydroxy-1,6-Naphthyridine	4.08	44
1-Hydroxyphenazine	1.44	44

5-Methyl-1-phenazone	4.9	44
10-Methyl-2-phenazone	3.0	44
1-Methyl-4-pteridone	1.25	44

Quinoline	**2--**	**3**	**4**	**5**	**6**	**7**	**8**	**Ref.**
H-	4.85*	4.80	4.69*					2
H_2N-	7.25*	4.86*	9.08*	5.37*	5.54*	6.56*	3.90*	2
HO-	-.36	4.30	2.27	5.20	5.17	5.48	5.13	44
	11.74	8.06	11.25	8.54	8.88	8.85	9.89	44
CH_3	5.42	5.14	5.20	4.62	4.92	5.08	4.60	2
	5.8		5.6		5.2		5.0	2
F-		2.36*		3.68*	4.00*	4.04*	3.08*	2
Cl-					3.73*			2
HO_2C	4.96*	4.62*	4.53*	4.81*	4.98*	4.97*	7.20*	2
NO_2		1.03^{88}						

Quinoline		
2,4-Dihydroxy-	5.86, 0.76	39
4-Methoxy-	6.65	59
1-Methyl-4-quinolone	2.46	39
2,4-Diamino-	9.45	19
Quinazoline	3.51, 3.2[a]	19
2-Amino-	4.43	19
6-Amino-	3.2[a]	19
2-Hydroxy-	10.69, 1.30	39
6-Hydroxy-	8.19, 3.12	39
3-Methiodide	7.26	39
2-Methoxy-	1.31	39
2-Methoxy-	3.17	39
1-Methyl-2-quinolone	-0.71	39
4-Amino-	9.44, 9.17	19, 41
8-Quinolinol	5.13, 9.89	6
3-Cl	--, 2.46	88, 44
3-Br	2.61	88
4-Amino-	5.73	19
8-Amono-	2.4[a]	19
4-Hydroxy-	9.81, 2.12	39
8-Hydroxy-	8.65, 3.41	39
2,4-Dihydroxy-	9.78, 2.5	39
4-Methoxy-	3.13	39

*Thermodynamic

Heterocyclics		
Quinoxaline	0.8, 0.56	19, 39
2-Amino-	3.96	19
6-Amino-	2.95	19
2-Hydroxy-	9.08, -1.37	39
1-Methiodide	5.74	39
2,3-Dihydroxy-	9.52	39
5-Hydroxy-1-methylquioxalinium chloride	5.74	44
Riboflavin	9.93	77
Sulphadiazine	6.48	6
Sulphapyridine	8.43	6
2-Aminothiazole	5.39	41
1,3,5-Triazine	--	39
2,4-Dihydroxy-	6.5	39
1,4,6-Triazanaphthalene	2.5	39
4-Hydroxy-	11.05, 0.78	39
5-Amino-	2.62	19
2,3-Diamino-	4.70	19
5-Hydroxy-	8.65, 0.9	39
6-Hydroxy-	7.92, 1.40	39
1,5-Naphthyridine	2.91	39
4-Hydroxy	10.01, 2.85	39
Sulphaquanidine	11.25	6
Sulphathiazole	7.12	6
Terramycin	3.10, 7.26, 9.11	77
Tetramethylenediamine	10.7	4
1,4,5-Triazanaphthalene	1.20	39
8-Hydroxy-	8.76, 0.60	39

SPECIAL NITROGEN COMPOUNDS

Hydroxylamines		
Hydroxylamine	5.97*	12
N-Methyl-	5.96*	12
O-Methyl-	4.60*	12
Trimethyl-	3.65*	12
N-Dimethyl-	5.20*	12
N,O-Dimethyl-	4.75*	12

Hydrazines (30°)

Hydrazine	8.07	13
Methyl-	7.87	13
N,N'-Dimethyl-	7.52	13
Tetramethyl-	6.30	13
N,N-Diethyl-	7.71	13
Phenyl-	5.21 (15°)	14
Glycylhydrazide	2.38, 7.69	15
N,N-Dimethyl-	7.21	13
Trimethyl-	6.56	13
Ethyl-	7.99	13
N,N'-Diethyl-	7.78	13
Acet-	3.24	15
Isonicotinhydrazide	1.85, 3.54, 10.77	77

Hydrazones Hydrazone of:

Benzophenone	3.85	16
p,p'-Dimethoxy-	4.38	16
p-Chloro-	4.38	16
p-Methoxyacetophenone	4.94	16
p,p'-Dichloro-	3.13	16
Phenyl-2-thienyl ketone	3.80	16

Semicarbazones of:

Semicarbazide	3.66	
Furfural	1.44	14
Benzaldehyde	0.96	14
Acetone	1.33	14
Acetaldehyde	1.10	14
Pyruvic acid	0.59	14

Amidoximes

Ox-	3.02	17
Benz-	4.99	17
α-Phenylacet-	5.24	17
Succin-	3.11, 5.97	17
o-Tolu-	4.03	17
p-Tolu-	5.14	17
Malon-	~4.77	17

Other

Diphenylthiocarbazone	4.5	6
Phthalimide	8.30	18
Nitrourethane	3.28	18
Acetylguanidine	8.33	19
Acetamidine	12.52	19
O-Methylisourea	9.80	20
Dimedone	5.23	18
Nitrourea	4.57	18
Guanidine	13.71	19
Phenylguanidine	10.88	19
Benzamidine	11.6	19
N-Phenyl-O-methylisourea	7.3	20

Nitrogen compounds, miscellaneous

Diguanide^{--}	3.07, 13.25	77
Dithiooxamide (rubeanic acid, $H_2NCSCSNH_2$)	10.62	77
Ethylenediguanide	1.74, 2.88, 11.34, 11.76	77
Phenyldiguanide	2.16, 10.71	77

Other

S-Methylisothiourea	9.83	20
N-Phenyl-S-methylisothiourea	7.14	20

Cinchona Alkaloids (in 80% aqueous methyl cellosolve)

Quinine	7.73	2
Quinidine	7.95	2
Ephedrine	9.14	2
N-Methylephedrine	8.50	2
Epiquinine	8.44	2
Epiquinidine	8.32	2
ψ-Ephedrine	9.22	2
N-Methyl-ψ-ephedrine	8.81	2

Acetamide	-0.51	4
Urea	0.18	4
Thiourea	-0.96	4

Thiols

N-Dimethyl-cysteamine	7.95, 10.7	7
N-Dipropyl-cysteamine	8.00 10.8	5
N-β-Mercaptoethyl-morpholine	6.65, 9.8	
1-Diethylamino-butan- (4)	10.1	5
Methyl-[β-diethylamino-ethyl]-sulfide	9.8	5
Methyl thioglycolate	7.8	23
Mercaptoethylamine	8.6, 10.75	23
N-trimethyl cysteine	8.6	23
Glutathione	2.12, 3.59, 8.75, 9.65	23
N-Diethyl-cysteamine	7.8, 10.75	5
N-B-Mercaptoethyl-piperidine	7.95, 11.05	5
1-Diethylamino-propan- (3)	8.0, 10.5	5
1-Diethylamino-hexan- (6)	10.1	5

p-Nitrobenzenethiol	5.1	58
Thioglycolic acid	3.67, 10.31	23
Mercaptoethanol	9.5	23
Cysteine	1.8, 8.3, 10.8	23
Cysteinylcysteine	2.65, 7.27, 9.35, 10.85	23

X=	**-H**	**-S⁻**	**-SH**
$X(CH_2)_2SH$	12.0	13.96	10.75
$X(CH_2)_4SH$	12.4	13.25	11.50
$X(CH_2)_3SH$	13.24	11.14	
$X(CH_2)_5SH$		13.27	11.82

o-Mercapto-phenylacetic acid	4.28, 7.67	59
Ethyl mercaptan	10.50	81
I-Thio-D-sorbitol	9.35	91
2-mercaptoethanesulfonate	7.53 (9.1)	81
o-aminothiophenol	6.59	81
Thiophenol	8.20[a], 7.8, 6.52	59, 81, 82
B-Mercaptopropionic acid	10.27	81
Methyl cysteine	6.5 (7.5) 81	
p-Cl-thiophenol	7.50	81

Mercaptans, RSH

R		
CH_3CCH_2-	7.86	32
$C_6H_5CH_2$-	9.43	82
$HOCH_2CH(OH)CH_2$-	9.51	82
CH_2=$CHCH_2$-	9.96	82
n-C_4H_9-	10.66	82
t-C_5H_{11}-	11.21	82
$C_2H_5OCOCH_2$-	7.95	82
$C_2H_5OCH_2CH_2$-	9.38	82
$HOCH_2CH(OH)CH_2$-	9.66	82
n-C_3H_7-	a10.65	82
t-C_4H_9-	11.05	82

CARBON ACIDS

Acetone	~20	24
Acetylacetone	8.95	24
Diacetylacetone	6	24
Hydrocyanic acid	9.21	25
1-nitropropane	9	18
Saccharin	1.6	18
Tri-methylsulfonyl-methane	strong	24
Dicyanomethane	12	2
Acetonitrile	c. 25	24
Benzoylacetone (anol)	8.23	24
Dimethylsulfone	14	24
Nitroethane	8.6	18
2-nitropropane	7.74	18
Tricyanomethane	strong	24
Trinitromethane	strong	24
Nitromethane	strong	25

Bis-(β-Diketones):$[(RCO)(R'CO)CH]_2CHR$ (in 50% dioxane) (ref. 28)

R	**R'**	**R"**	**pK**	**pK**
CH_3	CH_3	$(CH_2)_5CH_3$	11.33	12.52
CH_3	CH_3	C_6H_5	11.10	12.49
CH_3	CH_3	2-ClC_6H_4	11.04	12.73
CH_3	CH_3	2-C_5H_4N	9.80	12.46
CH_3	CH_3	2-$CH_3OC_6H_4$	11.47	12.44
CH_3	CH_3	3,4-$CH_2O_2C_6H_3$	11.39	12.60
CH_3	CH_3	3-C_5H_4N	10.29	12.63
CH_3	CH_3	4-$CH_3OC_6H_4$	11.62	12.61
CH_3	CH_3	4-$(CH_3)_2NC_6H_4$	11.50	12.45
CH_3	CH_3OCH_2	C_6H_5	11.54	12.27
CH_3	CH_3OCH_2	2-C_5H_4N	10.95	12.49
CH_3	CH_3OCH_2	4-$(CH_3)_2NC_6H_4$	12.13	12.31
CH_3	CH_3OCH_2	4-$CH_3OC_6H_4$	11.74	12.49
	$CH_3OCH_2COCH_2COCH_3$		9.66	
	$(CH_3CO)_2CH(CH_2)_3CH_3$		12.07	

Bis-(β-Diketones) (RCO)-(R'CO)CH-Y-CH(COR)(COR') (in 50% dioxane) (ref. 26)

R	R'	Y	pK	pK
CH_3	CH_3		9.43	13.54
CH_3	CH_3	$(CH_2)_4$	11.99	12.48
CH_3	CH_3	$(CH_2)_{10}$	12.01	12.07
CH_3	CH_3	1,4-$(CH_3)_2C_6H_4$	11.27	12.15

Bis-(β-Diketones) $RCOCH_2CO$-Y-$COCH_2COR$ (in 75% dioxane) (ref. 26)

R	**Y**	**pK**	**pK**
C_6H_5	$(CH_2)_4$	12.47	13.09
C_6H_5	$(CH_2)_5$	12.72	13.46
C_6H_5	$(CH_2)_6$	12.60	13.46
C_6H_5	$(CH_2)_7$	13.1 (est.)	
C_6H_5	$(CH_2)_3$	12.58	13.69
CH_3	$(CH_2)_5$	12.29	13.00
CH_3=$CH(CH_3)_2$	$(CH_2)_5$	12.95	13.60

CH_3NO_2	10.29	74
$CH_3CHClNO_2$	7	74
$CH_3COCH_2\ NO2$	5.1	74
$CH(NO_2)_3$	strong	74
$CH_3COCHCl_2$	15	74
$CH_3COCHC_2H_5CO_2C_2H_5$	12.7	74
$CH_3COCHCH_3COCH_3$	11	74
$CH_3COCH_2COC_6H_5$	9.4	74
$C_6H_5COCH_2COCF_3$	6.82	74
CH_3COCH_2CHO	5.92	74
$CH_3\ COCH2\ CO2CH_3$	10	74
$CH_3SO_2CH_2SO_2CH_3$	14	74
$CH_3SO_2CH(COCH_3)_2$	4.3	74
$C_2H_5NO_2$	8.6	74
$C_2H_5O_2CCH_2\ NO2$	5.82	74
$CH_2(NO_2)_2$	3.57	74
CH_3COCH_2Cl	c. 16.5	74
$CH_3COCH_2CO_2C_2H_5$	10.68	74
$CH_3COCH_2COCH_3$	9	74
$CH_3COCHBrCOCH_3$	7	74
$CH_3COCH_2COCF_3$	4.7	74
$C_6H_5COCH_2NC_5H_5$	10.51	74
$CH(COCH_3)_3$	5.85	74
$CH_3SO_2CH_3$	c. 23	74
$CH(SO_2CH_3)_3$	strong	74
$CH_2(CN)_2$	11.81	74
$C_2H_5O_2CCH_2CN$	9	74
$CH_3CO_2C_2H_5$	~ 24.5	74
$CHC_2H_5(CO_2C_2H_5)_2$	15	74
CH_3CONH_2	~ 25	74
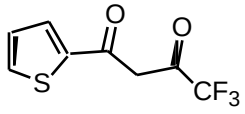	6.10	74
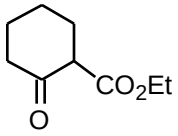	10.96	74
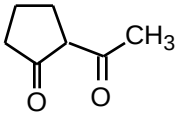	7.82	74
Dinitromethane	4	2
Potassium cyanide	9.21	2
$CH(CN)_3$	strong	74
$CH_2(CO_2C_2H_5)_2$	13.3	74
CH_3CO_2H	~ 24	74
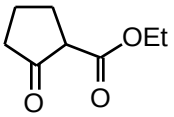	10.5	74
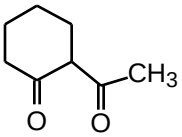	10.1	74
$CH_2(CHO)_2$	5	74

Indicators

Tropeoline OO	2.0	28
Bromocresol green	4.9	28
Thymol blue (1)	1.65	28
Methyl orange	3.45	28
Methyl yellow	3.25	28
Neutral red 7.4	28	
Bromophenol blue	4.1	28
Bromothymol blue	7.3	28
Thymol blue (2)	9.2	28
Methyl red (1)	2.3	28
Methyl red (2)	5.0	28

References

1. Hall, H.K., Jr. *J. A.m. Chem. Soc.* **1957**, *79*, 5441.
2. Brown, H.C. et al., in Braude, E.A. and F.C. Nachod *Determination of Organic Structures by Physical Methods*, Academic Press, New York, 1955.
3. Hall, H.K., Jr. *J. Am. Chem. Soc.* **1957**, *79*, 5439.
4. Handbook of Chemistry and Physics, Editor in Chief, Charles D. hodgman, M.S.; Chemical Rubber Publishing Company, Cleveland, OH, 1951, p. 1636-7.
5. Franzen, V. *Chem. Ber.* **1957**, *90*, 623.
6. Dawson, R.M.C. et al., *Data for Biochemical Research*, Oxford, Clarendon Press, 1959.
7. Buist, G.J.; Lucas, H.J. *J. Am. Chem. Soc.* **1957**, *79*, 6157.
8. Stevenson, G.W.; Williamson, D. *J. Am. Chem. Soc.* **1958**, *80*, 5943.
9. Soloway, S.; Lipschitz, H. *J. Org. Chem.* **1958**, *23*, 613.
10. Bissell, E.R.; Finger, M. *J. Org. Chem.* **1959**, *24*, 1256.
11. Tuckerman, M.M.; Mayer, J.R.; Nachod, F.C. *J. Am. Chem. Soc.* **1959**, *81*, 92.
12. Bissot, T.C.; Parry, R.W.; Campbell, D.H. *J. Am. Chem. Soc.* **1957**, *79*, 796.
13. Hinman, R.L. *J. Org. Chem.* **1958**, *23*, 1587.
14. Conant, J.B.; Bartlett, P.D. *J. Am. Chem. Soc.* **1932**, *54*, 2881.
15. Lindegren, C.R.; Niemann, C. *J. Am. Chem. Soc.* **1949**, *71*, 1504.
16. Harnsberger, H.F.; Cochran, E.L.; Szmant, H.H. *J. Am. Chem. Soc.* **1955**, *77*, 5048.
17. Pearse, G.A., Jr.; Pflaum, R.T. *J. Am. Chem. Soc.* **1959**, *81*, 6505.
18. Bell, R.P.; Higginson, W.C.E. *Pro. Royal Soc.* **1949**, *197*, 141.
19. Albert, A.; Goldacre, R.; Phillips, J. *J. Chem. Soc.* **1948**, 2240.
20. Dippy, J.F.J.; Hughes, S.R.C.; Rozanski, A. *J. Chem. Soc.* **1959**, 2492.
21. Edsall, J.T.; Martin, R.B.; Hollingworth, B.R. *PN'As* **1958**, *44*, 505.
22. Martin, R.B.; Edsall, J.T.; Wetlaufer, D.B.; Hollingworth, B.R. *JBC* **1958**, *233*, 1429.
23. Edsall, J.T.; Wyman and Jeffries, *Biophysical Chemistry*, Academic Press, Inc., New York, 1958.
24. Pearson, R.G.; Dillon, R.L. *J. Am. Chem. Soc.* **1953**, *75*, 2439.
25. Ang, K.P. *J. Chem. Soc.* **1959**, 3822.
26. Martin, D.F.; Fernelius, W.C. *J. Am. Chem. Soc.* **1959**, *81*, 1509.
27. Ellenbogen, E. *J. Am. Chem. Soc.* **1952**, *74*, 5198.
28. Kolthoff, *Treatise on Analytical Chemistry*, New York, Interscience Encyclopedia, Inc., 1959.
29. Edwards, J.O. *J. Am. Chem. Soc.* **1954**, *76*, 1540.
30. Bailey, N.A.; Carrington, K.A.; Lott, K.; Symons, M.C.R. *J. Chem. Soc.* **1960**, 290.
31. Brownstein, S.; Stillman, A.E. *J.P.C.* **1959**, *63*, 2061.
32. Schwarzenbach *Helv. Chem. Acta.* **1957**, *40*, 907.
33. Ingham, J.W.; Morrison, J. *J. Chem. Soc.* **1933**, 1200.
34. Hildebrand, J.H. *Principles of Chemistry*, New York, The Macmillan Company, 1940.
35. Baddiley, in Chargaff, *The Nucleic Acids*, vol. I, New York, Academic Press, 1955.
36. Pabst, OR 1.
37. Bendich, in Chargaff, etc.
38. Jordan, in Chargaff, etc.
39. Albert, A.; Phillips, J.N. *J. Chem. Soc.* **1956**, 1294.
40. Elliott, J.J.; Mason, S.F. *J. Chem. Soc.* **1959**, 2352.
41. Angyal, S.J.; Angyal, C.L. *J. Chem. Soc.* **1952**, 1461.
42. Edward, J.T.; Nielsen, S. *J. Chem. Soc.* **1957**, 5075.
43. Bruice, T.C.; Schmir, G.L. *J. Am. Chem. Soc.* **1958**, *80*, 148.
44. Mason, S.F. *J. Chem. Soc.* **1958**, 674.
45. Linnell, R.H. *J. Org. Chem.* **1960**, *25*, 290.
46. Jones, R.A.; Katritzky, A.R. *J. Chem. Soc.* **1959**, 1317.
47. Jaffe, H.H.; Doak, G.O. *J. Am. Chem. Soc.* **1955**, *77*, 4441.
48. Clarke, K.; Rothwell, K. *J. Chem. Soc.* **1960**, 1885.
49. Keyworth, D.A. *J. Org. Chem.* **1959**, *24*, 1355.

50. Gawron, O.; Duggan, M.; Grelechi, C.J. *Anal. Chem*. **1952**, *24*, 969.
51. Sims, P. *J. Chem. Soc.* **1959**, 3648.
52. Fickling, M.M.; Fischer, A.; Mann, B.R.; Packer, J.; Vaughan, J. *J. Am. Chem. Soc.* **1959**, *81*, 4226.
53. Wold, F.; Ballou, C.E. *JBC* **1957**, *227*, 301.
54. McElroy, W.D.; Glass, B. *Phosphorus Metabolism*, Vol. I, Baltimore, Johns Hopkins University Press, 1951.
55. Kumler, W.D.; Eiler, J.J. *J. Am. Chem. Soc.* **1943**, *65*, 2355.
56. VanWazer, J. *Phosphorus and Its Compounds*, Vol. I, New York, Interscience Encyclopedias, Inc., 1958.
57. Freedman, L.D.; Doak, G.O. *Chem. Rev*. **1957**, *57*, 479.
58. Ellman, G.L. *Arch. Biochem. Biophys*. **1958**, *74*, 443.
59. Pascal, I.; Tarbell, D.S. *J. Am. Chem. Soc.* **1957**, *79*, 6015.
60. Bascombe, K.N.; Bell, R.P. *J. Chem. Soc.* **1959**, 1096.
61. Gawron, O.; Draus, F. *J. Am. Chem. Soc.* **1958**, *80*, 5392.
62. Mukherjee, L.M.; Grunwald, E. *JPC* **1958**, *62*, 1311.
63. Ballinger, P.; Long, F.A. *J. Am. Chem. Soc.* **1959**, *81*, 1050.
64. Ballinger, P.; Long, F.A. *J. Am. Chem. Soc.* **1960**, *82*, 795.
65. Haszeldine, R.N. *J. Chem. Soc.* **1953**, 1757.
66. Deno, N.C.; Berkheimer, H.E.; Evans, W.L.; Peterson, H.J. *J. Am. Chem. Soc.* **1959**, *81*, 2344.
67. Gardner, J.N.; Katritzky, A.R. *J. Chem. Soc.* **1957**, 4375.
68. Wise, W.M.; Brandt, W.W. *J. Am. Chem. Soc.* **1955**, *77*, 1058.
69. Fortnum, D.H.; Battaglia, C.J.; Cohen, S.R.; Edwards, J.O. *J. Am. Chem. Soc.* **1960**, *82*, 778.
70. Everett, A.J.; Minkoff, G.J. *TFS* **1953**, *49*, 410.
71. Bauer, L.; Miarka, S.V. *J. Am. Chem. Soc.* **1957**, *79*, 1983.
72. Green, A.L.; Sainsbury, G.L.; Saville, B.; Stansfield, M. *J. Chem. Soc.* **1958**, 1583.
73. Burkhard, R.K.; Sellers, D.E.; DeCou, F.; Lambert, J.L. *J. Org. Chem*. **1959**, *24*, 767.
74. Bell, R.P., *The Proton in Chemistry*, Ithica, Cornell University Press, 1959.
75. Stewart, T.D.; Maeser, S. *J. Am. Chem. Soc.* **1924**, *46*, 2583.
76. Jencks, W.P.; Carriuolo, J. *J. Am. Chem. Soc.* **1960**, *82*, 1778.
77. Bjerrum, J., et al. *Stability Constants*, Chemical Society, London, 1958.
78. Parsons, R. *Handbook of Electrochemical Constants*, London, Butterworths, 1959.
79. Bower, V.E.; Robinson, R.A. *JPC* **1960**, *64*, 1078.
80. Candlin, J.P. *J. Chem. Soc.* **1960**, 4236.
81. Danehy, J.P.; Noel, C.J. *J. Am. Chem. Soc.* **1960**, *82*, 2511.
82. Kreevoy, M.M. et al. *J. Am. Chem. Soc.* **1960**, *82*, 4899.
83. Kabachnik, M.I., et al. *Tetrahedron* **1960**, *9*, 10.
84. Bjerrum, J., et al. *Stability Constants*, Chemical Society, London, 1958.
85. Crutchfield, M.M.; Edwards, J.O. *J. Am. Chem. Soc.* **1960**, *82*, 3533.
86. Lane, T.J.; Quinlan, K.P. *J. Am. Chem. Soc.* **1960**, 2994, 2997.
87. Moeller, T.; Ferrus, R. *JPC* **1960**, *64*, 1083.
88. Bryson, A. *J. Am. Chem. Soc.* **1960**, *82*, 4558, 4862, 4871.
89. Henderson, W.A., Jr.; Streuli, C.A. *J. Am. Chem. Soc.* **1960**, *82*, 5791.
90. Edwards, J.O. et al. *J. Am. Chem. Soc.* **1960**, *82*, 778.
91. Bell, R.P.; McTigue, P.T. *J. Chem. Soc.* **1960**, 2983.
92. Li, N.C. et al. *J. Am. Chem. Soc.* **1960**, *82*, 3737.
93. Cohen, W.; Erlanger, B.F. *J. Am. Chem. Soc.* **1960**, *82*, 3928.
94. Olson, D.C.; Margerum, D.W. *J. Am. Chem. Soc.* **1960**, *82*, 5602.
95. Ratner, S.; Clarke, H.T. *J. Am. Chem. Soc.* **1937**, *59*, 200.
96. Porter, G.R.; Rydon, H.N.; Schofield, J.A. *Nature* **1958**, *182*, 927.

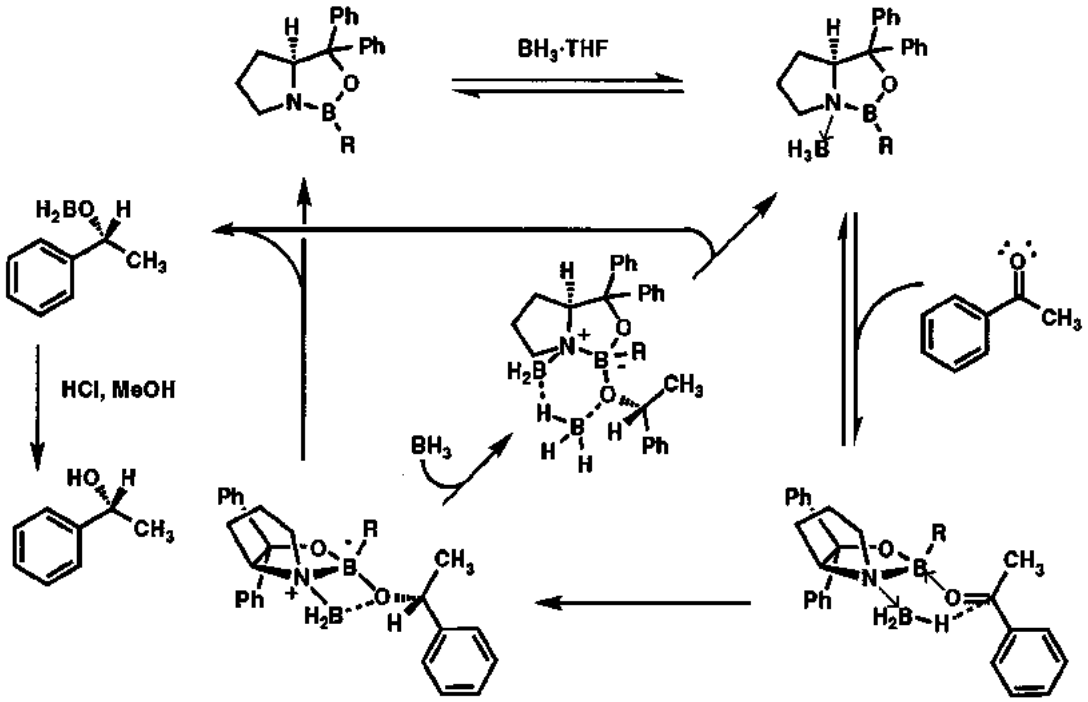

Remarkable advances in catalytic methods for enantioselective synthesis of chiral organic molecules have made the past decade truly momentous for organic chemistry. Great progress has been made not only in the discovery of useful new reactions, but also in our understanding of the fundamental mechanistic principles underlying enantioselective catalysis.

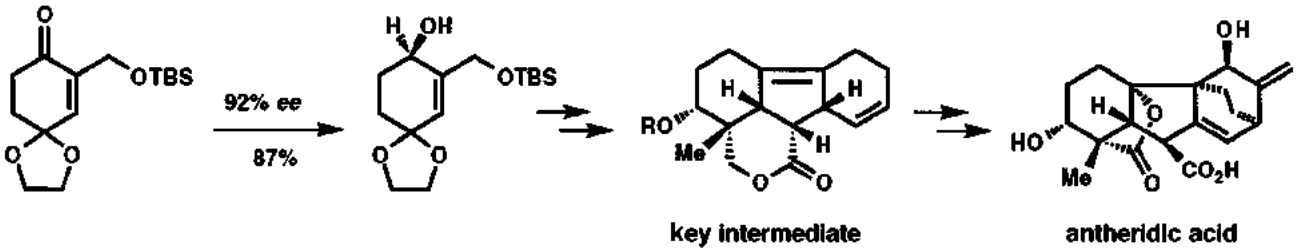

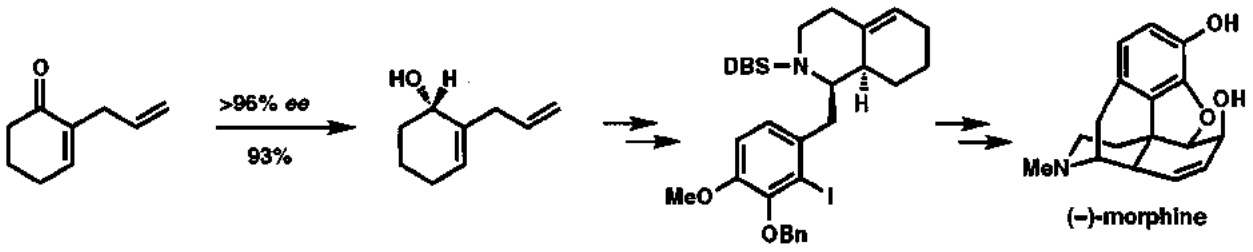

Reduction of Carbonyl Compounds with Chiral Oxazaborolidine Catalysts: A New Paradigm for Enantioselective Catalysis and a Powerful New Synthetic Method**

Elias J. Corey* and Christopher J. Helal

The introduction of complex metal hydrides such as lithium aluminum hydride and sodium borohydride into synthetic organic chemistry half a century ago greatly accelerated progress in this field. For many years, efforts to combine these reducing agents with various chiral ligands for the purpose of achieving efficient asymmetric synthesis proved disappointing. However, promising results obtained by Itsuno and his collaborators in the 1980s with mixtures of chiral 1,2-amino alcohols and borane paved the way for the discovery of oxazaborolidines as chiral catalysts for the borane-mediated enantioselective reduction of a wide variety of achiral ketones (CBS reduction). The well-defined structure of the catalyst and the straightforward reaction pathway have allowed the rapid expansion of the scope of the CBS reduction and the rational modification of catalyst structure to achieve optimal enantioselectivity for a particular type of substrate. This enantioselective catalytic reduction is now established as a major synthetic method for the asymmetric synthesis of chiral medicinals, catalytic ligands, complex natural products, and synthetic intermediates.

Keywords: asymmetric catalysis · boron · ketones · reductions · total synthesis

1. Introduction

The introduction of aluminum and boron hydrides for the reduction of carbonyl groups half a century ago had an enormous impact on the field of synthetic chemistry, and helped to usher in a golden age for the rationally planned multistep construction of complex organic molecules.[1] These reagents not only provided predictable site selectivity in multifunctional substrates, but often predictable diastereoselectivity as well. The versatile parent compounds $LiAlH_4$,[2] AlH_3,[3] $NaBH_4$,[4] and $BH_3 \cdot THF$[5] have been modified in almost every conceivable way to generate a large collection of derivatives, each of which has a special reactivity and utility, for example $NaBH(OMe)_3$, $NaBH(OAc)_3$, $NaBH_3CN$, $LiBH(sBu)_3$, Cl_2BH, $(cyclohexyl)_2BH$, catecholborane, $(RS)_2BH$, $NaBH_4 \cdot CeCl_3$, $LiAlH(OtBu)_3$, $LiAlH(OMe)_3$, $NaAlH_2(OR)_2$, and iBu_2AlH.[6] The literature on carbonyl reduction by this extensive family of hydride/hydrogen donors is so vast that a comprehensive review would require several large volumes. However, despite five decades of research and countless thousands of applications of hydride donors, much remains to be learned regarding detailed reaction mechanisms and transition-state structures.[6, 7] One consequence of this primitive understanding of transition-state structure is that it is difficult to predict how a new reagent will behave.

In view of the enormous utility of Al–H and B–H reagents for the reduction of carbonyl groups, it is natural that the modification of these structures by the emplacement of chiral ligands would be investigated for the purpose of achieving absolute stereochemical control (*re*- or *si*-face selectivity) in the synthesis of chiral alcohols. For more than thirty years there have been numerous studies of mixtures of $LiAlH_4$, $NaBH_4$, or $BH_3 \cdot THF$ with chiral 1,2-diols, 1,2-amino alcohols, or 1,2-diamines as reagents for enantioselective carbonyl reduction.[8] Specific examples of such "mixture reagents" include *cis*-2,3-pinanediol and $LiAlH_4$;[9a] (2*S*,3*R*)-4-dimethylamino-3-methyl-1,2-diphenyl-2-butanol (Darvon alcohol) and $LiAlH_4$;[9b, c, d] (−)-*N*-methyl-*N*-(1-phenylethyl)amine · HCl and $LiAlH_4$;[9e] hydroxymethyl oxazolines and $LiAlH_4$;[9f] (−)-*N*-methylephedrine, various phenols, and $LiAlH_4$;[9g, h, i] (*S*)-leucine methyl ester · BH_3 and BF_3;[9j] 2,2′-dihydroxy-1,1′-binaphthol, ethanol, and $LiAlH_4$ (BINAL-H);[9k, l] (*S*)-2-(*N*-arylaminomethyl)pyrrolidines and $LiAlH_4$;[9m] (*S*)-4-anilinyl-3-methylamino-1-butanol and $LiAlH_4$;[9n, o] 2,2′-dihydroxy-6,6′-dimethylbiphenyl, $BH_3 \cdot THF$, and various amines;[9p] (−)-*N*-methylephedrine, 2-alkylaminopyridines, and $LiAlH_4$;[9q] *N*-

[*] Prof. E. J. Corey, Dr. C. J. Helal
Department of Chemistry and Chemical Biology
Harvard University
12 Oxford Street, Cambridge, MA 02138 (USA)
Fax: (+1) 617-495-0376
E-mail: corey@chemistry.harvard.edu

[**] A list of abbreviations used is provided in the Appendix.

  1433-7851/98/3715-1987 $ 17.50+.50/0

benzoylcysteine, $LiBH_4$, and *tert*-butyl alcohol;[9r] and (1*S*,2*S*)-2-amino-3-methoxy-1-phenyl-1-propanol and $BH_3 \cdot Me_2S$.[9s]

While good levels of enantioselectivity have been reported for some of these early empirical studies, these reducing systems have seen very limited use in synthesis. In addition, because the reactive species are generally unknown, and in many cases insoluble as well, there has been no reliable information on the mechanistic basis for enantioselectivity. This is the situation for the Darvon alcohol – $LiAlH_4$ complex, introduced by Mosher and Yamaguchi,[9b] and used with some success by others.[9c, d] It is probably the best known of these mixture reagents. The Noyori reagent BINAL-H[9k, l]—which is made from (*S*)- or (*R*)-BINOL, $LiAlH_4$, and ethanol, and seems to be structurally better defined—also has seen very little use although it reacts with very high enantioselectivity with certain substrates; clearly high cost and marginal practicality are factors which detract from the usefullness of this reducing system.

After a survey of the extensive literature of these mixture reagents for hydride reduction and in an attempt to rationalize the basis for the observed enantioselectivities, we became very interested in a system introduced by Itsuno et al. in 1981.[10] In this initial work, the authors reported the novel finding that mixtures of chiral amino alcohols such as (*S*)-valinol and $BH_3 \cdot THF$ in a ratio of 1:2 in THF at 30 °C effected the enantioselective reduction of a number of achiral ketones to chiral secondary alcohols in nearly 100 % yield with enantiomeric excesses in the range of 10 – 73 % *ee*.[11] The most thoroughly studied substrate, butyrophenone, was reduced by this reagent to (*R*)-1-phenylbutan-1-ol with 69 % enantiomeric purity. Upon screening numerous amino alcohols, it was discovered that the tertiary amino alcohol **1** derived from (*S*)-valine together with two equivalents of $BH_3 \cdot THF$ at -78 to 0 °C over several hours converted acetophenone into (*R*)-1-phenylethanol with a much improved enantiomeric excess (94 %, Scheme 1).[12] The dependence of the enantioselectivity of this process on the ratio of BH_3 to amino alcohol, the quantity of hydride present in the reagent, and the steric bulk of the ketone substituents was studied. However, no mechanistic rationale was proposed by Itsuno et al. for either the sense or magnitude of this surprisingly good enantioselectivity. No applications were reported by other groups. Studies of this intriguing reaction were initiated by our group on the basis of mechanistic insights which were subsequently confirmed and which led to a new and powerful catalytic version of the original stoichiometric Itsuno reduction.

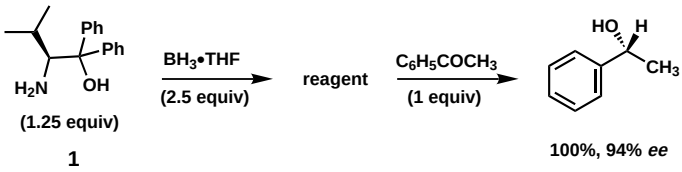

Scheme 1. Highly enantioselective ketone reduction reported by Itsuno.

2. Development of the CBS Catalytic Enantioselective Reduction[13]

From the outset it appeared reasonable that the primary reaction product of the tertiary amino alcohol **1** would be an oxazaborolidine of structure **2**. This was confirmed in 1986 – 1987 by Bakshi and Shibata of our laboratories. They found that the reaction of amino alcohol **1** with two equivalents of BH_3 in THF at 35 °C produced two equivalents of hydrogen gas and the oxazaborolidine **2**, which was obtained in pure form upon sublimation (105 – 130 °C, 0.05 Torr) after removal of the solvent and excess BH_3 in vacuo (see Scheme 2). Its structure was demonstrated by FT-IR and ^1H and ^{11}B NMR spectroscopy and mass spectrometry (EI). Although solutions of **2** in THF did not reduce acetophenone after several hours at 23 °C, mixtures of **2** and $BH_3 \cdot THF$ (0.6 equiv) effected the rapid reduction of acetophenone in less than one minute at 23 °C to afford (*R*)-1-phenylethanol in 94.7 % *ee*, which is

Elias J. Corey, born in 1928 in Methuen, 30 miles north of Boston, MA, studied chemistry from 1945 to 1950 at the Massachusetts Institute of Technology, where he gained his doctorate for work on synthetic penicillins under the supervision of John C. Sheehan. In 1951 he joined the University of Illinois at Urbana-Champaign as an Instructor in Chemistry and was promoted in 1956 to full Professor. Since 1959 he has been at Harvard University. For as long as he can remember he has enjoyed study, adventure, and discovery.

Christopher J. Helal, born in 1969 in Columbus, OH, received his Bachelor of Science degree in chemistry in 1991 from the Ohio State University. He enrolled in the graduate program at Harvard University, where he was a National Science Foundation Graduate Fellowship recipient. He earned his doctorate in 1997 under the direction of Professor E. J. Corey on the investigation of novel electronic and steric effects in the enantioselective oxazaborolidine-catalyzed reduction of ketones, and is currently employed at Pfizer Central Research, Groton, CT, where he is involved in drug discovery.

E. J. Corey

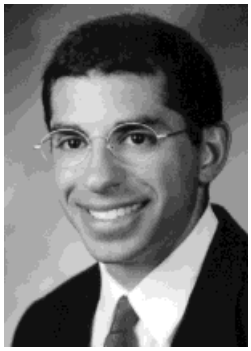

C. J. Helal

comparable to the results reported by Itsuno.[12] In the absence of **2**, acetophenone was reduced relatively slowly with $BH_3 \cdot THF$ at 23 °C. The rate acceleration with **2** immediately suggested that substoichiometric quantities of **2** could effect an asymmetric reduction of a ketone. This was readily verified by an experiment with 2.5 – 5 mol % of **2** and 1.2 equivalents of $BH_3 \cdot THF$, which produced (*R*)-1-phenylethanol with 94.7 % *ee* (Scheme 2). Thus, the careful investigation of an impressive yet, in the original report, poorly understood reaction led to the discovery of a highly enantioselective *catalytic* reduction of ketones mediated by an *isolable* and *structurally defined* catalyst.

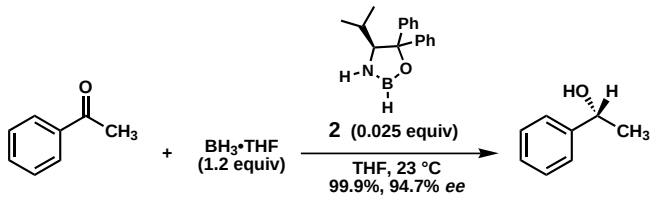

Scheme 2. Oxazaborolidine-catalyzed reduction with borane.

The demonstration of the catalytic activity of oxazaborolidine **2** and mechanistic considerations (see Section 3) led to the expectation that oxazaborolidine **4** should be a superior reagent (Scheme 3). Treatment of amino alcohol **3**[14a, b] with

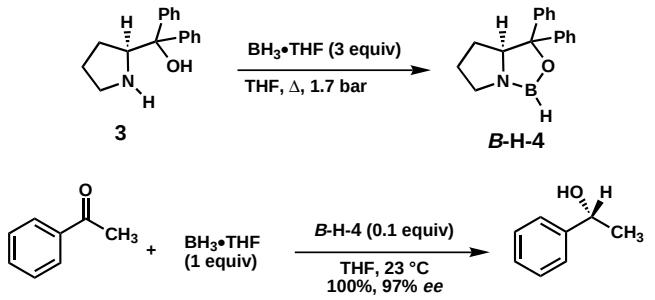

Scheme 3. A superior oxazaborolidine catalyst for the enantioselective reduction of ketones.

$BH_3 \cdot THF$ gave oxazaborolidine *B*-H-**4** (CBS catalyst named after *C*orey, *B*akshi, and *S*hibata), which was characterized by ^1H and ^{11}B NMR spectroscopy and mass spectrometry (EI).

Oxazaborolidine **4** was indeed found to be generally superior to **2** as an enantioselective reduction catalyst. For example, the reduction of acetophenone with 1.2 equivalents of $BH_3 \cdot THF$ and 0.1 equivalents of *B*-H-**4** in THF at 25 °C gave (*R*)-1-phenylethanol with 97 % *ee* and in quantitative yield.

The methyl-substituted oxazaborolidine *B*-Me-**4** was prepared as shown in Scheme 4 and characterized by ^1H and ^{11}B NMR spectroscopy and mass spectrometry (EI). An improvement in the selectivity and practicality of the CBS reduction was realized with this catalyst relative to the *B*-H analogue. The reduction of ketones with *B*-Me-**4** as the catalyst frequently resulted in appreciably higher enantioselectivity than with *B*-H-**4**. Additionally, *B*-H-**4** is extremely air- and moisture-sensitive, and its formation requires extended heating with BH_3 under increased pressure. On the other hand, *B*-Me-**4** is less sensitive and can be stored in closed containers, weighed or transferred in air, and is readily formed by heating **3** and methaneboronic acid at reflux in toluene for 4 h with removal of water.

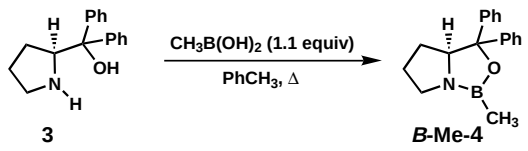

Scheme 4. A more stable and enantioselective catalyst.

Table 1 summarizes the results for the reduction of a variety of different ketones with *B*-Me-**4** as the catalyst.[13b] These data show that the CBS reduction process results in excellent enantioselectivities, near quantitative yields, and short reaction times, and leads to a product whose absolute configuration can be predicted from the relative effective steric bulk of the two carbonyl appendages. Another notable attribute of

Table 1. CBS reduction of ketones catalyzed by *B*-Me-**4**.[13b]

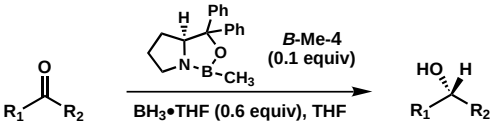

Ketone	Config. (*ee* [%])	*T* [°C]
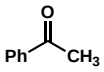	*R* (96.5)	2
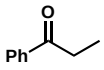	*R* (96.7)	– 10
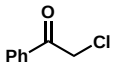	*S* (95.3)	32
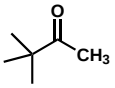	*R* (97.3)	– 10
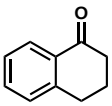	*R* (86)[a]	– 15
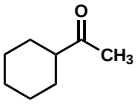	*R* (84)	– 10
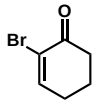	*R* (91)	23
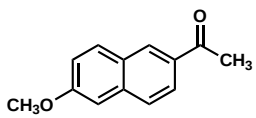	*R* (97.6)	23
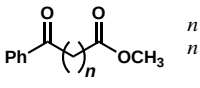	$n = 2$: *R* (94) $n = 3$: *R* (96.7)	$n = 2$: 0[b] $n = 3$: 0[b]

[a] 0.25 equiv of *B*-Me-**4**. [b] The reaction time was 25 min.

this methodology is the easy recovery of the catalyst precursor **3** by precipitation from organic solvent as the hydrochloride salt and efficient recycling.[14c]

3. Mechanistic Rationale[13, 15]

The general mechanistic model which was developed for reduction of ketones with oxazaborolidine catalyst **4** (and analogous catalysts such as **2**) is outlined in Scheme 5. The

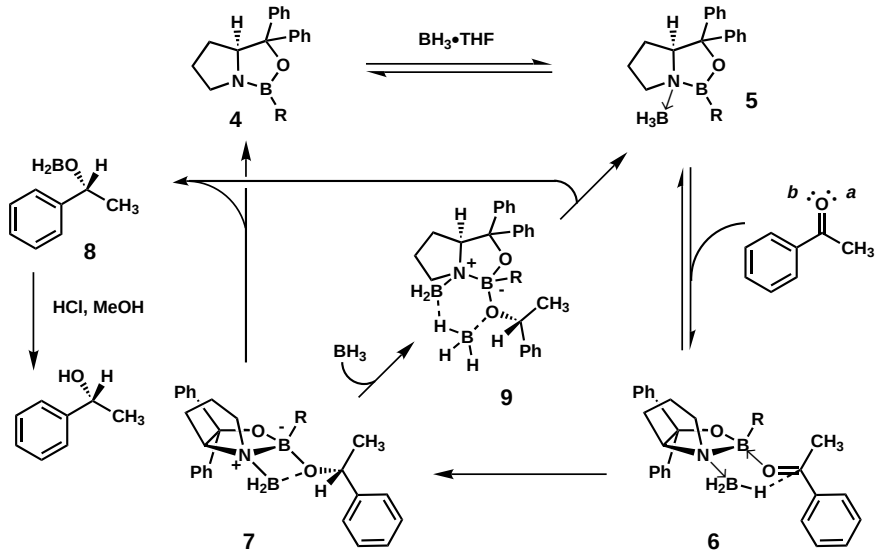

Scheme 5. Proposed mechanism for the catalytic enantioselective reduction of ketones by oxazaborolidines **4**.

mechanistic model explains 1) the absolute stereochemistry of the reduction, 2) the outstanding enantioselectivity obtained for the reduction, 3) the exceptional rate enhancement of the reduction, and 4) the turnover of the catalyst.

The initial step in the pathway is the rapid (and probably reversible) coordination of BH_3 to the Lewis basic nitrogen atom on the α face of oxazaborolidine **4** to form the *cis*-fused oxazaborolidine $\cdot$ BH_3 complex **5**. Unambiguous support for the initial step comes from the observation by ^{11}B NMR spectroscopy[16] that **4** and $BH_3 \cdot THF$ form the 1:1 complex *B*-H-**5** and the fact that crystalline *B*-Me-**5** (**5**, R = Me) can be isolated and structurally defined by single-crystal X-ray diffraction analysis.[17] The coordination of the electrophilic BH_3 to the nitrogen atom of **4** serves to activate BH_3 as a hydride donor and also to increase strongly the Lewis acidity of the endocyclic boron atom. The strongly Lewis acidic complex **5** then readily binds to the ketonic substrate, for example acetophenone, at the more sterically accessible electron lone pair (*a* in the case of acetophenone) and *cis* to the vicinal BH_3 group ($\rightarrow$**6**). This manner of binding minimizes unfavorable steric interactions between the oxazaborolidine and the ketone, and aligns the electronically deficient carbonyl carbon atom and the coordinated BH_3 for stereoelectronically favorable, face-selective hydride transfer via a six-membered transition state to form the reduction product **7**. Thus, the rate enhancement for the oxazaborolidine-catalyzed reduction is due to the activation of the stoichiometric reducing agent BH_3 by coordination with the Lewis basic nitrogen atom of **4** with simultaneous intensification of the Lewis acidity of the boron atom in the heterocycle for coordination to the ketone. This leads to subsequent enthalpically and entropically favorable face-selective intramolecular hydride transfer.[18]

Dissociation of the reduction product from **7** to regenerate the oxazaborolidine catalyst may occur by two different pathways: 1) reaction of the alkoxide ligand attached to the endocyclic boron atom with the adjacent boron atom of **7** to regenerate **4** and form the borinate **8** by cycloelimination;[13d, 15] or 2) by the addition of BH_3 to **7** to form a six-membered BH_3-bridged species **9**, which decomposes to produce the catalyst – BH_3 complex **5** and borinate **8**.[19, 20] The facile disproportionation of **8** to afford dialkoxyborane $(RO)_2BH$ and BH_3 allows the efficient use of the three hydrogen atoms of the stoichiometric reductant.[21]

The mechanism proposed in Scheme 5 provides a simple explanation for the superior effectiveness of oxazaborolidine **4** relative to **2**. As shown in Scheme 6, the selective binding of BH_3 to one face of **2** is the result of a steric preference for a *trans* relationship between the isopropyl substituent and BH_3. Competing formation of the *cis* adduct leads to lower enantioselectivity of the reduction. The rigid [3.3.0] ring system of **4**, however, strictly requires the α coordination

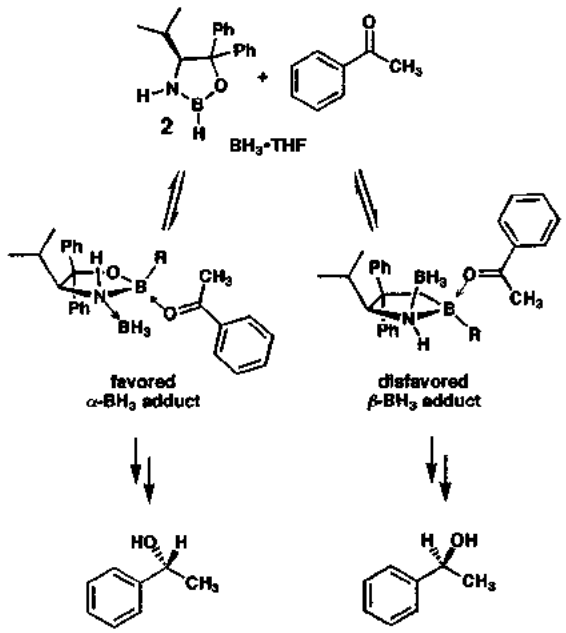

Scheme 6. A possible reduction pathway for catalyst **2** with low enantioselectivity.

of BH_3 to the Lewis basic nitrogen atom (see **6**); β coordination would result in a very strained (by ca. 10 kcal mol^{-1}) *trans*-fused [3.3.0]pentalane. Thus, production of the undesired alcohol enantiomer through a diastereomeric BH_3 coordination mode is energetically precluded with CBS catalyst **4**.

A final issue posed by the mechanistic model in Scheme 5 is whether the complexation of the ketone by **5** or the subsequent hydride transfer to form **7** is the rate-limiting step of the reduction. To answer this question, the rates of reduction of acetophenone and the *p*-NO_2 and *p*-MeO derivatives catalyzed by *B*-Me-**4** were measured.[22a] The relative rates of reduction were 3.4 (*p*-NO_2), 1.8 (*p*-MeO), and 1.0 (*p*-H).[22b] This implies that the coordination of the ketone to **5** is not strictly rate-limiting for these substrates. Additional information was obtained from the $^1H-^2H$ kinetic isotope effect (k_H/k_D) for hydride transfer, which was measured with an excess of a 1:1 mixture of B^1H_3 and B^2H_3 (6 equiv of each) in THF with two equivalents of oxazaborolidine B-Me-**4** and one equivalent of acetophenone. The ratio of ^1H to ^2H in the reduction product 1-phenylethanol at low conversion was determined by mass spectrometry to be 1.7, which is then the approximate value of k_H/k_D.[22a] This low value is indicative of an early transition state for highly exothermic transfer of hydride from the boron atom to the carbonyl group. Thus, both association to the carbonyl comound and hydride transfer are probably fast and comparably rate-limiting. In agreement with these experimental results, semiempirical molecular orbital calculations with the AM1 Hamiltonian provided similar transition state enthalpies for ketone complexation and hydride transfer.[18c] The calculated kinetic isotope effect for the oxazaborolidine-catalyzed reduction of 2-propanone was 1.8 at 23 °C, which is in agreement with the experimentally determined value of 1.7.[23]

4. Further Studies in the Optimization of the CBS Reduction

The high enantioselectivity, generality, and profound mechanistic understanding of the CBS reduction have led to a number of other studies aimed at further elucidating in ever increasing detail the effect of five variations in the structure of the oxazaborolidine catalyst on enantioselectivity over a wide range of substrates. Described in the following are results from investigations of varying 1) the oxazaborolidine ring system, 2) the *gem*-diphenyl substituents, 3) the group on the endocyclic boron atom, 4) the stoichiometric reducing agent, and 5) the mode of catalyst preparation.

4.1. Variations in the Oxazaborolidine Ring System

Subsequent to the discovery of the high enantioselectivity imparted by the proline-derived oxazaborolidine catalyst **4** in the reduction of ketones with BH_3, many other fused bicyclic oxazaborolidines have been prepared by other research groups and by our own to demonstrate the relationship between catalyst structure and enantioselectivity. The effectiveness of the various oxazaborolidine catalysts for the enantioselective reduction of acetophenone is summarized in Table 2. For example, the aziridine (entries 1 and 2),[24] azetidine (entry 3),[25] and pyrrolidine catalysts (entry 4, **4**)[13] afford (*R*)-1-phenylethanol in very high enantiomeric excess (94–97%). The structurally constrained tricyclic oxazaborolidine in entry 5 is among the most effective of all the oxazaborolidines synthesized, as it has demonstrated exceptional enantioselectivity for the reduction of acetophenone (98% *ee*) as well as numerous other substrates.[26] The use of a catalyst with a more flexible [4.3.0] ring system (entry 6) resulted in lower enantioselectivity.[27] Entry 7 reveals that the

Table 2. Fused bicyclic oxazaborolidine catalysts for the enantioselective reduction of acetophenone.

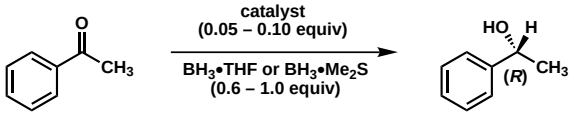

Entry	Catalyst	R	*ee* [%]	Solvent, *T* [°C]
1	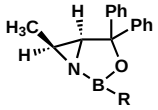	H	94	THF, 23
2	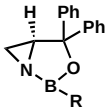	H	94	$PhCH_3$, 23
3	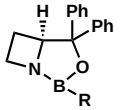	H Me	97 75	THF, 23 $PhCH_3$, 23
4	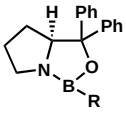	H Me	97 97	THF, 23 THF, 23
5	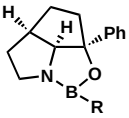	Me	98	THF, 0
6	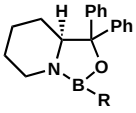	H	87	THF, 0
7	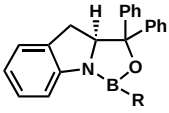	H Me	96 92	THF, 23 $PhCH_3$, 27
8	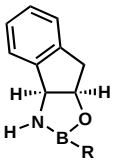	Me	86	THF, 0
9	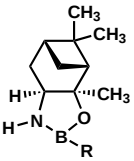	H Me	94 93	THF, 25–30 THF, 0–5

enantioselectivity of the reduction is not strongly affected by decreased Lewis basicity of the endocyclic nitrogen atom of the catalyst owing to conjugation with the fused aromatic ring (up to 96% *ee* for the reduction of acetophenone).[28] Industrial interest in the large-scale application of CBS reductions has led to the search for other inexpensive and readily available enantiopure amino alcohols as precursors to chiral oxazaborolidines. Towards this end, enantiopure *cis*-1-amino-2-indanol (entry 8, prepared in four steps from indene)[29] and an amino alcohol derived from α-pinene (entry 9, prepared from α-pinene)[30] have been used to generate bicyclic oxazaborolidine catalysts which mediate the reduction of acetophenone with high enantioselectivity (86 and 94% *ee*, respectively).

4.2. Variation of the Carbinol Substituents

The effects of the *gem*-diphenyl substituents of the carbinol center (R′) on the enantioselectivity of acetophenone reduction are summarized in Table 3. Replacing the phenyl group (entry 1, *B*-Me-**4**) by the somewhat bulkier β-naphthyl group (entry 2) leads to a slight increase in enantioselectivity (98% *ee*) in this and some other cases.[31] The use of still bulkier *ortho*-substituted aromatic groups such as α-naphthyl (entry 3),[25c] *ortho*-tolyl (entry 4),[32] or *ortho*-anisyl (entry 5),[32] however, results in considerably lower enantioselectivity, as does the use of the smaller 2-thienyl group (entry 6).[32] Substitution with straight-chain alkyl (*n*-butyl, entry 7)[25c] and spiroalkyl groups (entries 8 and 9),[33] did not provide useful catalysts. However, a catalyst containing the rigid spiro-2-indanyl substituent (entry 10) afforded the reduction product with high enantioselectivity (96% *ee*).[34] Emplacement of two strongly electron-withdrawing trifluoromethyl groups on the oxazaborolidine ring system (entry 11), which should inductively increase the Lewis acidity of the heterocyclic boron atom, led to a catalyst which provided relatively poor enantioselectivity.[35, 36]

4.3. Variation of the Substituent on the Heterocyclic Boron Atom

The group R on the heterocyclic boron atom can play an important role in determining the selectivity of complexation by the catalyst to the two possible ketone electron lone pairs. Because of differential steric interactions between R and the carbonyl substituents (see **6**, Scheme 5), a discrimination is crucial to the enantioselectivity of the reduction. Table 4 lists several groups which have been studied as boron substituents in our laboratory[37] for the CBS reduction of a range of ketonic substrates. Besides the compounds *B*-H-**4** (entry 1) and *B*-Me-**4** (entry 2) previously discussed, a variety of other catalysts containing *n*-alkyl (entries 3,[38] 4,[39] 5[35]), 3-phenylpropyl (entry 6),[40] allyl (entry 7),[37] *s*-alkyl (entry 8),[40] and β-branched attachments both with chiral centers (entry 9)[41] and without (entries 10[40] and 11[42]) have been synthesized and tested in the enantioselective reduction. In general, the R group exerts a steric effect in proximity to the boron atom to which it is attached that can influence the selectivity of binding at one of the oxygen lone pairs. In addition, it has been possible to design substituents, such as trialkylsilylmethyl (entry 12)[43] and *p*-substituted aryl groups (entry 13),[44] which interact sterically with more remote sites on the coordinated ketone and thus influence dramatically the enantioselectivity of reduction (see Sections 5, 6.3, and 6.4). The optimal R group for enantioselective reduction can be expected to depend on the structure of the substrate, as discussed in Section 5.

Table 3. Influence of the substituents R′ at the carbinol center.

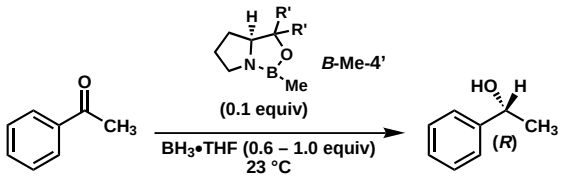

Entry	R′	*ee* [%]
1		97
2	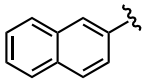	98
3	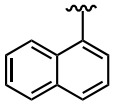	62
4	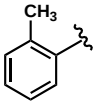	76
5	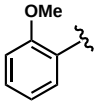	28
6		82
7	$CH_3CH_2CH_2CH_2$	55
8[a]		67
9[a]		71
10[a]	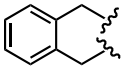	96
11[b]	CF_3	60

[a] The oxazaborolidine (0.15 equiv) was formed from the corresponding precursor by reaction with $BH_3 \cdot THF$ and contains a hydrogen atom on boron instead of the methyl group. The reduction was carried out at 0 °C. [b] The group on the oxazaborolidine boron atom was *n*-pentyl.

Table 4. Boron substituents in CBS catalysts.

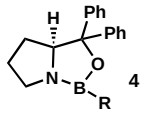

4

Entry	R
1	H
2	CH_3
3	CH_2CH_3
4	$CH_2CH_2CH_2CH_3$
5	$CH_2CH_2CH_2CH_2CH_3$
6	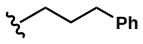
7	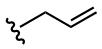
8	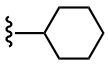
9	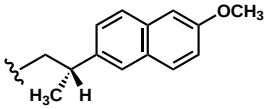
10	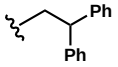
11	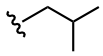
12	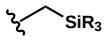
13	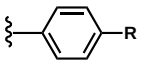

4.4. Variation of the Stoichiometric Reducing Agent

Since the initial use of $BH_3 \cdot THF$ as the stoichiometric reductant in the CBS reduction, a number of other BH_3 complexes have been employed—including $BH_3 \cdot Me_2S$,[44b] $BH_3 \cdot$ 1,4-thioxane,[45] and $BH_3 \cdot$ diethylaniline[46]—all of which lead to comparable enantioselectivity. An advantage of these reagents over $BH_3 \cdot THF$ is lower sensitivity to moisture and oxygen. The coordination of Me_2S, THF, etc. to BH_3 generally does not effect the level of enantioselection except at temperatures below $-30\,^{\circ}C$.[47] At this temperature the equilibria between BH_3, the coordinated ligand, the oxazaborolidine catalyst, and the ketone are sufficiently altered to allow the intervention of competing reduction pathways; this then results in diminished enantioselectivity. The use of catecholborane,[48] a less reactive monohydridic reagent that requires no ancillary ligand for stabilization, permits CBS reductions to occur at temperatures as low as $-126\,^{\circ}C$ in noncoordinating solvents (CH_2Cl_2 or toluene) with excellent enantioselectivity.[31, 47] Furthermore, the decreased reactivity of catecholborane as compared to BH_3, especially at lower temperatures, minimizes both uncatalyzed ketone reduction and hydroboration of sensitive functional groups (e.g., C=C, C≡C, C=O) within the ketonic substrate.

4.5. Variations in Oxazaborolidine Formation

The preparation of chiral oxazaborolidines in pure form was vital to the discovery of the CBS catalyst *B*-H-**4** and the demonstration of the mechanism outlined in Scheme 5. Catalyst purity is essential for the attainment of high enantioselectivity and reproducibility in the reduction of ketones. As a result, considerable effort has been extended towards the development of effective procedures for the generation of pure oxazaborolidines without the need for a purification step. The first-generation CBS catalyst *B*-H-**4** was originally prepared by the extended heating of amino alcohol **3** with three equivalents of $BH_3 \cdot THF$ under argon (1.7 bar) followed by sublimation.[13a] Subsequently, a more convenient procedure was developed for the synthesis of *B*-H-**4** that consists of heating **3** and $BH_3 \cdot Me_2S$ in toluene at reflux for 17 h and then removing solvent in vacuo without further purification.[49, 50] The alkyl- and aryl-substituted oxazaborolidines (Section 4.3) are easily prepared by heating a solution of **3** and the corresponding boronic acid $RB(OH)_2$ or boroxine $(RBO)_3$ at reflux in toluene for 12–24 h with removal of water with molecular sieves.[51] To shorten the time required for complete catalyst formation, the more reactive boronic acid equivalents bis(trifluoroethyl)alkyl boronates ($RB(OCH_2CF_3)_2$) have been developed; they allow for quantitative oxazaborolidine formation in less than one hour.[52]

5. Scope of Oxazaborolidine-Catalyzed Reductions

The well-defined mechanistic pathway of the enantioselective reduction of ketones mediated by chiral oxazaborolidine **4** greatly simplified application of this reaction to the enantioselective reduction of many different types of ketones and to the expansion of its scope and generality. As shown in Table 5, many conjugated aryl ketones of varying structure undergo highly enantioselective reduction with BH_3 or catecholborane in the presence of the proline-derived oxazaborolidine **4**. For example, acetophenone[46] and derivatives with functional groups on the alkyl side chain such as $P(O)(OiPr)_2$[53] or Cl[44a] are reduced with high enantioselectivity, as are the *para*-,[17b] *meta*-,[13b, 54] and *ortho*-substituted[55] aryl ketones and the cyclic aryl ketones 1-tetralone,[46] 1-indanone,[17b] and 1-benzosuberone.[17b] The presence of nitrogen and other heteroatoms in the ketonic substrate is tolerated in the oxazaborolidine-catalyzed reduction, but often requires the use of an additional equivalent of the stoichiometric reductant L_2BH to coordinate to the Lewis basic site.[50a, 56] Representative procedures for the CBS reduction of acetophenone and α-chloroacetophenone are detailed in reference [57].

Recently, the oxazaborolidine-catalyzed reduction of essentially isosteric electronically biased benzophenones[58, 59] as well as *ortho*-substituted benzophenones[59] and 2-benzoyl pyridinium triflates[59] has been shown to be strikingly selective as a result of gearing effects between the aromatic rings. This reaction provides an efficient route to optically active benzhydrols (Table 6).[60] The presence of an *ortho*-substituent on the aromatic ring also proved to be very

Table 5. Oxazaborolidine-catalyzed reduction of aryl ketones.

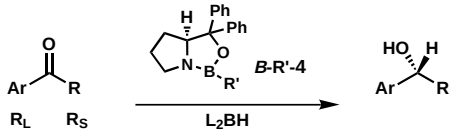

Ketone	*ee* [%]	Catalyst	L_2BH	*T* [°C]	Ketone	*ee* [%]	Catalyst	L_2BH	*T* [°C]
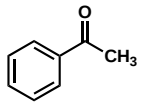	99[46]	*B*-Me-**4**	BDEA	30	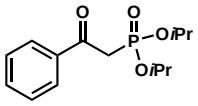	91[53]	*B*-*n*Bu-**4**	CB	−20
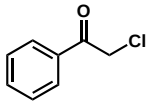	98[44a]	*B*-Me-**4**	BDEA	31	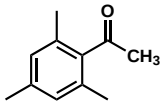	99.7[55a]	*B*-*n*Bu-**4**	CB	−78
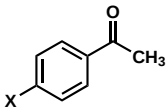	97 (X = F)[17b] 99 (X = OMe)[17b]	*B*-Me-**4** · BH_3	BMS	−20	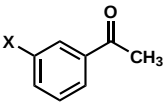	96 (X = Br)[54] 97 (X = OMe)[54]	*B*-Me-**4**	BTHF	23
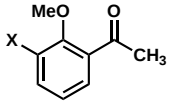	97 (X = OMe)[55b] 94 (X = H)[55b]	*B*-Me-**4**	BMS	23	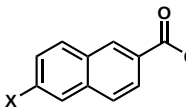	96 (X = H)[54] 98 (X = OMe)[13b]	*B*-Me-**4**	BTHF	23
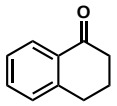	≥ 99[46]	*B*-Me-**4**	BDEA	20	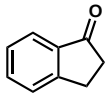	98[17b]	*B*-Me-**4** · BH_3	BMS	−20
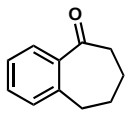	99[17b]	*B*-Me-**4** · BH_3	BMS	−20	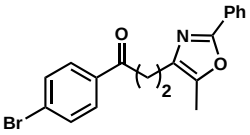	94[56]	*B*-Me-**4**	BMS	25
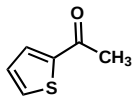	94[56]	*B*-Me-**4**	BMS	25	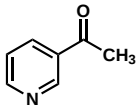	99[50a]	**3** + $(MeO)_3B$	BMS	23

important for the enantioselective reduction of aryl diisopropylphosphono ketones.[53]

α,β-Enones have been extensively investigated as CBS reduction substrates since enantiopure allyl alcohols are extremely versatile intermediates which can participate in many useful synthetic elaborations, for example the Claisen rearrangement or S_N2' displacement reactions with organometallic reagents that allow transfer of chirality by cleavage of C–O bonds and formation of C–C bonds to new chiral centers. It is interesting to note that in the case of acyclic enones (Table 7) the olefinic portion generally behaves as the large group R_L, especially in the presence of a β substituent such as aryl,[58] trimethylsilyl, tri-*n*-butylstannyl,[61] or alkyl groups.[62b–f]. Even an α substituent[62a, f] (see below) can serve to reinforce the intrinsic preference for lone pair coordination. For cyclic α,β-enones with endocyclic unsaturation, α substitution of the C–C double bond with alkyl[47, 63] or halogen[64] is crucial for effective steric differentiation of the carbonyl oxygen electron lone pairs (Table 8). The reduction of cyclic α,β-enones with an exocyclic double bond has not been extensively studied. However, it can be expected that β substitution is not crucial for high enantioselectivity, but helps to minimize reduction of the conjugated double bond.[65, 66]

The oxazaborolidine-catalyzed reduction of α,β-ynones to afford propargyl alcohols of high optical purity has recently been accomplished by two different reaction protocols (Table 9). The use of (*S*)-*B*-Me-**4** as catalystand $BH_3 \cdot Me_2S$ as reductant in THF leads to (*S*)-alcohols, with ethynyl behaving as the small group R_S.[67] In contrast, the use of (*S*)-*B*-CH_2SiMe_3-**4**[43] or (*S*)-*B*-*p*-*t*BuC_6H_4-**4**[44a] and catecholborane in CH_2Cl_2 for the reduction of triisopropylsilyl or trimethylsilylacetylene ketones furnishes (*R*)-propargyl alcohols, with ethynyl behaving as the large group R_L.[68] This intriguing reversal in the enantioselectivity of the reduction is the consequence of repulsive interactions between the remotely situated bulky substituents on the triple bond and the heterocyclic boron atom of the catalyst.[43]

Ketones with two sp^3-hydridized carbon atoms attached to the carbonyl center can also be reduced with high enantio-

Table 6. Oxazaborolidine-catalyzed reduction of diaryl- and aryl diisopropylphosphono ketones.[a]

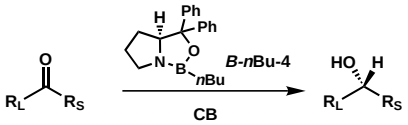

Ketone	*ee* [%]	*T* [°C]
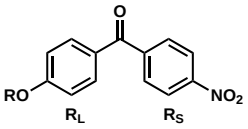	95[58]	– 78
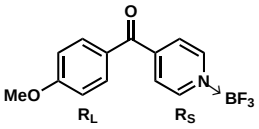	93[59]	– 78
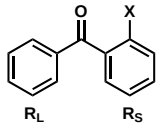	97 (X = Br,Me)[59]	– 40
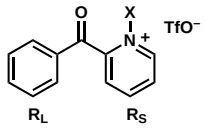	> 90 (X = Me)[59] 99 (X = allyl)[59]	– 40
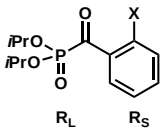	91 – 97 (X = F,Cl,Br,I,Me)[53]	– 20

[a] A procedure for the CBS reduction of *N*-allyl-2-(4-chlorobenzoyl)-pyridinium triflate is provided in reference [60].

Table 8. Oxazaborolidine-catalyzed reduction of cyclic α,β-enones.

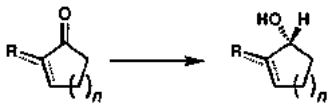

Enone	*ee* [%]	Catalyst	L_2BH	*T* [°C]
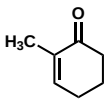	93[47]	*B*-*n*Bu-**4**	CB	– 78
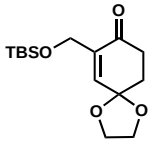	92[63a]	*B*-*n*Bu-**4**	BTHF	37
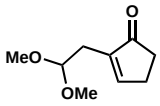	93[63b]	*B*-Me-**4**	BTHF	10
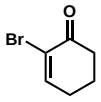	96[64a]	*B*-Me-**4**	BMS	– 15
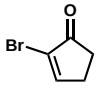	90[64b]	*B*-Me-**4**	BTHF	23
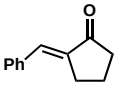	96[65]	*B*-Me-**4** · BH_3	BMS	– 20

Table 7. Oxazaborolidine-catalyzed reduction of acyclic α,β-enones.[a]

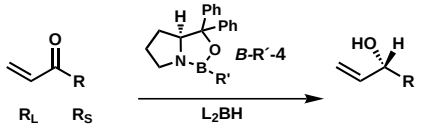

Enone	*ee* [%]	Catalyst	L_2BH	*T* [°C]
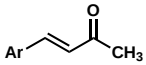	97 (Ar = Ph)[58] 95 (Ar = 4-$MeOC_4H_4$)[58]	*B*-*n*Bu-**4**	CB	– 78
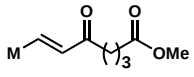	94 (M = $SiMe_3$)[61] 88 (M = $SnBu_3$)[61]	*B*-CH_2SiMe_3-**4**	CB	– 78 – 60
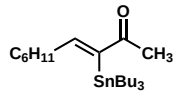	94[62a]	*B*-*n*Bu-**4**	CB	– 78
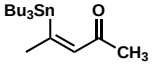	85[62b,c]	*B*-Me-**4**	CB	– 30
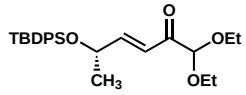	95[62d,e]	*B*-*n*Bu-**4**	BMS	23
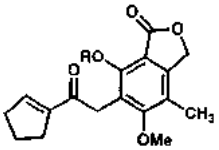	92 – 97[62f]	*B*-Me-**4**	BMS	– 30

[a] A procedure for the CBS reduction of (*E*)-4-(4′-methoxyphenyl)-3-buten-2-one is provided in reference [66].

Table 9. Oxazaborolidine-catalyzed reduction of α,β-ynones.

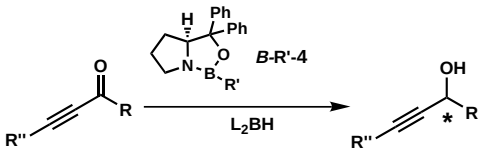

Ynone	*ee* [%]	Catalyst	L_2BH	*T* [°C]
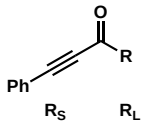	71–88 (R = *n*-alkyl)[67] 94–96 (R = *s*-alkyl)[67]	*B*-Me-**4**[a]	BMS	–30
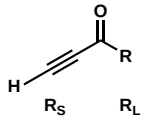	95 (R = *n*-alkyl)[67] 98 (R = *c*-Hexyl)[67]	*B*-Me-**4**[a]	BMS	–30
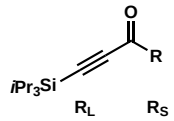	90–97 (R = *n*-, *s*-alkyl)[43]	*B*-CH_2SiMe_3-**4**	CB	–78
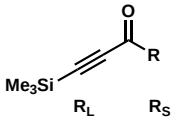	91–97 (R = CH_3, *n*-alkyl)[44a]	*B*-*p*-*t*BuC_6H_4-**4**	CB	–40

[a] 2 equiv of *B*-Me-**4**.

selectivity whenever there are substantial differences in the accessibility of the two oxygen electron lone pairs for coordination (Table 10). For example, ketones having a *tert*-alkyl group and a primary or *n*-alkyl-type group as carbonyl appendages can be reduced with high enantioselectivity.[44a, 46] The reduction of some ketones, especially those in which the carbonyl group is quite hindered, often proceeds with better stereoselectivity at higher temperatures (30–120 °C), possibly due to accelerated removal of the bulky boronate product from the oxazaborolidine.[55a, 69a, b] The highly enantioselective reduction of *s*-alkyl ketones such as cyclohexyl methyl ketone and isopropyl methyl ketone was recently accomplished by the use of $BH_3 \cdot$ diethylaniline as stoichiometric reductant.[46] In the CBS reduction of cyclopropyl isopropyl ketone, the strong influence of electronic factors is clearly evidenced, as the π electron rich cyclopropyl group behaves as R_L in comparison to the sterically similar isopropyl group.[58] Methyl *n*-alkyl ketones are reduced with modest selectivity with *n*-alkyl as R_L,[70] but the factors responsible for enantiodifferentiation of di-*n*-alkyl ketones can be quite subtle;[71] further study of the reduction of such challenging substrates represents an attractive area for future research.

Table 10. Oxazaborolidine-catalyzed reduction of dialkyl ketones.

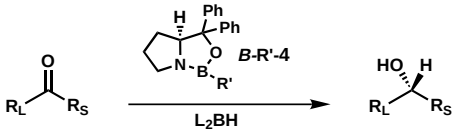

Ketone	*ee* [%]	Catalyst	L_2BH	*T* [°C]	Ketone	*ee* [%]	Catalyst	L_2BH	*T* [°C]
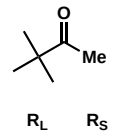	97.4[46]	*B*-Me-**4**	BDEA	20	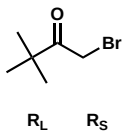	97[44a]	*B*-*n*Bu-**4**	BMS	23
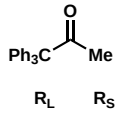	97[55a]	*B*-Me-**4**	BTHF	120	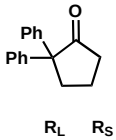	92[69a]	*B*-Me-**4**	BMS	40
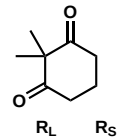	93[70]	*B*-*n*Bu-**4**	CB	25	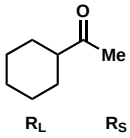	≥ 99[46]	*B*-Me-**4**	BDEA	20
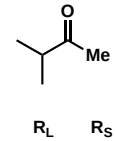	91[46]	*B*-Me-**4**	BDEA	20	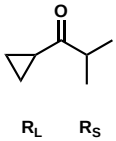	91[58]	*B*-*n*Bu-**4**	CB	–78
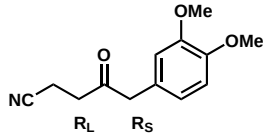	82[71]	*B*-Me-**4**	BMS	–15	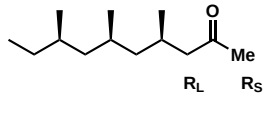	–[a]	*B*-Me-**4**	BTHF	23

[a] 70 % *de*.[70]

Transition metal π complexes of achiral ketones can often be reduced with high enantioselectivity. Thus, the CBS reduction of a variety of ketones π-complexed with chromium,[72] cobalt,[58] iron,[73] or ruthenium[73b] has been investigated with outstanding results (Table 11). The resulting optically active products are useful for the synthesis of pharmaceutically important compounds[72] and chiral ligands for asymmetric catalysis.[73]

The study of trihalomethyl ketones has provided deep insights into the connection between ketone conformation and reactivity.[22, 74] The electron-withdrawing nature of the trihalomethyl group results in a stereoelectronically favorable deformation of the carbonyl group towards CX_3. Together with the steric bulk of the trihalomethyl group, this leads to highly selective catalyst binding *anti* to CX_3 and subsequent fast hydride transfer[22] to furnish trihalomethyl carbinols of high enantiopurity across a wide range of ketonic structures (Table 12).[75]

Primary alcohols deuterated in the 1-position have been prepared by the reduction of the corresponding aldehydes with [D_1]catecholborane at low temperature (Scheme 7).[31] 1-Octanal (90% *ee*) and cyclohexanecarbaldehyde (92% *ee*) also undergo highly selective reduction under these conditions.

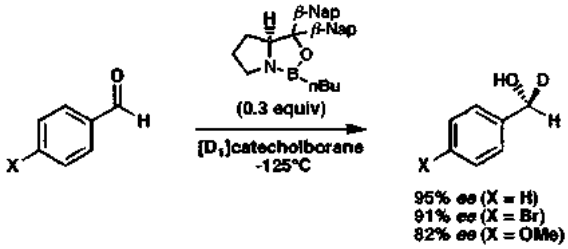

Scheme 7. Preparation of primary alcohols deuterated in the 1-position.

6. Applications of the Oxazaborolidine-Catalyzed Reduction of Ketones

The ever-increasing need for absolute stereochemical control in the construction of organic molecules has resulted

Table 11. Oxazaborolidine-catalyzed reduction of ketones in ligands of metal complexes.

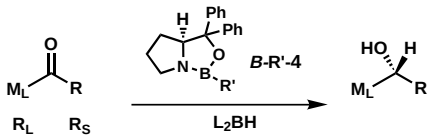

Complex	*ee* [%]	Catalyst	L_2BH	*T* [°C]
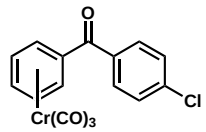	98[72]	*B*-*n*Bu-**4**	CB	– 40
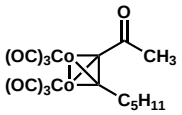	97[58]	*B*-CH_2SiMe_3-**4**	CB	– 78
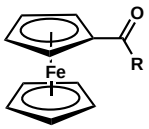	> 95 (R = Me, Et, Ph, *i*Pr)[73a]	*B*-Me-**4**	BTHF	0
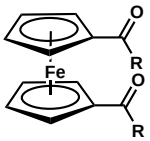	> 99 (R = *n*-, *s*-alkyl, Ph)[a][73b]	*B*-Me-**4**	BTHF	0
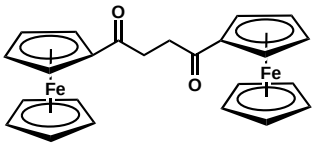	> 98[b][73c]	*B*-Me-**4**	BTHF	0
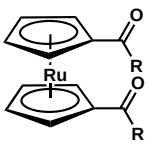	> 99 (R = Me, *n*-pentyl)[c][73b]	*B*-Me-**4**	BTHF	0

[a] 74 – 94% *de*. [b] 74% *de*. [c] 68 – 78% *de*.

Table 12. Oxazaborolidine-catalyzed reduction of trihalomethyl ketones.

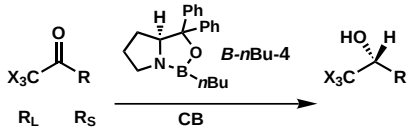

Ketone	*ee* [%]	*T* [°C]
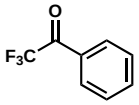	90[47]	– 78
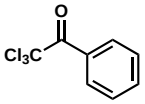	96[22]	– 23
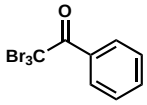	98[22]	– 23
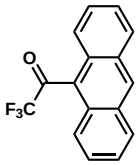	94[47]	– 78
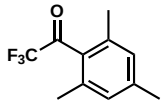	100[55a]	– 78
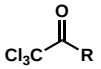	92 – 98 (R = *n*-, *s*-, *t*-alkyl)[75]	– 23 bis – 78

in a large number of applications of the CBS reduction to asymmetric synthesis. These applications include the preparation of 1) chiral ligands for enantioselective synthesis, 2) highly useful chiral intermediates, 3) synthetic bioactive compounds, and 4) natural products.

6.1. Preparation of Enantiopure Ligands for Asymmetric Synthesis

The CBS reduction of 1-mesityl trifluoromethyl ketone provided the corresponding (*R*)-alcohol with greater than 99.8% *ee* (Scheme 8).[55a] This product served as a useful chiral controller in Lewis acid catalyzed Diels – Alder reactions. The corresponding acrylate and fumarate esters react with cyclopentadiene to form Diels – Alder adducts with excellent diastereoselectivity.[76]

The Sharpless asymmetric dihydroxylation (AD) of olefins is broadly useful in organic synthesis. To increase the scope of this reaction, the DHQD-PYDZ-(*S*)-anthryl ligand (designed under guidance from the dihydroxylation mechanism) was prepared from enantioenriched *tert*-butyl anthryl alcohol (Scheme 9).[77] This catalyst has a deep binding pocket that can accommodate olefinic substrates with remote binding

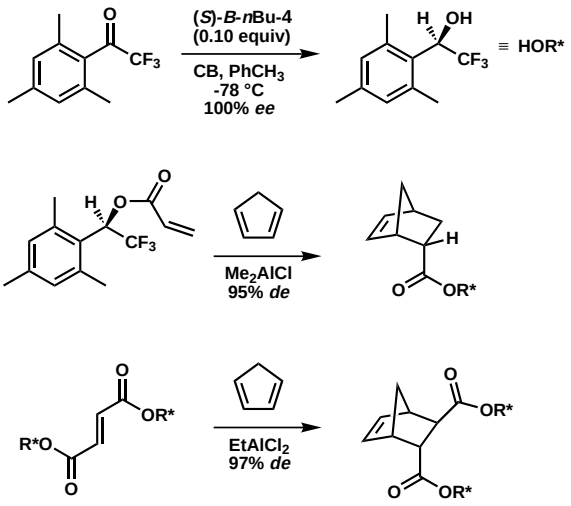

Scheme 8. Synthesis of (*R*)-(–)-mesityl-2,2,2-trifluoroethanol, an outstanding chiral auxiliary for the Lewis acid catalyzed Diels – Alder reaction.

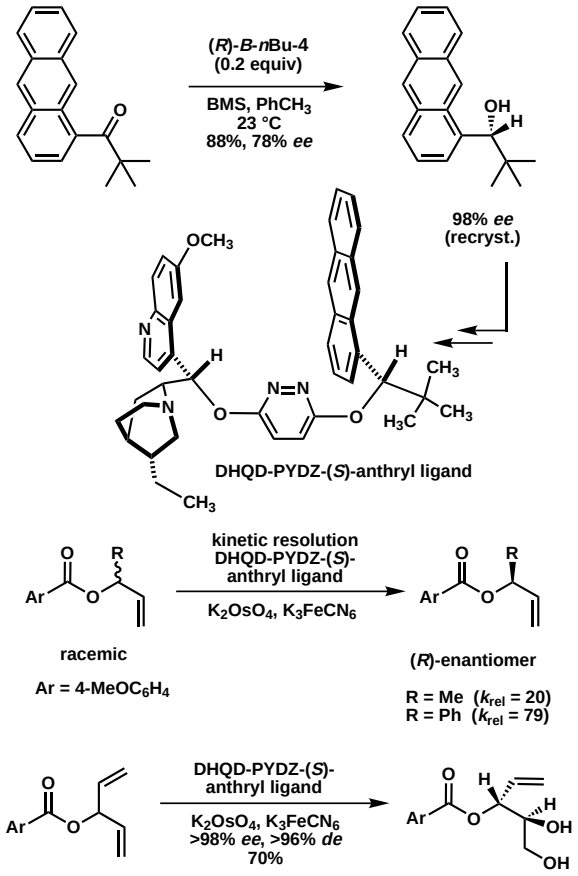

Scheme 9. Highly selective kinetic resolution of allyl alcohol derivatives with a catalyst for asymmetric dihydroxylation.

groups, such as allyl 4-methoxybenzoates.[78] It is highly effective for kinetic resolution of racemic allyl 4-methoxybenzoate (Scheme 9).

Chiral 1,2-diols have been extensively utilized as ligands and chiral controllers for the asymmetric preparation of C – X and C – C stereocenters. The CBS reduction of 1,2-diketones, in particular benzil derivatives and heterocyclic analogues, with $BH_3 \cdot Me_2S$ in the presence of (*S*)-*B*-H-**4** furnishes

the optically active (*S*,*S*)-hydrobenzoins with outstanding enantiomeric excess and good diastereomeric excess (Scheme 10).[79]

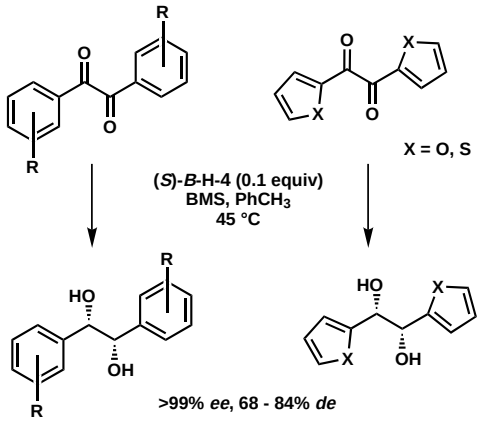

Scheme 10. Enantioselective reduction of 1,2-diketones to valuable chiral 1,2-diols.

The oxazaborolidine-catalyzed reduction of ferrocenyl ketones, F_CCOR, proceeds with excellent enantioselectivity (>95% *ee*, Scheme 11 and Table 11).[76] The resultant optically active ferrocenyl carbinols can be converted into chiral ferrocenylamines with complete retention of configuration. This affords useful chiral bases for asymmetric deprotonation or chiral ligands for transition metal catalyzed reactions.

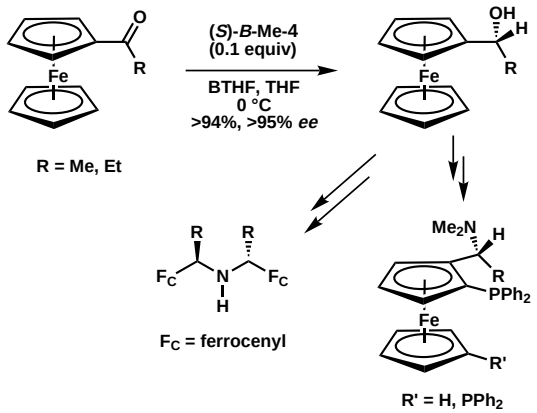

Scheme 11. CBS reduction of acylferrocenes to useful chiral ligands.

The asymmetric reduction of 1,2-bis(ferrocenoyl)ethane occurs with high enantioselectivity (>98% *ee*) and diastereoselectivity (74% *de*) to form a diol which was converted into a chiral C_2-symmetric pyrrolidine. This is a useful chiral auxiliary for diastereoselective alkylation (Scheme 12).[73c]

(*R*)-2,2-Diphenylcyclopentanol was obtained by oxazaborolidine-catalyzed reduction (92% *ee*) and converted into vinyl ethers for Lewis acid promoted [4+2] cycloaddition with 2-substituted 1-nitroalkenes. Hydrogenation of the resulting cycloadducts affords a route to chiral 3,4-disubstituted pyrrolidines (Scheme 13).[69a, 80]

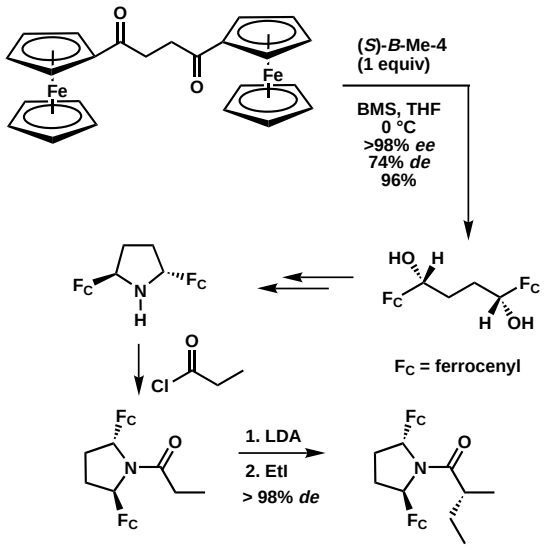

Scheme 12. A C_2-symmetric ferrocenylpyrrolidine is an effective chiral auxiliary.

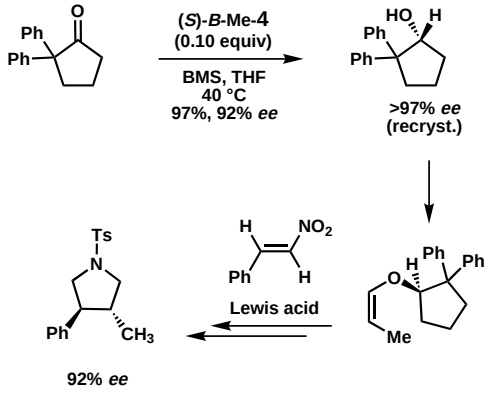

Scheme 13. Preparation of a useful auxiliary for nitroalkene–vinyl ether cycloadditions.

6.2. Preparation of Useful Chiral Building Blocks

Enantiopure amino alcohols are of interest because of their biological activity and value as chiral ligands in metal-catalyzed organic reactions. The catalytic oxazaborolidine-mediated reduction of α-keto oximes results in reduction of C=O followed by C=N to give primarily the *cis*-amino alcohol (Scheme 14).[81]

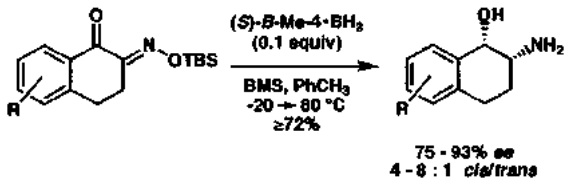

Scheme 14. One-step synthesis of optically active *cis*-amino alcohols.

In a particularly striking example of the broad applicability of the CBS methodology, the enantioselective reduction of axially prostereogenic biaryl lactones affords one atropisomer

in a ratio of 97:3 or higher (Scheme 15).[82] It was proposed that the product-determining step is the selective reduction of an equilibrating mixture of enantiomeric hydroxy aldehydes.

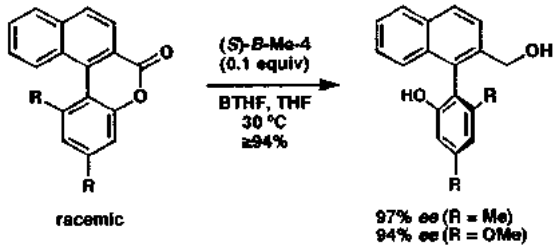

Scheme 15. Selective ring opening to an atropisomer of axially chiral biaryl compounds.

The chiral stannylated allyl alcohol shown in Scheme 16 was readily obtained by CBS reduction and transformed into a chiral allene by fluoride-catalyzed elimination.[62a]

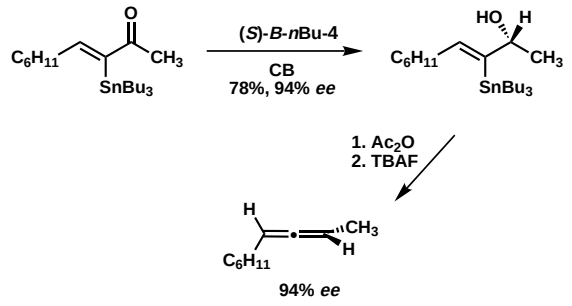

Scheme 16. A different route to optically active allenes.

Whereas chiral C–O stereocenters can be readily accessed by oxazaborolidine-catalyzed reduction of ketones, the asymmetric reductions of other heteroatom–carbon double bonds are not as efficient. To overcome these limitations, the displacement of the hydroxyl group of chiral secondary alcohols from the CBS reduction with either nitrogen or sulfur nucleophiles under Mitsunobu-type conditions has been investigated and found to occur by S_N2 inversion; this yields optically active nitrogen[54, 83] and sulfur compounds[86] (Scheme 17). These results are especially noteworthy considering the tendency of benzyl substrates to undergo S_N1 displacement with loss of configuration.

The dithiane protecting group for ketones has been utilized as a steric control element in the CBS reduction to differentiate the carbonyl oxygen electron lone pairs (Scheme 18).[85] The reductions were highly enantioselective for both acyclic and cyclic compounds. Subsequent desulfurization (with Raney Ni) gave aliphatic carbinols, whereas hydrolysis gave α-hydroxy ketones.

The desymmetrization of a *meso*-imide by the selective reaction of one of the two prochiral carbonyl groups is extremely powerful as three new chiral centers result. As shown in Scheme 19, oxazaborolidine-catalyzed reduction accomplishes this transformation with good enantiomeric excess (90% *ee*). This provides a route to enantioenriched starting materials for *N*-acyliminium ion chemistry.[86]

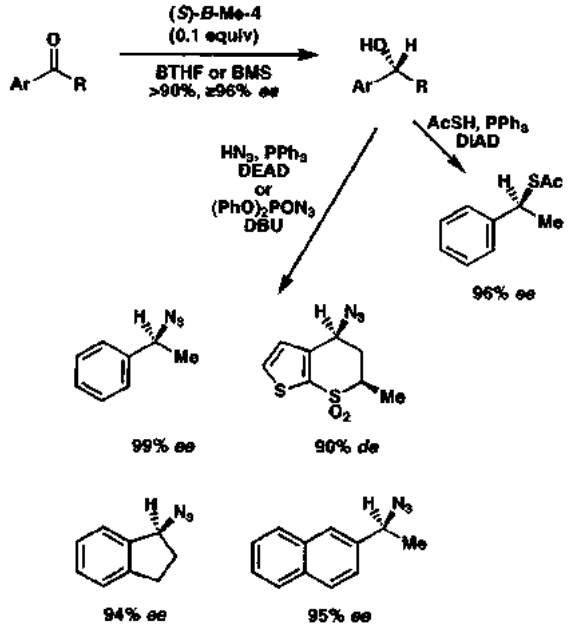

Scheme 17. The Mitsunobu route to chiral nitrogen and sulfur compounds.

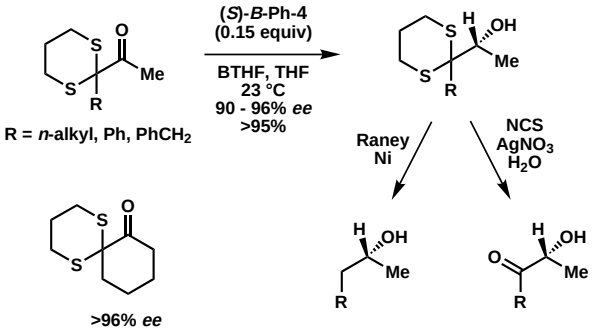

Scheme 18. Dithiane as the large group R_L in the CBS reduction.

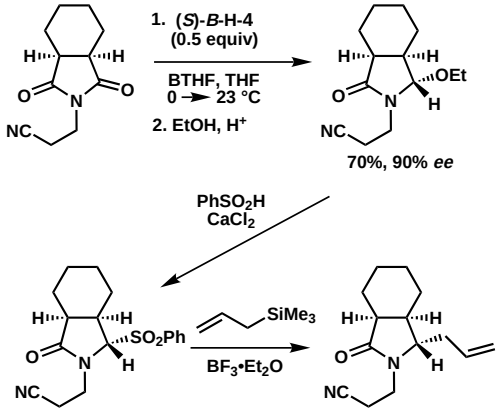

Scheme 19. CBS reduction of *meso*-imides yields chiral pyrrolidinones.

Trichloromethyl carbinols, which are available with very high levels of enantioselectivity by the asymmetric reduction of achiral trichloromethyl ketones,[87] are readily converted into α-amino,[75] α-hydroxy,[88] and α-fluoro acids[89] under basic conditions via a highly reactive 1,1-dichloro epoxide (Scheme 20). The selective dechlorination of trichloromethyl carbinols to chlorohydrins followed by ring closure provides a straightforward route to optically active terminal oxiranes.[90]

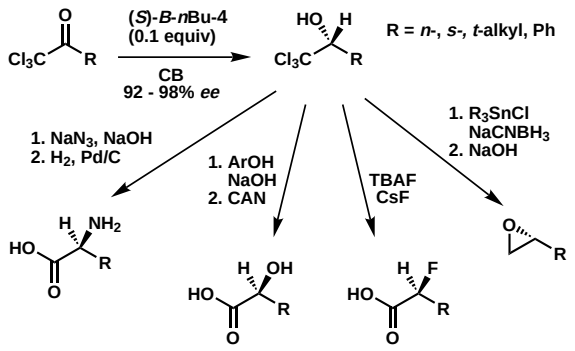

Scheme 20. Trichloromethyl alcohols give access to many useful chiral intermediates.

6.3. Synthesis of Bioactive Compounds

Many β-agonists, which are useful in the treatment of asthma and bronchitis, are currently sold as racemates despite the demonstration of enhanced efficacy of the *R* isomers. The oxazaborolidine-catalyzed reduction of α-haloacetophenones has permitted the highly efficient preparation of a number of β-agonists in enantiomerically pure form by amination of the corresponding optically active styrene oxide or O-silyl halohydrin (Scheme 21).[91]

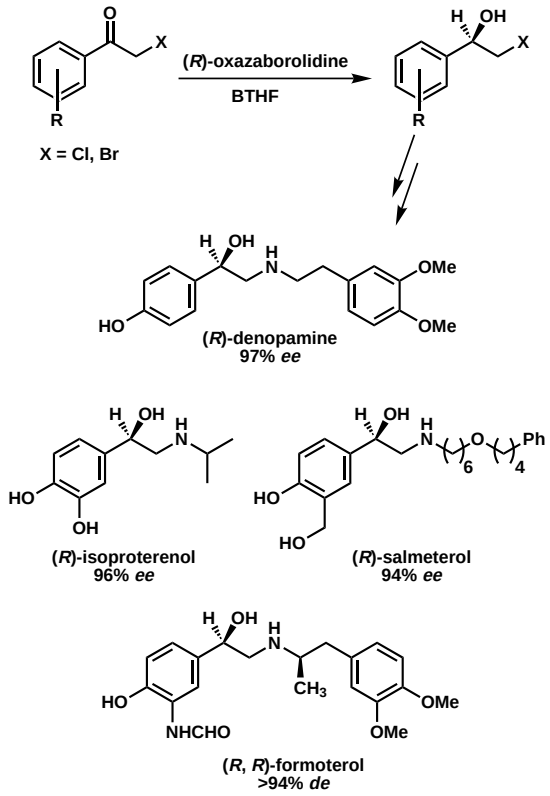

Scheme 21. Enantioselective synthesis of β-agonists.

The commercial histamine antagonist carbinoxamine has been prepared as essentially a single enantiomer (98 % *ee*); the key steps are a CBS reduction of *N*-allyl-2-(4-chlorobenzoyl)pyridinium triflate followed by in situ deallylation (Scheme 22).[59, 60] The allyl group serves both to prevent coordination of the pyridine nitrogen atom to the stoichiometric reductant catecholborane and/or the oxazaborolidine catalyst, and to provide the necessary steric bias for the selective binding of one of the carbonyl oxygen electron lone pairs to the catalyst.

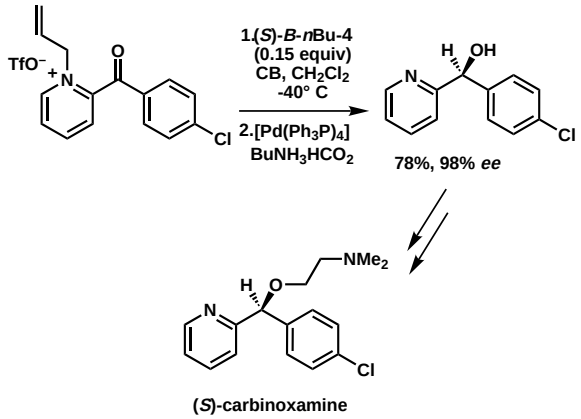

Scheme 22. Enantioselective synthesis of (*S*)-carbinoxamine.

Cetirizine hydrochloride (zyrtec), an antihistamine that is notable for its nonsedating properties and potency, contains an amino-substituted benzhydril stereocenter. This stereocenter has been established by a highly selective CBS reduction of a benzophenone – $Cr(CO)_3$ π complex (Scheme 23).[75] The complexed $Cr(CO)_3$ group behaves as R_L both for steric and electronic reasons, and functions as a controller for the enantiospecific displacement of the hydroxyl group by amine with retention of configuration.

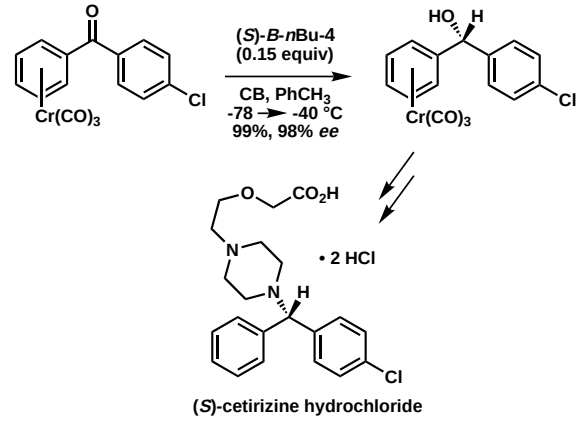

Scheme 23. Enantioselective synthesis of (*S*)-cetirizine hydrochloride.

The antidepressant fluoxetine hydrochloride (prozac, Eli Lilly) has been synthesized in enantiomerically pure form by the oxazaborolidine-catalyzed reduction of β-chloropropiophenone as a key step (Scheme 24).[92] This four-step synthesis proceeds in high overall yield (77 – 82 %) and does not require chromatographic purification.

Chiral *trans*-2,5-diaryltetrahydrofurans, inhibitors of the platelet activating factor, have been prepared by CBS

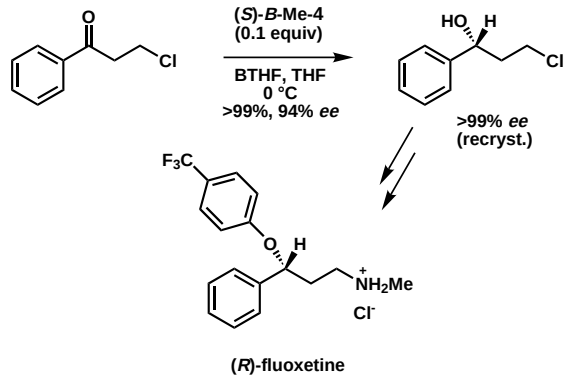

Scheme 24. Enantioselective synthesis of (*R*)-fluoxetine.

reduction of a γ-ketoester followed by lactonization, reduction, and stereoselective arylation (Scheme 25).[93]

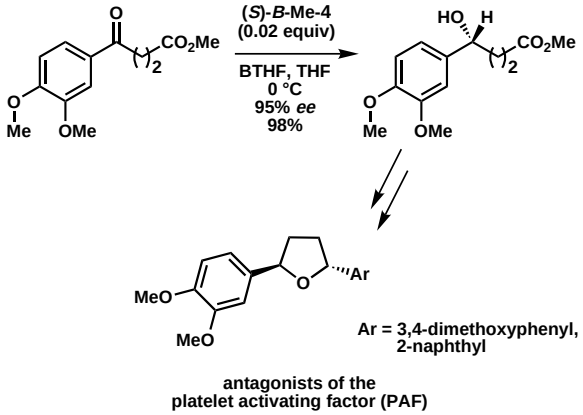

Scheme 25. Enantioselective synthesis of antagonists of the platelet activating factor (PAF).

The chiral thioether L-691,698, an antagonist of leukotriene D_4, has also been synthesized by the oxazaborolidine-catalyzed reduction (Scheme 26).[94]

The carbonic anhydrase inhibitor MK-0417 has been prepared on a large scale by the oxazaborolidine-catalyzed reduction of the heterocyclic ketone shown in Scheme 27.[44b]

The synthesis of the potassium channel blocker MK-0499 utilized a variant of the CBS reduction in which one equivalent of 2-propanol was added prior to $BH_3 \cdot SMe_2$ (Scheme 28).[21] The use of 2-propanol as additive increased the diastereoselectivity from 93 to 98%.

The CBS reduction of the acyclic α,β-enone shown in Scheme 29 proceeded diastereoselectively to form the corresponding allyl alcohol, which was used for the synthesis of an isomer of colletallol.[62d, e]

Oxazaborolidine-catalyzed reduction of the α,β-enone in Scheme 30 to the optically pure allyl alcohol provided the first chiral center in the synthesis of the antiinflammatory and immunosuppressive agent RS-97613.[62f] Subsequent stereoselective orthoester Johnson–Claisen rearrangement, diastereoselective α-methylation, and hydrolysis completed the synthesis of this analogue of mycophenolic acid.

The 3-deoxy-3-thia analogue of vitamin D was synthesized by CBS reduction of the cyclic α,β-enone shown in Scheme 31.

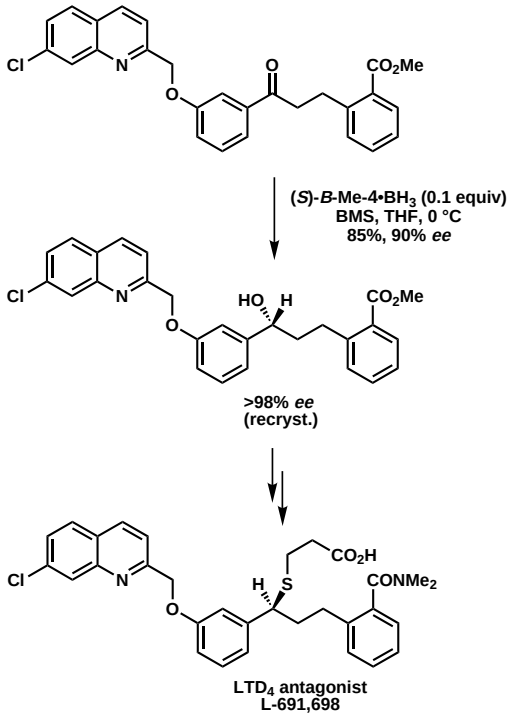

Scheme 26. Enantioselective synthesis of a leukotriene D_4 antagonist.

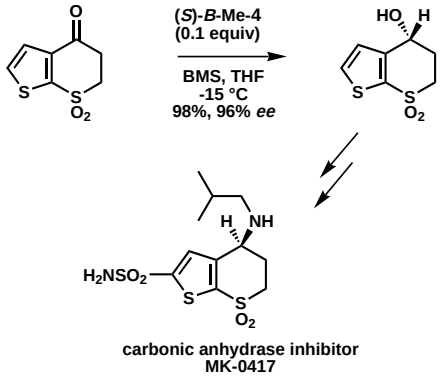

Scheme 27. Enantioselective synthesis of a carbonic anhydrase inhibitor.

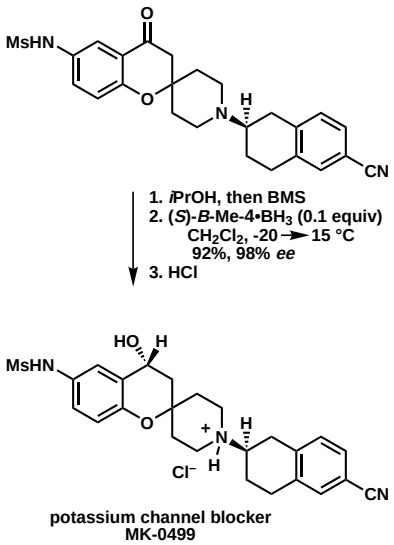

Scheme 28. Enantioselective synthesis of a potassium channel blocker.

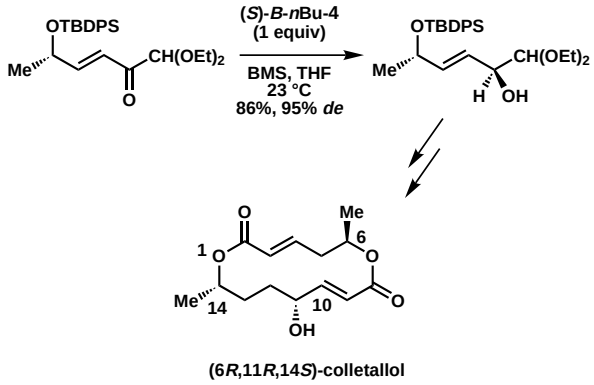

Scheme 29. Asymmetric synthesis of (6*R*,11*R*,14*S*)-colletallol.

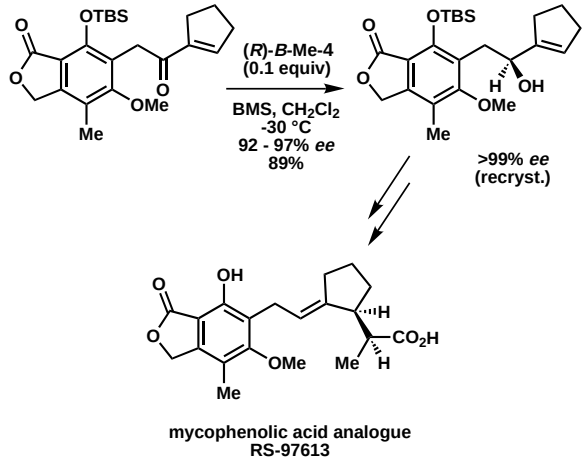

Scheme 30. Enantioselective synthesis of an immunosuppressive and antiinflammatory agent.

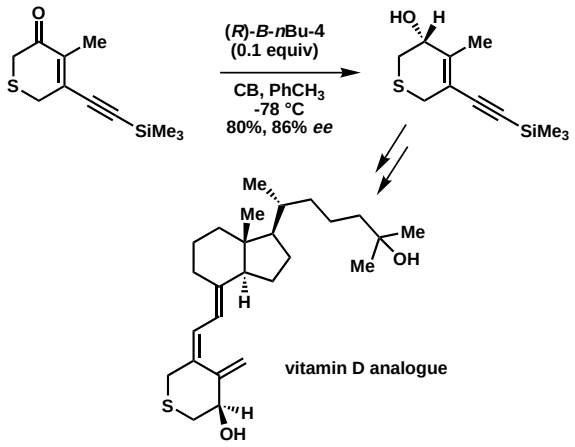

Scheme 31. Asymmetric synthesis of a vitamin D analogue.

This provided a chiral allyl alcohol corresponding to the A ring.[95]

Cicaprost, an orally active, metabolically stable prostaglandin I_2 (PGI_2) analogue, contains a complex side chain which was constructed by oxazaborolidine-catalyzed reduction (Scheme 32).[96] Long-range steric interactions between *n*-butyl group on the boron atom of the catalyst and the triisopropylsilyl group of the ketonic substrate cause ethynyl to behave as the large group R_L. The chirality of the starting ketone does not affect the selectivity of the reduction since

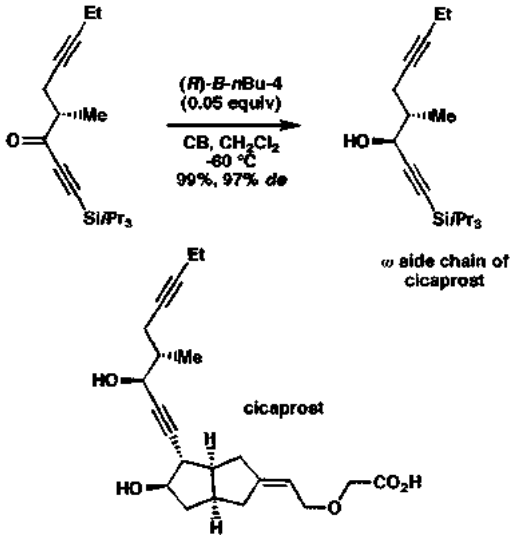

Scheme 32. Asymmetric synthesis of the ω side chain of cicaprost.

the use of the enantiomeric (*S*)-oxazaborolidine catalyst gave the other diastereomer with high diastereomeric excess (96%).

The dopamine D1 agonist A77636 was recently prepared in optically pure form by oxazaborolidine-catalyzed reduction of adamantyl bromomethyl ketone (Scheme 33).[97] Conversion of the chiral bromohydrin into the corresponding epoxide, ring opening with an aryllithium reagent, intramolecular acetal cyclization, and deprotection gave the desired product in very good yield.

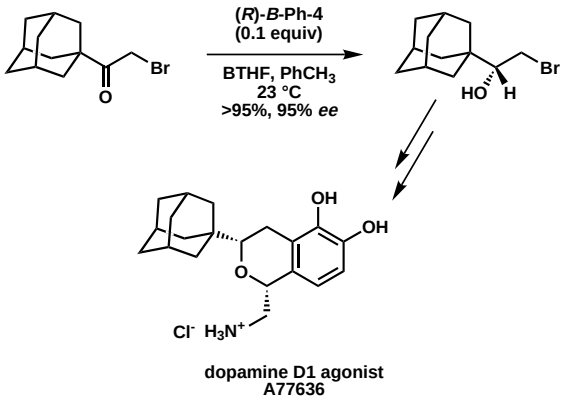

Scheme 33. Asymmetric synthesis of A77636.

6.4. Synthesis of Natural Products

The antiinfective compounds 7,8-dihydroxycalamenene and 7,8-dihydroxy-11,12-didehydrocalamenene were synthesized by CBS reduction of 5,6-dimethoxy-1-tetralone, hydroxyl-directed face-selective complexation of a $Cr(CO)_3$ moiety, and subsequent hydrogenolysis, metalation/alkylation, and decomplexation (Scheme 34).[98]

The tetrahydroisoquinoline (*S*)-salsolidine was prepared efficiently by oxazaborolidine-catalyzed reduction of a substituted acetophenone followed by Mitsunobu displacement

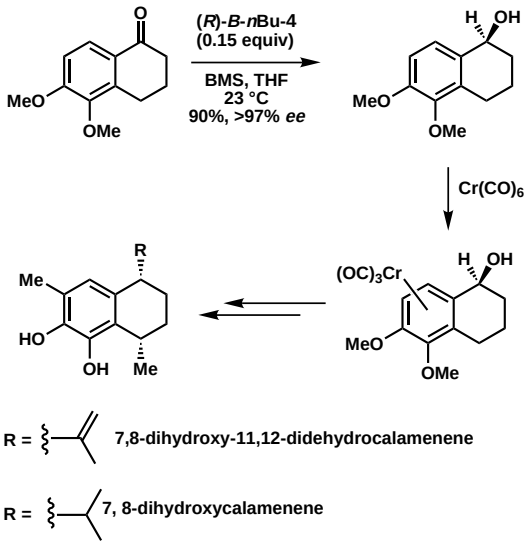

Scheme 34. Enantio- and stereocontrolled synthesis of chiralen antiinfective tetralins.

of the hydroxyl group with a sulfonamide and intramolecular cyclization (Scheme 35).[99] This approach should be applicable to the synthesis of a number of enantiopure tetrahydroisoquinoline derivatives.

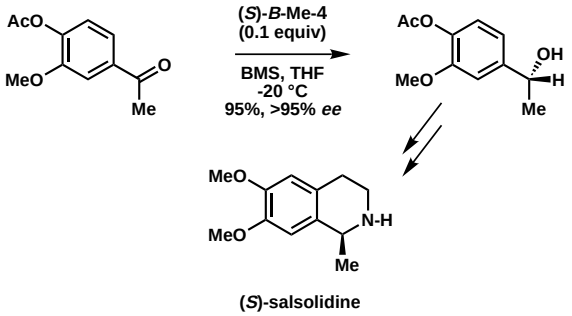

Scheme 35. Enantioselective synthesis of (*S*)-salsolidine.

In a recent total synthesis of the sesterterpene dysidiolide, a marine sponge metabolite that has been shown to exhibit antitumor activity, oxazaborolidine-catalyzed reduction afforded greater than 10:1 selectivity for the required alcohol; the 3-furyl group acted effectively as R_L, and the bicyclic ring system as R_S (Scheme 36).[100] Importantly, this route permitted conversion of the *S* diastereomer into the desired *R* isomer by oxidation and subsequent asymmetric reduction. Mitsunobu displacement of the hydroxyl group of the *S* diastereomer was nonstereoselective.

The fern hormone antheridic acid was initially synthesized in racemic form. An enantioselective synthesis of a key intermediate was achieved by the oxazaborolidine-catalyzed reduction and subsequent conversions depicted in Scheme 37.[63a]

Two different routes to optically active intermediates for the synthesis of forskolin, a potent activator of adenylate cyclase, have been devised utilizing CBS reduction of the dieneones shown in Scheme 38.[101, 102]

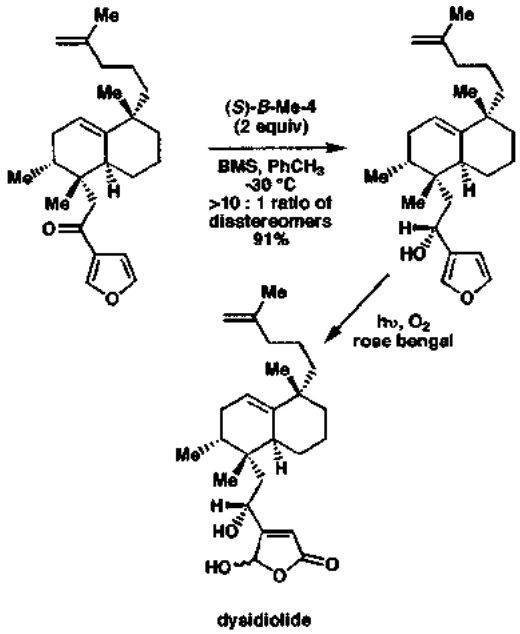

Scheme 36. Enantioselective synthesis of dysidiolide.

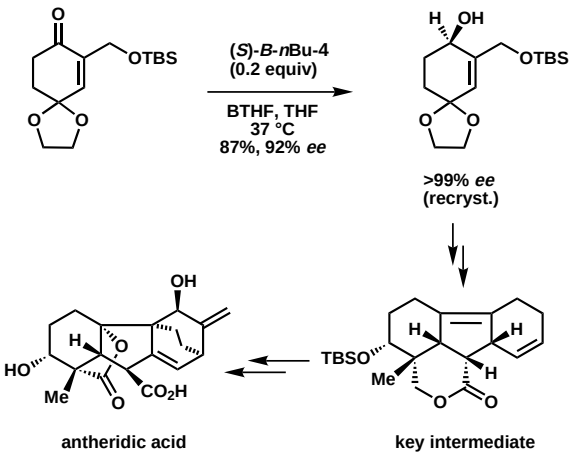

Scheme 37. Enantioselective synthesis of antheridic acid.

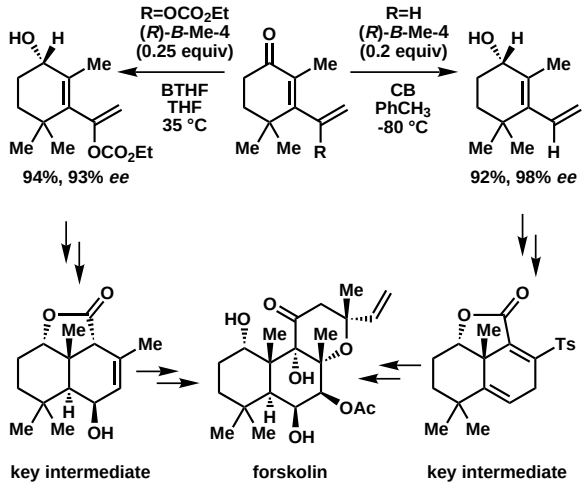

Scheme 38. Enantioselective synthesis of forskolin.

Ginkgolide B, a potent antagonist of the platelet activating factor, has been synthesized enantioselectively by CBS reduction of a α-functionalized cyclopentenone to introduce chirality (Scheme 39).[63b] The resulting optically active allyl

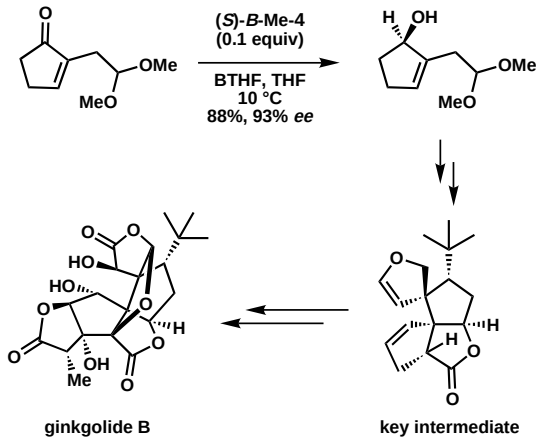

Scheme 39. Enantioselective synthesis of ginkgolide B.

alcohol was then elaborated in a stereocontrolled fashion via a tetracyclic lactone to ginkgolide B. The CBS reduction of 2-bromo-2-cyclopentenone served as a key step in the synthesis of a truncated analogue of ginkgolide B (Scheme 40).[64b]

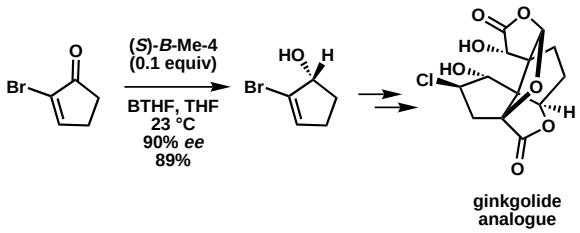

Scheme 40. Enantioselective synthesis of a ginkgolide analogue.

An asymmetric synthesis of bilobalide, an unusual substance produced by the gingko tree *Ginkgo biloba*, has been carried out starting from the bicyclic enone depicted in Scheme 41.[103] Attempts to reduce this chiral ketone to the α-

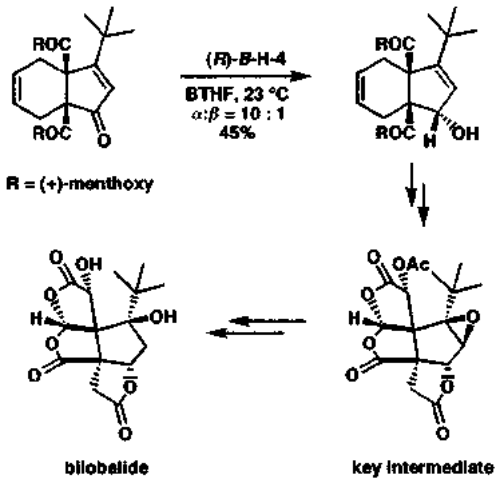

Scheme 41. Enantioselective synthesis of bilobalide.

epimer with a number of reagents ($NaBH_4$, $Zn(BH_4)_2$, SmI_2 in THF/MeOH, $BH_3 \cdot THF$, Na powder in 2-propanol/toluene) gave unsatisfactory results. The oxazaborolidine-mediated reduction of this substrate, however, provided greater than 10:1 selectivity for the α-epimer, which was then transformed into bilobalide via the tetracyclic trilactone shown.

The important fragrance (*S*)-α-damascone could be prepared by a sequence involving CBS reduction of the cyclic α-methyl-α,β-enone shown in Scheme 42, transfer of chirality from C–O to C–C by the Still variant of the [2,3] Wittig rearrangement to set the tertiary chiral center, oxidation, and introduction of the side chain.[104]

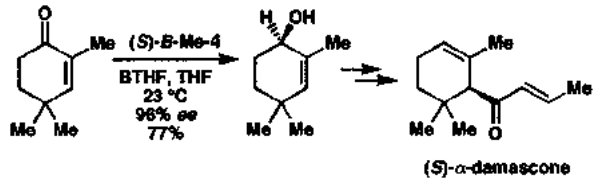

Scheme 42. Enantioselective synthesis of (*S*)-α-damascone.

A recent elegant synthesis of (−)-morphine also employed a highly enantioselective CBS reduction (Scheme 43).[105] Stereospecific conversion of the hydroxyl group into dimethylphenylsilyl and the terminal vinyl moiety into an amino

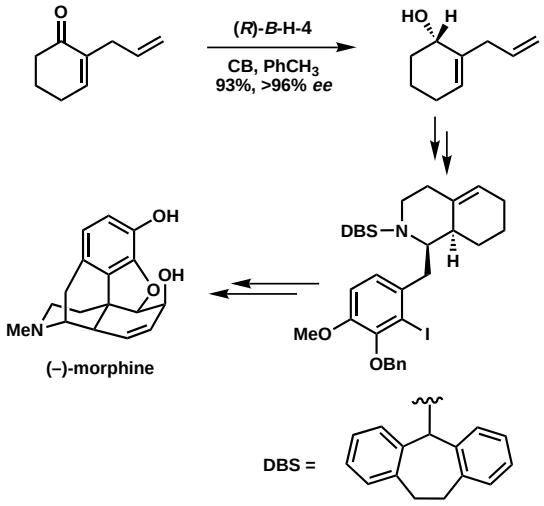

Scheme 43. Enantioselective synthesis of (−)-morphine.

substituent (*N*-DBS) set the stage for an intramolecular iminium ion – allylsilane cyclization to give the bicyclic system shown in Scheme 43. The bridgehead ring system was established by an intramolecular Heck reaction.

In the synthesis of the powerful immunosupressive agent (−)-rapamycin, oxazaborolidine-catalyzed reduction of 2-bromo-2-cyclohexen-1-one was used to generate the functionalized cyclohexyl subunit (Scheme 44).[64a, 106]

Two conceptually similar routes to the A ring of taxol have been developed by CBS reduction of functionalized cyclohexenones (Scheme 45).[107]

While many conjugated cyclic α,β-enones with *endocyclic* (*s-trans*) unsaturation have been reduced to allyl alcohols in

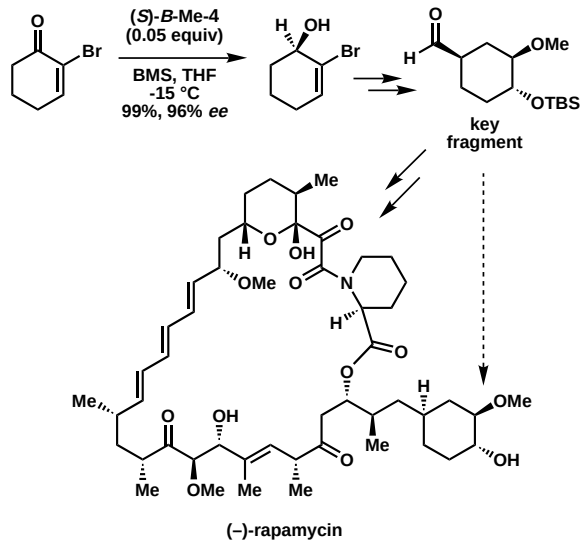

Scheme 44. Asymmetric synthesis of the cyclohexyl moiety of (−)-rapamycin.

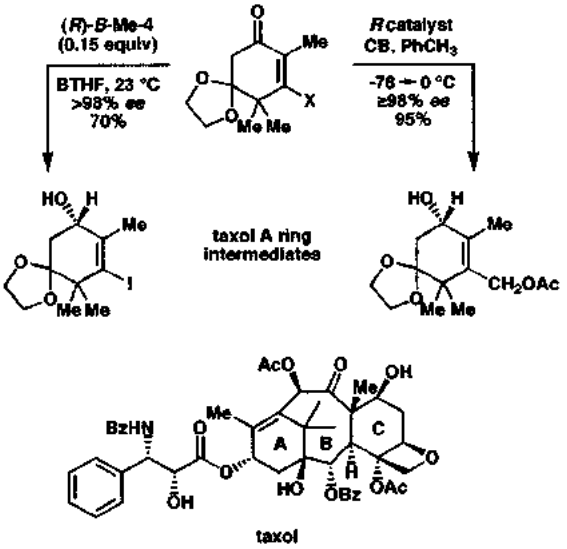

Scheme 45. Enantioselective synthesis of taxol A ring intermediates.

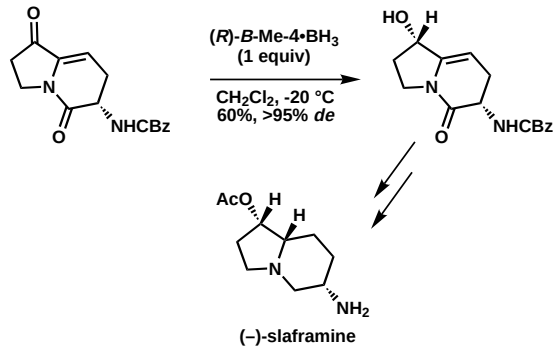

Scheme 46. Asymmetric synthesis of (−)-slaframine.

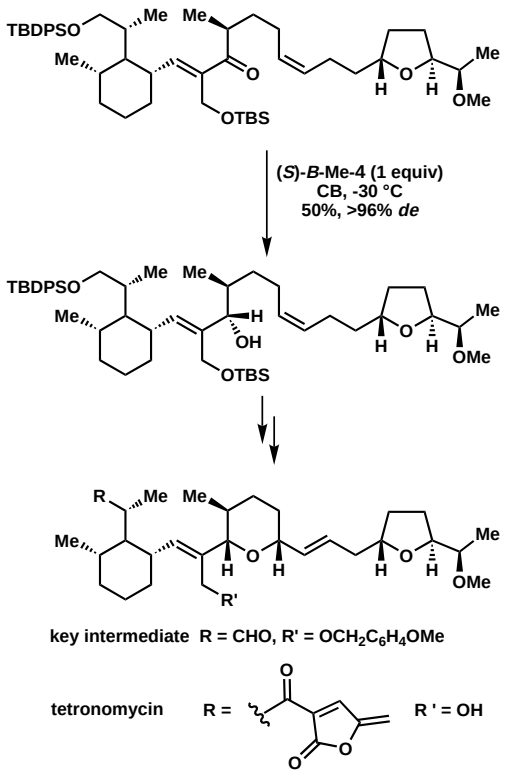

Scheme 47. Diastereoselective CBS reduction of a chiral ketone on the way to tetronomycin.

the presence of chiral oxazaborolidines, the reduction of such compounds with *exocyclic* (*s-cis*) double bonds has been reported only recently in connection with the synthesis of the alkaloid (−)-slaframine.[108] The chiral α,β-enone shown in Scheme 46 was reduced with one equivalent of the (*R*)-*B*-Me-**4**$\cdot BH_3$ complex (*B*-Me-**5**) to provide the required allyl alcohol with excellent diastereomeric purity. In contrast, the use of the enantiomeric oxazaborolidine–BH_3 complex afforded the other diastereomer with high selectivity.

An approach to the synthesis of the ionophore antibiotic tetronomycin utilized the CBS reduction outlined in Scheme 47[109] (>96% *de*) followed by an intramolecular Pd^{II}-mediated cyclization to establish the central *cis*-substituted tetrahydropyran ring. Attempts to prepare the same allyl alcohol by addition of vinyllithium to an aldehyde yielded a 1:2 ratio of desired to undesired diastereomeric alcohols.

The naturally occurring adenosine diphosphate transport inhibitor atractilygenin was originally synthesized as the racemate; the first key chiral intermediate in the enantioselective CBS reduction is the substituted 1,3-cyclohexadiene shown in Scheme 48.[61] The use of the β-trialkylstannyl substituent on the enone to provide temporary steric bulk and the CH_2SiMe_3 group on the boron atom of the catalyst to maximize long-range steric interactions were crucial for high enantioselectivity in the oxazaborolidine-catalyzed reduction. Subsequent steps including a Claisen rearrangement effected the transfer of chirality from C–O to C–C to form the quaternary carbon stereocenter of the key intermediate.

A recent study on the synthesis of heteroyohimbine alkaloids utilized a CBS reduction of the acyclic α,β-enone shown in Scheme 49 to the allyl alcohol; the *B*-*n*Bu-oxazaborolidine catalyst (93% *ee*) was superior to the *B*-Me-oxazaborolidine catalyst (81% *ee*).[110] Orthoester Johnson–

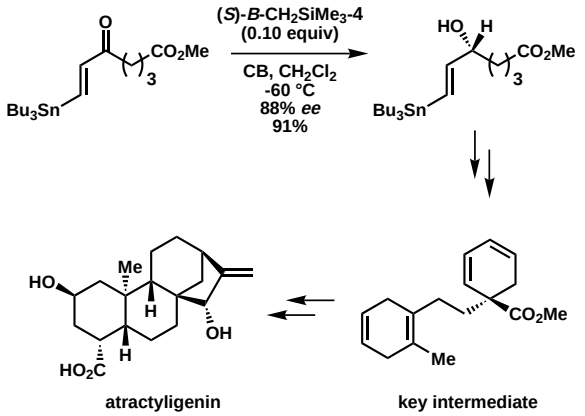

Scheme 48. Enantioselective synthesis of atractyligenin.

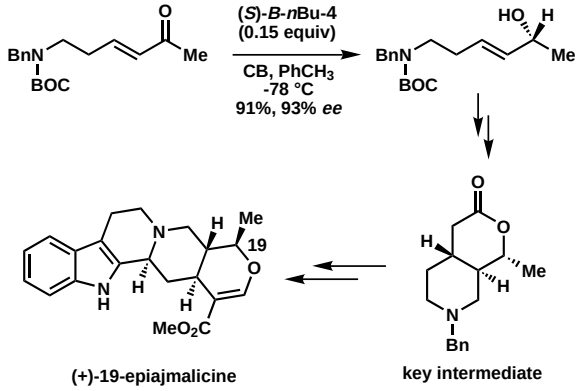

Scheme 49. Asymmetric synthesis of a key intermediate on the way to (+)-19-epiajmalicine.

Claisen rearrangement and iminium ion biscyclization provided the bicyclic amino lactone.

The relative and absolute configurations of the marine alkaloid hennoxazole A, which actively inhibits the herpes simplex virus, were unambiguously determined by enantioselective total synthesis. CBS reduction of the *cis*-β-stannylenone as depicted in Scheme 50 followed by hydroxyl activation and stereospecific displacement with a propenyl cuprate gave the indicated chiral 1,4-diene fragment.[62b, c] Transmetalation of this key coupling fragment from the tin to the zinc derivative facilitated a palladium-mediated coupling with an allyl bromide to afford the carbon framework of the natural product.

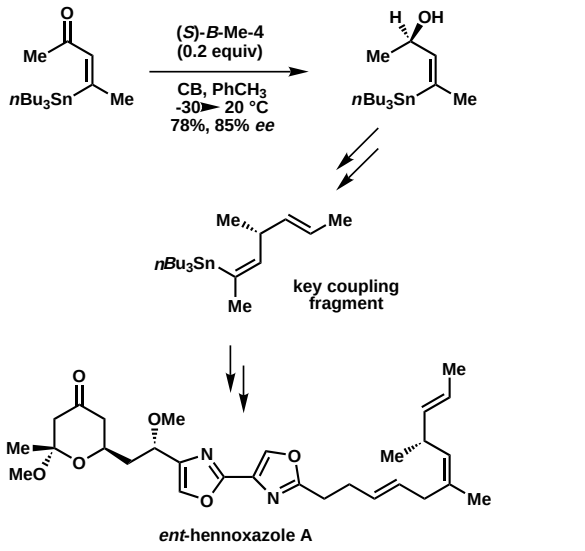

Scheme 50. Enantioselective synthesis of *ent*-hennoxazole A.

A long-standing challenge in the synthesis of prostanoids has been the selective introduction of the C(15) hydroxyl-bearing stereocenter by reduction of the α,β-enone. While a number of reagents and reaction conditions have been designed to effect this transformation, the CBS reduction provides a pleasing catalytic solution, and furnishes a 10:1 ratio of the diastereomeric alcohols under exceedingly mild conditions (Scheme 51).[13b]

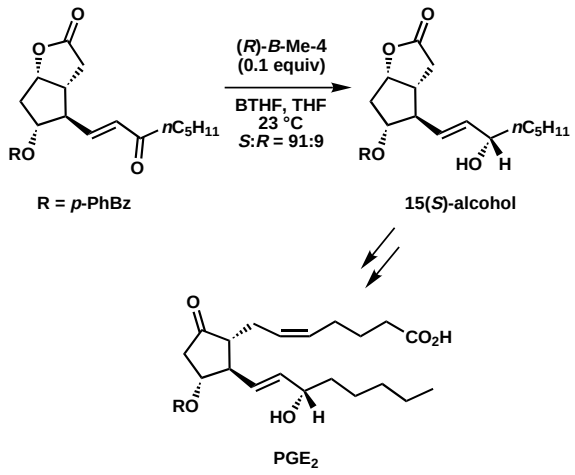

Scheme 51. Asymmetric synthesis of prostaglandins.

The scarce marine natural product (+)-discodermolide has been observed to possess impressive immunosuppressive activity and, as a result, has been the object of total synthesis. Oxazaborolidine-catalyzed reduction of the propargylic ketone shown in Scheme 52 gave a 10:1 mixture of isomers with the desired antipode predominating.[111] The alkynyl group behaved as R_L in this CBS reduction in a nonpolar solvent and with catecholborane as stoichiometric reductant, which is in agreement with other studies (see Table 9).[43]

(3*S*)-2,3-Oxidosqualene is the biosynthetic precursor to numerous steroids and polycyclic triterpenoids. Asymmetric reduction of the α-fluoro ketone shown in Scheme 53 followed by oxirane ring closure gave (3*S*)-2,3-oxidosqualene with 92% *ee*.[42] The choice of α-fluoro ketone was crucial for high enantioselectivity in the reduction, since the use of the α-chloro or β-bromo ketone resulted in slow reaction rates and only modest enantioselectivities. The magnitude and sense of enantioselectivity were highly dependent on temperature: The enantiomeric ratio *S*:*R* is 96:4 at 35 °C, 93:7 at 23 °C, and 20:80 at −23 °C.

In a recent improved synthesis of the right half of halichondrin B, a potent antitumor agent, a Nozaki–Kishi coupling of vinyl iodide with aldehyde afforded a 4:1 ratio of diastereomers favoring the desired alcohol.[112] Dess–Martin oxidation of the mixture of alcohols to the α-substituted α,β-

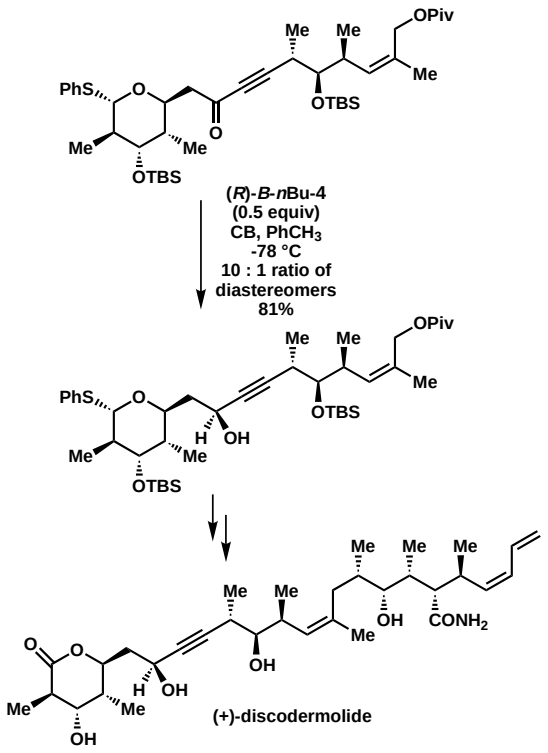

Scheme 52. Enantioselective synthesis of discodermolide.

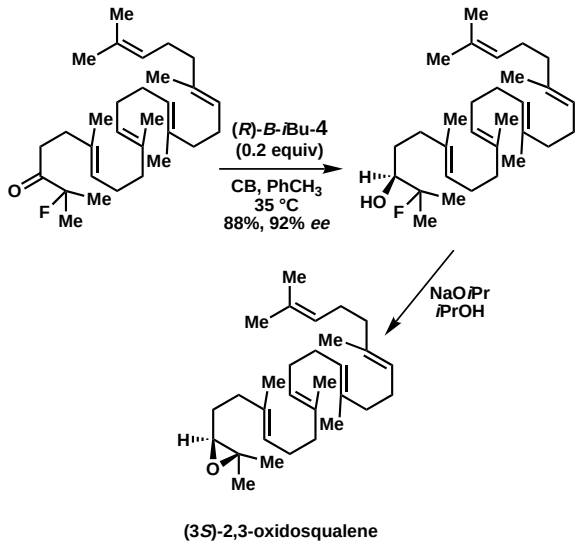

Scheme 53. Enantioselective synthesis of (3*S*)-2,3-oxidosqualene.

enone followed by CBS reduction gave a much improved 17:1 ratio of diastereomers at the carbinol center and permitted the efficient stereoselective construction of the central pyran unit of the right-half diol fragment (Scheme 54).

7. Summary and Outlook

Chiral oxazaborolidine-catalyzed reduction of ketones with coordinated borane or catecholborane as stoichiometric reductant provides access to a broad range of chiral secondary alcohols. These products, in turn, can serve as key intermediates for the synthesis of an enormous range of compounds with regard to functionality, size, and topological complexity. Thus, many types of chiral natural products and bioactive molecules can be synthesized efficiently without the need for optical resolution. The applications of this methodology continue to increase rapidly in number and could become commercially important.

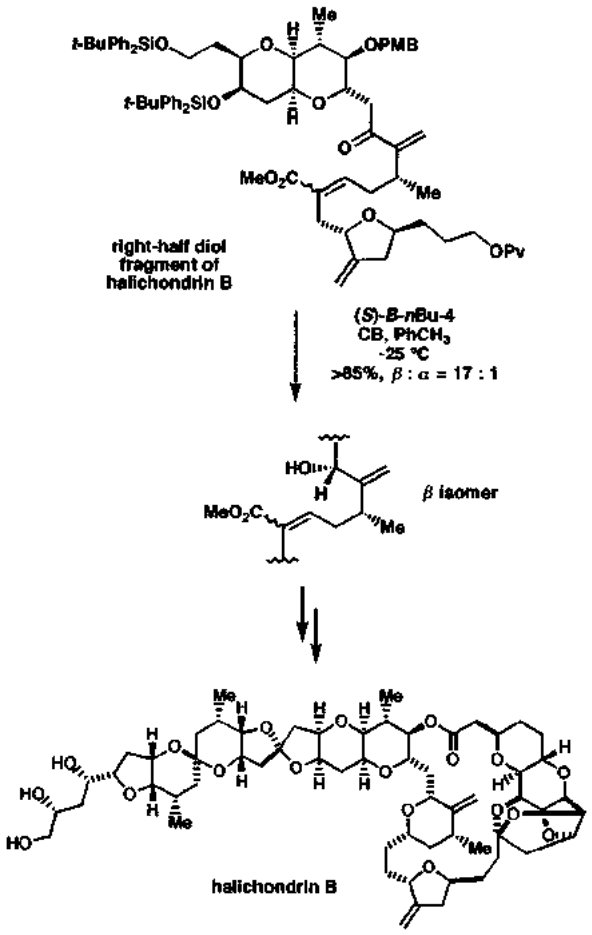

Scheme 54. Asymmetric synthesis of halichondrin B.

Appendix: Abbreviations Used

BDEA = $BH_3 \cdot$ diethylaniline, BMS = $BH_3 \cdot Me_2S$, Bn = benzyl, BOC = *tert*-butoxycarbonyl, BTHF = $BH_3 \cdot$ THF, Bz = benzoyl, CAN = cerammonium nitrate, CB = catecholborane, DBU = 1,8-diazabicyclo[5.4.0]undec-7-ene, DEAD = diethyl azodicarboxylate, DIAD = iiisopropyl azodicarboxylate, Ms = methanesulfonyl, Nap = naphthyl, NCS = *N*-chlorosuccinimide, Piv = pivaloyl, PMB = *p*-methoxybenzyl, TBAF = tetrabutylammonium fluoride, TBDPS = *tert*-butyldiphenylsilyl, TBS = *tert*-butyldimethylsilyl, Tf = trifluoromethylsulfonyl.

We are grateful to the National Institutes of Health and the National Science Foundation for generous financial support.

Received: October 28, 1997 [A258IE]
German version: *Angew. Chem.* **1998**, *110*, 2092 – 2118

[1] General reviews: a) N. G. Gaylord, *Reduction with Complex Metal Hydrides*, Interscience, New York, **1956**; b) *Reduction Techniques and Applications in Organic Synthesis* (Ed.: R. L. Augustine), Marcel Dekker, New York, **1968**; c) A. Hajos, *Complex Hydrides in Organic Synthesis*, Elsevier, New York, **1979**; d) M. Hudlicky, *Reductions in Organic Chemistry*, *Vols. 1 and 2*, Ellis Harwood, Chichester, **1984**.

[2] a) W. G. Brown, *Organic Reactions*, **1951**, *6*, 469 – 509; b) *Encyclopedia of Reagents for Organic Synthesis*, *Vol. 5* (Ed.: L. A. Paquette), Wiley, New York, **1995**, pp. 3009 – 3014.

[3] a) K. N. Semenko, B. M. Bulychev, E. A. Shevlyagina, *Russ. Chem. Rev.* **1966**, *35*, 649 – 658; b) H. C. Brown, S. T. Krishnamurthy, *Tetrahedron* **1979**, *35*, 567 – 607.

[4] a) E. Schenker, *Angew. Chem.* **1961**, *73*, 81 – 106; b) reference [3b].

[5] H. C. Brown, *Boranes in Organic Synthesis*, Cornell University Press, Ithaca, NY, **1972**.

[6] For a brief summary of the uses of such reagents in synthesis, see M. Greeves in *Comprehensive Organic Synthesis*, *Vol. 8* (Ed.: B. M. Trost), Pergamon Press, Oxford, **1991**, pp. 1 – 24.

[7] D. C. Wigfield, *Tetrahedron* **1979**, *35*, 449 – 462.

[8] Reviews: a) E. R. Grandbois, S. I. Howard, J. D. Morrison, *Asymmetric Synthesis*, *Vol. 2*, Academic Press, New York, **1983**, pp. 71 – 90; b) J. W. ApSimon, T. L. Collier, *Tetrahedron* **1986**, *42*, 5157 – 5254; c) H. Haubenstock, *Topics in Stereochemistry*, *Vol. 14* (Eds.: N. L. Allinger, E. L. Eliel, S. H. Wilen), Wiley, New York, **1983**, pp. 231 – 300; d) T. Mukaiyama, M. Asami in *Topics in Current Chemistry*, *Organic Chemistry*, *No. 127* (Ed.: F. L. Boschke), Springer, Berlin, **1985**, pp. 133 – 167.

[9] a) R. Haller, H. J. Schneider, *Chem. Ber.* **1973**, *106*, 1312 – 1318; b) S. Yamaguchi, H. S. Mosher, *J. Org. Chem.* **1973**, *38*, 1870 – 1877; c) R. S. Brinkmeyer, V. M. Kapoor, *J. Am. Chem. Soc.* **1977**, *99*, 8339 – 8341; d) N. Cohen, R. J. Lopresti, C. Neukom, G. Saucy, *J. Org. Chem.* **1980**, *45*, 582 – 588; e) G. M. Giongo, F. Di Gregorio, N. Palladino, W. Marconi, *Tetrahedron Lett.* **1973**, *14*, 3195 – 3198; f) A. I. Meyers, P. M. Kendall, *Tetrahedron Lett.* **1974**, *15*, 1337 – 1340; g) I. Jacquet, J. P. Vigneron, *ibid.* **1974**, *15*, 2065 – 2068; h) J. P. Vigneron, I. Jacquet, *Tetrahedron* **1976**, *32*, 939 – 944; i) J. P. Vigneron, V. Bloy, *Tetrahedron Lett.* **1980**, *21*, 1735 – 1738; j) M. F. Grundon, D. G. McCleery, J. W. Wilson, *ibid.* **1976**, *17*, 295 – 296; k) R. Noyori, I. Tomino, Y. Tanimoto, M. Nishizawa, *J. Am. Chem. Soc.* **1984**, *106*, 6709 – 6716; l) R. Noyori, I. Tomino, M. Yamada, M. Nishizawa, *J. Am. Chem. Soc.* **1984**, *106*, 6717 – 6725; m) M. Asami, H. Ohno, S. Kobayashi, T. Mukaiyama, *Bull. Chem. Soc. Jpn.* **1978**, *51*, 1869 – 1873; n) T. Sato, Y. Goto, T. Fujisawa, *Tetrahedron Lett.* **1982**, *23*, 4111 – 4112; o) T. Sato, Y. Gotoh, Y. Wakabayashi, T. Fujisawa, *ibid.* **1983**, *24*, 4123 – 4126; p) H. Suda, S. Kanoh, N. Umeda, T. Nakajo, M. Motoi, *ibid.* **1983**, *24*, 1513 – 1516; q) M. Kawasaki, Y. Suzuki, S. Terashima, *Chem. Lett.* **1984**, 239 – 242; r) K. Soai, T. Yamanoi, H. Oyamada, *ibid.* **1984**, 251 – 254; s) A. K. Mandal, T. G. Kasar, S. W. Mahajan, D. G. Jawalkar, *Synth. Commun.* **1987**, *17*, 563 – 574.

[10] A. Hirao, S. Itsuno, S. Nakahama, N. Yamazaki, *J. Chem. Soc. Chem. Commun.* **1981**, 315 – 317.

[11] S. Itsuno, A. Hirao, S. Nakahama, N. Yamazaki, *J. Chem. Soc. Perkin Trans. 1* **1983**, 1673 – 1676.

[12] a) S. Itsuno, K. Ito, A. Hirao, S. Nakahama, *J. Chem. Soc. Chem. Commun.* **1983**, 469 – 470; b) S. Itsuno, M. Nakano, K. Miyazaki, H. Masuda, K. Ito, A. Hirao, S. Nakahama, *J. Chem. Soc. Perkin Trans. 1* **1985**, 2039 – 2044.

[13] a) E. J. Corey, R. K. Bakshi, S. Shibata, *J. Am. Chem. Soc.* **1987**, *109*, 5551 – 5553; b) E. J. Corey, R. K. Bakshi, S. Shibata, C.-P. Chen, V. K. Singh, *J. Am. Chem. Soc.* **1987**, *109*, 7925 – 7926; c) E. J. Corey, S. Shibata, R. K. Bakshi, *J. Org. Chem.* **1988**, *53*, 2861 – 2863; d) E. J. Corey, *Pure Appl. Chem.* **1990**, *62*, 1209 – 1216.

[14] For improved preparations of amino alcohol **3**, see a) D. J. Mathre, T. K. Jones, L. C. Xavier, T. J. Blacklock, R. A. Reamer, J. J. Mohan, E. T. Turner Jones, K. Hoogsteen, M. W. Baum, E. J. J. Grabowski, *J. Org. Chem.* **1991**, *56*, 751 – 762; b) J. V. B. Kanth, M. Periasamy, *Tetrahedron* **1993**, *49*, 5127 – 5132; c) for an earlier review of oxazaborolidine-catalyzed reduction of ketones, see V. K. Singh, *Synthesis* **1992**, 605 – 616.

[15] J. O. Link, Ph.D. thesis, Harvard University (USA), **1992**.

[16] Interestingly, the treatment of oxazaborolidine **2** with $BH_3 \cdot THF$ under the same conditions reveals only a small proportion of the $BH_3 \cdot$ **2** complex relative to free **2**.[13a]

[17] a) E. J. Corey, M. Azimioara, S. Sarshar, *Tetrahedron Lett.* **1992**, *33*, 3429 – 3430. Researchers at Merck have used *B*-Me-**5** as a stoichiometric reagent and as a catalyst with stoichiometric amounts of $BH_3 \cdot Me_2S$ to effect the enantioselective reduction of ketones: b) D. J. Mathre, A. S. Thompson, A. W. Douglas, K. Hoogsteen, J. D. Carroll, E. G. Corley, E. J. J. Grabowski, *J. Org. Chem.* **1993**, *58*, 2880 – 2888.

[18] It has not been proven if the hydride transfer occurs via a boat or a chair transition state. Both conformations, however, are consistent with the mechanistic model in Scheme 5: a) D. A. Evans, *Science* **1988**, *240*, 420 – 426; for computational studies, see b) D. K. Jones, D. C. Liotta, I. Shinkai, D. J. Mathre, *J. Org. Chem.* **1993**, *58*, 799 – 801; c) L. P. Linney, C. R. Self, I. H. Williams, *J. Chem. Soc. Chem. Commun.* **1994**, 1651 – 1652; for computational studies concerning different oxazaborolidines, see d) G. J. Quallich, J. F. Blake, T. M. Woodall, *J. Am. Chem. Soc.* **1994**, *116*, 8516 – 8525.

[19] For the initial report proposing the direct conversion of **7** into **5**, see a) reference [13a]; for computational studies, see b) V. Nevalainen, *Tetrahedron: Asymmetry* **1994**, *5*, 289 – 296; c) reference [18c].

[20] A recent low-temperature NMR study was inconclusive in determining the detailed mechanism by which **7** is recycled to the active catalytic species: A. W. Douglas, D. M. Tschaen, R. A. Reamer, Y.-J. Shi, *Tetrahedron: Asymmetry* **1996**, *7*, 1303 – 1308.

[21] For studies detailing the role of the borinate **8** in effecting product enantioselectivity, see a) D. M. Tschaen, L. Abramson, D. Cai, R. Desmond, U.-H. Dolling, L. Frey, S. Karady, Y.-J. Shi, T. R. Verhoeven, *J. Org. Chem.* **1995**, *60*, 4324 – 4330; b) Y.-J. Shi, D. Cai, U.-H. Dolling, A. W. Douglas, D. M. Tschaen, T. R. Verhoeven, *Tetrahedron Lett.* **1994**, *35*, 6409 – 6412.

[22] a) E. J. Corey, J. O. Link, R. K. Bakshi, *Tetrahedron Lett.* **1992**, *33*, 7107 – 7110. b) If ketone complexation was the rate-limiting step, then the relative rates of reduction should have been *p*-MeO > *p*-H > *p*-NO_2; if hydride transfer was the rate-limiting step, then the relative rates should have been *p*-NO_2 > *p*-H > *p*-MeO.

[23] The calculated kinetic isotope effect for the direct reduction of 2-propanone with $BH_3 \cdot THF$ was 1.3.[18c]

[24] J. G. H. Willems, F. J. Dommerholt, J. B. Hammink, A. M. Vaarhorst, L. Thijs, B. Zwaneburg, *Tetrahedron Lett.* **1995**, *36*, 603 – 606.

[25] R = H: a) A. V. Rama Rao, M. K. Gurjar, V. Kaiwar, *Tetrahedron: Asymmetry* **1992**, *3*, 859 – 862; b) W. Behnen, C. Dauelsberg, S. Wallbaum, J. Martens, *Synth. Commun.* **1992**, *22*, 2143 – 2153; R = Me: c) E. J. Corey, V. K. Singh, unpublished results.

[26] E. J. Corey, C.-P. Chen, G. A. Reichard, *Tetrahedron Lett.* **1989**, *30*, 5547 – 5550.

[27] A. V. Rama Rao, M. K. Gurjar, P. A. Sharma, V. Kaiwar, *Tetrahedron Lett.* **1990**, *31*, 2341 – 2344.

[28] R = H: a) Y. H. Kim, D. H. Park, I. S. Byun, I. K. Yoon, C. S. Park, *J. Org. Chem.* **1993**, *58*, 4511 – 4512; b) J. Martens, C. Dauelsberg, W. Behnen, S. Wallbaum, *Tetrahedron: Asymmetry* **1992**, *3*, 347 – 350. R = Me: c) reference [25c].

[29] a) Y. Hong, Y. Gao, X. Nie, C. M. Zepp, *Tetrahedron Lett.* **1994**, *35*, 6631 – 6634; b) B. Di Simone, D. Savoia, E. Tagliavini, A. Umani-Ronchi, *Tetrahedron: Asymmetry* **1995**, *6*, 301 – 306; c) C. M. Bellucci, A. Bergamini, P. G. Cozzi, A. Papa, E. Tagliavini, A. Umani-Ronchi, *Tetrahedron: Asymmetry* **1997**, *8*, 895 – 902.

[30] M. Masui, T. Shioiri, *Synlett* **1996**, 49 – 50.

[31] E. J. Corey, J. O. Link, *Tetrahedron Lett.* **1989**, *30*, 6275 – 6278.

[32] E. J. Corey, S. Shibata, unpublished results.

[33] A. S. Demir, E. Mecitoglu, C. Tanyeli, V. Gülbeyaz, *Tetrahedron: Asymmetry* **1996**, *7*, 3359 – 3364.

[34] The spectral characterization of the spiro-2-indanyl catalyst (entry 10) has not been published.[33]

[35] E. J. Corey, J. O. Link, unpublished results.

[36] Heating a mixture of (*S*)-prolinol (R′ = H) and $BH_3 \cdot THF$ in toluene at reflux effected the enantiocontrolled reduction of acetophenone in moderate yield (95% *ee*, *R* isomer, 59% yield). The exact nature of the reducing agent as well as the precise mode of reduction under these conditions is not clear, however, as the treatment of (*S*)-prolinol with $BH_3 \cdot THF$ results in the formation of dimeric species: a) J. M. Brunel, M. Maffei, G. Buono, *Tetrahedron: Asymmetry* **1993**, *4*, 2255 – 2260; b) A. Lang, H. Nöth, M. Schmidt, *Chem. Ber.* **1997**, *130*, 241 – 246.

[37] Upon treatment with $BH_3 \cdot Me_2S$, the allyl group (entry 7) undergoes hydroboration to afford a novel internally bound reducing agent: R.

Berenguer, J. Garcia, J. Vilarrasa, *Tetrahedron: Asymmetry* **1994**, *5*, 165 – 168.
[38] E. J. Corey, J. O. Link, *Tetrahedron Lett.* **1992**, *33*, 4141 – 4144.
[39] E. J. Corey, J. O. Link, *Tetrahedron Lett.* **1990**, *31*, 601 – 604.
[40] E. J. Corey, R. K. Bakshi, S. Shibata, unpublished results.
[41] E. J. Corey, C.-P. Chen, R. K. Bakshi, S. Shibata, unpublished results.
[42] E. J. Corey, K. Y. Yi, S. P. T. Matsuda, *Tetrahedron Lett.* **1992**, *33*, 2319 – 2322.
[43] C. J. Helal, P. A. Magriotis, E. J. Corey, *J. Am. Chem. Soc.* **1996**, *118*, 10938 – 10939.
[44] a) E. J. Corey, C. J. Helal, unpublished results; b) a number of oxazaborolidine catalysts with *p*-substituted aryl groups on the boron atom of the catalyst have been prepared: T. K. Jones, J. J. Mohan, L. C. Xavier, T. J. Blacklock, D. J. Mathre, P. Sohar, E. T. Turner Jones, R. A. Reamer, F. E. Roberts, E. J. J. Grabowski, *J. Org. Chem.* **1991**, *56*, 763 – 769.
[45] G. B. Stone, *Tetrahedron: Asymmetry* **1994**, *5*, 465 – 472.
[46] A. M. Salunkhe, E. R. Burkhardt, *Tetrahedron Lett.* **1997**, *38*, 1523 – 1526.
[47] E. J. Corey, R. K. Bakshi, *Tetrahedron Lett.* **1990**, *31*, 611 – 614.
[48] For a recent in situ preparation of catecholborane, see Y. Suseela, M. Periasamy, *J. Organomet. Chem.* **1993**, *450*, 47 – 52.
[49] Preparation of *B*-H-**4**: A solution of amino alcohol **3** (126 mg, 0.5 mmol, azeotropically dried with toluene (2 × 2 mL)) in dry toluene (3 mL) at 0 °C was treated dropwise with $BH_3 \cdot Me_2S$ (110 μL, 1.1 mmol, 10 M, neat) to afford a white precipitate. After the mixture was stirred for 20 min, the solvent was removed in vacuo. Dry toluene (3 mL) was added to the white solid, and the mixture was heated at reflux, which resulted in dissolution of the solid. After 17 h the solution was allowed to cool to 23 °C, and the solvent was removed in vacuo to afford a glassy oil. The addition of dry toluene (5 mL) provided a 0.1 M solution of *B*-H-**4** (> 95 % conversion as determined by ^{1}H NMR spectroscopy); ^{11}B NMR (96 MHz, $CDCl_3$): $\delta = 28.3$; E. J. Corey, K. A. Cimprich, C. J. Helal, unpublished results.
[50] Numerous in situ preparations of *B*-H-**4** have recently been reported which result in excellent enantioselectivity for the reduction of a number of different ketones, but which do not provide physical characterization of the catalyst system: a) M. Masui, T. Shioiri, *Synlett* **1997**, 273 – 274; b) K. R. K. Prasad, N. N. Joshi, *Tetrahedron: Asymmetry* **1996**, *7*, 3147 – 3152; c) M. Periasamy, J. V. B. Kanth, A. S. B. Prasad, *Tetrahedron* **1994**, *50*, 6411 – 6416; d) G. J. Quallich, T. M. Woodall, *Synlett* **1993**, 929 – 930.
[51] a) Preparation of (*S*)-*B*-*n*Bu-**4**: Toluene (15 – 20 mL) was added to amino alcohol **3** (253 mg, 1 mmol) and nBuB(OH)$_2 \cdot n$H$_2$O (164 mg) in a 25-mL round-bottom flask fitted with a Dean – Stark apparatus (sidearm filled with 4-Å molecular sieves) and a reflux condenser. The mixture was vigorously heated at reflux for 12 h. The toluene was removed by distillation through the Dean – Stark sidearm until about 3 mL were left. After the reaction mixture was cooled to 23 °C, the Dean – Stark apparatus was replaced by a rubber septum and the remaining toluene was removed in vacuo at 40 °C. Toluene (5.0 mL) was added to provide a 0.20 M solution of (*S*)-*B*-*n*Bu-**4** (> 95 % conversion as determined by ^{1}H NMR spectroscopy). Spectral data were indentical to that reported in the literature.[14a] The catalyst was stored by placing an additional rubber septum on the flask followed by cooling the solution to − 78 °C under a positive pressure of nitrogen. The nitrogen source was removed, and the catalyst solution was stored in a jar containing Drierite at − 20 °C. This precooling procedure prevents possible introduction of air into the flask due to a pressure difference. b) nBuB(OH)$_2$ was prepared by a known method (H. C. Brown, T. E. Cole, *Organometallics* **1983**, *2*, 1316 – 1319) except that aqueous 1 N HCl was used instead of anhydrous HCl in the workup. The amount of water in the nBuB(OH)$_2$ prepared by this method varies. Therefore, ^{1}H NMR analysis of the catalyst formation is required to ascertain the exact amount of the boronic acid necessary for complete catalyst formation. Once this is known for a specific batch of nBuB(OH)$_2$, however, the proper amount of boronic acid (1.05 equiv) can be added at the start of the reaction. c) Preparation of *B*-Me-**4**: The catalyst was prepared from amino alcohol **3** (253 mg, 1 mmol) and MeB(OH)$_2$ (72 mg, 1.2 mmol) as described above for (*S*)-*B*-*n*Bu-**4**, except that 1) the reaction mixture was heated at 60 °C for 1 h before heating at reflux temperature and 2) heating at reflux was maintained for 5 h. The material so obtained showed identical spectral properties with those reported.[14a]
[52] a) Reference [38]; for a related procedure with alkyl boronic amides RB(NR$_2$)$_2$, see b) P. Y. Chavant, M. Vaultier, *J. Organomet. Chem.* **1993**, *455*, 37 – 46.
[53] C. Meier, W. H. G. Laux, *Tetrahedron: Asymmetry* **1995**, *6*, 1089 – 1092.
[54] C.-P. Chen, K. Prasad, O. Repic, *Tetrahedron Lett.* **1991**, *32*, 7175 – 7178.
[55] a) E. J. Corey, X.-M. Cheng, K. A. Cimprich, S. Sarshar, *Tetrahedron Lett.* **1991**, *32*, 6835 – 6838; b) T. S. Kaufman, *ibid.* **1996**, *37*, 5329 – 5332.
[56] G. J. Quallich, T. M. Woodall, *Tetrahedron Lett.* **1993**, *34*, 785 – 788.
[57] a) Reduction of acetophenone with *B*-Me-**4** as catalyst and $BH_3 \cdot$ diethylaniline (BDEA) as stoichiometric reductant (from reference [46]): A dry 100-mL two-necked flask equipped with an addition funnel, magnetic stirring bar, thermocouple, and septum inlet was charged with a solution of (*R*)-*B*-Me-**4** (0.84 mmol, 0.084 M in toluene, 10 mL) followed by BDEA (2.74 g, 16.8 mmol). The reaction vessel was immersed in a water bath, and acetophenone (2.0 mL, 16.6 mmol) in toluene (5 mL) was added through the addition funnel over 1 – 1.5 h. After ketone addition was complete, the reaction mixture was stirred for an additional hour. MeOH (5 mL) was then slowly added (hydrogen evolution) followed by aqueous 1 N HCl (10 mL). After 15 – 20 min the organic and aqueous layers were separated, and the aqueous layer was extracted with toluene or Et_2O (3 × 10 mL). The combined organic layers were washed with aqueous 1 N HCl (2 × 10 mL), water, and brine, and then dried ($MgSO_4$). Analysis of the organic layer by gas chromatography (CDX-B column, 30 m × 0.25 mm, J&W Scientific) showed the product to be (*S*)-1-phenylethanol with 94.7 % *ee*. Removal of the solvent in vacuo followed by distillation gave (*S*)-1-phenylethanol that was spectroscopically identical with an authentic sample. b) Reduction of α-chloroacetophenone with *B*-*n*Bu-**4** as catalyst and $BH_3 \cdot Me_2S$ (BMS) as stoichiometric reductant: This protocol requires the *simultaneous* addition of ketone and BMS to a solution of the catalyst (0.01 equiv) in order to suppress uncatalyzed reduction pathways and is practical on multigram scale. Dry THF (10 mL) was added to (*S*)-*B*-*n*Bu-**4** (0.647 mmol, 0.2 M in toluene, 3.2 mL) and BMS (65 μL, 0.65 mmol, 10 M (neat)) under nitrogen. Separate solutions of α-chloroacetophenone (10 g, 64.7 mmol, azeotropically dried with benzene) in dry THF (40 mL) and BMS (4.5 mL, 45 mmol, 10 M (neat)) in dry THF (40 mL) were then added simultaneously to the solution of the oxazaborolidine catalyst over 1 h. After addition of ketone and BMS was complete no starting material remained, as determined by thin-layer chromatography. A solution of HCl in MeOH (0.5 M, 1.5 mL, 1.2 equiv; prepared by adding acetyl chloride to MeOH at 0 °C) was then slowly added (hydrogen evolution), and the solution was stirred for 30 min. THF was removed in vacuo, Et_2O (75 mL) added, and the HCl salt of the amino alcohol that precipitated as a white solid removed by filtration. The Et_2O layer was washed with saturated aqueous $NaHCO_3$ (2 × 10 mL) and brine (2 × 10 mL), dried ($MgSO_4$), filtered, and concentrated in vacuo. HPLC analysis (Chiralcel OD, 2-propanol/hexane 2.5/97.5, 1 mL min^{-1}, $\lambda = 254$ nm) showed the product to be of 98.5 % *ee*; t_R: 17.2 min, major; 22.5 min, minor isomer. Purification by filtration through a small plug of silica gel with hexanes/EtOAc (4/1) afforded 10 g (99 %) of (*S*)-2-chloro-1-phenylethanol. See reference [13c] for the first report of this procedure with (*S*)-*B*-Me-**4** as catalyst and $BH_3 \cdot$ THF (BTHF).
[58] E. J. Corey, C. J. Helal, *Tetrahedron Lett.* **1995**, *36*, 9153 – 9156.
[59] E. J. Corey, C. J. Helal, *Tetrahedron Lett.* **1996**, *37*, 5675 – 5678.
[60] CBS reduction of *N*-allyl-2-(4-chlorobenzoyl)pyridinium triflate and in situ deallylation: A flame-dried flask was charged with a solution of (*S*)-*B*-*n*Bu-**4** (370 μL, 0.074 mmol, 0.20 M in toluene), and the toluene was removed in vacuo. CH_2Cl_2 (370 μL) was added followed by catecholborane (104 μL, 0.98 mmol). The solution was cooled to − 78 °C, and *N*-allyl-2-(4-chlorobenzoyl)pyridinium triflate (200 mg, 0.49 mmol, azeotropically dried with CH_2Cl_2) in CH_2Cl_2 (2 mL) was added. After 5 min the heterogeneous mixture was warmed to − 40 °C and vigorously stirred for 36 h, over which period the mixture became homogeneous. MeOH (300 μL) was added, the solution was warmed to 23 °C, and [Pd(PPh$_3$)$_4$] (30 mg, 0.025 mmol) and *n*-butylammonium

formate (300 μL) were added. The solution was stirred for 3 h at 23 °C, and Et_2O (60 mL) was then added. The organic layer was washed with buffer (pH = 13) until the aqueous washings were colorless. The solution was then washed with brine (2 × 10 mL), dried ($MgSO_4$), filtered, and concentrated in vacuo. Purification by chromatography (silica gel, hexane/EtOAc 4/1 →2/1) provided 84 mg (78 %) of (*S*)-(4-chlorophenyl)-2-pyridylmethanol as a colorless oil. $[\alpha]_D^{23} = +119$ (c = 0.50 in $CHCl_3$, literature value for the *R* isomer: $[\alpha]_D^{16} = -132.5$ (c = 0.7 in $CHCl_3$)); ^{1}H NMR (400 MHz, $CDCl_3$): $\delta = 8.55$ (d, $J = 4.8$ Hz, 1H), 7.63 (td, $J = 1.7$, 7.7 Hz, 1H), 7.33 – 7.28 (m, 4H), 7.20 (dd, $J = 5.0$, 7.5 Hz, 1H), 7.12 (dd, $J = 0.4$, 7.9 Hz, 1H); ^{13}C NMR (100 MHz, $CDCl_3$): $\delta = 160.426$, 147.987, 141.789, 137.023, 133.666, 128.774, 128.457, 122.678, 121.283, 74.338. HPLC analysis (Chiralpak AD, 2-propanol/hexane 5/95, 1 mL min^{-1}, $\lambda = 254$ nm) showed the product to be of 98 % *ee*; t_R: 17.7 min, major; 23 min, minor isomer.

[61] E. J. Corey, A. Guzman-Perez, S. E. Lazerwith, *J. Am. Chem. Soc.*, in press.

[62] a) T. Konoike, Y. Araki, *Tetrahedron Lett.* **1992**, *33*, 5093-5096; b) P. Wipf, S. Lim, *Chimia* **1996**, *50*, 157 – 167; c) P. Wipf, S. Lim, *J. Am. Chem. Soc.* **1995**, *117*, 558 – 559; d) S. J. Amigoni, L. J. Toupet, Y. J. Le Floc'h, *J. Org. Chem.* **1997**, *62*, 6374 – 6378; e) H. Dumartin, Y. Le Floc'h, R. Grée, *Tetrahedron Lett.* **1994**, *35*, 6681 – 6684; f) D. B. Smith, A. M. Waltos, D. G. Loughhead, R. J. Weikert, D. J. Morgans, Jr., J. C. Rohloff, J. O. Link, R. Zhu, *J. Org. Chem.* **1996**, *61*, 2236 – 2241.

[63] a) E. J. Corey, H. Kigoshi, *Tetrahedron Lett.* **1991**, *32*, 5025-5028; b) E. J. Corey, A. V. Gavai, *ibid.* **1988**, *29*, 3201 – 3204.

[64] a) K. C. Nicolaou, P. Bertinato, A. D. Piscopio, T. K. Chakraborty, N. Minowa, *J. Chem. Soc. Chem. Commun.* **1993**, 619 – 622; b) E. J. Corey, K. S. Rao, *Tetrahedron Lett.* **1991**, *32*, 4623 – 4626.

[65] A. F. Simpson, P. Szeto, D. C. Lathbury, T. Gallagher, *Tetrahedron: Asymmetry* **1997**, *8*, 673 – 676.

[66] CBS reduction of *E*-4-(4′-methoxyphenyl)-3-buten-2-one: (*E*)-4-(4′-methoxyphenyl)-3-buten-2-one (50 mg, 0.28 mmol, azeotropically dried with toluene) was treated with (*S*)-*B*-*n*Bu-**4** (86 μL, 0.043 mmol, 0.20 M in toluene) and toluene (900 μL). Upon being cooled to − 78 °C the solution became heterogeneous. Catecholborane (51 mg, 46 μL, 0.43 mmol) in toluene (138 μL) was added directly into the rapidly stirred reaction mixture, and the color immediately turned dark red (this is unique for 4-aryl-3-buten-2-ones). After the mixture was stirred for 20 h at − 78 °C the dark red color had faded to light pink. MeOH (200 μL) was added down the side of the flask, and the solution was warmed to 23 °C, diluted with Et_2O (40 mL), and washed with buffer (pH = 13, 1N NaOH/saturated $NaHCO_3$ 2/1) until the aqueous washings were colorless. The dark aqueous washes were extracted with Et_2O (2 × 10 mL). The combined organic layers were washed with brine (2 × 5 mL), dried ($MgSO_4$), filtered, and concentrated in vacuo to a volume of about 10 mL. A solution of HCl in MeOH (0.5 M, 86 μL, 0.043 mmol) was added, the HCl salt of the amino alcohol removed by filtration, and the solution concentrated in vacuo. Purification by chromatography (silica gel, hexane/EtOAc 4/1) provided 44 mg (88 %) of the alcohol as a while solid. $[\alpha]_D^{22} = +36.9$ (c = 1.15 in $CHCl_3$); m.p. 96 – 97 °C; ^{1}H NMR (400 MHz, $CDCl_3$): δ = 7.30 (d, $J = 8.7$ Hz, 2H), 6.85 (d, $J = 8.8$ Hz, 2H), 6.50 (d, $J = 15.9$ Hz, 1H), 6.12 (dd, $J = 6.6$, 15.9 Hz, 1H), 4.46 (m, 1H), 3.80 (s, 3H), 1.78 (br s, 1H), 1.36 (d, $J = 6.3$ Hz, 3H); ^{13}C NMR (100 MHz, $CDCl_3$): δ = 159.25, 131.43, 129.44, 129.01, 127.65, 114.01, 69.11, 55.31, 23.48. HPLC analysis (Chiralcel OD, 2-propanol/hexane 2.5/97.5, 1 mL min^{-1}, λ = 254 nm) showd the product to be of 95 % *ee*; t_R: 42.2 min, major; 49.3 min, minor isomer.

[67] K. A. Parker, M. W. Ledeboer, *J. Org. Chem.* **1996**, *61*, 3214 – 3217.

[68] CBS reduction of 1-trimethylsilyl-1-octyn-3-one: A flame-dried flask was charged with (*S*)-*B*-4-*t*BuC_6H_4-**4** (0.128 mmol, 1.28 mL, 0.1 M in toluene), the solvent was removed in vacuo, and a solution of 1-trimethylsilyl-1-octyn-3-one (500 mg, 2.55 mmol, azeotropically dried with benzene) in CH_2Cl_2 (5 mL) was added. The solution was cooled to − 40 °C, and catecholborane (364 mg, 324 μL, 3.06 mmol) in CH_2Cl_2 (2.2 mL) was added down the side of the flask over 30 min. After 1 h MeOH (2 mL) was added, and the solution was warmed to 23 °C. The reaction solution was diluted with Et_2O (150 mL), washed with buffer (pH = 13) until the aqueous washings were colorless and then with brine (10 mL), dried ($MgSO_4$), filtered, and concentrated in vacuo. The addition of Et_2O (10 mL) followed by HCl in MeOH (0.5 M, 256 μL, 0.128 mmol) resulted in precipitation of the HCl salt of the amino alcohol as a fine powder, which was removed by filtration. The Et_2O was removed in vacuo, and the residue was passed through a short column of silica gel (hexane/Et_2O 10/1) to provide 480 mg (96 %) of (*R*)-trimethylsilyl-1-octyn-3-ol as a colorless oil. $[\alpha]_D^{23} = +12$ (c = 0.15 in benzene); ^{1}H NMR (400 MHz, $CDCl_3$): $\delta = 4.34$ (t, J = 6.4 Hz, 1H), 2.05 – 2.00 (br s, 1H), 1.73 – 1.62 (m, 2H), 1.50 – 1.40 (m, 2H), 1.35 – 1.25 (m, 4H), 0.88 (t, $J = 6.8$ Hz, 3H), 0.16 (s, 9H); ^{13}C NMR (100 MHz, $CDCl_3$): $\delta = 107.08$, 89.28, 62.94, 37.71, 31.45, 24.82, 22.56, 13.99, − 0.08. Conversion of the alcohol into the *p*-nitrobenzoate (p-nitrobenzoyl chloride, dimethylaminopyridine, CH_2Cl_2, 23 °C) and HPCL analysis (Whelk-O1, 2-propanol/hexane 0.5/99.5, 1 mL min^{-1}, $\lambda = 254$ nm) showed the product to be of 94 % *ee*; t_R: 21.3, major; 25.8 min, minor isomer. The absolute configuration of the product was determined by desilylation (1.1 equiv of tetrabutylammonium fluoride, THF, 0 °C, 5 min, > 95 %) and comparison of the optical rotation ($[\alpha]_D^{23} = +6.0$ (c = 2.25 in CH_2Cl_2)) with the literature value ($[\alpha]_D^{23} = +6.5$ (c = 2.0 in CH_2Cl_2)). b) (*S*)-*B*-4-*t*BuC_6H_4-**4** was prepared from **3** (1 equiv) and *p*-*tert*-butylphenylboroxine ($(ArBO)_3$, 0.35 equiv) according to the literature procedure.[51]

[69] a) S. E. Denmark, M. E. Schnute, L. R. Marcin, A. Thorarensen, *J. Org. Chem.* **1995**, *60*, 3205 – 3220; b) E. J. Corey, A. Huang, unpublished results; c) for a study of the effect of temperature on the enantioselectivity of the oxazaborolidine-catalyzed reduction of acetophenone and cyclohexylmethyl ketone, see reference [45].

[70] M. Morr, C. Proppe, V. Wray, *Leibigs Ann.* **1995**, 2001 – 2004.

[71] O. W. Gooding, R. P. Bansal, *Synth. Commun.* **1995**, *25*, 1155 – 1166.

[72] E. J. Corey, C. J. Helal, *Tetrahedron Lett.* **1996**, *37*, 4837 – 4840.

[73] a) J. Wright, L. Frambes, P. Reeves, *J. Organomet. Chem.* **1994**, *476*, 215 – 217; b) L. Schwink, P. Knochel, *Tetrahedron Lett.* **1996**, *37*, 25 – 28; c) *ibid.* **1997**, *38*, 3711 – 3714; d) M. Woltersdorf, R. Kranich, H.-G. Schmalz, *Tetrahedron* **1997**, *53*, 7219 – 7230; e) A. Ohno, M. Yamane, T. Hayashi, N. Oguni, M. Hayashi, *Tetrahedron: Asymmetry* **1995**, *6*, 2495 – 2502.

[74] E. J. Corey, J. O. Link, S. Sarshar, Y. Shao, *Tetrahedron Lett.* **1992**, *33*, 7103 – 7106.

[75] E. J. Corey, J. O. Link, *J. Am. Chem. Soc.* **1992**, *114*, 1906 – 1908.

[76] E. J. Corey, X.-M. Cheng, K. A. Cimprich, *Tetrahedron Lett.* **1991**, *32*, 6839 – 6842.

[77] E. J. Corey, M. C. Noe, M. J. Grogan, *Tetrahedron Lett.* **1994**, *35*, 6427 – 6430.

[78] E. J. Corey, M. C. Noe, A. Guzman-Perez, *J. Am. Chem. Soc.* **1995**, *117*, 10817 – 10824.

[79] K. R. K. Prasad, N. N. Joshi, *J. Org. Chem.* **1996**, *61*, 3888 – 3889.

[80] S. E. Denmark, L. R. Marcin, *J. Org. Chem.* **1995**, *60*, 3221 – 3235.

[81] R. D. Tillyer, C. Boudreau, D. Tschaen, U.-H. Dolling, P. J. Reider, *Tetrahedron Lett.* **1995**, *36*, 4337 – 4340.

[82] a) G. Bringmann, D. Vitt, *J. Org. Chem.* **1995**, *60*, 7674 – 7681; b) G. Bringmann, T. Hartung, *Tetrahedron* **1993**, *49*, 7891 – 7902; c) *Angew. Chem.* **1992**, *104*, 782 – 783; *Angew. Chem. Int. Ed. Engl.* **1992**, *31*, 761 – 762.

[83] A. S. Thompson, G. R. Humphrey, A. M. Demarco, D. J. Mathre, E. J. J. Grabowski, *J. Org. Chem.* **1993**, *58*, 5886 – 5888.

[84] E. J. Corey, K. A. Cimprich, *Tetrahedron Lett.* **1992**, *33*, 4099 – 4102.

[85] a) M. P. DeNinno, R. J. Perner, L. Lijewski, *Tetrahedron Lett.* **1990**, *31*, 7415 – 7418; b) K. Kanematsu, A. Nishizaki, Y. Sato, M. Shiro, *Tetrahedron Lett.* **1992**, *33*, 4967 – 4970.

[86] a) M. Ostendorf, R. Romagnoli, I. Cabeza Pereiro, E. C. Roos, M. J. Moolenaar, W. N. Speckamp, H. Hiemstra, *Tetrahedron: Asymmetry* **1997**, *8*, 1773 – 1789; b) R. Romagnoli, E. C. Roos, H. Hiemstra, M. J. Moolenaar, W. N. Speckamp, *Tetrahedron Lett.* **1994**, *35*, 1087 – 1090.

[87] For the preparation of trichloromethyl ketones, see E. J. Corey, J. O. Link, Y. Shao, *Tetrahedron Lett.* **1992**, *33*, 3435 – 3438.

[88] E. J. Corey, J. O. Link, *Tetrahedron Lett.* **1992**, *33*, 3431 – 3434.

[89] A. P. Khrimian, J. E. Oliver, R. M. Waters, S. Panicker, J. M. Nicholson, J. A. Klun, *Tetrahedron: Asymmetry* **1996**, *7*, 37 – 40.

[90] E. J. Corey, C. J. Helal, *Tetrahedron Lett.* **1993**, *34*, 5227 – 5230.

[91] Denopamine: a) E. J. Corey, J. O. Link, *J. Org. Chem.* **1991**, *56*, 442 – 444; isoproterenol: b) reference [39]; salmeterol: c) R. Hett, R. Stare, P. Helquist, *Tetrahedron Lett.* **1994**, *35*, 9375 – 9378; formoterol (the oxazaborolidine derived from *cis*-(1*R*, 2*S*)-aminoindanol (Table 2, entry 8) was used): d) R. Hett, Q. K. Fang, Y. Gao, Y. Hong, H. T. Butler, X. Nie, S. A. Wald, *ibid.* **1997**, *38*, 1125 – 1128.
[92] E. J. Corey, G. A. Reichard, *Tetrahedron Lett.* **1989**, *30*, 5207 – 5210.
[93] a) E. J. Corey, C.-P. Chen, M. J. Parry, *Tetrahedron Lett.* **1988**, *29*, 2899 – 2902; b) reference [13].
[94] R. D. Larsen, E. G. Corley, A. O. King, J. D. Carroll, P. Davis, T. R. Verhoeven, P. J. Reider, M. Labelle, J. Y. Gauthier, Y. B. Xiang, R. J. Zamboni, *J. Org. Chem.* **1996**, *61*, 3398 – 3405.
[95] A. S. Lee, A. W. Norman, W. H. Okamura, *J. Org. Chem.* **1992**, *57*, 3846 – 3854.
[96] E. J. Corey, C. J. Helal, *Tetrahedron Lett.*, in press.
[97] M. P. DeNinno, R. J. Perner, H. E. Morton, S. DiDomenico, Jr., *J. Org. Chem.* **1992**, *57*, 7115 – 7118.
[98] a) H.-G. Schmalz, J. Hollander, M. Arnold, G. Dürner, *Tetrahedron Lett.* **1993**, *34*, 6259 – 6262; b) H.-G. Schmalz, M. Arnold, J. Hollander, J. W. Bats, *Angew. Chem.* **1994**, *106*, 77 – 79; *Angew. Chem. Int. Ed. Eng.* **1994**, *33*, 109 – 111.
[99] V. L. Ponzo, T. S. Kaufman, *Tetrahedron Lett.* **1995**, *36*, 9105 – 9108.
[100] E. J. Corey, B. E. Roberts, *J. Am. Chem. Soc.*, in press.
[101] a) E. J. Corey, P. Da Silva Jardine, T. Mohri, *Tetrahedron Lett.* **1988**, *29*, 6409 – 6412; b) D. Calvo, M. Port, B. Delpech, R. Lett, *ibid.* **1996**, *37*, 1023 – 1024.
[102] E. J. Corey, P. Da Silva Jardine, *Tetrahedron Lett.* **1989**, *30*, 7297 – 7300.
[103] E. J. Corey, W.-g. Su, *Tetrahedron Lett.* **1988**, *29*, 3423 – 3426.
[104] K. Mori, M. Amaike, M. Itou, *Tetrahedron*, **1993**, *49*, 1871 – 1878.
[105] C. Y. Hong, N. Kado, L. E. Overman, *J. Am. Chem. Soc.* **1993**, *115*, 11028 – 11029.
[106] K. C. Nicolaou, E. J. Sorensen, *Classics in Total Synthesis*, VCH, Weinheim, **1996**, pp. 616 – 617.
[107] a) M. J. DiGrandi, D. K. Jung, W. J. Krol, S. J. Danishefsky, *J. Org. Chem.* **1993**, *58*, 4989 – 4992; b) K. C. Nicolaou, C.-K. Hwang, E. J. Sorenson, C. F. Clairborne, *J. Chem. Soc. Chem. Commun.* **1992**, 1117 – 1118.
[108] P. Szeto, D. C. Lathbury, T. Gallagher, *Tetrahedron Lett.* **1995**, *36*, 6957 – 6960.
[109] M. F. Semmelhack, W. R. Epa, A. W-H. Cheung, Y. Gu, C. Kim, N. Zhang, W. Lew, *J. Am. Chem. Soc.* **1994**, *116*, 7455 – 7456.
[110] M. Lögers, L. E. Overman, G. S. Welmaker, *J. Am. Chem. Soc.* **1995**, *117*, 9139 – 9150.
[111] a) D. T. Hung, J. B. Nerenberg, S. L. Schreiber, *J. Am. Chem. Soc.* **1996**, *118*, 11054 – 11080; b) J. B. Nerenberg, D. T. Hung, P. K. Sommers, S. L. Schreiber, *ibid.* **1993**, *115*, 12621 – 12622.
[112] D. P. Stamos, S. S. Chen, Y. Kishi, *J. Org. Chem.*, in press.

Enantioselective catalysis with partially resolved chiral auxiliaries

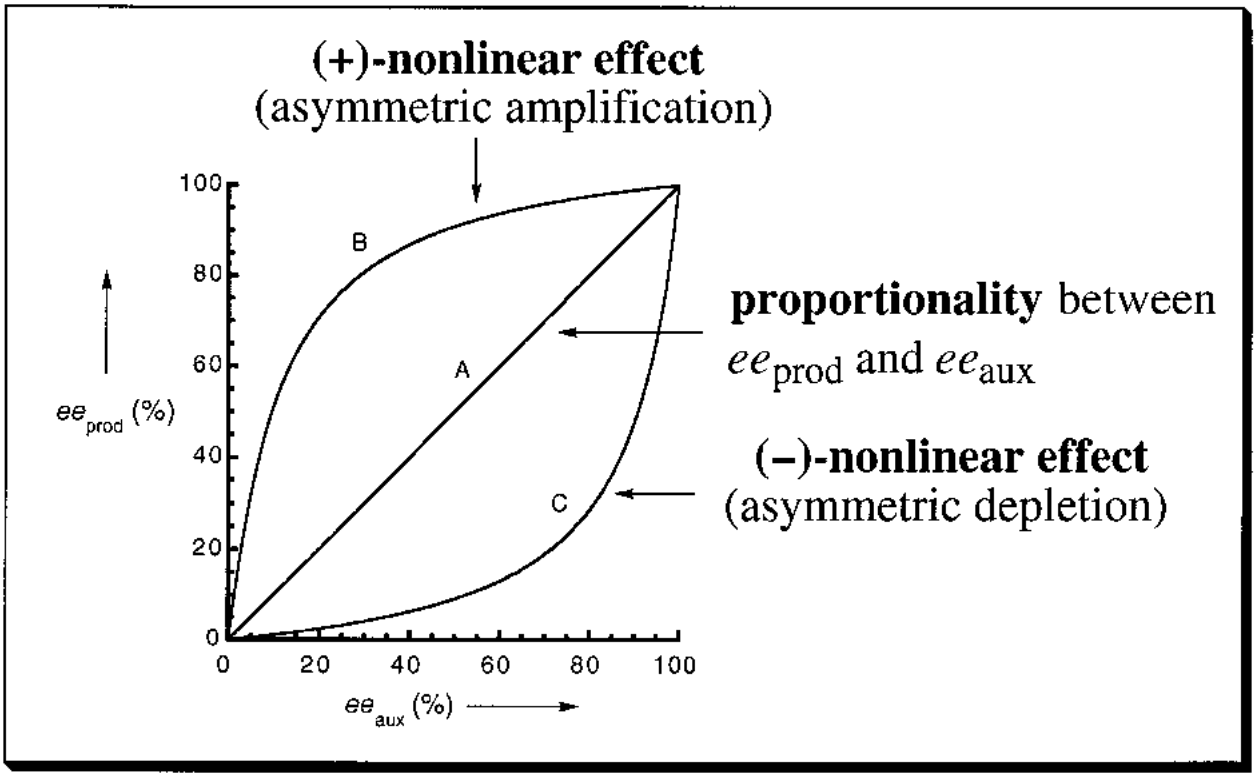

In many enantioselective reactions ee_{prod} *is not always proportional* to ee_{aux}.

Nonlinear Effects in Asymmetric Synthesis and Stereoselective Reactions: Ten Years of Investigation

Christian Girard and Henri B. Kagan*

Dedicated to Professor Dieter Seebach on the occasion of his 60th birthday

The first preoccupation of organic chemists was to develop their ability to reproduce the organization of atoms in natural products. This incursion in nature's laboratory gave rise to numerous techniques to transform matter but led to the discovery of her subtle way of producing substances with chirality and the preference of one enantiomer over the other in the living matter gave a lesson in perfection. The development of asymmetric synthesis gave the opportunity to elaborate methods, reagents, and reactions in order to prepare enantiomerically pure compounds. But this journey is far from being over, and there is a lot of surprises left. No chemist would have thought that an enantiomerically impure chiral auxiliary or ligand could give a stereoselection higher than its own and even equivalent to the pure one. Molecules can behave in numerous ways in solution; aggregation or organization can occur depending on the nature of the molecule or its environment. These phenomena give rise to modification of the anticipated enantiomeric excess (*ee*) of the reaction product. The relation between the *ee* value of the auxiliary or ligand and the *ee* value of the product deviates from linearity to give what we now call nonlinear effects (NLEs). The nonlinear effects in asymmetric synthesis and stereoselective reactions reflect molecular interactions and complexity in reaction mechanisms. They can be used to generate products with high *ee*'s from an enantiomerically impure, and more economical to prepare, chiral auxiliary or ligand. Furthermore, the NLEs can also act as a probe to obtain information on the subtle mechanisms by which the enantioselectivity is generated.

Keywords: asymmetric amplification · asymmetric catalysis · asymmetric synthesis · autocatalysis · chiral auxiliaries

1. Introduction

In the early years of organic chemistry chemists became aware of the importance of chirality in nature. Differences between biological activities of two enantiomers were soon uncovered and the importance of producing mainly or exclusively one enantiomer was highlighted. From the study of enantiomeric mixtures, behavioral differences between racemic and enantiomerically pure compounds were discovered.

In 1848 Pasteur demonstrated that tartaric acid rotated the plane of polarized light, but in a different way depending on its origin.[1] This discovery triggered the use of polarimetry as the technique for gathering information on the enantiomeric purity of compounds, since enantiomers of opposite absolute configuration gave the same degree of deviation of the plane of light, but in opposite sign. Mixtures of enantiomers that differed from racemic composition were therefore analyzed in this fashion and the relative amounts of each constituents were deduced from the total rotation.[2]

However, exceptions to this method were found to be more than a few. Horeau's work on 1-ethyl-1-methylsuccinic acid showed that its specific rotation in chloroform was not strictly related to enantiomeric composition.[5] The phenomenon was explained on the basis of diastereomeric associations by hydrogen bonding that gave rise to a nonlinear relationship between the enantiomeric excess (*ee*) of the acid and its optical purity (*op*). When methanol was used as a solvent for recording this optical property a strictly linear interrelation ($ee = op$) was observed as a consequence of the solvent preventing the aggregation.

The general problem of diasteromeric interactions in a solution of a mixture of enantiomers was discussed in 1974 by Horeau and Guetté.[6] The physicochemical properties of such mixtures may be modified with a change of enantiomeric composition. For example the ^{1}H NMR spectrum (in solution)

[*] Prof. Dr. H. B. Kagan
Laboratoire des Réactions Organiques Sélectives
Institut de Chimie Moléculaire d'Orsay
Bâtiment 420, Université de Paris-Sud, F-91405 Orsay Cedex (France)
Fax: (+33) 169-15-46-80
E-mail: kagan@icmo.u-psud.fr
Dr. C. Girard
Laboratoire de Vectorisation Moléculaire et Cellulaire
Ecole Nationale Supérieure de Chimie de Paris
11, rue Pierre et Marie Curie, F-75231 Paris Cedex (France)
E-mail: cgirard@ext.jussieu.fr

  1433-7851/98/3721-2923 $ 17.50+.50/0

of a racemic mixture or of an enantiopure compound may differ, as found for the first time by Uskokovic et al. in the case of dihydroquinine.[7] Recently the first example of fractionation by distillation of a non racemic mixture of enantiomers was discovered.[8] Isopropyl trifluorolacetate is highly associated by hydrogen bonding, it also shows variation in the infrared absorptions in the liquid (neat) phase. The enantiomeric composition of a non racemic mixture may also be modified significantly by chromatography with achiral stationary and mobile phases. There are several examples in the literature that were explained by diastereomeric associations in the mobile and (or) the stationary phases.[9–14] A mathematical simulation of this phenomenon has been performed.[15]

A nonideal behavior of a mixture of enantiomers may have some consequences on chemical reactions in solution. Wynberg and Feringa pointed out in 1976 that, based on symmetry considerations and free energy arguments, the surroundings of a given *R* enantiomer should be different if it is an enantiopure material or a racemic mixture.[16] In the latter *R/S* interactions may develop, which are absent in the enantiopure system. The authors proposed the following principle: *When a chiral substance undergoes a reaction, the reaction rate and the product ratio will depend—inter alia—upon the enantiomeric excess present in the starting material*. Wynberg and Feringa found some cases that are in agreement with the above principle. The diasteroselectivity of the $LiAlH_4$ reduction of camphor, the McMurry coupling of camphor, and the *ortho*-coupling of a phenol derivative were compared for the enantiopure and racemic systems. Significant differences could be observed. For example, the ratio of isoborneol to borneol was 90.2:9.8 or 88.7:11.3 for the reduction of (+)-camphor or racemic camphor, respectively. In the above publication there were no cases of reactions dealing with chiral substrates having an *ee* value different from 0 or 100%, nor discussion on the quantitative variation of the diastereoselectivity as a function of the *ee* of the substrate.

The chiral auxiliary that is needed in asymmetric synthesis is always of nonracemic composition, preferably of 100% *ee*. One may wonder if an enantiomeric excess lower than 100% will lower the enantiomeric excess of the product in a proportional manner, or if the *ee* of the product will have an unexpected value (as in the Wynberg and Feringa examples) because of a perturbation generated by the *ee* of the chiral auxiliary. This problem had almost never been questioned by the practitioners of asymmetric synthesis.[17] It was in 1986 that the quantitative aspects of the influence of the *ee* value of the chiral auxiliary on the corresponding *ee* value of the product were discussed and studied experimentally.[19] This review article will summarize the main results obtained in that area.[20] The cases of asymmetric catalysis, stoichiometric asymmetric synthesis, and diastereoselective reactions (with a chiral substrate) will be developed successively.

2. Asymmetric Catalysis

2.1. The First Examples—1986

In 1986 Kagan, Agami et al. considered the case of asymmetric synthesis with a chiral catalyst or auxiliary that was not enantiomerically pure.[19] The well accepted assump-

Henri B. Kagan was born in Boulogne-Billancourt (France) in 1930. He graduated from the Sorbonne and Ecole Nationale Supérieure de Chimie de Paris in 1954. He did his doctorate with Prof. J. Jacques, as his first student, and obtained his diploma for work on modified steroids. He then joined Prof. A. Horeau at the Collège de France in Paris in 1962 as a research associate and became involved in studies on stereochemistry and asymmetric synthesis. In 1965 he worked with Prof. T. Mabry at the University of Texas, Austin (USA). He was appointed assistant professor in 1968 at the Université de Paris-Sud, Orsay (France); where he became full professor in 1973. Kagan has been the recipient of several French and international awards and distinctions over the years. He was elected a member of the Académie des Sciences of the Institut de France in 1991 and is a member of the Institut Universìtaire de France.

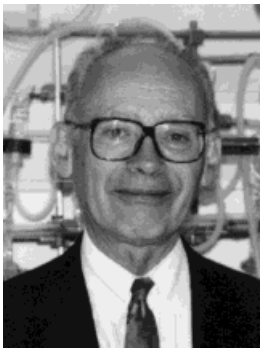

H. B. Kagan

C. Girard

Christian Girard was born in Grandes-Bergeronnes (Québec, Canada) in 1966. After graduating from the François-Xavier Garneau College with an Health Sciences diploma in 1985, he studied chemistry at the Université Laval (Québec, Canada) where he obtained his B. Sc. (1988) and M. Sc. (1990) with Prof. P. Brassard for work on quinonoid compounds. He then moved to Université de Montréal (Canada) where he completed his Ph. D. in 1994 with Prof. S. Hanessian on the use of samarium(II) iodide in carbohydrate chemistry. The same year, having been granted a Chateaubriand Postdoctoral Fellowship, he then joined Prof. H. B. Kagan at Université de Paris-Sud, Orsay (France) where he became involved in the study of nonlinear effects in asymmetric synthesis. Since 1996, he has been working as a post-doctoral fellow with Prof. J.-P. Genêt at Ecole Nationale Supérieure de Chimie de Paris, Paris (France), where he has been recently appointed as Maitre de Conférence.

tion that the *ee* value of the product (ee_{prod}) of an asymmetric synthesis is linearly correlated to the *ee* value of the chiral auxiliary (ee_{aux}) was questioned. The usual procedure to get an approximation of the experimental *ee* value (ee_{prod}) by correction, knowing the maximum *ee* value of the product (ee_o) is reached with the enantiopure chiral catalyst or auxiliary, was to use Equation (1). This linear relationship is

$$ee_{prod} = ee_o\, ee_{aux} \quad (1)$$

represented for an $ee_o = 100\,\%$ as Curve A in Figure 1. Equation (1) takes into account only the highest enantioselectivity (ee_o) reached with the chiral auxiliary. This linearity

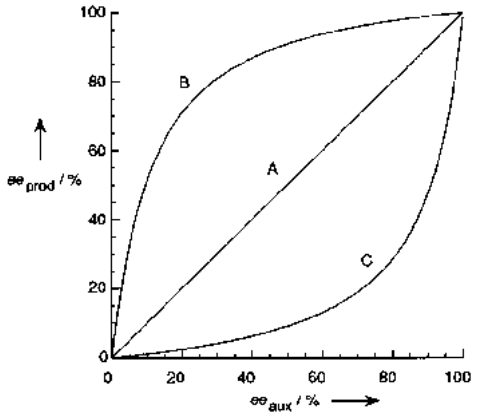

Figure 1. Typical curves for positive (B) and negative (C) nonlinear effects.

was theoretically not to be encountered in systems subjected to other influences, such as interaction between the catalytic species. If the linear relationship is not followed one can expect a plain curve above (curve B, positive nonlinear effect, abbreviated as (+)-NLE) or below (curve C, negative nonlinear effect or (−)-NLE) the straight line, respectively (Figure 1). By convention, all graphs of NLE will be presented as in Figure 1, whatever the absolute configuration of the chiral auxiliary and the product. We will not consider negative coordinates unless there is a special need.

The nonlinearities shown in Figure 1 may in principle arise by auto association or association around a matrix of the initial chiral species, which give diastereomeric perturbations. Those perturbations should then be added to Equation (1) as a multiplication factor to divert the relation between ee_{prod} and ee_{aux} from linearity. Equation (1) must then to be used with caution.

Three systems were studied in 1986 to test this hypothesis.[19] The results that emerged from the data collected provided clear indications that in several cases such nonlinear effects were to be encountered.[20] The first reaction studied was the asymmetric Robinson annulation (Hajos-Parrish-Wiechert reaction[25]) of the triketone **1** using (*S*)-proline as a catalyst (Figure 2). When the *ee* value of (*S*)-proline (ee_{aux}) was plotted against the *ee* value of the *cis*-ketol **2** (ee_{prod}) a slight (−)-NLE was observed, as depicted in Figure 2. Mechanistic investigations by Agami et al. suggested that the reaction proceeds through the formation of a chiral enamine followed by a complexation with a molecule of

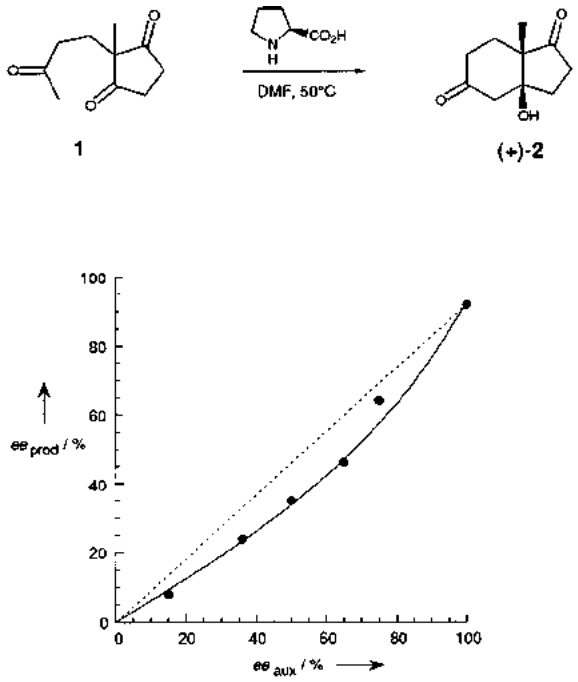

Figure 2. (−)-NLE in the Hajos-Parrish-Wiechert reaction of **1** to **2** catalyzed by (*S*)-proline (3 mol %).

catalyst. This was confirmed by a kinetic model based on a second-order reaction in respect to proline.[26] Furthermore, the (−)-NLE was explained by the fact that, by considering the complexes **3** as intermediates, the reaction involving heterochiral complexes proceed twice as fast as the one of homochiral complexes (Figure 3).

A different effect was however observed in the Sharpless epoxidation[27] of geraniol (**4**) during this investigation.[19] A positive nonlinear effect takes place in this reaction with (*R,R*)-(+)-diethyl tartrate ((*R,R*)-(+)-DET) of various *ee*'s

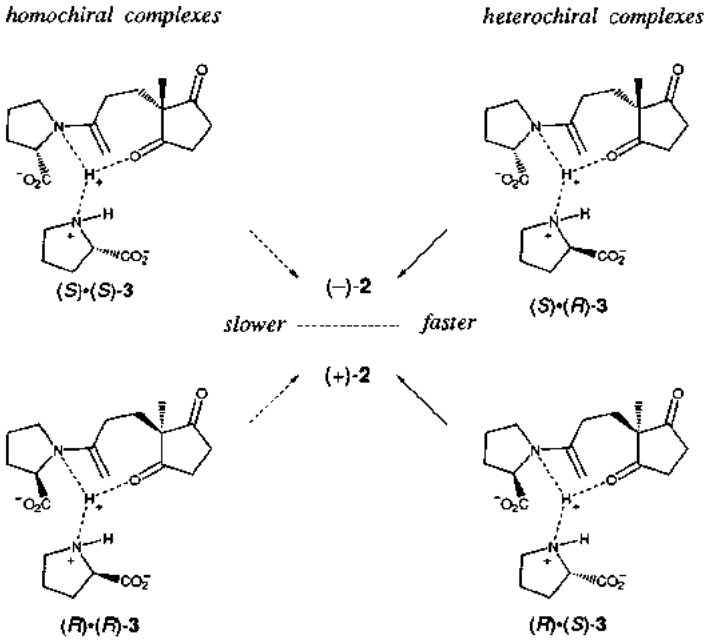

Figure 3. Intermediate complexes **3** in the asymmetric Robinson annulation of **1** to **2**.

(Figure 4). The enantiomeric excess of the produced epoxide **5** (ee_{prod}) when plotted as a function of the *ee* of (+)-DET (ee_{aux}) was indeed greater than expected. The use of a dimeric heterochiral species that is less reactive, and thus more stable,

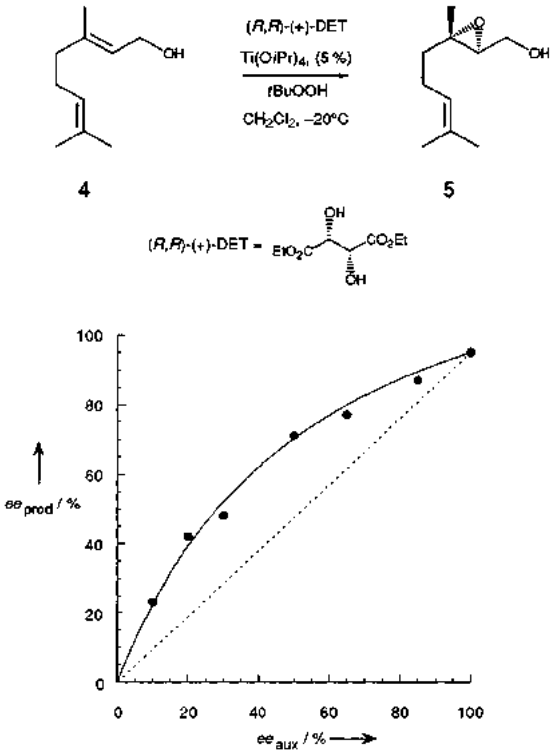

Figure 4. (+)-NLE in the Sharpless epoxidation of geraniol (**4**).

than its homochiral counterparts provides a way of understanding the (+)-NLE of the reaction, since some racemic DET will be retained in the inactive complex. This proposal is compatible with the Sharpless mechanism of asymmetric epoxidation, which indicates the intervention of a dimeric complex that introduces two tartrate units in the active species.[27b] The (+)-NLE discovered here for the first time has been found subsequently in many reactions and has been named "asymmetric amplification" by Oguni et al.[28]

A water-modified Sharpless reagent has been developed by Kagan et al. for the asymmetric oxidation of sulfides by hydroperoxides.[29] The oxidation of methyl-*p*-tolyl sulfide **6** to sulfoxide **7** is quite unexpected by comparison with the results previously discussed (Figure 5). The relation between the *ee*'s is clearly a (−)-NLE, but this effect affects the enantioselectivity until the value of 70% *ee* is reached for the diethyl tartrate. The linear relationship then prevails until enantiomerically pure DET is used. This perturbed behavior is indicative of a quite complicated structure for the water-modified reagent.[30]

These first experiments were a revelation in the behavior of mixtures of enantiomeric reagents or catalysts. They were an indication that some complex and subtle interactions were taking place in solutions with participation from a diastereomeric species. Furthermore, the analysis of the perturbations on the enantioselectivity of the reaction generated by mixing

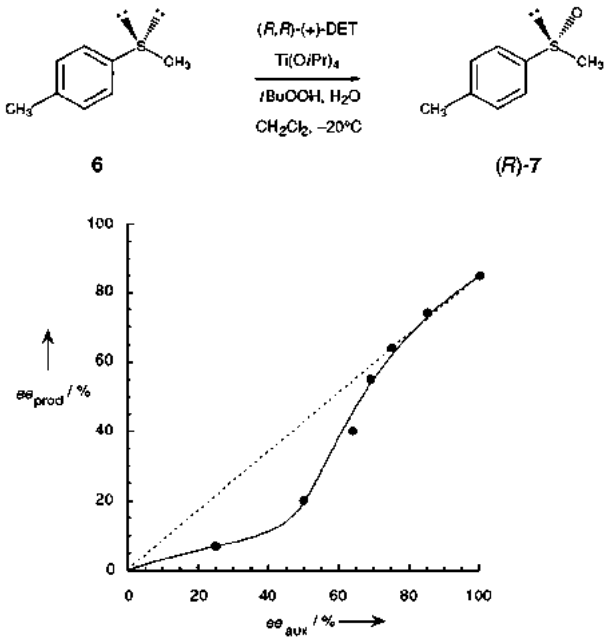

Figure 5. (−)-NLE in the asymmetric oxidation of sulfide **6** with a chiral titanium reagent.

various amounts of enantiomers also gave information about the reaction itself. It became clear that the search for nonlinear effects in a given system also becomes a probe for analyzing the nature of the catalytic species or the nonreacting species involved in an asymmetric synthesis.

2.2. Models and Principles

To get a better understanding and to have some insight into the behavior of catalysts during the course of a reaction that leads to a NLE, simplified mathematical models were developed by Kagan et al. in 1994.[31] These models were discussed in the cited article and will not be explained here in detail. The systems, equations, and the resulting curves will be presented in this section to demonstrate their usefulness.

2.2.1. The ML_2 System

The first model is based on a system in which a fast ligand exchange occurs at a metallic center (M) of a reactive species bearing two chiral ligands (L_R and L_S): the ML_2 system (Figure 6). The following discussion can easily be applied to $(ML)_2$ systems as well to reversible dimerization in the absence of the metal (e.g. association by hydrogen bonding). The model was based on the assumption of a steady state for the three expected complexes ML_RL_R, ML_SL_S, and ML_RL_S (in

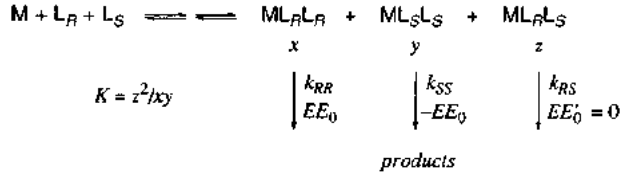

Figure 6. Illustration of the ML_2 system to explain NLEs.

the relative concentrations x, y, and z, respectively), a final irreversible step with pseudo-first order constants k_{RR}, k_{SS} ($=k_{RR}$), and k_{RS}, and a zero-order dependence with respect of the substrate. Furthermore, the *meso* catalyst (ML_RL_S) generated racemic product while the homochiral complexes gave enantiomeric products. It became easy to evaluate the *ee* of a product formed from this kind of system by obtaining the mathematical formula describing it. Equation (2) permits the

$$EE_{\text{prod}} = EE_0 \cdot ee_{\text{aux}} \frac{1+\beta}{1+g\beta} \tag{2}$$

ee value of the product (EE_{prod}) to be calculated for each value of ee_{aux} by knowing the maximum value reached with enantiopure catalyst (EE_0) and the parameters for the studied system. The new parameters introduced in this equation are β, the relative amounts of the complexes ($\beta = z/(x+y)$), and g, the relative reactivities of the hetero- over the homochiral catalysts ($g = k_{RS}/k_{RR}$).

If $\beta = 0$ (no *meso* catalyst) or $g = 1$ (identical reactivities of hetero- and homochiral species), then Equation (2) is simplified to Equation (1) and a linear relationship is observed. In other situations the correction factor $(1+\beta)/(1+g\beta) \neq 1$ is needed and a nonlinear relation takes place. When this factor is greater than one the system displays a (+)-NLE; the amplitude of which will depend on the size of the value of this factor. This will be the case of systems where g is less than one, in which a less reactive heterochiral complex exists. However, if g is greater than one the system will present a (−)-NLE as a consequence of a greater reactivity of the *meso* catalyst. In order to calculate curves from this model it was necessary to transform Equation (2) in terms of ee_{aux} and the relative amounts of the complexes by using the variable $K = z^2/(xy)$ (which is the equilibrium constant if these complexes are in fast interconversion during their formation). The ratio β of the hetero- and homochiral species then becomes available from Equation (3).

$$\beta = \frac{-Kee_{\text{aux}}^2 + \sqrt{-4\,Kee_{\text{aux}}^2 + K(4+ee_{\text{aux}}^2)}}{4+Kee_{\text{aux}}^2} \tag{3}$$

It was then possible to evaluate the EE_{prod} by using Equations (2) and (3) and to plot curves derived from this model. In Figure 7 the results for two cases in which $K = 9$ and 2500 are presented. The curves are generated for different values of g. In the particular case where the ligands are statistically distributed between the complexes a simplification occurs and K becomes equal to four. Furthermore, the term β is also simplified and, from Equation (3), is given by $\beta = (1-ee_{\text{aux}}^2)/(1+ee_{\text{aux}}^2)$. By introducing these new values and formula into Equation (2), EE_{prod} can be calculated from the resulting Equation (4).

$$EE_{\text{prod}} = EE_0\, ee_{\text{aux}} \frac{2}{1+g+(1-g)\,ee_{\text{aux}}^2} \tag{4}$$

The maximum (+)-NLE that can be encountered in this system will be obtained at $g = 0$, when none of the heterochiral species reacts. Linearity could be observed here as well for $g = 1$. At greater g values the NLE will be negative. The computer-calculated curves for this model are presented in Figure 8.

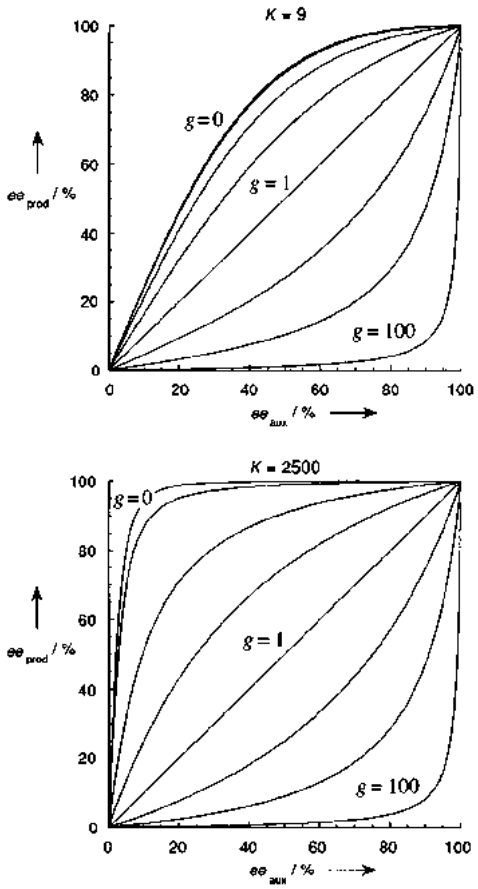

Figure 7. Computer-calculated curves for the ML_2 system for $K = 9$ and 2500.

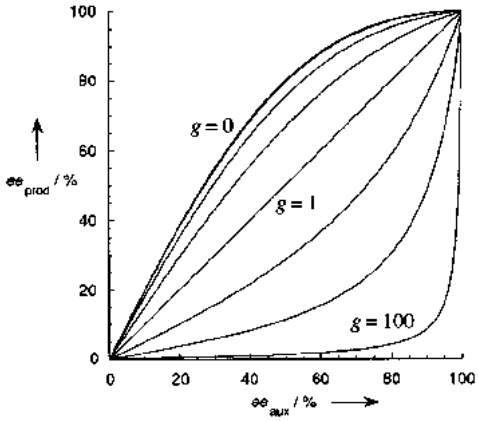

Figure 8. Computer-calculated curves for the ML_2 system with a statistical distribution of the ligands.

Good fits of experimental data can often be achieved from the nonstatistical distribution model, for example Equations (2) and (3).[30] For example, in the asymmetric epoxidation of geraniol (**4**) discussed in Section 2.1; the curve that corresponds well to the data is the one with $EE_0 = 95\,\%$, $K = 1000$, and $g = 0.35$ (Figure 4). These findings imply that the *meso* titanium complex is less reactive ($g = k_{RS}/k_{RR} \approx 1/3$) and much more abundant once the equilibrium is reached ($K = z^2/(xy) = 1000$). This example demonstrates that this model can be of some use in the study of NLEs and, furthermore,

provides some parameters for the discussion of the possible catalysts involved in enantioselective reactions.

A useful development to the ML_n model was reported recently by Blackmond.[20] The author showed that this model could be used to predict some relative reaction rates. These kinetic predictions may then be compared with the experimental data and provide an independent confirmation of the postulated model. For example, the calculations performed for the ML_2 model need to obtain the relative amounts (x, y, z) for the three complexes of Figure 6 as a function of ee_{aux} for a given K value. The overall rate may then be easily computed and compared to the rate for the homochiral complex ($ee_{aux} = 100\,\%$). The calculation has been carried out for the NLE of Figure 4 and showed a strong diminution of the reaction rate when ee_{aux} decreases. As often found in subsequent examples of this review a (+)-NLE usually comes at the cost of the rate of formation of the product.

2.2.2. M*L_2 System

A model, similar to the ML_2 system previously discussed, can be elaborated for the case in which the introduction of chiral ligands on M creates a center of chirality. In such a model, the *meso* complex ML_RL_S encountered in the preceding section becomes $M^*L_RL_S$. The stereochemistry on M is generated by the sequential introduction of the ligands, first producing the monoligated complexes M_RL_R, M_RL_S , M_SL_R, and M_SL_S. Subsequent reaction of those complexes with L_R and L_S finally gives the four pairs of enantiomers as illustrated in Figure 9. Here the heterochiral complexes such as $M_RL_RL_S$

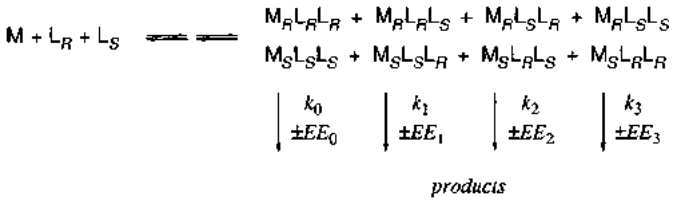

Figure 9. Another model for the NLEs: the M^*L_2 system.

and $M_SL_SL_R$ are enantiomers. Each stereoisomer in Figure 9 has its respective reactivity (k_i) and selectivity (EE_i) and will contribute to the final EE_{prod}. By using the same hypotheses as for the ML_2 system, the M^*L_2 model can be treated with Equations (2) and (3), the only difference being in the definition of the parameters K, g, and EE_o.

This model can be applied to reactions such as the asymmetric Robinson annulation (Section 2.1, Figure 2). The intermediates illustrated in Figure 3 are of the M^*L_2-type and for example, in a complex such as $M_RL_RL_S$, M_R symbolizes the creation of an asymmetric carbon atom with R configuration during the formation of the enamine with the first proline (L_R), and L_S is the second proline molecule involved in the formation of the complex. In this particular situation, where only four stereoisomers are formed, the system can be treated with a statistical distribution as with the ML_2 model. Equation (4) gave, with $EE_0 = 93\,\%$ and $g(=k_{RS}/k_{RR}) = 2$, a curve fitting the experimental results. The same value was found by Agami et al. in their kinetic analysis of the reaction ($k_{homo}/k_{hetero} = 0.5$).[26]

The equations found for the ML_2 systems can be applied to cases where ML_RL_R, ML_SL_S, and ML_RL_S complexes dissociate irreversibly to ML_R and ML_S, with or without the influence of the substrate, that are implicated in the final irreversible catalytic step. This approximation gives fair results but will not be discussed here.[31]

2.2.3. ML_3 System

A model in which species of the type ML_3 or $(ML)_3$ are active catalytic species can be proposed. At least four entities may be responsible for the catalysis: $ML_RL_RL_R$, $ML_SL_SL_S$, $ML_RL_RL_S$, and $ML_SL_SL_R$. The heterochiral complexes encountered here are always chiral and an enantiomerically enriched product is generated simultaneously from homo- and heterochiral species (Figure 10). Calculation of EE_{prod} as

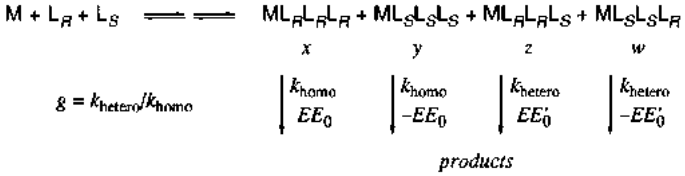

Figure 10. The more complex description of NLEs by the ML_3 system.

a function of ee_{aux} is much more complex in this case. However, the assumption of a statistical distribution of the chiral ligands between the four complexes gives a simplified function (Equation (5)). In this formula, EE_0 and EE'_0 are the

$$EE_{prod} = EE_0 ee_{aux} \frac{3 + 3g\,EE'_0/EE_0 + (1 - 3g\,EE'_0/EE_0)ee^2_{aux}}{1 + 3g + 3(1-g)ee^2_{aux}} \qquad (5)$$

enantiomeric excesses of the product from homochiral and heterochiral complexes (of 100 % *ee*). The parameter $g = k_{hetero}/k_{homo}$ is defined as for the ML_2 system. Figure 11 shows some curves selected for a case where homochiral complexes are more selective ($EE_0 = 100\,\%$) than their heterochiral counterparts ($EE'_0 = 50\,\%$).

From these curves one can observe that if the homochiral complexes are more reactive ($0 \le g < 1$) a (+)-NLE takes

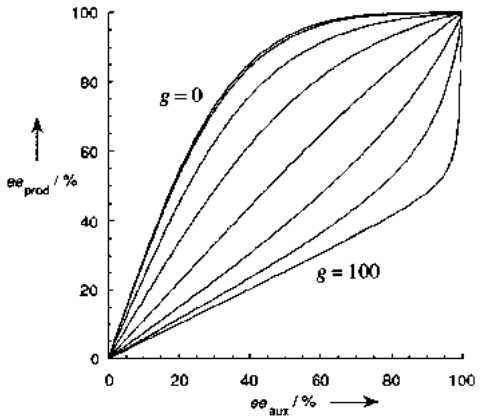

Figure 11. Computer-calculated curves for the ML_3 system with $EE_0 = 100\,\%$ and $EE'_0 = 50\,\%$.

place. If the less selective heterochiral complexes react faster ($g > 1$), a (−)-NLE will then be observed. If the heterochiral complexes are more enantioselective than the homochiral ones, the situation will be quite different. By selecting $EE_0 = 50\,\%$ and $EE'_0 = 100\,\%$, the curves produced by the use of Equation (5) were plotted for various values of g (Figure 12).

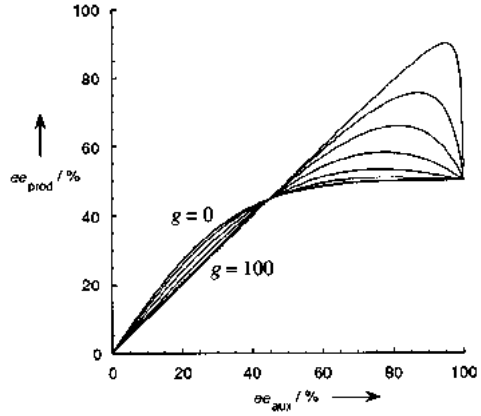

Figure 12. Computer-calculated curves for the ML_3 system for $EE_0 = 50\,\%$ and $EE'_0 = 100\,\%$.

For g values less than one, the curves display a similar behavior as in Figure 11. However, an interesting phenomenon occurs in this mathematical model for larger values of g. The EE_{prod} can be higher at lower ee_{aux} than at 100 % ee_{aux}; at which it drops to the EE_0 (= 50 %) value. If a system can fit this model, the chiral auxiliary will be much more efficient when partially resolved than when enantiomerically pure!

2.2.4. ML_4 System

In an even more complicated scenario the complex can bear up to four chiral ligands to become a ML_4 or $(ML)_4$ system. This will generate the five following complexes: $M(L_R)_4$, $M(L_S)_4$, $M(L_R)_3L_S$, $M(L_S)_3L_R$, and $M(L_R)_2(L_S)_2$. If the $M(L_R)_2(L_S)_2$ complex is assumed to be a *meso* complex (which gives a racemic product), that no additional stereoisomers involving the M center are present, and that, finally, the ligands are distributed on the center in statistical mode, the system is greatly simplified. By introducing the relative reactivities of the two heterochiral complexes (g and f) and taking into account the enantioselectivities of enantiopure homo- (EE_0) and heterochiral (EE'_0) complexes, Equation (6)

$$EE_{prod} = 8\,EE_0\,ee_{aux}\,\frac{1 + ee_{aux}^2 + 2\,g\,(1 - ee_{aux}^2)\,EE'_0/EE_0}{(1 + ee_{aux})^4 + (1 - ee_{aux})^4 + 8\,g\,(1 - ee_{aux}^4) + 6\,f\,(1 - ee_{aux}^2)^2} \quad (6)$$

is obtained. When there is no statistical distribution between the four complexes, two additional parameters are needed to define the relative contribution of the complexes[31]

The ML_4 model can efficiently describe the behavior of catalysts such as the one used in the asymmetric oxidation of methyl-*p*-tolyl sulfide (**6**, Figure 5). A calculated curve that fits the experimental data can thus be obtained. The parameters used mean that an active, but poorly, selective heterochiral species and a large predominance of a weakly active *meso* complex are involved. Quite complicated curves can be generated by the use of the ML_4 model. As an example, two triple-shaped curves are presented in Figure 13.[31]

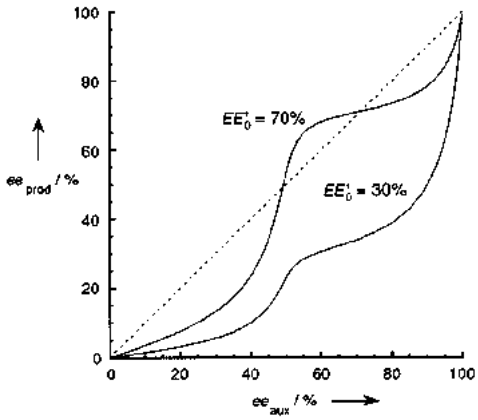

Figure 13. Computer-generated curves for the ML_4 system for $EE'_0 = 30\,\%$ or $EE'_0 = 70\,\%$, $K = 1000$, $K' = 1$, $g = 10$, and $f = 100$.

2.2.5. The Reservoir Effect

The use of a partially resolved chiral ligand in asymmetric catalysis can produce some perturbations generated by the formation of diasteromeric complexes, either within the catalytic cycle or at its periphery. Such perturbation in the cycle cannot be deduced from the sole behavior of the catalyst prepared from the enantiopure complexant. A more detailed analysis is needed and a model in which the active and inactive complexes are taken into account can better describe the system. The model presented here is based on the formation of those two types of catalysts (Figure 14).

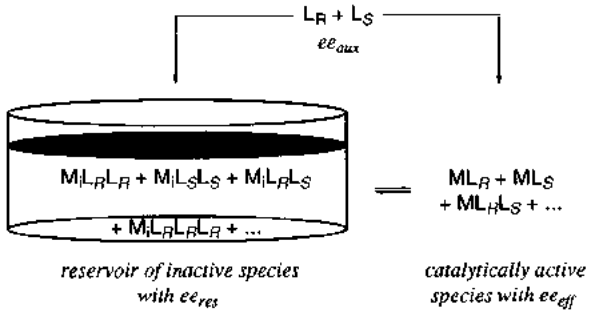

Figure 14. A large pool of unproductive complexes: the reservoir effect model. ee_{res} and ee_{eff} are for the ligands overall.

When a molar amount of ligand with a defined ee_{aux} reacts to form the different species, a part of this (α) can be diverted towards a reservoir; a pool of unproductive complexes with an ee_{res}. This storage will affect the resulting *ee* value of the active portion of the catalysts in such a way that a new value for the *ee* of the $1 - \alpha$ portion of the catalyst left will be attained and called the effective enantiomeric excess (ee_{eff}). This new value can be easily calculated from Equation (7). Such a reservoir

$$ee_{eff} = \frac{ee_{aux} - \alpha\,ee_{res}}{1 - \alpha} \quad (7)$$

can be created through several kind of processes. For example, aggregation can take place before, or in parallel with, the catalytic cycle reaching its steady state. The complexes can thus be stored in inactive oligomeric species, with the one with low aggregation numbers behaving as the catalyst or the catalyst precursor. A reservoir of racemic composition is more easily created by the formation of a heterodimer (*meso*), which is thermodynamically stable and catalytically inactive. Most of the reported (+)-NLEs presented in this review can be explained in such a way. In this simplified model ee_{eff} replaces ee_{aux} in Equation (1), and gives a fair approximation when used to draw curves that fit experimental data.[31]

The models presented in this section can be very useful in the understanding of the behaviors of catalysts. The mathematical expressions are in these cases utilized to extract quantitative parameters relative to the different oligomeric catalytic species that exist in solution. This approach is a mere mathematical interpretation of the experimental data recorded. The following Sections will present some of the results obtained by several groups in search of nonlinear effects in asymmetric synthesis.

2.3. Enantiomeric Catalysts

2.3.1. Addition of Organozincs to Aldehydes

One useful method of alkylating carbonyl compounds is the use of organozinc compounds coupled with a catalyst, which is needed for any reaction to be observed. During their work on the alkylation of benzaldehyde (**8**) by diethylzinc, Oguni et al. discovered in 1988 that a nonlinear effect was present when chiral β-amino alcohols were used as catalysts.[28] Figure 15 shows the results of alkylation in the presence of various chiral amino alcohols. All catalysts exhibited a (+)-NLE in this reaction (called asymmetric amplification by the authors). In Figure 15 (as in all the graphs of this article) positive values will be arbitrarily attributed to the ee_{prod}; such as here where (−)-PDB (or (−)-DDB) and (+)-P_yDB give alcohols of opposite absolute configuration. The (+)-NLE was explained by the authors by the formation of dimeric species in solution. This was confirmed by cryoscopic molecular weight measurements on catalysts generated by the treatment of diethylzinc on enantiomerically pure PDB and racemic PDB. Furthermore, kinetic experiments showed that the reaction with a catalyst prepared with 60% *ee* PDB was 5.5 times faster than the one from racemic PDB.

From these results one can assume that dimers, similar to those discussed in the preceding section, should participate in this amplification of the ee_{prod}. In this alkylation by diethylzinc, it is logical to conclude that if dimers are formed the heterochiral species that retains the minor enantiomer of the catalyst should be less implicated in the reaction; thus leaving the homochiral-enriched dimer free to operate as the active agent or its precursor. Oguni's system with PDB (Figure 15) may be described by the ML_2 model with $EE_0 = 94\%$, $K = 4000$ and $g = 0.015$ ($k_{RS}/k_{RR} \approx 1.5/100$), which shows again the lower reactivity and higher abundance of the heterochiral

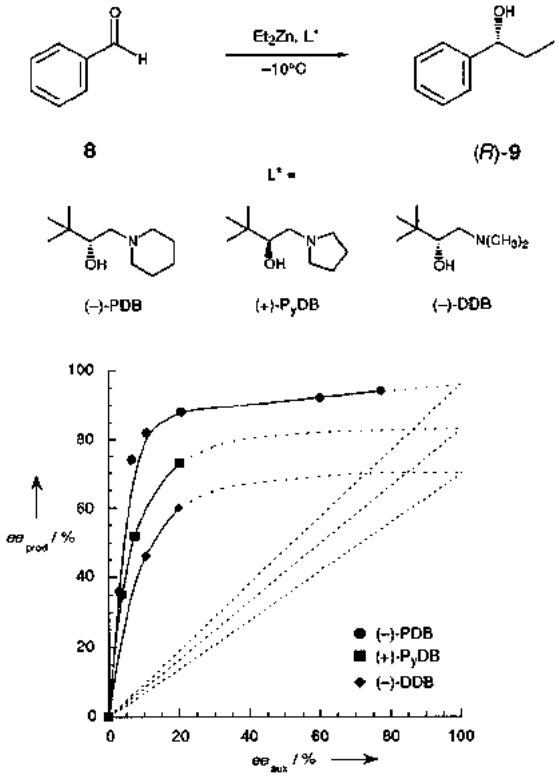

Figure 15. (+)-NLEs on addition of diethylzinc to benzaldehyde (**8**) in *n*-hexane catalyzed by aminoalcohol ligands L* (2 mol%).

catalytic species. If the reservoir effect model is used instead the results are fitted by the use of similar parameters ($EE_0 = 94\%$, $ee_{res} = 0\%$ and $\alpha = 0.87$).

In 1989 Noyori et al. published a mechanistic study on their system of catalyzed addition of organozinc complexes to aldehydes.[32] They also observed a strong (+)-NLE by using various *ee*'s of (−)-3-*exo*-(dimethylamino)isoborneol ((−)-DAIB) as a catalyst (Figure 16). This effect is even more important than the preceding one, with the maximum enantioselectivity of the reaction being reached at a very low *ee* of DAIB (curve ●). Thus, 1-phenylpropanol ((*S*)-**9**) can be prepared in high enantiomeric purity (95% *ee*) with a very impure catalyst (15% *ee*). A similar but less pronounced effect was also observed when dimethylzinc (curve ■) was used in the alkylation. Noyori et al. supposed that this strong (+)-NLE was a result of auto association of the chiral reagent generated by the reaction between (−)-DAIB and the organozinc compound. The organometallic DAIB–zinc complex formed undergoes dimerization as depicted in Figure 17. When a mixture of (−) and (+)-DAIB was used, two types of dimeric species were formed: homochiral ((−)·(−)-**10** and (+)·(+)-**10**) and heterochiral ((−)·(+)-**10**); the signs refer to the enantiomer of the chiral ligand included in the complex. The enantiomeric monomers DAIB–ZnR (R = Me or Et) are the active catalysts in this reaction and each one produces predominantly one enantiomer of alcohol **9**.

In a study on the influence of the amount of chiral catalyst on the outcome of the reaction, (−)-DAIB in 14% *ee* was used and the ee_{prod} of (*S*)-**9** was plotted as a function of the relative amount (mol%) of the catalyst (Figure 18). From

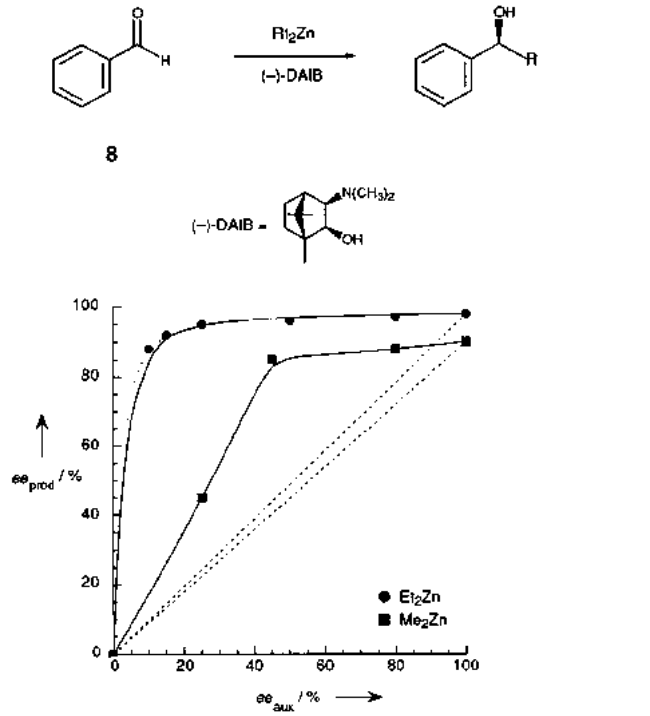

Figure 16. (+)-NLEs in the DAIB-catalyzed (8 mol%) addition of dialkylzinc compounds to benzaldehyde (**8**) in toluene.

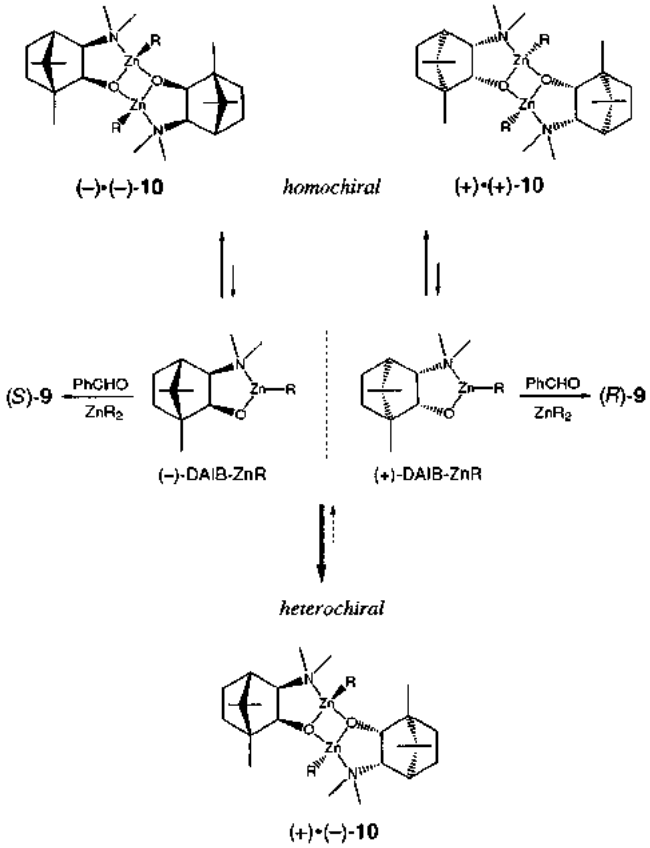

Figure 17. Homochiral and heterochiral dimers formed by the DAIB-alkylzinc reagent.

these results, the turnover efficiency of the homochiral precatalyst was estimated to be 1200 times greater than that of the heterochiral one.

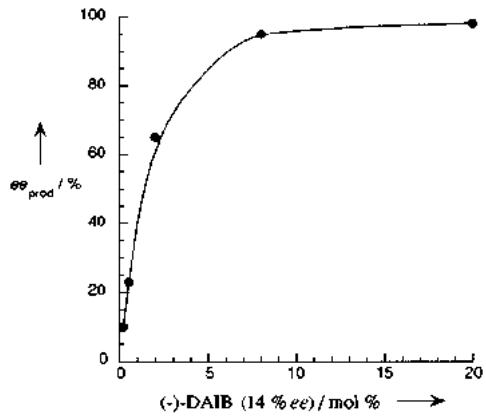

Figure 18. Variation in the ee_{prod} for (*S*)-**9** as a function of the amount of (–)-DAIB (14% *ee*) used in the addition of diethylzinc to benzaldehyde (**8**).

The existence and behavior of the dimeric species were well confirmed by numerous experiments. Cryoscopic molecular weight measurements demonstrated that DAIB – ZnR existed effectively as dimers in solution. NMR measurements of homochiral and heterochiral reagents gave insights as to the relative stability of the dimeric organozinc compounds. Noticeable changes were observed in the NMR spectrum of the homochiral dimer (–)·(–)-**10** upon addition of benzaldehyde, whereas the spectrum of the heterochiral complex (+)·(–)-**10** remained the same, thus revealing a greater stability.

The differences were understood by X-ray diffraction analysis of each of the dimers obtained by treatment of dimethylzinc with the chiral catalyst (Figure 19). The homo

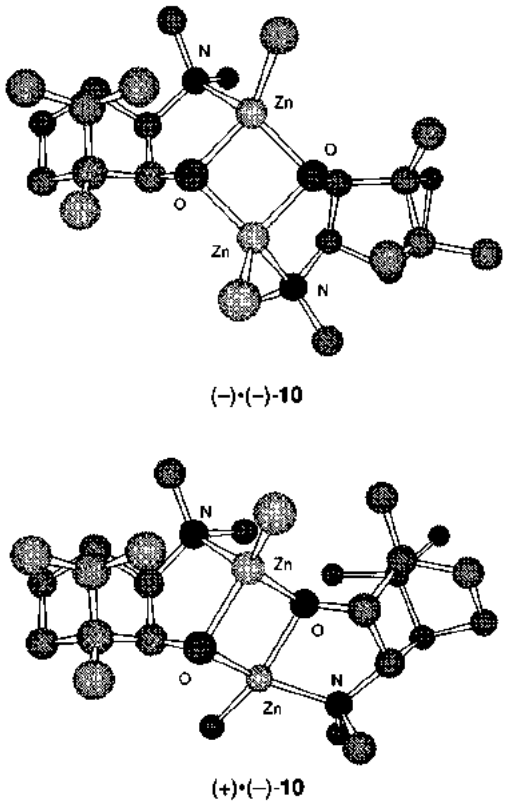

Figure 19. Three-dimensional models of the dimers of (–)-DAIB-methylzinc: (–)·(–)-**10** (homochiral) and (–)·(+)-**10** (heterochiral).

chiral species $(-)\cdot(-)$-**10** ($R = CH_3$) possesses a C_2 symmetry with a Zn_2O_2 four-membered ring with a *syn* relationship between the methyl groups on the zinc atoms. This ring is "*endo* fused" relative to the DAIB–Zn system. The heterochiral dimer $(+)\cdot(-)$-**10** ($R = CH_3$) also has a Zn_2O_2 cycle "*endo* fused" to the structure but the methyl groups on the metallic centers, as well as the DAIB fragments, are oriented in an *anti* fashion, which explains the greater thermodynamical stability of this dimer. This was later complemented by energetic calculations on simpler models by the same group.[32b]

If the ML_2 model is used for the reaction performed by Noyori et al. with their DAIB catalyst, the values of $EE_0 = 98\,\%$, $K = 5000$, and $g = 0.01$ ($k_{RS}/k_{RR} \approx 1/100$) give a curve that fits the experimental results. The results may also be analyzed using the reservoir effect model. Noyori's system approximates better to $EE_0 = 98\,\%$, $ee_{res} = 0\,\%$, and $\alpha = 0.88$. The values extracted hereby confirm a greater stability ($k_{RS}/k_{RR} \approx 1/100$) of the heterochiral complex, and its preponderance ($K = 5000$), in regard to the homochiral one.

Bolm et al. worked on this alkylation reaction as well but used a substituted pyridine alcohol as the chiral catalyst (Figure 20).[33] The ethylation of benzaldehyde (**8**) was very

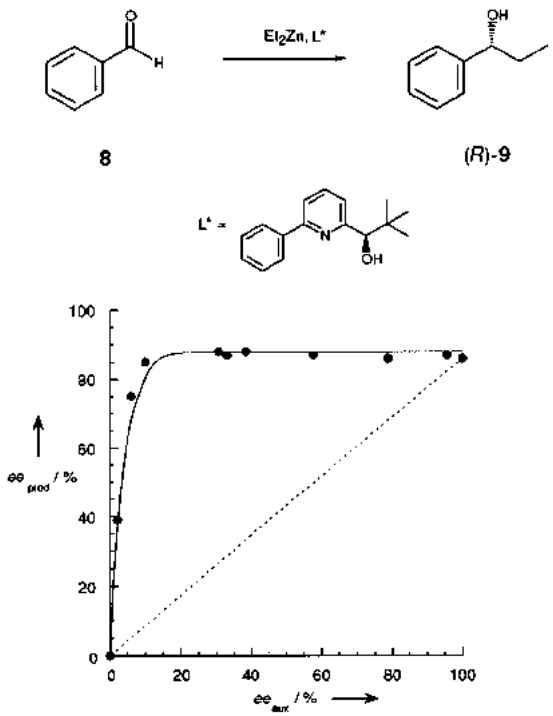

Figure 20. (+)-NLEs in the addition of diethylzinc to benzaldehyde (**8**) with a pyridine alcohol as the catalyst.

efficient with 5 mol% of the catalyst and Et_2Zn and gave access to (*R*)-1-phenylpropanol ((*R*)-**9**). By varying the *ee* value of the pyridine catalyst, they discovered that a (+)-NLE was taking place, as seen in Figure 20.

The (*R*)-cat-ZnEt and the (*S*)-cat-ZnEt can interact in solution to give the homochiral dimers $(R)\cdot(R)$-**11** and $(S)\cdot(S)$-**11** and the heterochiral species $(R)\cdot(S)$-**11** (Figure 21). If the heterochiral complex is favored over the homochiral ones,

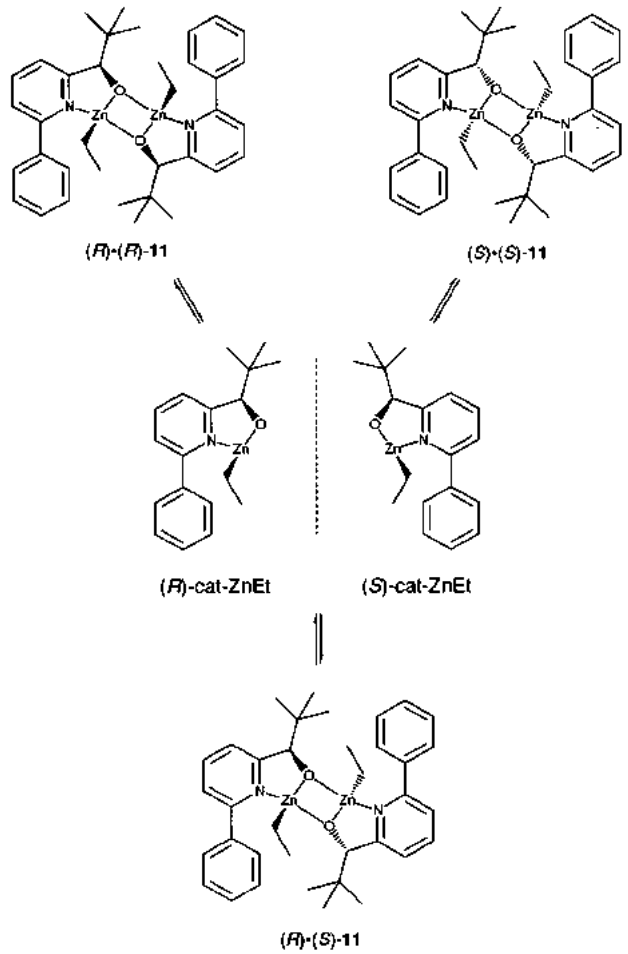

Figure 21. The different dimers formed in solution between the enantiomeric pyridine alcohol–ethylzinc reagents.

the effect of diverting the minor enantiomer from the reaction mixture will be a net increase in the *ee* value of the active catalyst, thus generating this strong (+)-NLE.

Bolm et al. observed the formation of a white precipitate when the pyridine alcohol was treated with an excess of diethylzinc. Starting with a (*R*)-catalyst in 50% *ee*, filtering off the resulting solid, and hydrolyzing both mother liquor and precipitate, two fractions of the ligand catalyst were obtained. The one from the crystalline material, and corresponding to 74% of the starting materials, had a value of 44% *ee*. However, the ligand recovered from the filtrate (26% yield) was of 84% *ee*. This was a clear indication of enrichment of the major enantiomer by predominant precipitation of the *meso* complex and suggested a possible greater stability of this species.

When the precipitation was conducted independently with the (*R*)-catalyst and its racemic form, the solid from the enantiopure pyridine alcohol was very unstable while the one from the racemic alcohol was stable enough to be isolated. The structure of the crystallized solid was determined by X-ray analysis and proved to be the one of a C_i-symmetric dinuclear zinc complex composed of each of the enantiomeric catalysts around a central Zn_2O_2 four-membered cycle; namely the heterochiral dimer $(R)\cdot(S)$-**11** (Figure 22). The ethyl and *tert*-butyl substituents on each subunit are *syn* to

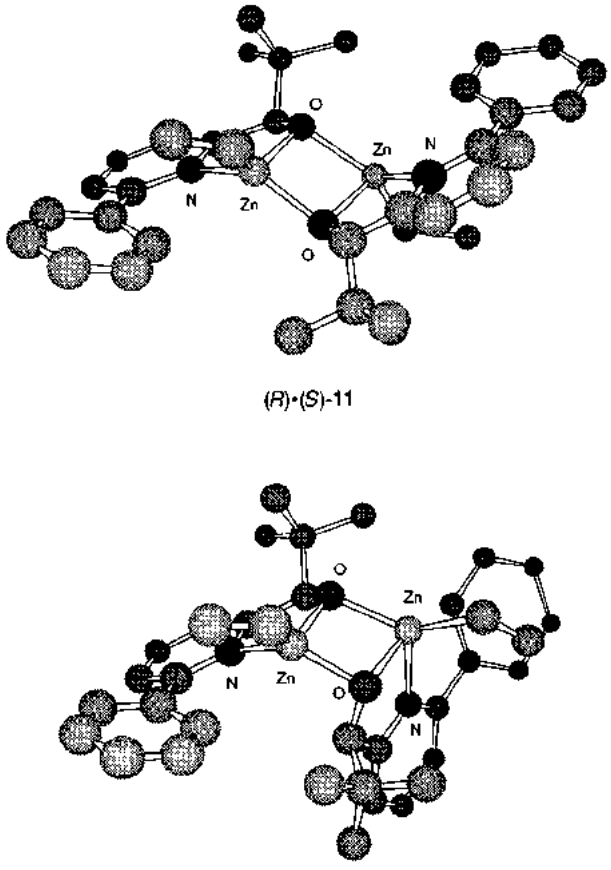

Figure 22. Structure of the dimeric species $(R)\cdot(S)$-**11** in the crystal and proposed structure of $(R)\cdot(R)$-**11**.

each other, but they end up *anti* to the substituents of the other unit in the global structure as a result of the overall symmetry. The speculated structure of the homochiral dimer is also presented in Figure 22. The $(R)\cdot(R)$-**11** complex has C_2 symmetry with the usual Zn_2O_2 cycle. The alkyl chains on the subunits are still *syn* to each other but the complex system presents a molecular cavity. The steric congestion generated by this geometry, in conjunction with the fact that the zinc atoms are relatively exposed on the convex surface of the dimer, can be an explanation of its lower stability and high reactivity towards air and moisture.

The dimeric structure was easily detected by mass spectrometry. However, the solid isolated from the (*R*)-catalyst showed no evidence of such dimeric species with the molecular ion peak in the mass spectrum being very weak in intensity. This indicates that, if the homodimer is formed, it possess a low stability. The exact structure was not elucidated, but NMR spectroscopy of homo- and hetero-dimeric zinc compounds were reported to be different.

Another example of nonlinear effects in this area is the work of Kellogg et al. on derivatives and analogues of ephedrine as catalysts.[34] The reactions were performed with 5 mol% of *N*-methylephedrine (NME), *N*-methylephedrine disulfide (NMED), and *N*-methylephedrinethiol chlorhydrate (NMET·HCl) as shown in Figure 23. The ethylation of benzaldehyde (**8**) under those conditions leads to the alcohol

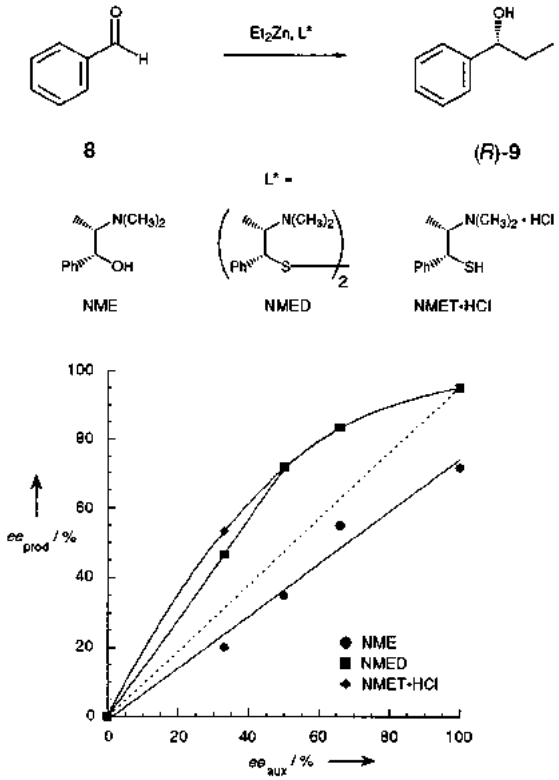

Figure 23. NLEs observed in the 1,2-addition of diethylzinc to benzaldehyde (**8**) catalyzed by derivatives and analogues of ephedrine (5 mol%, toluene, $-20\,^{\circ}C$).

(*R*)-**9** in all cases. The use of NME showed no particular irregularities in the linear relationship between its *ee* value and the *ee* value of (*R*)-**9** alcohol. However, when using NMED or NMET·HCl an evident (+)-NLE was observed, which was almost identical regardless of the catalyst used.

In order to understand the differences between the catalysts cryoscopic molecular weight measurements were done with NME and NMET·HCl after reaction with various amounts of Et_2Zn. With one equivalent of diethylzinc, oligomeric structures seem to exist in solution in both cases. NME was expected to give rise to an equal mixture of dimer and tetramer based on the results, while NMET·HCl only gave the molecular weight of a tetrameric complex. Addition of an extra equivalent of the dialkylzinc compound only resulted in a total breakdown of the oligomeric structures, with only monomers being detected with the two chiral compounds. It was then proposed by the authors that, in order to observe any NLE, heterochiral (*meso*) aggregates have to be stable to extra diethylzinc and generate an aggregation-induced enrichment of the major enantiomer of the catalyst.

2.3.2. 1,4-Addition of Organozinc Compounds

The use of alkylzinc compounds, far from being limited to the 1,2-addition reported in the preceding section, can also be extended to conjugated additions on α,β-unsaturated carbonyl compounds. This can be achieved by using nickel in catalytic amounts, the dialkylzinc compound, and a chiral catalyst in order to perform an asymmetric version of the reaction.

Bolm and his group studied this reaction with pyridine alcohol acting as the catalyst precursor (Figure 24).[35] The addition of diethylzinc to chalcone (**12**) in the presence of

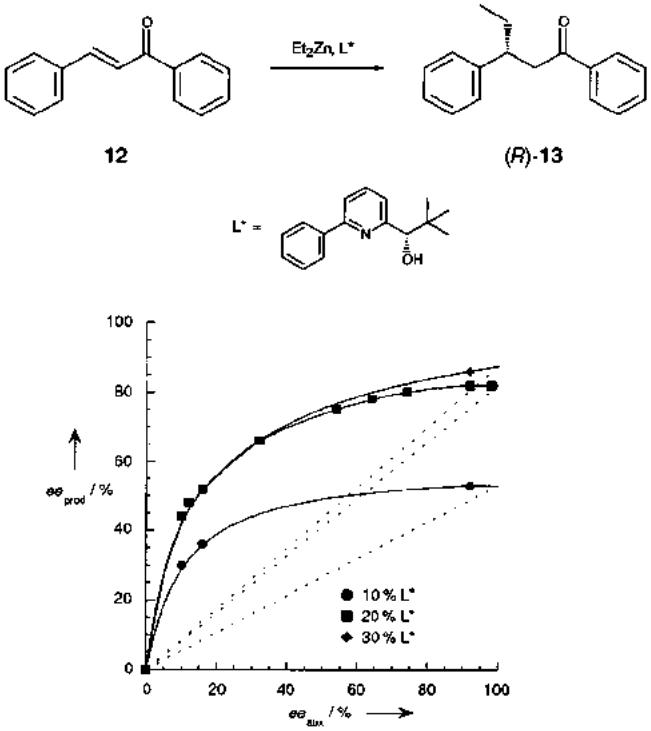

Figure 24. (+)-NLEs encountered in the pyridine alcohol (20 mol %) catalyzed asymmetric 1,4-addition of diethylzinc to chalcone (**12**) (1 mol % $[Ni(acac)_2]$, acetonitrile, $-30\,^{\circ}C$).

20 mol % of the catalyst and 1 mol % of $[Ni(acac)_2]$ gave efficient access to the ketone (*R*)-**13** (acac = acetylacetone acetate). When the catalyst was used in various enantiomeric excesses under these conditions, a strong (+)-NLE was observed. Moreover, the use of different quantities of the catalyst had an influence on the resulting curves. While 30 mol % gives essentially the same shape as with 20 mol % (curves ◆ and ■, respectively), a smaller amount of catalyst (10 mol %, curve ●) lowers the enantioselectivity and modifys the appearance of the curve.

The positive influence of the concentration of the catalyst was also confirmed by performing the reaction with the chiral pyridine ligand in 16 % *ee* at various mol %. The results are shown in Figure 25 a) and the plot against ee_{prod} clearly demonstrates the increased selectivity of larger amounts of the catalytic species, which reaches a maximum at 30–40 mol %. The asymmetric amplification was also tested against the time until the reaction was complete (Figure 25 b). When a 19 % *ee* catalyst was used in this reaction the ee_{prod} was shown to strongly decrease with the conversion. The use of the substituted pyridine with 89 % *ee* also demonstrated a time dependence of the ee_{prod}, but in a less pronounced fashion.

The (+)-NLE was initially explained on the basis of the results and studies done by this group during the course of their research on the 1,2-addition of organozinc compounds.[33] Formation of dimeric zinc catalysts (Figure 21) is sufficient to understand the phenomenon taking place. The stable heterochiral dimer, which acts as a trap for the minor enantiomer, increases the *ee* value of the major one (reservoir effect). The more reactive homochiral dimers left should then react with nickel(II) to form the active catalyst with an *ee* value greater than the one of the chiral pyridine introduced to the mixture. The concentration effect can be explained by a shift in the equilibrium between monomers and dimers. The more concentrated the catalyst becomes, the more dimers should form and thus increase the (+)-NLE.

However, the use of coordinating solvents such as acetonitrile, needed for the nickel catalysis, has deleterious effects on enantioselectivities in carbonyl alkylation reactions. This is possibly the result of the solvent preventing the dimerization of the catalyst–zinc species. Another explanation was thus necessary and was offered by Bolm et al. (Figure 26). A similar type of homo and heterochiral relationship between the two molecules of catalyst implicated can be found here, but the metal complexation is quite different. In this case, it has been postulated that the chiral pyridine first reacted with $[Ni(acac)_2]$ to form the two enantiomeric (*S*)- and (*R*)-**14**. These react further with another molecule of the pyridine with the same (homo) or the opposite (hetero) configuration. This leads to the formation of homochiral mononuclear complexes (*S*)·(*S*)-**15** and (*R*)·(*R*)-**15** and the heterochiral complexes (*S*)·(*R*)-**15**. The reaction of diethylzinc with these nickel complexes should proceed with the less stable ones and, from the (+)-NLE observed in this particular case, it has to be the homochiral (*S*)·(*S*)- and (*R*)·(*R*)-**15** dimers. A *meso*, or heterochiral species{(*S*)·(*R*)-**15**}, diverts the minor enantiomer from the catalytic pathway and generates this positive nonlinear effect.

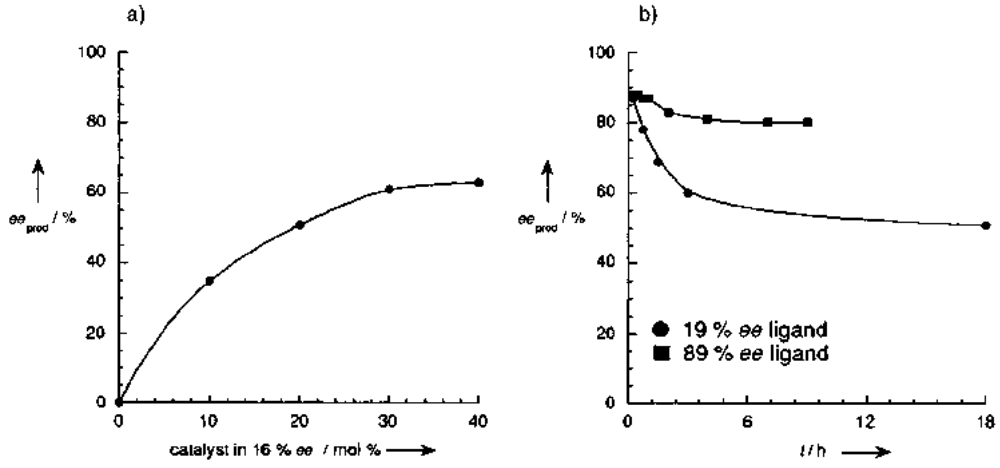

Figure 25. *ee* of product (*R*)-**13** as a function of a) the quantity of pyridine alcohol (16 % *ee*) and b) the reaction time with the ligand in 19 and 89 % *ee*.

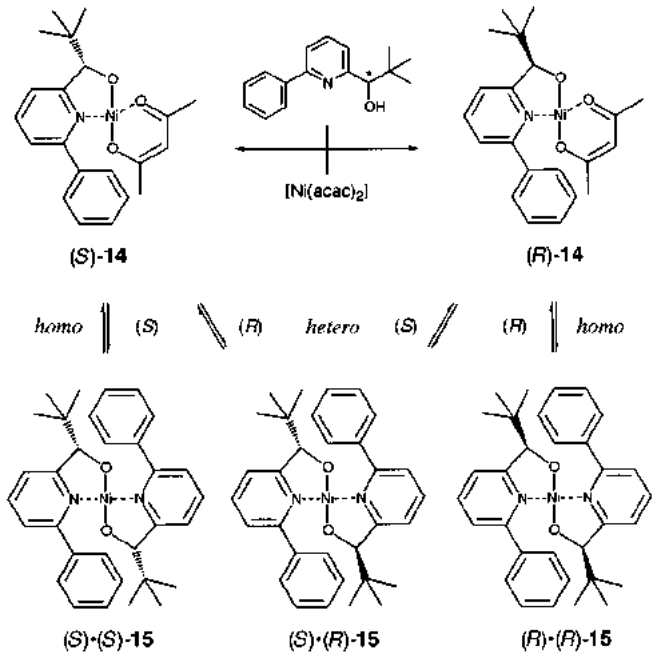

Figure 26. Proposed equilibrium between the monomers and dimers in the catalyzed addition of dialkylzinc compounds in the presence of nickel(II).

Since the formation of the heterochiral dimer reduces the total amount of active catalyst in solution, the decrease in the reaction rate on using a catalyst with a low *ee* value can be explained. One can see from the curves of Figure 25 that a reaction completed in 9 h with a 89% *ee* catalyst takes twice this time with a catalyst in 19% *ee*, because of the presence of a larger amount of the less reactive *meso* dimer. Even if the heterochiral complex is much more stable than the homochiral species longer reaction times seem to permit its dissociation, since ee_{prod} drops with conversion. The 89% *ee* catalyst, in which a lower amount of heterochiral dimeric structure is present, shows only a slight drop in the *ee* value while the one from 19% *ee* falls quite abruptly.

Bolm's 1,4-addition of diethylzinc to chalcone (Figure 24) displayed an $EE_0 = 82\%$, $K = 1000$, and $g = 0.1$ ($k_{RS}/k_{RR} \approx 1/10$) if one uses the ML_2 model to describe the system. These values and the experimental data are in accordance with the more stable *meso* complex hypothesis. The same reaction was studied by Feringa et al. but with (−)-DAIB as the chiral catalyst (Figure 27).[36] The 1,4-addition reaction to chalcone (**12**) was run with 16 mol% of DAIB. By varying its *ee* value and constructing a plot against the measured *ee* value of the resulting ethylated product (*R*)-**13** it was easy to visualize a (+)-NLE. This NLE was shown to be dependent on the concentration, as for Bolm's system, but in this case the influence of the amount of Ni^{II} salt was investigated. While the amount of DAIB was kept constant (16 mol%), the quantity of $[Ni(acac)_2]$ used for the reaction was of 1, 7, and 8 mol% (curves ●, ■, and ◆, respectively). The effect of increasing the nickel ratio was deleterious for both maximum enantioselectivity and the amplitude of the NLE.

It was suggested that two equivalents of DAIB reacted with $[Ni(acac)_2]$ as illustrated in Figure 28. Such an introduction of two molecules of the chiral auxiliary should give rise to three

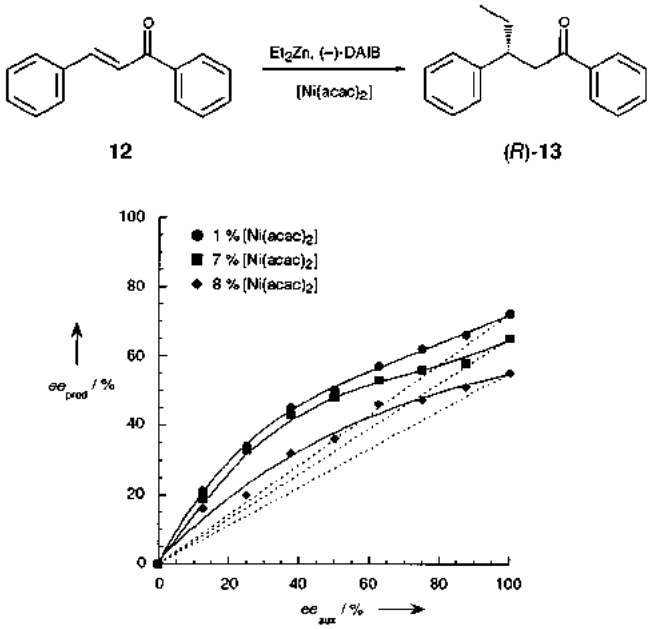

Figure 27. (+)-NLEs in DAIB-catalyzed (16 mol%) 1,4-addition of diethylzinc compounds to chalcone (**12**) (acetonitrile, −30 °C).

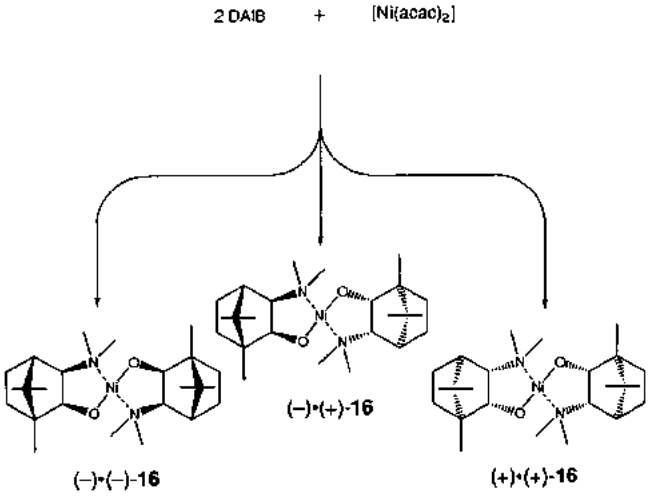

Figure 28. Intermediate dimeric species formed during the DAIB-catalyzed 1,4-addition.

possible complexes: homochiral (−)·(−)-**16** and (+)·(+)-**16** entities and the heterochiral complex (−)·(+)-**16**. The (+)-NLE taking place here implies, as it was seen before, a greater stability of the *meso* (−)·(+)-**16** species. The structures shown in Figure 29 can help to understand structural differences

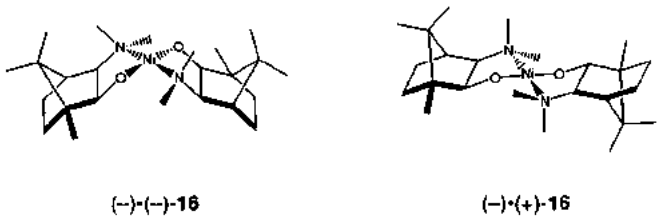

Figure 29. Perspective structural formulas of the DAIB – nickel complexes (−)·(−)-**16** and (−)·(+)-**16**.

between (−)·(−) and (−)·(+)-**16**. In the latter the two enantiomeric aminoisobornyloxy moieties are antiperiplanar, which assures lower steric interactions than its (−)·(−) analogue. The less stable homochiral structures should then be implicated more readily in the reaction than the heterochiral one, which keeps the minor enantiomer away in a thermodynamically-driven dimerization process.

2.3.3. 1,4-Addition of Cuprates

Nonlinear effects in 1,4-addition reactions are not restricted to the reagents discussed previously, but can also be encountered when cuprates are used. In 1994 Pfaltz and Zhou reported a (−)-NLE in the addition of isopropylcuprate to cycloheptenone (**17**, Figure 30).[37] The use of a chiral copper

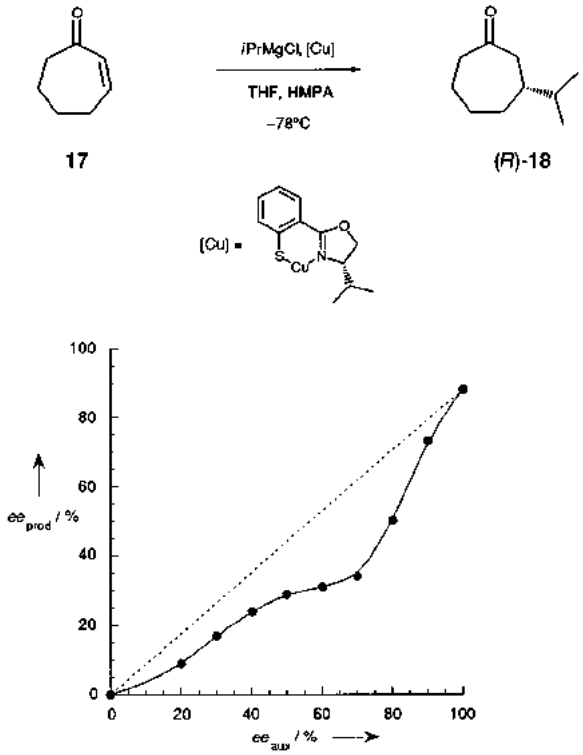

Figure 30. (−)-NLE observed in the copper catalyzed 1,4-addition of *i*PrMgCl to **17**.

oxazolinethiolate as the catalyst in this reaction gave access to the substituted suberone (*R*)-**18**. The *ee* value of this product was, for all ee_{aux}, lower than it should be, and thus generates the multishaped curve in Figure 30. This (−)-NLE is a clear indication of a different behavior of the copper catalyst when compared with the results of the 1,4-addition presented in the preceding section. Even if no explanation was given for this NLE, one can suggest that the aggregation of cuprates, which is usually more complex than with other organometallic reagents, is responsible for this effect. However, more information on the structure of the catalytic species involved is necessary to get a better understanding of this phenomenon.

This behavior seems to be a constant in cuprate addition reactions (at least with analogous catalysts); van Koten et al. discovered a multishaped NLE while working on the methylation of benzylideneacetone (**19**).[38] Thus, the chiral, aromatic copper aminothiolate (Figure 31) permits an effective alkylation and gives rise to the product (*S*)-**20**. A nonlinear effect that is just above the linear relation relation-

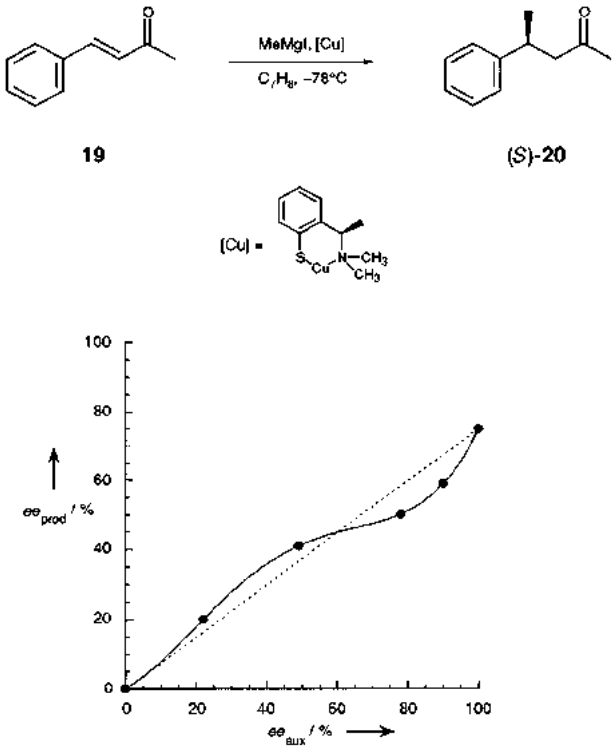

Figure 31. NLE in a copper-catalyzed 1,4-addition of MeMgI to benzylideneacetone (**19**).

ship between ee_{prod} and ee_{aux} was observed from 0 to 50% *ee*; at higher *ee* values, it becomes a moderate (−)-NLE. The intervention of multinuclear species as being responsible for this NLE has been invoked, but no exact explanation can be given here. The oligomeric structures should influence the *ee* value of the catalyst, and leave a mononuclear species with a modified enantiomeric excess. The curves of Figure 30 and 31 are reminiscent of those discussed for the ML_4 model.

2.3.4. Glyoxylate – Ene Reaction

One of the earliest and striking reports of nonlinear effects was published in 1990 by Mikami, Nakai et al.[39] In their study of the glyoxylate – ene reaction, mediated by chiral Lewis acid catalysts, they encountered a very strong (+)-NLE with the titanium catalyst derived from 1,1′-bi-2-naphthol (BINOL). Figure 32 depicts the reaction of α-methylstyrene (**21**) and methyl glyoxylate (**22**). The *ee* value of (*R*)-**23** was plotted against the one of (*R*)-BINOL (ee_{aux}). From the curves it can be observed that the effect is almost identical for catalysts prepared from (*R*)-BINOL and $(i\text{-PrO})_2TiBr_2$ (curve ●) or $[Ti(OiPr)_2Cl_2]$ (curve ○).

A series of studies were undertaken by this group and proved to be very helpful in understanding the exact nature of the catalyst in solution.[39c] The BINOL should react first with $[Ti(OiPr)_2X_2]$ (X = Cl, Br) to form, by alkoxy exchange, both

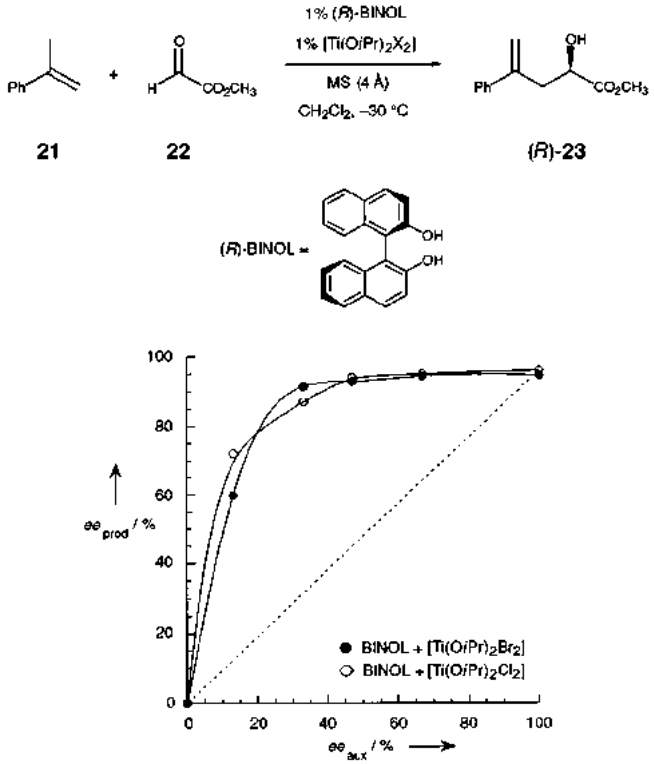

Figure 32. (+)-NLEs in the BINOL–titanium catalyzed ene reaction between **21** and **22**. MS = molecular sieve.

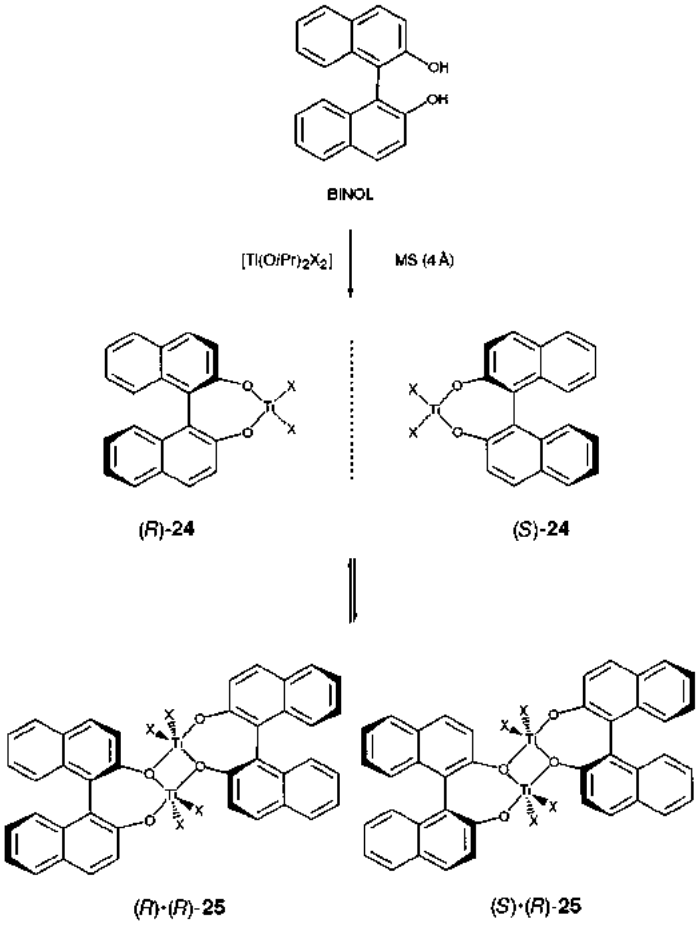

Figure 33. Homochiral ((*R*)·(*R*)-**25**) and heterochiral ((*S*)·(*R*)-**25**) dimers formed between the enantiomeric BINOL–titanium catalysts.

enantiomers of BINOL-TiX_2, (*R*)- and (*S*)-**24** (Figure 33). Those monomers then become implicated in an equilibrium with their dimers (*R*)·(*R*)-**25**, (*S*)·(*S*)-**25** (not shown here), and (*S*)·(*R*)-**25**. The same behavior discussed previously must be encountered to generate the (+)-NLE. Vapor pressure osmometry measurements showed that dimers are formed. Furthermore, the molecular weight of the complex prepared from enantiomerically pure (*R*)-BINOL (homochiral) was concentration dependent, whereas the one from *rac*-BINOL (heterochiral) does not change at all with dilution. This observation is an indication of a greater stability of the *meso* dimer. Kinetic measurements showed (*R*)·(*R*)-**25** to be 35 fold more active than (*S*)·(*R*)-**25**. Since the monomeric species are held responsible for the catalysis, these experiments clearly show that the homochiral dimeric structures dissociate more readily than the corresponding heterochiral ones.

Stability differences can be understood by simply looking at three-dimensional representations of the dimers proposed by the authors (Figure 34). Both structures possess a central four-membered Ti_2O_2 ring around which are organized the chiral

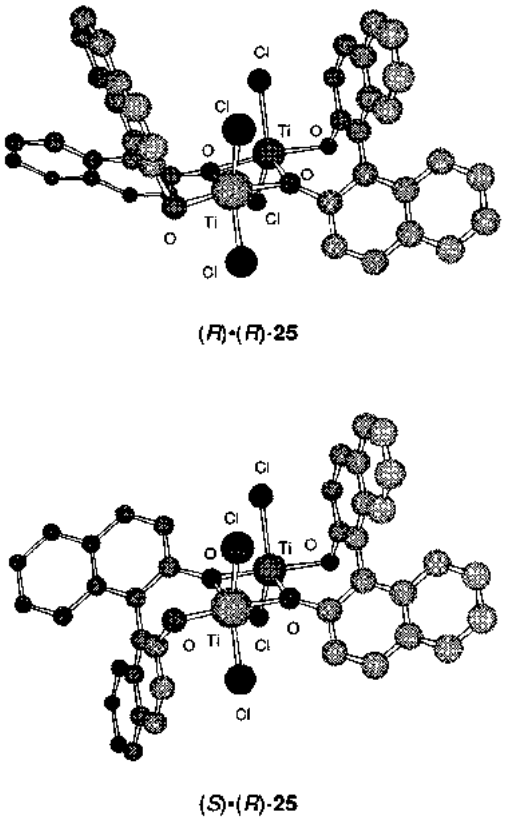

Figure 34. Structures of the dimeric species (*R*)·(*R*)-**25** and (*S*)·(*R*)-**25**.

units. Steric interactions are much more important in the C_2 symmetrical dimer (*R*)·(*R*)-**25**, since the binaphthyl moieties are *syn*-periplanar and close together. However, in the heterochiral complex (*S*)·(*R*)-**25**, which has a C_i symmetry and a coplanar instead of distorted Ti_2O_2 ring, the spatial orientation of the ligands (*anti*-periplanar) seems in fact to offer a greater stability.

The effect of the amount of catalyst on the NLE was also investigated. Various quantities of (*R*)-BINOL (31 % *ee*) ranging from 1 mol % to 100 mol % were introduced in the mixture and the ee_{prod} measured. Figure 35 shows that an

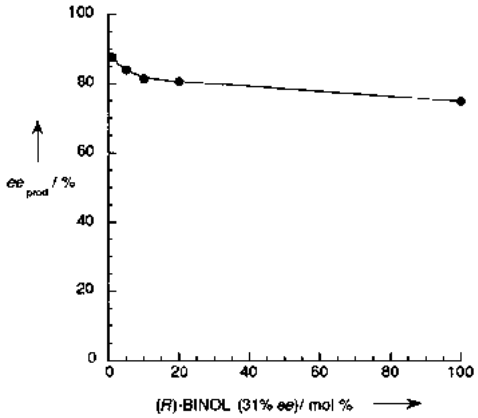

Figure 35. ee_{prod} of (*R*)-**23** as a function of the amount of (R)-BINOL (31 % *ee*).

increase in the amount of catalytic species, and thus its concentration, lowers the NLE. This observation is in total disagreement with the monomer/dimer equilibrium. This divergent behavior was, however, explained from molecular weight determinations on the catalyst prepared from 31 % *ee* BINOL by the appearance of a trimeric species at higher concentrations.[39c, d] The Mikami and Nakai ene-reaction with a BINOL-derived catalyst can however be described with the following parameters for the ML_2 system; $EE_0 = 98\,\%$, $K = 2300$ and $g = 0.005$ ($k_{RS}/k_{RR} \approx 1/200$), which give the best fit with the experimentally derived curve.

The glyoxylate – ene reaction can also be driven by another type of catalyst developed more recently. Mikami and Terada,[40] and later Nakai et al.,[41] reported the preparation of this new titanium catalyst **26** (Figure 36). Reaction of (*R*)-BINOL with either $[Ti(OiPr)_2X_2]$ (where X = Cl, Br) or

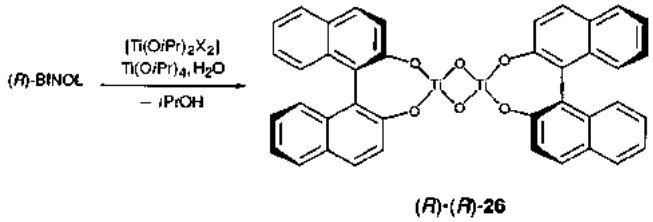

Figure 36. Synthesis of **26**.

$[Ti(OiPr)_4]$ and water, followed by heating and the azeotropic removal of isopropyl alcohol in refluxing toluene led to the formation of the μ-oxo titanium complex (*R*)·(*R*)-**26**. The existence of such a μ-oxo dimeric species in solution was confirmed by molecular mass measurements by vapor pressure osmometry and infrared spectroscopy,[40] as well as by mass spectrometry and NMR spectrocopy.[41] Moreover, the μ-oxo complex mass has a different behavior depending on the *ee* value of the BINOL used to prepare it.[40] When enantiomerically pure (*R*)-BINOL was utilized the apparent molecular weight was shown to be concentration-dependent; while with the racemic BINOL it remained unchanged upon dilution. This indicates a greater stability of the μ-oxo dimer prepared from *rac*-BINOL in solution over the homochiral complex (see above). This was an indication of a possible nonlinear behavior with this new catalyst.

When the ee_{prod} was tested in the glyoxylate – ene reaction against the *ee* value of the BINOL used to prepare the catalyst **26** a strong (+)-NLE was observed (Figure 37). The amount of

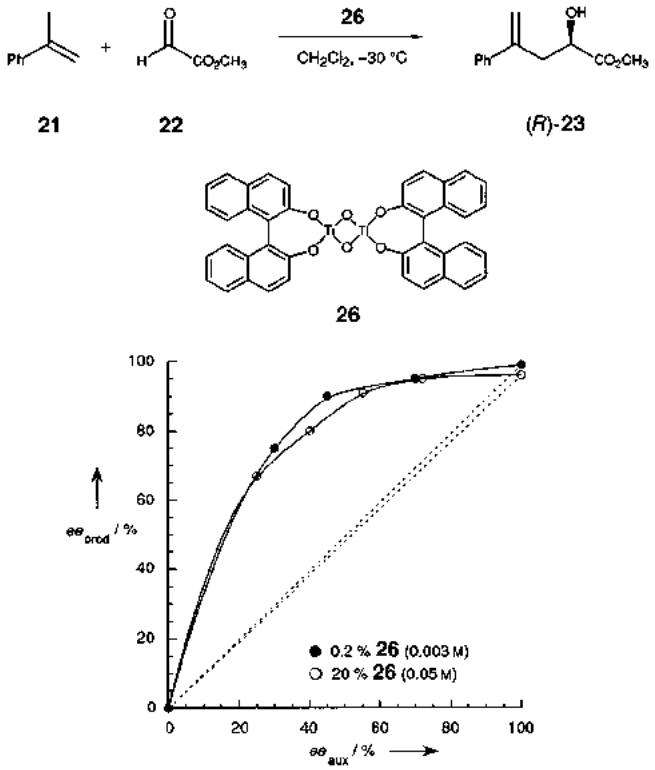

Figure 37. (+)-NLE observed in the ene reaction catalyzed by **26**.

the catalytic species had little effect on the amplifying phenomenon. The *meso* μ-oxo catalyst accounted for the increase of the *ee* value of the catalytic substance. In fact, the homochiral catalyst possessed a catalytic activity nine times superior to that of the heterochiral one. Furthermore, molecular modeling on the three-dimensional representations of the μ-oxo (*R*)·(*R*)- and (*S*)·(*R*)-**26** (Figure 38) showed the heterochiral (*S*)·(*R*)-**26** to be 1.08 kcal mol^{-1} lower in energy.[40]

2.3.5. *Trimethylsilylcyanation of Carbonyl Compounds*

Oguni et al. investigated the asymmetric cyanation of carbonyl compounds with trimethylsilylcyanide (TMSCN), as illustrated in Figure 39.[42]. The catalyst is prepared by freeze-drying a solution of an equimolar mixture of (+)-diisopropyl tartrate {(+)-DIPT} and $[Ti(OiPr)_4]$. It is then used in the reaction in the presence of isopropyl alcohol. This reaction gives trimethylsilylated cyanohydrines in both good chemical yields and enantioselectivity. For example, benzaldehyde (**8**) gives the corresponding compound (*R*)-**27**. This

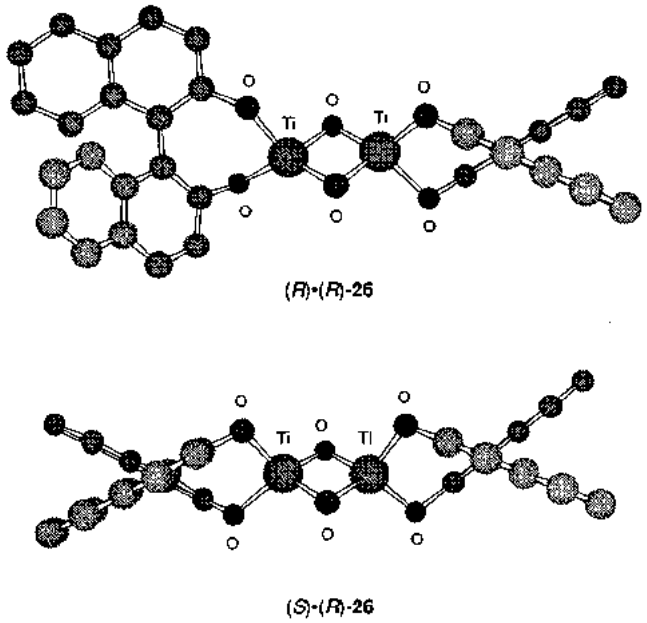

Figure 38. Three-dimensional representations of homo- and heterochiral μ-oxo-titanium complexes $(R)\cdot(R)$- and $(S)\cdot(R)$-**26**.

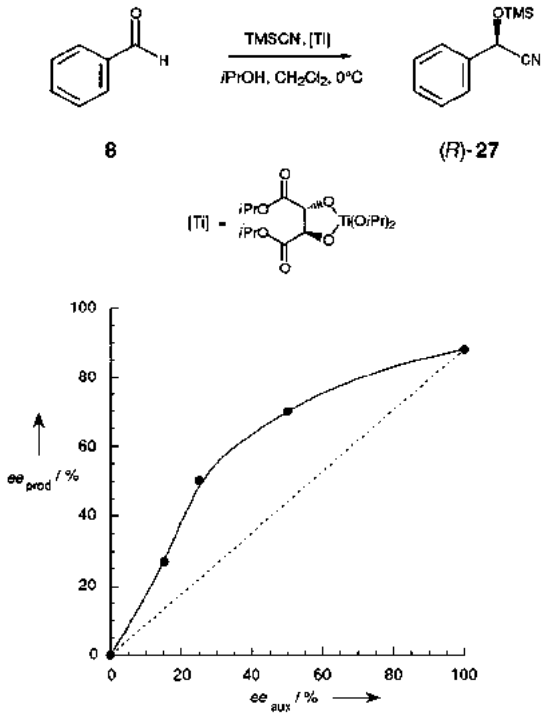

Figure 39. (+)-NLE in the trimethylsilylcyanation of benzaldehyde (**8**) with a chiral titanium catalyst (20–100 mol%).

asymmetric synthesis works well with 20 mol% of the catalyst, but selectivities are better with stoichiometric amounts. The authors tested the effect of the incorporation of partially resolved (+)-DIPT in the preparation of the catalyst. By using one equivalent of this species, the enantiomeric excesses of the product **27** were measured and a nonlinear effect observed (Figure 39). This effect was not explained because of the lack of information on the structure of the catalyst. However, the spectral analysis of the freeze-dried compound suggested an oligomeric structure of the type $[\{Ti(OiPr)_2(DIPT)\}_n]$, which breaks down to a simpler structure upon addition of the alcohol to the mixture.[42b] This NLE is reminiscent of the one encountered in the Sharpless epoxidation discussed in the Section 2.1.

2.3.6. Allylation and Aldol Condensation on Aldehydes

Keck et al. studied the asymmetric allylation and aldolization of aldehydes with a BINOL-derived titanium catalyst.[43] In their work they investigated the effect of using a chiral ligand that was not enantiomerically pure. In the allylation reaction furfural (**28**) was treated with tri-*n*-butylmethallylstannane (**29**) to give the product (*S*)-**30** (Scheme 1).[43a] When

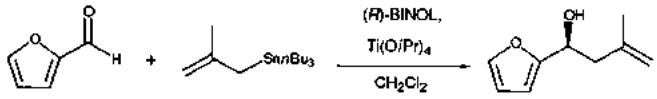

Scheme 1. The asymmetric BINOL–titanium catalyzed allylation of furfural (**28**) with a dependence of a NLE on the presence of molecular sieves.

the catalyst was prepared by the reaction of an equimolar mixture of BINOL and $Ti(OiPr)_4$, in the presence of molecular sieves (4 Å), a positive nonlinear effect could be detected when the reaction was performed at $-20\,^{\circ}C$. The use of 50% *ee* or 100% *ee* BINOL gave **30** with an *ee* of 88 or 99%, respectively. By comparison, simple mixing of BINOL and $Ti(OiPr)_4$ (in a 2:1 ratio) at room temperature without molecular sieves led to a strictly linear relationship between ee_{aux} and ee_{prod}. The departure from linearity can be explained as a result of the formation of the usual, more stable heterochiral dimer. The molecular sieves play an important role in the formation and interaction of the complexes, since in its absence no NLE is observed. The nature of the catalyst in the latter case is however unknown and maybe quite different from the one discussed previously.

The same catalyst was then used in the aldol condensation of aldehydes.[43b] Reaction of benzaldehyde (**8**) with the ketene acetal **31** gives access to the thioester (*S*)-**32** when 20 mol% of the BINOL-titanium catalyst, prepared in the presence of molecular sieves, is employed (Scheme 2). In this

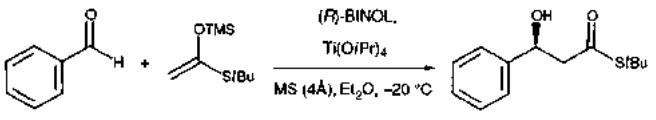

Scheme 2. Asymmetric aldol condensation of benzaldehyde (**8**) with **31**.

reaction the ee_{prod} varies nonlinearly with respect to different *ee*'s of the BINOL. A (+)-NLE takes place as expected for this type of catalyst, which is almost identical to the one presented in Scheme 1. The use of BINOL with 50% *ee* gave a product with an enantiomeric excess of 91% while the enantiopure diol gave the adduct with 97% *ee*.

Faller et al. and Tagliavini et al. were also interested in the allylation of aldehydes and reported a similar study of nonlinear effects in this reaction. A comparison was done between two types of BINOL-metal catalysts in the reaction of allyltributyltin (**34**) and aldehydes, as illustrated in Figure 40. Faller et al. prepared their catalyst by mixing (*R*)-BINOL with various *ee*'s with Ti(O*i*-Pr)$_4$ in the presence of

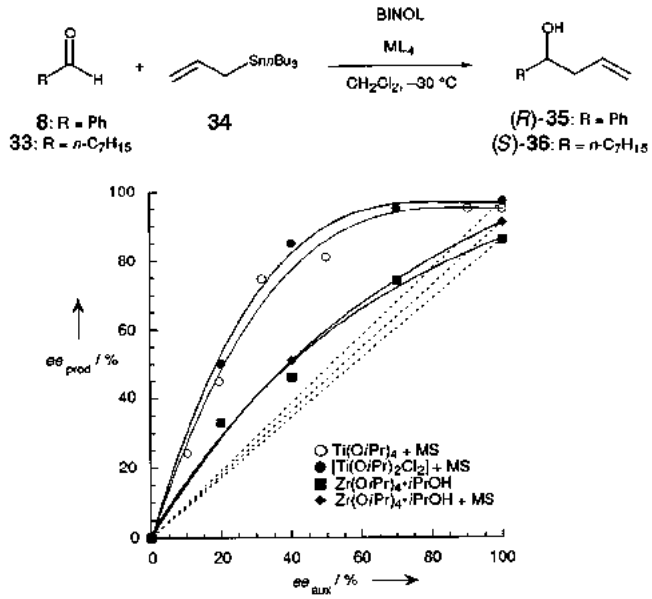

Figure 40. NLEs observed in the asymmetric allylation of aldehydes with various BINOL – metal catalysts (20 – 30 mol %).

4-Å molecular sieves.[44] The use 30 mol % of this catalyst in the allylation of benzaldehyde (**8**) gave rise to the usual (+)-NLE seen for BINOL catalysts (curve ○). Tagliavini et al. studied the reaction of octanal (**33**) catalyzed by 20 mol % of the complex that was prepared by reaction between (*S*)-BINOL and [Ti(O*i*Pr)$_2$Cl$_2$] in the presence of molecular sieves, and observed a pronounced (+)-NLE (curve ●).[45] A strong resemblance with the effect reported with the same catalyst in the ene reaction (Section 2.3.4.) is seen. In the allylation reaction the homochiral dimeric species was calculated to be 100 times more active than its heterochiral equivalent and, therefore, explains the NLE observed here.

When the chiral catalyst was prepared from Zr(O*i*Pr)$_4$ · *i*PrOH, with (curve ■) or without (curve ◆) the addition of molecular sieves, a moderate (+)-NLE could be recorded. The similarity of the results, for both methods of preparation, has been explained from the NMR analysis. While solutions of BINOL and [Ti(*i*PrO)$_2$Cl$_2$] remained unchanged if no molecular sieves are added, those of BINOL and Zr(O*i*Pr)$_4$ · *i*PrOH showed the formation of the catalyst [Zr(O*i*Pr)$_2$BINOL] with and without molecular sieves. Only a slight modification in the level of enantioselectivity takes place.

Kinetic experiments with the zirconium catalyst showed that the one prepared from pure (*S*)-BINOL needed four hours to complete the reaction, while the other catalyst derived from *rac*-BINOL was a little less active (10 h). The moderate deviation from the linear relationship was further explained by the activity of the homochiral zirconium complex being only two times greater. This value is quite small when compared to the activity difference in the case of the titanium catalysis. Tagliavini et al. found out, from the ML$_2$ model, that the BINOL – titanium catalyst possesses a $g = 0.01$ ($k_{RS}/k_{RR} = 1/100$), while the BINOL – zirconium one displays a $g = 0.6$ ($k_{RS}/k_{RR} \approx 1/1.7$).

Carreira et al. reported similar results from the allylation of pivalaldehyde with allyltrimethylsilane with a BINOL – Ti catalyst prepared from BINOL and TiF$_4$. In their case, the use of 50 % *ee* BINOL gave an allylic alcohol with 82 % *ee* while the enantiopure BINOL gave 95 % *ee* for the same alcohol.[46]

2.3.7. Asymmetric Epoxidation

In 1994 Kagan et al. reported an additional example of nonlinear effects during a Sharpless epoxidation (for geraniol epoxidation, see Section 2.1.) that involved the formation of the epoxide **38** from the allylic alcohol **37** (Figure 41).[31] A moderated amplification of the expected enantiomeric excess

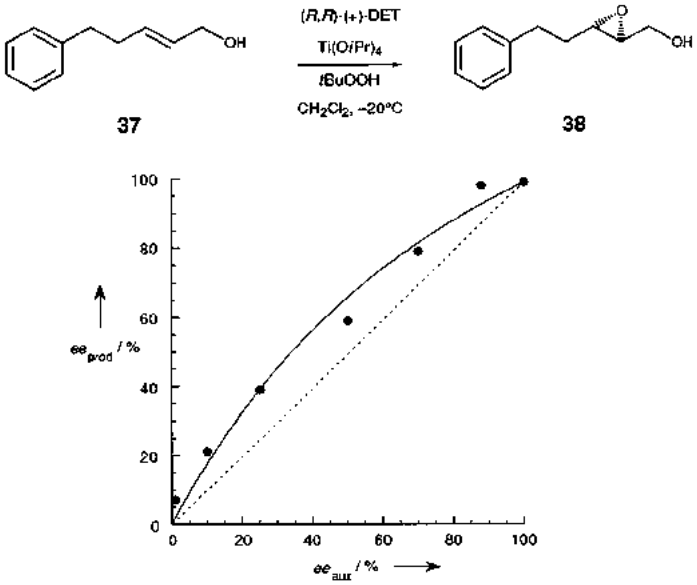

Figure 41. (+)-NLE in the Sharpless epoxidation of **37**.

was noted. Based on a model in which two chiral ligands are bound to the metallic center, this NLE was explained by the formation of the usual diasteroisomeric species. The heterochiral species was shown to possess half the catalytic activity of one of the homochiral complexes. On the basis of the ML$_2$ model, this asymmetric epoxidation of an allyl alcohol is described well by the parameters $EE_0 = 99\,\%$, $K = 1000$ and $g = 0.5$. The heterochiral species is slightly more stable ($k_{RS}/k_{RR} \approx 1/2$) and abundant ($K = 1000$).

2.3.8. Asymmetric Sulfoxidation

One of the first nonlinear effects was discovered by Kagan et al. during sulfide oxidation mediated by a chiral titanium complex.[19] The negative nonlinear effect resulting from this reaction was discussed in Section 2.1. Uemura et al. reported interesting results in their study of asymmetric oxidation of

sulfides promoted by a chiral BINOL–titanium catalyst.[47a] The method employs a reagent similar to Kagan's, but with BINOL as the chiral unit. This complex can be used at the catalytic level and sulfides such as **6** are efficiently transformed into sulfoxide (*R*)-**7** (Figure 42).

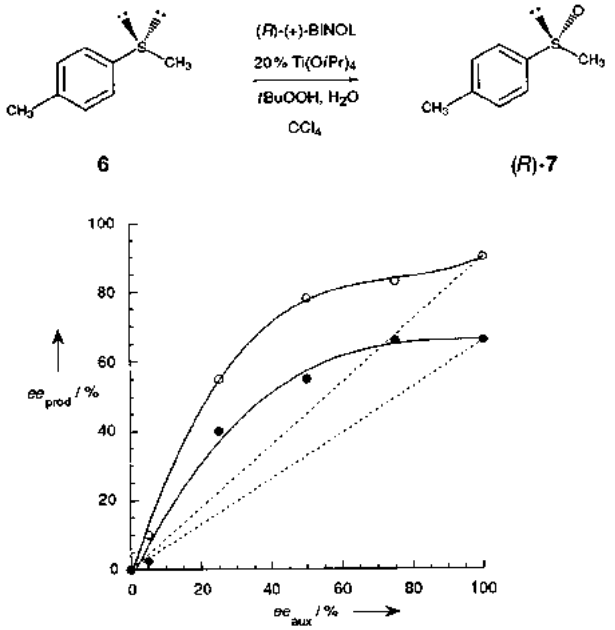

Figure 42. (+)-NLE in a BINOL–titanium catalyzed oxidation of sulfide **6** under various reaction conditions. Curve ●: Argon, −20 °C; curve ○: air, 0 °C.

The variation of the *ee* value of (*R*)-BINOL generated a (+)-NLE in the case of the two sets of experimental conditions, namely under argon at −20 °C (curve ●) and in air at 0 °C. When the reaction was performed under argon with a solution of *t*-BuOOH in toluene a moderate (+)-NLE was observed as well as a low selectivity at 100% *ee* of BINOL. The enantioselectivity of the transformation was however much better when the second method was employed; the use of 70% aqueous *t*-BuOOH at 0 °C with the reaction being carried out open to the atmosphere, generated higher levels of asymmetric induction as well as a stronger (+)-NLE (curve ○). The authors concluded that the existence of a (+)-NLE with this catalyst, in comparison with the negative effect observed with Kagan's reagent, was a result of a strong difference between the two catalysts. However, neither the NLE nor the structure of the catalyst itself was analyzed.

The presence of a NLE in this system can easily be understood if one takes into account the results already discussed with BINOL-metal catalysts (Sections 2.3.4 and 2.3.6). However, Uemura et al. discovered, by studying the evolution of the ee_{prod} over time, that a second reaction was also involved in the stereochemical outcome of the reaction.[47b] With the enantiopure BINOL, the *ee* value of the sulfoxide **7** was shown to increase considerably with the advancement of the reaction. This augmentation of the enantiomeric excess was accompanied by increased amounts of the overoxidation product, namely the corresponding sulfone. As the formation of the sulfone proceeds a process of kinetic resolution[48] takes place, which assures a better *ee* value of (*R*)-**7** over time. A study showed that racemic **7** indeed gave rise to a kinetic resolution in which there is some asymmetric amplification. The curves of Figure 42 are thus a complicated function of (+)-NLE for both the sulfoxidation and the subsequent kinetic resolution.[47b]

2.3.9. Allylic Oxidation

Feringa et al. reported that NLEs can be observed in the asymmetric allylic oxidation with copper salts and (*S*)-proline.[49] This NLE is however modified by the presence or absence of a catalytic amount of anthraquinone as seen in Figure 43. When proline of different enantiomeric excesses

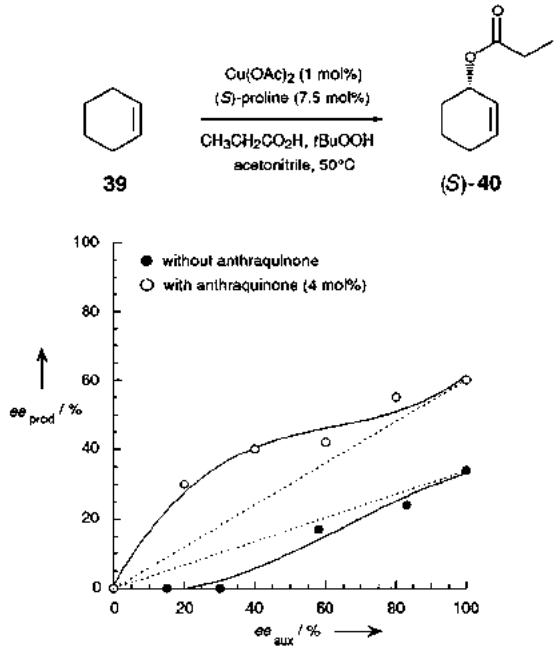

Figure 43. Modification of the NLE in an asymmetric allylic oxidation of **39** catalyzed by (**S**)-proline with the addition of anthraquinone.

was introduced alone into the reaction mixture a small (−)-NLE took place (curve ●) in this reaction of low enantioselectivity. When 4 mol% of anthraquinone was added to the mixture, an increase in the reaction selectivity as well as a moderate (+)-NLE were encountered. Both procedures transform cyclohexene (**39**) into (*S*)-2-cyclohexenyl propionate ((*S*)-**40**).

The authors stipulated that the generation of the (−)-NLE by the use of proline with copper(II) acetate was the result of more than one proline molecule being involved in the stereodiscriminating step, as was the case in the example from Agami (Section 2.1). It is also possible that dinuclear or oligonuclear catalytic complexes are implicated. The blue solution formed with the copper salt becomes more turbid when the *ee* value of proline is lowered. It was suggested that the precipitate was composed of the *meso*- or heterochiral complex (*R*)-prolinato-(*S*)-prolinato-copper(II). Moreover, the (*R*)·(*S*)-complex remaining in solution must be more

reactive than the homochiral ones, $(R)\cdot(R)$ and $(S)\cdot(S)$, in order to observe the negative effect.

Feringa et al. proposed that in the presence of anthraquinone a mechanistic or structural change occurred, which involved the interaction of the catalyst and quinone. The effect of anthraquinone cannot be ascertained, but since the reaction passes through a Cu^{III} intermediate, one can propose that it should play a role in the redox pathways of the reaction.

2.3.10. Diels–Alder Reaction

The Diels–Alder reaction, one of the most powerful methods for the synthesis of 6-membered rings, was studied in great detail and its asymmetric version developed with a certain success. Since chiral catalysts are utilized in the reaction, several groups tested the existence of nonlinear effects during its course.

As early as 1989 Narasaka et al. observed a peculiar behavior of a TADDOL-type diol when used with titanium as a catalyst in the Diels–Alder reaction illustrated in Scheme 3 (TADDOL = tetraaryldioxolanedimethanol.[50] When the 3-acyl-1,3-oxazolidin-2-one **41** was allowed to react

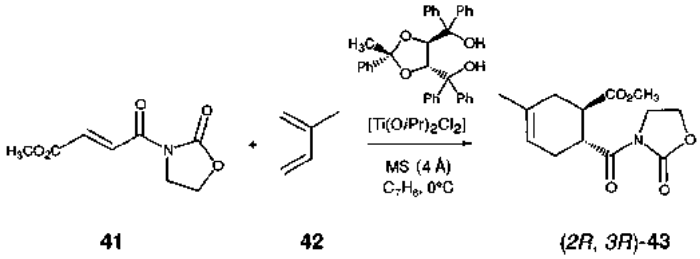

41 **42** **(2*R*, 3*R*)-43**

Scheme 3. Asymmetric Diels–Alder reaction between **41** and **42** with a TADDOL–titanium catalyst.

with 2-methyl-1,3-butadiene (**42**), in the presence of the catalyst generated by using the diol and $[Ti(OiPr)_2Cl_2]$, the product *(2R,3R)*-**43** derived from the *endo* transition state was isolated. When the authors took a diol with 25% *ee* for preparing the catalyst, the product **43** was isolated with an *ee* of 83%. Furthermore, a precipitate was observed during the preparation of the catalytic species. This observation was an indication of interactions in solution that lead to a NLE-type of behavior for the catalyst. This was further proved by admixing the diol (25% *ee*) and $[Ti(OiPr)_2Cl_2]$, removal of the precipitate, and performing the reaction with the supernatant solution. Once again the product **43** was isolated with 83% *ee*. The filtrated solid was hydrolyzed to retrieve the diol, which was in this case racemic. This result suggested that the species formed was at least dimeric, and the 1:1 ratio of enantiomers was an indication that the precipitated compound was the heterochiral complex.

Irrure et al. reported some years later a more complete study of NLE in the Diels–Alder reaction by using a similar diol as the chiral unit of the titanium catalyst.[51] With 10 mol% of the catalytic species, the cycloaddition of the oxazolidinone **44** and the diene **45** gave the expected product **46** (Figure 44). By varying the *ee* value of the diol, a (+)-NLE was observed for the *ee* of the product. The greater stability of

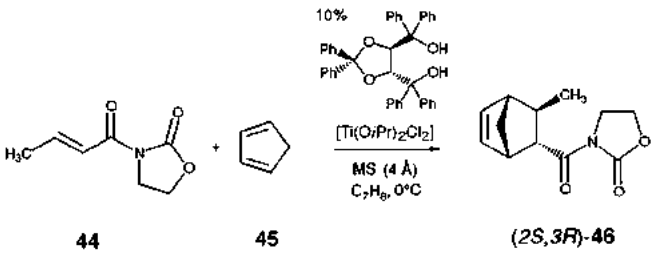

44 **45** **(2*S*,3*R*)-46**

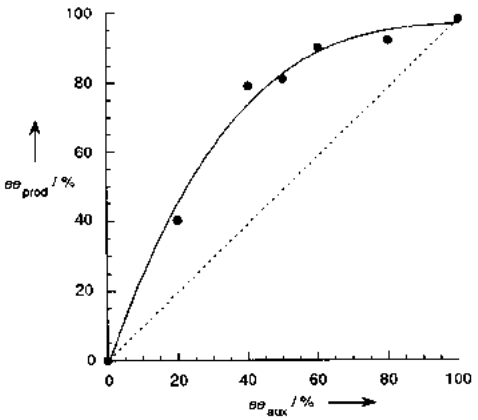

Figure 44. (+)-NLE in an asymmetric Diels–Alder reaction of **44** and **45** with a TADDOL–titanium catalyst.

the *meso*-dimeric species can be appreciated qualitatively by the formation of a precipitate when starting from the *rac*-diol, while enantiopure diol produced only a clear and limpid solution of the catalyst.

By keeping a constant amount of catalyst, and using the same reaction conditions, the influence of the enantiomeric purity of the diol on the chemical yield as well as the formation of the *endo* product **46** was evaluated (Figure 45). The racemic diol generates a poor catalytic system and, after 21 h at 0 °C, only 6% of **46** was obtained with a diastereoselectivity of 58% in favor of the *endo* isomer. This suggested that the very insoluble heterochiral dimer was very stable and thus, less easily implicated in a catalytic cycle. The enantiopure diol-derived catalyst is however much more efficient. Since it is constituted only of totally soluble homochiral dimeric species, it gave under the exact same conditions 68% of **46** at 87% *de* (diastereomeric excess). Figure 45 allows visualization of the effect of the variation of the *ee* value of the diol between 0 and 100% *ee* on the yield (a) and diastereoselectivity (b) in this reaction.

Mikami's group also studied an asymmetric Diels–Alder reaction but with their BINOL-titanium catalyst, and again obtained excellent results.[52] Condensation of the diene **47** with methacrolein (**48**) gave efficient access to the carbocycle **49**, as depicted in Figure 46. In this reaction, the (*R*)-BINOL/$TiCl_2$ catalyst ((*R*)-**24**) was prepared in the usual way (see Section 2.3.4.) and the molecular sieve filtered-off before using it for catalysis. To study NLEs in this reaction the authors decided to vary the *ee* value of the catalyst **24** using two methods: In the first, molecular sieve-free (*R*)-**24** and *rac*-**24**, prepared independently from enantiopure or racemic BINOL respectively, were admixed to reach the desired *ee*

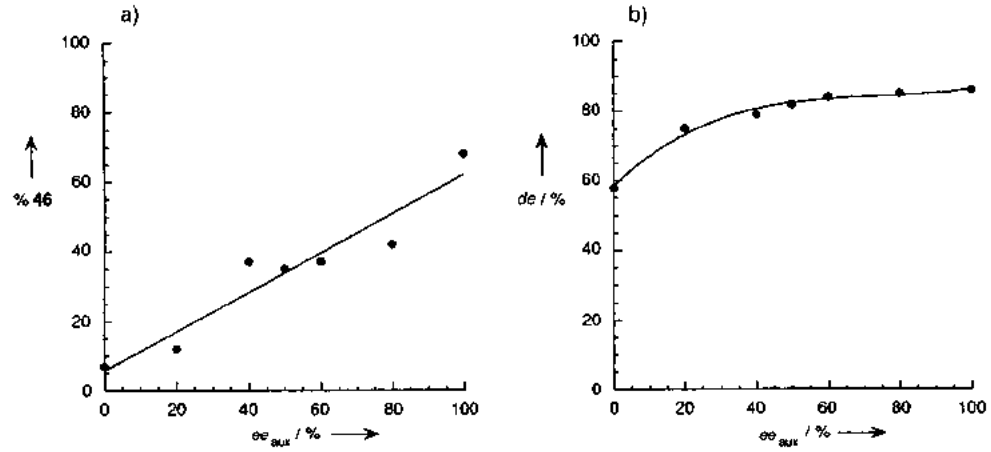

Figure 45. Yield and diasteromeric excess (*de*) of the product **46** with variation in the *ee* value of the diols.

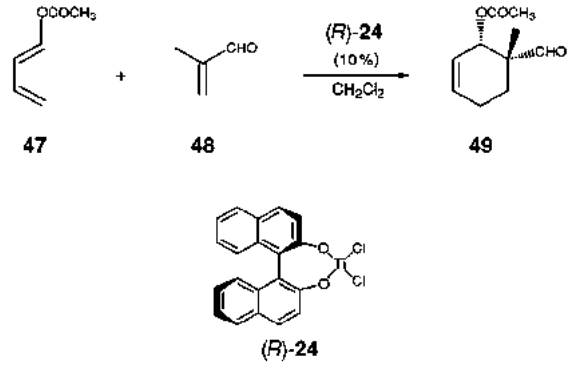

(*R*)-**24**

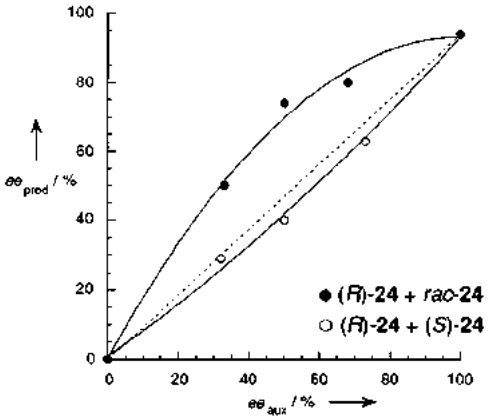

Figure 46. Variation of the NLE observed in a BINOL – titanium catalyzed Diels – Alder reaction with variation in the preparation of the catalyst.

value. The results of the asymmetric induction using this approach generated the curve ● of Figure 46, with a moderate (+)-NLE being observed.

In the second method, molecular sieve-free (*R*)-**24** and (*S*)-**24** were synthesized separately before using them to prepare the catalyst of various enantiomeric purities (curve ○). In this case, the relation was almost linear, which shows a strong difference with the preceding method of preparation and the results from Section 2.3.4. This result suggests that the presence of molecular sieves is important for establishing the equilibrium between the dimers. The fact that a mix of (*R*)-**24** and *rac*-**24** leads to a NLE, while (*R*)-**24** and (*S*)-**24** admixing gives a linear relationship, confirms that little exchange between the dimeric species takes place in the absence of molecular sieves. Thus in the first method catalyst *rac*-**24**, which exists as the more stable and less catalytically active heterochiral dimeric species, is mixed with the homochiral dimer generated from (*R*)-**24**. Since the exchange is almost nonexistent, the reaction will mainly be catalyzed by (*R*)-**24** that is readily liberated from the homochiral complex, with the *meso* complex acting mainly as a spectator. For the other technique homochiral dimers act independently in the reaction to give a product with an *ee* value reflecting the enantiomeric composition of the catalyst. It is intriguing that in this case the liberated monomeric (*R*)- and (*S*)-**24** seem to be implicated only in the catalysis and not in a heterochiral dimerization process. If the catalyst prepared from BINOL with 50% *ee*, followed by the filtration of molecular sieves, is used in this reaction, product **49** is isolated with an *ee* of 76%. This is the result of the formation of homo- and heterochiral species prior to removal of the molecular sieves.

The greater stability of the *meso* dimer was evaluated by kinetic experiments. The molecular sieve-free catalyst prepared from (*R*)-BINOL (curve ●) was shown to be five times catalytically more active than the one obtained from *rac*-BINOL (curve ○, Figure 47). The same group also

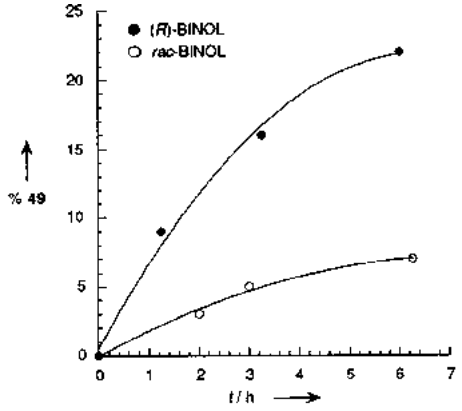

Figure 47. Yield of the product **49** as a function of reaction time for enantiomerically pure (*R*) and racemic BINOL.

observed a (+)-NLE of the same amplitude when using the catalyst prepared from (*R*)- and *rac*-**24** in an hetero-Diels – Alder reaction. The effect was examined in the reaction between the diene **50** and methyl glyoxylate (**22**) to afford the dihydropyrane **51** (Figure 48).

In their study of the asymmetric version of the Diels – Alder reaction Kobayashi et al. discovered various kinds of non-

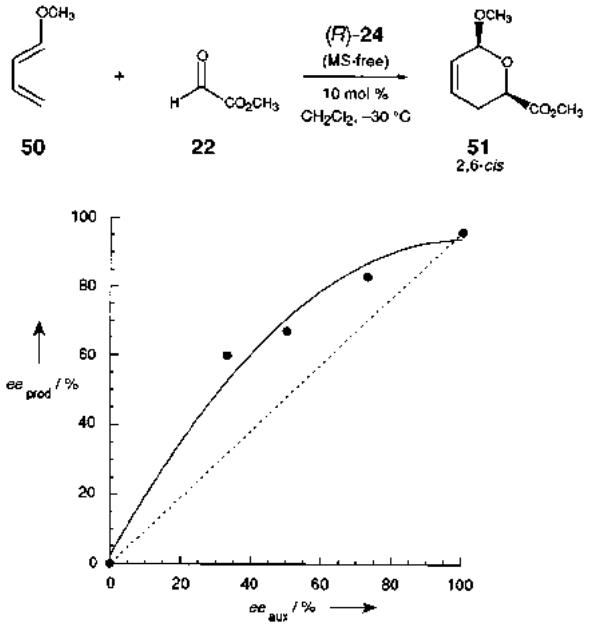

Figure 48. (+)-NLE in an asymmetric hetero-Diels–Alder reaction between **50** and **22** with a BINOL–titanium catalyst.

linear effects with some BINOL–lanthanide catalysts.[53] When (*R*)-BINOL was treated with scandium(III) triflate ($Sc(OTf)_3$) in the presence of *cis*-1,2,6-trimethylpiperidine (TMP) and molecular sieves, an efficient catalyst was prepared. The structure is the one of a simple chelate of the three constituents, namely $[Sc(tmp)_2((R)\text{-BINOL})]\cdot(OTf)_3$. When this catalyst was prepared from BINOL of various *ee* values, a (+)-NLE was observed for the *ee* value of the *endo* product **53** formed from the reaction between the acylated oxazolidinone **44** and cyclopentadiene (**52**), as seen in Figure 49 (curve ●).

The aging of the catalyst was proven to have deleterious effects on the selectivities of the reaction. While the scandium catalyst can be used as such in quick reactions, its ytterbium analogue needed stabilization in order to work properly. Furthermore, the additives used to stabilize the catalyst can even have a direct effect on the enantiofacial selectivity in this Diels–Alder reaction. When the Yb^{III} catalyst was prepared in the usual way, but with some 3-acetyl-1,3-oxazolidin-2-one (AOD) added as a stabilizer, the resulting nonlinear effect was much different from the preceding one. A (−)-NLE takes place with BINOL of to 60% *ee*, the value at which the linear relationship is observed for the enantiopure BINOL (curve ■). By changing the reaction temperature as well as the additive, in this case 3-phenylacetylacetone (PAA), a strong change was observed in the stereochemical outcome of this cycloaddition. Not only was the facial selectivity completely inverted, leading to (2*R*,3*S*)-**53** , but the NLE became strongly negative (curve □).

The differences between the scandium and ytterbium catalyst are the result of different levels of aggregation, especially when chelating additives are used. The perturbation created by the use of such compounds was shown to have a strong influence on the importance of the NLE.[53]

Seebach et al. studied the same reaction as Kobayashi's group, with the only difference being in the catalyst utilized.[54]

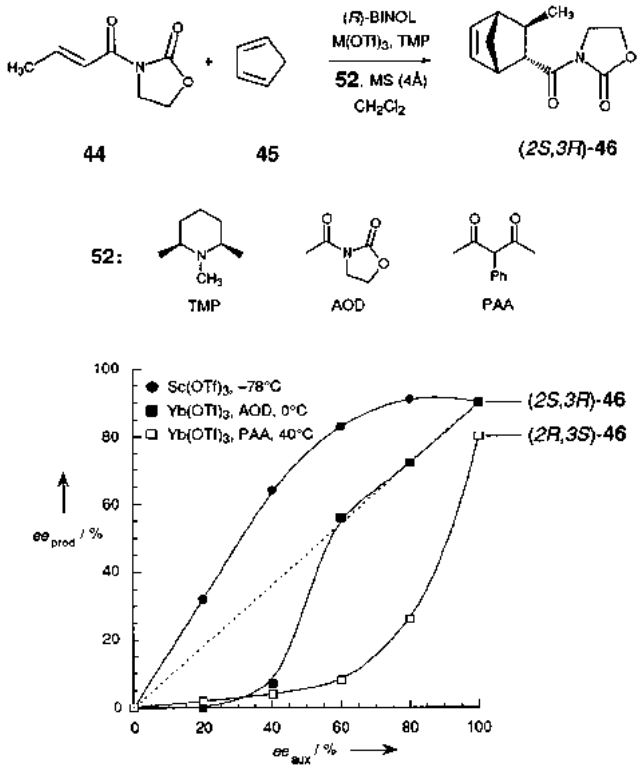

Figure 49. NLEs in a Diels–Alder reaction catalyzed by different BINOL–metal catalysts (20 mol%) in the presence of additives **52**.

The authors chose to use a highly hindered TADDOL-type diol to prepare the titanium catalyst needed to perform the Diels–Alder (Figure 50). When the diol of various *ee* values was allowed to react with $[Ti(OiPr)_2Cl_2]$ in order to form the

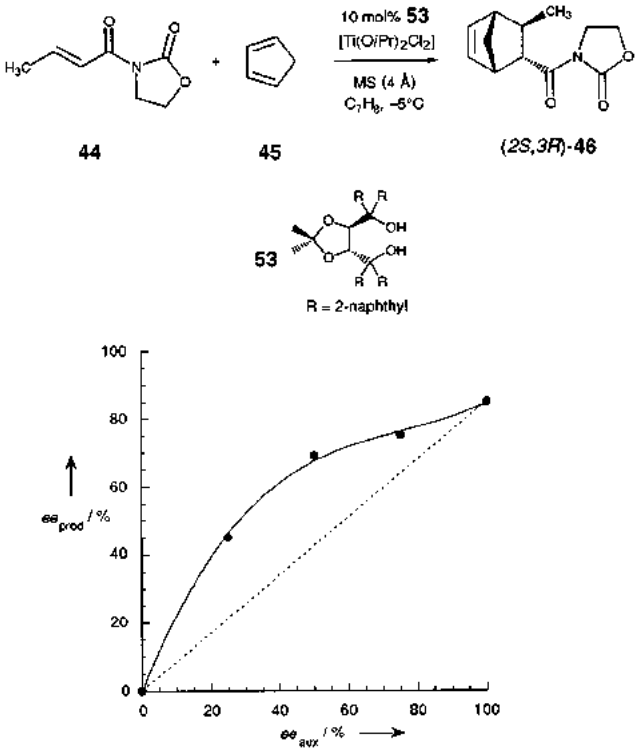

Figure 50. (+)-NLE in a titanium-catalyzed Diels–Alder reaction between **44** and **45**.

catalyst, which was then used in the reaction, a (+)-NLE was easy to observe. The same homo- and heterochiral species should be implicated here in the building of the amplification. However, unlike Narasaka's use of another TADDOL, there was no formation of a precipitate. The reaction mixture stayed homogeneous during the course of the transformation (except for the molecular sieves present in it) for all *ee*'s of the diol.

2.3.11. 1,3-Dipolar Cycloadditions

It has been found recently that Et_2Zn promotes the 1,3-dipolar cycloaddition of nitrile oxides to allyl alcohol in the presence of catalytic amounts of diisopropyl tartrate (DIPT).[55] From this method, 2-isoxazolines are obtained in good yields and up to 90% ee. A positive nonlinear effect has been observed during the reaction between allyl alcohol (**54**) and the nitrile oxide generated in situ from the hydroxymoyl chloride **55** to give the isoxazoline **56** (Figure 51). Presumably the (+)-NLE originates from soluble inactive zinc aggregates with DIPT. In this procedure, 1,4-dioxane is needed in order to avoid precipitation of highly aggregated complexes containing DIPT and zinc salts. The authors postulated that the key step of the cycloaddition involves the complex **57**.

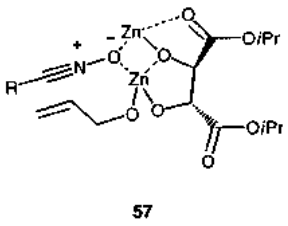

57

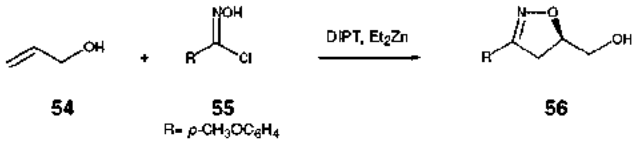

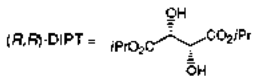

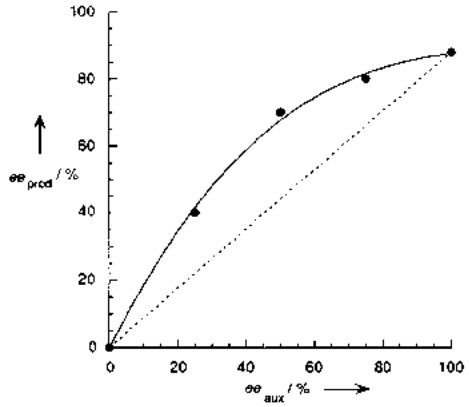

Figure 51. (+)-NLE in a 1,3-dipolar cycloaddition in the presence of DIPT (20 mol%) and Et_2Zn (dioxane, $CHCl_3$, 0 °C).

2.3.12. Nitroaldol Reaction

Shibasaki et al. reported that a BINOL–lanthanum complex is active in an asymmetric version of the Henry reaction (Scheme 4).[56] The nitroaldolization of α-naphthoxyacetaldehyde (**58**) in the presence of this enantiopure catalyst gave the nitroalcohol (*R*)-**59** in 87% *ee*. If the BINOL used to prepare the catalytic species was not enantiopure, in this case 56% *ee*, the enantiomeric excess of the product **59** was higher than expected (68% *ee*). This observation was an indication of an additional example of (+)-NLE for a BINOL-derived catalyst. The authors explained the NLE encountered with this lanthanum catalyst by its existence as an oligomer.

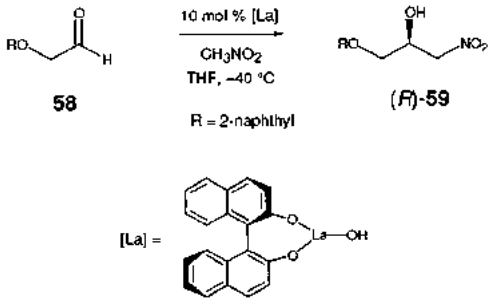

Scheme 4. Nitroaldolization of **58** with a BINOL–lanthanum catalyst.

2.3.13. Meerwein-Ponndorf-Verley Reduction

During the course of the elaboration of an asymmetric version of the MPV reaction, Evans et al. tested a chiral aminodiol-samarium(III) catalyst for NLEs (Scheme 5).[57] They discovered that the use of an aminodiol of 80% *ee* in the preparation of the catalyst, and its subsequent use in the reduction of *o*-chloroacetophenone (**60**), gave the product (*R*)-**61** in a higher *ee* value than expected (95% *ee*). The use of an enantiopure catalyst gave the product with 97% *ee*. A more stable heterochiral dimer $(R,R)\cdot(S,S)$ was suggested as a trap for the minor enantiomer, which thus increased the *ee* value of the major one that is implicated both in the homodimer formation and catalysis.

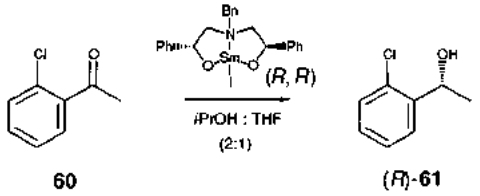

Scheme 5. Meerwein-Ponndorf-Verley reaction with a chiral samarium catalyst (5 mol%) at room temperature.

2.3.14. Ring-Opening of meso-Epoxides

Jacobsen et al. described a catalytic system for the asymmetric nucleophilic ring-opening of *meso* epoxides (Figure 52).[58] In their investigation in to the nature of the catalytic system, the authors discovered that the chiral (salen)chromium(III) complex used in this reaction showed a nonlinear behavior when its *ee* value was modified. The reaction of cyclohexene oxide (**62**) with the trimethylsilylated azidoalcohol **63** showed a (+)-NLE. On the basis of kinetic considerations and measurements, the authors postulated the formation of a bimetallic species to account for the observed

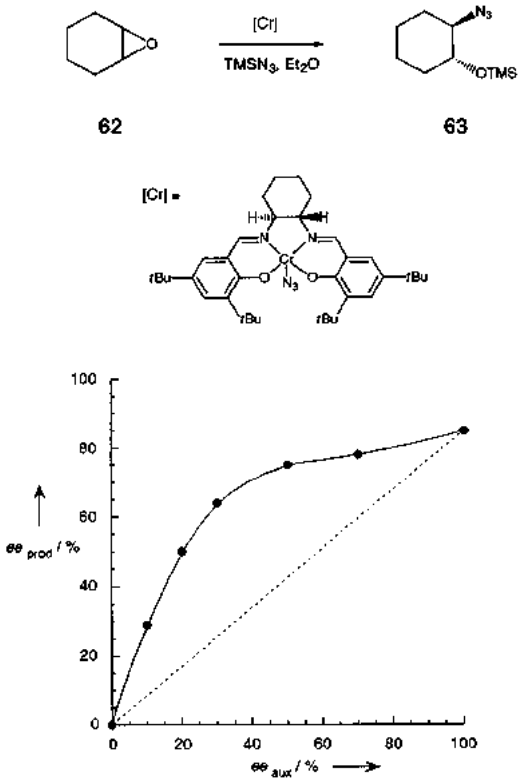

Figure 52. Ring-opening of *meso*-epoxide **62** catalyzed by a Salen–chromium catalyst (2 mol%).

NLE. The epoxide is activated by one chiral salen–chromium unit, while the nucleophilic attack involves a second azido salen–chromium entity. The rate-determining step involves the prefered homochiral combination. Thus the evaluation of the nonlinear effects gave confirmation of the suggested mechanism that the catalyst is a bimetallic species that can act as both a nucleophile and an electrophile.

2.3.15. Nonlinear Effects as a Probe

The preceding Sections clearly demonstrated that the study of nonlinear effects in asymmetric catalysis could be more than useful in understanding and getting quantitative information about the species involved in the catalytic cycle and their behavior in solution. This Section will now describe the qualitative use of NLEs by a number of groups to ascertain the nature of the catalytic entity responsible for the enantioselective reaction.

Yamaguchi et al. used NLE as a probe for the determination of the mechanism in asymmetric Michael additions with proline salts.[59] The 1,4-addition of diisopropyl malonate to cycloheptenone (**17**) by using a proline–rubidium salt gave them the opportunity to prepare the alkylated ketone (*R*)-**64** (Scheme 6). In contrast to the Hajos-Parrish-Wiechert reaction with proline presented in Section 2.1, the variation of the *ee* value of the proline salt resulted in a linear relationship with ee_{prod}. The authors concluded that the transition state of their reaction contained only one molecule of prolinate.

Seebach and Schmidt[60] used the NLE test to determine the nature of their catalytic species in diethylzinc addition on

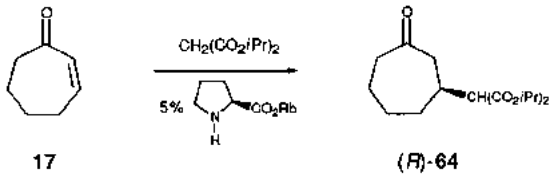

Scheme 6. 1,4-Addition of a malonate to the enone **17** catalyzed by a proline–rubidium salt ($CHCl_3$, room temperature).

aldehydes. Their experiments regarding benzaldehyde (**8**) are included in Scheme 7. By variation of the enantiomeric purity of the TADDOL-type diol used to prepare the spirotitanate

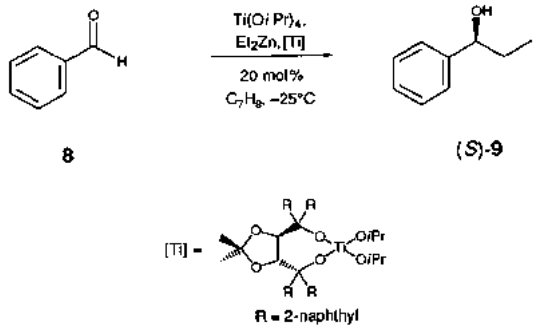

Scheme 7. TADDOL-titanium catalyzed addition of diethylzinc to benzaldehyde (**8**).

catalyst, and by determination of the resulting *ee* value of the product, they discovered that no NLE was present. A strict linear relationship was obtained, which suggested that only one chiral unit was involved in the stereochemical rate-determining step of the stereoselective reaction. These results are in sharp contrast to those they obtained with the same catalyst in the Diels–Alder reaction (Section 2.3.10, Figure 50), where a moderate (+)-NLE was observed.

Bolm et al.,[61] were interested in getting a better understanding of the catalyst used in the enantioselective addition of diethylzinc to aldehydes catalyzed by β-hydroxysulfoximines. The use of the enantiomerically pure sulfoximine illustrated in Scheme 8 for the addition to benzaldehyde (**8**),

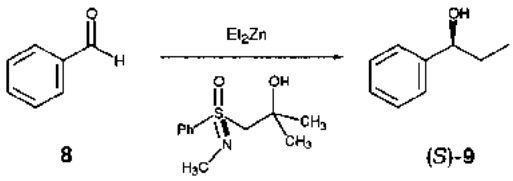

Scheme 8. Chiral sulfoximine (10 mol%) catalyzed 1,2-addition of diethylzinc to benzaldehyde (**8**).

gave the corresponding alcohol **9** with an *ee* of 85%. The nonmonomeric nature of the catalyst was proven by the authors by performing the same reaction with a sulfoximine of 23% *ee*, which gave rise to an alkylation product with an amplified *ee* of 70%.

The structure of the zinc species was later suggested to be dimeric in nature from NMR experiments.[61b] Furthermore, homochiral aggregates were estimated to react five times

faster than *meso* species, which explained the (+)-NLE observed in this case. The origin of the stability difference between the oligomers can be visualized by spatial representations of both *meso* and homochiral species (Figure 53). The

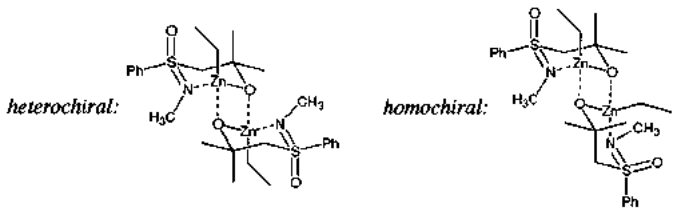

Figure 53. Dimers formed from the reaction shown in Scheme 8..

ethyl chains on the zinc atoms in the Zn–O four-membered cycle of the *meso* complex are *anti* to each other, whereas in the homochiral complex they end up *syn*, which has a destabilizing effect on the structure.

Another example of the addition of diethylzinc was performed by Fu and his group with a ferrocenyl chiral ligand (Scheme 9).[62] Despite several encounters with NLE in the

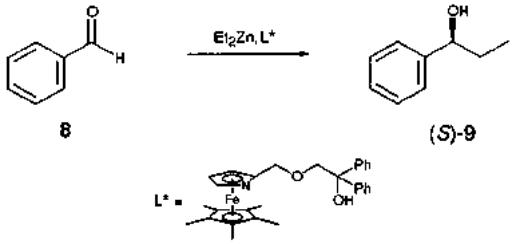

Scheme 9. Addition of diethylzinc to benzaldehyde (**8**) catalyzed by a chiral ligand (3 mol%, toluene, room temperature).

use of amino alcohols (Section 2.3.1.) the authors obtained a linear relationship in this case when their ligands with various *ee*'s were used.

During the course of the elaboration of a catalytic asymmetric epoxidation with a BINOL-derived catalyst, Shibasaki et al. tried to determine the exact structure of their catalyst.[63] Unfortunately, the spectroscopic analyses were unsatisfactory and the only conclusion was that the species were of oligomeric nature. In order to obtain more insights on the structure, the authors performed the NLE analysis. The chiral catalyst prepared from (*R*)-BINOL and Yb(O*i*Pr)$_3$ in the presence of molecular sieves was used in different *ee*'s in the epoxidation of benzylideneacetone (**19**) by *tert*-butylhydroperoxide (Figure 54). A (+)-NLE was observed in this case and the authors concluded that the oligomeric structure of the lanthanoid–BINOL complex should play a key role in their asymmetric epoxidation of enones. This type of NLE was not observed when chiral SALEN-type catalysts as reported by Schwenkreis and Berkessel were used, where perfect linearity is obtained.[64]

Bolm and Bienewald reported that in the asymmetric oxidation of sulfides the use of an imino alcohol chiral ligand with a vanadium salt and hydrogen peroxide oxidized methylphenyl sulfide (**66**) to sulfoxide **67** with a good

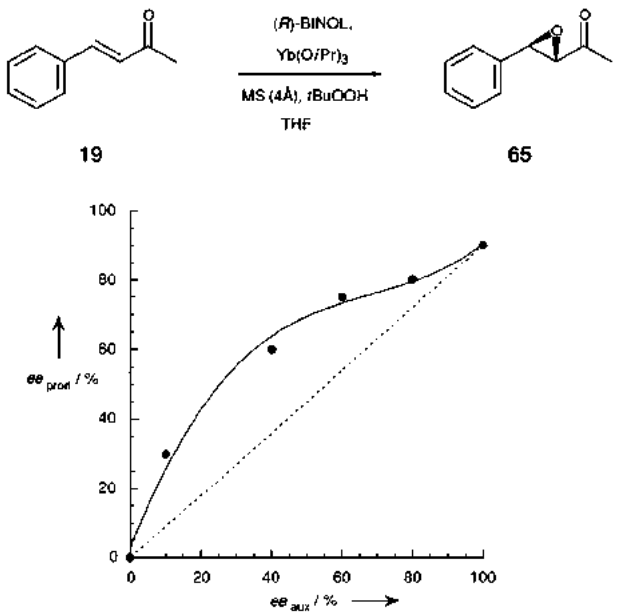

Figure 54. (+)-NLE in the asymmetric epoxidation of benzylideneacetone (**19**) catalyzed by a BINOL–ytterbium catalyst (5 mol%).

enantioselection (Scheme 10).[65] No NLEs were found in this system. The authors concluded that the catalyst contained only one molecule of chiral ligand.

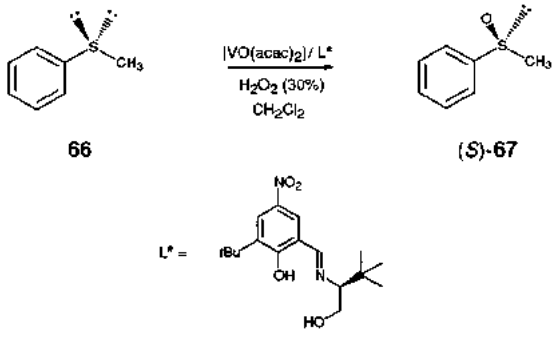

Scheme 10. Asymmetric oxidation of sulfide **66** with catalytic amounts (1 mol%) of a vanadium salt and a chiral iminoalcohol ligand.

Seebach et al., as part of their studies on the use of TADDOL-type ligands with titanium salts, were interested in probing the nature of the catalytic species that was involved in the [3+2] cycloaddition between **44** and the nitrone **68** to give **69** (Scheme 11).[66] The relationship between the *ee* value of the product and that of the chiral diol used to prepared the catalyst was strictly linear. This result was in sharp contrast with the (+)-NLE encountered with the same catalyst during a Diels–Alder reaction (Section 2.3.10, Figure 50).

Denmark and co-workers studied the cyclopropanation with a catalyst prepared from zinc salt and C_2-symmetrical disulfonamide (Scheme 12).[67] The use of this ligand in conjunction with bis(iodometyl)zinc permitted an enantioselective cyclopropanation of cinnamyl alcohol (**70**) to the corresponding carbocycle **71**. The relation between the *ee*'s of the ligand and the product was found to be perfectly linear. The authors interpreted these results as a consequence of only

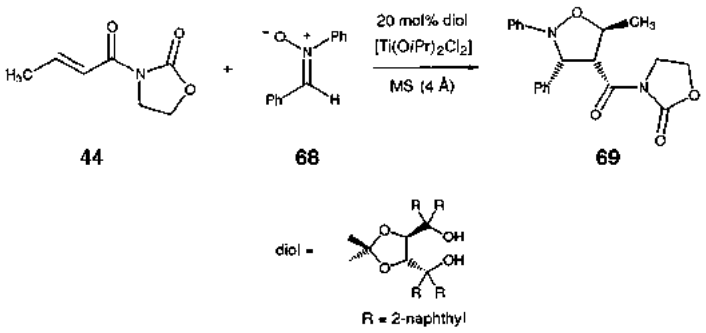

Scheme 11. [3+2] cycloaddition of **44** and **68** with a TADDOL–titanium catalyst (toluene, room temperature).

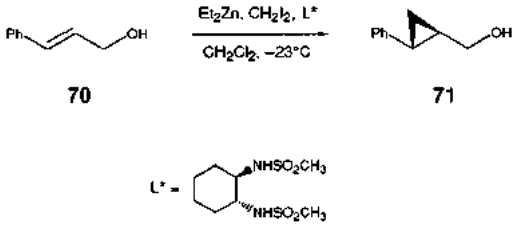

Scheme 12. Cyclopropanation of cinnamyl alcohol (**70**).

one molecule of ligand being present in the transition state responsible for the enantioselectivity, and that the stable species of all the ligand–zinc complexes is monomeric or dissociates with low activation energy.

Finally, Faller et al. reported the use of the NLE test to obtain information about the nature of the complexes implicated in some asymmetric hydrogenation reaction.[68a, 68b] The use of a cationic rhodium complex [Rh(norbornadiene)(chiraphos)]BF_4 in the hydrogenation of dimethyl itaconate (**72**) led to the corresponding methylsuccinate (*S*)-**73** in 98% *ee* (Scheme 13). When the chiraphos–rhodium complex

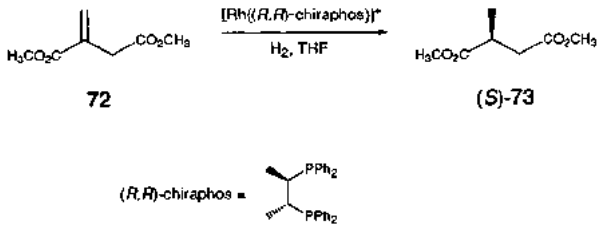

Scheme 13. Asymmetric hydrogenation of **72** with a rhodium catalyst (10 mol%).

used had a 33% *ee*, the product **73** was obtained in 60% *ee*, which was indicative of a (+)-NLE. This effect was explained by the formation of dimeric species generated by the hydrogenation of [Rh(norbornadiene)(chiraphos)]BF_4 into $[\{Rh(chiraphos)\}_2]^{2+}$.[68c–e] Accordingly to this scenario, the use of enantiomerically impure chiraphos should generate homo and heterochiral dimeric species. The authors reported that ^{31}P NMR studies in nonpolar solvents showed that the heterochiral dimer was the more stable. The dissociation of the dimers to give the monomeric, catalytically active species in this case explained the positive nonlinear effect observed. Burgess and van der Donk found that the use of a chiral rhodium catalyst incorporating DIOP in hydroboration reactions led however to linearity (DIOP = 2,3-*O*-isopropylidene-2,3-dihydroxy-1,4-bis(diphenylphosphanyl)butane).[69]

The results presented in this Section demonstrate that the study of the presence or absence of NLE in a catalytic system can complete the usual analyses, and can even be used as the sole analysis when all the others fail to give some insights into the nature of the involved species. However, this was limited to catalysis on mixtures of enantiomers. The Sections to come will present the study of NLEs in different systems and the information that can be extracted by this method of analysis.

2.4. Diastereomeric Catalysts

One may assume that the phenomena that are at the origin of nonlinear effects when using a mixture of *enantiomers* of chiral auxiliary, will remain if the chiral auxiliary is now a mixture of *diastereomers*. This assumption means that some deviations are expected from the predictions of the *ee*'s of the product as a result of the diastereomeric composition.

Noyori et al. have studied the mechanism of asymmetric amplification with DAIB as the promoter of the chiral catalyst (Section 2.3.1).[32] They concluded that a quite stable *meso* dimer of DAIB–zinc alcoholate was at the origin of the strong (+)-NLE, because of the storage of some racemic DAIB (reservoir effect). Recently these authors studied the effect of various mixtures of (−)- or (+)-DAIB and the *endo* diastereomer (*R*)-**74** or (*S*)-**74**.[70] These two catalysts gave (*R*)- or (*S*)-alcohols **9** with 94% *ee* while (−)-DAIB provided (*S*)-alcohol with 98% *ee*. Noyori et al. also compared the

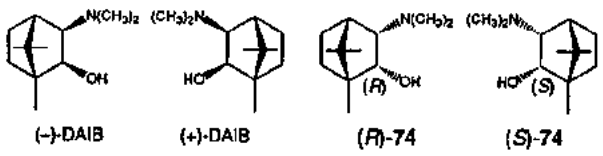

catalytic efficiency of these catalysts when enantiopure. Aminoalcohol **74** is 2.6 times more reactive as a promoter of the reaction than DAIB.

From the above data the authors computed the expected curves ee_{prod} as a function of the catalyst composition and initial rate v_0 as a function of the composition of the chiral auxiliary. They selected the mole equivalent amount (%) of one of the two components of the mixture as the chiral auxiliary composition. A curve and not a straight line was calculated for the relationship between ee_{prod} and the composition of the chiral auxiliary, but experimental data shows some significant departure to the calculated curve (Figure 55a).[71] The nonlinear effect is apparent for the mixture of (−)-DAIB with (*R*)-**74**, where the two individual catalysts generate alcohols of opposite absolute configuration. The catalysts prepared from (−)-DAIB or (*S*)-**74** gave alcohol (*S*)-**9** (see above) with similar rates of reaction. The mixture of these two catalysts showed almost perfect linearity for ee_{prod}. The formation of aggregates **10**, **76**, and **77**, with higher stability for the mixed dimer **76**, explains the above data (Figure 56). This was confirmed by measurements of the rates

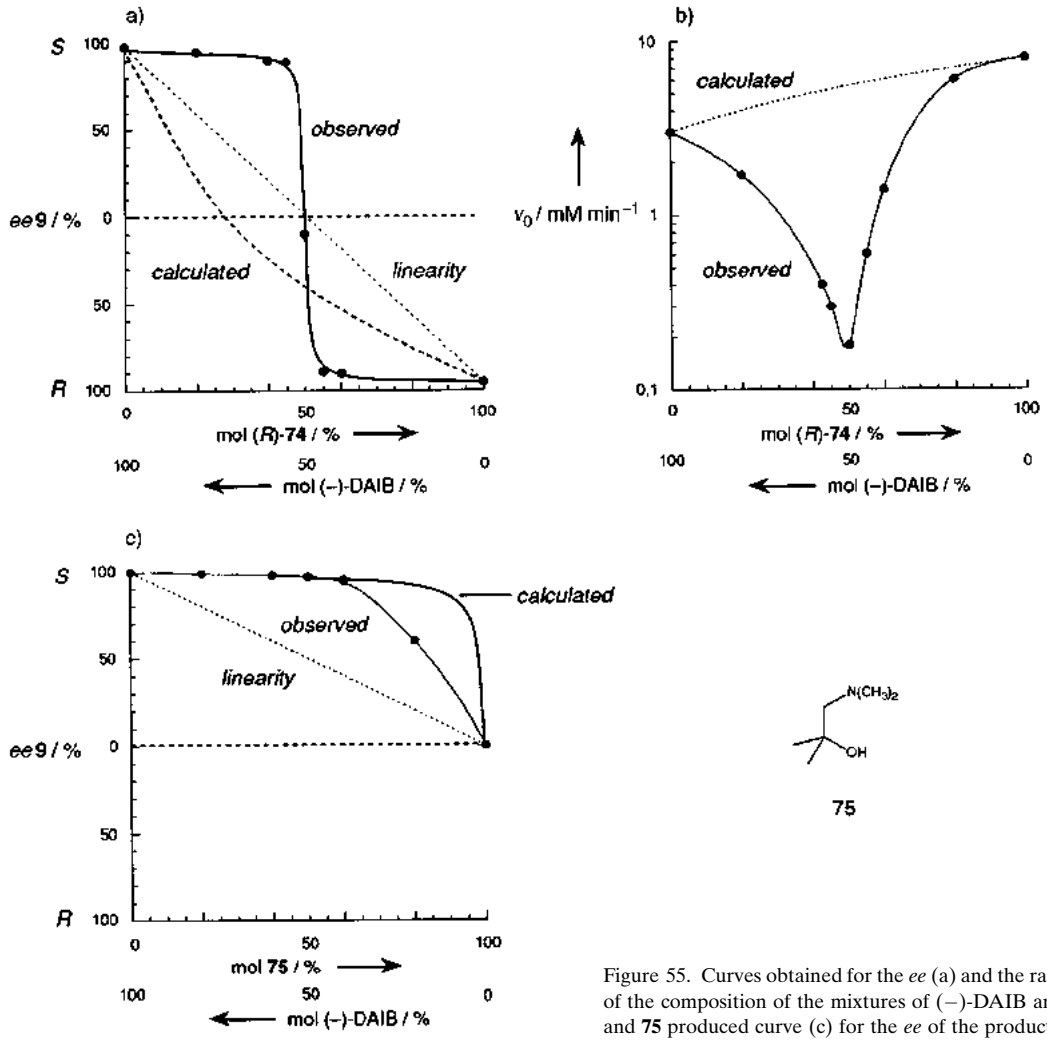

Figure 55. Curves obtained for the *ee* (a) and the rate of the reaction (b) as a function of the composition of the mixtures of (−)-DAIB and (*R*)-**74**. Mixtures of (−)-DAIB and **75** produced curve (c) for the *ee* of the product.

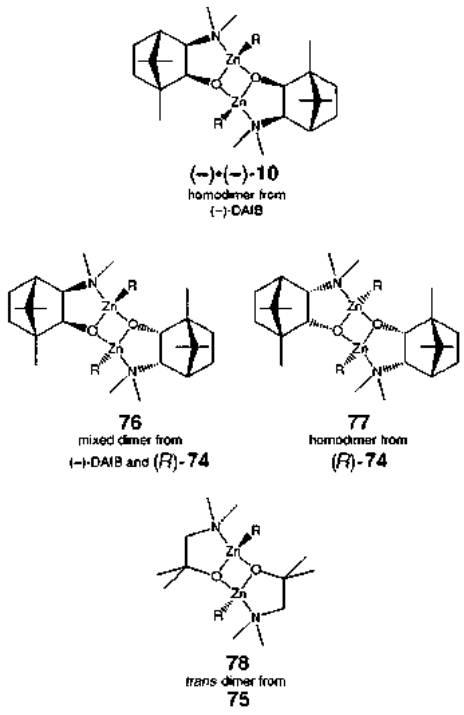

Figure 56. Some of the various dimers formed in the mixtures of DAIB and other aminoalcohols.

as a function of the catalyst composition. For example a mixture of (−)-DAIB and its diastereomer (*R*)-**74** showed a sharp minimum around a 1:1 composition, indicative of the preferred formation of heterodimer **76** of low reactivity (Figure 55b). In an additional experiment the enantioselectivity of (−)-DAIB in the presence of various amounts of the *achiral* β-aminoalcohol **75** was investigated (Figure 55c). The curve has been interpreted by the occurrence of *trans* dimer **78**, which is more stable than the *cis* dimer (not represented); which is itself more stable than homodimer **10**.

Kagan et al.[72] studied the Sharpless asymmetric dihydroxylation (AD)[73] of dibromostilbene (**79**) since several classes of diastereomeric ligands based on alkaloids are easily available. The *p*-chlorobenzoate of dihydroquinine (PCB–DHQ) gave (*S,S*)-diol **80** in 97% *ee*. The ligands of the second generation, namely phthalazine bisdihydroquinine ($PHAL(DHQ)_2$) and quinidine ($PHAL(DHQD)_2$) led to (*S,S*) and (*R,R*)-diols **80** in 98–99% *ee* in a faster reaction. Mixtures of $PHAL(DHQ)_2$ and $PHAL(DHQD)_2$ gave a curve very close to a straight line (Figure 57a), as expected from two pseudoenantiomeric ligands (similar reaction rates and similar enantioselectivities, but of opposite chirality). This experiment is in agreement with the reaction proceding through independent catalysts, and not through or involving a mixed

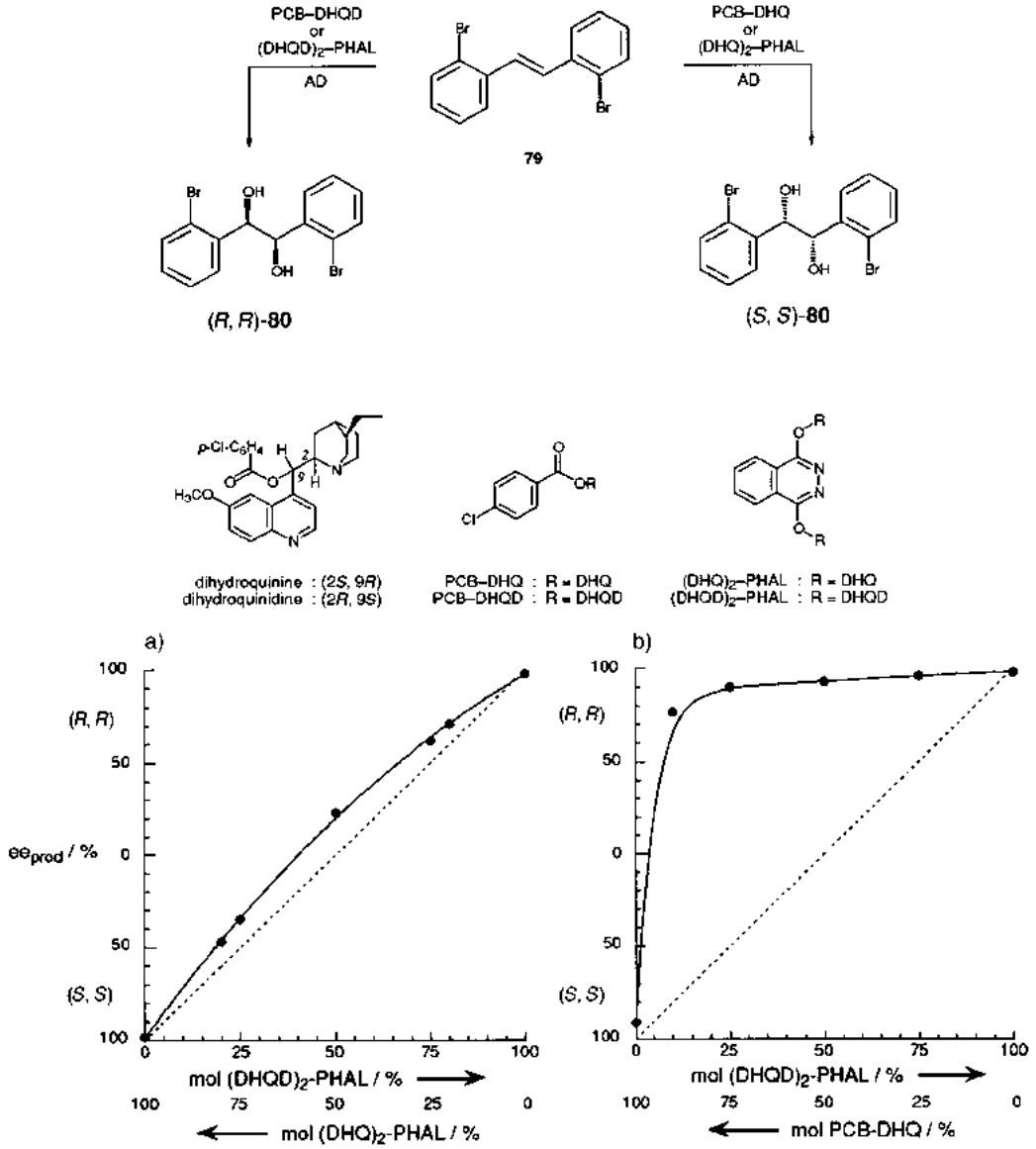

Figure 57. Curves of the *ee* of **80** obtained in the asymmetric dihydroxylation of **79** by mixing $(DHQD)_2PHAL$ with (a) $(DHQ)_2PHAL$ and (b) PCB–DHQ.

species. The mixture of PCB–DHQ and $PHAL(DHQD)_2$ gave a very strong nonlinear behavior (Figure 57b). This observation reflects the higher reactivity of the catalyst based on $PHAL(DHQD)_2$, presumably because of the larger affinity of this ligand (with respect to PCB–DHQ) towards OsO_4, as well as by the rate-acceleration given by the "chiral pocket mechanism" which has been established with the phthalazine ligands.[73]

Corey et al. evaluated the relative reactivities of some osmium catalysts, prepared from two different ligands derived from alkaloids, for AD.[74] They also used ligands (1:1 mixture) of opposite enantioselectivities in AD of styrene derivatives as a way to study these systems.

Marks et al. prepared diastereomeric chiral lanthanide complexes **81** and **82** as catalysts for the enantioselective hydrogenation of alkenes or hydroamination/cyclization of amino olefins.[75] Surprisingly the enantioselectivity in hydroamination reactions is insensitive to the metallocene chirality, since a 1:1 mixture of the two complexes gave the same ee_{prod} as diastereomerically pure **81**. This behavior has been

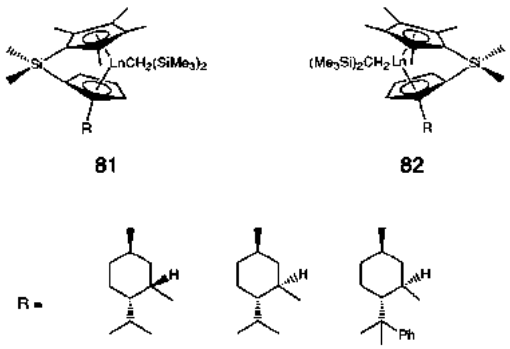

explained by epimerization around the lanthanide center (equilibrium of decomplexation and complexation during the reaction). In the hydrogenation of 2-phenyl-1-butene there is a significant difference between of **81** and **82**, in both rates and enantioselectivities. The 1:1 mixture of the two complexes gives rates and ee_{prod} that are very close to the calculated values. Obviously there are no NLE effects with these catalysts that act independently from each other.

2.5. Autocatalytic Systems

The reactions where a compound catalyzes its own formation were considered for a long time as important in prebiotic chemistry. They are of special interest in the generation and propagation of optical activity on earth.[76, 77] In the ideal case where a chiral compound (100 % *ee*) replicates with 100 % *ee* one may consider that the problem is solved. Actually the most efficient chiral catalysts presently known seldom reach enantioselectivities higher than 99.9 % *ee* (enantiomer ratio: *er* = 1999). These spectacular levels of efficiency are however unsatisfactory for the large scale production of chiral compounds by asymmetric autocatalysis. This is easily demonstrated by considering a simplified description of an asymmetric catalysis (Figure 58) where the

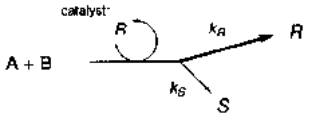

Figure 58. The asymmetric autocatalysis process.

two enantiomeric products *R* and *S* are derived from a chiral catalyst *R* (100 % *ee*). A rough computation may be done by an iterative process.

If the rate ratio k_R/k_S is high (1999) 1 mol equivalent of the product (by respect to catalyst) will be considered to be formed after one catalytic cycle with *ee* = 99.9 % (*er* = 1999). After mixing this product with 1 mole equivalent of the initial *R* catalyst (*ee* = 100 %, *er* = ∞) one ends up with 2 mole equivalent (*ee* = 99.95 %, *er* = 3999). The next catalytic cycle will provide 4 mole equivalents of catalyst (*ee* = 99.85 %, *er* = 1337). There is an endless erosion of the enantiomeric excess of the product which ineluctably will accumulate in a large amount, but in racemic composition.

Kinetics models have been proposed to overcome the above inherent tendency of *ee* degradation in asymmetric autocatalysis. Frank[76] first described a simple model where each enantiomer catalyzes its own formation but is competitively deactivated by interaction with the enantiomer of opposite configuration (Figure 59). In this model complete

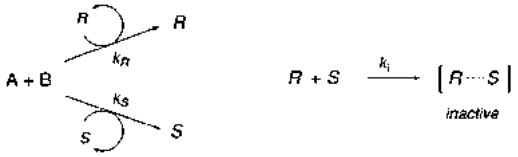

Figure 59. Frank's model with deactivation by dimerization.

enantioselectivity is assumed during the catalysis by the *R* or *S* enantiomer. The initial *R*/*S* enantiomeric ratio of the catalyst (close to 1) is amplified because of the autocatalysis (which ensures the growth of the amount of catalyst), which is combined to a continuous removal of a racemic material. In conclusion asymmetric autocatalysis from a small amount of enantiopure catalyst has no chance of propagating molecular chirality on a large scale unless it is sustained by additional reactions (such as the mutual inhibition of enantiomers in the Frank model). The situation is even worse if the initial catalyst is of low enantiomeric excess.

In that context a (+)-NLE superposed onto the autocatalytic reaction could be a convenient way to both amplify the initial *ee* value and to maintain it at a high level through the whole course of the autocatalytic reaction. There are quite a few identified asymmetric autocatalytic reactions.[78] Addition of a dialkylzinc compound to aromatic aminoaldehydes was the reaction pioneered by Soai et al. in the search of autocatalytic systems. In 1990 they discovered that pyridyl alcohol **84** is able to catalyze asymmetrically its own formation (Scheme 14).[80] The important point is that (*R*)-alcohol **84** (86 % *ee*) catalyzes formation of (*R*)-**84**, although with a low enantioselectivity (35 % *ee*, calculated by removal of the contribution of the initial catalyst).

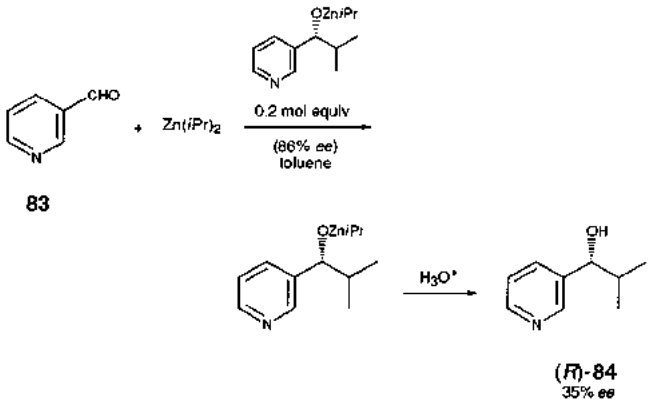

Scheme 14. Autocatalysis in the addition of diisopropylzinc to pyridine-3-carbaldehyde (**83**).

Subsequent investigations of Soai et al. on various types of aromatic aldehydes allowed the *ee* value of the product to be increased, which was also obtained with the same absolute configuration as the initiator. Ferrocene carboxaldehyde (**85**, Scheme 15) and diisopropylzinc in the presence of 0.2 mol equivalent of alcohol (*S*)-**86** (97.3 % *ee*) gave 4.75 times more alcohol (*S*)-**86** (29 % *ee*).[81]

A significant improvement was made recently in the reaction of quinoline-3-carboxaldehyde (**87**) with diisopropyl

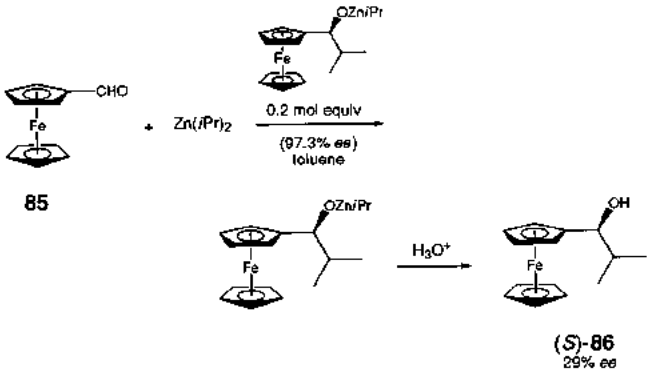

Scheme 15. Autocatalysis in the addition of diisopropylzinc to ferrocene-carbaldehyde (**85**).

zinc catalyzed by alcohol (*R*)-**88** (Scheme 16).[82] By optimization of the experimental conditions (1.2 mol equivalent of $Zn(iPr)_2$ instead of 2 mol equiv, a proper dilution to give a

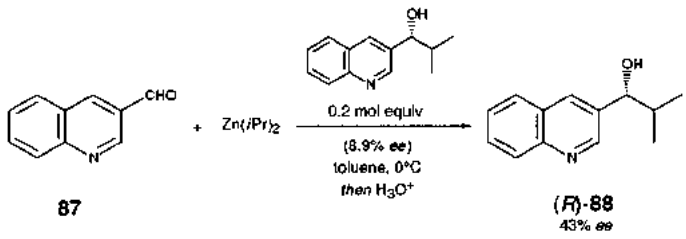

Scheme 16. Autocatalysis in the addition of diisopropylzinc to quinoline-3-carbaldehyde (**87**).

4 mM concentration of the initial catalyst) it was discovered that **88** (93.6 % *ee*) replicates 3.2 times into **88** (89.7 % *ee*).[83a] These experimental conditions were selected to study the influence of the initial *ee* value of **88** on the *ee* value of the additional **88** produced; in this particular case there is a strong (+)-NLE. For example 8.9 % *ee* of **88** generates 2.8 times more **88** (43.3 % *ee*).

A further investigation has been conducted by using 5-pyrimidyl carboxaldehyde (**89**) and the alcohol **90** (Scheme 17).[84] Even with an initial *ee* of 2 % for the **90**

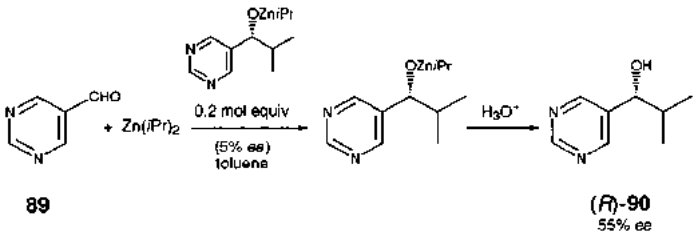

Scheme 17. Autocatalysis in the addition of diisopropylzinc to pyrimidyl-5-carbaldehyde (**89**).

formed, a plot of the *ee* value of newly formed **90** (ee_{prod}) versus the *ee* of the starting catalyst **90** (ee_{aux}) showed a typical (+)-NLE, with a strong amplification. The authors also made a correlation between their experimental data by taking the enantiomer ratios instead of the *ee*'s as parameters.[85] The above experiments have been performed by taking an initial catalyst of low *ee* and reusing the resulting product (with amplified *ee*) as a catalyst in a new reaction. By such a cycle of reactions the authors could use a sample of 2 % *ee* and reached a level of 88 % *ee* in five consecutive cycles. When the same procedure was applied to quinoline carboxaldehyde (**87**), by using the alcohol **88** with an initial 8.9 % *ee*, the enantiomeric excess obtained for (*R*)-**88** at the end of the cycle was 88 % as well (Scheme 16).[83a] A one-pot asymmetric autocatalytic reaction with a remarkable amplification (from 0.2 % *ee* to 90 % *ee*) was obtained recently in the formation of **90** by a special experimental procedure.[83b]

A catalytic enantioselective autoinductive reaction is a process that may be of interest to propagate high *ee*'s. This process is based on stereoselective reactions in which the products initially formed may influence the stereoselectivity of the proceding reaction (catalytic or stoichiometric). Albert and Wynberg coined the expression "enantioselective" autoinduction during their studies of a stoichiometric enantioselective reaction.[88]

The first example of enantioselective autoinduction in a catalytic reaction seems to be the report of Danda et al.[89] on the formation of cyanhydrine in the presence of small amounts of cyclic dipeptide **93** (Scheme 18). The authors

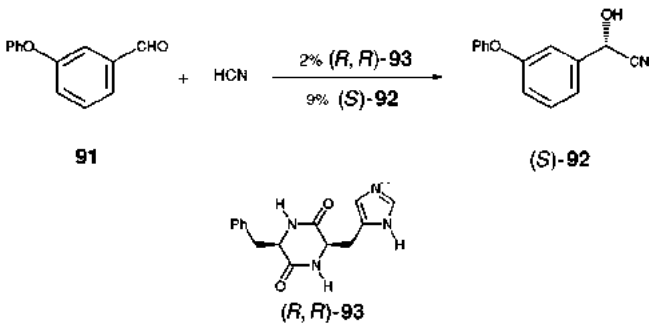

Scheme 18. Autoinduction in cyanohydrine formation in the presence of a cyclic dipeptide (**93**) (toluene, 5 °C).

found that the initial catalyst **93** is replaced in situ by the combination of **93** with product **92**. This has been established by adding a small amount of (*S*)-**92** with high *ee* value to the cyclic dipeptide **93** (enantiopure or of small *ee* value) at the beginning of the reaction. It is the enantiomeric purity of (*S*)-**92** that is the stereocontrolling factor on the catalytic production of cyanohydrine (*S*)-**92**. For example, in a given set of experimental conditions 0.022 mol equivalent of catalyst (*R,R*)-**93** (2 % *ee*) gave product (*S*)-**92** (81.6 % *ee*) in 43 % yield from the corresponding aldehyde **91**. The initially added (*S*)-**92** acts as a chiral co-catalyst. Interestingly, the catalyst prepared from **93** (66.8 % *ee*) and (*S*)-**92** (92.0 % *ee*) was able to generate (*S*)-**92** in 89 % yield with 96.0 % *ee* (which is higher than the *ee* of both components of the catalyst). The mechanistic details of the reaction, which works in heterogeneous conditions as a gel are not well understood, several mechanisms have been proposed.[90]

Soai et al. recently studied a catalytic enantioselective reaction with autoinduction in the particular case of addition of diisopropylzinc on an aromatic dialdehyde **94** (Scheme 19).[91] The catalyst is a chiral titanium complex

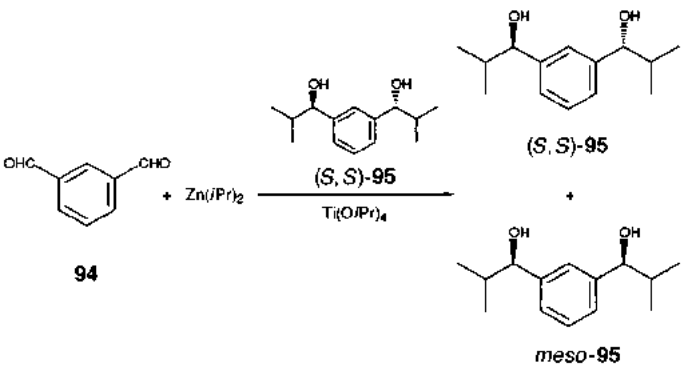

Scheme 19. Autoinduction in the double addition of diisopropylzinc with **94**.

presumably with a 1:2 stoichiometry, formed from the combination of $Ti(OiPr)_4$ with the chiral diol **95**. This chiral catalyst is different from the chiral zinc alkoxide which is derived from **95**, hence the expression "autoinduction". Here again the absolute configuration of the product **95** is the same as for the initiator **95** engaged in the catalyst. Unfortunately the product is obtained in lower *ee* value (30% *ee*) than the initial *ee* value of **95** (>99% *ee*), together with a large amount of *meso* diol.[92]

In conclusion asymmetric autocatalysis seems to be a promising area of investigation, as stated earlier by Wynberg.[93] The possibility of asymmetric amplification has been well established recently[84] and seems a consequence of the intervention of positive nonlinear effects (most presumably by a reservoir effect, see Section 2.2).[94]

3. Stoichiometric Asymmetric Synthesis

3.1. Principles

A chiral reagent may be prepared by modification of an achiral reagent with a chiral auxiliary X_c that will be bound covalently (**96**) or not (**97**) to the reagent Y (Figure 60). A

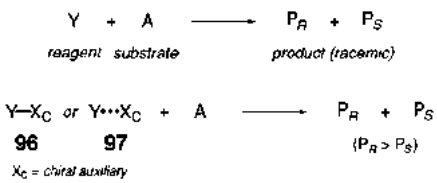

Figure 60. Formation of covalently bound (**96**) or associated (**97**) species in noncatalyzed asymmetric synthesis.

chiral silane R^*_3SiH (R^* = chiral group) or the combination *sec*-BuLi, sparteine (for asymmetric deprotonation) are examples of chiral reagents of type **96** ($Y{-}X_c$) or **97** ($Y\cdots X_c$).

Two basic situations are described in Figure 61. In the first case reagent $Y{-}X_c$ (**96**) is transformed into an inert by-

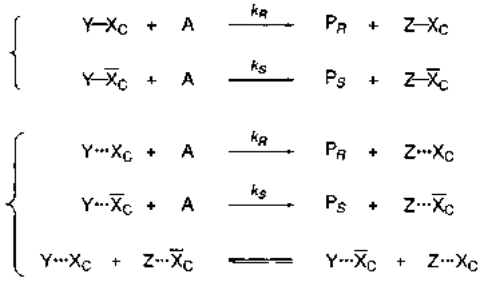

Figure 61. Two possible pathways in the noncatalyzed asymmetric synthesis. Xc and $\bar{X}_c$ = chiral intermediates of opposite configuration, Z = reagent that replaces Y.

product $Z{-}X_c$, the auxiliary is then removed from the reaction simultaneously to the formation of the product. When reagent $Y\cdots X_c$ (**97**) is used it may behave as above if the by-products $Z\cdots X_c$ and $Z\cdots \bar{X}_c$ retain their structures and do not exchange the X_c and $\bar{X}_c$ fragments with the reagents. If there are some exchanges of these groups (for example, as chiral ligands of some organometallic compounds) one may end up in the situation of asymmetric catalysis where there is a fast exchange of ligands (see Section 2). The enantioselectivity of the reaction must be independent of the conversion, with or without NLE that arises from the the number of X_c groups around Y, and of the relative reactivities of the diastereomeric species. One expects the same general behavior and the same models as discussed in Section 2.

The covalent reagent **96** gives a different scenario. If it involves only one X_c group the initial enantiomer ratio will remain constant during the course of the reaction and no NLE will appear. If this reagent gives rise to some aggregation one finds again the general features discussed for catalytic reactions (Section 2), some diastereomeric aggregates may be unreactive and the reaction will proceed through a monomeric reagent or a given diastereomer. NLE will be produced by a reservoir effect or through the $(ML)_n$ model.[96] The nonlinear effect will depend on conversion because the enantiomeric composition of the reagent should change if diastereomeric aggregates are of different reactivities. For example, if an heterochiral dimer is less reactive, the reaction will start with a (+)-NLE and in the latter stages of the reaction it will very much slow down with the generation of the racemic product. A constant (+)-NLE is expected if a large excess of reagent (in respect to substrate) is used. A reactive heterodimer will provide a strong (−)-NLE, and an excess of reagent will enhance this trend.

A special case, which is worth mentioning, is the use of a chiral reagent obtained by the permanent linking of two chiral fragments X_c to the achiral reagent Y. If the enantiopure reagent $Y(X_c)_2$, or $Y(\bar{X}_c)_2$, or the mixture of these enantiomeric reagents can be used in asymmetric synthesis, one would expect perfect linearity (unless aggregation occurs). However if the chiral reagent is prepared by the reaction of a mixture of X_c and $\bar{X}_c$ with Y there is the possibility that some heterochiral reagent $Y(X_c)(\bar{X}_c)$ will be generated. We then have a mixture of diastereomeric reagents in which the more reactive diastereomer has a chance to operate during part of the reaction, and provide an invariant NLE.

3.2. Asymmetric Reaction of Boron Compounds

Until now there were very few experimental data on NLE in stoichiometric asymmetric synthesis. One of the first examples seems to be an asymmetric synthesis at Merck in 1994 of an alcohol, which is a useful intermediate in the synthesis of a LTD_4 antagonist.[98, 99] It was found that Ipc_2BCl, prepared from (−)-α-pinene and BH_2Cl, reduced the ketone **98** to give alcohol **99** in 97% *ee* or 95% *ee* with (+)-α-pinene of 98% *ee* or 70% *ee* (Figure 62). It was hypothesized that three reagents (two homochiral and one *meso*) are in statistical distribution, with the *meso* borane being very sluggish to react. More recently the authors studied in detail the relationships between the *ee* value of the alcohol **99** and the *ee* value of the α-pinene (Figure 62). There is a good agreement between the calculated curve and experimental data, when the hypothesis of a statistical distribution and an

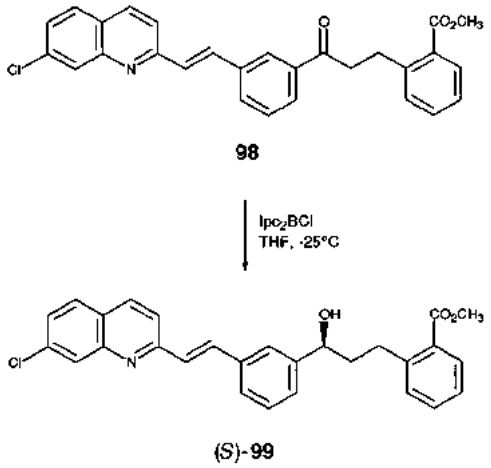

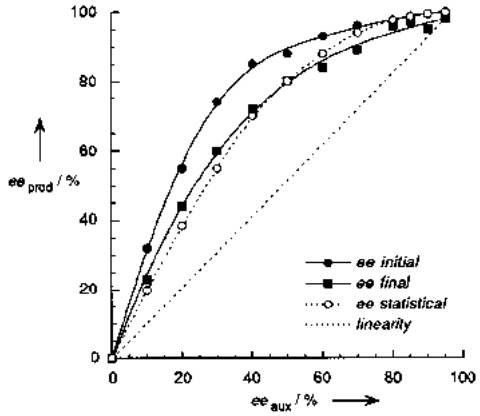

Figure 62. (+)-NLE in Ipc_2BCl reduction of the ketone **98**. Ipc = isopinocampheyl.

unreactive *meso* Ipc_2BCl is employed.[99] However, a quite large deviation has been observed at low conversion giving a higher *ee* value of **99** than after complete reduction.

In 1995 Kagan and Girard studied the asymmetric reduction of acetophenone by Ipc_2BCl (4 equiv) by using a reagent derived from (−)-α-pinene (**100**).[100] Ipc_2BCl was prepared according to the procedure of Brown and Joshi.[101] The way the reagent was synthesized was very important for the outcome of the reduction of acetophenone (**102**, Scheme 20). The separate preparation of Ipc_2BCl (**101**) from enantiopure α-pinenes gave "*ll*"-**101** and "*dd*"-**101**, which were then mixed in various amounts to reach the desired ee_{aux}. The other procedure starts from a mixture of (−)- and (+)-α-pinene in the required *ee*'s

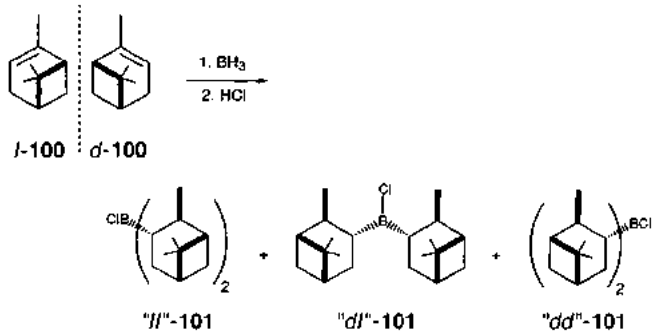

Scheme 20. Homochiral ("*ll*"- and "*dd*"-**101**) and heterochiral ("*dl*"-**101**) reagents generated during the formation of Ipc_2BCl (**101**).

(*l*- and *d*-**100**) to give rise to the formation of three boranes: "*ll*"-**101,** "*dd*"-**101** and "*dl*"-**101.** The first procedure gave perfect linearity between ee_{aux} and ee_{prod} (Figure 63a), while the second method generated a strong (+)-NLE, the asymmetric amplification being especially good above 30% *ee* for α-pinene (Figure 63b). The linear relationship indicates that each of the enantiomeric reagents acts independently in the reduction process. The (+)-NLE is in agreement with a very low reactivity of the *meso* reagent "*dl*"-**101**, which is presumably formed in quite a large amount.

As an added proof, the recent study by the Merck group demonstrated that the *ee* value of their reduction product was time-dependent.[102] The NLE was indeed more pronounced at lower conversion than after completion of the reaction. The curves however keep the same shape during the course of the reduction; which is close to the calculated curve based on a statistical distribution of the pinene on the boron atom. Kagan and Girard also presented another study where the stoichiometry of Ipc_2BCl (**101**) was varied from one to four equivalents.[103] The curves had the same shape, but the NLE increased with the amount of reductant used. These complementary results suggest that a higher *ee* value at the beginning

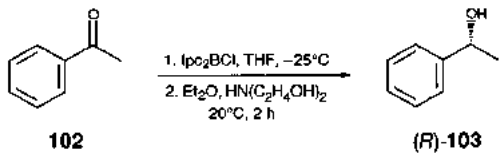

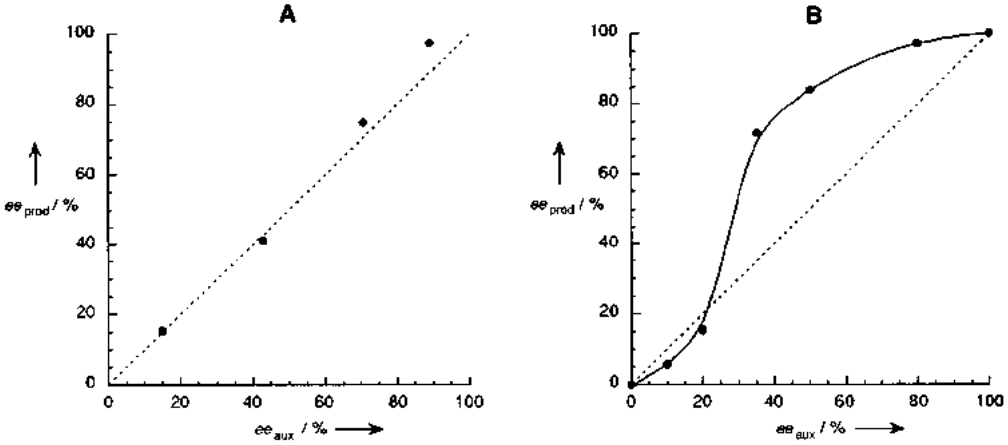

Figure 63. Variation in the *ee* value of (*R*)-**103** with the *ee* value of α-pinene (see text for further details).

of the reaction will be provided by the more reactive homochiral species or by the use of a larger quantity of reagent. But as soon as the amount of this species drops, with time or by using less reagent, the "unreacting" heterochiral borane becomes involved in the reduction, which lowers slightly the *ee* value of the product.

Apart from mechanistic interest, the possibility of creating a strong (+)-NLE in Ipc_2BCl reductions allows the expensive enantiopure α-pinene to be avoided, and instead cheaper α-pinene of *ee*'s lower than 90% can be used.[98, 99]

3.3. Cuprate Addition

Tanaka et al. studied an asymmetric synthesis of muscone **105** by the 1,4-addition of a methylcuprate complexed by the chiral bidentate ligand MPATH to the enone **104**.[104] An interesting NLE was observed, the data given in the paper allows to draw a two-shaped curve (Figure 64). The authors

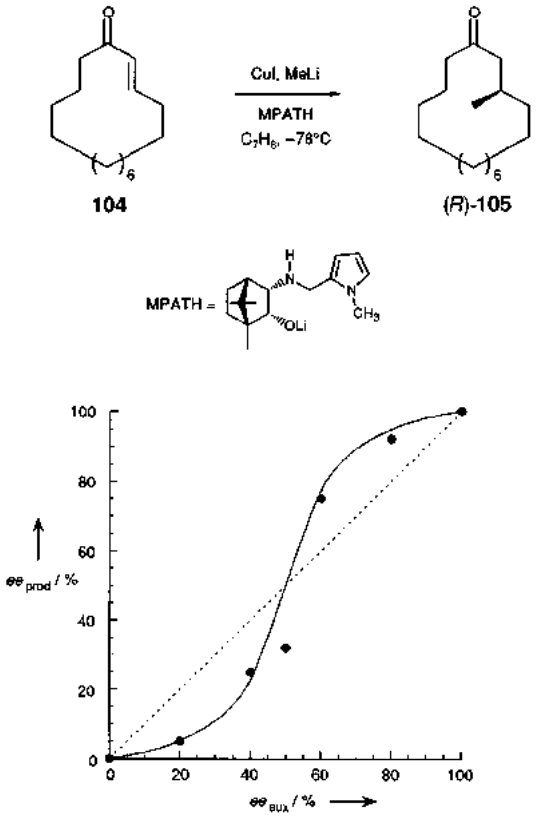

Figure 64. Two-shaped NLE curve observed in the synthesis of muscone (**105**) from **104**.

postulated the formation of dimeric species such as **106**. The curve was accurately reproduced by using the $(ML)_4$ model,

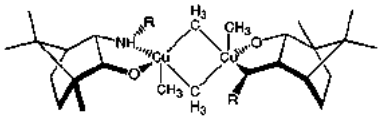

106

which could mean the involvement of an aggregation of dimers.[31]

Rossiter et al. observed a (+)-NLE in the asymmetric addition of a *n*-butylcuprate to 2-cycloheptenone (**17**) by using the lithium salt of an aminoalcohol chiral ligand, (*S*)-mapp (Figure 65).[105] The authors assumed a statistical

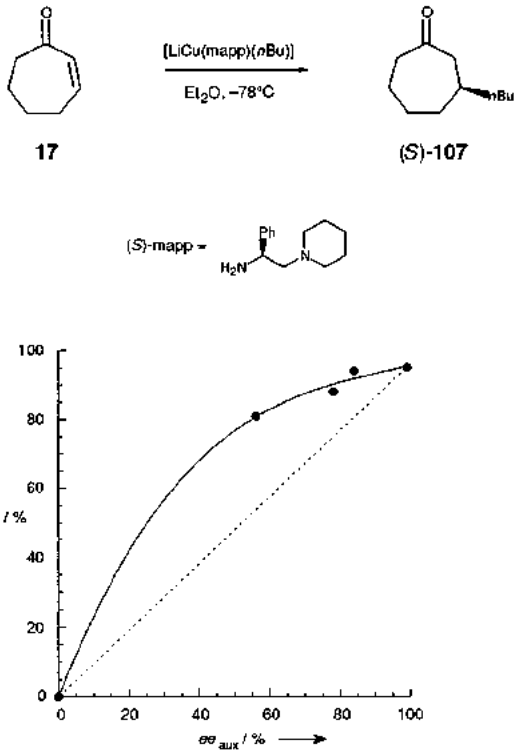

Figure 65. (+)-NLE observed in the mapp-catalyzed cuprate addition to **17**.

distribution of ligands into dimers such as the unreactive *meso* dimer **108**. Calculations are in good agreement with these hypotheses. For example, enantiopure ligand in this case gave 96% *ee* of product, while the (*S*)-MAPP at 56% *ee* provided a product with 81% *ee* (instead of 54% *ee* for linearity and 81.9% *ee* calculated with the above hypotheses). When the reaction was performed in diethyl ether with additives such as HMPA or solvents such as THF, which break the dimeric structure by lithium solvation, suppression of the enantioselectivity, presumably by generation of non-enantioselective monomers, was observed (HMPA = hexamethylphosphoramide). The cases of 1,4-additions of Grignard reagents in the presence of catalytic amounts of chiral copper complexes were discussed in Section 2.3.3.

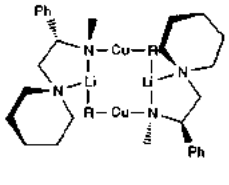

108

3.4. Asymmetric Protonation

A (+)-NLE has been observed in the asymmetric protonation of a lithium enolate **109** to (*S*)-γ-damascone ((*S*)-**111**)

by a 1:2 mixture of the amino alcohol **110**-OH and its corresponding lithium alkoxide **110**-OLi (Scheme 21).[106] The use of an enantiopure protonating agent (100 % *ee*) gave the product **111** with 75 % *ee*, while the use of 50 % *ee* mixture of

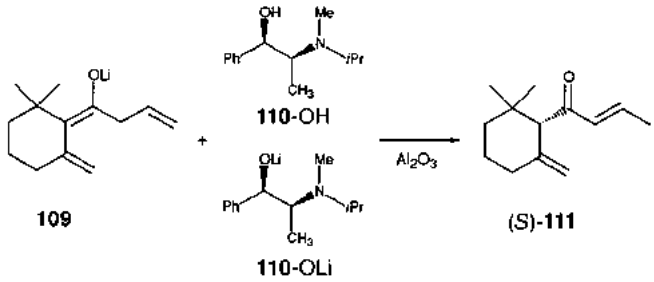

Scheme 21. Asymmetric protonation of **110** to (*S*)-γ-damascone (**111**).

110 gave the product with the same 50 % enantiomeric excess. The chiral protonating agent was proposed to form a complicated and dimeric structure, which is in agreement with the observed nonlinear effect prevailing in the present case.

4. Diastereoselective Reactions

In this section the reactions of chiral substrates that give rise to isolable diastereomers are considered. The reactions may be realized with an achiral or a chiral reagent, or with a chiral catalyst. If during the course of the reaction some aggregation occurs it may generate perturbations, as observed in enantioselective reactions. These perturbations should be reflected by nonlinearities between the diastereomeric excess and the *ee* value of the substrate or the reagent. Until now there were very few reports in that area. Wynberg and Feringa discovered that the $LiAlH_4$ reduction of racemic or enantiopure camphor gave different values for the isoborneol/borneol ratio[16] (see Section 1) but there were no data with camphor of intermediate *ee*'s, and then no knowledge of the variation of *de* of the product with the *ee* of the camphor.

Rautenstrauch et al. carefully investigated the reduction of camphor by potassium in liquid ammonia (Scheme 22).[107] They looked at the diastereomeric composition of the resulting alcohols (*dc*, percentage of the major

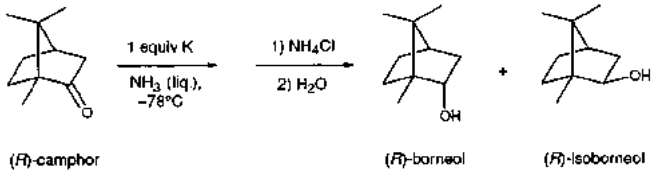

Scheme 22. Reduction of (*R*)-camphor by potassium in liquid ammonia.

diastereomer) as a function of the enantiomeric composition (*ec*, percentage of the major enantiomer) of camphor. Surprisingly, borneol is the major product when one starts from racemic camphor, while borneol slightly predominates if enantiopure camphor is the starting material.

In Figure 66 the *dc* of the alcohol versus *ec* of the camphor is shown. It is easy to establish that the relationships $de_{product} = EE_0\,ee_{substrate}$ and $dc_{product} = EC_0\,ec_{Substrate}$ are equivalent (EE_0 and EC_0 are the enantiomeric excess or the enantiomeric composition of the major alcohol derived from reduction of an enantiopure substrate).[108] There is almost a linear behavior for the diastereoselectivity of the reaction (Figure 66 a), while a strong nonlinear effect has been

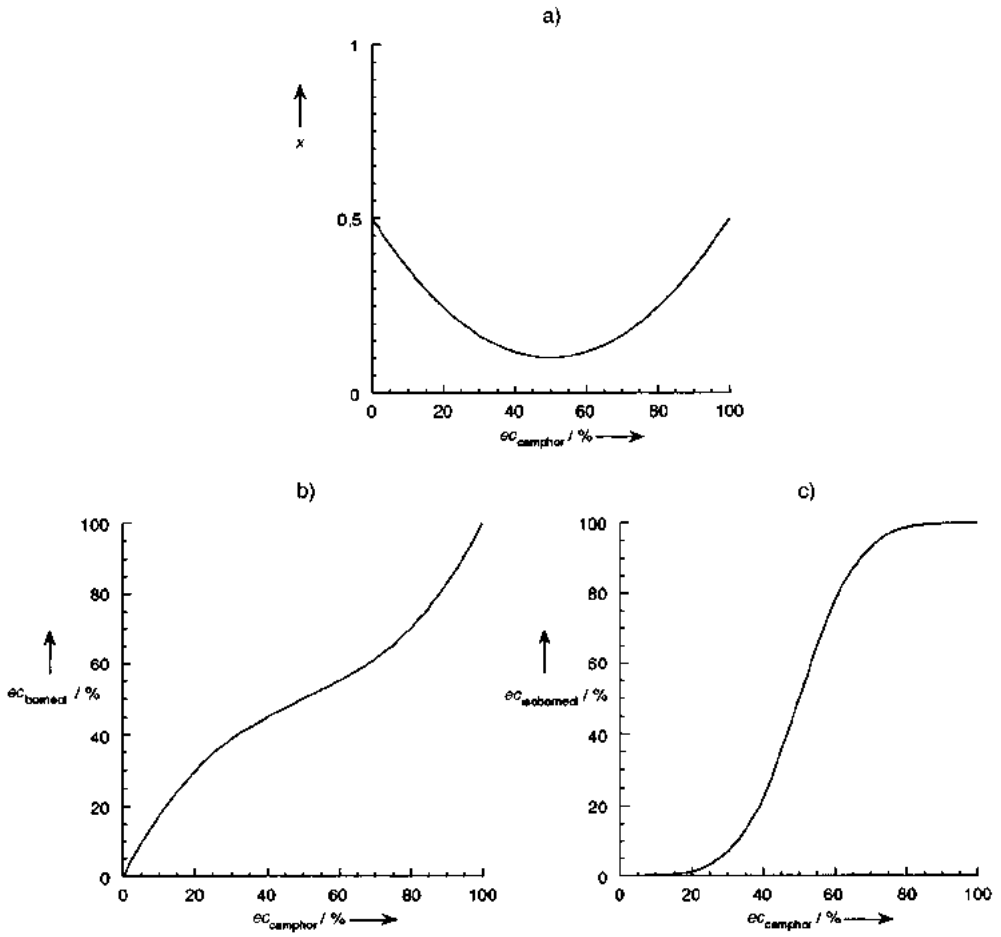

Figure 66. a) Mole fraction x of isoborneol and also the *ec* of b) borneol and c) isoborneol as functions of the enantiomeric composition of camphor.

observed for the enantiomeric composition of borneol or isoborneol (Figures 6b, c). These observations have been explained by a mechanism that involves the initial formation of a ketyl anion radical (as a dimeric species). Experimental results have shown that hydrogen transfers between two dimers **A** provide (after hydrolysis) equimolar amounts of alcohols and camphor (Scheme 23). A kinetic analysis of the

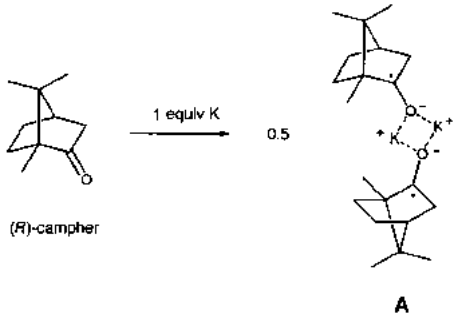

Scheme 23. The dimeric diastereomeric species **A** formed during the reduction of camphor.

results is in agreement with the reaction being fourth order in camphor (second order in respect to the dimers **A**). This analysis highlights the importance of associations of lithio species for stereochemical controls. The key factor that explains the deviation from linearity is the formation of diastereomeric species **A**, which give rise to new routes in the subsequent disproportionations into products.

The self-coupling reaction may give different products if the reactant is enantiopure or a mixture of enantiomers (homochiral or a mixture of homochiral and heterochiral coupling products are formed, respectively). Moreover the coupling reaction may create a new stereochemical unit (*E*/*Z*, *R*/*S*, *P*/*M*). It is this situation that has been investigated by Wynberg and Feringa in the case of McMurry coupling of camphor and the *ortho*-coupling of phenols with an asymmetric center[16] (Scheme 24). These reactions were only

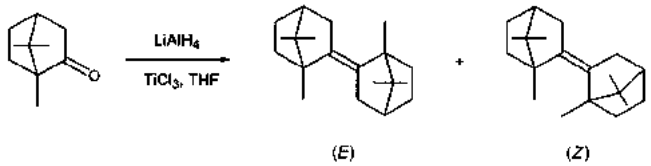

Scheme 24. McMurry coupling of camphor.

performed for 100% *ee* or 0% *ee*, and showed some stereochemical differences according to the initial *ee* value. For example, the McMurry coupling of enantiopure camphor gave homochiral dimers ($E/Z = 1.68$). McMurry coupling of racemic camphor provided homochiral dimers ($E/Z = 1.67$) and heterochiral dimers ($E/Z = 2.9$) in a ratio of 1.8:1

The oxidative coupling of enantiopure (*S*)-phenol **112** (Scheme 25) led to only one (>97.5%) configuration for the new atropoisomeric unit **113** (*P*), while the coupling of racemic **112** gave the following distribution of **113**: (*S*,*S*,*P*) + (*R*,*R*,*M*)/(*S*,*S*,*M*) + (*R*,*R*,*P*)/(*R*,*S*,*P*) + (*R*,*S*,*M*) in the relative

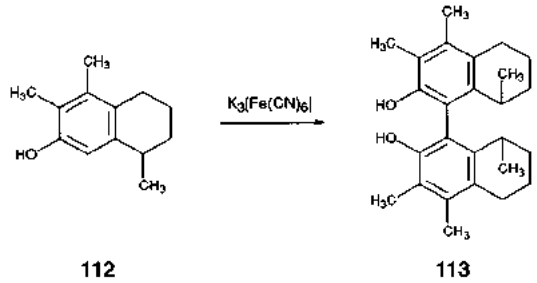

Scheme 25. Oxidative coupling of a phenol derivative **112**.

ratio of 66.0:7.9:26.1. In the above reactions, as well as in the reduction of camphor by $LiAlH_4$, it would be of interest to follow the various diastereoselectivities as a function of the enantiomeric excess of the substrate.

The condensation of a reagent (chiral or not) with a chiral substrate with the creation of an asymmetric center may also give rise to nonlinear effects if there is an external chiral auxiliary (in stoichiometric or catalytic amounts). A reagent control has been observed by Tanaka et al. in the catalyzed addition of diisopropylzinc on the steroid **114** (Scheme 26).[109]

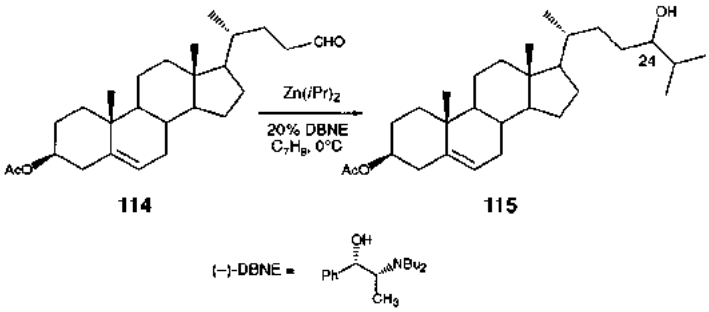

Scheme 26. DBNE-catalyzed addition of diisopropylzinc to the steroid **114**.

The chiral catalyst (a β-aminoalcohol of various *ee*'s) controls the configuration at C_{24}. The diastereoselectivity of the reaction is not proportional to ee_{aux}. The catalyst (−)-DBNE (100% or 21% *ee*) gave a product **115** with 24-(*R*) configuration (97.0% *de* in both cases) while with (+)-DBNE (100%) the (*S*)-product **115** (87% *de*) was obtained. These data are indicative of a positive nonlinear effect (asymmetric amplification) under reagent control.[110]

5. Summary and Outlook

In only a ten year period nonlinear effects have established themselves as an ubiquitous phenomenon in asymmetric reactions, especially in enantioselective catalysis. It provides a simple and additional tool to detect and to discuss aggregation and self-assemblies that may arise in given reactions. The generation of diastereomeric species is the key feature that gives deviation from linearity. Asymmetric amplification characterizes a (+)-NLE and is a useful property for a reacting system since enantioselectivity is higher than expected, which allows the convenient use in some cases of

enantiomerically impure chiral auxiliaries. It also paves the way to the possibility to build some autocatalytic systems with autoinduction. These systems could be synthetically useful or could suggest additional models for prebiotic generation of optical activity on earth.

The presence or not of nonlinear effects may depend of the experimental conditions in the preparation of the chiral catalyst or reagent. This may also enlighten some aspects of the reaction. The basic concepts, which are the roots of the nonlinear effects in enantioselective reactions, should apply as well to kinetic resolution[47b, 111] and diastereoselective reactions, for example in the creation of a new asymmetric center in enantiopure substrates under the influence of a chiral catalyst. The diastereoselectivity of the reaction may be influenced by the enantiomeric excess of the catalyst with a deviation from linearity. The burgeoning of the reports on NLEs for a wide range of reactions show how useful this concept is, and how it provides a kind of specific signature to a given process. One may anticipate that new developments will continue to accumulate in the near future.

Funds provided by the Centre National de la Recherche Scientifique de France and Institut Universitaire de France are greatly acknowledged. C.G. wants to thank the Ministère des Affaires Étrangères de France and the Ambassade de France au Canada for the Chateaubriand fellowship, which made his post-doctoral stay possible.

The curves, schemes, and molecular structures presented here are redrawn as accurately as possible from the original papers cited in this article.

Received: July 18, 1997 [A 245 IE]
German version: *Angew. Chem.* **1998**, *110*, 3088 – 3127

[1] L. Pasteur, *C. R. Acad. Sci. Paris* **1848**, *26*, 535.
[2] The optical purity (op) has been defined as the ratio of the observed specific rotation of the compound $[\alpha]^{D}_{obs}$ divided by the specific rotation of the enantiopure compound $[\alpha]^{D}_{max}$. It is easy to establish that $op(\%) = \frac{R-S}{R+S} \times 100$ (R = mole fraction of the major enantiomer), to give a way to calculate the relative amounts of the two enantiomers. Morrison and Mosher[3] proposed the use of the expression "enantiomeric" excess (*ee*) defined as $ee(\%) = \frac{R-S}{R+S} \times 100$. This definition has the advantage that *ee* coincides with op, even when the measurement is performed by nonpolarimetric methods. (See also ref. [4] for a discussion on that topic.)
[3] J. D. Morrison, H. S. Mosher, *Asymmetric Organic Reactions*, Prentice Hall, Englewood Cliffs, **1971**, p. 10.
[4] E. L. Eliel, S. H. Wilen, L. N. Mander, *Stereochemistry of Organic Compounds*, Wiley, New York, **1994**, p. 214.
[5] A. Horeau, *Tetrahedron Lett.* **1969**, 3121.
[6] A. Horeau, J. P. Guetté, *Tetrahedron* **1974**, *30*, 1923.
[7] T. Williams, R.G. Pitcher, P. Bommer, J. Gutzwiller, M. Uskokovic, *J. Am. Chem. Soc.* **1969**, *91*, 1871.
[8] T. Katagiri, C. Yoda, K. Furuhashi, K. Ueki, T. Kubota, *Chem. Lett.* **1996**, 115.
[9] a) K. C. Cundy, P. A. Crooks, *J. Chromatogr.* **1983**, *281*, 17; b) R. Charles, E. Gil-Av, *J. Chromatogr.* **1984**, *298*, 516.
[10] W.-L. Tsai, K. Hermann, E. Hug, B. Rohde, S. S. Dreiding, *Helv. Chim. Acta* **1985**, *68*, 2238.
[11] A. Dobashi, Y. Motoyama, K. Kinoshita, S. Hara, N. Fukasaku, *Anal. Chem.* **1987**, *59*, 2209.
[12] R. Matusch, C. Coors, *Angew. Chem.* **1989**, *101*, 624; *Angew. Chem. Int. Ed. Engl.* **1989**, *28*, 626.
[13] R. M. Carman, K. D. Klika, *Aust. J. Chem.* **1991**, *44*, 895.
[14] P. Diter, S. Taudien, O. Samuel, H. B. Kagan, *J. Org. Chem.* **1994**, *59*, 370.
[15] M. Jung, V. Schurig, *J. Chromatogr.* **1992**, *605*, 161.
[16] a) H. Wynberg, B. Feringa, *Tetrahedron* **1976**, *32*, 2831; b) H. Wynberg, *Chimia* **1976**, *30*, 445.
[17] However, Izumi and Tai pointed out that the measurement of the asymmetric induction in an asymmetric synthesis may not be necessarily correlated simply to the *ee* value of the chiral auxiliary, especially in asymmetric catalysis.[18]
[18] Y. Izumi, A. Tai, *Stereo-Differentiation Reactions*, Academic Press, New York, **1977**, p. 244.
[19] C. Puchot, O. Samuel, E. Duñach, S. Zhao, C. Agami, H. B. Kagan, *J. Am. Chem. Soc.* **1986**, *108*, 2353.
[20] There are a few review articles on some aspects of nonlinear effects.[21–24] For recent highlights and discussion on NLEs, see M. Avalos, R. Babiano, P. Cintas, J. L. Jiménez, J. C. Palacios, *Tetrahedron: Asymmetry* **1997**, *8*, 2997; M. Reggelin, *Nachr. Chem. Tech. Lab.* **1997**, *45*, 392, 622; D. G. Blackmond, *J. Am. Chem. Soc.* **1997**, *119*, 12934.
[21] R. Noyori, M. Kitamura, *Angew. Chem.* **1990**, *30*, 34; *Angew. Chem. Int. Ed. Engl.* **1990**, *30*, 49.
[22] R. Noyori, *Asymmetric Catalysis in Organic Synthesis*, Wiley, New York, **1994**, pp. 273 – 297.
[23] C. Bolm in *Advanced Asymmetric Synthesis* (Ed. G. R. Stephenson), Blackie Academic and Professional, New York, **1996**, pp. 9 – 26.
[24] H. B. Kagan, C. Girard, D. Guillaneux, D. Rainford, O. Samuel, S. Y. Zhang, S. H. Zhao, *Acta Chem. Scand.* **1996**, *50*, 345.
[25] a) U. Eder, G. Sauer, P. Wiechert, *Angew. Chem.* **1971**, *83*, 492; *Angew. Chem. Int. Ed. Engl.* **1971**, *10*, 496; b) Z. G. Hajos, D. Parrish, *J. Org. Chem.* **1974**, *39*, 1615.
[26] a) C. Agami, C. Puchot, *J. Mol. Cat.* **1986**, *38*, 341; b) C. Agami, *Bull. Soc. Chim. Fr.* **1988**, 499.
[27] a) K. Katsuki, K. B. Sharpless, *J. Am. Chem. Soc.* **1980**, *102*, 5974; b) M. G. Finn, K. B. Sharpless, *J. Am. Chem. Soc.* **1991**, *113*, 113.
[28] N. Oguni, Y. Matsuda, T. Kaneko, *J. Am. Chem. Soc.* **1988**, *110*, 7877.
[29] P. Pitchen, E. Duñach, M. N. Deshmukh, H. B. Kagan, *J. Am. Chem. Soc.* **1984**, *106*, 8188.
[30] For a simulation of the curve of Figure 5 under the assumption of a dimeric titanium species with four DET, see ref. [31].
[31] D. Guillaneux, S. H. Zhao, O. Samuel, D. Rainford, H. B. Kagan, *J. Am. Chem. Soc.* **1994**, *116*, 9430.
[32] a) M. Kitamura, S. Okada, R. Noyori, *J. Am. Chem. Soc.* **1989**, *111*, 4028; b) M. Yamakawa, R. Noyori, *J. Am. Chem. Soc.* **1995**, *117*, 6327; see also [21, 22].
[33] C. Bolm, G. Schlingloff, K. Harms, *Chem. Ber.* **1992**, *125*, 1191.
[34] K. Fitzpatrick, R. Hulst, R. M. Kellog, *Tetrahedron: Asymmetry* **1995**, *6*, 1861.
[35] a) C. Bolm, *Tetrahedron: Asymmetry* **1991**, *2*, 701; b) C. Bolm, M. Ewald, M. Felder, *Chem. Ber.* **1992**, *125*, 1205; c) C. Bolm, M. Felder, J. Müller, *Synlett* **1992**, 439.
[36] A. H. M. de Vries, J. F. G. A. Jansen, B. L. Feringa, *Tetrahedron* **1994**, *50*, 4479.
[37] Q.-L. Zhou, A. Pfaltz, *Tetrahedron* **1994**, *50*, 4467.
[38] G. van Koten, *Pure Appl. Chem.* **1994**, *66*, 1455.
[39] a) M. Terada, K. Mikami, T. Nakai, *J. Chem. Soc. Chem. Commun.* **1990**, 1623; b) K. Mikami, M. Terada, S. Narisawa, T. Nakai, *Synlett* **1992**, 255; c) K. Mikami, M. Terada, *Tetrahedron* **1992**, *48*, 5671; d) K. Mikami, *Adv. Asymmetric Synth.* **1995**, *1*, 1.
[40] M. Terada, K. Mikami, *J. Chem. Soc. Chem. Commun.* **1994**, 833.
[41] D. Kitamoto, H. Imma, T. Nakai, *Tetrahedron Lett.* **1995**, *36*, 1861.
[42] a) M. Hayashi, T. Matsuda, N. Oguni, *J. Chem. Soc. Chem. Commun.* **1990**, 1364; b) M. Hayashi, T. Matsuda, N. Oguni, *J. Chem. Soc. Perkin Trans.* **1992**, 3135.
[43] a) G. E. Keck, D. Krishnamurthy, M. C. Grier, *J. Org. Chem.* **1993**, *58*, 6543; b) G. E. Keck, D. Krishnamurthy, *J. Am. Chem. Soc.* **1995**, *117*, 2363.
[44] J. W. Faller, D. W. I. Sams, X. Liu, *J. Am. Chem. Soc.* **1996**, *118*, 1217.
[45] P. Bedeschi, S. Casolari, A. L. Costa, E. Tagliavini, A. Umani-Ronchi, *Tetrahedron Lett.* **1995**, *36*, 7897.

[46] D. R. Gauthier, Jr, E. M. Carreira, *Angew. Chem.* **1996**, *108*, 2521; *Angew. Chem. Int. Ed. Engl.* **1996**, *35*, 2363.
[47] a) N. Komatsu, M. Hashizume, T. Sugita, S. Uemura, *J. Org. Chem.* **1993**, *58*, 4529; b) N. Komatsu, M. Hashizume, T. Sugita, S. Uemura, *J. Org. Chem.* **1993**, *58*, 7624.
[48] H. B. Kagan, J.-C. Fiaud, *Top. Stereochem.* **1988**, *18*, 249.
[49] C. Zondervan, B. L. Feringa, *Tetrahedron: Asymmetry* **1996**, *7*, 1895.
[50] N. Iwasawa, Y. Hayashi, H. Sakurai, K. Narasaka, *Chem. Lett.* **1989**, 1581.
[51] J. Irurre, C. Alonso-Alija, A. Fernández-Serrat, *Afinidad* **1994**, *51*, 413.
[52] K. Mikami, Y. Motoyama, M. Terada, *J. Am. Chem. Soc.* **1994**, *116*, 2812.
[53] S. Kobayashi, H. Ishitani, M. Araki, I. Hachiya, *Tetrahedron Lett.* **1994**, *35*, 6325.
[54] D. Seebach, R. Dahinden, R. E. Marti, A. K. Beck, D. A. Plattner, F. N. M. Kühnle, *J. Org. Chem.* **1995**, *60*, 1788.
[55] M. Shimizu, Y. Ukaji, K. Inomata, *Chem. Lett.* **1996**, 455.
[56] H. Sasai, T. Susiki, N. Itoh, M. Shibasaki, *Tetrahedron Lett.* **1993**, *34*, 851.
[57] D. A. Evans, S. G. Nelson, M. R. Gagné, A. R. Muci, *J. Am. Chem. Soc.* **1993**, *115*, 9800.
[58] K. B. Hansen, J. L. Leighton, E. N. Jacobsen, *J. Am. Chem. Soc.* **1996**, *118*, 10924.
[59] M. Yamaguchi, T. Shiraishi, M. Hirama, *J. Org. Chem.* **1996**, *61*, 3520.
[60] B. Schmidt, D. Seebach, *Angew. Chem.* **1991**, *103*, 1383; *Angew. Chem. Int. Ed. Engl.* **1991**, *30*, 1321.
[61] a) C. Bolm, J. Müller, G. Schlingloff, M. Zehnder, M. Neuburger, *J. Chem. Soc. Chem. Commun.* **1993**, 182; b) C. Bolm, J. Müller, *Tetrahedron* **1994**, *50*, 4355.
[62] P. I. Dosa, J. C. Ruble, G. C. Fu, *J. Org. Chem.* **1997**, *62*, 444.
[63] M. Bougauchi, S. Watanabe, T. Arai, H. Sasai, M. Shibasaki, *J. Am. Chem. Soc.* **1997**, *119*, 2329.
[64] T. Schwenkreis, A. Berkessel, *Tetrahedron Lett.* **1993**, *34*, 4785.
[65] C. Bolm, F. Bienewald, *Angew. Chem.* **1995**, *107*, 2883; *Angew. Chem. Int. Ed. Engl.* **1995**, *34*, 2640.
[66] D. Seebach, R. E. Marti, T. Hintermann, *Helv. Chim. Acta* **1996**, *79*, 1710.
[67] S. E. Denmark, B. L. Christenson, S. P. O'Connor, *Tetrahedron Lett.* **1995**, *36*, 2219.
[68] a) J. W. Faller, J. Parr, *J. Am. Chem. Soc.* **1993**, *115*, 804; b) J. W. Faller, M. R. Mazzieri, J. T. Nguyen, J. Parr, M. Tokunaga, *Pure Appl. Chem.* **1994**, *66*, 1463; c) D. P. Fairlie, B. Bosnich, *Organometallics* **1988**, *7*, 936; e) D. P. Fairlie, B. Bosnich, *Organometallics* **1988**, *7*, 946; f) S. H. Bergens, P. Noheda, J. Whelan, B. Bosnich, *J. Am. Chem. Soc.* **1992**, *114*, 2121.
[69] K. Burgess, W. A. van der Donk, *Inorg. Chim. Acta* **1994**, *220*, 93.
[70] a) M. Kitamura, S. Suga, M. Niwa, R. Noyori, *J. Am. Chem. Soc.* **1995**, *117*, 4832; b) M. Kitamura, M. Yamakawa, H. Oka, S. Suga, M. Niwa, R. Noyori, *Chem. Eur. J.* **1997**, *2*, 1173.
[71] The authors used Equations (8) and (9) to draw the calculated curves: where v_0^A and v_0^B are the initial rates of pure cat_A- and cat_B-catalyzed reactions proceeding with enantioselectivities of ee_A and ee_B, respectively. The abscissa or the graphics are catalyst composition expressed as $100\,cat_A/([cat_A]+[cat_B])$ or $100\,cat_B/([cat_A]+[cat_B])$.

$$ee_{ber} = \frac{ee_A v_0^A [cat_A] + ee_B v_0^B [cat_B]}{[cat_A] + [cat_B]} \quad (8)$$

$$v_{0,ber} = \frac{v_0^A [cat_A] + v_0^B [cat_B]}{[cat_A] + [cat_B]} \quad (9)$$

[72] S. Y. Zhang, C. Girard, H. B. Kagan, *Tetrahedron: Asymmetry* **1995**, *6*, 2637.
[73] K. B. Sharpless, W. Amberg, Y. L. Bennani, G. A. Crispino, J. Hartung, K.-S. Jeong, H.-L. Kwong, K. Morikawa, Z.-M. Wang, X.-L. Zhang, *J. Org. Chem.* **1992**, *57*, 2768.
[74] E. J. Corey, M. C. Noe, *J. Am. Chem. Soc.* **1993**, *115*, 12579.
[75] a) M. A. Giardello, V. P. Conticello, L. Brard, M. R. Gagné, T. J. Marks, *J. Am. Chem. Soc.* **1994**, *116*, 10241; b) P.-F. Fu, L. Brard, Y. Li, T. J. Marks, *J. Am. Chem. Soc.* **1995**, *117*, 7157.
[76] F. C. Frank, *Biochim. Biophys. Acta* **1953**, *11*, 459.
[77] M. Calvin, *Chemical Evolution*, Clarendon, London, **1969**, Chap. 7.
[78] For a recent highlight on asymmetric autocatalysis with amplification of chirality, see ref. [79a]. For a possible asymmetric autocatalytic system (liquid phase autoxidation) see ref. [79b].
[79] a) C. Bolm, F. Bienewald, A. Seger, *Angew. Chem.* **1996**, *108*, 1767; *Angew. Chem. Int. Ed. Engl.* **1996**, *35*, 1657 and references therein; b) T. Buhse, D. Lavabre, J. C. Micheau, W. Thiemann, *Chirality* **1993**, *5*, 341.
[80] K. Soai, S. Niwa, H. Hori, *J. Chem. Soc. Chem. Commun.* **1990**, 983.
[81] K. Soai, T. Hayase, K. Takai, *Tetrahedron: Asymmetry* **1995**, *6*, 637.
[82] T. Shibata, K. Choji, T. Hayase, Y. Aizu, K. Soai, *Chem. Commun.* **1996**, 751.
[83] a) T. Shibata, K. Choji, T. Hayase, Y. Aizu, K. Soai, *Chem. Commun.* **1996**, 1235; b) T. Shibata, T. Hayase, J. Imamoto, K. Soai, *Tetrahedron: Asymmetry* **1997**, *8*, 1717.
[84] K. Soai, T. Shibata, H. Marioka, K. Choji, *Nature* **1995**, 767.
[85] For advantages or disadvantages of the use of the enantiomeric ratio (*er*) in stereochemical problems or Horeau amplification, see refs. [86, 87].
[86] H. B. Kagan, *Rec. Trav. Chim. Pays-Bas* **1995**, *114*, 203.
[87] V. Rautenstrauch, *Bull. Soc. Chim. Fr.* **1994**, *131*, 515.
[88] a) A. H. Alberts, H. Wynberg, *J. Am. Chem. Soc.* **1989**, *111*, 7265; b) A. H. Alberts, H. Wynberg, *J. Chem. Soc. Chem. Commun.* **1990**, 453.
[89] H. Danda, H. Nishikawa, K. Otaka, *J. Org. Chem.* **1991**, *56*, 6740.
[90] Y. Shvo, M. Gal, Y. Becker, A. Elgavi, *Tetrahedron Lett.* **1996**, *7*, 911, and references therein.
[91] K. Soai, Y. Inoue, T. Takahashi, T. Shibata, *Tetrahedron Asymmetry* **1996**, *7*, 13355.
[92] The interpretation of the reaction is complicated here by the possibility of a double asymmetric reaction.[87]
[93] H. Wynberg, *Chimia* **1989**, *43*, 150.
[94] A qualitative model for asymmetric autocatalytic processes has been proposed by Bailey.[95] It is based on the ML_2 model,[31] the reaction involving the formation of L. As discussed above it is possible to introduce a (+)-NLE, which makes this system useful for self-replication of chirality.
[95] P. D. Bailey, *J. Chem. Soc. Chem. Commun.* **1995**, 1707.
[96] Equations based on competitive reactions of Figure 60 have been developed to describe the various cases where stoichiometric asymmetric synthesis can give rise to NLE.[97]
[97] C. Girard, H. B. Kagan, manuscript in preparation.
[98] a) A. O. King, E. G. Corley, R. K. Anderson, R. D. Larsen, T. R. Verhoeven, P. J. Reider, Y. B. Xiang, M. Belley, Y. Leblanc, M. Labelle, P. Prasit, R. J. Zamboni, *J. Org. Chem.* **1993**, *58*, 3731; b) I. Shinkai, A. O. King, R. D. Larsen, *Pure Appl. Chem.* **1994**, *66*, 7551.
[99] Initial reports from Merck[98] indicated that NLE was observed for one value of *ee* of pinene. An excellent and complete study was published later.[102]
[100] C. Girard, H. B. Kagan, *Tetrahedron :Asymmetry* **1995**, *6*, 1881.
[101] H. C. Brown, N. N. Joshi, *J. Org. Chem.* **1988**, *53*, 4059.
[102] M. Zhao, A. O. King, R. D. Larsen, T. R. Verhoeven, P. J. Reider, *Tetrahedron Lett.* **1997**, *38*, 2641.
[103] C. Girard, H. B. Kagan, *Tetrahedron: Asymmetry* **1997**, *23*, 3851.
[104] K. Tanaka, J. Matsui, Y. Kawabata, H. Suzaki, A. Watanabe, *J. Chem. Soc. Chem. Commun.* **1991**, 1632.
[105] a) R. E. Rossiter, M. Eguchi, A. E. Hernandes, D. Vickers, J. Medich, J. Marr, D. Heninis, *Tetrahedron Lett.* **1991**, *32*, 3973; b) R. E. Rossiter, G. Miao, N. M. Swingle, M. Eguchi, A. E. Hernandez, R. G. Patterson, *Tetrahedron: Asymmetry* **1992**, *3*, 231.
[106] a) C. Fehr, J. Galindo, *J. Org. Chem.* **1988**, *53*, 1828; b) C. Fehr, J. Galindo, *Helv. Chem. Acta* **1995**, *78*, 539; c) C. Fehr, *Angew. Chem.* **1996**,*108*, 2726; *Angew. Chem. Int. Ed. Engl.* **1996**, *35*, 2567.
[107] V. Rautenstrauch, P. Mégard, B. Bourdin, A. Furrer, *J. Am. Chem. Soc.* **1992**, *114*, 1418.
[108] For the advantages and disadvantages of the use of *ee*, *ec*, or *er* in various problems, see ref. [86].
[109] M. Okamoto, M. Tabe, T. Fujii, T. Tanaka, *Tetrahedron: Asymmetry* **1995**, *6*, 767.
[110] S. Masamune, W. Choy, J. S. Petersen, L. R. Sita, *Angew. Chem.* **1985**,*97*, 1; *Angew. Chem. Int. Ed. Engl.* **1985**, *24*, 1.
[111] C. Girard, T. Luukas, H. B. Kagan, unpublished results.

Structure and Reactivity of Lithium Enolates. From Pinacolone to Selective *C*-Alkylations of Peptides. Difficulties and Opportunities Afforded by Complex Structures

By Dieter Seebach*

The chemistry of lithium enolates is used to demonstrate that complex structures held together by noncovalent bonds ("supramolecules") may dramatically influence the result of seemingly simple standard reactions of organic synthesis. Detailed structural data have been obtained by crystallographic investigations of numerous Li enolates and analogous derivatives. The most remarkable features of these structures are aggregation to give dimers, tetramers, and higher oligomers, complexation of the metal centers by solvent molecules and chelating ligands, and hydrogen-bond formation of weak acids such as secondary amines with the anionoid part of the enolates. The presence in nonpolar solvents of the same supramolecules has been established by NMR-spectroscopic, by osmometric, and by calorimetric measurements. The structures and the order of magnitude of the interactions have also been reproduced by ab-initio calculations. Most importantly, supramolecules may be product-forming species in synthetic reactions of Li enolates. A knowledge of the complex structures of Li enolates also improves our understanding of their reactivity. Thus, simple procedures have been developed to avoid complications caused by secondary amines, formed concomitantly with Li enolates by the common methods. Mixtures of achiral Li enolates and chiral Li amides can give rise to enantioselective reactions. Solubilization by LiX is observed, especially of multiply lithiated compounds. This effect is exploited for alkylations of N-methylglycine (sarcosine) CH_2 groups in open-chain oligopeptides. Thus, the cyclic undecapeptide cyclosporine, a potent immunosuppressant, is converted into a THF-soluble hexalithio derivative (without epimerization of stereogenic centers) and alkylated by a variety of electrophiles in the presence of either excess lithiumdiisopropyl amide or of up to 30 equivalents of lithium chloride. Depending on the nature of the LiX additive, a new stereogenic center of (*R*) or (*S*) configuration is created in the peptide chain by this process. A structure–activity correlation in the series of cyclosporine derivatives thus available is discussed.

Nowadays, the molecular program of
chemistry has arrived at its successful termination.
H. Primas, ETH Zürich (1982)

1. Introduction—from α-Carbonyl Carbanions to Metal Enolates

Carbon-carbon bond formation in α-carbonyl positions is one of the most important processes for elaboration of carbon skeletons ("backbone of organic synthesis"). From the very beginning,[1] the variety of reactions of this type carried out under alkaline conditions was described as involving enolates which were drawn with the negative charge on carbon, pragmatically so, because that is where they react (Scheme 1). This notation continued to be used, especially in teaching, even when these reactions were no longer carried out in aqueous or other protic media, where solvent-separated "free" ions occur, and even though one realized that the negative charge is located on the more electronegative oxygen atom. The decisive role of the metal was appreciated when silyl enol ethers ("silyl enolates") were discovered for synthetic purposes[2]—they can be activated[3,4] by transmetalation or by treatment with fluoride ion, and they combine with electrophiles in reactions mediated by Lewis acids—and when the correlation between the configuration of the Li, B, Mg, and Sn[11] enolate double bond and the steric course of aldol additions[5–7] and other reactions[8] was disclosed.[9,10] Most of these reactions are

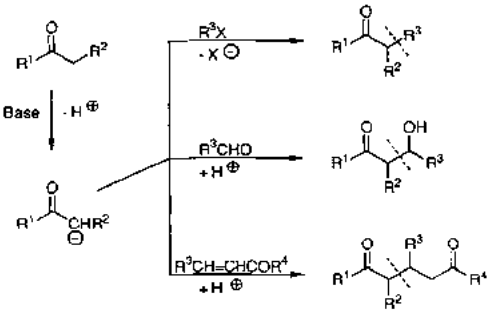

Scheme 1. Three classical reactions of carbonyl compounds: α alkylation, aldol addition, and Michael addition.

[*] Prof. Dr. D. Seebach
Laboratorium für Organische Chemie der
Eidgenössischen Technischen Hochschule
ETH-Zentrum, Universitätstrasse 16, CH-8092 Zürich (Switzerland)

performed in nonpolar solvents (hydrocarbons, chlorohydrocarbons, open-chain or cyclic ethers, amines),[11] preferably at low temperatures, i.e., under conditions disfavoring the formation of ions, the separation of charges.[12–14]

While the important role of the metal in aldol additions quickly became part of synthetic planning, another property of the polar alkali and alkaline-earth enolates remained the "esoteric science" of only a few specialists: *the aggregation to higher-order structures.* It was known that potassium *tert*-butoxide is tetrameric in the solid state and in the gas phase[15] and that alkali enolates, even of β-diketones, form dimeric aggregates in the crystalline state.[16–18] It was concluded from ebullioscopic measurements[19] and from NMR spectra[20,21] that Li and Na enolates and phenolates are dimeric or tetrameric[22] in nonpolar solvents.[11] It is especially in the footnotes of early synthetic papers where one finds speculative suggestions that such enolate aggregates may be influential in product formation. In contrast, it has been well known for almost 30 years that aggregates of organolithium compounds with carbon–lithium bonds *may be* the product-forming species.[23,24] References are found in a classical monograph on the structure and reactivity of alkali and alkaline-earth metal derivatives[25] and in more recent books[26–36] and review articles (general,[37–41] NMR spectroscopy,[42–46] crystal structure analysis[47–53]).

In this article we describe results of the past decade which not only increased our knowledge of Li enolates[53] but also enlarged the scope of these most important reagents and their nitrogen analogues, which are widely applied in research laboratories as well as in industrial development and production of drugs, pesticides, and fine chemicals. The choice of examples to be discussed is necessarily influenced by the personal experiences of the author and his collaborators: by making structural investigations on synthetically relevant reagents we try to reduce frustration originating from the fact that part of our group keeps discovering highly selective transformations which we do not understand at all.[54–57] Thus, the route of the sorcerer's apprentice is described, as indicated by the sequence of formulae in Scheme 2.

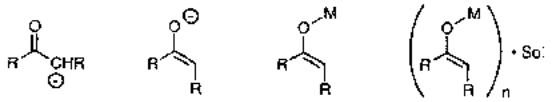

Scheme 2. From the deprotonated carbonyl derivative, via the metal enolate (M = metal), to aggregates, solvated and complexed by additives ("supramolecules" [58]). Sol = solvent molecules (ligands) in the coordination sphere of the metal.

2. The Complex World of Li Enolates—in Crystals and in Solution

Today's standard method of doing enolate reactions involves deprotonation of carbonyl compounds by lithium amide bases, for instance, lithium diisopropylamide (LDA),[59] tetramethylpiperidide (LTMP),[60] or hexamethyldisilazanide (LHMDS)[61] in THF, possibly in the presence of a cosolvent[8,62–65] or of a complexing agent.[26,32,66] The enolate solution thus obtained is combined with an electrophile. For CC bond formation this is usually an alkyl halide (Scheme 3) or a carbonyl compound (aldehyde/ketone,[67] Scheme 4). During these procedures, mixtures of the species shown inside the boxes of Schemes 3 and 4 are present. Since the first crystal structure analyses of ketone Li enolate aggregates[68] in 1981, numerous aggregates and complexes between these species have been isolated as single crystals suitable for X-ray analysis and/or have been

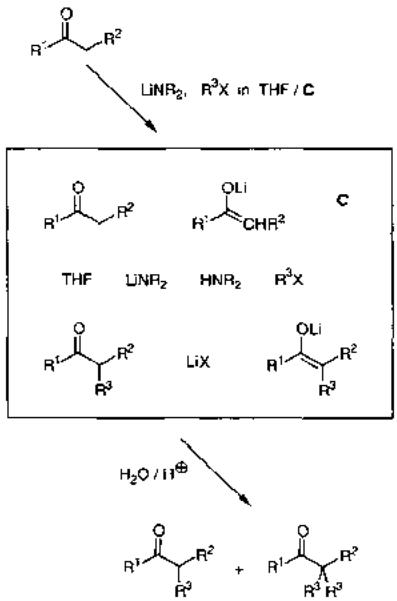

Scheme 3. Components which may coexist in a reaction mixture under the normal alkylation conditions of carbonyl compounds. C should be taken to represent an additive [cosolvent, complexing agent, e.g., hexamethylphosphoric triamide (HMPT) [62], "*N,N'*-dimethylpropyleneurea" (1,3-dimethyltetrahydropyrimidin-2(1*H*)-one, DMPU) [63], *N,N,N',N'*-tetramethylethylenediamine (TMEDA) [26], *N,N,N'*-trimethylethylenediamine (TriMEDA) [66], pentamethyldiethylenetriamine (PMDET) [26], dimethoxyethane (DME)].

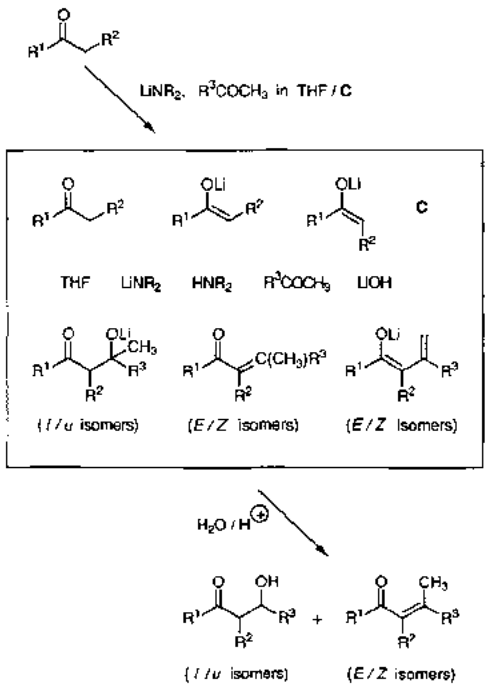

Scheme 4. Components that may occur in an aldol reaction performed with an enolate generated by R_2NLi. C is an additive (see caption to Scheme 3)

detected in solution. Thermochemical data were collected and force-field calculations, as well as quantum-mechanical "investigations", were performed. This will form the subject of the following sections, before we turn to the question of whether these complex structures are involved in product-forming steps.[69]

2.1. Li enolates and "Ingredients" in the Crystalline State

... la virtùe della geometria esser il più potente strumento d'ogni altro per acuir l'ingegnio e disporlo al perfettamente discorrere e specolare.[*]
Galileo Galilei

All crystalline Li enolates for which an X-ray structure analysis has been successfully performed so far are dimeric, tetrameric, or hexameric aggregates, the degree of aggregation depending less upon the particular enolate structure than upon solvent and added complexing or chelating agents (Figs. 1–12). Dimers tend to be favored in the presence of ethylenediamines and tetramers with ethers such as THF; a hexamer was crystallized from a non-donor hydrocarbon solvent. Lithium enolates of pinacolone (3,3-dimethyl-2-butanone, Figs. 1–3) and its derivatives (Figs. 7, 8, 10) prevail among the structures solved, for obvious reasons (high stability, only one enolate possible).

Lithium enolates of esters are unstable even in the crystalline state, due to their decomposition to ketenes and alkoxides.[72,73] Special techniques are required for the generation and isolation of suitable single crystals at low temperatures[5,67c,87] (Figs. 4 and 13). Amide enolates are much more stable (Figs. 5 and 6, compare the leaving groups $LiNR_2$ and LiOR). Again, dimeric and tetrameric aggregates are present in the crystals of these Li enolates containing additional heteroatoms. Other components of the mixtures present during generation and during reactions of Li enolates with electrophiles have been crystallized and successfully subjected to X-ray crystal structure analysis in recent years. Oligomeric aggregates of Li amides (Fig. 9, dimer), of an aldolate (Fig. 7, tetramer), and of a dienolate (Fig. 8, dimer) were found, the Li atoms of which are solvated by the oxygens of ethers (Figs. 2, 6, 9) or carbonyl compounds (Fig. 7, 8, 11), by the oxygens of HMPT (Fig. 12), or by the nitrogens of secondary or tertiary amines (Figs. 3–5). The formation of aggregates, $[(LiX)_n]$, is not limited to identical components; mixed aggregates $[(LiX)_n(LiY)_m]$ may also be formed from different components, for instance, the complex skeleton assembled from LDA and a siloxy-substituted Li enolate (Fig. 10).

Since lithium is *usually* tetracoordinated, it is possible—with due care—to deduce the degree of aggregation of Li enolates, alkoxides, phenolates,[90] and their nitrogen analogues from the stoichiometric composition of isolated samples. In order to achieve tetracoordination, one, two, or three "external" ligand atoms are present per lithium in a tetramer, dimer, or monomer, respectively. The ratios given in Table 1 confirm that aggregation of LiX in the crystalline state is a general phenomenon, also by this criterion. Furthermore, inspection of Table 1 reveals that lithiated nitriles (Li ketene imines) and iminoesters (Li enamides) are also aggregated, which was confirmed by crystal structure analysis:[98] see Table 2 and Figures 14 and 15, showing a lithio "bis-lactim ether" (reagent for enantioselective amino acid synthesis[99,100]) and the HMPT-solvated lithio malononitrile, respectively.

The structures of sodium, magnesium, aluminum, and zinc enolates (Figs. 16–19) exemplify the fact that aggregation is by no means a peculiarity of Li derivatives, but is a general phenomenon in polar metal enolates.[115]

Many a crystallographer and inorganic chemist does not quite share the excitement of us organic chemists about the structures described here; these colleagues live with the fact that aggregates and clusters are "ubiquitous all over the periodic table".[115] For synthetic organic chemists[116]

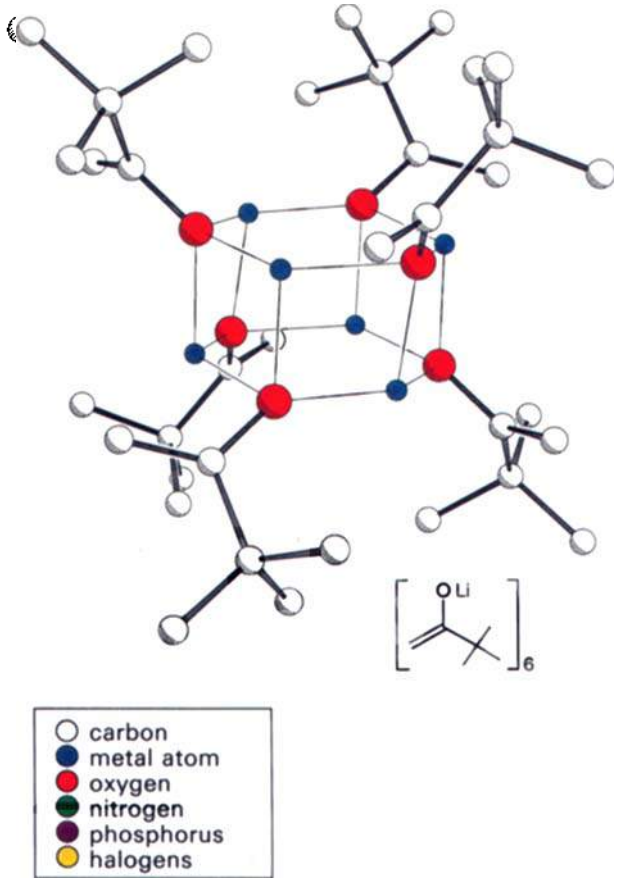

Fig. 1. Hexameric lithium enolate derived from pinacolone (enolate generated with LDA in heptane) [70, 71]. The crystal does not contain any solvent. The Li atoms are only threefold coordinated. Three square units of dimers are assembled in a hexagonal prism. A threefold axis runs perpendicularly to the hexagonal basis plane. The coordinates are stored in the *Cambridge Structural Database (CSD)* under the code CUYVOH. Here, and in all other illustrated structures (Figs. 1–12, 14–20, 23, 25, as well as the structures in [115]), the atoms are color-coded according to the key shown above. Other, non-carbon atoms are signified by their chemical symbol. The first coordination sphere of the metals is represented throughout by thin connection lines—for clarity, the neutral ligands or solvent molecules are not drawn to the same scale—while the anionic ligands are emphasized by bolder connection lines and larger spheres for the atoms.

[*] ... whoever has a grasp of geometry is capable of understanding this world.

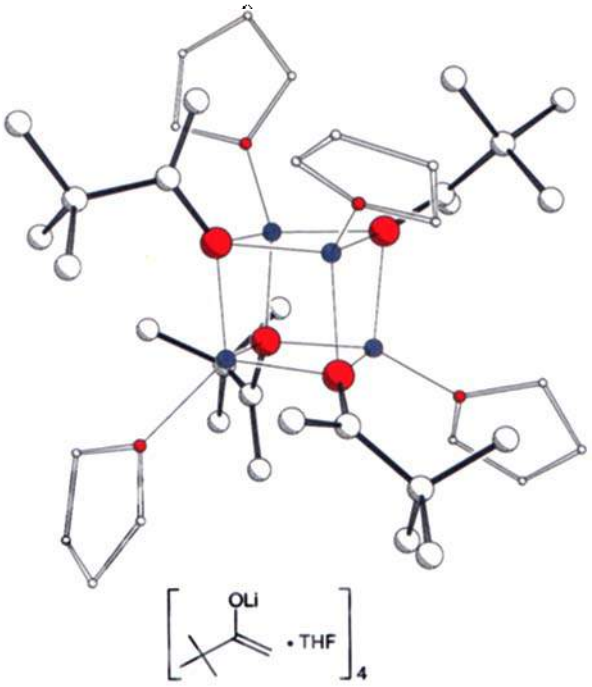

Fig. 2. Tetrameric Li enolate of pinacolone, crystallized from tetrahydrofuran. An almost perfect cube of four Li and four O atoms is surrounded by a "shell" of organic units—the enolate carbon skeleton and the THF molecules. The Li atoms are each surrounded by three enolate oxygens and one THF oxygen, so that a distorted tetrahedral coordination sphere results [68] (*CSD*: BEDYOY). The structure of the analogously arranged cyclopentanone-derived Li enolate is described in the same publication [68]; the corresponding coordinates are deposited under the *CSD* code BEDYUE.

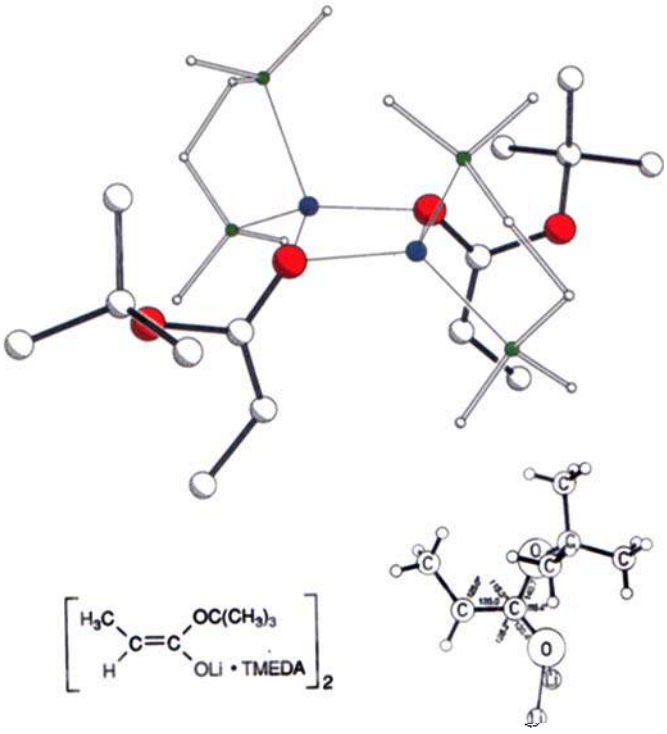

Fig. 4. Dimeric lithium (*Z*)-enolate of *tert*-butyl propionate, crystallized in the presence of TMEDA. The two enolate units are *cis* to each other on the LiOLiO four-membered ring through the center of which runs a C_2 axis of the dimeric aggregate. Even in the crystal, the ester enolate is unstable above −30°C. Its decomposition to a ketene [72, 73] and lithium *tert*-butoxide is perhaps indicated by the different C–O bond lengths (141 vs. 130 pm) and C=C–O bond angles (ca. 115 vs. 128°) at the trigonal O-substituted center of the double bond [73]. The *tert*-butyl group stands nearly perpendicular to the enolate plane (*CSD*: DEDXEP).

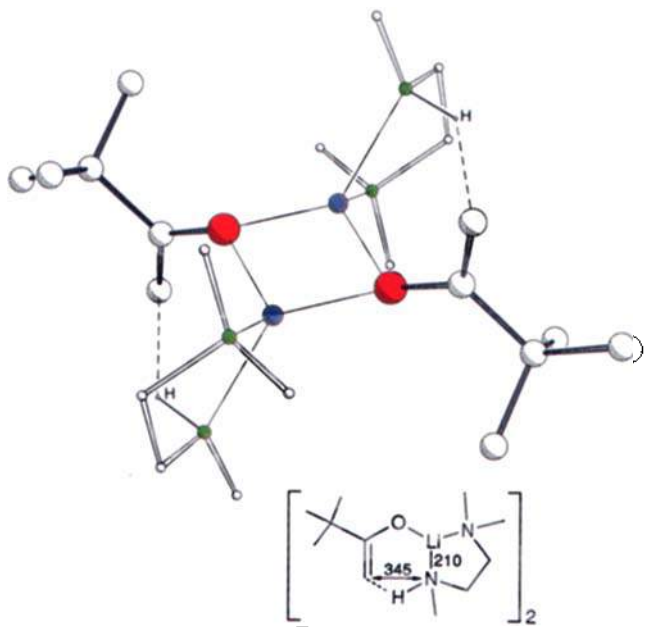

Fig. 3. Dimeric Li enolate of pinacolone crystallized in the presence of TriMEDA [66]. The nitrogens of the bidentate chelate ligand and two enolate oxygen atoms form a pseudo-tetrahedral arrangement around the Li atom. The distance between the NH hydrogen of the secondary amino group and the terminal C atom of the enolate double bond amounts to ca. 260 pm. The plane in which the atoms H···C–C lie forms an angle of ca. 60°C with that of the double bond. In the center of the LiOLiO quadrangle, there is a center of symmetry (*CSD*: DETRAV) [66], i.e., the enolate units are *trans* to each other (like the TriMEDA complex in Fig. 5 and the dienolate in Fig. 8, but unlike the dimers "solvated" with TMEDA or THF in Figs. 4 and 6).

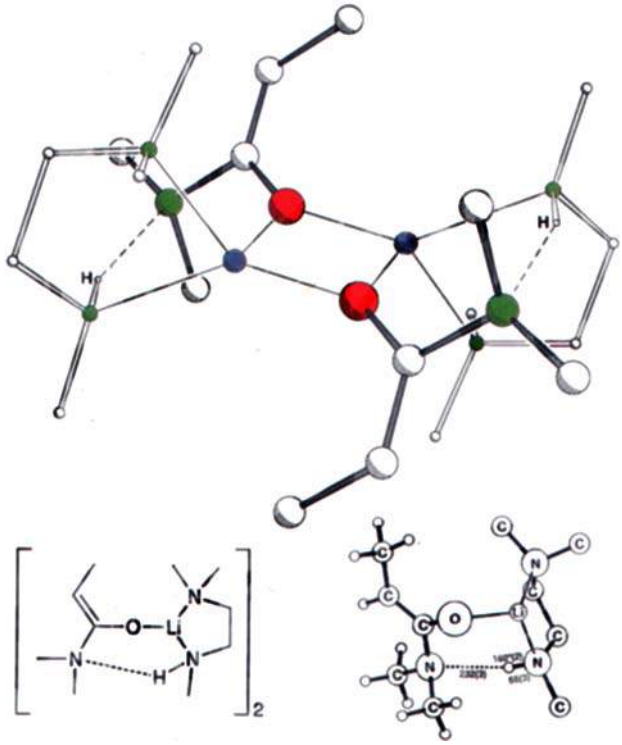

Fig. 5. *N,N*-Dimethylpropionamide lithium (*Z*)-enolate dimer, crystallized with TriMEDA. The center of the LiOLiO quadrangle is a center of inversion in the aggregate. The dimethylamino group of the enolate is like that in enamines [74], but much more strongly pyramidalized; the H atom of the secondary amino group lies in the direction of the virtual electron pair on this enamine nitrogen (lengths of hydrogen bonds, see [75, 76]) (*CSD*: DETPUN) [66].

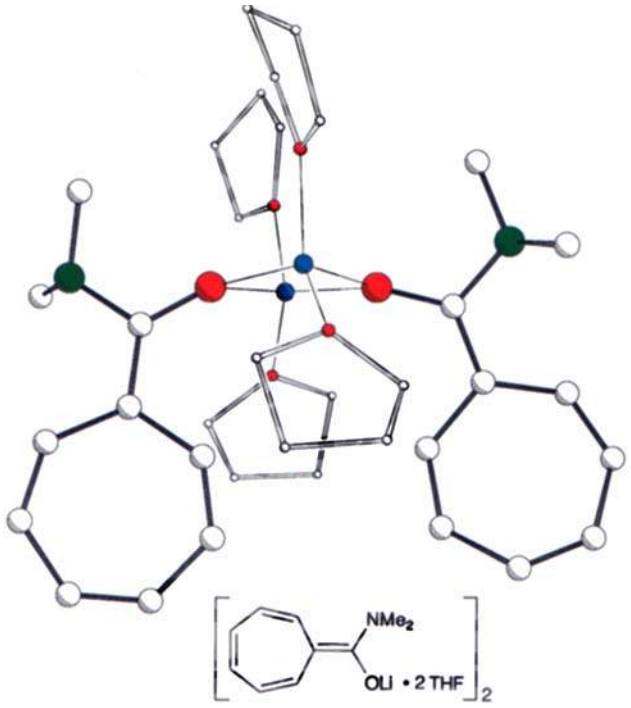

Fig. 6. Dimeric lithium enolate of *N,N*-dimethylcycloheptatrienecarboxamide, crystallized from THF [77]. As in the dimeric Li enolates of esters (Fig. 4), the enolate units are *cis* to each other at the LiOLiO quadrangle (with a C_2 axis through the ring center). THF molecules occupy quasi-axial and quasi-equatorial positions at the Li atoms of the folded four-membered ring (puckering angle between OLiO planes 68.6°, between the LiOLi planes 47.3°). The extended π systems do not participate in the complexation of the Li atoms. The Me_2N groups are turned out of the π plane, and the nitrogen is pyramidal (Δ = 36.5 pm) as in the propionamide enolate of Fig. 5.

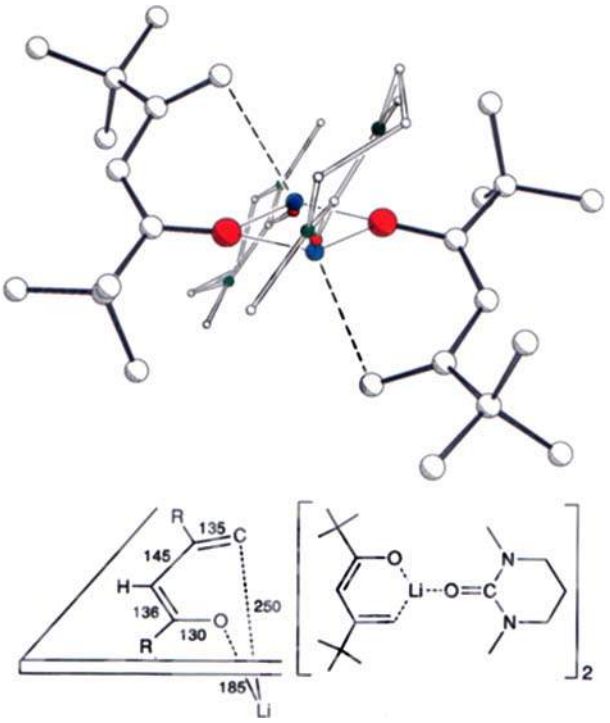

Fig. 8. Dimeric lithium (*Z*)-dienolate of 2,2,5,6,6-pentamethylhept-4-en-3-one (the product of aldol condensation between two pinacolone molecules), crystallized in the presence of DMPU [79]. The carbonyl oxygens of the cyclic urea and the terminal C atom of the dienolate (LiC bond distance 250 pm; cf. that in trityllithium, 223 pm [80]), as well as two oxygen atoms of the LiOLiO ring, surround the Li atom in the centrosymmetric dimeric aggregate (*CSD*: DIXWIQ).

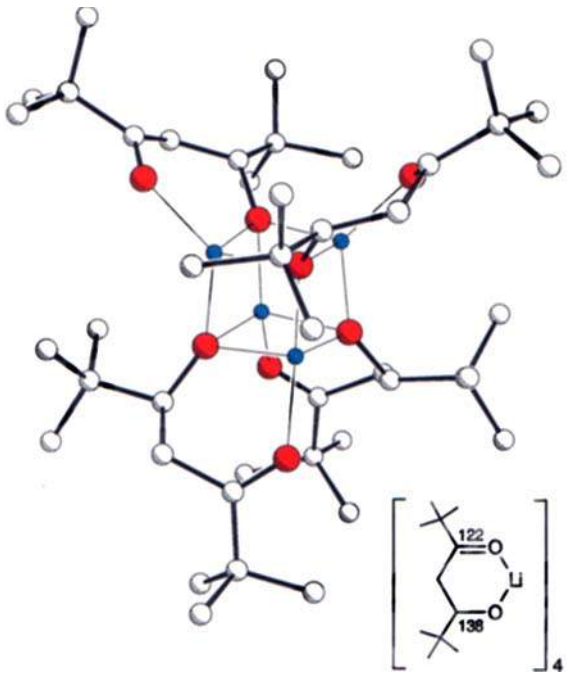

Fig. 7. Tetrameric aggregate of the Li aldolate from pinacolone and pivalaldehyde [78]. The negatively charged alkoxide oxygens and four Li atoms form a distorted cube (LiO distances 191–195 pm). The carbonyl oxygens of the aldolates are bonded to the Li atoms from outside (LiO distance 197 pm), as in other cases with the oxygen atoms of the solvent or nitrogen atoms of the ethylenediamine unit. In this arrangement, four "external" six-membered rings are formed, fused to alternating edges of the cube. The tetramer crystallized from pentane (*CSD*: DEWBIQ).

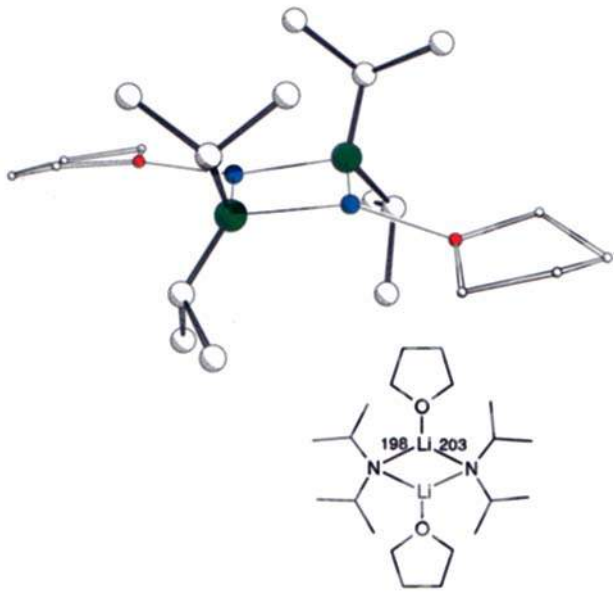

Fig. 9. Dimeric lithium diisopropylamide, obtained from THF [$(LDA)_2$·$(THF)_2$] [81]. The methyl groups of the isopropyl units point inwards, i.e., towards the LiNLiN four-membered ring. The Li atoms are each threefold coordinated as in other lithium amides (steric hindrance?). Additional $LiNR_2$ structures (monomer, four-membered ring dimer, six-membered ring trimer, and eight-membered ring tetramer) are shown in a review article on Li structures [47]; among these are also found lithium tetramethylpiperidide and hexamethyldisilazanide. (For more recent structure determinations of lithium anilide derivatives, see [82–84].)

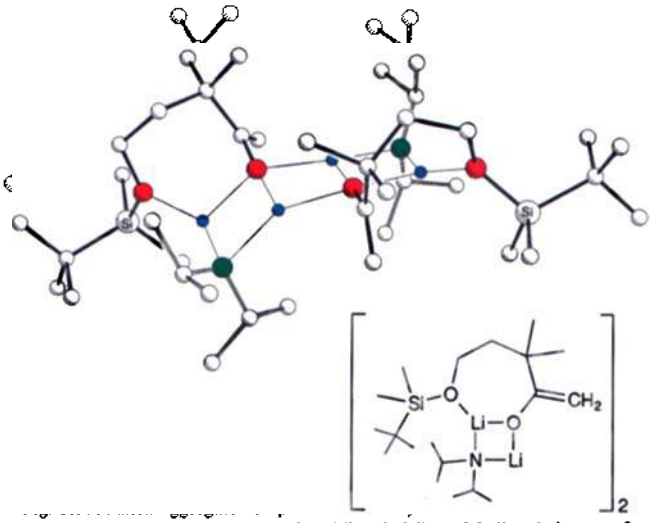

(from a methyl ketone, 5-(*tert*-butyldimethylsiloxy-3,3-dimethylpentan-2-one) and LDA. Three LiXLiY four-membered rings are fused to form a step-like structure. The siloxy oxygen serves as an "external" ligand to Li [85].

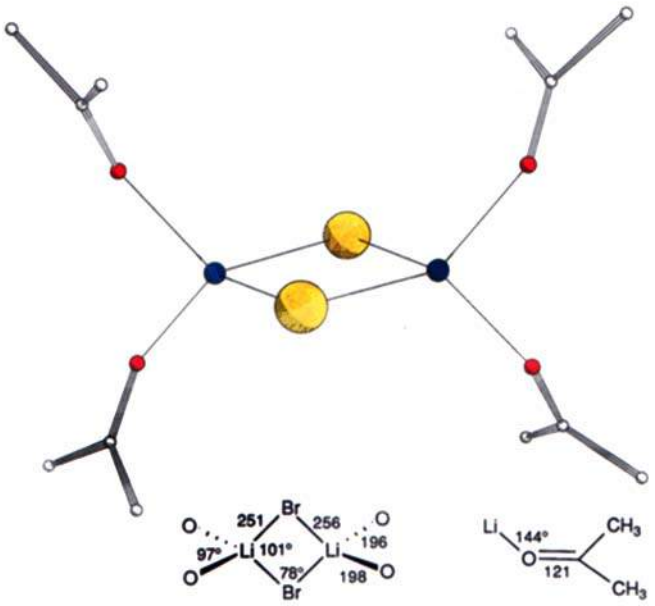

lithium atoms form a rhombus with acute angles at the bromine atoms. As in the case of protonated carbonyl compounds, the bond angle at oxygen is less than 180° in this complex between a ketone and LiBr (*CSD*: DECXEO 01). (See also the other adducts involving alkali-metal derivatives and carbonyl compounds in Figs. 7, 8, and 16 and in Tables 1, 2, 4, and 7 as well as the discussions in [79] and in Sections 2.3, 3, and 4.)

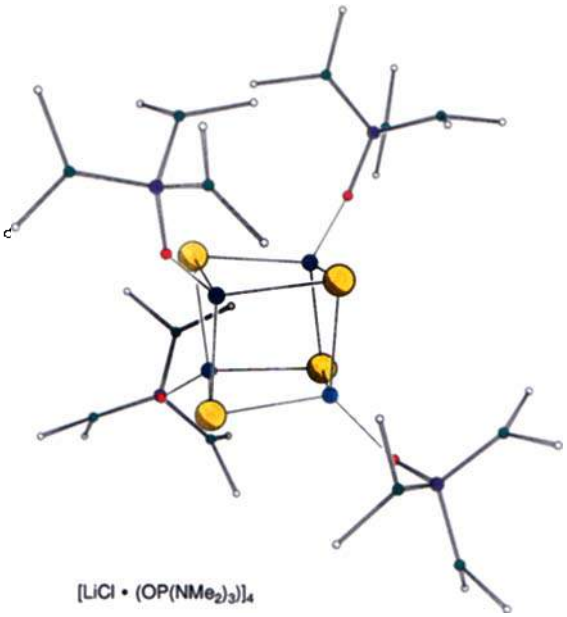

Fig. 12. Lithium chloride tetramer with four HMPT molecules, which are bonded to lithium via oxygen (from an "utterly fortuitous in situ preparation in high yield" involving $LiNCBu_2$, HMPT, $AlCl_3$ (1 : 1 : 0.3) in hexane/ether) [86] (*CSD*: CAWSIC). (For additional crystal structures with HMPT as "solvating ligand", see the review in [47], cf. also Fig. 15.)

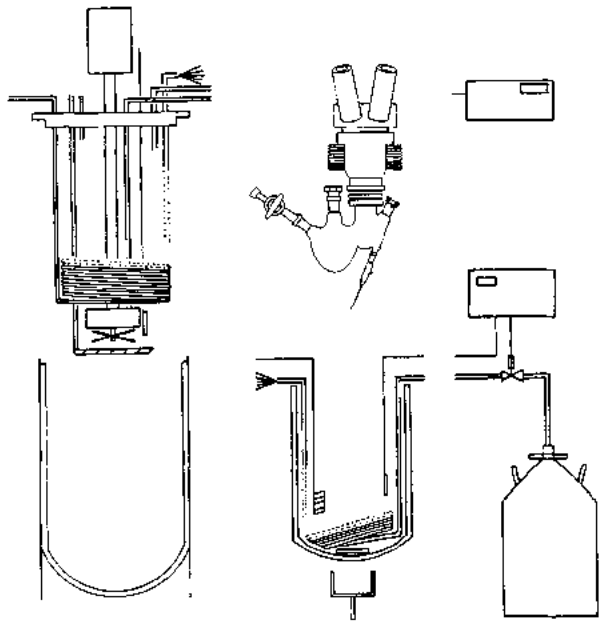

Fig. 13. Apparatus for the preparation of single crystals at low temperatures under inert atmosphere following the procedure in [67c, 73]. In this way, crystals of the ester enolates [73] (Fig. 4) and of a very unstable lithiated allyl thioether [87] were obtained; cf. also the X-ray structure analyses of aliphatic carbocation derivatives [88, 89] and the review article cited above [51].

these structures are of enormous importance for the following reasons: (1) With an accuracy provided only by X-ray crystal structure analysis, we finally have structural parameters of the reactive intermediates used in the most important CC bond-forming synthetic methods. (2) Applications of the structure-reactivity correlation principle[117–124] lead to conclusions about mechanistic details of the reactions of these species, and these conclusions become more and more reliable with an increasing number of structures. (3) The less stable these species are, the more their structures hint at their reactivity; reaction trajectories can be read from distortions of the molecules as they occur in the crystalline state.[73, 87–89] (4) Finally, knowing the rich complexity of the reagents involved, we can use these structures to reconsider and discuss in a more systematic way the jumble of excellent preparative results, useful recipes, and procedures.

Before doing so, the results of structural investigations of Li enolates in solution will be briefly discussed.

Table 1. Composition of crystalline samples of Li enolates and nitrogen analogues. The samples were obtained in the course of attempted preparations of single crystals for X-ray structure analysis. The solvent content was determined, after drying the crystals under high vacuum, by addition of excess CD_3COOD in an NMR tube and integration of appropriate signals in the resulting spectra [91–94]; for further examples see [66].

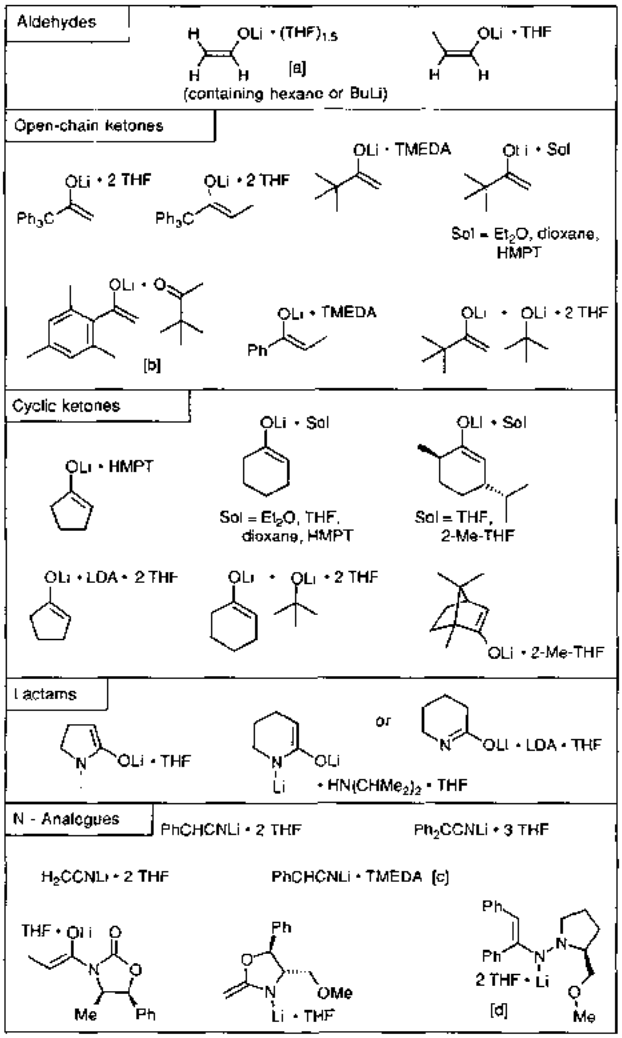

[a] Beautiful looking crystals separated from THF to which BuLi/hexane had been added [95]. Unfortunately, the crystals are not suitable for X-ray crystal structure analysis. [b] Compare with the Na enolate solvated by pinacolone (Fig. 16). [c] In the meantime, the dimeric Li phenylacetonitrile-TMEDA complex solvated by one molecule of benzene per aggregate unit was isolated and successfully subjected to X-ray crystal structure analysis [96]. [d] For the crystal structure of the Li enehydrazide of the hydrazone obtained from 2-naphthyl methyl ketone and *N*-aminoprolinol methyl ether, see [97] (monomeric, with two THF oxygens and the oxygen of the prolinol ether unit surrounding the Li atom).

Table 2. Schematic representation of some crystal structures of N-analogues of Li enolates. The PLUTO plots of two further structures of this type are shown in Figures 14 and 15 (see also a review article [47] covering the literature up to the beginning of 1984).

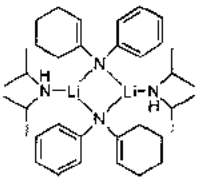	Li enamide of the product formed from cyclohexanone and aniline [102]
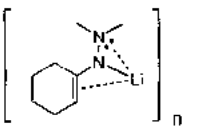	Polymeric Li enehydrazide of the product formed from 1,1-dimethylhydrazine and cyclohexanone [102]
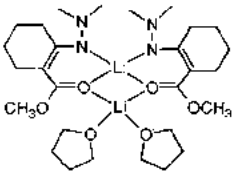	Dimeric Li enehydrazide of the product formed from 1,1-dimethylhydrazine and 1-oxocyclohexanecarboxylate. The compound contains two "very different" Li atoms [101a] (cf. Fig. 14)
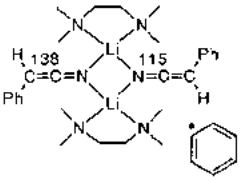	Dimeric Li ketenimide formed from phenylacetonitrile and TMEDA. A molecule of "crystal benzene" [96, 98] is present (for "simple" Li imides see [103–105])
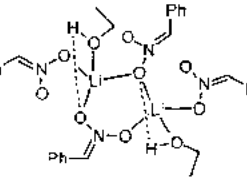	Section of the polymeric structure of the Li nitronate of phenylnitromethane $[PhCH{=}NO_2Li \cdot EtOH]_n$ [106]

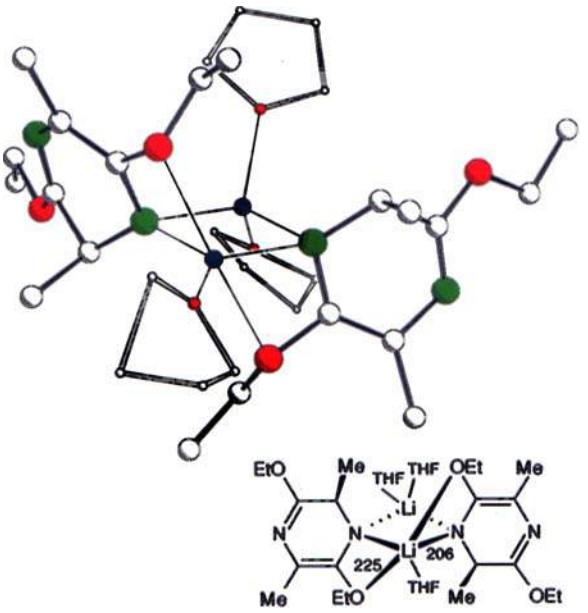

Fig. 14. Dimeric aggregate of the lithium bis-lactim ether derived from alanine [107] (*CSD*: CIFBOI). The two lithium atoms have very different environments; if the Li–Li neighborhood is not included, one Li atom is fivefold coordinated, the other fourfold. In this way, the diastereotopic faces of the dihydropyrazine ring are differentiated more strongly than by the methyl group at the stereogenic center (cf. the structure of the lithiated oxocyclohexanecarboxylic acid derivative in Table 2).

2.2. Li Enolate Structures in Solution—Not Simple Either!

2.2.1. *Osmometric Measurements—Colligative Properties*

From effects which ideally depend upon the number of particles per volume, the average molecular weight can be calculated, in the present case the degree of aggregation of Li enolates in solution. Ebullioscopy, vapor pressure osmometry, differential vapor pressure barometry, and cryoscopy applied to enolate solutions thus led to aggregation numbers between 1.0 and 4.0 (in certain cases several hundred), depending upon the type of enolate, the solvent,

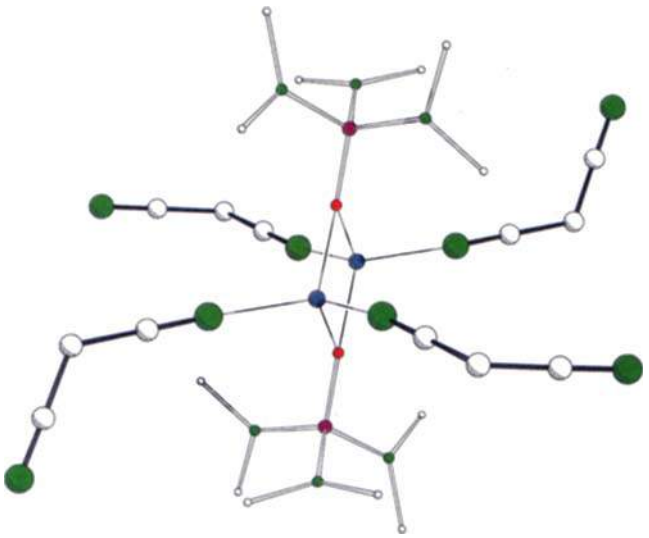

Fig. 15. Section of the polymeric structure of lithiated malononitrile $[LiCH(CN)_2 \cdot HMPT]_n$, which crystallized from a mixture of HMPT, hexane, and THF [108]. It is striking that the LiXLiX four-membered ring is not built up from the heteroatoms of the counterion (here the nitrogen) with the Li atoms, as usual, but from the oxygens of the HMPT. The nitrogen atoms of the dicyanomethanide lie "outside" of the aggregate. In the LiCl structure of Fig. 12, the HMPT oxygens are "outside". (Compare the structures in Fig. 12 and in Fig. 15 with a possible interpretation [69] of the HMPT effect on enolate reactions given in 1981, when there was no structural information about HMPT complexes. See also Scheme 9.)

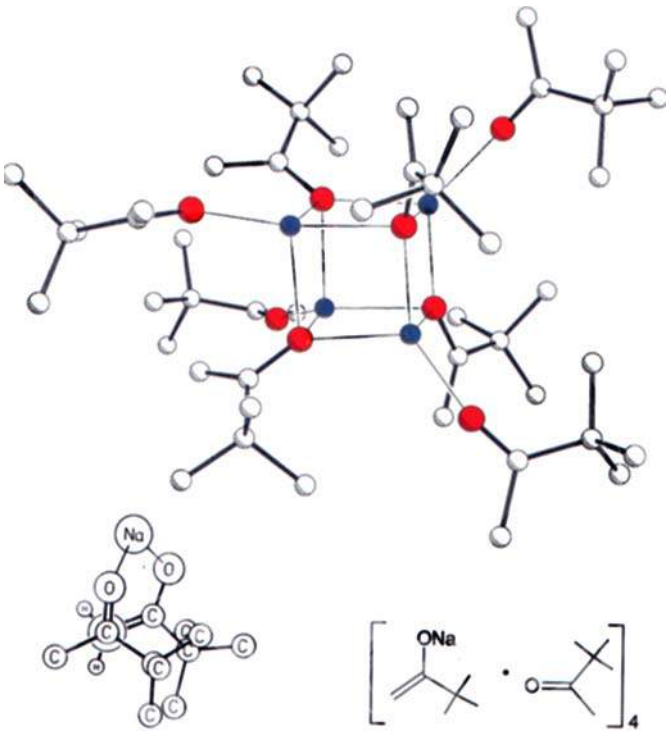

Fig. 16. Tetrameric sodium enolate of pinacolone, with pinacolone as "solvate molecule" (*CSD*: DIPSAW) [71]. A section shows that the planes of the π systems of the enolate and the ketone (bound together by the sodium) are more or less parallel, as they would have to be in a reaction between the electrophilic carbonyl carbon and the nucleophilic enolate one (separation distance 380 pm). The structure of the hexameric pinacolone K enolate solvated with THF, $[tBuC(OK)CH_2 \cdot THF]_6$, is described in the same publication (*CSD*: DIPSEA). A complete collection of the structures of Na, K, Rb, and Cs organometallic compounds was published in 1987 [48].

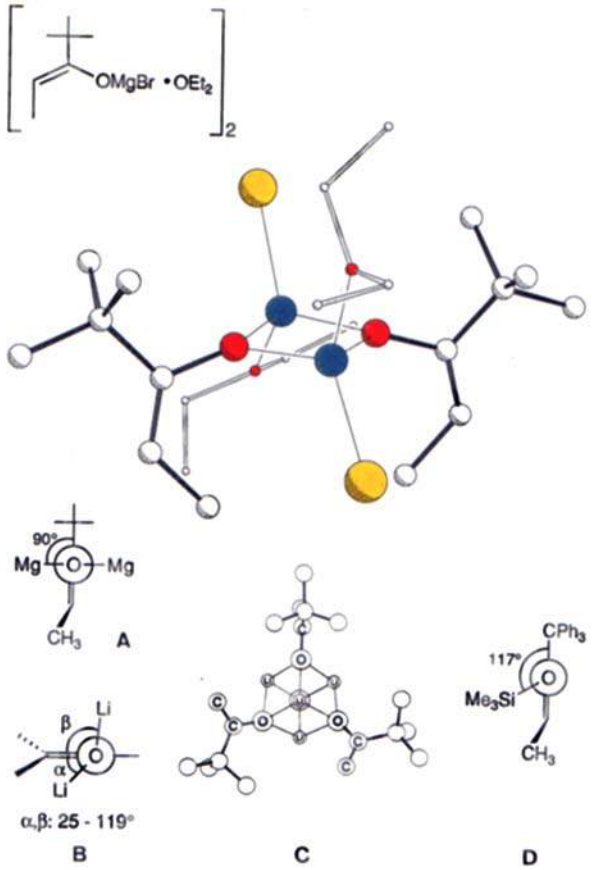

Fig. 17. Dimeric bromomagnesium (*Z*)-enolate of *tert*-butyl ethyl ketone (2,2-dimethylpentan-3-one), crystallized from diethyl ether (*CSD*: DILPUJ) [109]. The plane of the MgOMgO four-membered ring and that containing the enolate double bond are more or less perpendicular to each other (A). In the Li enolate dimers, the Li atoms lie outside the plane of the double bonds (Figs. 3–6) with very different LiOC=C torsion angles (B). In the tetramer (Fig. 2), however, a lithium atom does lie in the plane of the enolate (C). In a crystalline silyl enol ether (*CSD*: DIWXOW), the Si–O bond forms an angle of 117° with the plane of the enolate double bond [110a] (D).

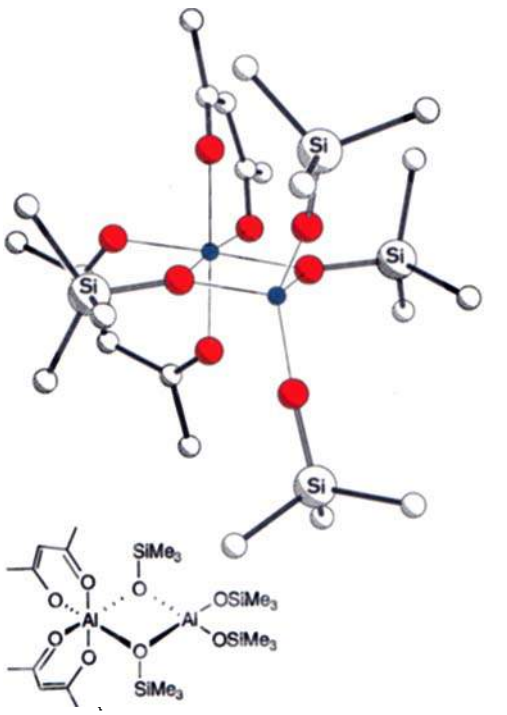

Fig. 18. Crystal structure of $[Al(OSiMe_3)_2(acac)]_2$, with two very different aluminum atoms (*CSD*: CIRMOF) [111]. In the opinion of the authors, the unexpectedly complex structure of these kinds of Al derivatives has to be borne in mind when considering their application as catalysts and as precursors of ceramic materials!

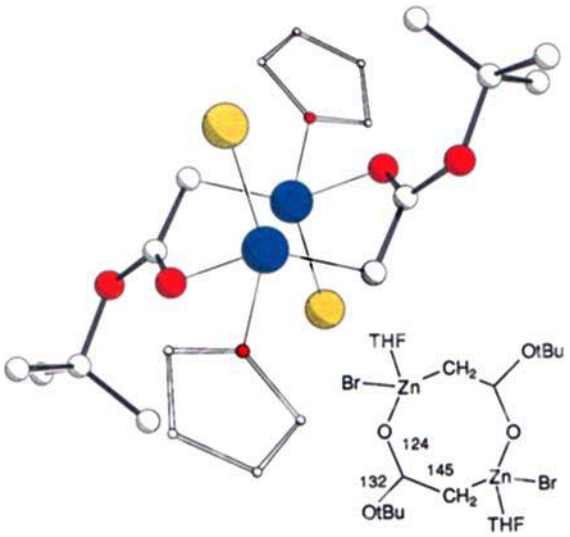

Fig. 19. Crystal structure of a Reformatsky reagent, $[BrZnCH_2COO(tBu)\cdot THF]_2$, crystallized from THF (*CSD*: BUDKAM) [112]. Two each of Zn, CH_2, C(O-*t*Bu), and O form an eight-membered ring. Each Zn bears a Br and a THF as substituents. In contrast to the alkali and Mg enolates, where the metal atoms are always bound to oxygens, the Zn atom here is simultaneously attached to the CH_2 group of one unit and the CO group of the other (see also the C-C and C-O bond lengths of the eight-membered ring). A discussion on the structures of cyclopropane and aziridine carboxylic ester enolates in which α-metallocarbonyl derivatives may also be present instead of the usual metal enolates can be found in [113, 114]. It is noteworthy that the Zn is σ-coordinated to oxygen, but π-coordinated to carbon (torsion angle Zn-O-C-O 164°, Zn-C-C-O −83°, respectively).

and the temperature.[22,25,27,30,94,125,126] Since many Li enolate reactions are preferentially carried out at dry-ice temperature in THF, the melting-point depressions measured[94] in this solvent (m.p. −107 °C) are especially "realistic". Of the numerous measurements only one will be referred to here: the Li enolate of cyclopentanone, which crystallizes as a tetramer from THF (see Fig. 2[68]), gives an aggregation number of 2.6-2.8 in THF solution at −107 °C, corresponding to a tetramer/dimer mixture of ca. 1:2. Vapor pressure measurements at higher temperature indicate that Li phenolates are largely tetrameric in ether solvents[127] (with polar organometallic compounds the entropy term may be such that larger aggregates—fewer solvent molecules bonded per Li—prevail at higher temperature and smaller ones at lower temperature[42c]).

2.2.2. *NMR Spectroscopy—More Detail*

By definition (*W. Wundt* and *W. Ostwald*) it is not possible to obtain information about the structure of aggregates in solution from colligative effects. Today's method of choice for studying solution structures is NMR spectroscopy. With the modern techniques (2D, 3D[128-131]) proximity between *nonbonded nuclei* (nuclear Overhauser effects) is detected, relaxation times are measured, quadrupole resonance spectra are obtained, dynamic processes are studied at very low temperatures, and the sensitivity is increased by isotopic labeling (^{6}Li, ^{13}C, ^{15}N, ^{17}O). All of this has provided a vast amount of detailed information about the species present in solution and the equilibria between them.[132] With *C*-metalated, "true" organolithium compounds the direct ^{6}Li,^{13}C coupling is the most valuable source of information about bonding between these two nuclei, about aggregation and the lifetime of aggregates (the multiplicity of the ^{13}C signals reveals the number of Li atoms bonded to the observed carbon[133]). Corresponding ^{6}Li,^{15}N coupling was used most recently for the determination of $LiNR_2$ aggregation in weakly polar solvents.[101b,132b,132c,134,135] There are no reports about Li,O coupling in enolates and phenolates; the investigation of Li enolates in solution by NMR spectroscopy is more difficult. So far, we owe the measurements in this area essentially to a single research group.[21,22,127,136-140] From elaborate studies, especially of isobutyrophenone Li enolate and of Li phenolates, rather stable representatives of this type of species, many structural details have been deduced. Not only was the equilibrium between dimeric and tetrameric aggregates discovered, but also the presence of mixed aggregates between Li enolates or phenolates and LiBr, LiCl, and $LiClO_4$ in solution (all of this work has been carefully described; for an early review article on structure and reactivity of Li enolates see Ref. [22]). From hitherto unpublished ^{1}H and ^{13}C NMR measurements of the Li (*Z*)-enolate of propiophenone in THF, the following conclusions were drawn:[141] (1) There is an equilibrium between dimers and tetramers. (2) The dimer, but not the tetramer, forms a mixed aggregate with LDA. (3) Complexes between the Li enolate and diisopropylamine are formed; most likely these are more stable with the tetramer than with the dimer. (4) Addition of HMPT does not destroy the dimeric and tetrameric aggregates. (5) Mixed aggregates are formed upon addition of LiCl to the Li enolate solution. Also from NMR measurements, it is known that the parent compound, the Li enolate of acetaldehyde, is tetrameric in THF solution[142] (cf. Table 1 and Section 3), and that dimeric aggregates and mixed aggregates with LiBr exist in solutions of lithium amides.[101b,102b,132b,132c,143]

2.2.3. *ate Complexes—Also of Li Enolates?*

In the early fifties, *Wittig* interpreted the fact that organolithium compounds self-associate as arising from the formation of "autocomplexes"[144a] ("triple ions"). He ranked the dimeric phenyllithium in ether as $[Ph_2Li]Li$ in a series with the complexes $[Ph_3Be]Li$ and $[Ph_4B]Li$. Subsequently, such species were called *ate* complexes,[144b] by analogy with *onium* salts (cf. $[Me_4N]Cl$). When the first X-ray crystal structure analyses of Li,C and Li,O compounds appeared, it was realized that ate complexes form especially in those cases in which different metal cations or different anions are involved. In both the crystal[145,146] (Fig. 20) and in solution[21] organolithium compounds with lithium halides were shown to be present as mixed aggregates rather than ate complexes, the formation of the latter being accompanied by charge separation.[150] Under these circumstances it is questionable whether ate complexes are present in solutions of Li enolates under the usual conditions, i.e., in nonpolar solvents and at low temperatures. Indeed, the only Li enolates for which ate complex-type structures have been detected are derived from β-dicarbonyl compounds (e.g., acetylacetone, acetoacetic esters; see the examples in Refs. [22, 47]). Some recent examples of Li ate complexes are collected in Table 3; cryptands and HMPT seem to favor their formation.

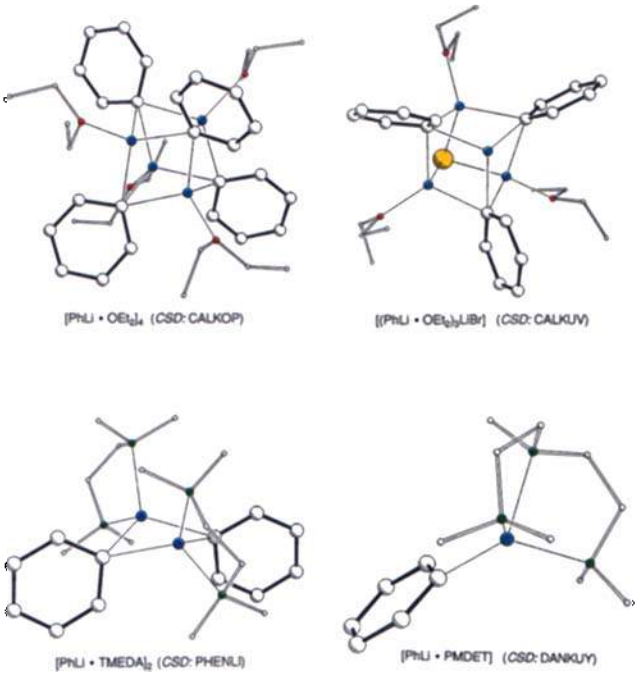

Fig. 20. Four different forms of phenyllithium in the crystalline state. From ether, a tetrameric aggregate crystallizes; in its center there are two "intertwined" tetrahedra, a larger one of four carbons and a smaller one of four lithiums [145]. In the presence of LiBr, a mixed tetrameric aggregate of three PhLi and one LiBr was crystallized from ether; three of the four Li atoms are complexed by ether oxygens, the fourth one, diagonally across the cube from the bromide, is not [145]. With TMEDA, a dimeric aggregate crystallizes [147], with PMDET a monomer was isolated [148] (for recent papers on PhLi structures in solution see Ref. [42a, 94, 149]). Until now, the "de-aggregation" of Li derivatives by addition of the tridentate PMDET has hardly been used by preparative organic chemists as a simple means of avoiding complications caused by aggregation.

Table 3. Some Li ate complexes detected in the solid state and in solution. In the examples chosen, oxygen-, nitrogen-, or carbon-centered anionic ligands are present.

Li ate complex ("triple ion")	Method	Ref
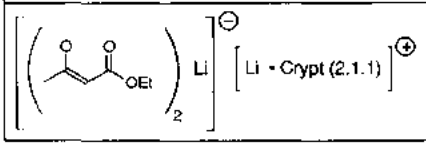	NMR	[151]
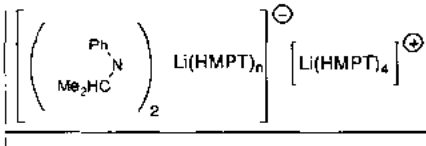	NMR	[135]
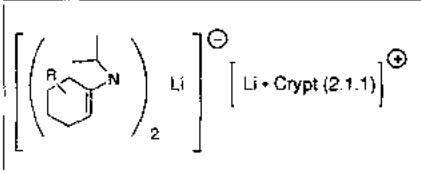	NMR	[102b]
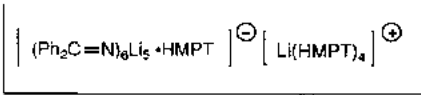	X-ray crystal structure	[103]
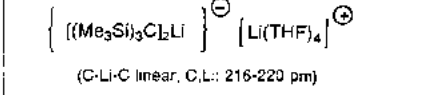 (C-Li-C linear, C,Li: 216-220 pm)	X-ray crystal structure	[152]
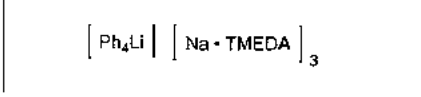	X-ray crystal structure	[153]

There are mixtures of bases (see Scheme 5) which exhibit properties drastically different from those of the components. It is not clear at this point[158] whether this is due to ate complexes or to dimeric, tetrameric, or even higher-order aggregates.

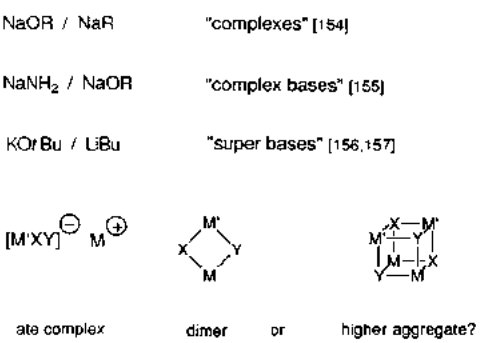

Scheme 5. Mixtures of bases may cause rate enhancements of deprotonations or eliminations in THF by several orders of magnitude as compared to the individual components.

2.3. Thermodynamic Data

Some thermodynamic data relevant to our discussion are listed in Tables 4–6. Again, many more measurements have been performed with Li,C than with Li,O derivatives.[122–53, 150] The most simple model for explaining the formation of aggregates may be to assume that it is caused by charge attraction. Lithium may be considered a small sphere of high positive charge density. In a Li enolate dimer each Li is "neutralized" by two counterions (and *vice versa*), and in a tetramer, by three (cf. the Madelung energy stabilization in an ionic crystal lattice). The large solvation energy of $Li^{\oplus}$ (interestingly, it is 7 kcal mol^{-1} more with NH_3 than with H_2O) is a consequence of the high charge density, and so is the exothermicity of LiX dimerization—the first step in formation of an ionic inorganic crystal lattice (Table 4).

The heats of deprotonation of carbonyl compounds by Li amides and of formation of an aldolate from Li enolate and aldehyde were measured only very recently (Table 5). The latter reaction is exothermic by 18 kcal mol^{-1} in THF and by 30 kcal mol^{-1} in cyclohexane (the calculated average bond energy change is $\Delta mBE = -19.4$ kcal mol^{-1}, i.e., the difference between a CC double and two CC single bonds).

The contributions of charge neutralization and complexation of the Li atoms by oxygens is clearly evident from these calorimetric measurements. Some of the reactions are so highly exothermic that their transition states should be more similar to the starting material than to the product (cf. the more selective deprotonations by LHMDS with the smaller heat of reaction!).

Some properties of Li enolates, such as the equilibrium ratios between regioisomers and between *E*/*Z* isomers (cf.

Table 4. Enthalpies of solvation, dimerization, and complexation of $Li^{\oplus}$ and LiX, respectively.

Gas-phase solvation enthalpies ΔH_{sol} (kcal mol^{-1}) of the lithium cation with water [159] and with ammonia [160]

$Li^{\oplus} + n\,H_2X \longrightarrow [Li{\bullet}(H_2O)_n]^{\oplus}$ or $[Li{\bullet}(NH_3)_n]^{\oplus}$

n	1	2	3	4	5	6
$\Delta H_{sol}^{H_2O}$	-34	-60	-81	-97	-111	-123
$\Delta H_{sol}^{NH_3}$	-39	-72	-93	-109	-121	-130

Gas-phase dimerization enthalpies ΔH_{dim} (kcal mol^{-1}) of lithium halides [161]

$2\ LiX \longrightarrow$ 

X	F	Cl	Br	I
ΔH_{dim}	-60	-49	-48	-43

Complexation of LiX with amides

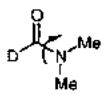

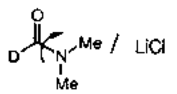

Rotation barrier [162]			
E_a	21.6	25.0	kcal mol^{-1}
$\Delta G^{\neq}$	21.2	21.8	kcal mol^{-1}
$\Delta S^{\neq}$	-1.0	+5.8	cal K^{-1} mol^{-1}

Equilibrium constant [163]

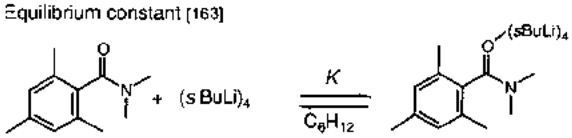

$K = 300 \pm 50$ (25°C)

Table 5. Calorimetric determination of the different steps of the aldol reaction of Li enolates at 25°C by *Arnett* et al. [164]. All the ΔH values are given in kcal mol^{-1} (compare with the structures in Figs. 3, 5, 7, 8, 11, and 16). ΔH_{dep}, enthalpy of deprotonation; ΔH_{comp}, enthalpy of complexation; ΔH_{ald}, enthalpy of aldol addition.

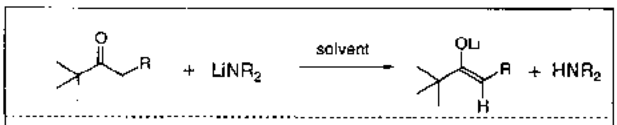

	LDA		LHMDS	
	in C_6H_{12}	1 eq. THF [b] in C_6H_{12}	in C_6H_{12}	in THF [c]
ΔH_{dep} R = H [a]	-29.6	-30.9	-22.6	-10.4
ΔH_{dep} R = $COCMe_3$ [a]	-50.9	-46.2	-38.7	-30.0

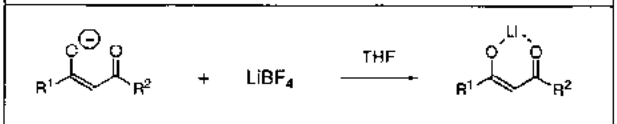

[K•Crypt (2.2.2)]$^{\oplus}$ [K•Crypt (2.2.2)]$^{\oplus}$ $BF_4^{\ominus}$

R^1	*t*Bu	*t*Bu	C_6H_5	OCH_3	CH_3
R^2	*t*Bu	OCH_3	C_6H_5	OCH_3	OCH_3
ΔH_{comp}	-26.2	-25.7	-24.9	-22.4	-16.6

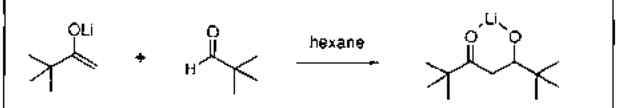

	without additive	1 eq. TMEDA	1 eq. DME	1 eq. THF
ΔH_{ald}	-30.2	-20.9	-19.0	-17.9

[a] pK_a (DMSO scale [165]) of pinacolone, 27.7; of dipivaloylmethane, 15.4. [b] Other ketones and 1,3-dicarbonyl compounds give similar values under the same conditions: cyclohexanone, −34.9; dimethyl malonate, −52.5 kcal mol^{-1}. [c] Under these conditions, enthalpies for the deprotonation (ΔH_{dep}) of phenylethanol [$PhCH(OH)CH_3$] and of ephedrine derivatives [$PhCH(OH)CH(CH_3)NR_2$] are between −18.7 and −20.6 kcal mol^{-1}, thus, there is no indication of (OLi···N) chelation (see, however, Refs. [166–169]).

the correlation between enolate and product configuration in aldol and other addition reactions[5–10, 72a, 173, 174]), are collected in Table 6.

3. Computational Studies of Formation and Reactions of Li Enolates—Contributions from Force-Field Calculations and Quantum Mechanics

In view of the availability of more and more powerful (super) computers, and of ab-initio[175] and force-field programs with an increasing number of improved parameters,[176] it is not surprising to see that almost all of the renowned research groups in this area of theoretical chemistry have contributed calculations of ground-state and transition-state geometries of Li and other polar metal enolates and of their reactions. It is impossible to do justice to this work in these pages and it is hoped that the accompanying Tables 7 and 8 and Figure 21 may suffice for the presentation of some of the results.

The examples in Table 7 and Figure 21 show that very large supramolecular structures have become subject to computational studies. These confirm the decisive role of solvation in the structures of polar Li derivatives; reasonable results, i.e., compatibility with experimental parameters, are frequently not obtained unless Li is given a solvent shell or is "removed" from an intramolecular chelating heteroatom by fixing the geometry otherwise (see the Li dienolate and the dioxanone Li enolate in entries 4 and 5, respectively, of Table 7). Table 8 contains the results of modeling, MNDO, and ab-initio calculations of reaction coordinates involving enolates. The layman certainly has cause to marvel at the ability of theory to reach conclusions about the structures of extremely complex arrangements of atoms, including those of higher periods such as zinc.

With the calculations, we have gone on to the gas phase in which minimum-energy structures may deviate from those in solution even more noticeably than in the crystalline state. It is evident that computations have become so

Table 6. Rotational barriers in Li enolates and relative stabilities of isomeric Li enolates as determined by equilibrium studies under various conditions.

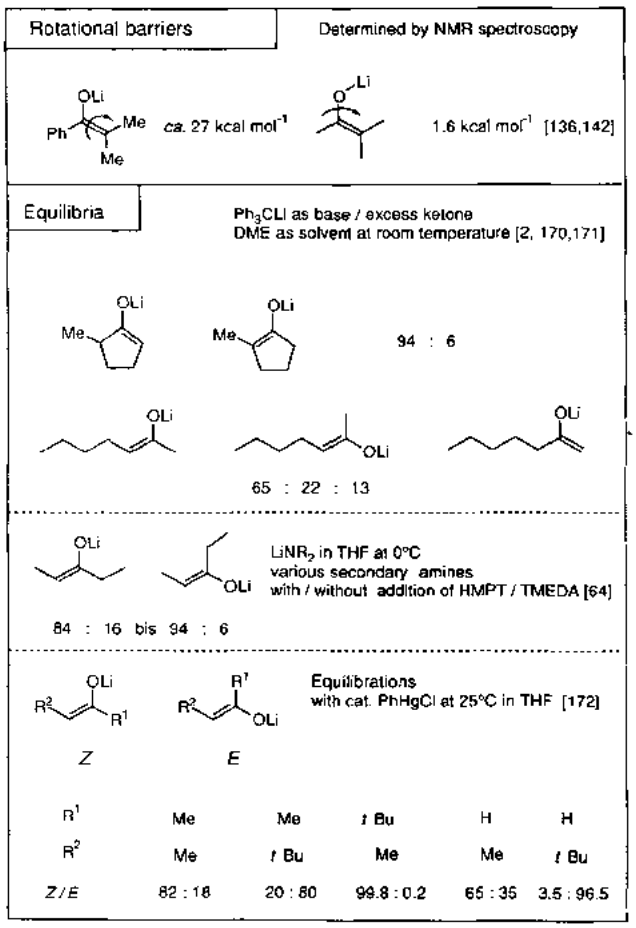

Table 7. Calculations on complexation and aggregation of LiX derivatives and on the structures of Li enolates.

Calculated structure, remarks, and references to the experimental results	Method (basis set)	Ref.
Linear structure most stable (cf. Figs. 7, 8, 11,16)	3-21G 6-31G*	[177a]
4 LiX → (LiX)4 X F OH NH2; Δ H -188 -190 -167 kcal mol⁻¹; more stable for X = NH2; more stable for X = F, OH; (see references in Fig. 9) (cf. Figs. 1-12 and Table 4)	6-31G + sp + d// 3-21G	[177b]
Force-field parameters for Li enolates [a]	MM2	[172]
Calculation and comparison with NMR data (cf. Fig. 8) [b]	STO-3G	[178] [179]
Pyramidalization and reactivity (cf. Figs. 4 and 17)	3-21G	[182]
Modeling and ab initio calculation (cf. also Figs. 2 and 21)	Modeling 3-21G	[183] [184]

[a] From isomerization equilibria and crystal structure data. [b] Compare also with 3-21+G, 4-31G and 6-31+G* calculations of lithiated acetaldoxime [180], of *E/Z*-isomeric enamide, enehydrazide, and oximate anions [181], and of lithiated thioallyl ethers [87].

powerful that solvent molecules can also be included. It is to be expected that discrepancies between calculated and observed values will eventually vanish. So far, theory has reproduced experimental results in this area. As far as I know, there is no instance of an organometallic reaction mechanism being put forward solely on the basis of calculation which was not first proposed, prior to calculation, on grounds of structural investigations in the solid or liquid phase,[199] or on the basis of preparative results, or of chemical intuition.

4. Reactions of Li Enolates—Supramolecules as Product-Forming Species

The behavior and properties of any organized system arise not only from its parts but also from the manner in which they are arranged.[200]

The fact that Li enolates are found to be more or less aggregated in solution and crystals does not, of course, tell us anything about the actual reactive species, at this point. As with Li,C derivatives,[24,25] it is not at all easy to furnish proof for the participation of aggregates in product-forming steps. Elaborate kinetic measurements of fast reactions of air-sensitive compounds at low temperature are necessary. NMR spectroscopy is the method of choice, and it was used early on, in a masterly manner,[21,137,138,201] to demonstrate that Li enolate aggregates *may* be directly involved in reactions, rather than being the pre-equilibrium precursors of monomeric reactants: the degree of aggregation and the presence of Li salts were clearly correlated with ratios of isomeric products formed (e.g., *C*- vs. *O*-alkylation of Li enolates[21,137,138]), the conclusion being that "ion-pair aggregates are the true reactants".[137] Dimeric aggregates turn out to be more reactive than tetrameric ones, according to these measurements.[138]

A new dimension of mechanistic details was made accessible by a new NMR technique, the method of rapid injection (RINMR):[202,203] reactants are quickly mixed in an NMR tube—also possible at very low temperatures—and the first spectrum can be taken after a few milliseconds.[204-206] This allows one to see different species, as well as transient ones, disappearing and appearing in the reaction mixture. Thereby, it was found[141] that the reac-

Table 8. Calculations on various nucleophilic additions to carbonyl groups, including the aldol addition of Li enolates and the Reformatsky reaction.

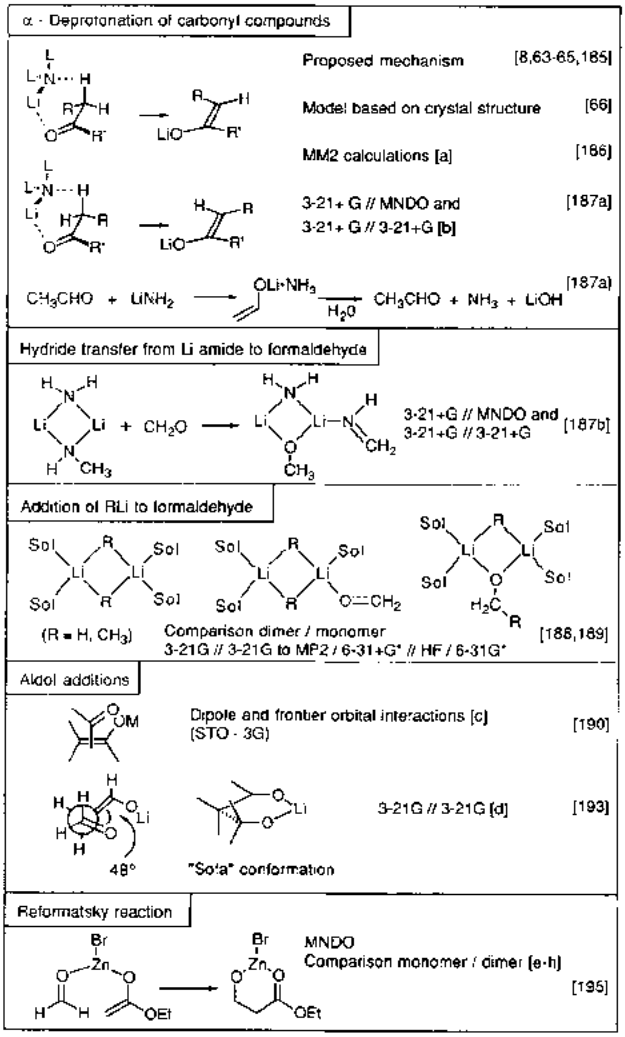

[a] Calculations without consideration of experimental results. [b] The protonation of the enolate-ammonia complex was also calculated (cf. the discussion in Section 3.1 (R_2NH effect)). [c] Compare the model of "unsuccessful cycloaddition" [191], earlier comments on the significance of HOMO-LUMO interaction [192], the chelate model [5, 12], and the general topological rules for coupling of trigonal centers following the Bürgi-Dunitz trajectory,[13, 14] see also: D. Seebach, V. Prelog, *Angew. Chem. 94* (1982) 696–702; *Angew. Chem. Int. Ed. Engl. 21* (1982) 654–660. [d] For MNDO calculations of the aldol addition of *E*/*Z*-isomeric boron enolates to aldehydes, see Ref. [194]. [e] According to this calculation, reactions starting from the dimeric Reformatsky reagent, as present in the crystal (Fig. 19), have an activation energy at least 15 kcal mol^{-1} higher than those with the monomeric reagent. [f] According to the calculation, a reaction starting from the α-Zn-ester (*C*-metalated enolate), a formal [3,1]-sigmatropic rearrangement, has a higher activation barrier (by ca. 15 kcal mol^{-1}). [g] A general comparison of aldol addition and other reactions of metal derivatives in nonpolar solvents with pericyclic processes (Woodward-Hoffmann type) is certainly apparent [102c, 195]. The present example would have to be called a [3,3]-sigmatropic rearrangement [196], a metallo-oxa-Claisen, or a metallo-dioxa-Cope reaction [197]. However, considering the involvement of strongly polar (ionic?) bonds and, more importantly, the presence of an element of the higher periods (Zn), this comparison should be regarded as a formalism. [h] According to the formalism proposed by *Baldwin* [198], a metal-atom-involving aldol addition between the two trigonal carbon atoms of the carbonyl and the enolate double bond may be regarded as an "allowed bis-(6-*endo*-*trig*) process". On the other hand, the 1,3-shift mentioned in footnote [f] would be a "forbidden (4-*endo*-*trig*) process"!

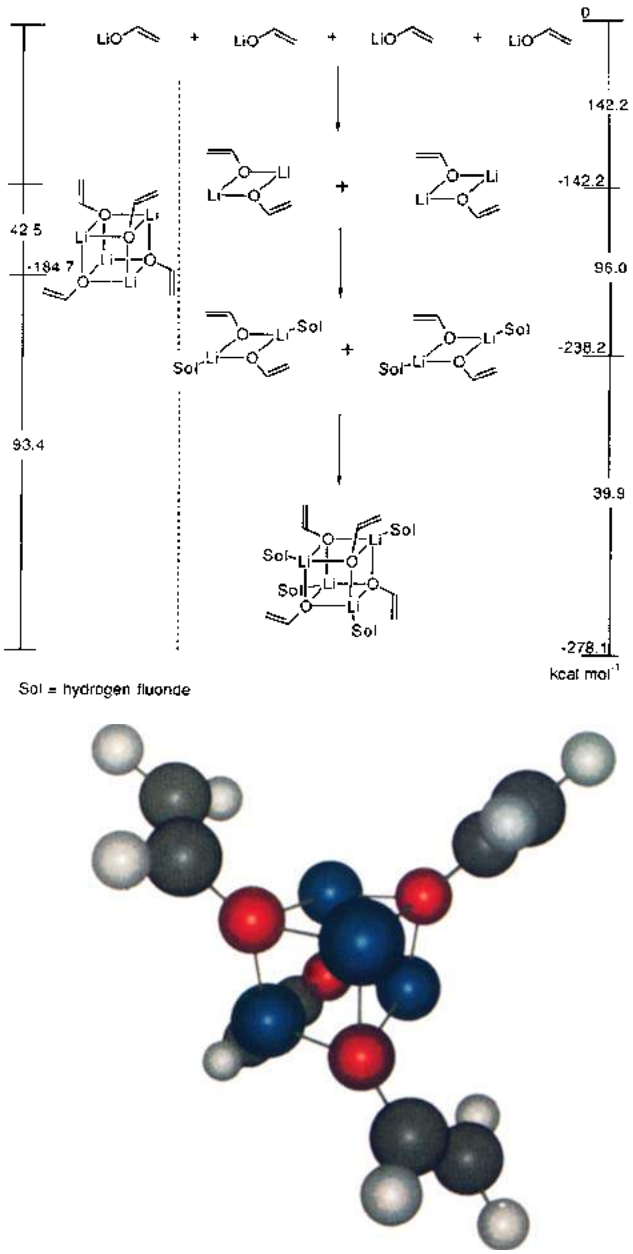

Fig. 21. Calculated (ab-initio 3-21G) aggregation and solvation enthalpies of the Li enolates of acetaldehyde (cf. Table 1) with HF as solvent molecule (Sol) [184]. According to this calculation, 33.5 kcal mol^{-1} of energy is liberated upon complexation of two additional solvent molecules to the dimer $[(EnOLi)_2Sol_2]$→$(EnOLi_2)\cdot Sol_4$} (En = CH_2=CH); therefore, without consideration of the entropy effect [42c], the difference in the stability between the dimer and the tetramer would be 27 kcal mol^{-1}, the latter being more stable. In THF, this difference is found to be significantly smaller: one often observes both species coexisting (see also Section 2.2). The color picture of the tetramer was generated from the calculated coordinates with the program *MacModel* [184].

tion of a dimeric Li enolate aggregate with an added aldehyde is much faster than its regeneration from the equilibrium with the tetrameric aggregate. The higher reactivity of the dimer may be attributed to less steric hindrance and more negative charge density, the enolate moiety being "neutralized" by two, rather than three, Li counterions; a monomeric Li enolate would be expected to be even more reactive,[207] and an ate complex should exhibit further increased reactivity (enolate "neutralized" by only 1/2 Li!).[208, 209]

It is much easier for the chemist dealing with synthetic and preparative aspects of Li enolate reactions to demonstrate that complex structures rather than a simple reagent

molecule *must* be responsible for an observed result. On the other hand, he or she has very little choice but to speculate exactly which species did it! Little fantasy is required to imagine what a wealth of complications can be caused by aggregations and complexations in processes as fundamental as deprotonation of a carbonyl compound (Scheme 6), aldol addition (Scheme 7), alkylation in the α-position of a carbonyl group (Scheme 8), with (Scheme 9) or without addition of a polar aprotic cosolvent.[216] An almost confusing situation results[2,7] in which a great variety of structurally different Li enolates of different reactivity may arise in the course of a simple transformation such as the reaction of an enolate with an electrophile[216]—a nightmare for the synthetic chemist, just like the one a crystallographer may experience, who, by pushing the wrong button, generates the chaos shown in Figure 22 instead of a beautiful three-dimensional representation of a structure. After all, it is surprising how well we fared with the simple model, how forgiving the Li enolates are! In the following sections I will describe results to show not only how we might reduce but also how we might exploit the complexity we gained. Once again, it must be emphasized

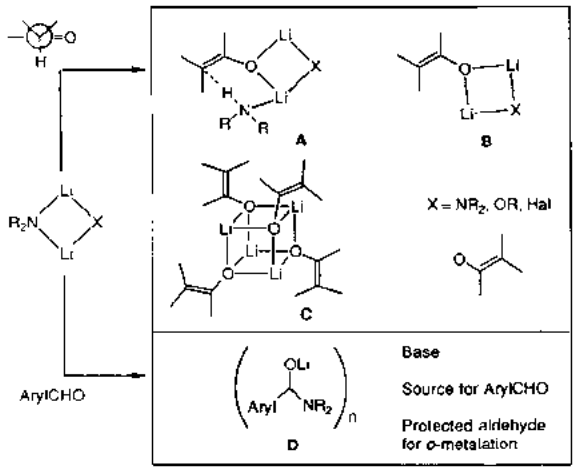

Scheme 6. Reaction of a carbonyl compound with LDA or with an LDA/Li halide or Li alkoxide mixture (cf. the structures in Figs. 2–4, 9, 10). **A**: Dimeric Li enolate or mixed aggregate complexed with a secondary amine. **B**: Pure or mixed aggregate from two LiX units. **C**: Tetrameric aggregate. **D**: Adducts of Li amides with nonenolizable, aromatic aldehydes [210–212].

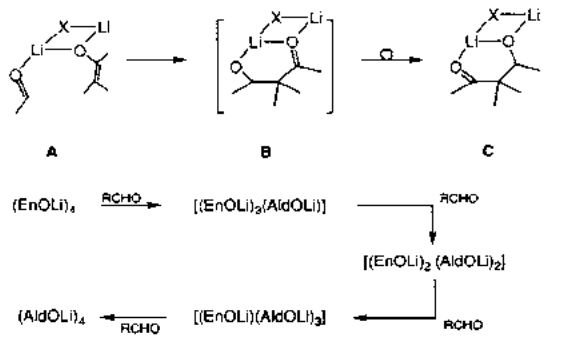

Scheme 7. Possible reactions of Li enolate aggregates with an aldehyde (cf. structures in Figs. 2, 7, 16). In the process of C-C bond formation, complex **A** is converted, through adduct **B** with the negative oxygen in an "outer position", into the aldolate **C**. The reaction of a Li enolate tetramer $(EnOLi)_4$ may take place over four steps to give the aldolate tetramer! (Cf. the structure in Fig. 7.)

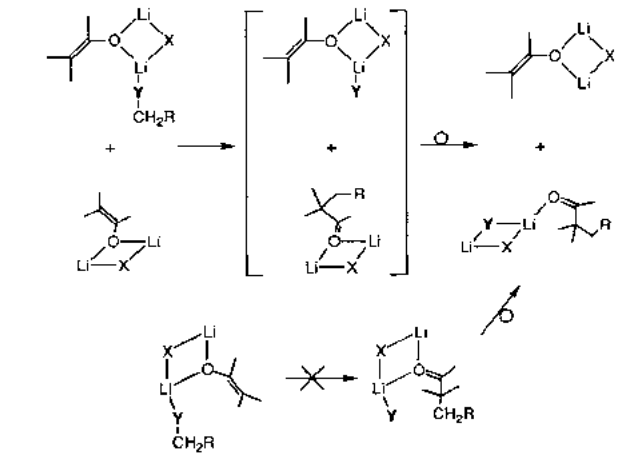

Scheme 8. Formulation of a reaction between two Li enolate aggregates and an alkyl halide to give an α-alkylated ketone and Li halide (cf. the structures in Figs. 11, 20). Because the alkylation of Li enolates occurs with inversion at the alkylating C atom [213], it should not be able to take place in an "intrasupramolecular" ("intraaggregate") fashion (linear S_N2 transition state!) [214].

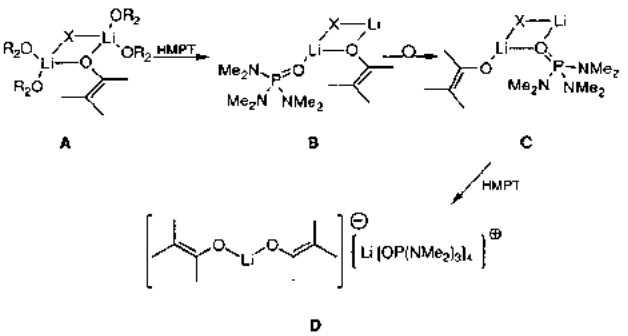

Scheme 9. Structures that may be formed from a Li enolate by addition of HMPT with enhancement or alteration of reactivity as compared to nonpolar solvent systems. The enolate unit in **A** (enolate inside, cf. Figs. 3–6) can attain increased charge density through complexation of the Li with an HMPT oxygen (**B**), the enolate O atom being still "neutralized" by two $Li^{\oplus}$ (cf. the tetrameric LiCl with HMPT complexation in Fig. 12). Through reorganization, the HMPT oxygen may become part of the aggregate nucleus (**C**), the enolate oxygen outside being "neutralized" only by one $Li^{\oplus}$, which should increase the nucleophilicity/basicity (cf. Fig. 15). In the ate complex **D** (cf. Table 3), the enolate would be even more activated. Very much the same effects are observed with the nonmutagenic cyclic urea DMPU as with HMPT (see Fig. 8 and Ref. [63]) [215].

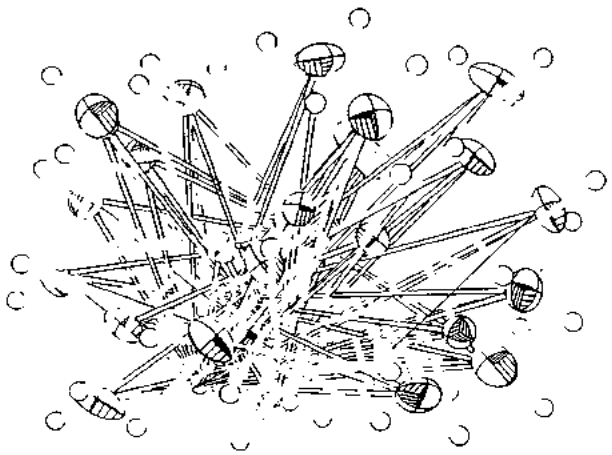

Fig. 22. Unsuccessful ORTEP plot, due to erroneous data input, of the structure of the TriMEDA-complexed amide enolate shown in Fig. 5.

that other polar organometallic compounds behave similarly, so that the discussion of Li enolates will lead to quite general conclusions.[219,220]

4.1. The Effect of Secondary Amines

It has been known since the beginning of the LDA era[59,221] that the secondary amine concomitantly generated with the Li enolate from a carbonyl compound and LDA *may* have an effect upon the reactivity of the enolate.[62b,222–224] In many reactions with electrophiles the amine-free Li enolate solution gives better results; examples for the generation of amine-free solutions are given in Scheme 10—note that some of these methods are "pre-LDA"!

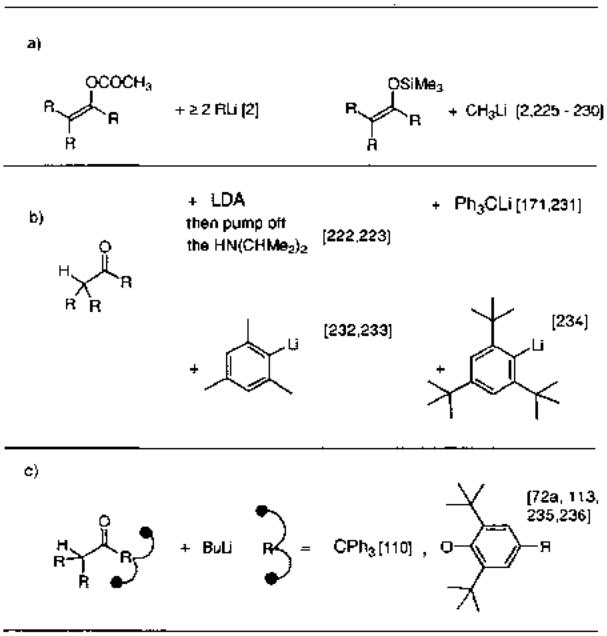

Scheme 10. Generation of amine-free Li enolate solutions. a) From enol esters and silyl enol ethers. b) From carbonyl derivatives and LDA (pumping off the secondary amine formed), or with sterically hindered, and therefore regioselective, organolithium compounds (with formation of a hydrocarbon). c) From a compound having a sterically hindered, but electronically effective [237] carbonyl group, with butyllithium [238].

Recently, a number of cases have come to light in which totally unexpected results were obtained with Li enolate reactions in the presence of secondary amines, mostly diisopropylamine: Addition of deuterating or alkylating reagents (DX and RX, respectively) does not furnish the desired α-deuterio or α-alkyl carbonyl compound, but a more or less completely α-protonated product, i.e., starting material, and it was shown that the proton stems from the secondary amine.[239] The expected products are often isolated in high yields if butyllithium is added prior to the electrophiles. The amine as a proton source for much too weak bases was observed especially with substrates having more than one acidic proton (effect of the "hidden proton").[240] The general effect is pictured in Scheme 11, which also contains some examples from the recent literature. Obviously, the complexes that we have discovered in crystals[66] (Figs. 3, 5) are also present in solution, and are much more stable than anticipated. Under quenching conditions the "intra-supramolecular" proton transfer from the diisopropylamine to the Li enolate, which are linked together by Li–N complexation and hydrogen bonding,[247,248] competes successfully with the expected intermolecular attack of the electrophile.[249] Formally, huge isotope effects occur in such deuterolysis experiments

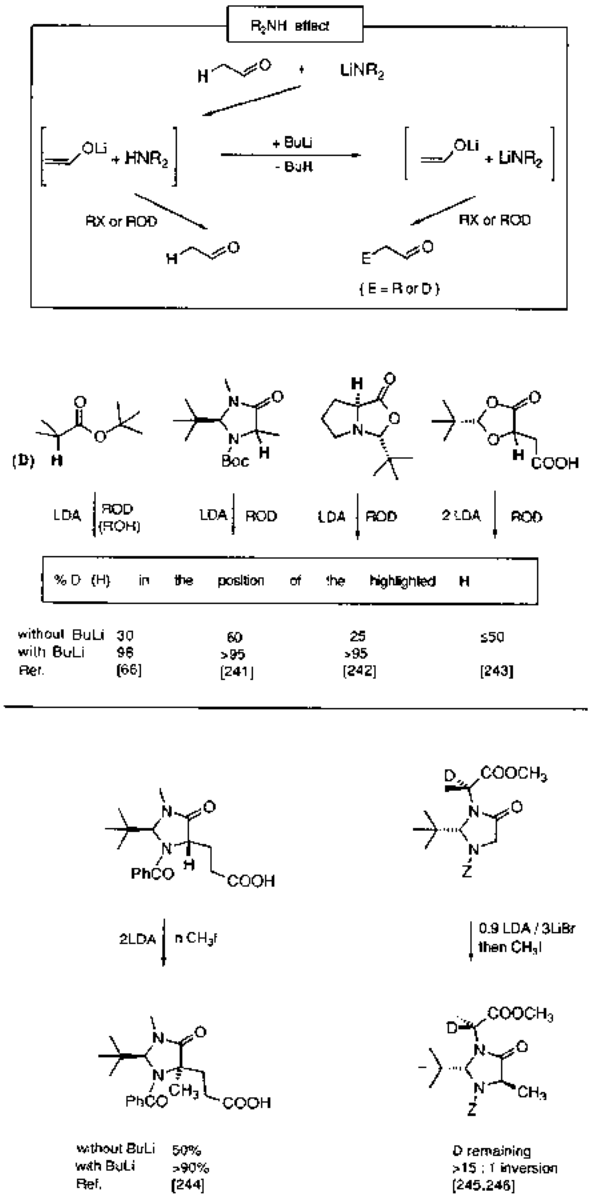

Scheme 11. Reactions of Li enolate–diisopropylamine complexes (in THF). *Top:* In the enolate–amine complex, a (partial) reprotonation occurs under the influence of the electrophile; by removal of the amine with BuLi, the yield of the desired product may be improved. *Middle:* Examples of deuterolyses; only after removal of the NH proton is a good deuterium incorporation achieved; a control experiment with the deuterated precursor and hydrolysis gives a complementary result (D replaced by H only after treatment of the enolate–DNR_2 with BuLi). *Bottom:* Examples for methylation of LDA-generated enolates with iodomethane. *Left:* Only after removal of the R_2NH proton is a high yield of the α-methylglutamic acid derivative obtained. *Right:* The deuterated imidazolidinone derived from glycylalanine is epimerized and alkylated, without loss or scrambling of deuterium over the two α-carbonyl positions, by treatment with LDA/LiBr (LDA alone does not cause a clean conversion, see Section 4.3) and CH_3I (with acetic acid instead of CH_3I as an electrophile, the starting material is recovered without loss of the D and without epimerization!).

when the Li enolate/amine solution in THF is added dropwise to a many thousandfold excess of perdeuteroacetic acid. The "internal return" of the originally removed proton is reminiscent of an effect termed *conducted-tour mechanism* coined many years ago by *Cram* to characterize the stereochemical course of certain ion-pair reactions,[250–252] and of proton-transfer mechanisms[253,254] discussed for active sites of enzymes (cf. serine proteases[255]).

Treatment of an LDA-generated enolate with BuLi is, of course, a drastic cure for removal of the villainous NH proton. Since an LDA/enolate *mixture* is formed, the product will be exposed to the base LDA; furthermore, an enolate results which may have quite different properties as compared to the original one, due to the presence of LDA (see Section 4.2). This is why the methods collected in Scheme 10 for the generation of amine- and amide-free Li enolate solutions should be kept in mind. To avoid many a complication, the use of sterically more hindered Li amides such as lithium *tert*-butyl(1,1,3,3-tetramethylbutyl)amide (also called LOBA ≡ *l*ithium-*tert*-*o*ctyl-*tert*-*b*utyl-*a*mide[65]) or of the less basic, but also less highly aggregated, disilazanides[256] (LHMDS, KHMDS; cf. the heats of deprotonation in Table 5), producing the poorer complexing $HN(SiMe_3)_2$ in the deprotonation step, is recommended.

The complexes of Li enolates and secondary amines dealt with here are probably also involved in some of the processes discussed in the following section, when achiral enolates are generated by chiral Li amides.

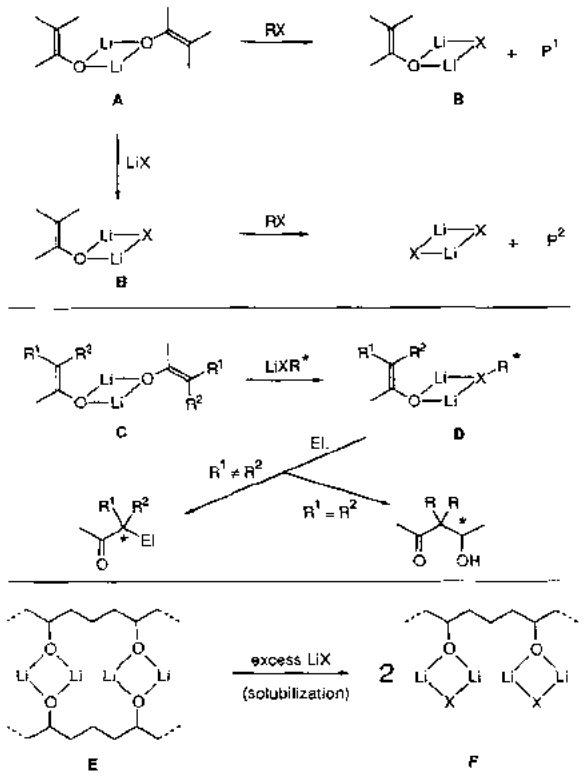

Scheme 12. Addition of LiX to an enolate solution could lead to formation of a mixed aggregate (**A**→**B**), and therefore change the product ratio P^1/P^2. A chiral additive puts an achiral enolate in a chiral environment (**C**→**D**), which may lead to the formation of enantiomerically enriched products. The LiX addition can have a solubilizing effect with a polylithiated derivative (**E**→**F**).

4.2. The LiX Effect in Li Enolate Reactions

Gedanken ohne Inhalt sind leer,
Anschauungen ohne Begriffe sind blind.[*]
Immanuel Kant

If the result of Li enolate reactions, carried out under the usual conditions in nonpolar solvents and at low temperatures, does depend upon the complex processes indicated in Schemes 6–8, then we not only need to worry about the secondary amine being a component of the mixture (Section 4.1); the formation of mixed aggregates may cause the following additional phenomena:

(1) The properties of Li amides used for deprotonations might be influenced by LiX additives, especially with more complex substrates.

(2) An enolate may exhibit different reactivity at the beginning ("pure" aggregate) and at the end ("mixed" aggregate with the LiX formed) of a reaction.

(3) The mode of addition and large excesses of one reactant in small-scale runs may strongly influence the results.

(4) LiX additives that are not part of the stoichiometric equation may decisively change the properties of an enolate.

In the three parts of Scheme 12 these effects are exemplified. *Firstly*, a Li enolate dimer may be converted into a mixed dimer by addition of LiX, which is formed in alkylations by alkyl halides or sulfonates. Assuming that the dimeric enolate gives rise to one product, the mixed aggregate of Li enolate and LiX another one; in the absence of interaggregate exchange, this would lead to formation of the two products in a 1 : 1 ratio. On the other hand, addition of excess LiX could convert all of the "pure" into the "mixed" aggregate so that a single product would be formed. *Secondly*, addition of a chiral Li derivative LiXR* to the dimer of an achiral Li enolate should give a chiral mixed aggregate, the enolate component of which has diastereotopic faces or, depending upon the substitution pattern of its double bond, can differentiate enantiotopic faces of a reactant. *Thirdly* (bottom part of Scheme 12), a polylithiated, self-aggregated compound (insoluble) may be converted into a mixed aggregate with added LiX and thus be solubilized (a kind of cross-linking is disrupted).

Of course, the LiX effect as sketched here is oversimplified, perhaps in a single-minded way: especially when added in large amounts, Li halides, thiolates, alkoxides, enolates, and amides will also change the medium itself,[257] rendering it more polar ("salt effect").[150] In addition, formation of ionized species[258] (ate complexes, ion pairs) will be more likely even at low temperatures. Still, the concept of mixed-aggregate formation turned out to be extremely fruitful in the course of our own work, some of which will be outlined in the following sections.

[*] Thoughts without content are empty, intuitions without concepts blind. *Critique of Pure Reason*. Edited and translated by W. Schwarz, Scientia Verlag, Aalen 1982, p. 29.

4.3. Achiral Enolates for the Preparation of Enantiomerically Enriched Products—Making a Virtue of Necessity

In Section 4.1, methods of avoiding the problems caused by the complexation of Li enolates with secondary amines were discussed. Here, we turn our attention to potentially very useful transformations which depend on the complexation between Li enolate and Li amide. For an enantioselective reaction, instead of coupling an enolate with a chiral auxiliary covalently, which requires a cleavage later on, the components are joined through a complexation, an interaction which is simply broken during aqueous workup! Just like in a chiral solvent,[259, 260] two achiral reactants, such as an enolate and an aldehyde, may thus be coupled to give enantiomerically enriched products (Scheme 12, middle). This procedure is fundamentally different from the use of a chiral Li amide[261] for enantioselective deprotonations or of a chiral acid for protonations[262, 263] (Scheme 13). A number of examples are collected in Table 9. As can be seen, metals other than Li can be employed. Chiral alkoxides are less effective than amides. Usually a Li enolate/$LiNR^*_2$ ratio of 1:3 gives rise to the highest enantiomer excesses.[278] Most of the chiral Li amides used are prepared from 1-phenylethyl amine or from amino acids and are thus readily available. Since there is very little structural information (Fig. 10) about complexes of Li amides with Li enolates, all attempts toward interpretations of these results are highly speculative, and we refrain from reproducing them here.

Enantioselective deprotonation to chiral enolate

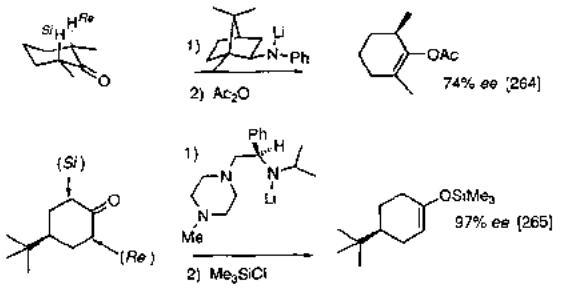

Enantioselective protonation of an achiral enolate

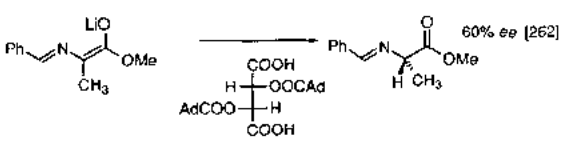

Scheme 13. Enantioselective protonations/deprotonations involving Li enolates. The chiral reagent (base or acid) selectively attacks enantiotopic groups or faces [266-268]. (With the protonations, the R_2NH effect discussed in Section 4.1 may be involved as well; with the deprotonations, the LiX effect may be operative—carefully excluded only in one case [264, 269].)

5. Alkylations of Sarcosine Units in Peptides—from Expectation to Surprise

What we learned about structure and reactivity of Li enolates was found to be successfully applicable to a seemingly unrelated project. For several years now, our group has been engaged in the development of new methods for the preparation of nonproteinogenic amino acids.[56, 100] These are required for incorporation into peptides whose biological properties are to be modified.[279] Normally, a separate synthesis is necessary for every peptide analogue [Scheme 14, route (a)]. A method by which a glycine unit in a given oligopeptide could be converted into other amino acid moieties by direct *C*-alkylation would not only be much more efficient; it would no doubt provide valuable information about the influence of chirality centers of neighboring amino acid units on the formation of a new stereogenic center in an open-chain peptide[280] [Scheme 14, route (b)].

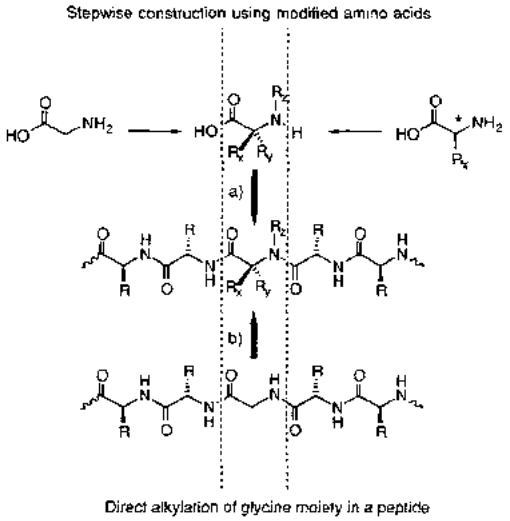

Scheme 14. Synthesis of modified peptides. a) By stepwise construction from the appropriately modified amino acid building blocks. b) Elaboration of an amino acid by introduction of side chains; many analogous derivatives could thus be obtained from a common precursor peptide.

The notion of generating an enolate in a peptide chain seems to be absurd:

Firstly, there is an acidic amide NH hydrogen ($pK_a < 20$) per amino acid unit to be removed before the CH_2 group of a glycine moiety can be deprotonated (there are even more acidic hydrogens in side-chain functionalized amino acids).

Secondly, strongly basic conditions are bound to be applied for such a CH deprotonation under which epimerizations of stereogenic centers might occur (in an n-oligopeptide a maximum of 2^n different diastereoisomers could be formed!).

Thirdly, it is usually necessary to generate Li enolates in an aprotic medium at low temperatures, conditions in which an oligopeptide itself, and even more so a polylithiated one, might be expected to have little solubility.

At the outset of our investigations in this area, we did not entertain such reflections; rather, a gifted young chemist[281] did a bold and careful experiment with an already rather large oligopeptide. For reasons of systematization, let us start with the simple cases, reversing the order of events.

Table 9. Enantioselective aldol additions, Michael additions to a nitroolefin, carboxylation, and alkylation of achiral enolates in the presence of chiral lithium alkoxides or amides. The examples 1–12 and 16 are taken from our own work [53, 91–93, 270–273], whereas we owe the results in entries 13 [274], 14 [275], and 15 [276] to research done by others. Enolate solutions free of amine were obtained either by addition of BuLi to enolates generated with $LiNR_2^*$ or by use of the silyl enol ether/methyllithium procedure. The configurations shown and the enantiomer ratios given were determined by NMR spectroscopy or with chiral HPLC columns [277].

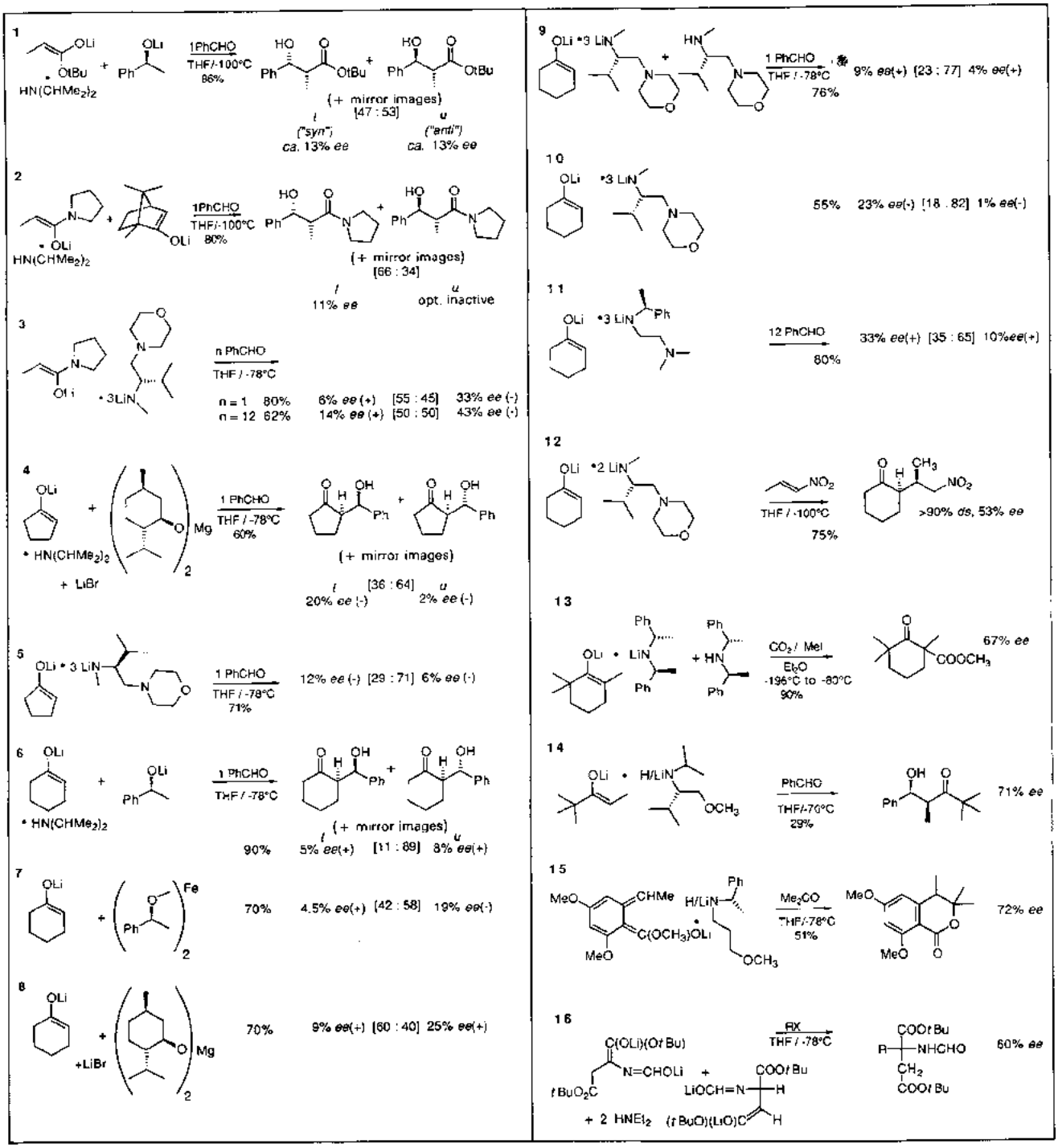

Two nonpeptide examples pictured in Scheme 15 may be used to demonstrate the LiX effect. The (*R*)-*N*-benzoyl-3-aminobutyrate shown in the upper part of Scheme 15 can be alkylated through a dilithium derivative in the 2-position.[141, 282] At dry-ice temperature the reaction mixture in THF is heterogeneous; warming is necessary to complete the reaction with iodomethane. In contrast, the reaction takes place in homogeneous solution if LiCl[285] is added, with greatly improved result! Other Li salts such as LiBr, $LiClO_4$, $LiOSO_2R$ have similar effects (cf. the lower part[283] of Scheme 15).

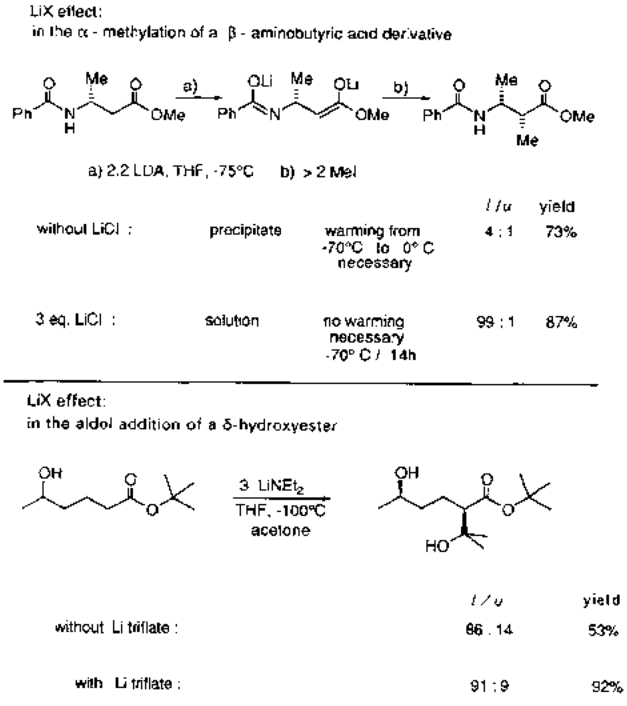

Scheme 15. LiX effect on the generation and behavior of two dilithium derivatives [41i, 282, 283]. In the case of the *N*-benzoyl β-amino acid ester the reagent to be alkylated is rendered soluble by addition of LiCl [41i]. In both cases, yields and stereoselectivities are increased. (C=C and C=N configurations here, in Schemes 16–21, and in Fig. 24 are drawn arbitrarily! [284].)

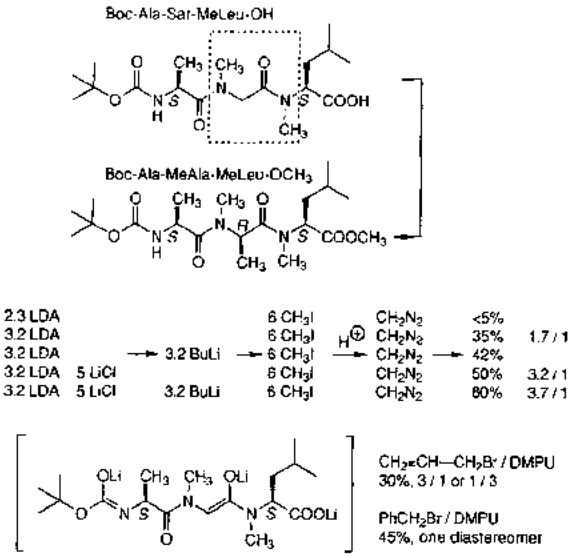

Scheme 16. Diastereoselective alkylations of the sarcosine unit in a Boc-protected tripeptide [286]. For the allylation and benzylation reactions, the co-solvent DMPU [63] had to be added to afford the yields shown.

5.1. Open-Chain Tri-, Tetra-, and Hexapeptides

For *C*-alkylations of open-chain peptides we first chose those containing (1) a sarcosine (*N*-methylglycine) substructure (shown in Scheme 16, sarcosine = *N*-methylglycine), (2) a Boc-protected amino end group (Boc = *tert*-butoxycarbonyl), and (3) a nonprotected carboxylic acid end group. Upon mixing of such peptides with the prerequisite number of equivalents of LDA, a more or less dense precipitate is formed. An enolate at the methylglycine (sarcosine) component of the tripeptide shown in Scheme 16 must arise when slightly more than three equivalents of LDA is added, because subsequent addition of iodomethane furnishes a new tripeptide with *N*-methylalanine at the former sarcosine position.

Removal of the diisopropylamine with butyllithium (cf. Section 4.1) led to marginal improvement of the yield, but addition of LiCl *and* BuLi (after LDA deprotonation) led to the isolation of the new peptide in 80% yield. More importantly, the reaction is diastereoselective (*R*-MeAla/*S*-MeAla almost 4 : 1), and it occurs without epimerization at the two stereogenic centers which were present in the starting material! The configuration was proved by comparison with authentic samples.[286–288]

Likewise, with the hexapeptide depicted in Scheme 17, containing four acidic OH and NH hydrogens besides a sarcosine CH_2 group, a precipitate is formed upon addition of the stoichiometric amount of LDA. Twice the calculated amount of LDA[289] or LiCl[285] causes the solid to dissolve.[290] A homogeneous, nonviscous, slightly yellow THF solution results, readily stirred at dry-ice temperature, and typical of polylithiated compounds under these conditions. Methylation again produces, in yields ranging from 30 to 67%, a new *N*-methylalanine unit in the peptide chain, the yield increasing in the presence of LiCl and with diisopropylamine deprotonation by BuLi.[285] Again, the reaction is diastereoselective, with the *R* configuration at the newly created stereogenic center prevailing (by comparison with authentic samples[288]). The hexalithio hexapeptide that ought to give rise to the observed product is shown at the bottom of Scheme 17.

Inspection of the *formulae* in Schemes 16 and 17 reveals that the peptides used have two characteristic features in common: (1) adjacent to each and every stereogenic center a deprotonation has occurred, rendering a certain protection from further deprotonation, i.e., from epimerization (see Scheme 18); (2) the peptides employed carry aliphatic side chains and are thus lipophilic, which should increase the solubility of their Li derivatives in the nonpolar THF. Had these properties been found to be essential for successful application of the above alkylation procedure, the method would be rather limited. The following two examples show that this is not the case.

The Boc-protected alanyl-glycyl-glycyl-glycine was selected as an example of an especially hydrophilic oligopeptide which, in fact, can hardly be retrieved from water. This also led to the discovery of a quite different LiX effect. As evident from the data in Scheme 19, the peptide, which itself is very insoluble in THF at room temperature, and LiCl form an extremely soluble complex. Furthermore, addition of five equivalents of LDA neither causes precipitation nor decomposition; hydrolysis leads to recovery of the peptide in optically active form. The possibility of carrying out reactions with the solutions thus obtained is currently being investigated. While the great solubility of peptide-LiCl complexes in an organic solvent is very surprising, the fact that anhydrous crystalline adducts

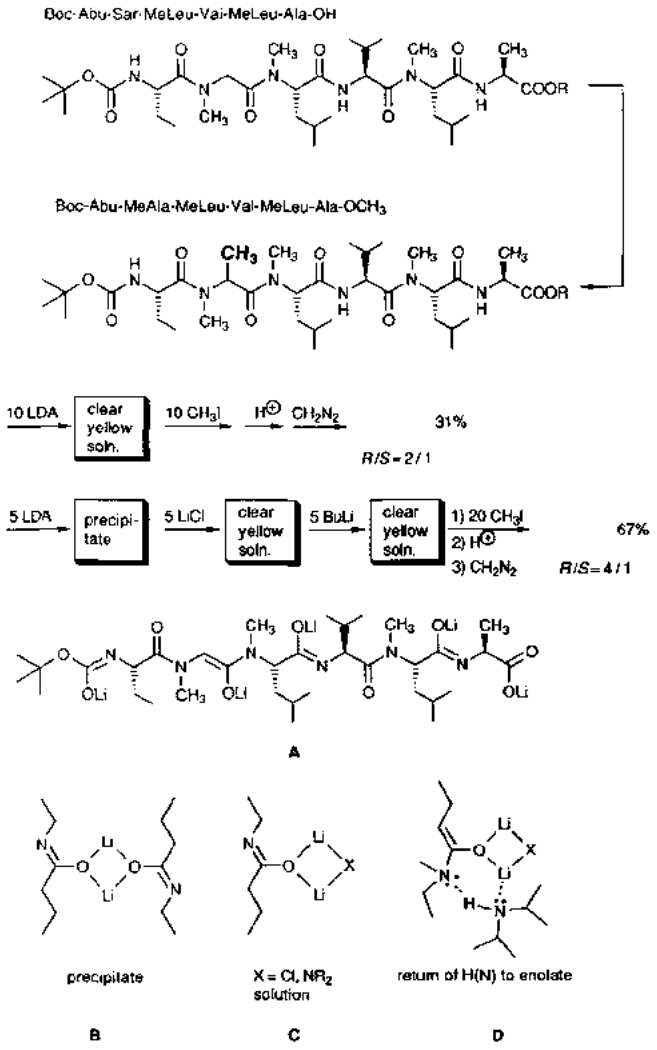

Scheme 17. Fivefold deprotonation of a Boc-protected hexapeptide (consisting of three *N*-methyl and three normal amino acid building blocks) by LDA and diastereoselective methylation at a sarcosine unit [285]. The yields shown were recorded after simple column chromatography and refer to the sum of the two epimers [2-(*R*-MeAla) and 2-(*S*-MeAla)]; the configurations at the other stereogenic centers are the same as in the starting material. **A**, pentalithium derivative; **B**, aggregates of **A**, poorly soluble; **C**, solubilization with LDA or LiCl, probably by formation of mixed aggregates (cf. Figs. 10, 20); **D**, complexation with diisopropylamine results in "reprotonation", i.e., lower yields without subsequent BuLi "treatment" (cf. Fig. 5 and Section 4.1).

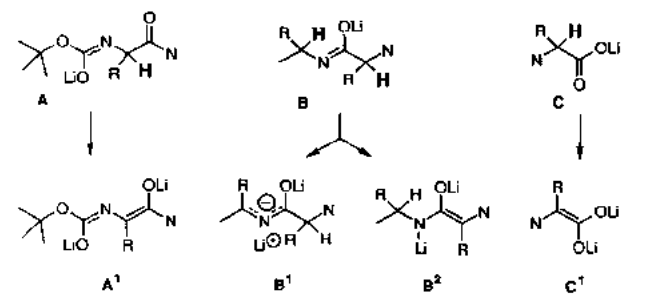

Scheme 18. Deprotonation of the carboxylic acid, carbamate, and amide groups of Boc-peptides, as applied to the reactions shown in Schemes 16 and 17, results in protection of the adjacent stereogenic center from epimerization. The highlighted hydrogens are less acidic in these structures than those in which a neighboring antionoid group is absent. The generation of doubly lithiated systems A^1, B^1, B^2, and C^1 from the respective precursors **A**, **B**, and **C** is indeed possible, as shown with simple molecules [126, 248, 291–293], but demands harsher conditions. (Protection of carbonyl groups against metal hydride reduction, and against addition of MeLi, by directed Li enolate formation in di- and tricarbonyl compounds has been well known for a long time [294, 295].

of Li salts with peptides may separate from aqueous solutions has been known since the beginning of this century (*Pfeiffer*'s "Neutralsalzverbindungen der Polypeptide und Eiweisskörper"[298]).[299] Furthermore, the solubilization in water of a protein antigen by addition of LiBr is described in a patent.[300] Some amide, peptide, and urea complexes of Li salts have been subjected to X-ray crystal structure analysis;[303] one such structure is shown in Figure 23.[303]

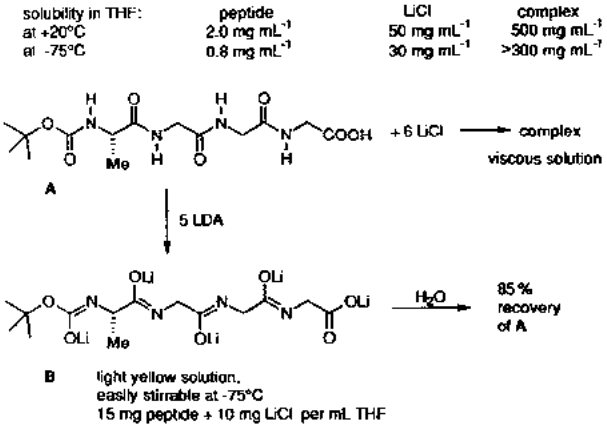

Scheme 19. Enormous increase in the solubility of a 1:6 mixture of Boc-Ala-Gly-Gly-Gly-OH and anhydrous LiCl in THF compared to that of the components. After removal of the solvent (5 h/10^{-3} torr/20°C), a solid residue is left which contains peptide, LiCl, and THF in the ratio 1:6:2.5. Adding five equivalents of LDA to the mixture of A and LiCl, at −75°C, produces a clear solution which probably contains the pentalithio derivative **B** [296, 297].

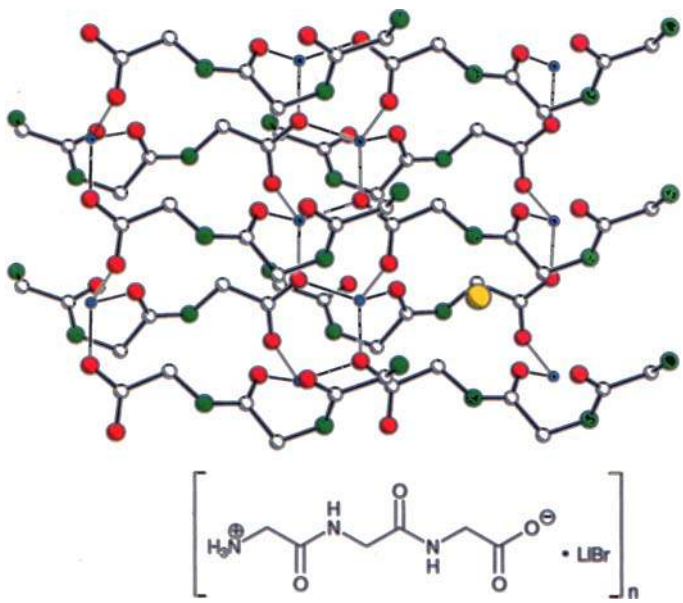

Fig. 23. Crystal structure of the LiBr complex of glycyl-glycyl-glycine [302] (section of the polymeric arrangement; *CSD*: GLYLIB). Cf. the LiX complexes with amides in Table 4, and the structures in Figs. 8, 11, and 16. The "addition ability" of Li salts toward amino acids decreases in the following series: Li > Na > K and I > Br > Cl (after *Pfeiffer*) [299].

5.2. Cyclosporine A

Nescire quaedam magna pars est sapientiae[304][*]

So far, the largest peptide in which we have been able to alkylate a sarcosine unit is cyclosporine A (CyA)[305, 306] and some of its analogues.[307–311] CyA contains a series of amino acid moieties which are not protected against epimerization in the way indicated in Scheme 18. CyA is a novel immunosuppressive drug,[312] the discovery and use of which is as important as skilled surgery for the recent rapid developments in organ transplantations. CyA is a cyclic undecapeptide containing seven *N*-methyl amino acids (Fig. 24), four of which are adjacent to each other

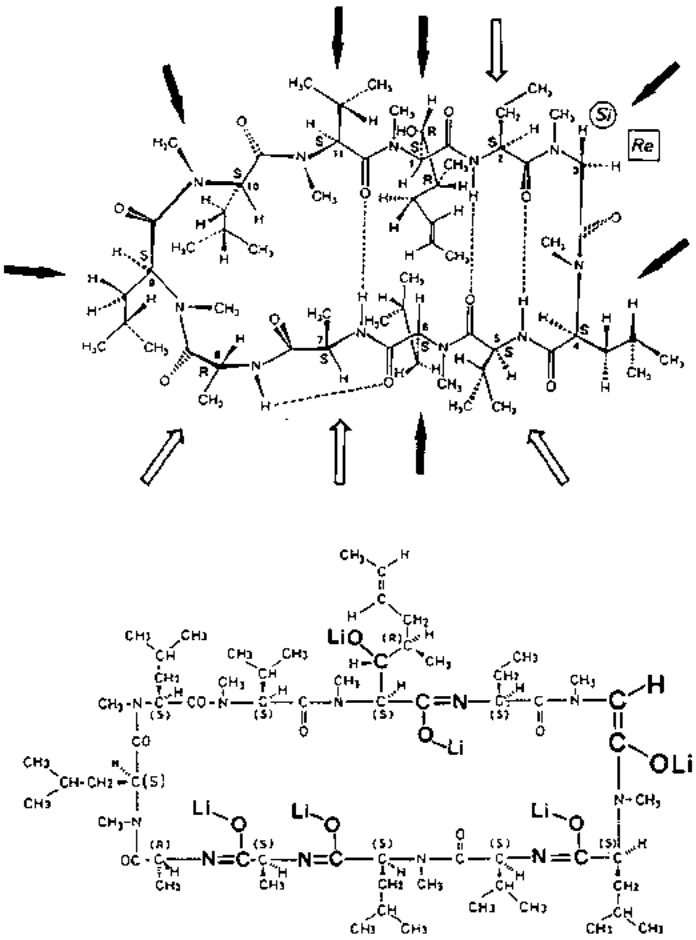

Fig. 24. Cyclosporine A (top) and the hexalithio derivative (bottom). The seven *N*-methyl amino acid building blocks are indicated by solid arrows, the four normal ones by open arrows. The conformation of CyA is identical in the crystal [306] and in solution [130a, 313], except for the orientation of the side chains of amino acids No. 1 and No. 11. There is no structural information available for the Li derivative (*E*/*Z* configuration at CC and CN double bonds is drawn arbitrarily). The Li derivative exists in THF solution in the presence of diisopropylamine, or LDA, or of LiCl, or mixtures of all three. The yellow solution (≥ 20 g L^{-1}), generated at −75°C, can be warmed up to +20°C without decomposition, at least for a short period of time.

(Nos. 9, 10, 11, 1). The amino acid No. 3 is sarcosine, which is followed by another *N*-methyl amino acid, MeLeu. CyA is highly lipophilic and insoluble in water due to the aliphatic side chains and the presence of transannular hydrogen bonds between opposite NH and CO groups in the pleated-sheet-type part of the molecule. In organic solvents CyA exhibits extremely high solubility (> 600 mg mL^{-1} in THF at room temperature and > 300 mg mL^{-1} at −75°C), and with LiCl a complex is formed, as evidenced gravimetrically or NMR spectroscopically[314] (cf. the LiBr complex of the cyclic decapeptide antamanide in Fig. 25).

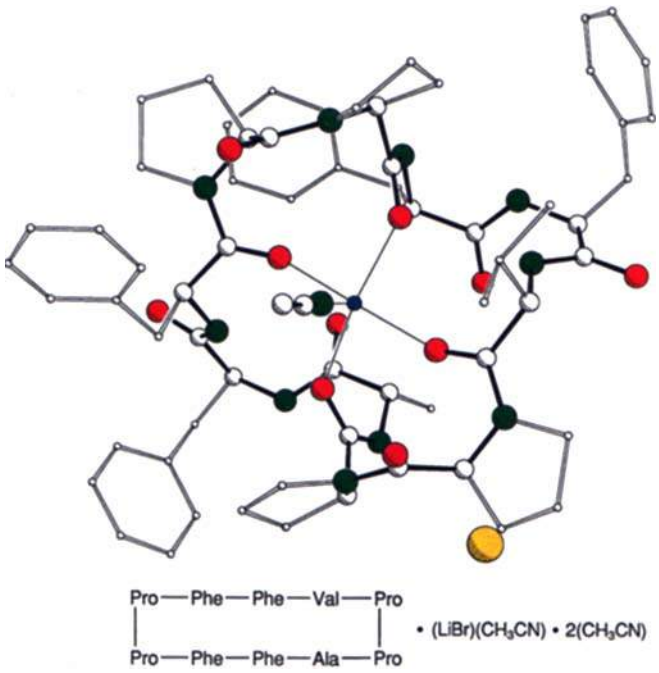

Fig. 25. LiBr complex of antamanide, *cyclo*(Val-Pro-Pro-Ala-Phe-Phe-Pro-Pro-Phe-Phe), crystallized from acetonitrile (*CSD*: ANTAML 10) [315]. The four carbonyl oxygens bound to Li form the base of a nearly square pyramid, with the acetonitrile nitrogen at the apex. The cyclic decapeptide originates from the green death cup mushroom *(Amanita phalloides)* [316]. There are two additional molecules of CH_3CN per cyclic peptide in the crystal.

When treated with the required number of equivalents of LDA (≥ 6) in THF, CyA is deprotonated at the sarcosine unit to give a Li enolate without destruction of the peptide ring. Reactions with electrophiles give derivatives with substituents in the former sarcosine position.[281, 285, 286, 289, 314, 317] With CyA and LDA alone a precipitate or a viscous mixture, which may solidify as a gel, results at −78°C. If an amount of LDA exceeding the six equivalents required (for removal of one OH, one CH_2, and four NH protons) is added (up to 15 equivalents), a clear, yellow, readily stirred solution is obtained, quenching of which with water leads to the recovery of more than 90% CyA. Epimerizations are observed only to a very small extent, and they do indeed occur mainly at the amino acids Nos. 9, 10, and 11, those lacking the protection discussed above. Simple column chromatography readily frees CyA from the impurities thus generated. With electrophiles other than water, products of substitution of the diastereotopic *Re* hydrogen (≤ 90% *ds*) in the sarcosine unit (Sar^3)

[*] Not knowing is the essence of wisdom.

are formed in yields ranging from 10 to 50%, with a large amount of unreacted CyA being recovered. Some of the substituents that were introduced into CyA by this procedure are indicated in Scheme 20.

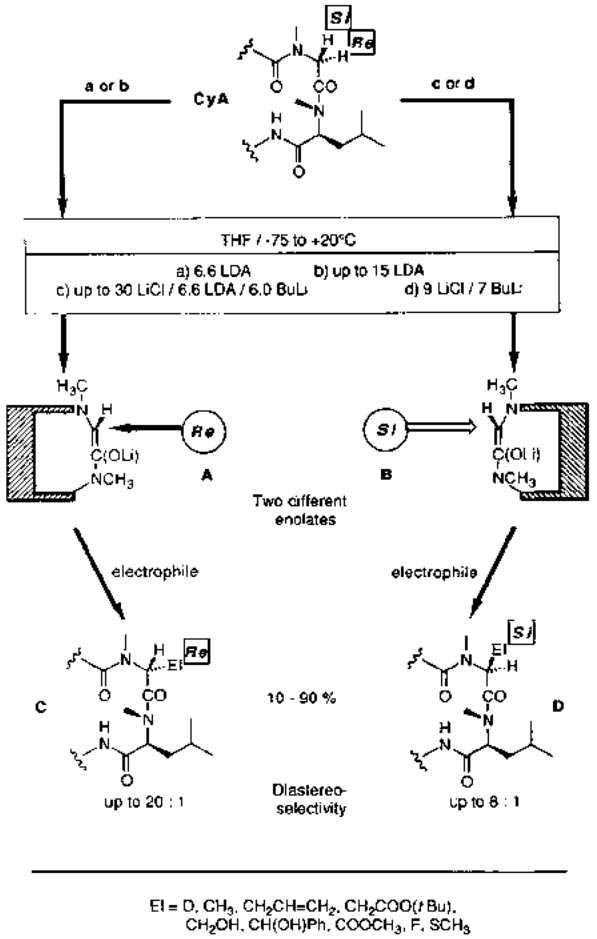

El = D, CH_3, $CH_2CH{=}CH_2$, $CH_2COO(t\,Bu)$, CH_2OH, CH(OH)Ph, $COOCH_3$, F, SCH_3

Scheme 20. Alkylation of CyA on the sarcosine unit via the Li enolate shown in Fig. 24 [317]. Depending on the conditions of deprotonation either an enolate **A** is generated that is preferentially attacked from the *Re* side, or an enolate **B** with *Si* selectivity (see the products **C** and **D**, respectively) [318]. The highest yields were recorded under "amine-free, LiCl conditions" [c and d], and the best selectivities under the "LDA conditions" [a and b]. CD_3CO_2D, MeI, alkyl bromides, aldehydes, CO_2/CH_2N_2, $FClO_3$, and disulfides were used in excess as electrophiles. The products **C** and **D** can be separated by flash chromatography and isolated in pure form.

We were overjoyed that the products derived from replacement of the diastereotopic *Si* hydrogen can also be obtained selectively; yields of over 90% may be obtained if the deprotonation of CyA by LDA is carried out in the presence of large amounts of LiCl (up to 30 equivalents), and if the diisopropylamine is removed by BuLi addition. We do not know whether the enolates generated under the two different sets of conditions are configurationally different (*E*/*Z* on C=N and/or C=C) or whether they differ only by different LiX effects exerted by LDA and LiCl. At any rate, the *Re* face of the enolate double bond must be hindered in one case, the *Si* face in the other, by the arrangement of the macrocyclic ring (see Scheme 20).

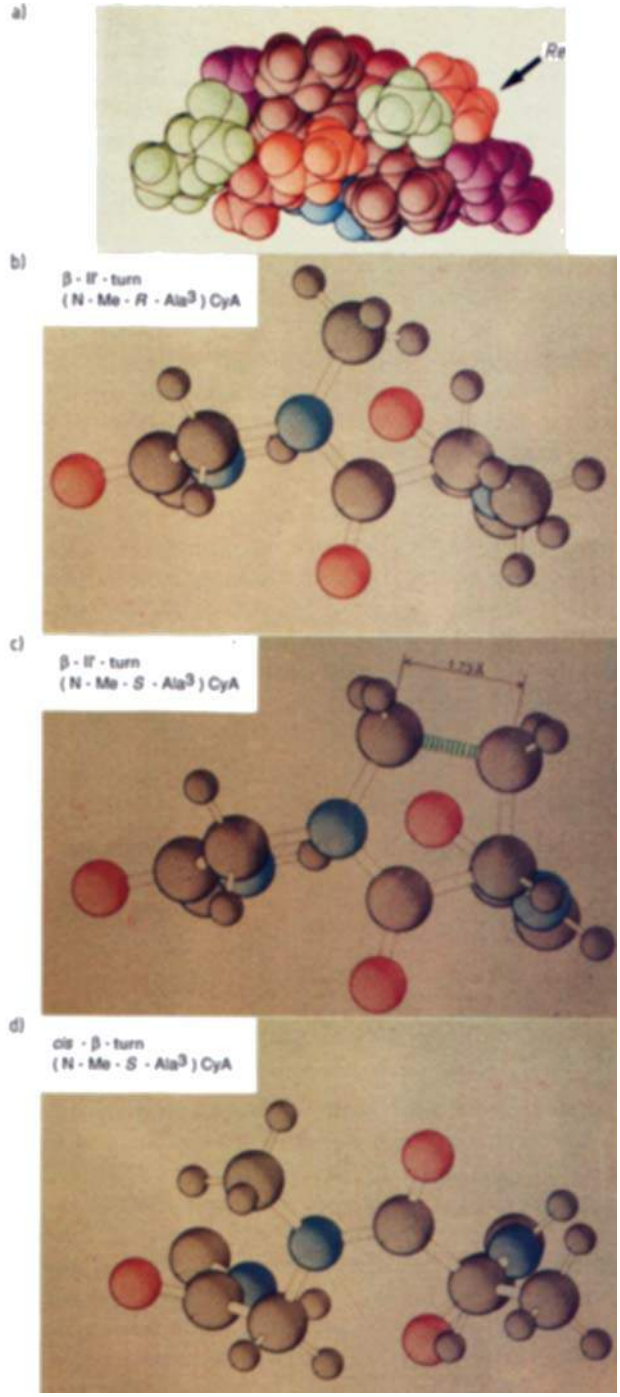

Fig. 26. Space-filling model of CyA generated with the data of the structure analysis, and ball-and-stick model of the partial structure around the β-turn at which the stereoselective alkylation through a Li enolate occurs (Fig. 24, Scheme 20). a) Overview, in which the *Re* hydrogen on sarcosine is emphasized; the *Si* hydrogen and the neighboring NCH_3 group are quasi-1,3-diaxial to each other as viewed by the reader. b) H(*Re*) substituted by CH_3, no steric hindrance [the NMR spectra of CyA and (*N*-Me-(*R*)-Ala^3)CyA are superimposable over wide regions]. c) H(*Si*) substituted by CH_3, strong penetration of van der Waals radii of the two CH_3 groups in maintaining the β-II'-turn. d) Equatorial (*Si*)-CH_3 group in a *cis* β-turn, with formation of a *cisoid* peptide bond [the NMR spectra of the (*R*) and (*S*) derivatives differ greatly].

The pure products are readily isolated by medium-pressure chromatography on SiO_2. Miraculously, CyA ($M_r = 1202$) and the two diastereomeric products of methylation [N-Me-(*R*)-Ala^3)CyA and (N-Me-(*S*)-Ala^3)CyA,

$M_r = 1216$] clearly separate on a simple analytical silica gel thin-layer plate![319] (The structural assignment of the two methyl derivatives was arrived at by comparison of the NMR spectra with those of authentic samples.[287,288])

Cleavages of the CyA peptide backbone or alkylations of amino acids other than the sarcosine occur only to a very small extent. Upon treatment of CyA with BuLi in the presence of LiCl (Scheme 20, d) appreciable amounts of a butyl ketone may be isolated, if desired, which results from attack at the carbonyl group of amino acid No. 9 (an "unprotected" site!).

The biological activity of the products thus available follows a simple rule: derivatives with substituents in the *Re* position still have immunosuppressive properties comparable to CyA, those substituted in the *Si* position do not. The reason for this is obvious from modeling as shown in Figure 26; the *Re* hydrogen of the sarcosine in CyA occupies a quasi-equatorial position, the *Si* hydrogen a quasi-axial one; introduction of a substituent into the latter position imposes such severe steric hindrance by van der Waals overlap with the NCH_3 group of the adjacent amino acid that the peptide chain must adopt a different conformation, causing the shape of the entire molecule to change.

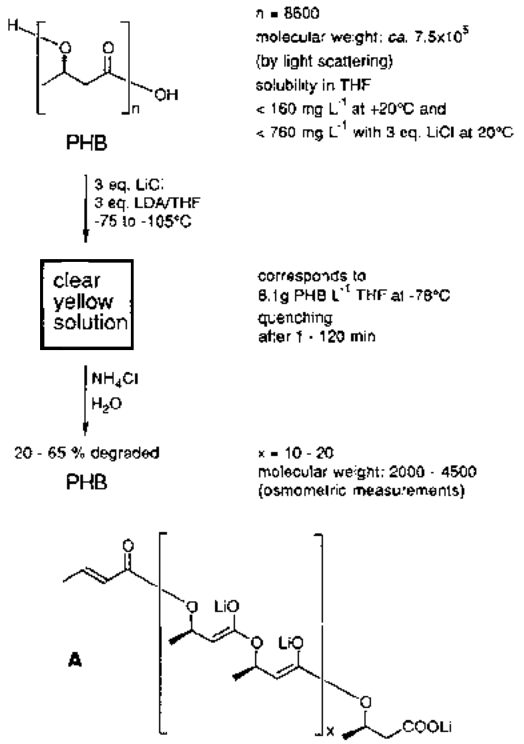

Scheme 21. Deprotonating solubilization and partial degradation of poly-[(*R*)-3-hydroxybutyrate], PHB, with LDA/LiCl in THF at low temperature. The solubilities described for PHB in THF are upper limits, which have been extrapolated from experiments in volumes of much less than 1 L. The upper limit of the solubility accessible by addition of LDA/LiCl was not investigated. The enolate could also decompose by α-elimination (72) (lithium oxybutyrate end group) instead of β-elimination (crotonate terminal group). There is no indication of a direct attack by LDA on the ester carbonyl groups of the polymer (aminolysis, resulting in formation of carboxamide end groups).

6. Outlook—on to Even More Complex Systems

An experiment is in progress
but it is uncertain
if we are in control
or just observers
Roald Hoffmann[320]

Encouraged by the solubilization of polylithiated organic compounds, such as peptides, by addition of inorganic Li salts, we also investigated other systems. We found, for instance, that when a suspension of the biopolymer PHB (polyhydroxybutyrate, $M_r = 7.5 \times 10^5$), which itself is totally insoluble both in water and THF, was treated with excess LDA in the presence of LiCl at low temperature, a clear, slightly yellow THF solution was obtained. Subsequent quenching with water leads to recovery of up to 65% of a polymer of lower molecular weight (Scheme 21).[321,322] The fact that decomposition of the polyester polyenolate does not take place all the way to the monomer (Li crotonate), but that an unexpectedly long-lived species containing ca. 30 units persists, suggests the answer must have something to do with the structure of this species—which we do not know.[323]

Our excursion into the world of Li enolate aggregate structures and the quest for proof of their involvement in product-forming steps did not only furnish important new knowledge, but led us continuously back to the laboratory. There, we have arrived at systems of a complexity with which we could not have hoped to cope at the outset; they exhibit reactivities which we observe with pleasure and with excitement, but which we again do not understand.

Lesson: Even the synthetic organic chemist must consider very complex structures, supramolecules in *Lehn*'s terminology, in his everyday work. I have nothing to add to the statement of *Lord Todd*:[324]

> Apart from consideration of the hydrogen bond, we organic chemists have really paid little attention to linkages other than the purely covalent. I believe that it will be the duty of organic chemists in the future to study the weak non-bonding interactions which are of enormous importance in the large natural macromolecules. Such studies will lead to a new blossoming of organic chemistry in the future.
>
> *Lord Alexander R. Todd*

My sincere thanks go to the co-workers who have contributed to the work described here; their names are given in the list of references. Collaboration with them was and still is a source of great pleasure for me. I thank my colleague Jack Dunitz for many enlightening discussions. The preparation of this review article would not have been possible without the help and dedication of Silvia Sigrist (typing), Albert K. Beck (list of references), Bernd Lamatsch and Thomas Maetzke (figures), Gerhard Stucky and Geo Adam (schemes and tables), Ulf Misslitz (corrections), Hans-Jörg Gründler (application of the programs WORD® and ChemDraw®), and Edward Dziadulewicz, Robert Fitzi, and Soo Y. Ko (parts of the English version).

Received: September 14, 1988 [A 702 IE]
German version: *Angew. Chem. 100* (1988) 1685

[1] Articles on this topic worth reading: A. Lapworth, *J. Chem. Soc. 79* (1901) 1265; *ibid. 121* (1922) 416 (reactivity and alternating polarity); R. Robinson in H. Grossmann (Ed.): *Sammlung chemischer und chemisch-technischer Vorträge, Neue Folge, Heft 14*, F. Enke Verlag, Stuttgart 1932; C. K. Ingold, *Chem. Rev. 15* (1934) 225–274 (electronic theory of organic reactions); C. R. Hauser, D. S. Breslow, *J. Am. Chem. Soc. 62* (1940) 2389; H. B. Watson, *Trans. Faraday Soc. 37* (1941) 707; V. Franzen, *Chem.-Ztg. 80* (1956) 446 (aldol additions and condensations), Sir Robert Robinson, *Memoirs of a Minor Prophet (70 Years of Organic Chemistry)*, Elsevier, Amsterdam 1976; D. Seebach, *Angew. Chem. 91* (1979) 259–278; *Angew. Chem. Int. Ed. Engl. 18* (1979) 239–258 (reactivity umpolung—also of carbonyl compounds).

[2] H. O. House: *Modern Synthetic Reactions, 2nd ed.*, W. A. Benjamin, Menlo Park 1972.

[3] T. Mukaiyama, *Org. React. 28* (1982) 203–331.

[4] R. Noyori, I. Nishida, J. Sakata, *J. Am. Chem. Soc. 105* (1983) 1598; I. Kuwajima, E. Nakamura, *Acc. Chem. Res. 18* (1985) 181.

[5] a) P. Fellmann, J.-E. Dubois, *Tetrahedron 34* (1978) 1349; b) C. H. Heathcock: *The Aldol Addition Reaction* in J. D. Morrison (Ed.): *Asymmetric Synthesis, Vol. 3*, Academic Press, Orlando, FL 1984, pp. 111–212.

[6] D. A. Evans: Stereoselective Alkylation Reactions of Chiral Metal Enolates in J. D. Morrison (Ed.): *Asymmetric Synthesis, Vol. 3*, Academic Press, Orlando, FL 1984, pp. 1–110.

[7] Double Asymmetric Synthesis and a New Strategy for Stereochemical Control in Organic Synthesis: S. Masamune, W. Choy, J. S. Petersen, L. R. Sita, *Angew. Chem. 97* (1985) 1–31; *Angew. Chem. Int. Ed. Engl. 24* (1985) 1–30.

[8] R. E. Ireland, R. H. Mueller, A. K. Willard, *J. Am. Chem. Soc. 98* (1976) 2868.

[9] T. Mukaiyama, K. Inomata, *Bull. Chem. Soc. Jpn. 44* (1971) 3215; T. Mukaiyama, T. Inoue, *Chem. Lett. 1976*, 559.

[10] E. Shimada, K. Inomata, T. Mukaiyama, *Chem. Lett. 1974*, 689.

[11] The effect of polar cosolvents like hexamethylphosphoric triamide (HMPT) or *N,N'*-dimethylpropyleneurea (DMPU), of chelating additives, or of crown ethers or cryptands will be discussed further below; see Schemes 3, 5, 9, Table 3, Figs. 12, 15, and Section 2.2.3.

[12] H. E. Zimmerman, M. D. Traxler, *J. Am. Chem. Soc. 79* (1957) 1920.

[13] D. Seebach, J. Goliński, *Helv. Chim. Acta 64* (1981) 1413.

[14] M. A. Brook, D. Seebach, *Can. J. Chem. 65* (1987) 836.

[15] E. Weiss, H. Alsdorf, H. Kühr, H.-F. Grützmacher, *Chem. Ber. 101* (1968) 3777.

[16] F. A. Schröder, H. P. Weber, *Acta Crystallogr. B31* (1975) 1745.

[17] D. Bright, G. H. W. Milburn, M. R. Truter, *J. Chem. Soc. A 1971*, 1582.

[18] D. E. Fenton, C. Nave, M. R. Truter, *J. Chem. Soc. Dalton Trans. 1973*, 2188.

[19] H. D. Zook, T. J. Russo, *J. Am. Chem. Soc. 82* (1960) 1258; H. D. Zook, W. L. Gumby, *ibid. 82* (1960) 1386.

[20] H. O. House, M. Gall, H. D. Olmstead, *J. Org. Chem. 36* (1971) 2361.

[21] L. M. Jackman, N. Szeverenyi, *J. Am. Chem. Soc. 99* (1977) 4954.

[22] Review article: *Structure and Reactivity of Alkali Metal Enolates*: L. M. Jackman, B. C. Lange, *Tetrahedron 33* (1977) 2737–2769.

[23] Reaction of benzoyl chloride with ethyllithium (hexamer) in benzene: R. West, W. Glaze, *J. Chem. Phys. 34* (1961) 685.

[24] Reaction of ethylene with *tert*-butyllithium (tetramer) in diethyl ether/hexane: P. D. Bartlett, C. V. Goebel, W. P. Weber, *J. Am. Chem. Soc. 91* (1969) 7425.

[25] M. Schlosser: *Struktur und Reaktivität polarer Organometalle*, Springer, Berlin 1973.

[26] A. W. Langer (Ed.): *Polyamine-Chelated Alkali Metal Compounds, Adv. Chem. Ser. 130* (1974) ACS, Washington DC (USA).

[27] B. J. Wakefield: *The Chemistry of Organolithium Compounds*, Pergamon Press, Oxford 1974.

[28] *Organolithium Compounds in Organic Synthesis.* Recent developments: D. Seebach, K.-H. Geiss: *J. Organomet. Chem. Libr. 1* (1976) 1–92.

[29] J. C. Stowell: *Carbanions in Organic Synthesis*, Wiley, New York 1979.

[30] B. J. Wakefield in D. H. R. Barton, W. D. Ollis (Eds.): *Comprehensive Organic Chemistry, Vol. 3*, Pergamon Press, Oxford 1979, Part 15, pp. 943–1012.

[31] M. E. O'Neill, K. Wade, J. L. Wardell, N. A. Bell, W. E. Lindsell in G. Wilkinson, F. G. A. Stone, E. W. Abel (Eds.): *Comprehensive Organometallic Chemistry, Vol. 1*, Pergamon Press, Oxford 1982, pp. 1–252; B. J. Wakefield, *ibid. Vol. 7*, pp. 1–110.

[32] R. B. Bates, C. A. Ogle: *Carbanion Chemistry*, Springer, Berlin 1983.

[33] R. O. Bach (Ed.): *Lithium-Current Applications in Science, Medicine and Technology*, Wiley, New York 1985.

[34] Symposium on Advances in Carbanion Chemistry, Division of Petroleum Chemistry, ACS Meeting, Chicago (September 1985): *Prepr. Div. Pet. Chem. Am. Chem. Soc. 30* (1985) No. 4.

[35] L. Brandsma, H. Verkruijsse: *Preparative Polar Organometallic Chemistry 1*, Springer, Berlin 1987.

[36] C. Elschenbroich, A. Salzer: *Organometallchemie*, Teubner, Stuttgart 1986.

[37] Heteroatom-Facilitated Lithiations: H. W. Gschwend, H. R. Rodriguez, *Org. React. 26* (1979) 1–360.

[38] Lithium Halocarbenoids—Carbanions of High Synthetic Versatility: H. Siegel, *Top. Curr. Chem. 106* (1982) 55–78.

[39] Stereo- and Regiocontrol by Complex Induced Proximity Effects: Reactions of Organolithium Compounds: P. Beak, A. I. Meyers, *Acc. Chem. Res. 19* (1986) 356–363.

[40] Oxygen- and Nitrogen-assisted Lithiation and Carbolithiation of Non-aromatic Compounds: Properties of Non-aromatic Organolithium Compounds Capable of Intramolecular Coordination to Oxygen and Nitrogen: G. W. Klumpp, *Recl. Trav. Chim. Pays-Bas 105* (1986) 1–21.

[41] Some review articles on polylithiated compounds: a) T. M. Harris, C. M. Harris, *Org. React. 17* (1969) 155–211; b) E. M. Kaiser, J. D. Petty, P. L. A. Knutson, *Synthesis 1977*, 509–550; c) D. Seebach, E.W. Colvin, F. Lehr, T. Weller, *Chimia 33* (1979) 1–18; d) D. Seebach, M. Pohmakotr, *Tetrahedron 37* (1981) 4047–4058; e) P. von R. Schleyer, *Pure Appl. Chem. 56* (1984) 151–162; f) B. Bogdanović, *Angew. Chem. 97* (1985) 253–264; *Angew. Chem. Int. Ed. Engl. 24* (1985) 262–273; g) A. Maercker, M. Theis, *Top. Curr. Chem. 138* (1987) 1–61; h) K. Müllen, *Angew. Chem. 99* (1987) 192–205; *Angew. Chem. Int. Ed. Engl. 26* (1987) 204–217; i) D. Seebach, H. Estermann, *Helv. Chim. Acta 71* (1988), in press.

[42] a) Low-Temperature ^{13}C NMR Spectroscopy of Organolithium Derivatives.—$^{13}C,^{6}Li$-Coupling, a Powerful Structural Information: D. Seebach, R. Hässig, J. Gabriel, *Helv. Chim. Acta 66* (1983) 308–337; b) Low Temperature ^{13}C-NMR Spectra of ^{6}Li- and ^{13}C-Labelled Sulfur- and Selenium-Substituted Organolithium Derivatives: D. Seebach, J. Gabriel, R. Hässig, *ibid. 67* (1984) 1083–1099; c) J. Heinzer, J. F. M. Oth, D. Seebach, *ibid. 68* (1985) 1848–1862.

[43] The Structure and Dynamic Behaviour of Organolithium Compounds in Solution, ^{13}C, ^{6}Li, and ^{7}Li-NMR: G. Fraenkel, H. Hsu, B. M. Su, see [33], Chapter 19, pp. 273–290.

[44] High-Resolution Metal-NMR Spectroscopy of Organometallic Compounds: R. Benn, H. Rufińska, *Angew. Chem. 98* (1986) 851–871; *Angew. Chem. Int. Ed. Engl. 25* (1986) 861–881.

[45] Aggregation States and Exchange Properties of Alkyllithium Compounds in Hydrocarbon Solvent from ^{13}C–^{6}Li Coupling: R. D. Thomas, R. M. Jensen, T. C. Young, *Organometallics 6* (1987) 565.

[46] Modern NMR Spectroscopy of Organolithium Compounds: H. Günther, D. Moskau, P. Bast, D. Schmalz, *Angew. Chem. 99* (1987) 1242–1250; *Angew. Chem. Int. Ed. Engl. 26* (1987) 1212–1220.

[47] X-Ray Structural Analyses of Organolithium Compounds: W. N. Setzer, P. von R. Schleyer, *Adv. Organomet. Chem. 24* (1985) 353–451.

[48] Sodium, Potassium, Rubidium and Cesium—X-Ray Structural Analysis of Their Organoalkali Compounds: C. Schade, P. von R. Schleyer, *Adv. Organomet. Chem. 27* (1987) 169–278.

[49] High-Resolution X-ray Crystallography—an Experimental Method for the Description of Chemical Bonds: K. Angermund, K. H. Claus, R. Goddard, C. Krüger, *Angew. Chem. 97* (1985) 241–252; *Angew. Chem. Int. Ed. Engl. 24* (1985) 237–247.

[50] Unsaturated Molecules Containing Main Group Metals: M. Veith, *Angew. Chem. 99* (1987) 1–14; *Angew. Chem Int. Ed. Engl. 26* (1987) 1–14.

[51] Low-Temperature X-ray Structure Techniques for the Characterization of Thermolabile Molecules: M. Veith, W. Frank, *Chem. Rev. 88* (1988) 81–92

[52] Free Inorganic, Organic, and Organometallic Ions by Treatment of Their Lithium Salts with 12-Crown-4: P. P. Power, *Acc. Chem. Res. 21* (1988) 147–153.

[53] A preliminary report on our work, which received only little attention, appeared in a conference volume; Crystal Structures and Stereoselective Reactions of Organic Lithium Derivatives: D. Seebach, *Proc. Robert A. Welch Found. Conf. Chem. Res. 27: Stereospecificity in Chemistry and Biochemistry* (November 7–9, 1983), Houston, TX 1984, pp. 93–145.

[54] Review article: B. Weidmann, D. Seebach, *Angew. Chem. 95* (1983) 12–26; *Angew. Chem Int. Ed. Engl. 22* (1983) 31–45.

[55] D. Seebach, B. Weidmann, L. Widler in R. Scheffold (Ed.). *Modern Synthetic Methods, Vol. 3*, Salle + Sauerländer, Aarau/Wiley, New York 1983, pp. 217–353.

[56] D. Seebach, R. Imwinkelried, T. Weber in R. Scheffold (Ed.): *Modern Synthetic Methods, Vol. 4*, Springer, Berlin 1986, pp. 125–259.

[57] D. Seebach, S. Roggo, J. Zimmermann in W. Bartmann, K. B. Sharpless (Eds.): *Stereochemistry of Organic and Bioorganic Transformations, Workshop Conferences Hoechst, Vol. 17*, VCH Verlagsgesellschaft, Weinheim 1987, pp. 85–126.

[58] Review article, Nobel lecture: J.-M. Lehn, *Angew. Chem. 100* (1988) 91–116; *Angew. Chem. Int. Ed. Engl. 27* (1988) 89–112.

[59] G. Wittig, H. Reiff, *Angew. Chem. 80* (1968) 8; *Angew. Chem Int. Ed. Engl. 7* (1968) 7; G. Wittig, A. Hesse, *Org. Synth. 50* (1970) 66.

[60] R. A. Olofson, C. M. Dougherty, *J. Am. Chem. Soc. 95* (1973) 581, 582.

[61] M. W. Rathke, *J. Am. Chem. Soc. 92* (1970) 3222.

[62] H. Normant, *Angew. Chem. 79* (1967) 1029–1050; *Angew. Chem. Int. Ed. Engl. 6* (1967) 1046–1067.

[63] Replacement of the mutagenic phosphoric amide HMPT by DMPU and other cosolvents (see also Scheme 3): T. Mukhopadhyay, D. Seebach, *Helv. Chim Acta 65* (1982) 385; D. Seebach, *Chem. Br. 21* (1985) 632.

[64] Z. A. Fataftah, I. E. Kopka, M. W. Rathke, *J. Am. Chem. Soc. 102* (1980) 3959.

[65] E. J. Corey, A. W. Gross, *Tetrahedron Lett. 25* (1984) 495.

[66] T. Laube, J. D. Dunitz, D. Seebach, *Helv. Chim. Acta 68* (1985) 1373.

[67] Special precautions have to be taken in synthesizing 1,3-dicarbonyl compounds via lithium enolates to avoid double addition. a) A well-known method especially applied to synthesizing methyl ketones is the use of Li carboxylates as acylating agents. Review article: M. J. Jorgenson, *Org. React 18* (1970) 1–97. b) The acylation succeeds directly with acid chlorides by (inverse) addition of Li enolates at very low temperatures, even with 3-nitropropanoyl and 4-nitrobutanoyl chloride: D. Seebach, T. Weller, G. Protschuk, A. K. Beck, M. S. Hoekstra, *Helv. Chim. Acta 64* (1981) 716. c) Review article on "Synthese bei Temperaturen unter −80°C": D. Seebach, A. Hidber, *Chimia 37* (1983) 449–462. d) A trick that avoids complications is the reaction of the enolate with acyl cyanides, which at first results in cyanohydrin derivatives: S. Hünig, R. Schaller, *Angew. Chem. 94* (1982) 1–15; *Angew. Chem. Int. Ed. Engl. 21* (1982) 36–49 (review). L. N. Mander, S. P. Sethi, *Tetrahedron Lett. 24* (1983) 5425.

[68] R. Amstutz, W. B. Schweizer, D. Seebach, J. D. Dunitz, *Helv. Chim. Acta 64* (1981) 2617.

[69] D. Seebach, R. Amstutz, J. D. Dunitz, *Helv. Chim. Acta 64* (1981) 2622.

[70] P. G. Williard, G. B. Carpenter, *J. Am. Chem. Soc. 107* (1985) 3345.

[71] P. G. Williard, G. B. Carpenter, *J. Am. Chem. Soc. 108* (1986) 462.

[72] a) R. Häner, T. Laube, D. Seebach, *J. Am. Chem. Soc. 107* (1985) 5396; b) H. R. Seikaly, T. T. Tidwell, *Tetrahedron 42* (1986) 2587–2613 (review); c) C. Fehr, J. Galindo, *J. Org. Chem. 53* (1988) 1828.

[73] D. Seebach, R. Amstutz, T. Laube, W. B. Schweizer, J. D. Dunitz, *J. Am. Chem. Soc. 107* (1985) 5403. The structures of the *tert*-butyl 2-methylpropionate lithium enolate (dimer with TMEDA; *CSD*: DEDXIT) and of the tetrameric methyl 3,3-dimethylbutyrate lithium (*Z*)-enolate solvated by four THF molecules (*CSD*: DEDXOZ) are described in the same paper. It is striking that in all dimeric ester and amide enolates with THF and TMEDA as ligands to Li, the two enolate units are on the same side of the OLiOLi quadrangle, as if it were a bisected cube in which the enolates are necessarily *cis* to each other

[74] a) L. Ghosez, J. Marchand-Brynaert in H. Böhme, H. G. Viehe (Eds.): *Iminium Salts in Organic Chemistry, Part 1*, Wiley, New York 1976, pp. 421–532, especially pp. 465–467; b) K. L. Brown, L. Damm, J. D. Dunitz, A. Eschenmoser, R. Hobi, C. Kratky, *Helv. Chim. Acta 61* (1978) 3108; c) A. Kümin, E. Maverick, P. Seiler, N. Vanier, L. Damm, R. Hobi, J. D. Dunitz, A. Eschenmoser, *ibid. 63* (1980) 1158; d) S. J. Blarer, W. B. Schweizer, D. Seebach, *ibid. 65* (1982) 1637; e) Latest comprehensive review on the structure of enamines: A. G. Cook (Ed.): *Enamines*, 2nd ed., Marcel Dekker, New York 1988, Chapter 1, pp. 1–101.

[75] Hydrogen Bond Geometry in Organic Crystals: R. Taylor, O. Kennard, *Acc. Chem. Res. 17* (1984) 320–326.

[76] W. Saenger: *Principles of Nucleic Acid Structure*, Springer, Berlin 1984.

[77] W. Bauer, T. Laube, D. Seebach, *Chem. Ber. 118* (1985) 764.

[78] P. G. Williard, J. M. Salvino, *Tetrahedron Lett. 26* (1985) 3931.

[79] R. Amstutz, J. D. Dunitz, T. Laube, W. B. Schweizer, D. Seebach, *Chem. Ber. 119* (1986) 434.

[80] J. J. Brooks, G. D. Stucky, *J. Am. Chem. Soc. 94* (1972) 7333.

[81] P. G. Williard, *J. Am. Chem. Soc. 110* (1988), in press. I thank Professor *Williard* for sending us the manuscript and the coordinates prior to publication of the structure of $[(LDA)_2(THF)_2]$.

[82] T. Fjeldberg, P. B. Hitchcock, M. F. Lappert, A. J. Thorne, *J. Chem. Soc. Chem. Commun. 1984*, 822.

[83] R. Hacker, E. Kaufmann, P. von R. Schleyer, W. Mahdi, H. Dietrich, *Chem. Ber. 120* (1987) 1533.

[84] D. Barr, W. Clegg, R. E. Mulvey, R. Snaith, D. S. Wright, *J. Chem. Soc. Chem. Commun. 1987*, 716.

[85] P. G. Williard, M. J. Hintze, *J. Am. Chem. Soc. 109* (1987) 5539. I thank Professor *Williard* for transmitting the coordinates of this structure prior to their entry in the Cambridge Structural Data Base.

[86] D. Barr, W. Clegg, R. E. Mulvey, R. Snaith, *J. Chem. Soc. Chem. Commun. 1984*, 79.

[87] Isolation of a lithiated allyl thioether, unstable above −30°C: D. Seebach, T. Maetzke, R. K. Haynes, M. N. Paddon-Row, S. S. Wong, *Helv. Chim. Acta 71* (1988) 299.

[88] T. Laube, *Angew. Chem. 98* (1986) 368; *Angew. Chem. Int. Ed. Engl. 25* (1986) 349.

[89] T. Laube, *Angew. Chem. 99* (1987) 580; *Angew. Chem. Int. Ed. Engl. 26* (1987) 560.

[90] Examples of crystal structure analyses of Li-phenolate aggregates can be found in the following two papers: a) B. Cetinkaya, I. Gümrükcü, M. F. Lappert, J. L. Atwood, R. Shakir, *J. Am. Chem. Soc. 102* (1980) 2086; b) J. C. Huffman, R. L. Geerts, K. G. Caulton, *J. Crystallogr. Spectrosc. Res. 14* (1984) 541.

[91] R. Amstutz: *Struktur und Reaktivität von Lithiumorganischen Verbindungen, Dissertation Nr. 7210*, ETH Zürich 1982.

[92] T. Laube: *Beiträge zu Struktur und Reaktivität von Ester- und Amid-Lithiumenolaten, Dissertation Nr. 7649*, ETH Zürich 1984.

[93] J. Hansen: *Beiträge zu Struktur und Reaktivität aggregierter Lithiumorganischer Verbindungen, Dissertation Nr. 7863*, ETH Zürich 1985.

[94] W. Bauer, D. Seebach, *Helv. Chim. Acta 67* (1984) 1972.

[95] R. B. Bates, L. M. Kroposki, D. E. Potter, *J. Org. Chem. 37* (1972) 560.

[96] G. Boche, M. Marsch, K. Harms, *Angew. Chem. 98* (1986) 373; *Angew. Chem. Int. Ed. Engl. 25* (1986) 373.

[97] D. Enders, G. Bachstädter, K. A. M. Kremer, M. Marsch, K. Harms, G. Boche, *Angew. Chem. 100* (1988) 1580; *Angew. Chem. Int. Ed. Engl. 27* (1988) 1522.

[98] Review articles on the structures of lithiated nitriles, nitroalkanes, sulfides, sulfoxides, and sulfones (with emphasis on the work of *G. Boche* and *H.-J. Gais*): G. Boche, *Angew. Chem. 101* (1989) and *Angew. Chem. Int. Ed. Engl. 28* (1989), in press.

[99] U. Schöllkopf, *Top. Curr. Chem. 109* (1983) 65–84.

[100] Tetrahedron Symposia-in-Print Number *33* on the methods to synthesize α-amino acids with CC bond formation at the stereogenic center: *Tetrahedron 44* (1988) 5253–5614.

[101] a) X-ray structure analysis: R. A. Wanat, D. B. Collum, G. Van Duyne, J. Clardy, R. T. De Pue, *J. Am. Chem Soc. 108* (1986) 3415; b) ^{6}Li, ^{13}C, ^{15}N NMR investigation of the same compound: N. Kallman, D. B. Collum, *ibid. 109* (1987) 7466.

[102] a) X-ray structure analysis: D. B. Collum, D. Kahne, S. A. Gut, R. T. De Pue, F. Mohamadi, R. A. Wanat, J. Clardy, G. Van Duyne, *J. Am. Chem. Soc. 106* (1984) 4865; b) ^{6}Li,^{23}Na NMR of the alkali-metal derivatives: A. S. Galiano-Roth, D. B. Collum, *ibid. 110* (1988) 3546; c) Kinetic measurements: R. A. Wanat, D. B. Collum, *ibid. 107* (1985) 2078.

[103] D. Barr, W. Clegg, R. E. Mulvey, R. Snaith, *J. Chem. Soc. Chem. Commun. 1984*, 226.

[104] D. Barr, W. Clegg, R. E. Mulvey, R. Snaith, *J. Chem. Soc. Chem. Commun. 1984*, 285.

[105] D. Barr, W. Clegg, R. E. Mulvey, R. Snaith, K. Wade, *J. Chem. Soc. Chem. Commun. 1986*, 295.

[106] G. Klebe, K. H. Böhn, M. Marsch, G. Boche, *Angew. Chem. 99* (1987) 62; *Angew. Chem. Int. Ed. Engl. 26* (1987) 78.

[107] D. Seebach, W. Bauer, J. Hansen, T. Laube, W. B. Schweizer, J. D. Dunitz, *J. Chem. Soc. Chem. Commun. 1984*, 853.

[108] K. Jens, J. Kopf, N. P. Lorenzen, E. Weiss, *Chem. Ber. 121* (1988) 1201.

[109] P. G. Williard, J. M. Salvino, *J. Chem. Soc. Chem. Commun. 1986*, 153.

[110] a) D. Seebach, M. Ertas, R. Locher, W. B. Schweizer, *Helv. Chim. Acta 68* (1985) 264; b) M. Ertas, D. Seebach, *ibid. 68* (1985) 961.

[111] J. H. Wengrovius, M. F. Garbauskas, E. A. Williams, R. C. Going, P. E. Donahue, J. F. Smith, *J. Am. Chem. Soc. 108* (1986) 982; M. F. Garbauskas, J. H. Wengrovius, R. C. Going, J. S. Kasper, *Acta Crystallogr. Sect. C 40* (1984) 1536.

[112] J. Dekker, J. Boersma, G. J. M. van der Kerk, *J. Chem. Soc. Chem. Commun. 1983*, 553; J. Dekker, P. H. M. Budzelaar, J. Boersma, G. J. M. van der Kerk, A. L. Spek, *Organometallics 3* (1984) 1403.

[113] R. Häner, T. Maetzke, D. Seebach, *Helv. Chim. Acta 69* (1986) 1655.

[114] R. Häner, B. Olano, D. Seebach, *Helv. Chim. Acta 70* (1987) 1676.

[115] Some structures, in part also important in biology, with (metal)$_2$X$_2$ four-membered ring units of Si, Sn, and transition metals are: the step-like arrangement in **A** and the distorted cube in the solvent-free **B**, the distorted cube in **C** (only those C atoms of the butyl and cyclohexyl groups which are coordinated to the metal are drawn), the dimer of a dimethyl titanate in **D**, the dimer of the general formula **E**, a model for the (FeS)$_2$ units in the oxo-transferases with iron (**F**) or molybdenum (**G**) in the active site. **A**, **B**: M. Veith, F. Goffing, V. Huch, *Chem. Ber. 121* (1988) 943, see also [50]; **C**: K. C. K. Swamy, R. O. Day, R. R. Holmes, *J. Am. Chem. Soc. 109* (1987) 5546 (We thank Professor *R. O. Day* (University of Massachusetts, Amherst, MA) for transmitting the coordinates of structure **C** to us prior to publication); **D** (*CSD*: MPTIDM): A. Yoshino, Y. Shuto, Y. Iitaka, *Acta Crystallogr. Ser. B 26* (1970) 744; **E** (*CSD*: XLDTSF), **F**: R. H. Holm, *Acc. Chem. Res. 10* (1977) 427–434; **G** (*CSD*: CESXIH): T. Shibahara, H. Kuroya, K. Matsumoto, S. Ooi, *J. Am. Chem. Soc. 106* (1984) 789. Further examples see [50] and the review article "*Clusters of Valence Electron Poor Metals—Structure, Bonding, and Properties*": A. Simon, *Angew. Chem. 100* (1988) 163–188; *Angew. Chem. Int. Ed. Engl. 27* (1988) 159–183.

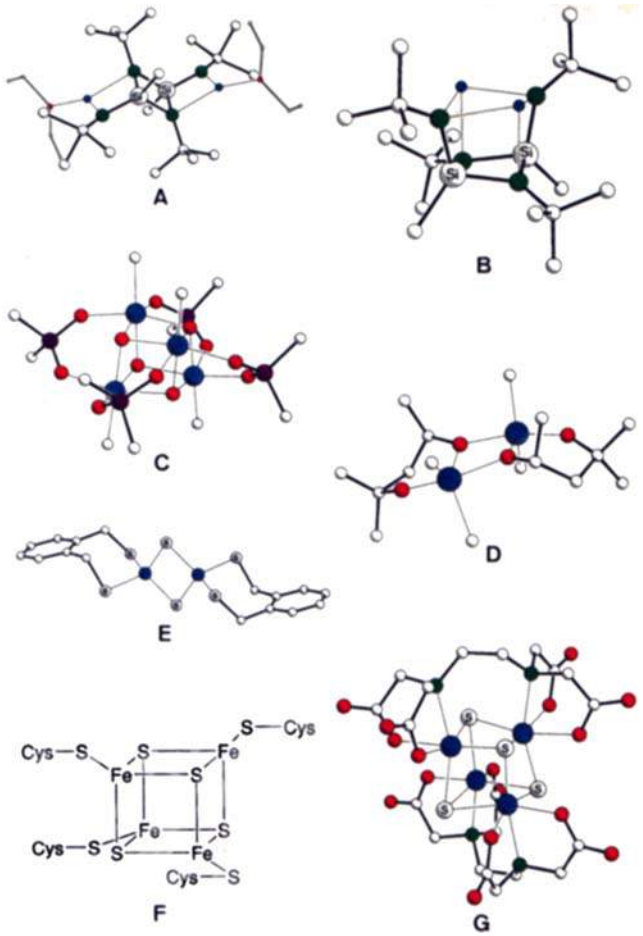

$[(t\mathrm{BuN})_2(\mathrm{CH_3Si})\mathrm{Li}]_2 \cdot 2\mathrm{OEt_2}$ **A**
$[(t\mathrm{BuN})_2(\mathrm{CH_3Si})\mathrm{Li}]_2$ **B**
$[\mathrm{BuSn(O)O_2P(C_6H_{11})_2}]_6$ **C**
$[\mathrm{Me_2TiOC(Me_2)CH_2CH(Me)O}]_2$ **D**
$[(\mathrm{R,S})_2\mathrm{FeS}]_2$ **E**
For **F**, **G**, see text

[116] *It might be appropriate at this point to mention that, in the discussion of structures, we draw formulae and use a language not according to the usual conventions in organic chemistry but rather according to those in crystallography. A line between two atoms thereby does not correspond to an electron pair but indicates that their distance is smaller than the sum of the van der Waals' radii. Here, we do not observe the octet rule; otherwise we would have to add a ⊖ charge to all the oxygens of the THF molecules bound to Li. We also speak of an X atom not of a $Li^{\oplus}$ cation or an $RO^{\ominus}$ anion! (See also the remarks in the caption of Fig. 1.)*

[117] H.-B. Bürgi, *Angew. Chem. 87* (1975) 461 496; *Angew. Chem. Int. Ed. Engl. 14* (1975) 460-473.

[118] J. D. Dunitz: *X-Ray Analysis and the Structure of Organic Molecules*, Cornell University Press, Ithaca 1979, Chapter 7, pp. 301-390.

[119] H.-B. Bürgi, J. D. Dunitz, *Acc. Chem. Res. 16* (1983) 153-161.

[120] P. G. Jones, A. J. Kirby, *J. Am. Chem. Soc. 106* (1984) 6207.

[121] H.-B. Bürgi, J. D. Dunitz, *J. Am. Chem. Soc. 109* (1987) 2924; H.-B. Bürgi, K. C. Dubler-Steudle, *ibid. 110* (1988), in press.

[122] H.-B. Bürgi, K. C. Dubler-Steudle, *J. Am. Chem. Soc. 110* (1988) 4953; H.-B. Bürgi, J. D. Dunitz, *Acta Crystallogr. Ser. B 44* (1988) 445.

[123] See also the discussion about protonation/deprotonation in our paper about TriMEDA-Li enolate complexes [66].

[124] Application of the structure-reactivity correlation to reactions of α,β-unsaturated carbonyl compounds (D. Seebach, J. Zimmermann, U. Gysel, R. Ziegler, T.-K. Ha, *J. Am. Chem. Soc. 110* (1988) 4763) and to the addition to carbonyl groups (T. Laube, H. U. Stilz, *ibid. 109* (1987) 5876).

[125] J. L. Wardell in G. Wilkinson, F. G. A. Stone, E. W. Abel (Eds.): *Comprehensive Organometallic Chemistry, Vol. 1*, Pergamon Press, Oxford 1982, Chapter 2, pp. 43-120.

[126] As to doubly lithiated carboxylic acids $R_2C{=}C(OLi)_2$ in THF, degrees of aggregation of 65-250 have been measured ("colloidal" solutions): P. E. Pfeffer, L. S. Silbert, *J. Org. Chem. 36* (1971) 3290.

[127] L. M. Jackman, C. W. DeBrosse, *J. Am. Chem. Soc. 105* (1983) 4177.

[128] a) Two-Dimensional NMR Spectroscopy: A Powerful Tool for the Investigation of Molecular Structure and Dynamics: R. R. Ernst, *Chimia 41* (1987) 323-340; b) K. Wüthrich: *NMR of Proteins and Nucleic Acids*, Wiley-Interscience, New York 1986.

[129] W. R. Croasmun, R. M. K. Carlson (Eds.): *Two Dimensional NMR Spectroscopy*, VCH Verlagsgesellschaft, Weinheim 1987.

[130] a) Conformation and Biological Activity of Cyclic Peptides: H. Kessler, *Angew. Chem. 94* (1982) 509-520; *Angew. Chem. Int. Ed. Engl. 21 (1982) 512-523; b) Two-Dimensional NMR Spectroscopy: Background and Overview of the Experiments: H. Kessler, M. Gehrke, C. Griesinger, Angew. Chem. 100* (1988) 507-554; *Angew. Chem. Int. Ed. Engl. 27* (1988) 490-536.

[131] 3D NMR techniques: C. Griesinger, O. W. Sørensen, R. R. Ernst, *J. Magn. Reson. 73* (1987) 474; *J. Am. Chem. Soc. 109* (1987) 7227; H. Oschkinat, C. Griesinger, P. J. Kraulis, O. W. Sørensen, R. R. Ernst, A. M. Gronenborn, G. M. Clore, *Nature (London) 332* (1988) 374.

[132] See the general reviews mentioned above [34, 42-46] and special papers [101b, 102b] as well as: a) W. Bauer, G. Müller, R. Pi, P. von R. Schleyer, *Angew. Chem. 98* (1986) 1130; *Angew. Chem. Int. Ed. Engl. 25* (1986) 1103 (^{6}Li,^{1}H-2D HOESY); b) A. S. Galiano-Roth, E. M. Michaelides, D. B. Collum, *J. Am. Chem. Soc. 110* (1988) 2658 (^{6}Li,^{13}C,^{15}N NMR of lithium cyclohexylisopropylamide); c) J. S. DePue, D. B. Collum, *ibid. 110* (1988) 5524. d) J. S. DePue, D. B. Collum, *ibid. 110* (1988) 5518.

[133] a) As the following details of the ^{13}C NMR spectra (A^1 and A^2) show, the content of dimeric aggregate increases by cooling a solution of butyllithium (THF), and dynamic processes that "smear out" the ^{6}Li, ^{13}C coupling at −70°C are frozen out at −90°C, so that the coupling of two ^{6}Li ($I = 1$) with the neighboring ^{13}C atom can be recognized from the quintet splitting [42a, c]. b) Mixed aggregates $(R^1\mathrm{Li}\cdot n\,R^2\mathrm{Li})_m$ are formed by addition of Bu^6Li to a solution of ^{6}Li,^{13}C-labeled lithium phenylacetylide: the pure acetylide dimer (B^1) first equilibrates with the mixed dimer (B^2) and, after addition of 6 equiv. of BuLi, only the mixed tetramer (B^3) is present: R. Hässig, D. Seebach, *Helv. Chim. Acta 66* (1983) 2269.

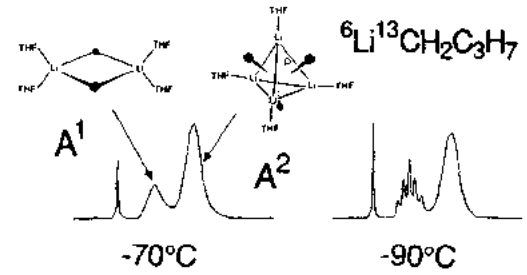

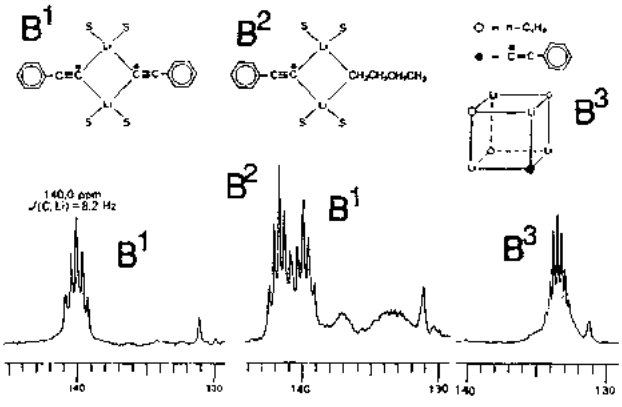

[134] L. M. Jackman, L. M. Scarmoutzos, *J. Am. Chem. Soc. 109* (1987) 5348.

[135] L. M. Jackman, L. M. Scarmoutzos, W. Porter, *J. Am. Chem. Soc. 109* (1987) 6524.

[136] L. M. Jackman, R. C. Haddon, *J. Am. Chem. Soc. 95* (1973) 3687.

[137] L. M. Jackman, B. C. Lange, *J. Am. Chem. Soc. 103* (1981) 4494.

[138] L. M. Jackman, T. S. Dunne, *J. Am. Chem. Soc. 107* (1985) 2805.

[139] L. M. Jackman, L. M. Scarmoutzos, C. W. De Brosse, *J. Am. Chem. Soc. 109* (1987) 5355.

[140] L. M. Jackman, B. D. Smith, *J. Am. Chem. Soc. 110* (1988) 3829.

[141] R. R. Hunma, R. Cloux, A. Haider, University of Lausanne, unpublished work. I thank the aforementioned colleagues as well as Professor *H. Dahn* for sharing his results prior to publication.
[142] J. Q. Wen, J. B. Grutzner, *J. Org. Chem. 51* (1986) 4220.
[143] This footnote must be sufficient for the remark that the N-analogues of the Li enolates also form aggregates, mixed aggregates, and all the complex arrangements in solution, as has been shown especially by *Collum* and his group [101, 102, 132]. Higher alkali metals can also be present within complex structures in solution (see also the discussion about ate complexes in Section 2.2.3). In the pK_a determination of cesium ion pair acidities in THF (Streitwieser scale) aggregation effects also occur: M. J. Kaufman, A. Streitwieser, Jr., *J. Am. Chem. Soc. 109* (1987) 6092.
[144] a) G. Wittig, F. J. Meyer, G. Lange, *Justus Liebigs Ann. Chem. 571* (1951) 167; G. Wittig, R. Ludwig, R. Polster, *Chem. Ber. 88* (1955) 294; b) Reviews: G. Wittig, *Angew. Chem. 70* (1958) 65–71; *Q. Rev. Chem. Soc. 20* (1966) 191–210; W. Tochtermann, *Angew. Chem. 78* (1966) 355–375; *Angew. Chem. Int. Ed. Engl. 5* (1966) 351–371.
[145] H. Hope, P. P. Power, *J. Am. Chem. Soc. 105* (1983) 5320.
[146] H. Schmidbaur, A. Schier, U. Schubert, *Chem. Ber. 116* (1983) 1938 (X-ray structure of $[Li_2(cyclopropyl)Br\cdot(OEt_2)_2]_2$, a tetrameric aggregate of 2 LiBr and 2 cyclopropyllithium).
[147] D. Thoennes, E. Weiss, *Chem. Ber. 111* (1978) 3157.
[148] U. Schümann, J. Kopf, E. Weiss, *Angew. Chem. 97* (1985) 222; *Angew. Chem. Int. Ed. Engl. 24* (1985) 215.
[149] L. M. Jackman, L. M. Scarmoutzos, *J. Am. Chem. Soc. 106* (1984) 4627.
[150] M. Szwarc (Ed.): *Ions and Ion Pairs in Organic Reactions, Vol. 1 and 2*, Wiley, New York 1972 and 1974, respectively.
[151] C. Cambillau, M. Ourevitch, *J. Chem. Soc. Chem. Commun. 1981*, 996.
[152] C. Eaborn, P. B. Hitchcock, J. D. Smith, A. C. Sullivan, *J. Chem. Soc. Chem. Commun. 1983*, 827.
[153] U. Schümann, E. Weiss, *Angew. Chem. 100* (1988) 573; *Angew. Chem. Int. Ed Engl. 27* (1988) 584.
[154] A. A. Morton, C. E. Claff, Jr., F. W. Collins, *J. Org. Chem. 20* (1955) 428.
[155] Reviews on "complex bases": P. Caubère, *Acc. Chem. Res. 7* (1974) 301–308; *Top. Curr. Chem. 73* (1978) 49–124; *Angew. Chem. 95* (1983) 597–611; *Angew. Chem. Int. Ed. Engl. 22* (1983) 599–613; *Pure Appl. Chem. 57* (1985) 1875–1882. Two recent papers about interesting applications of complex mixtures of NaH/NaOR/MX_n (with or without Me_3SiCl): A. Feghouli, Y. Fort, R. Vanderesse, P. Caubère, *Tetrahedron Lett. 29* (1988) 1379, 1383.
[156] L. Lochmann, J. Pospíšil, J. Vodňanský, J. Trekoval, D. Lim, *Collect. Czech. Chem. Commun. 30* (1965) 2187; L. Lochmann, J. Pošpišil, D. Lim, *Tetrahedron Lett. 1966*, 257.
[157] M. Schlosser, *J. Organomet. Chem. 8* (1967) 9; M. Schlosser, J. Hartmann, M. Stähle, J. Kramar, A. Walde, A. Mordini, *Chimia 40* (1986) 306.
[158] More and more structural information about the cuprates (copper ate complexes, Gilman reagents) has been made available in recent times. Reference to the X-ray structures by *Hope* and *Power* as well as by *van Koten* and NMR investigations by *Lipshutz* and *Bertz* are compiled in a recently published communication: S. H. Bertz, G. Dabbagh, *J. Am. Chem. Soc. 110* (1988) 3668.—Enantioselective cuprates: E. J. Corey, R. Naef, F. J. Hannon, *ibid. 108* (1986) 7114; R. K. Dieter, M. Tokles, *ibid. 109* (1987) 2040; K. Yamamoto, M. Kanoh, N. Yamamoto, J. Tsuji, *Tetrahedron Lett. 28* (1987) 6347.—A comprehensive review about structures of organocopper reagents is also found in: *Gmelin, Handbook of Inorganic Chemistry*, 8th edition, Part 1–4, Springer, Berlin 1983–1987.
[159] P. Kebarle, *Annu. Rev. Phys. Chem. 28* (1977) 445.
[160] A. W. Castleman, Jr., P. M. Holland, D. M. Lindsay, K. I. Peterson, *J. Am. Chem. Soc. 100* (1978) 6039.
[161] V. G. Solomonik, K. S. Krasnov, *Russ. J. Phys. Chem. (Engl. Transl.) 53* (1979) 161, and references cited therein.
[162] K. G. Rao, E. D. Becker, C. N. R. Rao, *J. Chem. Soc. Chem. Commun. 1977*, 350. Rotation barrier of dimethylacetamide: M. Feigel, *ibid. 1980*, 456.
[163] From IR-spectroscopic "stop-flow" measurements: M. Al-Aseer, P. Beak, D. Hay, D. J. Kempf, S. Mills, S. G. Smith, *J. Am. Chem. Soc. 105* (1983) 2080.
[164] E. M. Arnett, F. J. Fisher, M. A. Nichols, *22nd Reaction Mechanism Conference, Pittsburgh, June 12-16, 1988* (Poster Session 1, 1); also reported at the ACS Fall Meeting in Los Angeles, September 1988. See also earlier work of this group: E. M. Arnett, S. G. Maroldo, S. L. Schilling, J. A. Harrelson, *J. Am. Chem. Soc. 106* (1984) 6759, and references cited therein. I thank Professor *Arnett* (Duke University, Durham, NC) for a detailed summary of his lectures prior to publication.
[165] F. G. Bordwell, *Pure Appl. Chem. 49* (1977) 963–968; a more recent paper on acidity in DMSO: F. G. Bordwell, D. J. Algrim, *J. Am. Chem. Soc. 110* (1988) 2964.
[166] Chelation in the reaction of α-alkoxy ketones with Grignard reagents: S. V. Frye, E. L. Eliel, R. Cloux, *J. Am. Chem. Soc. 109* (1987) 1862.
[167] P. J. A. Geurink, G. W. Klumpp, *J. Am. Chem. Soc 108* (1986) 538; G. W. Klumpp, M. J. Sinnige, *Tetrahedron Lett. 27* (1986) 2247.
[168] P. Beak, B. Siegel, *J. Am. Chem. Soc. 96* (1974) 6803.
[169] The "cyclic model" of *Cram*'s rule, today called "chelation control" was formulated 30 years ago: a) D. J. Cram, K. R. Kopecky, *J. Am. Chem. Soc. 81* (1959) 2748. b) M. T. Reetz, *Angew. Chem. 96* (1984) 542–555; *Angew. Chem. Int. Ed. Engl. 23* (1984) 556–569 ("Chelation or Non-Chelation Control in Addition Reactions of Chiral α- and β-Alkoxy Carbonyl Compounds").
[170] H. O. House, V. Kramar, *J. Org. Chem. 28* (1963) 3362.
[171] H. O. House, B. M. Trost, *J. Org. Chem. 30* (1965) 1341.
[172] G. W. Spears, C. E. Caufield, W. C. Still, *J. Org. Chem. 52* (1987) 1226.
[173] R. Häner, T. Laube, D. Seebach, *Chimia 38* (1984) 255.
[174] R. Häner, W. B. Schweizer, P. Seiler, D. Seebach, *Chimia 40* (1986) 97.
[175] W. J. Hehre, L. Radom, P. von R. Schleyer, J. A. Pople: *Ab Initio Molecular Orbital Theory*, Wiley, New York 1986; R. D. Amos, J. E. Rice: *The Cambridge Analytical Derivatives Package*, Issue 4.0, Cambridge 1987.
[176] N. L. Allinger, *J. Am. Chem. Soc. 99* (1977) 8127; U. Burkert, N. L. Allinger: *Molecular Mechanics, ACS Monogr. 177* (1982); W. C. Still, *MacroModel*, Columbia University, New York 1986.
[177] a) J. E. Del Bene, M. J. Frisch, K. Raghavachari, J. A. Pople, P. von R. Schleyer, *J. Phys. Chem. 87* (1983) 73; b) A.-M. Sapse, K. Raghavachari, P. von R. Schleyer, E. Kaufmann, *J. Am. Chem. Soc. 107* (1985) 6483.
[178] a) See also the interesting dienolate of cyclogeraniol and the discussion of possible structures, which might explain the reactivity: C. Fehr, J. Galindo, *J. Org. Chem. 53* (1988) 1823 and [72]; b) C. Fehr, J. Galindo, *J. Am. Chem. Soc.* (1988), in press (*I* thank Dr. *Fehr* for sending us the manuscript).
[179] A. Bongini, M. Orena, S. Sandri, *J. Chem. Soc. Chem. Commun. 1986*, 50.
[180] R. Glaser, A. Streitwieser, Jr., *J. Am. Chem. Soc. 109* (1987) 1258.
[181] K. N. Houk, R. W. Strozier, N. G. Rondan, R. R. Fraser, N. Chuaqui-Offermanns, *J. Am. Chem. Soc. 102* (1980) 1426.
[182] J. Zimmermann, D. Seebach, T.-K. Ha, *Helv. Chim. Acta 71* (1988) 1143.
[183] J. H. Horner, M. Vera, J. B. Grutzner, *J. Org. Chem. 51* (1986) 4212.
[184] S. D. Kahn, lectures and poster: *The Third Chemical Congress of North America*, Toronto, June 5–11, 1988; *22nd Reaction Mechanism Conference*, Pittsburgh, June 12–16, 1988. I thank Professor *Kahn* (School of Chemical Sciences, University of Illinois at Urbana-Champaign, Urbana) for sending us a manuscript and for permission to cite the data prior to publication and to reproduce here the color picture generated by the program *MacModel* and printed out with a Tektronix 4693 D.
[185] A. S. Narula, *Tetrahedron Lett. 22* (1981) 4119.
[186] D. W. Moreland, W. G. Dauben, *J. Am. Chem. Soc. 107* (1985) 2264.
[187] a) M. L. McKee, *J. Am. Chem. Soc. 109* (1987) 559. b) M. L. McKee, *ibid. 107* (1985) 7284.
[188] E. Kaufmann, P. von R. Schleyer, K. N. Houk, Y.-D. Wu, *J. Am. Chem. Soc. 107* (1985) 5560. Similar calculations concerning the addition of LiH and $LiCH_3$ to ethylene and acetylene: K. N. Houk, N. G. Rondan, P. von R. Schleyer, E. Kaufmann, T. Clark, *ibid. 107* (1985) 2821.
[189] S. M. Bachrach, A. Streitwieser, Jr., *J. Am. Chem. Soc. 108* (1986) 3946; correction: *ibid. 109* (1987) 5888.
[190] N.-T. Anh, B.-T. Thanh, *Nouv. J. Chim. 10* (1986) 681.
[191] J. Mulzer, G. Brüntrup, J. Finke, M. Zippel, *J. Am. Chem. Soc. 101* (1979) 7723.
[192] G. Kyriakakou, A. Loupy, J. Seyden-Penne, *J. Chem. Res. Synop. 1978*, 8.
[193] Y. Li, M. N. Paddon-Row, K. N. Houk, *J. Am. Chem. Soc. 110* (1988) 3684.
[194] C. Gennari, R. Todeschini, M. G. Beretta, G. Favini, C. Scolastico, *J. Org. Chem. 51* (1986) 612.
[195] M. J. S. Dewar, K. M. Merz, Jr., *J. Am. Chem. Soc. 109* (1987) 6553.
[196] R. B. Woodward, R. Hoffmann, *Angew. Chem. 81* (1969) 797–869; *Angew. Chem. Int. Ed. Engl. 8* (1969) 781–853.
[197] W. von E. Doering, W. R. Roth, *Tetrahedron 18* (1962) 67–74; *Angew. Chem. 75* (1963) 27–35; *Angew. Chem. Int. Ed. Engl. 2* (1963) 115–122.
[198] J. E. Baldwin, *J. Chem. Soc. Chem. Commun. 1976*, 734.
[199] Complex structures are present not only according to the calculations mentioned in Section 3 [15, 25] but also in the gaseous state; see the dimer $[LiN(SiMe_3)_2]_2$, discovered by electron diffraction in the gas phase [82], or the mass spectroscopically identified oligomers of polylithiated alkanes [41g] and: L. A. Shimp, J. A. Morrison, J. A. Gurak, J. W. Chinn, Jr., R. J. Lagow, *J. Am. Chem. Soc. 103* (1981) 5951; J. A. Gurak, J. W. Chinn, Jr., R. J. Lagow, *ibid. 104* (1982) 2637; F. J. Landro, J. A. Gurak, J. W. Chinn, Jr., R. M. Newman, R. J. Lagow, *ibid. 104*

(1982) 7345; H. Kawa, B. C. Manley, R. J. Lagow, *ibid. 107* (1985) 5313.

[200] R. E. Dickerson, I. Geis: *Chemistry, Matter and the Universe*, 3rd Printing, Benjamin, Menlo Park CA, 1979, p. 458

[201] Accordingly, "dramatic induction periods" in reactions of Li derivatives with alkyl halides have been reported; the generated lithium halide acted as an "accelerator" [102b, 132d].

[202] J. F. McGarrity, J. Prodolliet, T. Smyth, *Org. Magn. Resonance 17* (1981) 59.

[203] J. F. McGarrity, J. Prodolliet, *J. Org. Chem. 49* (1984) 4465.

[204] J. F. McGarrity, C. A. Ogle, *J. Am. Chem. Soc. 107* (1985) 1805.

[205] J. F. McGarrity, C. A. Ogle, Z. Brich, H.-R. Loosli, *J. Am. Chem. Soc. 107* (1985) 1810.

[206] By this method the rate of equilibration [204, 205] between dimeric and tetrameric BuLi in THF (cf. [42a,c, 133]) was measured at −60 to −85°C as well as that of the reaction of butyllithium with oxygen [204], with cyclopentadiene, and with benzaldehyde [205]. Most important findings: no indication of monomeric BuLi down to concentrations of 10^{-4} M; $(BuLi)_2$ as well as the mixed aggregate $[Bu_2(BuO)_2Li_4]$ react about ten times faster with PhCHO than does $(BuLi)_4$; the alkoxide $PhCH(OLi)C_4H_9$, formed from BuLi and PhCHO, adds to benzaldehyde to give the alkoxide of a hemiacetal (cf. Scheme 6 and references cited there). See also the RINMR measurement of the addition of Grignard compounds to alkoxy ketones [166].

[207] In the case of Li enehydrazide it was concluded from kinetic measurements of the alkylation that the monomeric species forms product, not the aggregate, though the latter is the predominant species in solution [102c].

[208] See Schemes 5 and 9, Table 3, and Section 2.2.3.

[209] A "free" anion (not neutralized by *any* Li) must of course be even more reactive. A "fairly free" carbanion was recently proposed as the product-forming species from results obtained for Sn/Mg exchange processes in the reaction of Me_3Sn-substituted aryl bromides: H. J. R. de Boer, O. S. Akkerman, F. Bickelhaupt, *Angew. Chem. 100* (1988) 735; *Angew. Chem. Int. Ed. Engl. 27* (1988) 687.

[210] a) $LiNR_2$ adducts to aromatic aldehydes for *ortho*-metalations: U. Michael, S. Gronowitz, *Acta Chem. Scand. 22* (1968) 1353; D. L. Comins, J. D. Brown, *Tetrahedron Lett. 22* (1981) 4213; D. L. Comins, J. D. Brown, N. B. Mantlo, *ibid. 23* (1982) 3979; b) $LiNR_2$ adducts to aromatic aldehydes for aminative alkylations and reductive aminative coupling with low-valent titanium: D. Seebach, M. Schiess, *Helv. Chim. Acta 65* (1982) 2598; D. Seebach, A. K. Beck, M. Schiess, L. Widler, A. Wonnacott, *Pure Appl. Chem. 55* (1983) 1807–1822; D. Seebach, C. Betschart, M. Schiess, *Helv. Chim. Acta 67* (1984) 1593; C. Betschart, D. Seebach, *ibid. 70* (1987) 2215.

[211] $LiNR_2$ and LiOR adducts [*t*BuOCH(OLi)R] to nonenolizable aldehydes as bases and precursors for the in-situ liberation of an aldehyde: D. Seebach, T. Weber, *Tetrahedron Lett. 24* (1983) 3315; *Helv. Chim. Acta 67* (1984) 1650.

[212] Sulfur analogues [Aryl$CH(SLi)SR$]: D. Seebach, K.-H. Geiss, *Angew. Chem. 86* (1974) 202; *Angew. Chem. Int. Ed. Engl. 13* (1974) 202; K.-H. Geiss, D. Seebach, B. Seuring, *Chem. Ber. 110* (1977) 1833.

[213] L. M. Jackman, B. C. Lange, *J. Org. Chem. 48* (1983) 4789.

[214] L. Tenud, S. Farooq, J. Seibl, A. Eschenmoser, *Helv. Chim. Acta 53* (1970) 2059.

[215] See also the amide complexes in Table 4, urea and amide complexes of Li in crystals [47], and the discussion about LiX effects on peptides in Section 5.

[216] Most of the reaction paths via aggregates shown in Schemes 6–9 had been proposed by us already in 1981 and 1983 [53, 69]; only the complexity, not the principle, is changed if the reaction is formulated for tetrameric aggregates instead of dimeric ones as done here.

[217] The scenario is even extended if one considers that single-electron transfers (SET) become more probable with increasing degree of aggregation of polar organometallic compounds; a supramolecule can more likely donate an electron (as in the present case), or accept one, than one of its components, because the resulting charge deficiency is distributed over a larger area (higher lying HOMO, lower LUMO). Accordingly, for example, it was recently proved that the tendency of single-electron transfer to occur from a Li amide strongly increases with its degree of aggregation (P. Renaud, M. A. Fox, *J. Am. Chem. Soc. 110* (1988) 5702). An SET mechanism with participation of the aggregate (Fig. 14) was also proposed [56] to explain the reversal of stereoselectivity of reactions of the Li enamides of diketopiperazine-bislactim ethers when going from "normal" electrophiles [99] to C_2Cl_6 (U. Schöllkopf, H.-J. Neubauer, M. Hauptreif, *Angew. Chem. 97* (1985) 1065; *Angew. Chem. Int. Ed. Engl 24* (1985) 1066).

[218] In the case of participation of aggregates in product-forming steps, different results are possible depending on the use of the respective enolates as racemic mixtures (which can form diastereomeric aggregates) or of enantiomerically pure reagents! Compare the nonlinear dependence of the product *ee* values in numerous enantioselective reactions on the enantiomeric purity of the reagents used. Several examples can be found in the following references: [53]: A. Horeau, *Tetrahedron Lett. 1969*, 3121; C. Agami, C. Puchot, H. Sevestre, *ibid. 27* (1986) 1501; C. Puchot, O. Samuel, E. Dunach, S. Zhao, C. Agami, H. B. Kagan, *J. Am. Chem. Soc. 108* (1986) 2353; Review on *Kinetic Resolution*. H. B. Kagan, J. C. Fiaud, *Top. Stereochem. 18* (1988) 249.

[219] Two "aggregate effects" may prove this. a) In the reaction of *gem*-dibromocyclopropane with an excess of butyllithium and subsequent addition of an excess of electrophile, products of double substitution

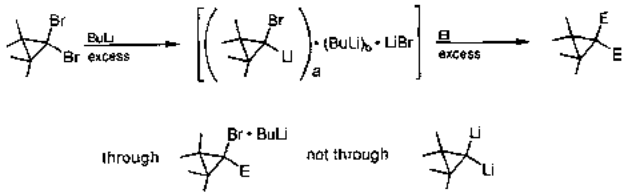

are formed which originally was seen as proof for the occurrence of *gem*-dilithiocyclopropanes. These species, however, could not be detected by NMR spectroscopy of ^{6}Li- and ^{13}C-labeled samples. It turns out that a mixture of bromolithium carbenoid and BuLi is present instead. The added electrophiles react faster with the carbenoid than with BuLi, and "interaggregate" Br/Li exchange leads to the observed result. See flow chart (R. Dammann, *Dissertation Nr. 6277*, ETH Zürich 1978). b) In the reaction of phenylacetonitrile with 2 BuLi (see structure

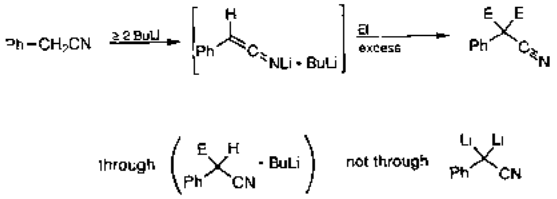

in Table 2) it is not a dilithium derivative that is responsible for the formation of double substituted products, but a fast "interaggregative" proton transfer during addition of electrophile (P. J. Crowley, M. R. Leach, O. Meth-Cohn, B. J. Wakefield, *Tetrahedron Lett. 27* (1986) 2909). c) Cf. also the discussion in: P. Beak, T. J. Musick, C. Chen, *J. Am. Chem. Soc. 110* (1988) 3538.

[220] Representations from publications by *Schlosser* show what has been concluded from kinetic measurements of the HCl elimination with potassium alkoxides: "Alcoholate Clusters ("Aggregates") and Their Role in Alkyne-Forming Elimination Reaction." M. Schlosser, T. D. An, *Angew. Chem. 93* (1981) 1114; *Angew. Chem. Int. Ed. Engl. 20* (1981) 1039; M. Schlosser, C. Tarchini, T. D. An, R. Ruzziconi, P. J. Bauer, *ibid. 93* (1981) 1116 and *20* (1981) 1041, respectively

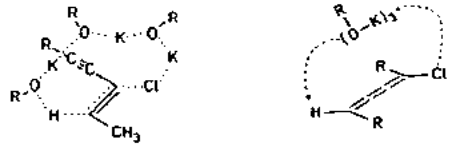

[221] G. Wittig, *Top. Curr. Chem. 67* (1976) 1–14.

[222] M. Schlosser, G. Heinz, *Chem. Ber. 102* (1969) 1944.

[223] D. Seebach, V. Ehrig, M. Teschner, *Liebigs Ann. Chem. 1976*, 1357.

[224] R. P. Woodbury, M. W. Rathke, *Tetrahedron Lett. 1978*, 709.

[225] G. Stork, P. F. Hudrlik, *J. Am. Chem. Soc. 90* (1968) 4462, 4464.

[226] J. K. Rasmussen, *Synthesis 1977*, 91–110.

[227] E. Colvin: *Silicon in Organic Synthesis*. Butterworths, London 1981.

[228] E. W. Colvin: Preparation and Use of Organosilicon Compounds in Organic Synthesis, in F. R. Hartley (Ed.): *The Chemistry of the Metal-Carbon Bond, Vol. 4*, Wiley, New York 1987, Chapter 6, pp. 539–621.

[229] E. W. Colvin: *Silicon Reagents in Organic Synthesis*. Academic Press, London 1988.

[230] W. P. Weber: *Silicon Reagents for Organic Synthesis*. Springer, Berlin 1983.

[231] P. J. Reider, R. S. E. Conn, P. Davis, V. J. Grenda, A. J. Zambito, E. J. J. Grabowski, *J. Org. Chem. 52* (1987) 3326.

[232] A. K. Beck, M. S. Hoekstra, D. Seebach, *Tetrahedron Lett. 1977*, 1187.

[233] D. Seebach, T. Weller, G. Protschuk, A. K. Beck, M. S. Hoekstra, *Helv. Chim. Acta 64* (1981) 716.

[234] M. Yoshifuji, T. Nakamura, N. Inamoto, *Tetrahedron Lett. 28* (1987) 6325.

[235] C. H. Heathcock, M. C. Pirrung, S. D. Young, J. P. Hagen, E. T. Jarvi, U. Badertscher, H.-P. Märki, S. H. Montgomery, *J. Am. Chem. Soc. 106* (1984) 8161, and earlier papers of the same group cited therein.

[236] R. Häner, D. Seebach, *Chimia 39* (1985) 356; D. Seebach, R. Häner, T. Vettiger, *Helv. Chim. Acta 70* (1987) 1507.

[237] T. Hassel, D. Seebach, *Helv. Chim. Acta 61* (1978) 2237, and earlier papers of our group cited therein.

[238] P. Beak, D. B. Reitz, *Chem. Rev. 78* (1978) 275–316; P. Beak, W. J. Zajdel, D. B. Reitz, *ibid. 84* (1984) 471–523.

[239] In this case alkylated diisopropylamine can be formed under conditions, under which pure diisopropylamine would not be alkylated (−80°C, in THF); thus, one must conclude that the amine is activated by the Li enolate for the alkylation to the tertiary amine! (See [244].)

[240] a) The effect of the "hidden proton" has been observed in substrates with several acidic sites also in the absence of secondary amines: see, e.g., the results of protonation of Schiff bases of penicillamine benzyl esters: R. A. Firestone, N. Schelechow, D. B. R. Johnston, B. G. Christensen, *Tetrahedron Lett. 1972*, 375; R. A. Firestone, N. S. Maciejewicz, R. W. Ratcliffe, B. G. Christensen, *J. Org. Chem. 39* (1974) 437; R. A. Firestone, B. G. Christensen, *J. Chem. Soc. Chem. Commun. 1976*, 268. b) Doubly deprotonated species—bis(enolates)—can be more stable than the corresponding simply deprotonated ones; see the following newer papers and the references cited therein: K. G. Bilyard, P. J. Garratt, R. Hunter, E. Lete, *J. Org. Chem. 47* (1982) 4731; K. Furuta, A. Misumi, A. Mori, N. Ikeda, H. Yamamoto, *Tetrahedron Lett. 25* (1984) 669. Solvation and chelation (see Tables 4,5) can invert the normal order of acidity: S. M. Bachrach, *J. Am. Chem. Soc. 108* (1986) 6406. But also here, as a warning, we must point to the intraaggregate effects mentioned in [219].

[241] E. Dziadulewicz, postdoctoral fellow, ETH Zürich 1987/88, hitherto unpublished results.

[242] D. Seebach, M. Boes, R. Naef, W. B. Schweizer, *J. Am. Chem. Soc. 105* (1983) 5390.

[243] P. Strazewski, C. Tamm, *Helv. Chim. Acta 69* (1986) 1041; P. Strazewski, *Dissertation*, Universität Basel 1986.

[244] J. D. Aebi, D. Seebach, *Helv. Chim. Acta 68* (1985) 1507.

[245] R. Polt, D. Seebach, *Helv. Chim. Acta 70* (1987) 1930; *J. Am. Chem. Soc. 111* (1989), in press.

[246] Cf. the protonations and alkylations of Schiff base enolates formed from amino acids and hydroxypinanone; under otherwise identical conditions, the epimeric precursors give rise to two enolates, **A** and **B**, that behave very differently (both should have the (*E*) configuration of the enolate double bond!); A. El Achqar, M.-L. Roumestant, P. Viallefont, *Tetrahedron Lett. 29* (1988) 2441.

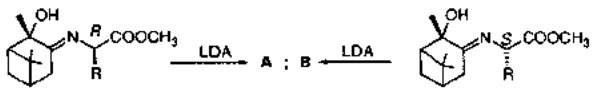

[247] Cf. the cooperative hydrogen bonds [76] in many biologically important structures in which, for example, three hydrogen bonds are arranged in a cyclic array, **A**, with the complexes **B** and **C** (Figs. 3, 5, Table 2). Here, as there, the bond strength is greater than anticipated from simple O···HO, N···HN or πC···HN hydrogen bonds. Much stronger are hydrogen bonds between ions, and between ions and neutral molecules, see [250, 251, 252c].

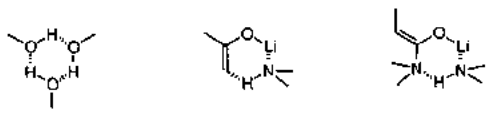

[248] The effect of the complexation of Li carboxylate (or the [RR'C=CO_2Li]Li derivative) with the secondary amine and the return of the proton in attempted deuterations of doubly metalated toluic acids as well as aliphatic or alicyclic carboxylic acids was already discussed at the beginning of the 1970s: P. L. Creger, *J. Am. Chem. Soc. 92* (1970) 1396; P. E. Pfeffer, L. S. Silbert, J. M. Chirinko, Jr., *J. Org. Chem. 37* (1972) 451.

[249] Reports on the observation of such effects in carbonyl additions, which occur much faster than nucleophilic substitutions, are not known to us. The enolate **A** generated with LDA, e.g., adds smoothly to acetaldehyde to give the expected product **B** (84%), while with CH_3I a 3:1 product **C**, R = CH_3, is generated in ca. 50% yield, which was attributed to the existence of tetrameric aggregates [183].

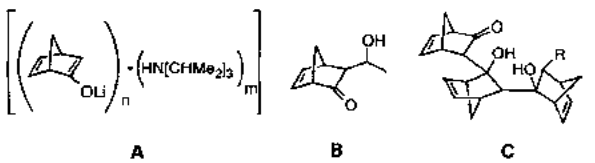

[250] D. J. Cram: *Fundamentals of Carbanion Chemistry*, Academic Press, New York 1965. In spite of the protic medium, the rate of racemization ($k_{rac.}$) is greater than that of the D/H exchange ($k_{exch.}$) via an ion pair. The formulae show the "conducted tour mechanism" (*Cram*), $k_{rac.}:k_{exch.} = 20:1$. Cf. also: A.-M. Weidler, G. Bergson, *Act. Chem. Scand. 18* (1964) 1487; K. Bott, *Tetrahedron Lett. 1965*, 4569.

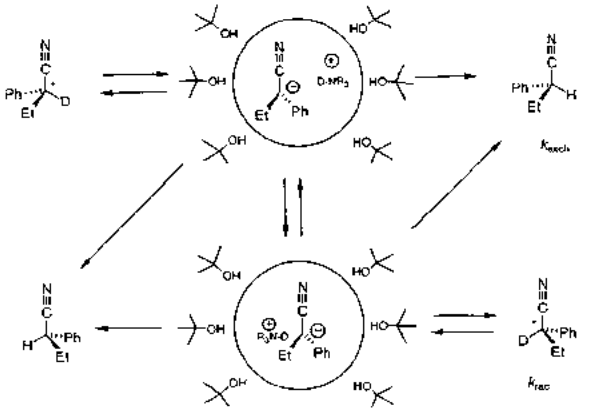

[251] There are very strong hydrogen bonds formed between ammonium or oxonium ions and π systems: C. A. Deakyne, M. Meot-Ner (Mautner), *J. Am. Chem. Soc. 107* (1985) 474 (measurements and ab-initio calcula-

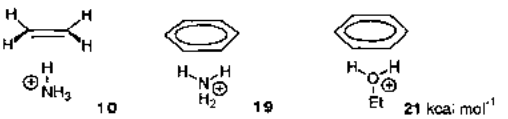

tions), cf. also [257]. Hydrogen bonds between an amine NH and the fluorenyl carbanion: S. Buchholz, K. Harms, M. Marsch, W. Massa, G. Boche, *Angew. Chem. 101* (1989) No. 1; *Angew. Chem. Int. Ed. Engl. 28* (1989) No. 1. Intramolecular hydrogen bonds between an OH group and an indenyl carbanion: P. Ahlberg, B. Johnsson, I. McEwen, M. Rönnqvist, *J. Chem. Soc. Chem. Commun. 1986*, 1500.

[252] Recent reviews on hydrogen bonds see [75, 76] and: a) A. C. Legon, D. J. Millen, *Acc. Chem. Res. 20* (1987) 39; b) E. B. Wilson, Z. Smith, *ibid. 20* (1987) 257; c) H. A. Staab, T. Saupe, *Angew. Chem. 100* (1988) 895–909; *Angew. Chem. Int. Ed. Engl. 27* (1988) 865–879.

[253] C. F. Bernasconi, D. E. Fairchild, C. J. Murray, *J. Am. Chem. Soc. 109* (1987) 3409, and earlier papers of this group cited therein.

[254] Theoretical Studies of Proton Transfers: S. Scheiner, *Acc. Chem. Res. 18* (1985) 174–180.

[255] S. Sprang, T. Standing, R. J. Fletterick, R. M. Stroud, J. Finer-Moore, N.-H. Xuong, R. Hamlin, W. J. Rutter, C. S. Craik, *Science (Washington, DC) 237* (1987) 905; C. S. Craik, S. Rozcniak, C. Largman, W. J. Rutter, *ibid. 237* (1987) 909.

[256] See [47, 61, 82], Table 5, and papers about basicity [LDA (pK_a 35.7)/$LiN(SiMe_3)_2$ (pK_a 29.5)] and about aggregation in solution: B. Y. Kimura, T. L. Brown, *J. Organomet. Chem. 26* (1971) 57; R. R. Fraser, T. S. Mansour, *J. Org. Chem. 49* (1984) 3442.

[257] Effect of $LiClO_4$ on the Diels–Alder reaction: R. Braun, J. Sauer, *Chem. Ber. 119* (1986) 1269. In the presence of $LiClO_4$ the equilibrium constant of the deprotonation of tropolone with pyridine in Et_2O is raised by a factor of 12500; this finding was related to ion pairs and aggregates of the Li salt: Y. Pocker, J. C. Ciula, *J. Am. Chem. Soc. 110* (1988) 2904. Influence of $LiClO_4$ on the *C*- vs. *O*-alkylation of Li enolates, see [138]; on the addition of MeLi to ketones: E. C. Ashby, S. A. Noding, *J. Org. Chem. 44* (1979) 4371; on the S_N2 reaction of MeLi with vinyloxiranes: J. C. Saddler, P. L. Fuchs, *J. Am. Chem. Soc. 103* (1981) 2112.

[258] Mixtures of LiBr and a tertiary amine can be applied for the α-alkylation of special base-labile and/or polymerization-prone carbonyl compounds. In these cases "complexes" such as **A** and **B** are proposed as the reactive species (cf. the data in [251]). **A**: O. Tsuge, S. Kanemasa, M. Yoshioka, *J. Org. Chem. 53* (1988) 1384. **B**: M. A. Blanchette, W.

Choy, J. Davis, A. P. Essenfeld, S. Masamune, W. R. Roush, T. Sakai, *Tetrahedron Lett. 25* (1984) 2183; M. W. Rathke, M. Nowak, *J. Org.*

Chem. 50 (1985) 2624; T. Rosen, C. H. Heathcock, *J. Am. Chem. Soc. 107* (1985) 3731. Cf. also an enantioselective version: T. Yamashita, H. Mitsui, H. Watanabe, N. Nakamura, *Bull. Chem. Soc. Jpn. 55* (1982) 961.

[259] D. Seebach, H. Dörr, B. Bastani, V. Ehrig, *Angew. Chem. 81* (1969) 1002; *Angew. Chem. Int. Ed. Engl. 8* (1969) 982; D. Seebach, H.-O. Kalinowski, B. Bastani, G. Crass, H. Daum, H. Dörr, N. P. DuPreez, V. Ehrig, W. Langer, C. Nüssler, H.-A. Oei, M. Schmidt, *Helv. Chim. Acta 60* (1977) 301, D. Seebach, W. Langer, *ibid. 62* (1979) 1701.

[260] Cf. also chiral ethylenediamine derivatives of proline (with and without alkoxide group) for the enantioselective addition of Li compounds and of tin enolates to aldehydes (in part very high *ee*), see references cited in T. Mukaiyama: *Organic Synthetic Reactions*, Tokyo Kagaku Dojin, Tokyo 1987 (ISBN 4-8079-0286-5), Chapter 11.3 and 13.2, respectively. (An English translation of this book published in Japanese, is being prepared. Its title will be *Challenges in Synthetic Organic Chemistry*.) Chiral binaphthyl-substituted ethylenediamine for enantioselective addition of alkyllithium to aldehydes: J.-P. Mazaleyrat, D. J. Cram, *J. Am. Chem. Soc. 103* (1981) 4585.

[261] J. K. Whitesell, S. W. Felman, *J. Org. Chem. 45* (1980) 755.

[262] L. Duhamel, J.-C. Plaquevent, *J. Am. Chem. Soc. 100* (1978) 7415. Review: L. Duhamel, P. Duhamel, J.-C. Launay, J.-C. Plaquevent, *Bull. Soc. Chim. Fr. 1984*, II 421–430.

[263] H. Hogeveen, L. Zwart, *Tetrahedron Lett. 23* (1982) 105.

[264] N. S. Simpkins, *J. Chem. Soc. Chem. Commun. 1986*, 88.

[265] R. Shirai, M. Tanaka, K. Koga, *J. Am. Chem. Soc. 108* (1986) 543.

[266] Further enantioselective protonations of achiral enolates and N-analogues with chiral acids or in the presence of chiral amines/Li amides: [178b, 262, 263] and L. Duhamel, S. Fouquay, J.-C. Plaquevent, *Tetrahedron Lett. 27* (1986) 4975; U. Gerlach, S. Hünig, *Angew. Chem. 99* (1987) 1323; *Angew. Chem. Int. Ed. Engl. 26* (1987) 1283; *Tetrahedron Lett. 28* (1987) 5805.

[267] Diastereoselective protonations: H. E. Zimmerman, *Acc. Chem. Res. 20* (1987) 263–268; ... of nitronates: D. Seebach, A. K. Beck, T. Mukhopadhyay, E. Thomas, *Helv. Chim. Acta 65* (1982) 1101; T. M. Williams, R. Crumbie, H. S. Mosher, *J. Org. Chem. 50* (1985) 91; M. Eyer, D. Seebach, *J. Am. Chem. Soc. 107* (1985) 3601; U. Brändli, M. Eyer, D. Seebach, *Chem. Ber. 119* (1986) 575.

[268] Further enantioselective deprotonations have been performed, e.g., with the bases **A**–**C** (see also Table 9 and N. S. Simpkins, lecture held at the Society of Chemical Industry Symposium "Chirality Recognition in Synthesis", London, March 17, 1988). For **A**, see [261, 263, 264] and

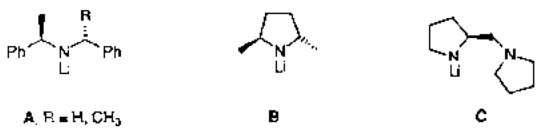

A, R = H, CH_3 **B** **C**

J. A. Marshall, J. Lebreton, *Tetrahedron Lett. 28* (1987) 3323; *J. Am. Chem. Soc. 110* (1988) 2925; L. Duhamel, A. Ravard, J.-C. Plaquevent, D. Davoust, *Tetrahedron Lett. 28* (1987) 5517; For **B** see [26]; For **C**, see M. Asami, *Chem. Lett. 1984*, 829; *Tetrahedron Lett. 26* (1985) 5803; M. Asami, H. Kirihara, *Chem. Lett. 1987*, 389; S. K. Hendrie, J. Leonhard, *Tetrahedron 43* (1987) 3289.

[269] When the precursor of the achiral enolate is a mixture of enantiomers and a chiral base is used for the deprotonation, a kinetic resolution may be responsible for the optical activity of the product; this has to be considered especially in cases of yields below 50%, see for example: M. B. Eleveld, H. Hogeveen, *Tetrahedron Lett. 27* (1986) 631, and review article cited in [218].

[270] M. Simpson, *Diplomarbeit*, ETH Zürich 1982.

[271] T. Mukhopadhyay, Postdoctoral fellow at the ETH Zürich 1981–1982.

[272] D. Wasmuth, *Dissertation Nr. 7033*, ETH Zürich 1982.

[273] D. Seebach, D. Wasmuth, *Angew. Chem. 93* (1981) 1007; *Angew. Chem. Int. Ed. Engl. 20* (1981) 971.

[274] H. Hogeveen, W. M. P. B. Menge, *Tetrahedron Lett. 27* (1986) 2767.

[275] A. Ando, T. Shioiri, *J. Chem. Soc. Chem. Commun. 1987*, 1620; cf. also *ibid. 1987*, 656.

[276] A. C. Regan, J. Staunton, *J. Chem. Soc. Chem. Commun. 1983*, 764; cf. also T. A. Carpenter, G. E. Evans, F. J. Leeper, J. Staunton, M. R. Wilkinson, *J. Chem. Soc. Perkin Trans. 1 1984*, 1043; A. C. Regan, J. Staunton, *J. Chem. Soc. Chem. Commun. 1987*, 520. It is not clear from these papers if and which excess of $LiNR_2$ has been used. Cf. also the complexes of Li toluic acid diamion derivatives and diisopropylamine [248].

[277] With the aldol-type products (Nos. 1–11), chiral shift reagent [Eu(dmc)$_3$] and the Mosher method or Pirkle columns [93] were used. With the nitroketone (No. 12), Eu(tfc)$_3$ was used, the product being compared with that of an authentic racemic sample [173] by NMR [93].

[278] It has not been investigated to what extent the adducts **D** shown in Scheme 6 are involved in the aldol additions to benzaldehyde (Nos. 1–11 from Table 9), which proceed most selectively by using a large excess of aldehyde (Nos. 3, 11).

[279] a) A. F. Spatola in B. Weinstein (Ed.): *Chemistry and Biochemistry of Amino Acids, Peptides, and Proteins, Vol. 7*, Marcel Dekker, New York 1983, pp. 267–357.—See also the articles by *Benner, Fersht*, and *Kaiser* in: S. A. Benner (Ed.): *Redesigning the Molecules of Life*, Springer-Verlag, Berlin 1988. b) M. Mutter, *Trends Biochem. Sci. 13* (1988) 260. I thank Professor *Mutter* for kindly allowing us to reproduce the following cartoon (drawn by the graphic division of the journal *Trends in Biochemical Sciences* ("TIBS") after a draft of Prof. *Mutter*).

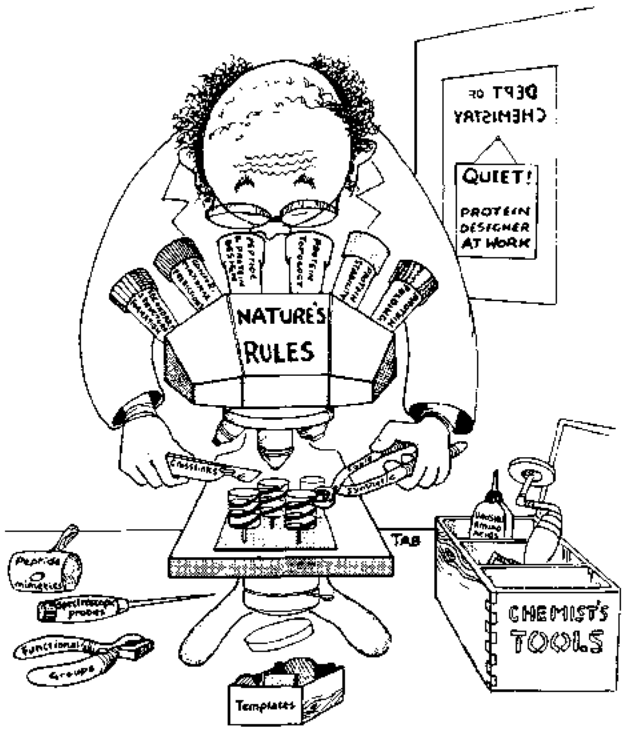

[280] Cf. the path via the cyclic dipeptide derivatives, Scheme 11 (bottom right) and [245].

[281] R. Naef, ETH Zürich 1983, hitherto unpublished results.

[282] D. Seebach, H. Estermann, *Tetrahedron Lett. 28* (1987) 3103.

[283] K. Narasaka, Y. Ukaji, K. Watanabe, *Chem. Lett. 1986*, 1755.

[284] The configuration of the CC and CN double bond of the enolate drawn in Scheme 15 is, as with all deprotonated peptides in this section (Schemes 15–19 and 24), chosen arbitrarily (or better, by the "technique of illustration"). There are no structural investigations of such species known to us. There is probably no doubt about the position of the Li at the more electronegative heteroatom oxygen (**A**–**C** vs. **D**). Of the four possible geometric isomers of the butyric acid derivative, **A** seems to be especially "attractive". Besides the *Z* isomer **B**, the *E* isomer **C** may be also considered for the lithiated peptides. See also entry 16 in Table 9.

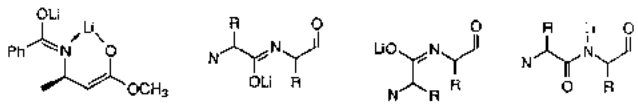

A (*E,E*) **B** (*Z*) **C** (*E*) **D**

[285] The first experiments on solubilization and alkylation of polylithiated open-chain peptides in the presence of LiCl have been performed in our laboratory by *S. Shoda* (Postdoctoral fellow at the ETH Zürich 1984–1986).

[286] H. Gründler, Part of the projected *Ph. D. thesis*, ETH Zürich.

[287] a) R. M. Wenger, *Helv. Chim. Acta 67* (1984) 502; b) *Angew. Chem. 97* (1985) 88–96; *Angew. Chem. Int. Ed. Engl. 24* (1985) 77–85; *Progr. Chem. Org. Nat. Prod. 50* (1986) 123–168; *Prog. Allergy 38* (1986) 46–64; R. M. Wenger, T. G. Payne, M. H. Schreier, *Prog. Clin. Biochem. Med. 3* (1986) 157–191.

[288] I sincerely thank Dr. *R. M. Wenger* of Sandoz AG, Basel, for the temporary acceptance of co-workers of my group into his laboratory, for

numerous discussions about oligopeptides and about cyclosporine, and for authentic samples and help in the identification of our products. Dr. *Wenger* has also kindly provided us with the color prints of Fig. 26.

[289] The solubilizing effect of an excess of LDA on polylithiated peptides was first observed in our laboratory by *C. W. Murtiashaw* (Postdoctoral fellow at the ETH Zürich 1983–1984).

[290] Probably other highly aggregated lithium derivatives can also be solubilized in this way, e.g., the geminal enediolates $R_2C=C(OLi)_2$, derived from carboxylic acids, for which "polymerization degrees" of up to 250 in THF were reported [126].

[291] A. P. Krapcho, E. A. Dundulis, *Tetrahedron Lett. 1976*, 2205.

[292] D. A. Evans, P. J. Sidebottom, *J. Chem. Soc. Chem. Commun. 1978*, 753.

[293] A general discussion of 4-atom 6-electron and of 6-atom 8-electron π systems is found in [41c, d] and in: R. Schlecker, D. Seebach, *Helv. Chim. Acta 60* (1977) 1459.

[294] D. H. R. Barton, R. H. Hesse, M. M. Pechet, C. Wiltshire, *J. Chem. Soc. Chem. Commun. 1972*, 1017.

[295] D. J. Goldsmith, A. J. Lewis, W. C. Still, Jr., *Tetrahedron Lett. 1973*, 4807.

[296] A. Thaler, *Diplomarbeit*, ETH Zürich 1987.

[297] D. Seebach, A. K. Beck, A. Thaler, *Helv. Chim. Acta 71* (1988), in press.

[298] a) P. Pfeiffer, J. von Modelski, *Hoppe Seyler's Z. Physiol. Chem. 81* (1912) 331; *85* (1913) 1; b) P. Pfeiffer, *ibid. 135* (1924) 22.

[299] One can imagine that the complexation of Li with peptides is linked to the application of Li salts in the long-term treatment of depressions; the mechanism is unknown to date, see [33] and: F. N. Johnson: *The History of Lithium Therapy* and *The Psychopharmacology of Lithium*, Macmillan Press, London 1984.

[300] T. H. Haskell, S. Hanessian, US Patent 3405218 (Oct. 8, 1968); *Chem. Abstr. 68* (1968) 89875p.

[301] See [47] and references [113, 122, 123, 135] therein.

[302] R. Meulemans, P. Piret, M. van Meerssche, *Acta Crystallogr. Sect. B 27* (1971) 1187.

[303] The solubilization of proteins in aqueous/organic solvent mixtures is an important method in protein chemistry. Review: P. Douzou, C. Balny, *Adv. Protein Chem. 32* (1978) 77–189.

[304] P. T. d'Holbach (pseudonym: J. B. Mirabaud): *Système de la nature ou des lois du monde physique et du monde moral* (First edition 1770, London).

[305] Cyclosporine A (CyA): A. Rüegger, M. Kuhn, H. Lichti, H.-R. Loosli, R. Huguenin, C. Quiquerez, A. von Wartburg, *Helv. Chim. Acta 59* (1976) 1075.

[306] X-ray structure of a derivative of CyA: T. J. Petcher, H.-P. Weber, A. Rüegger, *Helv. Chim. Acta 59* (1976) 1480.

[307] CyC: R. Traber, M. Kuhn, A. Rüegger, H. Lichti, H.-R. Loosli, A. von Wartburg, *Helv. Chim. Acta 60* (1977) 1247.

[308] CyB,D,E: R. Traber, M. Kuhn, H.-R. Loosli, W. Pache, A. von Wartburg, *Helv. Chim. Acta 60* (1977) 1568.

[309] CyE,F,G,H,I: R. Traber, H.-R. Loosli, H. Hofmann, M. Kuhn, A. von Wartburg, *Helv. Chim. Acta 65* (1982) 1655.

[310] CyK–*L*: R. Traber, H. Hofmann, H.-R. Loosli, M. Ponelle, A. von Wartburg, *Helv. Chim. Acta 70* (1987) 13.

[311] For the total synthesis of CyA and of analogues, see [287] and D. H. Rich, M. K. Dhaon, B. Dunlap, S. P. F. Miller, *J. Med. Chem. 29* (1986) 978; R. D. Tung, M. K. Dhaon, D. H. Rich, *J. Org. Chem. 51* (1986) 3350; I. J. Galpin, A. K. A. Mohammed, A. Patel, *Tetrahedron Lett. 28* (1987) 6517.

[312] J. F. Borel in D. J. G. White (Ed.): *Cyclosporine*, Elsevier, Amsterdam 1982, pp. 5–17.

[313] H. Kessler, H.-R. Loosli, H. Oschkinat, *Helv. Chim. Acta 68* (1985) 661; H.-R. Loosli, H. Kessler, H. Oschkinat, H.-P. Weber, T. J. Petcher, A. Widmer, *ibid. 68* (1985) 682.

[314] A. Thaler, part of the projected *Dissertation*, ETH Zürich.

[315] I. L. Karle, *J. Am. Chem. Soc. 96* (1974) 4000.

[316] More alkali-metal complexes of cyclic peptides are collected in the following monograph: M. Dobler: *Ionophores and Their Structures*, Wiley, New York 1981.

[317] D. Seebach, P. Bollinger, C. Gerber, H. Gründler, S. Y. Ko, M. Krieger, H.-R. Loosli, C. W. Murtiashaw, R. Naef, S. Shoda, A. Thaler, R. M. Wenger, *Helv. Chim. Acta*, in preparation; hitherto unpublished experiments, ETH Zurich and Sandoz AG, Basel.

[318] With all other El groups shown, except $COOCH_3$, the new amino acid has *R* configuration in **C**, and *S* configuration in **D**. By the change of the CIP order of priority, the afore mentioned assignment is inverted with the aminomalonic acid moiety (El = $COOCH_3$), a demonstration that the pro-*R*/pro-*S* specification is not constitutionally invariant! In the products with El = F and El = SCH_3 the newly introduced substituents have highest priority, so that **C** is *R* and **D** *S*. Generally, substitution of the C^{Re} ligand on a tetrahedral center $XABC_2$ by a new group **D** (→ XABCD) will lead to *R*-specification in exactly 50% of all cases, depending upon whether D is No. 1, 2, 3, or 4 in the priority sequence!

[319] R_f values with 10% MeOH in Et_2O: (*R*)-Ala^3 0.56, (*S*)-Ala^3 0.51, CyA 0.47.

[320] Taken from the poem "Flag of Poland" in *The Metamict State*. Poems by Roald Hoffmann, University Presses of Florida 1987.

[321] U. Brändli, *Dissertation No. 8680*, ETH Zürich 1988.

[322] D. Müller, *Diplomarbeit*, ETH Zürich 1988.

[323] a) There are indications, that LiCl formed in situ increases the solubility of polybenzamides in an aprotic solvent (e.g., DMF) ("solubility mediator"): F. Schultze-Gebhart in B. von Falkai (Ed.): *Synthesefasern*, Verlag Chemie, Weinheim 1981, Chapter II, p. 452; Z. A. Rogowin: *Chemiefasern*, Thieme Verlag, Stuttgart 1982, Chapter 30, p. 375. b) The solubilization and reaction of polyamides with electrophiles by deprotonation of the amide groups with NaH in the aprotic polar solvent DMSO has recently come into use to modify the properties of polymers: M. Takayanagi, T. Katayose, *J. Polym. Sci. Polym. Chem. Ed. 19* (1981) 1133; D. R. Moore, L. J. Mathias, *J. Appl. Polym. Sci. 32* (1986) 6299; M. Takayanagi, S. Ueta, W.-Y. Lei, K. Koga, *Polym. J. 19* (1987) 467. c) The effect of the deprotonation, and solubilization with LiX, is reminiscent of the xanthate-method in the production of artificial silk from cellulose: M.-L. Kehren, A. Reichle: *Cellulose-Chemiefasern* in *Ullmanns Enzyklopädie der technischen Chemie, 4th ed., Vol. 9*, Verlag Chemie, Weinheim 1975, pp. 213–226.

[324] Taken from a speech given in Frankfurt, see [130a].

Pergamon

Tetrahedron: *Asymmetry* 9 (1998) 357–389

TETRAHEDRON: *ASYMMETRY*

TETRAHEDRON: ASYMMETRY REPORT NUMBER 33

Catalyzed enantioselective aldol additions of latent enolate equivalents

Scott G. Nelson

Department of Chemistry, University of Pittsburgh, Pittsburgh, Pennsylvania 15260, USA

Received 10 October 1997; accepted 25 November 1997

Contents

1	Introduction	357
2	Sn(II) catalyst systems	360
2.1	Sn(II)–diamine reaction promoters	360
2.2	$Sn(OTf)_2$-based catalysts	361
3	Boron heterocycle catalysts	363
3.1	(Acyloxy)borane complexes	363
3.2	Oxazaborolidine catalysts	367
4	Early transition metal catalysts: Ti(IV)	372
4.1	Introduction	372
4.2	Ti(IV)[BINOL]-catalyzed aldehyde ene reactions	373
4.3	$Ti(O\textit{i}\text{-}Pr)_4$[BINOL] catalyst systems	376
4.4	Ti(IV)–Schiff base catalysts	377
5	Late transition metal catalysts: Cu(II)	381
5.1	Cu(II)[pyridine(bisoxazoline)]-catalyzed additions to α-benzyloxyacetaldehyde	381
5.2	Cu(II)[bisoxazoline]-catalyzed additions to pyruvate esters	381
6	Group 2B, lanthanide and other late transition metal catalysts	384
7	Nucleophilic (Lewis basic) catalysts	385
7.1	Additions of (trichlorosilyloxy)alkenes	385
7.2	Additions of latent enolate equivalents derived from ketene	386
8	Conclusion	387

1. Introduction

Aldol addition reactions are among those transformations that have greatly simplified the construction of asymmetric C–C bonds and, thus, satisfy the most stringent of requirements for salient asymmetric organic synthesis methodology. Numerous examples attesting to the strategic nature of asymmetric aldol reactions exist in the context of both complex molecule synthesis and the preparation of optically active small molecule building blocks.[1] Demand within the pharmaceutical and fine chemical industries for efficient and economical methodologies for the asymmetric synthesis of both simple and complex target molecules has resulted in new developments in aldol-based reaction technology being increasingly

PII: S0957-4166(97)00634-4

shaped by concerns for potential industrial applicability. As a consequence, an increasing emphasis has been placed on developing catalyzed asymmetric aldol bond constructions as a means of addressing the issues of cost and operational simplicity inherent in industrial-scale chemistry. Catalytic variants of the aldol addition reaction have evolved primarily from reaction design strategies that employ preformed, latent enolates that require some activating agent, often substoichiometric quantities of a Lewis acid, to undergo addition to the electrophilic reaction component. Investigations that have successfully implemented this reaction design strategy to the execution of asymmetric catalytic cross aldol reactions are the subject of the present account.

Many of the fundamental issues that confronted initial development of chemoselective cross aldol reactions are inherent to the design of catalyzed variants of this important bond construction. Establishing procedures for achieving chemo- and regioselective enolization, an essential prerequisite to chemoselective aldol addition reactions, was among the seminal achievements that ultimately led to aldol bond constructions reaching their current level of sophistication.[2] Reaction designs for catalyzed aldol reactions must similarly incorporate mechanisms for selective enolate formation and the controlled reaction of the resulting nucleophile with aldehyde electrophiles. It is not surprising, therefore, that the most widely explored strategy for executing catalyzed and, ultimately, asymmetric aldol additions exploits preexisting stoichiometric methodologies for generating the desired enolate structures. This design strategy shares with stoichiometric protocols the procedural requirement for making enolate formation (enolization) and C–C bond construction (addition) separate and distinct chemical operations (Scheme 1). However, the catalyzed reaction schemes necessarily require a reaction catalyst to initiate and mediate the reaction of the resulting enolate, thus presenting the catalyst as a vehicle for influencing reaction stereoselection. Implementing this reaction design, therefore, required the identification of suitable latent enolate equivalents that would add to aldehyde electrophiles only upon the intervention of a suitable activating agent (catalyst). (Silyloxy)alkenes were first recognized as the requisite latent enolate equivalents, undergoing addition to aldehydes in the presence of Lewis acid activators, a process ultimately to become known as the Mukaiyama aldol reaction (Eq. 1).[3] The reaction parameters enumerated by Mukaiyama's initial investigations provided a reaction platform and a mechanistic guideline for the subsequent design and development of chiral catalysts for asymmetric variants of these aldol addition reactions.

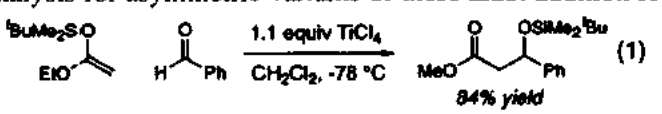

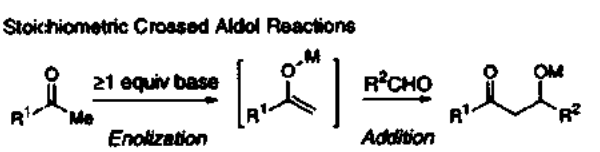

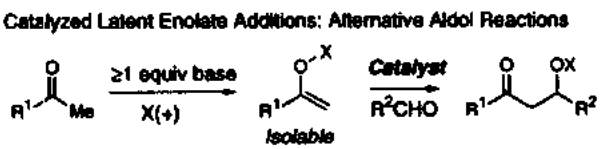

Scheme 1.

The primary objective of this review is to present a comprehensive survey of catalyzed enantioselective aldol reactions in which asymmetric induction is derived solely from the catalyst complex. Catalyzed aldol reactions that translate preexisting chirality in one of the reaction partners to the bond

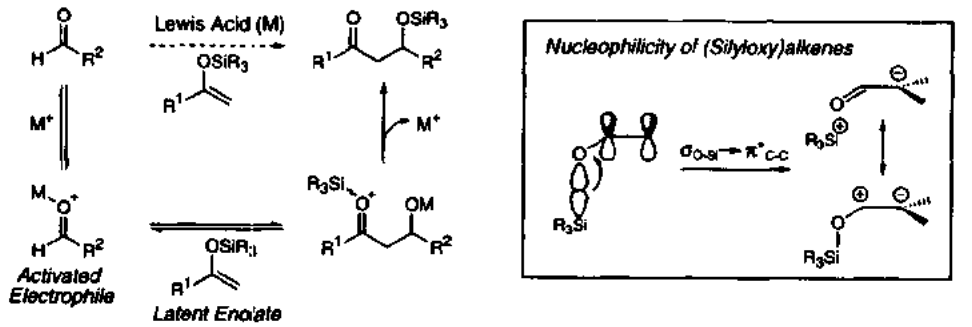

Fig. 1. Lewis acid-catalyzed additions of (silyloxy)alkenes

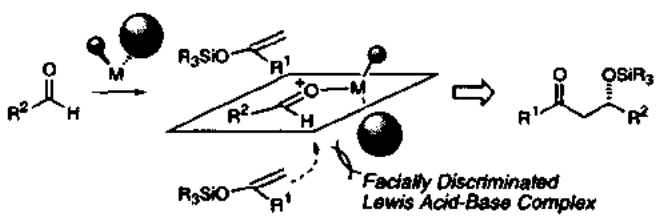

Fig. 2. Asymmetric aldol reactions catalyzed by chiral Lewis acids

construction event (diastereoselective reactions) are, therefore, not included. Furthermore, reactions requiring stoichiometric quantities of a chiral reaction promoter are discussed only as they pertain to the subsequent development of catalytic reaction variants. Many of the studies pertinent to this review appeared nearly concurrently from a number of research groups. Therefore, rather than attempt to present these investigations in rigorous chronological order, the present account organizes these studies according to the structure and function of the various catalyst systems.

Analysis of the C–C bond construction resulting from the Lewis acid-mediated reaction of (silyloxy)alkenes with aldehydes suggests addition of the latent enolate to a Lewis acid activated aldehyde complex to be a viable mechanistic hypothesis for Mukaiyama aldol reactions (Fig. 1). Silylated enolates possess significant nucleophilic character owing to electron donation to the alkene π-system derived from resonance interaction with the oxygen lone pairs and the β-silicon effect.[4] Thus, Lewis acid activation of the aldehyde elicits enolate addition with subsequent transfer of the silicon residue to the aldolate oxygen or direct hydrolysis of the metal alkoxide intermediate providing the silylated or unsilylated aldol adducts, respectively. While succeeding investigations would reveal the mechanistic profile of Mukaiyama aldol reactions to be considerably more complex, this mechanistic paradigm implicated reaction designs employing optically active Lewis acid complexes to create facially discriminated aldehyde electrophiles as a strategy for effecting asymmetric catalyzed aldol reactions (Fig. 2).[5]

In 1986, Reetz provided the first indication that asymmetry in catalyzed Mukaiyama aldol reactions could be induced by substoichiometric quantities of chiral Lewis acid complexes. The Ti(IV)–BINOL complex **1** and the Al(III)-based Lewis acids **2** and **3** were evaluated as chiral catalysts for the addition of 1-methoxy-1-trimethylsilyloxy-3-methylpropene (MTMP; **4**) to aliphatic aldehydes.[6] Especially encouraging levels of enantioselection were obtained in reactions employing the Al(III)-pinanediol catalyst system **2** (~20 mol% catalyst loading), providing the aldol adduct **5** with 66% ee (Eq. 2).

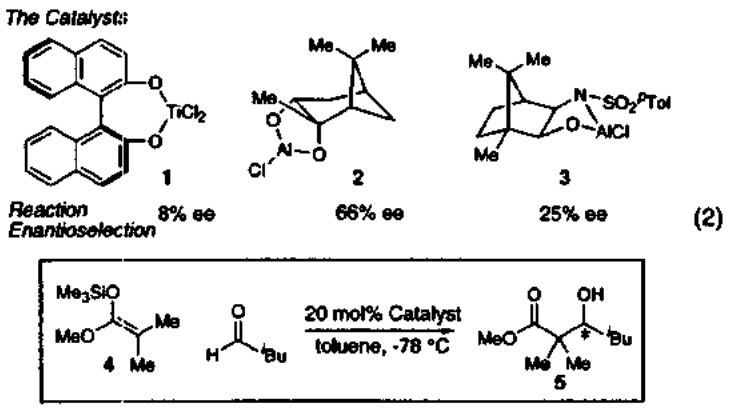

The poor enantioselection realized in reactions catalyzed by the Ti(IV)–BINOL complex 1 contrasts sharply with the high levels of asymmetric induction that would ultimately be derived from catalyst systems that are nearly identical in composition. Furthermore, despite the promising levels of asymmetric induction achieved in this study using Al(III)-derived Lewis acid catalysts, no aluminum-based catalyst systems that elicit highly enantioselective aldol reactions have been reported subsequently. Collectively, these preliminary investigations foreshadow the considerable sensitivity of enantioselection in Lewis acid-catalyzed aldol reactions to subtle variations in the preparative details of catalyst generation, the solution-state structure of the catalytically active species, and minor variations in reaction conditions that would be encountered repeatedly in subsequent studies.

2. Sn(II) catalyst systems

2.1. Sn(II)–diamine reaction promoters

Divalent tin complexes modified with chiral, chelating diamine ligands provided some of the earliest indications that absolute stereochemical control could be established in Mukaiyama aldol reactions using non-covalently bound chiral controllers integrated into the metal-based reaction promoter.[7] The development of these catalyst systems was predicted on the preliminary finding that substoichiometric quantities of $SnCl_2$ in combination with trityl chloride function as a catalyst for the aldol addition reaction of silyl thioketene acetals and aldehydes; substoichiometric quantities of either constituent of this catalyst system do not promote the addition reaction.[8] This observation implicated a cationic Sn(II) species, generated by cocatalyst-induced halide abstraction, as the active reaction promoter and resulted in divalent tin complexes emerging as templates for developing chiral aldol catalysts. Stoichiometric quantities of Sn(II) triflate and specific combinations of optically active chelating diamines and Lewis acidic cocatalysts, typically Sn(IV) salts, provided excellent yields and enantioselectivities in the addition of ketene acetals to various aldehyde electrophiles (Eq. 3).

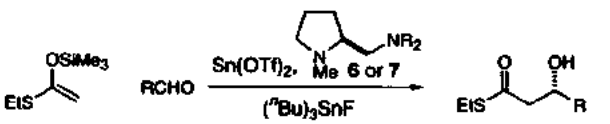

(3)

R = Ph, $(CH_2)_2Ph$, ^iPr, ^tBu

diamine	NR_2	% yield	% ee
6		70-90	78->98
7	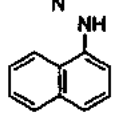	50-52	81-92

Reaction enantioselectivity proved to be especially sensitive to the structure of both the Lewis acid cocatalyst and the diamine ligand, with the most effective promoters being derived from either *n*-Bu_3SnF or *n*-Bu_2SnOAc_2 as cocatalysts and the proline-derived diamine ligands **6** and **7**. Near-perfect levels of relative and absolute stereochemical control were achieved in the aldol reactions of the (*Z*)-*O*-propionate enolate equivalent **8** and both unsaturated and aliphatic aldehydes using this chiral promoter system; *syn* propionate aldol adducts **9** emerged from these reactions with high optical purity (≥98% ee), generally in excess of 85% chemical yield (Eq. 4).[9]

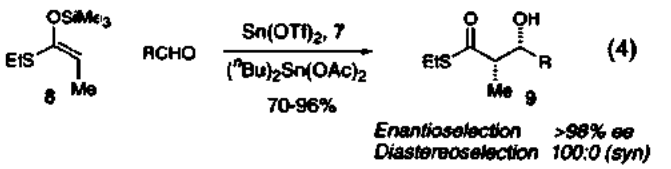

(4)

2.2. *Sn(OTf)$_2$-based catalysts*

2.2.1. *Reaction design*

Subsequent attempts to elucidate the mechanism of the Sn(II)/Sn(IV)-promoted aldol reactions revealed that a catalytic cycle for the addition of silyl thioketene acetals to benzaldehyde could be established using substoichiometric quantities of Sn(II) triflate.[10] The sensitivity of enantioselection in the Sn(II)[diamine]-promoted aldol reactions to the identity of the Sn(IV) cocatalyst was ultimately ascribed to the Sn(IV) cocatalyst functioning as a scavenger of TMSOTf generated during the course of the addition reaction (Fig. 3).[7] Trialkylsilyl triflates are sufficiently Lewis acidic to promote the aldol addition reaction and, therefore, offer a reaction manifold that is independent of the diamine chiral controller, resulting in attenuated reaction enantioselection.[11] It was reasoned that substoichiometric quantities of the Sn(II) triflate–diamine complex might provide useful levels of enantioselection provided a reaction protocol that precluded the intervention of the 'silicon-catalyzed' pathway could be established. Indeed, the $Sn(OTf)_2$–diamine complex **10** (20 mol%) catalyzes the addition of silyl thioketene acetals to aldehydes with enantioselectivities approaching those obtained for the stoichiometric Sn(II)-promoter system. Realizing optimum enantioselection in the Sn(II)-catalyzed propionate aldol reactions require the slow addition of the enolate equivalent to a propionitrile solution of aldehyde and catalyst. The initial events in the catalytic reaction cycle are proposed to parallel those of the Sn(II)-promoted reaction with the tin aldolate adduct **11** emerging from ketene acetal addition to a Lewis acid activated aldehyde (Fig. 4).[12] Silyl group transfer to the aldolate oxygen regenerates the chiral tin catalyst **12** in providing the silylated aldol product **13**. Alternatively, ligand exchange in **11** can occur to liberate TMSOTf, a mechanistic

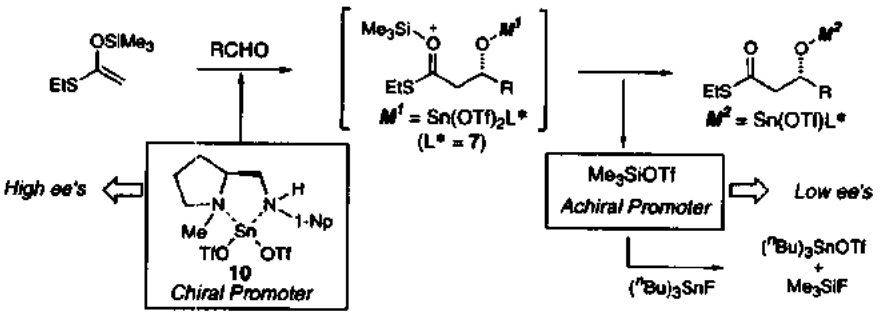

Fig. 3. Mechanism of Sn(II)/Sn(IV)-promoted aldol reactions

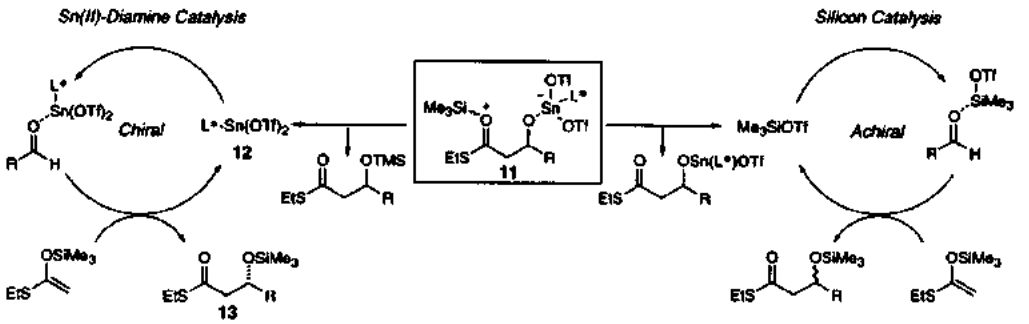

Fig. 4. Competing Sn(II) versus TMSOTf-catalyzed reaction pathways

scenario that rationalizes the procedural requirement for slow substrate addition in order to obtain high enantioselectivities. Specifically, a build-up of TMSOTf resulting from direct addition of the silylketene acetal to the aldehyde–catalyst complex results in partioning of the reaction mechanism between the chiral Sn-mediated process and an achiral TMSOTf-catalyzed reaction manifold. Slow substrate addition allows transmetallation of the initial tin aldolate **11** to remove free TMSOTf from the reaction mixture, thus shunting the achiral reaction pathway. Accelerated rates of aldolate silylation precipitated by Lewis base coordination to the metal ion, and the resulting amplified alkoxide nucleophilicity, have been suggested as an explanation for improved reaction enantioselection and turnover frequencies in propionitrile relative to dichloromethane reaction solvents.[13]

2.2.2. *Acetate and propionate aldol reactions*

The optimized Sn(II) triflate–diamine catalyst system has been successfully applied to the aldol addition of the silyl thioketene acetals, representing propionate and acetate enolate equivalents, with a wide variety of aldehyde electrophiles.[13] The complex derived from a 1:1.1 mixture of $Sn(OTf)_2$ and diamine 7 (20 mol%, EtCN, −78°C) catalyzes the addition reaction of the (*E*)-*O*-ketene acetal **8** to aryl, α,β-unsaturated, and aliphatic aldehydes with excellent relative and absolute stereochemical control: *syn*:*anti*=89:11–100:0, ee=89–>98% (Table 1).[14] The reactions of the corresponding (*Z*)-*O*-ketene acetals are not reported, presumably due to the poor diastereo- and enantioselectivity afforded by these nucleophiles in the Sn(II)–diamine promoted reactions. The catalyst derived from $Sn(OTf)_2$ and diamine **15** affords the acetate aldol adducts **16** with high optical purity via the addition of the unsubstituted ketene acetal **14** to several aliphatic aldehydes (90–93% ee); however, conjugated aldehydes afford considerable variability in enantioselection (68–88% ee) (Table 2).[15]

The sense of asymmetric induction in the preceding reactions can be rationalized by assuming that the reaction proceeds via the intermediacy of the square pyramidal aldehyde–Sn(II) complex **17** (Fig. 5).[10]

Table 1
Sn(II)–diamine catalyzed additions of thioketene acetals

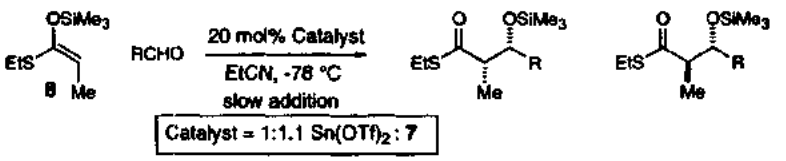

entry	aldehyde	% yield	*syn*:*anti*	% ee (*syn*)
a	C_6H_5CHO	77	93:7	90
b	$CH_3(CH_2)_6CHO$	80	100:0	>98
c	$^cC_6H_{11}CHO$	71	100:0	>98
d	4-$CH_3C_6H_4CHO$	75	89:11	91
e	(*E*)-CH_3CH=$CHCHO$	76	96:4	93
f	(*E*)-^nBuCH=$CHCHO$	73	97:3	93

Table 2
Sn(II)–diamine catalyzed additions of acetate enolate equivalents

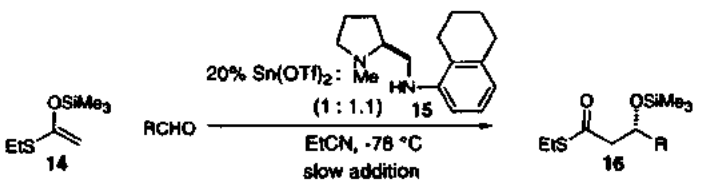

entry	aldehyde	% yield	% ee
a	$CH_3(CH_2)_3CHO$	79	93
b	$^cC_6H_{11}CHO$	81	92
c	Me_2CHCHO	48	90
d	$^tBuCCCHO$	68	88
e	$Me_3SiCCCHO$	75	77

Orientation of the amine and triflate ligands arrayed about the Sn ion to minimize mutual non-bonded interactions result in adjacent ligands shielding opposite faces of the square planar $Sn(OTf)_2$–diamine complex **10**. Lewis acid–base association occurs preferentially at the more accessible apical coordination site on tin, opposite the pyrrolidine and triflate ligands. The resulting Lewis acid–base complex orients the 1-naphthyl substituent to efficiently shield the (*re*) aldehyde diastereoface, thus affording aldol adducts having the (*S*) configuration (R^L=Ph) at the hydroxyl-bearing stereocenter. Addition of β-substituted ketene acetals to the activated Sn–aldehyde complex **17** via an open transition state that minimizes developing gauche interactions rationalizes the fidelity of these reactions for the production of the *syn* aldol diastereomer.

3. Boron heterocycle catalysts

3.1. (Acyloxy)borane complexes

Chiral boron heterocycles have proven to be among the most successful platforms for developing chiral Lewis acids with applications to organic synthesis. Mukaiyama aldol addition reactions are among the

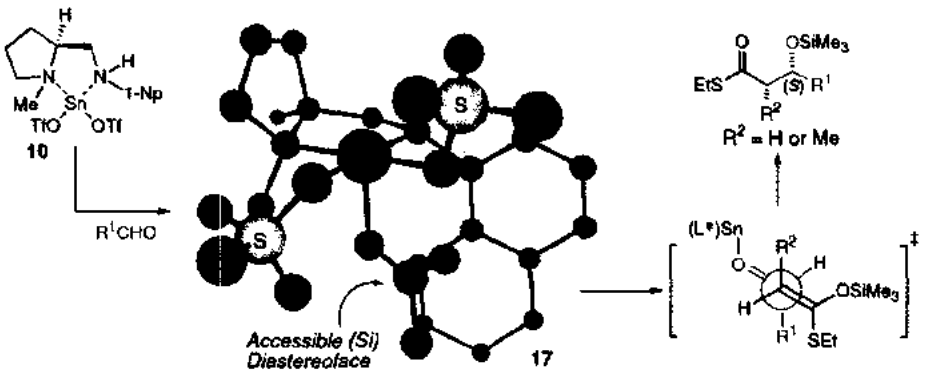

Fig. 5. Chiral Sn(II)[diamine]–aldehyde complex

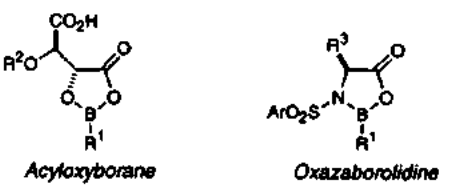

Fig. 6. Chiral boron heterocycle Lewis acids

numerous asymmetric bond constructions catalyzed by acyloxyborane and oxazaborolidine complexes, prototypical examples of boron heterocycles that are readily obtained in optically active form (Fig. 6). Reaction of the mono-arylester of tartaric acid **18** with borane or a suitable boronic acid provides the chiral (acyloxy)borane (CAB) complexes **19–21** (Eq. 5).

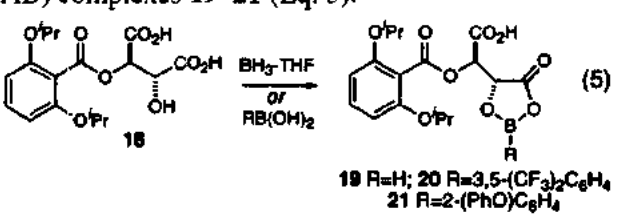

(5)

The parent CAB complex **19** affords good levels of relative and absolute stereoselection in the catalyzed addition of various enol silane and silyl ketene acetal nucleophiles with a limited number of aldehyde electrophiles.[16,17] Terminal enol silane **22** affords enantioselectivities ranging from 80–85% ee in the CAB-catalyzed addition reactions with aromatic or aliphatic aldehydes (70–98% yield) (Eq. 6).

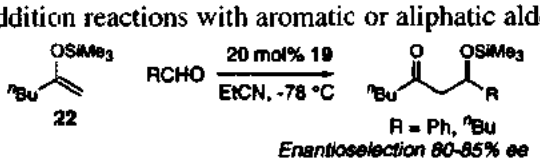

(6)

Internal enol silanes **23** and **24** afford similarly high levels of enantioselection and commensurately high relative stereocontrol in CAB-catalyzed additions to benzaldehyde (Eqs. 7 and 8).

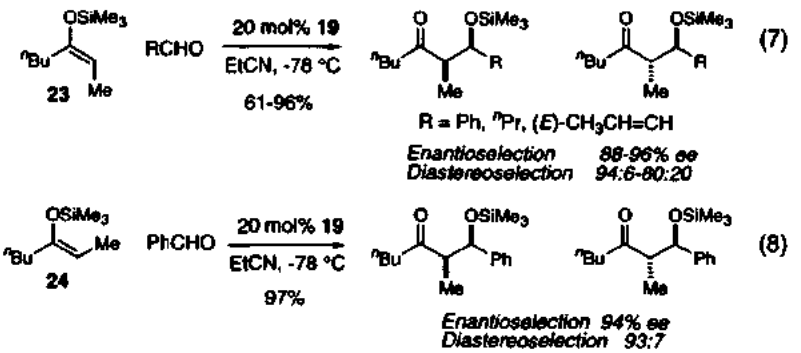

Lower catalyst loadings (10 mol%) may be used and modest increases in enantioselection are achieved when the arylboronic acids **20** and **21**, respectively, are employed as catalysts.[16b] Analogous aldol additions employing aliphatic aldehyde electrophiles suffer from attenuated levels of diastereo- and enantioselectivity relative to those values obtained using benzaldehyde. Reaction diastereoselection is insensitive to the stereochemistry of the substituted enolate equivalents; both (*E*) and (*Z*) enol ethers selectively provide the *syn* aldol diastereomer (Fig. 7). This result is suggested to provide evidence that these reactions are proceeding via open, extended transition states; minimization of close contact between the enolate substituent R_1 and the aldehyde alkyl residue R_2 in the transition state lead, preferentially, to the *syn* aldol adducts regardless of the initial enolate geometry.[18]

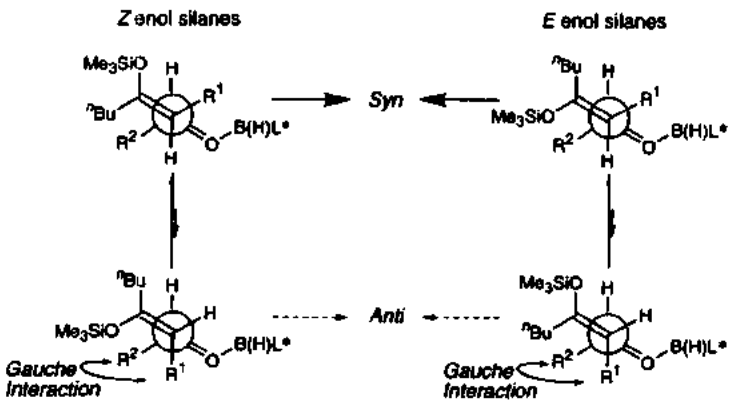

Fig. 7. Transition states for CAB-catalyzed additions of β-substituted enol silanes

An investigation into the effectiveness of silyl ketene acetals as nucleophiles in CAB-catalyzed Mukaiyama aldol reactions revealed an interesting relationship between reaction stereoselectivity and the identity of the ketene acetal *O*-alkyl substituent. Under the reaction conditions optimized for catalyzed enol silane additions (20 mol% CAB catalyst, EtCN, −78°C), aldol reactions employing *O*-ethyl silyl ketene acetals provided stereorandom mixtures of diastereomeric aldol adducts.[19] In contrast, the phenyl acetate-derived enolate equivalent **25** provided good to moderate asymmetric induction in CAB-catalyzed aldol reactions (Table 3). Analogous levels of enantioselection were achieved using the β-substituted silyl ketene acetal **26**, with α,β-unsaturated aldehydes providing optimum chemical yields and stereoselectivity, delivering aldol adducts with both diastereo- and enantioselection in excess of 90% (entries f and g). The role that *O*-phenyl substitution within the enolate plays in influencing the stereochemical course of these reactions (the 'phenyl ester effect') is currently undefined; however, this effect subsequently proved to be operative in other Lewis acid catalyzed aldol reactions. Silyl ketene acetal **27a**, derived from the commercially available 1,3-dioxin-4-ones, has been investigated as another

Table 3
CAB-catalyzed aldol additions of silyl ketene acetals

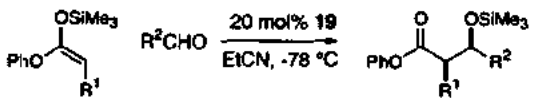

entry	ketene acetal	aldehyde	% yield	*syn*:*anti*	% ee (*syn*)
a	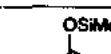 25	PhCHO	63	NA	84
b		^{n}PrCHO	49	NA	76
c	 26	PhCHO	83	79:21	92
d		^{n}PrCHO	57	65:35	68
e	26	^{i}PrCHO	45	64:36	79
f	26	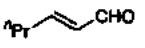	97	96:4	97
g	26	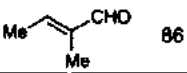	86	>95:5	94

class of nucleophile in CAB-catalyzed aldol reactions with limited success; reactions require high catalyst loadings and deliver only moderate levels of enantioselectivity (Eq. 9).[20,21]

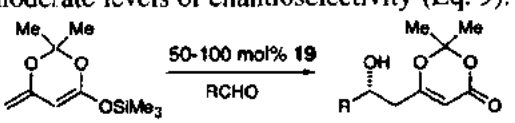

27a

Enantioselection 36-73% ee

Acyloxyborane catalyst systems share several of the procedural requirements for achieving highly stereoselective aldol additions associated with the $Sn(OTf)_2$-diamine catalysts. Lewis basic solvents such as propionitrile or nitromethane were found to elicit optimum catalyst efficiency, suggesting that Lewis base accelerated silicon-transfer to the putative aldolate intermediate is required to facilitate catalyst turnover in both the CAB and Sn(II) catalyst systems. Furthermore, relatively high catalyst loadings ($\geq$20 mol%) are required to achieve the indicated levels of stereoinduction. Whether these catalyst loadings reflect an attempt to ensure the chiral catalyzed reaction kinetically dominates competitive catalysis by adventitious Lewis acidic species (silicon catalysis), or are indicative of an inherent lack of catalytic competency of the CAB complexes, with higher loadings being required to drive the reaction to completion, is unclear.

A transition state model that rationalizes the observed sense of asymmetric induction in acyloxyborane-catalyzed aldol reactions has been developed in the context of related CAB-catalyzed Diels–Alder cycloadditions (Fig. 8). Solution and solid state conformational analysis of CAB complexes of various α,β-unsaturated aldehydes by NOE measurements and X-ray crystal structure determination, respectively, reveal that the Lewis acid–base complexes adopt a folded conformation that aligns the aldehyde and aromatic π-systems to engage in face-to-face π-stacking interactions.[22] Similar conformational preferences in the activated (*R*,*R*)-CAB catalyst–aldehyde complex **28** would expose the aldehyde (*re*) diastereoface to nucleophilic attack, delivering the observed aldol adduct **29**.

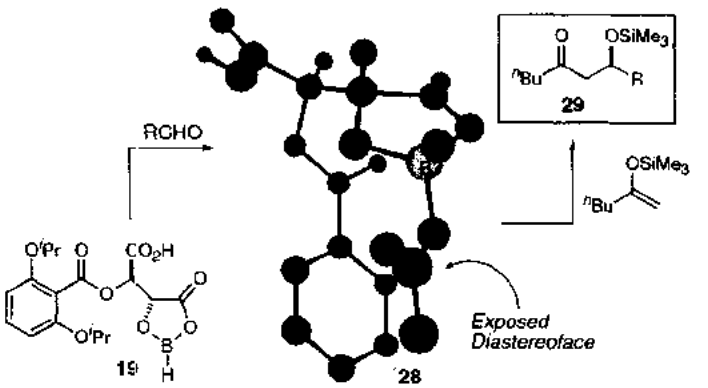

Fig. 8. Chiral (acyloxy)borane–aldehyde complex

3.2. Oxazaborolidine catalysts

3.2.1. Catalysts incorporating α,α-disubstituted amino acids

Oxazaborolidine complexes share considerable structural homology with (acyloxy)borane Lewis acids and, accordingly, have been investigated as catalysts for effecting asymmetric Mukaiyama aldol addition reactions. Structurally similar oxazaborolidine complexes have been investigated by several research groups as potential aldol catalysts. In one of these studies, optically active α,α-disubstituted amino acids were identified as essential components of catalytically competent oxazaborolidine aldol catalysts based upon speculation regarding the mechanism by which oxazaborolidine complexes would mediate Mukaiyama-type bond constructions.[23] Either of the catalyst complexes **30** and **31**, derived from relatively easily obtained α,α-disubstituted α-amino acids, provide near-perfect enantioselection (≥97% ee) in addition reactions of the disubstituted silyl ketene acetal **32** with unbranched aliphatic aldehydes (Eq. 10).

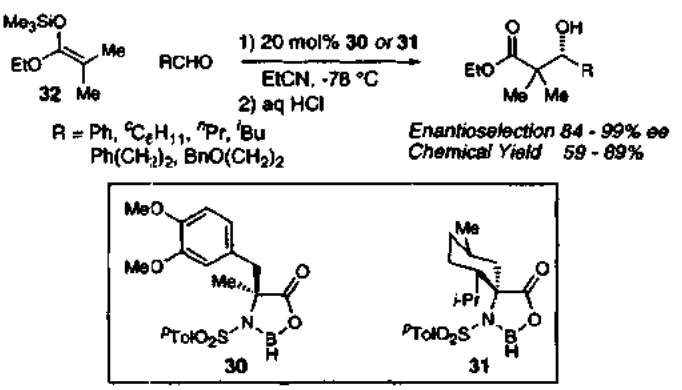

(10)

In contrast to the Sn(II)-based aldol catalysts, oxazaborolidine complexes are proposed to offer an active mechanism for scavenging electrophilic silicon species generated during the reaction cycle, an event previously determined to be imperative for achieving efficient chirality transfer and catalyst turnover (Fig. 9). Specifically, the silyl oxocarbenium ion **33** that emerges from initial nucleophilic addition situates the boron carboxylate to effect intramolecular silicon transfer in providing the boron aldolate **34**, thereby precluding the potential for silicon (achiral) catalysis that might be initiated by such electrophilic silicon species. Regeneration of the five-membered boron heterocycle provides an enthalpic impetus for ensuing silicon transfer to the aldolate oxygen, thereby liberating the silylated

aldol adduct with concomitant turnover of the oxazaborolidine catalyst. Catalyst liberation from the aldolate intermediate was postulated to be the rate-limiting step and, thus, disubstitution of the catalyst's amino acid backbone was considered a mechanism for facilitating catalyst turnover by accelerating oxazaborolidine ring closure, and the attendant silicon transfer event, by virtue of the Thorpe–Ingold effect. The efficiency of the essential intramolecular silicon transfer event is questionable, however, as slow addition of the nucleophile to the reaction mixture is still required to achieve high enantiomeric excesses.

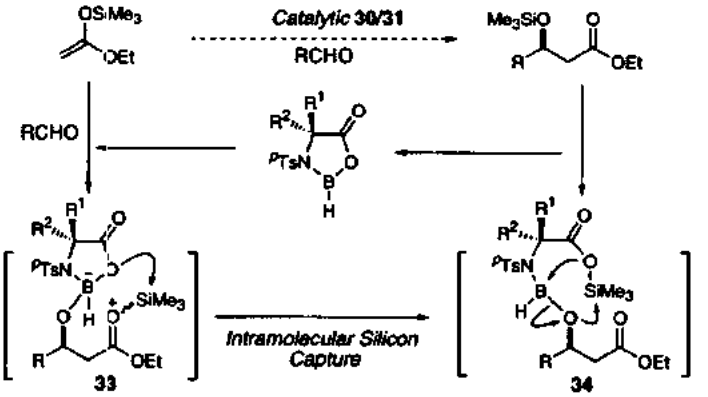

Fig. 9. Silicon-shuttle mechanism for oxazaborolidine-catalysis

Enantioselection in the oxazaborolidine catalyzed aldol reactions exhibits a pronounced dependence on nucleophile structure, with some attenuation of asymmetric induction being derived from ketene acetals other than **32**.[24] The *O*-phenyl or *S*-*t*-butyl silyl ketene acetals **25** and **35** provide the derived acetate aldol adducts **36** (R^1=OPh or S*t*-Bu) with enantiomer ratios ≥91:9; the menthone-derived catalyst **31** provided optimum enantioselection in addition reactions employing these ketene acetal nucleophiles (Table 4). Furthermore, the 'phenyl ester effect' enumerated by Yamamoto proved to be operative in these oxazaborolidine-catalyzed reactions as other *O*-alkyl-substituted ketene acetals afforded little to no stereoinduction. Propionate aldol products can also be obtained from the catalyzed aldol reactions employing (*E*) propionate enolate equivalents **37**; however, useful levels of relative and absolute stereoinduction are achieved in a limited number of cases (Eq. 11).

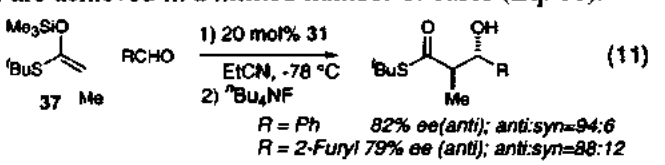

(11)

Diastereo- and enantioselectivity in the propionate aldol reactions are highly variable, exhibiting a marked dependence on the identity of both the nucleophilic and electrophilic reaction components. In fact, the highest levels of asymmetric induction are achieved in the minor diastereomeric aldol adduct. The predominance of the *anti* aldol diastereomer derived from the catalyzed propionate aldol reactions is in contrast to the diastereoselection observed in CAB and Sn(II)[diamine]-catalyzed reactions of β-substituted enolate equivalents that uniformly provide the *syn* aldol adduct as the major reaction product.

3.2.2. Valine-derived complexes

Kiyooka[25] and Corey[26] have independently developed oxazaborolidine complexes derived from simple, naturally occurring α-amino acids as effective catalysts for the addition of ketene acetals and enol

Table 4
Oxazaborolidine **31**-catalyzed acetate aldol reactions

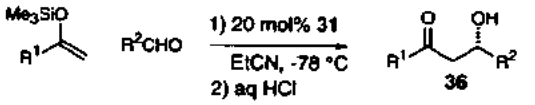

entry	R^1	aldehyde	% yield	% ee
a	S^{t}Bu (35)	PhCHO	86	87
b	OPh (25)	PhCHO	77	93
c	S^{t}Bu	$Ph(CH_2)_2CHO$	77	91
d	OPh	$Ph(CH_2)_2CHO$	78	85
e	S^{t}Bu	$^cC_6H_{11}CHO$	75	81
f	OPh	$^cC_6H_{11}CHO$	87	84
g	S^{t}Bu		91	82
h	S^{t}Bu	(2-furyl)CHO	98	95

silanes, respectively, to various aldehyde electrophiles. In an initial disclosure, stoichiometric quantities of oxazaborolidine **38a** were reported to mediate the addition of **32** to hydrocinnamaldehyde with relatively high optical and chemical yields (87% yield, 93% ee).[27] More significantly, the product distribution derived from the oxazaborolidine-mediated aldol reactions was found to be sensitive to the structure of the ketene acetal silyl group. Trimethylsilyl ketene acetal **32** provided the anticipated aldol adducts **39** exclusively (83–93% ee), while the *t*-butyldimethylsilyl ketene acetal **40** afforded the silyl acetal **41** as the predominant reaction product (92–98% ee) (Eq. 12)

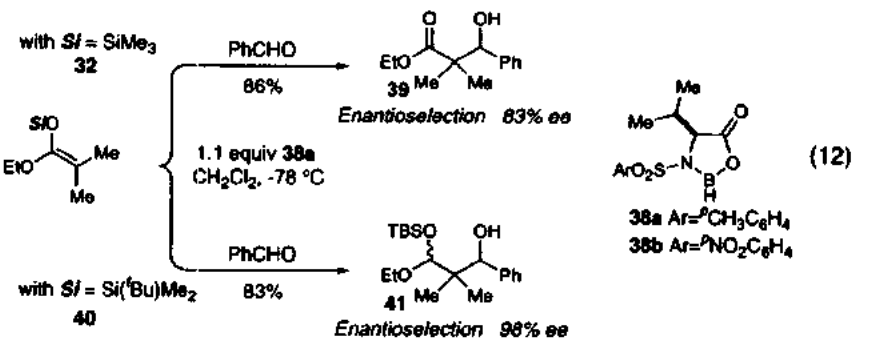

Acetal formation results from a partitioning of the reaction pathway that typically leads to aldol adducts (c.f., Fig. 9) elicited by slow transmetallation of the boron–aldolate intermediate **42** (Fig. 10). Reaction variables that function to slow silyl transfer to the aldolate oxygen, such as the poor migratory aptitude of *t*-butyldimethylsilyl groups, allow hydride migration to the carbonyl carbon to compete effectively with the silicon transfer event that affords the typical aldol adducts. Hydrolysis of the resulting azaborate **43** upon work-up provides the observed β-hydroxy acetal **41**.

These observations have led to the direct preparation of optically active *syn* 1,3-diols by the tandem asymmetric aldol addition–diastereoselective carbonyl reduction promoted by optically active oxazaborolidine complexes.[28] Oxazaborolidine-mediated (1.0 equiv **38a**, EtCN, −78°C) addition of terminal enol silanes **44** to a limited number of aldehydes afford the derived *syn* diols **45** as the major reaction products (53–70%), regardless of silyl group structure, with the corresponding aldol adduct **46** com-

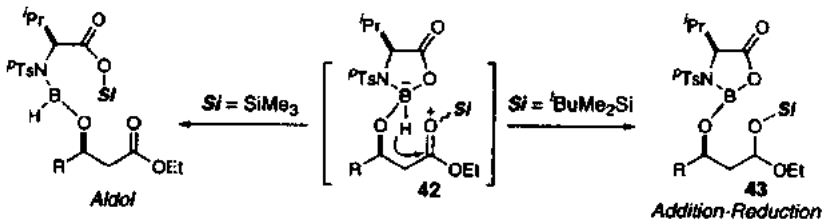

Fig. 10. Mechanism for competing addition–reduction reactions

Table 5
Oxazaborolidine-mediated tandem asymmetric aldol–reduction reaction

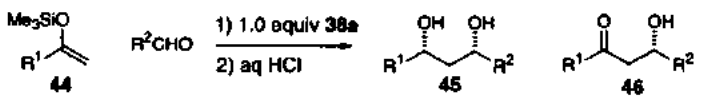

			45		46	
entry	R^1	R^2	% yield (*syn*:*anti*)	% ee (*syn*)	% yield	% ee
a	Ph	$^iC_3H_7$	65 (97:3)	99	17	60
b	BnO(CH$_2$)$_2$	$^iC_3H_7$	55 (89:11)	86	15	67
c	$^nC_6H_{13}$	$^iC_3H_7$	70 (90:10)	99	23	60
d	$^nC_6H_{13}$	$^nC_3H_7$	66 (90:10)	98	25	49
e	$^nC_6H_{13}$	Ph	53 (97:3)	85	18	72

prising the remainder of the product mixture (6–25%) (Table 5). Selectivity for the formation of the *syn* diol diastereomer is high (*syn*:*anti*=89:11–97:3) with enantioselection generally exceeding 94% ee. The enantiomeric purity of the 1,3-diols is substantially higher than that of the accompanying aldol products suggesting that reduction of the intervening diastereomeric β-keto azaborate complexes (c.f., **47**) is subject to double stereodifferentiation (Fig. 11). While several transition state models rationalizing diastereoselectivity for the carbonyl reduction are advanced, reaction via a non-chelated transition state **48** in which hydride is delivered to the silicon-activated carbonyl residue finds considerable precedence in closely related (triacetoxy)borohydride-mediated reductions of similar β-hydroxy carbonyls.[29] In addition to being a more reactive electrophile, the silyl oxocarbenium ion may also serve to create a conformational preference for orienting the silyloxy function in the pseudo-equatorial position in transition state assembly **48**. In the absence of such conformational perturbations, the related substrate-directed reductions of β-hydroxy ketones exhibit a strong proclivity for providing the 1,3-*anti* diol adducts via the transition state assembly **49** in which the carbonyl oxygen occupies the pseudo-axial orientation.

Solvent also plays an important role in defining the mechanistic course of these oxazaborolidine-mediated ketene acetal–aldehyde addition reactions.[25] Aldol addition of MTMP (**4**) that requires stoichiometric quantities of **38a** in CH_2Cl_2 could be executed in high yield with 20 mol% of **38b** if nitroethane was substituted as the reaction solvent. While the mechanistic details of the reaction were not investigated, nucleophilic assistance provided by the Lewis basic solvent was postulated to sufficiently accelerate silyl transfer to the intervening boron aldolate such that catalyst turnover was realized. This hypothesis is consistent with the notion that Lewis acid–base association of nitroethane and boron in the aldolate intermediate would amplify the nucleophilicity of the alkoxide oxygen. Under these reaction conditions, **38b** catalyzes the addition of MTMP (**4**) to a limited set of aldehyde electrophiles with enantioselection exceeding 90% ee. However, the unsubstituted ketene acetal **25** and/or α,β-unsaturated

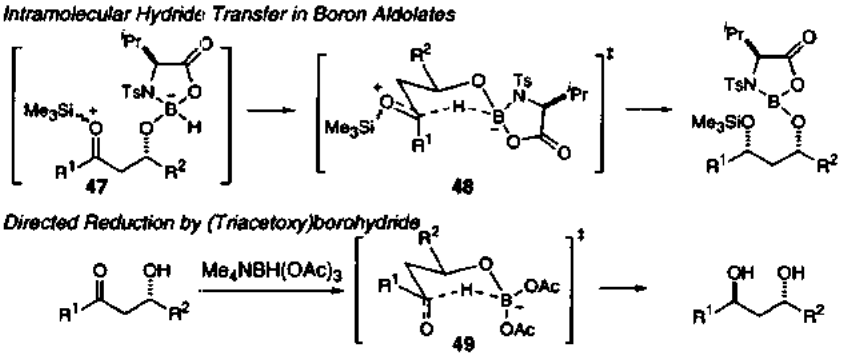

Fig. 11. Diastereoselective reduction of boron aldolates

or α-branched aldehydes afford significantly eroded levels of asymmetric induction (Eq. 13). Moreover, the (*E*) enolate equivalent **26** provides low levels of diastereoselection, although asymmetric induction in the major diastereomer is relatively good (90% ee) in one trial.

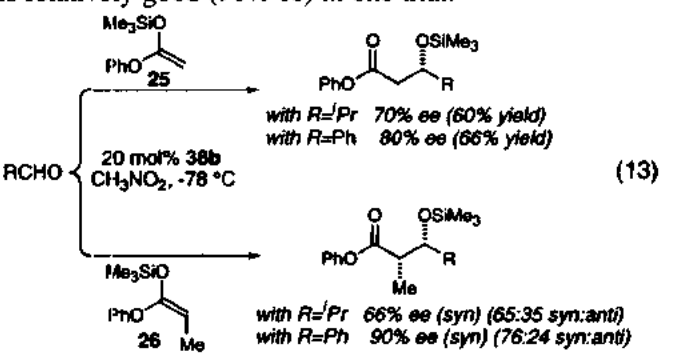

3.2.3. Tryptophan-derived complexes

Tryptophan-derived oxazaborolidine **50** has also undergone development as a catalyst for the asymmetric addition of trimethylsilyl enol ethers to various aldehydes.[26] Enantioselectivity in the catalyzed aldol reactions utilizing terminal enol silanes **23** and **51** is superior to that obtained in analogous CAB-catalyzed additions, with enantioselection generally exceeding 89% ee (Eq. 14). However, the oxazaborolidine **50** shares the relative lack of catalyst efficiency common to other boron-derived aldol catalysts, a fact alluded to by the high catalyst loadings required for these reactions and the high percentages of unreacted aldehyde that are recovered in several instances. Nonetheless, the oxazaborolidine catalyst **50** provides an expedient entry to optically active dihydropyrone derivatives via aldol addition reactions of dienyl enol silanes. Nucleophilicity of the silyloxy diene **52** is expressed exclusively by the enol silane terminus, providing the vinylogous ester **53** upon catalyzed aldol addition; acid-promoted cyclization then affords the dihydropyrone **54** with good to moderate levels of optical purity (Eq. 15).

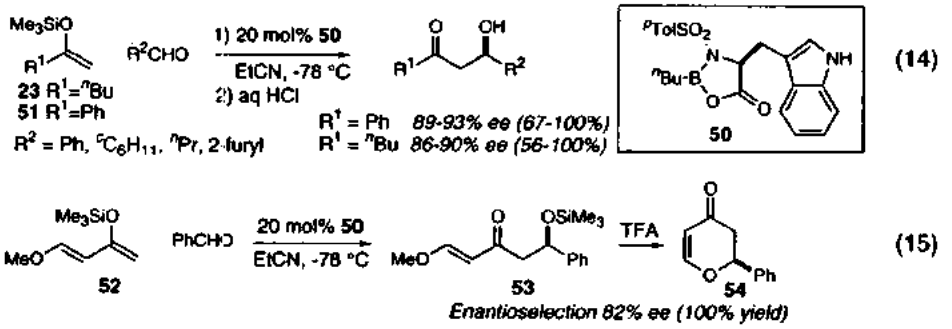

Despite the structural homology existing among the various oxazaborolidine Lewis acids, an analysis of aldol stereoselection derived from each of these catalysts reveals some divergence in the operative stereochemical control elements. Enantioselectivity in aldol reactions catalyzed by the disubstituted oxazaborolidines **30** and **31** or the valine-derived complex **38b** is consistent with steric shielding provided by the amino carboxylate alkyl substituent forcing aldehyde association to occur from the opposite face of the oxazaborolidine ring (Fig. 12). Pyramidalization of the sulfonamide nitrogen due to 'gearing' interactions with the backbone alkyl substituent in the resulting Lewis acid–base complex **55** then orients the sulfonamide residue to effectively shield the (*re*) aldehyde diastereoface.[30] In contrast, Lewis base coordination to boron in the tryptophan-derived catalyst **50** occurs *syn* to the indole substituent, suggestive of an attractive π–π interaction between the carbonyl and indole moieties in the activated aldehyde complex **56**.[31] The resulting preorganization of the coordinated aldehyde leaves the aldehyde (*re*) face exposed to nucleophilic attack.

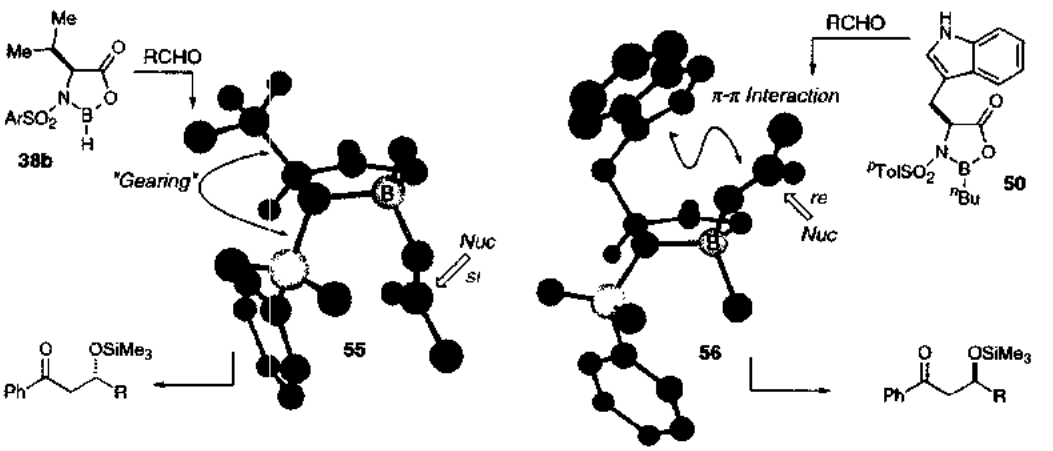

Fig. 12. Origin of enantioselectivity in oxazaborolidine-catalyzed aldol reactions

4. Early transition metal catalysts: Ti(IV)

4.1. Introduction

Titanium-based complexes are among the most widely utilized Lewis acids in organic chemistry and, as such, have undergone considerable development as vehicles for effecting asymmetric catalytic

Mukaiyama aldol reactions.[32] Indeed, the Ti(IV)-promoted addition of silyl ketene acetals to carbonyl compounds was among Mukaiyama's initial observations during preliminary investigations of these C–C bond constructions.[3c] Subsequent studies revealed that even relatively weak Lewis acids efficiently promoted these reactions, implicating modified Ti(IV) complexes possessing substantially attenuated Lewis acidities relative to $TiCl_4$ as potential catalysts for aldol addition reactions.[8b] As a result, tetra(alkoxy)titanium complexes were identified as effective catalysts for addition reactions employing a variety of silylated enolate equivalents. Furthermore, tetra(alkoxy)titanium complexes provided for the expedient synthesis of chiral catalyst structures by exploiting the facile substitution of monodentate alkoxide ligands for chelating optically active diols.

Among the numerous chiral Ti(IV) complexes that are available from optically active chelating diols, Lewis acids derived from binaphthol have undergone the largest degree of development as catalysts for the Mukaiyama aldol reaction.[33] Reetz was the first to report enantioselective Mukaiyama aldol reactions catalyzed by Ti(IV) complexes modified with chiral ligands.[6] The Ti–BINOL complex **1**, obtained by the substitution reaction of $TiCl_4$ with the bis-lithium alkoxide of (*S*)-binaphthol, catalyzed (20 mol%) the addition of MTMP (**4**) to isobutyraldehyde with minimal enantioselection (8% ee) (Scheme 2). A close structural analog to the putative Ti–BINOL catalyst investigated by Reetz, the chiral (BINOL)Ti–oxo complex **57**, catalyzes the addition of *t*-butyldimethylsilyl thioketene acetals to a limited number of aromatic and α,β-unsaturated aldehydes with good to modest levels of enantioselection.[34] These two early studies portend an observation that would pervade subsequent development of Ti-based Lewis acids as catalysts for asymmetric aldol reactions: reaction enantioselection is highly sensitive to minor variations in catalyst preparation and, presumably, the solution-state structure that is derived therefrom, resulting in nearly identical catalyst systems providing dramatically different results, ranging from negligible to nearly perfect asymmetric induction.

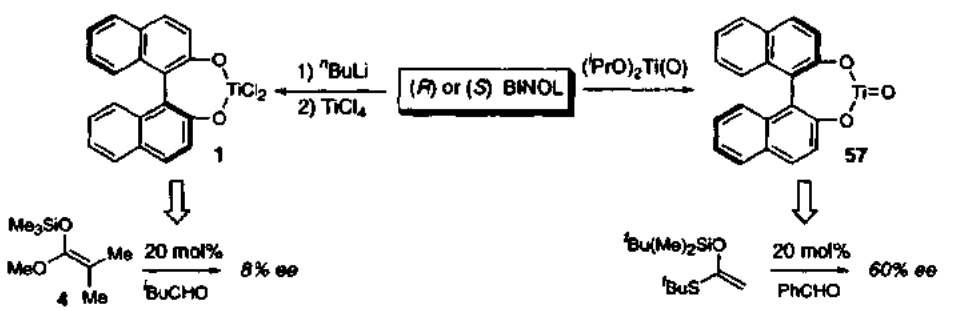

Scheme 2.

4.2. *Ti(IV)[BINOL]-catalyzed aldehyde ene reactions*

4.2.1. *Ene addition reactions of enolsilanes*

The Ti(IV)-BINOL complex **58** provides an exceptionally efficient catalyst for the asymmetric addition of silyl enol ethers to glyoxylate esters and silyl ketene acetals to aldehydes.[35,36] The Ti(IV) complex **58**, prepared by the exchange reaction of (*R*)-BINOL with $Cl_2Ti(O\textit{i}\text{-}Pr)_2$ in the presence of 4 Å molecular sieves, catalyzes (5 mol%) the addition of the enol silanes **59a–d** to alkyl glyoxylate esters to afford the homoallylic alcohols **60** with ≥99% ee (54–75% yield) (Table 6).[37] Isolation of the enol silanes **60** as the sole products from these reactions was inconsistent with the mechanistic paradigm previously associated with Mukaiyama aldols, indicating Mukaiyama-type addition reactions to be mechanistically more complex than originally believed. A Lewis acid catalyzed ene reaction pathway was offered as

Table 6
Ti[BINOL]-catalyzed ene addition reactions

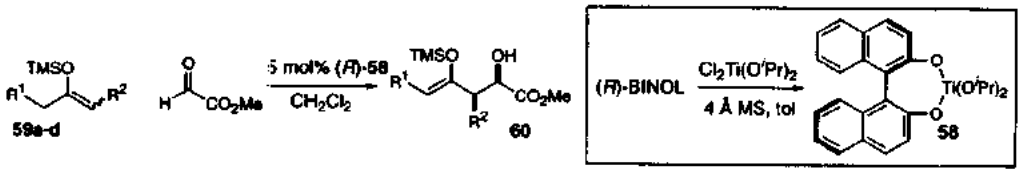

entry	enol silane	% yield	*syn*:*anti*	(Z):(E)	% ee
a	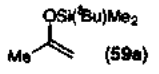 (59a)	75	NA	NA	>99
b	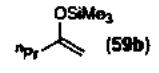 (59b)	67	NA	95:5	>99
c	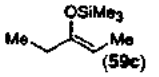 (59c)	58	98:2	94:6	99
d	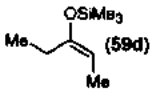 (59d)	54	98:2	94:6	99

a mechanistic alternative that accommodated the salient characteristics of these reactions including product structure, the olefin geometry of the derived enol silane adducts, and the insensitivity of reaction diastereoselection to enolate geometry (Fig. 13).[38] Thus, terminal enol silanes **59a** and **59b** provide the corresponding ene products with near perfect asymmetric induction and, in the latter case, high selectivity for the formation of the *Z* olefin isomer (*Z*:*E*=95:5). Substituted silyl enol ethers **59c** and **59d** afford analogously high enantiomeric excesses and excellent fidelity for the formation of the *syn* aldol diastereomer.

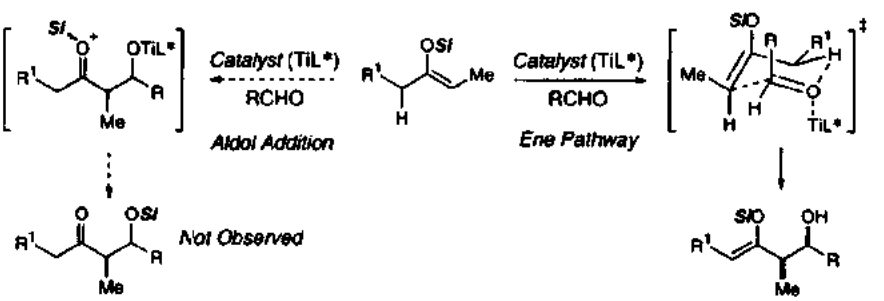

Fig. 13. Ene reaction pathway for enol silane addition reactions

The stereoselection exhibited by these reactions has been proposed to derive from the intrinsic conformational preferences associated with the competing ene reaction transition states (Fig. 14).[35] Reaction of *E* enol silanes provide *Z*, *syn* addition products **61** via the closed transition state assembly **62** that alleviates the developing *syn*-pentane interaction incurred between the pseudoaxial alkyl substituent (R_2) and titanium ion in the alternate assembly **63**. In the absence of incipient transannular interactions, the developing gauche interaction incurred between the ester residue and the enol silane substituent (R_2) in **64** appears to be the dominant influence in the reaction of *Z* enolate equivalents; the closed transition state **65** that eliminates this non-bonded interaction predicts the observed sense of stereoselection. There must exist a relatively subtle interplay of interactions that operate to differentiate the various transition

structures as reactions of *E* enol silanes appear to proceed via a chelated Lewis acid–glyoxylate complex (**62**) while a non-chelated Ti(IV)–aldehyde complex (**65**) seems involved in the reaction of *Z* enol silanes.[39] For example, the transannular interaction incurred in **63** is apparently sufficient to destabilize the transition state involving the monodentate Ti(IV)–glyoxylate complex, but is insufficient to disrupt organization of the alternative transition state **62** that incorporates the chelated glyoxylate complex. Furthermore, transition structure **65** neglects consideration of the transannular interaction that would exist between the pseudoaxial silyloxy and ester groups, raising as a possible reaction manifold addition of *Z* enol silanes via an open transition state that mitigates such steric interactions.[40]

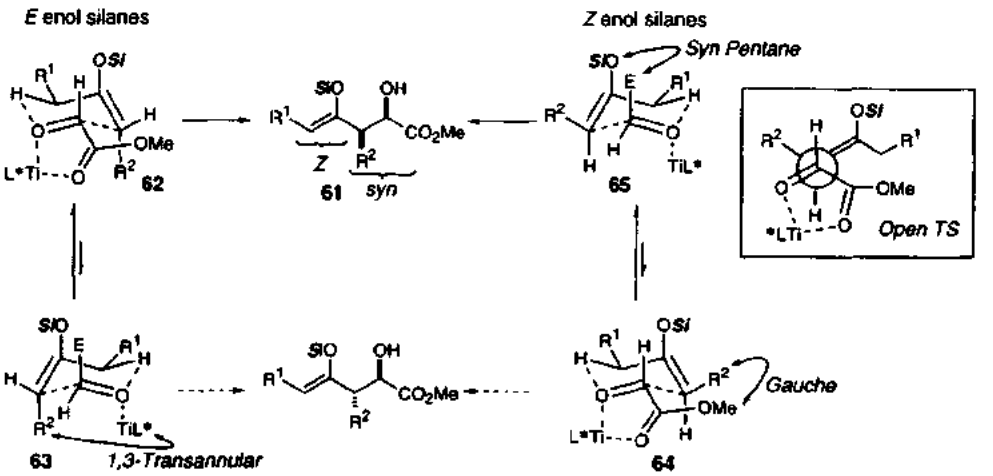

Fig. 14. Competing transition states for Ti[BINOL]-catalyzed ene reactions

4.2.2. *Silatropic ene reactions of silyl ketene acetals*

Mikami has also found a related ene reaction pathway to be operative in the Ti[BINOL]-catalyzed addition of silyl ketene acetals to aldehydes.[41] Low catalyst loadings of the titanium complex **58** (5 mol%) mediate the addition of thioacetate-derived enolate **14** to a number of functionalized aldehydes with uniformly high levels of enantioselectivity (Eq. 16).[42] A silatropic ene reaction pathway was hypothesized to be operative in these reactions based on a series of crossover experiments involving 'labeled' ketene acetal nucleophiles (Eq. 17).

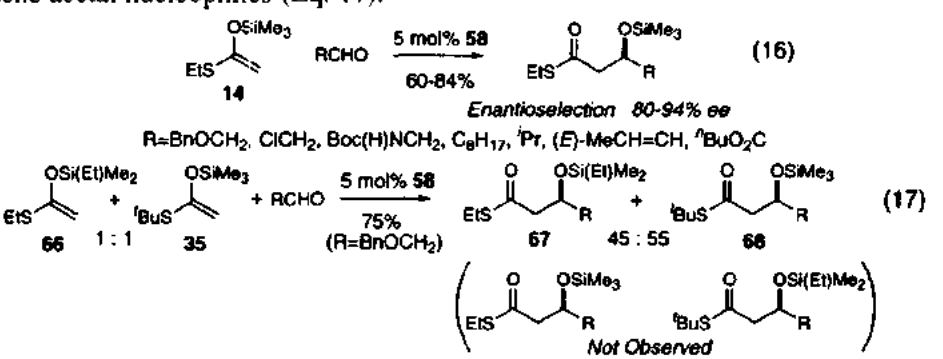

The catalyzed addition of an equimolar mixture of silyl ketene acetals **35** and **66** to α-benzyloxy acetaldehyde affords a ~1:1 mixture of the two aldol products **67** and **68**, while none of the crossover products were detected. This result provides persuasive evidence for a reaction mechanism that proceeds

with concerted silyl group transfer to the incipient aldolate oxygen; a silatropic ene reaction (Scheme 3). Thus, C–C bond construction proceeds via the Zimmerman–Traxler transition state assemblies **69** and **70** involving concerted silicon transfer from the enolate to the electrophile oxygen. Relative stereocontrol in these reactions, (*Z*)-*O*-enolate equivalent **71** affords *anti* aldol adducts **72** while (*E*)-*O*-ketene acetal **8** provides the *syn* diastereomers **73**, is consistent with the documented relationship existing between metalloenolate geometry and aldol reaction diastereoselectivity derived from Zimmerman–Traxler transition states.[2] In order for the proposed closed transition structures to be operative, the coordination geometry typically associated with Lewis acid–aldehyde complexes must be relaxed to accommodate titanium coordiantion *syn* to the aldehyde alkyl residue or, at least, significantly out of the carbonyl π-plane.[43]

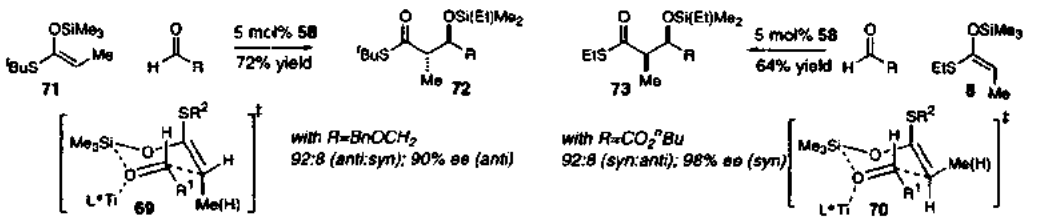

Scheme 3.

4.3. *Ti(Oi-Pr)4[BINOL] catalyst systems*

The striking contrast in results obtained in the Reetz and Mikami investigations of closely related reactions employing catalyst systems that are proposed to be nearly identical in constitution, highlights the pronounced sensitivity to reaction variables that characterize asymmetric Ti(IV)-catalyzed aldol reactions. This aspect of Ti-based Mukaiyama aldol catalysts was further emphasized during Keck's development of Ti(IV) complexes derived from Ti(O*i*-Pr)$_4$ and BINOL [1:1 Ti(O*i*-Pr)$_4$:BINOL=Catalyst A] as catalysts for the enantioselective addition of acetate enolate equivalent **25** to aldehydes (Table 7).[44,45] Ultimately, the derived catalysts were found to provide excellent levels of enantioselectivity for aldol additions employing an array of structurally diverse aldehydes. Some generality in nucleophile structure is also offered by these catalyst systems as silyloxy(dienes) **52** also add to aldehydes with good to excellent asymmetric induction using a similar Ti(O*i*-Pr)$_4$[BINOL]-derived catalyst system [2:1 Ti(O*i*-Pr)$_4$:BINOL=Catalyst B] (Eq. 18).[46] The resulting β-hydroxy vinylogous esters **74** are converted to the corresponding optically active dihydropyrone derivatives **75** upon treatment with acid. However, optimum chemical and optical yields in the Ti(O*i*-Pr)$_4$[BINOL]-catalyzed aldol reactions are achieved only within a narrow reaction parameter window; conversion and enantioselection are extremely sensitive to the method of catalyst preparation, reaction solvent, and catalyst loadings. Relatively minor deviations from this optimized reaction protocol (e.g., use of 10 mol% catalyst rather than the 20 mol% specified) result in reduced conversion and/or enantioselection.

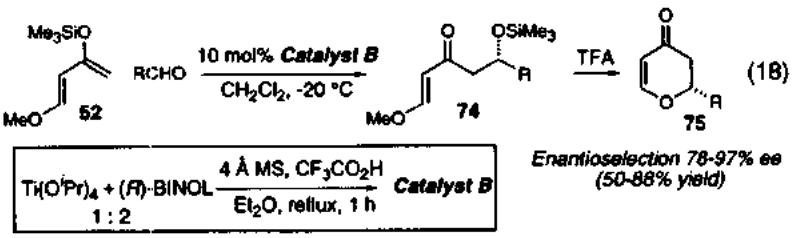

Keck emphasizes, and these sentiments are reinforced here, that little to no conclusive evidence exists concerning the solution state structures of the Ti(IV)[BINOL] complexes utilized in this study or the

Table 7
Ti(O*i*-Pr)$_4$[BINOL]-catalyzed Mukaiyama aldol reactions

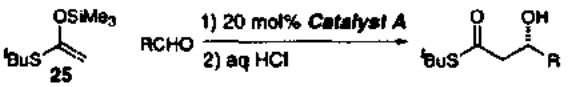

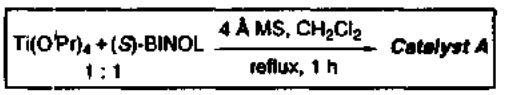

entry	aldehyde	% yield	% ee[a]
a	PhCHO	90	97
b	PhCHO	71	97[b]
c	PhCHO	45	92[c]
d	$Ph(CH_2)_2CHO$	80	97
e	$^nC_8H_{17}CHO$	74	98
f	(2-furyl)CHO	88	>98
g	$^cC_6H_{11}CHO$	70	89
h	(*E*)-PhCH=CHCHO	76	89
i	$BnOCH_2CHO$	82	>98

[a]Reported values are for reactions employing 20 mol% catalyst and 0.25M in aldehyde, except entries b and c. [b]Reaction using 10 mol% catalyst. [c]Reaction 0.50M in PhCHO.

other investigations involving Ti-based catalyst systems. The structural representations of the presumed Ti-based catalysts presented herein are intended to represent only the metal:ligand stoichiometry used in the published preparation of these catalysts and are not intended to depict solution-state structures of the catalytically active species. Indeed, the nonlinear relationship that exists between catalyst optical purity and reaction enantioselection documented by Keck[47] and Mikami[48] in related Ti–BINOL-catalyzed reactions is indicative of catalyst aggregation in solution.

Dienyl ketene acetal **27a** and **b**, prepared from the corresponding dioxinone derivative, provide limited degrees of success in Ti(O*i*-Pr)$_4$[BINOL]-catalyzed addition reactions (Eq. 19).[49] Chemical and optical yields of the β-hydroxy dioxinone aldol adducts **76** vary considerably with chemical yields generally below 60% and enantioselection exceeding 90% ee in only two instances. The dioxinone aldol products **76** can be converted to the corresponding acetone aldol adducts **77** upon thermolysis in water.

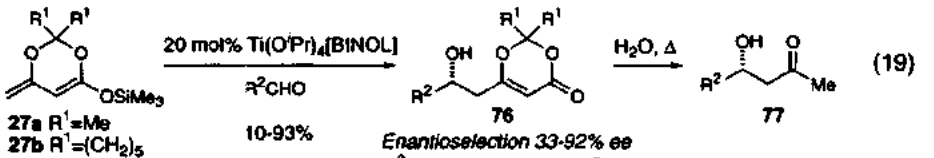

(19)

4.4. *Ti(IV)–Schiff base catalysts*

4.4.1. *Salicylate-modified complexes for silyl ketene acetal additions*

Analysis of the preceding investigations reveals a conspicuous lack of catalyst systems that effectively mediate the aldol addition of simple *O*-alkyl ketene acetals with uniformly high enantioselection. The amplified reactivity and sensitivity of *O*-alkyl silyl ketene acetals relative to their thioketene and silyl enol ether analogs is considered a contributory factor in the generally inferior results obtained in catalyzed Mukaiyama aldol reactions employing this class of nucleophile.[50] Mechanistic investigations suggest that the intervention of a silicon-catalyzed reaction manifold that is independent of the initial

chiral metal catalyst is responsible for the observed lack of asymmetric induction derived from *O*-alkyl ketene acetal addition reactions.[12] These mechanistic considerations proved instrumental in the design and development of chiral Ti–Schiff base complexes that are remarkably efficient catalysts for the enantioselective addition of simple *O*-alkyl ketene acetals to a wide array of functionalized aldehyde electrophiles.[51] The parent Ti(IV) catalyst is prepared by the reaction of the axially chiral Schiff base **78** with Ti(O*i*-Pr)$_4$ to provide the putative catalyst structure **79** (Eq. 20). In a preliminary investigation, **79** was found to catalyze the aldol addition of the ethyl acetate derived ketene acetal **80**, affording a mixture of unsilylated and silylated aldol adducts, **81** (78% ee) and **82** (64% ee), respectively (Eq. 21).

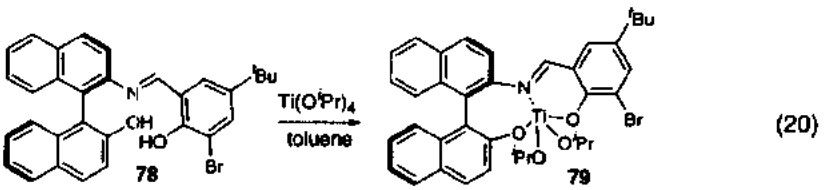

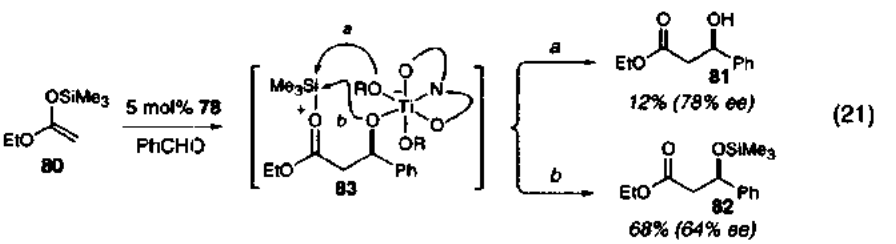

Isolation of the carbinol **81** was consistent with a reaction mechanism proceeding through Ti–aldolate **83** in which indiscriminate silicon transfer to either an isopropoxide ligand or the aldolate would account for the observed product distribution. Efficient transfer of the silicon residue to the aldolate oxygen had previously been identified as a prerequisite for limiting silicon-catalyzed reaction pathways that might be initiated by silyl oxocarbenium ion intermediates similar to **83**. As a means of engineering catalyst structures that would provide a mechanism for facilitating the requisite silicon-to-aldolate oxygen transfer, modified catalyst complexes incorporating salicylic acid-derived ligands were investigated (Fig. 15). Indeed, the Schiff base complex **84** incorporating the 3,5-di-*t*-butylsalicylic acid ligand afforded dramatically enhanced yields, enantioselectivity, and catalyst efficiency relative to the parent Schiff base complex **79**. The salicylic acid ligand is postulated to function as a silyl group shuttle, scavenging electrophilic silicon species at the stage of the silyl oxenium ion intermediate **85**. The resulting silyl carboxylate **86** is then suitably disposed to provide for eventual silylation of the aldolate oxygen, the most nucleophilic of the oxygen ligands arrayed about the Ti ion. Thus, aldolate silylation liberates the protected aldol adduct and reestablishes the salicylic acid chelate in regenerating the catalyst complex **84**. This mechanistic construct finds a close analogy to the silicon shuttle mechanism proposed to be operative in oxazaborolidine-catalyzed aldol reactions.[23]

The Ti(IV)–Schiff base catalyst system **79** developed by Carreira is unique among the aldol catalysts reported to date in terms of operational simplicity, catalyst efficiency, chirality transfer, and substrate generality. Enolate equivalents derived from inexpensive, readily available methyl or ethyl acetate (**87**) react with alkenyl, alkynyl, aromatic, and functionalized aliphatic aldehydes using the Ti–salicylate catalyst **84** to afford the corresponding β-hydroxy esters **88** with near perfect enantioselection (≥94% ee) (Table 8). Furthermore, high yields of the enantiomerically enriched aldol adducts are obtained using catalyst loadings as low as 2 mol% and do not require slow addition protocols. The Ti(IV)–Schiff base catalyst exhibits similarly high activity and enantioselectivity in addition reactions employing the dienyl

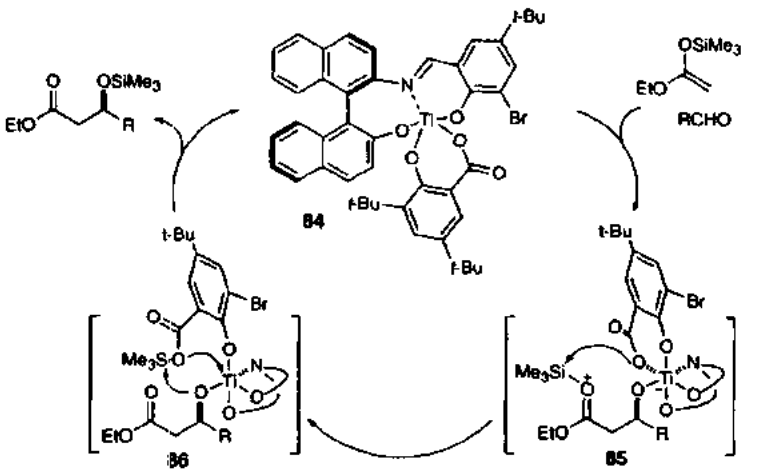

Fig. 15. Silicon shuttle mechanism for Ti(IV)–salicylate catalyzed aldol

Table 8
Ti[salicylate]-catalyzed addition of silyl ketene acetals

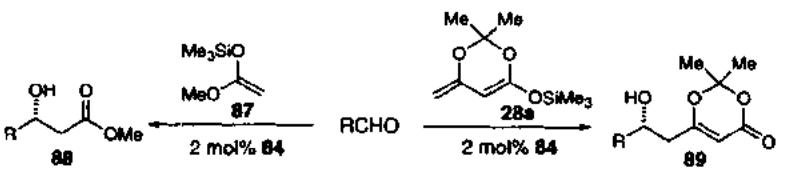

entry	aldehyde	ketene acetal 87 % ee[a]	ketene acetal 28a % ee[a]
a	$^{i}Pr_3Si$—≡—CHO	97	91
b	$TBSOCH_2$—≡—CHO	96	—
c	TBSC—⌒—CHO	—	94
d	Ph—⌒—CHO	94	80
e	PhCHO	96	84
f	$^{c}C_6H_{11}CHO$	95	—
g	Me—⌒—⌒—CHO	98	92

[a]Yields for two steps (addition and desilylation) range from 72 to 98%.

ketene acetal **28a**; the derived optically active β-hydroxy dioxinones **89** represent masked acetoacetate aldol adducts and provide versatile precursors to δ-hydroxy-β-keto esters, amides and β-keto-δ-lactones (Eq. 22).[52]

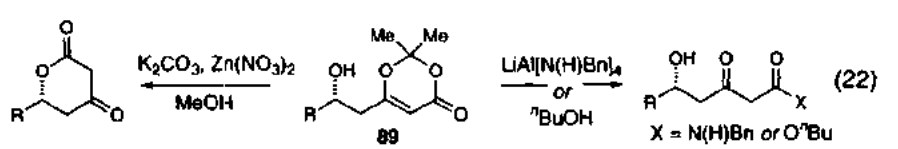

(22)

The enantioselective acetate aldol bond constructions accessed by Ti–salicyclate **84**-catalyzed Mukaiyama aldol additions have been exploited in the context of several total syntheses. Catalyzed addition of the acetate enolate equivalent **87** to the highly functionalized aldehyde **90** provides the

all *syn* triol **91**, thereby installing the C_{29} stereocenter in a major segment of the macrolide antibiotic roflamycoin (**92**) (Eq. 23).[53]

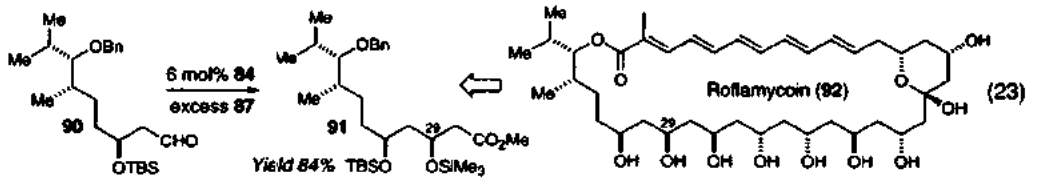

Significantly, reaction stereoselection is consistent with the catalyst complex operating as the sole stereochemical control element and does not appear to be complicated by resident chirality within the aldehyde reaction component.[54] The Carriera catalyst also serves as the chiral source for introduction of the only stereogenic center derived from non-natural sources in the total synthesis of the antitumor depsipeptide FR-901,228 (**93**) (Eq. 24).[55]

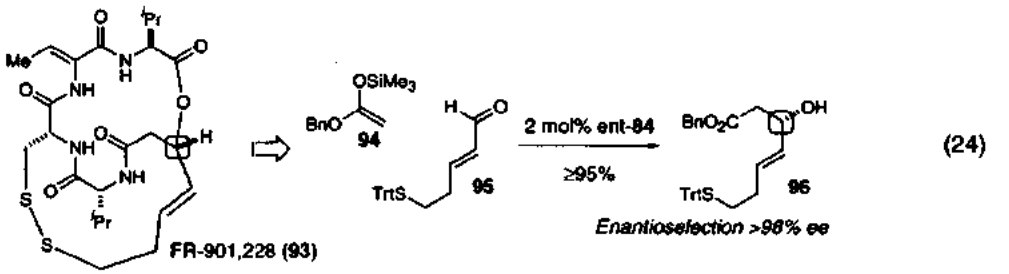

Thus, addition of the *O*-benzyl silyl ketene acetal **94** to the α,β-unsaturated aldehyde **95** proceeds to afford the optically active heptenoic acid derivative **96** with near-perfect enantioselection (>98% ee, ≥95% yield).

4.4.2. Catalyzed additions of O-alkyl enol ethers

Aldol reaction protocols that would eliminate the procedural requirement for generating the enolate equivalent in a separate operation, either by incorporating enolate formation into the catalytic cycle or by using commercially available enolate surrogates, would impart considerable operational simplification to Mukaiyama aldol reactions. The latter strategy has been successfully implemented in the context of Ti–Schiff base catalyzed aldol additions employing commercially available 2-methoxypropene as the requisite latent enolates (Table 9).[56] The acetone aldol adducts **97**, derived from the hydrolysis of the initial enol ether adduct, are produced with very high enantioselectivity in reactions employing a variety of functionalized aldehydes. In addition to the acetone aldols **97**, the initial enol ether reaction products **98** provide a conduit to a number of aldol adducts upon differential functionalization of the enol ether function, including the methyl acetate aldol **99** and the α-hydroxyacetone aldol adduct **100** (Eq. 25).

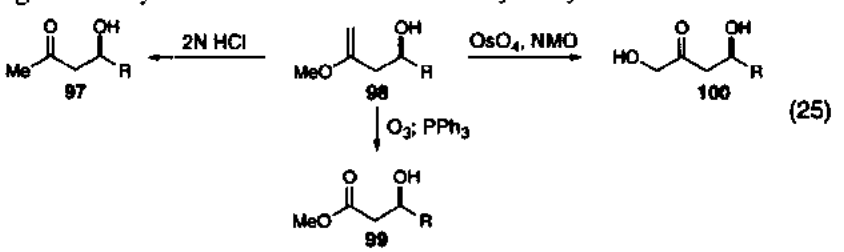

The catalyst complex **79** required for executing these reactions further distinguishes them from their Mukaiyama aldol counterparts; reactions employing the 2-methoxypropene nucleophile do not offer

Table 9
Catalyzed additions of 2-methoxypropene

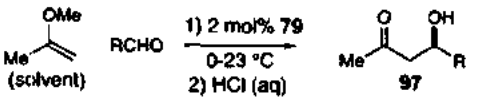

entry	aldehyde	% yield	% ee
a	$Ph(CH_2)_3$—≡—CHO	99	96
b	$TBSOCH_2$—≡—CHO	85	93
c	Ph—≡—CHO	99	91
d	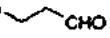	98	90
e	PhCHO	83	66
f	$^cC_6H_{11}CHO$	79	75

the potential for establishing a competitive silicon-catalyzed reaction pathway thus obviating the need for catalyst structures incorporating the salicylic acid ligand. The modest attenuation in electrophile generality (Table 9, entries e and f) associated with the 2-methoxypropene additions relative to the Mukaiyama reactions suggest that the salicylic acid ligand may play a small role in defining the stereochemical outcome of the catalyzed silyl ketene acetal aldol reactions.

5. Late transition metal catalysts: Cu(II)

5.1. Cu(II)[pyridine(bisoxazoline)]-catalyzed additions to α-benzyloxyacetaldehyde

Cationic Cu(II) complexes are among the rare examples of late transition metal Lewis acid catalysts that have been successfully applied to organic reaction methodology. Cationic Cu(II)-complexes incorporating chiral pyridine–bisoxazoline (pybox) and bidentate bisoxazoline ligands, **101** and **102** respectively, provide exceptional levels of asymmetric induction in Mukaiyama aldol reactions employing a variety of structurally diverse enolate equivalents (Table 10).[57] Low catalyst loadings (5 mol%) of the cationic Cu(II) complex **101** mediate the addition of *S*-alkyl and *O*-alkyl silyl ketene acetals, and the acetoacetate enolate equivalents **27a** and **103** to α-benzyloxyacetaldehyde (**104**) with enantioselectivities exceeding 92% ee (≥90% yield). Substituted enolate equivalents are also functional nucleophiles providing the derived propionate aldol adducts with excellent relative and absolute stereochemical control (entries d and e). Electrophilic reaction components capable of engaging in five-membered chelates with the catalyst appear to be a prerequisite for attaining high levels of asymmetric induction as non-chelating electrophiles, or those providing expanded chelate sizes, afford significantly reduced enantioselection (≤56% ee).

5.2. Cu(II)[bisoxazoline]-catalyzed additions to pyruvate esters

Mukaiyama aldol reactions employing carbonyl electrophiles other than aldehydes are relatively rare and, as a result, reactions utilizing ketone electrophiles as a means of preparing optically active tertiary alcohol derivatives have received little attention.[58] Copper(II)[bisoxazoline]-catalyzed aldol additions to pyruvate esters successfully address this issue and provide an efficient synthesis of optically active tertiary alcohols.[59] Acetate and propionate enolate equivalents, **8** and **14** respectively, undergo catalyzed

Table 10
Cu(II)[pybox]-catalyzed aldol reactions

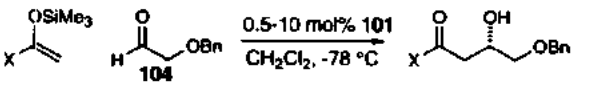

entry	ketene acetal	product	% yield	% ee
a	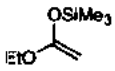	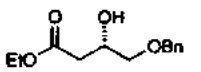	99	98
b	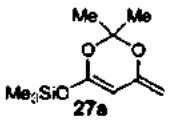	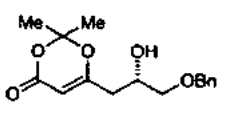	94	92
c	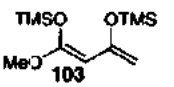	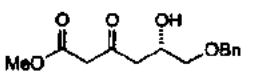	99	97
d	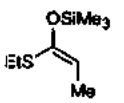	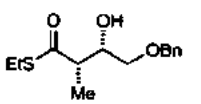	90	97
e	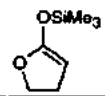	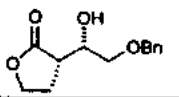	95	95

addition to various pyruvate ester electrophiles (**105**) to afford the derived optically active succinate ester derivatives **106** with excellent absolute and, in the latter case, relative stereochemical control (Eq. 26).

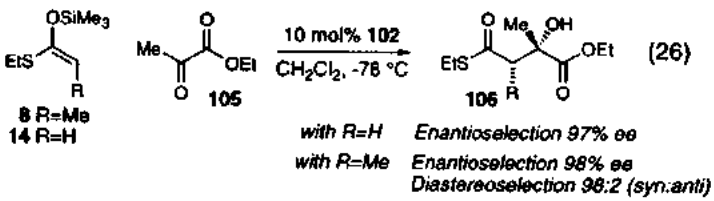

Reaction enantioselection is insensitive to structural variations in the pyruvate ester, tolerating a number of *O*-alkyl and ketone substituents; only branching at the ketone terminus results in significant erosion of enantioselection. However, these reactions exhibited an especially pronounced sensitivity to subtle steric perturbations about the reacting centers within the electrophile; catalyzed ketene acetal addition to 2,3-pentanedione (**107**) occurs almost exclusively at the methyl ketone terminus (Eq. 27).

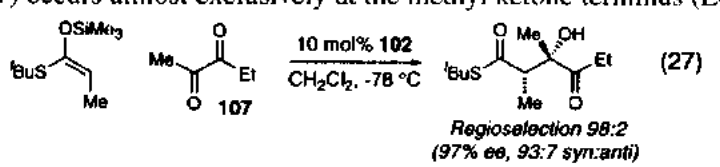

The mechanistic details of these Cu(II)-catalyzed Mukaiyama aldol reactions are especially intriguing in considering that preceding investigations unanimously agreed upon the deleterious effect of adventitious silicon catalysis has on asymmetric induction. Crossover experiments reveal that intermolecular silyl group transfer is a general phenomenon in Cu(II)-catalyzed aldol reactions, indicating that electrophilic silicon species are available for intermolecular reaction processes, including silicon-catalyzed reaction pathways. The fact that high levels of asymmetric induction are attained despite

this phenomenon suggests that electrophilic silicon species are not competitive catalysts relative to the chiral Cu(II) complexes. Indeed, addition of TMSOTf to the Cu(II)[bisoxazoline]-catalyzed addition of hindered nucleophiles to pyruvate esters accelerated aldol reaction rates with no loss in enantioselectivity; silylation of the intervening copper aldolate and the resulting catalyst turnover has been suggested as the origin of the observed rate acceleration.

Catalyst–electrophile structures have been proposed as predictive models for the Cu(II)-catalyzed α-benzyloxyacetaldehyde and pyruvate ester aldol reactions (Fig. 16). The regular square pyramid geometry of the Cu(II)[pybox]–aldehyde complex **108**, alluded to by ESR spectroscopy, results in effective shielding of the *re* aldehyde face by the pybox phenyl substituent, affording the observed (*S*)-β-hydroxy ester aldol adducts. Asymmetric induction derived from Cu(II) complexes incorporating bidentate bisoxazoline ligands is consistent with the reaction proceeding via the intermediacy of a square planar Cu(II)-α-diketone complex **109**. Projection of the proximate alkyl substituent over the π-system of the reacting carbonyl function effectively differentiates the prochiral faces of the pyruvate electrophiles.

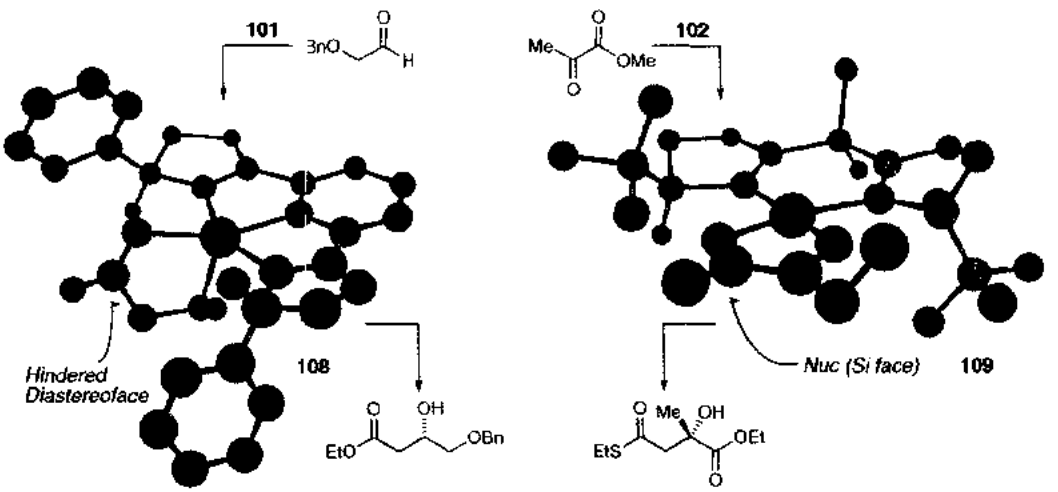

Fig. 16. Cu(II)[bisoxazoline]-electrophile complexes

Divalent tin complexes have also been developed as effective catalysts for aldol additions involving α-dicarbonyl electrophiles.[60,61] The Sn(II)–pyridyl bisoxazoline complex **110** catalyzes the highly enantioselective *S*-alkyl ketene acetal–pyruvate aldol addition with a complete reversal in diastereoselection (99:1 *anti:syn*) relative to the analogous *syn*-selective Cu(II)–bisoxazoline catalyzed reaction (Eq. 28). The Sn(II)–bisoxazoline complex **111** is an equally efficient catalyst for the pyruvate aldol additions as well as ketene acetal additions to glyoxylate esters, each providing the 2,3-*anti* aldol adducts characteristic of these Sn(II)-catalyzed reactions (Eq. 29).

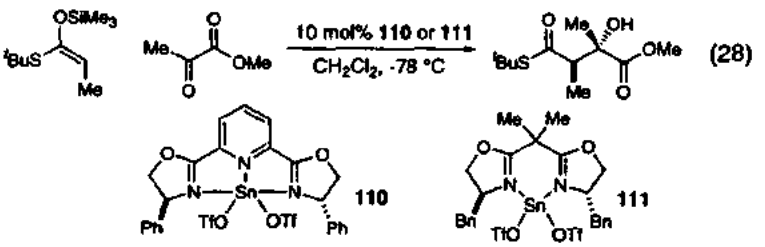

catalyst	*anti:syn*	% ee	% yield
110	99:1	99	94
111	92:8	94	—

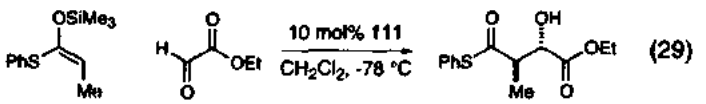

Enantioselection 95% ee
Diastereoselection 90:10 (anti:syn)

6. Group 2B, lanthanide and other late transition metal catalysts

Limited degrees of success have been achieved in developing optically active Rh(I)-,[62] Zn(II)-,[63] and lanthanide-based[64] complexes as catalysts for enantioselective Mukaiyama aldol reactions. Divalent zinc complexes modified with α-amino acid derived triflamide ligands mediate the addition of *O*-alkyl silyl ketene acetal **112** to a variety of aldehydes. However, the Zn(II)-catalyzed aldol reactions impose especially rigid constraints on aldehyde structure as only α,α,α-tribromoacetaldehyde (**113**) provides highly enantiomerically enriched aldol adducts (Eq. 30).

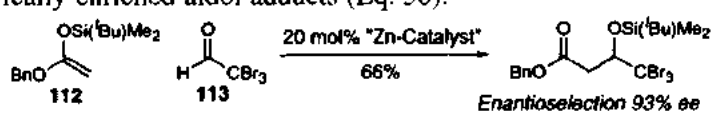

Enantioselection 93% ee

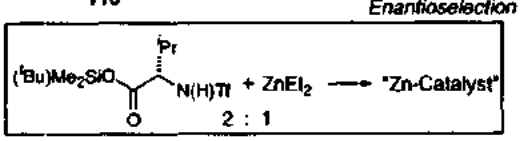

Chiral lanthanide-based catalysts derived from the corresponding lanthanide triflates and optically active bis(triflamide) ligands provide only moderate optical and chemical yields in the standard test reaction involving MTMP (**4**)/aryl aldehyde aldols (Eq. 31). The complex coordination chemistry associated with the lanthanide metals makes meaningful predictions concerning catalyst or transition state structure exceedingly difficult for this catalyst system. Cationic Rh(I) complexes incorporating chiral chelating bisphosphine ligands exhibit modest catalytic activity in the identical MTMP (**4**)/benzaldehyde addition reaction, but afford negligible enantioselection (≤12% ee) (Eq. 31).[65]

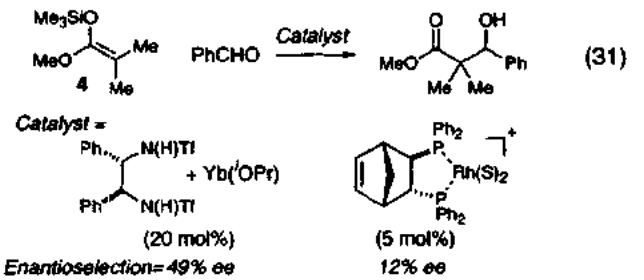

7. Nucleophilic (Lewis basic) catalysts

7.1. Additions of (trichlorosilyloxy)alkenes

Catalytic asymmetric aldol reaction design has been predicated almost exclusively on generating activated, facially discriminated electrophiles by virtue of complexation with a chiral Lewis acid catalyst. A less explored strategy for catalyzing Mukaiyama-type bond constructions involves the transient activation of the latent enolate equivalent via Lewis base coordination to the enolate silicon residue (Fig. 17).[66] Latent enolate equivalents incorporating trichlorosilyl groups are subject to this type of Lewis base activation, an observation that has resulted in the realization of Lewis base catalyzed aldol additions.[67] The addition of (trichlorosilyloxy)alkenes (enol ethers and ketene acetals) to aldehyde electrophiles is initiated by Lewis acid–base preassociation of the nucleophile and electrophile, dictating that the reaction proceeds through a closed, Zimmerman–Traxler transition state (Eq. 32).

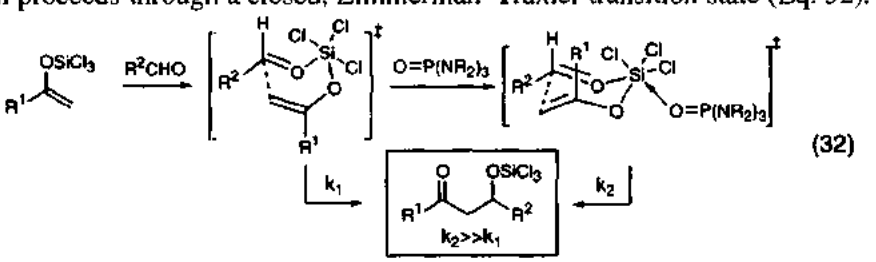

While reaction of the resulting nucleophile–electrophile aggregate is often spontaneous, aldol reaction rates are substantially accelerated by substoichiometric quantities of Lewis base addends. Based on these observations, a series of optically active Lewis basic catalysts have been developed for asymmetric aldol addition reactions involving (trichlorosilyloxy)alkenes; the optically active phosphoramide **114** catalyzes the highly stereoselective addition of the trichlorosilyl enolate **115** to aryl and α,β-unsaturated aldehydes (84–96% ee) (Eq. 33). Enantioselection in reactions employing the trichlorosilyl ketene acetal nucleophile **116** is eroded considerably relative to the enol silane aldols, presumably due to the intervention of the uncatalyzed reaction pathway (Eq. 34). Computational investigations of Lewis base promoted aldehyde additions of allyl trichlorosilanes suggest that amplified alkene nucleophilicity engendered upon silicon–phosphoramide association and/or the spatial compression of the reacting centers elicited by the accompanying change in silicon geometry from trigonal bipyramidal to octahedral is responsible for the observed Lewis base acceleration.[68]

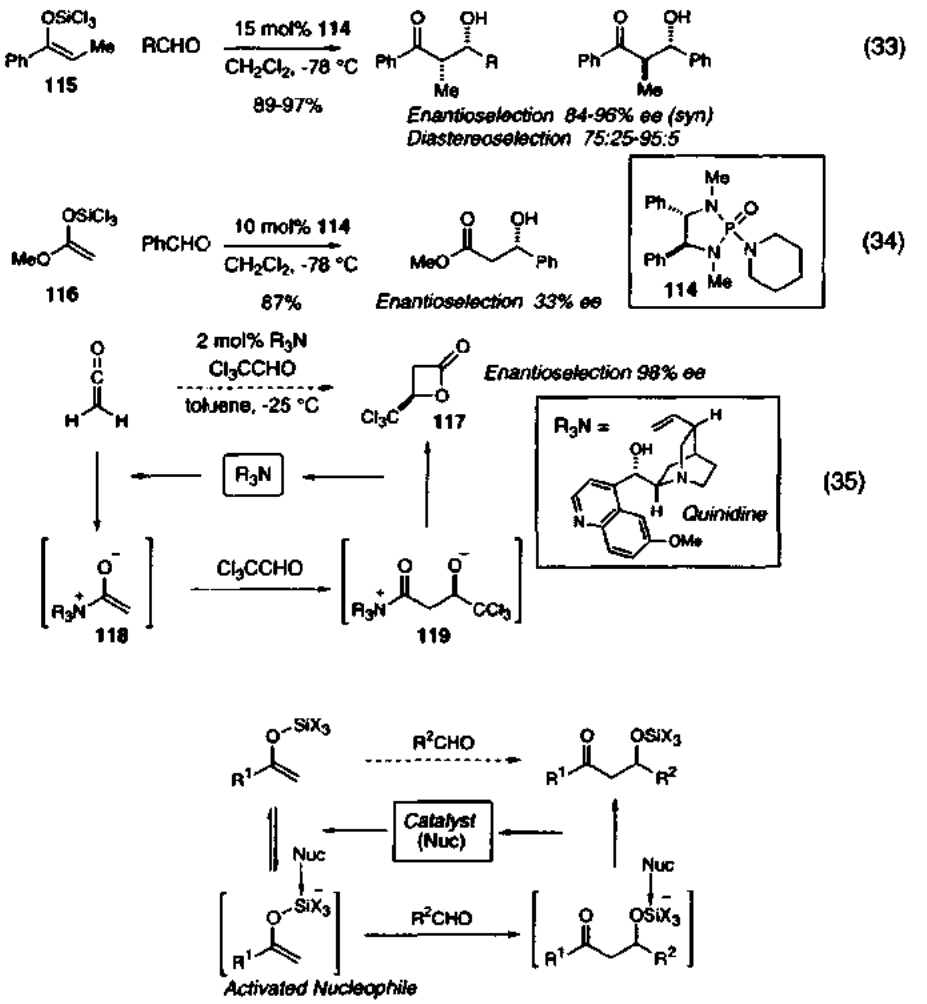

Fig. 17. Lewis base-catalyzed aldol additions of (silyloxy)alkenes

7.2. *Additions of latent enolate equivalents derived from ketene*

Optically active tertiary amine bases (quinine and quinidine) catalyze the addition of ketene to electron-deficient aldehydes and ketones, providing the derived 2-oxetanones **117** with high optical purity (Eq. 35).[69] The chiral ammonium enolate **118** resulting from nucleophilic addition of the amine catalyst to ketene is postulated to be the reactive species in these processes. Subsequent to enolate addition, lactonization ensues upon addition of the aldolate oxygen to the acyl ammonium ion **119** with concomitant regeneration of the amine catalyst. These cyclocondensation reactions represent an interesting example in which the latent nucleophilic reaction component is not derived from an enol ether functionality.[70]

8. Conclusion

Substantial progress has been realized in rendering asymmetric catalytic aldol reactions as reliable, easily executed organic reaction methodology. While efficiency and selectivity provide the benchmarks by which the various catalysts systems are evaluated, the extent to which each of these investigations built upon and benefited from the data and observations accumulated in preceding studies cannot be underappreciated. Similarly, the investigations detailed in this account will undoubtedly serve to accelerate research directed toward addressing the issues that confront further development of these important C–C bond constructions. The fact that little if any information exists regarding the structure of the catalytically active species or the mechanism by which these catalysts translate chirality to the incipient C–C bond is among the most prominent of these issues. Insights in these areas will greatly facilitate further developments of catalyst systems that will provide high levels of stereoselection in aldol reactions involving a broad range of enolate and electrophile structures. Future developments toward the reliable and efficient production of propionate aldol adducts with well-defined relative and absolute stereochemistry, and the preparation of optically active materials derived from latent enolate additions to eletrophiles other than aldehydes (e.g., ketones, acetals, imines) will serve to further expand the already considerable impact of these reactions on asymmetric organic synthesis.

Acknowledgements

Financial support provided by the University of Pittsburgh is gratefully acknowledged.

References

1. For a review of asymmetric aldol bond constructions, see: (a) Heathcock, C. H. The Aldol Reaction: Group I and II Enolates. In *Comprehensive Organic Synthesis: Additions to C–X π-Bond Part 2*; Trost, B. M.; Fleming, I.; Heathcock, C. H., Eds.; Pergamon Press: New York, 1991; Vol. 2, Chapter 1.6, pp. 181–238. (b) Kim, B. M.; Williams, S. F.; Masamune, S. The Aldol Reaction: Group III Enolates. In *Comprehensive Organic Synthesis: Additions to C–X π-Bond Part 2*; Trost, B. M.; Fleming, I.; Heathcock, C. H., Eds.; Pergamon Press: New York, 1991; Vol. 2, Chapter 1.7, pp. 239–275. (c) Paterson, I. The Aldol Reaction: Transition Metal Enolates. In *Comprehensive Organic Synthesis: Additions to C–X π-Bond Part 2*; Trost, B. M.; Fleming, I.; Heathcock, C. H., Eds.; Pergamon Press: New York, 1991; Vol. 2, Chapter 1.9, pp. 301–319. (d) Caine, D. in *Comprehensive Organic Synthesis: Additions to C–X σ-Bond*; Trost, B. M.; Fleming, I.; Heathcock, C. H., Eds.; Pergamon Press: New York, 1991; Vol. 3, Chapter 1.1, pp. 1–110.
2. (a) Evans, D. A.; Nelson, J. V.; Taber, T. R. *Top. Stereochem.* **1982**, *13*, 1–115. (b) Heathcock, C. H. in *Asymmetric Synthesis*, Morrison, J. D. Ed.; Academic Press New York, 1984; Vol. 3, pp. 111–212.
3. (a) Mukaiyama, T.; Narasaka, K.; Banno, K. *Chem. Lett.* **1973**, 1011–1014. (b) Mukaiyama, T.; Banno, K.; Narasaka, K. *J. Am. Chem. Soc.* **1974**, *96*, 7503–7509. (c) Saigo, K.; Osaki, M.; Mukaiyama, T. *Chem. Lett.* **1975**, 989–990.
4. Wierschke, S. G.; Chandrasekhar, J.; Jorgensen, W. L. *J. Am. Chem. Soc.* **1985**, *107*, 1496–1500.
5. In addition to the mechanistic alternatives discussed later in this text, silyl ketene acetals transmetallate with $TiCl_4$ under certain reaction conditions and undergo aldol addition via the derived (trichloro)titanium enolates, see: Nakamura, E.; Shimada, J.; Horiguchi, Y.; Kuwajima, I. *Tetrahedron Lett.* **1983**, *24*, 3341–3342.
6. Reetz, M. T.; Kyung, S.-H.; Bolm, C.; Zierke, T. *Chem. Ind.* **1986**, 824.
7. (a) Kobayashi, S.; Mukaiyama, T. *Chem. Lett.* **1989**, 297–300. (b) Mukaiyama, T.; Uchiro, H.; Kobayashi, S. *Chem. Lett.* **1989**, 1001–1004. (c) Mukaiyama, T.; Kobayashi, S.; Sano, T. *Tetrahedron* **1990**, *46*, 4653–4662. (d) Kobayashi, S.; Uchiro, H.; Fujishita, Y.; Shiina, I.; Mukaiyama, T. *J. Am. Chem. Soc.* **1991**, *113*, 4247–4252, and references cited therein.
8. (a) Iwasawa, N.; Mukaiyama, T. *Chem. Lett.* **1987**, 463–466. (b) Mukaiyama, T.; Kobayashi, S.; Tamura, M.; Sagawa, Y. *Chem. Lett.* **1987**, 491–494. See also: Mukaiyama, T.; Sugumi, H.; Uchiro, H.; Kobayashi, S. *Chem. Lett.* **1988**, 1291–1294, and references cited therein.

9. For a recent application of related chiral Sn(II)–diamine promoters to aldol additions employing β-alkoxy silyl ketene acetals, see: Kobayashi, S.; Horibe, M. *J. Am. Chem. Soc.* **1994**, *116*, 9805–9806. See also: Mukaiyama, T.; Uchiro, H.; Shiina, I.; Kobayashi, S. *Chem. Lett.* **1990**, 1019–1022.
10. Mukaiyama, T.; Kobayashi, S.; Uchiro, H.; Shiina, I. *Chem. Lett.* **1990**, 129–132.
11. (a) Noyori, R.; Murata, S.; Suzuki, M. *Tetrahedron* **1981**, *37*, 3899–3910. (b) Noyori, R.; Murata, S.; Suzuki, M. *Tetrahedron* **1988**, *44*, 4259–4275.
12. (a) Carriera, E. M.; Singer, R. A. *Tetrahedron Lett.* **1994**, *35*, 4323–4326. (b) Denmark, S. E.; Chen, C.-T. *Tetrahedron Lett.* **1994**, *35*, 4327–4330. (c) Hollis, T. K.; Bosnich, B. *J. Am. Chem. Soc.* **1995**, *117*, 4570–4581.
13. Kobayashi, S.; Fujishita, Y.; Mukaiyama, T. *Chem. Lett.* **1990**, 1455–1458.
14. A similar catalyst system derived from tin(II) oxide, TMSOTf, and the chiral diame **7** has been reported. Asymmetric induction in the reaction depicted in Table 1 using this catalyst is dramatically inferior to that achieved using the $Sn(OTf)_2$–**7** catalyst (**10**) (21% ee). See: Mukaiyama, T.; Uchiro, H.; Kobayashi, S. *Chem. Lett.* **1990**, 1147–1150.
15. Kobayashi, S.; Furuya, M.; Ohtsubo, A.; Mukaiyama, T. *Tetrahedron: Asymmetry* **1991**, 2, 635–638.
16. (a) Furuta, K.; Maruyama, T.; Yamamoto, H. *J. Am. Chem. Soc.* **1991**, *113*, 1041–1042. (b) Ishihara, K.; Maruyama, T.; Mouri, M.; Gao, Q.; Furuta, K.; Yamamoto, H. *Bull. Chem. Soc. Jpn* **1993**, *66*, 3483–3491.
17. The term 'CAB' is used in Ref. 16a as an acronym for 'chiral (acyloxy)borane' and is used herein for the purposes of convenience.
18. Addition reactions of structurally related allylsilane nucleophiles proceed via similar extended transition state structures, see: Hayashi, T.; Kabeta, K.; Hamachi, I.; Kumada, M. *Tetrahedron Lett.* **1983**, *24*, 2865–2868.
19. Furuta, K.; Maruyama, T.; Yamamoto, H. *Synlett* **1991**, 439–440.
20. Sato, M.; Sunami, S.; Sugita, Y.; Kaneko, C. *Chem. Pharm. Bull.* **1994**, *42*, 839–845.
21. Barrett, A. G. M.; Kamimura, A. *J. Chem. Soc., Chem. Commun.* **1995**, 1755–1756.
22. Ishihara, K.; Gao, Q.; Yamamoto, H. *J. Am. Chem. Soc.* **1993**, *115*, 10412–10413.
23. Parmee, E. R.; Tempkin, O.; Masamune, S.; Abiko, A. *J. Am. Chem. Soc.* **1991**, *113*, 9365–9366.
24. Parmee, E. R.; Hong, Y.; Tempkin, O.; Masamune, S. *Tetrahedron Lett.* **1992**, *33*, 1729–1732.
25. Kiyooka, S.; Kaneko, Y.; Kume, K. *Tetrahedron Lett.* **1992**, *33*, 4927–4930.
26. Corey, E. J.; Cywin, C. L.; Roper, T. D. *Tetrahedron Lett.* **1992**, *33*, 6907–6910.
27. Kiyooka, S.; Kaneko, Y.; Komura, M.; Matsuo, H.; Nakano, M. *J. Org. Chem.* **1991**, *56*, 2276–2278.
28. Kaneko, Y.; Matsuo, T.; Kiyooka, S. *Tetrahedron Lett.* **1994**, *35*, 4107–4110.
29. (a) Evans, D. A.; Chapman, K. T. *Tetrahedron Lett.* **1986**, *27*, 5939–5942. (b) Evans, D. A.; Chapman, K. T.; Carreira, E. M. *J. Am. Chem. Soc.* **1988**, *110*, 3560–3578 and references therein.
30. For a discussion of 'gearing' in related bis(sulfonamide) ligands, see: Corey, E. J.; Imwinkelried, R.; Pikul, S.; Xiang, Y. B. *J. Am. Chem. Soc.* **1989**, *111*, 5493–5495.
31. Corey, E. J.; Loh, T.-P.; Roper, T. D.; Azimioara, M. D.; Noe, M. C. *J. Am. Chem. Soc.* **1992**, *114*, 8290–8292.
32. Narasaka, K. Chiral Titanium Complexes in Asymmetric Construction of Carbon Skeletons. In *Stereocontrolled Organic Synthesis*; Trost, B. M. Ed.; Blackwell: Oxford, 1994; pp. 17–36.
33. (a) Boyle, T. J.; Eilerts, N. W.; Heppert, J. A.; Takusagawa, F. *Organometallics* **1994**, *13*, 2218–2229, and references therein. (b) Gau, H.-M.; Lee, C.-S.; Lin, C.-C.; Jiang, M.-K.; Ho, Y.-C.; Kuo, C.-H. *J. Am. Chem. Soc.* **1996**, *118*, 2936–2941.
34. Mukaiyama, T.; Inubushi, A.; Suda, S.; Hara, R.; Kobayashi, S. *Chem. Lett.* **1990**, 1015–1018.
35. Mikami, K.; Matsukawa, S. *J. Am. Chem. Soc.* **1993**, *115*, 7039–7040.
36. For a review of asymmetric ene reactions catalyed by the Ti(IV)[BINOL] complex **58**, see: Mikami, K. *Pure & Appl. Chem.* **1996**, *68*, 639–644.
37. The relationship between catalyst efficiency and the procedural details of preparing complex **58** have been investigated in the context of asymmetric catalyzed ene reactions, see: Mikami, K.; Terada, M.; Nakai, T. *J. Am. Chem. Soc.* **1990**, *112*, 3949–3954.
38. Shoda, H.; Nakamura, T.; Tanino, K.; Kuwajima, I. *Tetrahedron Lett.* **1993**, *34*, 6281–6284.
39. Non-chelated Lewis acid–glyoxylate complexes have been envoked to rationalize the *syn* diastereoselection derived from related Lewis acid promoted ene reactions, see: Mikami, K.; Loh, T.-P.; Nakai, T. *Tetrahedron Lett.* **1988**, *29*, 6305–6308.
40. While the addition of enol silane **59** via an open transition state seemingly does not accomodate the formal ene-type products that emerge from these reactions, this fact does not necessarily preclude the intervention of the non-concerted reaction pathway represented by an open transition state structure.
41. Mikami, K.; Matsukawa, S. *J. Am. Chem. Soc.* **1994**, *116*, 4077–4078.
42. Matsukawa, S.; Mikami, K. *Tetrahedron: Asymmetry* **1995**, *6*, 2571–2574.

43. For a review of the structural aspects of Lewis acid–carbonyl complexes, see: Shambayati, S.; Schreiber, S. L. Lewis Acid Carbonyl Complexation. In *Comprehensive Organic Synthesis: Additions to C–X π-Bond Part 1*; Trost; B. M.; Fleming, I.; Heathcock, C. H., Eds.; Pergamon Press: New York, 1991; Vol. 1, Chapter 1.10, pp. 283–324.
44. Keck, G. E.; Krishnamurthy, D. *J. Am. Chem. Soc.* **1995**, *117*, 2363–2364.
45. Reference to 'Catalyst A' and 'Catalyst B' is consistent with the nomenclature used in references 44 and 46 to describe the Ti(O*i*-Pr)$_4$–BINOL catalysts derived from a particular experimental procedure. For experimental details on the preparation of the various Ti(O*i*-Pr)$_4$–BINOL catalyst systems, see: (a) Keck, G. E.; Tarbet, K. H.; Geraci, L. S. *J. Am. Chem. Soc.* **1993**, *115*, 8467–8468. (b) Keck, G. E.; Geraci, L. S. *Tetrahedron Lett.* **1993**, *34*, 7827–7828.
46. Keck, G. E.; Li, X.-Y.; Krishnamurthy, D. *J. Org. Chem.* **1995**, *60*, 5998–5999.
47. Keck, G. E.; Krishnamurthy, D.; Grier, M. C. *J. Org. Chem.* **1993**, *58*, 6543–6544.
48. Terada, M.; Mikami, K.; Nakai, T. *J. Chem. Soc., Chem. Commun.* **1990**, 1623–1624.
49. Sato, M.; Sunami, S.; Sugita, Y.; Kaneko, C. *Heterocycles* **1995**, *41*, 1435–1444.
50. Bach, T. *Angew. Chem. Int. Ed. Engl.* **1994**, *33*, 417–419.
51. (a) Carreira, E. M.; Singer, R. A.; Lee, W. *J. Am. Chem. Soc.* **1994**, *116*, 8837–8838. (b) Carreira, E. M.; Singer, R. A. *Drug Discovery Today* **1996**, *1*, 145–150.
52. Singer, R. A.; Carreira, E. M. *J. Am. Chem. Soc.* **1995**, *117*, 12360–12361.
53. Rychnovsky, S. D.; Khire, U. R.; Yang, G. *J. Am. Chem. Soc.* **1997**, *119*, 2058–2059.
54. Lewis acid promoted additions of enol silanes to chiral β-alkoxy aldehydes, transformations analogous to the reaction depicted in Eq. 23, afford the 1,3-*anti* aldol diastereomer selectively. See: Evans, D. A.; Dart, M. J.; Duffy, J. L.; Yang, M. G. *J. Am. Chem. Soc.* **1996**, *118*, 4322–4343.
55. Li, K. W.; Wu, J.; Xing, W.; Simon, J. A. *J. Am. Chem. Soc.* **1996**, *118*, 7237–7238.
56. Carreira, E. M.; Lee, W.; Singer, R. A. *J. Am. Chem. Soc.* **1995**, *117*, 3649–3650.
57. Evans, D. A.; Murry, J. A.; Kozlowski, M. C. *J. Am. Chem. Soc.* **1996**, *118*, 5814–5815.
58. Kobayashi, S.; Fujishita, Y.; Mukaiyama, T. *Chem. Lett.* **1989**, 2069–2072.
59. Evans, D. A.; Kozlowski, M. C.; Burgey, C. S.; MacMillan, D. W. C. *J. Am. Chem. Soc.* **1997**, *119*, 7893–7894.
60. Evans, D. A.; MacMillan, D. W. C.; Campos, K. R. *J. Am. Chem. Soc.* **1997**, *119*, 10859–10860.
61. Despite the organizational scheme of this review, these Sn(II) catalysts are discussed here to allow a more effective comparison to the structurally related Cu(II)–bisoxazoline catalyst complexes discussed in the preceeding section.
62. (a) Sato, S.; Matsuda, I.; Izumi, Y. *Tetrahedron Lett.* **1986**, *27*, 5517–5520. (b) Reetz, M. T.; Vougioukas, A. E. *Tetrahedron Lett.* **1987**, *28*, 793–796.
63. Mukaiyama, T.; Takashima, T.; Kusaka, H.; Shimpuku, T. *Chem. Lett.* **1990**, 1777–1780.
64. Uotsu, K.; Sasai, H.; Shibasaki, M. *Tetrahedron: Asymmetry* **1995**, *6*, 71–74.
65. For a detailed investigation of Rh(I)-catalyzed addition reactions of silyl enol ethers that involve nucleophile rather than electrophile activation, see: Slough, G. A.; Bergman, R. G.; Heathcock, C. H. *J. Am. Chem. Soc.* **1989**, *111*, 938–949.
66. Lewis base accelerated aldehyde additions of allylic trichlorosilanes have been reported, see: (a) Denmark, S. E.; Coe, D. M.; Pratt, N. E.; Griedel, B. D. *J. Org. Chem.* **1994**, *59*, 6161–6163. (b) Kobayashi, S.; Nishio, K. *J. Org. Chem.* **1994**, *59*, 6620–6628.
67. (a) Denmark, S. E.; Winter, S. B. D.; Su, X.; Wong, K.-T. *J. Am. Chem. Soc.* **1996**, *118*, 7404–7405. (b) Denmark, S. E.; Wong, K.-T.; Stavenger, R. A. *J. Am. Chem. Soc.* **1997**, *119*, 2333–2334.
68. (a) Kira, M.; Sato, K.; Sakurai, H.; Hada, M.; Izawa, M.; Ushio, J. *Chem. Lett.* **1991**, 387–390. (b) Hada, M.; Nakatsuji, H.; Ushio, J.; Izawa, M.; Yokono, H. *Organometallics* **1993**, *12*, 3398–3404.
69. (a) Wynberg, H.; Staring, E. G. J. *J. Org. Chem.* **1985**, *50*, 1977–1979. (b) Wynberg, H. *Top. Stereochem.* **1986**, *16*, 87–130.
70. The author wishes to thank a referee for suggesting the relevance of this process to catalyzed additions of latent enolates.